



Al-Mustansiriyah

ISSN 1814 - 635X

Journal of Science

Vol. 21, No. 6, 2010



Issued by College of Science - Mustansiriyah University

Al- Mustansiriyah Journal of Science

Issued by College of Science- Al- Mustansiriya
University

Special Edition
Researchs of The 6th Conference College Of
Science Al-Mustansiriyah University
From 9-10 February

Head Editor

Prof. Dr. Redha I. AL-Bayati

General Editor

Asst. Prof. Dr. Ikbal khider Al- joofy

Editorial Board

Dr. Iman Tarik Al -Alawy	Member
Dr. Ramzy Rasheed Al-Ani	Member
Dr. Inaam Abdul-Rahman Hasan	Member
Dr. Awni Edwar Abdulahad	Member
Dr. Majid Mohammed Mahmood	Member
Dr. Saad Najm Bashikh	Member
Dr. Hussain Kareem Sulaiman	Member

Consultant Committee

Dr. Kadhim Hasan H. Al-Mossawi	Member
Dr. Tariq Salih Abdul-Razaq	Member
Dr. Mehdi Sadiq Abbas	Member
Dr. Abdulla Ahmad Rasheed	Member
Dr. Hussein Ismail Abdullah	Member
Dr. Muhaned Mohammed Nuri	Member
Dr. Monim Hakeem Kalaf	Member
Dr. Amir Sadiq Al-Malah	Member
Dr. Tariq Suhail Najim	Member
Dr. Yosif Kadhim Al-Haidari	Member

CONTENTS

ITEM	Page No.
Impact Parameter Dependence of Electronic Energy Loss of Fast Ions Khalid A. Ahmad, Riayhd K. Ahmad and Muthanna M. Mahmood	1-7
Effect of Electron Beam Irradiation on Optical and electrical Properties of Tin Dioxide Thin Film Raad S. Sabry	8-14
Tribological Characteristic Of Graphite-Novolac Composites: Experimental And Simulation Approach Bahjat B. Kadhim	15-21
Ionizing radiation impacts the powerful antioxidant activity of Zingiber officinale Rosc. extracts: <i>in vitro</i> study Zainab Wahbee Abdul Lateef	22-32
Using Maximum Likelihood Technique to Classify and Recognized the Voices of Spoken Words Ahmed Humod Flieh	33-38
Study Text Image Resolution Using Soble Operator Ahlam Mjeed Kadhum, Farah Jawad Kadhum and Ban Sabah	39-48
Influence of Copper Sulfate Additives on Some Optical Properties of PMMA films Sami Salman Chiad, Amer Basim Shaalan and Nadir Fadhil Habubi	49-56
The Extrapolation Of The Lateral Distribution function Approximation Of Cherenkov Radiation At The Energy Range 10^{16} - $2 \cdot 10^{18}$ eV Ahmed Aziz Ahmed And Sabah Toma Murad	57-62
Effect of Structural Properties Variation on the Ethanol Sensing of ZnO Thin Films Ali Jasim Mohammed	63-68
Study The Effect of Lightness on The Good Vision of Written text in the class room Ali A. D. Al-Zuky, Salema S. Salman and Ahlam M.Kadhum	69-84
Some Optical Properties of the Sputtered SnO ₂ Thin Film Affected by Gamma Radiation Ali J. Mohammad, Salah K. Hazaa, Ali N. Mohammed	85-89
Study The Resolution of the Written Text on the Whiteboard Based on the Criterion of Contrast for Different Illumination Conditions Salema Sultan Salman	90-105
Synthesis of Pyrazoline-5-one Compounds Derivative From 4-Aminobenzoic Acid Rafah F.Al-Smaisim, Redha E. Al-Bayati and Abdul Hussain K. Sharba	106-116
Preparation of new HPLC stationary phase and study of their chromatographic performance towered the separation of amino acids and poly aromatic compounds. Noor M. Ali, Shahbaz A. Maki and Hadeel S. Abd Al- wahab	117-128
Simple and Rapid Method for Determination of Vitamin C, in pharmaceutical Preparations Hadi.H.Jasim	129-133
Determination of The Carboxylic Group Using Ion Selective Electrode Souhaila K.Syhood,Adnan A.Hussain, Kafa K.Hammud and Abtesam A.kudar,Lamiaa Hussain	134-138
Synthesis and Characterization of Mixed Ligand Complexes of Some Transition Metals with Alanine and 8-Hydroxyquinoline Taghreed.H.AL-Noor, Shatha.M.Obed and Eqbal.R.Hana	139-151

Synthesis and Characterization Of Some Dioxo – Rhenium (V) Complexes Shemaa. A.S.Jabar, Mahmmad. Jaber, Atiaf K. Hammed, Dunia. N. Jihad and Samaa. A.S. Jabar	152-159
Copolymerization of 1,2:3,4-di-o-isopropylidene-5,6-exo- α -d-galactosene Monomer Yousif Ali Al-Fattahi, Salah M. Aliwi and Hammed H. Mohamed	160-169
Construction of New Ethambutol Selective Electrodes for Determination Ethambutol in Pharmaceutical Drugs Nabil S. Nassory, Abdul-Muhsin A. Al-Haideri and Souhaila K. Sayhood	170-178
Preparation and Study of Cephalexin Selective Electrodes and Their Application in Pharmaceutical Drugs Khaleida H. Al-Saidi, Nabil S. Nassory and Shahbaz A. Maki	179-191
Simultaneous Determination of Paracetamol and Cephalexin Binary mixtures by Using Derivative Spectrophotometry and H-point Standard Addition Methods Khaleida Hamid Al-Saidi, Firyal Waly Askar and Asraa Abed AL-Abaas	192-203
Inhibitive Action of Ellagic acid on Corrosion behavior of SS 316L in Artificial saliva Murtdha A. Siyah., Amar .M. hmud, Riyadh sh. Al- Hussein, and Jamal. F. Hamodi.	204-211
Preparation and Potentiometric Study of Amiloride Hydrochloride Selective Electrodes and Their Application in Determining Some Drugs Khaleida, H. Al-Saidi and Maha Abdulateef yahya	212-229
Assessment of Cancer Risk to the Human Tissues Related to Public Exposure to Cesium-137 Nabeel Hashim Ameen Al-Tameemi	230-243
Study Of Protein Profile In Patients With Bladder Cancer Israa G. Zainal and Shaema S. AL-Janabi	244-250
Synthesis and Spectroscopic Studies of New Heterocyclic Azo Dye and Their Complexes with Selected Metal Ion Amer. J. Jarad, Khalida. F. Suhail And Ahmed. L. Hussien	251-257
<i>In vitro</i> and <i>In vivo</i> Effect of <i>Myrtus communis</i> Extracts on <i>Staphylococcus</i> <i>aureus</i> Isolated from Patients with UTI Rukia Muhammad. Al-Barzinji and Sazan Khalid Esmahil	258-267
Chromosomal Aberrations In Patients With Recurrent Spontaneous Abortion Rafid Abdulwahed, A, Abdul amer naser G., kareem .M lilo and rushdi sadi	268-274
The Adhesion of <i>Candida albicans</i> to Epithelial Cells in Diabetes Mellitus Patients Najah Ali Mohammed, Bara'a Jawad Kadhim, and Ibtisam Mohammad Hussain	275-280
The Minimal Degree of a Faithful Representation of $G = SL(2, q)$ Afra M. Ibraheem, Dunya M. Hamed and Maysa'a'Z. Salman	281-290
Single Machine with Multicriteria Problems Tariq Salih Abdul-Razaq and Fadia Mohammed Salman	291-303
$\Gamma(m,n)$ - $\Gamma(m,n)$ -Quasi-ASI-Injective Modules Mehdi Sadik Abbas and Akeel Npasir Kadhim	304-317
Reflection Arrangement which is neither Hypersolvable nor supersolvable Michel Jambu, Abid A. Al-Taai, Rabeaa G.A. AL-Aleyawee	318-328
Exact Solution for a Spherical Symmetric Perfect Fluid Model of Embedding Class Two ¹ Mahmood K. Jasim, ² Inaam A. Malloki and ³ Arwa A. Abd Al-Hameed	329-341
Solving combinatorial optimization problem by using genetic algorithm	342-362

Degree of Best Approximation of Bounded μ - Measurable Function by Means of K- Functional Sahib K. AL- Saigy and Zainab Esa Abdul Naby	363-373
On Relative Pure Injective Modules* Mehdi Sadik Abbas and Mohanad Farhan Hamid	374-382
Comparison of Approximation Algorithms for Unrelated Parallel Machines to Minimize the Weighted Makespan Tariq S.Abdul-Razaq and Najwa Raheem Mustafa	383-391
Fully Stable Modeles Relative To An Ideal Mehdi Sadik Abbas and Anaam Moter Sharky	392-400
On reverse *-centralizer of prime and semiprime ring with involution Abd Al- Rahman.H.Majeed and Ali Abd Abeed.AL-Tay	401-407
S* - Order continuous Ali Hussain Battor and Falah Hasan Sarhan	408-411
On The θ -Convergence of Net and Filter in Bitopological space Bassam Jabbar AL-Asadi and Amer Ismael Al-Saeed	412-422
Coincidence Points of Two Maps In Banach Spaces Zena Hussein Mabeed	423-428
The Escape Time Dimension of the Filled Julia Set Adil Mahmood Ahmed, Abdul Al-Samee Al-Janabi and Arkan Jassim Mohammed	429-440
Some Topological Properties of I(X)-Spaces Amal Ibrahim Al-Attar and Habeeb Kareem Abdullah	441-456
On Prime and Semiprime Rings With Derivations Mehsin Jabel Atteya	457-465
Approximately Projective Modeles and The Endomorphism Ring of Approximately Projective Models Mehdi Sadik Abbas and Maha Abdulazeez Al	466-481
Special Injective Modules and Their Endomorphishm Ring Mehdi Sadik Abbas and Shaimaa Noori Abd-alridha	482-500
Using Genetic Algorithm and Local Search to Solve Flow shop NP - comple Tariq S. Abdul-Razaq and Lika Z. Hummady	501-518
Estimating Global Solar Radiation on Horizontal Surfaces Using Different Correlation Formulas for Baghdad City Ali.M. AL-Salihi, Kais. J. Al-Jumaily, Osama. T. Al-Taai	519-530
The Relationship between Surface Air Temperature and Ground Surface Temperature for Selected Station in Iraq Dheyaa .A. Al-Hassani and Kais J.AL-Jumaily	531-535
Solar Radiation and Longwave Radiative Climatology for Selected Stations in Iraq Dheyaa Azeez Bilal Al-Hassani	536-541
Authentication for Remote voting via visual cryptography Musaab R. Abdulrazzaq and Dina R. Abdulrazzaq	542-551
Coins Recognition Using Complex Moments and Feed Forward Neural Network Loay E. George and Narjes M. Shaty	552-566

Impact Parameter Dependence of Electronic Energy Loss of Fast Ions

Khalid A. Ahmad, Riayhd K. Ahmad and Muthanna M. Mahmood
Department of Physics, College of Science, Al-Mustansiriya University

الخلاصة

في هذا البحث تمت دراسة اعتماد معامل التصادم على فقدان الطاقة للأيونات السريعة مثل الهيدروجين في الهيدروجين ، والهليوم في النيون .. باستخدام تقريب الالتفاف الإضطرابي والذي يعتمد على نظرية الإضطراب بالحد الأول . تم الحصول على نتائج جيدة مع الاعمال السابقة .

ABSTRACT

The dependence of impact parameter of energy loss of fast ion like H in H, He and Ne is investigated in the present work using perturbation convolution approximation (PCA) which is based on first-order perturbation theory. Good agreement is achieved with previous works.

INTRODUCTION

The electronic energy loss has been studied for many years because of its direct applications in problems concerning material damage, ion beam analysis and plasma physics. The theoretical treatment of the energy loss in atomic collisions has been greatly improved over the last decades. Calculations of the electronic energy loss have been performed by using traditional methods known from atomic physics investigations such as the plane wave Born approximation (PWBA) (1).

The energy loss of the light ions slowing down in matter is dominated by electronic processes at projectile velocities higher than the mean electron velocity. The basic mechanisms of the energy loss of a swift projectile are ionization and excitation of target atoms, well described in the frame work of perturbation theory. The well known Z_p - projectile charge dependence of the electronic energy loss per unit path, the electronic stopping power, follows immediately from such a treatment (1). Also, the Beth formula (2) which yields the asymptotic high-energy limit of the stopping power may be derived directly from first-order perturbation theory. By decreasing the ion energy higher-order effects come into play.

In order to describe the energy loss properly, the contribution due to projectiles carrying bound electrons must be considered. The problem of the stopping screened projectiles was first studied by Dalarno and Griffing (3) in the (PWBA) for the most simple collision system (H on H) in the mid 1950s and has been extended for other atomic collision systems using the Bethe theory (4-5). Sigmund (6) has developed a model for the charge-dependent electronic stopping of swift heavy ions in the framework of Bohr's classical theory and Bethe-Bloch stopping theory.

Energy loss and convolution theory

In order to calculate the energy loss due to target ionization and excitation we have to consider the amplitude of each electronic transition from ground state $|0\rangle$ with energy E_0 to a final state $|f\rangle$,

$$a_f(\vec{b}) = -i \int_{-\infty}^{\infty} dt e^{i(E_F - E_0)t} \langle f | V(\vec{r} - \vec{R}(t)) | 0 \rangle \quad (1).$$

Where $V(\vec{r} - \vec{R}(t))$ is the Coulomb interaction potential between the bare projectile ion with nuclear charge Z_p and a target electron. The ion trajectories are described by straight lines

$$\vec{R}(t) = \vec{v}t + \vec{b} \quad (2)$$

Where \vec{v} is the projectile velocity and \vec{b} is the impact parameter vectors of the collision.

At large impact parameter the so called

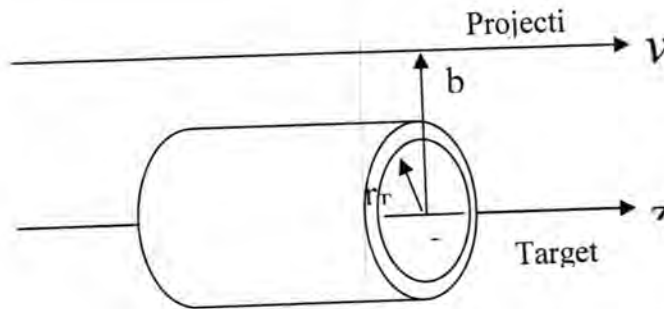


Fig. -1: shows the collision geometry of target and nucleus with impact parameter \vec{b} and velocity \vec{v} . The cylinder represents the integrated electronic density along the ion flight direction (7).

dipole approximation for $V(\vec{r} - \vec{R}(t))$ is used, where

$$V(\vec{r} - \vec{R}(t)) = -\frac{Z_p}{|\vec{r} - \vec{R}(t)|} \approx -\frac{Z_p}{R(t)} - \vec{r} \cdot \frac{\vec{R}(t)Z_p}{R^3(t)} \quad (3), \quad 3$$

And thus, and analytic expression for the energy loss $\Delta E(b)$ has been derived (8):

$$\Delta E(b) = \frac{2Z_p^2}{v^2 b^2} \sum_i f_i g\left(\frac{\omega_i b}{v}\right) = T_1(b) \sum_i f_i g\left(\frac{\omega_i b}{v}\right) \quad (4) \quad \text{Where } T_1(b) = 2Z_p^2 / (v^2 b^2)$$

$$\text{And, } g(x) = x^2 (K_0^2(x) + K_1^2(x)) \quad (5)$$

K_0 and K_1 are the modified Bessel functions, ω_i are the transition energies and f_i are dipole oscillator strength, which fulfill the sum rule $\sum_i f_i = 1$ (10). From the

properties of modified Bessel function Eq.(5) has the following limits (9):

$$g(x) = x^2 (K_0^2(x) + K_1^2(x)) \approx 1 \quad \text{for } x \leq 1, \\ \approx \left(1 + \frac{1}{\gamma^2}\right) \frac{\pi}{2} x e^{-2x} \quad \text{for } x \gg 1 \quad (6)$$

Where $\gamma = (1 - \beta^2)^{-1/2}$

Eq.(4) gives exact solution for asymptotic large values of b , but it is completely inadequate for small impact parameters, where multiple new term is important. According to the property given in Eq. (6) the energy loss given in Eq. (4), $\Delta E(b)$,

turn to be equal the classical form of energy loss when $b \rightarrow 0$, when the projectile velocity or maximum energy transfer approaches infinity (this is called sudden approximation) (8). A computer program *ghshl.f90* is written in Fortran-90 using a software Compaq Visual Fortran 6.6 (CVF) for compiling, linking and executing the program.

The variation of the function $g(\omega b/v)$ with $(\omega b/v)$ is shown in Fig. (2). The function $g(\omega b/v)$ increases slightly from the value of one to a shallow maximum at $(\omega b/v \approx 0.2)$ and at larger parameter $(\omega b/v)$ values the function $(g(\omega b/v) \rightarrow 0)$ exponentially.

For intermediate impact parameter b (somewhat larger than the shell radius r_{shell}) and at higher velocities, the collision time $\tau = r_{shell}/v$ is small compared to $1/\omega$. Thus, it is possible to sum over all final states analytically by using the closure relation to obtain (7),

$$\Delta E(b) = \int d^3 r_T T_1(\vec{b} - \vec{r}_T) \int dz \rho(\vec{r}_T, z) \quad (7)$$

As shown in Fig.(1) \vec{r}_T is perpendicular to z , the direction of projectile motion, $\int dz \rho(\vec{r}_T, z)$ is the electronic density integrated along the ion path. Eq. (7) agrees with the classical sudden approximation of the energy loss for electrons at rest.

The influence of the target potential can be neglected for small impact parameters at high projectile energies. In this case an analytical formula for $\Delta E(b)$ can also be obtained by replacing the final target continuum states by plane waves (11). The energy loss $\Delta E(b)$ can be written as:

$$\Delta E(b) = \int d^3 r_T T_2(\vec{b} - \vec{r}_T) \int dz \rho(\vec{r}_T, z) \quad (8)$$

With,

$$T_2(b) = T_1(b) h(2vb) = \left(\frac{2Z_p^2}{v^2 b^2} \right) h(2vb) \quad (9)$$

$$h(x) = \frac{x^2}{2} \int_0^1 y dy K_0(xy^2) J_0(xy\sqrt{1-y^2}) \quad (10)$$

Where J_0 is the Bessel function with zero-order (9). Eq. (10) has been solved numerically using Simpson's rule together with a program *ghshl.f90*

From the variation of $h(2vb)$ with $(2vb)$ as shown in Fig.(3), the following points can be concluded:

- (i) The function $h(2vb) \rightarrow 0$ for $b \ll 1/v$ i.e for $2vb \ll 1$.
- (ii) $h(2vb) \rightarrow 1$ for large values of b i.e $2vb \gg 1$.

In what follows, the energy loss for all impact parameter is:

$$\Delta E(b) = \int d^3 r_T T_{12}(\vec{b} - \vec{r}_T) \int dz \rho(\vec{r}_T, z) \quad (11)$$

With,

$$T_{12}(\vec{b} - \vec{r}_T) = T_2(\vec{b} - \vec{r}_T) \sum_i f_i g(\omega_i b/v) \quad (12)$$

This function joins smoothly small, intermediate and large impact parameters. The first two terms in Eq.(12) describe the violent binary collisions and the last term accounts for the long-range dipole transitions. The first integral in Eq. (11)

$\int d^2r T_{12}(\vec{b} - \vec{r}_T)$ describes a convolution with the initial electron density also outside the projectile path yields nonlocal Contributions to the energy ions.

For large impact parameters ($b \gg r_{shell}$) the convolution from Eq.(11) can be separated as follows:

$$\begin{aligned} \Delta E(b) &\approx \int d^2r_T T_{12}(b) \int dz \rho(\vec{r}_T, z) \\ &= T_{12}(b) \end{aligned} \quad = \int \left[\int d^2r_T \rho(\vec{r}_T, z) \right] dz T_{12}(b) \quad (13)$$

Also according to Fig.(3), at high impact parameters and velocity (i.e $2vb \gg 1$), the function $h(2vb) \rightarrow 1$, therefore Eq.(13) reduces to Eq.(4). Finally according to Figs.(2,3), the higher the projectile velocity v the better separation of small and large impact parameters, where the functions g and h approaches to zero.

RESULTS AND DISCUSSION

Fig. 4(a, b, c) shows the impact parameter b dependence of the energy loss $\Delta E(b)$ in eV for Hydrogen ion, H, in Hydrogen, H, Helium, He and Neon, Ne, at different incident energies, 100, 300, 500 and 600 keV. The oscillator strengths are taken from Ref. (10). The energy loss, $\Delta E(b)$ decreases smoothly with increasing impact parameter, also $\Delta E(b)$ decreases faster when incident ions increases as shown in Fig.4. At high impact parameter, $b > 3$ for H-target, $b > 2$ for He-target and $b > 1$ for Ne-target, the energy loss, $\Delta E(b)$ decrease linearly with increasing impact parameters.

Good agreement between present calculations of energy loss, $\Delta E(b)$ with the previous work of References (7,12) as shown in table (1).

Table (1) Energy loss $\Delta E(eV)$ calculated

As a function of impact parameter $b(A^0)$ for H-ions with energies 100, 300 and 500 keV in H (7,12).

b(A®)	$\Delta E(eV)$		
	100 keV	300 keV	500 keV
1	4	2	0.8
2	0.7	0.4	0.2
2.5	-----	-----	0.1
3	0.2	0.12	-----
4	0.04	0.04	-----

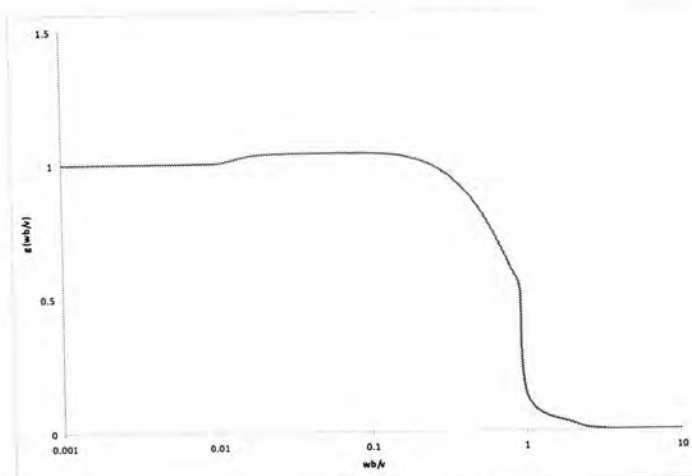
$g(Wb/v)$ 

Fig-2: The functions $g(x)$ and $h(x)$ from Eqs.(5) and (10) that describe the dipole terms and quasifree collisions. At high Wb/v velocities the flat parts of function

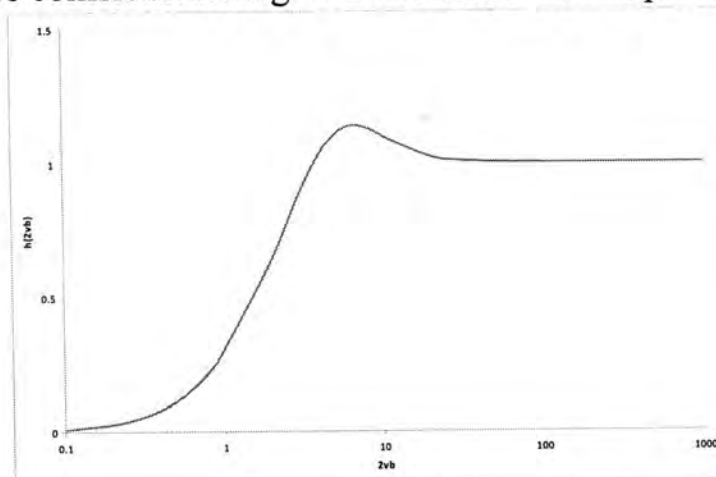
 $h(2vb)$ 

Fig-3: The function $h(x)$ from Eq-(10) that describe the quassifree collisions. At high ion velocities the flat parts of function.

 $2vb$

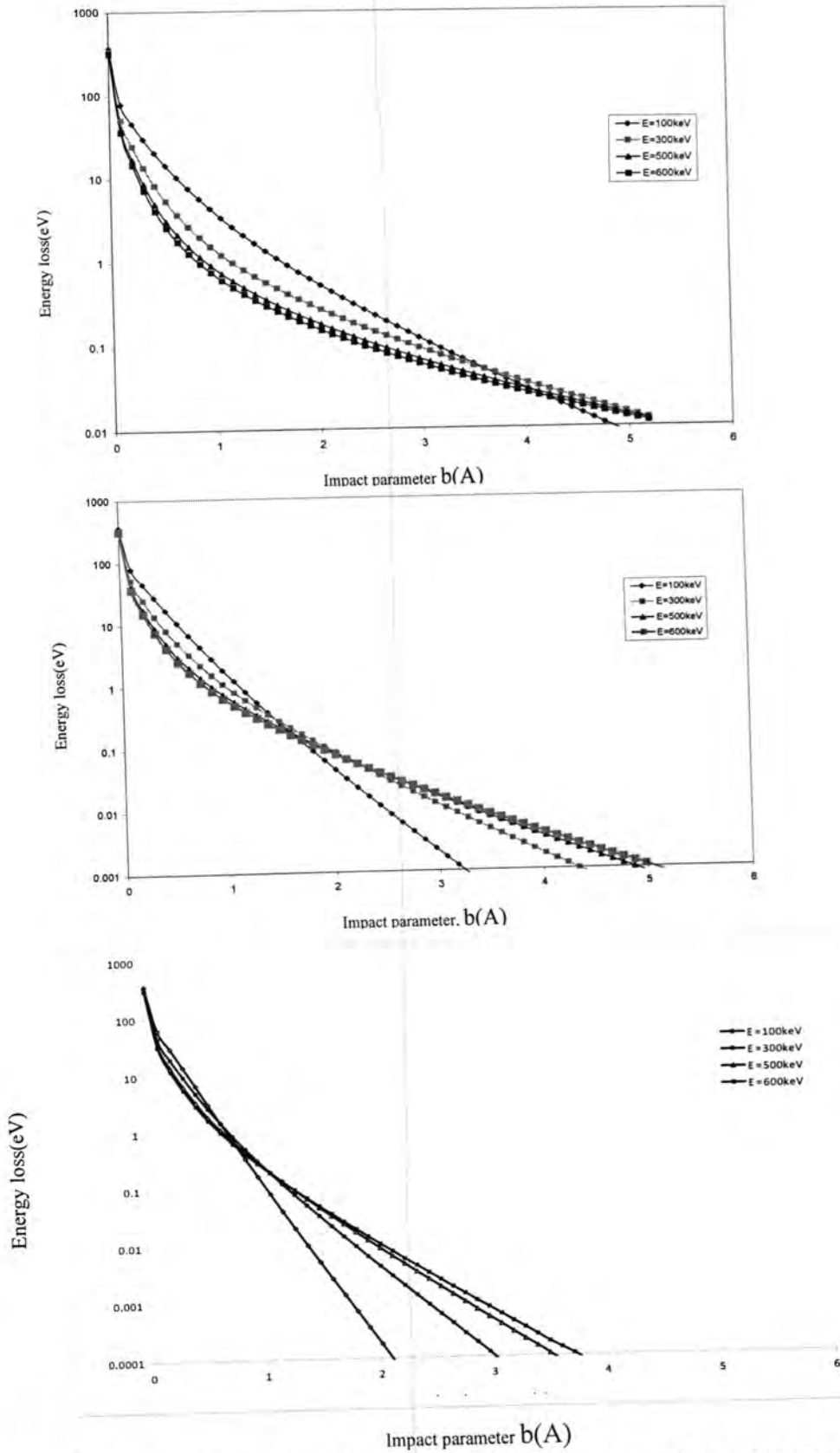


Fig.-4: The electronic energy loss E (eV) as a function of impact parameter b (Å) for bar H-ion at incident energy $E=100,300,500$ and 600 keV

REFERENCES

1. Bethe, H. A., Jackiw, R. W., Intermediate Quantum Mechanics, 2nd. Edition, Benjamin, W. A., New York, (1968).
2. Bethe, H., Ann. Phys. (Leipzig) 5 (1930) 325. Cited by Grande, P. L. and Schiwietz, G., 'Impact parameter dependence of electronic energy loss and straggling of incident bare ions', Phys. Rev. A58, :3796(1998).
3. Dalgarno, A., Griffing, G. W., Proc. R. Soc. London Ser. A232 :423(1955).
4. Kim, Y. K., Cheng, K. T., 'Stopping power for partially stripped ions' Phys. Rev. A22 :61(1980).
5. Cabrera-Trujillo, R., Cruz, S. A., Oddershede, J., Sabin, 'A Bethe theory of stopping incorporating electronic excitation of partially stripped projectiles', J. R., Phys. Rev. A55 :2864(1997).
6. Sigmund, P., 'Charge dependent electronic stopping of swift ions', Phys. Rev. A56 3781(1997).
7. Grande, P. L. and Schiwietz, G., 'Impact parameter dependence of electronic energy loss and straggling of incident bare ions', Phys. Rev. A58 :3796(1998)
8. Jackson, J. D., Classical Electrodynamics, 2nd. Edition, John Wiley & Sons, Inc., New York, (1975).
9. Handbook of Mathematical Functions, Edited by Abramowitz and I. A. Stegun (Dover, New York, 1974).
10. Oddershede, J, and Sabin, J. R., Atomic Data and Nuclear Data Tables 31 :275(1984)
11. Vries, L., in case studies in atomic structure calculations (Prentice-Hall Englewood Cliffs, NJ, (1963)
12. Azevedo, G. dze M, Grand, P. L. and Schiwietz, G., Nucl. Instr. & Meth. B164-165 :203-211(2000)

Effect of Electron Beam Irradiation on Optical and electrical Properties of Tin Dioxide Thin Film

Raad S. Sabry

Al-Mustansiyrhah University, College of Science , Physical department

الخلاصة

تم تحضير اغشية SnO_2 الرقيقة على قواعد زجاجية باستخدام طريقة الرش الكيميائي الحراري وتم تشعيع اغشية SnO_2 حزمة الكترونية مستقرة ($2500\mu\text{A}$) وبعرض ($1-1.5\text{mm}$) وبأزمان تشعيع ($3,6,9\text{min}$)، درست الخصائص البصرية والكهربائية قبل وبعد التشعيع من خلال النتائج المستحصلة من دراسة الخصائص البصرية وتبين ان فجوة الطاقة البصرية (E_g) تقل من (3.46eV) إلى (3.05eV) مع زيادة زمن التشعيع ومن خلال قياس التوصيلية الكهربائية المستمرة (DC) لوحظ ان المقاومة للاغشية تقل من ($7.8 \times 10^3 \Omega \cdot \text{cm}$) قبل الشيع إلى ($1.2 \times 10^2 \Omega \cdot \text{cm}$) للاغشية المشعة بزمن (9min) وكذلك فان طاقة التنشيط تقل من (0.33) إلى (0.2) مع زيادة زمن التشعيع.

ABSTRACT

SnO_2 thin film have been prepared on glass substrates using the simple pyrolytic (spray) method, the SnO_2 film was irradiated by a stable electron beam of $2500\mu\text{A}$ and width ($1-1.5\text{A}$) at different times ($3,6,9\text{ min}$). Optical and electrical properties were investigation before and after irradiation, from optical measurement it was found that optical band gap decreases with increasing irradiation time form (3.46 eV) to (3.05 eV). DC electrical conductivity measurements showed that the resistivity of films decreases from ($7.8 \times 10^3 \Omega \cdot \text{cm}$) as deposited to ($1.2 \times 10^2 \Omega \cdot \text{cm}$) for 9 min irradiation time, the activation energy decreases from (0.33) to (0.2) with increases of irradiation time.

INTRODUCTION

Transparent conducting oxide (TCO) semiconductor exhibit in general high transmission in the visible region, high reflectance in the infrared region and high electrical conductivity. Due to these properties, the TCO materials have been used in a wide range of applications in science and technology, including solar cells(1) heat reflecting mirrors(2), antireflection coatings(3), gas sensors (4) and a variety of electro-optical devices such as flat panel display devices(5,6).

TCO thin films have been deposited by a variety of techniques such as, magnetron sputtering (7), chemical vapor disposition CVD(8), reactive evaporation(9) and spray pyrolysis(10) particularly attractive among these techniques is the spray deposition technique successfully used for TCO thin films; this technique is simple, cheap, and easily adaptable for large area deposition.

Interaction of electron with matter

When the electrons of a given energy impinge on substance, these electrons are changed into transmitted electrons, back scattered electrons (reflected electrons), and absorbed electrons (absorption) by interaction with the atoms of these substance (11).

The transmitted electrons may be classified into two types:

1. Elastically scattered electrons; which change direction due to atomic collisions but retain their energy.

2. In elastically scattered electrons; which suffer a change in direction and partial energy loss.

When the energy of an incident electron exceeds the energy gap of the substance, the electron can produce a individual electron transitions from the (V.B) to the (C.B). (11,12).

The electrons irradiation can change the structural, electrical and optical properties of solids by causing displacement damage or through ionization effects (13, 14).

Incident particles on polycrystalline material can create dislocations and/or displace atoms from their lattice sites, creating electronic traps into the band gap, and so altering the electronic characteristics of the semiconducting layer, the displacement damage depends on the non-ionizing energy loss (NIEL) which is the energy and momentum transfer to lattice atoms, depending on the mass and energy of the incident quant (14).

This paper presents the results related to the effect of electron irradiation on optical and electrical properties of SnO_2 thin films.

MATERIALS AND METHODS

SnO_2 thin films were sprayed on ultra sonically clean glass substrates using SnCl_4 dissolution in water typical spray mixture which gane a good results consists of a 0.4M solution, it has been found that the following deposition parameters given good stoichiometric films with good transparency and uniform surface (i) substrate temperature of about 450°C (ii) spray rate of 4ml/min (iii) distance between sprayer nozzle and substrate of 26 cm the glass substrates are placed on the hot plate for about 20min before the spraying process, so the glass substrate are nearly at the same temperature as the hot plate, each spraying period lasts for about 15sec followed by 2.5min waiting period to avoid excessive cooling of the hot substrate due to the spraying process.

After depositing the SnO_2 films and measuring the optical and electrical properties of them, the SnO_2 films were positioned inside the electron gun chamber above the anode electrode at a distance of 6mm instead of the collector electrode, the SnO_2 film was irradiated by a stable electron beam of $2500\mu\text{A}$ having the energy of a 600eV and width of (1-1.5mm) at different times of irradiation (Tirr) (3,6,9min), by using home made a triode electron gun system.

A (Double Beam Spectrophotometer UV.210A) was used to record the transmittance and absorbance spectrum (before and after irradiation) at room temperature, in range between (300-800nm).

Before electrical measurement, the frontal metal electrode is formed by sequentially evaporation (400nm) of (Al) under 10^{-5} torr.

RESULTS AND DISCUSSION

Optical properties

Optical measurements on the SnO_2 thin films were performed on a shimadzu uv-210 spectrophotometer. During scanning a blank glass slide with film deposit was

in the other beam's direction. Thus, the absorption spectrum displayed by spectrophotometer was a result of film deposited on the glass slide.

Figure (2) shows the transmission spectra of the SnO₂ thin films as deposited without irradiation and the films were irradiated with different times (3,6,9)min, it was found that films are highly transparent, also, it was found that the transmission decrease with increase the irradiation time, this gives the possibility to explain the change in the film color from being transparent before irradiation in to being light brown after irradiation, the darkness in the film color increases with increases of the time of irradiation.

The details of the mathematical determination of the absorption coefficient can be found in literature (15) while the plots absorption coefficient against photon energy is shown in figure (3).

These absorption spectra, which are the most direct and perhaps simplest method for probing the band structure of semiconductors, are employed in the determination the energy gap (E_g). The films show an increase in absorbance and a decrease in transmission after irradiation the films. E_g was calculated using the following relation(16).

$$\alpha = A(h\nu - E_g)^n / h\nu \quad (1)$$

where (A) is a constant and (n) is a constant, equal (1/2) for direct band gap semiconductors. The estimated band gaps from the plots of $(\alpha h\nu)^2$ versus $(h\nu)$ are shown in figure (4) for as deposited and irradiated SnO₂ films, the linear nature of the plot indicates the existence of the direct transition.

The band gap (E_g) was determined by extrapolating the straight portion of the energy axis at $\alpha=0$. It was found to be (3.46eV) for as deposited SnO₂ films which are similar to the reported elsewhere (1, 17), it is also clear from table (1) that the optical band gap gradually decreases with increasing irradiation time, the value decrease from (3.46eV) for SnO₂ without irradiation to (3.05eV) (9min).

Table -1: Different parameters observed to SnO₂ thin films with different irradiation

Sample	E _g (eV)	P(Ω.cm)	ΔE ₁	ΔE ₂
Without	3.46	7.8x10 ³	0.05	0.33
3 min	3.17	2.5 x10 ²	0.048	0.3
6 min	3.1	2.1x10 ²	0.04	0.25
9 min	3.05	1.2 x10 ²	0.02	0.2

Blue shift of absorption coefficient (α) and decreases in Band gap (E_g) with increasing irradiation time is due to increasing the defects caused by irradiation, increasing irradiation time will not only cause defects in depth, but also in a wider area in the same layer(4,18).

Electrical properties

resistivity of SnO₂ thin films as deposited and with irradiation was measured at room temperature. Electrical resistivity was also measured from room temperature to 200°C.

Resistivity of the samples decreases with the increase of temperature showing a negative temperature coefficient.

Depending on irradiation time resistivity decreases from (7.8×10^3) to $(1.2 \times 10^2) \Omega \cdot \text{cm}$ values of resistivity are shown in table (1).

Figure (5) shows the temperature dependence of dark conductivity (σ) of SnO₂ (before and after irradiation) the activation energy has been calculated using the relation (15).

$$\sigma = \sigma_0 \exp\left(\frac{\Delta E}{K_B T}\right) \quad (2)$$

Where σ_0 is the pre exponential factor indicating high temperature limit of σ or when ΔE vanishes. ΔE is the so called activation energy for dc conduction and K_B is the Boltzmann constant using Fig.(5) and equation (2). The values of σ and ΔE for the set of samples have been calculated and are given in table (1).

The results suggest that there are two competing conduction mechanisms. The first term with lower temperature, corresponds to the hopping conduction involving the localized state induced by the structural and/or chemical disorder in the band gap the second, dominating in the high temperature range corresponds to the conduction band mechanism.

Electron irradiation can affect from sport across the grain boundaries by increasing the density of free carriers throughout the material, decreasing the inter grain barrier height by changing the inter grain states charge and increasing the probability of tunneling through the inter grain barriers by decreasing the depletion layer widths in the adjacent grains.

The resistance shift of SnO₂ thin film of after electron beam irradiation was decreases slowly. The electron beam irradiation will not change the chemical composition of the semiconductor but produces structural defects, its changes occupancy of the defects but electrons and holes, changes the concentration of adsorption on the surface of the semiconductor, these factors caused the decrease of resistance and activation energy of SnO₂ thin film.

We can conclude:

The chemical spray pyrolysis prepared tin dioxide thin film where treated by electron beam irradiation.

The results show that the energy gap, transmission, activation energy, and resistance decrease with increasing irradiation time.

These results give a good perspective for the application of SnO₂ in the fabrication of thin film heterojunction solar cell and gas sensors.

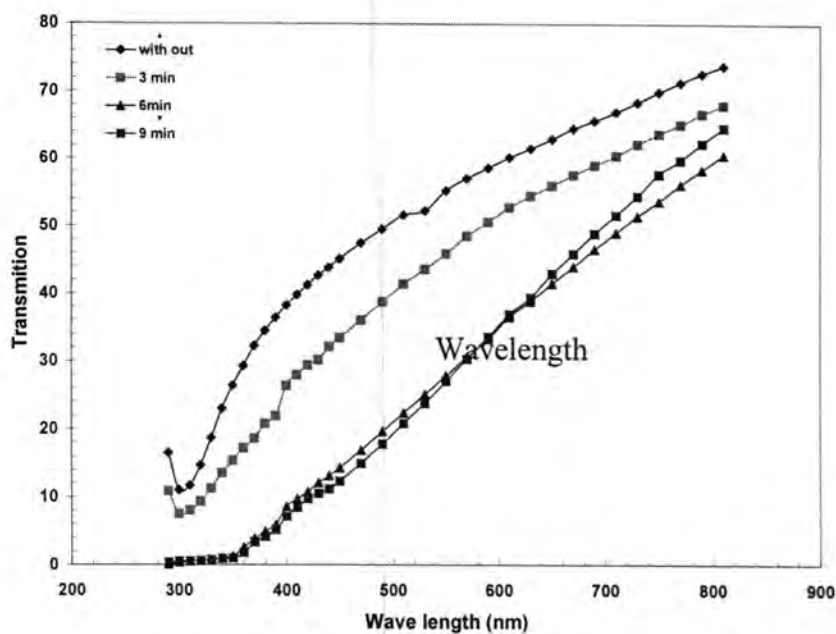


Fig.-1: Plots of transmittance against wavelength for SnO₂ thin films at various irradiation times

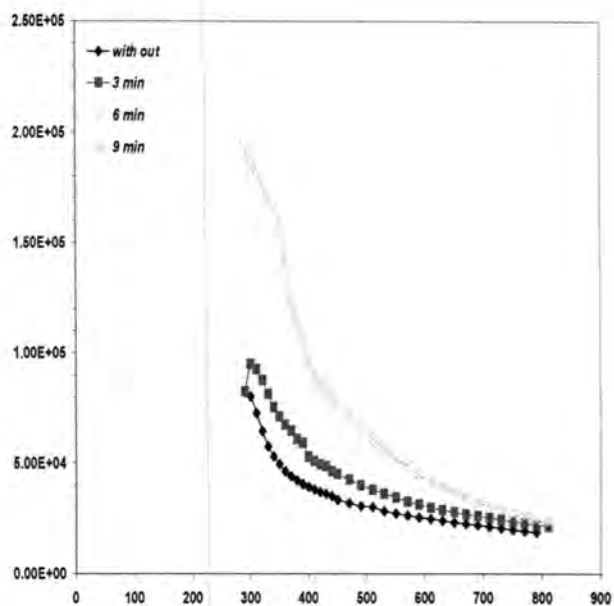
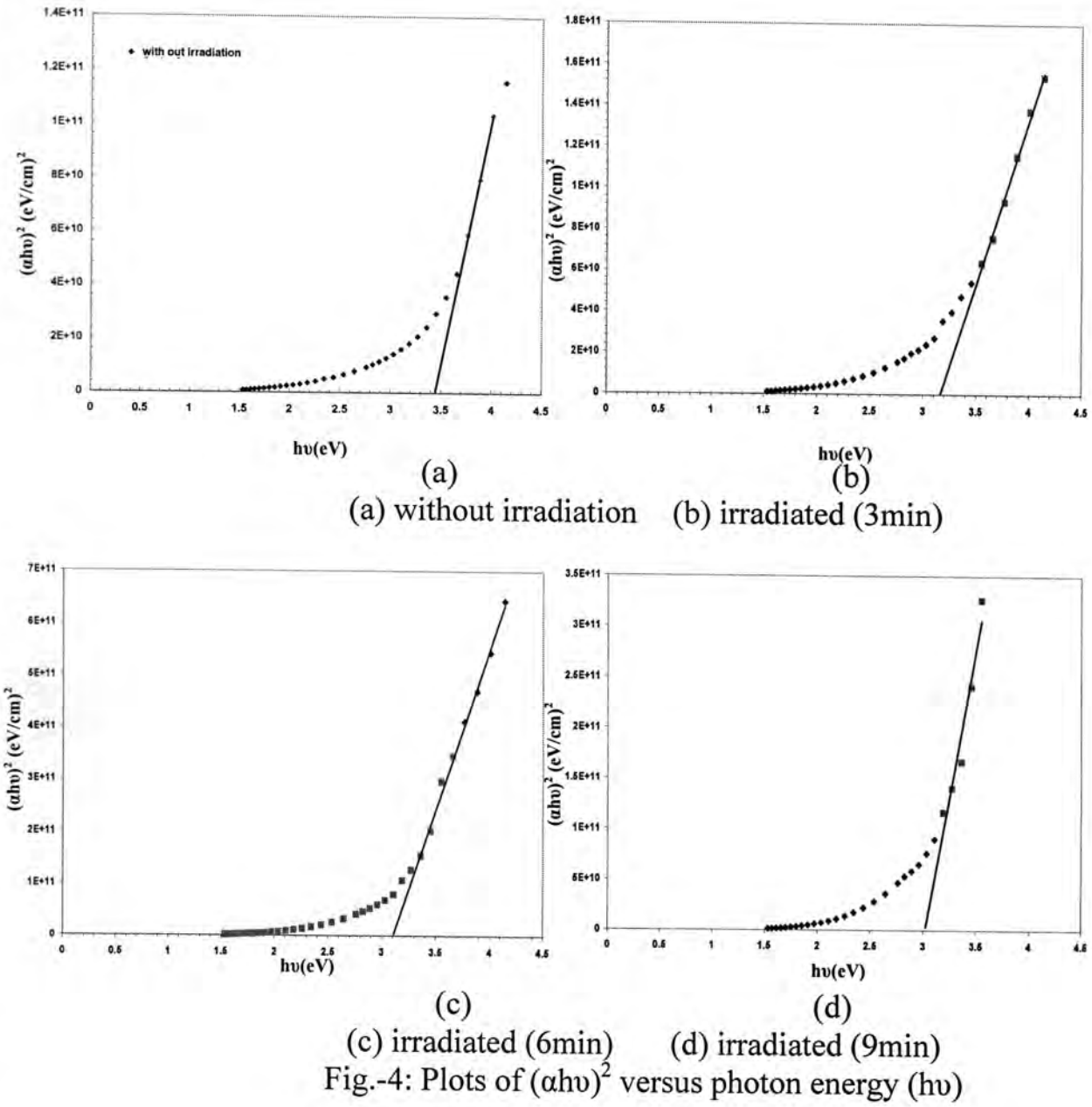
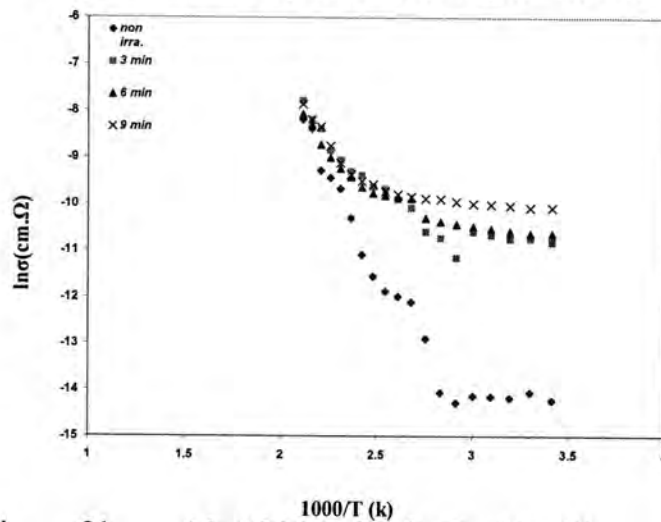


Fig.-3: Variation of absorption coefficient with wavelength for SnO₂ thin films at various irradiation times

Fig.-4: Plots of $(\alpha h\nu)^2$ versus photon energy ($h\nu$)Fig.-5: Variation of $\ln \sigma$ with $1000/T$ for SnO₂ thin films with different irradiation times

REFERENCES

1. R.Riveros,E. Romero and G. Cordillo, "Synthesis and characterization of highly transparent and conductivity $\text{SnO}_2\text{:F}$ and $\text{In}_2\text{O}_3\text{:Sn}$ thin films deposited by spray pyrolysis", Brazillian Journal of Physics,36, (3B)(2006).
2. K.L Chopra, S.R. Dass, (thin film solar cells) CPenu press New York) (1983).
3. H.L.Hartangel,A.L Dawar, H.K. Jain and C. Jagadis, (Semiconducting transparent thin films), Institute of Physics, Philadelphia (1995).
4. Z.Jiao,X.Wan,B.Zhao,A.Guo,T.Liu and M. Wa, Effect of electron Beam irradiation on tin oxide gas sensors).
5. J.E. Costellamo, (handbook of display technology), Academic Press, New York (1992).
6. Kyung-Hwan Kim, (The preparation of indium tin oxide films as a function of oxygen gas flow rate by facing target sputtering system), Journal of ceramic Processing research, 8.(1) : 19-21 (2007).
7. W. Wohlmuth, I. Adesida, "Properties of R.R magnetron sputtered cadmium-Tin-Oxide and indium-Tin oxide thin films", thin solid films,479:223(2005).
8. R.G. Dhere, H.R. Moutinho, S.Ashev, O.Young, X.Li, R. Ribel in ad T-Gesext, (characterization of SnO_2 films prepared using Tin Tetrachloride and tetramethyl Tin precursors), NREL/CR52-25733 (1998).
9. M.G.L.Sabino, V.d. Falco, C.P. Guerra, A.S.Dinz, J.RI,-Bgreative electron Beam Evaporation technique), revista Brasileira Apicacoes vacuo, 26(1)(2007).
- 10.E.Elangovan and K. Ramamurti, (studies ceramic structural and electrical properties of spray-deposition fluorine-doped tin oxide thin films from low-cost precursor), thin solid films, 476, ISSUE.2, (2005).
- 11.E. J. Pharhan, (Designing and constructing an electron gun system and some of it's applications), Al-Mustansiriyah University, College of Sciecne, Physics Department, thesis (2001).
- 12.J.P.Ganachoud,A.Mokrani (theoretical study of the secondary electron emission of insulting targets),surface science,334:329-341 (1995).
- 13.H. Yasuda, H. Mori and J.G. Lee, (Electron-irradiation-induced phase separation in GaSb nanoparticles), physical review B70, 214105, (2004).
- 14.A. Romeo, D.L.Batzner, H. Zogg and A.N. Tiwari, (Potential of CdTe thin film solar cells for space applications), 17th European Photovoltaic conference and exhibition, 99-96 October –Germany, (2001).
- 15.M.G.M.Choudhaury, M.R. Islam, M.M.Rahman, M.O. Hakim M.K.R. Khan, K.J. Kao, G.R.. lai, (Preparation and characterization of ZnSe:Al thin films), acta physica solvaca ,54(4) :417-425(2004).
- 16.F.I.Ezema, A.B.C. Ekwelior and R.U. Osuji, (Effect of thermal Annealing on the Band Gap and optical properties of chemical Batti. Deposited ZnSe thin films), Turk.J.Phys., 30:157-163(2006).
- 17.Preparation of indium tin oxide films and doped tin oxide films by an ultrasonic spray cub, Process).
- 18.S.Amtone, L. Ion, V.A. Anotone, (the effect of the electron irradiation on the structural and electrical properties of $\text{A}^{\text{II}}\text{-B}^{\text{VI}}$ thin polycrystalline films,Journal of optoelectronic and advanced materials,5,(4):801-16 (2003).

Tribological Characteristic Of Graphite-Novolac Composites: Experimental And Simulation Approach

Bahjat B. Kadhim

Department of Physics, College of Science, The University of Mustansiriya.

الخلاصة

المميزات الترابولوجية لمتراكبات النوفولاك المدعمة بدقائق الكرافيت قد درست بدلالة معاملات الاحتكاك - البلى لتغيرات الكسر الحجمي للكرافيت , استخدمت تقنية الكبس الحار لتحضير المتراكبات ونماذج النوفولاك باستخدام القوالب المارقة تحت الظروف القياسية , استخدمت ماكينة امزلة لتعيين معاملات الاحتكاك والبلى لمتراكبات نوفولاك - كرافيت ونماذج النوفولاك المنزقة على قرص صلب من الفولاذ الغير مزيت . نفذت المحاكاة لحساب معدل البلى بثلاث ابعاد لاختبار الاحتكاك - البلى باستخدام طريقة الفروقات المحددة , ووظفت الصور البصرية (المجهرية) بالاقتران مع الصلادة الدقيقة والكثافات للمساعدة في تفسير النتائج . اظهرت النتائج العملية بان دقائق الكرافيت قد حسنت المميزات الترابولوجية لمتراكبات النوفولاك . ان معامل الاحتكاك يهبط تزايديا بتعاقب زيادة الكسر الحجمي لدقائق الكرافيت , ويستقر عند قيم ثابتة للاحمال العالية . يسلك معامل البلى كاوفا قيمة عند اعلى كسر حجمي للكرافيت . تعرض علاقة الاحتكاك - البلى متزايدة , الاولى تكون الية التآكل بالحرث في بداية الحركة , والثانية تكون الية التآكل بالتصاق التي ترافق الاحتكاك المستقر . جاءت قيم نتائج للمحاكاة اعلى من قيم النتائج العملية , وقد فسر ذلك بسبب تاثير السطح البيني للمتراكبات , الذي كان ذو متانة وقوة ارتباط عالية , وقيم الكثافات والصلادة تدل على ذلك . معاملات البلى للمتراكبات تعتمد بقوة على التوزيع الحجمي لدقائق الكرافيت , الصلادة , ومحتوى الكرافيت (الكسر الحجمي) . يمكن استنتاج بان الكرافيت يعمل عمل مزدوج , فهو مزيت صلب فعال بين السطوح المتماسكة ومادة جيدة مشتتة للحرارة .

ABSTRACT

Tribological characteristics of novolac composites reinforce with graphite particles were investigated in terms of friction - wear coefficients subject to changes in different graphite volume fraction. Hot press technique was used to prepare the composites as well as novolac specimens using flash molds at standard conditions. Amslar machine in conforming geometry was used to determine friction and wear coefficients of novolac and graphite - novolac composites specimens slide against un lubricated steel disc. Simulation program of wear rate in three dimensions of friction - wear test were carried out using finite difference method. Optical microscopy coupled with auxiliary micro - hardness, and densities were employed to aid interpretation of results. Experimental results show that graphite particles improve the tribological characteristics of novolac composites. The coefficient of friction drops progressively and settles at constant values by succession of graphite volume fraction for high normal loads. The wear coefficient was behaved as being lowest for high graphite volume fraction. The friction - wear relationship displays two associated mechanisms, the first was ploughing wear mechanism, which is associated with run - in period, and the second was adhesion wear mechanism, which is associated with steady friction. Simulation results values coming higher than experimental results values, and this could be explained as the interface affect of composites, which had high strength and strong bond face. Densities and hardness values are evidenced to that. The wear coefficients of composites are strongly dependent on graphite particles distribution, hardness, and graphite content. We can conclude that the graphite plays dual work, as a solid lubricating media within the contacting surfaces as well as good heat dispersion element.

Key word: Tribology, Friction, wear, Lubricant, and Novolac composites.

INTRODUCTION

Material and energy conservation are becoming increasingly important. The ever - increasing demand, reliability and long life of materials is one of the main problems of contemporary engineering; obviously due to economic reasons (1). Friction is a principal cause of energy dissipation and considerable, saving is

possible by improving frictional control. Wear (the progressive loss of substance from the operating surface of body as a result of relative motion at the surface) is major cause of material wastage, so any reduction of wear can affect considerable savings. Wear can be minimized by modifying the surface properties of solids by one or more of "surface engineering" processes (also called surface finishing) or by use of lubricants (for frictional or adhesive wear). Thus, tribology (which is the science and technology of friction, lubrication and wear) is considerable importance in material and energy conservation (2).

The sliding friction coefficients of many engineering materials tend to decrease as temperature increases, which mainly due to a reduction of shear strength at higher temperature. But under some special conditions, other factors such as oxide layer development may dominate the friction and wear behavior and alter the influence of temperature on the friction (3). So, thermal property is meant the response of material to the application of tribology. As a solid absorbs energy in the form of heat, its temperature rises, and its dimensions most of the time increase. Thermal conductivity, thermal expansion, and heat capacity are properties that are often critical in the practical utilization of solids (4).

There have been several attempts to correlate wear resistance with various mechanical properties of polymers and composites (5-13). The dependence of wear rate up on mechanical properties is complicated because deformation caused by erosive particles is associated with high strain rates and the stress state is complex(14). Also, a survey of literature indicates that the effect of fiber and /or filler on wear of polymers /composites is a complex and unpredictable phenomenon(15). Hence, the dependence of erosive wear rate on the experimental parameters is difficult to model physical effects such as fiber or particle fragmentation; debonding, pullout, etc. affect the behavior of polymer composites subjected to the erosive wear process. It is also difficult to predict their relative contribution because various other mechanisms influence the wear process. The prediction of wear rate of polymer/composites is an important requirement if it is likely to operate under erosion conditions. Meng and Ludema(16) published an article providing the information about the existing models and equations for predicting the wear rates of various types of materials. However, these models and equations are not possible to use for the prediction on all the situations because of certain limitations.

THEORETICAL APPROACH

The understanding, simulation and prediction of the behavior of contacting systems with friction are very important in both theory and practical applications. Some of the general friction theories which have been proposed to explain the nature of dry friction are: mechanical inter locking molecular attraction, electrostatic forces, welding / shearing and ploughing (17).

Any apparatus for measuring friction must be capable of supplying relative motion between two specimens, of applying a measurable normal load of measuring the tangential resistance to motion. There are a number of methods available and the choice will depend largely on the exact conditions of rubbing

contact under investigation. Among different methods for the determination of coefficient of friction, is the conforming contact geometry provided by Amsler machine which offers a realistic friction behavior (18). According to the conditions of Amsler machine, the coefficient of friction (μ) can be calculated by using the following relationship (18):

$$\mu = \frac{\tau}{L \times r} \dots \dots \dots (1)$$

where L is the applied normal load in (N), r is the radius of lower steel disc in (m), and τ is friction torque in (Nm). The τ value is obtained from the integration disc counter before and after the test.

Wear occurs as a natural consequence when two surfaces with relative motion interact with each other. Several mechanisms may be involved in wear. The wear of rubbers and polymers are no less complex than wear of metals, being dependant on the combination of mechanical, thermal, and chemical processes (17). The coefficient of wear, k , are calculated using an Archard - type wear equation (19):

$$k = \frac{VH}{LS} \dots \dots \dots (2)$$

where V is the wear volume, L is the normal load, S is the total distance slid and H is the hardness of the specimen.

MATERIALS AND METHODS

Phenol – formaldehyde resin material (Novolac type) designed by (PFN) in form of solid manufactured by F.C.F. was used as a matrix in preparation of composite materials. Graphite (from Hoechst, Germany) of particle size distribution between 100 to 150 microns is used as a particulate reinforced novolac composites. The volume fraction of graphite included in the novolac are (10,20,30,40, and 50) Vol.%. Well mixing of constituent powders of graphite and novolac with the hardener (14 Vol. %) of Hexamethylene – Tetramine (HMTA) is done before molding for all specimens to ensure homogeneity. Molding of specific mixing ratio into disc shape of diameter (40 mm) and (10 mm) in width is carried out in flash mold using (Hot – press) technique. The disc shape novolac and novolac composite molds are arch and hole machined to dimensions that are purposed for friction-wear testing. The steel disc were machined from soft-annealed (1045) steel to about (44 mm) in diameter and (10 mm) in width, which is commonly known as high quality journal material.

SIMULATION APPROACH

The modeling of wear found in the literature can broadly be classified into two main categories (20-23) namely, (i) mechanistic models, which are based on material failure mechanism e.g., ratcheting theory for wear (24) and (ii) phenomenological models, which often involve quantities that have to be computed using principle of contact mechanics e.g., Archard's wear model. Archard's wear model is simple phenomenological model, which assumes a linear relationship between the volume of material removed, V , for a given sliding distance, S , an applied normal load, L , and the hardness (normal load over

projected area) of the softer material, H . Proportionality constant, the wear coefficient, k , characterizes the wear resistance of the material. The simulation of wear test of a frictional material is considered an important process since it reduces many efforts, time and raw materials that are used in trail and error of the experimental procedure. This simulation is performed by using the values of friction as well as thermal parameters of specific material. The simulation supposes a certain load at which the specimen is removed by gravity or the mechanical effect of the load. The analysis of the friction-wear system is based upon Newton's law in torsional form (25):

$$\tau = I\alpha \dots \dots \dots (3)$$

Where, τ , is torque, I , is moment of inertia, and α is angular acceleration. The elastic torque, τ_E , due to the twisting of the machine-wear testing shaft is:

$$\tau_E = -q\theta \dots \dots \dots (4)$$

Where, θ , is an angular displacement and q is constant and the minus sign is indicating that the resistance is always in opposition to the velocity. The friction torque, τ_F , is:

$$\tau_F = -C \frac{d\theta}{dt} \dots \dots \dots (5)$$

$$T_i = T_0 \cos \omega t \dots \dots \dots (6)$$

Where, T_i , is the impressed torque, ω , is angular velocity, T_0 and C are constants. Since the angular acceleration is $(d^2\theta/dt^2)$, on substituting into Newton's law, equation (3), we have a completely familiar differential equation:

$$I \frac{d^2\theta}{dt^2} + C \frac{d\theta}{dt} + q\theta = T_0 \cos \omega t \dots \dots \dots (7)$$

RESULTS AND DISCUSSIONS

The comparison influence of Gr. Vol. % on the friction coefficient, μ of individual matrix, PFN and various Vol. % of Gr. – PFN composites by simulation operation with the experimental results of fixed load (100 N) slid against steel disc at room temperature is shown in Fig. (1) respectively. According to the Fig. (1) , the friction coefficient of graphite reinforced novolac composites of experimental as well as simulation operation were nearly the same and they smoothly decreased from about 0.62 and 0.66 for pure novolac to about 0.22 and 0.26 for the composites including 50 Gr. Vol. % for experimental and simulation results respectively. The maximum load that specimen can endure depend on the graphite volume fraction , and at a fixed load of 100 N , the friction coefficient values vary as inverse- linear relationship with the Gr. Vol.% added the novolac matrix as shown in Fig.(1) . For the high Gr.Vol.%, the low μ values of the composites specimens is due to the lubrication nature of graphite .As the Vol.% of graphite is increased , the fraction of its mating surface become larger , this leads to further decrease in the μ values .

Archards wear equation expresses the generally observed proportionality between the wear coefficient and the product of normal load and sliding distance. Thus the wear coefficients computed via Archards equations are plotted against load times sliding distance .Fig. (2) show a substantial decrees in the wear

coefficient with the increasing normal load , approaching nearly a constant value above about 80×10^3 Nm . This consistent with the previously reported results for polymer composites in which the wear coefficient decreased rapidly during run – in and achieved a steady value for continued sliding (25) . Above 80×10^3 Nm the values of wear coefficient indicate that the test at the heavier loads was conducted primarily under steady state wear conditions. It is interesting to note that the wear of the largest vol. % of graphite composite specimen being the smallest at the high loads, which is may be due to the action of aspirates of the rubbing surfaces which is presumably large at low loads. Also, it can be seen from the Fig.1 and Fig. 2 that the experimental values were lowered then simulation values, which may be explained according to Fig.3. Where, Fig.3 shows load distribution after 15 min. when 50 Gr. Vol.% of novolac matrix is ploughing by simulation operation of friction-wear mechanism, the reason of this may be due to interface effect which is composed between graphite particles and the matrix, moreover, the influence of aspirates located between the contact surfaces .

The pictures presented in Fig. (4) show the worn surfaces of pure novolac and its composites (10 Vol.% and 50 Vol.% graphite-novolac composites) . It has been seen in Fig. (4a) that the slightly deformation flow accrued on the worn surface of pure novolac . This indicated that adhesion was the main wear mechanism of pure Novolac. For the composites reinforced with graphite particles Fig. 4 and Fig.6) , ploughing was the main characterization on their worn surface, and the composites reinforced with 10 Vol.% graphite particles showed wider and deeper ploughing groves that extend the length of the wear track than the composites reinforced with 50 Vol.% graphite particles .

We can conclude:

The Wear coefficients of composites filled with graphite particles decreased with the increase of graphite filler content. Graphite addition plays the dual work as a sold lubricating media within the contacting surfaces as well as good heat dispersion element. SEM pictures reveal that material removal takes place by ploughing and adhesion mechanisms. Artificial Amsler wear technique in conforming geometry was applied to predict the friction – wear coefficient of graphite – novolac composites. The results show that the predicted data are well acceptable when comparing then to simulation values, which is coming higher than experimental results values, this could be evidenced to the interface affect of composites.

Acknowledgments

The work reported in this paper was supported by labrotaries of University of Technology, Iraq, Center of Materials Science, Ministry of Science and Technology, Iraq, University of Baghdad, and the University of Mustansiriya.

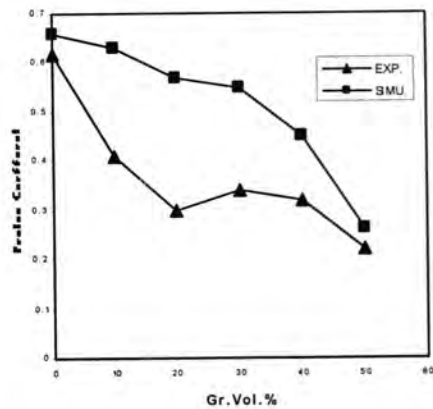


Fig.1: Comparison of Gr. Vol.% on the friction coefficient of PFN .

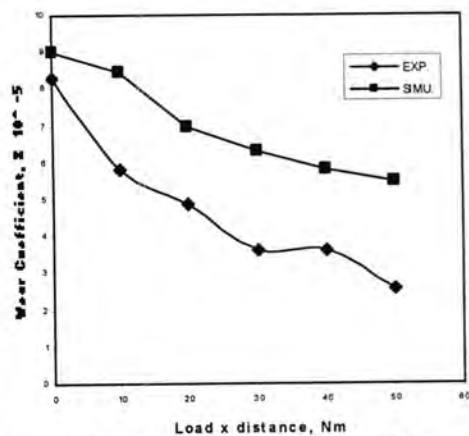


Fig.2: Comparison influence of Gr. Vol.% on the wear coefficient of PFN composites.

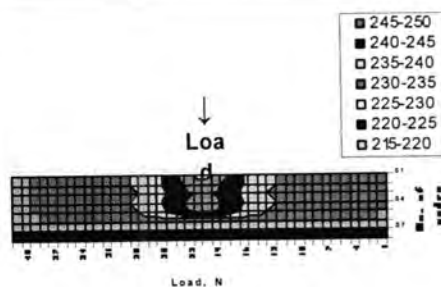
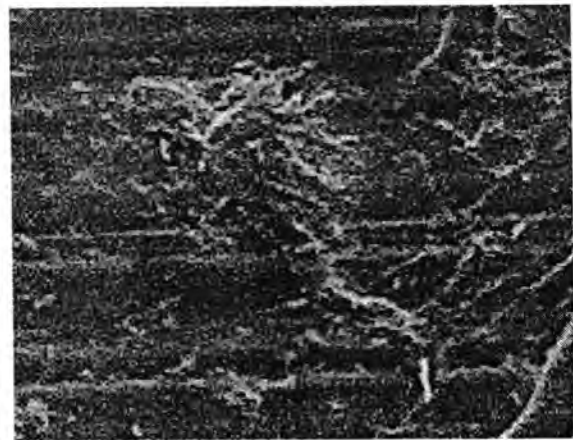
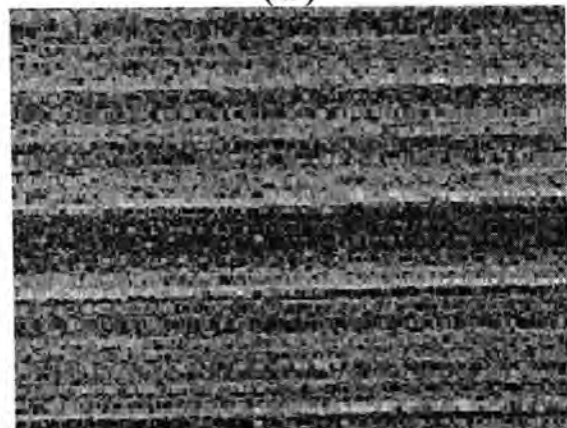


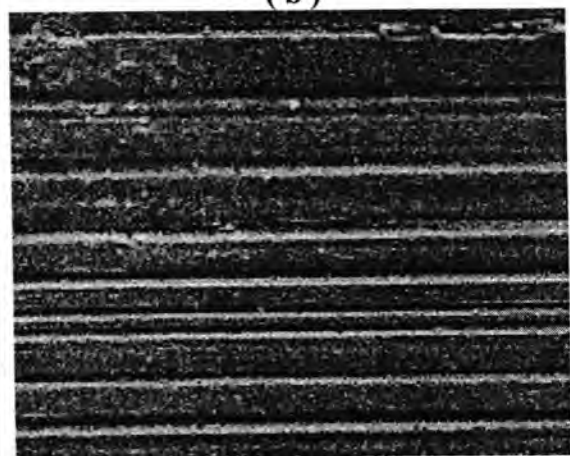
Fig.3: Load distribution after 15 min. when 50 Gr. Vol.% of PFN is ploughing by simulation in operation of friction - wear mechanism.



(a)



(b)



(c)

Fig.-4:Optical microscopy of wear surfaces:(a) the worn surfaces of pure novolac,(b) 10 Gr.Vol.%,and (c) 50 Vol. %

REFERENCES

1. I.V.Kragelsky,M.N.Dobychin and V.S.Kombalov, "Friction and Wear Calculation methods ", Pergamon Press, Oxford, (1982).
2. M.H.Jones&D.Scott(E.d)"Industrial Tribology,The Practical Aspect of Friction ,Lubrication,& Wear"(Elsevier,Tribology Series8,(Amsterdam)(1983)).

3. Mori(eds),A.A.Balkema "Simulation of Materials Processing ;Theory ,Methods and Applications": 91– 96(2001).
4. W.D.Callister,"Materials Science Engineering An Introduction"John Wiley and Sons,Inc.,New York,: 2,40,193 and 475(2000) .
5. P.V.Rao,D.H.Buckley,Angular particle impingement studies of thermoplastic materials at normal incidence,ASLE Trans.29:283–298 (1986).
6. K.Friedrich,Erosive wear of polymer surfaces by steel ball blasting,J. Mater. Sci. 21: 3317–3332(1986).
7. S.M.Walley,J.E.Field,M.Greengrass,An impact and erosion study of polyetheretherketone,Wear 114: 59–71(1987).
8. I.M.Hutchings,D.W.T.Deuchar,A.H. Muhr, Erosion of unfilled elastomers by solid particle impact, J. Mater. Sci. 22: 4071–4076(1987).
9. J.Li,I.M. Hutchings,Resistance of cast polyurethane elastomers to solid particle erosion, Wear 135: 293–303(1990).
- 10.Manish Roy,B.Vishwanathan,G.Sundararajan,The solid particle erosion of polymer matrix composites,Wear171:149–161(1994).
- 11.J.J. Rajesh, J. Bijwe, U.S. Tewari, B. Venkataraman, Erosive wear behavior of various polyamides, Wear 249: 702–714(2001).
- 12.A.P. Harsha, A.A. Thakre, Investigation on solid particle erosion behavior of polyetherimide and its composites, Wear 262:807–818(2007).
- 13.S. Arjula,A.P.Harsha, M.K. Ghosh, Solid-particle erosion behavior of high performance thermoplastic polymers, J. Mater. Sci. 43 :1757–1768(2008).
- 14.H.C.Meng,K.C. Ludema,Wear models and predictive equations: their form and content,Wear 181–183: 443–457(1995).
- 15.K.Velten,R.Reinicke,K. Friedrich,Wear volume prediction with artificial neural networks, Tribol. Int. 33: 731–736(2000).
- 16.D.F.Moore,Principle and Applications of Tribology,Pergamon Press,Oxford, (1975).
- 17.B.K.Amsler,A.G.Prufmaschinen, & C.H.Merishauser, Operating Instructions – Amsler "Wear Testing Machine A135" Schaffhausen, Berlin,(1985).
- 18.C.P.Micheal , N.Saka, and R.Ernest , Wear , 127: 15(1988) .
- 19.Meng,H.C.,Wear modeling: evaluation and categorization of wear models. PhD Thesis, University of Michigan, Ann Arbor, MI, USA, (1994).
- 20.Meng,H.C.& Ludema,K. C., Wear models and predictive equations: their
- 21.form and content. Wear,:443-457(1995).
- 22.Hsu,S.M.,Shen,M.C.,&Ruff, A.W.Wear prediction for metals. Tribology. Int.,30:377-383(1997).
- 23.Blau,P.J.Fifty years of research on the wear of metals Tribology Int.,30:332-331 (1997).
- 24.Kapoor, A. Wear by plastic ratcheting. Wear, 212, :119-130(1997).
- 25.C.R.Wylie, Advanced Engineering Mathematics, 3rd Ed.McGraw – Hill Kogakusha ,Ltd.,Tokyo, :146(1966).
- 26.M.W.Paseoe,Plain and Filled Plastics Materials in Bearings:areview, Tribology Int. 6: 184(1973).

Ionizing radiation impacts the powerful antioxidant activity of *Zingiber officinale* Rosc. extracts: *in vitro* study

Zainab Wahbee Abdul Lateef

Department of Physiology / Medical Physics/College of Medicine
Al-Mustansiriya University

الخلاصة

تظهر أعشاب محددة صفة الحماية من الأشعاعات الأيونية وغير الأيونية إلا أن القليل من الدراسات تفحصت تأثير الأشعاع على مكونات الفينولات المتعددة والفلافوناد للأعشاب. هدفت هذه الدراسة للتقصي عن تأثير الأشعاع المتأين (أشعة أكس) على مكونات محددة من مستخلصات الزنجبيل أخذين بنظر الاعتبار طبيعة تحضير المستخلص. تم تحضير مستحضرات الزنجبيل المائي المعقم، المائي، إيثانول، والميثانول بنسبة (1%) و تعرضها إلى أشعة أكس بجرعة نسبتها 1,9 كري / دقيقة عند درجة حرارة الغرفة. تم مسح المستخلصات قبل وبعد الأشعاع بواسطة مقياس الطيف الضوئي وكذلك الصفات الفيزيوكيميائية المتضمنة الأس الهيدروجيني، التوصيل و الاملاح الذائبة. وتضمنت الفحوصات الكيميائية مركبات الفينولات المتعددة، الفلافوناد، الانتوين وقابلية تحرر اكسيد النتريك. تسبب الأشعاع الأيوني في فقدان قمم الامتصاصية عند طول موجي 277 – 278,5 نانومتر مع تغيرات في الصفات الفيزيوكيميائية للمستخلصات ذات علاقة بطبيعة تحضير المستخلص. وقد تدنت مستويات الفينولات المتعددة في المستخلصات المائي المعقم، المائي، وإيثانول في حين تدنت مستويات الفلافوناد في جميع المستخلصات بفعل الأشعاع الأيوني، وقد تلطفت مستويات الانتوين وقابلية تحرر اكسيد النتريك قليلا بالتشعيع الأيوني. يستنتج من ذلك أن تأثير التشعيع المؤذي لمستخلصات الزنجبيل اعتمد على طبيعة تحضير المستخلص وعلى نوعية محتويات المستخلص، وأن مستخلص الميثانول أقل عرضة للتأثير مقارنة ببقية المستخلصات.

ABSTRACT

Certain herbs showed radio-protective against ionizing and non-ionizing radiation. Few studies investigated the effect of radiation on the polyphenols and flavonoids constituents of herbs. This study is aimed to investigate the effect of ionizing radiation (X-ray) on the certain constituents of *Zingiber officinale* Rosc. extracts taking in considerations the nature of preparation of extracts. Hydro-distilled, aqueous, ethanol and methanol extracts (1%) were prepared and exposed to X-ray radiation at dose rate of 1.9 Gy / min at room temperature. UV-visible scan of each extract was achieved and the physiochemical properties including pH, conductivity and total dissolved salts were determined for irradiated and non irradiated extracts. Biochemical testing including total polyphenolic compounds, total flavonoids, allantoin, and nitric oxide generation were also determined. Ionizing radiation resulted in disappearance of UV-peak at 277-278.5 nm and changes in the physiochemical properties of extracts that were related to the nature of extract. Total polyphenolic compounds were reduced in irradiated hydro-distilled, aqueous, and ethanol extracts while total flavonoids were reduced in all tested extracts. Allantoin level and the ability to donate nitric oxide were slightly improved by ionizing radiation. It concluded that the deleterious effects of ionizing radiation *Zingiber officinale* Rosc. extracts is depended on the nature of extract and on the nature of the constituents of each extract. Methanol extract is less affected by ionizing radiation compared with other extracts.

Key words: *Zingiber officinale* Rosc, ionizing radiation

INTRODUCTION

Ginger, the rhizomes of *Zingiber officinale* Roscoe (Zingiberaceae), has widely been used as a spice. Ginger is native to India and China and took its name from the Sanskrit word *stringa-vera*, which means "with a body like a horn", as in antlers. It has a long history of medicinal use for the treatment of a variety of human ailments including common colds, fever, rheumatic disorders, gastrointestinal complications, motion sickness, diabetes, cancer, etc (1,2). Ginger contains several nonvolatile pungent principles viz. gingerols, shogaols, paradols and zingerone which account for many of its health beneficial effects (3-5). Ginger is a strong antioxidant substance and may either mitigate or prevent generation of free radicals (6). The main pharmacological actions of ginger and/or isolated compounds were immuno-modulatory, anti-tumorigenic, anti-inflammatory, anti-apoptotic, anti-hyperglycemic, anti-lipidemic and anti-emetic actions (1, 7-11).

It is well known that when ionizing radiation passes through aqueous solution, electrons are removed from neutral water molecules to produce H_2O^+ ions. Between three and four water molecules are ionized for every 1.2×10^5 KJ/Mol of energy absorbed in the form of ionizing (X-ray) radiation. The radicals formed when ionizing radiation passes through water are among the strongest oxidizing agents that can exist in aqueous solution. Most literatures were investigated the effect of γ - rays radiation rather than X-ray radiation on the biological tissues and antioxidants related to herbs (12). Degradation of chalcones, , the natural antioxidants that present in fruit and vegetables, in the methanol radiolysed solution was observed (13).

The more water concentration in irradiated methanol/water mixture contained antioxidant by γ -radiolysis using a ^{60}Co source, the more degradation of antioxidants (14). On the other hand, Kozlowski et al investigated theoretically the formation of a new series of antioxidants from flavonoids in methanol and ethanol solutions irradiated with γ -rays(15).

The aim of this study is to test the hypothesis that the effect of ionizing radiation on the *Zingiber officinale* Rosc. extracts is varied with the extracted solvent.

MATERIALS AND METHODS

This study was conducted in Department of Pharmacology, College of Medicine, Al-Mustansiriya University in cooperation with X-ray Unit in Al-Yarmouk teaching hospital in Baghdad, Iraq during May 2009.

Extracts preparation

Hydro-distilled extract of *Zingiber officinale* Rosc. was prepared by simple distillation. In brief 1 g of tuberous fine powder in 100 mL distilled water (1%) was boiled, and the vapor separated and condensed to obtain clear colorless liquid that was more concentrated in the more volatile components. Also, aqueous, ethanol and methanol extracts were prepared. A 1 g dried tuberous fine powder was extracted with 100 mL of distilled water (aqueous extract), absolute ethanol or 100 methanol i.e. (1%) for 24 hours in dark place at room temperature 25°C. The extraction was followed by filtration. The UV-Visible spectra of full strength aqueous and hydro-distilled extracts, and 1:80 v/v ethanol or methanol / distilled water extracts were obtained by scanning the extract using UV-Visible spectrophotometer (Aquarius, France, Cecil series with scanning ability).

Radiation of *Zingiber officinale* Rosc. extracts

A total number of 32 tubes (10 mL) contained extracts solutions within 20 x 20cm were exposed to conventional X-ray radiation with the following specifications: X-ray tube distance from upper level of extract was 80 cm, accelerated potential 120 KpV (calculated effective energy 30.976 KeV and the absorbed dose 1.9 Gy/min), at room temperature 22°C.

Physiochemical properties of extracts

The physiochemical properties of each extract (radiated and non radiated) including pH, conductivity ($\mu\text{S}/\text{cm}$), and total dissolved salts (TDS) (ppm) were determined using pH/ °C/ EC/ TDS meter.

Determination of the amount of total polyphenolic compounds

This was carried out as described previously (16). Briefly 1 mL of each extract was mixed with 5 mL distilled water and 0.5 mL of Folin-Ciocalteu reagent (50%). Then allowed the mixture to stand and after 5 minutes 1 mL of Na_2CO_3 (2%) was added. Subsequently the mixture was shaken for 1 hour at room temperature in dark place. Afterward the absorbance was measured at 725 nm. Gallic acid was used as the standard for calibration curve and phenolic content were expressed as μg gallic acid equivalent /mg dry weight.

Quantification of total flavanoids

The method is based on the quantification of the yellow color produced by the interaction of flavonoids with AlCl_3 reagent (17). Aliquots of 1.5 mL of extracts were added to equal volumes of a solution of 2% $\text{AlCl}_3 \cdot 6\text{H}_2\text{O}$ (2 g in 100 mL methanol). The mixture was vigorously

shaken, and absorbance at 367 nm was read after 10 min of incubation. The flavonoids content were calibrated using the linear equation base on the calibration curve quercetin. Flavonoids content were expressed as μg quercetin equivalent/mg dry weight.

Determination of allantoin

This was carried out as described previously (18) using Ehrlich's reagent, which consists of 1 g *p*-dimethylaminobenzaldehyde (*p*DMAB) in a mixture of 25 mL concentrated HCl and 75 mL methanol. 1 mL of each extract was mixed with Elrich's reagent (1:2 v/v), incubated at room temperature and read the absorbance at 440nm. The allantoin content was calibrated using the linear equation based on the standard allantoin calibration curve

Nitric oxide assay

Nitric oxide donating activity was determined as describe by Newaz et al [19] using Griess's reagent. Briefly, 3 mL of each extract (1: 2 v/v distilled water) was added to 50 μL HCl (6.5M) and 50 μL sulfunalic acid (37.5mM), After incubation of 10 min, 50 μL naphthylethylenediamine hydrochloride (12.5 mM) was added and incubated for further 30 min, centrifuged for 10 minutes at 3000 rpm. The reference nitric oxide donating compound was 5 mM sodium nitroprusside. The absorbance was immediately recorded at 540nm. Experiments were performed in triplicate.

Statistical analysis

The results are presented as absolute numbers and percents.

RESULTS AND DISCUSSION

Fig 1 showed that Each extract of non radiated ginger solution had specific UV-Visible peak and they are shared with certain peaks but differed in their magnitudes. All extracts shared with the peaks ranged 191.5-196 nm, 277-278.5 nm and 578.5-579.5 nm [Fig. 1]. Irradiated ginger extracts showed the presence of one peak ranged 191.5 -196 nm with higher magnitudes than corresponding non radiated except aqueous extract [Fig. 1]. Ionizing radiation caused shifting to higher values in the pH [Fig. 2 A] for all extracts except hydro-distilled extract compared with non radiated extract solutions. The conductivity and the solubility of aqueous extract were also increased by ionizing radiation [Fig. 2 B& C]. The effect of ionizing radiations on the variable related to the free radicals was shown in Table 1. The highest concentration levels of polyphenols were found in ethanol and methanol extracts. Ionizing radiation caused depletion of polyphenols in aqueous extract and reducing

it to 78% of non radiated level of ethanol extract. Methanol extract responded to ionizing radiation by increase rather than decrease of polyphenols that amounted 2.5 times of non radiated methanol extract. Total flavonoids were reduced by ionizing radiation to reach 16.6%, 84.7% and 80.1 % for aqueous, ethanol and methanol extracts respectively (Table1). It is of great interest to find that *Zingiber officinale* Rosc. extracts had considerable levels of allantoin. Ionizing radiation reduced the levels of allantoin in hydro-distilled and aqueous extracts while it caused a slight increase in allantoin levels in alcoholic extracts (Table 1). A minute levels of nitric oxide was released in ethanol and methanol extracts which further induced by ionizing radiation (Table 1)

This *in vitro* study shows that extracts of *Zingiber officinale* Rosc, other than methanolic extract, are affected by ionizing radiation and lost their beneficial effects.

The prominent effect of ionizing radiation is the disappearance the peak of 6-gingerol on the UV-Visible scan at 277-278.5 nm in aqueous, ethanol and methanol extracts.

There is no doubt that radiation causes changes in physiochemical properties of irradiated solution including pH, conductivity and total dissolved salts (20). In this study, a slight changes in pH is observed in mirror image fashion i.e. hydro-distilled extract (free from the peak of 6-gingerol), the pH is decreased rather than increased as with aqueous, ethanol, and methanol extracts. Once again the conductivity and total dissolved salts alterations were observed in aqueous extract (20). There is no doubt that polyphenols of whatever source protect the biological tissues from the effects of ionizing radiation or ultraviolet radiation (21,22). Few articles deal with the effect of radiation *per se* on the polyphenols (23,24). In this study, other than methanol extract, irradiated extracts showed lower levels of polyphenols compared with non radiated polyphenols. The irradiated methanol extract shows 2.5 folds increase rather than decrease polyphenols This finding is in agreement with the study of Marfak who found that the radiolytic process of the flavonoid (quercetin) in methanol solution is completely differed from that in aqueous solution i.e. formation of new depsides of quercetin via process other than oxidation (25).

Flavonoids were severely exhausted in irradiated aqueous extract and to less extent in ethanol or methanol extract. This finding was previously reported by others (15). The thermal effect of ionizing radiation shared in degradation of 6-gingerol, a thermo-labile antioxidant, in the studied extracts (5).

There are few herbs that contained allantoin like comfrey (0.6-0.7%) which acts as peroxynitrite scavenger (26). In this study, the allantoin constituent in ginger is higher in methanol extract than other

extracts and even than comfrey. It is of great interest that the level of allantoin is reduced by 50% in irradiated aqueous extract but is slightly increased in irradiated ethanol or methanol extract. The possible explanation of this increment is possibly related to the oxidation of uric acid by hydroxyl radical generated by ionizing radiation (27). In cell culture, Ginger inhibits the nitric oxide synthesis in activated mouse macrophages due to its content of 6-gingerol (28). In living tissue, ionizing radiation, can mimic cytokine signals, is known to increase the activity of the transcription factor NF- κ B (29). It is well-established that NF- κ B activity accelerated the synthesis of the inducible nitric oxide synthase (iNOS) which increases, in turn, nitric oxide levels (30). Irradiated Murine macrophages produce more nitric oxide in response to either interferon- γ or lipopolysaccharide but radiation alone (0.5-50 Gy) did not induce nitric oxide (31). The results of this study are in agreement with others in that irradiated ethanol or methanol extract showed a slight increase in nitric oxide production and this is possibly due to degradation of 6-gingerol by ionizing radiation that is demonstrated in the UV-Visible spectra in this work. One of the limitation of the study is the isolation and determination of 6-gingerol and its new depsides. It concludes that ionizing radiation causes deleterious effects upon the antioxidants constituents and physiochemical properties of *Zingiber officinale* Rosc extracts. Methanol extract is less affected by ionizing radiation compared with other extracts.

Table-1: The effect of ionizing radiation on the variables related to antioxidants and nitrogen species radicals.

	Hydro-distilled extract		Aqueous extract		Ethanollic extract		Methanolic extract	
	Before	After	Before	After	Before	After	Before	After
Total polyphenolics (μ g/mg)	0	0	4.43	0	52.6	41.1	50	126
Total flavonoids (μ g/mg)	0	0	187.2	31.1	92.4	78.3	95.2	76.3
Allantoin (μ g/mg)	0.25	0.04	5.1	2.5	7	7.61	11.5	12.8
Nitric oxide release (μ mol/mg)	0	0	0	0	0.35	0.42	0.37	0.38

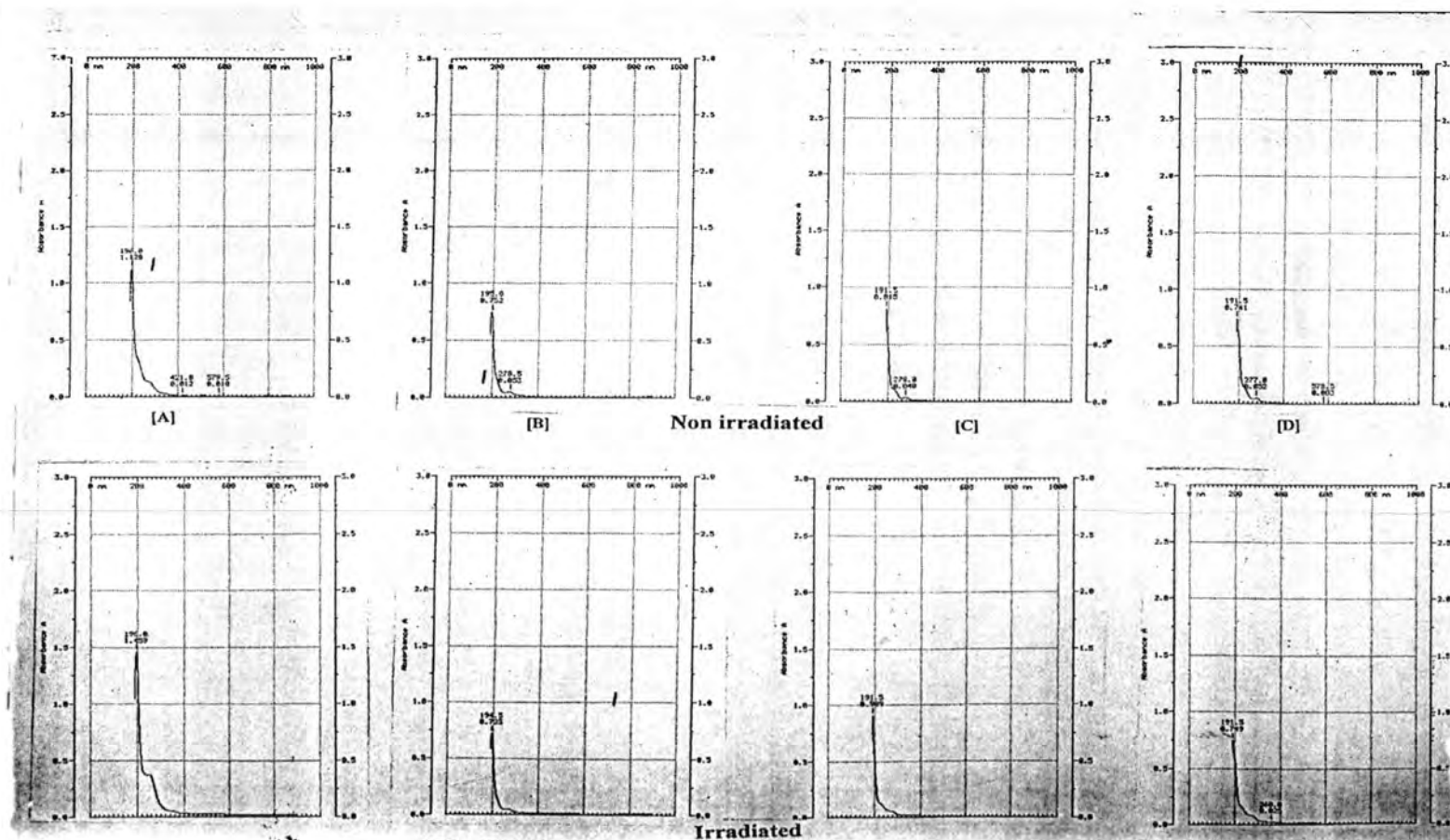


Fig-1: UV-visible scan of *Zingiber officinale* Rosc. Extracts [A] hydro-distilled, [B] aqueous, [C] ethanol and [D] methanol

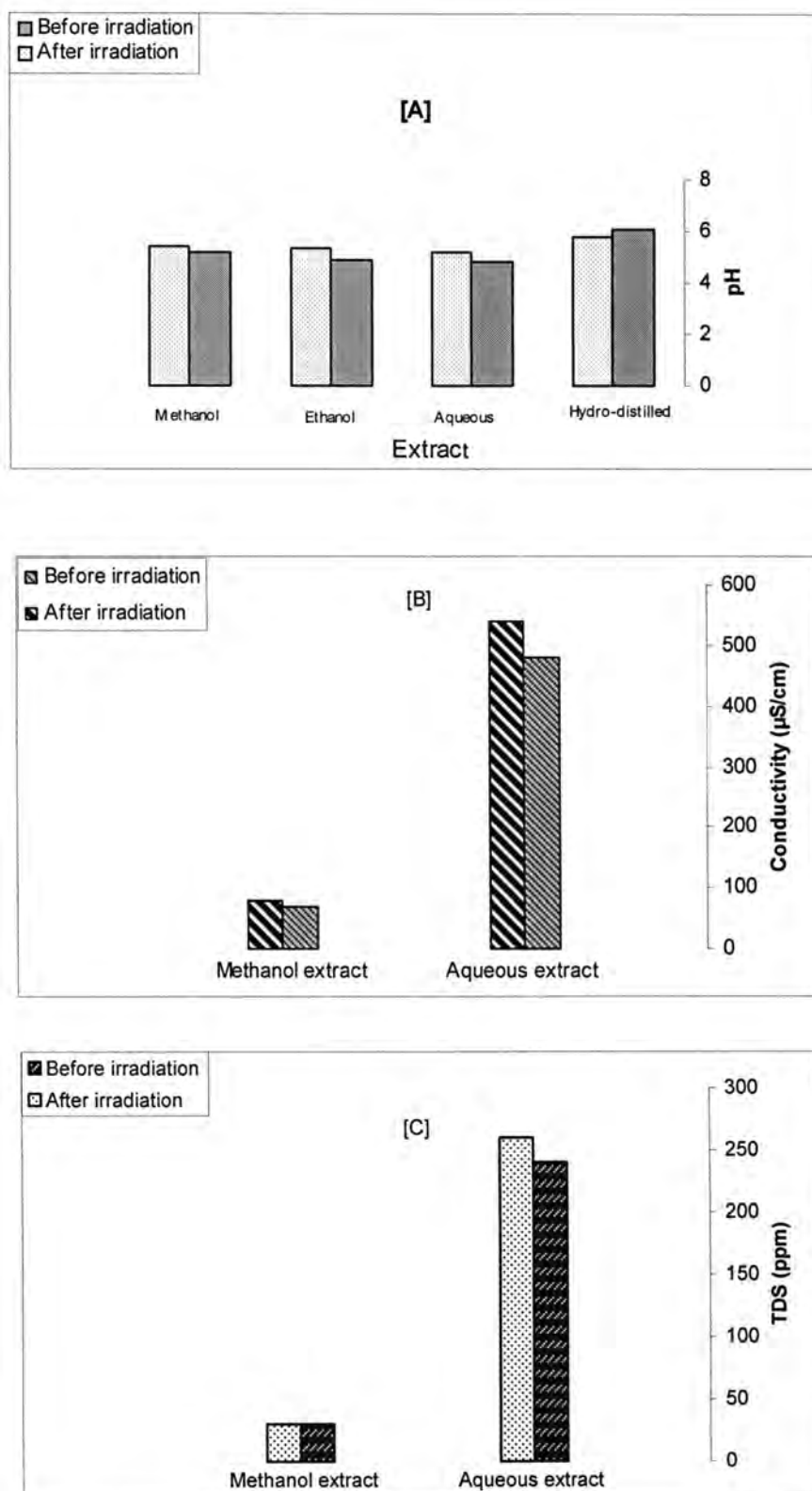


Fig- 2: The effect of ionizing radiation on the physiochemical properties of *Zingiber officinale* Rosc. extracts [A] pH, [B] conductivity and [C] total dissolved salts

REFERENCES

1. Ali BH, Blunden G, Tanira MO, Nemmar A. Some phytochemical, pharmacological and toxicological properties of ginger (*Zingiber officinale* Roscoe): a review of recent research. *Food Chem Toxicol* **46**: 409-420 (2008).
2. Ghayur MN, Gilani AH. Pharmacological basis for the medicinal use of ginger in gastrointestinal disorders. *Dig Dis Sci* **50**:1889-1897 (2005).
3. Funk JL, Frye JB, Oyarzo JN, Timmermann BN. Comparative Effects of Two Gingerol-Containing *Zingiber officinale* Extracts on Experimental Rheumatoid Arthritis (perpendicular). *J Nat Prod*. Feb 13 (2009)
4. Singh G, Kapoor IP, Singh P, de Heluani CS, de Lampasona MP, Catalan CA. Chemistry, antioxidant and antimicrobial investigations on essential oil and oleoresins of *Zingiber officinale*. *Food Chem Toxicol* **46**:3295-3302 (2008).
5. Jiang H, Solyom AM, Timmermann BN, Gang DR. Characterization of gingerol-related compounds in ginger rhizome (*Zingiber officinale* Rosc.) by high-performance liquid chromatography/electrospray ionization mass spectrometry. *Rapid Commun Mass Spectrom* **19**: 2957-2964 (2005).
6. Adhikari S, Indira Priyadarsini K, Mukherjee T. Physico-chemical studies on the evaluation of the antioxidant activity of herbal extracts and active principles of some Indian medicinal plants. *J Clin Biochem Nutr* **40**:174-183 (2007).
7. Grzanna R, Lindmark L, Frondoza CG. Ginger--an herbal medicinal product with broad anti-inflammatory actions. *J Med Food* **8**:125-132 (2005).
8. Al-Amin ZM, Thomson M, Al-Qattan KK, Peltonen-Shalaby R, Ali M. Anti-diabetic and hypolipidaemic properties of ginger (*Zingiber officinale*) in streptozotocin-induced diabetic rats. *Br J Nutr* **96**: 660-666 (2006).
9. Wei QY, Ma JP, Cai YJ, Yang L, Liu ZL. Cytotoxic and apoptotic activities of diarylheptanoids and gingerol related compounds from the rhizome of Chinese ginger. *J Ethnopharmacol* **102**: 177-184 (2005).
10. Hickok JT, Roscoe JA, Morrow GR, Ryan JL. A Phase II/III Randomized, Placebo - Controlled , Double - Blind Clinical Trial of Ginger (*Zingiber officinale*) for Nausea Caused by Chemotherapy for Cancer: A Currently Accruing URCC CCOP Cancer Control Study. *Support Cancer Ther* **4**:247-250 (2007).
11. Liu H, Zhu Y. Effect of alcohol extract of *Zingiber officinale* rose on immunologic function of mice with tumor. *Wei Sheng Yan Jiu* **31**: 208-209 (2002)
12. Jagetia G, Balliga M, Venkatesh P. Ginger (*Zingiber officinale* Rosc.), a dietary supplement, protects mice against radiation-induced lethality: mechanism of action. *Cancer Biother Radiopharm* **19**: 422-435 (2004).
13. Morkini R, Trouillas P, Kaouadji M, Champavier Y, Houée-Lévin C, Fangère C, Duroux JL. Reactivity of Chalcones with 1-hydroxymethyl radicals. *Radiat Res* **166**: 928-941 (2006).

14. Marfak A, Trouillas P, Allais DP, Champavier Y, Calliste CA, Duroux JL. Radiolysis of Kaempferol in water/methanol mixtures. Evaluation of antioxidant activity of kaempferol and products form. *J Agric Food Chem* **51**: 1270-1277 (2003)
15. Kozłowski D, Marsal P, Steel M, Mokrini R, Durox JL, Lazzaroni R, Trouillas P. Theoretical investigation of the formation of a new series of antioxidant depsides from the radiolysis of flavanoid compounds. *Radiat Res* **168**: 243-252 (2007).
16. Chandler SF, Dodds JH. The effect of phosphate, nitrogen and sucrose on the production of phenolics and solasidine in callus cultures of *Solanum laciniatum*. *Plant Cell Reports* **2**:1005-1110 (1993).
17. Lamaison, J.L.C. and A. Carnet. Teneurs en principaux flavonoids des fleurs de *Crataegus monogyna* Jacq et de *Crataegus laevigata* (Poiret D.C) en fonction de la vegetation. *Pharm Acta Helv* **65**:315-320 (1990).
18. Vrbaski M, Injac GB, Gajic A. A new method for allantoin determination and its application in *Agrostemma githago* L. seed. *Analytical biochemistry* **91**: 304-308 (1978).
19. Newaz MA, Yousefipour Z, Nawal N, Adeeb N. Nitric oxide synthase activity in blood vessels of spontaneously hypertensive rats: Antioxidant protection by gamma-tocotrienol. *J Physiol Pharmacol* **54**: 319-327 (2003)
20. Singh A, Yang Y, Adelstein SJ, Kassis AI. Synthesis and application of molecular probe for detection of hydroxyl radicals produced by Na(125)I and gamma-rays in aqueous solution. *Int J Radiat Biol* **84**:1001-1010 (2008).
21. Bors W, Michel C. Chemistry of the antioxidant effect of polyphenols. *Ann N Y Acad Sci* **May**:57-69 (2002)
22. Liu ML, Yu LC. Potential protection of green tea polyphenols against ultraviolet irradiation-induced injury on rat cortical neurons. *Neurosci Lett* **444**:236-239 (2008).
23. Anderson RF, Fisher LJ, Hara Y, Harris T, Mak WB, Melton LD, Packer JE. Green tea catechins partially protect DNA from $\cdot\text{OH}$ radical-induced strand breaks and base damage through fast chemical repair of DNA radicals. *Carcinogenesis* **22**: 1189-1193 (2001).
24. Anderson RF, Amarasinghe C, Fisher LJ, Mak WB, Packer JE. Reduction in free-radical-induced DNA strand breaks and base damage through fast chemical repair by flavonoids. *Free Radic Res* **33**: 91-103 (2000).
25. Marfak A, Trouillas P, Allais DP, Champavier Y, Calliste CA, Duroux JL. Radiolysis of quercetin in methanol solution: observation of depside formation. *J Agric Food Chem* **50**: 4827-4833 (2002).

26. Gafițanu C, Popescu C, Singurel G, Macocinschi D. Physical and chemical characterization of allantoin-beta-cyclodextrin inclusion complex. *Rev Med Chir Soc Med Nat Iasi* **108**:173-176 (2004).
27. Hicks M, Wong LS, Day RO. Identification of products from oxidation of uric acid induced by hydroxyl radicals. *Free Radic Res Commun* **18**:337-351 (1993).
28. Ippoushi K, Azuma K, Ito H, Horie H, Higashio H. [6]-Gingerol inhibits nitric oxide synthesis in activated J774.1 mouse macrophages and prevents peroxynitrite-induced oxidation and nitration reactions. *Life Sci* **73**:3427-3437 (2003).
29. Ibuki Y, Mizuno S, Goto R. c-Irradiation-induced DNA damage enhances NO production via NF- κ B. *Biochim Biophys Acta* **1593**:159-167 (2003).
30. Pall ML. Post-radiation syndrome as a NO/ONOO⁻ cycle, chronic fatigue syndrome-like disease. *Medical hypotheses* **71**:537-541 (2008).
31. McKinney LC, Aquilla EM, Coffin D, Wink DA, Vodovotz Y. Ionizing radiation potentiates the induction of nitric oxide synthase by IFN- γ and/or LPS in murine macrophage cell lines: role of TNF- α . *Journal of Leukocyte Biology* **64**: 459-466 (1998).

Using Maximum Likelihood Technique to Classify and Recognized the Voices of Spoken Words

Ahmed Humod Flieh

Thi-Qar University/ Science College. /Physics Dept.

الخلاصة

يمتلك نظام التمييز طورين أساسيين وهما طور التدريب و طور التصنيف والمطابقة ولهذا قد ركزنا لاستخدام تقنية تصنيف لنحصل على نتائج جيدة, وبذلك استخدمنا تقنية الاحتمال الأعظم كنموذج للتصنيف الذي سيحدث ويحسن بشكل نستطيع استخدامه بفعالية اكبر في نظام تمييز الكلام, ان معدل النتائج العملية أظهرت ان النسبة المؤية للنظام المقترح هي بحوالي (78.57%) وكذلك ان احتمال الصنف المحدد يمتلك قيم تمييز عالية, ان هذا يشير إلى أن نظام التمييز هو فعال في عملية التصنيف.

ABSTRACT

The recognition system has two elementary phases, training phase and classification and matching phase, So we are concentrate to use classification technique to get good result, Therefore we are using maximum likelihood technique as a pattern for classification, also this model will update and enhanced in a form, we can be use it more effective in speech recognition system, the average of experimental results shown that the percentage of recognition of proposed system is about (78.57%). Also the likelihood of specific class has high values, this indicated that the system is efficient in classification process.

INTRODUCTION

Designing a machine that mimics human behavior, particularly the capability of speaking naturally and responding properly to spoken language, has intrigued scientists and engineers for centuries. Since the 1930s, when Homer Dudley of Bell laboratories propose a system model for speech analysis and synthesis, the problem of automatic speech recognition (ASR) has been approached progressively, from a simple machine that responds to a small set of sound to a sophisticated system that responds to fluently spoken natural language and takes into account the varying statistics of the language in which the speech is produced. Based on major advance in statistical modeling of speech in the 1980s, ASR systems today find widespread application in tasks that require a human-machine interface, such as automatic call processing in telephone network and query-base information systems that do things like provide updated travel information, stock price quotations, weathers reports, ...etc.(1)

Basic Structure of a Speech Recognition System

Like most pattern recognition problems, a speech recognition system can be partitioned into two modules: feature extraction and classification. The

classification module has two components: pattern matching and decision. Figure (1) depicts a generic speech recognition system (1).

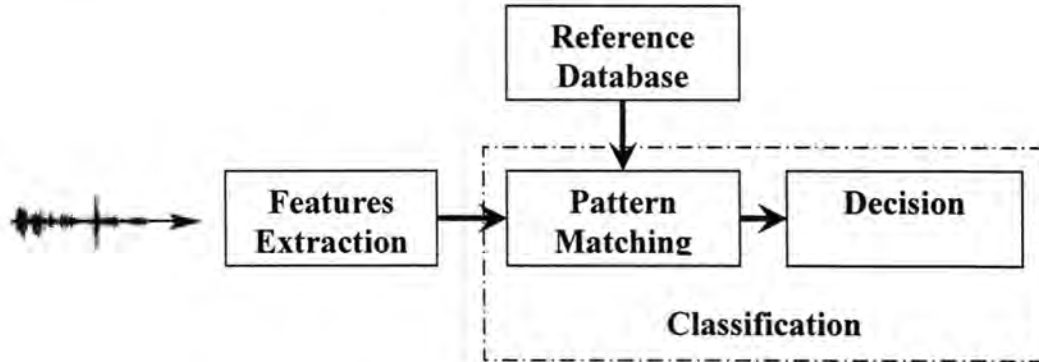


Fig.-1: depicts a generic speech recognition system.

Acoustic Features

All audio processing techniques start by converting the raw speech signal into a sequence of acoustic feature vectors carrying characteristic information about the signal. This preprocessing module (feature extraction) is also referred to as “front-end” in the literature. The most commonly used

Acoustic vectors are Mel Frequency Cepstral Coefficients (MFCC)(2) , this feature are based on the spectral information derived from a short time windowed segment of speech. MFCC features are derived directly from the FFT power spectrum as shown in figure (2):

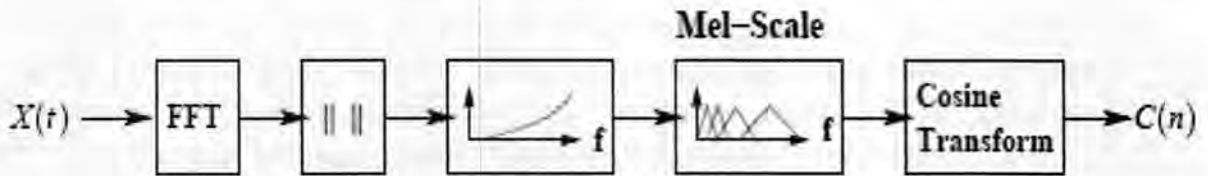


Fig.-2: illustrated MFCC method

Maximum a posteriori probability classifier (MAP)

A decision rule that used in the recognition process is a maximum a posteriori probability classifier (MAP). The MAP classifier will select tone i for the feature vector β of the unknown speech input if the posteriori probability (3) :

$$P(w_i|\beta) > P(w_j|\beta) \quad , \quad \forall j \neq i \quad (1)$$

where w_0, w_1, w_2, w_3 and w_4 are the class of tone. This probability can be determined from:

$$P(w_i|\beta) = \frac{P(w_i|\beta)P(w_i)}{P(\beta)} \quad (2)$$

where $P(w_i)$, the priori class probability, is assumed to be equal for all tone. The PDF (Probability Density Function) of feature vectors is determined from the summation of all conditional PDF given each class, that is

$$P(\beta) = \sum P(\beta|w_i) \quad (3)$$

Notice that the quantity $P(w_i)$ and $p(\beta)$ are common to all class-conditional probabilities; therefore, it represents a scaling factor that may be eliminated. Thus the decision algorithm become:

$$\text{select tone if } P(\beta|w_i) > P(\beta|w_j), \forall j \neq i \quad (4)$$

we assume the class-conditional PDF to be D-dimensional Gaussian PDF. Therefore (3):

$$P(\beta|w_i) = \sqrt{\frac{1}{2\pi}} |\Sigma_i|^{-\frac{1}{2}} \exp \left[-\frac{1}{2} (\beta - \mu_i) \Sigma_i^{-1} (\beta - \mu_i) \right] \quad (5)$$

where β is $d \times 1$ with mean vector $k \mu$ and covariance matrix $k \Sigma$ for class k . MAP is the value of the parameter which maximizes the likelihood Which we can write this as:

$$K = \text{Arg max} (P(\beta|w_i)) \quad (6)$$

MATERIALS AND METHODS

There are two elementary phase that the ASR depends on two fundamental phases:

1. training phase : in this phase the voice signal feature will be extracted and then enhanced as be in useful form that could be regarded as basic distinguishing features. We extract the cepstral coefficient (one of the frequency domain features) using MFCC method, this method is one of the most practicable methods in voice recognition system. The MFCC method has been enhanced by (4) using the normalization and smoothing of spectrum extracted from the voice signal

2. classification phase : the classification phase plays a great role in the recognition process. We used the Gaussian probabilities in calculating the probability of features, then they will be compared to get the most probable class.

The algorithm depend in this features is :

- i. calculating the Gaussian probability for each vector using sliding window.
- ii. Repeating the forming of vector for each layer (the layer is a set of voice files recorded in deferent position and times but have the same eliephone) to form one vector for each layer.
- iii. Comparison among the layer and choosing the most probable one.

The figure (3) illustrates how to estimate the maximum likelihood.

RESULTS AND DESCUSION

After applied the proposed system on isolated words that consist fourteen words, these word represent some of computer command, The experimental results of the word recognition ratios for classical and suggested method are shown in table (1), which are put in appendix (A), the average of experimental results shown that the percentage of recognition of proposed system is about 90%. Also the likelihood of specific class has high values and this indicated that the system is efficient in classification process.

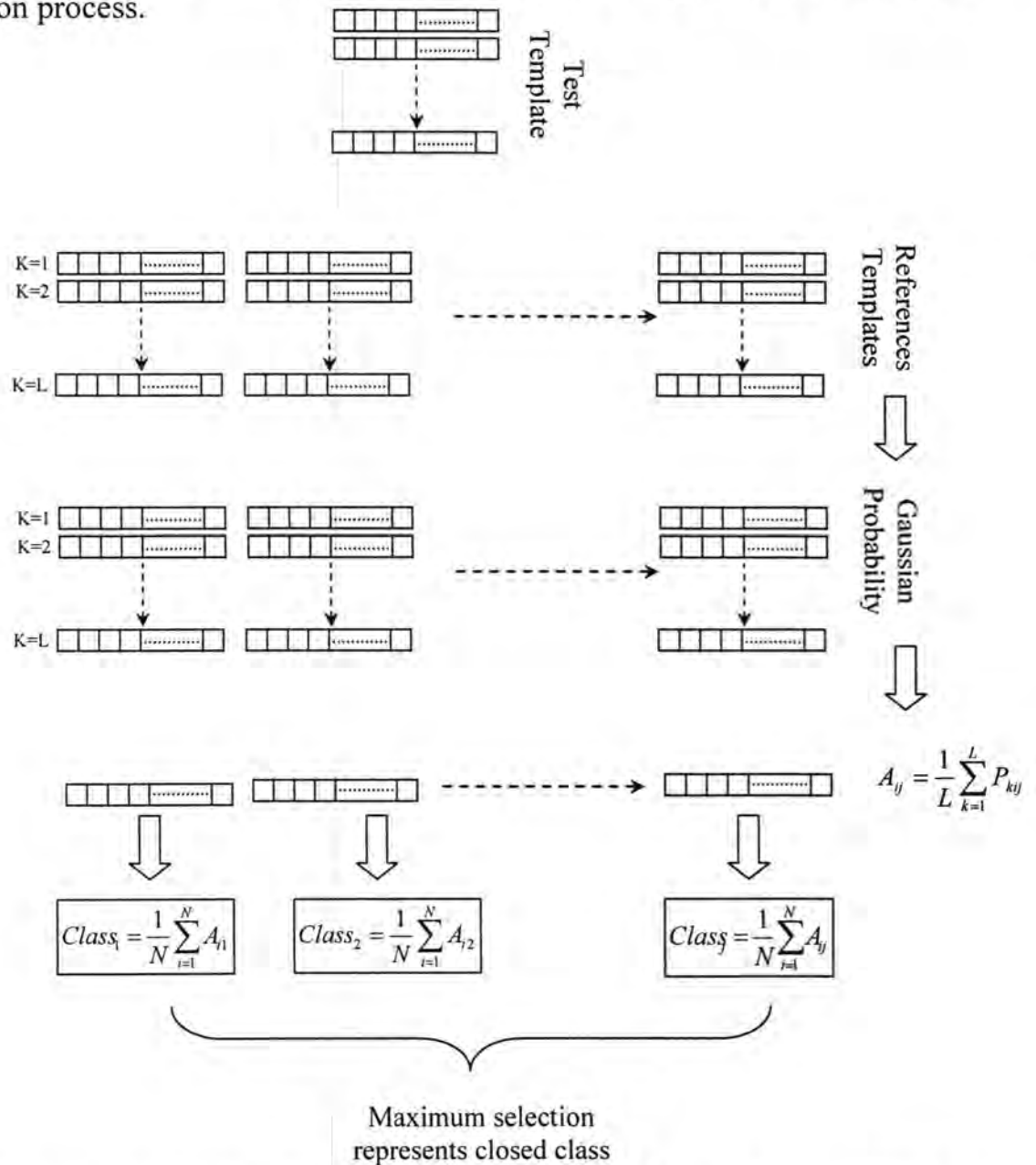


Fig.-3: illustrated the used method to applied maximum likelihood probability in speech recognition system.

Table-1: Results of isolated words recognition.

	Open	New	Print	Tool	Edit	View	Option	Close	Cut	Help	Paste	Play	Refresh	Start
Open	0.3158	0.0587	0.0338	0.0694	0.0067	0.0404	0.1718	0.0269	0.0241	0.0206	0.069	0.0295	0.0632	0.013
New	0.1221	0.1694	0.0987	0.0973	0.0386	0.1176	0.0435	0.0881	0.0095	0.0691	0.0165	0.0534	0.1214	0.0712
Print	0.0314	0.0342	0.2656	0.047	0.0647	0.0881	0.0268	0.0748	0.0032	0.0854	0.1416	0.0602	0.0529	0.1156
Tool	0.071	0.1154	0.0886	0.1447	0.1058	0.0723	0.014	0.159	0.0034	0.1313	0.0201	0.13	0.139	0.1377
Edit	0.0424	0.0599	0.0541	0.0666	0.1478	0.0302	0.0537	0.0476	0.0755	0.0417	0.0389	0.1231	0.0648	0.0541
View	0.0704	0.1337	0.0456	0.0612	0.0668	0.1637	0.0141	0.0394	0.022	0.0744	0.0144	0.1763	0.0549	0.028
Option	0.0929	0.0984	0.0068	0.0407	0.0189	0.0265	0.5242	0.0061	0.1071	0.0074	0.032	0.0141	0.0625	0.0049
Close	0.0375	0.0659	0.0502	0.1021	0.1528	0.1392	0.0098	0.127	0.0098	0.1086	0.0098	0.083	0.0857	0.0869
Cut	0.0076	0.0005	0.0045	7E-05	0.0451	0.0068	0.0059	0.0008	0.4003	0.0074	0.1338	0.0002	0.0104	0.0011
Help	0.0143	0.0138	0.1305	0.1287	0.0924	0.0217	0.0047	0.1732	0.0183	0.1553	0.0914	0.0481	0.0527	0.2206
Paste	0.0217	0.0008	0.0286	0.0005	0.0336	0.0083	0.0103	0.0063	0.2064	0.0463	0.3675	0.0039	0.0362	0.0056
Play	0.1122	0.1206	0.0338	0.0184	0.1391	0.1376	0.0086	0.0365	0.0028	0.0472	0.0075	0.1752	0.0679	0.0429
Refresh	0.0519	0.1232	0.0235	0.1126	0.0342	0.123	0.0984	0.029	0.1096	0.0592	0.0307	0.0507	0.1464	0.0245
Start	0.0089	0.0055	0.1356	0.1107	0.0535	0.0246	0.0142	0.1853	0.0079	0.1461	0.0268	0.0524	0.042	0.1941

REFERENCES

1. Qin Jin, "Robust Speaker Recognition", Language Technologies Institute, School of Computer Science, Carnegie Mellon University, Ph.D Thesis:4(2007).
2. Davis S., and Mermelstein P., "Comparison of Parametric Representations for Monosyllabic Word Recognition in Continuously Spoken Utterances", IEEE Transactions on Speech and Audio Processing, 28:357–366(1980) .
3. Greene W. "Econometric Analysis" 6th ed. Prentice Hall. Ch.(16)(2008) .
4. AL_zuky A.&Fleih A.&Hani M "Enhancement of Isolated_words Recognition System" Journal of Education, Al_Mustasriyah University (2008).

Study Text Image Resolution Using Soble Operator

Ahlam Mjeed Kadhum , Farah Jawad Kadhum and Ban Sabah
Physic Department L College of Science / Mustansiriyah University.

الخلاصة

يعد التصوير الملون مجالاً فعالاً وغنياً بالبحوث العلمية وهو في حالة تقدم مستمر نتيجة للتطور السريع الحاصل في عالم الكمبيوتر ودراسة الصورة النصية هي جزء من هذا التطور. في هذا البحث صورنا ثلاث صور لنصوص مكتوبة باللغة العربية مكتوبة على خلفية بيضاء صورت النصوص باستخدام كاميرا رقمية وتم التصوير بإضاءة جيدة في غرفة الصف تم استخدام مؤثر سوبل لتحديد نقاط الحافات في الصورة النصية المختلفة تم بعد ذلك حساب التباين بطريقتين الأولى حساب التباين المباشر والثانية حساب التباين لمعدل العناصر حول نقاط الحافات وتم حساب معدل التباين لعناصر الصورة ولكلا الطريقتين ودرس معدل التباين كدالة لبعث الكاميرا عن الصورة.

ABSTRACT

Color imaging effective field for since research it is continue development as a result of fast development that happened in computer world. The studies text image is apart of this development .In this research we are imaging three text which are writing in Arabic language on white background by digital camera in good lightness. Then we used Soble operator to determine image edges for the different text images then we are study the contrast mean for the image edges as a function of the distance between the white bored and camera.

INTRODUCTION

In the last three decades, color image processing and analysis has been, and now is, a very active field of research. Nowadays, the amount of color image processing and analysis methods is growing quickly. A large number of algorithms can be classified in this field, which gives the solution to problems such as color image segmentation, image compression, image enhancement , and image indexing (1).

Some of these techniques, such as color image segmentation, are natural operations for the human visual system (2). This complex system is a perfect interconnection network between the environment and our brain. A basic task of this system is image description. Given an image, our visual human system is able to detect the meaningful objects in the image and to describe the image by means of these elements. In the color case, color names are associated to these meaningful objects improving the description of the image.

- Ambbrozial and Russell. (3), in 1985, they used (HIS) color system (intensity, hue, and saturation) that to enhance and analyse the satellite images.
- Paul Muther (4), in 1987, he was concerned with one specialized area of remote sensing. He suggested a number of enhancement techniques such as,

altering the contrast, and converting to hue, saturation, and intensity, and adjusted them by using contrast-stretching methods.

- Robin N. Strickland (5), in 1987, he found that color saturation as well as luminance, can have an important role in achieving a good image enhancement. His technique is based on the observation that the saturation color component often has high frequency data that are not presented in the luminance color component.

Color: Description and Representation

The study of Color involves several branches of knowledge: physics, psychology, mathematics, art, biology, physiology... Each one of these disciplines contributes with different information's, but the way towards the absolute understanding of color has just begun. Color is:

- a. An attribute of things that results from the light they reflect, transmit, or emit in
so far as this light causes a visual sensation that depends on its wavelength.

- b. The aspect of visual perception by which an observer recognizes this attribute.

- c. The quality of the light producing this aspect of visual perception.

This definition illustrates the complexity of the notion of color and roughly sketches the three factors on which color depends: light, physical objects and our visual system.

Color does not exist by itself; only colored objects exist (6). Three elements are necessary for the existence of color:

- A light source, to light the scene.
- The objects, which reflect, spread, absorb or diffract the light.
- A receptor, which captures the spectrum reflected by the object.

Color basically depends on these three elements, in such a way that, if one of them is not present, then we are not able to perceive color. On one hand, color is a physical attribute,

due to its dependence on a light source and on physical characteristics of the objects; on the other hand, it is a psychophysical and physiological attribute, since it depends on our visual perception.

Physical Meaning of Light

Light consists of a flux of particles called photons, which can be regarded as tiny electromagnetic waves (7). These waves must have a length between 380nm and 780 nm to stimulate our visual system. The wavelength content of a light beam can be assessed by measuring how much light energy is

contained in a series of small frequency intervals. The light can then be described by its spectral distribution of energy.

This spectral distribution characterizes each light source. For instance, the distribution of solar light is virtually at since it has the same quantity of all visible wavelengths (8). The distribution of the light emitted by a light bulb or tungsten is more intense for the longer wavelengths than for the short ones. Our perception of color may change depending on the scene illumination, since the wavelengths reflected by the objects depend on the light source.

The color of an object is defined and measured by its reflection spectrum(7). When light hits an object, the following three phenomena can happen: the light can be absorbed and the energy converted to heat, as when the sun warms something; it can pass through the object, as when the sun's rays hit water or glass; or it can be reflected, as in the case of a mirror or any light-colored object. Often two or all three of these phenomena occur simultaneously. Moreover, the same object can have different colors", depending on the light source, on the geometry of the light devices, or on the change of some of its physical characteristics (8).

The practical part

To study lighting quality, its distribution in the class, the effect of the use color in specifying the three texts written on the white board along with study of distance effect in specifying good view of the written texts, the texts illustrated in Figure (1) was imaged using Sony – Digital Camera and the color of the pen used in study is (black, green, blue)

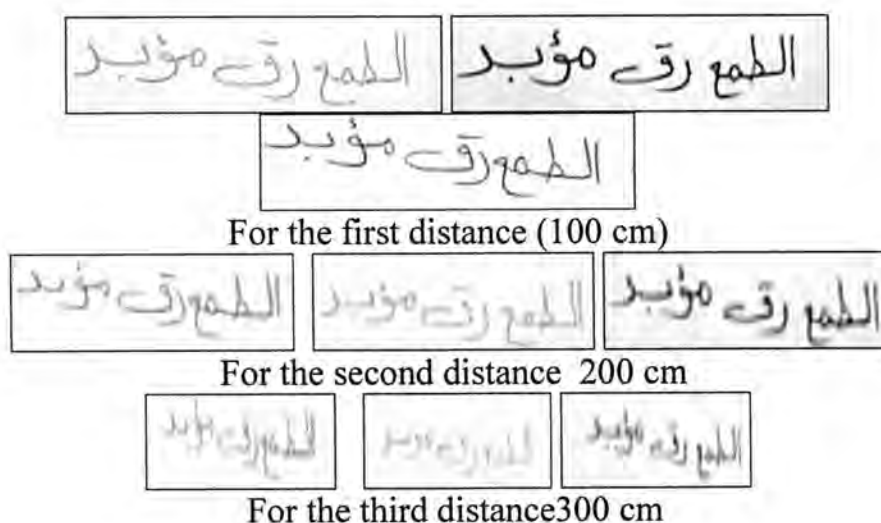
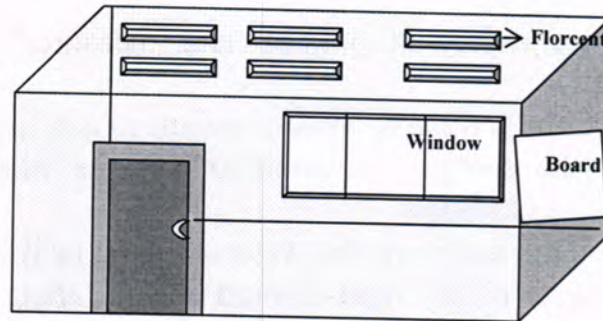


Figure -1 : Text images for three distance between the camera and white board

(Dry-Eraser) for different distances 100, 200, 300 cm. Imaging process was made at 10:00 AM of 14-04-2009 according to the geometry of classroom illustrated in Figure (2). Hence we used the indirect sun light enter the room from the window and the florcent in the room.



**Figure -2: classroom geometry
Direct image contrast**

Contrast is the difference in optical characteristics that make the written text recognizable. In optical detection of image, contrast is determined through the difference

in color band and lightness. The general relation of lightness contrast given by (1)

$$CT = \frac{L_{\max} - L_{\min}}{L_{\max} + L_{\min}} \quad \text{----- (1)}$$

Lux_{\max} and Lux_{\min} represent higher and lower reading of the photometer in Lux unit by difference in spotlight of photometer direction in relation to the classroom geometry, as illustrated in Figure (3).



Figure -3: photometer using to determined lighting intensity

Table (1) shows luminance and contrast values of opposite spotlight direction according to classroom geometry in case with no Fluorescent light i.e (used only indirect sun light).

Table -1: luminance and contrast values of class room lightness

<i>Direct</i>				
Lux (1)	Lux(2)	Lux(3)	Lux(4)	Lux(average)
197	236	222	192	211.75
C1	C2	C3	C4	
0.09	0.072	0.012	0.03	

<i>Right</i>				
z	Lux(2)	Lux(3)	Lux(4)	Lux(average)
116	122	118	130	121.5
C1	C2	C3	C4	
0.025	0.048	0.056	0.016	

<i>Left</i>				
Z	Lux(2)	Lux(3)	Lux(4)	Lux(average)
270	300	272	254	274
C1	C2	C3	C4	
0.052	0.034	0.03	0.048	

<i>Upper</i>				
Lux (1)	Lux(2)	Lux(3)	Lux(4)	Lux(average)
218	257	261	233	242.25
C1	C2	C3	C4	
0.082	0.056	0.033	0.007	

<i>Down</i>				
z	Lux(2)	Lux(3)	Lux(4)	Lux(average)
63	73	64	58	64.5
C1	C2	C3	C4	
0.073	0.049	0.041	0.065	

The contrast of the written text was determined by adopting edges' points which are specified by (Sobel operator) for edge detection depending upon four procedures Contrast determination by adopting direct contrast of edges elements. The equation of image edge contrast is:

$$CT = \frac{I_{\max} - I_{\min}}{I_{\max} + I_{\min}} \quad \text{-----} \quad (2)$$

When I_{\max} : maximum image edge intensity
 I_{\min} : minimum image edge intensity

Figures (4, 5,6 and 7) show the results of this technique. In case of lighting from the right side classroom, contrast average was charted as a function of the distance between the camera and the white board. When using different thresholds of Sobel operator, we see, from the figures that increasing the distance lead to decrease in contrast. Also, we may note that by increasing the threshold value of Sobel operator the contrast increases, we may see that the line converges together for different soble thresholds; we get best image quality best resolution at high contrast for the blue and black written text.

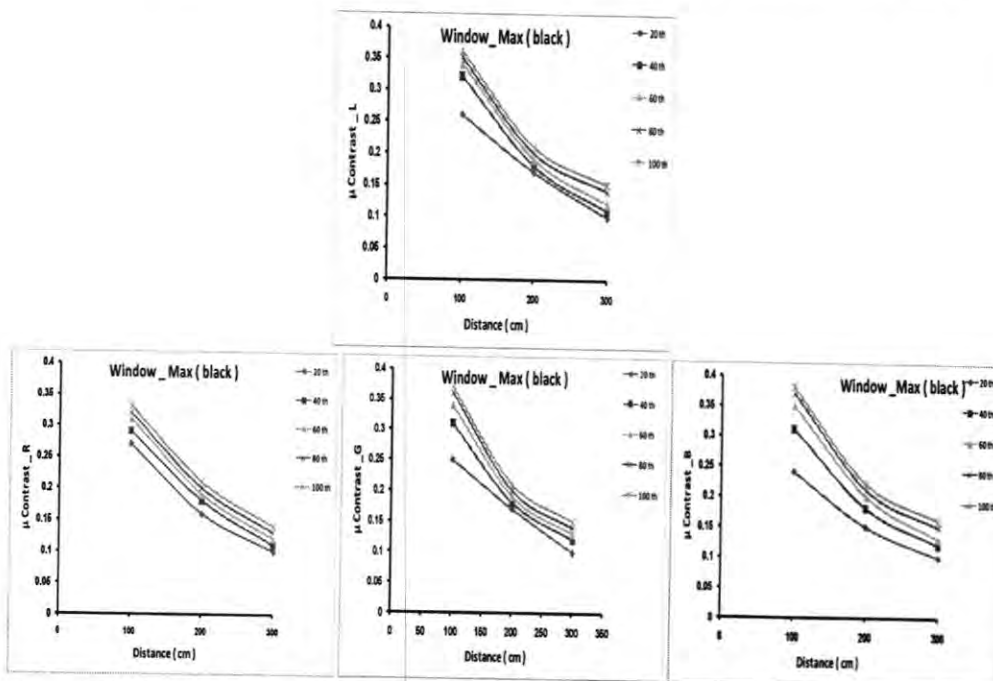


Figure -4: The relation between direct contrast as a function to distance digital camera and White board for black text for the band(RGB)

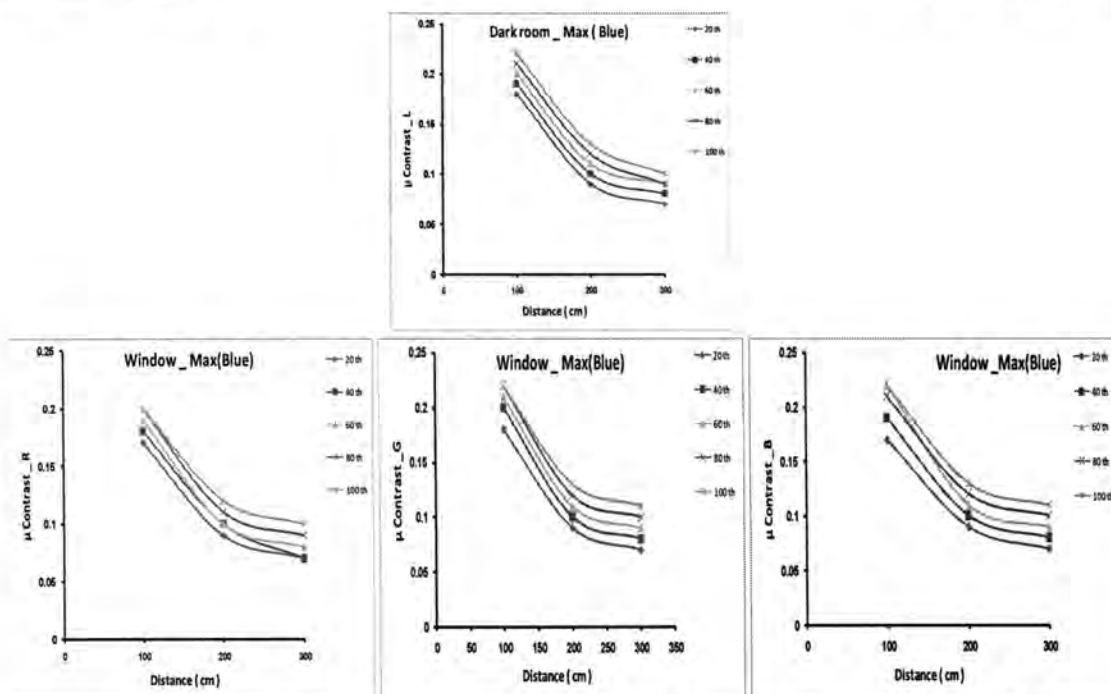


Figure-5: The relation between direct contrast as a function to distance digital camera and White board for blue text for the band(RGB)

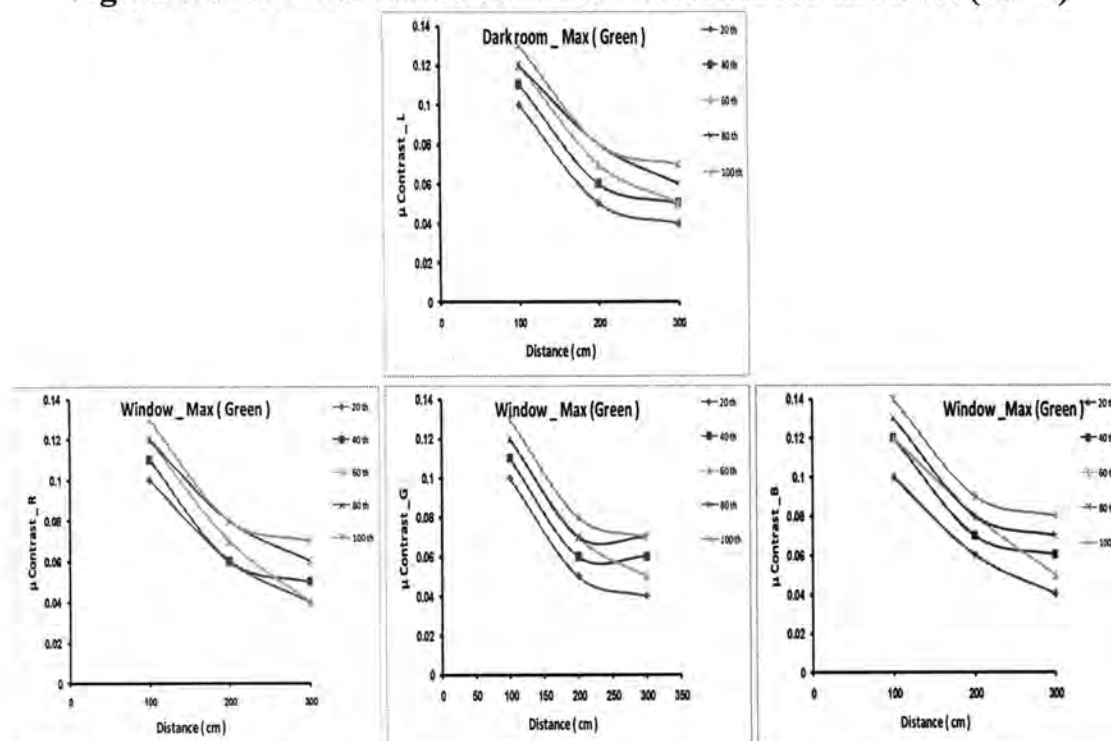


Figure-6: The relation between direct contrast as a function to distance digital camera and White board for green text for the band(RGB)

Determined contrast of minimum value with central mask element

In this case we research for minimum neighbor elements (I_{\max}) to central mask element which represent edge in trinal window , maximum value represent central mask element ($I_{\min} = I_{\text{center}}$) , figure (5) shows to diagram of this technique, contrast equation in this technique is found by the relation [1]:

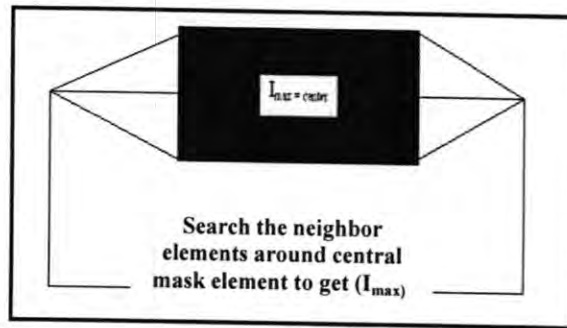


Figure -7: the (3*3) mask around image element

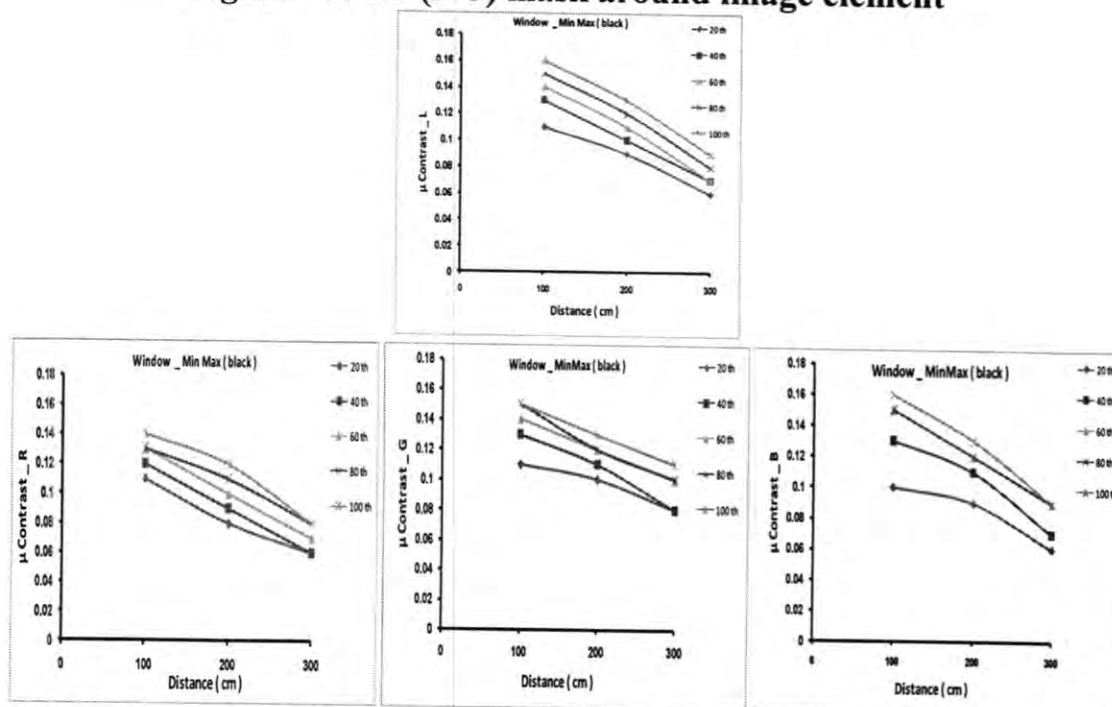


Figure -8: the relation between minimum and maximum contrast as a function of distance digital camera and White board for black text for the band (RGB)

The results of contrast calculation of edges points using larger and smaller element of edges elements technique. Shown in figures (9,10 and 11), for the three colors bands and luminance compound of written text in non-uniform

lightness (lighting from the right side). Contrast average was charted as a function of distance between camera and written text on the white board. We note that by increasing distance, calculated contrast values of written text on the white board decrease and by increasing threshold value of Sobel Effect the contrast values of the written text in black on the white board increased.

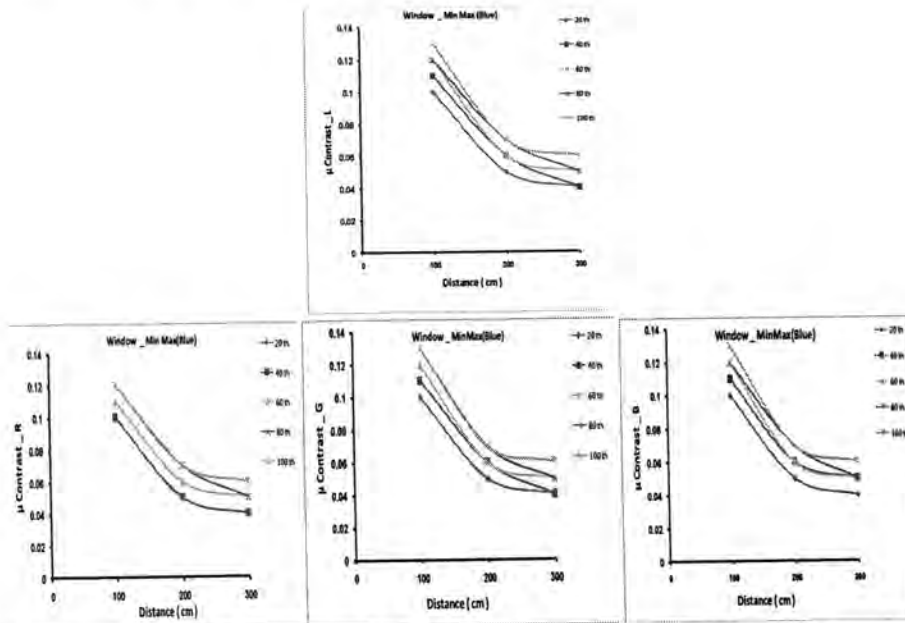


Figure-9: The relation between minimum and maximum contrast as a function of distance digital camera and White board for blue text for the band(RGB)

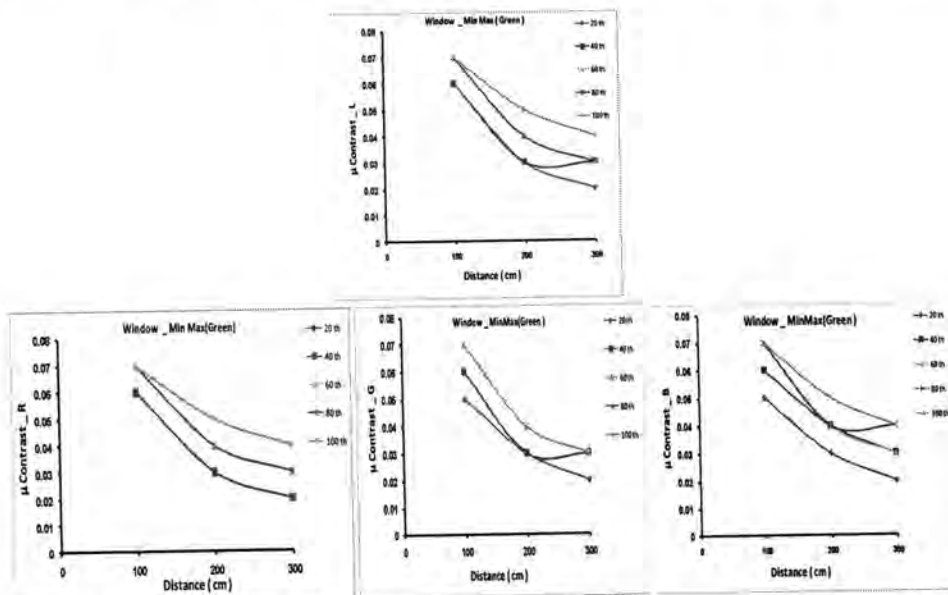


Figure-10: The relation between minimum and maximum contrast as a function of distance digital camera and White board for green text for the band(RGB)

We can conclude

The mean contrast increasing as a function of increasing soble operator thresholds, we can see stability contrast values in large distance for the blue and green text. The good contrast obtained for using blue and black texts .i.e. get high resolution image can be recognize the text for large distances.

REFERENCES

1. R. Schettini, G. Ciocca, and S. Zu_. A survey of methods of colour image indexing and retrieval in image database. In *Color Imaging Science: Exploiting Digital Media*,: 183{211. John Wiley & Sons (2002).
2. D. Hubel. *Eye, Brain and Vision*. Paperback,(2000).
3. Ambroziak and Russell,"Operational use of color perception to Enhance satellite image quality", conference title:" Image quality Overview" (1985).
4. Mather M., "Computer processing of remote sensing images: an Introduction", (1987).
5. Robin N. Strickland, "Digital Image enhancement based on the Saturation component", Society of optical instrumentation engineers, 1987.
6. Tremeau, C. Fernandez-Maloigne, and P. Bonton. *Image numerique couleur, de l'acquisition au traitement*. Dunod, (2004).
7. G. Wyszecki and W.S.Stiles. *Color Science: Concepts and Methods, Quantitative Data and Formulae*. Wiley, (1984)
8. E.B. Goldstein. *Sensacion y Perception*. Editorial Debate,(1999).

Influence of Copper Sulfate Additives on Some Optical Properties of PMMA films

¹Sami Salman Chiad , ²Amer Basim Shaalan and ¹Nadir Fadhil Habubi

¹Al Mustansiriya University, College of Education, Physics Department

²Muthana University, College of Science, Physics Department

الخلاصة

حضرت أغشية البولي مثيل ميثاكريلات (PMMA) النقية والأغشية المضاف إليها كبريتات النحاس بتركيزات مختلفة بطريقة الصب. سجل طيفي النفاذية (T) والامتصاصية (A) ولكافة الأغشية وذلك لغرض دراسة بعض الثوابت البصرية، مثل معامل الانكسار (n)، معامل الخمود (k)، التوصيلية الضوئية (σ)، ثابت العزل بجزئية الحقيقي (ϵ_r) والخيالي (ϵ_i). المضافات قد أثرت على كافة العوامل قيد الدراسة وحسنت من صفاتها وخصوصا حافة الامتصاص البصري عندما كانت الاضافة بتركيز 8 %.

ABSTRACT

Film of PMMA and a variable concentrations of copper sulfate additives were prepared by casting method.

The absorbance and transmittance spectra have been recorded for all the deposited films in order to study the optical constants such as, refractive index, extinction coefficient, optical conductivity, real and imaginary parts of dielectric constant, these additives affect all the parameters under study and enhance their values especially the optical absorption edge for 8% additive concentration.

INTRODUCTION

Polymethyl methacrylate (PMMA) could be tailored in many application due to its unique properties for its high chemical resistance, advantageous optical properties, simple synthesis low cost (1,2), therefore pure PMMA and PMMA composites has been widely used in many field of technology, such as photoresist for direct – write e-beams (3), in photonic of nanotechnology because of the uniform optical index of its structure (4), and in prosthetic composites used in dentistry because of its excellent cell adhesion and biocompatibility (5), as a gate insulator because it can be easily formulated into uniform and mechanically flexible layers over a large area (6), as an intraocular lens material that's is used in cataract surgery (7), chemical sensing (8), muscle – like actuators (9), it is also used in consumer products due to excellent mechanical properties and performance under various processing conditions (10).

The properties of composites mostly depend on size and shape of filler particles, their concentration as well as the type of interaction with polymer matrix. Also polymer composites take advantage of desired properties of host polymers such as possibility to be designed in various shapes, long term stability and reprocess ability (11).

The aim of this work is to investigate the effect of copper sulfate an additive on optical properties of PMMA films.

MATERIALS AND METHODS

Thin layer of pure PMMA and copper sulfate as an additive (2, 4, 6, 8) % weight to weight, were prepared by the dispersed polymer dissolved in chloroform. The polymer solution and the additives of copper sulfate were casted as thin layers, dried at room temperature for 24 hours.

Thin layer thickness were measured using (indicating micrometer 0.25 mm) with an error not exceeding $\pm 5\%$ and find to be in the range of $20 \pm 1 \mu\text{m}$, the layers were clear, transparent, free from any noticeable defect and showing light bluish color.

The absorbance and transmittance spectra were recorded using double beam shimadzu UV/VIS-160⁰ Å in the wavelength range (300-900) nm, all measurements were carried out at room temperature.

RESULTS AND DISCUSSION

Fig. (1) Shows the optical transmission of pure PMMA and with different concentration of additive copper sulfate. High transmittance above 80 % is exhibited in the visible region for pure PMMA, while the addition of 8 % copper sulfate decreases the transmittance to 70 %. All the films have sharp absorption edge in the UV range, which shift to longer wavelength as the concentration of copper sulfate increase.

Fig. (2) Shows the absorptance versus wavelength for all the samples under investigation, the absorption edge were shifted toward lower wavelength (blue shift) as the concentration of CuSO_4 increased.

The complex refractive index (n^*) of a material can be expressed as (12):

$$n^*(\lambda) = n(\lambda) + ik(\lambda) \quad \text{----- (1)}$$

Where (n) is refractive index and (k) is the extinction coefficient.

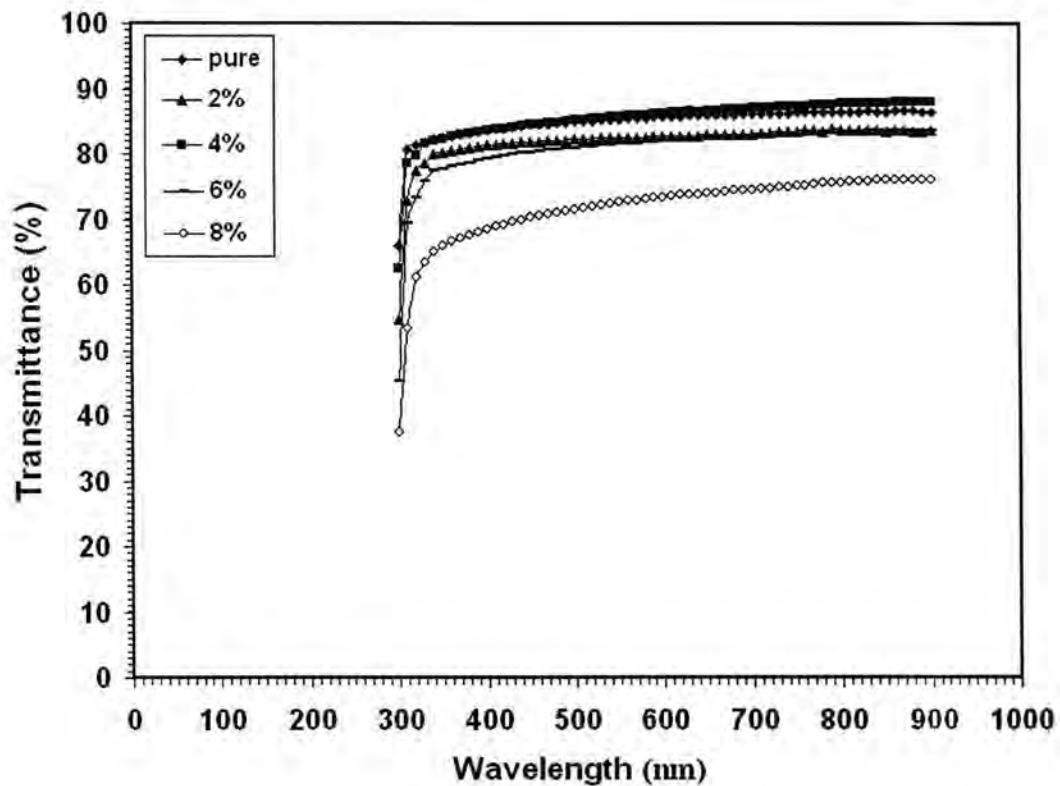


Fig. -1: Transmittance versus wavelength for the as deposited films.

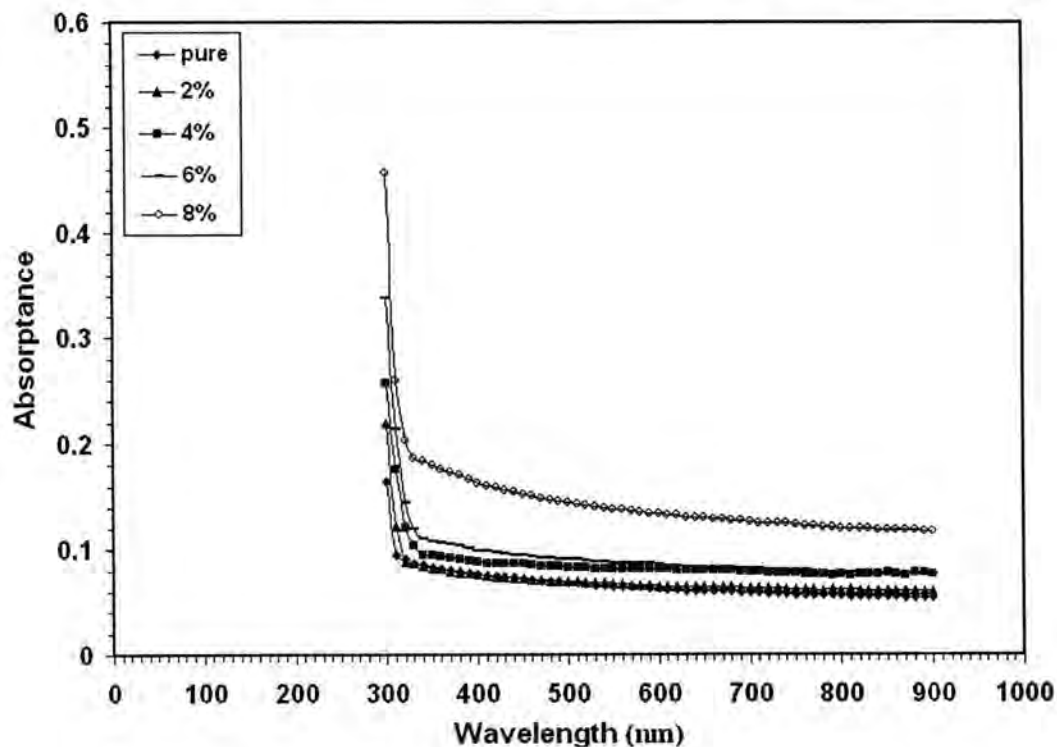


Fig. -2: Absorbance versus wavelength for the as deposited films.

Fig. (3) Shows the dependence of the refractive index of the as deposited films against photon energy, it can be seen that the refractive index

increase with increasing the additive concentration and this could be attributed to the increase of optical absorption in the visible and ultra violet region.

It is known that the extinction coefficient (k) and absorption coefficient (α) can be related by (13):

$$k = \frac{\alpha \lambda}{4 \pi} \quad \text{----- (2)}$$

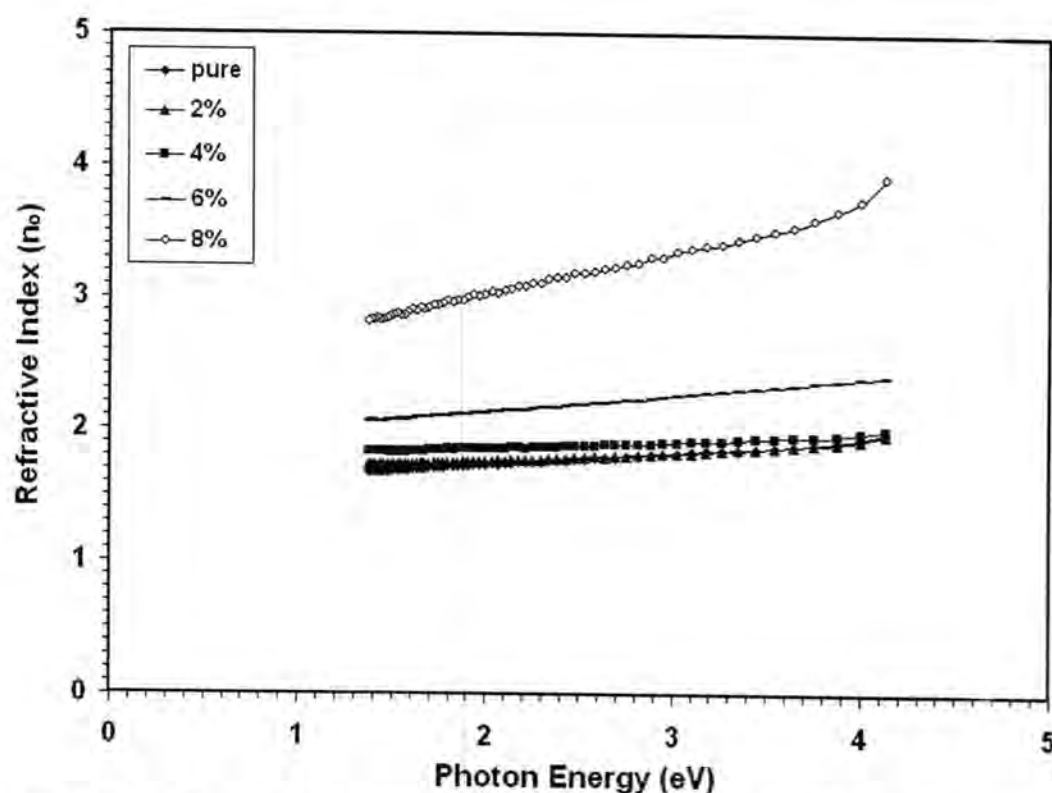


Fig. -3: Refractive indices versus photo energy for the as deposited films.

From Fig. (4) we can easily obtain the extinction coefficient of the deposited films it can be seen that the extinction coefficient increase as the additive concentration increased.

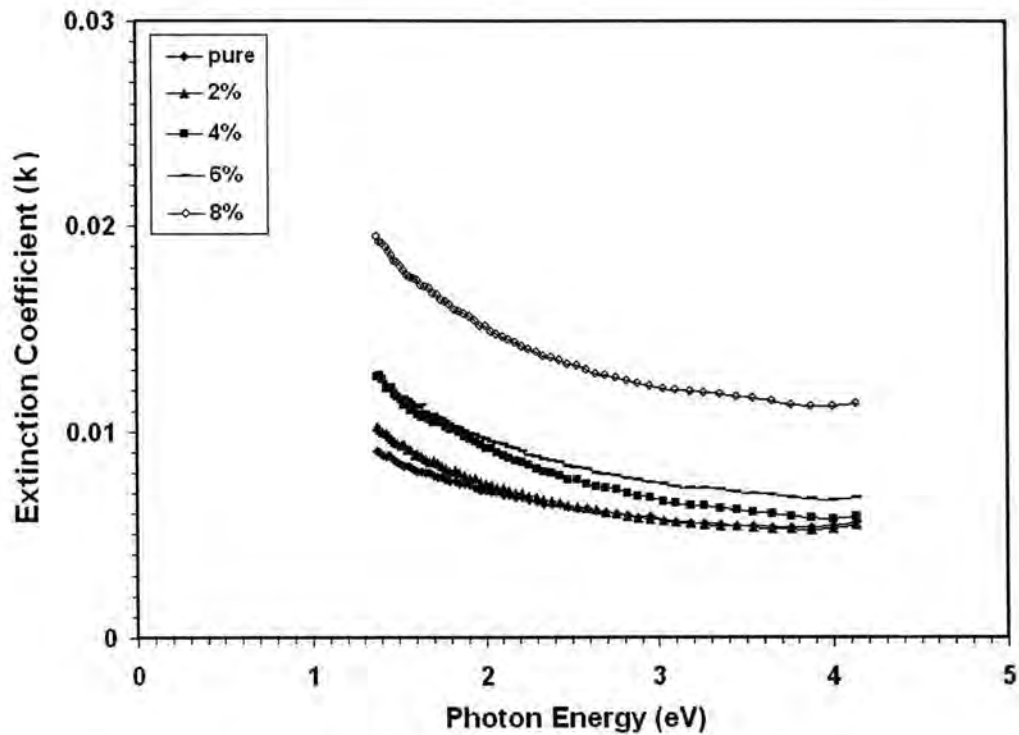


Fig. -4: Extinction coefficient versus photo energy for the as deposited films.

Fig. (5) Shows the variation of optical conductivity with the incident photon energy.

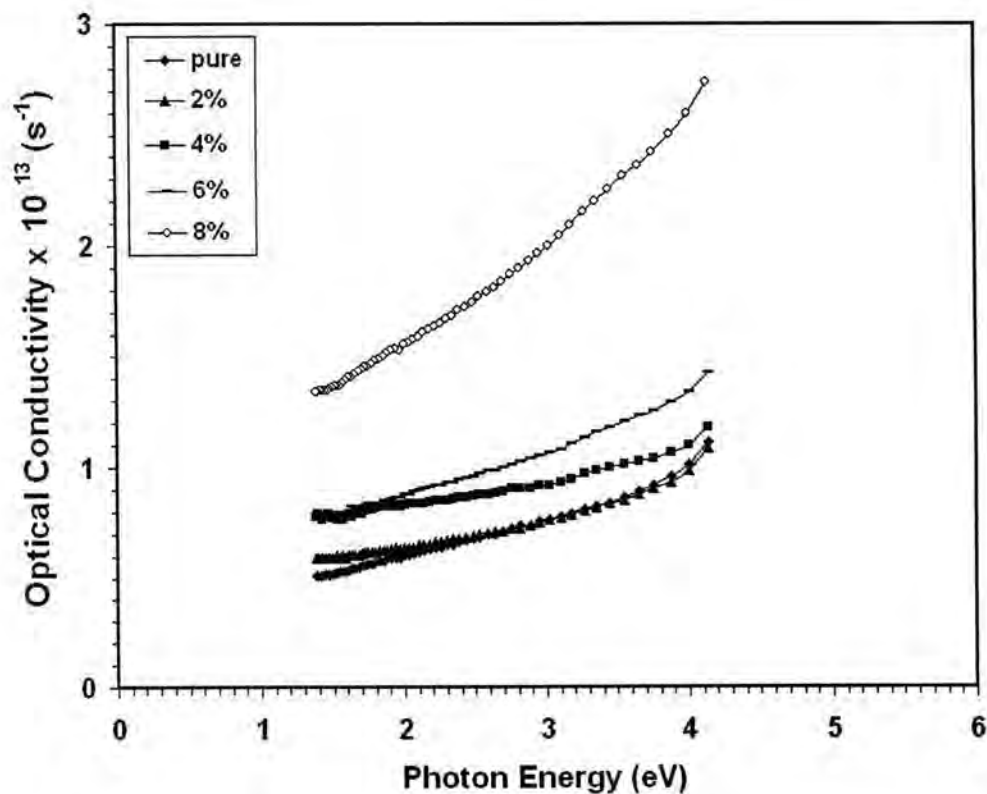


Fig. -5: Optical conductivity versus photo energy for the as deposited films.
The optical conductivity is determined using the relation^[14]:

$$\sigma = \frac{\alpha n c}{4 \pi} \quad \text{-----} (3)$$

Where (c) is the velocity of light.

The optical conductivity directly depends on the absorption coefficient (α) and found to increase sharply in 8 % additive concentration.

Fig. (6) and Fig. (7) Shows the variation of the real and imaginary part of dielectric constant for the deposited films. The real part of it ,is associated with the term that how much it will slow down the speed of light in the material, the imaginary part gives that how a dielectric absorb energy from electric filed due to dipole motion.

The real and imaginary parts of the dielectric constant were determined using the relation (15):

$$\epsilon_r = n^2 - k^2 \quad \text{-----} (4)$$

$$\epsilon_i = 2nk \quad \text{-----} (5)$$

The real and imaginary parts of the dielectric constant were increase as the concentration increased.

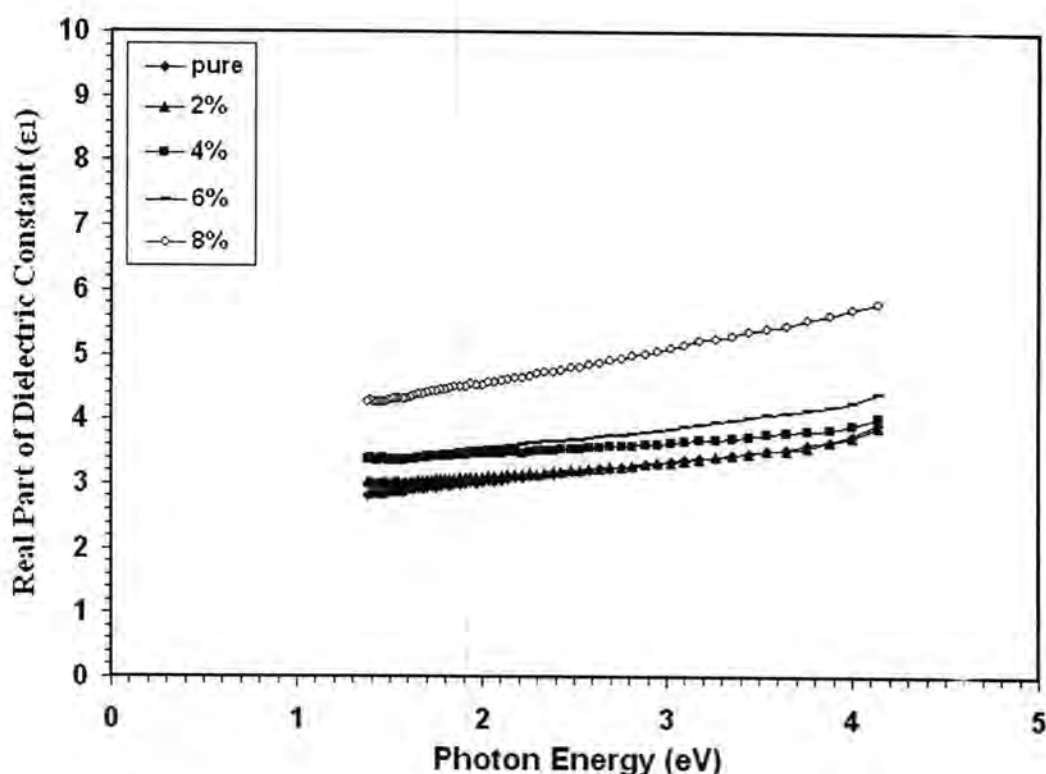


Fig. -6: Real part versus photo energy for the as deposited films.

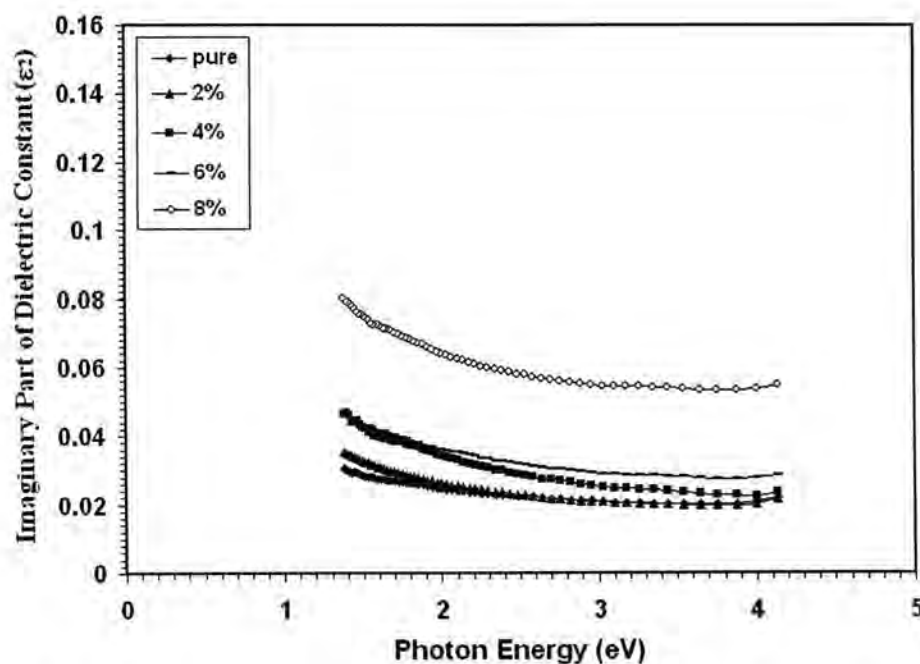


Fig. -7: Imaginary part versus photo energy for the as deposited films.

We can conclude

The transmission approximately remains constant at visible region; this makes the deposited films a good candidate to use as an antireflection coating within this spectral range.

It is clearly seen from the absorbance spectra that the absorption edge shifts toward shorter wavelengths (blue Shift).

From refractive index curve it is seen that the refractive index for pure PMMA and (2, 4, 6, 8) % Concentration of copper sulfate remain approximately constant at ultra violet and visible region and this behavior represents optical stability with this spectral region.

REFERENCES

1. Yadav J.B.,Puri R.K.&Puri V.,Improvement In Mechanical and Optical Properties of Vapour Chopped Vacuum Evaporated PANI/PMMA Composite Thin Film,Applied Surface Science,254:1382 (2007).
2. Nie Z.,Lee H.,Shin H.,Lee Hy.,Optical Properties and Spectroscopy Parameters of Sm (DBM)₃ Phen-Doped Poly(Methyl Methacrylate),Lim Ki-Soo and Lee M., Spectrochimia Acta Part A and Biomolecular Spectroscopy, 72 (3): 554(2009).
3. Tsai T.,Lin C.,Guo G.&Chu T., Effects of Microwave-Assisted Digestion on Decomposition Behavior of Poly (Methyl Methacrylate) (PMMA), Materials Chemistry and Physics, 108: 382(2008).
4. Nakajima M.,Yoshikawa T.,Sogo K.and Hirai Y.,Fabrication of Multi-Layered Nano-Channels by Reversal Imprint Lithography, Micro Electron. Eng., 83: 876 (2006).

5. Ciffi M.O.H., Voorwald H.J.C. and Mota R.P., Surface Energy Increase of Oxygen-Plasma-Treated PET, *Mater. Charact.*, 50:209 (2003).
6. Pyo S., Son H., Choi K-Y., Yi M. H. and Hong S. K., Low-Temperature Processable Inherently Photosensitive Polyimide as A Gate Insulator for Organic Thin-Film Transistors, *Appl. Phys. Lett.*, 86, : 133508(2005).
7. Zhang L., D. Wu, Chen Y., Wang X., Zhoo G., Wan H. and Huang C., Surface Modification of Polymethyl Methacrylate Intraocular Lenses by Plasma for Improvement of Antithrombogenicity and Transmittance, *Applied Surface Science*, 255: 6840 (2009).
8. Convertino A., Capobianchi A., Valentine A., and Cirillo E., A New Approach to Organic Solvent Detection: High Reflectivity Bragg Reflectors Based on A Gold Nanoparticle/Teflon-Like Composite Material, *Advanced Materials*, 15 (13):1103(2003).
9. Shahinpoor M., Bar-Cohen Y., Simpson Jo. and Smith J., Ionic Polymer-Metal Composites (Ipmcs) as Biomimetic Sensors, Actuators and Artificial Muscles - A Review, *Smart Mater. Struct.*, 7: 15(1998).
10. Deng B. L., Hu Y. S., Chiu W. Y., Chen L.W., and Chiu Y. S., Thermal Degradation Behavior and Physical Properties for Poly (Methyl Methacrylate) Blended With Propyl Ester Phosphazene, *Polymer Degradation And Stability*, 57:269 (1997).
11. M-Cincovic M., Popovic M. C., Novakoic M. and Nedeljkovic J. M., The Influence of B-Feooh Nanorods on The Thermal Stability of Poly(Methyl Methacrylate), *Polymer Degradation and Stability*, 92:70 (2007).
12. Xue S. W., Zu X. T., Zhou W. L., Deng H-X., Xiang X., Zhang L. and Deng H., Effects of Post-Thermal Annealing on The Optical Constants of ZnO Thin Film, *Journal of Alloys and Compounds*, 448 :21 (2008).
13. Chakraborty A., Mondal T., Bera S. K., Sen S. K., Chosh R. and Paul G. K., Effects of Aluminum and Indium Incorporation on The Structural and Optical Properties of ZnO Thin Films Synthesized by Spray Pyrolysis Technique, *Materials Chemistry and Physics*, 112: 162 (2008).
14. Sharma P., Sharma V. and Katyal S. C., Variations of Optical Constants in $\text{Ge}_{10}\text{Se}_{60}\text{Te}_{30}$ Thin Film, *Chalcogenide Letters.*, 3 (10) : 73 (2006).
15. Wooten F., *Optical Properties of Solids*, Academic Press, New York (1972).

The Extrapolation Of The Lateral Distribution function Approximation Of Cherenkov Radiation At The Energy Range 10^{16} - $2 \cdot 10^{18}$ eV

Ahmed Aziz Ahmed (a75a2000@yahoo.co.uk), Sabah Toma Murad
Al-Mustansiriyah university, college of science, department of physics

الخلاصة

لقد تم حساب دالة التوزيع الفراغية لإشعاع جيرينكوف لوابل من الجسيمات الناتجة من البروتونات الأولية لطاقت عالية جدا ($E \geq 10^{16}$ eV) باستخدام برنامج كورسيكا، وبالاعتماد على النتائج التي تم الحصول عليها تم ايجاد تقريب لدالة التوزيع الفراغية والذي يسمح لنا تحديد نوع وطاقة الجسيم الناشئ نتيجة لتفاعل البروتونات مع نوى ذرات الهواء داخل الغلاف الجوي الأرضي. لقد تم الأخذ بنظر الاعتبار توسيع تقريب دالة التوزيع الفراغية لإشعاع جيرينكوف ضمن مدى الطاقة ($10^{16} - 2 \cdot 10^{18}$ eV).

ABSTRACT

The Lateral distribution function (LDF) of Cherenkov radiation from particles of Extensive Air Showers (EAS) with ultra high energies ($E \geq 10^{16}$ eV) was simulated for primary protons by the computer code CORSIKA. The approximation, that constructed on the basis of this simulation have allowed us to reconstruct the events, that is, to reconstruct the type and energy of the particle that generated EAS from signal amplitudes of Cherenkov light registered with the Tunka-25 facility. The extrapolation of the Cherenkov light LDF approximation at the energy range ($10^{16} - 2 \cdot 10^{18}$ eV) was taken into account.

INTRODUCTION

The determination of the energy spectrum and mass composition of the ultrahigh energy cosmic rays ($E > 10^{16}$ eV) is one of the greatest challenges in cosmic ray measurements. Using the atmosphere as a large target, Detectors are capable of tracing the development of the size of the Extensive Air Shower (EAS) through the atmosphere (1, 2). Large-scale experiments, like the Yakutsk EAS array (3), AGASA (4) HiRes (5), Pierre Auger Observatory (6) and Tunka-133 (7) focus on the precise determination of the energy spectrum, mass composition and arrival direction distribution of ultrahigh-energy cosmic rays. The analysis of the characteristics of the detected longitudinal profiles is currently the most reliable way for extracting some information about the primary cosmic ray mass composition. One of the main techniques for observing EAS is effectively investigated by the method of Cherenkov light EAS registration (8, 9). The main tools for calculating of EAS characteristics and experimental data analyzing (Direction of the shower axis, determination of the primary particle energy and type from the characteristics of Cherenkov radiation of

secondary charged particles) are codes of numerical simulation by the Monte Carlo method. Reconstruction of the primary particle characteristics initiating the atmospheric cascade from Cherenkov radiation of secondary particles at the energy ranges (10^{16} - 10^{18}) eV calls for the creation of a library of shower patterns, when this requires much computation time.

In the present work, the CORSIKA software package (10) in which hadron interactions are simulated using the QGSJET (11) and GHEISHA codes (12) simulates lateral distributions of Cherenkov light emitted by atmospheric cascades initiated by primary high-energy cosmic ray protons and nuclei. Simulation of Cherenkov radiation using the CORSIKA code requires very long computation time for a single shower with energy of 10^{18} eV for a processor with a frequency of a few GHz. Therefore, the development of fast modeling algorithms and the search for approximations of the results of numerical modeling are important practical problems.

Parameterization of the lateral distribution function (LDF) of Cherenkov radiation versus the distance R from the EAS axis and the primary particle energy E that can be used to approximate the results of numerical simulation of LDFs of Cherenkov photons emitted by EAS initiated in the Earth's atmosphere by the cosmic ray particle having a very high energy was taken. In the present work, we use this parameterization to describe results of numerical simulation of EAS by the CORSIKA code and of Cherenkov light emitted by EAS measured with the Tunka-25 facility (13).

THE CHERENKOV LIGHT LDF APPROXIMATION

The simulation of the Cherenkov light LDF in EAS is obtained using CORSIKA code for primary protons at the highest energies ($E \geq 10^{16}$) eV. For parameterization of simulated Cherenkov light LDF, we used the proposed function as a function of the distance R , from the shower axis and the energy E_0 of the initial primary particle, which depends on four parameters a , γ , σ and r_0 (14, 15):

$$Q(E, R) = \frac{C\sigma e^a \exp\left(\frac{R/\gamma + (R-r_0)/\gamma + (R/\gamma)^2 + (R-r_0)^2/\gamma^2}{\gamma[(R/\gamma)^2 + (R-r_0)^2/\gamma^2 + R\sigma^2/\gamma]}\right)}{m^{-2}}, \quad (1)$$

where $C=10^3 \text{ m}^{-1}$; R is the distance from the shower axis; a , γ , σ and r_0 are parameters of Cherenkov light LDF. The energy dependences of the parameters, γ , σ and r_0 is shown on Fig.1 for primary proton.

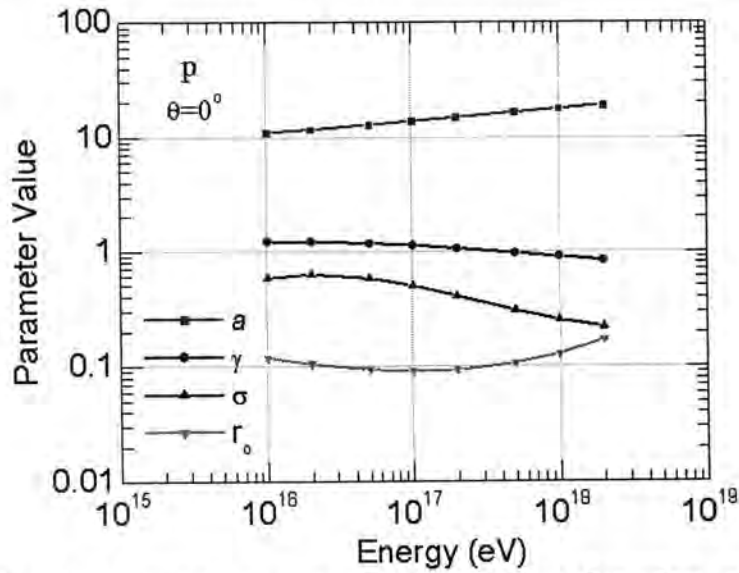


Figure-1: The fit parameters a , γ , σ and r_0 as a function of the primary energy of the initiating primary proton for vertical EAS.

The simulated data and the approximated formula (Eq.(1)) for vertical showers are presented on Fig. 2. for primary protons at the energies 10^{16} , $2 \cdot 10^{16}$ and $5 \cdot 10^{16}$ eV. In Fig. 3. one can see the extrapolation of the Cherenkov light LDF parameterization of the obtained data with CORSIKA program at the energies 10^{17} , $2 \cdot 10^{17}$, $5 \cdot 10^{17}$, 10^{18} and $2 \cdot 10^{18}$ eV. The accuracy of the Cherenkov light LDF approximation for vertical showers for primary protons is better than 15 % at the distances 80-120m from the shower axis, and close to 5 % for the other distances.

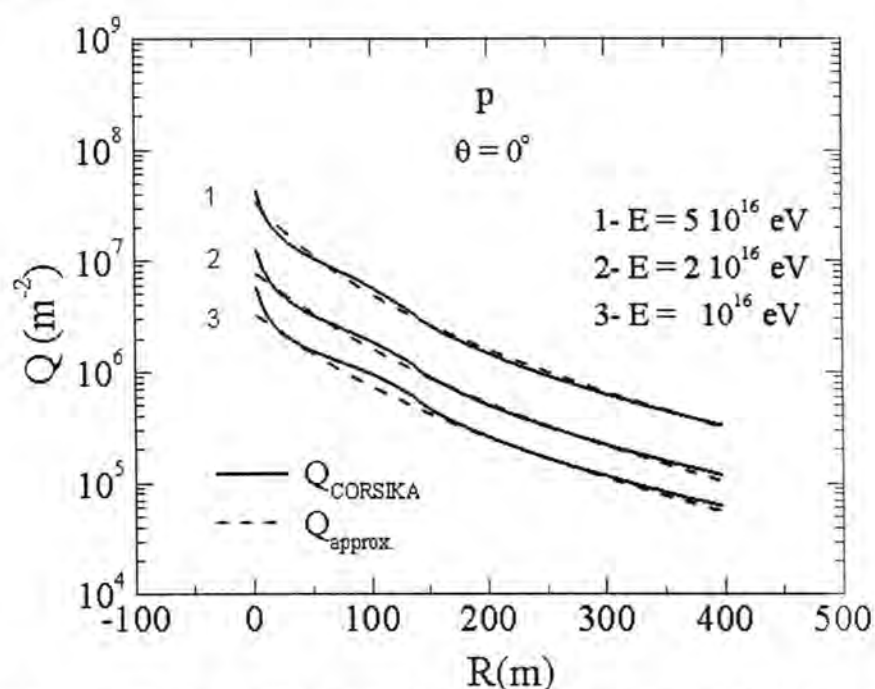


Figure- 2: Lateral distribution of Cherenkov light which simulated with CORSIKA code (solid lines) and one calculated (Eq. (1)) (dashed lines) for vertical showers initiated by primary protons at 10^{16} , $2 \cdot 10^{16}$ and $5 \cdot 10^{16}$ eV.

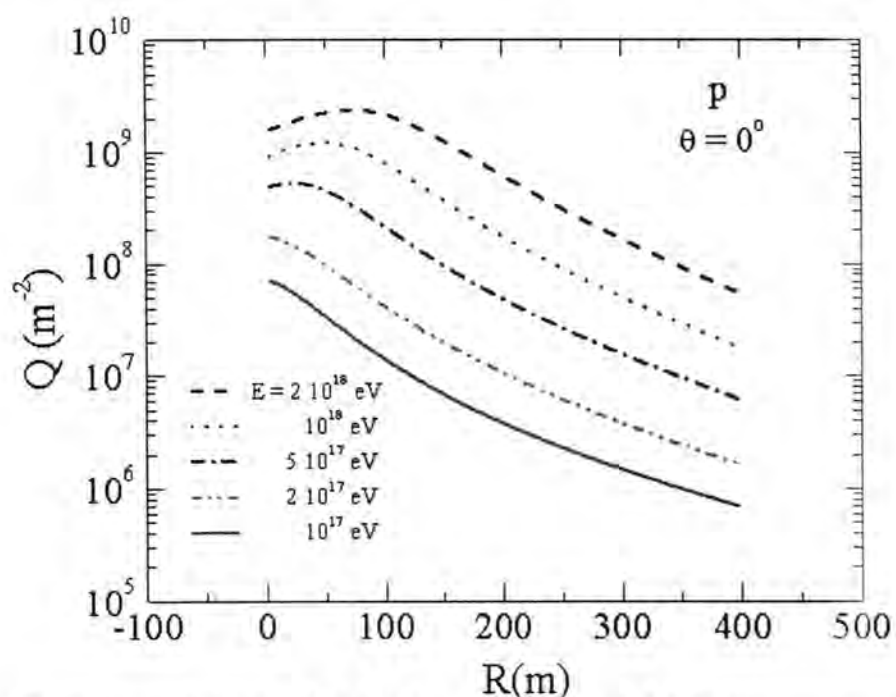


Figure -3: Extrapolation of the Cherenkov light LDF parameterization at energies 10^{17} , $2 \cdot 10^{17}$, $5 \cdot 10^{17}$, 10^{18} and $2 \cdot 10^{18}$ eV with the help of Eq.(1).

CONCLUSION

On the basis of simulated events for primary protons with CORSIKA code is obtained the lateral distribution function of atmospheric Cherenkov light in extensive air showers for configuration of the Tunka-25 EAS array at the highest energies $E \geq 10^{16}$ eV. Using results of this simulation we obtained the parameters of lateral distribution function of the Cherenkov radiation as a functions of the primary energy for primary protons. The extrapolation of the Cherenkov light LDF parameterization of the obtained data with CORSIKA program at the energy range 10^{16} - $2 \cdot 10^{18}$ eV is obtained.

The main advantage of the given approach consists of the possibility to make a library of LDF samples which could be utilized for analysis of real events which detected with the ultrahigh energy EAS arrays and reconstruction of the primary cosmic rays energy spectrum and mass composition.

REFERENCES

1. Engel R. Very high energy cosmic rays and their interactions // Nucl. Phys. B. Proc. Suppl. 151, : 437-461 (2006).
2. Giller M., Stojek H., Wieczorek G. Extensive air shower characteristics as functions of shower age // Int.J.Mod.Phys. A., 20, (29) : 6821-6824 (2005).
3. Ivanov A.A., Knurenko S.P. Analysis of the energy estimation algorithm of UHECRs detected with the Yakutsk array // Proc. 28th ICRC, Tsukuba, July 31-Aug. 7 : 385-388 (2003).
4. Shinozaki K., Chikawa M., Fukushima M. et al. Chemical composition of ultra-high energy cosmic rays Observed by AGASA // Proc. 28th ICRC, Tsukuba, July 31-Aug. 7: 401-404(2003).
5. Bellido J., Belz J., Dawson B. et al. Anisotropy studies of ultra-high energy cosmic rays as observed by the High Resolution Fly's Eye (HiRes) // Proc. 27 ICRC, Hamburg, 7-15 Aug., : 364-366(2001).
6. Unger M., Pierre Auger Collaboration , Composition Studies with the Pierre Auger Observatory // www.arXiv: astro-ph/0902.3787(2009).
7. Budnev N.M., Chvalaev O.B., Gress O.A. et al. Tunka-133 EAS Cherenkov Array: Status of 2007 // www.arXiv: astro-ph/0801.3037(2008).
8. Nikolsky S.I. Cherenkov detectors in cosmic rays studies // Nucl. Instrum. Meth. Phys. Res. A., 248: 214-218(1986).
9. Fomin Yu.A., Khristiansen G.B. Study of the longitudinal development of individual EAS inferred from the Cherenkov light pulse shape: method and results // Nucl. Instrum. Meth. Phys. Res. A., 248, : 227-233(1986).
10. Heck D., Knapp J., Capdevielle J.N. et al. CORSIKA: A Monte Carlo Code to Simulate Extensive Air Showers. Report FZKA 6019. Forschungszentrum Karlsruhe. 90 p., (1998).

11. Heck D., Engel R. Influence of low-energy hadronic interaction programs on air shower simulations with CORSIKA // Proc. 28th ICRC, Tsukuba, July 31-Aug. 7, : 279-282 (2003)
12. Ostapchenko S. QGSJET-II: Towards reliable description of very high energy hadronic interactions //Nucl. Phys. B. Proc. Suppl.,151,:143-146 (2006).
13. Budnev N., Chernov D., Galkin V. et al. Tunka EAS Cherenkov array - status 2001 // Proc. 27 ICRC, Hamburg, 7-15 Aug., : 581-584 (2001).
14. Alexandrov L., Mavrodiev S.Cht., Mishev A. Estimation of the primary cosmic radiation characteristics // Proc. 27 ICRC, Hamburg, 7-15 Aug. : 257-260 (2001).
15. AL-Rubaiee A.A., Gress O.A., Kochanov A.A. et al. Parametrization for Cherenkov light lateral distribution function in Extensive Air Showers // Proc. 29 ICRC, Pune, India, 03-10 Aug. Tata Institute of Fundamental Research, Mumbai, 6, : 249-252 (2005).

Effect of Structural Properties Variation on the Ethanol Sensing of ZnO Thin Films

Ali Jasim Mohammed

Department of Physics, College of Science, Al-Mustansiriya University

الخلاصة

ان تحليل شكل الخط الناتج عن طريق حيود الاشعة السينية يعطي فكرة واضحة عن الخصائص التركيبية الدقيقة وذلك بحساب الحجم الحبيبي , التعريض , معامل الترابط ومعامل شكل الخط الناتج . ان هذه الدراسة تتضمن تحليل شكل القمة الناتجة وخصوصا للمستوي التفضيلي (002) وبأسماء مختلفة لغشاء اوكسيد الزنك (ZnO) وتأثيرها على قابلية التحسس لابخرة المواد الكيميائية والمعتمدة على دراسة تحليلية للتعريض الحاصل في القمم باتباع طريقة التعريض التكاملي والتي من خلالها يمكن حساب حجم التشاكة , كثافة الانخلاعات والاجهاد الحاصل داخل المادة . من خلال مقارنة النتائج لتقنية حيود الاشعة السينية والتحسس لبخار الايثانول ولعدة اسماء تبين ان هنالك علاقة تربط احدهما الاخرى , فزيادة سمك الغشاء ومع زيادة تركيز الايثانول حصلت زيادة لجميع الخصائص التركيبية انفة الذكر , وكذلك زيادة في تيار التحسس وبالنسبة للتحسس حصلت زيادة مع السمك ونقصان مع التركيز . من ذلك يتبين ان معدل الحجم الحبيبي يؤدي الى تضاول حدود الحبيبات والتي تقود الى انخفاض حاجز الجهد بين الحبيبات مما يسمح لعبور حاملات الشحن والتي تؤدي الى تنامي تيار التحسس والتحسسية .

ABSTRACT

The microstructure characterization by X-ray line profile analysis is possible for determination of crystallite size , broadening (integral breadth), texture coefficient and shape factor . This study presents the X-ray diffraction peaks shape analysis and their broadening of ZnO thin films affected the chemical vapor sensing depending on the analysis of broadening of the peaks by integral breadth method which gives the coherent domain size, dislocation density and micro-strain present in the material . The comparable results from the X-ray techniques and ethanol sensing method with different thicknesses are related each other . For preferred orientation (002) with increasing ethanol concentration , increasing in thickness yields to increase all the previous structural properties and the measured ethanol sensing current will increase also and the sensitivity will increase with thickness and decreased with vapor concentration . The average grain size increasing , decreased the grain boundaries leads to decrease the barrier between the grains , and crossing this barrier by the charge carriers will be allowed and the sensing current , sensitivity will be grown .

Keyword : line-profile analysis , structural properties , chemical sensing .

INTRODUCTION

ZnO is one of the few metal oxides which can be used as a transparent conducting oxide. It has some advantages over other possible materials such as In_2O_3 , or SnO_2 due to its unique combination of interesting properties: non-toxicity, good electrical, optical and piezoelectric behavior (1) . It has good electrical and optical properties, in combination with their large bandgap, abundance in nature and absence of toxicity (2) . The properties exhibited by ZnO thin films depend on the non-stoichiometry of the films, resulting from the presence of oxygen vacancies and interstitial zinc (3) . It can be widely used in various applications such as light-emitting diodes (LEDs), flat-panel displays, and solar cells (4).

ZnO is a low cost and abundant material and with a band gap of 3.3 eV it shows an excellent transparency for the entire visible spectrum. Low resistivity and highly transparent layers have been deposited with a variety of deposition methods such as metal organic chemical vapor deposition,(5) laser ablation,(6) spray

pyrolysis,(7) the sol-gel technique,(8) and sputtering.(9) The electrical conductivity of ZnO is controlled by intrinsic defects, i.e., oxygen vacancies(10) and zinc interstitials,(11) which act as n-type donors.

The mechanism of gas or chemical sensing based on the reduction and oxidation (redox) reactions with gas species caused to change the electrical conductance .(12) The effect of grain boundary in the polycrystalline thin film metal oxide sensors was studied and showed that it limits the repeatability and long term stability(13),and the crystalline structure also can be affected the sensitivity of the chemical sensor(14,15) The gas sensing depending on the variation of resistivity of ZnO thin film was studied by (M. Schuisky,et. al.)(16), the measured values showed that sensitivity was extremely high for ultrathin ZnO films .

MATERIALS AND METHODS

ZnO films were prepared on glass substrates by a homemade spray pyrolysis system. The different molarities of spray solution (0.5, 0.6 and 0.7)M of zinc chloride ($\text{ZnCl}_2 \cdot 2\text{H}_2\text{O}$) were dissolved in distilled water and the solution was carried by the compressed air as a carrier gas then fed into a spray nozzle. The flow rate of solution was 10ml/min flows from a 0.5mm diameter nozzle at a distance of 25cm to the substrate. The substrate temperature was kept constant at (350°C). The single spraying time was (5sec) with different number of sprays , the thickness of samples are (0.94 , 1.026 and 1.21) μm respectively .

Polycrystalline ZnO thin films show a preferred orientation in the (002) direction perpendicular to the substrate . This plane is strongly dependent on the deposition conditions , diffraction patterns preliminary recorded on the film indicated that all investigated films were polycrystalline . Diffraction pattern was recorded for a range of 2θ from 10° to 60° at 2° glancing angle . The film was crystallized in the wurtzite phase and presents a preferential orientation along the c-axis , the strongest peak observed at $2\theta = 34.3^\circ$ ($d = 0.260 \text{ nm}$) .

The measurements of chemical sensing was carried out by measuring the variation in (resistivity or conductivity) through measuring the output current resulting from exposing the film surface to the chemical vapor (ethanol)carried by the nitrogen gas . Ethanol was evaporated by heating it to 38°C , the temperature was recorded by a k-type thermocouple (XB 9208B). The bias voltage was supplied by (FARNELL E350) power supply. The output current was recorded by (Tektronix CDM 250) multimeter , and the carrier gas flow rate was measured by the flow meter (0 – 1 Ltr/min) .

RESULTS AND DISCUSSIONS

The line profiles of the reflections of various planes during X-ray diffraction are characteristic of the state of the material. The shapes of line profiles are also affected by instrument and sample shape, which is referred to as instrumental broadening. This instrumental broadening needs to be eliminated to obtain broadening exclusively due to metallurgical effects. Once such data is obtained, estimation of coherent domain size, micro strains within these domains, density of dislocation ,

Coherent domain size (D) is the size of coherently diffracting region within a grain , representing fault free region between dislocations (of the order of 100–1000 Å), higher the ρ lower the D . Depending on the XRD resultant patterns as in figure (1) we can calculate the average grain size . Figure (2) shows the dependent of the average grain size (g) (evaluated by using well known Scherrer's equation below) with the thickness :

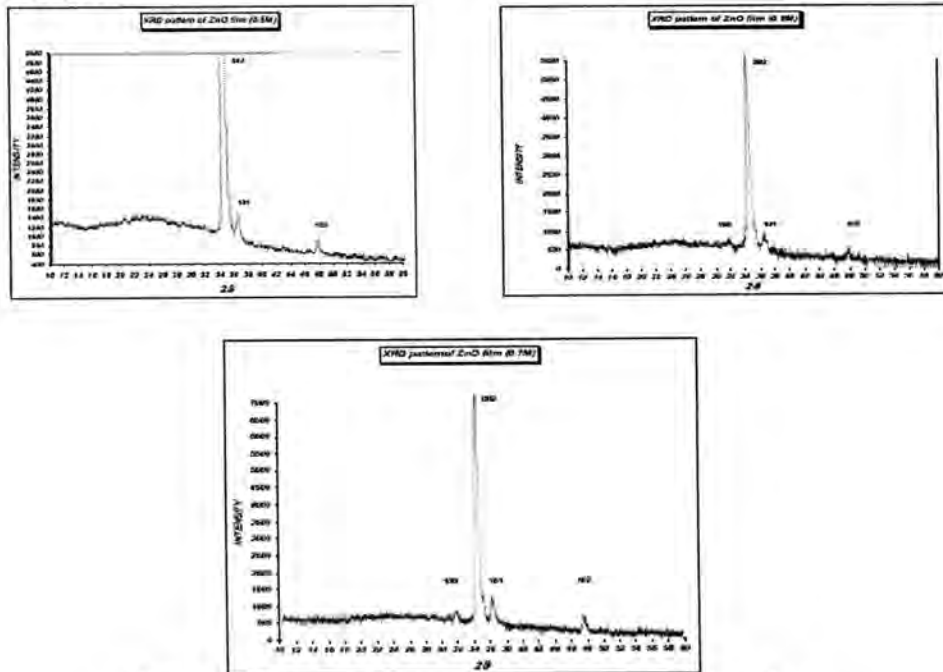


Fig.-1: XRD patterns of the prepared samples .

$$g = \frac{0.9\lambda}{\Delta \cos \theta} \dots \dots \dots (1)$$

Where λ is the incident wavelength , Δ is the full width at half maximum of the line and θ is the diffracted angle . Increasing in thickness caused to increase (g) , while the coherent domain (D) and the strain (ϵ) could be calculated from the plot of $(\beta \cos \theta / \lambda)^2$ vs $(\sin \theta / \lambda)^2$ follows (17):

$$\text{Intercept} = 1/D^2$$

$$\text{Slope} = 16 \epsilon^2$$

when the corrected broadening (β) could be calculated from the relation (17):

$$\beta = \Delta - (b^2 / \Delta) \dots \dots \dots (2)$$

b is the instrumental broadening could be evaluated from most often the original relation (17):

$$b^2 = u \tan^2 \theta + v \tan \theta + w \dots \dots \dots (3)$$

where u , v and w are constants obtained from the second polynomial equation find out from the plot of (b^2) vs $\tan (\theta)$. The observed broadening in X-ray line profiles is due to the D and ϵ present in the material. Once the D and ϵ are determined from the broadening, the dislocation density can be estimated(17):

$$\rho_D = \frac{3\eta}{D^2} \dots \dots \dots (4)$$

where ρ_D is the domain density and $\eta = 1$

$$\rho_\epsilon = 2k\epsilon^2 / b^2 \dots \dots \dots (5)$$

where : ρ_{ε} is the strain density , $k = 2\sin \theta/\lambda$ and ε is a micro strain
then :

$$\rho = \rho_D \rho_{\varepsilon} \dots\dots\dots(6)$$

Increasing the grain size caused to decreased the coherent domains , this effect will be shown in the figure (3) . Due to dislocations, micro strain (\square) is present between the atomic planes (of the order of 10^{-3}) , figure (4) shows the effect of grain size on the strain , the micro strain gradually decreased up to 130 Å grain size and then sharply increased for grains of grater sizes , while the dislocation density decreased with the same order of the strain as illustrated in the figure (5).

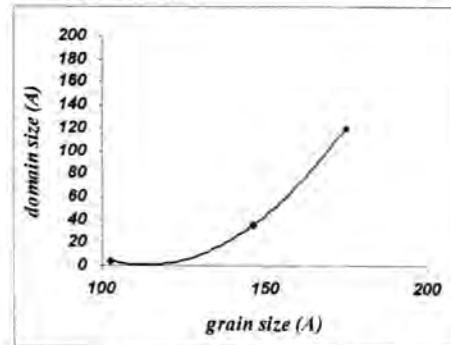
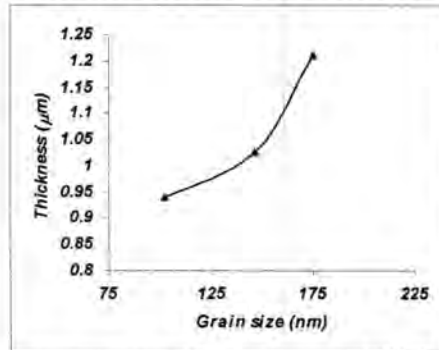


Fig.-2: Thickness vs grain size .

Fig.-3: Effect of grain size on the domain size

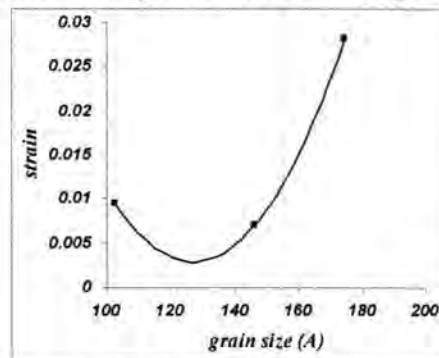


Fig.-4: the effect of grain size on the strain .

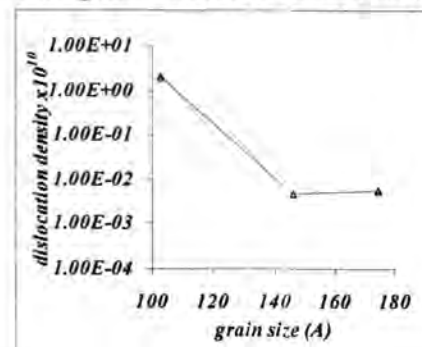


Fig.-5: dislocation density as a function
Of grain size .

The sensing current of the ethanol vapor depending on the grain size , for smaller grains (below 150 Å) clearly increased at 5% concentration , but with a lower concentrations (3%) , the current will increased with a few (μA) , while for grains greater than 150 Å , saturated sensing current appeared for higher concentrations , but for lower concentrations , higher increasing in the current will be caused as shown in the figure (6) .

The sensitivity is defined as the relative variation of the resistance of the sensitive thin film in per cent per ppm of applied gas concentration (12):

$$S = [(R_g - R_a) / nR_a] \cdot 100\% \dots\dots\dots(7)$$

Where R_g , R_a are the electric resistance of the film in presence of gas and in air , n is the density of ambient air (almost 1) . Our results of sensitivity depends on the current with an applied voltage of (3 volts) , the results show that no effect of grain size at higher concentrations , while for lower concentrations , increasing in grain size (g) , increasing in sensitivity (S) as shown in the figure (7)

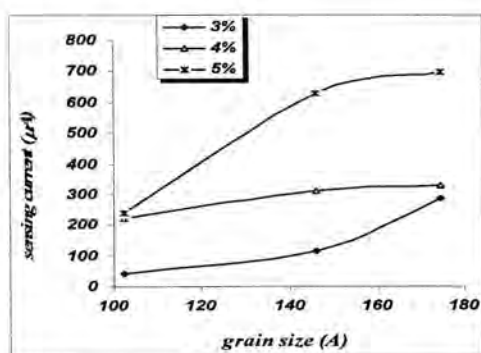


Fig. -6: sensing current vs grain size .

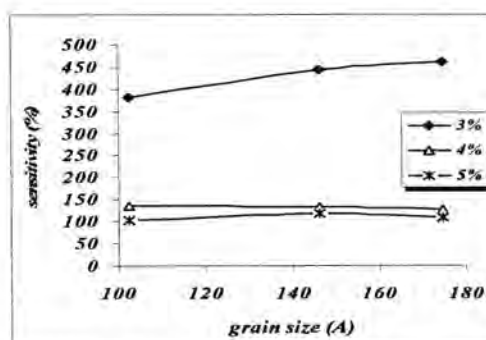


Fig. -7: the sensitivity vs grain size .

The effect of thickness on the domain density shown in the figure (8) , the domain density was decreased with increasing thickness .The sensitivity was increased with increased domain size up to 50 Å and also with the increased of dislocation density as shown in figures (9 , 10) respectively .

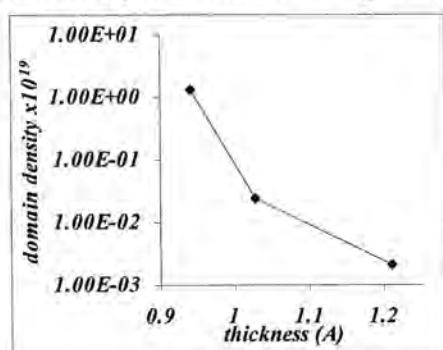


Fig.-8: the effect of thickness on the domain density .

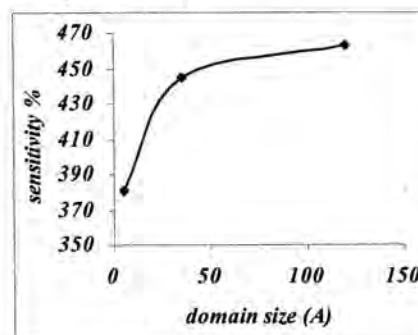


Fig.-9: effect of domain size on the sensitivity .

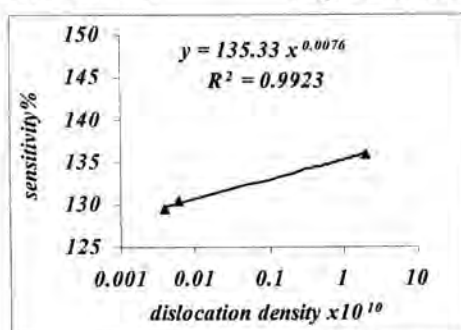


Fig.-10: sensitivity as a function of dislocation density .

We can conclude:

The diffraction pattern gives information about imperfections in the material i.e. dislocations, small crystallite (domain) size, microstrains within the grains due to small crystallite size and strain due to dislocations and stacking faults. The analysis of the shape of the peaks for obtaining information about the material is referred to as line profile analysis (LPA). Dislocation density (ρ_D) is an important material property, which gives the length of the dislocations present per unit volume (m/m^3) in the material. It has a strong influence on the other properties like optical , electrical , thermal and sensing properties . X-ray line broadening technique has been used widely to estimate the dislocation density. But use of this technique requires careful experimentation , sample preparation and calculations.

REFERENCES

1. Seeber W.T., Abou-Helal M.O., Barth S., Beil D., Höche T., Afify H.H., and Demian S.E., "Transparent semiconducting ZnO:Al thin films prepared by spray pyrolysis", *Mater. Sci. Semi. Proc.* 2 :45 -55(1999).
2. Jeong S.H., Lee J.W., Lee S.B. & Boo J.H. "Optical and electrical properties of Al doped ZnO films prepared by RF magnetron sputtering" *Thin Solid Films* 435,78 (2003).
3. Major S., Chopra K.L. "In-doped ZnO films as transparent electrode for solar cells" *Sol. Energy Mater.*, 17, 319 (1998).
4. Li X., Yan Y., Gessert T.A., DeHart C., Perkins C.L., Young D., and Coutts T.J., "P-type ZnO thin films formed by CVD reaction of Diethyl Zinc and NO gas" *Electrochemical and Solid State Letters*, 6(4):C56-C58(2003).
5. Wang A., Dai J., Cheng J., Chudzik M.P., Marks T.J., Chang R.P., and Kannewurf C.R. "Charge transport optical transparency, microstructure & processing relations in transparent conductive Indium-Zinc Oxide films grown by low pressure metal-organic chemical vapor deposition" *Appl. Phys. Lett.* 73, 327 (1998).
6. Ma X.M., Yang X.T., Wang C., Yang J., Gao X.H., Liu J.E., Jing H., Du G.T., Liu B.Y., and Ma K. "ZnO thin film grown on glass by metal-organic chemical vapor deposition" *Nanoelectronics Conf. 2nd IEEE* :833-835(2008).
7. Studenikin S.A., Golego N. & Cocivera M. "Carrier mobility and density contributions to photoconductivity transients in polycrystalline ZnO films" *J. Appl. Phys.*, 87, 2413 (2000).
8. E. Jimenez Gonzalez A.E., Jose A., and Suarez Parra R. "Optical and electrical characteristics of Al-doped ZnO thin films prepared by sol-gel technique" *J. Cryst. Growth*, 192, (3-4) :430-438(1998).
9. Minami T. "Transparent and conductive multicomponent oxide films prepared by magnetron sputtering" *J. Vac. Sci. Technol.*, A17, 4, 1765(1999).
10. Schoens J., Kanazawa K., and Kay E., "Band and hopping conduction in high-resistivity ZnO" *J. Appl. Phys.*, 48, 6, 2537(1977).
11. Minami T., Sato H., Nanto H., & Takata S. "Optical properties of Al-doped ZnO thin films prepared by RF magnetron sputtering" *Jpn. J. Appl. Phys. Part 2*, 24, 8, L781 (1985).
12. Marian S., Tsiulyanu D., Marian T., and Liess H.D. "Chalcogenide-based chemical sensors for atmospheric pollution control" *Pure Appl. Chem.* 73, 12, (2001).
13. Ruhland R., Becker Th., and Muller G., "Gas kinetic interaction of nitrogen oxides with SnO₂ surfaces", *Sens. Actuators*, B50, 85(1998).
14. Jin Z., Zhou H.J., Jin Z.L., Savinell R.F., & Liu C.C. "Electrical & CO gas sensing properties of ZnO-SnO₂ composites" *Sens. Actuators, B: Chem.* 52, 188(1998)(2003).
15. Schuisky M., Elam J.W. & Georg S.M. "In situ resistivity measurements during the atomic layer deposition of ZnO & W thin films" *Appl. Phys. Lett.* 81, 180 (2002).
16. Kapoor K., Lahiri D., Rao S., Sanyal T., & Kashyap B. "X-ray diffraction line profile analysis for defect study in Zr-2.5 % Nb material" *Bull. Mater. Sci.*, 27, 1:59-67(2004).

Study The Effect of Lightness on The Good Vision of Written text in the class room

¹ Ali A. D. Al-Zuky, ² Salema S. Salman and ¹ Ahlam M.Kadhum

¹ Physics Deptment , College of Science/ Al-Mustansiriyah

² Department of Clinical Laboratory Science/ College of Pharmacy/ Baghdad University

الخلاصة

ان مدى النصوص والتباين تعتبر من خصائص الضوء التي تلعب دور رئيسا في وضوح الرؤية البصرية . تتميز خاصية النصوص بين الإضاءة العالية أو العتمة للنص المكتوب على السبورة حيث يمتلك اللون الأسود نصوص واطى ويمتلك اللون الأبيض نصوص عالي ، اما خاصية التباين فهي تمثل النسبة بين إضاءة الرمز (النص) والخلفية (السبورة) . فإذا كان هنالك تجانس في توزيع شدة إضاءة قاعة الدرس (إضاءة منتظمة) فان قيم التباين للنص المكتوب على السبورة تتأثر بالمسافة بين الكاميرا والسبورة فعند المسافات البعيدة تقل قيم التباين للنصوص بسبب تكون غشاوة حول النص بزيادة المسافة بين الكاميرا والسبورة . لذا توجهنا في هذه الدراسة الى اقتراح أساليب متعددة لحساب التباين في صور النص المكتوب على السبورة لشروط الإضاءة المختلفة . حيث تم دراسة النصوص والتباين لصورة النص والنتائج بينت ان الطرائق المقترحة لحساب التباين بالاعتماد على نقاط الحافات ذات كثافة عالية في تحديد التباين لصورة النص ومن خلال هذه النتائج يمكن ملاحظة ان تباين صورة النص يقل بزيادة المسافة بين الكاميرا والسبورة .

ABSTRACT

The range of brightness and contrast is one of the light characteristics that plays a major role in the resolution of optical vision. Brightness property discriminate between high light or darkness of written text on the whiteboard. The black color has a low brightness and the white color has a high contrast. However, contrast property represents the rate between lighting the symbol (The text) and the background (The Whiteboard). If there is a consistency in the light intensity distribution of classroom (uniform lighting), the contrast values of written text on the whiteboard is affected by the distance between camera and whiteboard. In case of far distances, contrast values will decrease due to the blur appearing around the text by increasing the distance between camera and whiteboard. Hence, we aimed, in this study, to suggest various methods to calculate contrast in the images of written text on the whiteboard in different lighting conditions.

Brightness and contrast of text image were examined. Results shows that the suggested methods to calculate contrast edges points were enjoying high efficiency in specifying the contrast of text in mage. We may not, through these results, that text image contrast decreases by increasing the distance between camera and whiteboard.

INTRODUCTION

Light Quality is the most important characteristic of light for the photographer for it sets the mood of a shot. Quality of light breaks down into two types hard or soft light. Hard light throws distinct shadows. It comes from a point light source such as the sun or an electronic flash. It is a harsh light and often can cause the subject if it is a person to squint or need to put on sun glasses. Soft light is the opposite and comes from a reflected source or a broad source. It is often indirect light and is

frequently found in the shade as light that reflects into the shade from the surroundings. Light quality is affected mostly by change in subject or camera position or the use of reflectors or fills flash. Hard light can give a dramatic effect strong, bold or angry (1) . A soft light is used for more subtle effects. Hard light can further be broken down according to its direction where it might come from the front, side, back or top of the subject. The direction of light will determine where shadows will be. By looking at the shadows in a picture, you can determine where the light comes from. This direction, more than any other light feature will affect the look of a picture. Directions of light are given from the subject's point of view, thus back light points into the camera lens. There are no rules about which direction to use, the main reason for study of them is to control their effect on our subject. Front light is used to show detail. Few good outdoor shots use this type of light because it eliminates texture (1,2) . This type of light is what comes out of a flash attachment and evenly lights our subject. It is the worst of the hard light types and would be better as soft light if a choice is possible. Side light emphasizes texture and shape. A strong side light from a window or a sunset causes long shadows and a dark side and light side relationship on a subject. To meter such a light the photographer may want to average a close up meter reading of both the bright side and the dark side. Backlight softens the quality of the light as the subject gets mostly reflected light on its surface. If the light is placed directly behind the subject a rim light can be the result. This is the most dramatic type of light. This type of light does a good job of separating the subject from the background but requires careful metering. If the meter sees mostly the bright light in the background the exposure will be adjusted lower to compensate which will result in an underexposed subject who has less light falling on it from the reflected light reaching it from the front (3,4) . Many former studies concerned with the illuminance and contrast effect on the image quality:

- **Eli Peli et.al** (5) conducted a study on 1996 for contrast enhancement through the changes in luminance intensity and spatial frequency. The study adopted contrast sensing over the threshold by using contrast analogy.
- **William B. et.al** (6).suggested on 2003 an algorithm to enhance image in night scenes by a technique of making the images taken in the day light as if they were taken in night images through decreasing the contrast and brightness for all of the image, adding a distortion to the image and present the night image characterized with high noise, loss in optical acuity along with distortion size taking place in it

visual task generally becomes easier with increased contrast. too much contrast causes glare and makes the visual task much more difficult. You can reduce glare or luminance ratios by not exceeding suggested light levels and by using lighting equipment designed to reduce glare. A louver or lens is commonly used to block direct viewing of a light source. Indirect lighting, or uplighting, can create a low glare environment by uniformly lighting the ceiling (12) .

Contrast

In this section we will mainly be concerned with the lighting of objects. Diffuse illumination, that is light coming equally from all directions will enable an object to be seen but will not reveal the form or texture because of a lack of shadows. The gradation of reflected light over the surface of an object reveals its three-dimensional nature and texture can be expressed or expressed by applying light at an appropriate angle (13) .

The degree of diffusivity in a space can be expressed as the vector-scalar ratio with a value between 1.2 and 1.8 giving satisfactory modeling of faces. If an unnatural emphasis is required, that is effects variously described on a scale ranging from subtle to dramatic, the ratio between object and display illuminance is set out in the table (1) (14) .

Table -1: explain the ratio between objective and display illuminance

Display Effect	Objective display illuminance ratio	Subjective apparent Brightness ratio
Subtle	5 : 1	2.5 : 1
Moderate	15:1	5:1
Strong	30:1	7:1
Dramatic	50:1	10:1

It is defined elsewhere in terms of the luminance contrast ,C, given by (13):

$$C = \frac{L_t - L_b}{L_t + L_b} \quad (2)$$

Where L_t is the target object luminance and L_b is the background luminance

Uniformity of Illuminance

The uniformity of illuminance is a quality issue that addresses how evenly light spreads over a task area. Although a rooms average illuminance may be appropriate, two factors may compromise uniformity (4) :

- * improper fixture placement based on the luminaries spacing criteria (ratio of maximum

Brightness

Another measurement of light is luminance, sometimes called brightness. This measures light leaving a surface in a particular direction, and considers the illuminance on the surface and the reflectance of the surface(10) .

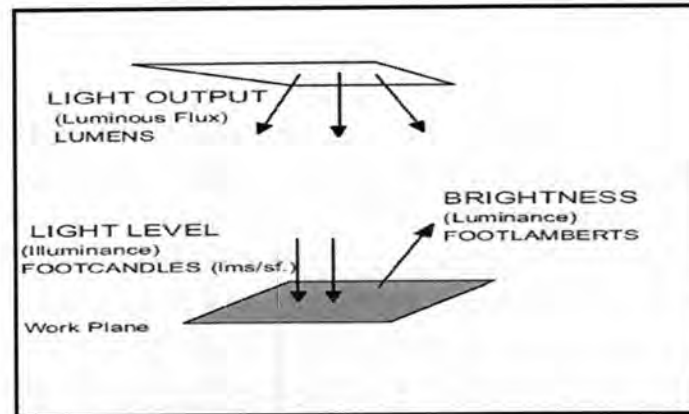


Figure – 1: shows the interaction between light output, light level, and brightness.

Glare

Glare has been previously categorized into disability and discomfort glare. The former gives rise to visual impairment while the latter causes discomfort but no apparent visual impairment. Disability glare is said to be caused by light scatter in the eye causing veiling reflections on the retina. The cause of discomfort glare remains unclear. Recent studies have however challenged the idea that they are two separate phenomena and showed that discomfort glare could be explained by the increase in light scattering in the eye with ageing. The maximum luminance ratio is given by (11) :

$$Luminance = \frac{Luminance_{Source}}{Luminance_{background}} \quad (1)$$

to avoid discomfort glare was estimated as 1000:1 for people at the age of 21 and 100:1 for people age 51. Therefore no luminance ratio should exceed this in a persons field of view within a room. Perhaps the most important factor with respect to lighting quality is glare. Glare is a sensation caused by luminances in the visual field that are too bright. Discomfort, annoyance, or reduced productivity can result. A bright object alone does not necessarily cause glare, but a bright object in front of a dark background, however, usually will cause glare. Contrast is the relationship between the luminance of an object and its background. Although the

- **Norman Carver** (7), in 1997 , he explore the relations between blackboard-based and belief network approaches to interpretation problems. In this way we begin to reinterpret the blackboard model, to show how it can be explained in terms of modern AI concepts.
- **Truus de Bruin et. Al.** (8), in 2002 , they design possibilities for an optimum use of daylight. However, a classroom is a difficult space to light with daylight, because of the depth of the classroom and the different tasks which must be performed in it. At the university of Delft research has been done in order to optimize the daylight access by the design of classrooms. In a first step the luminances and illuminances in a number of existent schools were measured. From this, nine possible design models of classrooms have been draw up.
- **Paulsson et .al**(9) in 1980 he proposed A method is presented for quantitative measurements of the glare effect of light scattered, in the ocular media. The contrast sensitivity function is measured with a television display system. A bright light source is introduced into the field of vision, and the resultant decrease in contrast sensitivity is measured.

Quantity of Illumination

Figure (1) shows the interaction between light output, light level, and brightness. Although they are quantitative measures, they directly affect the quality of illumination (9).

Light Output

The most common measure of light output (or luminous flux) is the lumen. Light sources are labeled with an output rating in lumens. For example, a T12 40-watt fluorescent lamp may have a rating of 3050 lumens. Similarly, a light fixtures output can be expressed in lumens. As lamps and fixtures age and become dirty, their lumen output decreases (i.e., lumen depreciation occurs). Most lamp ratings are based on "initial" lumens (i.e., when the lamp has been operated for 100 hours) (5,10).

Light Level

Light intensity measured on a plane at a specific location is called illuminance. Illuminance is measured in foot candles, which are work plane lumens per square foot. You can measure illuminance using a light meter located on the work surface where tasks are performed. Using simple arithmetic and manufacturers' photometric data, you can predict illuminance for a defined space. (Lux is the metric unit for illuminance, measured in lumens per square meter. To convert foot candles to lux, multiply foot candles by 10.76) (9) .

recommended fixture spacing distance to mounting height above task height) .

- fixtures that are retrofit with reflectors or louvers that narrow the light Distribution

Non-uniform illuminance

causes several problems:

- * inadequate light levels in some areas .
- * visual discomfort when tasks require frequent shifting of view from underlit to overlit areas .
- * bright spots and patches of light on floors and walls that cause distraction and generate a low-quality appearance .

Color Rendition

The ability to see colors properly is another aspect of lighting quality. Light sources vary in their ability to accurately reflect the true colors of people and objects. The color rendering index (CRI) scale is used to compare the effect of a light source on the color appearance of its surroundings. A scale of 0 to 100 defines the CRI. A higher CRI means better color rendering, or less color shift. CRIs in the range of 75-100 are considered excellent, while 65-75 are good. The range of 55-65 is fair, and 0-55 is poor. Under higher CRI sources, surface colors appear brighter, improving the aesthetics of the space. Sometimes, higher CRI sources create the illusion of higher illuminance levels. The CRI values for selected light sources are tabulated in table (2) (3) .

Table -2: Typical CRI Values For Selected Light Sources

Source	Typical CRI Value
Incandescent / Halogen	100
Fluorescent	
Cool White T12	62
Warm White T12	53
High Lumen T12	73 – 85
T8	75 – 85
T 10	80 – 85
Compact	80 – 85
Mercury Vapor (clear / coated)	15/50
Metal Halide (clear / coated)	65 /70
High – Pressure Sodium	
Standard	22
Deluxe	65
White HPS	85
Low – Pressure Sodium	

System work (for evaluation of text quality with different lighting and distance)

Adopted in this study, the writing on the blackboard using color of the pen in this study is black (Dry – Eraser) , the text illustrated by using Sony – Digital camera , where the distance between the camera and the whiteboard (100, 200, 300) cm and two lighting different light from the right (Window) and the other from the left (Door) and figure (1) shows the images from the camera. Imaging process was made at 10:00 AM of 14 – 4 – 2009 according The geometry of classroom illuminated in figure (2). where the recorded values of the intensity of lighting, depending on the direction of measurement of detector light detector , figure (3) & (4) shows the difference in the values of the intensity of lighting for both the cases of non – uniform lighting and direction of a detector measuring intensity of light, respectively. As seen from Figure (3) that the values of the intensity of lighting from the right to be the highest in the case of the direction of the detector around the window .

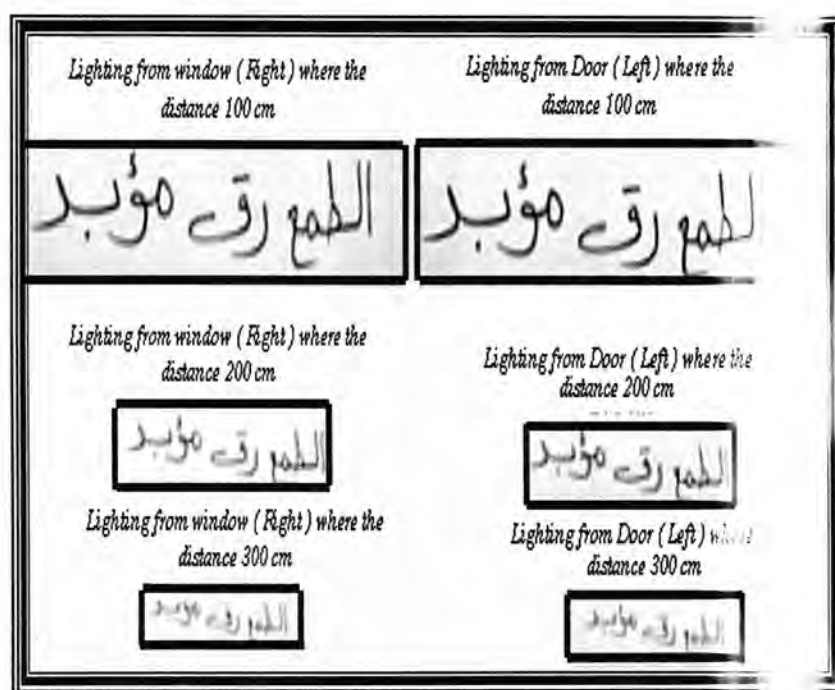


Figure-1: Images of the text written in black for two different lighting conditions (one side lighting from window or door) and at distances are 100, 200, 300 cm

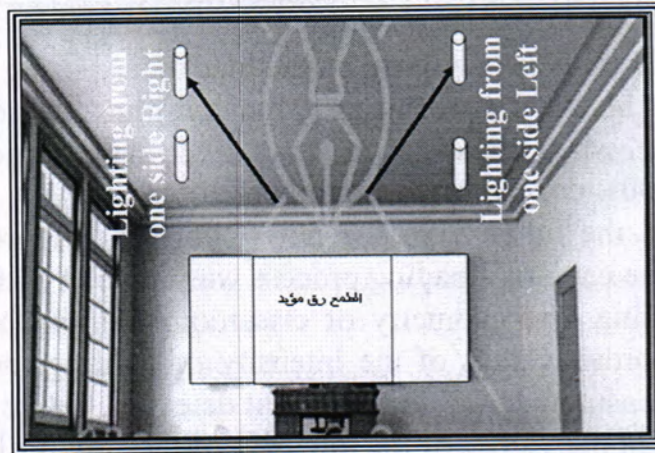


Figure -2: classroom geometry

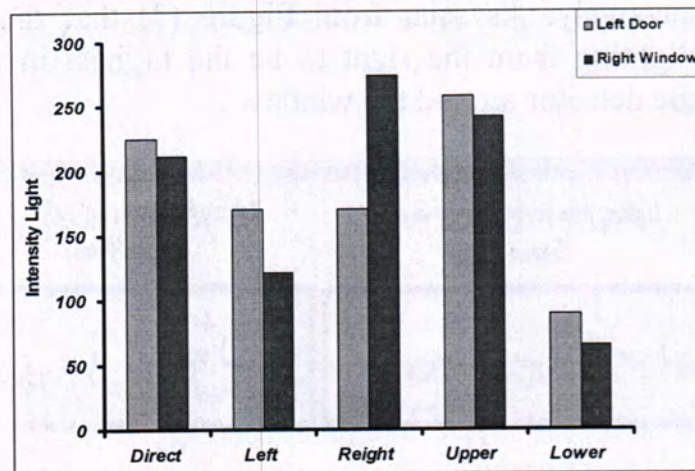


Figure-:3 Represents the difference in illuminance values toward the spotlight for classroom geometry at non uniform lighting

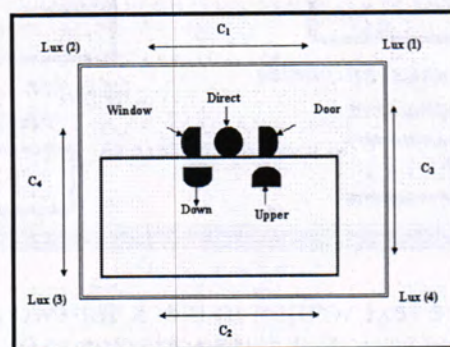


Figure -:4 represents Luxmeter spotlight direction according to classroom geometry

The contrast of the written text is a measure of the acuity visual, texts of the high contrast of the visual point of view plain , text of the low contrast is

difficult to see optical . contrast can be defined as the ratio between text and illumination lighting the whiteboard as the relationship (1)

$$c = \frac{Lux_{max} - Lux_{min}}{Lux_{max} + Lux_{min}} \quad (3)$$

By equation application (3) for calculating the contrast from the read device by measuring the intensity of the lighting direction of the detector, as shown in table (3, 4) the lighting of the left and right respectively.

Lux (1)	Lux(2)	Lux(3)	Lux(4)	Lux (average)
234	226	207	232	24.75
C1	C2	C3	C4	
0.0173	0.056	0.004		0.043

Door (Left)

Lux (1)	Lux(2)	Lux(3)	Lux(4)	Lux (average)
161	171	182	168	170.5
C1	C2	C3	C4	
0.03	0.04	0.02		0.03

Window (Right)

Lux (1)	Lux(2)	Lux(3)	Lux(4)	Lux (average)
154	162	199	165	170
C1	C2	C3	C4	
0.025	0.093	0.034		0.1

Upper (roof)

Lux (1)	Lux(2)	Lux(3)	Lux(4)	Lux (average)
273	261	243	255	258
C1	C2	C3	C4	
0.022	0.024	0.034		0.035

Lower (Floor)

Lux (1)	Lux(2)	Lux(3)	Lux(4)	Lux (average)
89	100	87	80	89
C1	C2	C3	C4	
0.058	0.04	0.053		0.069

Table - 3 : illuminance and contrast values in case of illumination from left classroom (non – uniform darkness) We note the value of illumination from the door and roof is highest Direct

Lux (1)	Lux(2)	Lux(3)	Lux(4)	Lux(average)
197	236	222	192	211.75
C1	C2	C3	C4	
0.09	0.072	0.012	0.03	

Door (Left)

Lux (1)	Lux(2)	Lux(3)	Lux(4)	Lux(average)
116	122	118	130	121.5
C1	C2	C3	C4	
0.025	0.048	0.056	0.016	

Window (Right)

Lux (1)	Lux(2)	Lux(3)	Lux(4)	Lux(average)
270	300	272	254	274
C1	C2	C3	C4	
0.052	0.034	0.03	0.048	

Upper (roof)

Lux (1)	Lux(2)	Lux(3)	Lux(4)	Lux(average)
218	257	261	233	242.25
C1	C2	C3	C4	
0.082	0.056	0.033	0.007	

Lower (Floor)

Lux (1)	Lux(2)	Lux(3)	Lux(4)	Lux(average)
63	73	64	58	64.5
C1	C2	C3	C4	
0.073	0.049	0.041	0.065	

Table- 4 : illuminance and contrast values in case of illuminated from Right (window)classroom (non – uniform darkness We note the value of illuminane from the window and roof is highest Direct

Contrast Determination Procedures

The contrast of written text was determined by adopting edges points which are specified by (soble operator) for edge detection using upon four procedure : -

1- Contrast Direct

Contrast determination by adopting larger and smaller element of edge elements . Figure (5,6) shows the results of this technique . in case of illuminated from door and window (non – uniform) of classroom , where contrast average plotted as a function of the threshold soble operator. when depending different distance between the camera and whiteboard . We note from the figures ,that increasing the distance leads to decrease in

contrast . Also we may note that by increasing the threshold operator the calculated contrast increases

of soble

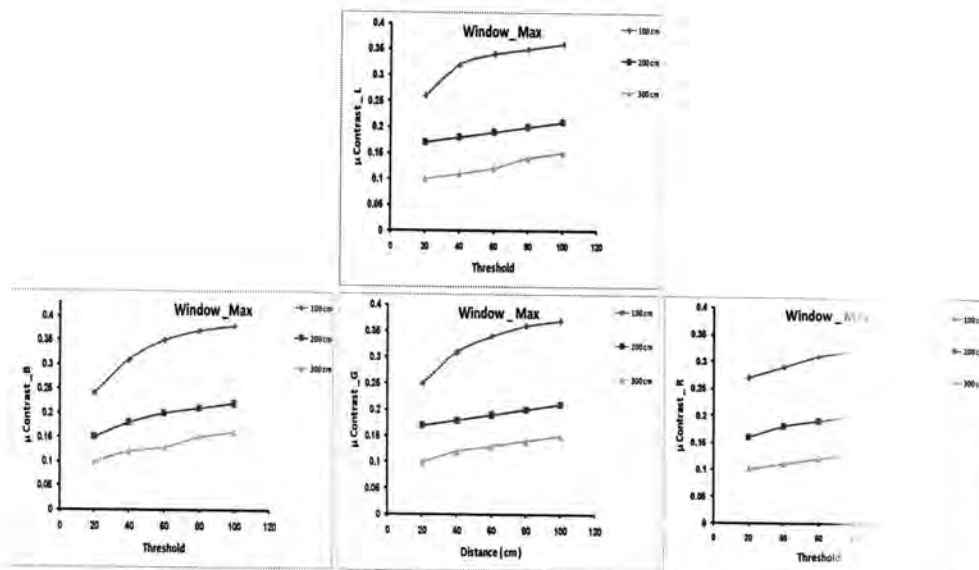


Figure-5 : Direct contrast technique in condition of classroom from Right (window)for the color band and lighting component, using different distance (100,200, 300)cm

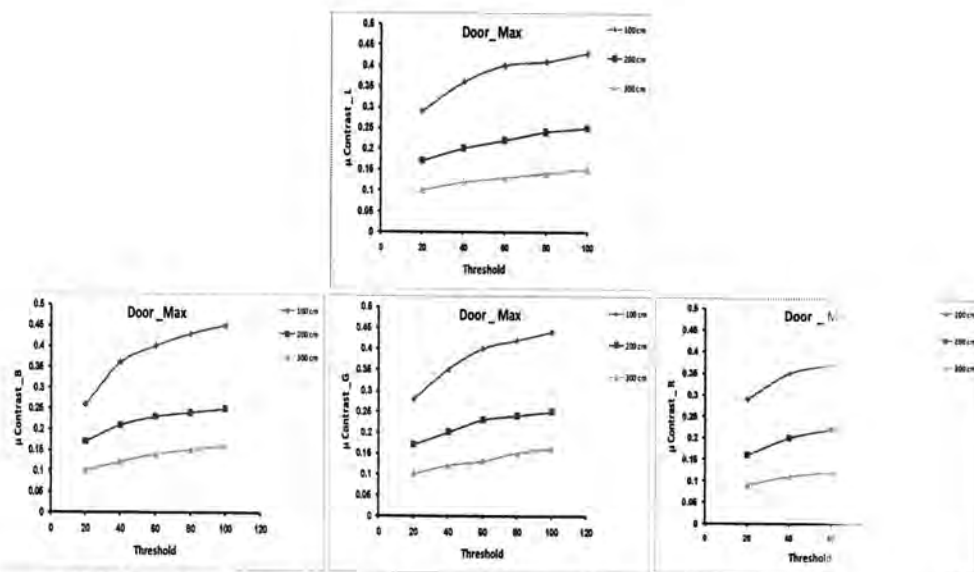
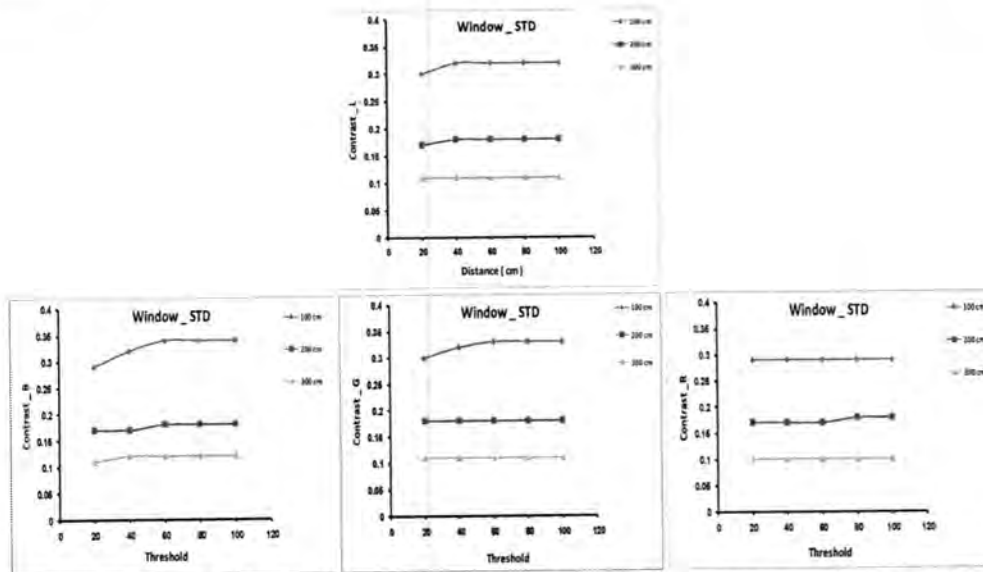


Figure- 6: Direct contrast technique in condition of classroom from Left direction (Door)for the color band and lighting component, using different distance (100,200,300)cm

- 2- Contrast Calculation by adopting statistical characteristics of edges points (standard deviation and average). Figure (7,8) shows the results of this technique for the three color bands and lighting compound of written text in two conditions of non - uniform lighting from one side (window or door). Contrast was charted as a function of threshold value of Soble operator when depending different distance (100,200,300)cm between camera and written text in whiteboard increasing the distance leads to decrease in contrast. From the figure, we note that by increasing threshold value of Soble operator the calculated contrast increases.



Figure— 7 : Statistical contrast technique in condition of classroom illuminated from Right (window)for the color band and lighting compound , using different distance (100,200, 300)cm

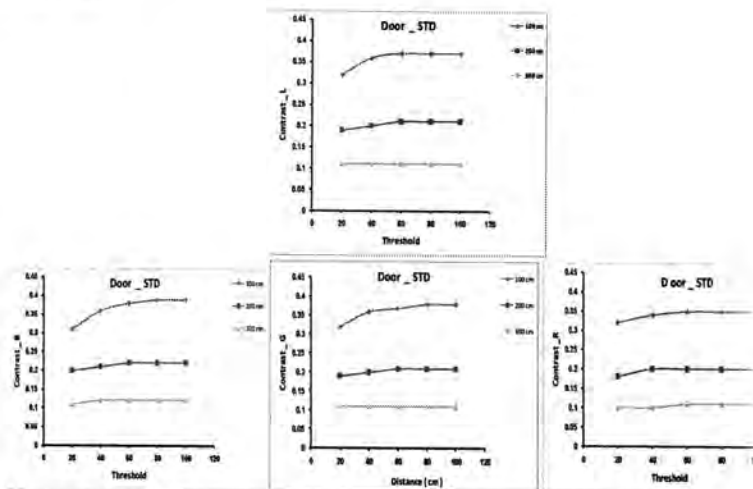


Figure-8 : Statistical contrast technique in condition of classroom from Left direction (Door)for the color band and lighting component, using different distance (100,200,300)cm

- 3- Contrast calculation of edges points using vertical contrast technique. The total elements of the first and third column for the triangular window, except for the column that includes edges element and result showed in figure (9,10), for the three color bands and lighting component of written text in two conditions of non - uniform lighting (full brightness and lighting). Contrast average was charted as a function of threshold value of Sobel operator when depending different distance (100, 200, 300)cm between camera and written text in whiteboard increasing distance leads to decrease in contrast. From the figure, we note that increasing threshold value of Sobel operator the calculated contrast increases.

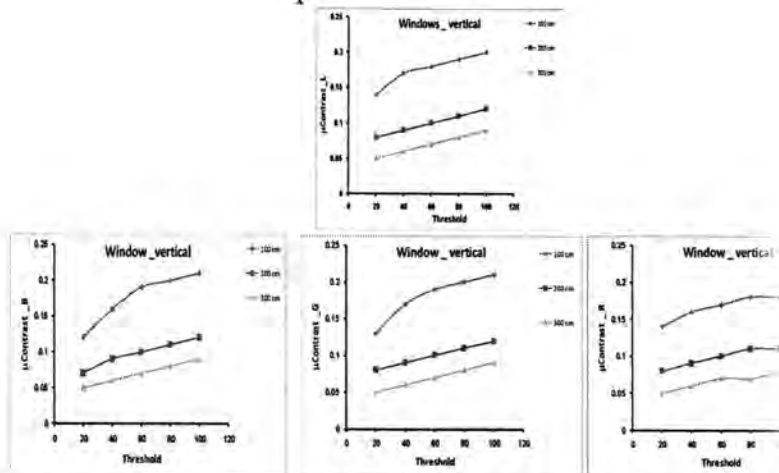


Figure-9 : Vertical contrast technique in condition of classroom from Right (window)for the color band and lighting component, using different distance (100,200, 300)cm

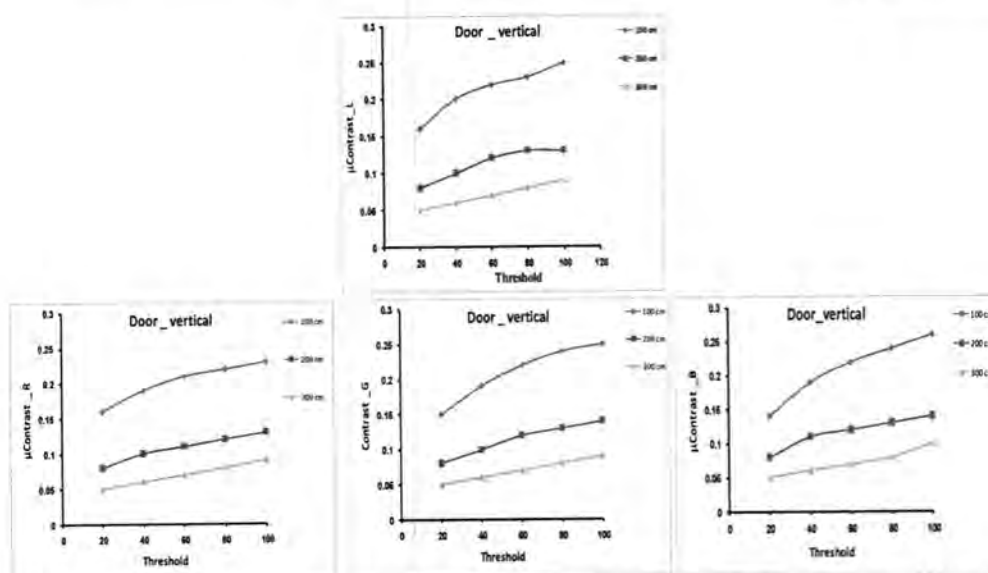


Figure -10 : Vertical contrast technique in condition of classroom illuminated from Left direction (Door)for the color band and lighting compound , using different distance (100,200,300)cm

- 4- Diameter Calculation by adopting edges points. triangular window is set around edges element and, then, the total of elements on the to the bottom of the main diameter. Figure (11,12) shows the results of this technique for the three color bands and lighting compound of written text in two conditions of non - uniform lighting (window or Door lighting). Contrast average was charted as a function of threshold of soble operator, when the distance between camera and written text on the white board (100,200 ,300)cm. We note, form the figures, that by increasing the distance, contrast decrease and by increasing threshold value of Soble operator the calculated contrast increases .

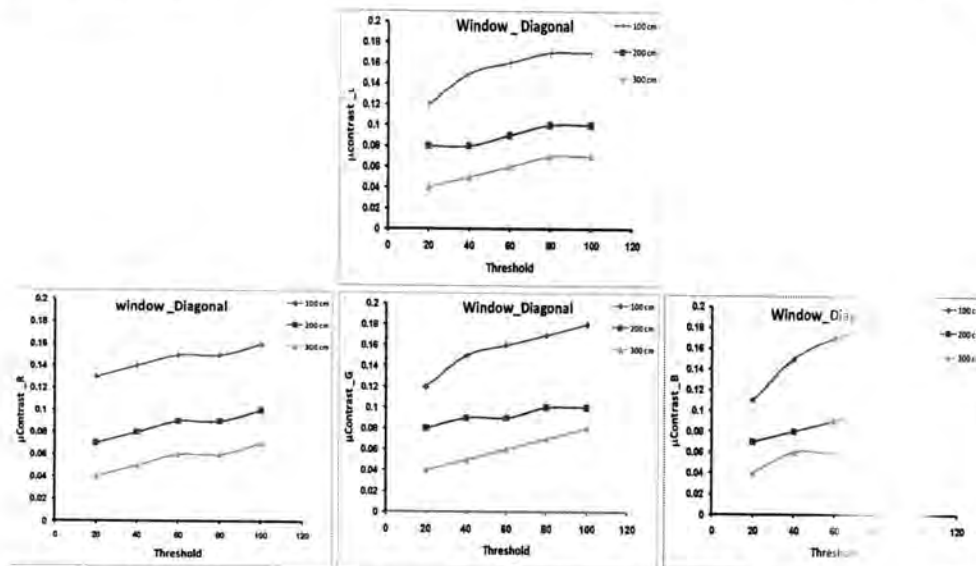


Figure -11 : Diameter contrast technique in condition of room illuminated from Right (window)for the color band and lighting compound , using different distance (100,200, 300)

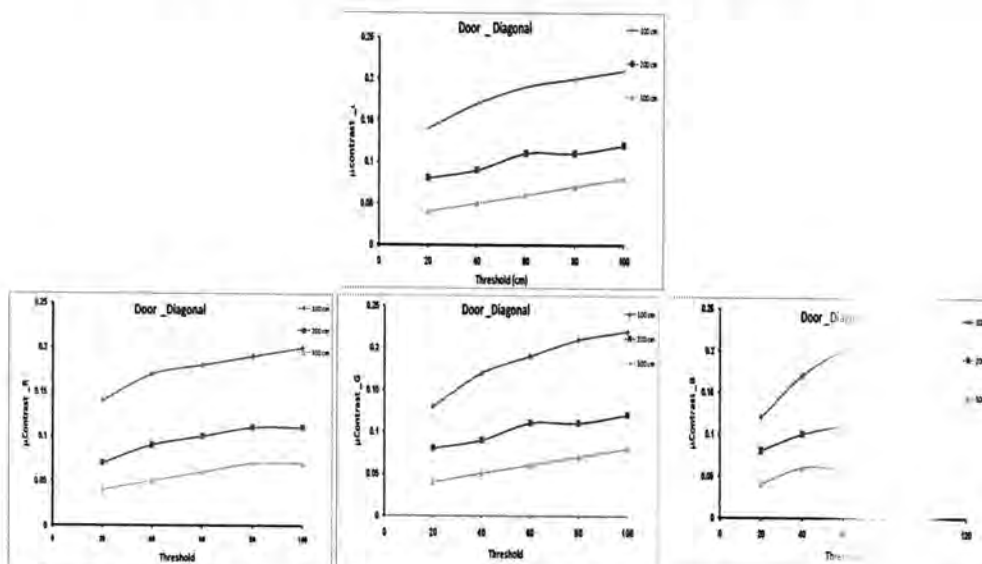


Figure -12 : Diameter contrast technique in condition of room illuminated from Left direction (Door)for the color band and lighting compound , using different distance (100,200,300)

We can conclude :

- 1- Observing the simulations of the illuminances and the luminance we see that the roof window' model has a good performance. As a comment, however, has to be made. The luminance simulations in this study have only shown the situation from one camera position. In case of classroom design with a roof window it is reasonable to make more simulations with

different camera positions, looking from the different student seats, in order to provide, with a further specification of the design, for a visual comfortable situation for all students.

- 2- Contrast techniques were of high efficiency in calculating contrast of text image and no difference appeared in determining of contrast values of written text on the white board, by difference in distance of lighting for classroom .

REFERENCES

1. John J." Lighting For Digital Video and Television " 2nd,printed in united states of America ,ISBN:1-57820-251-5,www.cmpbooks. com, (2004) .
2. Harry C., "Set Lighting Technicians hand Book" 3rd, film Lighting equipment, practices, and electrical distribution, 3rd, ISBN0-240-80495-3 (pbk:alk.paper) (2003) .
3. Bliain B." Motion Picture and video Lighting" 2nd edition (2007).
4. "Journal of illuminating engineering Institute of Japan (IEIJ) " , ISSN: 00019 – 2341/0019 – 2341,92(12)(2008) .
5. Peli E . , Arend L . , Labiance T . , " Contrast Perception a Cross Changes in Luminance and Spatial Frequency " , Opt.Soc.Am.A , vol.13, no.10/October 1996/J.Opt.Soc.Am.A (1996) .
6. William B.and Shirly P.and Ferwerda J., "A spatial Post Processing algorithm for Images of Night Scenes " Author Address : University . of Utah and Cornell University (2003) .
7. Norman C. " A Revisionist View of Blackboard Systems" From: MAICS - 97 Proceedings. , AAAI (www.aaai.org). All rights reserved , (1997) .
8. Trus de B. and E Ilie de G. , " Lighting in School " , Journal of the illuminating Engineering Society "25(2) :562–577(2002).
9. Paulsson E. and Sjostrand J. " Contrast Sensitivity in the Presence of a Glare Light " , S- 10401 Stockholm , widen Mar.26, (1980) .
10. Susan W. " Fundamentals of Lighting Paperback " , 1 edition, ISBN-10: 1563675285 ,(2007) .
11. The illuminating Engineering Society North America(IES) (1994) .
12. Holick M."Photochemistry and Photobiology of Vitamin D" Photome - dicine, Regan and Parrish (eds)195– 218, Plenum, New York (1982) .
13. Perry M. " Re – investigation of Causal Links Between Light Scatter and Discomfort Glare" Proc CIBSE National Lighting Conference ,Bath,UK: 280 – 292 (1996) .
14. Julian.W.&Surybrata J"Glare & Distraction–Are They one Phenomenem" Preceding CIBSE National Lighting Conference,Bath,UK:269–279 (1996)

refractive index, and hence reflectance, is relatively higher than that of the real refractive index.

In order to determine the type of energy gap in the prepared SnO_2 sample, $(\alpha h\nu)^n$ was plotted versus the incident photon energy, and the linear behavior was obtained from the relation between $(\alpha h\nu)^2$ and $(h\nu)$ as shown in Fig. (4). It is explained that the prepared SnO_2 sample has a direct bandgap and the allowed absorption processes are the dominant. Extrapolation of the linear portion of the plot to the energy axis yielded the bandgap value of about (3.3)eV, the radiation caused to lowering the energy gap to (3.25 eV). In the photonic processes, light incident on a sample is absorbed in a length characterized by the optical skin depth (ξ), which is given by:

$$\xi = \frac{\lambda}{2\pi k_{ex}} \dots\dots\dots(3)$$

In this optical skin depth, electrons can be excited to ionization states and are eventually emitted. The behavior of the skin depth with the incident wavelength is just a reciprocal to that of the absorption coefficient multiplied by 2. Fig. (5) shows the variation of skin depth (ξ) with the incident wavelength, it was increased in the visible region up to maximum value around 700nm then decreased in the IR region

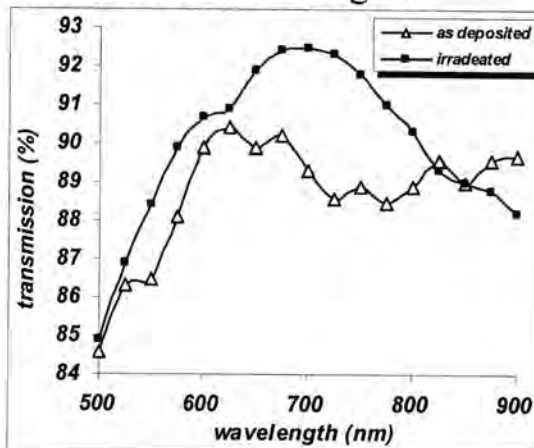


Fig.-1: The transmission of the sample

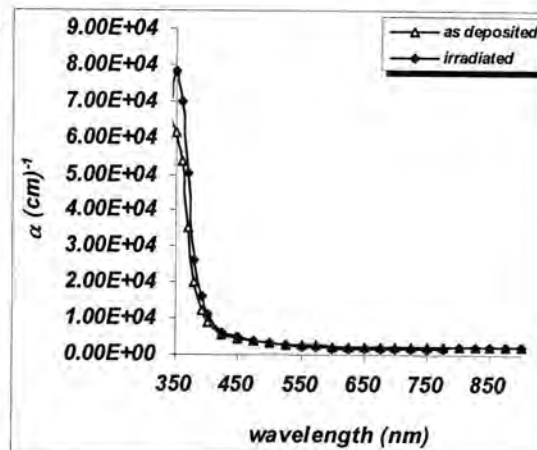


Fig.-2: The absorption coefficient

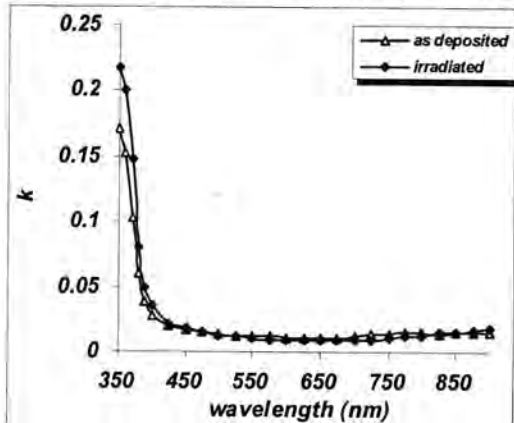


Fig.-3: The extinction coefficient

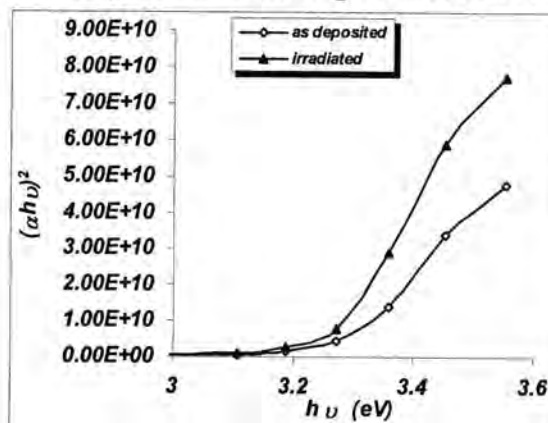


Fig.-4: plot of $(\alpha h\nu)^2$ vs photon energy .

variable range hopping conduction (8). Bipolar on hopping conduction appears to be affected less by ion-irradiation and is quite effective to modify the electrical transport behavior of the glass (9). The work on amorphous selenium (a-Se) showed that the disorder in the material increases upon light irradiation(10).

MATERIALS AND METHODS

SnO₂ films were prepared by dc magnetron sputtering . Argon gas 99.9998 % is used as sputter gas in pressure 6×10^{-2} Torr. Substrate temperature equals to 200°C, and deposition time 30 minute . Target-anode distance (30 mm) .The film was deposited on (glass) with thickness (~1µm). The data of the experiment and the specifications for X-ray test were as follows: Tube anode: Cu, Wavelength [Å]: 1.54060, Divergence slit : 1°. The optical constants were determined from transmittance (T), which were carried out at normal incidence using a double beam Spectrophotometer (Shimadzu UV 210A) operating in the UV/VIS over the wavelength range 350 nm - 900nm .

Irradiation for thin film sample with dose (3.7MBq) was performed using a Cs¹³⁷ gamma ray source exposed the sample film for (50 days) .

The transmission , absorption coefficient , extinction coefficient , energy gap and skin depth for unirradiated and irradiated sample were carried out .

RESULTS AND DISCUSSION

Transmittance is explained in figure (1) as a function of the incident wavelength for radiated and unirradiated SnO₂ thin film sample. The optical properties of the sputtered SnO₂ film similar to those produced by using other methods. It is clear that there are two effects caused by irradiation , the first is the blue shift , the other is the increasing in the transmittance up to 800 nm and then decreased in the NIR region .

Consequently, the absorption coefficient (α) is determined by the following relation(11) :

$$\alpha = -(\ln T) / t \dots\dots\dots (1)$$

where t is the film thickness , figure (2) shows the calculated absorption coefficient rapidly decreasing with the increasing incident wavelength (λ) and the sample has close value for α at NIR wavelengths.

It is worth to mention that the absorption coefficient is necessarily determined by overall preparation conditions . The extinction coefficient (kex) is determined by the following relation (11):

$$k_{ex} = \frac{\alpha \lambda}{4\pi} \dots\dots\dots (2)$$

So, its behavior with wavelength shown in figure (3) is the same as for the absorption coefficient (α). The effect of the extinction coefficient on the

Some Optical Properties of the Sputtered SnO₂ Thin Film Affected by Gamma Radiation

¹Ali J. Mohammad, ²Salah K. Hazaa, ¹Ali N. Mohammed

¹Department of Physics, College of Science, Al-Mustansiriya University, Baghdad, Iraq .,

²Department of Physics, College of Education, Al-Mustansiriya University, Baghdad, Iraq .,

الخلاصة

في هذا البحث تم دراسة بعض الخصائص البصرية كالنفاذية , معامل الامتصاص , معامل الخمود , فجوة الطاقة والعمق السطحي لغشاء اوكسيد القصدير المحضر بطريقة الترنيد قبل وبعد التشعيع ناشعاع كاما المنبعث من مصدر السيزيوم (¹³⁷Cs) ولمدة خمسون يوما .

النتائج بينت بان تأثير التشعيع هو زيادة في النفاذية والعمق السطحي وكذلك نقصان في معامل الامتصاص ومعامل الخمود خصوصا في المنطقة المرئية وايضا نقصان في فجوة الطاقة البصرية .

ABSTRACT

In the present work , some of optical properties of the sputtered SnO₂ thin film before and after irradiated by γ -radiation like transmission , absorption coefficient , extinction coefficient , energy gap and skin depth were studied . The results indicated that the influence of the γ -radiation from Cs ¹³⁷ gamma ray source exposed the sample film for (50 days) caused to increase the transmission and the skin depth , while decreased the absorption coefficient , extinction coefficient especially in the visible region and lowering the optical energy gap

Keywords: SnO₂ films , Sputtered Thin Films , TCO film , Matter-Radiation Interaction

INTRODUCTION

Last ten years the energy-dispersive spectroscopy of high-energy radiation such as X-rays, γ -rays, and other uncharged and charged particles has improved dramatically (1). This is of great importance in a wide range of applications including medical imaging, industrial process monitoring, national security and treaty verification, environmental safety and remediation, and basic science. The influence of γ -radiation onto different types of thin films has been discussed (2,3).

Crystal structure and optical properties of metal oxide thin films were the subjects of numerous theoretical and experimental studies (4, 5).

High-energy radiations, such as γ -rays, change the physical properties of the materials they penetrate. The changes are strongly dependent on the internal structure of the absorbed substances. It is believed that ionising radiation causes structural defects (called color centers or oxygen vacancies in oxides) leading to their density change on the exposure to γ -rays (6). The influence of radiation depends on both the dose and the parameters of the films including their thickness: the degradation is more severe for the higher dose and the thinner films (7)

The absorption of γ -radiation in the thin films depends strongly upon their electronic structure which in turn changes by the interaction with photons. Ion-irradiation induced defect states near the Fermi level play a dominant role in the

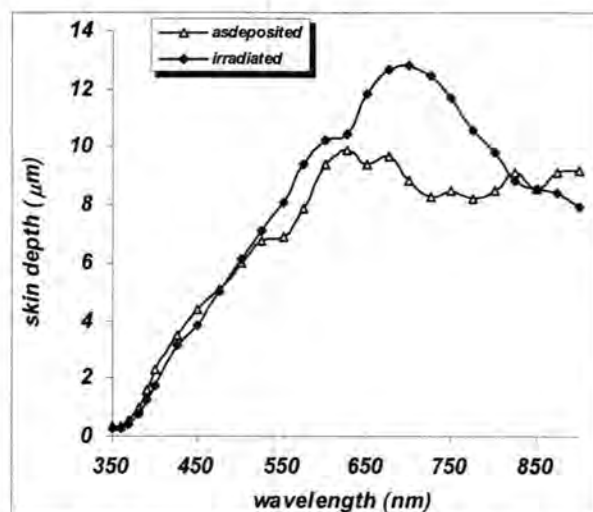


Fig.-5: The skin depth before and after irradiation .

We can conclude:

The small sensitivity in the optical properties of material to radiation or fluence in the saturation region has been attributed to the generation of high structural disorder , this damage may create a large enough concentration of localized levels , which reduces the sensitivity of parameters to further irradiation . High concentration of dangling bonds makes disordered semiconductors insensitive to doping or irradiation (11, 12).

The effects on the optical properties may be due to the increase of the disorder of the samples by irradiation . The disordered energy decreases at about 3 MBq dose and increases as the radiation doses increase for all compositions showing the increase of disorder and compaction.

The optical properties are influenced by irradiation . The blue shift and transmittance increased with the wavelength increasing , the absorption coefficient decreases, the same behavior for the optical energy gap E_{opt} shifted to lower energy . Also the skin depth increased with the increasing wavelength due to the absorption decreasing . So we can conclude that - doses cause the breaking of bonds leading to the increase of dangling bonds and of defects, as well as the trapping of the generated carriers "

REFERENCES

- 1.Schlesinger T.E., Toney J.E., Yoon H., Lee E.Y., Brunett B. A., Franks L., and James R.B. " Cadmium zinc telluride and its use as a nuclear radiation detector material ".Materials Science and Engineering, R: Reports,32,103,(2001) .
- 2.Kolobov A. V. , Oyanagi H.and Tanaka K.,MRS-Bulletin,24,1, 32,(1999)
- 3.Shpotyuk O.I."Amorphous chalcogenide semiconductors for dosimetry of high-energy ionizing radiation ".Radiation Physics and Chemistry,46,1279(1995) , .
- 4.Champarnaud-Mesjard J.C., Blanchandin S.,Thomas P., Mirgorodsky A., Merle-Méjean T., and Frit B. , " Crystal structure. Raman spectrum and lattice

- dynamics of a new metastable form of tellurium dioxide : γ -TeO₂ " . Journal of Physics and Chemistry of Solids , 61 , 1499(2000) .
5. Mirgorodsky, A.P., Merle-Méjean T., Champarnaud J.-C., Thomas P., and Frit, B. " Dynamics and structure of TeO₂ polymorphs: model treatment of paratellurite and tellurite; Raman scattering evidence for new γ - and δ -phases " . Journal of Physics and Chemistry of Solids , 61, 501, (2000) .
 6. Zhu, R.Y. " Radiation damage in scintillating crystals. Nuclear Instruments and Methods in Physics Research", Section A: Accelerators, Spectrometers, Detectors and Associated Equipment , 413 , 297(1998) .
 7. Tanassova E., Paskaleva A., Konakova R., Spassov D. and Mitin V. F. " Influence of γ -radiation on thin Ta₂O₅-Si structures " . Microelectronics Journal , 32 , 553(2001).
 8. Inagawa I., Morimoto S., Yamshita T., and Shirotani I., Japanese-Journal of Applied-Physics, 36, 4A , 2229(1997).
 9. Singh M., Bhatia K. L., Kishore N. , and Kundu R. S., Kanjilal-D , "Nuclear-Instruments & Methods-in-Physics-Research" , Section-B, 140: 3-4, 349(1998).
 10. Phillips, G.W., Readshaw, A.K., Brown, G.O., Weiss R.G., Guardala, N.A., Price, J.L., Mueller, S.C., and Moscovitch, M. , " Observation of radiation effects on three-dimensional optical random-access memory materials for use in radiation dosimetry " , Applied Radiation and Isotopes , 50 , 875(1999) .
 11. Gumus C. , Ozkendir O. , Kavak H. , Ufuktepe Y. , " Structural and optical properties of zinc oxide thin films prepared by spray pyrolysis method " , J. Optoele. And Advanc. Mat. , 8 , 1 , 299(2006).
 12. Croitoru, N., Gubbini, E., Rancoita, P.G., Rattaggi, M., and Seidman, A. " Influence of damage caused by Kr ions and neutrons on electrical properties of silicon detectors " Nuclear Instruments and Methods in Physics, Res. Sec. A 426 , 477(1999).
 13. Mott, N. "Conduction in Non-Crystalline Materials" Oxford Science Publications, Clarendon Press, Oxford , 83 (1993).

Study The Resolution of the Written Text on the Whiteboard Based on the Criterion of Contrast for Different Illumination Conditions

Salema Sultan Salman

College of Pharmacy/Department of Clinical Laboratory Science/Baghdad University

الخلاصة

أن جودة توزيع الإضاءة بشكل جيد ومنتظم تلعب دور رئيساً في الإدراك الحسي البصري للإنسان . حيث أن تجانس توزيع الإضاءة في قاعة الدرس لها دور مهم في وضوح النص المكتوب على السبورة . أن الغاية من إضاءة قاعة الدراسة بإضاءة صناعية بالإضافة إلى ضوء الشمس من النوافذ هي توفير مستوى إضافي لوضوح الرؤية للنصوص المكتوب . لذا توجّهنا في هذه الدراسة إلى حساب التباين للنص المكتوب للحزم اللونية ومركبة الإضاءة بالاعتماد على مناطق الحافات ، وقد استخدم مؤثر سوبل للكشف الحافي ، أن نتائج هذه الدراسة بينت أن التباين للنص المكتوب على السبورة يقل بازدياد المسافة بين الكاميرا والسبورة وكذلك يقل التباين للنص كلما كانت الإضاءة قليلة (غير كافية) .

ABSTRACT

Good quality of light plays a significant role in the psychological and biological processes of human beings. We know that performances of students increase by a good visual environment. Besides that, energy use by electric lighting is one of the important energy for classroom . We calculate the contrast as a function of illumination to the text which writing in the whiteboard by using pen of color black . The results of study show that the contrast based on text edge regions decreases with decreasing illumination and increasing distance between the camera and whiteboard .

INTRODUCTION

Three main rules govern both the appearance and the behavior of light for photographic purposes. These rules are essential knowledge for photographers. (1) .

• Properties of light

The larger the light source, the softer the light. For the quality of the light to change, the surface of the light source must change first, either in terms of size, color, reflectance or a combination of 2 or 3 of these elements. In practice, and for landscape photography, this means that direct light from the sun alone will be much harsher than light coming from the entire sky on an overcast day. This is because the sun, although a giant star, is actually a very small light source when seen from the earth. On the opposite, on an overcast day, the cloud-filled sky becomes a giant light reflector the size of the entire sky above us. A small light source, such as the sun, produces a very harsh light with bright highlights and deep shadows. A large light source, such as the entire sky on a cloudy day, produces a very soft and even light with little or no shadows (2).

- **Reflected Light**

If the light is reflected, the light will take the color of the reflector on which it bounces. This is best exemplified by the lighting situation in the canyon country of the Southwestern United States. In a canyon, the light reflected off one side of the canyon bounces onto the other side the opposite wall of this same canyon. While direct light is basically colorless, the light bouncing from one canyon wall to the other takes the color of the canyon wall off which it bounces. This bounced light is tinted red or orange and in turns adds this color to the other canyon wall. The result is that the wall lit by this bounced light is much warmer in color much redder to the eye and much redder on film than the wall lit by direct sunlight (2,3)

- **Intensity of Light**

The intensity of the light on any given surface decreases in a manner inversely proportional to the square of the distance between the light source and the subject. Doubling the distance between the light source and the subject is equivalent to reducing the quantity of light reaching the subject by 1/4th of the original illumination. This rule is very important in a studio situation where artificial lights can be moved at will closer or further to the subject being photographed. In an outdoor, natural light situation, it is mostly academic since we cannot move the sun, the clouds, or the canyon walls (4) . Many former studies concerned with the illuminance and contrast effect on the image quality:

- **Eli Peli et.al** (5) conducted a study on 1996 for contrast enhancement through the changes in luminance intensity and spatial frequency. The study adopted contrast sensing over the threshold by using contrast analogy.

- **Thompson W . et.al** (6)suggested on 2003 an algorithm to enhance image in night scenes by a technique of making the images taken in the day light as if they were taken in night images through decreasing the contrast and brightness for all of the image, adding a distortion to the image and present the night image characterized with high noise, loss in optical acuity along with distortion size taking place in it .

- **Norman Carver** (7) in 1997 , he explore the relationship between blackboard-based and belief network approaches to interpretation problems. In this way we begin to reinterpret the blackboard model, to show how it can be explained in terms of modern AI concepts.

- **Truus de Bruin et. Al.** (8) in 2002 , they design possibilities for an optimum use of daylight. However, a classroom is a difficult space to light with daylight, because of the depth of the classroom and the different tasks which must be performed in it. At the university of Delft research has been done in order to optimize the daylight access by the design of classrooms. In a first step the luminances and illuminances in a number of existent schools were measured. From this, nine possible design models of classrooms have been draw up.
- **Paulsson et .al**(9) in 1980 he proposed A method is presented for quantitative measurements of the glare effect of light scattered, in the ocular media. The contrast sensitivity function is measured loith a television display system. A bright light source is introduced into the field of vision, and the resultant decrease in contrast sensitivity is measured.

2- Lighting Quality

Good lighting adds accuracy, comfort, and aesthetics to the viewing task. The characteristics of high-quality lighting vary by the task being illuminated. For example, the kind of lighting necessary for a writing task differs significantly from that needed for visual display terminals (VDTs). Many light sources can be adjusted to provide high-quality lighting. Because lighting needs are task-specific, it is important to consider several factors when evaluating lighting, including color, contrast, shadow, luminance ratios, glare, and illumination levels (10) .

Contrast is the difference in brightness or color between various objects. The greater the contrast between objects, the more readily the eye distinguishes between them. Proper lighting can fine-tune contrast between objects--even black and white ones such as pencil marks on white bond paper. An example of good color contrast is a beautiful vista at sunset, which is eye-catching because of the generous interplay of colors enhanced by the setting sun. Improved contrast also helps weak eyes see better. Many people wear glasses to correct their eyesight, but the appropriate amount of contrast provided by proper lighting also improves vision by resolving images on the retina (4) .

3- Shadow

Depending on the application, shadow may be deliberately used or consciously avoided in high-quality lighting. Highlighting and shadowing can effectively contrast the various surfaces of an object to enhance it aesthetically or give it more definition. For instance, when illuminating a sculpture, or even the measuring lines of a vernier caliper, a "grazing" light beam uses shadows to

emphasize certain surfaces, giving the sculpture more texture and making the caliper lines easier to read. But this type of lighting will not enhance a two-dimensional object, such as the writing on a piece of paper. The readability of the pencil marks depends on a combination of the lighting and how the task reflects this illumination (2,3).

4- Luminance Ratios

The luminance ratio--the ratio of task brightness to that of the surrounding area--can significantly affect user comfort. Too high a luminance ratio within the field of view can create too great a contrast, making vision difficult and uncomfortable. In fact, extreme luminance ratios between parts of the viewing area can induce frequent eye adaptations (pupil adjustments), which may cause eye fatigue. Proper task illumination ensures that the shadowing of the task area, even by a writing hand, does not impair visibility. Too low a luminance ratio, such as the dim light at dusk, fails to enhance important details in objects, such as the lines on a highway (6) .

Light Contrast Illusions

When looking at the image figure (1) to the left , can you determine what colors the two gray squares are? Is the left square 2, 3 or the right square 4 , 5 Surely, the square on the right has to be darker than the square on the left. Right Actually, both the right and left squares are same color as number 4. What makes them look like two different colors is **light contrast**, a phenomenon closely related to Lateral Inhibition.

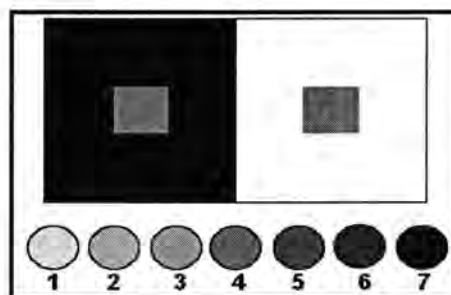


Fig -1:Image different contrast (6)

To understand light contrast you must first understand the difference between lightness and intensity see figure (2). Although both are measures of the strength

of light reflecting off an object, intensity is a physical and constant measure while lightness is a perceptual and subjective measure. The level of an object's lightness depends on the amount of light reflected from the surface of that object. The level of an object's intensity remains constant no matter how much light is reflected from the surface. With ON-Center receptive fields, if light is detected solely by the light photoreceptors in the center portion of a receptive field (e.g., field A to the left), the response of that field increases proportionately to any increase in light level. However, if light is also detected by the dark photoreceptor surround, the two regions conflict with one another and it takes a greater amount of light for the field to respond (6,11)

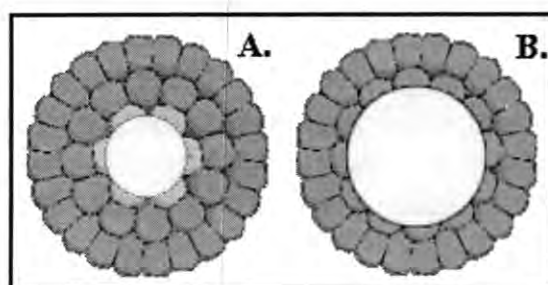


Figure – 2: explain the different between the lightness and intensity(11)

The greater the amount of light shined on the surround the more conflicted the center and surround of the receptive field becomes. Because of this, a receptive field could view a single color with the same intensity differently depending on the amount of light detected by the field's surrounding photoreceptors. Similar to the Mach Bands illusion, **Lateral inhibition** can cause objects identical in intensity to appear different in lightness. This is the illusory phenomenon of **light contrast**. Returning to the figure (1) above, by looking only at the squares without the surrounding colors, you will see that they are both identical in lightness (4 , 12) .

5- Illumination Levels and Glare

The amount (or level) of illumination is an important element of lighting quality. Too little light can cause eye strain; too much light can waste energy and cause glare. The Illuminating Engineering Society (IES) publishes recommended illumination levels for specific tasks, based on a consensus of expert opinion. These IES recommendations should be initially included in any illumination analysis (13) . Two types of glare reduce lighting quality: disability glare and discomfort glare. Disability glare is light that masks an object--the light from a window reflected off the slick page of a magazine--without necessarily irritating the eyes. Discomfort glare, however, is an annoying and uncomfortable light

source directly in the field of view. In some cases, both types of glare can occur at the same time, such as when the sun is low in the sky, shining through the windshield and masking the road. Sparkle is a type of glare that actually enhances viewing. A classic example of sparkle is a "brilliant" cut diamond that comes to life when illuminated by a high-intensity point source. A more affordable example is a display of shiny red apples glistening under the man-made light of a grocery store or the natural sunlight at a roadside stand (5).

6- Light Source and Application

It is important to note that all of the lighting characteristics described above are affected by lighting design. Installation of a high-quality lamp does not automatically ensure proper lighting. The appropriate lighting components--luminaries, lenses, louvers, etc. must be carefully selected and installed. Developing a high-quality lighting system takes considerable time and effort. That time and effort, however, can pay off in improved productivity, user comfort, and overall cost-effectiveness (3,4).

7- Work geometry (for Evaluation of lighting quality)

To study lighting quality, its distribution in the class, the effect of the use color in specifying the text written on the white board along with study of distance effect in specifying good view of the written text, the text illustrated in Figure (3) was imaged using Sony – Digital Camera and the color of the pen used in study is black (Dry-Eraser) for different distances between the board and the camera 100, 200, 300 cm and two lighting conditions in the classroom, present of fluorescent light effect (full lighting) and absence of fluorescent light effect (darkness). Imaging process was made at 10:00 AM of 14-04-2009 according to the geometry of classroom illustrated in Figure (4). Values of illuminance was recorded for both lighting conditions (full lighting and full darkness). Scheme (1) represents the difference in illuminance values for two different lighting conditions in relation to classroom geometry. From the scheme, it is obvious that maximum illuminance appears when classroom is in full lighting and from upper side for classroom geometry.

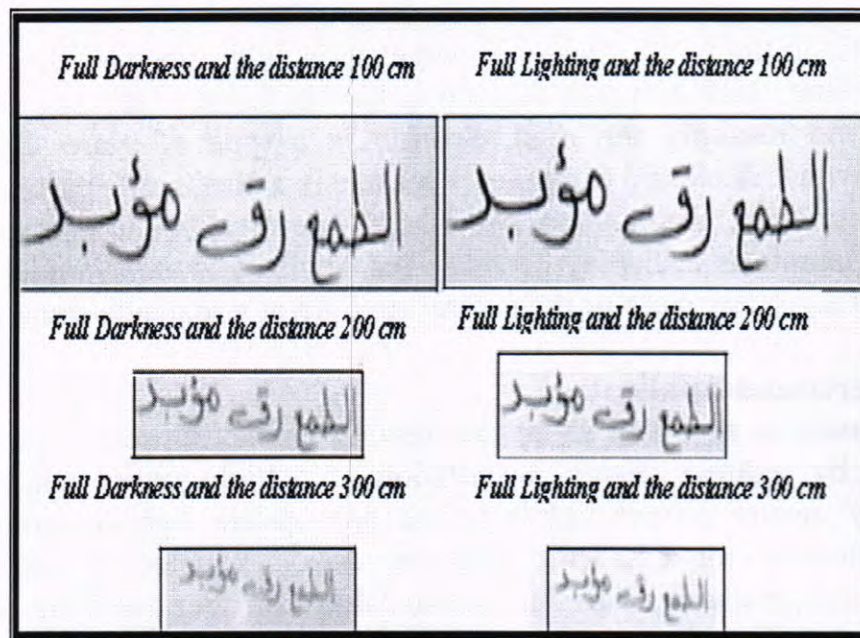
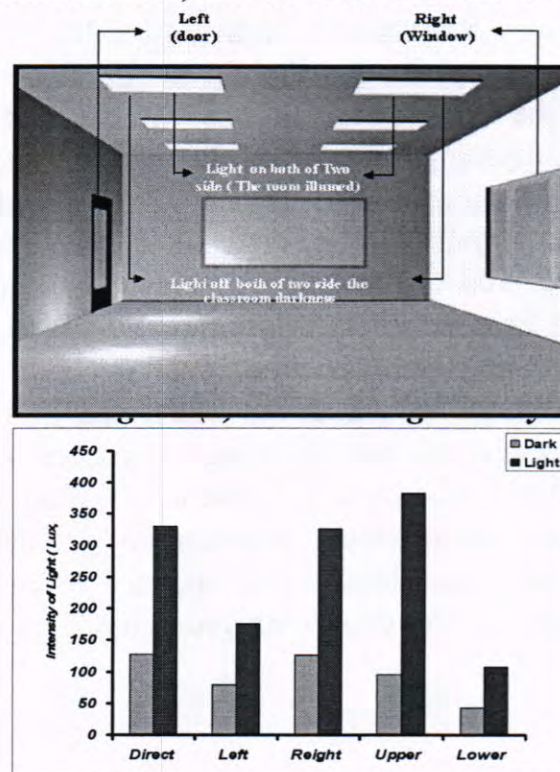


Figure -3: Images of the text written in black for two different lighting conditions (full lighting and full darkness) and at distances are 100,200, 300cm



Scheme -1: Represents the difference in illuminance values toward the spotlight for classroom geometry at full lighting and full darkness

Contrast is the difference in optical characteristics that make the written text recognizable in terms of different elements or background. In optical detection of image, contrast is determined through the difference in color and lighting. So, contrast is found by the relation (14).

$$c = \frac{Lux_{\max} - Lux_{\min}}{Lux_{\max} + Lux_{\min}} \quad (1)$$

Lux_{\max} and Lux_{\min} represent higher and lower reading of the photometer in Lux unit by difference in spotlight of photometer direction in relation to the classroom geometry, as illustrated in Figure (5). Table (1) shows illuminance and contrast values by difference in spotlight direction according to classroom geometry in case of no effect of fluorescent light (full darkness). Table 2 shows illuminance and contrast values by difference in spotlight direction according to classroom geometry in case of effect of fluorescent light (full lighting).

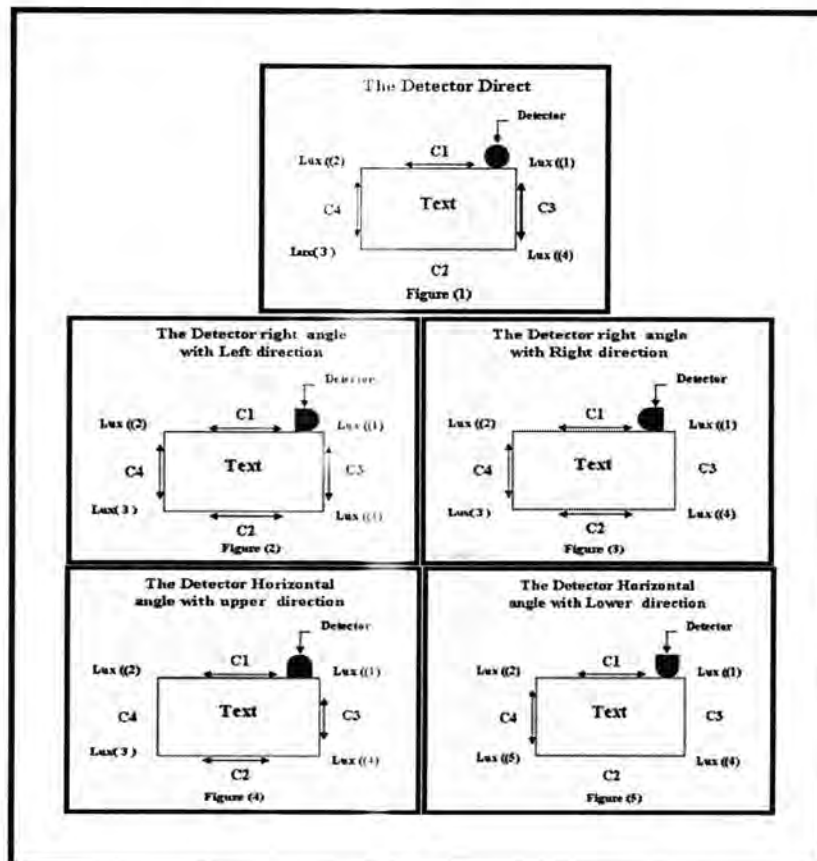


Figure-5: represents Luxmeter spotlight direction according to classroom geometry

Table-1: illuminance and contrast values in case of dark classroom (uniform darkness)

Direct

We note that the horizontal and vertical contrast values are equal due to equivalence in illuminance fallen onto the spotlight

Lux (1)	Lux(2)	Lux(3)	Lux(4)	Lux(average)
128	129	127	129	128.25
C1 (Horizontal)	C2(Horizontal)	C3(Vertical)	C4(Vertical)	
0.0038	0.0078	0.0038	0.0078	

Right (Window)

We note that there is a difference horizontal and vertical contrast values since the light is comes from window's direction in respect to classroom and from top of the written text

Lux (1)	Lux(2)	Lux(3)	Lux(4)	Lux(average)
82	87	76	77	80.5
C1 (Horizontal)	C2(Horizontal)	C3(Vertical)	C4(Vertical)	
0.029	0.0065	0.067	0.0065	

Left (Door)

We note that the horizontal and vertical contrast values are equal due to the equivalence in illuminance fallen onto the spotlight

Lux (1)	Lux(2)	Lux(3)	Lux(4)	Lux(average)
133	124	123	124	126
C1 (Horizontal)	C2(Horizontal)	C3(Vertical)	C4(Vertical)	
0.035	0.004	0.035	0.004	

(Upper)

We note that there is a difference horizontal and vertical contrast values since the light comes from window's direction in respect to classroom and from top of the written text

Lux (1)	Lux(2)	Lux(3)	Lux(4)	Lux(average)
101	96	93	95	96.25
C1 (Horizontal)	C2(Horizontal)	C3(Vertical)	C4(Vertical)	
0.025	0.0053	0.03	0.015	

(Down)

We note that illumination values are almost equal, so there is no difference in the horizontal and vertical contrast

Lux (1)	Lux(2)	Lux(3)	Lux(4)	Lux(average)
43	44	42	41	42.5
C1 (Horizontal)	C2(Horizontal)	C3(Vertical)	C4(Vertical)	
0.011	0.012	0.011	0.023	

Table (2): Illumination and contrast values in case of lighted classroom

Uniform lighting

Direct lighting

We note that the horizontal contrast is higher than vertical contrast since illumination values are higher in respect to the written text in the top

Lux (1)	Lux(2)	Lux(3)	Lux(4)	Lux(average)
344	348	334	305	332.7
C1 (Horizontal)	C2(Horizontal)	C3(Vertical)	C4(Vertical)	
0.005	0.045	0.06	0.02	

Right (Window)

We note that illumination values between the text in the top and in the bottom , so there is a difference in the horizontal and vertical contrast

Lux (1)	Lux(2)	Lux(3)	Lux(4)	Lux(average)
181	192	170	162	176.25
C1 (Horizontal)	C2(Horizontal)	C3(Vertical)	C4(Vertical)	
0.029	0.024	0.055	0.06	

Left (Door)

We note that the horizontal and vertical contrast are not equivalent due to non-equivalence in illumination of the written text

Lux (1)	Lux(2)	Lux(3)	Lux(4)	Lux(average)
371	336	309	292	327
C1 (Horizontal)	C2(Horizontal)	C3(Vertical)	C4(Vertical)	
0.049	0.028	0.11	0.041	

(Upper)

We note that there is a difference horizontal and vertical contrast values since the light comes from window's direction in respect to classroom and from the top according to the room's geometry

Lux (1)	Lux(2)	Lux(3)	Lux(4)	Lux(average)
391	395	383	364	383.25
C1 (Horizontal)	C2(Horizontal)	C3(Vertical)	C4(Vertical)	
0.005	0.025	0.035	0.015	

(Down)

We note that illumination values in the top are higher than illumination values in the bottom, so there is a difference in the horizontal and vertical contrast

Lux (1)	Lux(2)	Lux(3)	Lux(4)	Lux(average)
118	117	105	92	108
C1 (Horizontal)	C2(Horizontal)	C3(Vertical)	C4(Vertical)	
0.004	0.065	0.12	0.054	

8- Contrast Determination Procedures

The contrast of the written text was determined by adopting edges points which are specified by (Soble effect) for edge detection depending upon four procedures:

- 1- Contrast determination by adopting maximum and minimum element of edges elements. Figure (6-7) shows the results of this technique. In case of darkness and lighting (uniform lighting) of classroom, contrast average was charted as a function of the distance between the camera and the white board. When using different thresholds of Soble Effect. We see, from the figures, that increasing the distance leads to decrease in contrast. Also, we may note that by increasing the threshold value of Soble Effect the calculated contrast increases.

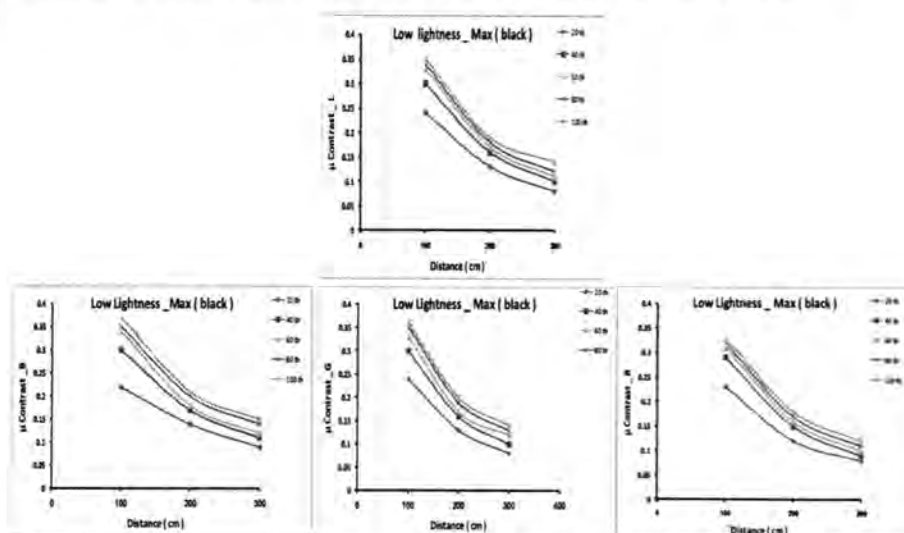


Figure -6: Direct Contrast Technique in condition of classroom full darkness for the color bands and lighting compound, using Soble Effect with thresholds values (th= of 20, 40, 60, 80 and 100).

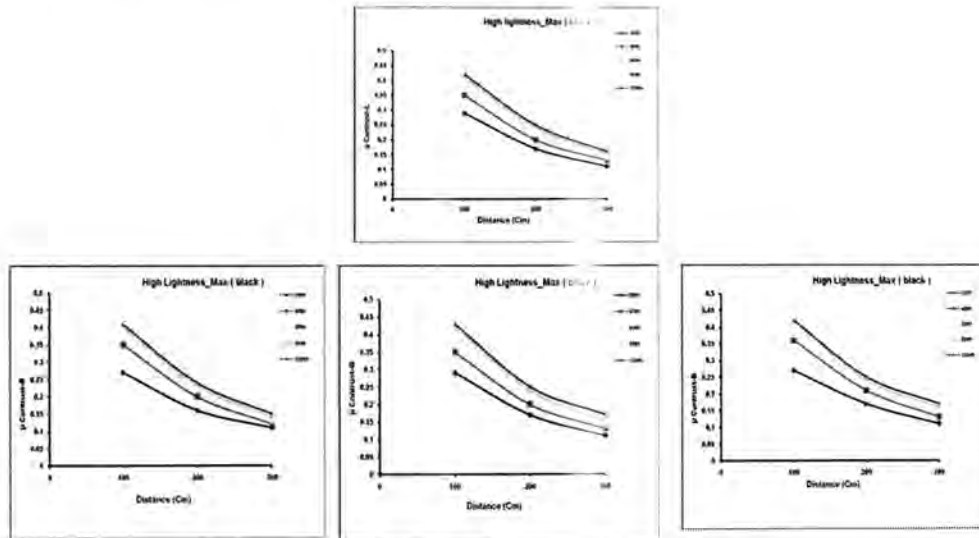


Figure -7: Direct Contrast Technique in condition of classroom full Lighting for the color bands and lighting compound, using Sobel Effect with thresholds values (th= of 20, 40, 60, 80 and 100).

2- Contrast Calculation by adopting statistical characteristics of edges points (standard deviation and average). Figure (8-9) shows the results of this technique for the three color bands and lighting compound of written text in two conditions of uniform lighting (full darkness and lighting). Contrast average was charted as a function of distance between camera and written text in black. From the figure, we note that by increasing threshold value of Sobel Effect the calculated contrast increases.

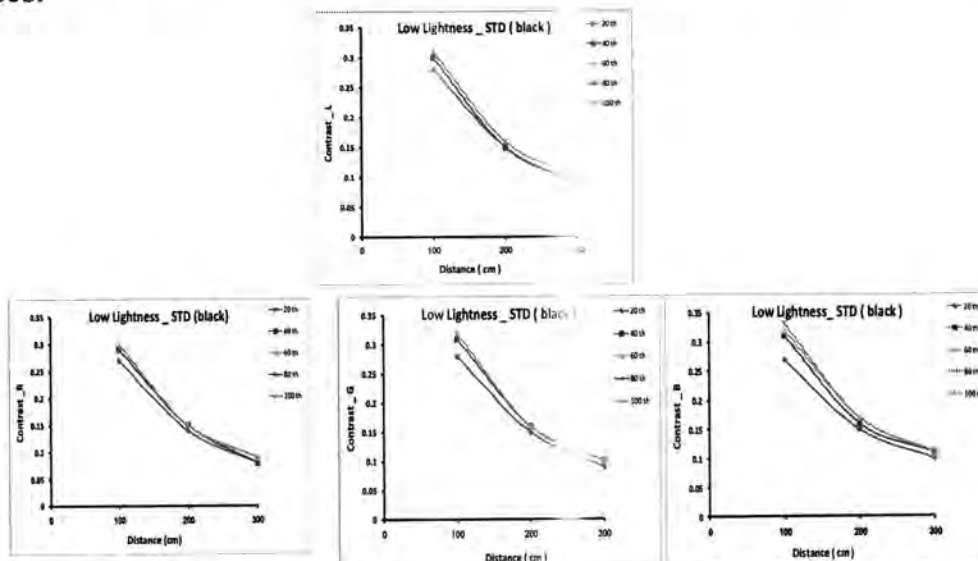


Figure -8: Statistical Contrast Technique in condition of classroom full darkness for the color bands and lighting compound, using Sobel Effect with thresholds values (th= of 20, 40, 60, 80 and 100)

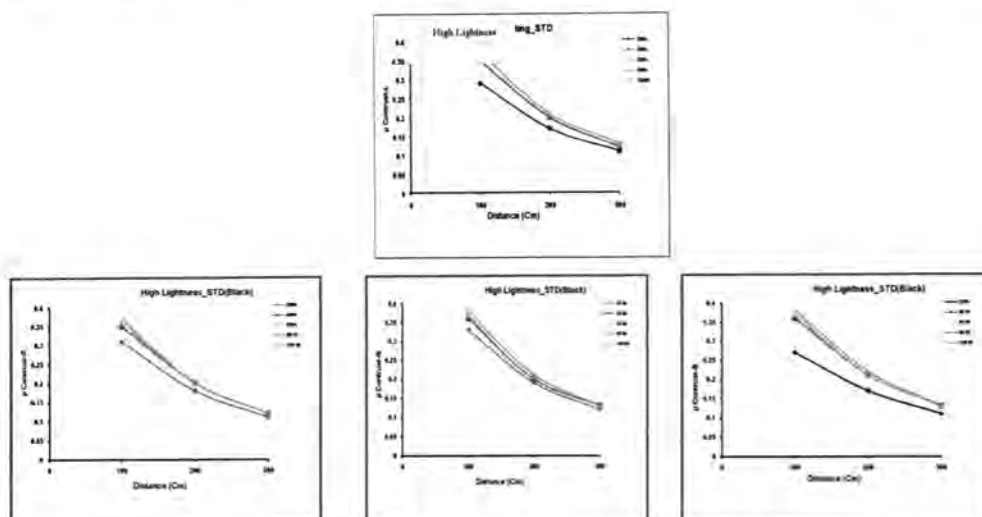


Figure -9: Statistical contrast technique in condition of classroom full lighting for the color bands and lighting compound, using Sobolev Effect with thresholds values of 20, 40, 60, 80 and 100

- 3- Contrast calculation of edges points using vertical contrast technique. The total elements of the first and third column for the triangular window, except for the column that includes edges element and results, showed in figure (10-11), for the three color bands and lighting compound of written text in two conditions of uniform lighting (full darkness and lighting). Contrast average was charted as a function of distance between camera and written text on the white board. We note that by increasing distance, calculated contrast values of written text on the white board decrease and by increasing threshold value of Sobolev Effect the contrast values of the written text in black on the white board increase.

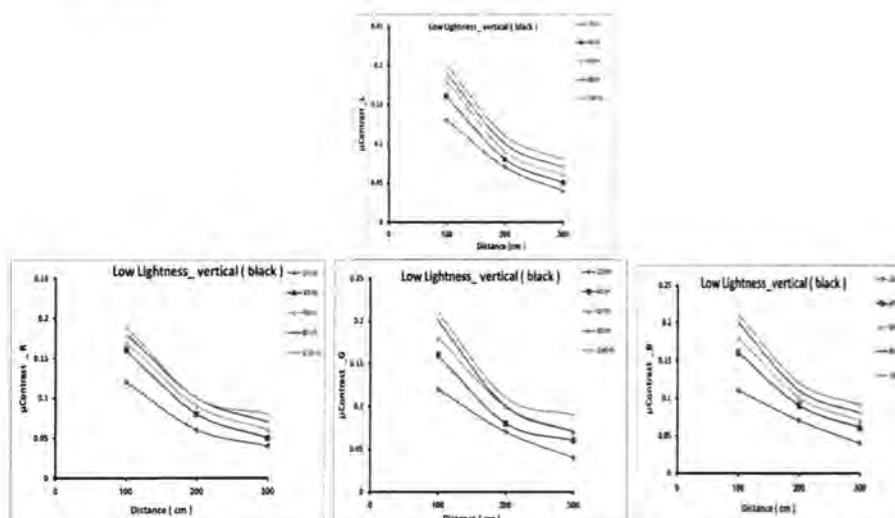


Figure -10: Vertical contrast technique in condition of classroom full lighting for the color bands and lighting compound, using Sobolev Effect with thresholds values of 20, 40, 60, 80 and 100.

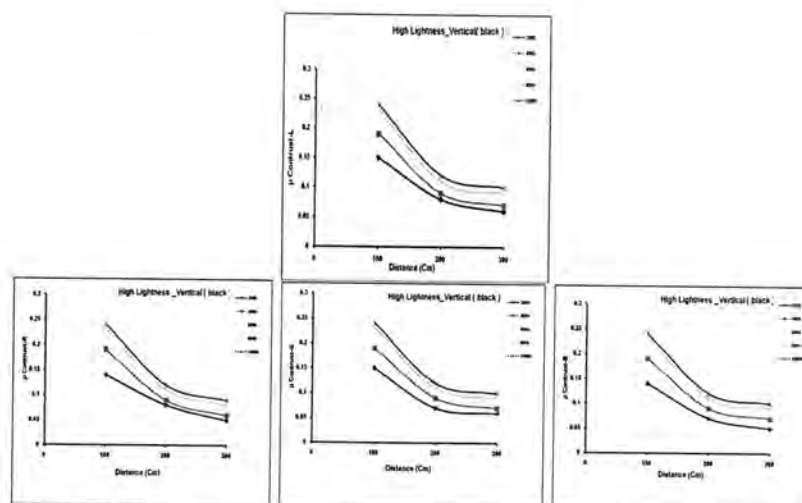


Figure -11: Vertical Contrast Technique in condition of classroom full darkness for the color bands and lighting compound, using Soble Effect with thresholds values of 20, 40, 60, 80 and 100.

- 4- Diameter Calculation by adopting edges points. triangular window is set around edges element and, then, the total of elements on the to the bottom of the main diameter. Figure (12 and 13) shows the results of this technique for the three color bands and lighting compound of written text in two conditions of uniform lighting (full darkness and lighting). Contrast average was charted as a function of distance between camera and written text on the white board, using different thresholds of Soble Effect. We note, form the figures, that by increasing the distance, contrast decrease and by increasing threshold value of Soble Effect the calculated contrast increases.

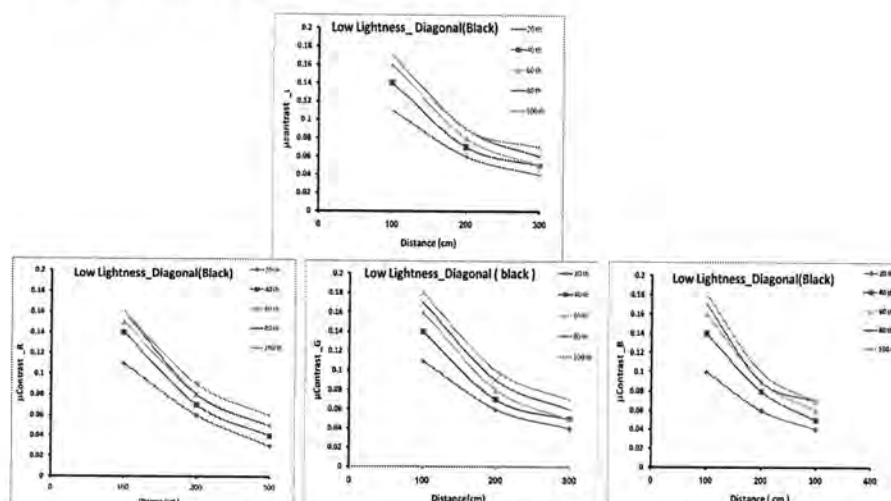


Figure -12: Diameter Contrast Technique in condition of classroom full darkness for the color bands and lighting compound, using Soble Effect with thresholds values of 20, 40, 60, 80 and 100.

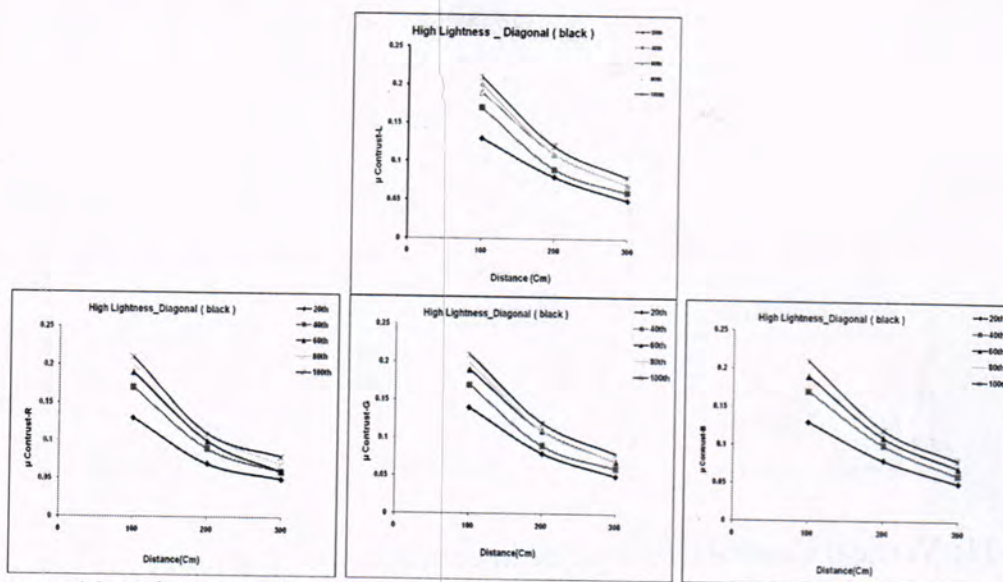


Figure -13: Diameter Contrast Technique in condition of classroom full lighting for the color bands and lighting compound, using Sobel Effect with thresholds values of 20, 40, 60, 80 and 100.

We can conclude

1. Contrast techniques were of high efficiency in calculating contrast of text image and no difference appeared in determining of contrast values of written text on the white board, by difference in distance of lighting for classroom.
2. Classroom illumination values from to top and from window direction are the best in determining the resolution of the written text on the white board.

REFERENCES

1. John J. , " Introduction For Digital Video and Television "(2004) .
2. Harry C. , " Set Lighting Technicians hand Book "(2003).
3. Bliain B. " Motion Picture and video Lighting " 2nd edition "(2007) .
4. "Journal of illuminating engineering Institute of Japan (IEIJ) " , ISSN: 00019 – 2341/0019 – 2341 ,92 (12) (2008) .
5. Peli E . , Arend L. , Labianca T." Contrast Perception a Cross Changes in Luminance and Spatial Frequency "Optical Society America,13, (10) / October 1996/J.Opt.Soc.Am.A (1996) .
6. Thompson W. and Shirly P. and Ferwerda J., " A spatial Post Processing algorithm for Images of Night Scenes " , Anthers Address : University . of Utah and Cornell University (2003) .
7. Norman C. "A Revisionist View of Blackboard Systems" From: MAICS-97 Proceedings., AAAI (www.aaai.org). All rights reserved , (1997) .

8. Trus de B. and E Ilie de G. "Lighting in School" Journal of the Illuminating Engineering Society "(25).2 :562 – 577 (2002) .
9. Paulsson E. and Sjostrand J. " Contrast Sensitivity in the Presence of a Glare Light " , S- 10401 Stockholm , widen Mar.26, 1980 .
10. Susan W. " Fundamentals of Lighting Paperback " (2007) .
11. The Illuminating Engineering Society North America (IES) , (1994) .
12. Holick M. "Photochemistry and Photobiology of Vitamin D" Photomedicine, Regan and Parrish (eds)195–218, Plenum, New York (1982) .
13. Perry M. " Re – investigation of Causal Links Between Light Scatter and Discomfort Glare " Proc CIBSE National Lighting Conference, Bath, UK:280–292 (1996) .
14. CIBSE Code for Interior Lighting London (1994) .

Synthesis of Pyrazoline-5-one Compounds Derived From 4-Aminobenzoic Acid

Rafah F. Al-Smaisim¹; Redha E. Al-Bayati² and Abdul Hussain K. Sharba³

¹ Al-Mustansiriya University of \College of Pharmacy

^{2,3} Al-Mustansiriya University \College of Science/ Chemistry Department

الخلاصة

تناول هذا البحث تحضير بعض مركبات البايرازولين المشتقة من ملح كلوريد الدايزونيوم للمركب 4-امينو حامض البنزويك. تم تحضير مركبات الازو عن طريق مفاعلة ملح كلوريد الدايزونيوم مع مركبات حاوية على مجموعة المثليين الفعالة مثل (ethylcyanoacetate), (ethyl acetoacetate) و (malonitrile) باستخدام الايثانول كمذيب بوجود خلاص الصوديوم حيث تم الحصول على المشتقات [3-1]. تضمن البحث ايضاً تكاثف حلقي للمركبات [3-1] مع الفينيل هيدرازين [6-4] و الهيدرازين [9-7] في الايثانول عند درجة غليانه للحصول على مشتقات البايرازولين للمركب 4-امينو حامض البنزويك. بعدها اجري تفاعل المركب [9] مع كلوريد الثايونيل للحصول على مشتق حامض الكلوريد [10], و تم تحويل هذا المشتق الى مشتق الهيدرازيد [11] بالمفاعلة مع الهيدرازين. تضمن البحث ايضاً تحضير عدد من قواعد شف [12-15], بمعاملة المركب [11] مع عدد من الالديهيدات و الكيتونات الاروماتية المختلفة, و من ثم غلق حلقي لاثنين من هذه القواعد بمفاعلتها مع (α -mercapto acetic acid) للحصول على [16,17]. أخيراً تم تحضير مشتق الاوكسادايازول [18] من تصعيد مشتق هيدرازيد الحامض مع CS_2 و KOH في الايثانول المطلق.

ABSTRACT

In this work pyrazolin derivatives were prepared from the diazonium chloride salt of 4-aminobenzoic acid. Azo compounds were prepared from the reaction of an ethanolic solution of sodium acetate and calculated amount of active methylene compounds namely, (ethyl cyanoacetate), (ethyl acetoacetate) و (malonitrile) to obtain the corresponding hydrazono derivatives [1-3]. Cyclocondensation reaction of compounds [1-3] with phenyl hydrazine [4-6] and hydrazine hydrate [7-9] in ethanol affording the corresponding pyrazoline-5-one derivatives of 4-aminobenzoic acid. Then compound [9] was reacted with thionyl chloride to give the corresponding acid chloride derivative [10], followed by conversion into the corresponding acid hydrazide derivative [11] carboxylic acid when treated hydrazine hydrate. Schiff's bases [12-15] were prepared by refluxing of compound [11] with different aromatic aldehydes and ketons, then two compounds from the Schiff's bases were cyclized with α -mercapto acetic acid to give [16,17]. Finally, oxadiazole derivative [18] has prepared by condensation of its acid hydrazide derivative with carbon disulfide in basic medium.

INTRODECTION

Heterocyclic compounds represent an important class of biologically active molecules. Specifically, those containing the pyrazole nucleus have been shown to possess high biological activities as herbicides, fungicides, analgesics, etc (1). Pyrazole derivatives have attracted particular interests during the last twenty five years due to the use of such ring system as the core structure in many drug substances, covering wide range of pharmacological applications (2-4). Some novel pyrazole derivatives containing sulfonamide moieties as anti microbial agents (5). Various sulfa drugs were coupled with active methylene compounds to give various hydrazones, then novel series of pyrazoles derivatives (6). Moreover; reaction of azo compounds with substituted acetoacetic ester derivatives using acetic acid as solvent (7). Azo pyrazolone derivatives were used for this purpose instead of inorganic pigment (8), have prepared an azo pyrazolone compound such as barium, strontium, magnesium, manganese,

sodium, and especially calcium. The reaction of monosubstituted hydrazides with 1,3-dicarbonyl compound is widely used for the synthesis of pyrazoles. (9).

MATERIALS AND METHODS

Apparatus and Chemicals

Electrothermal 9100 melting point apparatus, Perkin-Elmer 1310 infrared spectrophotometer or a Shimadzu FTIR-800, as KBr discs or thin films, UV-Visible Varian UV-Cary-100 spectrophotometers were used in this work. ¹H-NMR spectra was recorded on spectrometer (200MHz) at Silicone Research Center at Wisconsin University, USA. Tetramethylsilane was used as an internal reference and DMSO as solvent. All the chemicals used were supplied by Merck, Fluka and BDH chemicals. The solvents were purified by distillation and dried with anhydrous calcium chloride.

Synthesis of compounds:

Synthesis of hydrazone derivatives [1 - 3] (10)

To an ice-cooled mixture of the appropriate active methylene compound (malonitrile, ethyl cyanoacetate and ethyl acetoacetate) of each (0.01 mole) and sodium acetate (0.05 mole, 4.10 g) in ethanol (50 ml), was added dropwise with stirring to a cooled solution of the diazonium salt over 15 minute. The solid product was collected and recrystallized from ethanol.

General procedure for the synthesis of [4-6] (10)

To a solution of compound [1 - 3] (0.01 mole) in glacial acetic acid (30 ml), phenyl hydrazine (0.012 mole, 1.3 g) and anhydrous sodium acetate (0.01 mole, 0.82 g) was added. The reaction mixture was heated under reflux for 4 hours. The mixture was poured into ice-cold water and stored in a refrigerator for 12 hours. The crude product, which is separated, was washed with water, dried and recrystallized from appropriate solvent.

General procedure for the synthesis of [7-9] (10)

A mixture of azo derivative [1 - 3] (0.01 mole) and hydrazine hydrate (95 %) (0.012 mole, 0.35 g) in ethanol (30 ml) was heated under reflux for 4 hours. The reaction mixture was concentrated and the reaction product was allowed to cool. The separated product was filtered off, washed with water, and recrystallized from the appropriate solvent.

Synthesis of 4-[(3-methyl-5-oxo-4,5-dihydro-1H-pyrazol-4-yl)diazenyl] benzoyl chloride [10]

A mixture of compound [9] (0.01 mole, 2.46 g) and thionyl chloride (7 ml) was gently refluxed for 2 hours. After cooling, excess thionyl chloride was removed under reduced pressure. The product was recrystallized from benzene.

Synthesis of 4-[3-methyl-5-oxo-4,5-dihydro-1H-pyrazol-4-yl)diazenyl] benzohydrazide [11]

To a stirred solution of compound [9] (0.005 mole, 1.32 g) in dry benzene (15 ml), a mixture of hydrazine (95 %) (0.01 mole, 0.35 gm) and benzene (10 ml) was added dropwise. The mixture refluxed for 2 hours, cooling, excess benzene was removed under reduced pressure. The product was collected and recrystallized from the appropriate solvent.

Synthesis of Schiff's bases derivatives of 4-(3-Methyl-5-oxo-4,5-dihydro-1H-pyrazol-4-ylazo)-benzoic acid hydrazide [12-15]

To a stirred solution of compound [11] (0.01 mole, 2.6 g) in absolute ethanol (30 ml), the appropriate aldehyde or ketone was added (0.01 mole). The mixture was refluxed for 3 hours and cooled to room temperature. The precipitate was filtered and recrystallized from ethanol.

Synthesis of thiazolidine derivatives [16 and 17]

A solution of α -mercaptoacetic acid (0.01 mole, 0.92 g) in (15 ml) dry benzene was added slowly with stirring to a solution of compounds [12 and 13] (0.01 mole) in (15 ml) of dry benzene. The mixture was refluxed for 10 hours. The solution were concentrated and neutralized with sodiumbicarbonate solution (10 %). The solid product was filtered and recrystallized from appropriate solvent.

Synthesis of 4-[4-(5-Mercapto-[1,3,4]oxadiazol-2-yl)-phenylazo]-5-methyl-2,4-dihydro-pyrazol-3-one [18]

To a mixture of compound [11], (0.01 mole, 2.6 g) in a solution of potassium hydroxide (0.01 mole, 0.56 g), (100 ml) of ethanol (96 %) was added. carbon disulfide (0.2 mole, 12 ml) was added slowly with stirring. The mixture was refluxed for (5-6 hours). The mixture was cooled, concentrated under vacuum, poured slowly with stirring onto ice (60 g). The solution was acidified with dilute hydrochloric acid (10 %) to (pH 5-6); the resulting precipitate was recrystallized from the appropriate solvent.

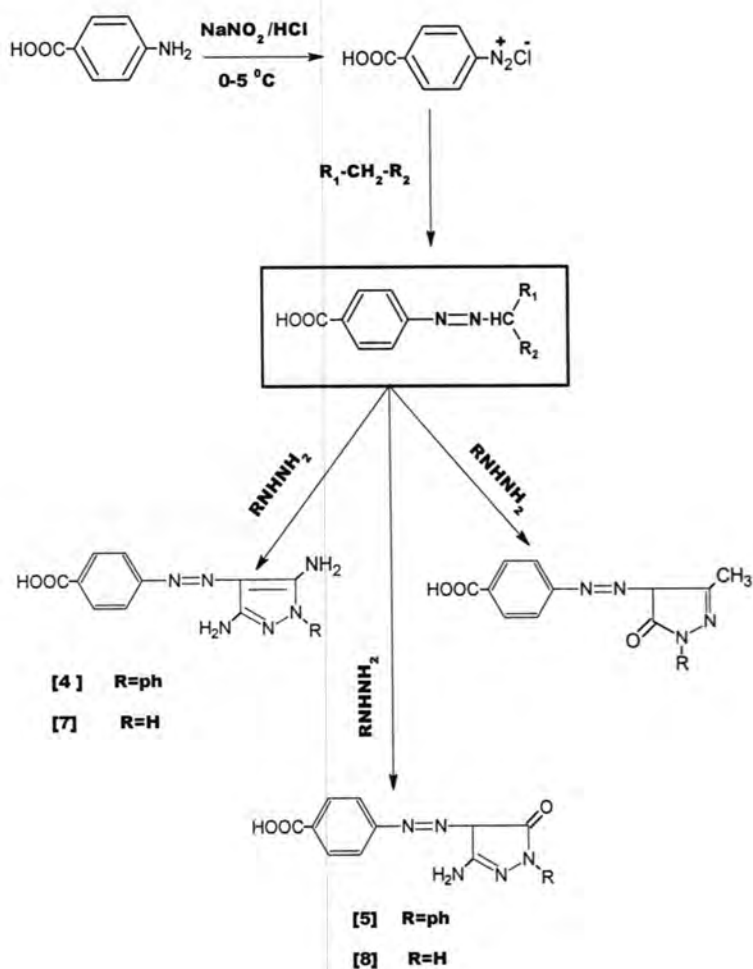
Table -1: The physical properties of compounds [1-18]

Compound Number	Molecular Formula	M.P/ °C	Color	Purification solvent	Yield (%)
1	C ₁₀ H ₆ N ₄ O ₂	180-182	Yellow	Chloroform	82
2	C ₁₂ H ₁₁ N ₃ O ₄	195-197	Yellow	Benzene	76
3	C ₁₃ H ₁₄ N ₂ O ₅	201-203	Green	Ethanol	88
4	C ₁₆ H ₁₄ N ₆ O ₂	273-275	Pale Brown	Chloroform	50
5	C ₁₆ H ₁₃ N ₅ O ₃	262-265	Orange	Benzene	43
6	C ₁₇ H ₁₄ N ₄ O ₃	240-243	Deep-Orange	Ethanol	83
7	C ₁₀ H ₁₀ N ₆ O ₂	235-237	Pale Brown	Chloroform	46
8	C ₁₀ H ₉ N ₅ O ₃	218-220	Pale Brown	Benzene	40
9	C ₁₁ H ₁₀ N ₄ O ₃	240-242	Orange-Yellow	Ethanol	68
10	C ₁₁ H ₉ ClN ₄ O ₂	217 dec.	Deep-Green	Benzene	82
11	C ₁₁ H ₁₂ N ₆ O ₂	250-252	Pale Brown	Ethanol	70

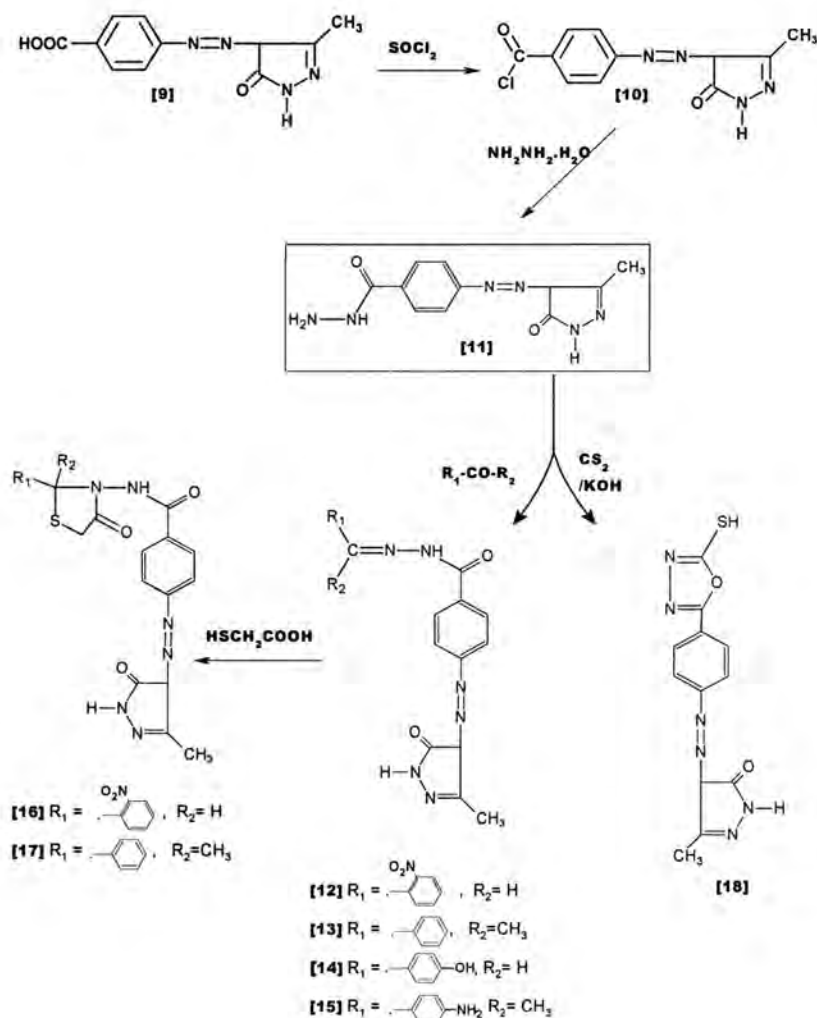
12	C ₁₈ H ₁₅ N ₇ O ₄	280-282	Brown	Ethanol	73
13	C ₁₉ H ₁₈ N ₆ O ₂	257-259	Yellow	Ethanol/water 1:1	62
14	C ₁₈ H ₁₆ N ₆ O ₃	233-235	Pale-green	Ethanol/water 1:1	77
15	C ₁₉ H ₁₉ N ₇ O ₂	271 dec.	Yellow	Ethanol	78
16	C ₂₀ H ₁₆ N ₇ O ₅ S	295dec	Deep-Green	Chloroform	43
17	C ₂₀ H ₁₇ N ₆ O ₄ S	290 dec.	Brown	Chloroform	57
18	C ₁₁ H ₁₀ N ₆ O ₂ S	225-228	Brown	Chloroform	57

RESULTS AND DISCUSSION

For the synthesis of the target 4-aminobenzoic acid derivatives in this work, the reaction sequences are outlined in schemes (1 and 2).



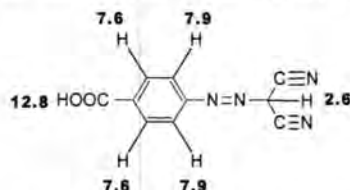
Scheme (1)



Scheme (2)

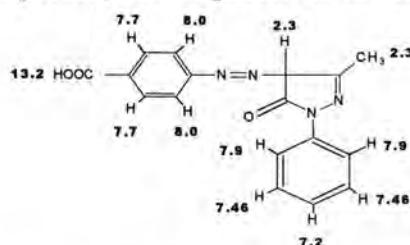
The prepared diazonium chloride of 4-aminobenzoic acid was added to an ethanolic solution of sodium acetate and calculated amount of some active methylene compounds, namely, malonitrile, ethyl cyanoacetate, and ethyl acetoacetate to afford the corresponding hydrazono derivatives [1- 3] as shown in Scheme (1). The IR spectrum of compound [1] it shows a characteristic (CN) stretching band at (2260cm^{-1}), at (1700 cm^{-1}) due to ($\text{C}=\text{O}$) stretching vibration of carboxylic acid while the band at ($2600\text{-}3200\text{ cm}^{-1}$) due to OH stretching vibration, also the band at (1570) refer to azo group stretching vibration. The IR spectrum of compound [2] shows a characteristic (CN) stretching band at (2240 cm^{-1}) and absorption band at (1720 and 1690 cm^{-1}) due to ($\text{C}=\text{O}$) stretching vibration of ester and carboxylic acid, respectively. The spectrum also shows a band at (1550 cm^{-1}) corresponding to the stretching vibration of the azo group. The IR spectrum of compound [3] shows a characteristic band at (1735 cm^{-1}) for the carboxylic ester moiety, while bands at (1715 cm^{-1}), and (1685 cm^{-1})

corresponding to the characteristic ($\text{C}=\text{O}$) of acetyl and carboxylic acid, respectively. The band at (1530 cm^{-1}) corresponds to the stretching vibration of the azo group, and the broad band at ($2600\text{--}3200\text{ cm}^{-1}$) refers to stretching vibration of hydroxyl group. The $^1\text{H-NMR}$ spectrum of compound [1] showed signals at δ (2.6 ppm) integrated for one proton, which was assigned for the proton of the malonic group. Aromatic protons appeared as AB quartet at δ (7.6-7.9) integrated for four protons. A signal at δ (12.8 ppm) integrated for one proton, may be attributed to the proton of the carboxylic acid group.

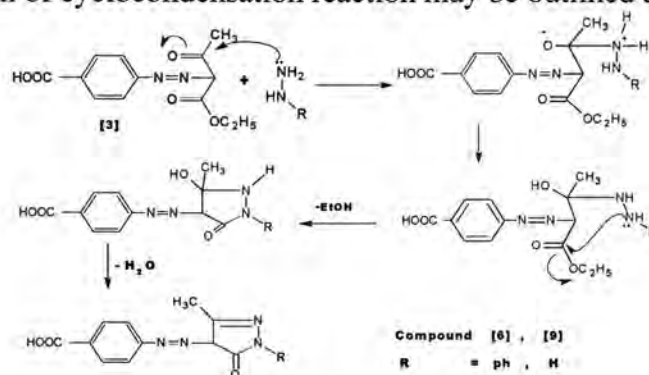


Hydrazons are easily undergoing cyclocondensation reaction with hydrazine hydrate or phenyl hydrazine in boiling ethanol afford to the corresponding pyrazoline-5-one derivatives of p-aminobenzoic acid. Thus cyclization of [1-3] with phenyl hydrazine yielded the corresponding products [4-6]. On the other hand reactions of [1-3] with hydrazine hydrate afford the corresponding derivatives [7-9], respectively (scheme 1). The IR spectrum of compound [4], shows the disappearance of the characteristic band of (CN) stretching vibration at (2260 cm^{-1}) and appearance of a band at ($3400\text{--}3300\text{ cm}^{-1}$) attributed to the stretching vibration of (NH_2) group and band at (1290 cm^{-1}) due to (N-Ph) stretching vibration which give a good indication for the cyclization⁽¹¹⁾. The U.V. spectrum of this compound, has λ_{max} (MeOH) at (377 nm and 250.0 nm) due to ($\pi\text{--}\pi^*$) transitions. The IR spectrum of compound [6] shows the disappearance of the characteristic band of acetyl carbonyl group and carboxylic acid ester at (1740 and 1715 cm^{-1}), and appearance of a band at (1610 cm^{-1}) refer to ($\text{C}=\text{N}$) bond stretching vibration and band at (1270 cm^{-1}) due to (N-Ph) stretching vibration. The IR spectrum of compound [8], shows the disappearance of the characteristic band of (CN) stretching vibration at (2240 cm^{-1}), and appearance of two bands at (3300 , 3200 and 3160 cm^{-1}) attributed to the stretching vibration of (NH , NH_2) groups and appearance of a band at (1647 cm^{-1}), due to ($\text{C}=\text{O}$) stretching vibration of the ring system, finally the band at (1610 cm^{-1}) is due to ($\text{C}=\text{N}$) stretching vibration. The IR spectrum of compound [9], shows the disappearance of the characteristic bands of the acetyl carbonyl group and carboxylic acid ester at (1735 , 1715 cm^{-1}), and the appearance of strong bands in the (3450 cm^{-1}), attributed to (N-H) stretching vibration and the bands of ($\text{C}=\text{O}$) carboxylic acid appeared at (1680 cm^{-1}), pyrazolinone ring ($\text{C}=\text{O}$) stretching vibration appeared at (1650 cm^{-1}) and (OH_{st}) appear at ($2600\text{--}3300\text{ cm}^{-1}$). On the other hand, in compounds [4, 5, 7, and 8] we noted the disappearance of (CN) stretching vibration band at (2200 cm^{-1}) and appearance of bands at ($3400\text{--}3300\text{ cm}^{-1}$)

attributed to the stretching vibration of NH_2 group. The ^1H -NMR spectrum of compound [6] showed a singlet at δ (2.3) ppm integrated for three protons assigned for the methyl group protons. The signal at δ (2.31) ppm integrated for one proton of the pyrazol ring. Aromatic protons appeared as AB quartet for the p-substituted ring at (7.7-8.0) ppm, (7.9) ppm as doublet, (7.46) ppm as triplet, (7.46) ppm as triplet and (7.23) ppm as triplet for the other ring. A signal at δ (13.2) integrated for one proton, for the proton of the carboxylic acid group.



The mechanism of cyclocondensation reaction may be outlined as follows:



Scheme (3)

The IR spectrum of compound [10] shows the disappearance of the hydroxyl group of the starting material and appearance of the new ($\text{C}=\text{O}$) band at (1780 cm^{-1}), for the acetyl chloride. The spectrum also shows an absorption band at (700 cm^{-1}) referring to ($\text{C}-\text{Cl}$) band ⁽¹²⁾. The U.V. spectrum of this compound, has λ_{max} (MeOH) at (240 and 344 nm) responsible for ($\pi-\pi^*$). The IR spectrum of compound [11], shows an absorption band at (1700 cm^{-1}) for ($\text{C}=\text{O}$) stretching vibration which appears at (1780 cm^{-1}) in the acid chloride derivatives and at (3300) for ($\text{N}-\text{H}$) and ($3450-3500\text{ cm}^{-1}$) for (NH_2) stretching vibration. The Schiff's bases [12-15] have been synthesized by the condensation of [8] with appropriate aromatic aldehydes or ketones in the presence of absolute ethanol as a solvent. The IR spectrum of compound [12], shows the characteristic band at (3300 and 3165 cm^{-1}) due to (NH) stretching vibrations, at (1658 cm^{-1}) for ($\text{C}=\text{O}$) of amide group and at (1635 cm^{-1}) due to ($\text{C}=\text{N}$) stretching vibration. Other

bands of the synthesized Schiff's bases [12-15] are listed in table (2). In general, the thiazoline-4-one have been obtained by treatment of the corresponding Schiff's bases [12] and [13] with mercaptoacetic acid in dry benzene as a solvent. The IR spectrum of compound [17] revealed a strong band around (1710 cm^{-1}) for amide carbonyl group of thiadiazole-4-one and (1690 cm^{-1}) for the carbonyl of the pyrazolone ring. The IR spectrum of compound [18], shows absorption band at (3350 cm^{-1}) which corresponds to (NH) stretching vibration, the spectrum also shows a band at (1640 cm^{-1}) due to (C=N) stretching vibration. Another band for (C-O-C) stretching vibration appears at (1180 cm^{-1}). The U.V. spectrum of this compound, has λ_{max} (MeOH) at (410 nm and 289.0 nm) due to ($\pi - \pi^*$) transition.

Table -2: Spectral data for compounds [1-18]

Compound Number	UV λ_{\max} (nm)	$\nu(\text{C=O})$	$\nu(\text{C=N})$	N(N=N)	$\nu(\text{C-H})_{\text{al}}$	$\nu(\text{C-H})_{\text{ar}}$	Others
1	356 348	1700 (acid)	-----	1570	2950asy 2820 sy	3080	2600-3200(OH) _{st} 2260(C \equiv N)
2	362 290	1720(ester) 1690(acid)	-----	1550	(2950)asy (2850)sy	3050	2240(C \equiv N) 2600-3100(OH)
3	362 238	1735(ester) 1715(acetyl) 1685 (acid)	-----	1530	(2970)asy (2850) sy	3050	2600-3200 OH) _{st}
4	377 250	1680(acid)	1623	1540	2950 asy 2850 sy	3050	3400-3300 (NH ₂) _{st} 2600-3100 OH) _{st} 1290(N-Ph)
5	360 245	1650(ring) 1690(acid)	1610 interfere with C=C	1540	(2950)asy (2800)sy	3070	2600-3600(O-H) 1310 (N-Ph)
6	300 258	1650 (ring) 1685 (acid)	1610 interfere with C=C	1535	(2900)asy (2800)sy	3050	2600-3200(O-H) 1270(N-Ph)
7	295	1650(acid)	1620 interfere with C=C	1560	2950 asy 2820 sy	3030	3400-3500 (NH,NH ₂) _{st} 2700-3600(OH) _{st}
8	260	1647(ring) 1680(acid)	1610 interfere with C=C	1540	2950 asy 2800 sy	3070	2600-3600(O-H) 3400-3500 (NH ₂) _{st}
9	285 261	1650(ring) Interfere with 1680(acid)	1620 interfere with C=C	1580	(2920) asy (2850) sy	3090	2600-3300(O-H) Interfere with 3450(NH) _{st}
10	344 240	1780 1660(ring)	1610 interfere with C=C	1550	(2950)asy (2800) sy	3050	700 (C-Cl) _{st} 3350 (N-H) _{st}
11	320	1700 Interfere with 1685 (ring)	1610 interfere with C=C	1555	(2970) asy (2820) sy	3080	3450-3500 (NH) _{st} 3300 (NH) _{st}
12	331 227	1658	1635	1540	(2995) asy (2850) sy	3040	3165-3300 (N-H) _{st} 1360, 1515 (NO ₂) _{st}
13	316 215	1650	1620	1550	(2950) asy (2850) sy	3090	3250 (N-H) _{st}
14	333	1655	1620 Interfere with C=C	1545	(2950) asy (2820)sy	3075	3230 (N-H) _{st}
15	290	1665	1620	1550	(2940) asy (2800) sy	3030	3300-3425 (NH ₂) _{st} Interfere with 3275(NH) _{st}
16	390 285	1705 1680	1638	1520	(2960)al	3020	-----
17	409 294	1710(thia) 1690(amid) Interfere with 1685 (ring)	1660	1550	(2950)al	3050	-----
18	410 289	1640 (ring)	1640 interfere with C=O	1550	(2970)asy (2800) _{sy}	3080	1180 (C-O-C) _{st} 2750(SH) _{st} 1200 (C=S) _{st} 3350 (NH)

REFERENCES

1. X. Ren, H. Li., C. Wu and H. Yang, " Synthesis of a small library containing substituted pyrazoles" *Arkivoc* (xv) :59-67(2005).
2. E. S. Othman " Some nucleophilic cyclization reaction with 3-[4-(benzo[1,3]dioxolyl methylene) pyrazolyl]quinolone", *Acta Chim, Slov.*, 50:15-28(2003).
3. M. Shalaby, O. A. Fathalla, E. M. M. Kassem, and M. E. A. Zaki "Synthesis of new 5-N-pyrazolol amino acids, pyrazolo-pyrimidines and pyrazolopyridines derevatives ", *Acta. Chim. Slov.*, 74 :187-203(2000).
4. O. Prakash, K. Pannu and A. Kumar "Synthesis of Some New 2-(3-Aryl-1-phenyl-4-pyrazolyl)-benzoxazoles Using Hypervalent Iodine Mediated Oxidative Cyclization of Schiff's Bases", *Molecules*, 11 : 43-8(2006).
5. M. S. A. El-Gaby, N. M. Taha, J. A. Micky and M. A. El-Sharief, " Preperation of some new novel 3,5-diaminopyrazole, pyrazolo[1,5-a][1,3,5]triazine derevatives containing sulfonamide moities as antimicrobial agents "*Acta, Chim, Slov.*, 49 :159-71(2002).
6. S. A. El-Assiery, G. H. Sayed, A. Foude " Synthesis of some new annulated pyrazolo-pyrido (or pyrano) pyrimidine, pyrazolopyridine and pyranopyrazole derivatives", *Acta Pharm*, 54 :143-50(2004).
7. V. V. Dabhakar and R. P. Gavand " Amicrowave-catalyzed rapid, efficient and ecofriendly synthesis of substituted pyrazol-5-ones Short communication)", *J. Serb. Chem. Soc.* 68(10) :723-27(2003) .
8. A. P. Chorlton and J. Mason "Azo pyrazolone pigments", *U.S. Patent*, 5,919,915 (1999).
9. Z. Teter, D. Zicane, I. Ravina, M. Petrowa, E. Gudrinece and U. Kalejs "1-(1-Carboxy-2-R-4-methylcyclohex-4-enyl)carbonyl- and 1-(2-R-4-Methylcyclohex-4-enyl)carbonyl-3,5-dimethyl (diphenyl) pyrazoles", *Chemistry of Heterocyclic Compounds*,38(6):677-81 (2002).
10. M. A. Saleh, M. F. Abdel-Mageed, M. A. Abdo and A. B. M. Shoker "Synthesis of Novel 3H-Quinazolin-4-ones Containing

- Pyrazolinone, Pyrazole and Pyrimidinone Moieties", **Molecules**, 8 :363-73(2003).
11. A. K. Mittal and O. P. Singhal "isoxazolines as possible biological agents" **J. Ind. Chem. Soc.**, LIX, may :711-13(1982).
12. V. M. Parikh, "**Absorption Spectroscopic of Organic Molecules**"
Translated by A. H. Khuthier, J. M. A. Al-Rawi, M. A. Al-Iraqi,
Mousul University (1985).

Preparation of new HPLC stationary phase and study of their chromatographic performance towered the separation of amino acids and poly aromatic compounds.

¹Noor M. Ali, ²Shahbaz A. Maki and ¹Hadeel S. Abd Al- wahab

¹Al-Nahrain University, College of Medicine, Medical Research Center, Al-Nahrain University, Iraq

²Al-Nahrain University, College of Science, Department of Chemistry, Al-Jaderia, Baghdad, Iraq.

الخلاصة

تم في هذا البحث تحضير طور ثابت جديد لغرض استخدامه في الفصل الكروماتوغرافي سائل عالي الإيداء وذلك من خلال تفاعل راتنج المتبادل الأيوني الأمبرلايت مع صبغة الأليزارين الحمراء. أثبت تحاليل اشعة الحمراء ارتباط الصبغة مع الراتنج مثلما دل عليه المظهر الخارجي للراتنج الجديد وتغيير في صفاته الكروماتوغرافية.

تم قياس السعة الكروماتوغرافية للطور الثابت الجديد وتغيير في صفاته ووجد أن السعة للراتنج تساوي 6.65 meq./g الذي هو ضعف السعة للراتنج الأمبرلايت الأصلي الذي يساوي 3.05 meq./g .

تم تعبئة الطور الثابت في عمود من الفولاذ المقاوم للصدأ خاص بـ HPLC بواسطة طرق التعبئة الخاصة تم تحليل الأحماض الأمينية مثل tryptophan, histidine, phenylalanine, tyrosine بواسطة عمود الأمبرلايت- الأليزارين استخدام طور متحرك مائي حامضي pH= 2.5 وقاعدي pH= 8.6 وكان زمن احتجاز الأحماض الأمينية كالاتي histidine 2.18 دقيقة, phenylalanine 2.49 دقيقة, tyrosine 2.75 دقيقة و tryptophan 3.10 دقيقة عند استخدام طور متحرك مائي حامضي pH= 2.5 وأما عند استخدام طور متحرك مائي قاعدي pH= 8.6 فإن زمن الاحتجاز كان histidine 2.45 دقيقة, phenylalanine 2.94 دقيقة, tyrosine 3.14 دقيقة و tryptophan 3.79 دقيقة. وتم تحليل المركبات الحلقية الهيدروكربونية مثل naphthalene, Acenophthene, anthracene, phenatherene و flourine بواسطة عمود الأمبرلايت- الأليزارين استخدام طور متحرك methanol pH= 2.5 و pH= 8.6 وكان زمن احتجاز المركبات الحلقية الهيدروكربونية كالاتي naphthalene 1.26 دقيقة, 1.78 Acenophthene دقيقة, anthracene 1.54 دقيقة, phenatherene 1.90 دقيقة و flourine 2.82 دقيقة عند استخدام طور متحرك مائي حامضي pH= 2.5 وأما عند استخدام طور متحرك مائي قاعدي pH= 8.6 فإن زمن الاحتجاز كان naphthalene 1.37 دقيقة, acenophthene 1.95 دقيقة, anthracene 1.74 دقيقة و phenatherene 2.29 دقيقة و flourine 3.79 دقيقة.

ABSTRACT

A new stationary phase was prepared by adsorption of Alizarin Red-S solution on Amberlite anion exchanger. The capacity of new prepared resin was 6.65meq./g which is approximately twice as those of Amberlite resin, 3.05meq./g. The resulted polymer has high rigidity with high stability and used as stationary phase for HPLC column. Amino acids (histidine, phenylalanine, tyrosine and tryptophan) were examined with this column with isocratic elution distilled water adjusted pH at 2.5 and 8.6 as a mobile phase with flow rate of 1.4ml/min and UV detection of 254nm. The retention times for histidine, phenylalanine, tyrosine and tryptophan were 2.18 min, 2.49 min, 2.75min and 3.10 min, respectively at pH 2.5. And when adjusted the pH of mobile phase at 8.6 the retention time. The retention times for these amino acids were 2.45 min, 2.94 min, 3.41min and 3.79 min, respectively. Furthermore some of poly aromatic compounds, such as naphthalene, acenophthene, anthracene, phenatherene and flourine were analyzed with this stationary phase. The eluent 100% methanol and also adjusted pH at 2.5 and 8.6 and with the same

condition of flow rate. The retention times for naphthalene, acenophthene, anthracene, phenanthrene and fluorine were 1.26 min, 1.78 min, 1.54min, 1.9min and 2.82 min, respectively at pH 2.5. and when adjusted the pH of mobile phase at 8.6 the retention time. The retention times for polyaromatic compounds were 1.37 min, 1.95 min, 1.74min, 2.29min and 3.79 min, respectively.

INTRODUCTION

The packing materials have been developed in which the stationary phase is chemically bonded to an insoluble matrix (solid support). BPC involved a relatively non-polar stationary phase used in conjugation with polar mobile phase to separate a wide variety of less polar solutes (1). Dohtsu(2) prepared silica material modified with anthracene and phthalimide-containing groups and used these stationary phases for the separation of mononucleotide and pentadecamer oligonucleotides. They proposed that the nucleic base stacking interactions were important for the separation obtained and proposed directions for the further development of such stationary phases. Tanaka (3) prepared alkylated stationary phases for reversed phase liquid chromatography based on polymer particles with aliphatic backbones, having hydroxyl groups. The chromatographic properties were examined in terms of steric selectivity and its preference toward aromatic and saturated compounds. Polymer support stationary phases were less hydrophobic than silica-based phases, but it showed preferential retention of aromatic compounds. Snyder and coworkers(4) showed that most samples exhibit significant changes in band spacing based on solvent strength optimization. Fetizer and Biggs(5) compared the elution strength of 11 common LC solvents using a marker set polycyclic aromatic hydrocarbons. With the exception of THF, they found the pure solvent and blended mixtures behaved quite differently. The preference shown by the polymer-based stationary phases toward rigid, compact molecules over flexible and/or bulky molecules can be explained by the contribution of the polymer network structure, to the retention process. The polymer-based stationary phases showed greater variation of selectivity due to changes in the composition of the mobile phase (1). In this work Amberlite - Alizarin Red-S was prepared and used as a new stationary phase for HPLC column. It is used for analysis of several aromatic amino acids and poly aromatic compounds. Isocratic and elution programs were applied for separation as well as the percent composition of the mobile was studied.

MATERIALS AND METHODS

Equipments

High performance liquid chromatography type Shimadzu (Japan) which consisted of a system controller model SCL-10 Avp, a degasser model DGU-RA, a liquid delivery pump model LC-8Avp, UV-Visible detector model SPD-10Avp and Rheodune manual injector model 3298(USA) equipped with 5 μ l sample loop was used. The HPLC system has been interfaced with computer via a Shimadzu class-VP5 chromatography data system program supplied by the manufacturer; Epson LQ-300 Printer model P852A (Japan). Shimadzu Fourier transforms infrared model FTIR 8300 (Japan) was used to measure the IR spectra for resins. Combination glass electrode was used to measure the pH of polymer solutions (Germany). Sonicator Sonerex model Super RK103H Mandolin (Germany). Two blank stainless steel columns of dimensions 25 \times 0.4cm (i.d.).

Preparation of triethanolamine- glycerol-maleate polymer:

Four grams of Amberlite resin was first rinsed with 50ml deionized water in a 100ml beaker. A 10ml of 2.9×10^{-3} M Alizarin Red-S was then added with stirring to the beaker. A 10ml of 0.1M of NaOH solution was added drop-wise to the content of the beaker with continuous stirring. The color of the resin has been changed from yellow to deep blue. The content of the beaker was left to settle for period of time. The solution was then decanted and discarded. The resin was washed few times with deionized water, then rinsed with ethanol and dried in oven at 50°C over-nights and kept in desiccator for further. The FTIR spectrum for this resin was measured.

Preparation of standard:

A stock solution of 100ppm of standard amino acids and poly aromatic compounds were prepared by dissolving 10mg histidine in 0.1M of NaOH and diluted to 100ml with distilled water. The same procedure was followed in the preparation of phenylalanine, tyrosine and tryptophan stock solutions. Other standard solutions were prepared by subsequent dilution of the stock solutions. The solvent used to prepare these solutions before injection into HPLC was the mobile phase employed for their separation. A stock solution of 100ppm of standard polyaromatic compounds were prepared by similarly.

RESULTS AND DISCUSSIONS

Stationary phase in this work was done via adsorption of Alizarin Red-S on amberlite resin in which produces a hard and rigid. The resin was identified by FTIR in which the appearance of absorption band was different. The solubility

has been examined using different solvents such as acetonitrile, benzene, chloroform, dioxane, DMF, DMSO, hexane, methanol and water. It is found that the polymer insoluble and undecompose in all the above solvents and it is very stable. Column packing was done by using the slurry formed by mixing 4gm of resin powder with 15ml of deionized water and homogenized in an ultrasonic bath and placed in the slurry reservoir and the column was packed using down-flow packing system.

The study was carried out for the analysis of amino acids, histidine, phenylalanine, tyrosine and tryptophan by using the amberlite-Alizarin-Red-S column (25 x 0.4 cm). The retention times of amino acids gave a good sharp peak using distilled water adjusted pH at 2.5 and 8.6. Each amino acid injected alone and then made mixture of these compounds and also injected as shown in figure 1. The capacity factor K' for amino acids compounds chromatographed on the Amberlite-Alizarin-Red-S column were ranged from 1.67-3.13 in pH 2.5 and 1.78-2.51 at pH 8.6 as shown in table 1. These indicate that good competitive interaction between these compounds and stationary phase and mobile phase in both cases.

Table -1: Capacity K' , separation α factors and peaks asymmetry variation with changing the pH of mobile phase for amino acids using Amberlite-Alizarin-Red-S column (25x0.4 cm (id)).

Compounds		Retention time t_R	Capacity factor K'	Separation factor α	Peaks Asymmetry
Name	Mobile phase pH				
Histidine	2.5	2.18	1.67	-	1.36
	8.6	2.45	1.75	-	0.99
Phenylalanine	2.5	2.49	2.16	1.29	1.09
	8.6	2.94	1.98	1.11	1.16
Tyrosine	2.5	2.75	2.59	1.19	1.22
	8.6	3.14	2.24	1.13	1.56
Tryptophan	2.5	3.10	3.13	1.21	0.98
	8.6	3.79	2.51	1.12	1.36

- Not detected

The separation factor (α) values for histidine, phenylalanine, tyrosine and tryptophan were ranged from 1.21-1.29 at pH 2.5 and ranged from 1.11-1.13, at pH 6.0, 7.0, 8.0 and 9.0 respectively. These variations in capacity and separation factors of these analytes may indicate separation at the pH 2.5 buffer is the best pH buffer that can use for separating compounds. Also the study was carried out for analysis of poly aromatic compounds, naphthalene, acenophthene, anthracene, phenatherene and flourine by using the same column. The retention times of amino acids gave a good sharp peak using distilled methanol adjusted pH at 2.5 and 8.6. Each poly aromatic compounds injected alone and then made mixture of these compounds and also injected as shown in figure 2. The capacity factor K' for poly aromatic compounds chromatographed on this column were ranged from 1.26-2.82 in pH 2.5 and 1.37-3.12 at pH 8.6 as shown in table 2.

Table 2 Capacity K' , separation α factors and peaks asymmetry variation with changing the pH of mobile phase for amino acids using column.

Compounds		Retention time t_R	Capacity factor K'	Separation factor α	Peaks Asymmetry
Name	Mobile phase pH				
Naphthalene	2.5	1.26	1.12	-	2.48
	8.6	1.37	1.61	-	1.08
Acenophthene	2.5	1.78	2.50	1.49	1.46
	8.6	1.95	1.92	1.19	1.18
Anthracene	2.5	1.54	2.13	1.28	1.07
	8.6	1.74	2.49	1.14	1.01
Phenathrene	2.5	1.91	2.47	1.16	1.61
	8.6	2.29	2.81	1.13	0.98
Fluorine	2.5	2.82	2.76	1.13	1.76
	8.6	3.12	2.51	1.12	1.98

- Not detected

The separation factor (α) values for naphthalene, acenophthene, anthracene, phenatherene and flourine were ranged from 1.13-1.49 at pH 2.5 and ranged

from 1.12-1.19, at pH 6.0, 7.0, 8.0 and 9.0 respectively. These variations in capacity and separation factors of these analytes may indicate separation at the pH 2.5 buffer is the best pH buffer that can use for separating compounds. Quantitative analysis was studied from the construction of calibration curves for the amino acids and poly aromatic compounds. The linear calibration curves for these compounds are shown in figure 3 and 4. The linear equations and concentration range with the detection limit using Amberlite-Alizarin-Red-S column, eluent distilled water at pH 2.5 and pH 8.6, are listed in table 3 and 4.

Table -3: Linear equation, correlation coefficient and detection limits for the amino acids using two types of pH buffer.

Eluent at pH 2.5				
Compounds	Linear Equation $Y^*=mx^*+b$	Linear Conc. Range	correlation coefficient (R)	Detection Limit (ppm)
Histidine	$Y=92.806x+867.83$	0.05-50	0.9993	0.05
Phenylalanine	$Y=4880.3x+8309.50$	0.10-50	0.9996	0.10
Tryptophan	$Y=3009.4x+386.86$	0.10-50	0.9992	0.10
Tyrosine	$Y=26987X+736.83$	0.05-50	0.9998	0.05
Eluent at pH 8.6				
Compounds	Linear Equation	Linear Conc. Range	correlation coefficient (R)	Detection Limit (ppm)
	$Y=314.86x+983.59$	0.05-50	0.9991	0.05
Phenylalanine	$Y=11548x+1786.10$	0.10-50	0.9993	0.10
Tryptophan	$Y=7124x+2995.10$	0.10-50	0.9997	0.10
Tyrosine	$Y=31951X+9364.10$	0.05-50	0.9996	0.05

The slopes for the linear calibration curves using Amberlite-Alizarin-Red-S column ranged from 92.806 – 26987 depends upon the kind of amino acids when using buffer at pH 2.5. The correlation coefficients ranged from 0.9992 – 0.9998 with detection limit ranged from 0.05 to 0.10 ppm. While when using buffer at pH 8.6, the slopes for the linear calibration curves of the analyzed amino acids ranged from 314.86– 31951. The correlation coefficients ranged from 0.9991 – 0.9997 with detection limit for the three drugs was 0.05 ppm.

Table -4: Linear equation, correlation coefficient and detection limits for the poly aromatic compounds using two types of pH buffer.

Eluent at pH 2.5				
Compounds	Linear Equation $Y=mx^*+b$	Linear Conc. Range	correlation coefficient (R)	Detection Limit (ppm)
Acenophthene	$Y=29313x+29683.0$	0.1-50	0.9996	0.10
Anthracene	$Y=17197x+2045.4$	0.1-50	0.9998	0.10
Fluorine	$Y=50435x+49950.0$	0.10-50	0.9993	0.10
Naphthalene	$Y=38271x+7304.9$	0.10-50	0.9993	0.10
Phenathrene	$Y=77290x+3993.0$	0.05-50	0.9990	0.05
Eluent at pH 8.6				
Compounds	Linear Equation	Linear Conc. Range	correlation coefficient (R)	Detection Limit (ppm)
Acenophthene	$Y=29541x+21971.0$	0.10-50	0.9998	0.10
Anthracene	$Y=27343x+2945.4$	0.10-50	0.9997	0.10
Fluorine	$Y=50230x+5755.0$	0.05-50	0.9990	0.05
Naphthalene	$Y=38017x+14973.0$	0.10-50	0.9995	0.10
Phenathrene	$Y=77284x+4995.0$	0.10-50	0.9994	0.10

The slopes for the linear calibration curves using Amberlite-Alizarin-Red-S column ranged from 17197 – 77290 depends upon the kind of poly aromatic

Preparation of new HPLC stationary phase and study of their chromatographic performance towered the separation of amino acids and poly aromatic compounds.

Noor , Shahbaz and Hadeel

compounds when using buffer at pH 2.5. The correlation coefficients ranged from 0.9990 – 0.9998 with detection limit ranged from 0.05 to 0.10 ppm. While for when using buffer at pH 8.6, the slopes for the linear calibration curves of the analyzed drugs ranged from 29541 – 77284. The correlation coefficients ranged from 0.9990 – 0.9998 with detection limit for the three amino acids was 0.05ppm.

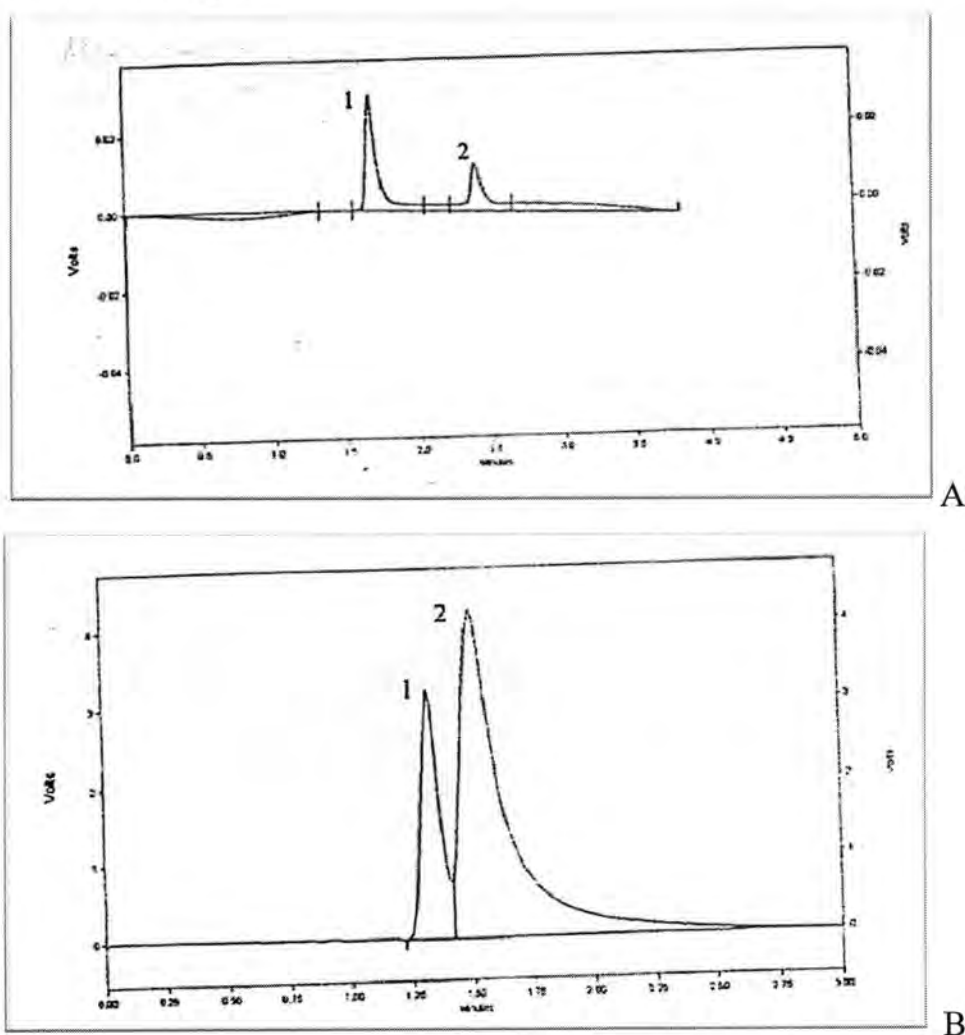


Figure-1:Chromatogram of amino acids (1) Histidine 25ppm, (2) Phenylalanine 25ppm. Using Amberlite-Alizarin-Red-S column, detection wavelength 254nm, and using distilled water as mobile phase (A) Adjusted at pH=2.5. (B) Adjusted at pH=8.6.

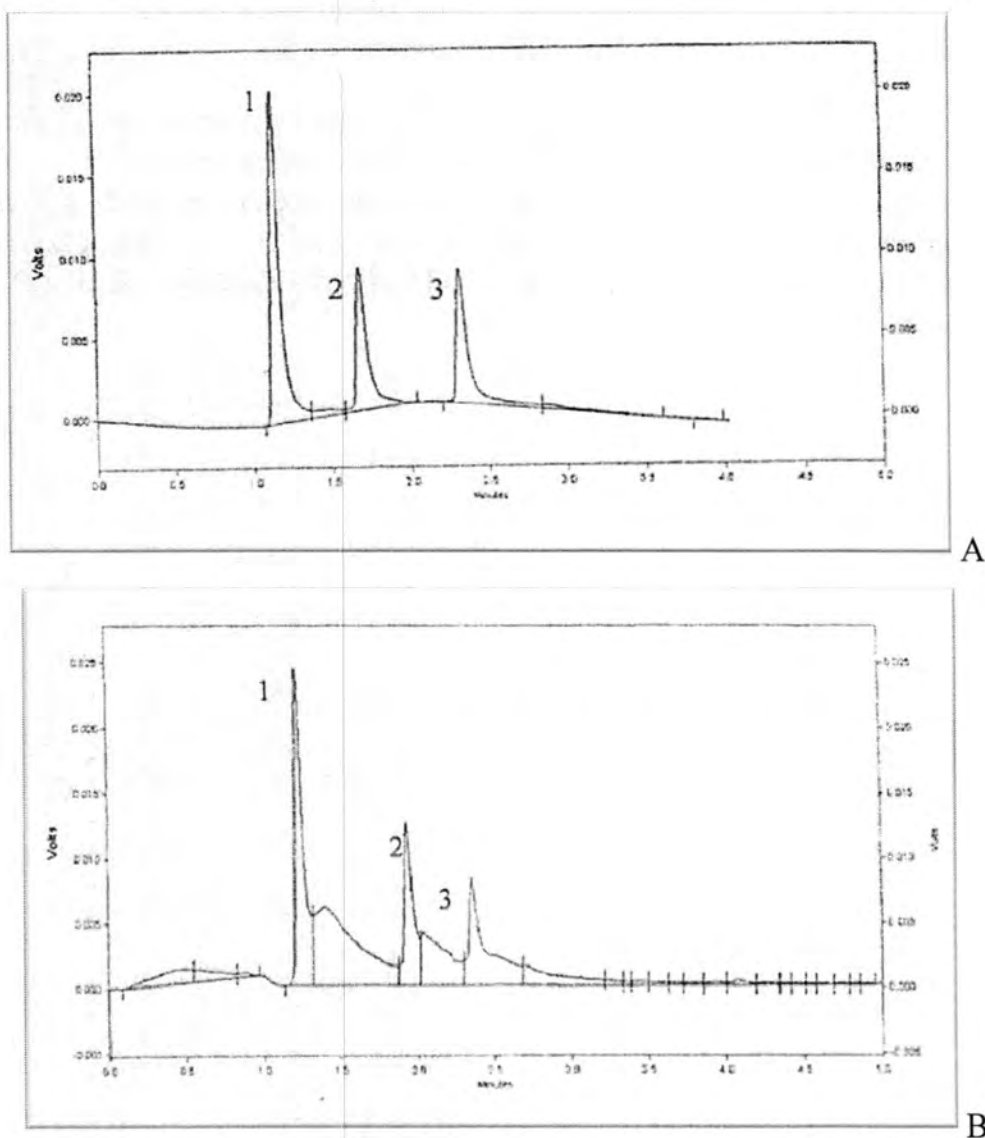


Figure-2: Chromatogram of poly aromatic compounds (1) Naphthalene 25ppm, (2) Acenophthene 25ppm and (3) Flourine 25ppm. Using Amberlite-Alizarin-Red-S column, detection wavelength 254nm, and using distilled water as mobile phase (A) Adjusted at pH=2.5. (B) Adjusted at pH=8.6.

Preparation of new HPLC stationary phase and study of their chromatographic performance towered the separation of amino acids and poly aromatic compounds.

Noor , Shahbaz and Hadeel

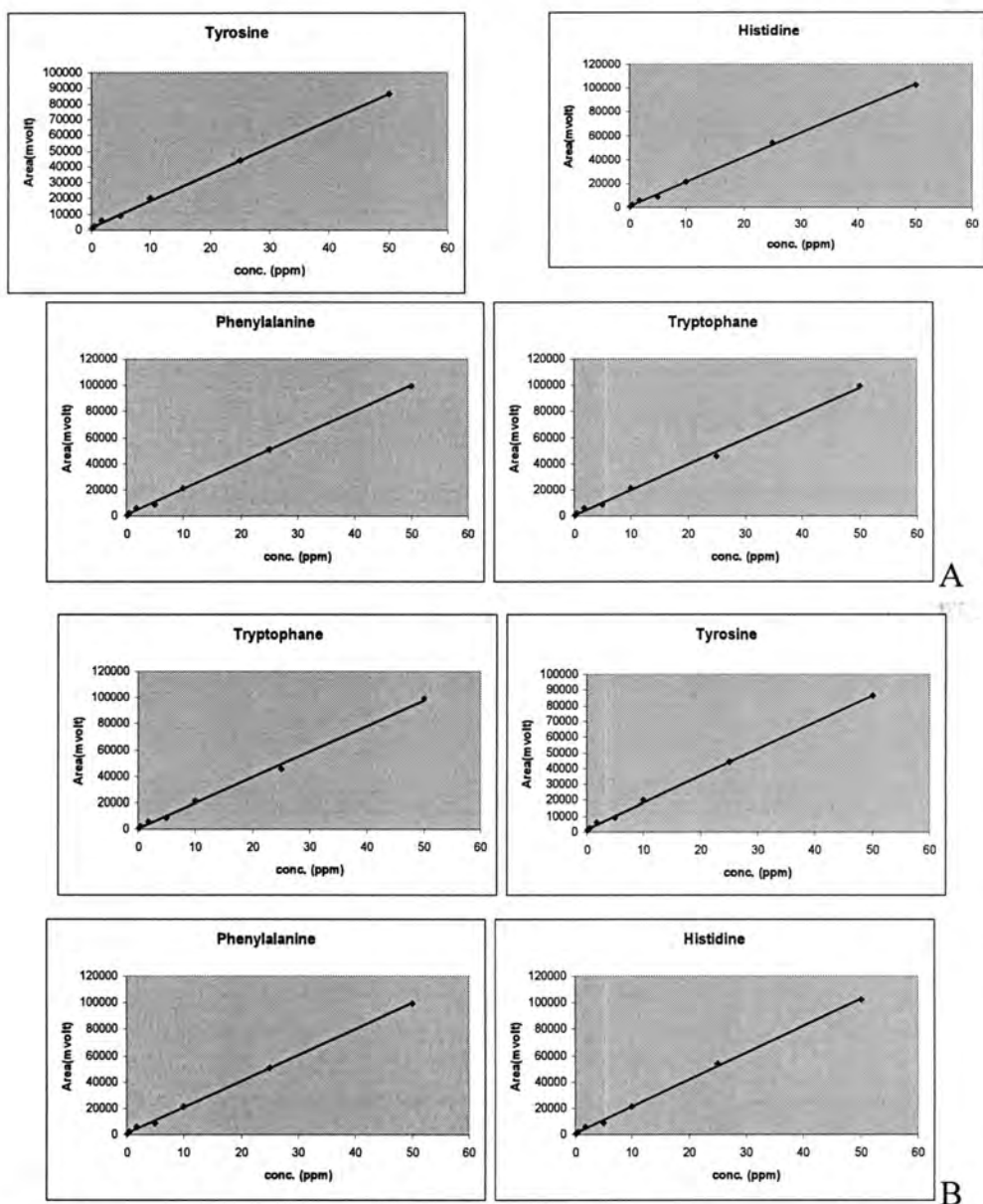


Figure-3: calibration curves of amino acids using column, and using distilled water as mobile phase (A) Adjusted at pH=2.5. (B) Adjusted at pH=8.6.

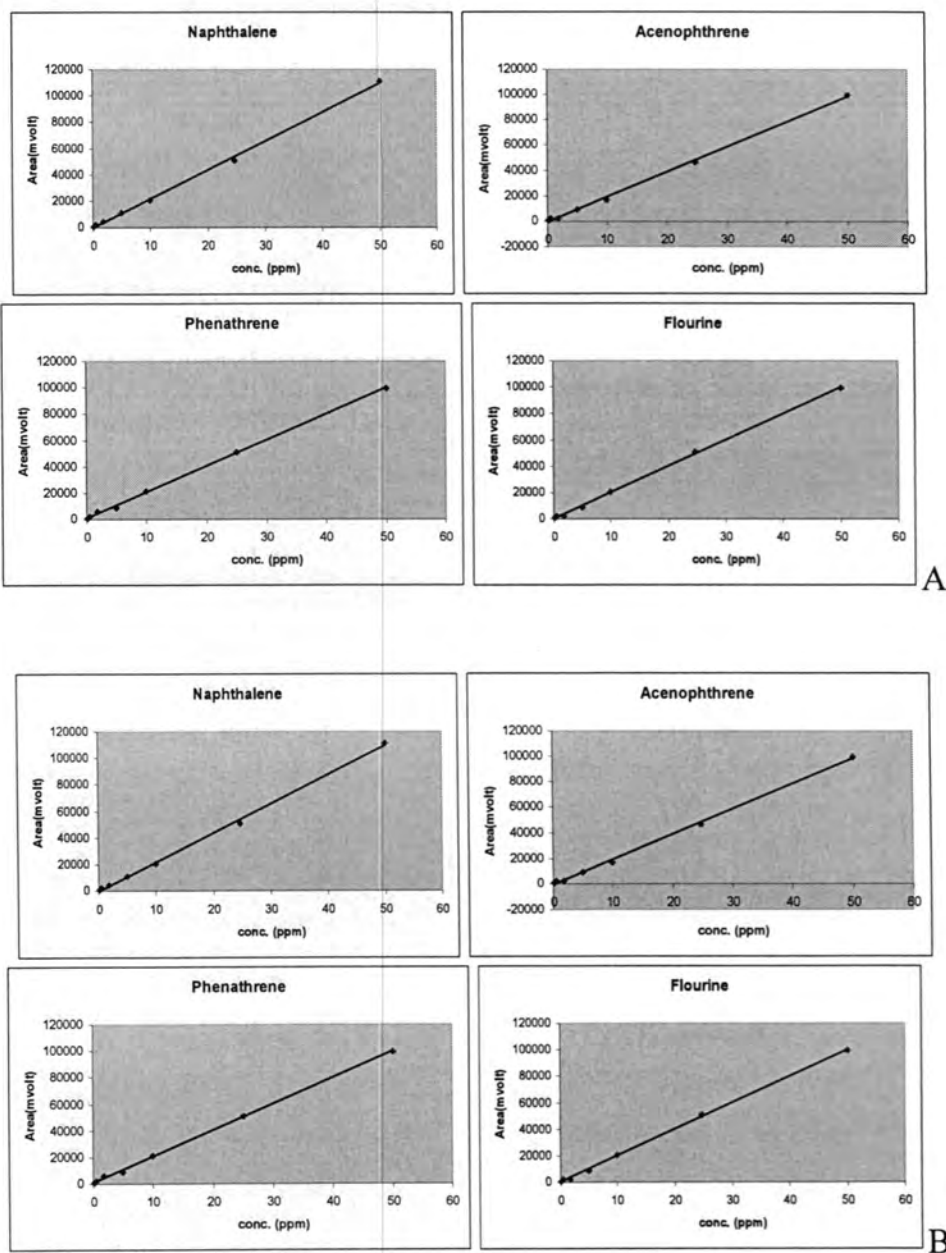


Figure-4: calibration curves of poly aromatic compounds using column, and using distilled water as mobile phase (A) Adjusted at pH=2.5. (B) Adjusted at pH=8.6.

Preparation of new HPLC stationary phase and study of their chromatographic performance toward the separation of amino acids and poly aromatic compounds.

Noor , Shahbaz and Hadeel

REFERENCES

1. Raithwaite, A. B., Smith, F. J. "chromatographic methods" Fourth edition, Chapman and Hall, London (1985).
2. Dohtsu K., Ohmori K., Fukuda R., Takenaka S., Takagi M., Analytical Sciences, 4, 371(1988).
3. Tanaka, N. Ebata T. Hashizume, K., Hosoya, K. Araki, M., J. Chromatography. 475,195(1989).
4. Snyder L., Qurry M., Glajch A., J. Chromatogr., 24, 33, (1989).
5. Fretzer J., Biggs W., J. Chromatographia, 27, 118(1989).

Simple and Rapid Method for Determination of Vitamin C, in pharmaceutical Preparations .

Hadi.H.Jasim

Chemistry Department, College of Science, Al-Mustansyriah University

الخلاصة

هذه الدراسة هي طريقة سهلة وسريعة لتقدير فيتامين (C) في مختلف المستحضرات الصيدلانية على هيئة حبوب او كبسولات وذلك من خلال التسحيح مع كلورامين -T (CAT) بوجود يوديد البوتاسيوم واستخدام النشاء كدليل وحيد خلال الدراسة . ان احتواء المحلول على بعض الايونات الفلزية مثل الخارصين والحديد والنحاس فانها لا تسبب أي تداخل ولا تؤثر على طريقة القياس ولكن احتواء المحلول المحضر على الكبريت او مركبات الكبريت والهاليد فانها تسبب تداخل ممكن التخلص من هذا التداخل باستخدام عوامل الحجب الكيميائي مثل الفورفورل والاكريلونتريل كما قدر في هذه الدراسة الفيتامين (C) مع السيستين والكبريت.

ABSTRACT

This study is simple and rapid method for determination of vitamin C in any pharmaceutical preparations (Tablets or capsules) by titration with a suitable titrant (Sodium N-chloro-4 toluenesulfonamide trihydrate) chloramine -T in the presence of potassium Iodide and starch as indicator . If the solution contains sulfite or sulfhydryl compounds interfere severely , but if the solution contains Zn^{+2} , Fe^{+2} , Ca^{+2} does not interfere . When using masking agent by a preaction with 2- furfuraldehyde and acrylonitrile, respectively. In this study Mixture of sulfite and cysteine are analyzed too .

INTRODUCTION

Vitamin C we can determined by much methods (1,2), chemical method for the determination of vitamin C are based on the reducing properties of its 1,2- diol group⁽¹⁾ . A number of these methods have been reviewed . Oxidation with 2,6-dichloro phenolindophenol is the extensively used method , however it is vitiated by the susceptibility of the dye to react with other reducing materials , like glutathione and cysteine , which are frequently present in biological fluids , Fe^{+2} which is particularly found in food stuffs (3) or sulfite commonly added as a preservative in soft drinks . Titration with N-bromosuccinimide has been reported to tolerate Fe^{+2} (4,5) , albeit the reagent is only unstable and reacts with cysteine , glutathione and sulfite (6) .

We can use chloramine -T as titrant for determination of Vitamin. Test solution are titrated in the presence of either acidified potassium iodide and starch . Iron(II) does not interfere in this method but sulfite interfere in this method . but when treatment the solution with acrylonitrile before titration to mask sulfite and sulfhydryl compounds (sulfite and sulfhydryls both can be nonreducing by prereaction with acrylonitrile) .

In the presence of these substances we can determine vitamin C (8,9) .

MATERIALS AND METHODS

Reagents and Apparatus

All stock solutions were prepared by using analytical grade reagents from BDH company – In this study the UV. Spectrophotometer used was a Perkin – Elmer model 305B. PH-meter used was Philips model 212K .

Standard solutions of the compound were prepared by dissolving the amounts of high purity materials in deionized water, solution of vitamin C were standardized by titration with 2,6-dichlorophenolindophenol of sodium sulfite with iodine and of sulfhydryl substances with O-iodosobenzoate (9,10,11). Solution of 0.2 M chloramine – T prepared by dissolving 5.62g of sodium N- Chloro -4-toluenesulfonamid trihydrate in two liters of water and standardized iodometrically (8). Phosphate buffer (PH = 7) was prepared by dissolving 58.8 g grams of dipotassium hydrogen orthophosphate and 22.05 grams of potassium dihydrogen orthophosphate in one liter water (10).

Sodium tetrathionate 0.025 M, was made afresh by titrating 50 ml of 0.2M sodium thiosulfate with 0.05 M iodine to the first appearance of iodine color which is bleached by dropwise addition of 1×10^{-2} M thiosulfate, this solution stored in a dark bottle.

Procedure :

Two tablets or one of the capsule from any pharmaceutical preparations was stirred with about 50 ml of deionized water which containing two drops of glacial acetic acid. After 10 min. the residual precipitate is filtered and washed by 10 ml deionized water.

The filtrate is diluted to 40 ml in suitable flask and mixed with 0.6 gr KI, Two small drops of starch, and 1 ml of 0.2 M H_2SO_4 and titrated with 0.02 M chloramines – T to the appearance of a blue color.

RESULTS AND DISCUSSION

Table -1: Vitamin C take and found in pharmaceutical preparations .

No.	Sample	Content	Name	Vitamin C taken mg(b)	Vitamin C found mg
	Paracetamol	500 mg	Panacare*	3.5	3.45
	Mefenamic acid	500 mg	Mefril- 500 *	1.5	1.5
	Ibuprofen BP	400 mg	Jazofen- 400 *	1.5	1.48
	Diazepam	5 mg	Valiapain -5 *	2.5	2.47
	Omerprazol	20 mg	A prazole – 20 ^a	2.5	2.36
	Cebexin	500 mg	Cebexin ^a	1.5	1.40

* : T ablets, a: capsules, b: Average of five determination.

Determination of Vitamin C in Presence of sulfhydryl substances .

A 10 ml of solution is treated with 5 ml of phosphate buffer and one drop of acrylonitrile. The mixture left for 10 min, when sulfhydryl substances are present with vitamin C. The contents are mixed with 10 ml of 0.05 M H_2SO_4 , 0.4 gr KI, and two drops of starch and titrated with 0.05 M chloramines – T to a blue color.

Determination of Vitamin C in Presence of sulfite .

A 10 ml of Test solution is treated with 4 ml of 2- furfuraldehyde and allowed to stand for about 12 min. . The mixture is diluted to 20 ml and mixed with 0.4 gr KI, one drop of starch, and 3 ml of 0.05 M H_2SO_4 . The vitamin C is titrated with 0.05 M chloramines – T to the appearance of a blue color.

Table -2: Determination of Vitamin C in Presence of sulfite .

No.	Weight of vitamin C taken (mg)	Sulfite (mg)	added	Vitamin C Found (mg)	Masking agent (mg)	CV
	3.25	4.68		4.59	0.4 mg	0.45
	4.61	7.85		7.79	2- furfal	0.42
	6.24	5.21		5.20	Aldehyde	0.30
	8.52	3.50		3.36	Four	0.81
	10.14	4.88		4.65	Each sample	0.79

Table (2) vitamin C found is average of three determination , CV = coefficient of variation .

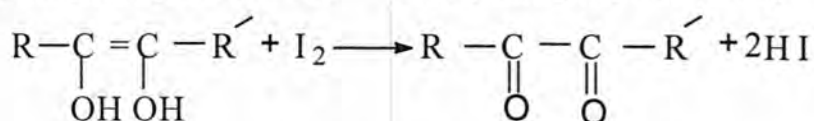
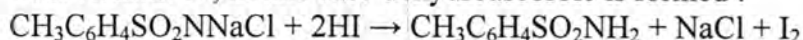
Determination of Mixture of vitamin C with cysteine and sulfite.

To determine atotal of three compounds , an aliquot of mixture (10 ml) is mixed with 5 ml of phosphate buffer and 12 ml of tetrathionate . The contents are shaken for two min. and then mixed with 0.4 gr KI, one drop of starch , and 4 ml of 0.05 H₂SO₄ and titrated with 0.02 M chloramines -T to a blue color . A second aliquot of mixture is treated with 5 ml of 2- furfuraldehyde for 12 min. to tie sulfite.The above method using tetrathionate is repeated to yield atotal of vitamin C and cysteine (sec. titer). Sulfite is obtained by difference of (first titer and th second). Athird but equal aliquot of mixture is reacted with 1 ml of acrylonitrile and there after mixed with 4 ml of 0.05 M H₂SO₄, 0.4 gr KI, and one drop of starch and titrated with 0.02 M chloramine-T to a blue color to yield vitamin C alone (titer III) . Cysteine is obtained from the difference of titer II and III .

Table-3: Determination of Mixtures of vitamin C with sulfite and cystine .

No	mg taken			mg found					
	Sulfite I	Vitamin C II	Cystine III	Sulfite I	Vitamin C II	Cystine III	CV _I	CV _{II}	CV _{III}
	3.24	2.1	5.20	3.22	2.01	5.12	0.05	0.09	0.02
	2.65	3.2	7.05	2.68	3.15	6.85	0.12	0.30	0.25
	3.54	4.5	8.50	3.57	4.35	8.42	0.30	0.25	0.32
	4.62	6.7	10.10	4.61	6.65	9.56	0.25	0.35	0.41
	2.75	7.9	12.62	2.68	7.85	11.98	0.4	0.42	0.32

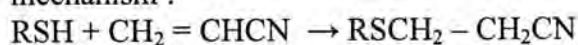
Chloramine-T reacts with hydroiodic acid to yields iodine ⁽¹¹⁾ which reacts with vitamin C , in this case dehydroascorbic is formed .



Substances which do not interfere with either indicator when present up to 10-fold molar excess of vitamin C include, urea , FeSO₄ , starch citric acid , lactose , tartaric acid , and maleic acid sulfanil amide , hydrazide and cystine when present in the not interfere when iodide and starch are used but vitiate the results badly

with methyl red and bromide even when present in traces . Amounts equal to that of vitamin C of 4- hydroxyl benzoic acid , salicylic acid and N- acetyl -4- amino phenol high results when methyl red and bromide are used but can be tolerated up to 20- foldmolar excess of the determinant with the other indicator . Thiosulfate , thiouracay sulfide and other strongly reducing species , e.g. hydrazine and hydroxylamine interfere with indicator . Sulfite forms unusual complex with 2- furfuraldehyde or acrylonitrile by nucleophilic addition to activated π orbital of carbonyl or olefinic group ($C=O$), ($C=C-$) yielding anion reducing product . Formaldehyde reacts with vitamin C affecting its reducing properties and therefore cannot be employed to tie sulfite .

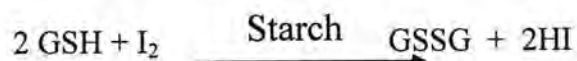
Sulphydryl substances undergo cyanoethylation with acrylonitrile via the same mechanism .



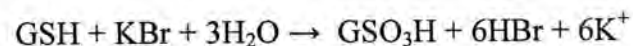
The reducing thiol group is blocked . Alkali hydroxides and tetra alkyl ammonium hydroxides are powerful catalysts for cyanoethylation (12,13) but in their presence vitamin C deteriorates .

Phosphate buffer of pH = 7 was found to catalyze the reaction , although less readily (2 min. with hydroxides as compared to 15 min. with phosphate buffer), but the vitamin C is unaffected .

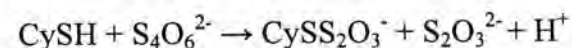
Glutathione when present with vitamin C can be oxidized smoothly to its disulfide when potassium iodide and starch are used .



If potassium bromide and methyl red are employed the oxidation goes further yielding a sulfonic acid (14) .



A method based on these two reactions of different stoichiometry has been reported to analyze mixtures of vitamin C and glutathione or cystine however , inaccuracy results due to the difference between a small and large titer . This is avoided in the present method by blocking the thiol group through cyanoethylation cysteine gives variable recoveries when determined under the condition used for glutathione . This is ostensibly due to the ready conversion of cysteine to a number of oxidation states the tetrathionate method has been found to determine cystine accurately , the reaction being (15) .



The thiosulfate liberated in an amount equal to that of cysteine is in fact titrated so that measured amounts of tetrathionate need not be added provided there is a sufficient excess to complete the above reaction . In Table (1) results are given for the determination of vitamin C in Pharmaceutical preparations and

compared with those obtained by using N- bromosuccinimide . Quantitative data for the titration of vitamin C in the presence of thiol and sulfite are given in table (2), where as results for the analysis of their mixtures are presented in tables (3).

REFERENCES

1. Krishna K. and Anil K. Gulati ,Determination of Different Types of Vitamin C by Chromatographic Method. Anal. Chem., 52:2336-2338(1980) .
2. Danehy J.P.; Dester, M.Y.J. X-Ray Fluorescence Spectrometry used for Determination two types of Vitamin C . org. Chem. 32:1491 (2007) .
3. Kreshk Jov A. P. and L.B. Oganessyan . Reducing Materials (Glutathione and Cysteine) using for Determination of some Vitamin in Soft drink . Anal . Khim. 28 : 2260 (1973) .
4. Basford R.E. and F.M. Huennekens ,Determination of Alkali Element by Field Desorption Mass Spectrometry. J.Am. Chem . Soc., 3873 (1992) .
5. Basu K.P. and M.C. Nath ,Separation of Vitamins by High Pressure Liquid Chromatography . J.Indian Chem . Soc. 15 :133(2002) .
6. Penney J.R. and Zilva , Liquid- Liquid Extraction of Protein with Bis(diethyldithiocarbamate) S.S. J. Biochem.,39:392 (2005) .
7. Evered D.F. Determination of Vitamin C by Gas Chromatography and Infrared Spectrophotometry . Analyst (London) 85 : 515 (1990) .
8. Verma K.K. and S.Z. Bose, Interference in the Determination of some Vitamins by Fluorescence Emission Spectrometry. Anal .Chem. 274:126(2005).
9. Franke W. and J.M. Harris , Acid Interference in Determination of Arsenic by Atomic Absorption Spectrometry . Anal .Chem . 52 :295-702 (2001) .
10. Vogel A.I., A Text – Book of quantitative inorganic Analysis, London :383 (1978) .
11. Verma K.K. and S.Z. Bose Fluorometric Detection in High – Pressure Liquid Chromatography of Peptide and Vitamin . Analysis (London) 100:366(2002).
12. Misra G.S. and R.S. Asthana, Cyanoethylation of Sulfhydryl with Acrylonitrile . J. Pract. Chem.,4 :270(1997)
13. Wronski M. Tetra Alkylammonium Hydroxides Powerful catalyst for cyanoethylation . Analyst (London) , 85 :526(1980) .
14. Barakat M.Z., and L.A. Decker , Oxidation of Vitamin C by Iodometric Method in presence of Glutathione . Anal . Chem., 47:299-307.
15. Gupta D. and P.D. Sharma , Determination of Cystine by the Oxidation of Tetrathionate Talanta , 22 :913(1975) .

Determination of The Carboxylic Group Using Ion Selective Electrode

Souhaila K.Syhood, Adnan A.Hussain, Kafa K.Hammud and Abtesam A.kudar, Lamiaa Hussain
Ministry of Technology and Science

الخلاصة

في هذه الدراسة تم تعيين المجاميع الكربوكسيلية باستخدام الأقطاب الانتقائية باستخدام قطب الفضة الانتقائي. تم تطبيق الطريقة على مواد قياسية تحتوي على مجموعة الكربوكسيل. أظهرت النتائج نسبة خطأ (0.5-1) عن ما هو محسوب نظرياً بالنسبة للحمض الساليسليك و 1.5 بالنسبة لـ acetyl salicylic. طبقت هذه الطريقة على مواد صيدلانية وأعطت نتائج بنسبة استرجاع 99%.

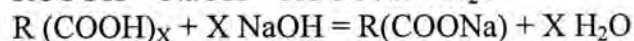
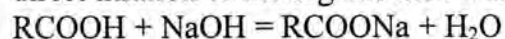
ABSTRACT

simple, rapid and sensitive method for determining the concentration of carboxylic acid group by reaction of this group with potassium hydrogen sulfide titration and titration with silver nitrate in room temperature using silver/sulfide electrode. This method applied with pharmaceutical materials (Asprin, Locaslen, White) with recovery.

INTRODUCTION

The carboxyl group, COOH, presents in organic compounds may be determined by numbers of micro methods.

1. Acidic methods (Direct Neutralization) which preferred by Calkibs (1) is the direct titration of the organic acid with standard alkali:



where R is either aliphatic or aromatic

The method gives not only the amount of carboxyl, but also-called neutralization equivalent, or number of grams of substance required to neutralize one liter of normal alkali. The neutralization equivalent is equal to the molecular weight divided by the number of acidic groups present.

2. Chromatographic methods

Block (2) described the estimation of the amino acids in paper chromatography. The quantity of colour –as measured by a simple photoelectric densitometer – developed by ninhydrin or other reagents in each spot of these chromatograms, is proportional to concentration of the substance in that spot. This observation had been used as a basis of estimation of the amino acid in less than 0.1 mg of casein nitrogen, the chromatographic methods used for the separating amino acids.

Clabron (3) determined lactic and succinic acids in foods using : ether extraction, precipitation of barium succinate in 80% alcohol, isolation of lactic acid from the filtrate and succinic acid from the insoluble fraction by partition chromatography, titration of the acids with barium hydroxide, and identification by microscopic examination of the barium salts.

The small amounts of volatile fatty acids containing four to ten carbon atoms were determined by semimicro methods based on the principle of the chromatographic methods.

3. Colorimetric methods

Bergold (4) described a quantitative colorimetric method for the determination of glycolic and oxalic acids, devised from the sensitive qualitative spot test based on the colour produced with 2, 7- dihydroxy naphthalene in acidic solution, and determination pyruvic acid in blood and urine using colorimetric procedure.

Nekhorocheff and Wajer determined citric acid by micro-color procedure while Gordon determined citric and other α - hydroxy carboxylic acids by indirect colorimetric micro-oxidation (KMnO_4). Pratt and Corbitt (5) determined desoxycholic acid in the presence of certain other bile acids.

Tsao Baumann and other workers determined lactic acid in urine by oxidation to acetaldehyde which was measured by colorimetric means. The colorimetric micro-procedure described the simultaneous determination of pyruvic and α - ketoglutaric acids in mixture. The yellow colour of the 2, 4-dinitrophenyl hydrazone and the red colour with alkalis were measured.

4.Electrical methods

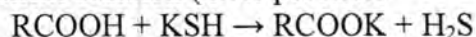
Furter and Gubes(5) make of conductivity cell with 5-30 mg.Sampie in 10-14 ml initial volume and titrate with 0.1 N aqueous sodium or lithium hydroxide. The solvent is aqueous ethanol chosen in such concentration as to provide the maximum initial dissociation of the minimum hydrolysis the acid ,and the minimum solution of the resulting, for moncarboxyl,25-75%ethanol is used for dicarboxyl, absolute ethanol,and polycarboxyl,85-95%ethanaol.The results give on 14 mono carboxyl, 6 dicarboxyl ,and 11 polycarboxyl(3-5carboxyl),theerror ranging from 0.1-3.0%of the theoretical

5-Other methods

Carboxylic acid group, may be determinated by ^{31}P - NMR spectroscopy(7) ,NIR-PLS-R(8) UV(9) .

MATERIALS AND METHODS

Carboxylic acid immediately disengage hydrogen sulfide gas from aqueous potassium hydrogen sulfide solution (mole per mole



The reaction was carried out at room temperature with a known sulfide concentration. After the reaction was completed, the remaining sulfide was potentiometrically titrated with silver nitrate using the silver /sulfide electrode results

within $\pm 1\%$ of the theoretical were obtained

Lead perchlorate solution

0.1M orion cat. No. 94-82-06 for titration of sulfide standard solution. Sulfide standards were prepared from a stock solution of saturated sodium sulfide by dissolving approximately 100 g reagent – grade $\text{Na}_2\text{S} \cdot 9\text{H}_2\text{O}$ in 100 ml distilled water then shaken well and let to stand over night store tightly stoppered bottle.

Weekly sulfide standard solution was prepared by mixing 10 ml of the

stock solution with 500 ml SAOB II and diluting to the mark of 1L volumetric flask with distilled water. To determine the exact concentration, 10 ml of the standard titrated with 0.1 M lead perchlorate and calculated with $(C=3200(V_t, V_s))$ where V_t = volume of the titrant end point V_s = volume of the standard (10 ml)

The other standards daily prepared by serial dilution of the weekly standard to-fold dilution, 10 ml of the standard with 45 ml SAOB II were diluted to 100 ml with distilled water.

Procedure:

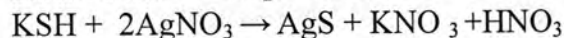
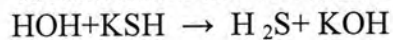
1. Accurately 0.1-4 gm of the carboxylic acid weighted, dissolved in 2 ml of bi-distilled water and 1.0 ml added of the potassium hydrogen sulfide reagent (aromatic carboxylic acids do not dissolve in water but become soluble upon the addition of the alkali sulfide reagent).
2. 40 ml of bi-distilled water added with stirring for 4 minutes.
3. The silver/ sulfide and reference electrodes system immersed in the solution with nitrogen gas.
4. Titration with 0.01 M silver nitrate solution was carried out.
5. Blank was carried out under identical condition.

RESULTS AND DISCUSSION

Table-1: Determination of the COOH group in the blank

mV	Volume	mV	Volume
-425.2	0.0	-182.3	3.0
-311.2	0.5	-136.6	3.5
-275.9	1.0	-75.6	4.5
-259.7	1.5	-2.1	4.5
-220.3	2.0	+13.4	5.0
-212	2.5		

Table (1) show that the increasing in volume of the blank increases the voltage measurement due to formation of silver sulfide from the reaction silver nitrate



Resid

Table-2: Salicylic acid titrate with 0.01M AgNO₃

mV	Volume Of AgNO ₃	mV	Volume Of AgNO ₃
-312.6	0.5	-213.4	3.0
-292.0	1.0	-96	3.5
-274.3	1.8	-35	4.0
-265.7	1.5	-1.2	4.5
-260.1	2.5		

Calculate the Carboxylic content according to the relation

$$\text{COOH}\% = 45 \cdot M \cdot (V_b - V_a) \cdot 100 / W$$

Where V_b V_a and volume (ml) of silver nitrate consumed in the blank and

experiment, respectively, M the molarity of silver nitrate, and W is the sample weight.

$$\text{COOH}\% = 45 \times 0.01 \times (0.5) \times 100 / 0.63 = 35.7\%$$

where weight of sample = 0.63 g, the error = (0.5-1.1)% of the theoretical

this result indicates the reaction is fast and complete and the salicylic acid which contains carboxylic group reacts with potassium hydrogen sulfide to form the acid salt and the reaction potassium hydrogen sulfide reacts silver nitrate. The volume of AgNO_3 titrate in standard materials (salicylic acid) is less than the blank because of the residue of S^{2-} ion less than the blank (table 2)

Table -3: Acetyl salicylic acid titrate with 0.01 M silver nitrate solution

mV	ml of AgNO_3
-320	0.0
-295.3	0.5
-262.5	1.5
-201.9	2.0
-87.9	2.5
-31.3	3.0
-2.5	4.5
+1.6	4.55

Weight of the sample = 0.85 g, The results with $\pm 1.5\%$ of the theoretical value. In table (3) the acetyl salicylic (ester) had more error value than its acid because of its weakly dissociation.

Application: the analytical method used was applied on drugs as illustrated in table (4).

Table-4: Application: the analytical method used was applied on drugs.

Name of drug	COOH% theoretical	COOH% practical	Recovery
Asprin	0.03	0.0298	99.3
Asprin	0.07	0.0701	100.1
Locasalen	0.97	0.964	99.3
White	9%	8.97	99.6

Table (5) Determine COOH Group concentration by Standard curve

mV	Concentration(M)
-765.3	1×10^{-4}
-795.5	1×10^{-2}
-851.8	1×10^{-1}
-725.3	salicylic acid

From table (5) standard curve can not be used to estimate in drugs and direct measurement gave better because of low sensitivity and the concentration of the sample is below the LOD. results.

REFERENCES

1. Calkins, V.P., Anal. Chem "Micro method for estimation of sulfonamides, seimper manet color standards, 15,762(1943).
2. Block, R.J., Anal. Chem., "Estimation of Amino Acids and Amines on paper chromatograms" 22,1327(1955).
3. Claborn, H.V. and Patterson, W.I., J. Assoc. Official Agr. Chem., 31,134(1958).
4. Bergold, G. & Pister, L., Z. Naturforsch., 3b, 406(1948); C.A., 43, 8420(1949). Organic analysis, II(1986).
5. Instruction manual, sulfide ion electrode, silver electrode model 94-16
6. A. Spyros, Journal of Applied Polymer, "Quantitative Determination of Distribution of free Hydroxyl carboxylic Group in unsaturated polyester and alkyd Resins by ^{31}P -NMR Spectroscopy" 83:1635-1645, (2009).
7. Henniges UTE, Schwanninger Manfred, Potthast Antje, Carbohydrate Polymers, "Non destructive determination of cellulose functional groups and molecular weight in pulp hand sheets and historic papers by NIR-PLS-IR: 76:374-380, (2009).
8. Jerry A. Leenleer, Robert L. Wershaw, and M. Reddy, Environmental Science & Technology, "Strong-Acid carboxyl-Group structures in fulvic Acid from the Suwannee River, Georgia, 1 minor structures" 29:393-397(1995).

Synthesis and Characterization of Mixed Ligand Complexes of Some Transition Metals with Alanine and 8-Hydroxyquinoline

¹Taghreed.H.AL-Noor , ¹Shatha.M.Obed and ²Eqbal.R.Hana

¹Chemistry Department, Ibn -Al-Haithem College of Education, University of Baghdad

Biology Department, College of Science , University of Baghdad

الخلاصة

تضمن هذا البحث تحضير وتشخيص معقدات ذات لكاندات مختلطة من حامض الالانين (L-Ala) و 8-هايدروكسي كوينولين مع أيونات العناصر الانتقالية الآتية:

Mn(II), Co(II), Ni(II), Cu(II), Zn(II), Cd(II) and Hg(II)

تم دراسة المعقدات بالطرائق الآتية : الدراسات الطيفية (UV-Vis , FT-IR , AAS) فضلا عن قياس درجات الانصهار والتفكك ، الذوبانية ، التوصيلية الكهربائية

كما تم دراسة الفعالية البايولوجية للمعقدات المحضرة إذ كانت بعض المركبات لها فعالية بايولوجية وانعدمت للبعض منها .

ABSTRACT

The mixed ligand complexes of Mn(II), Co(II), Ni(II), Cu(II), Zn(II), Cd(II) and Hg(II) with alanine and 8-hydroxyquinoline (Oxine) were synthesized and characterized by FT-IR ,spectra electronic, flam-AAS] along with conductivity measurements , solubility , melting point , magnetic susceptibility.

The synthesized complexes were tested in vitro for antimicrobial activity. The results obtained indicated that some of these complexes are more active than with others.

INTRODUCTION

8-hydroxyquinoline (oxine) is well-characterized organic chelating ligand, which can form covalent compounds with over 60-metal ions under controlled pH-conditions ,and its preference for transition and heavy metal cations over alkali and alkaline-earth cations is well known.(1)

Chemical properties of quinoline and its derivatives are of interest due to their biological activity(2),coordination capacity(3) and their use as metal extracting agents.(4)

A.Z.Ei-Sonbatai and Co-worker were prepared several new coordination compound of Cu(II), Ni(II), Co(II), Mn(II), Fe(II), Sn(II), Hg(II), UO₂ and Fe(III) with schiff base derived from 8-hydroxyquinoline and 2-aminophenol or 2-aminopyridine .The ligand and the complexes have been characterization by elemental analysis, IR,UV, H¹-NMR and C-¹³ NMR spectra.(5)

Numerous complexes of amino acid –based schiff bases with various metal ions such as Cu (II), Ni (II), Zn(II), Pd(II), Sn (IV),V(IV), lanthanide ions were prepared .(6-13)

Mixed-ligand transition metal complexes of Pt (IV) ions were synthesized, where, Phthalic acid as a primary ligands and hetero cyclic amine bases as a secondary ligands have been used, respectively.(14) Moreover, mixed-ligand transition metal complexes of Ni (II) ions were also synthesized by the same way, which, mentioned before except Ni(II)ions used instead of Pt (IV) ions. Their

conventional physical and chemical analysis had been done. Their anti-bacterial and anti-fungal activity had been evaluated. Disc diffusion methods were employed for anti-microbial assays against fourteen pathogenic bacteria (five gram positive and nine gram negative) and fourteen fungi. The complexes containing 8-hydroxyquinoline as secondary ligand were much more microbial active than the other complexes. In addition, the complexes; $[Pt(IV)(PA)(Q)_2]$ shows the highest anti-bacterial activity against all bacteria tested (where, $PA = C_8H_4O_4$ and $Q = C_9H_6NO$)

In this paper we present the synthesis and study of some transition metal complexes with paper we present the synthesis and study of some transition metal complexes with 8-hydroxyquinoline as a primary ligands and amino acid (L-alanine) as a secondary ligands have been used, respectively.

MATERIALS AND METHODS

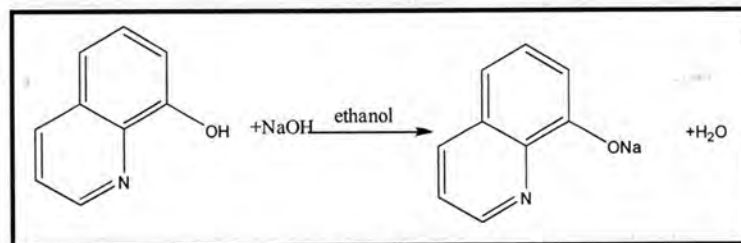
a- Reagents and instruments: L-alanine and 8-hydroxyquinoline were purchased from (Merck) , metals chloride and solvents from (B.D.H). The reagents were used without further purification .

b- Instruments: FT-I.R spectra were recorded as KBr discs using Fourier transform Infrared Spectrophotometer Shimadzu 24 FT-I.R 8400s. Electronic spectra of the prepared complexes were measured in the region (200- 1100) nm for 10^{-3} M solutions in DMF at 25°C using shimadzu-U.V-160 . A Ultra Violet Visible- Spectrophotometer with 1.000 ± 0.001 cm matched quartz cell. While metal contents of the complexes were determined by Atomic Absorption (A.A)Technique using Japan A.A-67G Shimadzu. Electrical conductivity measurements of the complexes were recorded at 25°C for 10^{-3} M solutions of the samples in DMF using pw9527 Digital conductivity meter (Philips). Melting points were recorded by using Stuart melting point apparatus.

The proposed molecular structure of the complexes were determined by using chem. office prog, 3DX (2004).

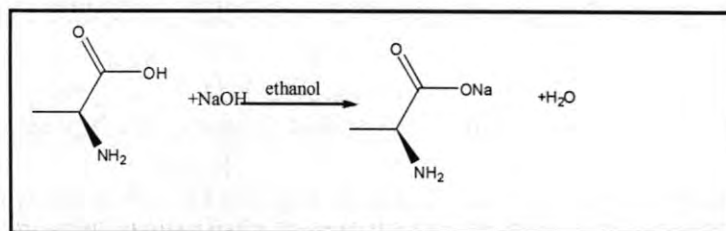
General Method for the Synthesis

a- Sodium-8-oxyquinolate: [0.145 gm, 1mmol] 8-hydroxyquinoline (QH) with [0.04 gm (1mmol)] sodium hydroxide in ethanol was deprotonated according to the following reaction: (scheme -1)



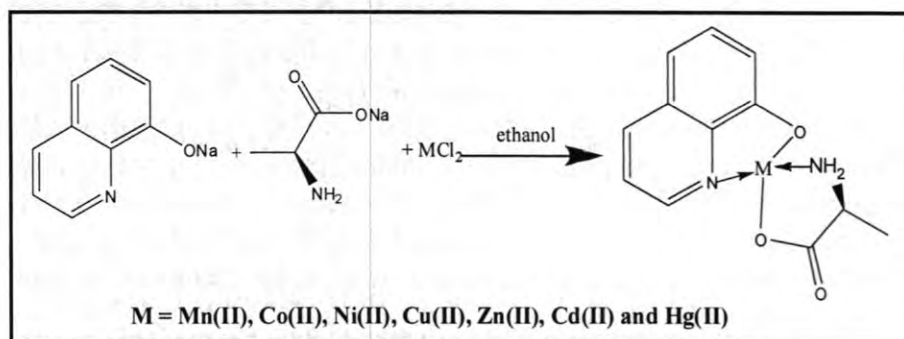
scheme -1 : sodium-8-oxyquinolate

b- Sodium alaninate: [0.089 gm(1mmol)] with [0.04 gm (1mmol)] sodium hydroxide in ethanol was deprotonated according to the following reaction (scheme -2)



scheme -2 : Sodium alaninate

c- Synthesis of complexes: An aqueous solution of the metal salt was added to the solution of the ligand in ethanol respectively using stoichiometric amounts (1:1:1) (metal: ligand: ligand)(M:Q:A) molar ratio, the mixture was stirred for half an hour at room temperature, crystalline precipitates observed. The resulting precipitates were filtered off ,re crystallized from ethanol and dried at room temperature according to the following reaction : (scheme -3) :



scheme -3: Synthesis of the mixed complexes

The antibacterial activity of the synthesized complexes was determined in vitro using paper disc method (agar plate diffusion method) against four pathogenic microorganism viz., Staphylococcus aureus (Gram +ve) , Salmonella typhi (Gram -ve), Escherischea coli (Gram -ve) and Bacillus cereus (Gram+ve). The solvent used was dimethyl sulfoxide (DMSO)and sample from 1 to 200 $\mu\text{g/mL}$ were used. The plates were incubated for 24 hours at 37 C⁰ and after 3-years.

RESULTS AND DISCUSSION

The Physical properties listed in Table (1). All the complexes are colored, non-hygroscopic, and appears as powders with high melting points .They are not soluble in water. All complexes dissolved in DMF solvent.

The molar conductance values of the complexes in DMF at 10^{-3} M concentration are found to be (2.23 - 15.38) $\mu\text{S.cm}^{-1}$, indicating their non-electrolytic nature.(15)

The atomic absorption measurements (Table-1) for all complexes gave approximated values for theoretical values.

The Electronic Spectra

The electronic spectra of all compounds (Ligand and complexes) are listed in (Table -2) figs (1-3) together with the proposed assignments and suggested geometries. The spectrum of the free ligand (Ala) in DMF solvent show two high intensity band in wave length 304 nm (32894 cm^{-1}) ϵ max ($391\text{ l.mol}^{-1}.\text{cm}^{-1}$) and 277 nm. (36101 cm^{-1}) ϵ max ($343\text{ l.mol}^{-1}.\text{cm}^{-1}$) assigned ($n \rightarrow \pi^*$) and ($\pi \rightarrow \pi^*$) transition respectively .(16,17) and the spectrum of the free ligand (8-HQ) in same solvent show signal at 317 nm (31545 cm^{-1}) ϵ max ($200\text{ l.mol}^{-1}.\text{cm}^{-1}$) assigned to the ($n \rightarrow \pi^*$).

The (UV-Vis) spectra of the all complexes displayed absorptions at (213-342)nm assigned for ligand field

In the $\text{Mn}(\text{C}_{12}\text{H}_{12}\text{N}_2\text{O}_3)$ Complex:

Exhibits additional (for ligand field) broad peak at (400nm) (25000 cm^{-1}), which assigned to ($6\text{ A}_1 \rightarrow 4\text{T}_2$) transition in a tetrahedral geometry. (16,17)

In the $\text{Co}(\text{C}_{12}\text{H}_{12}\text{N}_2\text{O}_3)$ Complex:

Showed another two peaks , the first weak peak at (352 nm) 28409 cm^{-1} is due to the (Charge. Transfer) , while the second weak broad peak at (415nm) (24096 cm^{-1}) was assigned to ($4\text{T}_{1p} \rightarrow 4\text{A}_2$) transition in a tetrahedral geometry .(16)

In the $\text{Ni}(\text{C}_{12}\text{H}_{12}\text{N}_2\text{O}_3)$ Complex :

Showed another two peaks, the first weak peak at (357 nm) (28011 cm^{-1}) is due to the (Charge. Transfer) while the second weak broad peak at (400 nm) (25000 cm^{-1}) was assigned to ($\text{B}_{2g} \rightarrow \text{B}_{1g}$) transition in a square planar geometry.(16)

In the $\text{Cu}(\text{C}_{12}\text{H}_{12}\text{N}_2\text{O}_3)$ Complex:

Showed another two peaks, the first peak at (351 nm) (28490 cm^{-1}) is due to the (Charge.Transfer), while the second weak broad peak at (415 nm) (24096 cm^{-1}) was assigned to ($2\text{E} \rightarrow 2\text{T}_2$) transition in a tetrahedral geometry.(16,17)

The complexes $[\text{Zn}(\text{C}_{12}\text{H}_{12}\text{N}_2\text{O}_3)]$, $[\text{Cd}(\text{C}_{12}\text{H}_{12}\text{N}_2\text{O}_3)]$ and $[\text{Hg}(\text{C}_{12}\text{H}_{12}\text{N}_2\text{O}_3)]$ exhibited an additional weak peak at (355nm) (28169 cm^{-1}), (384nm) (26041 cm^{-1}) and (387nm) (25839.79 cm^{-1}) was assigned to the charge transfer (C.T). The geometry of the complex are tetrahedral.(17)

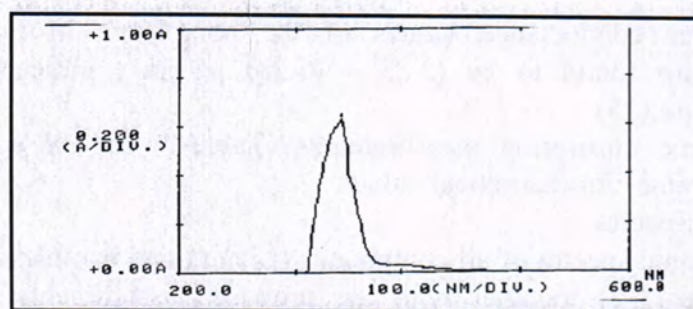


Fig. -1: Electronic Spectrum L-alanine

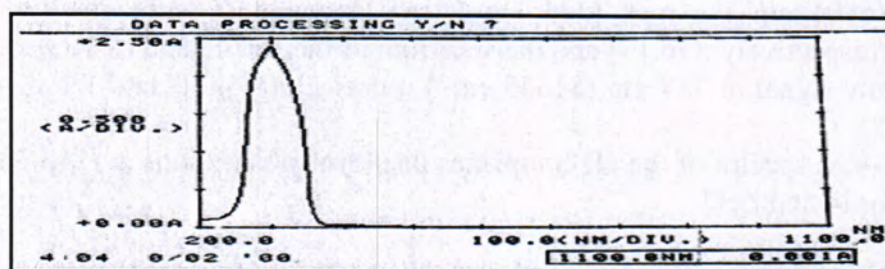
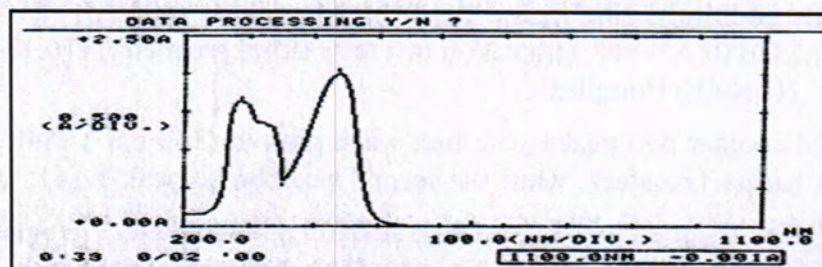


Fig- 2: Electronic Spectrum of 8-hydroxyquinoline

Fig -3: Electronic spectrum of complex $\text{Mn}(\text{C}_{12}\text{H}_{12}\text{N}_2\text{O}_3)$

Infrared spectra and mode of coordination :

The most important infrared spectral bands that provide conclusive structural evidence for the coordination of the ligands to the central metal ions .

The characteristic vibrations and assignments of ligands (QH) and (Ala) and their complexes as KBr spectrum discs are described (Table -3) , Figs(4-6)

The infra red spectrum of free ligand (Ala) exhibited a strong band around $(3378) \text{ cm}^{-1}$ that corresponds to the stretching vibration of $\nu(\text{N-H}) + \nu(\text{O-H})$, while another strong absorption band at $(1618) \text{ cm}^{-1}$ is appeared which could explained as $\nu(\text{OCO})$ asym where the $\nu(\text{OCO})$ sym was noticed at $(1411) \text{ cm}^{-1}$. An important feature of infra-red spectra of metal complexes with 8-HQ is the absence of the band at $(3240-3047) \text{ cm}^{-1}$ due to the O-H stretching vibration of the OH group of HQ (18). Fig (4). This observation leads to the conclusion that the complex formation takes place by deprotonation of the hydroxyl group of HQ moiety .

Charles et al.(19) reported that for several metal complexes with HQ, the $\nu(\text{C-O})$ band is observed at $\sim 1120 \text{ cm}^{-1}$. The position of this band varies depending on metal complex under study. A strong $\nu(\text{C-O})$ band observed at $\sim 1104 \text{ cm}^{-1}$ indicates the presence of oxine moiety in the complexes coordinated through its nitrogen and oxygen atoms as uninegative bidentate ligand.(18) The $\nu(\text{C=N})$ mode observed at 1577 cm^{-1} in the spectra of free HQ ligand is found to be shifted to lower wave number i.e. $\sim 1500 - 1497 \text{ cm}^{-1}$ in the spectra of complexes. A negative shift in this vibrational mode on complexation indicates the coordination through the tertiary nitrogen donor of HQ. Some new bands of weak intensity observed in the regions around $(648 - 630) \text{ cm}^{-1}$ and $(436 - 516) \text{ cm}^{-1}$ may be ascribed to M-N and M-O vibrations, respectively. (20, 21) It may be noted that, these vibrational bands are absent in the spectra of the ligands.

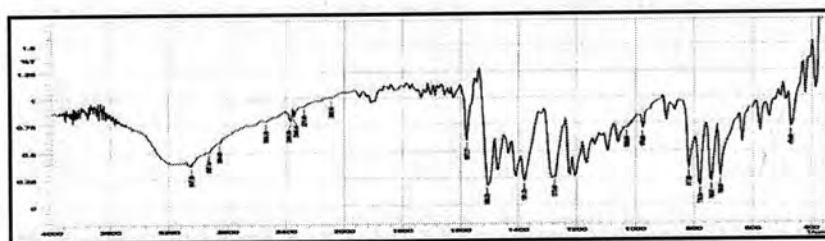


Fig -4: FT- Infrared spectrum of (8-Hydroxyquinoline)

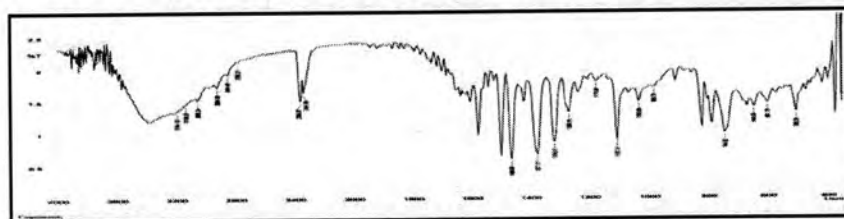


Fig-5: FT- Infrared spectrum of (alanine)

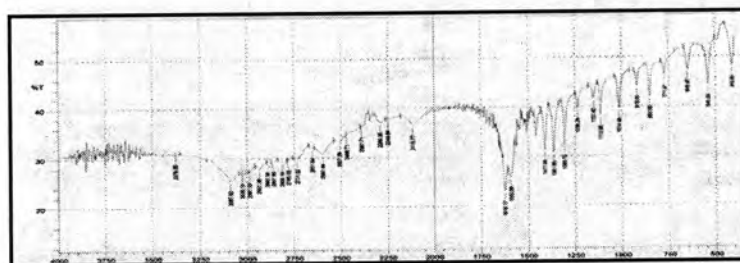


Fig -6: FT- Infrared spectrum of $\text{Na}[\text{Mn}(\text{C}_9\text{H}_6\text{NO})(\text{C}_5\text{H}_8\text{NO}_2)_2]$

Biological activity:

The zone inhibition of bacterial growth were measured in mm depending upon the diameter as shown in Table (4) Fig (7)

Nomenclature of prepared complexes :

Table(5)shows empirical formula and nomenclature (IUPAC) with abbreviated .

Table -1: The physical properties of the compounds

Compounds	M.wt	Colour	M.p (de) °C	Λ_m $\mu\text{S.cm}^{-1}$	Metal %	
					Thory	Exprement
Alanin (Ala)	89.09	White	314	1.0	-	-
8-hydroxyquinoline (8-HQ)	145.16	Pale-yellow	77		-	-
Mn(C ₁₂ H ₁₂ N ₂ O ₃)	287.17	Dark-brown	> 350	12.78	19.13	18.22
Co(C ₁₂ H ₁₂ N ₂ O ₃)	291.02	Pale-brown	> 350	15.38	20.24	21.66
Ni(C ₁₂ H ₁₂ N ₂ O ₃)	290.93	green	> 350	8.08	20.17	20.99
Cu(C ₁₂ H ₁₂ N ₂ O ₃)	295.02	green	312	2.86	21.48	21.00
Zn(C ₁₂ H ₁₂ N ₂ O ₃)	297.01	Yellow-green	>350	2.56	21.97	20.98
Cd(C ₁₂ H ₁₂ N ₂ O ₃)	344.65	Yellow-green	> 350	7.98	32.62	31.56
Hg(C ₁₂ H ₁₂ N ₂ O ₃)	432.83	Dark-yellow	> 350	2.53	46.34	-----

8-hydroxyquinoline = C₉H₇NO , Λ_m = Molar Conductivity , Ala = C₃H₇NO₂
 de = decomposition

Table 2: Electronic data for the ligand and there complexe

Compound	λ nm	ν cm ⁻¹	ϵ_{\max} l.mol ⁻¹ .cm ⁻¹	Assignments	Suggested structure
Ala= (C ₃ H ₇ NO ₂)	277 304	36101 32894	343 391	$\pi \rightarrow \pi^*$ $n \rightarrow \pi^*$	—
8-yhydroxyquinoline	317	31545	200	$n \rightarrow \pi^*$	—
Mn(C ₁₂ H ₁₂ N ₂ O ₃)	280 400	35714 25000	420 1653	Ligand field ${}^6A_1 \rightarrow {}^4T_2$	Tetrahedral
Co(C ₁₂ H ₁₂ N ₂ O ₃)	277 338 352 415	36101 29585 28409 24096	108 467 740 1671	Ligand field Ligand field Charge transfer ${}^4T_1 p \leftarrow {}^4A_2$	Tetrahedral
Ni(C ₁₂ H ₁₂ N ₂ O ₃)	342 357 400	29239 28011 25000	152 836 1397	Ligand field Charge transfer $B_{2g} \rightarrow B_{1g}$	Square planar
Cu(C ₁₂ H ₁₂ N ₂ O ₃)	336 351 415	29761 28490 24096	1178 582 1887	Ligand field Charge transfer ${}^2E \rightarrow {}^2T_2$	Tetrahedral
Zn(C ₁₂ H ₁₂ N ₂ O ₃)	213 833 355	46948 29585 28169	412 631 1371	Ligand field Ligand field Charge transfer	Tetrahedral
Cd(C ₁₂ H ₁₂ N ₂ O ₃)	257 327 384	38910.50 30581.03 26041.66	162 40 21	Ligand field Ligand field Charge transfer	Tetrahedral
Hg(C ₁₂ H ₁₂ N ₂ O ₃)	223 276 387	44843.04 36231.88 25839.79	419 141 29	Ligand field Ligand field Charge transfer	Tetrahedral

Table -3: represent the antimicrobial activity of chemical compound against some pathogenic bacteria

Compound	NH _{sym} str	CH _(py) str	(CH) _{cycl}	ν (C=N)	ν (C=C)	ν(C-O)	ν _d (C-O)	ν(-COO ⁻)		M-N	M-O
								asym	sym		
Ala ⁻	3379m							1618 vs	1411 s	-	-
8-HQ	3240- 3047br	-	-	1577	1508	-	-			-	-
[Mn(Ala) (Q)]	3168w-	3136s 2854w	2974m	160w	1573vs	1283m	457m	1465s	1323s	640m	450m
[Co(Ala) (Q)]	3194br-s	3136m 2854w	2924w	1590s	1570s	1269m	505m	1465 v s	1377vs	648m	450w
[Ni(Ala) (Q)]	3356 br s	3240 br- s	2989w	1620s	1520w	1284m	497m	1497vs 1423 s	1373s	644m	503w
[Cu(Ala) (Q)]	3384 br	3058m	2925w	1581vs	1504m	1284m	588s	1469vs	1377vs	632m	516m
[Zn(Ala) (Q)]	3315s	3085m	2927w	1577vs	1500 vs	1282s	583w	1467vs- 1423 s	1371vs- 1328vs	642m	503m
[Cd(Ala) (Q)]	3313br-s	3178m	2977sh-m	1573vs	1500s	1284m	505s	1498s- 1465s	1390vs- 1323vs	640m	436w
[Pd(Ala) (Q)]	3194br-s	3055m	2927w	1620m	1577vs	1273m	597vs	1496s- 1465vs	1384vs- 1323vs	630m	436w
[Hg (Ala) (Q)]	3384 br	3172 m	2927w	1575s	1500s	1282w	597m	1465vs	1363s 1325s	635w	503w

Sym: symmetric, asy: asymmetric, am: amide, py: pyridine, o.p: out of plane, str: stretching, v.s: very strong,
s: strong, m: medium, w: week, sh: shoulder

	Complexes No. In figure	Complexes	Pathogenic Bacteria			
			E. coli	Bceraus	S. typhi	Stap. epidermades
After 24 hours	1	[Mn(A) Q]	-	10	-	9
	2	[Ni (A) (Q)]	20	25	22	18
	3	[Hg (A) (Q)]	15	30	24	20
	4	[Cd (A) (Q)]	-	25	11	12
	5	[Zn (A) (Q)]	-	22	13	12
	6	[Co (A) (Q)]	11	15	14	10
	7	[Cu (A) (Q)]	11	23	11	12
After three years	8	[Zn (A) (Q)]	10	25	-	16
	9	[Ni (A) (Q)]	-	20	10	15
	10	[Mn(A) (Q)]	4	20	-	13
	11	[Co (A) (Q)]	-	18	-	10
	12	[Cd (A) (Q)]	13	35	12	15
	13	[Hg (Ala) (Q)]	15	25	14	13
	14	[Cu (Ala) (Q)]	12	25	20	20

Table-4: represent the antimicrobial activity of chemical compound against some pathogenic bacteria

Note :

Highly active = Inhibition zone > 20 mm , Moderately active = Inhibition zone > 11- 20 mm

Slightly active = Inhibition zone > 4 -10 mm , Inactive = - , Q⁻ = oxinate ion = C₉H₇NO⁻ , Ala⁻ = alaninate ion = C₃H₆NO₂⁻

Table -5: Nomenclature of prepared complexes

Complexes	Name	Abbreviation
Mn (C ₁₂ H ₁₂ N ₂ O ₃)	AlaninatoOxinateManganese (II) or Alaninato(8-oxyquinolate) Manganese (II)	Mn(A) (Q)
Co(C ₁₂ H ₁₂ N ₂ O ₃)	AlaninatoOxinate Cobalt (II) or Alaninato(8-oxyquinolate) Cobalt (II)	Co(A) (Q)
Ni(C ₁₂ H ₁₂ N ₂ O ₃)	AlaninatoOxinateNickel(II) or Alaninato(8-oxyquinolate) Nickel (II)	Ni(A) (Q)
Cu(C ₁₂ H ₁₂ N ₂ O ₃)	AlaninatoOxinateCopper (II) or Alaninato(8-oxyquinolate) Copper (II)	Cu(A) (Q)
Zn(C ₁₂ H ₁₂ N ₂ O ₃)	AlaninatoOxinateZinc (II) or Alaninato(8-oxyquinolate) Zinc (II)	Zn(A) (Q)
Cd(C ₁₂ H ₁₂ N ₂ O ₃)	AlaninatoOxinateCadmium (II) or Alaninato(8-oxyquinolate) Cadmium (II)	Cd(A) (Q)
Hg(C ₁₂ H ₁₂ N ₂ O ₃)	alaninatoOxinateMercury (II) or Alaninato(8-oxyquinolate) Mercury (II)	Hg(A) (Q)

Oxine (HQ) = 8-Hydroxyquinoline = C₉H₇NO , Q = C₉H₆NO

Ala =Alanine = C₃H₇NO₂ , A⁻ = C₃H₆NO₂⁻

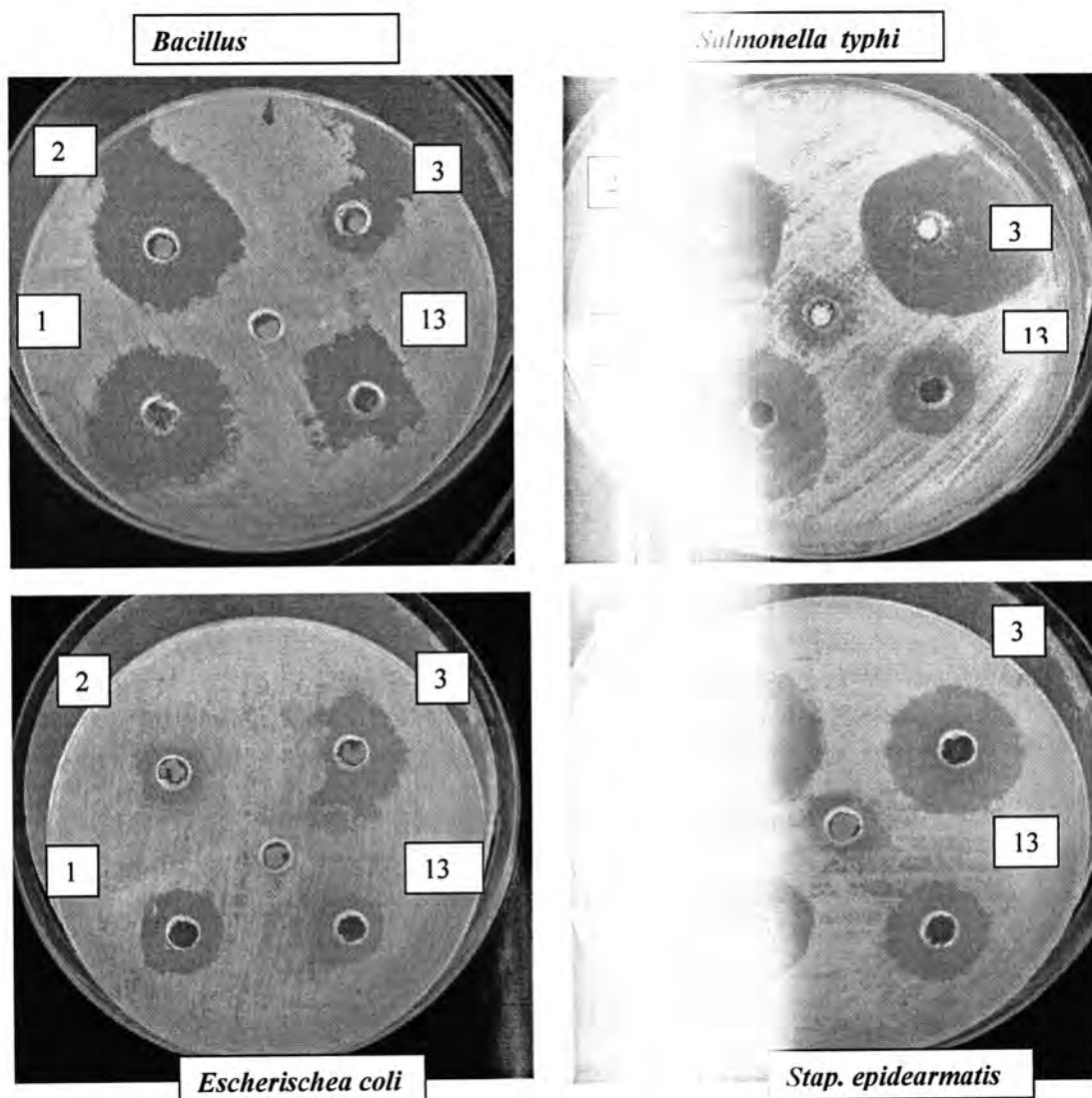


Fig-7: shows the antimicrobial activity of the inhibition zones against some pathogens

REFERENCES

1. Rao T.P, and Gladis G.M., preconcentration Agents in flow in molecular spectrometric techniques, Analyst, 107 (2002).
2. Harane R. and Cairin J., Protonated coordination behaviour towards some metal ions, Inorg. Chem. Acta, 46, : 63 (1980).
3. Sonbati A.Z, E.I., synth. React. for the determination of metal ions, Inorg. Met.- Org. Chem. Lett., 1, :459 (1997).

compounds (2,3,12,13) appear

and its derivatives as coupled to atomic and molecular spectroscopy (2002).

Salicylidene (N-benzoyl)its metal ions glycol hydrazone and

electrodes, potentiometric determination (1991), Spectroscopy Lett., 30,

4. Sonbati A.Z, Ei, El-Bindary A.A., El-Mosalamy E.H., And E.M. El-Santawy, Thermodynamics of Substituted Pyrazolone VIII. Potentiometric, Spectrophotometric, and Conductometric Studies of 4-(4-Nitrophenylazo)-3-methyl-1-(2-hydroxy-3-morpholinopropan-1-yl)-2-pyrazolin-5-one and its Metal Complexes , Springer's Journal Volume 56, Number 5 (2002).
5. Sonbati A.Z, Ei- and Ei-Bindary, Stereochemistry of New Nitrogen Containing Heterocyclic Aldehydes. III. Novel Bis-Bidentate Azodye Compounds Polish, J. Chem, 74 : 621-630, (2000).
6. Boghaei, M.D. & Lachanizadajene, M. Metal complexes of non symmetric tetradentate Schiff bases derived from N-(1-hydroxy-2-acetonephthone-amino-2-phenyleneimine). Synthesis and Reactivity in Inorganic and Metal Organic Chemistry, 30(8): 1535- 1540 (2000).
7. Pattison D.I., Lay P.A. and Davies, M.J The effect of divergent-bite ligands on metal-metal bond distances in some paddlewheel complexes , Inorg. Chem., 39, :2729. (2000)
8. Raman, N., Rahay, P. & Kulandaisory A. Preparation and characterization of Co(II), Ni(II) , Cu(II) and Zn(II) complexes. Indian Academy of Science, 113(3): 183-185. .(2001).
9. Sonmez, M. & Sekerel, M. . Synthesis and spectroscopic Investigation of some Schiff base complexes. Polish Journal of Chemistry, 76, 907– 914. (2002)
10. Hassan, A.M.A. "Co (II) and Fe (III) Chelates derived from isatin and some amines Journal of Islamic Academy Sciences, 4(4): 271- 274. (1999).
11. Carraher Jr., F. Li, D. Siegmann-Louda, Butler, C.S. Harless and F. Pflueger, Biological Activity of Organotin Polymers Containing p-Aminobenzoic Acid and Ampicillin Against Human Ovary Adenocarcinoma Cell Lines". Polym. Mater. Sci. Eng., 80, 363 (1999).
12. Kong, D., Chen, Q. Xie Y and. Zhou, X., Zhongguo Yaowu Huaxue Clinical value of Helicobacter pylori stool antigen test, ImmunoCard STAT HpSA, for detecting H pylori infection Clinical value of Helicobacter pylori stool antigen test, ImmunoCard STAT HpSA, for detecting H pylori infection Zazhi, 10, 13 (2000).
13. Sandow, M., May, B.L., C.J. Easton and S.F. Lincoln, Aust. " The study of properties of humic acids, and their separation" J. Chem., 53 :149 (2000).
14. Yeamin Reza , Belayet Hossain; " Antimicrobial Studies of Mixed Ligand Transition Metal Complexes of Phthalic acid and Heterocyclic amine Bases" Saidul Islam, Pakistan Journal of Biological Sciences , 6 Issue: 17 (2003).
15. Preti C. and Tosi , G. "Some observations on penta- and tri-hydro-complexes of iridium", J. Inorg. Nucl. chem, 36, : 3725 (1974) .
16. Lever. A.B.P. and Dodsworth E. S, in Comprehensive Coordination Chemistry, II, 2 Edited by A. B. P. Lever, Elsevier Publishers, (2004).

17. Lever. A.B.P. "Inorganic spectroscopy" 2nd ed publishing company London , New York. (1968).
18. Nakamoto; K "Infrared spectra of Inorganic and coordination compounds "4ED th ; J. Wiley and Sons, New york, (1996).
19. Panda S., Mishra R., Panda A.K., Satpathy S.C.: " Studies of Magnetic Field Effect on 9-Cyanophenanthrene-trans-1,2-dioxetane Exciplex Luminescence", J. Ind. Chem. Soc. 66, :472 (1989).
20. Klienstien, A. and Gabe ,I. An. "Solvent effects of benzophenone infrared spectrum" St. Univ, Lasi XIV, 139 (1968).
21. Chacko J, Parameswaran. G. " The effect of methanol and isopropanol on the mixed surfactant systems, ACS Proceeding on Surfaces and Colloids" Ind. J. Chem. 28A, :77 (1989).
22. Awetz, Melnick J. and Delbrgs, A , " Molecular Microbiology" M McGraw Hil- USA (2007).
23. Shivankar. V.S., Vaidya R.B., Dharwadkar. S., Thakkar N.V-23: Syn. React. Inorg. Metal-Org Chem. "Synthesis and biological activities of benzofuran antifungal agents targeting fungal N-myristoyl transferase " 33, 1597 (2003).

Synthesis and Characterization Of Some Dioxo – Rhenium (V) Complexes

Shemaa. A. S. Jabar¹, Mahmmad. Jaber², Atiaf K. Hammed¹, Dunia. N. Jihad¹, and Samaa. A. S. Jabar³

¹ Directorate of chemistry and petrochemical Industries Ministry of sciences and echnology

² Department of Chemistry, College of education, Ibn-Alhaitham, University of Baghdad

³ College of Education, University of Mustanceria

الخلاصة

تضمن البحث تحضير وتشخيص معقدات الرهنيوم خماسية الحالة التأكسدية وذات الصيغ التالية

- trans- $[(O)_2 Re (L^n)_2]X$; Where X=Cl, Br

n=2= L²= OPD= orthophenylene diamine

n=3= L³= HD = hexamethylene diamine

$[ReOX_3 (pPh_3)_2]$ where

X= Cl or Br

- cis $[Re O_2 (m- tolunitrile) bipy] Cl$

باستخدام المادة الأولية

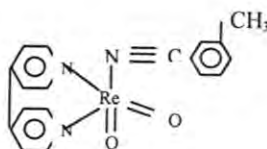
Re O₂ bipy

باستخدام المادة الأولية

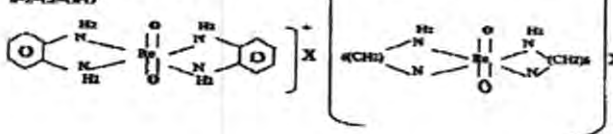
وبوجود مذيب الأسيتون أو الايثانول لمعقدات الترانس والتلوين لمعقدات الـ cis حضرت جميع المعقدات السالفة الذكر وبوجود الجو الخامل من غاز النيتروجين تم دراسة تشخيص تراكيب المعقدات المحضرة بالإضافة إلى دراسة الاستقرار الإشعاعية للمعقدات المحضرة تجاه أشعة كاما.

شخصت المعقدات المحضرة بواسطة التحليل الدقيق للعناصر (C,H,N)، أطيف الأشعة تحت الحمراء، أطيف الأشعة البنفسجية والمرئية، قياسات التوصيلية الكهربائية إضافة إلى استخدام تقنية HPLC لإيجاد زمن الاحتجاز والتعرف على عدد الإيزومرات ونقاوة المعقد المحضر، حيث أظهرت معظم المعقدات المحضرة قمة امتصاص واحدة والتي تبين نقاوة المعقد إضافة على وجوده بشكل ايزومر واحد في المحلول. ومن الدراسات أعلاه تبين أن الشكل الفراغي المقترح للمعقدات المحضرة هو ثنائي السطوح المشوه. تحتوي معقدات الرهنيوم ذات الصيغة العامة $[cis-ReO_2(m-tolunitrile)bipy]$ على مركز ثنائي الأوكسو وبموقع cis بينما تحتوي معقدات الرهنيوم ذات الصيغة العامة $trans-[(O)_2 Re (L^n)_2]X$ على مركز ثنائي الأوكسو وبموقع $[trans ReO_2]$ إضافة إلى كون هذه المعقدات أيونية وبالصيغ التركيبية المقترحة كالتالي:-

cis- $[ReO_2(L_1)bipy]Cl$



Trans- $[(O)_2 Re (L^n)_2]X$
n=2-L²=OPD



ABSTRACT

Two serious of rhenium (V) compounds were prepared: The first in trans- dioxo core with general formula:-

trans- $[(O)_2 Re (L^n)_2]X$

Where n=2=OPD= orthophenylene diamine

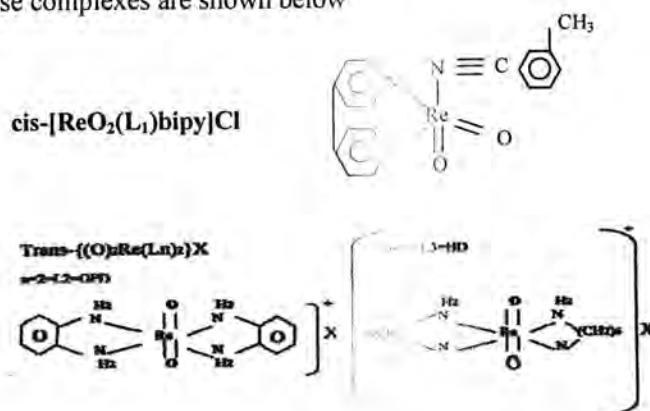
n=3=HD= hexamethylene diamine

These complexes were formed in high yield from reaction of $[\text{ReOX}_3(\text{pph}_3)_2]$ where $\text{X} = \text{Cl}$ and Br as a starting materials in Acetone once and another in ethanol.

The second compounds is cis-dioxo core with formula cis- $[\text{Re}(\text{O})_2(\text{m-tolunitrile})\text{bipy}] \text{Cl}$ was prepared by heating $[\text{ReO}_2 \text{ bipy Cl}]$ as a starting materials in toluene as a solvent. All reactions were carried out under nitrogen Atmosphere. The properties and structure of these complexes are discussed. Also the stability of these complexes have been examined towards γ - irradiation.

The structure of these complexes were confirmed by (C.H.N), I.R, (UV-Vis) spectra, electric conductivity measurements, along with HPLC technique to determine retention time (t_R) and find out the purity of complexes and the number of isomers in solution, these complexes displayed single species, which confirmed the purity of complexes and the presence of one isomer in solution.

This study show that all rhenium complexes have an octahedral structure. The proposed structures for these complexes are shown below



INTRODUCTION

We are currently studying the chemistry of complexes of rhenium containing rhenium nitrogen bonds(1), rhenium trichlorides (2, 3, 4). Our interests arises from the important of rhenium chemistry in radio pharmaceuticals chemistry (5,6,7).

Recently, we reported the synthesis of a new class octahedral rhenium complexes of the ReO_2CL_3 (8) type $[\text{ReO}_2(\text{L})_2]\text{X}$ where $\text{L} = \beta$ -Picoline, δ -picoline, β -amino pyridine were achieved under oxygen atmosphere(9).

In the work presented here in the synthesis of complexes containing dioxo core - rhenium (V)-with aryl and alkyl ligands are reported from the common starting material $[\text{ReOX}_3(\text{pph}_3)_2]$ where $\text{X} = \text{Cl}$ or Br and for preparing $\text{ReO}_2 [\text{m-tolunitrile bipy}] \text{Cl}$ from the starting material $[\text{ReO}_3\text{bipy}] \text{Cl}$.

MATERIALS AND METHODS

All reagents used were obtained from commercial sources and used as received $[\text{ReOX}_3(\text{pph}_3)_2]$, cis $[\text{ReO}_2 (\text{bipy}) \text{Cl}]$ was prepared by literature method as a starting material(10). The preparation of trans- $[(\text{O})_2\text{Re}(\text{L})_2]\text{X}$ and cis $[\text{ReO}_2(\text{m-tolunitrile})\text{bipy}]\text{Cl}$ were carried out under nitrogen atmosphere. I.R.

spectra were recorded on a perrkin – Elmer 1330 I.R. spectrophotometer in the $(4000-400)\text{cm}^{-1}$ range using KBr discs. UV-vis spectra were on a shimadzu UV-160 A. U.V-vis spectrophotometer in solution of the compounds in dichloromethane (CH_2Cl_2) at 25°C , using 1 cm width of quartz cell. HPLC were recorded carried out using a Gilson S50 DSI (octadecylsilane) column, with isocratic system and flow rate 1 cm min^{-1} with CH_2Cl_2 elution, Detection γ -irradiation was carried out using a ^{60}Co source type 220, canadion origin.

D- Trans – $[(\text{O})_2\text{Re}(\text{OPD})_2]\text{Cl}$

The complex $[\text{ReOCl}_3(\text{pph}_3)_2]$ (0.2gm, $2.4 \times 10^{-3}\text{mol}$), OPD (0.15gm, $1.38 \times 10^{-3}\text{mol}$) in acetone (15cm^3) were stirred under reflux for 90 min, during which time suspension green-yellow color mixture cooled to room temperature was removed under vacuum to dryness $\text{CH}_2\text{Cl}_2(10\text{cm}^3)$ along with ether (15cm^3) were added. Deep drank – green crystal of the required compound were obtained by slowly evaporation of the solution. This was collected by filtration washed with (5cm^3) of ether, and dried to give (0.1 gm, 89%), m.p = 115°C .

Found C = 30.65; H = 3.40; N = 11.92 $\text{C}_{12}\text{H}_{16}\text{ClReO}_2$

Require C = 30.60; H = 3.40; N = 11.85% I.R, $750_{\text{transvas}}\text{ReO}_2$,

$3310\delta(\text{N}-\text{H})$. U.V – vis, $\lambda_{\text{max}} = 316_{\text{nm}}$ $\epsilon = 494\text{ M}^{-1}.\text{S}^{-1}$, 384_{nm}

$\epsilon = 428\text{ M}^{-1}.\text{S}^{-1}$ (MLCT), $672\epsilon = 409\text{ M}^{-1}.\text{S}^{-1}$.

D₁ trans - $[(\text{O})_2\text{Re}(\text{OPD})_2]\text{Br}$

These complexes prepared by using the same method mentioned earlier but with (0.5gm, $5.1 \times 10^{-4}\text{mol}$) of $[\text{ReOBr}_3(\text{pph}_3)_2]$ in place of $[\text{ReOCl}_3(\text{pph}_3)_2]$. The complexes with formula trans- $[(\text{O})_2\text{Re}(\text{OPD})_2]\text{Br}$ as a green solid (0.098 gm, 92%).

E Trans – $[(\text{O})_2\text{Re}(\text{HD})_2]\text{Cl}$

The method used was analogous to that procedure given for compound (D) but with $[\text{ReOBr}_3(\text{pph}_3)_2]$ [$0.5\text{gm } 4.3 \times 10^{-3}\text{mol}$] in stead of $[\text{ReOCl}_3(\text{pph}_3)_2]$. The quantities of the other reagents were adjusted accordingly. The mixture was allowed to reflux for 90 min to give an orange colour solution, it was cooled in ice bath, and an orange compound was formed. The compound was recrystallised from $\text{CH}_2\text{Cl}_2/\text{n-hexane}$ and dried under vacuum yielded 0.10 gm of the required compound (m.p = 140°C , 86%) found C = 29.64, H = 6.58, N = 11.52; $\text{C}_{12}\text{H}_{32}\text{N}_4\text{O}_2\text{Re}$ requires, C = 29.59; H = 6.60; N = 11.50%, I.R, $710_{\text{transvas}}(\text{ReO}_2)$, $3310\delta(\text{N}-\text{H})$. U.V – vis, $\lambda_{\text{max}} 6211_{\text{nm}}$ $\epsilon = 2352\text{ M}^{-1}.\text{S}^{-1}$; 265.305_{nm} $\epsilon = 1661$, $1023\text{M}^{-1}.\text{S}^{-1}$ MLCT.

E₁ Trans – [(O)₂Re(HD)₂]Br

The method used to prepare this compound was similar to that from compound (E), but using (0.2gm, 2.0×10^{-4} mol) of $[\text{ReOBr}_3(\text{PPh}_3)_2]$ instead of $[\text{ReOCl}_3(\text{pPh}_3)_2]$. The compound as orange solid was obtained (0.95gm, 87%).

C [ReO₂ (m-tolunitrile) bipy] Cl

Under nitrogen atmosphere the complex $[\text{ReO}_3\text{Cl}(\text{bipy})]$ (0.1gm, 2.3×10^{-4} mol), m-tolunitrile (0.24ml, 1.9×10^{-3} mol) in toluene (10ml) were stirred under reflux for 90 min to give green – yellow, colour mixture solution. It was cooled in ice bath, and green yellowish was formed. The compound recrystallised from $\text{CH}_2\text{Cl}_2/\text{n-hexane}$ and dried under vacuum to dryness. (CH_2Cl_2) (10ml) along with ether (15ml) were added. Green yellowish crystals of the required compound were obtained by slowly evaporation of the solution. This was collected by filtration washed with 4cm^3 of ether, and dried to give (0.11gm, 92%) m.p = 349°C found C = 41.01; H = 2.84; N = 7.97; requires C = 40.00; H = 2.83; N = 7.75% I.R, 919, 760_{cis} (ReO_2); $1430\nu(\text{C}\equiv\text{N})$; $710\delta(\text{C}-\text{H})_{\text{ar}}$; $1025\nu(\text{Re}-\text{N})$, 1460 ($\text{C}=\text{N}$) U.V – vis λ_{max} 246nm $\epsilon = 119\text{M}^{-1}\text{C}^{-1}$; 312, $\epsilon = 531\text{M}^{-1}\text{S}^{-1}$.

RESULTS AND DISCUSSION

The complexes were prepared in good yield from reactions of the common rhenium precursor $[\text{ReOX}_3(\text{pPh}_3)_2]$, $[\text{ReO}_2\text{Cl}(\text{bipy})]$ in suitable solvent. The reactions were carried out in acetone, ethanol for trans-compound. These complexes are stable in the solid and in solution.

In the I.R spectra (D.E) compound, the most salient feature is the band at $750\text{--}760\text{cm}^{-1}$ is assigned to a symmetric stretching vibration of rhenium dioxo core at trans-arrangement which is expected to be the most sensitive band upon complexation. Also the absence of $[\text{Re}=\text{O}]$ at 968cm^{-1} and 981cm^{-1} which have been observed in the spectrum of the starting material while the (N–H) band appears at 3320cm^{-1} show lower value in compare with free ligand through nitrogen donor-set. Table (1) show additional bands in the spectrum of (L^2 , L^3 , C) which appears in the range of $1460\text{--}1440\text{cm}^{-1}$ which is attributed for bending vibration for group $\delta_{\text{sci}}(\text{CH}_2)_6$.

In additional I.R spectrum of compound show no band around 2000cm^{-1} for $\nu(\text{C}\equiv\text{N})$. on the other hand the strong band $\text{Ca.}1420\text{cm}^{-1}$ was attributed for the $\nu(\text{C}\equiv\text{N})$, such a shift to lower wave number is a result of redistribution of the electrons from the metal to the ligand orbital, forming π -back bonding ($d_\pi - p_\pi$) (11). In complex (C_1) the band at $\text{Ca } 919$ and 760cm^{-1} were assigned for the symmetric and a symmetric stretching vibration from cis dioxo rhenium, while the another band shift for lower frequency which is refers for coordination between metal and ligand. In the U.V-visi. Spectra, the complexes exhibit several bands at $\text{Ca.}240, 340\text{nm}$ due to the ligand and metal-Ligand charge transfer

respectively. While the absorption at Ca.460nm is attributed for (d-d) transition(12).

Figure (1), shows the HPLC chromatogram for complex E_1 . The spectrum displayed one absorbance band at retention time t_R 3.45 min with ration 1:1. This can be related to the presence of one isomer in the solution of distillation water.

Also the stability of complexes (D.E) and (C) have been examined towards γ -irradiation. The complexes show high stability and no change in the m.p, I.R and U.V-vis-visible spectra were observed. (Figure 2) shows the U.V-vis. Spectra of the irradiated complex (D) during different time. While (Figure 3) displayed the linear relationship between radiation time and the absorbance at λ_{max} (461 and 467)nm for complex (E_b , E_1) and (D_1) respectively.

Table -1: I.R. spectra of prepared compounds compare to their starting material

No. complex	$\nu_{as,s}(N-H)$	$\delta N-H$	$\nu(C-N)$	$\nu Re = O$	$\nu_{as trans}(ReO_2)$	$\nu(C\equiv C)_{arm}$	$\delta(C-H)_{arm}$	$\delta s(CH_2)$	cisReO ₂
L ²	3380,3360	1530	1340	-	-	-	-	-	-
M ₁	-			968		1550	690	-	-
D	3320	1445	1320		750	-	-	-	-
M ₂	-	-	-	981	-	-	690	-	-
D ₁	3300	1470	1310	-	780	-	-	-	-
L ³	3400, 3300	1525	1340	-	-	-	-	1465	-
E ₁	3310	1540	1310	-	900	-	-	1440	-
C ₁	-	-	-	-	-	-	-	-	919, 760

L² = O – phenylenediamine (OPD)

M₁ = [ReOCl₃(pph₃)₂], M₂ = [ReOBr₃(pph₃)₂]

D = trans – [(O)₂Re(L²)₂]Cl; D₁ = trans – [(O)₂Re(L²)₂]Br

L³ = hexamethy lenediamine (HD)

E₁ = trans – [(O)₂Re(L³)₂]Br, C₁ = [cis Re(O),bipy (m-tolunite)Cl]

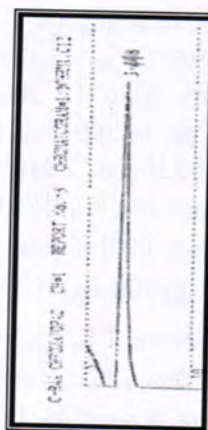


Fig.-1: The HPLC chromatogram for complex (E)

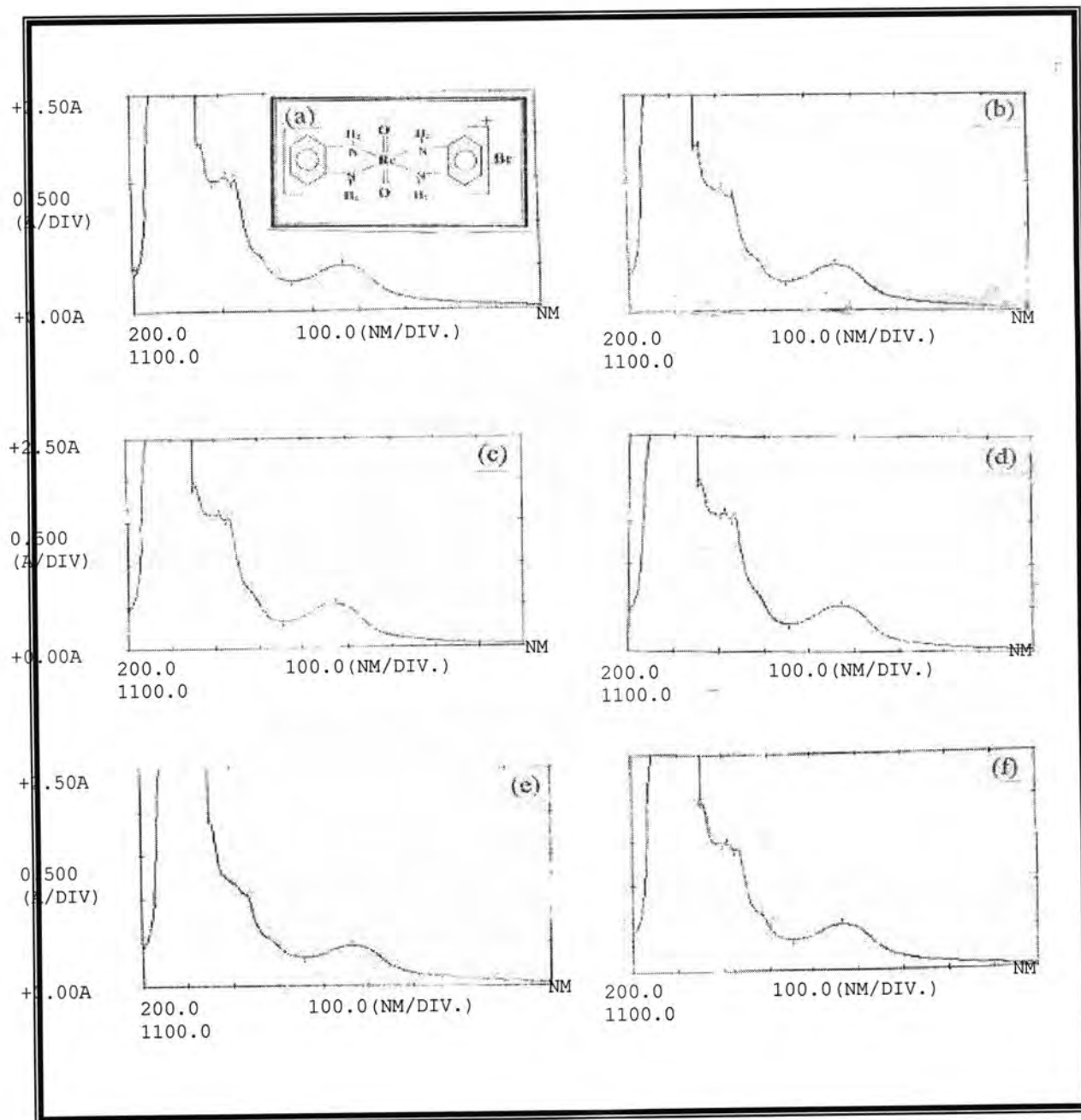


Fig.- 2: The U.V. visi. Spectra of complex $\text{trans-}[(\text{O})_2\text{Re}(\text{OPD})_2]\text{Br}$
 (a): before radiation.
 (b): after 5 minutes of g-radiation.
 (c): after 15 minutes of g-radiation.
 (d): after 60 minutes of g-radiation.
 (e): after 90 minutes of g-radiation.
 (f): after 120 minutes of g-radiation.

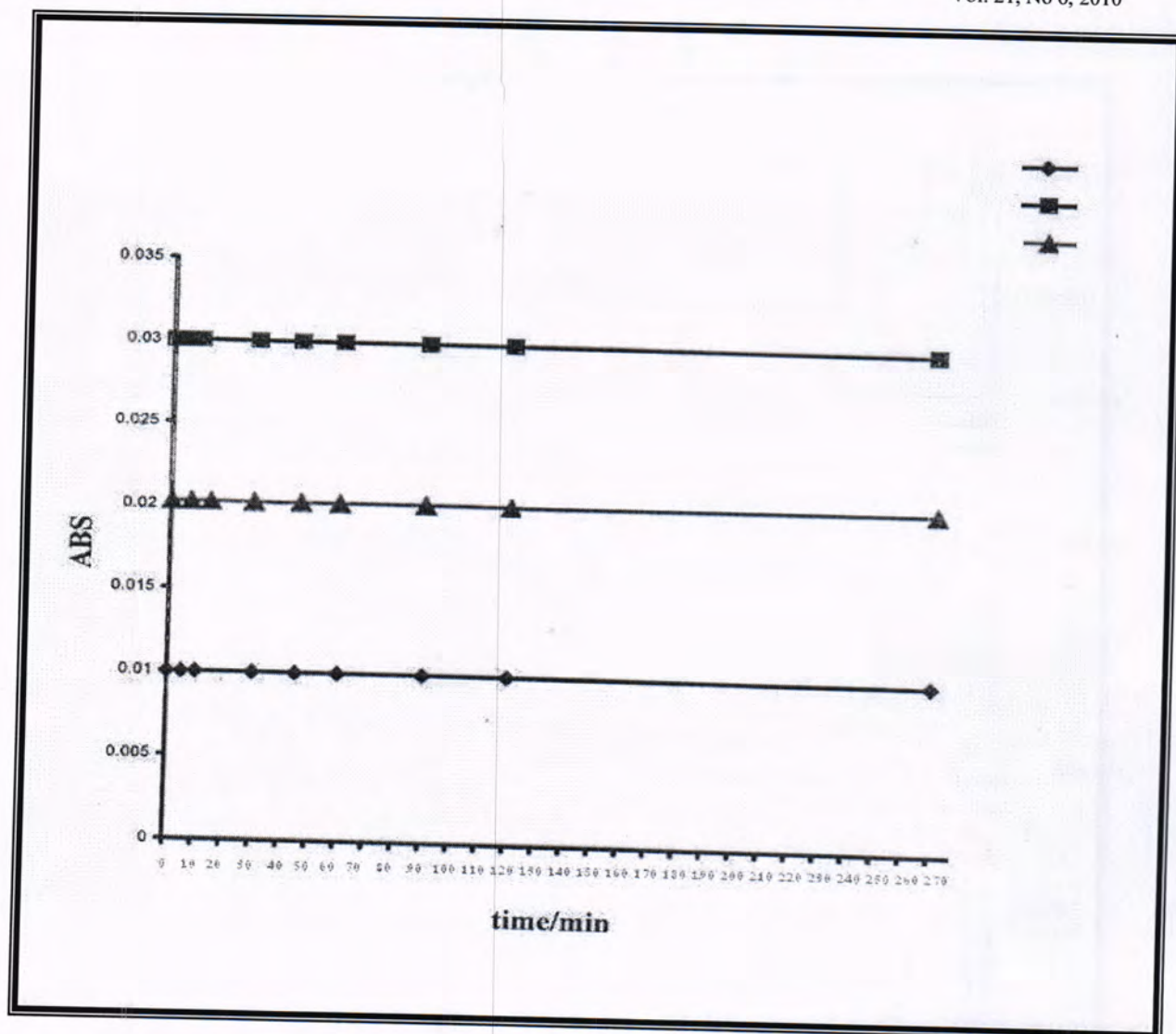


Fig.- 3: The relationship between the absorbance and radiation time of complexes (E_h, E_l) and D)

REFERENCES

1. Dilworth J.R. & Parrott S.J.,chem. Soc. Rev. "Thebiomedical chemistry of technetium and rhenium" 27, 43 (1998).
2. Abram.U.,Brucken.B.,Hagenbach.A.,Hecht.M.Kirmse.R.,&Voigt.A.J.of Inorga -nic "Reactions of rhenium and Technelium Nitrido complexes with ER₃ Fragments E=B,Ga, Al, C,P;R=H,Alkyl,Aryi" 629, issue 1:1560-1564 (2003).
3. Hunghuy.N.,Abram.U.J.of Ino. and general chemistry "Synthesis and Reactivity of structurally A nalogousphenylimido and oxo complexes of Rhenium V with N, N-Dialkyl- N- benzoylthioureas"634:1560-1564(2008).
4. Verma.S., Hanack. M., J. of Ino and general chemistry "Synthesis of Nitrido (Phthalocyaniato) metal Vcomplexes and New compounds with Nitrido- Bri

- gages between Rhenium and elements of the third Main Group" 629, issue 5 :880-892(2003).
5. Nicolini M., Bandoli G. and U. Mazzi "Technetium and Rhenium in nuclear medicine" 4. Padova, (1995).
 6. Housecroft.C., & sharpe A.G."Inorganic chemistry" 2nd Amesterdam,(2007).
 7. Ilsezolle"Technetium 99m. pharmaceutical: preparation and quality control in nuclear medicinie"(2007).
 8. Brown.D.&Colton.R.,J.of Nature,"preparation of Rhenium Tetrachloride" chem- istry Division,Atomic Energy Research Establishment,198,:1300–1301 (1963).
 9. Salah.A.A.M.Sc.,Thesis"Studying and mechanism of picolyime and theirdrivad -iue in different solvents"college of Ibn–Haitham Unicersity of Baghdad(2000).
 - 10.Al-Hamzawi.Sh.A.M.Sc.Thesis,"Synthesis and characterization of some rhenium III,V complexes,containg Nitrogen Donerjet Ligands,and their stability towards γ -irradiation"College of Ibn-Haitham, University of Baghdad (2000).
 - 11.Rouschias G.&G.Wjlkinson,J.Chem.soc.,A."The preparation and reactions of Trihalogeno (alkanonitrile) rhenium complexes": 993(1967).
 - 12.Lever,A.B.T.Inorganic Electronic spectroscopy,2nd Ed.,Elsevier,New York, :324 (1986).

Copolymerization of 1,2:3,4-di-o-isopropylidene-5,6-exo- α -D-galactosene Monomer

Yousif Ali Al-Fattahi¹, Salah M. Aliwi², and Hammed H. Mohamed³

¹ Department of Chemistry, College of Science, University of Baghdad

² Ministry of Higher Education & Scientific Research

³ Department of Chemistry, College of Science, University of Al-Mustansiriyah

الخلاصة

تم في هذا البحث اجراء البلمرة المشتركة للسكر غير المشبع: 1,2:3,4-di-o-isopropylidene-5,6-exo- α -D-galactosene مع الستايرين، خلاص الفانيل، مثيل اكريلات، انهريد المالك و اكريلونايتريل، وقد تم تحضير هذه البوليمرات في المحلول باستخدام ثنائي البنزويل بيروكسيد كبادئ وعند درجة حرارة 80 °C. شخّصت تراكيب السكريات البوليمرية المحضرة بواسطة الطرق الطيفية الأشعة تحت الحمراء (FT-IR) والرنين النووي المغناطيسي (¹H-NMR). وتم تحديد نسب الفعالية بطريقة (K-T) Kelen-Tüdös و (F-R) Finnan-Ross للستايرين (r_1) و السكر (r_2) وكانت القيم: $r_1 = 0.83$, $r_2 = 0.2$ (F-R) و $r_1 = 0.74$, $r_2 = 0.21$ (K-T) ومن خلال نسب الفعالية تم معرفة تركيب البوليمر الناتج وهو بوليمر عشوائي.

ABSTRACT

copolymerization of the 1,2:3,4-di-o-isopropylidene-5,6-exo- α -D-galactosene with vinyl monomer such as: styrene, vinyl-acetate, methylacrylate, maleic anhydride and acrylonitrile were carried out in toluene solution using dibenzoyl peroxide as initiator at 80 °C. The structures and compositions of the saccharide homo and co-polymers were established by ¹H-NMR and FT-IR spectroscopy.

Reactivity ratios of vinyl sugar (r_2) with styrene (r_1), (ratio of the rate constant for adding its own monomer to that for adding the other monomer) were determined by Fineman-Rose (F-R) and Kelen-Tüdös (K-T) methods. The values are $r_1 = 0.83$, $r_2 = 0.21$ for F-R method and $r_1 = 0.74$, $r_2 = 0.2$ for K-T method and the composition of copolymer was random copolymer.

INTRODUCTION

During recent years there has been an increasing interest in the use of renewable resources as organic raw materials(1), especially the use of carbohydrates for the preparation of polymers(2). Large amounts of carbohydrates are commercially available and a substantial part of the surplus of their agricultural production may be spent in this way. One possibility to prepare macromolecules from sugars makes use of the preparation of vinyl sugars and their polymerization 3.

The chemical or enzymatical synthesis of sugar monomers such as "vinyl saccharides" and their radical and / or cationic polymerization are well known in the literature (4,5,6).

The corresponding poly (vinyl saccharides) have been prepared from different vinyl saccharides such 1,3-dimethyl-5-glucopy-raneosyl-5-(4-vinyl benzyl) barbiurate (4).

A new exo-glucopyranoide(7),exo-fructofuranoid(8),exo-fructopyranoid(9), glucono- δ -lactone(10,11) derivatives were synthesized and investigated in chain polymerization reaction.

The corresponding saccharide polymers, homo-and copolymers,were synthesized under free radical conditions(11,12) new styryl-water-insoluble and methacryloyl-type water-soluble monomers were synthesized from the most common acidic saccharide, D-glucuronic acid(13), a new glycomonomer was synthesized from D-glucose(14).

The application of polymerizable vinyl sugar molecules for the preparation of special polymers was investigated. In one research project, hydrophilic surface are generated on standard polymers after copolymerization with low amounts of protected vinyl sugars.

The polymers might then find use as thickeners (15) (e.g. in the tertiary oil recovery), as flocculating agents(16), as polymeric detergents(15,16) as bioadhesive water soluble polymeric drug carriers(17) or for surface modification of standard polymers(18). They might also be of interest as models for intercellular recognition processes.

The aim of the present work is to synthesize vinyl sugar " 1,2: 3,4-di-O-isopropylidene-5,6- α -D-galactosene" and saccharide-co-polymers by either homopolymerization or copolymerization with different vinyl monomers. This type of copolymer and homopolymer have found useful applications: in medicine and industry. Study of their either UV-light degradation or biodegradation may give an understanding of their application as degradable saccharide-polymers .

MATERIALS AND METHODS

Preparation 1,2:3,4-di-O-isopropylidene-5,6- α -D-galactosene monomer

The monomer was prepared as described previously(19)

Copolymerization of 1,2:3,4-di-O-isopropylidene - 5,6- α -D-galactosene with active alkenes

1,2:3,4-Di-O-isopropylidene-5,6- α -D-galactosene(3)(0.03g;1.2mmole), alkene monomer (1.3mmole) and dibenzoyl peroxide (DBP) (0.006g ; 0.02mmole) were dissolved in toluene (5mL) and introduced to a 20mL polymerization tube and sealed. The mixture was heated at 80°C for 48 hr in an oil-bath, then the reaction solution was added to diethyl ether: petroleum ether (1:4) (35ml) to eject the precipitation of the copolymer.

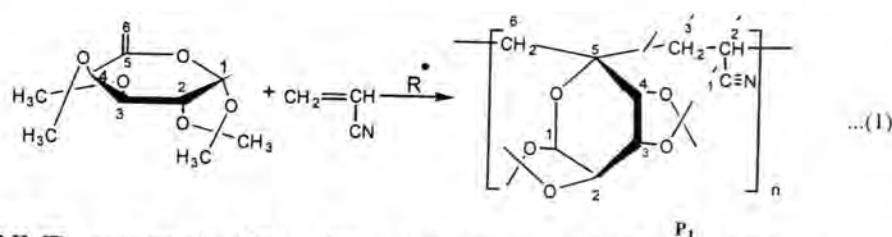
The copolymer produced was filtered off and dried overnight under reduced pressure at 40°C. It was purified by dissolving it in dichloromethane and was precipitated several times by diethyl ether-petroleum ether (1:4) to give pure copolymer. Physical properties and spectral details of the prepared copolymers are listed in table (1)

RESULTS AND DISCUSSION

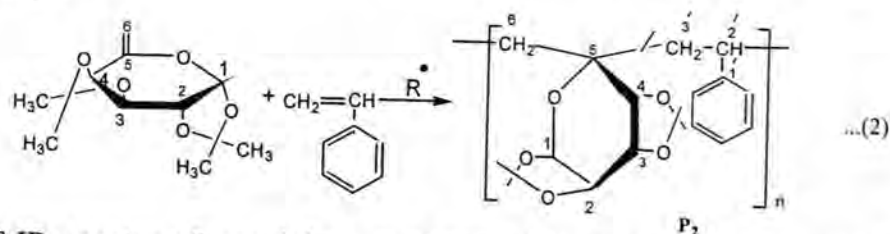
Copolymerization of 1,2:3,4-di-O-isopropylidene-5,6- α -D-galactosene

Although the radical homopolymerization of vinyl sugar seems to be quite difficult, copolymerization takes place readily with a range of commercially available vinyl comonomers (styrene, vinylacetate, acrylonitrile, methylacrylate and maleicanhydride). Vinyl sugar is easily copolymerized with the comonomers within a period of 48 hr using dibenzoyl peroxide as initiator and toluene as solvent at 80°C. The overall yields of the copolymerization of vinyl sugar are generally low, independent from polarity and / or reactivity of comonomers. These results are similar to other researches in literatures^{7,8} . The chemical structures of the saccharide copolymers were investigated with ¹HNMR and fourier transform

infrared (FT-IR) analysis. The ^1H NMR spectrum of poly (exo-galactosene-co-acrylonitril) P_1 [see equation 1], shows signals appeared in the spectral region between 3.14-3.38 ppm belong to the sugar protons of the pyranoid ring and methine protons of acrylonitril moiety (H-2'). The signal located in the range 2.1-2.5 ppm is a characteristic of methylene protons (H-6,H-3') of the polymeric chain and for the methyl protons of the isopropylidene groups respectively. The FT-IR spectrum of P_1 showed stretching band located at 2243 cm^{-1} for nitrile group ($\text{C}\equiv\text{N}$) and the disappearance the stretching bands at 1600 cm^{-1} for double bond ($\text{C}=\text{C}$).



The ^1H NMR spectrum) of poly(exo-galactosene-co-styrene) (P_2) [see equation 2] ,shows signals appeared in the spectral region between (3.65-4.1)ppm for sugar protons of pyranoid ring and methane protons of phenyl moiety (H-2'). The signal located in the range (1.1-2.3)ppm is a characteristic of methylene protons (H-6,H-3') of the polymeric chain and for the methyl protons of the isopropylidene groups respectively. Signals are located at (6.3-7.2)ppm which are characteristic of benzene ring protons. The FT-IR spectrum of P_2 showed stretching bands located at $3024\text{-}3100\text{ cm}^{-1}$ which are assigned to the C-H aromatic, stretching vibration and the bands located in the spectral range between $1025\text{ to }1255\text{ cm}^{-1}$ belong to the C-O-C groups.



The FT-IR spectra of remaining copolymers illustrate the disappearance of the stretching band of ($\text{C}=\text{C}$) located at 1600 cm^{-1} and the presence of stretching bands located between $1731\text{ to }1735\text{ cm}^{-1}$ for carbonyl group. Table(1) shows the physical properties and spectral details for the synthesized compounds and copolymers .

Table -1 : The physical properties and spectral details of the compounds

Number of compound	Melting point	Yield	FT-IR details	¹ H-NMR details
P ₁ Poly(galactosene-co-AN)	> 250 °C	35%	2939 cm ⁻¹ (C-H) m, 2243 cm ⁻¹ (CN) s, 1438-1456 cm ⁻¹ (CH ₂ bending)s, 1350-1390 cm ⁻¹ (C-H)m of pyranoid ring, 1072 - 1300 cm ⁻¹ (C-O-C) s	(2.1-2.5) ppm for isopropylidene protons and methylene protons(H-6, H-3), (3.14-3.38) ppm for sugar protons of the pyranoid ring and methine protons of acrylonitrile moiety (H-2)
P ₂ Poly(galactosene-co-St)	185-187 °C	40%	3024-3100 cm ⁻¹ (C-H aromatic) m, 2921 cm ⁻¹ (C-H aliphatic) m, 1600cm ⁻¹ (C=C stretching) m, 1452-1482 cm ⁻¹ (CH ₂ bending)s, 1330-1385 cm ⁻¹ (C-H)w of pyranoid ring, 1025 -1255 cm ⁻¹ (C-O-C) w	(1-2.3) ppm for isopropylidene protons and methylene protons (H-6, H-3) , (3.65-4.1) ppm for sugar proton of the pyranoid ring and methine protons of phenyl moiety (H-2) , (6.3-7.2) ppm for benzene ring protons
P ₃ Poly(galactosene-co-Vac)	> 200 °C decomposed	26%	2989-3089 cm ⁻¹ (C-H) w, 1735 cm ⁻¹ (C=O)s, 1450 cm ⁻¹ (CH ₂ bending)s, 1330-1395 cm ⁻¹ (C-H)m of pyranoid ring , 1024-1311 cm ⁻¹ (C-O-C) s	
P ₄ Poly(galactosene-co-MA)	> 200 °C decomposed	40%	2846-3053cm ⁻¹ (C-H) s, 1731 cm ⁻¹ (C=O) s, 1450 cm ⁻¹ (CH ₂ bending)s, 1350-1395 cm ⁻¹ (C-H)w of pyranoid ring , 1058-1268 cm ⁻¹ (C-O-C) m	
P ₅ Poly(galactosene-co-MAh)	>200 °C decomposed	33%	2906-3072 cm ⁻¹ (C-H) w, 1733 cm ⁻¹ (C=O) s, 1450 cm ⁻¹ (CH ₂ bending)s, 1330-1375 cm ⁻¹ (C-H)w of pyranoid ring , 1026-1234 cm ⁻¹ (C-O-C) m	
S :strong , m: medium , w: weak , AN :acrylonitril , St :styrene , Vac : vinyl acetate , MA : methyl acrylate , MAh : malice anhydrid				

Determination of reactivity ratios

The reactivity ratios (r_1, r_2) of poly (exo-galactosene-co-styrene) determined by u.v.spectrophotometer method using Fineman and Rose (F-R)²⁰, Kelen and Tüdös (K-T)²¹ equations. Copolymerization were carried out in low conversion conditions ($\leq 10\%$). Tables (2) ,(3) ,(4) and (5) shows the calculated values in feed and copolymer .

Table -2: The mole fraction of monomers in feed and copolymer.

Numbers of copolymer experiments	Mole fraction of monomers in feed		Mole fraction of monomers in copolymer	
	F_1 for styrene	F_2 for sugar	f_1 for styrene	f_2 for sugar
1	0.263	0.736	0.423	0.576
2	0.487	0.512	0.592	0.433
3	0.675	0.324	0.735	0.291
4	0.718	0.281	0.742	0.259
5	0.775	0.224	0.815	0.183

Table -3: Calculated values of the monomers mole fraction in feed.

Numbers of copolymer experiments	$F = F_1/F_2$	F^2
1	0.337	0.127
2	0.951	0.904
3	2.083	4.34
4	2.55	6.52
5	3.45	11.97

Table - 4: Calculated values of the monomers mole fraction in copolymer

Numbers of copolymer experiments	$f = f_1/f_2$	$f-1$
1	0.734	-0.265
2	1.360	0.36
3	2.525	1.525
4	2.864	1.864
5	4.45	3.45

Table -5 : The F-R and K-T parameters for copolymers

Numbers of copolymer experiments	F-R parameters		K-T parameters	
	$F(f-1)/f$	F^2/f	$\zeta = (F^2/f) / (F^2/f) + \alpha$	$\eta = F(f-1)/f / (F^2/f) + \alpha$
1	-0.128	0.173	0.189	-0.13
2	0.25	0.843	0.520	0.154
3	1.25	1.718	0.688	0.50
4	1.62	2.27	0.744	0.53
5	2.6	3.5	0.818	0.607

monomer reactivity ratios r_1 and r_2 (where 1 and 2 refer to styrene and vinyl sugar respectively) can be obtained from the well known Finmann-Rose equation:

$$F(f-1)/f = (r_1 F^2/f) - r_2 \quad \dots(1-1)$$

Where F and f are the mole fraction of monomers 1 and 2 in the initial monomer feed and initial copolymer respectively. By plotting $F(f-1)/f$ vs F^2/f (the plot shown in Fig. 1) a linear relationship is obtained, from which the r_1 and r_2 values are obtained from slope and intercept respectively (0.83 for r_1 and 0.21 for r_2).

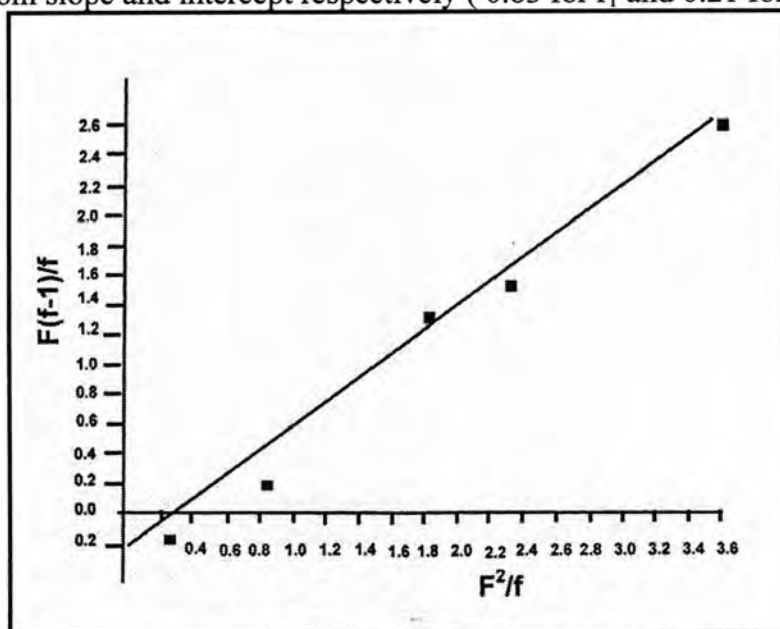


Figure -1: Fineman-Ross plot for copolymer of styrene with vinyl sugar

An alternative method of evaluating such results has been put forward by Kelen and Tüdös using equation (1-2):

$$\eta = (r_1 + r_2 / \alpha) - r_2 / \alpha \quad \dots\dots(1-2)$$

$$\text{Where } \eta = \frac{F(f-1)/f}{(F^2/f) + \alpha} \quad \dots\dots(1-3)$$

$$\zeta = \frac{(F^2/f)}{(F^2/f) + \alpha} \quad \dots\dots(1-4)$$

and (α) is an adjustable constant. The value of α was chosen using the equation:

$$\alpha = [(F^2/f)_{\max} * (F^2/f)_{\min}]^{1/2} \quad \dots\dots(1-5)$$

Where $(F^2/f)_{\max}$ and $(F^2/f)_{\min}$ represent the highest and lowest values of (F^2/f) in the range studied. values of (α) is found to be 0.77. Plot of η vs ζ are given in Fig (2) yield in a value of 0.74 for r_1 (slop= r_1+r_2/α) and 0.21 for r_2 (intercept = $-r_2/\alpha$).

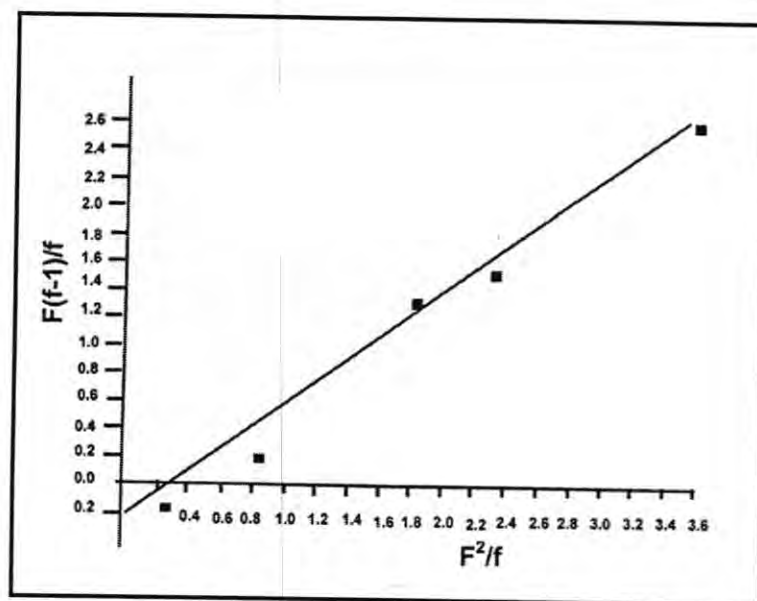


Figure-2: The Kelen and Tüdös plot for copolymer of styrene with vinyl sugar

The higher reactivity of styrene can be explained on the basis of π -electron availability and the radical stability by resonance, a conjugated monomer exhibits a strong tendency to add to a given radical because the resulting adduct radical will be strongly stabilized by resonance. On the other hand, an unconjugated monomer will exhibit a much weaker tendency to add to the same monomer given radical because the resulting adduct will be much less stabilized, these results are similar to the results reached in literature(8).

Copolymer composition for the copolymerization systems.

The composition of copolymer ($P_{2,5}$) can be obtained from plot of the mole fraction of styrene in feed and in the resulted copolymer as shown in Fig. 3. The figure shows the curve for styrene not met with straight line which presents random copolymer but near to it, i.e., its presents are random copolymerization where $r_1 r_2$ less the one ($r_1 r_2 = 0.22$).

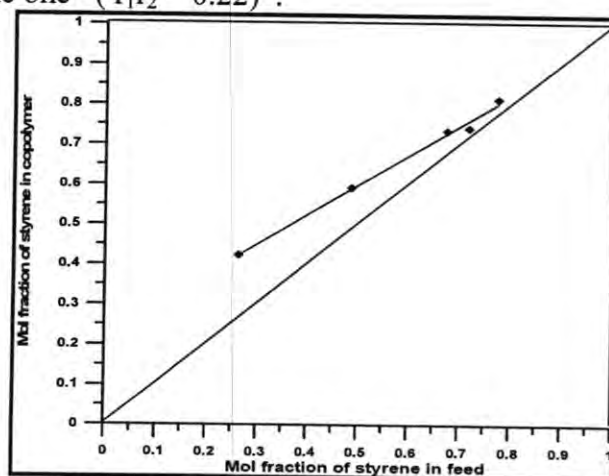


Figure-3 : The relationship between mole fraction of styrene in feed and in the copolymer

Sequence length distribution

The sequence length distribution was obtained from the following equations(22)

$$S_A = 1 + r_A \frac{[A]}{[B]} \quad \dots(1-6)$$

$$S_B = 1 + r_B \frac{[B]}{[A]} \quad \dots(1-7)$$

Where S_A and S_B present sequence length distribution for styrene (A) and vinyl sugar (B) respectively, r_A , r_B present reactivity ratios for styrene (A) and vinyl sugar (B). $[A]$ and $[B]$ present the number moles of monomers in feed. The S_A , S_B values are tabulated in table (6).

Table -6: Values of sequence length distribution for poly (exo-galactosene-co-styrene).

Numbers of copolymer experiments	[st]/ [sugar]	[sugar]/ [st]	S_A		S_B	
			Where $r_1 = 0.83$	Where $r_2 = 0.74$	Where $r_2 = 0.21$	Where $r_2 = 0.2$
1	0.337	2.798	1.279	1.249	1.559	1.587
2	0.951	1.051	1.706	1.703	1.216	1.220
3	2.083	0.48	2.728	2.541	1.096	1.100
4	2.55	0.39	3.116	2.887	1.078	1.081
5	3.45	0.28	3.86	3.55	1.056	1.058

From the above mentioned results one could notice that the copolymers are richer with styrene monomer as compared to the vinyl sugar monomer.

We can conclude:

This study shows that copolymers of a new type of C-C linked vinyl sugar monomer with technically interesting monomers (styrene, vinylacetate, acrylonitril, maleic anhydride and methylacrylate) could be conveniently prepared by radical copolymerization in solution. The chemical structure of the vinyl sugar monomer, copolymers of vinyl sugar monomer was determined by using ^1H NMR and FT-IR.

By applying Finmann-Rose (F-R) and Kelen-Tüdös (K-T) methodologies to the copolymers data obtained from ultraviolet-visible analysis of copolymers obtained at low conversions, the reactivity ratios of styrene (1) and sugar (2) were found to be $r_1 = 0.83$, $r_2 = 0.21$ (F-R method) and $r_1 = 0.74$, $r_2 = 0.2$ (K-T method). The differences in reactivity ratios are explained on the basis of π -electron availability and the radical stability. The composition of copolymer was random copolymer.

REFERENCES

1. Lichtenthaler F.W., Ed., "Carbohydrates as Organic Raw Materials" VCH, Weinheim, (1991).
2. Wulff G., Clarkson G., Diderichs H. and Gunz S., in "3 Symposium Nachwuchsende Rohstoffe-Perspektiven für die chemie", Schriftenreihe des Bundesministeriums für Ernährung, Landwirtschaft und Forsten, Reihe A, Landwirtschaftsverlag, Münster, :187, (1994).
3. Wulff G., Schmid J. and Venhoff T.P., "The preparation of new types of polymerizable vinyl sugars with C-C bonds between sugar and double bond", *Macromol. Chem., phys.*, 197, 259, (1996).
4. Wulff G. and Clarkson G., "New type of polyvinylsaccharides with N,N-dimethylbarbituric acid as a linker between sugar and styrene residue", *Macromol. Chem., phys.*, 195, 2603, (1994).
5. M.J.Donnely, "In vitro enzymic synthesis of polymers containing saccharides, lignins, proteins or related compounds: a review" *Polymer International*, 47, 257 (1999).
6. Al-Bagoury M., Buchholz K. & Yaacoub J. "Synthesis of well-designed polymers carrying saccharide moieties via RAFT miniemulsion polymerization" *Polymers for advanced technologies*, 18, 313, (2007).
7. Yaacoub E.J., Skeries B. and Buchholz K. "Synthesis and polymerization of exoglucal derivatives", *Macromol. Chem. Phys.*, 198, 899, (1997).
8. Wick S. and Yaacoub E. J., "Synthesis and polymerization of a 5,6-unsaturated fructofuranoid derivatives" *Macromol. Chem. Phys.* 201, 93, (2000).
9. Glümer A. & Yaacoub E.J., "Synthesis and polymerization of 1,2-unsaturated fructopyranoid derivatives", *Macromol. Chem Phys.*, 201, 1521, (2000).
10. Glümer A.G., Skeries B., and Buchholz K. "Synthesis and copolymerization of unsaturated Glucono- δ -lactone derivatives" *Macromol. Chem. Phys.*, 205, 73, (2004).
11. Boltres D., Schmalbruch B. and Buchholz K., "Copolymerization of unsaturated Glucono- δ -lactone derivatives", *Macromol. Chem. Phys.*, 205, 1508, (2004).
12. Yaacoub E.J., Wick S., & Buchholz K., "Synthesis and polymerization of methyl 5-deoxy-2,3-O-isopropylidene- β -D-erythro-pent-4-enofuranoside" *Macromol. Chem. Phys.*, 196, 3155, (1995).
13. Shimura Y., Hashimoto K., Yamanaka C. & Setojima D. "Synthesis and polymerization of new styryl and methacryloyl monomers containing acidic saccharide moieties" *J. of Polymer Science part A: Polymer Chemistry*, 39, 3893, (2001).
14. Shinde V.S. and Pawar V.U., "Synthesis of thermosensitive glycopolymers containing D-glucose residue: copolymers with N-isopropylacrylamide", *J. of Applied Polymer Science*, 111, 2607, (2008).
15. Kunz M., in "Nachwachsende Rohstoffe-Perspektiven für die chemie", M. Eggersdorfer, S. Warvel, G. Wulff, Eds., VCH, Weinheim, :367, (1993).
16. Klein J., Kunz M., in "Nachwachsende Rohstoffe: Polysaccharid Forschung", Edited in Commission of BMFT, Forschungszentrum Jülich. :198, (1993).
17. Rathi R.C., Kopeckova P., Rihova B. & Kopecek J., "N-(2-hydroxypropyl) methacrylamide copolymers containing pendant saccharide moieties : synthesis and

- bioadhesive properties" *J. of Polymer Science part A: Polymer Chemistry*, 29, 1895 (2003).
18. Kunz M., in: *Carbohydrates as Organic Raw Materials*, F.W. Lichtenfhler, Ed., VCH, Weinheim, :127, (1999).
 19. Al-Fattahi Y. A., Aliwi S. M., and Mohamed H. H., " Preparation and study the thermal initiation of poly vinyl isopropylidene D-galactose", *J. of College of Education*, 1, 45, (2009).
 20. Fineman M. and Ross SD., Linear method for determining monomer reactivity ratio in copolymerization, *J. Polym. Sci.*, 5(2), 259, (1950).
 21. Kelen T. and Tudos F., Analysis of linear methods for determining copolymerization reactivity ratios, *J. Macromol. Sci. chem. A.*, 9, 1, (1975).
 22. Sharba A.A.H., Tarik S.N. and Butti N.A., M.Sc. Thesis, "Free radical copolymerization of some vinyl monomers and determination of their composition by infra-red spectroscopy", AL-Mustansiriah University, (2005)

Construction of New Ethambutol Selective Electrodes for Determination Ethambutol in Pharmaceutical Drugs

Nabil S. Nassory, Abdul-Muhsin A. Al-Haideri and Souhaila K. Sayhood
Chemistry Department, College of Education (Ibn Al-Hatham), University of Baghdad,

الخلاصة

في هذه الدراسة حضرت اقطاب انتقائية لمادة الايثمبوتول الدوائية معتمدة على معقد الدواء مع dodeca-Tungstophoric acid مع مجموعة من المواد الملدن di-butyl phosphate (DBP), tri-butyl phosphate (TBP), di-butyl phthalate (DBPH), (NPOE) o -phenyl octyl ether octyl phthalate (DOPH). اظهرت الاقطاب مع الملدنات DOPH, TBP, DBP انحدار 34.5, 21.5, 27.5 mV/decade على التوالي ويحد تحسس 1.9×10^{-5} مولاري وبمدى تركيز خطي 10^{-1} - 10^{-4} مولاري ومدى دالة حامضية 3-8. اما الاقطاب للملدنات DBPH, NPOE, اظهرت استجابة غير نرنستية بانحدار 21.5 mV/decade. اظهرت الدراسة عدم وجود تداخل لعدد من الايونات الموجبة الاحادية والثنائية والثلاثية. تم تطبيق هذا القطب على المستحضرات الصيدلانية باستخدام قطب المستند على DOPH كملدن وقد اعطت نتائج جيدة.

ABSTRACT

Ethambutol selective electrodes were constructed based on ethambutol-phosphotungstate (EMB-PT) complex with different plasticizers; di-butyl phosphate (DBP), tri-butyl phosphate (TBP), di-butyl phthalate (DBPH), o-nitro phenyl octyl ether (NPOE) and di-octyl phthalate (DOPH). The electrodes based on DBP, TBP and DOPH plasticizers gave slopes near to Nernstian slope which are 27.5, 25.2 and 34.5 mV/decade with detection limit of 1.9×10^{-5} M and concentration range 10^{-1} to 10^{-4} M and pH range 3.0 – 8.0. The electrodes based on DBPH and NPOE showed non-Nernstian slopes, 21.5 mV/decade for both plasticizers. Interfering of some cations was investigated and shows no interfering with electrodes response. Potentiometric methods were used for measuring ethambutol in pharmaceutical drugs (tablets) and the electrode based on DOPH was used for determination. The recovery obtained from measuring was in good agreements with that given in British Pharmacopias.

Keywords: Ethambutol electrodes, Phosphotungstic acid ionophore, Potentiometric methods

INTRODUCTION

Ethambutol hydrochloride (EMB), $C_{10}H_{24}N_2O_2 \cdot 2HCl$, contains not less than 97.0% and not more than the equivalent of 101.0%. A white, crystalline powder, freely soluble in water, soluble in alcohol, it melts at about 202 °C(1). Ethambutol is an antibiotic; it prevents growth of the tuberculosis bacteria in the body and used to treat tuberculosis. Several papers were published for determination of ethambutol, a high-performance liquid chromatographic method for determination ethambutol in plasma has been developed by Suzuki et al.(2). Ion-pair reversed phase liquid chromatography with UV detection can be used for determination of ethambutol by Jiang et al.(3). A selective liquid chromatographic method has been developed by Nakano et al.(4) for assay of ethambutol in serum samples with fluorescence detection; the detection limit of ethambutol was 23 ng/ml serum and the method was selective enough to analyze ethambutol in rabbit serum. Ion selective electrodes (ISEs), which are applied for drug analysis due to their simplicity, fast response and easy to used. Kharitonov(5) reviewed a paper in using ion selective electrodes in organic

medicinal drug determination, including the optimization of the selective electrodes and mechanism of the response. Several papers were published using phosphotungstic acid as an ionophore for drug complex formation and used for construction of drug electrodes. Al-Haideri et al.(6) prepared and studied ampicilline selective electrodes on complexation of ampicilline with phosphotungstic acid as an active substances with different plasticizers. The best electrode was based on TBP plasticizer which gave a slope of 58.0 mV/decade and detection limit of 7.0×10^{-5} M and used for ampicilline determination in pharmaceutical drugs. Atenolol selective electrodes were prepared by Nassory et al.(7) based on complex of atenolol-phosphotungstate as an active material using various plasticizers. The best electrode was based on DOPH plasticizer with slope 55.9 mV/decade and standard deviation of ± 0.1 . Several amines and amiloride-selective electrodes were constructed by Nassory et al.(8). The amiloride electrode based on di-octyl phthalate plasticizer was excellently sensitive and was used for determination of amiloride in pharmaceutical drugs. A novel mebendazole PVC sensor was described by Kumar et al.(9) for fabrication, optimization and some possible applications of the mebendazole electrode. The membrane based on mebedazole-phosphotungstate complex with BEP plasticizer gave a slope of 55.8 mV/decade and detection limit of 6.3×10^{-7} M. In this work, new ethambutol selective electrodes were prepared based on phosphotungstic acid (PT) as an ionophore in PVC plastic membranes with different plasticizers. The study was carried out for determination, selectivity coefficients, pH range, and electrode parameters and used for determination of ethambutol in pharmaceutical drugs.

MATEREIALS AND METHODS

Orion EA-940 ion analyzer was used for measuring electrode response.

pH meter type pH M82 type Radio meter, Copenhagen.

Saturated calomel electrode type Gallenkam.

Silver wire coated with silver chloride used as internal reference electrode.

PVC powder type Breon S110/10 B.P.

All solutions were prepared using doubly distilled de-ionized water.

Chemicals and reagents

Ethambutol hydrochloride was a gift from the State Company of Drug Industries and Medical Appliances (Samara IRAQ-SDI).

Ethambutol tablets (400 mg ethambutol-HCl) was purchased locally (Ajanta Pharm. Limited, India).

Di-butyl phosphate 98.9%, di-butyl phthalate, 99%, tri-butyl phosphate, 97%, o-nitro phenyl octyl ether, 98% and di-octyl phthalate, were obtained from Fluka AG, Switzerland.

Stock solutions of 0.1 M in each of LiCl, NaCl, KCl, CaCl₂, MgCl₂, ZnCl₂, AlCl₃, CrCl₃ and FeCl₂ were prepared. More diluted solutions were prepared by subsequent dilution of stock solutions.

Solution of 0.1 M ethambutol hydrochloride was prepared by dissolving 1.386 g standard and completing the solution up to 50 ml water.

Phosphotungstic acid (PT), 0.1 M was prepared by dissolving 7.2 g in 25 ml water.

Procedures

Preparation of ion pair complex

EMB-PT ion pair was prepared by mixing with stirring equal volumes of 0.1 M phosphotungstic acid (PT) and 0.1 M ethambutol hydrochloride. The resultant precipitate was filtered, washed and dried.

Assembly the electrode

The construction of the electrode body and immobilization were done according to the method described by Davis et al.(10). The glass tube was $\frac{3}{4}$ filled with 0.1 M ethambutol solution as an internal filling solution. The membrane prepared by dissolving 0.04 g of ethambutol-phosphotungstate with 0.36 g plasticizer and 0.17 PVC in 6 ml THF. The mixture was poured into glass disc, 3.5 cm diameter and allowed to dry at room temperature.

Selectivity measurements:

A separate solution method was used for the selectivity coefficient measurement, and was calculated according to the equation(11):

$$\log K_{\text{pot}} = [(E_B - E_A) / (2.303 RT/z_F)] + (1 - z_A/z_B) \log a_A \dots\dots\dots(1)$$

E_A , E_B ; z_A , z_B ; and a_A , a_B are the potentials, charge numbers and activities for the primary A and interfering B ions, respectively, at $a_A = a_B$.

Also the selectivity coefficients were measured by match method according to equation (12).

$$K_{\text{pot}} = \Delta a_A / a_B \quad \Delta a_A = a_A' - a_A$$

RESULTS AND DISCUSSION

Ethambutol-phosphotungstate (EMB-PT) as an electro active complex was used to prepare new ethambutol selective electrodes. The characteristics of the electrode response based on (EMB-PT) and different plasticizers, di-butyl phthalate (DBPH), di-butyl phosphate (DBP), tri-butyl phosphate (TBP), o-nitro phenyl octyl ether (NPOE) and di-octyl phthalate (DOPH) were investigated. All the membranes were soaked in 0.1 M ethambutol solution for 2 hours in order to conditioning the membrane before used. The results of electrode parameters measurements for ethambutol selective electrodes are listed in Table 1. The physical properties of the membranes prepared are colorless, flexible and transparent except the membrane based on NPOE plasticizer gave a yellow colored. Electrodes based on DBP, TBP and DOPH plasticizers gave slopes near to Nernstian slope are 27.5, 25.2 and 34.3 mV/decade, respectively. The slope values indicate that the complex (EMB-PT) formed is 2:1, two molecules of ethambutol interact with one molecule of phosphotungstic acid, and interaction may be the two nitrogen atoms in ethambutol interact with phosphotungstic acid. Non-Nernstian slopes were obtained for electrodes based on DBPH and NPOE plasticizers was around 21.5 mV/decade, this may be attributed to the behaviors

of the plasticizers with ethambutol complex, such as a weak interaction, incompatibility of the plasticizers with the complex or the viscosity of the plasticizers which cause a leaching of the complex to the external solution during the measurements. The linear concentration range was ranged from 10^{-1} to 10^{-4} M and with excellent detection limit of 1.9×10^{-5} M. A typical plot for electrode response with concentrations of ethambutol is shown in Figure 1 for electrode based on tri-butyl phosphate plasticizer using Orion 7 cycle semilogarithmic paper for plot.

pH effect

The effect of pH on the response of the ethambutol electrodes was studied for three concentrations of ethambutol (10^{-2} , 10^{-3} and 10^{-4} M) by following the variation in potentials over pH range from 2.0 to 11.0 by addition dilute hydrochloric acid and sodium hydroxide. Fixed potentials (did not change in potentials) was noticed in the range 3.0 to 8.0. The results are listed in Table 2. Representation curve for pH plot with potentials is shown in Figure 2 for ethambutol electrode based on DBP plasticizer at 10^{-2} to 10^{-4} M ethambutol solutions.

Response time and life time

The response times at t_{95} for the electrodes at concentrations ranging from 10^{-1} to 10^{-5} M were calculated from the response with time plot. The values of response time were ranged from 6 s at concentration 10^{-1} M ethambutol solution and the values increases when the concentration of ethambutol increase and reach to about 35 s at 10^{-5} M. The fast response time of the electrodes indicates the more stability of the electrodes and can be used for quantitative measurements of the drugs with very good values of standard deviations. The life time of the electrodes was measured from the calibration of the electrode continuously every 2 days and behaviors of the slopes were investigated. The life time of the electrode ranged from 6 to 37 days. The short life time for electrode based on NPOE plasticizer is attributed to the leaching of the plasticizer (low viscosity 11.44 cSt) to the external solution during the measurements or incompatibility of the plasticizer with the active complex.

Selectivity measurements

The influence of some interfering inorganic cations, Li^+ , Na^+ , K^+ , Mg^{2+} , Ca^{2+} , Zn^{2+} , Al^{3+} , Cr^{3+} and Fe^{3+} on the electrode response was studied. The selectivity coefficients for the electrodes were measured by the separate solution method for the concentrations range from 10^{-1} M to 10^{-5} M. The values of the selectivity coefficients for electrodes based on DBP, TBP and DOPH plasticizers are listed in Table 3 for concentrations of ethambutol at 10^{-2} M and 10^{-4} M. As noticed from the Table 3 the interference was increases as the concentration of ethambutol decrease. None of the investigated cations interfere seriously with the electrode response. A match method was used for the electrodes based on DBPH and

NPOE plasticizers of the non-Nernstian slopes using the equation given in the experimental part. The selectivity coefficient can not be measured by this method because the cations show no interference with the electrode response. A typical plot for match method using electrode based on TBP and magnesium ion is shown in Figure 3.

Sample analysis

Potentiometric techniques were used for determination of ethambutol hydrochloride which includes (direct, standard addition and titration methods). Synthetic solutions of ethambutol at concentrations 10^{-3} , 5×10^{-3} and 5×10^{-4} M were used. The recoveries and linear equations for the electrodes obtained from the calibration curves are listed in Table 4. The results of direct, standard addition and titration methods for concentration of ethambutol at 1×10^{-3} M using electrode based on DOPH plasticizer are listed in Table 5. A phosphotungstic acid was used as a titrant for potentiometric titration. Determination of ethambutol in commercial drugs (Tablets) with electrode based on DOPH plasticizer by using potentiometric methods was studied. 10^{-3} M of ethambutol hydrochloride was taken from ethambutol tablets and the analysis showed that the recoveries and %RE obtained using direct, standard addition and titration methods are 102.1, 99 and 104% and 2.1, -1.0 and 4.0%, respectively. The values of the recovery of ethambutol in tablets are in good agreements with the results of British Pharmacopeias. A plot of standard addition method, antilog (E/S) versus ml of standard ethambutol addition is shown in figure 4.

Conclusion

New ethambutol selective electrodes were constructed based on phosphotungstic acid ionophore and different plasticizers. A good ethambutol electrode was based on DOPH plasticizer and used for determination of ethambutol in pharmaceutical formulations.

Table-1: Properties of constructed ethambutol electrodes with different plasticizers.

Electrode No.	Plasticizer	Slope mV/decade	Detection limit/M	Conc. range/M	Response time/s	Life time/day
I	DBPH	21.5 (0.9999)	1.9×10^{-5}	$10^{-1} - 10^{-4}$	6.0 – 32.0	~ 17
II	DBP	27.5 (0.9992)	1.9×10^{-5}	$10^{-1} - 10^{-4}$	7.0 – 34.0	~ 19
III	TBP	25.2 (0.9998)	1.9×10^{-5}	$10^{-1} - 10^{-4}$	5.0 – 22.0	~ 24
IV	NPOE	21.5 (0.9998)	1.7×10^{-5}	$10^{-1} - 10^{-4}$	5.0 – 25.0	~ 6.0
V	DOPH	34.5 (0.9998)	1.9×10^{-5}	$10^{-1} - 10^{-4}$	5.0 – 29.0	~ 37

Vales between the parentheses refer to r (correlation coefficient).

Table-2: pH values for the electrodes at different concentrations of ethambutol solutions

Electrode number	pH range		
	10^{-2} M	10^{-3} M	10^{-4} M
I	3.90 – 7.36	2.69 – 6.26	3.36 – 6.10
II	4.55 – 7.31	4.18 – 8.20	4.25 – 8.30
III	3.71 – 6.14	3.44 – 5.68	3.48 – 6.00
IV	3.79 – 7.42	3.66 – 7.72	4.79 – 8.02
V	3.71 – 6.19	4.96 – 6.68	3.74 – 6.70

Table-3: Selectivity coefficient values for ethambutol electrodes at 10^{-2} and 10^{-4} M concentrations of ethambutol and some cations

Interfering cations	Selectivity coefficient K_{etham}					
	DBP		TBP		DOPH	
	10^{-2} M	10^{-4} M	10^{-2} M	10^{-4} M	10^{-2} M	10^{-4} M
Li^+	2.32×10^{-3}	1.76×10^{-2}	8.37×10^{-4}	2.46×10^{-3}	2.57×10^{-2}	2.74×10^{-1}
Na^+	5.41×10^{-3}	2.17×10^{-1}	3.58×10^{-3}	2.63×10^{-2}	2.57×10^{-2}	1.97×10^{-1}
K^+	1.89×10^{-2}	3.90×10^{-1}	5.32×10^{-3}	8.56×10^{-2}	1.14×10^{-2}	4.39×10^{-1}
Mg^{2+}	8.66×10^{-3}	7.87×10^{-2}	2.42×10^{-4}	1.14×10^{-3}	4.51×10^{-3}	5.88×10^{-2}
Ca^{2+}	1.88×10^{-2}	7.24×10^{-2}	1.14×10^{-3}	4.93×10^{-2}	2.93×10^{-4}	7.59×10^{-3}
Zn^{2+}	1.88×10^{-2}	4.76×10^{-2}	9.56×10^{-4}	7.94×10^{-3}	3.95×10^{-3}	5.88×10^{-2}
Al^{3+}	6.47×10^{-4}	1.87×10^{-3}	3.29×10^{-4}	9.24×10^{-4}	8.64×10^{-4}	8.50×10^{-3}
Cr^{3+}	1.37×10^{-3}	2.87×10^{-3}	5.12×10^{-4}	7.52×10^{-3}	3.28×10^{-3}	4.99×10^{-3}
Fe^{3+}	7.94×10^{-4}	2.04×10^{-3}	6.57×10^{-3}	9.88×10^{-3}	2.35×10^{-3}	9.09×10^{-3}

Table-4: Recoveries and linear equations values for electrodes at different concentrations of ethambutol solutions.

Electrode No.	Conc. of ethambutol taken/M	Conc. of ethambutol found/M	%RE	%REC	Linear equation
I	5.0×10^{-3}	5.01×10^{-3}	0.2	100.2	$Y = 9.37 \text{Lin}X + 63.18$
	5.0×10^{-4}	4.99×10^{-4}	-0.2	99.8	
II	5.0×10^{-2}	5.01×10^{-3}	0.2	100.2	$Y = 12.01 \text{Lin}X + 58.11$
	5.0×10^{-3}	4.99×10^{-2}	-0.2	99.8	
III	5.0×10^{-3}	5.04×10^{-2}	0.8	100.8	$Y = 10.98 \text{Lin}X + 93.05$
	5.0×10^{-3}	5.04×10^{-2}	0.8	100.8	
IV	5.0×10^{-3}	4.90×10^{-2}	-2.0	98.0	$Y = 9.37 \text{Lin}X + 74.28$
	5.0×10^{-3}	4.91×10^{-3}	-1.8	98.2	
V	5.0×10^{-3}	5.01×10^{-3}	0.2	100.2	$Y = 15.02 \text{Lin}X + 112.9$
	5.0×10^{-4}	4.92×10^{-4}	-1.6	98.4	

Table-5: Analysis of ethambutol hydrochloride samples by potentiometric methods

Method	Conc. of ethambutol taken /M	Conc. of ethambutol found /M	%RE	%REC	%RSD
Direct	1.0×10^{-3}	1.01×10^{-3}	1.0	101.0	2.670*
Standard addition	1.0×10^{-3}	1.003×10^{-3}	0.3	100.3	0.351
Titration	1.0×10^{-3}	0.98×10^{-3}	-2.0	98.0	3.25

* Each value was an average of three measurements.

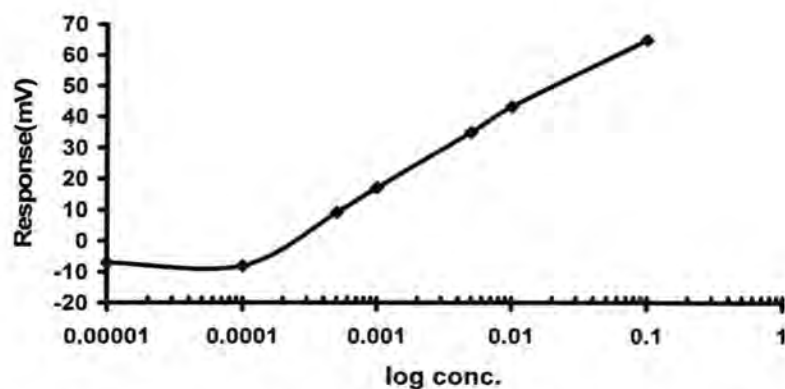


Fig.-1: Calibration curve of ethambutol selective electrode based on TBP plasticizer.

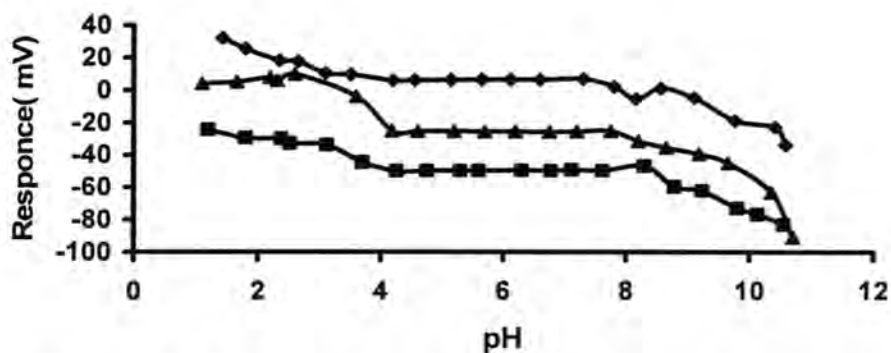


Fig-2: Plot of pH vs. electrode response of ethambutol electrode based on DBP plasticizer.

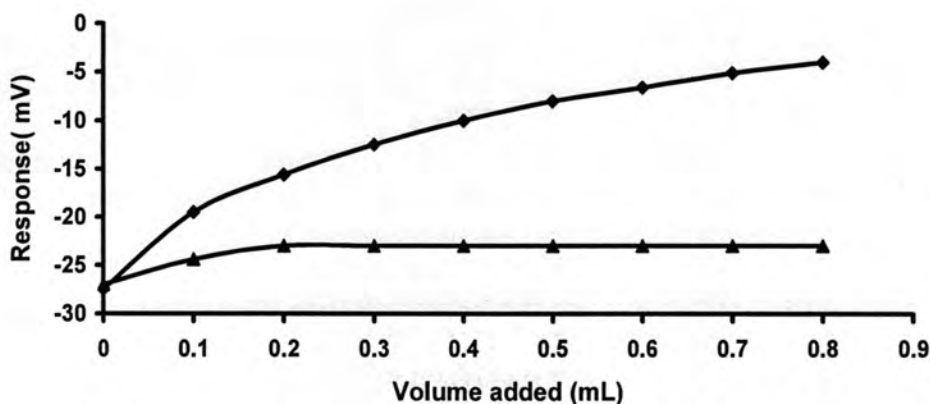


Fig.-3:Plot of selectivity by match method for electrode based on DBP plasticizer in present interfering Mg^{2+} ion.

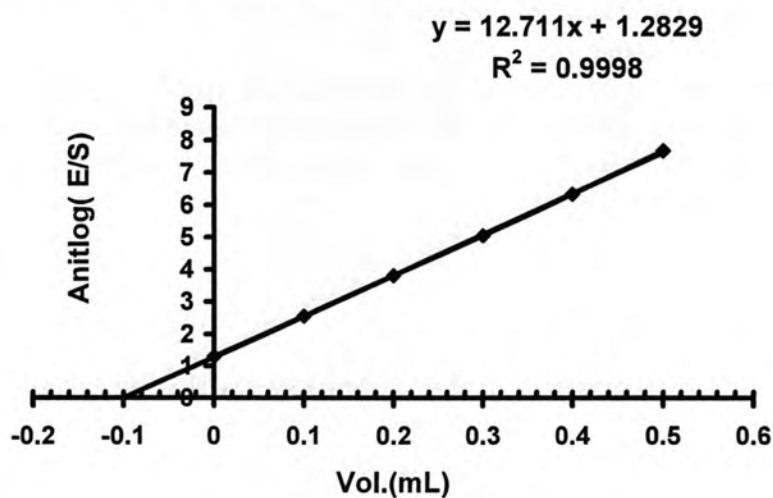


Fig.-4:Standard addition plot for determination $10^{-3}M$ ethambutol in tablets using electrode based on DBP plasticizer.

REFERENCES

- 1.The pharmaceutical codex, Principle and Practical of Pharmaceutical, 21st ed., The Pharmaceutical Press, London (1994).
- 2.M.Suzuki,T.Ono&S.Takitani,Analytical Sciences,"Determination of ethambutol in plasma by high-performance liquid chromatography with fluorescence detection", 7 :949- 950(1991).
- 3.Z.Jiang,H. Wang&D.C.Locke,Analytica Chimica Acta,456(2),189- 192(2002).

4. Y.Nakano, H.Nohta, H. Yoshida, K.Todoroki, T.Saita, H.Fujito, M.Mori & M.Yamaguchi, *Analytical Sciences*, "Liquid chromatographic determination of ethambutol in serum samples based on intramolecular excimer-forming fluorescence derivatization" 20(3):489(2004).
5. S.V.Kharitonov, *Russian Chemical Reviews*, "Ion-selective electrodes in medicinal drug determination" 76(4):361–395(2007).
6. A.M. Al-Haidery, N.S. Nasory and A.S.M. Al-Saadi, *Ibn-Al-Haitham J. of Pure and Applied Sciences (in Arabic)*, "preparation and characterization of ampicillin selective electrode" 19(4A):101–115(2006).
7. N.S.Nassory, S.A.Maki & M.A.Ali, *Turk.J.Chem.* "Preparation and characterization of an Atenolol selective electrode based on a PVC matrix membrane" 31:75–82 (2007).
8. N.S.Nassory, A.A.Al-Haidery & I.K.M.Al-Mashhadany, *Chem.Anal.(Warsaw)* "Preparation and characterization of an amiloride selective electrode based on a PVC matrix membrane, 52:55– 66(2007).
9. K.G.Kumar, S.Tohn, P.Augustin, P.Poduval & B.Sarawathyamma, *Analytical Sciences*, "Mebendazole selective membrane sensor and its application to pharmaceutical", 23, 291,(2007).
10. J.E.W.Davies, G.J.Moody & J.D.R. Thomas, *Lab. Practice*, 22, 20(1974).
11. Y. Umezawa, P. Buhlmann, K. Umezawa, K. Tohda and S. Amemiya, *Pure and Appl. Chem.*, "Potentiometric selectivity coefficients of ion –selective electrodes", 72:1851-2082, (2000).
12. K.Tohda, D.Drago, M.Shibata & Y.Umezawa, *Analytical Sciences* "Studies on the matched p-potential method for determining the selective coefficient of Ion – Selective electrodes based on neutral ionophores experimental and theoretical verification" 17:733-742(2001).

Preparation and Study of Cephalexin Selective Electrodes and Their Application in Pharmaceutical Drugs

Khaleda H. Al-Saidi, Nabil S. Nassory and Shahbaz A. Maki

Chemistry Department, College of Science, Al-Nahrain University.

الخلاصة

حضرت أقطاب إنتقائية للسيفالكسين بتحضير المادة الفعالة (السيفالكسين- فوسفوتنكستيت) Ceph-PT مع الملدنات المختلفة وهي داي بيوتيل فوسفيت (DBP), داي بيوتيل فثاليت (DBPH), داي اوكتيل فثاليت (DOP), تري بيوتيل فوسفيت (TBP) واورثو نيترو فثيل إيثر (NPOE) في غشاء اصله من بولي فائينيل كلورايد (PVC). الدراسة شملت خواص الأقطاب كتأثير الدالة الحامضية (pH), المحلول الداخلي للأقطاب, الانتقائية وحد التحسس ومدى الخطية. إن أفضل الأقطاب المحضرة هي باستعمال الملدنات (DBPH, DOP). والمحلول الداخلي (10^{-3} M Ceph + 10^{-3} M NaCl) حيث إن الميل لمنحني المعايرة هو (59.5 و 58.5 mV/decade) وبحدود تحسس (5×10^{-5} , 3×10^{-5} M) على التوالي ومدى خطية متساوي 10^{-4} – 10^{-2} M ولهما ثبوتية وتكرارية جيدة. إن هذه الأقطاب استخدمت لتقدير السيفالكسين في المستحضرات الدوائية الكبسول والمعلق الفموي وإن معدل الاسترجاع والانحراف المعياري كالآتي: (100.344 ± 0.120) (100.116 ± 0.393). تمت مقارنة النتائج المستحصلة من الأقطاب مع نتائج المشتقات الطيفية حيث تطابقت نتائج المشتقة الطيفية الأولى من حيث قيمة نسبة الاسترجاع والدقة وسهولة الطريقة.

ABSTRACT

A plastic membrane electrodes for the determination of cephalexin monohydrate were fabricated based on the use of cephaixin-phosphotungstate as an active substance, and with different plasticizers, di-butyl phosphate (DBP), di-butyl phthalate (DBPH), di-octyl phthalate (DOP), tri-butyl phosphate (TBP) and o-nitro phenyl octyl ether (NPOE) in PVC matrix membranes. The study was carried out to investigate the electrode parameters, effect of pH and selectivity. Internal filling solution of 10^{-3} M Ceph + 10^{-3} M NaCl was used to fill the electrodes. The best electrodes were based on DBPH and DOP plasticizer which gave a slope 59.5 and 58.5 mV/decade, linear concentration range 10^{-4} – 10^{-2} M and detection limit of 5×10^{-5} and 3×10^{-5} M, respectively displayed good stability and reproducibility. The electrodes were used to determine the cephalexin monohydrate in oral suspension and capsules, the average recovery and standard deviation were (100.116 ± 0.393) and (100.344 ± 0.120), respectively. The results were compared with UV-derivative spectrophotometry (DS) and the results for the drugs obtained by first derivative are quite comparable with the recovery obtained by cephalexin selective electrodes.

Keywords; cephaixin electrodes, phosphotungstic acid ionophore, Derivative spectrophotometry, cephaixin monohydrate determination

INTRODUCTION

The name of cephalexin monohydrate was changed to cefalexin in British pharmacopeia's 1999. It prepared as; capsules, oral suspension and tablets. Cephalexin monohydrate is an oral antibiotic which has a wide spectrum of antibacterial activity, which has the empirical formula ($C_{16}H_{17}N_3O_4 \cdot S, H_2O$), and the molecular weight 365.4g/mol(1). cephalexin monohydrate contains not less than 95.0% and not more than 100.1% with reference to the anhydrous substances(1). Cephalexin occurs as white, or almost white, crystalline monohydrate powder. It is soluble in water, practically insoluble in alcohol and in

ether, resistant to acid and well absorbed orally. Ion selective electrodes (ISEs) are used today in a wide range of applications and new uses constantly being reported in the literature. Characterization of bulk drugs becomes increasingly important in the pharmaceutical industry. Analytical techniques are commonly employed for this purpose by using drug-selective electrodes(2-7). Several different methods have been used for determination of cephalexin monohydrate including; High-performance liquid chromatographic(8-12), A capillary zone electrophoresis method(12), Parallax, a solid-phase fluorescence(13). Spectrophotometry and derivative spectrophotometry (DS) technique were utilized in determination of cephalexin (15,16). The methods for the determination of organic substances by the derivative spectrophotometry (DS) technique have been developed mainly for application in the analysis of pharmaceuticals and biochemical interesting systems. The general aspects of UV derivative spectrophotometry and its advantages and limitations with respect to normal spectrophotometry are reviewed.(17,18) and it's used in chemical and in pharmaceutical analysis. In this work several cephalexin selective electrodes were prepared using phosphotungstic acid ionophore with different plasticizers in PVC membranes. The electrodes based on DBPH and DOP used for determination cephalexin in oral suspension and capsules and to compare the results with UV derivative spectrophotometry.

MATERIALS AND METHODS

Apparatus

- 1-Double-beam UV-Visible spectrophotometer model (UV-1650 PC) SHIMADZU (Japan), interfaced with computer via a SHIMADZU UV probe data system program (Version 1.10).
- 2- Infrared spectrophotometer SHIMADZU, FTIR-8000 (Japan).
- 3- Expandable ion analyzer, ORION, model EA 940, (U. S. A.).
- 4- Reference electrode single junction, ORION, model 90-01
- 5- Combined glass electrode Orion No.91-02, (Swiss made).

Chemicals and reagents

- 1- Standard antibiotic drugs: cephalexin monohydrate, Amoxicillin trihydrate, cloxacillin sodium, and ampicillin trihydrate were gift from the State Company of Drug Industries and Medical Appliances (IRAQ-SDI- Samara).
- 2- Commercial drugs: cephalexin capsule 250 (ACFLEX)* and oral suspension of cephalexin (ACFLEX)* 125 were marketed by (The Arab Co. for Antibiotics Industries), all drugs were purchased from local pharmacies
- 3-The plasticizers are di-butyl phosphate, di-butyl phthalate, di-octyl phthalate, tributyl phosphate, o-nitro phenyl octyl ether and phosphotungstic acid were obtained from Fluka and BHD companies
- 4-Tetrahydrofuran (E.Merck).

5-Polyvinyl chloride (PVC) of relatively high molecular weight (Breon S 110/10 B.P Chemical U. K. Ltd).

All chemicals and solvents were of an analytical reagent grade obtained from BDH, Fluka and Aldrich companies. Deionized distilled water was used throughout the study.

Procedure

The stock standard solutions of 0.01M cephalexin monohydrate was prepared by dissolving 0.1827g standard drug, into 50 ml water by using ultrasonicator to dissolve the drug. Other standards were prepared by serial dilutions of the stock solution. Stock solution of phosphotungstic acid (0.01 M) was prepared by dissolving 1.44 g of the acid in 50 ml of water.. 0.1M stock solutions of each interfering salts. NaCl, NH₄Cl, KCl, CaCl₂, MgCl₂, CuSO₄ and Fe(NO₃)₃.3H₂O were prepared by dissolving 0.2922, 0.2672, 0.3729, 0.5550, 0.4761, 0.7980 and 2.0201 gm in 50 ml of water respectively. 0.01M solutions were prepared for amoxicillin trihydrate, cloxacillin sodium, ampicillin trihydrate, sucrose and gelatin. The pharmaceutical drugs oral suspension cephalexin 125 BP (ACFLEX) solution was prepared by dissolving all content to 1L with vigorous shaking followed by filtration the first part was rejected, the resultant concentration of drug is 125 µg/ml (0.342×10^{-3} M). 0.01 M cephalexin capsules (AEFLEX) capsules 250 BP was prepared similar to standard the content of ten capsules were mixed and homogenized and weighted accurately, the weight of one capsule was diluted to 1L of water.

Preparation of ion-pair compound

The ion-pair of cephalexin -phosphotungstate (ceph-PT) was prepared by mixing equal amounts of 0.01 M acidified solution of the drug with 0.01 M phosphotungstic acid with stirring. The resulting a yellow precipitate obtained was sediment by centrifugation and extensively washed with de-ionized water and dried for 2 days in evacuated desiccator's.

Fabrications of the membrane and electrode

The method of immobilization the ion-pair compound into the PVC matrix membrane was made as described by Craggs et al. (18). A 0.04 g of cephalexin -phosphotungstate mixed with 0.36 g plasticizer and 0.17 g PVC dissolved in 6 ml THF with stirring until a clear viscous solution was obtained. The resultant solution was poured into a glass casting ring about 35 mm in diameter, the solution was left for 2 days to allow slow evaporation of the solvent and formation a sensing membrane. Laboratory-made electrode body was used, which consisted of glass tube containing silver wire coated with silver chloride and internal filling solution. The electrode was made according to the procedure given in reference(20).

RESULTS AND DISCUSSION

Cephalexin -phosphotungstate as an electro active compound was used to prepare new sensors. The electroactive compound was confirmed by using FTIR, the coordination sites of cephalexin monohydrate involve in the bonding with phosphotungstic acid had been determined by comparison of the IR spectrum of the complex with that of the parent cephalexin monohydrate as in Figure 1. The potentiometric response characteristics based on (ceph-PT) and five plasticizers, DBP, DBPH, DOP, TBP and NPOE in PVC matrix were examined. The effect of the plasticizers was studied with respect to the slope, concentration range, detection limit, response time, life time and pH effect. All the membranes were soaked in 10^{-3} M cephalexin monohydrate solution for one hour in order to conditioning the membrane before use. Two different internal filling solutions were used; the first one was 10^{-3} M cephalexin + 10^{-3} M HCl to calibrate the electrodes from 10^{-2} M to 10^{-7} M cephalexin.. The second was 10^{-3} M + 10^{-3} M NaCl. The best conditions for determination cephalexin monohydrate were with internal filling solution of 10^{-3} M + 10^{-3} M NaCl. The slopes were near Nernstian slope with correlation coefficients around one for the electrodes based on DBPH, DOP, and NPOE. Therefore, this internal solution was fixed for all measurements. The results of electrode parameters measurements for cephalexin monohydrate selective electrodes are listed in Table 1. Electrode based on DBPH, DOP, and NPOE gave a very good Nernstian slopes equal to 59.5, 58.5 and 62.0 mV/decade and detection limit of 5.0×10^{-6} M, 3×10^{-5} M and 6×10^{-6} M respectively displayed good stability and reproducibility during the measurements. Also good electrode parameters were obtained for electrodes DBPH and DOP with life times around 20 and 30 days. The short life time for NPOE around 7 day. This short life time can be attributed to the behavior of the plasticizer with (ceph-PT) complex or may be the low viscosity of the plasticizers or incompatibility of the plasticizer with PVC matrix. A typical plot for calibration curves of electrodes based five plasticizers are shown in Figure 2.

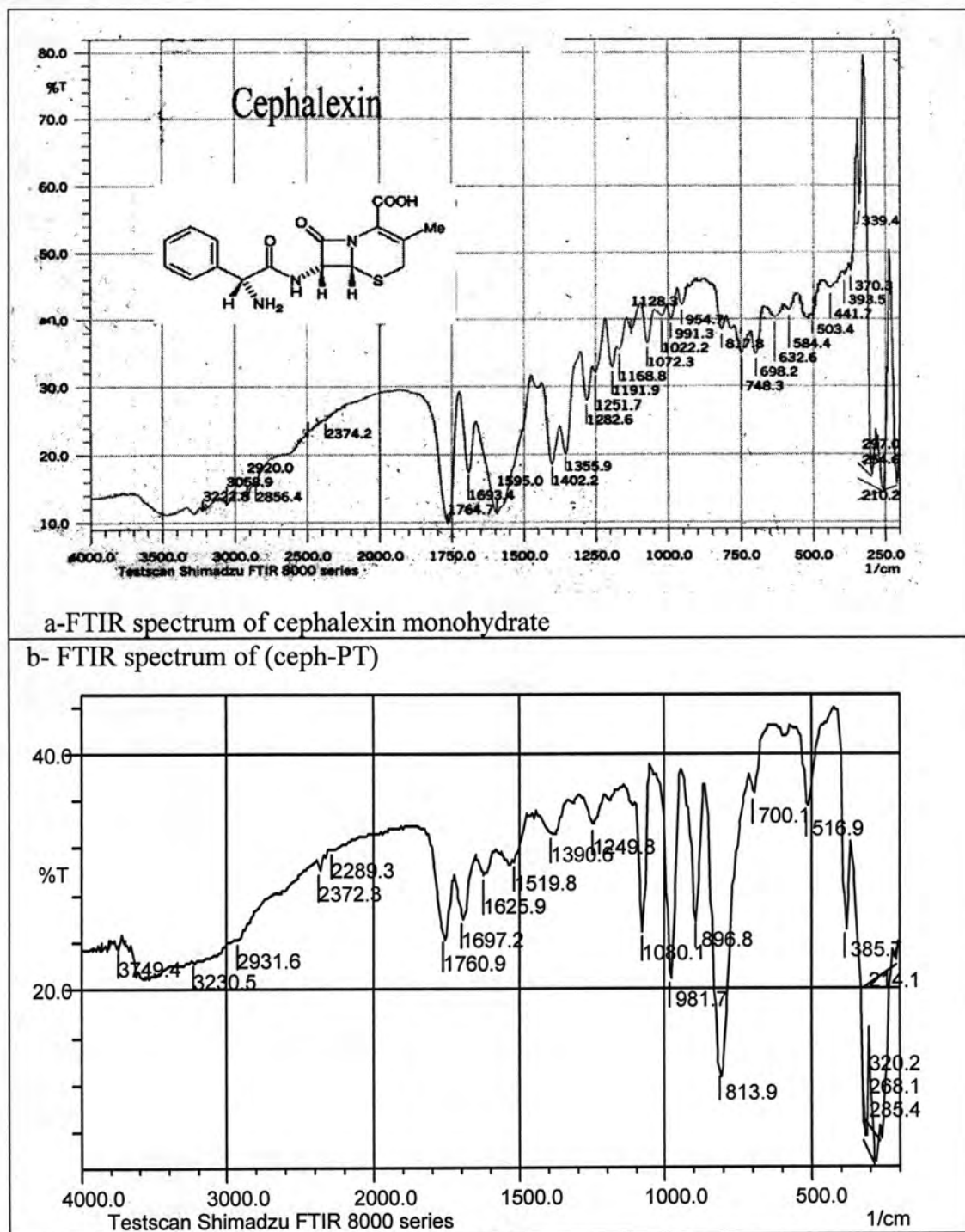


Fig.-1: a- FTIR spectrum of (ceph), b- FTIR spectrum of (ceph-PT).

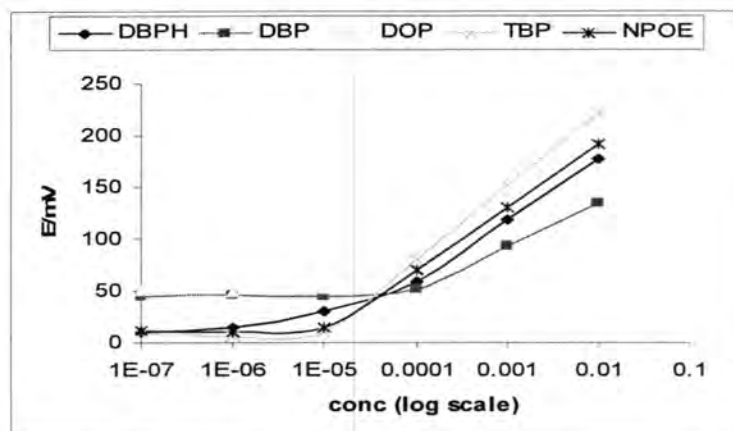


Fig. -2: The calibration curves for the five membranes: DBP, DBPH, DOP, TBP and NPOE.

Table -1: The characteristics parameters of cephalixin electrodes.

Membrane composition	Slope mV/decade	Concentration Range M	PH	Detection limit	Response /second		Life time/day
					10 ⁻³ M	10 ⁻⁴ M	
Ceph-PT +DBP	42.0	10 ⁻⁴ – 10 ⁻²	3.9- 5.1	5x10 ⁻⁵	40	60	40
Ceph-PT+DBPH	59.5	10 ⁻⁴ – 10 ⁻²	3.9- 5.1	5x10 ⁻⁵	15	30	20
Ceph-PT +DOP	58.5	10 ⁻⁴ – 10 ⁻²	3.9- 5.1	3x10 ⁻⁵	25	45	30
Ceph-PT +TBP	71.5	10 ⁻⁵ – 10 ⁻²	3.9- 5.1	8x10 ⁻⁶	10	35	4
Ceph-PT +NPOE	62.0	10 ⁻⁵ – 10 ⁻²	3.9- 5.1	6x10 ⁻⁶	20	35	7

Effect of pH

The effect of pH on the response was examined by measuring the pH from 1.0 to 11.0 for the two concentrations of cephalixin monohydrate 10⁻² and 10⁻³ M respectively. The pH range are listed in Table 2, At the strongly acid solution pH< 3 the drug undergoes a complex series of reactions leading to variety of inactive degradation products and protonated of the lacton nitrogen. At higher pH>6 the cephalixin monohydrate like other penicillin group drugs was hygroscopic and effected by pH of solutions. This may be attributed to the reactivity of the strained β -lactam ring, particularly to hydrolysis.

Table-2: Working pH ranges for cephalixin electrodes.

Membrane Composition.	pH range	
	10 ⁻² M	10 ⁻³ M
Ceph-PT+DBPH	3.0-6.5	2.5-6.0
Ceph-PT+DOP	3.0-6.5	3.0-6.0
Ceph-PT+NPOE	3.5-5.5	3.0-6.5

Selectivity

The influence of some inorganic cations and antibiotic of penicillin group on the response characteristics of the electrodes were investigated. Potentiometric selectivity coefficients were performed by separate solution method using 10^{-3} M concentration for both cephalixin and interfering species ($a_A = a_B = 10^{-3}$ M). The following equation was used to calculate the selectivity coefficients according to references (21) and (22).

$$\text{Log } K_{\text{ceph}}^{\text{pot}} = [(E_B - E_A) / (2.303 RT/zF)] + (1 - z_A / z_B) \log a_A$$

E_A , E_B ; z_A , z_B ; and a_A , a_B are the potentials, charge numbers and activities for the primary A and interfering B ions, respectively, the values were calculated at $a_A = a_B$. The results for selectivity coefficients were summarized in Table 3 using electrodes based on DBPH, DOP, and NPOE plasticizers and the potential of cephalixin monohydrate (a_A) at 10^{-3} M equal to 98, 102 and 95 mV respectively. The results in Table 3 show that the selectivity coefficients of monovalent cations are higher than divalent and trivalent cations. This may be attributed to the differences in ionic size, charge density, mobility and permeability. The values of selectivity coefficients for mono-valent (NH_4^+ and K^+) ranged from 0.227 to 0.685 for NH_4^+ , 1.264 to 2.934 for K^+ . Bad selectivity for Na^+ with K_{AB} ranged from 5.150 to 6.128 may be due to filling solution of the electrodes (10^{-3} M of NaCl). There is also an interference of amoxicillin, ampicillin and cloxacillin on responses of cephalixin selective electrodes. Other neutral species, sucrose and gelatin can not interfere with electrode response due to low values of selectivity coefficients, 0.092 and 0.272, respectively. None of the investigated species interfere seriously except monovalent ions.

Table-3: Selectivity coefficient values for the cephalixin electrodes.

Interfering Ion	Ceph-PT+DBPH		Ceph-PT+DOP		Ceph-PT+NPOE	
	LogK _{AB}	K _{AB}	LogK _{AB}	K _{AB}	LogK _{AB}	K _{AB}
amoxicillin	-0.305	0.274	-0.207	0.169	-0.113	0.771
Ampicillin	-0.169	0.677	-0.121	0.739	-0.274	0.532
Cloxacillin	0.372	2.360	0.138	1.374	0.548	3.535
Na^+	0.712	5.150	0.827	6.128	0.726	5.319
NH_4^+	-0.644	0.227	-0.621	0.685	-0.441	0.363
K^+	0.102	1.264	0.466	2.924	0.306	2.025
Cu^{2+}	-0.856	0.139	-0.845	0.046	-0.613	0.244
Ca^{2+}	-0.754	0.176	-0.586	0.073	-0.774	0.168
Mg^{2+}	-1.449	0.036	-1.552	0.019	-1.613	0.024
Fe^{3+}	-0.373	0.424	-0.569	0.326	-0.532	0.294
Sucrose	-0.983	0.103	-0.810	0.092	-0.563	0.272

Sample analysis

Quantitative determination of cephalexin monohydrate in solutions was used using potentiometric techniques, direct method and increment method which include single standard addition (SSA), multi standard addition (MSA) and Gran's plot. In increment method a 0.5 ml of cephalexin monohydrate standard solution 10^{-2} M was added to 20 ml of the sample. The results of quantitative measurements for the electrodes are listed in Table 4. The (MSA) for electrodes based on DBPH and DOP and a typical plot is shown in Figure 2 and 3 The Gran's plot was constructed by using Orion Gran's plot paper with 10% correction for electrodes based on DBPH and DOP and a typical plot is shown in Figure 4 for cephalexin concentration at 2.6×10^{-4} M and 2.0×10^{-4} M respectively.. Direct method was used for determination of cephalexin in cephalexin oral suspension and cephalexin capsules. From the results in Table 5, the average recovery and standard deviation of cephalexin oral suspension and cephalexin capsule were (100.116 ± 0.393) and (100.344 ± 0.120) , respectively These recoveries are quite comparable with that given in the certificate of British pharmacopeia's 2000 (1). Due to the interference of cephalexin monohydrate with the response of amoxicillin electrode or may be other drugs can be interfere. Therefore, UV-derivative spectrophotometry (DS), first, second, third and fourth derivatives were shown in Figure 5, used in this study for determination of cephalexin drug and to compare with cephalexin selective electrodes. The values of the wavelengths for normal spectrum and derivative spectra (1D , 2D , 3D and 4D) for cephalexin in the range 2 to 150 $\mu\text{g/ml}$ were determined and the results of applying the UV-derivatives for 40 $\mu\text{g/ml}$ cephalexin solution are listed in Table 6. As we noticed the accurate results were obtained by using all derivatives spectrophotometry. The accuracy of the method depending on the wavelength chose not just the order of derivative.

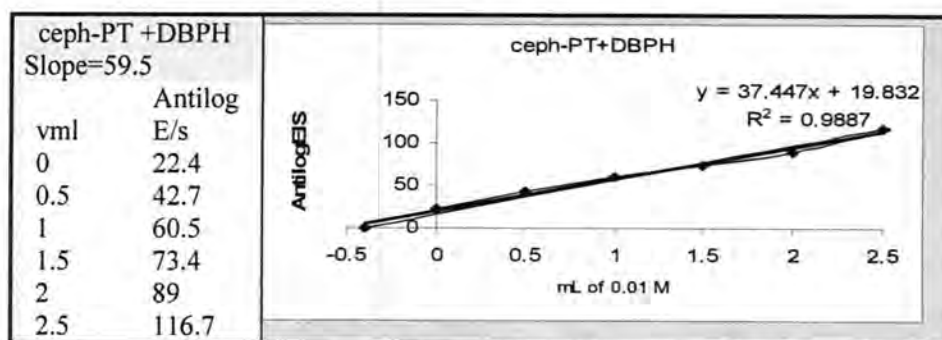


Fig.-3: Antilog (E/S) versus the volume of the added standard for the determination of cephalexin solution (2.6×10^{-4} M) MSM using electrode ceph-PT+DBPH.

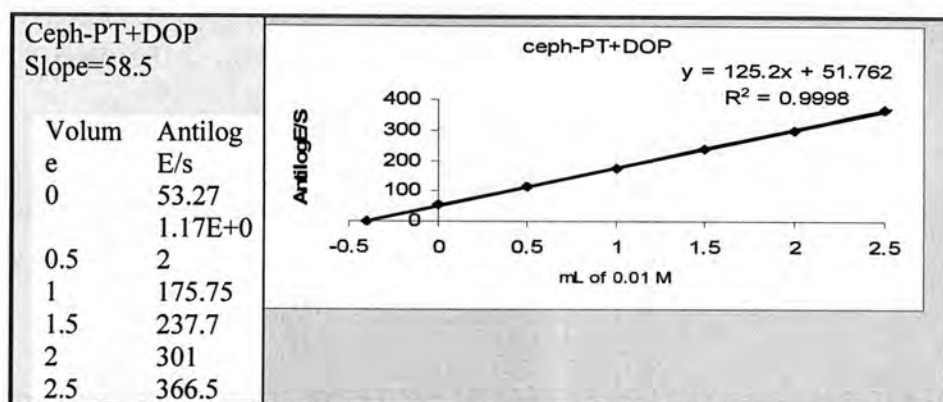


Fig.-4: Antilog (E/S) versus the volume of the added standard for the determination of cephalixin solution (2×10^{-4} M) by MSM using ceph-PT+DOP electrode.

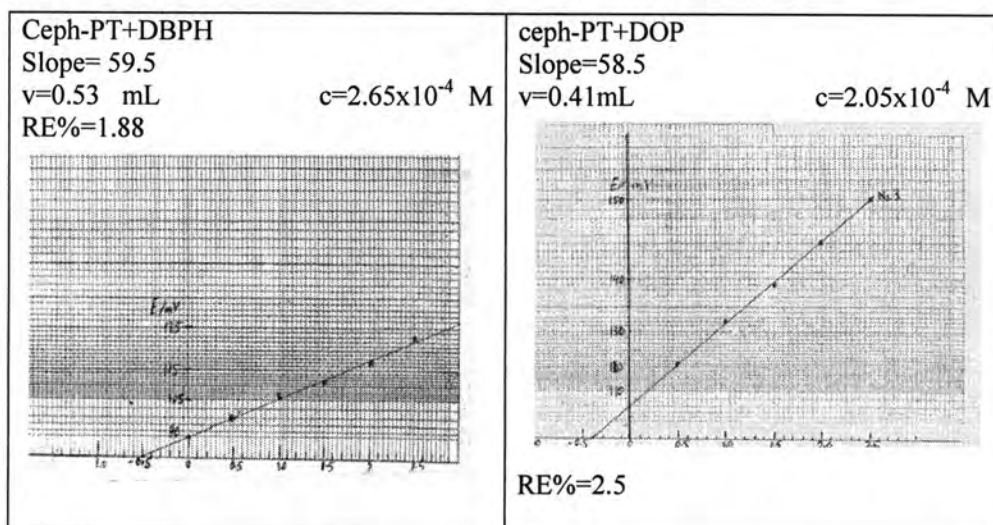


Fig.-5: Gran's plot for ceph-PT +DBPH and ceph-PT +DOP electrodes

Table-4: Determination of cephalixin sample using cephalixin electrodes.

Membrane composition	Ceph Conc./M sample	Measured concentration (M) Using potentiometric method					
		Direct*	gran's plot	SAM*	MSM	OPC*	TM*
Ceph-PT+DBPH	2.600x10 ⁻⁴	2.570x10 ⁻⁴	2.650x10 ⁻⁴	2.620 X 10 ⁻⁴	2.650 X 10 ⁻⁴	2.630x10 ⁻⁴	2.645x10 ⁻⁴
	RSD%	1.24		5.95		1.34	3.74
	RE%	-1.15	1.88	0.769	1.92	1.15	2.25
Ceph-PT+DOP	2.0x10 ⁻⁴	2.07x10 ⁻⁴	2.05x10 ⁻⁴	1.95 X 10 ⁻⁴	2.06x10 ⁻⁴	2.06x10 ⁻⁴	
	RSD%	2.21		1.687		1.87	
	RE%	3.5	2.5	-2.5	3.0	3.0	

*The result of five additions. *Each concentration represents an average of at least three measurements.

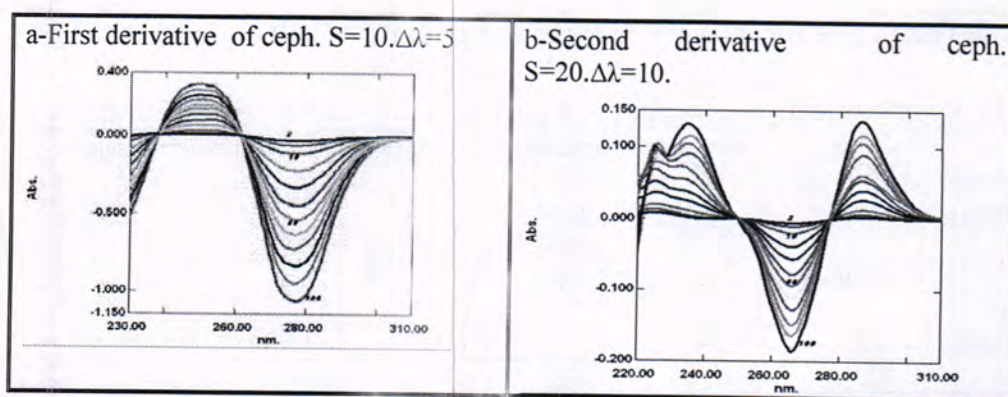
Table-5: sample analyses of pharmaceutical cephalexin using ceph-PT+ DBPH electrode.

pharmaceutical	cephalexin oral suspension BP		cephalexin capsules BP	
	Direct method	OPC	Direct method	OPC
Concentration	6.842×10^{-4}	6.842×10^{-4}	8×10^{-4}	8×10^{-4}
Found*	6.874×10^{-4}	6.852×10^{-4}	8.02×10^{-3}	8.03×10^{-3}
Recovery %	100.468	100.146	100.25	100.375
RE %	0.468	0.854	0.25	0.375
Concentration	1.368×10^{-3}	1.368×10^{-3}	2×10^{-3}	2×10^{-3}
Found*	1.372×10^{-3}	1.362×10^{-3}	2.01×10^{-3}	2.005×10^{-3}
Recovery %	100.292	99.561	100.50	100.25
RE %	0.292	-0.439	0.50	0.25

*Each concentration represents an average of at least three measurements.
Relative Standard deviation ranged 0.232 to 1.156

Comparison between ISE and DS

Cephalexin monohydrate was determined by First derivative using wavelength 249 nm. ($n=7$) and by ISE using ceph-PT+DBPH electrode ($n=5$). The values of F at 95% confidence level is 4.53, standard deviation (s) were 0.298 and 0.213 for the ISE and DS methods, respectively. Therefore, the resulting F is equal to 1.957. The results obtained by ISE were quite comparable with DS method and indicated no significant difference between the two methods. Other parameters for the methods are listed in Table 7, which show that two methods are equivalent in the accuracy and simplicity but differ in linear range and detection limit, which were not effected on determination of cephalexin in the pharmaceutical samples.



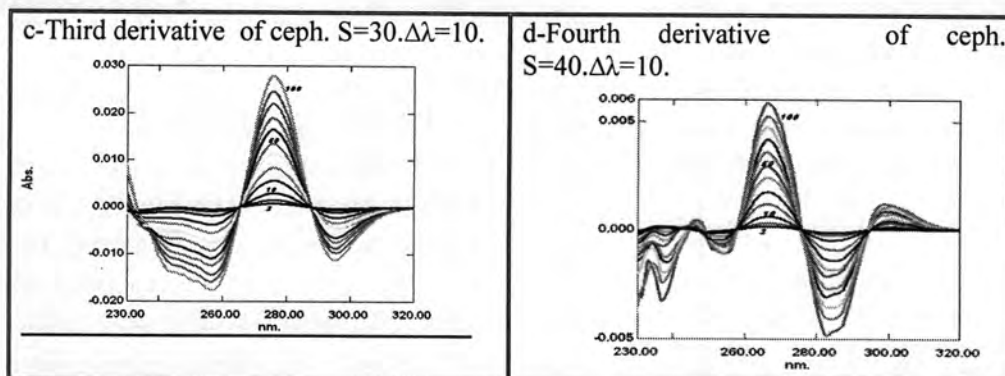


Fig.-6: The UV-derivatives: spectra first, second, third and fourth derivative for ceph.

Table-6: The equations and correlation coefficient of calibration curves for the suitable range of the cephalixin concentrations.

Method	Range mg/L	Wavelength nm	Linear equation	r
Normal	4-80	262	$Y=0.02296x+0.00639$	0.99974
¹ D	12-100	P=249	$Y=0.00211x-0.00042$	0.99953
	8-100	V=277	$Y=-0.00687x+0.00196$	0.99977
² D	10-50	P=286	$Y=0.00178x+0.00320$	0.98809
	10-50	P=236	$Y=0.00164x+0.00340$	0.99970
	8-80	V=268	$Y=-0.00067x+0.00037$	0.99971
³ D	8-60	P=270	$Y=0.00027x-0.00025$	0.99938
	8-100	V=297	$Y=-0.00020x-0.00047$	0.99938
⁴ D	8-100	P=268	$Y=0.00151x-0.00152$	0.99973
	8-60	P=297	$Y=0.00071x-0.00058$	0.99910
	8-100	V=286	$Y=-0.00148x+0.00382$	0.99951

Table-7: The parameters of ISE and DS methods to determine cephalixin monohydrate (60 mg/L).

parameter	ISE using ceph-PT+DBPH	DS using D1 at 249 nm
Linear range	1×10^{-4} - 1×10^{-2} M (36.5-365.4 mg/L)	2×10^{-6} - 2×10^{-2} M (8-100 mg/L)
Detection limit	5×10^{-5} M (14.6 mg/L)	4×10^{-6} M (2 mg/L)
Working pH range	$\approx 3.0 - 6.5$	3.0 - 7.0
Standard deviation	0.298	0.213
RSD%	0.812 - 1.99	0.103 - 0.214
S^2	0.0888	0.0454
ceph .found mg/L	60.288	60.137
RE%	0.48	0.228
Recovery%	100.48	100.228

We can conclude:

Several cephalexin selective electrodes can be prepared based on phosphotungstic acid as an ionophor with different plasticizers in PVC matrix membranes. Electrodes based on DBPH and DOP plasticizers with longer life times can be used for determination of cephalexin in drugs. The recovery obtained by the electrodes was good comparable with the recovery obtained by first derivative spectrophotometer. The proposed electrodes were successfully applied to the determination of cephalexin in the pharmaceutical preparation. The analytical method proposed proved to be a simple rapid and accurate method.

REFERENCES

1. The Pharmaceutical Codex, Principle and Practical of Pharmaceutical, 21st ed.,The Pharmaceutical Press, London (1994).,British pharmacopoeia, CD, ROM (2000).
2. Kharitonov S.V., "Ion-Selective in Medicing Drug Determinationinter" Russian Chemical Reviews, 76, 361 (2007).
3. Kumar K.G., John S., Popval P. and Saraswathyamma B., "Mebendazole Selective Membrane Sensor and its Application to Pharmaceutical Analysis" Analytical Sciences, 23: 291-294 (2007).
4. Nassory N.S., Maki S.A.and Ali M.A., "Preparation and characterization of an Atenolol Selective Electrode Based on PVC Matrix Membrane" Turk. J. Chem., 31: 75-82 (2007).
5. Nassory N.S., Al-Haderi A.M. and Al-Mashhadany I.K.M., "Preparation and Examination of Amine and Amiloride-Ion Selective Electrode with PVC Matrix Membranes", Chem. Anal., (Warsaw), 52, 55 (2007).
6. Al-Haideri A.M.,Nassory N.S. and Al-Saadi A.S.M., Ibn Al-Haitham,"Study the Polymeric Membrane Selective Electrodes for the Determination of Ampicillin Trihydrate"J. of Pure and Applied Sciences, 19: 101-115 (2006).
7. Al-Saidi, Kh. H. ; Nassory, N. S. and Maki, S. A., " Preparation and study of amoxicillin selective electrodes and their application with the derivative spectrophotometer in pharmaceutical drugs" JNUS, 12 (1): 29-37, (2009).
8. Ghidini, S.; Zanardi, E.; Varisco, G. and Chizzolini, R., "Residue of Beta-lactam antibiotics in bovin milk: confirmatory analysis by liquid chromatograph tanden mass spectrometry after microbial assay screening", Food-Addit-Cont., 20(6): 528-534, (2003),
9. Wu,Z.J.;Guo,W.B.;Zhang,Q.G.;Ni,K.Y.and;Lin, Y. S., "Studies on the simultaneous measurement of several cephalosporins by RP-HPLC"Se-Pu.17(6): 518-522 (1999).
10. Agbaba, D.; Eric, S.; Zivanov-Stakic, D. and Vladimirov, S., "HPLC assay of cephalexin and cefaclor in pharmaceuticals" Biomed-Chromatogr. ,12 (3) :133-135, (1998 May-Jun).
11. Farag-SA, "Simultaneous liquid chromatographic analysis of the beta-lactam antibiotics cefazolin , cefadroxil , cephalexin, ampicillin and cephradine in solution" J-AOAC- Int., 81(2): 381-375(1998).

12. Kovach, P. M., Lantz, R. J. & Brier, G., "High-performance liquid chromatographic determination of loracarbef, a potential metabolite, cefaclor and cephalixin in human plasma, serum and urine." *J-Chromatogr.* 567 (1) :129-139, (1991)
13. Long, H.; Ding, Q.; Wang, T. S.; Huang, A. J. and Sun, Y. L., "Purity analysis of cephalosporines with capillary zone electrophoresis" *Se-Pu.*, 17(6):570-572(1999).
14. Okerman, L.; De-Wasch, K.; Van-Hoof, J. & Smedts, W. "Simultaneous determination of different antibiotic residues in bovine and porcine kidneys by solid-phase fluorescence immunoassay." *J-AOAC-Int.* 86(2):236-240, Mar-Apr(2003).
15. Abdel-Hamid, M. E., Mahrous, M. S., Daabees, H. G. and Beltagy, Y. A., "A rapid First-derivative spectrophotometric analysis of cephalixin and cephradine in human urine". *J-Clin-Pharm-Ther.*, 17(2), 91-95, (1992).
16. Martinez, L. G.; Cabeza, A. S.; Falco, P. C. & Cabeza, A. S., "Comparison of several methods used for determination of cephalosporin, Analysis of cephalixin in pharmaceutical samples" *J-Pharm-Biomed-Anal.*, 29(3), 405-423, (2002).
17. Popovic G. V., Pfendt L. B. and Stefanovic V. M., "Analytical application of derivative spectrophotometry and their Analytical Applications". *J. Serb. Chem. Soc.*, 65(7), 547-4720 (2000).
18. El-Sayed A. Y. and N. A. El-Salem N. A., "Recent Developments of Derivative spectrophotometry", *Analytical Sciences*, 21, 595 (2005).
19. Craggs A., Moody G. J. and Thomas J. D. R., "PVC Matrix Membrane Ione-Selective Electrodes: Construction and Laboratory Experiments", *Chem. Educ.*, 51(8):541 (1974).
20. Moody G. J. and Thomas J. D. R., "Selective Ion Sensitive Electrodes", Merrow Publication Co. Ltd, (1970).
21. Umezawa Y., Umezawa K. and Sato H., "Selectivity Coefficients for Ion-Selective Electrodes Recommended Methods for Reporting $K_{pot}^{A,B}$ values", *Pure Appl. Chem.*, 67, 507-518 (1995).
22. Umezawa Y., Buhlmann P., Umezawa K., Tohda K. and Amemiya S., "Potentiometric Selectivity Coefficients of Ion-Selective Electrodes" *Pure Appl. Chem.* 72, 1851-2082 (2000).

Simultaneous Determination of Paracetamol and Cephalixin Binary mixtures by Using Derivative Spectrophotometry and H-point Standard Addition Methods

¹Khaleda Hamid Al-Saidi, ²Firyal Waly Askar and ¹Asraa Abed AL-Abaas

¹Al-Nahrain Unhversity, College of Science, Chemistry Department

²Al-Mustansiria Unhversity, College of Science, Chemistry Department

الخلاصة

استخدم في هذا البحث طريقتان لتعيين متعاقب لأمزجة من الباراستيمول والسيفالاكسين بتقنية المشتقات الطيفية وطريقة نانومتر 290.2 و 250.5. الطريقة الأولى اعتمدت على المشتقة الثانية في الأطوال الموجية H-PSAM وكانت الخطية لمنحني المعايرة 60-2 و 70-2 ملغ/لتر، بنتيجة ممتازة وبدرجة ثقة ودقة جيدة وأن نسبة الأسترجاع (أكبر من 98) و حد الكشف (1.5 ملغ/لتر) كذلك النسبة المئوية للانحراف المعياري بلغت (0.757 – 1.207) لكل من الباراستيمول والسيفالاكسين على التوالي.

أما الطريقة الثانية التي اعتمدت على الاختلاف في الممتصية لكل من الباراستيمول والسيفالاكسين في الطولين الموجيين (250.2-265 نانومتر). وكانت الخطية لمنحني المعايرة 35-2 و 50-2 ملغ/لتر، بنتيجة ممتازة وبدرجة ثقة ودقة جيدة وأن نسبة الخطأ تتراوح بين (0.605 إلى 0.164) و (1.230 إلى 1.43) وحد الكشف (2 و 3 ملغ/لتر) كذلك النسبة المئوية للانحراف المعياري بلغت (0.151 – 1.1775) لكل من الباراستيمول والسيفالاكسين على التوالي كانت الطريقتين دقيقتين وبسيطتين وسريعتين.

ABSTRACT

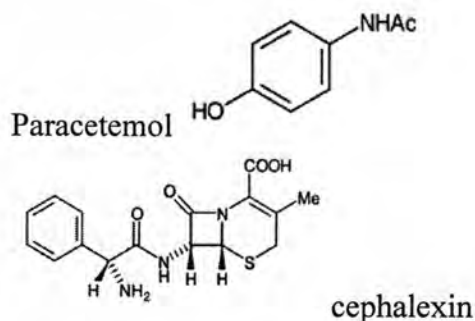
Two methods are applied for simultaneous determination of paracetamol (para) and cephalixin (ceph) in combined mixtures, derivative spectrophotometric technique and H-Point standard addition method (HPSAM) spectrophotometry. The first procedure is based on the use of the, second derivative ($2D$) and used the suitable wave lengths at zero crossing at valley 250.5 and 290.2 nm for determination paracetamol and cephalixin respectively.. Calibration graphs were established for 2-60 mg/L for Para and 2-70 mg/L for ceph in binary mixture. The proposed method were successfully applied to the determination of these drugs in synthetic mixtures, linearity was excellent ($r^2 > 0.999$) over the concentration tested (2–60 mg/L) with good precision and accuracy. Recoveries were good ($>98\%$) with limits of detection of 1 and 1.5 mg/L, (%R.S.D.= 0.757 - 1.207) for para and ceph, respectively.. The second procedure HPSAM was applied to the simultaneous determination of Para and ceph. respectively. (HPSAM) method was based on the difference in the absorbance of para and ceph.at choosing wavelengths (265 and 257 nm). Results of the analysis of the different mixtures in the proposed system revealed a dynamic range of 2-35 and 2-50 mg/L, with limits of detection of 2 and 3 mg/L for para and ceph, respectively. The relative error are between -0.605-1.64 and -1.230-1.43, for para and ceph respectively. RSD% 0.151-1.775 for para and ceph, respectively. The two methods were found to be precise, accurate, simple and rapid.

Keywords: zero crossing , derivative spectrophotometry, paracetamol, cephalixin, H-Point.

INTRODUCTION

Paracetamol is acetaminophen is the active metabolite of phenacetin, a so-called coal tar analgesic. Unlike phenacetin, paracetamol has not been shown to be carcinogenic in any way. It has analgesic and antipyretic properties, but,

unlike aspirin, it is not a very effective anti-inflammatory agent. It is well tolerated, lacks many of the side-effects of aspirin, and is available over-the-counter, so it is commonly used for the relief of fever, headaches, and other minor aches and pains. Paracetamol is also useful in the management of more severe pain, where it allows lower dosages of additional non-steroidal anti-inflammatory drugs (NSAIDs) or opioid analgesics to be used, thereby minimizing overall side-effects. It is a major ingredient in numerous cold and flu medications, including Tylenol and Panadol, among others. It is considered safe for human use at recommended doses; however, acute overdose can cause fatal liver damage often heightened with use of alcohol, and the number of accidental self-poisonings and suicides has grown in recent years¹. The words *acetaminophen* and *paracetamol* come from the chemical names for the compound: *para*-acetylaminophenol and *para*-acetylaminophenol. (The brand name Tylenol also derives from this name: *para*-acetylaminophenol.) In some contexts, it is shortened to APAP, for *N*-acetyl-*para*-aminophenol(1) It has the formula $C_8H_9NO_2$, molecular weight 151.2 and structure as follow.



Paracetamol is a white, crystalline powder, sparingly soluble in water (0.1-0.5 g/100mL at 20 C°), freely soluble in alcohol, very slightly soluble in ether and in methylene chloride(2).Paracetamol (acetaminophen) is widely used as an analgesic and as an antipyretic drug. Many assays have been described for acetaminophen including titrimetry(3), chromatography(4-9), fluorometry(10), colorimetry(11-14), UV spectrophotometry(15), and various modes of electrochemistry (16-24). Although the electrochemical oxidation of paracetamol at a glassy carbon electrode has been in the literature for some time(20) only a few applications of its use in differential pulse voltammetry have been reported; for determination of the drug in blood plasma and in a single type of tablet(21) and in a variety of drug formulations containing paracetamol(19). Recently the differential pulse voltammetric behaviour of some drugs including paracetamol at various conducting polymers (17) and at pumice mixed carbon electrodes(22) have been examined and reviewed(23). cyclic voltammetric(25). Derivative spectrophotometric technique and chemometric methods(26-27) The estimation of paracetamol and

orphenadrine citrate in a multicomponent pharmaceutical dosage form by spectrophotometric method has been reported. Because of highly interference in the spectra and the presence of non-linearity caused by the analyte concentrations which deviate from Beer and Lambert's law, partial least-squares (PLS) and artificial neural networks (ANN) techniques were used for the calibration(3) A micellar electrokinetic chromatography (MEKC) method was established for determination of paracetamol (PARA) and chlorpheniramine maleate (CPM) in cold tablets. Separation of both drugs rapid and efficient(4)

Cephalexin monohydrate contains not less than 95.0 per cent and not more than the equivalent of 101.0 percent of (6*R*,7*R*)-7-[(*R*)-2-amino-2-phenylacetamido]-3-methyl-8-oxo-5-thia-1-azabicyclo[4.2.0]oct-2-ene-2-carboxylic acid, calculated with reference to the anhydrous substance. The empirical formula of cephalexin was (C₁₆H₁₇N₃O₄ S, H₂O), and the molecular weight (365.4g/mol) (2). Cephalexin occurs as white, or almost white, crystalline monohydrate powder. It is soluble in water, practically insoluble in alcohol and in ether, resistant to acid and well absorbed orally. Several different methods have been used for determination of cephalexin monohydrate including; High-performance liquid chromatographic(28-31). A capillary zone electrophoresis method³². Fluorimetric Method(33,34).And Electroanalysis such as Polarography and voltametry(35,36). And there are several methods used for the determination of cephalexin(37). Recently Simultaneous Spectrophotometric determination using of Chemometrics methods(38).

The H-point standard addition method⁵ (HPSAM) permits both proportional and constant errors produced by the matrix of the sample to be corrected directly. This method was based on the principle of dual wavelength spectrophotometry and the standard addition method. The greatest advantage of HPSAM is that, it can remove the errors resulting from the presence of an interfering and blank reagent. Although HPSAM could remove the error resulting from the sample matrix, it cannot remove the constant error resulting from other components in the system. The requirements for the application of the method is that if necessary to work only at two wavelengths where the analytical signal due to the one of the species is constant and for another one to be as different as possible. By plotting the analytical signal versus the added analyte concentration, two straight lines are obtained that have a common point with coordinates H (–C_H, A_H), where –C_H is the unknown analyte concentration and A_H the analytical signal due to the interfering species.

Recently H.point standard addition (HPSAM) were used for simultaneous determination of binary mixture (39-47). In this work HPSAM Derivative spectroscopy(48) were employed for the resolution of binary mixtures of paracetamol and cephalexin . The suggested methods were successfully applied to the determination of these analytes in synthetic mixtures.

MATERIALS AND METHODS

Instruments and Equipments:

Double-beam UV-Visible spectrophotometer model (UV-1650 PC) SHIMADZ (Japan), interfaced with computer via a SHIMADZU UV probe data system program (Version 1.10), using 1.00 cm quartz cells, Ultra sonic devise (ultrasonicator) for dissolving samples, (SONOREX), (W. Germany), Ultra pure water manufacturing devise, (TORAYPURE), model LV-08 (Japan).

Chemicals

Standard drugs: cephalixin monohydrate ($C_{16}H_{17}N_3O_4S \cdot H_2O$; F.W. 365.4) and Paracetamol ($C_8H_9NO_2$; F.W. 151.2) were provide from the State Company of Drug Industries and Medical Appliances (IRAQ-SDI- Samara). All drugs were used as working standards without further purification and analyzed to one of the official methods or reported methods to determine their purity and compliance with the requirements.

Preparation of Stock and working Standard Solutions

1-Stock solutions (500 or 250 mg/L) of standard were prepared by dissolving an accurately weighed amount (50 or 25 mg) of the studied drugs in about 80 ml of the deionized water 100ml volumetric flask .using ultra sonic devise (ultrasonicator) for dissolving samples.The solution is then made up to the volume with deionized water the stock solutions were completed quantitatively with the deionized water to obtain the suitable working standard solutions according to the linear calibration range for each drug.

2- Two series of pure single standards drugs prepared by dilution from stock solutions with the deionized water to prepare suitable constrictions (2-70 mg/L)

3-Solutions for binary mixtures of standard drugs cephalixin monohydrate solutions and paracetmol were prepared by two series;

First series of mixture solutions were prepared by using a fixed concentration of (30 mg/L) for ceph with different concentrations (2, 5, 10, 20, 30, 40, and 50 mg/L) of para, second series of mixture contain a fixed concentration (30 mg/L) of para with different concentration of (2, 5, 10, 20, 30, 40, and 50 mg/L) of ceph.

RESULTS AND DISCUSSION

Derivative spectroscopic Methods:

Normal spectrum can not be used to determine each of para and ceph present in mixture, due to interference between the spectra, as shown in Fig.1a. Therefore, UV derivative can be used in this case. As shown in Fig.1 and 2, first derivative also can not used to determine ceph in the presence para by using zero crossing method .(22)

Fig.3 shows Second Derivative (2D) for 2-50 mg/L para spectra and 30 mg/L zero crossing ceph. at valley 250. nm and 2D spectra for 2-70 mg/L

ceph. with 30 mg/L para zero crossing at 290.2 nm for ceph., which were they are suitable for measuring para and ceph respectively.. The calibration curve of 2D with the range of concentrations (2-60 mg/L para) at 250.5 nm gave a linear equation with slope and the correlation coefficient and the relative errors for the mixtures for each drug were listed in Table1 and 2.. The relative standard deviation for each concentration represents an average of at least three measurements is between 0.781- 1.063. Cephalexin can be determined in the presence of para using 2D spectrum at 290.2 nm. The calibration curve of 2D for standard ceph solutions was ranged from 2 to 70 mg/L at 290.2 nm gave a linear equation with slope and the correlation coefficient and the relative errors for the mixtures each drug were listed in Table1 and 2. and the relative standard deviation for each concentration represents an average of at least three measurements. is between 0.757- 1.207.

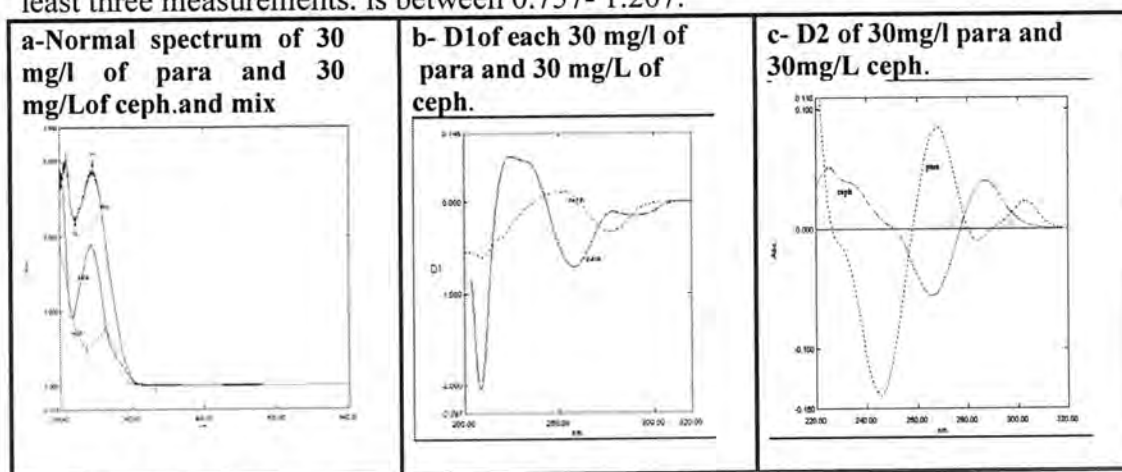


Fig.-1: The spectra: a- normal spectra of para and ceph $\Delta\lambda=5$, b- D1 of each para and ceph $S=10$, $\Delta\lambda=5$, c- D2 of each para and ceph $S=20$, $\Delta\lambda=5$.

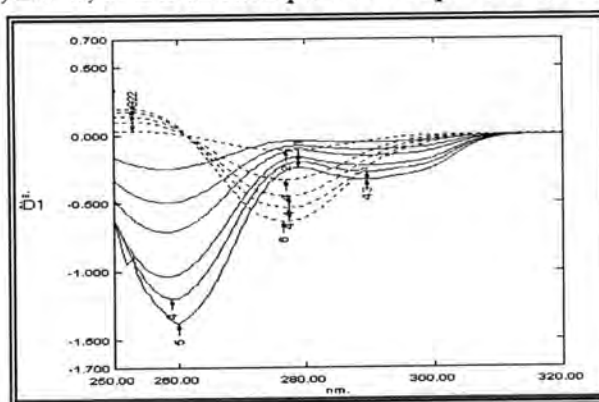


Fig.-2: 1D spectrum for 10-50 mg/L para and 1D spectra for 10-60 mg/L ceph

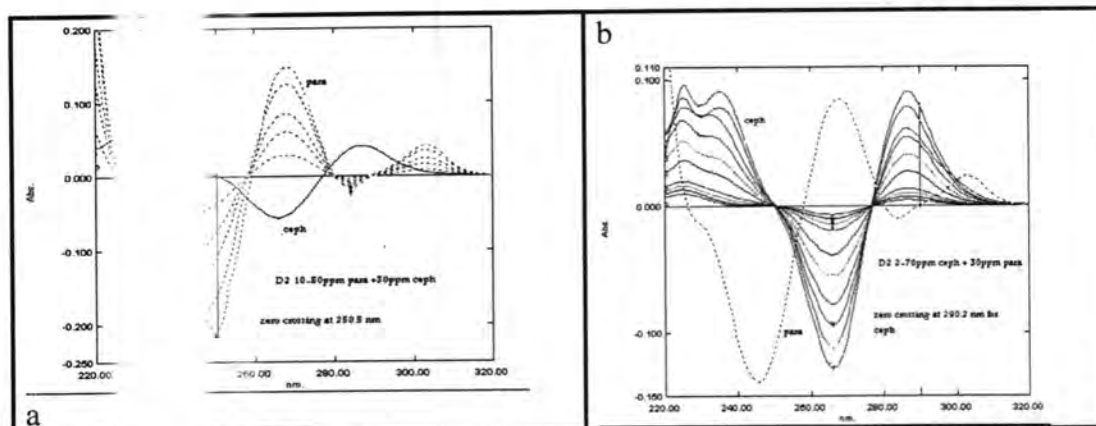


Fig.-3: or 2-50 mg/L para spectra and 30 mg/L ceph. at 250.5. b-²D 70 mg/L ceph. with 30 mg/L para zero crossing at 290.2 nm for ceph

Table-1

Drug
para
ceph

Methods using for determination binary mixture para and ceph

Method	Equation	Relative error for 50% mixture	r
² D Valley=250.5	$Y=0.0043X + 0.0074$	0.757	0.9996
² D Peak=250.5	$Y=0.0011X + 0.0013$	1.207	0.9995

Table-2: Relative error of ceph in the presence of para and the relative error of para in the presence of ceph using 2D spectrum at valley 290.2 nm and 250.5 respectively.

Ceph + amox mixtue	Ceph found* rmg/L	Relative error%	para + ceph mixture	Para found*	Relative error
10 ceph+00 para	9.831	-1.690	10 para.+00 ceph	10.212	+2.120
20 ceph+00 para	19.848	-0.760	20 para.+00 ceph	20.218	+1.090
30 ceph+00 amox	30.277	0.923	30 para.+00 ceph	30.261	+0.870
40 ceph+00 para	39.645	-0.888	40 para.+00 ceph	40.328	+0.820
50 ceph+00 amox	49.875	-0.250	50 para.+00 ceph	50.297	+0.594
10ceph +30 para	9.612	-3.880	10 para + 30 ceph	10.123	+1.230
20ceph +30 para	19.896	-0.520	20 para + 30 ceph	20.324	+1.620
30ceph +30 para	30.227	+0.757	30 para + 30 ceph	30.362	+1.207
40ceph +30amox	39.927	-0.183	40 para + 30 ceph	39.844	-0.390
50ceph +30 para	49.934	-0.132	50 para + 30 ceph	49.920	-0.160
30ceph + 10 para	30.129	+0.43	30 para + 10 ceph	30.263	+0.877
30ceph + 20 para	30.115	0.383	30 para + 20 ceph	30.345	+1.150
30ceph + 40 para	29.813	-0.623	30 para + 40 ceph	30.452	+1.501
			30 para + 50 ceph	30.763	+2.543

- each value is the mean at least three measurements

Applying HPSAM

In the proposed systems Para and Ceph are the analyte and interfering, respectively. As seen in Fig. 1, at the selected wavelengths of $\lambda_1 = 265$ and $\lambda_2 = 257$ nm, the Para signal increases linearly with the increase in concentration of para, whereas the cep signal does not change with the increase in analyte concentration. The concentration of para is determined by HPSAM using two wavelengths $\lambda_1 = 265$ and $\lambda_2 = 257$ nm, at which the interfering species, cep, should have the same absorbance. Known amounts of para are then added consecutively to the mixture. After each addition the absorbance (A) is measured at the two wavelengths, and expressed by the following equations⁴¹.

$$A_{265} = M_{265}C_{\text{para}} + b_0 + b \quad (1)$$

$$A_{257} = M_{257}C_{\text{para}} + A_0 + A' \quad (2)$$

The two straight lines obtained intersect at the H-point (para, ceph) (Fig. 5). To achieve simultaneous determination of ceph and para in a sample, several synthetic mixtures with different concentration ratios of para and ceph were analyzed using HPSAM as shown in fig 6 and table 3. Results of the analysis of the mixtures in the proposed system revealed a dynamic range and of 2-35 and 1-50 mg/L for para and ceph, respectively. The relative error are between 0.05-1.64 and -1.230-1.43, for para and ceph respectively. RSD% 0.151-2.71.

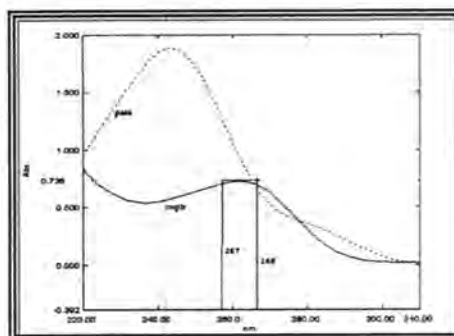


Fig-5 Normal spectra 30mg/L ceph , 30mg/L Para, at 265 and 257nm.

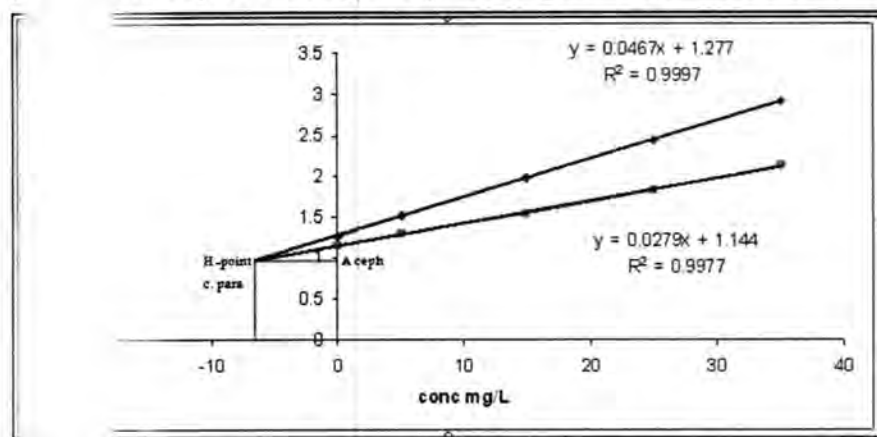


Fig -5 HPSAM for 30 mg cephalixin with 0.0 – 35 mg/L paracetamol at 265 and 257 nm.

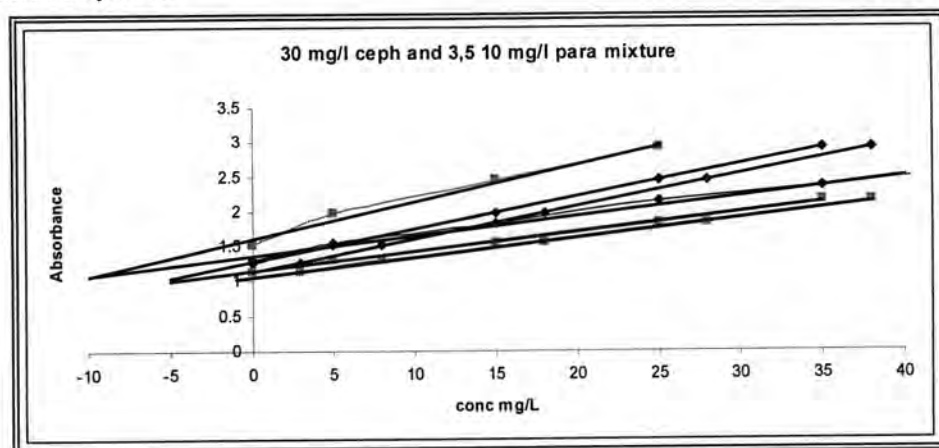


Fig.-6: H-point standard addition plot for simultaneous determination three mixtures of para and ceph with constant concentration of Ceph 30 mg/L and the para concentration of 2, 5, 10 mg/L para respectively.

Table-3: Relative error of ceph and para present in synthetic mixture using HPSAM..

Conc. Para +ceph	Para found* Mg/L	Relative error	Ceph found* mg/L	Relative error%
2 para + 30 ceph	2.024	+1.2	30.254	+0.887
5para + 30 ceph	5.082	+1.64	30.429	+1.430
10 para + 30 ceph	9.957	-0.43	29.818	- 0.607
20 para + 30 ceph	19.879	-0.605	29.631	-1.230

* each value is the mean at least three measurements standard deviation 0.0454-0.1153

We can conclude:

The above results show that HPSAM and Derivative spectroscopy allow rapid, accurate and simple resolution of paracetamol and cephalixin mixtures. The HPSAM can be used in the multi components samples with matrix effects because standard addition method has capability of removing these effects.

REFERENCES

1. Wikimedia Foundation, Inc., a U.S. registered, the free encyclopedia 09:57,3 March (2008).
2. Browse: British Pharmacopoeia CD-ROM British Pharmacopoeia, I, 1023-25 (2000)
3. Blake, M.I. & Shumaker, L.B. Differentiating Non-aqueous Titration of Mixtures Containig Acetaminopehen and Salicylamide, J. Ass. Off. Analyt. Chem., 56, :653-655 (1973).
4. Dalibor S, I.N.: Petr, S.H.: Sklen, I.M. & Concei, B.S. "Sequential injection chromatographic determination of paracetamol, caffeine, and acetylsalicylic acid in pharmaceutical tablets", J. Sep. Sci, 27:529-536 (2004).
5. Suntornsuk, L. Pipitharome, O. Wilairat, P. Simultaneous determination of paracetamol and chlorpheniramine maleate by micellar electrokinetic chromatography, Journal of Pharmaceutical and Biomedical Analysis, 33(3):441-449 (2003).

6. Senyuva H.Ozden T"Simultaneous high-performance liquid chromatographic determination of paracetamol,phenylephrine HCl,& chlorpheniramine maleate in pharmaceutical dosage forms.J Chromatogr Sci.40(2):97-100(2002).
7. Carroll, M. White, E.F. and Zarembo, J.E. Over-the-counter Drug Analyses with HPLC. *Analyt. Chem.*, 53, 1111A-1114A (1981).
8. [3] McSherry, W.O. and Savage, I.V.E. 1980 Simultaneous High-Pressure Liquid-Chromatographic Determination of Acetaminophen, Guaiphenesin and Dextromethorphan Hydrobromide in Cough Syrup, *J. Pharm. Sci.*69: 212-214.
9. Wang,J.&Dewald, H.D. Electrochemical Detector for Liquid Chromatography Based on a Reticulated Vitreous Carbon Electrode in a Thin-layer Cell, *J. Chromat.* 287:281-287(1984).
- 10.Oztunc,A. Fluorimetric Determination of Acetaminophen as Its Dansyl Derivative, *Analyst*, 107: 585-587(1982).
- 11.Afshari,J.T.&Liu,T.-Z. Rapid Spectrophotometric Method for the Quantitation of Acetaminophen in Serum, *Analyt. Chim. Acta*, 43: 165-169 (2001).
- 12.Belal, S.F. Elsayed, M.A.H., Elwalily, A. and Abdine, H. Spectrophotometric Determination of Acetaminophen and Salicylamide through Nitrosation and Subsequent Coupling, *Analyst*, 104: 919-927(1979).
- 13.Elsayed,M.A.H.,Belal,S.F.,Elwalily,A-f.M. & Abdine, H. Spectrophotometric Determination of Acetaminophen, Salicylamide and Codeine Phosphate in Tablets, *Analyst*, 104:620-625(1979).
- 14.Murfin, J.M. & Wragg, J.S. A Colorimetric Method for the Determination of Phenacetin and Paracetamol, *Analyst*, 97: 670-675(1972).
- 15.Das,S.,Sharma,S.C.,Talwar,S.K.&Sethi,P.D.Simultaneous Spectrophotometric Determination of Mefenamic Acid and Paracetamol in Pharmaceutical Preparations, *Analyst*, 114: 101-103(1989).
- 16.Bramwell, D.J. Mass, A.E.G., Gibbs, P.N.B. & Green, M.J. Method for Determining Paracetamol in Whole Blood by Chronoamperometry following Enzymatic Hydrolysis, *Analyst*, 115: 185-188 (1990).
- 17.Erdogdu, O. & Karagozler, A.E. Investigation and Comparison of the Electrochemical Behavior of Some Organic and Biological Molecules at Various Conducting Polymer Electrodes, *Talanta*, 44:2011-2018(1997).
- 18.Gilmartin, C.T. & Hart, J.P. Rapid Detection of Paracetamol Using a Disposable, Screen-Modified Screen-Printed Carbon Electrode, *Analyst*, 119: 2431-437 (1994).
- 19.Lau, O.W. S.-F. & Cheung, Y.P.M. Simultaneous Determination of Ascorbic Acid, Caffeine & Paracetamol in Drug Formulations by Differential-Pulse Voltammetry Using a Glassy Carbon Electrode, *Analyst*, 114: 1047-1051 (1989).
- 20.Miner, D. J. R., Riggan, R.M. & Kissinger, P.T. Voltammetry of Acetaminophen and its Metabolites, *Analyt. Chem.*, 53: 2258-2263 (1981).
- 21.Navarro, J. & Arjona, D., Roldan, E. & Rueda, M. Determination of Paracetamol in Tablets and Blood Plasma by Differential Pulse Voltammetry, *J. Pharm. Biomed. Anal.*, 6: 969-976 (1988).

22. Ozkan, S.A., Uslu, B. and Aboul-Enein, H.Y. Analysis of Pharmaceuticals and Biological Fluids Using Modern Electroanalytical Techniques, *Crit. Rev. Analyt. Chem.*, 33:155-181(2003).
23. Wang, C., Hu, C.X., Leng, Z., Yang, G. & Jin, G. Differential Pulse Voltammetry for Determination of Paracetamol at a Pumice Mixed Carbon Electrode, *Analyt. Lett.*, 34:2747-2759,(2001).
24. Zen, J.-M. & Ting, Y.-S. Simultaneous Determination of Caffeine and Acetaminophen in Drug Formulations by Square-Wave Voltammetry Using a Chemically Modified Electrode, *Analyt. Chim. Acta*, 342:175-180(1997).
25. Kanita Tungkananuruk Nipon Tungkananuruk and Duncan Thorburn Burns Cyclic voltammetric determination of acetaminophen in paracetamol tablets, *KMITL Sci. Tech. J.* 5(3) Jul.-Dec. (2005).
26. Erk, N., Ozkan, Y., Banoglu, E., Ozkan, S.A., Senturk, Z., "Simultaneous determination of paracetamol and methocarbamol in tablets by ratio spectra derivative spectrophotometry and LC" *Journal of Pharmaceutical and Biomedical Analysis*, 24 (3):469-475(2001)
27. Lawan SRATTHAPHUT1) and Nongluck RUANGWISES, "Determination of Paracetamol and Orphenadrine Citrate in Pharmaceutical Tablets by Modeling of Spectrophotometric Data Using Partial Least-Squares and Artificial Neural Networks" *YAKUGAKU ZASSHI*, 127(10):1723-1729 (2007).
28. S. Ghidini, E. Zanardi, G. Varisco, & R. Chizzolini, "Residues of beta-lactam antibiotic in bovine milk : confirmatory analysis by liquid Chromatography Tandem Mass spectrometry after microbial assay screening." *Food-Addit-Contm.*, 20, : 528-534(2003).
29. Chalermpon, T.; Boonsom, L.; Surapol, N & Saisunee, L., "High Performance Liquid Chromatographic (HPLC) Assay for the Determination of Cephalexin in Commercial Pharmaceuticals" 31st Congress on Science and Technology of Thailand at Suranaree University of Technology: 18 – 20 October (2005).
30. V.F. Samanidou, E.A. Hapeshi, I.N. Papadoyannis, "Rapid and sensitive high-performance liquid chromatographic determination of four cephalosporin antibiotics in pharmaceuticals and body fluids" *Journal of Chromatography B*, 788, Issue 1, 5 :147-158 (2003).
31. M. Dousa, & R. Hosmanova, "Rapid determination of amoxicillin in premixes by HPLC." *J. Pharm-Biomed-Anal.*, 37:373-377(2005).
32. C.E. Lin, H.W. Chen, E.C. Lin, K.S. Lin, & H.C. Huang, "Optimization of separation and migration behavior of cephalosporins in capillary zone electrophoresis," *J-Chromatogr-A*, 879:197-210(2000).
33. L. Okerman, K. De-Wasch, J. Van-Hoof, & W. Smedts, "Simultaneous determination of different antibiotic residues in bovine and in porcine kidneys by solid-phase fluorescence immunoassay." *J. AOAC-Int.*, 86:236-240(2003).
34. Quanli Ma; Jinghe Yang; Xia Wu; Fang Huang; Limei Sun "A Selective Fluorimetric Method for the Determination of Some β -Lactamic Antibiotics Supported by Natural Science Foundations of China and Shandong province" *Analytical Letters*, 33, Issue 13 :2689–2699(2000).

35. Maotian Xu, Huailing Ma, Junfeng Song, "Polarographic behavior of cephalexin and its determination in pharmaceuticals and human serum". *J Pharm Biomed Anal.* 3;35 (5):1075-81) (2004).
36. Orawon, CH.; Akira, F.; Pornpimol, T. & Hatai, S. "Electroanalysis of Glutathione & Cephalexin Using the Boron-Doped Diamond Thin-Film Electrode Applied to Flow Injection Analysis" *ANALYTICAL SCIENCES* 17:i419-i422(2001).
37. Gallo-Martinez, L.; Campins-Falco, P. & Sevillano-Cabeza, A. "Comparison of several methods for determination of cephalosporine analysis of cephalexin in pharmaceutical sample." *J. Pharm-Biomed-Anal.*, 29:405-423(2002)
38. Yong-Nian Ni; Wei-Qiang Xiao, " Simultaneous Kinetic Spectrophotometric Determination of Cephalexin and Trimethoprim in Pharmaceutical Preparation and Human Urine with the Aid of Chemometrics", *Chinese Chemical Letters*, 19,8:981-984(2008/08).
39. P.P.KAUR & U.GUPTA " H-Point Standard Addition Method for Simultaneous Determination of Maneb and Zineb" *Journal of Chemistry*, 6(1):106-112(2009).
40. H. Tavallali* & M. Sheikhaei, " Simultaneous kinetic determination of paracetamol and caffeine by H-point standard addition method" *Afr. J. Pure Appl. Chem.*, 3(1):011-019, January, (2009).
41. H.R. Pouretedala,* and M. Asefi " H-point Standard Addition Method for Simultaneous Determination of Cobalt(II) and Zinc(II) Ions" *J. Iran. Chem. Soc.*, 4, (4): 503-509(2007).
42. Mehdi Nekoei, a, b* Majid Mohammadhosseini and Kobra Zareic Simultaneous Kinetic Determination of Phosphate and Silicate by Spectrophotometric H-Point Standard Addition Method *Journal of the Chinese Chemical Society*, 55: 362-368 (2008) .
43. Kobra Zarei,* Morteza Atabati and Mahnaz Safaei, " Simultaneous Spectrophotometric Determination of Aluminum and Iron in Micellar Media by Using the H-Point Standard Addition Method" *Journal of the Chinese Chemical Society*, 54: 1395-1400(2007).
44. A. Doménech-Carbó . M. T. Doménech-Carbó & J. V. Gimeno-Adelantado . F. Bosch-Reig., " H-point standard addition method" *Anal Bioanal Chem.* ,385 :1552-1561 (2006).
45. Abbas Afkhami* and Nahid Sarlak "Simultaneous Determination of Salicylamide and Paracetamol by Spectrophotometric H-Point Standard Addition Method and Partial Least Squares Regression, *Acta Chim.Slov.* 52:98-103, (2005).
- 43 H. Abdollahi, S. Zeinali, " Spectrophotometric study of complexation equilibria with H-point standard and Spectroscopy, 49:309-313(2004).
46. El-Sayed, A.Y., and El-Salem, N.A. "Recent developments of Derivative spectrophotometry and their analytical applications" *Anal.Sci.*, 21, 595(2005).
47. addition and H-point curve isolation methods." *Talanta* 62 : 151-163(2004).
48. A.Safavia*, F. Towhidi a & H. Abdollahi "Simultaneous Kinetic Determination of V(IV) and Fe(II) by H-point Standard Addition Method", *Canadian Journal of Analytical Sciences*.

Inhibitive Action of Ellagic acid on Corrosion behavior of SS 316L in Artificial saliva

¹Murtdha A.Siyah., ¹Amar .M .hmud, ¹Riyadh sh. Al- Hussein, and ²Jamal. F.Hamodi.

¹Chemical Research and Petrochemical Industries, Ministry of Science and Technology

²Directorate of Materials Science, Ministry of Science and Technology.

الخلاصة

للاجك أسيد مادة مضادة للأكسدة وللسرطان استعمل في هذه الدراسة اللاجك كمثبط للتآكل البايولوجي للحديد المقاوم للصدأ في محلول اللعاب الصناعي الذي استعمل كوسط تجرى فيه اختبارات التآكل إذ تم تحديد درجة الحرارة لعمليات الاستقطاب الكهروكيميائية بحدود (37 ± 1 °C) باستخدام حمام مائي لمحاكاة درجة حرارة الجسم البشري حالياً التآكل للحديد المقاوم للصدأ خفض باستخدام لاجك أسيد إذ تم إضافة نسب مختلفة من مادة اللاجك إلى محلول اللعاب الصناعي من أجل مقارنة تأثير إضافة اللاجك على سلوك التآكل للحديد المقاوم للصدأ الذي تحرى عنه بالقياسات الكهروكيميائية أظهرت النتائج إن كثافة تيار التآكل للحديد المقاوم للصدأ تقل بزيادة إضافة مادة اللاجك إلى محلول اللعاب الصناعي .

ABSTRACT

Ellagic acid has antioxidant, anti-mutagen and anti-cancer properties. In this study we use them as inhibitor of bio corrosion of SS 316 L in Artificial saliva was used as the electrolyte The temperature of the polarisation test cell was maintained at 37 ± 1 °C by thermo stated water bath to simulate the human body temperature Recently the corrosion of SS316L was suppressed in solutions containing ellagic add in different concentrations of Ellagic acid. to compare The corrosion behavior investigated by electrochemical measurements. The result showed that corrosion current density of SS 316 L specimens in artificial saliva solution containing ellagic acid was much lower than the values obtained in artificial saliva solution without ellagic acid .

Key word : biocorrosion ,Ellagic acid ,biomaterial.

INTRODUCTION

Ellagic acid is a naturally occurring phenolic constituent in certain fruits and nuts. Research in the past decade confirmed that ellagic acid markedly inhibits the ability of other chemicals to cause mutations in bacteria. Ellagic acid from red raspberries has proven as an effective anti mutagen and anti carcinogen as well as an inhibitor of cancer and intioxidant and antiatherosclerosis (1). Ellagic acid has been found to occur naturally in 46 different foods, with the red raspberry having been identified as having the highest natural content. Ellagic acid is a phenolic compound found in plants in the form of hydrolysable tannins called ellagitannins. Ellagitannins are esters of glucose with hexahydroxydiphenic acid; when hydrolyzed, they yield ellagic acid, the dilactone of hexahydroxydiphenic acid. Ellagic acid is a very stable compound and is readily absorbed through the gastrointestinal system in mammals, including humans. (2).The ellagic acid is rapidly absorbed and subsequently metabolized(3) . The absorption of ellagic acid occurred mostly within two hours after oral administration and more than 53% of the orally

administered of ellagic acid remained in the gastrointestinal tract at 24h. (4). The ellagic acid has strong affinity for protein in small animals. Further studies investigated the presence of free ellagic acid in human plasma may be due to its release from the hydrolysis of ellagitannine, (5). Corrosion is the major problem affecting the service life of orthopedic implants. There are a number of ways to reduce corrosion, altering the environment using addition of inhibitors. Metals and alloys are used in restoration of anatomical structures for centuries owing to their superior mechanical properties. However, the degradation of most metals implanted in the human body has narrowed the choice of clinically usable metals and alloys to mainly-stainless steels, cobalt-chromium and titanium and its alloys (6,7). These metallic devices are unique that they are exposed to living cells, tissues and biological fluids which are not only dynamic but are also a hostile environment for the survival of the implant (8,9). Type SS 316L are widely used for implantation purposes in orthopaedic surgery owing to their corrosion resistance, mechanical properties and low cost. However, clinical experience has shown that they are susceptible to localised corrosion in the human body causing the release of metal ions into the tissues surrounding the implants with several incidences of failures(10,11).

MATERIALS AND METHODS

Ellagic acid

Ellagic acid was provided by sigma chemical – USA .

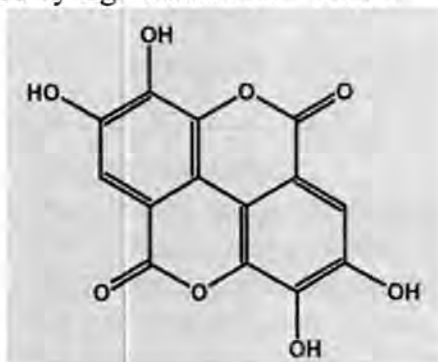


Figure- 1: Chemical formula of Ellagic acid

MW: 302.1 | Formula: $C_{14}H_6O_8$

Material

The material used in this work was austenitic SS 316L. Chemical analysis of this material was carried out using (ARL Spectrometer 3460) in Al-Nasser Company. Table (1) shows the nominal and the analytical chemical compositions of SS 316L used in this work.

Table -1: A nominal (12) and analytical chemical composition of SS 1316L

Element wt% Alloy	C	Cr	Ni	Mn	Si	P	S	Mo	N	Fe
Actual Value	0.03 Max	16-18	10-14	2.00 Max	0.75 Max	0.045 Max	0.03 Max	2-3	0.10 Max	Rem.
Analytical	0.027	16.18	11.81	1.61	0.67	0.02	0.01	2.2	0.08	Rem.

Surface condition of specimen plays an important role in corrosion resistance, hence, it is necessary to prepare uniform surface and requires careful specimen preparation. The specimens were cut out in dimensions of (10×10 mm) for electrochemical tests and (20×20 mm) and 2 mm thick for corrosion test.

The shaped specimens were molded using fast cold setting material up to 20 cm thick leaving the topside of the specimen exposed. The mounted specimens were allowed to set for half an hour and care was taken to ensure that the mould does not contain any cracks or bubbles at the mould / specimen interface. For electrochemical studies, suitable provision was made on the other side for electrical contact. The schematic diagram of the molded specimen for microstructure evaluation and electrochemical tests show the **figure (2)** . The mounted specimens were ground with SiC emery papers in sequence on 120, 180, 220, 320, 500, 800, 1000, and 1200 grit to get flat and scratch- free surface. The specimens were polished using polish cloth and alpha alumina 0.3µm and washed with distilled water. The polished specimens were degreased with acetone trichloroethylene and cleaned in the same solution. The degreased specimens were washed with deionized water, dried and kept in a dissector over a silica gel pad and used for electrochemical investigation.

Electrochemical Studies

In this work the Electrochemical measurements of the SS316L samples was carried out under simulated body fluid—Artificial saliva (Modified Carters solution) chemical composition in Table 2 with adjusted pH.7.4 and temperature 37 ± 1 ° C by means of a thermostated water bath to simulate the

human body. A saturated calomel electrode (SCE) and a platinised platinum black were used as the reference and auxiliary electrodes respectively. The area of the SS316L samples surface exposed to corrosion study was (1 cm²). The other sides of the electrode and its edges were masked with lacquer and were dried in air. The electrodes were further dipped into the electrolytic solution to study the corrosion process. The electrochemical measurements carried out with different concentration of Ellagic acid samples are open circuit potential (OCP)—time measurements, cyclic polarisation. The critical parameters like corrosion potential (E_{corr}), were evaluated from the polarisation curves. The samples were immersed in modified Carters solution with different concentration of ellagic acid and the OCP (E_{corr}) was monitored for half hour. During cyclic polarisation study, the potential was increased from 0.200 V below the OCP towards the noble direction at a rate of 10 mV/min until 0.200 V above the OCP. The sweep direction.

Table -2: Chemical composition of modified artificial Saliva(13).

O.	CONSTITUENT	WEIGHT (gm/l)
1	NaCl	0.70
2	KCl	1.20
3	KSCN	0.33
4	NaHCO ₃	1.50
5	Na ₂ HPO ₄	0.26
6	KH ₂ PO ₄	0.20
7	Urea	0.13

RESULTS AND DISCUSSION

The electrochemical behavior of SS 316L was investigated in simulated body fluid solution (artificial saliva) at 37 °C, the corrosion current for all specimens which mixed with Ellagic acid is more noble than that of the specimen with not add it show the figures (3, 4, 5 and 6).

And the Table.3. The figure (7) show the effect of Ellagic contraction on corrosion behavior of SS316L in the saliva solution compared to that for specimen immersed in the saliva with out Ellagic. The corrosion current density of SS316L decrease with increasing concentration of Ellagic, indicating Ellagic revealed a good corrosion inhibition.

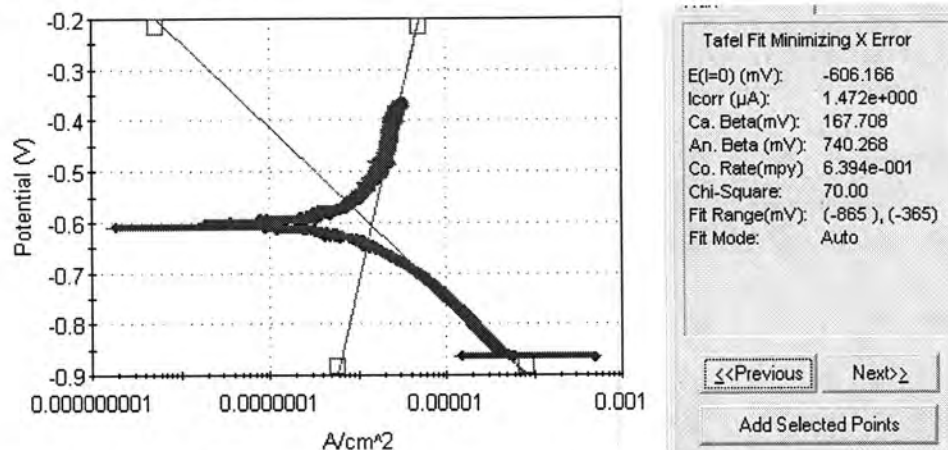


Figure -3: Tafel fit of Potentiodynamic Polarization of SS316L in Artificial Saliva without concentration of Ellagic.

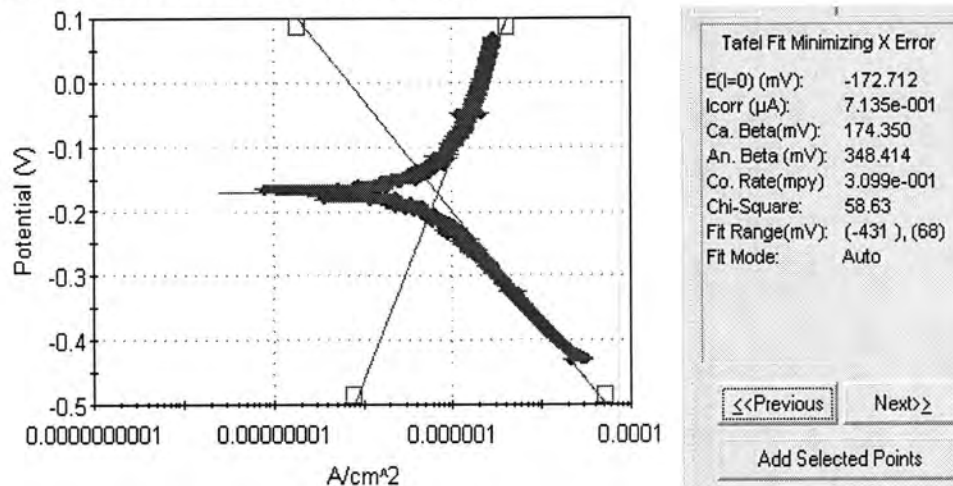


Figure -4: Tafel fit of Potentiodynamic Polarization of SS316L in Artificial Saliva with 0.02gm/l concentration of Ellagic.

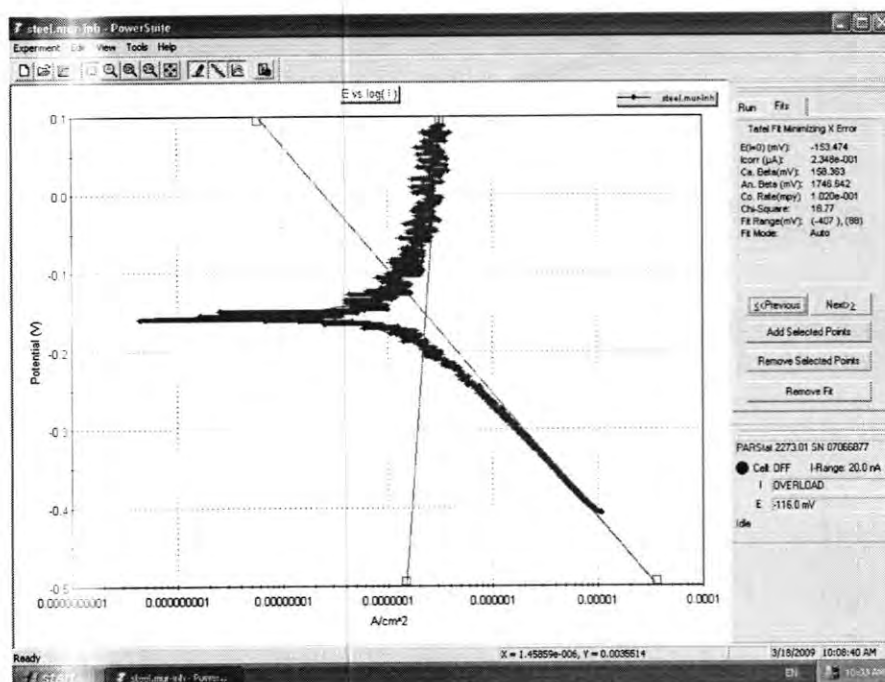


Figure -5: Tafel fit of Potentiodynamic Polarization of SS316L in Artificial Saliva with 0.04gm/l concentration of Ellagic.

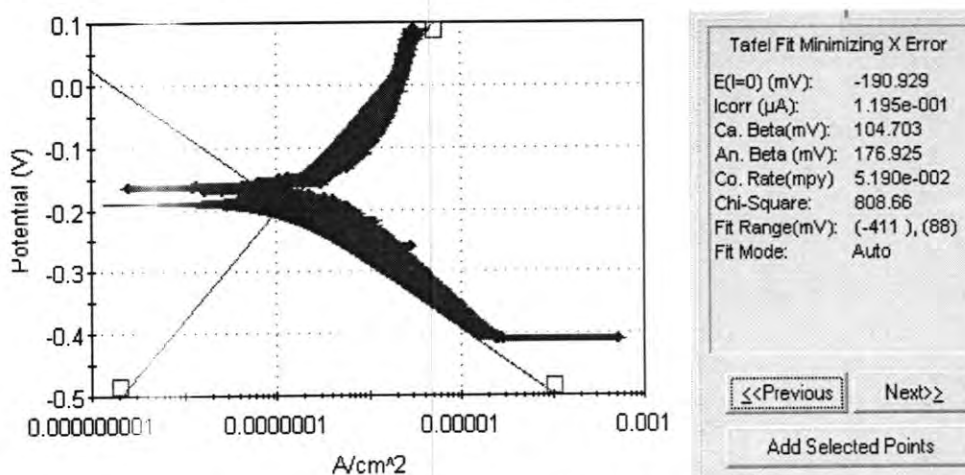


Figure -6: Tafel fit of Potentiodynamic Polarization of SS316L in Artificial Saliva with 0.06gm/l concentration of Ellagic.

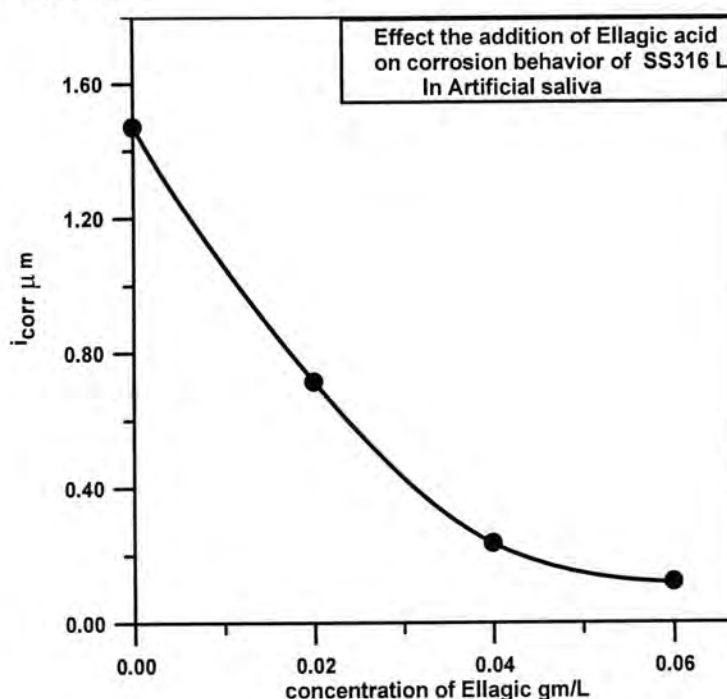


Figure-7:Corrosion Current Density of SS316L in Artificial saliva with different concentration of Ellagic Acid .

Table-3: Summary of electrochemical parameters for SS316L In artificial saliva with different concentration of Ellagic

We can conclude:-

1. The Ellagic acid can be used as an inhibitors for SS316Ldissolution but their effect depends on their concentration.
- 2.The corrosion current density of SS316L specimens in artificial saliva

Concentration of Ellagic Acid Gm\L	E corr mv	I corr μA	mpy
0	-606	1. 472	0.639
0.02	-172	0.715	0.309
0.04	-153	0.234	0.102
0.06	-190	0.119	0.05

containing Ellagic acid decreased in comparison with that in a artificial saliva solution without Ellagic addition . Adding Ellagic to the solution resulted in preventing the corrosion of the SS316L in artificial saliva.

- 3 . from these results the noble negative passive direction film for specimens immersed in the saliva solution mixed with Ellagic at different concentration

compared to those with out Ellagic, the effects of Ellagic are not only the protection of SS316L from chloride attack but also the suppression of dissolution of SS316L ions via

REFERENCES

1. Michael, A. ; Leslie, D. ; Mira, R.; Nina, V. ; Marielle, K.; Raymond, C.; Tony, H.; Dita, P. r and Bianca, F. Am. J. Clin. Nutr., 71:1062–1076. (2000).
2. Stephen T. Talcott and Jonn-Hee Lee . J. Agric. Food Chem, 50, 3186-192. (2002).
3. Doyle, B. and L. A. Griffiths Xenobiotic. 410 (4) PP 247-256. (1980) .
4. Robert, W. T. and Ronald, M. M. Xenobiotica, 18, (4) : 397 – 405. (1988) .
5. Navindra, P. S. ; Rupo, L. and David, H. Clinica. Chimica. Acta., 348 :63–68. (2004).
6. Joon B. Park and Joseph D. Bronzino. p. cm "Biomaterials principles and applications" Boca Raton London New York Washington, D.C., (2002).
7. T.M.Sridar, U. Kamachi, Mudali, M. Subbaiyan" J. Corrosion Science 45, : 237-252 (2003).
8. M. Sivakumar, U. Kamachi Mudali, S. Rajeswari, J. Mater. Eng. Perf. 3 (744) . (1994).
9. T.M.Sridar, U. Kamachi, Mudali, M. Subbaiyan J. Corrosion Science 45, : 237-252 (2003).
10. M. Sivakumar, U. Kamachi Mudali, S. Rajeswari, J. Mater. Sci. Lett. 13 (142). (1994).
11. O.E.M. Pholer, Failure of orthopaedic metallic implants, in: ASM Hand - book on Failure Analysis and Prevention, 9th ed., 11, ASM International, Metals Park, Ohio, :.670, (1986).
12. ASM, Metal Handbook, " Properties and Selection Irons and Steel ", 9th edition, 9, (1985).
13. Murtadha .A. siyah Msa Thesis Baghdad University (2009).

Preparation and Potentiometric Study of Amiloride Hydrochloride Selective Electrodes and Their Application in Determining Some Drugs

Khaleda, H. Al-Saidi and Maha Abdulateef yahya
Chemistry Department, College of Science, Al-Nahrain University

الخلاصة

تم تصنيع عدة أقطاب بوليمرية من مادة الهولي فاينيل كلورايد حساسة للاميلورايد هيدروكلورايد بالاعتماد على المعقد المحضر (Amiloride-phosphotungstate) والمعقد الثاني (Amiloride-tetraphenylborate) كمادة فعالة. هذه المادة الفعالة تكون مذابة في عدة مواد ملدنة منها:

Di-butylphthalate (DBPH), Di-octylphthalate (DOP), Tri-butyl phosphate (TBP), وقد تم دراسة خواص هذه الأقطاب والتي شملت (ميل منحني المعايرة ومعامل الارتباط ومدى التراكيز و حد التحسس و عمر القطب) ومن خلال الدراسة أظهرت النتائج أن أقطاب الاميلورايد: Amilo-PT+DOP, Amilo-PT+TBP, Amilo-TPB+ DBPH, Amilo-TPB + Amilo-PT+DBPH, 54.198, 52.759, 50.91, 49.007, 48.508, 48.501 ملفولت/حقبة على التوالي. و حد التحسس (1.5×10^{-5} , 7×10^{-6} , 6×10^{-7}) مولاري وإنحدار 1×10^{-2} - 1×10^{-5} مولاري و (35, 10, 12, 10, 30, 10) ثانية للتركيز 10^{-3} مولاري و عمر القطب (10, 15, 21, 30, 35, 45) يوم على التوالي. ومدى الدالة الحامضية وجد بحدود (1.9 - 7.8) لتركيز محلول الاميلورايد 10^{-3} مولاري باستخدام القطب (A) Amilo-PT+DBPH. أيضاً درست التداخلات لبعض الأيونات الأحادية والثنائية والثلاثية وتداخل نوع آخر من الأدوية المدرة مثل الهيدوكلووروثايزايد بواسطة طريقة المحاليل المنفصلة وطريقة المحاليل الممزوجة لتعيين معامل الانتقائية ($K^{pot}_{A,B}$) وكذلك استخدم القطب (A) في التقديرات الإجهادية لتعيين الاميلورايد في الأدوية التجارية و أظهرت النتائج بأن الطريقة المستخدمة بسيطة، سريعة ودقيقة مقارنة بطريقة الأطياف.

ABSTRACT

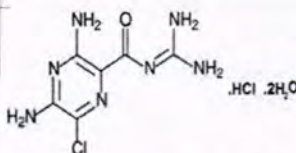
Amiloride hydrochloride ion-selective electrodes were constructed in polymeric membrane by using PVC and based on the use of active ion-pair (Amiloride-phosphotungstate) and the other ion pair (Amiloride- tetraphenyl -borate). The plasticizers used were Di-butyl phthalate (DBPH), Di-octylphthalate (DOP) and Tri-butyl phosphate (TBP). The electrodes (A, B and C) based on the ion pair (Amiloride -phosphotungstic acid) and (D, E and F) based on the ion pair (Amiloride - tetraphenylborate) and the plasticizers used DBPH, DOP and TBP respectively they gave approximately the same linear concentration range from (1×10^{-5} to 1×10^{-2}) M. The slopes are (54.198, 52.759, 50.910, 49.007, 48.508 and 48.501) mV/decade, and the detection limit were (6×10^{-7} , 1.5×10^{-6} , 7×10^{-6} , 1.75×10^{-5} , 7×10^{-6} and 1.5×10^{-5}) M, with the response time (10, 30, 10, 12, 10 and 35) Sec. and the lifetime were about (45, 35, 30, 21, 15 and 10) days respectively. And the working pH range found to be (1.9 - 7.8) for the concentration of Amiloride solution 1×10^{-3} M by using electrode A (Amilo-PT+DBPH). The measurement interferences in the presence of Na^+ , K^+ , Mg^{2+} , Mn^{2+} , Cu^{2+} , Fe^{3+} and Hydrochlorothiazide were studied using separate and mixed methods for selectivity coefficient determination. The pH and life time of the electrodes were also studied. The analytical methods results showed to be simple, rapid and with a good accuracy by comparing it with UV-spectrophotometric method by using F-test.

Key Words Amiloride hydrochloride ion-selective, phosphotungstic acid, tetraphenylborate, Amiloride determination.

INTRODUCTION

Amiloride Hydrochloride, an antikaliuretic-diuretic agent, is a pyrazine-carbonyl-guanidine(1) that is unrelated chemically to other known antikaliuretic or diuretic agents, it is a yellow solid crystal powder, odourless, it is solubility in water is 0.52 g/100 mL; in alcohol 1.96 g/100 mL at 25°C; freely soluble in

dimethylsulfoxid (DMSO)(2); practically insoluble in ether, acetone and chloroform, melting point 240.5 to 241.5°C, pH 3.8 to 5.2, it is the salt of a moderately strong base (pKa 8.7), Store in well-closed containers ideally between 15 to 30°C, Avoid freezing or a temperature greater than 40°C and protect from light(3). It is designated chemically as 3, 5 - diamino - 6 - chloro- N - (diaminomethylene) pyrazine carboxamide monohydrochloride, dihydrate and has a molecular weight of 302.12. Its empirical formula is $C_6H_8ClN_7O.HCl.2H_2O$ and its structural formula(4) .



There have been only a few reports on the determination of Amiloride in tablets or in biological fluids such as fluorescence spectrometry (5,6). The sequential injection analysis technique (SIA)(7) . A simple and fast method for the derivative spectrophotometry (8, 9). The chromatographic methods HPLC and GC/MS.(10-13).The electrochemical methods voltammetry(14) and Potentio - metry(15). UV spectrophotometry coupled with new chemometric regression techniques (16, 17). Potentiometric membrane ion-selective electrodes (IESs) have been used in pharmaceutical and biological analysis. This is mainly due to their simple design, low cost, adequate selectivity, good accuracy and wide concentration range (18).

Electroanalytical methods have a long history of development, progress in ISE development has occurred rapidly in the past 40 years, with promising innovations still on the horizon. (19). Analytical techniques are commonly employed for this purpose by using drug-selective electrodes (15, 20-25).

MATERIALS AND METHODS

Instruments and equipment:

- 1- Expandable ion analyzer, ORION, model EA 940, (U. S. A.).
- 2-FTIR-8300 Fourier transforms infrared spectrophotometer Shimadzu. (Japan).
- 3-Double-beam UV-Visible spectrophotometer model (UV-1650 PC) SHIMADZ (Japan), interfaced with computer via a SHIMADZU UV probe data system program (Version 1.10).

Reagents and solutions

- 1- Pure Standard Amiloride hydrochloride ($C_6H_8ClN_7O.HCl.2H_2O$ F.W.302.12) and Hydrochlorothiazide (HCT) $C_7H_8ClN_3O_4S_2$; F.W. 297.74) were a gift from the State Company of Drug Industries and Medical Appliances (Samara- IRAQ-SDI).
- 2-Commercial drugs: Saluretic tablets (Amiloride hydrochloride 5mg + Hydrochlorothiazide 50mg) made in Cairo-Egypt and the same content in Maduratic Indian tablets.

3-Dodeca –Tungstophosphoric acid (PT) ($\text{H}_3\text{PO}_4 \cdot 12\text{WO}_3 \cdot \text{XH}_2\text{O}$; F.W. 2880.2), (BDH).

4-Sodium tetraphenylborate (NaTPB) ($\text{C}_{24}\text{H}_{20}\text{BNa}$; F.W. 342.22)

5-Tetrahydrofuran ($\text{C}_4\text{H}_8\text{O}$; F.W. 72.11), (E.Merck).

6-Polyvinyl chloride (PVC) of relatively high molecular weight (Breon S 110/10 B.P Chemical U. K. Ltd).

7-The plasticizers were obtained from Fluka AG, (Switzerland), their composition and viscosity were tabulating in Table 1.

Table-1: Shows the plasticizer which were used and their chemical composition and their viscosity.

Plasticizer's name	Chemical composition	viscosity	company
Di-butylphthalate (DBPH)	$\text{C}_6\text{H}_4[\text{CO}_2\text{CH}_3(\text{CH}_2)_3]_2$	14.44 CST	Fluka
Di-octylphthalate (DOP)	$\text{C}_6\text{H}_4[\text{CO}_2\text{C}_8\text{H}_{17}]_2$	82.98 CST	Fluka
Tri-butylphosphate (TBP)	$(\text{C}_4\text{H}_9\text{O})_3\text{PO}$	3.114 CST	Fluka

8-Other chemicals such as hydrochloric acid (HCl; F.W. 36.45; sp.gr. 1.184; 37% HCl; $\approx 12\text{M}$), sodium hydroxide (NaOH; F.W. 40.00 pellets), sodium chloride (NaCl; F.W. 58.45), potassium chloride (KCl; F.W. 74.58), magnesium chloride ($\text{MgCl}_2 \cdot 6\text{H}_2\text{O}$; F.W. 203.218), manganese(II) sulfate, anhydrous (MnSO_4 ; F.W. 151), copper(II)sulfate, anhydrous (CuSO_4 ; F.W. 159.60) and Ferric(III) Sulfate ($\text{Fe}_2(\text{SO}_4)_3 \cdot 9\text{H}_2\text{O}$; F.W. 506.027). All chemicals and solvents were of an analytical reagent grade obtained from BDH, Fluka and Aldrich companies. Other needed to prepare was Hydrochlorothiazide (HCT) $\text{C}_7\text{H}_8\text{ClN}_3\text{O}_4\text{S}_2$; F.W. 297.74 that used in selectivity methods to find if it interfered with Amiloride drug, All solutions were prepared in doubly distilled water.

1-A stock standard solution of 0.01 M Amiloride hydrochloride was prepared by dissolving 0.151 g of standard Amiloride hydrochloride and completing the solution up to 50 ml, (ultrasonicator) equipment was used to assist the dissolving of the drug. The other

Amiloride standard solutions were prepared by serial dilution of the stock solution, ranged (10^{-7} - 10^{-2}) M.

2-The stock standard solution of 0.01M PT was prepared by dissolving 1.44g in distilled water and diluted up to 50 mL.

3- A stock standard solution of 0.01M NaTPB was prepared by dissolving 0.171g in distilled water and diluted up to 50 mL.

4-Stock solutions of 0.1 M of NaCl, KCl, $\text{MgCl}_2 \cdot 6\text{H}_2\text{O}$, MnSO_4 , CuSO_4 , and $\text{Fe}_2(\text{SO}_4)_3 \cdot 9\text{H}_2\text{O}$ were prepared by weighted (0.584, 0.745, 2.0311, 1.51, 1.596 and 5.056 g) respectively and dissolved by distilled water in 100mL volumetric flask. More diluted solutions were prepared by dilution from the stock solutions.

5-A solution of 0.01M Hydrochlorothiazide(HCT) prepared by dissolving 0.297g in methanol about 10 mL and completes the volume to 100 mL, another diluted solution prepared from the standard.

6-A solution of $\approx 0.1\text{M}$ HCl was prepared by diluting 0.833mL of 12M HCl concentrated stock solution to 100mL. 0.1M NaOH was prepared by weighing 0.4g of NaOH and dissolving to 100mL distilled water.

Preparation of pharmaceutical formulation:

Ten tablets were crushed, mixed in a mortar and weighed accurately it found that the weight of average was equal to 0.2334 and 0.2364g for Maduratic and Saluretic respectively. and the weight of three tablets (0.7002 and 0.7038 g) which contain approximately 0.015 mg from Amiloride hydrochloride (each one tablet contained 0.005g) it dissolved by deionized water and using ultrasonicator for $\sim 5\text{min}$ then filtrate and washing the precipitate, the filtrate was collected in 50 mL volumetric flask the resulting solution contain $\sim 0.001\text{ M}$ Amiloride hydrochloride

Procedure

Preparation of Ion-pair Compounds:

The Amiloride hydrochloride ion-selective electrode is prepared based on the use of ion-pair compound (Amilo-PT) as the electro-active substance. The preparation of ion-pair was performed by mixing 50 ml of 0.01 M solution of Amiloride hydrochloride with 50 ml of 0.01 M PT with stirring. The resulting precipitate was filtered off, washed with water, dried at room temperature for two days. The composition of the ion-pair compound (Amilo-PT) was confirmed using UV and FTIR spectra as shown in Fig. 1 and Fig 2 respectively.

The other ion-pair compound (Amilo-NaTPB) was prepared by the same way, mixing 50 ml of 0.01 M solution of Amiloride hydrochloride with 50 ml of 0.01 M NaTPB with stirring. The resulting precipitate was also filtered off, washed with water, dried at room temperature for two days. The composition of the ion-pair compound, (Amilo-NaTPB) was confirmed also by using UV and FTIR spectra as shown in Fig. 1 and Fig 2 respectively..

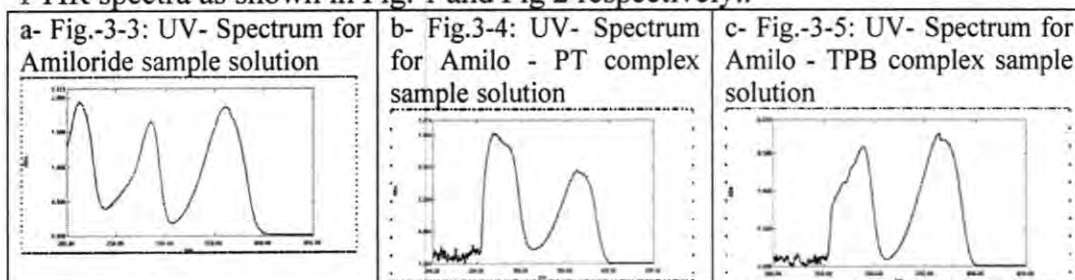
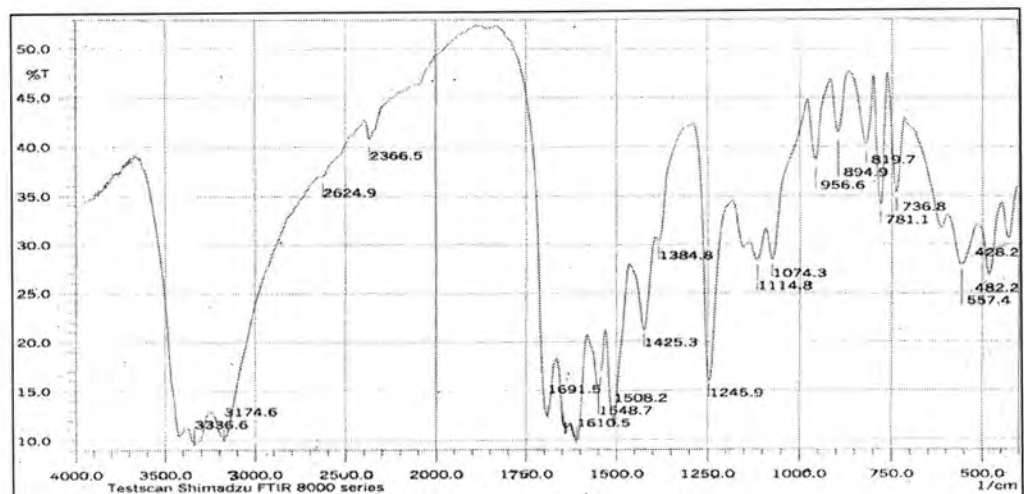
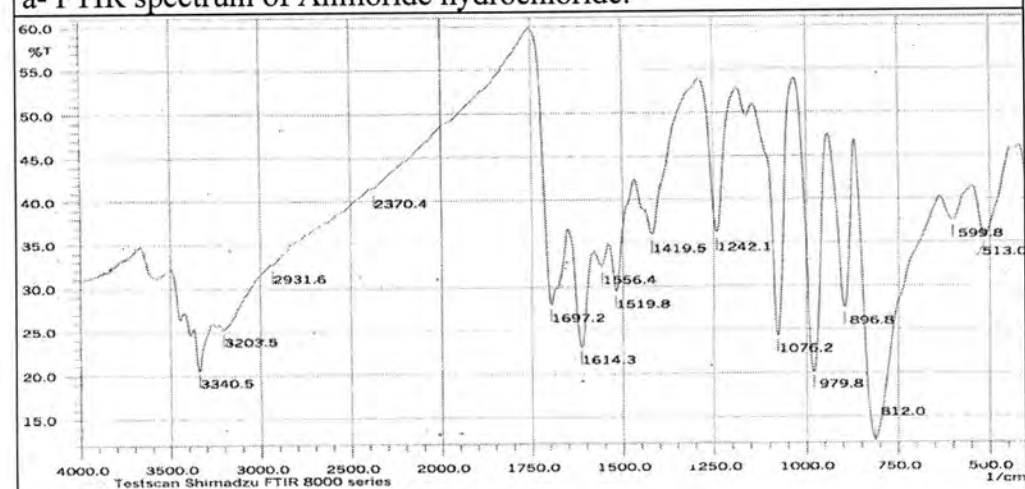


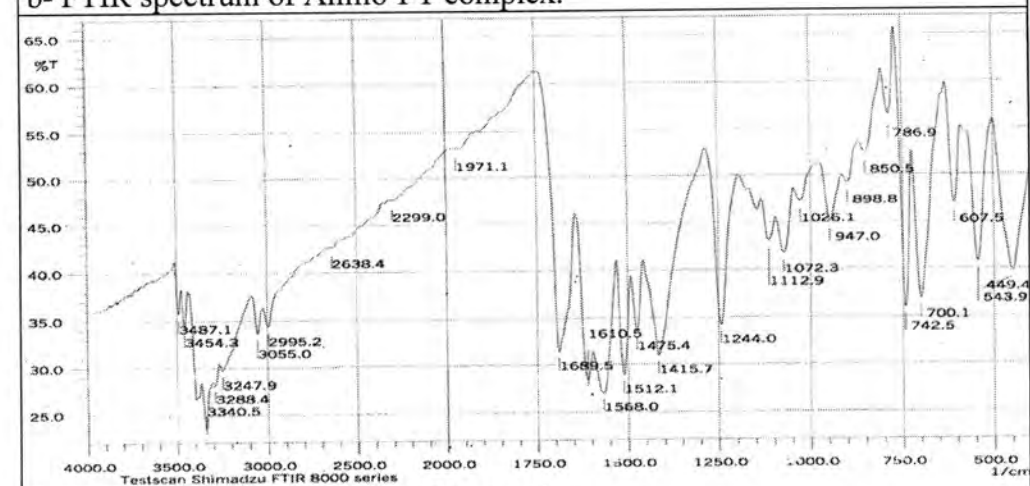
Fig.-1: UV spectra, a- Amiloride, b- Amilo-PT complex, c- Amilo-NaTPB



a- FTIR spectrum of Amiloride hydrochloride.



b- FTIR spectrum of Amilo-PT complex.



c- FTIR spectrum of Amilo-TPB complex.

Fig.-2:a- FTIR spectrum of (Amilo), b- (Amilo-PT), c- (Amilo-TPB) by using KBr.

Fabrication of the Electrodes:

The electrodes for Amiloride hydrochloride were prepared using electro active complexes (Amilo-PT), (Amilo-NaTPB) with different plasticizers showed in Table (1). The ISE nature and characteristics are considerably influenced by the nature and the amount of each component. As far as the polymeric membrane is concerned, it separates the test solution from the inner compartment, containing the target ion solution. The method of immobilization ion-pair compounds into the PVC matrix membrane as described by Craggs et al (26). A (0.040g) of Amilo-PT (ionophore or ion-pair) matrix was mixed with (0.360g) of plasticizer and (0.17g) of PVC powder; all were dissolved in (6-7 mL) of THF with stirring until a clear viscous solution was obtained. The same process was performed for the other ion-pair (Amilo-NaTPB). The resultant solution poured into a glass casting ring about (30 mm) in length and (35 mm) in diameter. It consists of two pieces; one of them was the glass cylinder and the other was glass plate. The two pieces was pasted together using PVC-THF viscous mixture to make sure no loss in the membrane mixture. The top side of the cylinder was covered with a pad of filter paper. Then all of the contents were left for two days to allow slow evaporation of the solvent and formation sensing membranes. A disc of the membrane was cut equal to the external diameter of a PVC tube (≈ 3 cm length, 6 mm i.d) The other side of the glass tube was assembled with plastic cover in which Ag/AgCl wire was inserted through it, tube was filled with 10^{-3} M Amiloride hydrochloride as internal solution before fixing the cover. The electrode was immersed in 10^{-3} M Amiloride solution for at least one hour before use. When not in use, they were stored in air. The master membrane was used to prepare several others

Selectivity measurements

A separate solution method was used for the selectivity coefficient measurement, and was calculated according to the equation(27, 28)

$$\log K_{pot} = [(E_B - E_A)/(2.303RT/zF)] + (1 - z_A/z_B) \log a_A \quad (1)$$

E_A , E_B ; z_A , z_B ; and a_A , a_B are the potentials, charge numbers, and activities for the primary A and interfering B ions, respectively, at $a_A = a_B$. The selectivity coefficients were also measured by the mixed solution method and was calculated according to the equation] (29-31)

$$K_{A,B}^{pot} = a_A / (a_B)^{z_A/z_B} \quad (2)$$

RESULTS AND DISCUSSION

The complexes were obtained by conversion Amiloride hydrochloride to Amilo-PT and Amlo-TBP characterized by their UV and FTIR spectra, , Amiloride phosphotungstate (Amilo-PT) light brown precipitate and the second complex is obtained by conversion Amiloride hydrochloride into Amiloride tetraphenylborate (Amilo-TPB) white precipitate the complex Amilo-PT, and

Amilo-TPB. were stable and water insoluble ion-pair complex though readily soluble in organic solvents such as tetrahydrofuran. The complex was incorporated into a PVC membrane and three plasticizers; di-n-butylphthalate (DBPH), di-octylphthalate (DOP) and tri-n-butylphosphate (TBP). The first ion-pair complex (Amilo-PT) used to construct three electrodes (A, B and C) by using three different plasticizers (DBPH, DOP and TBP respectively) which their calibration curves shown in Fig..3.

The second ion-pair complex (Amilo-TPB) used to construct other three electrodes (D, E and F) by using the same three different plasticizers (DBPH, DOP and TBP respectively). The working characteristics for the investigated A, B, C, D, E, F electrodes were assessed on the basis of the calibration curves which were obtained by measuring of the e.m.f. values of the set of Amiloride hydrochloride solutions ranged (10^{-2} – 10^{-7})M. These electrodes show sub-Nernstain response to the Amiloride hydrochloride activity in different concentration ranges depending on the properties of the plasticizers and ion-pair complexes, which their calibration curves shown in Fig. 4. The equations of the linear range and their slope, correlation coefficient and relative standard deviation of there were listed in Table 2.

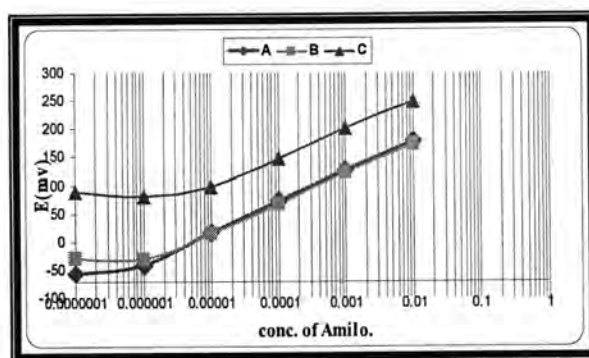


Fig.-3: Calibration curves of Amiloride hydrochloride selective electrodes (A, B and C) using (Amilo-PT) ion-pair complex.

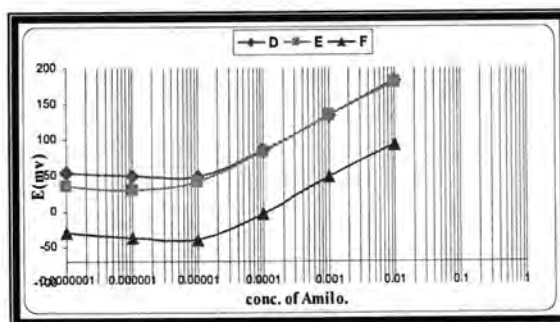


Fig.-4: Calibration curves of Amiloride hydrochloride selective electrodes (D, E and F) using (Amilo-TPB) ion-pair complex.

Table-2: The equation of calibration curves and their slope, Correlation coefficient and relative standard deviation of their slope.

Electrode Membrane	Linear equation	Slope (mV/Decade)	RSD%*	Correlation coefficient (R)
A-Amilo-PT +DBPH	$y = 23.534 \text{ Lnx} + 287.49$	54.198	0.275	0.9999
B-Amilo-PT +DOP	$y = 22.909 \text{ Lnx} + 277.75$	52.759	0.674	0.9998
C-Amilo-PT +TBP	$y = 22.106 \text{ Lnx} + 351.4$	50.910	0.836	0.9998
D-Amilo-TPB +DBPH	$y = 21.28 \text{ Lnx} + 280$	49.007	0.358	1.0000
E-Amilo-TPB +DOP	$y = 21.063 \text{ Lnx} + 277.83$	48.508	0.708	0.9995
F-Amilo-TPB +TBP	$y = 21.063 \text{ Lnx} + 191.17$	48.501	0.852	0.9991

* The result of three times repeated.

The parameters of Amiloride hydrochloride electrodes which include the slope, linear concentration range, detection limit, response time and life time of the six electrodes (A, B, C, D, E, F) are listed in Table 3, from the table electrode A (Amilo-PT with DBPH) is the best electrode which used to determined Amiloride.. Non-Nernstian slopes were obtained for electrodes non-Nernstian slope behaviors could be attributed to the high viscosity of plasticizers. slow down the ion exchange process between ion pair complex in membrane with the external solution of amiloride hydrochloride. Moreover, the steric effect of the alkyl group on the DBPH may decrease the bond strength of the ion pair complex. The TBP, which has a low viscosity (3.11 cSt), leads to leaching of the complex from the membrane or may have a high steric effect on methyl groups. Near Nernstian slopes, and there are several pharmaceutical application of ion selective electrode that have non- Nernstian slope proved that they can be used those electrodes in detection of drugs like the determination of Scopolamine(32) in Some Pharmaceutical Formulations by using ISE has a slope of 54.5 mV /decade, other ion selective membrane electrode forr PVC Membrane Sensors for potentiometric determination of Acebutolol(33) has slope 51.5 and 53 mV /decade, also the determination of Methacycline Hydrochloride(34) by using ISE has the slope equal 52.9 mV/decade and there was also Promethazine Hydrochloride (25) ion selective electrodes used in pharmaceutical preparations have a slopes of 40-56 mV /decade.

Table-3: The parameters of Amiloride hydrochloride electrodes.

Membrane Composition	Slope (mV/Decade)	Linear Concentration Range (M)	Detection Limit (M)	Response time (sec)			Lifetime (day)
				10^{-2} (M)	10^{-3} (M)	10^{-4} (M)	
A- Amilo-PT+DBPH	54.198	$10^{-5} - 10^{-2}$	6×10^{-7}	8	10	20	45
B- Amilo-PT+DOP	52.759	$3 \times 10^{-6} - 10^{-2}$	1.5×10^{-6}	20	30	35	35
C- Amilo-PT+TBP	50.910	$10^{-5} - 10^{-2}$	7×10^{-6}	5	10	15	30
D- Amilo-TPB+DBPH	49.007	$6 \times 10^{-5} - 10^{-2}$	1.75×10^{-5}	20	35	40	21
E- Amilo-TPB+DOP	48.508	$3 \times 10^{-5} - 10^{-2}$	7×10^{-6}	7	10	20	15
F- Amilo-TPB+TBP	48.501	$5 \times 10^{-5} - 10^{-2}$	1.5×10^{-5}	6	12	20	10

Effect of pH:-

The effect of pH on the response of the Amiloride electrode (A) was examined by measuring the variation in the potential against pH range from 0.7 to 11.0 by using 0.1M HCl to lower pH to 0.7 and by monitoring the potential stability with addition of 0.1M NaOH until the pH reach to 11, the pH effect studied for the three different Amiloride hydrochloride concentrations 10^{-4} , 10^{-3} and 10^{-2} M. The curves are shown in Fig.5.

At pH values lower than 1.0 or in very high acidity, the electrodes responses has been increased rather irregularly. This may be due to that the electrodes responses to H^+ activities as well as analyte ions. A drift in potential was noticed at $pH > 8$. This attributed to the poisoning of the membrane by formation a white precipitated tungsten oxides or sodium phosphotungstate. The working pH ranges of Amiloride electrode A are listed in Table 4.

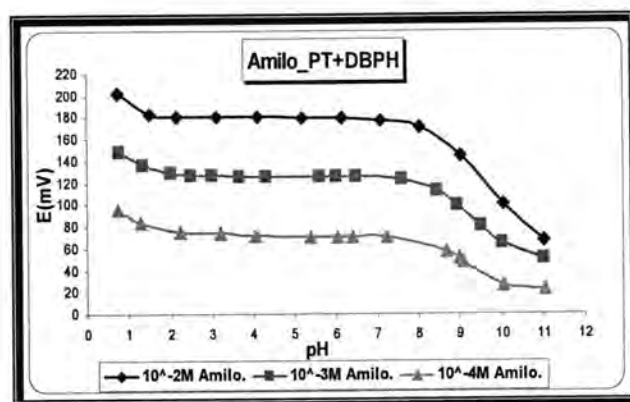


Fig.-5: Effect of pH on the potential of the electrode A (Amilo-PT+DBPH) at concentrations 10^{-2} , 10^{-3} and 10^{-4} M.

Table-4: Working pH ranges for Amiloride electrode A.

Membrane Composition	pH range		
Amilo-PT +DBPH	10^{-2}M	10^{-3}M	10^{-4}M
	1.8 – 7.8	1.9 – 7.8	2.3 – 7.2

Selectivity methods:

Separate solution methods (27,28):

The influence of some possible interfering inorganic cations such as Na^+ , K^+ , Mg^{2+} , Mn^{2+} , Cu^{2+} and Fe^{3+} and Hydrochlorothiazide drug which presented with amiloride in the pharmaceutical formulation for amiloride sensors (A, B, C, D, E and F) on the electrode response was studied. The selectivity of the electrodes based on DBPH, DOP and TBP were measured by the separate solution methods. The potentiometric selectivity coefficients were calculated using equation 1 at Amiloride and interfering concentrations were 10^{-3} . The values of the selectivity coefficients electrodes are listed in Table 5. The selectivity coefficients were very small. This means that there is no interference of these cations with the response of amiloride electrodes.

Table 5: Selectivity coefficient values for Amiloride electrode using - Separated solution methods

Sensors Interfering-Ion	A Amilo-PT+DBPH	B Amilo-PT+DOP	C Amilo-PT+TBP	D Amilo-TPB+DBPH	E Amilo-TPB+DOP	F Amilo-TPB+TBP
Na^+	1.320×10^{-3}	1.100×10^{-3}	1.770×10^{-3}	7.910×10^{-3}	5.140×10^{-3}	1.150×10^{-2}
K^+	3.699×10^{-4}	1.104×10^{-3}	9.024×10^{-4}	1.040×10^{-2}	5.660×10^{-3}	8.270×10^{-3}
Mg^{2+}	3.530×10^{-5}	4.344×10^{-5}	3.932×10^{-4}	3.643×10^{-4}	2.269×10^{-4}	5.59×10^{-4}
Mn^{2+}	2.212×10^{-5}	5.896×10^{-5}	3.433×10^{-4}	4.002×10^{-4}	2.617×10^{-4}	6.147×10^{-4}
Cu^{2+}	1.643×10^{-5}	5.403×10^{-5}	2.738×10^{-4}	2.0731×10^{-4}	2.164×10^{-4}	4.623×10^{-4}
Fe^{3+}	3.96×10^{-4}	7.872×10^{-5}	1.040×10^{-3}	8.289×10^{-4}	7.007×10^{-4}	8.076×10^{-4}
Hydrochlorothiazide	7.500×10^{-2}	7.900×10^{-2}	9.510×10^{-2}	7.540×10^{-2}	8.470×10^{-2}	7.000×10^{-2}

Mixed solution methods

By using the fixed interference method (FIM), (29-31) The potentiometry of a cell comprising an ion-selective electrode and a reference electrode (ISE cell) is measured for solutions of constant activity of the interfering ion (a_B) at first used $5 \times 10^{-2}\text{M}$ then mixed it with varying activity of the primary ion that is for the Amiloride (a_A). The potentiometry E (mV) values obtained are plotted vs. the logarithm of the activity of the primary ion. The intersection of the extrapolated linear portions of this plot indicates the value of (a_A) from Fig.6 as an example for all interfering ions, that is used to calculate $K^{\text{pot}}_{A,B}$ from equation (2) all results of $K^{\text{pot}}_{A,B}$ were in Table 6.

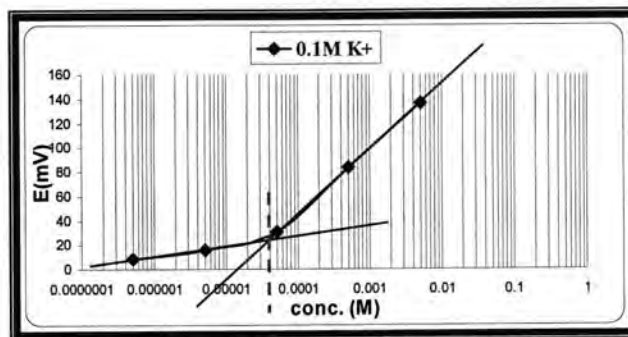


Fig.-6: FIM calibration curve for electrode A (Amilo-PT+DBPH), K^+ ($5 \times 10^{-2} M$) as interfering ion $a_A = 4 \times 10^{-5} M$.

Table-6: Values of $K_{A,B}^{pot}$ calculated from the equation $K_{A,B}^{pot} = a_A / (a_B)^{Z_A/Z_B}$ according to FIM.

Interfering ions	$a_B = (5 \times 10^{-2} M)$		$a_B = (5 \times 10^{-3} M)$	
	a_A	$K_{A,B}^{pot}$	a_A	$K_{A,B}^{pot}$
K^+	4.000×10^{-5}	8.000×10^{-4}	3.000×10^{-5}	6.000×10^{-3}
Na^+	7.000×10^{-5}	1.400×10^{-3}	2.000×10^{-5}	4.000×10^{-3}
Mg^{+2}	1.900×10^{-5}	8.497×10^{-5}	1.000×10^{-5}	1.414×10^{-4}
Mn^{+2}	5.000×10^{-5}	2.236×10^{-4}	2.000×10^{-5}	2.828×10^{-4}
Cu^{+2}	4.000×10^{-5}	1.788×10^{-4}	1.000×10^{-5}	1.414×10^{-4}
Fe^{+3}	2.000×10^{-5}	5.428×10^{-5}	8.000×10^{-6}	4.678×10^{-5}
Hydrochlorothiazide	—	—	1.500×10^{-5}	3.000×10^{-3}

Sample analyses:-

Four potentiometric techniques were used for the determination of Amiloride, direct measurement, standard addition (SAM), multi-standard addition (MSA) and titration by using electrode A. The recovery (RC %), relative error (RE %) and relative standard deviation (RSD %) for each method are calculated and listed in table 7.

Direct method

The calibration curve was constructed (for electrode A) in Fig.7, the concentration of the unknown was calculated from the linear equation $y = 23.534 \ln x + 287.49$ of the calibration curve which has the slope (S) $\square \square$ S.D. = 54.1988 ± 0.0177 and the intercept $\square \square$ S.D. = $287.49 \square \square \square \square \square \square \square \square$, for $n=5$, and the results are listed in Table 7.

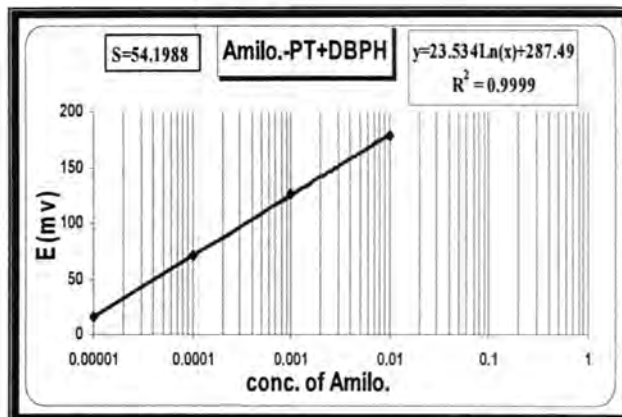


Fig.-7: Calibration curve of electrode A (Amilo-PT+DBPH).

Standard addition method (SAM)

That 0.5 ml increment of standard solution of 10^{-2} M Amiloride was added to 20 ml of unknown sample. By solving the following equation the unknown concentration can be obtained.

$$C_U = C_S / 10^{\Delta E/S} [1 + (V_U / V_S)] - (V_U / V_S)$$

Where: C_U : concentration of unknown solution, C_S : concentration of standard solution, V_U : volume of unknown solution, V_S : volume of standard solution, S : slope of electrode. The Recovery, Relative error and Relative standard deviation for five addition of Amiloride hydrochloride are listed in Table 7.

Multi standard addition method (MSA)

The calibration curve for MSA for electrode (A) was shown in Fig. 8 by plotting of $\text{antilog}(E/S)$ versus the volume of the five addition of Amiloride hydrochloride of 0.05 mL of 1×10^{-2} M. the analysis results RC% and RE% were listed in Table 7

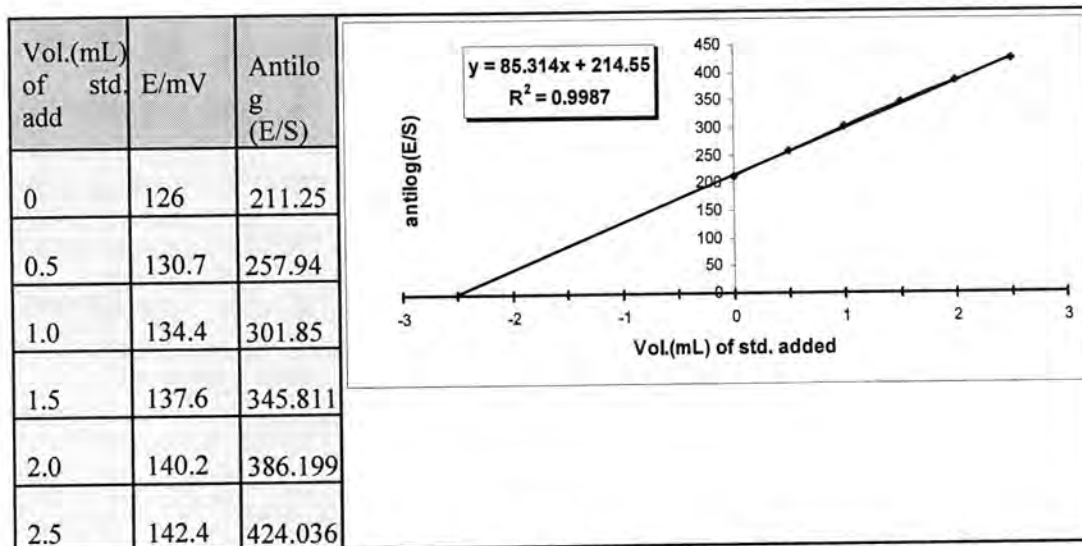


Fig.-8: Calibration curve of antilog (E/S) versus the volume added of standard (0.01 M) for determination of 25mL Amiloride hydrochloride solution 10^{-3} M by (MSA).

Titration method:

The potentiometric titration for 15 mL of 0.01M Amiloride hydrochloride sample solution with 0.01M phosphotungstic acid as titrant solution, using two methods for indication end point from potentiometric titration curves as shown in (Fig.8), the results of titration (RC%, RE% and RSD%) were listed in Table 7.

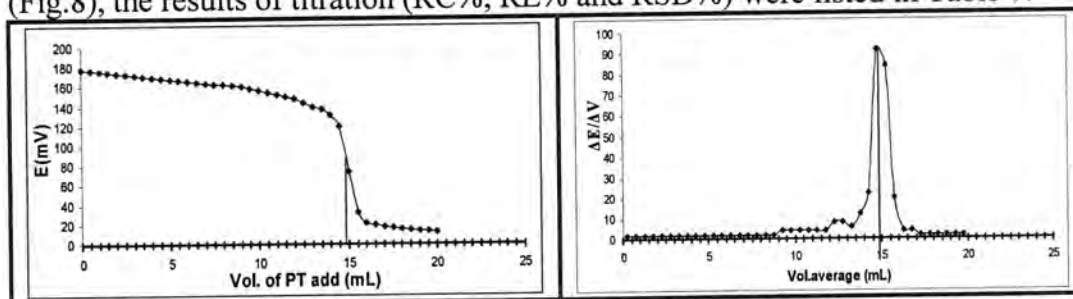


Fig.-9: Titration curve of electrode A (Amilo-PT+DBPH) for 15 mL sample solution 0.01 M Amiloride hydrochloride with 0.01 M of PT as a titrant solution.

Table -7: Determination of Amiloride in the standard sample (1.00×10^{-4} M) by potentiometric methods using Amiloride selective electrode A

Membrane.	Samples	potentiometric methods			
		Titration	Direct	SAM*	MSA*
A (Amilo-PT+DBPH)	1.00×10^{-4}	0.986×10^{-3}	0.999×10^{-3}	0.994×10^{-3}	1.006×10^{-3}
	RSD%	0.500%	0.366%	0.372%	4.280
	RE%	-1.33 %	-0.10%	-0.60%	0.60%
	%RC	98.66 %	99.900%	99.40%	100.60%

Each concentration represents an average of 3 measurements* The results of five additions

Analytical Application of the Selected Electrode:-

Accuracy of the proposed electrode was assisted by determining Amiloride's solutions using the above methods and the data obtained for pharmaceutical samples were listed in Table 8 for Maduratic and Saluretic tablets.

Table-8: Sample analyses of Maduratic and Saluretic tablets pharmaceutical Amiloride using electrode A (Amilo-PT +DBPH).

Parameter	Maduratic tablets				Saluretic tablets			
	Direct method	SAM	MSA	Titration method	Direct method	SAM	MSA	Titration method
Conc. (M)	1.000×10^{-3}	1.000×10^{-3}	1.000×10^{-3}	1.000×10^{-3}	1.000×10^{-3}	1.000×10^{-3}	1.000×10^{-3}	1.000×10^{-3}
Found(M)	0.995×10^{-3}	0.991×10^{-3}	1.008×10^{-3}	0.990×10^{-3}	0.986×10^{-3}	0.988×10^{-3}	1.01×10^{-3}	0.983×10^{-3}
RSD%*	0.474%	0.408%	-----	0.631%	0.576%	0.51%	-----	0.768%
RC%	99.5%	99.1%	100.8%	99%	98.6%	98.8%	101%	98.3%
RE %	-0.5%	-0.9%	0.8%	-1%	-1.4%	-1.2%	1%	-1.7%

*Each concentration represents an average of at least three measurements.

Sample analyses by using UV-Spectrophotometry:-

The standard methods detected in British pharmacopeia's 2000^[4] are spectrophotometric methods. UV spectrum of Amiloride hydrochloride as shown in Fig 9. and the equations and other parameters of the calibration curves are listed in table 9

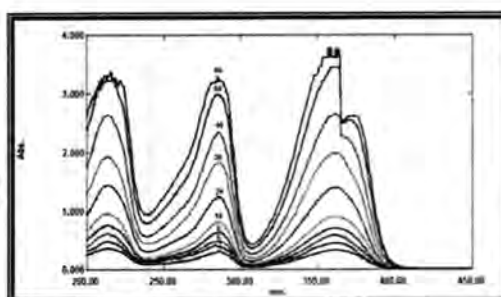


Fig.-10: UV- Spectra for Amilo. solutions at different concentration ranged from 2 to 60 mg/L.

Table -9 : The concentration range of the three wavelengths and their linear equations, correlation coefficient, standard deviation of slope and intercept respectively.

Wavelength (λ_{\max})/nm	Range of conc. mg/L	Linear equation	r^2	r	S.D of the slope	S.D of the intercept
361	2-40	$Y = 0.06208X + 0.22634$	0.99895	0.99947	2.511×10^{-4}	7.990×10^{-3}
286	2- 50	$Y = 0.05588X + 0.19580$	0.99936	0.99968	3.407×10^{-4}	4.0926×10^{-3}
213	2-40	$Y = 0.05877X + 0.25594$	0.99932	0.999664	3.214×10^{-4}	3.7004×10^{-3}

*The result of three times repeated.

The best wavelength 286 nm with high concentration range and best ($R^2 = 0.99936$) as shown in the calibration curve in Table 10 used to determine Amiloride hydrochloride sample solutions ($1 \times 10^{-4} M$ that equal to 30.2 ppm) by direct method. The analysis results of three samples are average recovery, relative error and relative standard deviation are 99.87%, -0.13% and 0.497 % respectively.

Comparison between ISE and UV-Spectrophotometric Methods:-

The comparison between ISE and UV-Spectrophotometric methods by using direct method are listed in Table 10 shows that the ISE method was better than UV- Spectrophotometric Method. The F value found equal to 1.863 that was smaller than the value in the table of F- test at 95% confidence level for (n-1) that was equal to 6.39 when n= 5 means that the newer ISE method was better than UV- spectrophotometry.

Table 10 :- The comparison between ISE and UV-Spectrophotometric Methods.

Parameters	ISE method	UV- spectrophotometric method
Linear range	$1 \times 10^{-5} - 1 \times 10^{-2}$	$6.62 \times 10^{-6} - 1.655 \times 10^{-4}$
Detection limit	6×10^{-7}	6.62×10^{-6}
RSD%*	0.366%	0.497 %
S^2	3.6469×10^{-7}	4.978×10^{-7}

*for five unknown concentrations of direct method of ISE and UV-spectro.

Conclusions:-

Amiloride-selective PVC membrane electrode (Amilo-PT +DBPH) was used for potentiometric determination. which gives excellent electrode parameters as well as good results in determination of Amiloride and no interference with several cations and (HCT drug),. The analytical method proposed proved to be simple, rapid and of good accuracy compared to the UV-spectrophotometric method by normal calibration curve.

REFERENCES

1. György, S. & Budvári-Bárány, Z., "Pharmaceutical Chemistry of Antihypertensive Agents", CRC Press, :92-98(1990).
2. Dhasmana, D., " Effect of amilorid on ouabain induced arrhythmias in vivo in guinea-pigs. Indian Journal of Pharmacology, 32:102-107 (2000).
3. Ellenhorn, M. & Barceloux, D., "Potassium-Sparing Diuretics", Medical Toxicology, New York, (1988).
4. "British pharmacopoeia on CD-ROM", version 4, Copyright by Crown Ltd., London,(2000).
5. Jose, A.; Murillo, P.; Aurelia, A. & Pablo, F., "Direct Determination of Amiloride in Urine Using Isopotential Fluorimetry" Analyst, 122:247-252(1997).
6. Murillo, P.; Alanon, M. & Fernandez, L. " Direct analysis of amiloride and triamterene mixtures by fluorescence spectrometry using partial-least squares calibration", Analytica chimica acta, 449:179 -187(2010).
7. Huclová, J.; Satínský, D.; Pavlíček, O.; Vedralová, L. and Karlíček, R., " Using on-line solid phase extraction for determination of amiloride in human urine by sequential injection technique", Analytica Chimica Acta., 573, : 376-82(2006).
8. Toral, M.; Pope, S.; Quintanilla, S. & Richter P., "Simultaneous determination of amiloride and furosemid in pharmaceutical formulation by first digital derivative spectrophotometry" International journal of pharmaceutics, 249, (2) : 117-126(2002).
9. Ortega-Barrales, P.; Pellerano, G.; Vazquez, F. & Molina-Díaz, A., "Rapid and sensitive determination of Amiloride by cation exchange pre-concentration and direct solid-phase UV detection." Analytical Letter, 35, :1491-1504(2002).
10. Schänzer, W.; Geyer, H.; Gotzmann, A. and Mareck-Engelke, U., " Recent advances in doping analysis" Sport und Buch Strauß, 8:197-202 (2000).
11. Min, S.; Taijun, H.; Hua, Z.; Li, W.; Ping, G. & Pengcheng, M., " Simultaneous determination of amiloride and hydrochlorothiazide in human plasma by liquid chromatography/tandem mass spectrometry with positive/negative ion-switching electrospray ionization", John Wiley & Sons, 21 Issue 21: 3427- 3434(2007).

12. Vincek, W.; Hessey, G.; Constanzer, M. & ayne . "Amiloride: Biological Fluid Analysis by Reverse-Phase HPLC" *Pharmaceutical Research*, 2:143-145 (1985).
13. Yip, M.; Coates, P. and Thiessen, J., " High-performance liquid chromatographic analysis of amiloride in plasma and urine," *J Chromatogr.*, 307, (2):43-50(1984)
14. El-Hefnawy, G.; El-Hallag, I.; Ghoneim, E. & Ghoneim, M., " Electrochemical behavior and determination of amiloride drug in bulk form and pharmaceutical formulation at mercury electrodes", *Journal of Pharmaceutical and Biomedical Analysis Journal of Pharmaceutical and Biomedical Analysis*, 34, Issue 5:899-907(2004)
15. Nassory, N.S., Al-Haderi A.M, A. & Israa, K., " Preparation and Examination of Amine and Amiloride-Ion Selective Electrodes with PVC Matrix Membranes " *Chem. Anal. (Warsaw)*, 52: 55-66(2007).
16. Lukasz, K., Robert, S., Agnieszka, G. & Agnieszka, O. " Simultaneous quantitation of amiloride hydrochloride and hydrochlorothiazide in tablets by UV spectrophotometry coupled with new chemometric regression techniques and artificial neural networks." *Annales Universitatis Mariae Curie - Sklodowska Ublin – Polonia*, 2: 139-144(2007).
17. Ferraro, M.; Castellano, P. & Kaufman, T., " Chemometric determination of amiloride hydrochloride, atenolol, hydrochlorothiazide and timolol maleate in synthetic mixtures and pharmaceutical formulations.", *J Pharm Biomed Anal.*, 34, (2):305-14(2004).
18. Buhlmann, P.; Pretsch, E. and Bakker, E., " Carrier-Based Ion-Selective Electrodes and Bulk Optodes. 2. Ionophores for Potentiometric and Optical Sensors", *Chem. Rev.*, 98: 1593-1687(1998).
19. Richard, P. and Erno, L., " Tracing the History of Selective Ion Sensors, " *Analytical Chemistry*, 97:88-100(2001).
20. Kharitonov S.V., "Ion-Selective in Medicing Drug Determination inter" *Russian Chemical Reviews*, 76, 361 (2007).
21. Kumar K.G., John S., Popval P. and Saraswathyamma B., "Mebendazole Selective Membrane Sensor and its Application to Pharmaceutical Analysis" *Analytical Sciences*, 23: 291-294 (2007).
22. Nassory N.S., Maki S.A. and Ali M.A., "Preparation and characterization of an Atenolol Selective Electrode Based on PVC Matrix Membrane" *Turk. J. Chem.*, 31: 75-82 (2007).
23. Al-Haideri A.M., Nassory N.S. and Al-Saadi A.S.M., Ibn Al-Haitham, "Study the Polymeric Membrane Selective Electrodes for the Determination of Ampicillin Trihydrate", *J. of Pure and Applied Sciences*, 19: 101-115 (2006).
24. Al-Saidi, Kh. H. ; Nassory, N. S. and Maki, S. A., " Preparation and study of amoxicillin selective electrodes and Their application with the derivative spectrophotometer in pharmaceutical drugs" *JNUS*, 12 (1): 29-37, (2009).

25. Nassory N.S; Maki, S.A & AL-Phalahy, B.A., "Preparation and Potentiometric Study of Promethazine Hydrochloride Selective Electrodes and Their Use in Determining Some Drugs" *Turk J Chem.*, 32:539– 548, (2008)
26. A. Craggs, G.J. Moody & J.D.R. Thomas, "PVC Matrix Membrane Ion-Selective Electrodes: Construction and Laboratory Experiments" *Chem. Educ.*, 51(8):541- 544, (1974)
27. Y. Umezawa, K. Umezawa and H. Sato, "Selectivity Coefficients for Ion-Selective Electrodes Recommended Methods for Reporting $K^{pot}_{A,B}$ values", *Pure Appl. Chem.*, 87(3): 507-518 (1995).
28. Y. Umezawa, P. Buhlmann, K. Umezawa, K. Tohda and S. Amemiya, "Potentiometric Selectivity Coefficients of Ion-Selective Electrodes", Part 1. Inorganic cations (Technical Report)" *Pure Appl. Chem.*, 72(10):1851-2082 (2000).
29. Lee Yook Heng, Loh Han Chern and Musa Ahmad, "A Hydrogen Ion-Selective Sensor Based on Non-Plasticised Methacrylic-acrylic Membranes" *Sensors*, 2 :339-346(2002).
30. Susan Sadeghi, Mohammad Taghi Vardini, Hossein Naeimi, Copper (II) Ion Selective Liquid Membrane Electrode Based on New Schiff Base Carrier, *Wiley Interscience journal*, 96 Issue 1-2: 65-74(2006).
31. Carlo Maccà and Joseph Wang, "Experimental procedures for the determination of amperometric selectivity coefficients" *Analytical Chemical Acta*, Volume 303, Issues 2-3, 10 March, : 265-274(1995).
32. Gamal, M.. "Potentiometric PVC Membrane Sensor for the Determination of Scopolamine in Some Pharmaceutical Formulations", *Analytical Sciences*, 18, (12):1335-1338(2002).
33. Gamal, M.; Mohamed, H. and Abdulrahman, A. "PVC Membrane Sensors for Potentiometric Determination of Acebutolol", *Sensors*, 7: 3272- 3286 (2007).
34. Hassan, A.; Xian, X. and Cheng, J., "Ion Selective PVC Membrane Electrode for the Determination of Methacycline Hydrochloride in Pharmaceutical Formulation", *Sensors*, 2: 424-431(2002).
35. Simultaneous Determination of Paracetamol and Cephalexin Binary mixtures by Using Derivative Spectrophotometry and H-point Standard Addition Methods

Assessment of Cancer Risk to the Human Tissues Related to Public Exposure to Cesium-137

Nabeel Hashim Ameen Al-Tameemi

Ministry of Science and Technology – Decommissioning of Destroyed Nuclear Facilities Center

الخلاصة

جرى في هذه الدراسة تقدير المخاطر الصحية الناجمة عن تعرض سكان المناطق السكنية المحيطة بموقع التوثبة للأبحاث النووية (حي الرياض وجسر ديالى) الى نويدة السيزيوم-137 عبر المسالك البيئية (الهواء والغذاء) باستخدام النموذج الاحصائي الخطي (LNT). جرى قياس تراكيز السيزيوم-137 في نماذج التربة مختبريا باستخدام منظومة تحليل اطياف جاما. وتم استخدام النماذج الرياضية ذات العلاقة في تقدير انتقال نويدة السيزيوم-137 من التربة الى الانسان عبر المسالك البيئية (انتقال نويدة السيزيوم-137 الى الخضراوات وعلف الحيوانات، استهلاك المحاصيل الزراعية والمنتجات الحيوانية الملوثة، واستنشاق دقائق السيزيوم-137 التي يعاد تعليقها من التربة). وجرى تقدير الجرعة الاشعاعية المكافئة للأشخاص المتعرضين من خلال تقدير كمية السيزيوم-137 التي سيتعرض اليها الفرد باستخدام معاملات تحويل الجرعة التي تعتمد على الوكالة الدولية للطاقة الذرية. بينت النتائج ان استهلاك المنتجات الحيوانية الملوثة هو المسلك الحرج واكثر أعضاء الجسم المتأثرة هي القولون. بينت نتائج النموذج الرياضي ان تعرض سكان منطقة الدراسة الى نويدة السيزيوم-137 ممكن ان يزيد احتمالية الاصابة بالاورام السرطانية بمعدل 2.172 لكل مليون شخص يستلمون السيزيوم-137 بمعدل 50.108 بكريل لكل سنة او ان هنالك احتمالية حصول حالة اصابة سرطانية واحدة لكل 460405 شخص يستلمون السيزيوم-137 بالمعدل المشار اليه اعلاه. كما اظهرت النتائج احتمالية حصول اضرار جينية وراثية للأشخاص المتعرضين بمعدل شخص واحد لكل 2304147 او اربعة اشخاص لكل عشرة ملايين شخص يتعرضون لنويدة السيزيوم-137، وبمقارنة مستويات الجرعة الخطورة الاشعاعية مع المعايير الدولية تبين تعرض عامة السكان للنشاط الاشعاعي لنويدة السيزيوم-137 ضمن الحدود والمعايير المسموح بها عالميا، ولاغراض الوقاية من الاشعاع، جرى في هذه الدراسة اشتقاق اعلى تراكيز مسموح بها للسيزيوم-137 في لحوم وحليب الحيوانات، بيض المائدة، لحوم الدجاج، الخضراوات والتربة الزراعية بالاعتماد على اعلى حد مسموح به لاستلام نويدة السيزيوم-137 سنويا.

ABSTRACT

Multi-step risk assessment process was used in characterization of probable health hazards caused by exposure of local inhabitants live in the urban areas that surrounds Al-Twaitha nuclear research site (Hay Al-Riyad and Jesr-Diyala sectors) to ^{137}Cs through environmental pathways (air and food) using a hypothetical linear no threshold (LNT) statistical model. The gamma-ray activity concentrations of ^{137}Cs in soil samples were measured using gamma-ray spectroscopy system. A typical model developed for radiological assessment was used to evaluate principal pathways for ^{137}Cs transfer from soil to human through environmental pathways (soil to vegetation transfer, ingestion of animal products, and inhalation of resuspended ^{137}Cs particles). The annual effective dose equivalents were determined from the annual intake of ^{137}Cs using dosimetric parameters based on International Atomic Energy Agency (IAEA) publications. The results of this study show that cesium-137 contributes about 0.622 $\mu\text{Sv/y}$ to the average annual total effective dose equivalent for the exposed population. The animal products pathway is found to be the most significant route and the most exposed organs are found to be the colon. The individual doses resulting from the consumption of animal products are one to two orders of magnitude higher than doses delivered from the consumption of vegetables. For the population as a whole, ingestion is a minor route of entry of ^{137}Cs into the body; food is generally the main source of intake. The results of this study indicate that exposure of respective population to ^{137}Cs cause considerable carcinogenic risks to a large number of people. The lifetime (70 years) fatal cancer risk to a population receives 50.108 Bq of ^{137}Cs per year is found to be about 2.172 expected fatal cancer case per million exposed individuals, or there is one additional death as a result of radiation-induced cancer incidence in a group of 460405 people if they would all receive ^{137}Cs at a rate of 50.108 Bq per year instantaneously. The probability of having a genetic damage by radiation for all generations is estimated to be about 1 per 2304147 or 4 per 10 million in parents who were irradiated before conception occurred. Direct comparison of the estimated

dose and radiation-derived risk with the guidelines indicates that people are exposed to ^{137}Cs radioactivity within acceptable dose and risk limits. The annual limit on ^{137}Cs intake established by the International Atomic Energy Agency is translated in this study into a corresponding derived maximum permissible concentration in food crops and agricultural soil through the use of environmental pathway modeling.

INTRODUCTION

Long-lived, artificial radionuclides were introduced into the environment due to human activities. The largest quantities of the radioactive elements were released as a result of test nuclear explosions, the ground and atmospheric ones in particular. The nuclear power plant breakdown in Chernobyl (Ukraine) was the latest substantial source of the radioactive contamination. Most of the radionuclides liberated into the atmosphere were later deposited on the ground surface, with ^{137}Cs being of primary importance among this group of isotopes (1). Another significant source of ^{137}Cs contamination in the surface soil of Baghdad city is the normal operation of the nuclear facilities located in Al-Twaitha site before destruction in 1991 war.

The aims of this study are:

- 1- Calculation of radiological doses and health risks to the body organs and tissues related to public exposure to ^{137}Cs through environmental transport pathways. The quantitative estimation of the radiation health risks is carried out in this study by using a hypothetical linear no threshold (LNT) statistical model. The LNT model indicates that any radiation dose, no matter how small, may result in human health effects, such as cancer and hereditary genetic damage.
- 2- Investigate the effect of the consumption of animal and agricultural products contaminated with ^{137}Cs on the increase of population intake of ^{137}Cs .

MATERIALS AND METHODS

Preparation of soil samples

Eight samples of surface soil were collected from the urban areas that surrounds Al-Twaitha nuclear research site (Hay Al-Riyad and Jesr-Diyala sectors). The soil sampling procedure involves cutting out a soil sample of about 1 kg weight at about 1 cm depth. The soil samples were collected from flat and undisturbed areas, then placed in polyethylene bags, labeled with the location code, date and time of sampling, and transferred to the analytical laboratory for analysis. At the laboratory, the soil material was crushed into small pieces, screened on a sieve of 1 mm mesh size and dried in an oven at 80°C for 4-hrs according to a procedure recommended by the International Atomic Energy Agency (IAEA). The dry mass of soil material is recorded. The soil samples were subjected later to radiometric analysis.

Quantative radiological analytical analysis of the soil samples

Radiometric analysis of the soil samples were performed in Marinelli type beakers of 1 liter volume using a gamma-ray spectrometric system (Fig.-1) composed of a pure germanium detector with 40% efficiency (Canberra, USA), coupled to an 8192 channel personal computer analyzer. Energy and efficiency

calibrations were carried out with a multi-gamma standard source (Canberra). The computer code Genie-2000 was used to determine the activity concentration of cesium-137 in the samples (3). Every sample is counted for 3600 seconds. The soil sampling process and laboratory measurements were carried out in 2008 in the laboratories of Hazardous Materials and Environmental Researches Directorate/ Ministry of Science and Technology.

Heal The Risk Assessment

Risk, may be defined as the chance of encountering the potential adverse effects of human or ecological exposures to environmental hazards. In general terms, risk is the probability of harm or loss, which may also be considered as a product of probability and the severity of consequences (4).

Risk assessment is the gathering of data that are used to relate response to dose. Such dose-response data can then be combined with estimates of likely human exposure to produce overall assessments of risk (5).

The National Academy of Sciences suggests that risk assessment be divided into the following four steps (6):

Hazard Identification

Radiation causes ionizations in the molecules of living cells. These ionizations result in the removal of electrons from the atoms, forming ions or charged atoms. The ions formed then can go on to react with other atoms in the cell, causing damage. An example of this would be if a gamma ray passes through a cell, the water molecules near the DNA might be ionized and the ions might react with the DNA causing it to break.

Human Exposure Assessment (Terrestrial Pathways)

The most important atmospheric transport mechanisms for radionuclides released to the atmosphere are illustrated in Fig.-2 (7).

Soil To Vegetation Transeer

The concentration of a radionuclide in vegetation attributable to root uptake is conventionally modeled as follows (8):

$$C_v = C_g \times B_v \quad \dots (1)$$

where:

C_g is the concentration of the radionuclide in the soil rooting zone (Bq/g).

C_v is the concentration of the radionuclide in type v vegetation (Bq/g).

B_v is the soil to plant transfer factor for the radionuclide to type v vegetation (Bq/g wet plant per Bq/g dry soil).

The concentration factors of ^{137}Cs in forage plants and vegetation are taken to be 0.042 and 0.03 (Bq/g wet plant per Bq/g dry soil) respectively (9).

Plant uptake of radionuclides from the soil is affected by numerous processes and factors. As a result, B_v may vary widely. Some of the influencing factors include: the physicochemical form of the radionuclide; type of vegetation; soil characteristics (including stable element concentrations and the presence of fertilizers, agricultural chemicals and chelating agents); and the distribution of radionuclides within the soil (8).

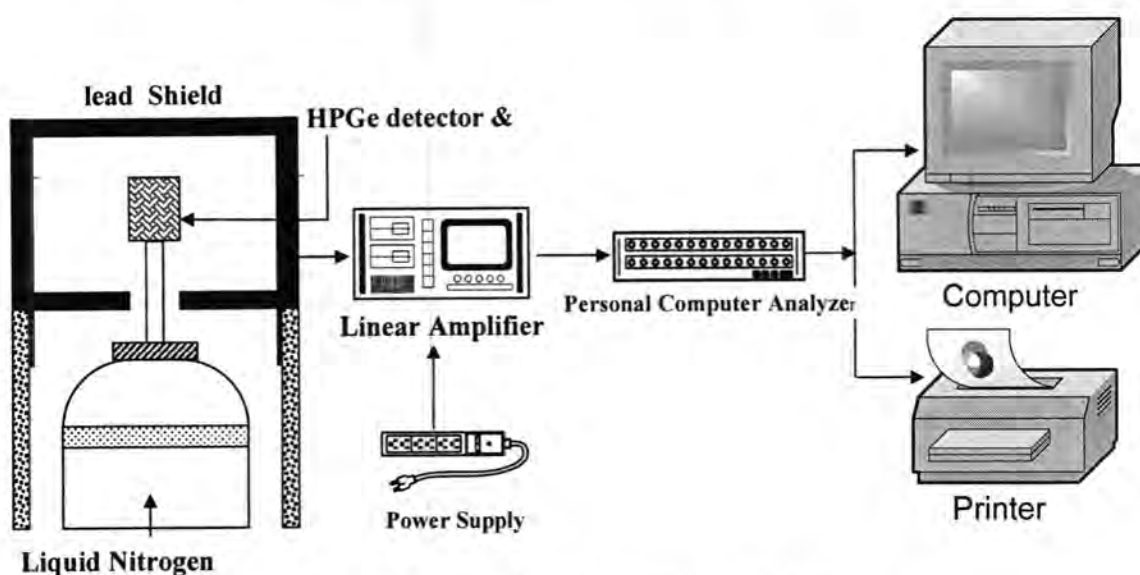


Fig.-1: Gamma Ray Spectrometry System

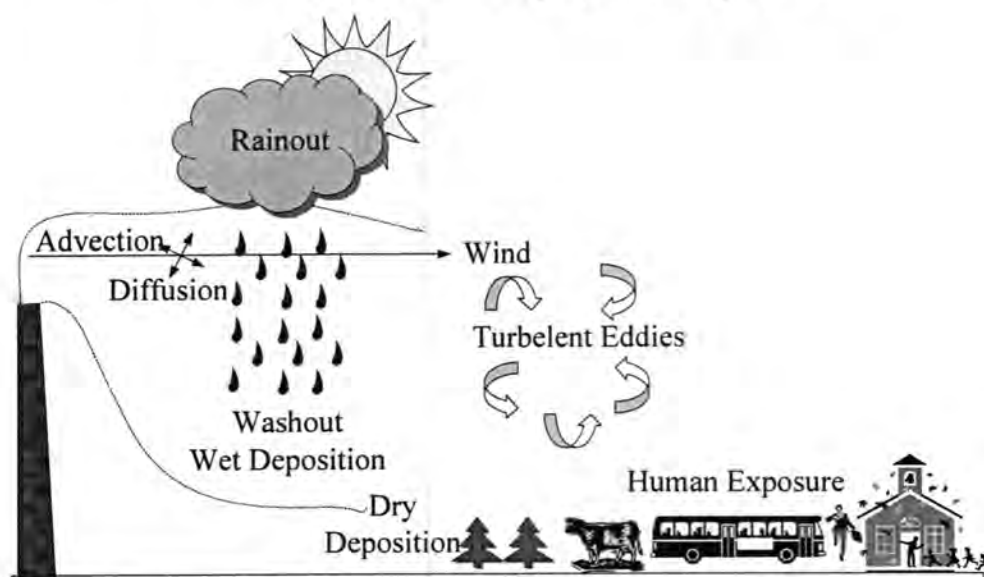


Fig.-2: The most important processes affecting the transport of radionuclides released to the atmosphere (7).

ANIMAL PRODUCTS

For equilibrium assessment models, transfer factors are most commonly used to specify the degree of transfer of a radionuclide from feed, forage and/or drinking water to animal products. The most general type of model is as follows(9):

$$C_p = f_p \sum_v (C_v Q_v + C_w Q_w) \quad \dots (2)$$

where:

C_p is the average concentration of the radionuclide in type p animal produce (Bq/kg, excepting milk, which is in Bq/L);

f_p is the transfer factor of the radionuclide from the daily intake to type p animal produce (d/kg, excepting milk, which is in d/L)(Table-1);

C_v is the concentration of the radionuclide in forages or type v feed ingested by the animal (Bq/kg);

Q_v is the average daily intake of contaminated forage or type v ingested by the animal, kg/d (Table-2);

C_w is the concentration of the radionuclide in the animal's water supply (Bq/L);

Q_w is the average daily intake of contaminated water by animal (L/d).

This model assumes that the radionuclide concentration in animal products is in equilibrium with the concentrations in the feed, forage, or water. The concentration of the radionuclide in the feed or forage must be specified in the same manner as the daily intake.

Table-1: Animal Product Transfer Factors for ^{137}Cs (10):

Animal Product / Intake	f_p	Units
Milk / Feed	0.058	d/L
Beef / Feed	0.05	d/kg
Egg/feed	0.4	d/kg
Chicken meat /Feed	10	d/kg

Table-2: Daily water and food intake by animals (8):

Animal	Daily Water Intake (L/d)	Daily Food Intake (kg/d)
Dairy cows	80	50
Beef Cattle	50	50
Chickens	0.3	0.1
Pigs	7	3
Caribou	11.5	7
Moose	36	27

RESUSPENSION

Mathematical models of resuspension have been developed based on wind erosion models and as a function of wind speed. Air concentration, C_{air} , can be approximated with the following model (11):

$$C_{\text{air}} = k(U - U_T) \frac{C_{\text{soil}}}{U} \quad \dots (3)$$

in which:

C_{air} is the air concentration, Bq/m³,

U is the wind speed in m/s,

U_T is the threshold wind speed for particle resuspension, m/s, and

C_{soil} is the surface contamination level in Bq/m².

Resuspension of material deposited on the surface of soil represents an important and often overlooked horizontal terrestrial transport mechanism. Resuspension results from wind or mechanical disturbance and is usually described in terms of the resuspension factor (RF) or resuspension rate. The

resuspension factor is defined as the ratio of the activity per unit volume in air at a reference height above the ground (usually 1 meter) (C_{air}) to the activity per unit area on the surface of the ground (C_{soil}). The air concentration of resuspended radionuclide is estimated by using equation below:

$$C_{air} = RF \times C_{soil} \quad \dots (4)$$

Thus, the RF has units of reciprocal length, and is usually expressed in units of m^{-1} . The resuspension factor is highly variable, depending on the freshness of the deposition, particle size, weather, and atmospheric variables including precipitation, humidity, wind speed, turbulence and temperature, and the ground roughness, moisture content, and other physical factors. Values ranging overall orders of magnitude from 10^{-13} to 10^{-2} have been reported in the literature, but the value of $10^{-6}/m$ appears to be suitable for general use outdoors for freshly deposited material (11). To calculate the surface contamination level in (Bq/m^2), the average radionuclide activity concentration (Bq/kg) is multiplied by the effective surface soil density that is a function of depth and soil characteristics. At the depth of (0-30) cm, soil density is equal to 400 kg/m^2 (8).

TOXICITY ASSESSMENT AND RISK CHARACTERIZATION (RISK ESTIMATES AND RADIOLOGICAL DOSE ASSESSMENT)

External exposure to large amounts of ^{137}Cs can cause burns, acute radiation sickness and even death. Exposure to ^{137}Cs can increase the risk of cancer because of exposure to high-energy gamma radiation. Internal exposure to ^{137}Cs , through ingestion or inhalation, allows the radioactive material to be distributed in the soft tissues, especially muscle tissue, exposing these tissues to the beta particles and gamma radiation and increasing cancer risk (12).

EXTERNAL EXPOSURE

Soils contaminated with radioactive material provide a potential for external exposure to nearby individuals. Estimates of soil contamination may be available from atmospheric deposition calculations or measurements of soil contamination levels.

Based on comprehensive radionuclide concentration on the ground, the effective dose from exposure to ground contaminants is given by the equation(13):

$$H = C_{ground} \times CF \quad \dots(5)$$

where:

H: effective dose from deposition for the period of concern, mSv,

C_{ground} : ground concentration of radionuclide, Bq/m^3 ,

CF : conversion factor from Table-3, effective dose per unit deposition of the radionuclide.

The following equation is used for estimating adjusted effective dose from eposition by taking into account shielding and partial occupancy (13):

$$H_{ext} = H [SF \cdot OF + (1 - OF)] \quad \dots(6)$$

where:

H_{ext} : Effective dose from deposition for the period of concern assuming shielding and partial occupancy, mSv,

SF : Shielding factor during occupancy,

OF: Occupancy fraction; fraction of time the shielding factor SF is applicable, e.g., the fraction of spent indoors; it is assumed that for the rest of the time, there is no shielding, default 0.6 (13).

INTERNAL DOSES

Calculation of internal doses due to intake by inhalation and ingestion is carried out by using equations below (14):

$$E_{ing,p} = C_{p,i} \times H_p \times DF_{ing} \quad \dots (7)$$

where $E_{ing,p}$ = the annual effective dose from consumption of nuclide i in foodstuff p (Sv/y),

$C_{p,i}$ = the concentration of radionuclide i in foodstuff p at the time of consumption (Bq/kg),

H_p = the consumption rate for foodstuff p (kg/y),

DF_{ing} = the dose coefficient for ingestion of radionuclide (Sv/Bq) (Table-3),

Irradiation from inhaled radionuclides is estimated from (14):

$$E_{inh} = C_A \times R_{inh} \times DF_{inh} \quad \dots (8)$$

where C_A = the radionuclide concentration in air (Bq/m³),

R_{inh} = the inhalation rate (m³/y),

DF_{inh} = the inhalation dose coefficient (Sv/Bq) (Table-3).

Estimation of the potential risk from low levels of ionizing radiation requires application of dose-to-risk conversion factors to an estimate of the dose. Dose and risk factors to different body organs and tissues as a result of ingestion, inhalation and external exposure to ¹³⁷Cs are listed in Table-3. Dose factors for external exposure (listed in Table-3) are for exposure to contaminated soil surface with ¹³⁷Cs to a depth of 1 cm. The relative sensitivity to harmful stochastic effects expressed as risk per Sv of the several organs and tissues that contribute to the overall health risk is shown in Table-3.

Risk assessment could be interpreted to mean simply multiplying the exposure (dose) by the potency to get individual risk, and then multiplying that by the number of people exposed to get an estimate of overall risk to some specific population (5). The linear no-threshold (LNT) dose-response equation for an individual exposed to ionizing radiation is:

$$\text{Lifetime risk for an individual} = \text{Average annual dose (mSv/y)} \times 10^{-3} \text{ (Sv/mSv)} \times \text{Lifetime (70 y)} \times \text{Risk factor (Sv}^{-1}\text{)} \quad \dots (9)$$

The annual limit on intake (ALI) for each isotope assumes exposure to no other isotope and no other pathway, as well as no external radiation exposure. Generally, a person who may be exposed to several different radioisotopes by inhalation and by ingestion and also to external radiation must meet the following criterion if he/she is to remain within the recommended dose limit (17):

$$\sum \frac{\text{Intake}_i(\text{inhaled})}{\text{ALI}_i(\text{inhalation})} + \sum \frac{\text{Intake}_i(\text{ingested})}{\text{ALI}_i(\text{ingestion})} + \sum \frac{\text{External dose}}{\text{Dose limit}} \leq 1 \quad \dots (10)$$

where the ALI for ingestion and inhalation of ¹³⁷Cs is 6*10⁶ Bq/y (19).

GENETIC INJURY OF RADIOLOGICAL EXPOSURE

The genetic injury or damage to Baghdad population from radiation exposure is estimated in this study from the total number of human-sieverts delivered to the gonads. It is thought that in the majority of cases the inherited change will have a deleterious effect on the individual. This may be premature death, inability to produce offspring, susceptibility to disease, or any number of changes of lesser or greater importance. The genetic risk coefficient for gonads is taken to be $4 \times 10^{-3} \text{ Sv}^{-1}$ for the first 2 generations (17) and 0.01 Sv^{-1} for all generations (14).

Table-3: Dose factors for public exposure to ^{137}Cs (15) and lifetime fatal probability coefficients in a population of all ages from specific fatal cancer after exposure to low doses (16):

Body Organ or Tissue	Dose Factors			Risk Factor (10^{-4} Sv^{-1})
	Ingestion (nSv.Bq^{-1})	Inhalation (nSv.Bq^{-1})	External Exposure ($\text{Sv per Bq s m}^{-3}$)	
Bone surfaces	12	7.9	$3.74\text{e-}21$	5
Breast	12	7.8	$1.52\text{e-}21$	20
Colon	14	9	-	85
Gonads	13.5	8.3	$1.43\text{e-}21$	-
Liver	14	8.6	-	15
Lungs	13	8.7	$1.18\text{e-}21$	85
Red bone marrow	13	8.2	$1.04\text{e-}21$	50
Thyroid	13	8	$1.18\text{e-}21$	8
Effective	13	8.5	$1.34\text{e-}21$	500
Remainder	-	-	$1.12\text{e-}21$	50
Skin	-	-	$9.03\text{e-}20$	2

RESULTS AND DISCUSSION

Multi-step risk assessment process is used in this study to analyze the environmental impact of ^{137}Cs particles released from nuclear facilities and to estimate the health risks to the local inhabitants living in the area of the study (Hay Al-Riyad and Jesr-Diyala sectors) associated with radiological exposure to ^{137}Cs . The first step is estimation of the internal exposure by evaluation of the annual intake of ^{137}Cs by a critical group of local inhabitants living in the area of the study. The second step is the estimation of the individual doses using the dose factors for particular organs and tissues. The key objective of such an analysis is the estimation of doses to individual members of the public from releases of radioactivity to the atmosphere in both the near and long term. The type of analysis used in this study relies heavily on predicted values produced by mathematical models. These models have been formulated to calculate the environmental transport of radionuclides, the exposure, and dose received by critical population. The last step is estimation of the risk of developing a fatal

cancer to various body organs and tissues as a result of radiation exposure by application of dose-to-risk conversion factors available in the literature data. Risk/dose is correlated in this study using the linear, no-threshold (LNT) dose-response model (Eq.-9).

The analytical laboratory in the Iraqi Ministry of Science and Technology/Hazmat and Environmental Researches Directorate reports a mean ^{137}Cs concentration of 1.933 ± 0.665 Bq/kg in the surface soil of the area of the study, which is less than the derived concentration guidance level (DCGL) proposed by the US Nuclear Regulatory Commission (NRC) of 407 Bq/kg, and less than the exemption, exclusion and clearance level established by the International Atomic Energy Agency (IAEA) of 100 Bq/kg (19). Radioactivity of ^{137}Cs was measured in eight different locations in the area of the study. The observed concentrations range from 1.39 to 2.99 Bq/kg. ^{137}Cs variability in the radiological measurements is due to random distribution and uncertainties in the measurement process since the extreme values of the records are found to be less than 3 standard deviations of the mean observed value. Therefore, there are no unusual or suspicious data. The total ^{137}Cs intake rate is estimated by using appropriate values for the parameters in equations (1), (2) and (4).

The first step in calculating internal exposure is to evaluate the annual intake through food chain pathways of ^{137}Cs by a critical group of local inhabitants living in the area of the study. Taking into account the annual consumption of the various foods under consideration [18]. Terrestrial food-chain mathematical models (Eqs.(1) and (2)) are used to forecast ^{137}Cs concentrations in the animal products and agricultural crops that are eaten by human or that serve as food for stock animals. The receptors annual ^{137}Cs intake through food chain pathway are given by the product of the respective concentrations of ^{137}Cs in the agricultural crops and animal products by the receptors annual intake of these foodstuffs. The mean ^{137}Cs content of locally produced foods has been evaluated using equations (1) and (2). A quantitative description of the routes by which human exposure to ^{137}Cs occurs is shown in Table-4. In the case of air, the receptors annual intake of ^{137}Cs is given by the product of the respective concentrations of ^{137}Cs and the receptors assumed annual local intake of air. In the case of vegetables and animal products, the calculations involve one extra step, namely the transfer of ^{137}Cs from the soil to these foodstuffs. ^{137}Cs activity concentration in vegetation can be used to predict ^{137}Cs intake from vegetables consumed by people and from pasture vegetation consumed by animals. The low ^{137}Cs content of surface soil is reflected in corresponding low ^{137}Cs concentrations in the foodstuffs.

The percentage contribution to the total ^{137}Cs intake is illustrated in Fig.-3. The main radiation-derived health hazard is due to ingestion of contaminated foodstuffs. The major ^{137}Cs transfer route to human is via the soil-grass-cow-milk-human chain (cow's milk is the largest contributor of ^{137}Cs to the Baghdad's population adult diet). A smallest contribution to dose (0.02%) arises from ingestion of contaminated egg contents. Food-chain contamination is likely to occur for relatively long-lived isotopes like ^{137}Cs because radioactive decay of

this radioisotope would not reduce the opportunity for the isotope to pass from the soil into the plants.

Table-4: The annual estimated intake rates of ^{137}Cs by adults in Baghdad:

Pathway	<u>Intake per person</u>	^{137}Cs Content (Bq/kg)	^{137}Cs intake per year (Bq/y)
Meat	13 kg/y	0.202923	2.638
Milk	150 kg/y	0.235433	35.315
Vegetable	90 kg/y	0.057989	5.219
Egg	3.2 kg/y	0.003125	0.010
Chickens meat	5.3 kg/y	0.081094	0.4298
Air	8400 m ³ /y	0.000773 Bq/m ³	6.494
Total			50.108

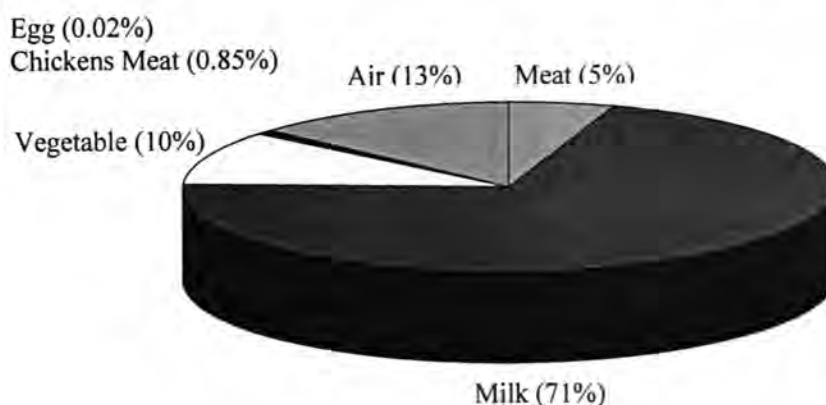


Fig.-3: The percentage contribution to the total ^{137}Cs intake

The estimated total annual ^{137}Cs intake per year (50.108 Bq/y) is found to be less than the annual limit on intake (ALI), 6×10^6 Bq/y established by the International Atomic Energy Agency (IAEA) (19). The combined exposure criterion is estimated using Eq.-10 to be 8.35×10^{-6} , less than one. This result suggests that the respective individuals are exposed to ^{137}Cs within the recommended dose limit. However, there is some possible adverse health effects related to population exposure to ^{137}Cs . The resulting contribution from ^{137}Cs intake to the annual effective dose is found to be $0.62 \mu\text{Sv/y}$, less than the recommended dose limit for the public (1 mSv/y). The whole-body ^{137}Cs dose of $0.62 \mu\text{Sv/y}$ is a small fraction of the U.S. Environmental Protection Agency (EPA) radiation dose standard to a member of the public of $100 \mu\text{Sv/y}$ from an atmospheric release (21). The effective dose equivalent from ingestion of food is calculated by summing the contributions from leafy vegetables, milk, meat and other animal products (such as eggs) to the diet. Eq.-9 is used to estimate the lifetime probability of dying as a result of lethal cancer (mortality) to the respective individuals induced by human intake of ^{137}Cs . Based upon the

metabolic and dosimetric models for ^{137}Cs recommended by the IAEA, it is possible to estimate the committed dose equivalents to the sensitive cells of the lower large intestine (the tissue most at risk in the gut (8)), the cells near bone surfaces, the bone marrow, and other soft tissues following ingestion of ^{137}Cs by adults, by multiplying these doses by risk coefficients for radiation induced fatal cancers for the different tissues (9). The likelihood or probability of developing extra cancer cases to the respective population as a consequence of ^{137}Cs exposure is evaluated in Table-5 using a linear, no-threshold (LNT) dose-response model (Eq.-9) and the risk factors listed in Table-3. The LNT dose-response model predicts the frequency with which radiation-derived health effects might occur. Public exposure to ^{137}Cs is due primarily to internal irradiation, and the external irradiation is not thought to be significant. The risk assessment data listed in Table-5 indicate that deposited ^{137}Cs particles provide a potential for external and internal exposure to nearby individuals and results in detrimental adverse health effects including increased incidence of fatal cancers. The linear, no-threshold (LNT) model postulates about 2.172 extra cancer cases among a population of 1 million people who received a whole body dose-equivalent of $0.62 \mu\text{Sv/y}$ from ^{137}Cs exposure. The cancer incidence rate to population owing to ^{137}Cs exposure is evaluated at 0.031 extra cancer case/million people/year. The risk of developing bone cancer is calculated to be about 4.7 in a group of 100 million exposed individuals. Radiation-induced cancer is predicted most frequently in the colon. The risk of leukemia as a result of irradiation of the bone marrow is calculated to be about 21.7 in a group of 100 million exposed individuals. The results of quantitative health risk assessment are written in Table-5 in statistical terms (risk = number of injuries or deaths per number of people exposed to hazard) in order to account for differences in sensitivity between the most sensitive individuals in the exposed human population such as pregnant women, babies, the elderly and normal (healthy) people and due to biological variability accounts for a difference in sensitivity among individuals and a wide variation in susceptibility to radiation damage exists among different types of cells and tissues.

If the entire breeding respective population received a radiation dose of $0.64 \mu\text{Sv.y}^{-1}$ to gonads from intake of ^{137}Cs , then the probability of having a genetic damage as a consequence of gonads irradiation for all generations is estimated to be about 1 per 2304147. In other words, a gonad dose of $0.64 \mu\text{Sv.y}^{-1}$ to each parent who was irradiated before conception occurred will lead to 4 additional genetic disorders cases per 10 million live births for all generations. The gonad dose of $0.64 \mu\text{Sv.y}^{-1}$ is found to be less than the population dose limit for genetic effects of 1.7 mSv/y proposed by the National Council on Radiation Protection and Measurements (NCRP) (19) and less than the dose limits for gonads of 5 mSv/y recommended by the International Commission on Radiological Protection (ICRP) (17). At present, there is no evidence of any connection between the cancer incidence and genetic damage occurs actually in the general population of Baghdad city and ^{137}Cs contamination. The health risks from

exposure to low-level ionizing radiation can be observed by studying large population groups such as Baghdad community. However, any somatic or genetic effects that may be ensue from ^{137}Cs radiation dose rate of $0.62 \mu\text{Sv/y}$ would be masked by other factors.

A maximum permissible concentrations (MPC) have been derived for ^{137}Cs in foodstuffs and agricultural soils (Table-6) based on the annual limit on ^{137}Cs intake ($6 \times 10^6 \text{ Bq/y}$) (19). These limits have been derived in order to control environmental health hazards associated with public exposure to ^{137}Cs . It should be emphasized here that the recommended maximum permissible environmental concentrations listed in Table-6 are upper limits only, and that, in all instances, planning for radiation protection should be based on radiation doses that are as low as reasonably achievable.

Table-5: Tissue dose and associated possible radiogenic cancer risk as a consequence of public exposure to ^{137}Cs :

Tissue	Radiological Dose ($\mu\text{Sv/y}$)	Radiation- derived risk
Bone surfaces	0.574813	0.047 per million
Breast	0.574813	0.08 per million
Colon	0.671463	0.399 per million
Gonads	0.640942	-
Liver	0.666376	0.069 per million
Lungs	0.625682	0.371 per million
Red bone marrow	0.620595	0.217 per million
Thyroid	0.620595	0.0345 per million
Effective	0.620595	2.172 per million
Remainder	0.569726	0.199 per million
Skin	4.578158	0.064 per million

Table-6: Derived (or proposed) maximum permissible concentrations (MPC) for ^{137}Cs in different foodstuffs and agricultural soil:

Foodstuff	MPC
Meat	23076 Bq/kg
Milk	28400 Bq/L
Egg	375 Bq/kg
Vegetable	6666 Bq/kg
Chickens meat	466 Bq/kg
Agricultural soil	222222 Bq/kg

We can conclude:

- (1) Analysis of the results shows that the individual doses from internal exposure are higher than those due to external exposure.
- (2) The animal products pathway (milk) is the greatest exposure pathway to ^{137}Cs and the most exposed organ is the skin.

(3) The individual doses resulting from the consumption of animal products are seven to eight orders of magnitude higher than doses delivered from the consumption of plants (vegetables).

(4) For the population as a whole, ingestion is a major route of entry of ^{137}Cs into the body; food is generally the main source of intake. Inhalation is a minor source of entry.

(5) The results of this study indicate that exposure of Hay Al-Riyad and Jesr-Diyala population to ^{137}Cs causes possible long term adverse health effects including increased incidence of fatal cancer and genetic damages to a large number of people. The results show that one extra fatal cancer case is expected for every 460405 persons living near Al-Twaitha nuclear research site related to lifetime (70 year) radiological exposure to ^{137}Cs , or there is 2.172 extra fatal cancer case (additional death as a result of cancer incidence) in a group of million people if they would all exposed externally to ^{137}Cs at 1.933 Bq/kg and receive ^{137}Cs internally at a rate of 50.108 Bq per year instantaneously. The chronic excess cancer risk estimates attributed to internal and external exposure to ^{137}Cs do not exceed the EPA's 1×10^{-5} level of concern (22) for all receptors evaluated.

(6) Radiation-induced cancer from ^{137}Cs exposure is predicted most frequently in the colon.

RECOMMENDATIONS

(1) Further radiological investigations (soil sampling and laboratory measurements) are recommended to assess environmental radioactivity of ^{137}Cs and associated radiation-derived hazards especially in undiscovered residential areas.

(2) The radioactivity of soil, local and imported foods need to be monitored in Iraq to prevent artificial radionuclides from becoming a major source of radiation hazard.

REFERENCES

1. Chibowski, S., Zygmunt, J., Klimowicz, Z., "Investigation of Adsorption and Vertical Migration of ^{137}Cs in Three Kinds of Soil at Lublin Vicinity", Journal of Radio analytical and Nuclear Chemistry, Elsevier Science B.V., Amsterdam, 242(2):287-295(1999).
2. IAEA, "Measurement of Radioactivity in Environmental Samples and Foods", Technical Reports Series-364 (1989)
3. Marouf, B., "Environmental Impact of Depleted Uranium (DU) contamination in Iraq", Conference on the effects of the use of Depleted Uranium Weaponry on Human and Environment in Iraq, Baghdad (2000).
4. Watts, Richard J., "Hazardous Wastes, Sources, Pathways, Receptors", John Wiley and Sons, Inc.:521-530(1998).
5. Masters, Gilbert M, "Introduction to Environmental Engineering and Science", Prentice-Hall, Inc.:191-215 (1991).
6. National Academy of Sciences, "Risk Assessment in the Federal Government: Managing the Process", National Academy Press, Washington, DC (1983).

7. IAEA, "Generic Models for Use in Assessing the Impact of Discharges of Radioactive Substances to the Environment" Safety Reports Series-14, (2001).
8. IAEA, "The Environmental Behavior of Radium" Technical Reports Series.2, (310) IAEA, Vienna: 345-355(1990).
9. IAEA, "Generic Models and Parameters for Assessing the Environmental Transfer Radionuclides from Routine Releases" Safety Series (1982).
10. IAEA, "Handbook of Parameter Values for the Prediction of Radionuclide Transfer in Temperate Environment" Technical Reports Series(364):35-37 (1994).
11. Kathren, Ronald, L., "Radioactivity in the Environment" 1st Edition, Hawood Academic Publishers: 240 (1984).
12. CDC, "Radioisotope Brief: Cesium-137 (Cs-137)" Centers for Disease Control and Prevention, Emergency Preparedness and Response (2003).
13. IAEA, "Generic Procedures for Assessment and Response During a Radiological Emergency", IAEA TECDOC-1162 (2000).
14. IAEA, "Radiation and Society: Comprehending Radiation Risk", Proceeding Series, Vol.1, Prepared by the Swedish Risk Academy, International Atomic Energy Agency, Vienna (1994).
15. UNSCEAR, "Sources and Effects of Ionizing Radiation", Report to the general Assembly, UN, New York (1993).
16. Rutherford, "Radiation Risk" A critical Look at Real and Perceived Risks from Radiation Exposure (2002).
17. Cember, H, "Introduction to Health Physics", Pergamon Press (1987).
18. FAO, (Food Agricultural Organization), Review of Food Consumption Surveys , 2, Africa, Latin America, Near East:181-183 (1979).
19. IAEA, "Application of the Concepts of Exclusion, Exemption and Clearance" International Atomic Energy Agency (IAEA) Safety Standards Series RS-G-1.7 (2004).
20. Eisenbud, M. "Environmental Radioactivity" 4th Edition, Academic Press (1997).
21. Peterson, S. "Appendix A. Methods of Dose Calculations", Lawrence Livermore National Laboratory (LLNL) Environmental Report (1999).
22. EPA, "Combustion Human Health Risk Assessment for Angus Chemical Company" Sterington, Louisiana, U.S. Environmental Protection agency, Center for Combustion Science and engineering, Dallas, Texas, Region 6:10 (2000).

Study Of Protein Profile In Patients With Bladder Cancer

Israa G.Zainal and Shaema S.AL-Janabi

AL-Mustansiriya University , College Of Science , Chemistry Department

الخلاصة

تم تحديد مستوى البروتين الكلي وصورة البروتين في مجموعتين من المرضى : (35 مريض بسرطان المثانة و 25 مريض بحصى المثانة كمجموعة سيطرة) و 25 من الأصحاء. لوحظ وجود نقصان واضح في مستوى البروتين الكلي في مرضى سرطان المثانة مقارنة بمجاميع السيطرة و الأصحاء. وكذلك وجود نقصان واضح في الالبومين و الجزء بيتا في مرضى سرطان المثانة مقارنة بالأصحاء وعدم وجود اختلاف في الجزء ألفا - 1 لمرضى سرطان المثانة ومجموعة السيطرة مقارنة بالأصحاء وزيادة واضحة بالجزء ألفا-2 وكما بمجموعة السيطرة مقارنة بالأصحاء .

ABSTRACT

Plasma levels of total protein and protein profile were estimated in three groups of patients with bladder cancer : 35 patients suffer from bladder cancer , 25 patients suffer from bladder stones disease as pathological controls and 25 normal subjects. There were significant decrease in total protein content of patients with bladder cancer as compared to pathological controls and normal subjects , and there were significant decreases in albumin and β – fractions in bladder cancer patients as compared to normal subjects , while significant increases in albumin and decreases in β – fractions in pathological control as compared to normal subjects , non significant difference in α_1 - fraction in patients with bladder cancer and pathological controls as compared to normal subjects , but there were significant increases in α_2 - fractions and γ – fractions in pathological controls as compared to normal subjects .

INTRODUCTION

Bladder cancer is the most common malignant tumor of the urinary system (1,2). It affects twice as many men as women , it is rare in people under 55 years of age and most common among those over 70 years (3). Bladder cancer is the fourth most common form of malignant disease worldwide, accounting for 4% of all cancer cases(4).

Proteins are substances made up of two smaller building blocks called amino acids(3).The major site of synthesis of the plasma proteins is the liver(5). Total protein level depends on the balance between their synthesis and their catabolism or loss from body (6). Total protein is significantly decreased in patients with bladder cancer (7). A total plasma protein test measures total amount of protein in blood plasma as well as the amounts of albumin, globulin and fibrinogen (8). Under the influence of an electrical field , charged molecules and particles migrate in the direction of the electrode bearing the apposite charge . Because of their varying charges and masses , different molecules and particles of a mixture will migrate at different speeds and will thus be separated into single fractions (9,10). Therefore, the electrophoresis is especially useful as an analytical method (11). The measurement of serum/plasma protein concentration is one of the most frequent routine analyses performed to investigate hydroelectrolytic

disorders, inflammatory or infectious diseases, colostrums intake, tumors, etc. Its determination is also prerequisite of protein electrophoresis (12).

The purpose of this article is to determine the total protein TP in plasma of bladder cancer Patients, pathological controls and normal subjects , evaluate the technique of quantitative and to investigate the effect of cancer on the plasma electrophoretic patterns in order to define average ranges . The advantage of reporting the qualitative appearances of the electrophoretogram with the concentrations of the electrophoretic bands , is indicated.

MATERIALS AND METHODS

All common laboratory chemicals and reagents were of analar grade , Twenty five samples of blood (15) male, (10) female were taken from physically normal volunteers used as controls age between (45-71) years. Thirty five samples of blood were taken from patients with bladder cancer aged (48-75) years. After being classified by senior surgery (patient suffering from any disease, that may interfere with our study were excluded). Blood was also collected from twenty five pathological controls (patients with bladder stones), aged (48-73) years..

All patients were admitted for treatment to specialized surgical hospital. Five milliliters (mL) of venous blood sample were taken by using plastic disposable syringes, and were added to EDTA tubes. Plasma was separated from blood by centrifugation at (1000Xg) for 15 mints. Plasma samples were aspirated and stored in capped sterilized tubes at -20oC until time of analysis. The method of Hartree (12) was used to determine plasma total protein, using (BSA) as standard. Protein concentration were expressed in g/dL of plasma. Figure (1) shows the standard curve of protein, which was constructed by plotting the absorbance at 650 nm against standard protein concentration.

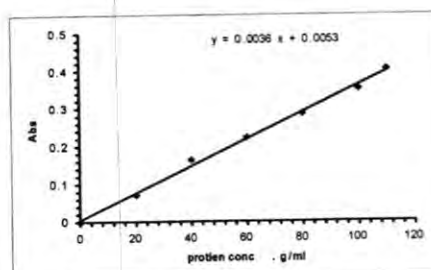


Fig.-1:Standard curve for the determination of plasma protein concentration.

The plasma proteins were determined by electrophoresis technique in patients of bladder cancer, pathological controls (bladder stones) and normal subjects by Sherwin and Kohn methods. (14,15) , and performed using cellulose stripe and barbital buffer with a pH of (8.6) and ionic strength (0.075). The buffer was prepared by dissolving (41.2)gm of sodium barbiton and (7.36)gm of diethyl barbituric acid in distilled water .Dye solution

(ponceau S) was made by dissolving (0.2)gm of (P) powder in (100)mL distilled water (solution A) and dissolving (3)gm of trichloro acetic acid in (100)mL distilled water (solution B) , and solutions A and B were mixed together . The washing solution (5%) was done by diluting (5 mL) of glacial acetic acid to (100 mL) in distilled water. The electrophoresis tank was filled with the buffer to the appropriate mark , the samples were placed in the cellulose acetate of the sheet .The sheet was placed in the tank , whereas the two end of the sheet floated in the buffer . Electrophoresis was done under constant current (150 mA) for (30 min) . The sheet was removed and treated with a staining reagent for at least (15 mins) .Then the sheet was passed through a washing solution and then allowed to dry. Finally the sheet was cut to five fractions and the dye was dissolved in appropriate solution (buffer) . The color was measured at (520 nm) .

Statistical analysis :

Descriptive statistics were used in analyzing the patients characteristics and laboratory parameters for each groups. In addition , unpaired student t – test was used to assess group differences , where appropriate .A statistical significant difference was accepted as p value less than 0.05 . All the statistical analysis in this study were made using SPSS 10.0 for windows program.

RESULTS AND DISCUSSION

The total protein TP levels expressed as (mean±SD) g/dl in plasma of patients with bladder cancer, pathological control (bladder stones) and normal subjects are shown in table (1) :

Table-1: Total protein level in plasma of patients with bladder cancer, pathological control and normal subjects.

Groups	g/dl (mean±SD)
Bladder cancer	6.93 ± 0.45
Pathological control	7.43 ± 0.54
Normal control	7.58 ± 0.41

The (mean ± SD) level of TP among normal groups was (7.58 ± 0.41) g/L , while the (mean ± SD) of TP concentration in plasma of patients with bladder cancer and pathological control were (6.93 ± 0.45), (7.43 ± 0.54)g / L, respectively. The results showed that their were significantly decrease (P<0.05) in TP conc. in patients with bladder cancer and pathological control (bladder stone) as compared to the normal subjects and so significantly decrease (P<0.05) for patients with bladder cancer as compared to the pathological control.

Additional useful information was gained from the qualitative appearance of the electrophoretogram , with the results being expressed as values

indicating concentrations of each fraction, table (2) show the results of (albumin, α_1 , α_2 , β and γ globulin) of (mean \pm SD) in the plasma of bladder cancer patients, pathological control and normal subjects. The results indicated the presence of significant decrease ($P < 0.05$) in albumin in bladder cancer patients and increase in albumin in pathological control as compared to normal subjects, While (α_1 -globulin) values showed non significant difference ($p > 0.05$) in bladder cancer patients and pathological control as compared to normal subjects.

There were a significant increase ($P < 0.05$) in α_2 level in pathological control as compared to normal subjects and no significant difference in bladder cancer patients as compared to normal subjects, the presence of significant decrease ($P < 0.05$) in β -level in both bladder cancer patients & pathological control as compared to normal subjects also there were a significant increase ($P < 0.05$) for γ -level in both bladder cancer patients and pathological control as compared to normal subjects.

Table -2: Plasma protein distribution in bladder cancer patients pathological control and normal subjects.

Groups	Albumin g%	α_1 g%	α_2 g%	β g%	γ g%
Bladder cancer	3.707 \pm 0.686	0.163 \pm 0.0144	1.377 \pm 0.274	0.81 \pm 0.0042	1.72 \pm 0.530
Pathologic al control	3.837 \pm 1.199	0.053 \pm 0.0018	0.9130 \pm 0.2990	0.693 \pm 0.020	1.51 \pm 0.248
Normal subjects	3.753 \pm 0.0421	0.11 \pm 0.0098	0.707 \pm 0.0065	0.877 \pm 0.0817	1.497 \pm 0.394

figure (2) shows the band of serum proteins of in plasma of patients with bladder cancer, pathological controls and normal subjects:

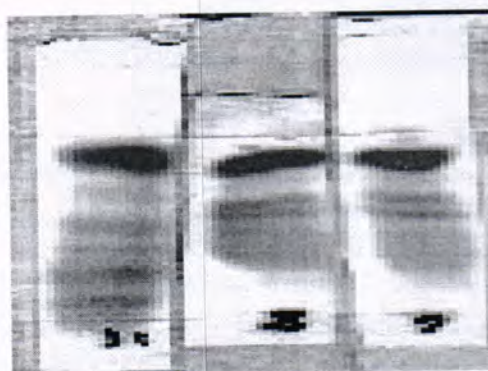
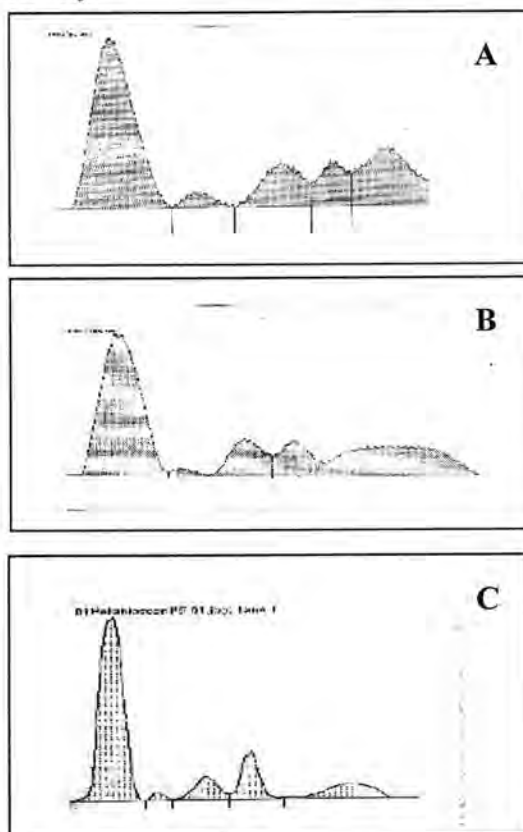


Figure-2: Plasma electrophoresis pattern of bladder cancer patients, pathological control and normal subjects. (Left):
1-bladder cancer 2- pathological control 3-normal subjects.

Figure -3:(A, B, C) shows proteins profile electrophoretically analyzed using cellulose acetate paper for bladder cancer patients, pathological control and normal subjects, respectively.



Figure(3)(A, B, C):- electrophoretic patterns for plasma proteins in patients with bladder cancer, pathological control and normal subjects, respectively. To our knowledge , few studies have been carried out to investigate total protein and the protein profile in cancer patients , the results of this study show that considerable variation in the concentration of TP and the five electrophoretic protein bands occurred in bladder cancer patients , pathological controls as compared to normal subjects.

The possible cause of decreased plasma total protein secondarily decreased synthesis of protein by the liver(16) or Perhaps because a development attributed to poor nutrition and restricted calorie diet(17).

The results of protein electrophoresis indicated the presence of significant decrease in albumin in bladder cancer patients and significant increase in pathological controls as compared to normal subjects , this agrees with the study of (Zainal 2001)(18) who found that the level of albumin decreased in patients with oral cancer , while α_1 - globulin values showed non significant difference in bladder cancer patients , pathological controls as compared to normal subjects and α_2 - globulin level showed a non

significant difference in bladder cancer patients and a significant increase in pathological controls as compared to normal subjects respectively, this disagrees with (AL – Zaid 'S MK 1981)⁽¹⁹⁾ in intestinal lymphoma disease. A significant decrease in β - level in both bladder cancer patients & pathological controls as compared to normal subjects, this agrees with (AL – Jassem 1990)⁽²⁰⁾, finally there were a significant increase in γ - level in both bladder cancer patients & pathological controls as compared to normal subjects, this agrees with the study of (Zainal 2001)⁽¹⁷⁾, (AL – Jassem 1990)⁽¹⁹⁾ and study of (AL – Zuhry SA 2005)⁽²¹⁾.

In protein electrophoresis each protein band, composed of several different proteins, respond to different physiological and pathological stimuli⁽²²⁾, perusal of the original electrophoretic strip by a person well versed in the variations of individual proteins in health and disease, has been recommended, therefore, the original electrophoretic strip should be perused by an examiner well – versed in the changes. The appearance of the electrophoretogram should be reported, depending on the qualitative electrophoretic appearances and the clinical findings. To assess the degree of abnormality, or to study minor changes, quantitative data are necessary and these may be obtained by quantitative immuno – electrophoresis.

REFERENCES

1. Jankovic'S.&Radosavljevic "S.Risk factors for bladder cancer", Tumori, 39: 4-12 (2007).
2. H.Katherine,K.Alex,C.Carole&B.Domininc.Metastatic Bladder Cancer Presenting as Duodenal Obstruction. Ann Acad Med Singapore, 38:914-5 (2009).
3. Greer P. serum protein electrophoresis.[http:// Webmd.Com/hw/health-myguide/atoz/hw43650.asp](http://Webmd.Com/hw/health-myguide/atoz/hw43650.asp).
3. Kaneko J.J.,Harvey J.W., & Bruss M.C. "Clinical Biochemistry of Domestic Animals " 5th ed. : 120 – 226 . Academic Press(1997)..
4. F.Y.Chit,N.K.Beng,R.G.Sirajudeen,C.W.William,T.H.Puay,L.K.Weber& O. Malini. Fluorescence detection of bladder cancer using urine cytology. INTERNATIONAL JOURNAL OF ONCOLOGY 31: 525-530(1976).
5. WWW.better health.vic.gov.au.
6. Michael L.,Janet L.,&Edward P."Clinical Chemistry"4th ed.P.172.Lippincott Williams and Wilking : 39:4-12(2002).
7. Yilmaz,I.A.,et al.: Relation between bladder cancer and protein oxidation. Urol. Nephrol . 35(3):345-350(2003).
8. Hermann E.,Schultze JF.&Hermann. Molecular biology of human proteins . P.3 .Publish Elsevier(1966). .
9. Drkaslow:Protein-albumin/globulin.<http://WWW.drkaslow.com/html/prot-eins-albumin-globulin.html>,(2004).

10. Westermeier R., Fichmann J. , and Granav S. "Electrophoresis in practice" .2^{ed} ed. ,P(1).VCH, a Wiley Company(1997).
11. Bishop, M.L., Pody,E.P., & Schoff, L. "Clinical chemistry: principles , procedures and correlations" . 5th ed.:105-106. Lippincott Williams and Wilkins(2005).
12. KANEKO J.J.: Serum proteins and dysproteinemia. In :Clinical biochemistry of domestic animals. 5th ed.(Kaneko J.J.Harvey J.W., Bruss M.L., Edrs)Academic Press,San Diego:117-138.(1997).
13. Hartree, E.E. Determination of protein; A modification of the Lowry method that gives a linear photometric response. Anal.Biochem. 48: 422-427 (1972).
- 14.Kohn,J.:Chromatographic and Electrophoretic Techniques,2:104, Heinemann Medical Books Ltd.London(1968).
- 15.Sherwin,R.M.,Moore , G.H: Microzone Electrophoresis of unconcentrated C.S.F. using cellulose acetate strips. Amer.J.Clin.Path.55:705-712.(1971).
- 16.Elizabeth,M.B.,Boonson C.,&Dorothy A.H. Total protein in α - thalassemia major. Arch.Dis.Child.,56(6): 476 – 477(1981).
- 17.Niani A.B.,Dickerson J.W. and Brown M.M. Preoperative And postoperative levels of plasma protein and amino acid esophageal and lung cancer patients .Cancer .62(2) :355 – 360(1981).
- 18.Zainal I.G. Biochemical studies on sialic acid derivatives in patients with oral cancer.Ph.D.Thesis.College of science,Baghdad University(2001).
- 19.AL-Zaidi M.K.Alkaline phosphatase in patients with intestinal Lymphoma. MS.C. Thesis.College of science , Baghdad University(1981).
- 20.AL-Jassem A.K. Major biochemical changes in patients with H.D.S., MS.C. Thesis.College of Medicine, Baghdad University(1990).
- 21.AL-Zuhry S.A.A."A Study of some clinical parameters in patients with-thalassemia MS.C.Thesis.College of science AL-Mustansiriya University (2005).
- 22.SHULMAN G. The value of quantitative protein electrophoresis. S.Afr. Med. J.50: 2059- 2063(1976).

Synthesis and Spectroscopic Studies of New Heterocyclic Azo Dye and Their Complexes with Selected Metal Ion

¹Amer. J. Jarad, ²Khalida. F. Suhail And ³Ahmed. L. Hussien

¹Department of Chemistry, Ibn Al-Haitham Education College, University of Baghdad

²Applied Chemistry Division, Department of Applied Science, University of Technology

³Ministry of Education

الخلاصة

حضر الليكاند 5-(4-amoina antipyrène)-8-hydroxyquinoline من تفاعل ازدواج 4-amoina antipyrène مع 8-hydroxyquinoline تمت مفاعلة الليكاند مع أيونات بعض العناصر الفلزية (Mn^{II} , Co^{II} , Ni^{II} , Cu^{II} and Zn^{II}) في وسط الايثانول وبنسبة (2:1) فلز: ليكاند للحصول على معقدات متعادلة ذات الصيغة العامة $[M(L)_2Cl_2]$. شخصت جميع المعقدات المحضرة باستخدام تقنية الامتصاص الذري الهبي، أطيف الأشعة تحت الحمراء والأشعة فوق البنفسجية – المرئية فضلاً عن قياسات الحساسية المغناطيسية والتوصيلية الكهربائية، كما تم تقدير محتوى الكلور باستخدام طريقة مور. ومن النتائج المحصول عليها تم اقتراح الشكل ثماني السطوح للمعقدات المحضرة.

ABSTRACT

Coupling reaction of 4-aminoantipyrène with 8-hydroxyquinoline gave the new bidentate azo ligand 5-(4-antipyrène azo)-8-hydroxyquinoline. Treatment of this ligand with the following metals ions (Mn^{II} , Co^{II} , Ni^{II} , Cu^{II} and Zn^{II}) in aqueous ethanol with a 1:2 M:L ratio yielded a series of neutral complexes of the general formula $[M(L)_2Cl_2]$. The prepared complexes were characterized using flame atomic absorption, FT-IR, UV-Vis spectroscopic as well as magnetic susceptibility and conductivity measurements. Chloride ion content were also evaluated by (Mohr Method).

From above data, the proposed molecular structure for these complexes as octahedral geometry.

INTRODUCTION

Azo dyes with the heterocyclic diazo-component from colored complexes with many metal ions in solution(1-5). Great number of spectro -photometric methods based on these reactions were developed and used in analytical chemistry(6). In recent years, a lot of publications deal with the investigations of the mechanism of azo-dyes adsorption on to the solid supports,(7) such as ion-exchangers, pvc, fabric, silica gel or cellulose.

About a half of global production of synthetic textile dyes are classified into azo compounds that have the chromophore of (-N=N-) group and over 15% of the textile dyes are lost in wastewater stream during dyeing operation. These azo dyes are known to be largely non-biodegradable in aerobic condition(8).

The development of new structures of azo dyes have been interested in the commercial application to polyester, poly amide or poly acrylic as well as their blends with other fibres(9). In this respect, an attempt has been made to synthesize and characterize azo bidentate ligand, derived from 4-aminoantipyrène as diazo component, and 8-hydroxyquinoline as coupling agent. The complexes of this ligand with some metal ions has also studied and characterized physicochemically.

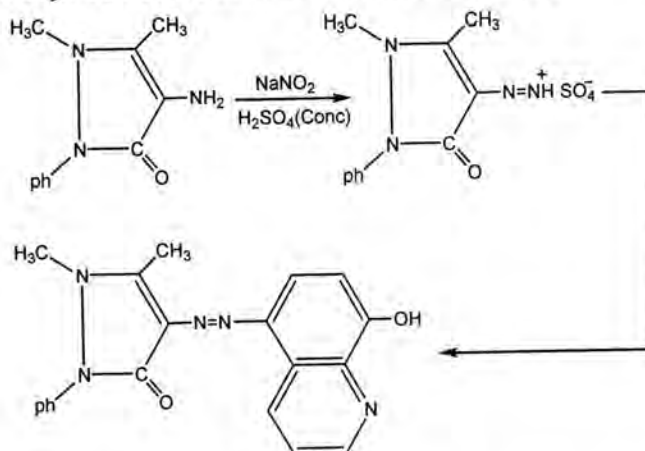
MATERIALS AND METHODS

A. Materials: All chemical used were of reagent grade and used without further purification $\text{MnCl}_2 \cdot 4\text{H}_2\text{O}$, $\text{CoCl}_2 \cdot 6\text{H}_2\text{O}$, $\text{NiCl}_2 \cdot 6\text{H}_2\text{O}$, $\text{CuCl}_2 \cdot 2\text{H}_2\text{O}$, ZnCl_2 (Fluka) 4-aminoantipyrene and 8-hydroxyquinolene (B.D.H).

B. Instrumentation: -FT.IR-spectra as KBr discs, in the range $(4000-400) \text{ cm}^{-1}$ were obtained using a (Shimadzu, FT.IR-8400 S were recorded in ethanol 10^{-3} M using (Shimadzu UV-160A) Ultra Vioet-Visble Spectrophotometer. Conductivity were measured for 10^{-3} M of complexes in ethanol at 25°C using (Philips Pw-Digital Conductimeter). Magnetic susceptibilities were performed using (Brucker Magnet B.M.6) instrument at 25°C . Melting points were obtained using (Stuart Melting Point Apparatus).

Preparation of the Ligand

The ligand was synthesized according to the general method(10) by dissolving (0.5g, 1mmole) of 4-aminoantipyrene in a mixture consisting of 2ml of sulphuric acid, 10ml ethanol and 10ml of distilled water. The solution mixture was cooled to 5°C . 10ml of 10% sodium nitrite was added dropwise with stirring in order to obtain the diazonium salt. After 30min the diazonium salt was slowly added to a cooled solution of 0.42g, 1mmol of 8-hydroxy quinolene to obtain the ligand. The dark colored mixture was neutralized by sodium hydroxide and the sold precipitate was filtered off and washed several times with 1:1 water ethanol, mixture then left to dry. The reaction is shown in scheme (1).



Scheme -1: Preparation of the ligand.

Preparation of Metal Complexes (General Procedure)

An aqueous solution of the metal salt contains 0.118g, 0.118g, 0.086g and 0.068g (1m mole) of $\text{MnCl}_2 \cdot 4\text{H}_2\text{O}$, $\text{CoCl}_2 \cdot 6\text{H}_2\text{O}$, $\text{NiCl}_2 \cdot 6\text{H}_2\text{O}$ and ZnCl_2 respectively was added gradually with stirring to the ethanolic solution of the ligand (0.347g, 2 mmole) using stichiometric amount (1:2) metal: ligand molar ratio, the mixture was stirring for half an hour at room temperature,crystalline

precipitates observed. The resulting precipitates were filtered off, recrystallized from ethanol and dried at 50C°.

RESULTS AND DISCUSSION

The isolated complexes were crystalline solid soluble in common solvents such as ethanol, methanol and dimethyl sulfoxide. They are relatively thermally stable. The conductivity measurements in ethanol (10^{-3} M) indicated the non-electrolyte behavior(11). The metal determination and chloride content (Mohr method) were found to be in agreement with calculated values. Table (1) include the physical properties. The effective magnetic moments of the complexes lies in the range (1.64-4.81) B.M.

This values refers to a parameters (high spin) which has been reported for most octahedral geometry. The I.R spectrum of the ligand Fig. (1) exhibited broad band at $(3414) \text{ cm}^{-1}$ indicated to ν (OH) vibration(12,13). Since no significant change in this band was noticed, the possibility that coordination occur via the donating atom in this group was excluded. Strong band in the ligand spectrum was observed at $(1678) \text{ cm}^{-1}$ due to ν (C = O)⁽¹⁴⁾, on complexation Fig. (2, 3) a shifted with change in shape were observed from main band, the significant change in this band may be a result of coordination with the metal ion. The strong characteristic band at $(1392) \text{ cm}^{-1}$ which was assigned to the (-N = N-) stretching(15, 16) suffered a great change in the intensity and in position, splitting to higher frequency was also observed on complexation with metal ion. This may suggest the participation of the azo nitrogen in this complexation. Two new stretching bands were noticed around $(580-497) \text{ cm}^{-1}$ and $(473-420) \text{ cm}^{-1}$ refers to metal oxygen and nitrogen respectively(17,18). Table (2) gives the characteristic absorption for the free ligand and its complexes.

Electronic Spectra

Free ligand peaks of maximum absorption and assignments related to the ligand(19,20) and its complexes are listed in Table (3). The ligand spectrum Fig. (4) exhibited an absorption peak at 242nm was assigned to the moderate energy $\pi - \pi^*$ transition of aromatic ring. The two peak at (399) nm was related to the $\pi - \pi^*$ transition of intermolecular charge- transfer taken through the azo group (-N = N-). The UV-Vis spectra of the complexes (Mn^{II} , Co^{II} , Ni^{II} , Cu^{II} , Zn^{II}) showed absorption peaks at (220, 304nm), (330nm), (304nm), (220, 298nm) and (220nm) which were assign to ligand field and charge transfer transition respectively. The peak at (390nm) and (459nm) on Mn^{II} complex Fig. (5) were caused by electronic transition ${}^6\text{A}_{1g} \rightarrow {}^4\text{T}_1(\text{p})$ and ${}^6\text{A}_{1g} \rightarrow {}^4\text{E}_{g(\text{D})}$ respectively The spectra of Co^{II} and Ni^{II} complexes appears two absorption peaks at (460nm) and (471nm) refers to electronic transition ${}^4\text{T}_{1g} \rightarrow {}^4\text{A}_{2g}$ and ${}^3\text{A}_{2g} \rightarrow {}^3\text{T}_{2g}$ respectively. The spectrum of Cu^{II} complex Fig. (6) gave absorption peak at (463nm) due to ${}^2\text{E}_g \rightarrow {}^2\text{T}_{2g}$ transition. Zn^{II} complex have no (d-d) transition because filled of the d-orbital. According to the results obtained may be suggest the octahedral structures of these complex.

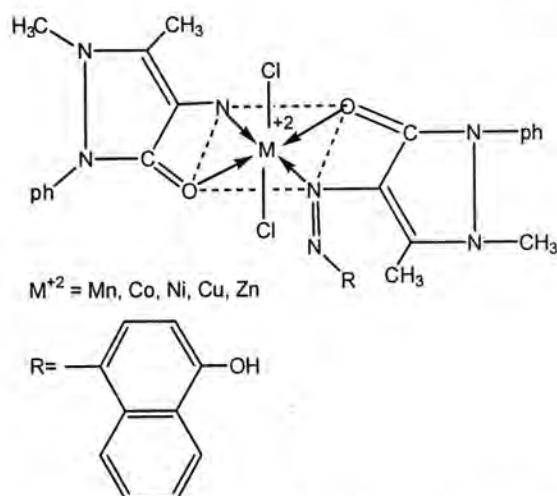


Table -1: Physical Properties of the Ligand and its Complexes.

Compounds	Color	M. P ^o C	M% Cal C. (found)	Cl%Cal C. (found)	A_m (ohm ⁻¹) .cm ² .mole ⁻¹ in absolute ethanol	μ_{eff} (B.M)
Ligand	Brown	185	-	-	-	-
[Mn(L) ₂ Cl ₂]	Reddish Brown	>360	7.13 (6.95)	9.20 (9.11)	6.79	4.81
[Co (L) ₂ Cl ₂]	Deep Brown	>360	7.61 (6.96)	9.16 (8.93)	6.97	3.72
[Ni (L) ₂ Cl ₂]	Red	>360	7.58 (7.12)	9.15(9.03)	8.66	3.08
[Cu (L) ₂ Cl ₂]	Yellowish Orange	>360	8.20 (8.04)	9.10 (8.87)	1.47	1.64
[Zn (L) ₂ Cl ₂]	Reddish Brown	>360	8.32 (7.88)	9.09 (8.95)	1.99	-

Table -2: The Main Frequencies of the Ligand and its complexes (cm⁻¹).

Compounds	$\nu(\text{OH})$	$\nu(\text{C}=\text{O})$	$\nu(\text{N}=\text{N}) + \nu(\text{C}=\text{N}-\text{N}=\text{C})$	$\nu(\text{M}-\text{O})$ $\nu(\text{M}-\text{N})$
Ligand	3414 br.	1678 V. S.	1392 S.	-
[Mn (L) ₂ Cl ₂]	3414 br.	1612 V. S.	1454 Sh. 1392 V.S.	580 W. 473 W.
			1462 Sh. 1427 Sho. 1384 S.	520 W. 420 W.
[Co (L) ₂ Cl ₂]	3414 br.	1585 S.	1454 Sh. 1427 Sh. 1388 S.	497 W. 450 W.
[Ni (L) ₂ Cl ₂]	3379 br.	1620 V. S.	1454 Sh. 1427 Sh. 1388 S.	497 W. 450 W.
		1585 S.	1458 Sh. 1438 Sho. 1384 S.	570 W. 466 W.
[Cu (L) ₂ Cl ₂]	3414 br.			
[Zn (L) ₂ Cl ₂]	3414 br.	1643 s.	1442 S. 1430 Sho.	580 W. 443

v.s = very strong, br = broad, sh= sharp, sho = shonlder.

Table -3: Electronic Spectra for The Ligand and Its Complexes.

Compounds	λ_{nm}	ABS	wave number(cm^{-1})	E max($L.Mol^{-1}.cm^{-1}$)
Ligand	242	1.465	41322.31	1465
	399	1.877	25062.65	1877
[Mn (L) ₂ Cl ₂]	220	1.637	45454.54	1637
	304	1.011	32894.73	1011
	390	1.325	25641.02	1325
	459	1.367	21786.49	1367
[Co (L) ₂ Cl ₂]	330	0.893	30303.03	893
	460	1.988	21739.13	1988
[Ni (L) ₂ Cl ₂]	304	0.620	32894.73	620
	471	0.916	21231.42	916
[Cu (L) ₂ Cl ₂]	220	1.732	45454.54	1732
	298	0.531	33557.04	531
	463	1.334	21598.27	1334
[Zn (L) ₂ Cl ₂]	220	1.121	45454.54	1121
	460	1.872	21739.13	1872

 λ = wave length in nanometers

Abs = Absorbance

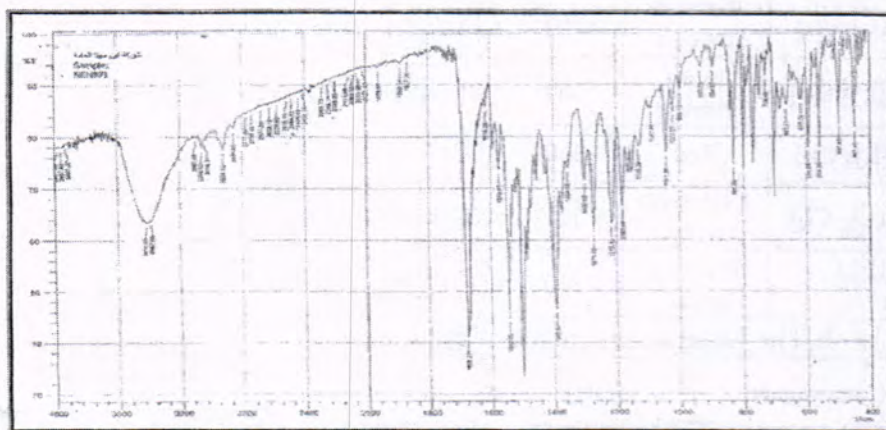


Fig.-1:FT-IR spectrum of the ligand

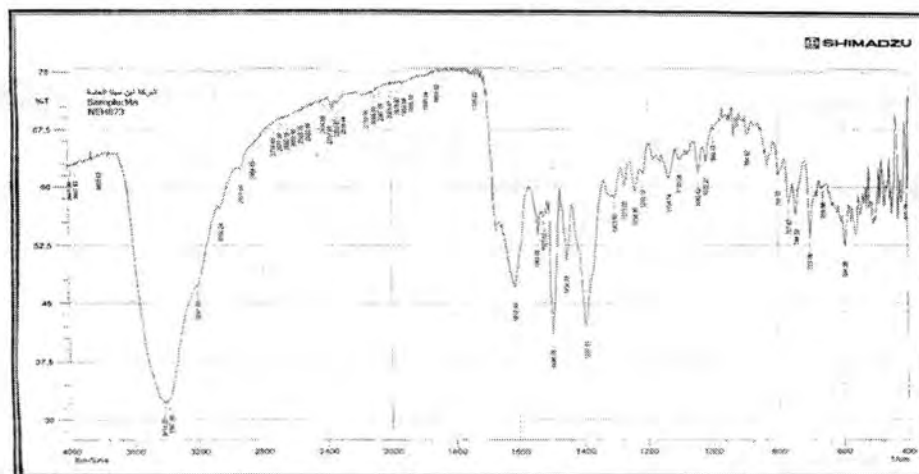


Fig.-2:FT-IR spectrum of the $[Mn(L)_2Cl_2]$ complex

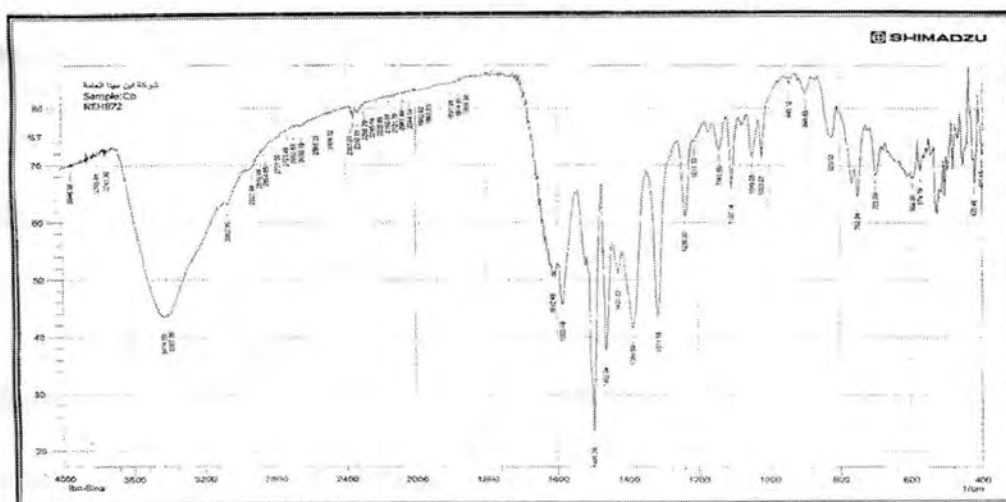


Fig.-3:FT-IR spectrum of the $[Mn(L)_2Cl_2]$ complex

REFERENCES

- 1.S. B. Savvin, V. P. Dedkoval and O.P.Shvoeva; Russ.Chem.Rev; 69:187-200(2000).
- 2.F. Lazaro, M. D. Luque and M. Valcarcel; Anal. Chim. Acta; 214 : 217-227(1988).
- 3.S. A. Morozko and V. M. Ivanov; Zh. Anal. khim; 50: 629-635(1995).
- 4.H. R. Maradia and V. S. Patel; J. Braz. Chem; Soc; 121:710(2001).
- 5.B.Kuswandi, A.A.Vaughan and R. Naray anaswamy; Anal. Sci; 17:181-186(2001).
- 6.J. Savic and V. Vasic; Acta. Chim. Slov; 53 : 36-42(2006).
- 7.K. L.Mutafichiev; Turk.J.Chem.27:619-626(2003).
- 8.H.Park & W.Choi; Journal of photo chemistry and photobiology; 159:241-247 (2003).
- 9.V. H. Patel, M. P. Patel and R. G. Patel; J. Serb. Chem. Soc; 67:727- 734(2002).
- 10.M. Panda, C. Das and C. Hung; J. Chem. Sci; 119:3-9(2007).
11. W. J. Geary; "coordination chemistry Reviews" 7: 110(1971).
- 12.E. Yildiz and H. Boztpe; Turk. J. Chem; 26(2002).
- 13.F.El-Saied, M.I. Ayad, R. M. Issa and S. A. Ally; Polish. J. Chem; 75 :773(2001).
- 14.R. M. Silverstein and F. X. Webster; "Spectrometric Identification of Organic Compounds"; 6th, New York, John Wiley and Sons, Inc, (1996).
- 15.R. Cabrillo, A. Castineirars, B. Covelog, J. Nicolas and E.N. Vazquez-Lopez; Polyhedron; 20(2001) 2415.
16. J. Pal, T. K. Misra and C. Sinha; Transition. Met. Chem.; 25 (2000) 333.
17. C. P. Gupta, D. K. Kanugo and P. K. Mehta; 56 (1979) 826.
18. A. K. Rona and J. R. Shah; 58 (1981) 1100.
19. K. B. Pandega and R. P. Singh; Ind. J. Chem; 14 (1976) 681-682.
20. M. Y. Al-Janabi; "The Physical Methods in Inorganic Chemistry" 1983.

***In vitro* and *In vivo* Effect of *Myrtus communis* Extracts on *Staphylococcus aureus* Isolated from Patients with UTI**

¹Rukia Muhammad. Al-Barzinji and ²Sazan Khalid Esmahil

¹Quia University /College of Pharmacy

¹Quia University / College of Science/Biology Department

الخلاصة

التهاب المجاري البولية يعرف بانها الحالة التي تصاب بها المجاري البولية بالمسببات المرضية كيكتريا *Staphylococcus aureus* مسببا للالتهاب. أجريت هذه الدراسة لتقييم تأثير مستخلص نبات اليأس خارج و داخل الجسم الحي على بكتريا *S. aureus* المعزولة من مرضى التهاب المجاري البولية. شملت الدراسة 350 مريضاً (125 ذكر و 225 أنثى) مصابين بالتهاب المجاري البولية من المراجعين للمستشفى التعليمي في مدينتي اربيل و السليمانية للفترة من آذار إلى أيار لسنة 2007. كذلك شملت الدراسة 25 فرداً من الاصحاء كمجموعة سيطرة. استخدمت طريقة الحفر في الأكار وطريقة الأقراص في الاختبار خارج الجسم الحي بينما استخدمت ثلاثة مجاميع من الفئران في اختبار داخل الجسم الحي. تم الحصول على نتائج زرعية موجبة في 119 (34%) من نماذج الإدرار. سجلت نسبة الإصابة بكتريا *S. aureus* 23 (17,82%) في مجموعة الذكور والاناث و السيطرة على التوالي. سجلت نسبة الإصابة بكتريا *S. aureus* 23 (17,82%). كان التأثير التثبيطي للمستخلص الكحولي للأس الأكثر كفاءة في تثبيط نمو *S. aureus* خارج و داخل الجسم الحي.

ABSTRACT

Urinary tract infection (UTI) defines as a condition in which the urinary tract is infected with different pathogens as *Staphylococcus aureus* (*S. aureus*) causing inflammation. This study was "carried out to evaluate the *in vivo* and *in vitro* effect of *Myrtus communis* (*M. communis*) plant extracts on *S. aureus* isolated from UTI. This study included 350 patients (125 males and 225 females) with signs and symptoms of UTI, who were referred to the Teaching Hospital in Erbil and Sulaimania cities, from March till May 2007. Also, 25 healthy individuals were included in the study as a control group. Agar well and disc diffusion assay were used for *in vitro* test while 3 groups of rats were used for *in vivo* test. The bacterial cultivations revealed positive results for 119 (34%) urine specimens; 56 (47.05 %), 63 (52.94 %) and 0 (0%) in males, females and control group respectively. The rate of uropathogenic *S. aureus* was 23(17.82%). Ethanol extract of *M. communis* was the most efficient to inhibit *S. aureus in vitro* and *in vivo*.

INTRODUCTION

A urinary tract infection is an infection caused by microorganisms mainly bacteria that may affect any part of the urinary tract(1). Most UTIs are caused by facultative anaerobes Gram-negative rods, especially *Escherichia coli*, *Proteus sp.*, *Klebsiella sp.*, *Pseudomonas sp.*, and certain Gram-positive cocci such as staphylococci(2). Some medicinal plants have potential sources of new antibacterial agents even against some antibiotic-resistant strains(3). *Myrtus communis* is taken either internally or externally, the former one in the treatment of urinary

infections, digestive problem, vaginal discharge, bronchial congestion, sinusitis, dry coughs, diabetes mellitus and inflammatory disorders(4,5).

MATERIALS AND METHODS

Urine samples had been taken randomly from 350 patients (inpatients and out patients) who were suffering from signs and symptoms of UTIs attending Hawler and Sulaimania Teaching Hospitals and 25 apparently healthy individuals were considered as a control group, during the period from March to May 2007.

Bacteriological agar media were used for detection isolated bacteria. However, stock solution was prepared by mixing 50 grams leaf of the plant powder with 250 ml of extractant (cold water, hot water, ethanol, acetone and diethyl ether). From the stock solution (200mg/ml percent), different concentrations of the plant extract (200, 100, 50 and 25 mg/ml) were prepared (6).

A standardized inoculum of $1-2 \times 10^7$ cfu/ml was inoculated into the surface of sterile Muller-Hinton agar plates. Discs were soaked in the above concentrations of the extract while the control disc was soaked in sterilized distilled water. At 37°C After 24 hour sensitivity and resistance of the bacteria to the plant extract were recorded through measurement of inhibition zones by ordinary ruler(7). Minimum inhibitory concentration (MIC) and the minimum bactericidal concentration (MBC) of the extracts were determined. The highest dilution that yielded no single bacterial colony on a solid medium was known as MBC(8).

In vivo study was done using a number of rats classified into 3 groups: Control negative group consist of 5 rats injected with normal saline, control positive group consist of 4 rats injected with *S. aureus* and orally tested group, consists of 4 rats injected with counted amount of isolated *S. aureus*.

Surgery was done for female albino rats weighing 170-200g according to(9). The abdomen of the rats cleaned with iodophore and opened by longitudinal midline incision from the xiphoid process towards the symphysis pubis by blade. 0.1ml of staphylococcal suspension (10^8 bac/ml) injected into bladders of groups 2 and 3 small volume of 0.1 ml of sterilized normal saline was injected into group1, then abdominal cavity was closed(10). Urine samples were collected after operation to check infected cases. Groups 1 and 2 were housed by standard chaw and tap water. However, group 3 for three weeks were taken standard chaw and solution of plant extract at concentrations of 200, 100, 50 and 25mg/ml instead of water. Urine culturing was done for all 3 groups.

RESULTS AND DISCUSSION

This study was carried out on 350 patients complaining of signs and symptoms of UTI and 25 apparently healthy individuals as control group. Only 119 patients (34%) were positive for bacterial infections whereas 231 patients (66%) had no bacterial infection. However, urine samples of control group were negative for bacterial cultures (0%).

Regarding the sex and age distribution of UTI patients. Out of 119 patients with positive bacterial cultures 56(47.05%) were males and 63(52.94%) were females ($p<0.01$) Table (1).

Table -1: Prevalence of UTI in relation to gender

Sex Bacterial infection	Male	Female	Total
Infected	56 (47.05%)	63 (52.94%)	119(34%)
Non-Infected	69 (29.87%)	162 (70.12%)	231(66%)
Chi-square	P<0.01		350(100%)

There is a significant difference in the UTI incidence regarding to sex and age Table (2). The incidence of UTI infection in males was significantly higher than in females only in the first age group 1-9 year.

Table -2: Prevalence of UTI in relation to age and gender

Sex Age (years)	Female	Male	Total
1-9	5 (7.93%)	23 (41.07%)	28
10-19	8 (12.69%)	7(12.5%)	15
20-39	28 (44.44%)	8 (14.28%)	36
≥40	22 (34.92%)	18(32.14%)	40
Total	63	56	119
Chi-square	P<0.01		

The percentage of *S. aureus* was more frequently than other isolates 17.82%, in pure culture 22(18.48 %) and 1(10 %) in mixed culture Table(3).

Table -3: Number of *S. aureus* isolates recovered from 119 patients with UTI

Bacterial isolates	Pure culture		Mixed culture		Total	
	No.	%	No.	%	No.	%
<i>Staphylococcus aureus</i>	22	18.48	1	10	23	17.82
Others	97	73.76	9	90	106	16.18
Total	119	92.24	10	7.75	129	34

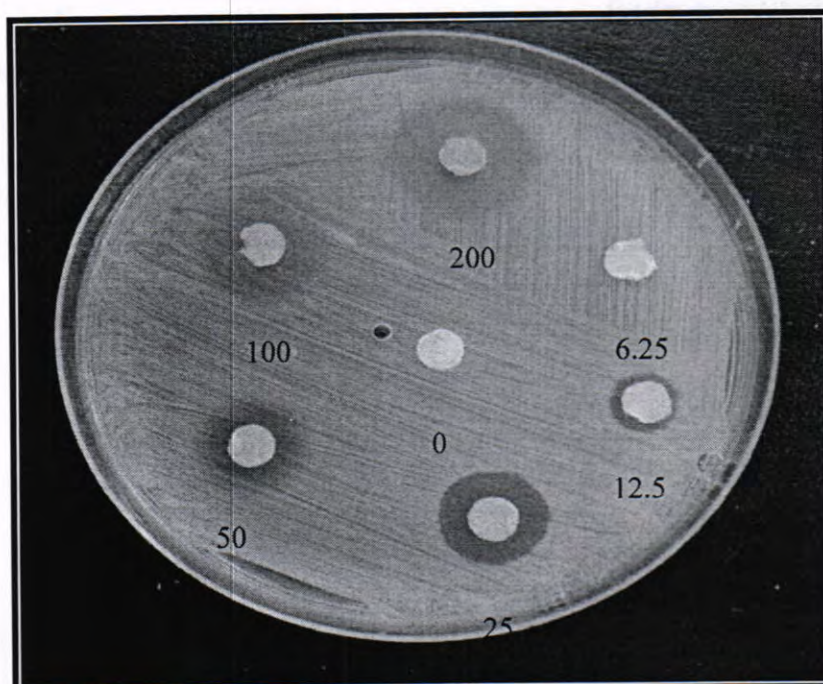
The results of plant extract revealed that *M. communis* showed different degrees of antibacterial effects when used with different extractants such as cold, hot water, ethanol, acetone and diethyl ether.

Ethanol extract had the greatest bactericidal action compared with other extractants on *S. aureus* 17.09. Indeed, the best inhibition zones were found by using a high concentration of *M. communis* (200mg/ml) by agar well diffusion for all types of extractants. The most average diameter of inhibition zone detected was 34.66mm by using ethanol compared with other type of extractants 28, 25.33, 22.33, and 22mm of diethyl ether, acetone, cold and hot water respectively. Additionally, the mean of inhibition zone in agar-well diffusion assay by using Least Significant Difference was significantly more than disc diffusion assay 18.29mm versus 8.43mm Table (4), Figure (1).

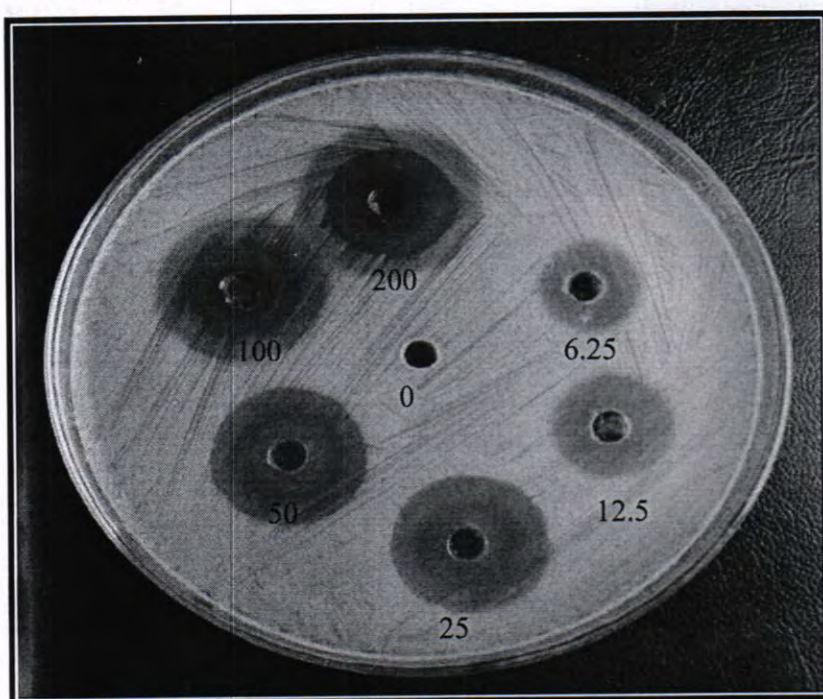
Table -4: Relation *S. aureus* with plant extract types, concentrations and inhibition method

Types of extract ant	Concentrations mg/ml	Inhibition zone (mm)		Mean of types of extractant	Mean of concentrations
		Disc	Well		
Cold water	0	0	0	12.36	0 0
	25	7	17.66		
	50	9	19		
	100	12.3 3	21.66		
	200	14.6 6	22.33		
Hot water	0	0	0	12.56	25 13.29
	25	7	15.33		
	50	10.6 6	19		
	100	14.3 3	21.33		
	200	16	22		
Ethanol	0	0	0	17.09	50 15.53
	25	10.3 3	25		
	50	10.6 6	28.33		
	100	14.3 3	31		
	200	16.6 6	34.66		
Acetone	0	0	0	15.29	100 18.63
	25	16	18.66		
	50	16	20.66		
	100	17.3 3	22.66		
	200	18.6 6	25.33		
Diethyl ether	0	0	0	10.76	200 20.63
	25	0	18.33		
	50	0	22		
	100	7	24.33		
	200	8	28		
Mean of inhibition zone		8.94	18.29		

- L.S.D 0.01 of types of extract ant = 1.583 concentration=1.583
Inhibition zone= 1.001



A- Disc diffusion assay



B- Agar-well diffusion assay

Figure (1) A and B: Effect of different concentration of *M. communis* acetone extract on growth of *S. aureus* by disc and agar diffusion methods

The MIC and MBC of *M. communis* affected *S. aureus* growth were in concentrations 100 and 150 µg/ml respectively.

Antibacterial effect of *M. communis* extract on *S. aureus* was tested *in vivo*. The control negative group of rats were only injected with normal saline, their urine cultures were negative for bacterial growth (0%). cultivation was done for urine of control positive group after 7 days and 3 weeks of orally administration tap water. The urine culture results of (-) control group were positive, after 7 days and 3 weeks of orally administration tap water. Also cultivation was done for urine of myrtle orally tested group after 3 weeks of orally administration myrtle extract, the culture was negative, table (5) figure(2).

Table -5: Effect of myrtle extract on *S aureus in vivo*

Study groups	No.	Type of injection	Growth after 7 day	%	Growth after 3 weeks of treatment	%
Control negative	5	normal saline	-	0%	-	0%
Control positive	4	<i>S. aureus</i>	+	100%	+	100%
Tested bacterial injected group	4	<i>S. aureus</i>	+	100%	-	100%
Total	13					

+ = positive - = negative



Figure -2: Injection of *S. aureus* into rat bladder by surgery

The percentage of positive UTI was 119 out of 350 (34%) however in other studies were 162 (75.42%) and 231 (66%) respectively (11). The failure of urine samples to give growth may be due to the effect of broad spectrum antimicrobial drugs which had been given to the patients. Indeed, using the outer sterilizer solutions had a great effect on reducing the rate of the bacterial isolations (12).

Other reasons of bacterial growth failure in urine samples could be to anaerobic bacteria, mold and other bacteria that can not be isolated by conventional methods used in this study and we need special technique for their isolation and growth(13).

Out of 119 UTI patients with positive bacterial cultures 56(47.05%) were males and 63(52.94%) were females and this result is in agreement with report of Al-Salammia(14).

Females may get UTI through sexual intercourse or from the bowel due to shortness of the female urethra and its close location to the perineal region. Indeed absence of prostatic secretion and pregnancy are risk factors for UTI(15). The incidence of bacterial infection in age group (1-9 years) in males was significantly higher than in females, because in uncircumcised boys bacteria established in the perpetual sac and provide a source of ascending infection(16). In age group 40 years and above the incidence of UTI in females were more than in males because after menopause period UTI may become more common in females due to the decrease in estrogen and reduced antimicrobial activity of genitourinary secretions(17).

S. aureus isolates were a common pathogen for UTIs 23(17.82%) out of 129 while the number of staphylococci isolate in the result of Al-Harti *et al.*, 1990 was 35(28.9%) 95(18). The variations in previous results might have been due to sample size, different communities of these studies and development of bacterial resistance as a result of the frequent usage of the antimicrobial drugs(18).

In general, ethanol extract of *M. communis* exerted greatest antibacterial activity against certain Gram-positive bacteria than other solvents at the same concentration with significant difference. Because most of the active compounds dissolved in ethanol so their inhibition increased, these observations may be attributed to nature of biological active components could be enhanced in the presence of ethanol. Furthermore, the stronger extraction capacity of ethanol could have produced greater number of active constituents responsible for antibacterial activity (8).

However, water extract had less antibacterial activity, since all of the plant components which are active against microorganisms are aromatic or saturated organic compounds. They are not water soluble and more often obtained by treatment with less polar solvents so the lower dissolving capacity produced a smaller number of active components and decrease the antibacterial effect of the extract(19).

More inhibition was found by using a higher concentration of the *M. communis* extract compared with lower concentration extract, as reported by Al-Barzinji in 2000(6). This is because some chemical

compounds have the inhibitory effect only at a higher concentration(20). Moreover, higher inhibition zone was present in agar-well diffusion assay as compared to disc diffusion assay which may be due to the diffusion property of extract solution within the medium in wells is greater than disc.

The inhibitory action of myrtle is related to phenolic and polyphenolic structure especially tannins as chemical constituents. The antimicrobial mechanisms of tannins can be summarized as follows: enzyme inhibition through reaction with sulfhydryl groups which cause denaturation of proteins and blockage of enzymes responsible for metabolic process (19). Also the ability of tannins to complex with bacterial cell wall and may disrupt microbial membrane and complex of membranes by tannins may account for tannin toxicity because tannin has a high great binding efficiency to iron and work like a siderophore to chelate iron from the medium and make iron unavailable to microorganisms and subsequently effect on their growth(21). The alkaloid binds tightly to DNA and behaves as a typical intercalating agent (9). Moreover terpinoids are active against many microorganisms as bacteria, fungi, viruses and protozoa during membrane disruption by lipophilic compound(19).

It could be concluded that *M. communis* extract inhibits growth of *S. aureus* by *in vivo* and *in vitro* tests due to its phenolic compounds.

REFERENCES

1. Kaper, J.B., Mobley, H.L. and Nataro, J.P. Pathogenic *Escherichia coli*. *N. Engl. J. Med.* 2(2):123-40(2004).
2. Roberts, D. Urinary Tract Infection .In: Practical Clinical Medicine; University of Manchester, MTP Press, 3rd ed.p.1-17 (1987).
3. Thakur, M. Pharmacological Screening of Some Medicinal Plants as Antimicrobial and Feed Additives. M.Sc. Thesis, Virginia polytechnic Institute and State University. Blacksburg. Virginia USA (2004).
4. Farnsworth, C., Franke, L., Appendino, G., and Werz, O. Identification of molecular targets of the oligomeric nonprenylated acylphloroglucinols from *Myrtus communis* and their implication as anti-inflammatory compounds, *Cell. and Mole. J. of pharm. and Exper. Therap.* Fast Forward. 315: 389-396(2005).
5. Cengiz, S., Timur, S., Okutucu, B. and Zihnioglu, F. Inhibition of alpha-glucosidase by aqueous extracts of some potent antidiabetic medicinal plants. *Prep Biochem. Biotech.* 35(1)29-36(2005).
6. Barzinji, R.M. Microbiological and Immunological study of the secondary infection of cutaneous Leshmaniasis and the effect of *Myrtus communis* extract on the bacteria. M.Sc. Thesis. College of Science. University of Al-Mustansiriyah (2000).

7. Nawas, F.E., Mawajedch, S., Dabnich, A., and Al-Omari, A. Invitro activities of antimicrobial agents *Proteus sp.* from clinical specimens. Br.J.Biomed.Sci. 2:95-96 (1994).
8. Akinymi K.O., Oladapo, O., Okwara, C.E. and Ibe,C.C. Screening of crude extracts of six medicinal plants used in South-Weast Nigerian unorthodox medicine for anti-methicillin resistant *Staphylococcus aureus* activity. JMC Complementary and Alternative medicine.5(6): 1-7 (2005).
9. Zhao, H., Li, X., Johnson, D.E. and Mobley, H.L. Idetification of protease and *rpoN*-associated genes of uropathogenic *Proteus mirabilis* by negative selection in a mouse model of ascending urinary tract infection. Micribiology. 145:185-195 (1999).
10. Rowett, I.G. The rat as a small mammal. John murray publisher. Ltd.1st ed.p12-130. (1974).
11. Jarjees, K. K. Study the resistance of bacterial species isolated from patients to the some antibiotics and new chemical compounds. M.Sc. Thesis. College of Science. University of Al-Mustansiriyah (2006).
12. Kriger, N., Kauser, D.L. and Wenzel, R.P. Nosocomial urinary tract infection, cause wound infections postoperativial in surgical patients. Surgery. 156:313-316 (1993).
13. Al-Salam, M.A. Isolation and Identification Two of Bacteria Causing Urinary Tract Infection and Studying the Effect of *Trigonella foenum gracum* L. and *Glycyrrhiza glabral* L. Extracts On it. M.Sc.Thesis. College of Science. University of Kufa (2004).
14. Al-Habib, A.M. Urinary tract infection among pregnant women in Al-Mukalla district. Yemen. East. Medit.Health. J. 11(3) (2005).
15. Thomas, B.N., Bernzweig, A.J., Takayama, I.J. and Pantell, H.R. Urine testing and urinary tract infection in febrile infants seen in office setting. Pediatrics. 156(1):44-54(2002).
16. Hofman, M.T. Urinary Tract Infections :How to manage nursing home patients with or without catheterization, Geriatrics. 57(5):49-52(2002).
17. Al-Habib, K.J., Hadithi, T.S. and Ani, Z. A Preliminary study on bacteriuria in pregnant women baghdad. J.Fac.Med.Bag. 32(3):361-366 (1999).
18. Collier, Carrie, A. P. and Harry, L.T. Pathogenesis of *Proteus mirabilis* in urinary tract infection. J. Micro. and Inf. 2:1497-1505 (2000).
19. Cowell, I.M. Plant products as antimicrobial agent, Clin. Microb. Revi. 12(3):571-582(1999).
20. Sasser, J., Balke, N.E. Plant growth response to several allelopathic chemicals. Weed scie. 31: 292-298 (1983).
21. Fadda, B., Phila, R., Bianchini, J., Madjebi, S. and Hnawia, E. Bioactive compounds from *Cunonia macrophylla*: An endemic cunoniaceae from Madagascar. J. Phytochem. 6: 241-247 (2005).

Chromosomal Aberrations In Patients With Recurrent Spontaneous Abortion

¹Rafid Abdulwahed; A, ²Abdul amer naser G., ³Kareem .M lilo and ⁴Rushdi sadi
¹Biochemical Engineering Dept, Al-khwarizimi Collage Engineering , Baghdad University
²Biomedical Engineering Dept, College of Science , Al-Mustansrya University
³Technical Center For Drug Control and Research/MOH
⁴Inter for Cancer and Medical Genetics Research.

الخلاصة

تعتبر التغيرات الكروموسومية من العوامل المهمة والمرتبطة ارتباطاً وثيقاً مع الإجهاض التلقائي المتكرر. 60% من النساء الحوامل. حيث وجدت الدراسات الحديثة أن 2-4% من الأزواج الذين يعانون من الأسب المتكرر أن أحد الأزواج على الأقل يحمل نوعاً معيناً من التغيرات الكروموسومية. في هذه الدراسة تم التحري عن دور التغيرات الكروموسومية في أحداث الأسقاط التلقائي المتكرر لدى الأز هذه الدراسة تحتوي على اثنان وثلاثون زوجاً (64 فرداً) من الذين يعانون من الأسقاط التلقائي المتكرر حيث كان لديهم على الأقل ثلاثة حالات إسقاط متكرر تم إرسالهم من قبل الطبيب المختص إلى المختبرات في مستشفى البرموك التعليمي في وحدة الوراثة الخلوية لأجراء الفحوصات الخلوية للتحري عن وجود كروموسومية، علماً أن بقية نتائج التحليلات الهرمونية والكيموحيوية والمرضية كانت ضمن المعدل للأشخاص الأصحاء. بينت نتائج هذه الدراسة وجود تغيرات كروموسومية عديدة وتركيبية عديدة شملت الزيادة في كل من الكروموسوم 6 والكروموسوم 15 والتغيرات التركيبية التي تمثلت بالانتقالات بين الكروموسومات الجنسية والكروموسومات بالإضافة إلى الكسور الكروماتيدية للكروموسومات الجنسية والجسمية عند المقارنة مع مجموعة الأصحاء. الدراسة أن التغيرات الكروموسومية في الإناث كانت أعلى من الذكور كشفت النتائج لهذه الدراسة أن الكروموسومية دوراً واضحاً في عملية حدوث الأسقاط التلقائي المتكرر لدى الأزواج الذين يحملون كروموسومية معينة.

ABSTRACT

Results detected the chromosomal aberrations has important role in spontaneous is for parents which suffered from chromosomal aberrations. acytogenetic factors are related to show association with recurrent spontaneous abortions RSA. In approximately 2-4% couples with recurrent pregnancy loss, one partner will have a genetically balanced structural chromosome rearrangement. Couples who are predisposed toward chromosomal abnormal conceptions will be at increased risk for Recurrent Spontaneous Abortion. This study an evaluation of the contribution of chromosomal anomalies in causing recurrent spontaneous abortions was made. The study included 32 couples (64 individuals) with a history of repeated spontaneous abortions who were referred for cytogenetic studies at the cytogenetic Department from the clinical laboratory in Al-Yarmook hospital in Baghdad for hormonal and Biochemical analysis which Considered in normal range of health persons. All the other clinical parameters of both the partners were within the normal range. The results showed numerical aberrations, in chromosome 6 and 15. The numerical aberrations, included a trans location also chromatide breaks in sex and somatic chromosomes when compared with health persons males or female. Chromosomal analysis is an important etiological investigation in couples with repeated spontaneous abortions as it helps in genetic counseling and deciding about further reproductive options. and associated with an increased risk of spontaneous abortion. Corresponding author: Rafid Abdulwahid Biochemical engineering Dept, Al-khwarizimi Collage Engineering, Baghdad University .

INTRODUCTION

Recurrent Spontaneous Abortion (RSA) can be define is the loss of three or more consecutive pregnancies before the 24th week of gestation. or can be define is the termination of pregnancy before 20 completed gestational weeks from the last menstrual period, or less than 500 g fetal weight. The rate of spontaneous abortion in women is about 15%–20% and increases with age, from 15% in women younger than 25 years and to 35% in women older than 38 years (1).

RSA occurs chiefly due to either there is something wrong with the pregnancy itself, such as chromosomal abnormality that prohibits the pregnancy from implanting/ growing properly or there is a problem within the environment in which the pregnancy grows. (2). The causes of RSA have been classified as infection (1%), anatomic abnormalities (5% to 10%), lutealphase defect (5% to 20%), chromosomal abnormalities (7% to 50%), immune mechanisms (50%), and unknown (15%). Some women have multiple reasons for RSA.(3). It is well known that lower implantation rate and higher spontaneous abortions rate are closely related with the chromosomal abnormalities of both parents. Cytogenetic factors are found to show association with RSA. In approximately 2-4% of couples with recurrent pregnancy loss, one partner will have a genetically balanced structural chromosome rearrangement. Couples who are predisposed toward chromosomal abnormal conceptions will be at increased risk for Recurrent Spontaneous Abortion. It has been accepted that at least 50% of clinical abortions result from chromosomal abnormalities. Pregnancy loss and fetal abnormalities depend on the size, location, and type of structural rearrangement. (4).

Recent studies demonstrated that Chromosomal translocation is the most common structural rearrangement involved in recurrent miscarriage. Cytogenetic screening of couples with recurrent abortion reveals that the prevalence of translocation in either parent is 3% to 5%, with the wife being affected twice as frequently as the husband. Numeric chromosomal abnormalities however, might be involved in both recurrent and sporadic losses.(5),the most common abnormality observed is trisomy (\square 30% of all losses), although sex chromosome monosomy and polyploidy account for the majority of the remaining chromosome abnormalities found (each contributing to \square 10% of total losses). However, the frequency of specific abnormalities depends strongly on the age of the study group members, because risks of most trisomies increase dramatically with increasing age of the mother, whereas sex-chromosome monosomy and polyploidy do not (6).Cytogenetic studies give considerable information about the genetic makeup leading to RSA and still remain an important tool. In the coming years, newer advanced techniques will help to increase our understanding of RSA resulting in new and expedient diagnosis and potential treatment (7).

MATERIALS AND METHODS

The study included 64 individuals (32 couples) with a history of repeated spontaneous abortion who were referred for cytogenetic studies at the cytogenetic Department in the educational laboratory, Al-Yarmook hospital in Baghdad, between June 2007 and June 2009. All the other clinical parameters of the partners were within the normal range. The obstetrical history of each couple was recorded on the report from the files of patients. Cytogenetic analysis of peripheral blood lymphocytes in these couples was performed. Peripheral blood lymphocyte culture was carried out according to the standard procedure with slight modifications (8). Five ml of blood was incubated in complete lymphocyte culture medium (RPMI 1640; Sigma,). Supplemented with 10% of fetal bovine serum (Sigma). To initiate the cultures 0.3 ml of phytohemagglutinin (Sigma) was added to the culture. The cultures were incubated at 37 °C in CO₂ incubator for 72h. Metaphases were harvested by adding colcemid (Sigma,) to the cultures to arrest the cell division at metaphase stage, followed by hypotonic KCl treatment and fixation. For each individual, a minimum of 50 metaphases were counted and cells were banded after standard G-banding that described by (9). With slight modifications, as the routine banding method.

RESULTS AND DISCUSSION

The study was carried out to assess the incidence of chromosomal aberrations in couples who suffer from recurrent spontaneous abortion. And to examine the relationship between spontaneous abortions and the presence of chromosomal aberrations.

The median age of male partners was 42.21 ± 3.6 and the median age of female partners was 36.23 ± 1.4 . In general, this study reported that the incidence of chromosomal abnormalities is higher in females than that in males (Five females and two male) which was a ratio of 2.5: 1. But paternal chromosomal abnormality may also have a role in the pathogenesis of spontaneous abortions. Fig (1) an almost similar male to female ratio has been found in most of the reported studies (10).

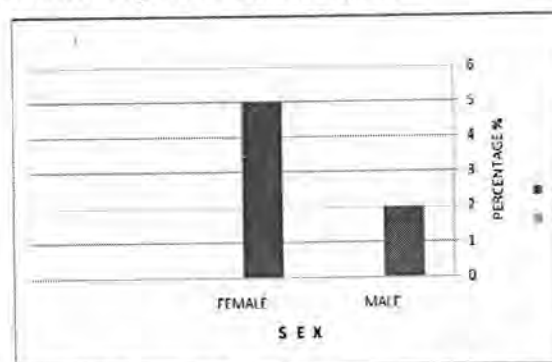


Fig-1: The incidence of chromosomal aberrations in couples

Karyotyping was successful in 45 cases (70.31%) of the 64 specimens and the remaining 19 cases (29.68%) were failed. Among these 45 specimens, 7 cases

(10.9 %) were found to be carriers of different chromosomal abnormalities and the remain 38 cases (59.37%) were chromosomally normal . The Chromosomal aberrations that found in these 7 subjects, can be classify into 2 cases (3.12 %) showed numerical aberrations, and 5 cases (7.81 %) carried structural abnormalities. Among these two numerical aberrations, a males partner (1.56) was detect to have trisomy of chromosome 15, and the other female partner (1.56) have trisomy of chromosome 6. From the other hand the result detected that structural aberration were seen in the karyotyping of the remain five cases involved breaks in the P arm of X chromosome in two females (3.12 %). , and one female (1.56) had a translocation in chromosome 21 and X chromosome $t(21,X)$ the other female (1.56) had a break in q arm of chromosome 18 , and the remain male (1.56) detected to have breaks in q arm of Y chromosome as shown in fig (2) .

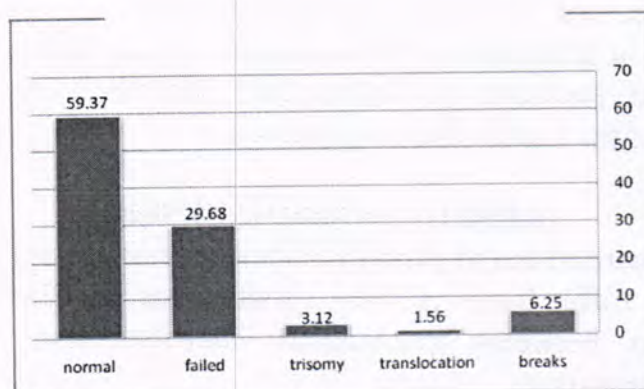


Fig.-1:Cytogenetic analysis of couples under the study

Data of different chromosomal analysis found in the specimens are postulated in Tables 1.

Table-1:Frequency of cytogenetically normal and abnormal individuals in the study.

Case No:	aberration	karyotyping	frequency	Age	Sex
1	Normal	46 XY	17	32-43	male
2	Normal	46 XX	21	25-40	female
3	Structural	breaks	1	33	female
4	numerical	47XX+ 6	1	42	female
5	structural	breaks	1	43	female
6	structural	breaks	1	40	male
7	structural	Translocation $t(X,21)$	1	41	female
8	structural	breaks	1	24	female
9	numerical	47 XY+15	1	38	male

Several studies have been carried out to determine the prevalence of chromosomal aberrations among couples with recurrent spontaneous abortion. (1) This study reported that the incidence of chromosomal abnormalities is higher in females than that in males. In addition the incidence of structural chromosomal aberrations is higher than the numerical chromosomes aberration that found in the cases under the study. An almost similar male to female ratio has been found in most of the reported studies about the recurrent spontaneous abortion (12).

That biological hypothesis has been epidemiologically investigated to explain the relationship between recurrent spontaneous abortion patients and chromosomal aberration, in our study two types of chromosomal aberration were found: numerical aberration included trisomy, structural aberration included breaks, translocation, in X and Y chromosome.

Y chromosome X chromosomes are essential for the male and female reproductive system. The human Y chromosome is not only the dominant sex determiner, but also plays an essential role in the genetic regulation of spermatogenesis, and the male-specific region of the Y chromosome (MSY) differentiates the sexes and comprises 95% of the chromosome length (13).

The long arm of the Y chromosome contains areas responsible for the regular spermatogenesis. And any breaks or deletions of the euchromatic part of the Y chromosome's long arm may affect spermatogenesis, because long arm has loci essential for spermatogenesis. And we hypothesized that breaks of Y chromosome may increase the risk of RSA in couples who had these types of aberrations, because Y chromosome plays a major role in transplantation (14). Autosomal chromosomes have a chance in RSA. The X chromosome plays a critical role in pregnancy from gamete formation to completion of development. And contains numerous genes essential to survival. Every major translocation or break of this chromosome has a lethal effect in the male sex. Translocations between the X chromosome and an autosome usually result in disturbed spermatogenesis, whereas inversions of the X chromosome do not substantially affect male fertility. (15). X chromosome is expected to be associated with an increased risk of spontaneous Abortion, some deletions or mutations on the X chromosome may be lethal to fetuses carrying the abnormal X chromosome, from another hand X-autosome translocations can lead to RSA, because some gametes may be deleted and/or duplicated for portions of each chromosome that are involved in the rearrangement (16). We proposed that for all the above reasons, that the aberration in sex chromosomes such as translocations or breaks can lead to the formation of unbalanced gametes and therefore carry a higher risk of increased spontaneous abortion. (17).

Abnormality of chromosome 6 was seen in one female of the patients under study. The short arm of this chromosome carries the Human Leukocyte Antigen (HLA) or (MHC) major histocompatibility complex and this antigen plays a critical role throughout pregnancy by influencing gamete development, cleavage, blastocyst and trophoblast formation, implantation, fetal

development and survival (18). And playing a role at the maternal-fetal interface. The fetus being semi-allogenic might face a rejection from the maternal antibodies if there is increase HLA sharing among the couple. And we think that this type of aberration (trisomy 6) may lead to a high gene density or lead to increased the frequency of gene rearrangements resulting in the formation of variant antigens. And these antigens play a major role in transplantation and are critical in pregnancy from gamete formation to completion of development and association with the RSA. (19).

REFERENCES

1. Aruna Meka and B. Mohan Reddy Recurrent Spontaneous Abortions: An Overview of Genetic and Non-Genetic Backgrounds .Int J Hum Genet, 6(2): 109-117(2006).
2. Andersen N, Wohlfahrt J, Christens P.: Maternal age and fetal loss: population based register linkage study. Br Med J., 320:1708-1712 (2000).
3. Penny J. Chong, MD, William L. Matzner, MD, Wendell T.W. Ching, MD. (1995). Immunology of Recurrent Spontaneous Abortion. THE FEMALE PATIENT. 20 : 1-5.(2006).
4. Stephenson MD, Sierra S. Reproductive outcomes in recurrent pregnancy loss associated with a parental carrier of a structural chromosome rearrangement. Hum Reprod.;21(4):1076-82(2006)..
5. Simona Farcas¹, Valerica Belengeanu¹, Cristina Popa¹, Roll of chromosome translocation in recurrent spontaneous abortion . Obstetrics & Gynecology ,(22)117 -121(2007).
6. W. P. Robinson,¹ D. E. McFadden,² and M. D. Stephenson³ The Origin of Abnormalities in Recurrent Aneuploidy/Polyploidy. Am. J. Hum. Genet. 69:1245-1254(2001).
7. Hossein Mozdarani, Anahita Mohseni Meybodi, Shabnam Zari-Moradi A cytogenetic study of couples with recurrent spontaneous abortions and infertile patients with recurrent IVF/ICSI failure. 14:(1) :1-6(2008).
8. Hungerford DA. Leucocytes cultured from small inocula of whole blood and the preparation of metaphase chromosomes by treatment with hypotonic KCl. Stain Technol;40:333-8(1965).
9. Sun NC, Chu CH, Chang CC. Staining method for banding patterns of human mitotic chromosomes. Caryologia;27:315(1973).
10. Celep F, Karagüzel A, Ozeren M, The frequency of chromosomal abnormalities in patients with reproductive failure. Eur J Obst Gyn Reprod Biol;127(1):106-9((2006).
11. SB Nair, G Mukundan, BM Paul, L Ramachandran, KK Gopinathan, (2006) Chromosome 12;15 rearrangements in patients with recurrent miscarriage .Indian J Hum Genet 12: (3).133-139(2005).
12. Nilüfer Karadeniz,¹ Kristin Mrasek,² and Anja Weise² Further delineation of complex chromosomal rearrangements in fertile male using multicolor banding. Bio. Med(1):1-17(2008).

- Bashamboo, Mohammed Mahidur Rahman, Aparna Prasad. Fate of PABY, DYS1, DYZ3 and DYZ1 loci in Indian patients harbouring chromosomal anomalies. *Molecular Human Reproduction* 11(2):117-126 (2005).
1. Toni M, Tüttelmann F, Gromoll J, Nieschlag E. Clinical consequences of deletions of the Y chromosome: the extended Münster experience. *Hum Reprod* 16:289-303 (2005).
15. Joly-Helas, C. de La Rochebrochard, N. Mousset. Complex chromosomal rearrangement and intracytoplasmic sperm injection: A case report. *Human Reproduction* 2007. 22(5):1292-1297 (2007).
16. Jensen AM, Garn ID, Aksglaede L, Juul A, Rajpert-De Meyts E. A simple screening method for detection of Klinefelter syndrome and other chromosome aneuploidies based on copy number of the androgen receptor gene. *Mol Hum Reprod* 13:745-50 (2007).
17. Tre M, Painter JN, Ulander VM, Kaaja R, Aittomäki K. Sex chromosome characteristics and recurrent miscarriage. *J Fertil Steril*; 90(6):2328-2332 (2008).
18. Sudhury SR, Knapp LA. Human reproductive failure II: Immunogenetic and interacting factors. *Hum Reprod Update*, 7: 135-145 (2001).
19. Se C, Steffensen R, Varming K, Christiansen OB. A study of HLA-DRB1*03:01 alleles in 588 patients and 562 controls confirms that HLA-DRB1*03 is associated with Recurrent Miscarriage. *Hum Reprod*, 19: 1215-1221 (2004).

The Adhesion of *Candida albicans* to Epithelial Cells in Diabetes Mellitus Patients

Najah Ali Mohammed ,Bara'a Jawad Kadhim ,and Ibtisam Mohammad Hussain

الخلاصة

تم تحديد نسبة التصاق المبيضات الفطرية على الخلايا الطلانية الفموية في مرضى السكري بطريقة الالتصاق الدائرية، حيث عزلت عزلة من المبيضات الفطرية من كل مريض بطريقة تركيز غسول الفم، وتم تقشير كل من الخلايا الطلانية الفموية والحنيكية لدراسة مدى تأثير كل من مصدر الكربون في الوسط الزرع، مصدر الخلايا الطلانية بالإضافة الى عاملي الجنس والتدخين في عملية التصاق المبيضات الفطرية على الخلايا الطلانية الفموية. استخدم كل من سكر الكلوكوز والسكرور واللاكتوز في الوسط الزرع كمصدر للكربون حيث وجد ان الخلايا الطلانية الفكية تحتفظ بشكل اكثر معنوية مقارنة بالخلايا الطلانية الفموية. وكان الالتصاق اكثر بوجود سكريات في الوسط الزرع. (in vitro) بالمبيضات الفطرية

ABSTRACT

We determined the adhesion of *Candida albicans* to oral epithelial cells in diabetic patients by an autologous adhesion assay with exfoliated buccal or palatal epithelial cells and one strain of *C. albicans* isolated from each patient by concentrated oral rinse technique, and investigated the influence of the carbon source of the growth medium, source of epithelial cells, and the influence of gender and smoking on the adhesion. Glucose, sucrose and galactose were used as the predominant carbon source of the growth medium. The autologous strain of *C. albicans* adhered selectively to the oral mucosa of diabetic patients. Palatal epithelial cells retained significantly more *C. albicans* in vitro and adhesion influenced by the availability of sugars in the growth medium.

INTRODUCTION

Candida albicans is the most common fungal pathogens isolated from the oral cavity. One of the main causes of oral candidiasis is the presence of grant amount of carbohydrates in the oral cavity (1). The susceptibility of diabetic patients to cutaneous vaginal and oral candidosis has been well documented (2) and has been linked to the ability of *C. albicans* to adhere to mucous membranes. The importance observation that in the presence of 20 mM glucose the expression of iG₃b receptor on *C. albicans* was doubled (3). This relevance in diabetic patients whose oral cavity is exposed to increased glucose levels in saliva (4). The capacity of yeast to disease depends on its ability to survive and thrive in special microenvironments within the host including the mucosa, and on a number of virulence factors that aid the pathogen's adherence to and invasion of host tissue and cells (5). This study investigated factors that may affect the adhesion of *C. albicans* to epithelial cells of insulin-using diabetic mellitus patients.

MATERIALS AND METHODS

The present study included 108 diabetic patients, none of whom had received antibiotic, corticosteroid or antifungal therapy. *Candida albicans* was isolated from each patient by concentrated oral rinse technique (6). *Candida albicans* was identified by germ-tube formation (7) and by yeast identification system API 20C (8).

Adhesion of the subjects' own strain of *C. albicans* to their buccal and palatal epithelial cells was determined by an autologous adhesion assay. The adherence of *C. albicans* to epithelial cells was measured *in vitro* after growth of the yeast to stationary phase in defined medium containing glucose, sucrose, and galactose as the carbon sources. An overnight culture of *C. albicans* in Sabouraud's dextrose was tested and adjusted to 10^7 *C. albicans* / ml, and 1 ml was incubated with 1 ml suspension containing 10^5 buccal and palatal cells obtained by gently rubbing the oral mucosa with sterile cotton swabs, followed by dispersion in sterile phosphate-buffered saline (PBS, pH 7.2) (9). The mixture was incubated in an orbital shaker operating at 100 rpm at 37°C for 1 hr. The epithelial cells with attached yeast were harvested and washed with 5 ml volumes of PBS on a polycarbonate filter. The filters were air-dried, fixed in methanol at room temperature, stained with Gram crystal violet and examined under a microscope. The number of *C. albicans* cells attaching to 100 single epithelial cells was counted.

The effects of addition of sugars to the growth medium and source of epithelial cells were evaluated in the adhesion assay. The reproducibility of the autologous assay was determined as was the association between the adherence of *C. albicans* and patient parameters such as gender and smoking. Candidal colonization was determined by counting the number of colonies on the primary isolation plate with a colony counter and converted to CFU/ml of oral rinse.

RESULTS AND DISCUSSION

The study group was 108 diabetic patients (20-70) years old, mean (45) years, female 69 (69%), male 39 (36.01%). *C. albicans* isolated from patients & identified by characters on Sabouraud's agar and identification system API 20C (figure 1).



(+ + + + + - + + - +)
 (+)=Positive. (-)=Negative.

Figure -1: Identification of *C.albicans* by API 20C AUX.

The adherence of *C.albicans* to epithelial cells was measured *in vitro* after growth the yeast to stationary phase in medium contains glucose, sucrose, and galactose as the carbon source. The rate of yeast formation grown in medium contains 500 mM concentration of the different sugars correlated well with the relative adherence of the *C.albicans* to epithelial cells (Table 1) compares the adherence of *C.albicans* grown in medium contains 500 mM concentration of different sugars as the carbon source.

Table-1: Adherence of *C.albicans* grown in media containing different sugars as carbon source to oral epithelial cells:

Carbon source	Mean (SD)/adhesion of yeast cells/100 epithelial cells
Sucrose 500m M	202 (124)*
Galactose 500mM	191 (101)
Glucose 500mM	104 (79)

* Significant at the ($P < 0.05$).

Adherence was enhanced according to the carbon source used. Sucrose & galactose were the most. The specific role of the organism to synthesize extracellular glucans from this effective sugars of these tested. The specific role of the organism to synthesis extracellular glucans from this sugars which inturn allow it to accumulate on the tooth surface.

The palatal epithelial cells retained more *C.albicans*, but there was no demonstrable association between the adhesion of *C.albicans* to buccal epithelial cells and oral candidiasis, (table 2), gender & smoking were not associated with a significant increase in the adhesion of *C.albicans* to buccal epithelial cells of patients.

Table Adhesion of *C.albicans* to oral epithelial cells:

Param		Mean (SD)number of yeast cells/epithelial cells
Buccal	epithelial cells	1.21 (2.11)
Palatal	epithelial cells	8.85(12.72)*

* Significant at the ($P<0.05$).

The current study revealed increase in the adhesion of *C. albicans* to buccal epithelial cells when sugars (sucrose, galactose) were added to the growths medium. Galactose was the most effective sugar of these tested, yeasts harvested from medium containing 500mM galactose showed more than 10 fold greater adherence than cells grown in medium with 50mM glucose (1,19). Mc Courtic and Douglas (12) reported a five-fold increase in adhesion when isolates *C. albicans* from patients with active infection were grown in broth containing 500mM sucrose. The effect of sugars can be due to the production of a mannose protein surface layer which is known to enhance adhesion (B), which is virtually absent in yeast grown in media containing 50mM glucose (14). It is possible that the accumulation of glycosylation products in epithelial cells may increase the number of receptors for *C. albicans* on epithelial cells surfaces. Also high secondary glucose levels which are commonly seen in diabetic patients (3,15) may produce increased resistance to intracellular killing by phagocytosis (16).

We used autologous adhesion assay system (i.e. both buccal cells and *C. albicans* isolated from the same patients). Epithelial cells were used because they represent a natural mucocutaneous surface which is a common site for candidal infection in vivo. A *Candida albicans* isolate from each patient was used as the test organism and also has been shown to adhere to buccal epithelial cells (8, 17).

This is in agreement with (15) that the present study observed that in vivo palatal cells retained significantly more *C. albicans* than buccal cells. *C. albicans* is most prevalent in the palate, tongue & gingival. The palatal cells which are more resistant to the stringent washing procedures used in autologous adhesion assay system and the palate is a common site for intraoral candidal infection.

The results of the present study could also be showed that the mean candidal adhesion to buccal epithelial cells of females was higher than in males but the difference between the groups was not significant. This has also been reported for healthy individuals (18). Smoking increased the number of *C. albicans* cells attaching to buccal epithelial cells of diabetic patients. It has been suggested that tobacco smoking may lead to localized epithelial alterations that facilitate *Candida* adherence (19).

REFERENCES

1. Pizzo, G., Giuliona, G., Milici, M.E and Glangreco, R.: Effects of dietary carbohydrates on the in vitro, epithelial adhesion of *Candida albicans*, *Candida tropicalis* and *Candida krusei*. New Microbiol. 23:36-71 (2000).
2. Lamey, P.J, Darwaza, A., Fisher, B.M., Samaranayake, L.P., Macfarlane, T.W., and Frier, B.M.: Secretor status candidal carriage and candidal infection in patients with diabetes mellitus, J. oral pathol. 17:354-357 (1988).
3. Hostetter, M.K.: Perspectives in diabetes. Handicaps to host defense: effects of hyperglycemia on C₃ and *Candida albicans*. Diabetes. 39:271-275 (1990).
4. Steele, C., Leigh, J., Swoboda, R., H., Ozenci, H., and Fidel, P.L.: Potential role for carbohydrate moiety in anti-candida activity of human oral epithelial cells. Infect. Immune. 69:7091-7099 (2001).
5. McCarron P.A., Donnelly, R.F., Canning, P.E., McGovern, J.G., and Jones, D.S.: Bioadhesive, non-drug-loaded nanoparticles as modulators of candidal adherence to buccal epithelial cells: a potentially novel prophylaxis for candidosis. Biomaterials 25:2399-2407 (2004).
6. Willis, A.M., Coulter, W.A., and Fulton, C.R. Oral candidal age and infection in insulin-treated diabetic patients. Diabetic Med. 16:675-679 (1962).
7. Mackenzie D .W.R. Serum tube identification of *C.albicans*. J.Clin. Pathol. 15:563-565 (1993).
8. Schuffenecker , I., Freydiere, A., de Montclus, H., Gille, Y. Evaluation of four commercial system for identification of medically important yeast. Eur. J.Clin.Microbiol .Infect. Dis. 12:255-260 (1993).
9. Kimura ,L.H., and Pearsall, N.N.I. Adherence of *Candida albicans* to human buccal epithelial cells. Infect. Immun. 21:64-68 (1978).
10. Nikawa ,H., Egusa, H., Makihira, S., Ishida, K., Furukawa, M., and Hamada, T. A novel technique to evaluation the adhesion of *Candida albicans* species to gingival epithelial cells. Mycoses. 46:384-389 (2002).
11. Cotter , G., and Kavanagh, K. Adherence mechanism of *Candida albicans* .Br.J.Biomed.Sci. 57:241-249 (2000).
12. McCourtie , J. and Douglas, L.J. Relationship between cell surface composition of *Candida albicans* and adherence to acrylic after growth on different carbon sources. Infect. Immun. 32:1234-1241 (1981).
13. McCourtie, M.J., Ross, B.C., and reDE, p.c. *Candida albicans*: a review of its history ,taxonomy, epidemiology, virulence attributes and methods of strain differentiation. Int. J.Oral maxillofac. Surg. 25:137-144 (1996).
14. Douglas, L.J. Adhesion of pathogenic species to host surfaces. Microbial Sci, 2:243-247 (1985).
15. Pizzo, G., Milici, M.E., and D Angelo. M. Effect of antimicrobial mouth rinses on the in vitro adhesion of *Candida albicans* to human buccal epithelial cells. Clin. Oral Invest. 5:172-176 (2001).

- 16.Liv ,H. Transcriptional control of dimorphism in *Candida albicans* .Curr. Opin.Microbiol. 4:728 -735(2001).
- 17.Sullivan , D.J.,Moran, G.P.,and Colemaqn, D.C.*Candida albicans* :Ten years on FEMS Microbiol.Lett.253:9-17(2005).
- 18.Arendorf ,T.M.,and Walker,D.M. Oral candidal population in health and disease.Br.Dent.J.147:267-272(1977).
- 19.Nair ,R.G.,and Samaranayke,L.P. The effect of oral commensal bacteria on candidal adhesion to human buccal epithelial cells *in vitro*.J.Med.Microbiol. 45 :179-185 (1996).

The Minimal Degree of a Faithful Representation of $G = SL(2, q)$

Afra M. Ibraheem , Dunya M. Hamed and Maysa`a`Z. Salman
Dep. of Mathematics, College of Education, Al-Mustansiriya University

الخلاصة

في هذا البحث قمنا بحساب الدرجة الدنيا $p(G)$ للتمثيل التبادلي الخالص للزمرة المنتهية G والدرجة الدنيا $C(G)$ للتمثيل الخالص عن طريق المصفوفات شبه التبادلية العقدية عندما تكون G الزمرة $SL(n, q)$ ، $q = p^k$ ، حيث p عدد أولي ، $k > 0$.

ABSTRACT

In this paper we calculate the minimal degree $p(G)$ of a faithful permutation representation of a finite group G and the minimal degree $C(G)$ of a faithful representation of G by complex quasi-permutation matrices, when G equal to $SL(2, q)$, $q = p^k$, p is a prime number, $k > 0$.

INTRODUCTION

Let G be a finite group and χ be an irreducible complex character of G . let $m_Q(\chi)$ denote the Schur index of χ over Q , and $\Gamma(\chi)$ be the Galois group $Q(\chi)$ over Q . It is known that by (1), corollary 10.2(b)] $\sum_{\alpha \in \Gamma(\chi)} m_Q(\chi) \chi^\alpha$ is a character of

an irreducible $Q(G)$ -module. In (2) a quasi-permutation matrix it mean a square matrix over the complex field C with non-negative integer trace. Thus every permutation matrix over C is a quasi-permutation matrix and its then simply a complex representation of G whose character values are rational and non-negative. Behraves and Ghafarra in (3) found the characters and quasi-permutation representation of 2-groups of order less than or equal to 32, and in (2) Behraves denote the minimal degree of a faithful permutation representation of G (or of a faithful representation of G by permutation matrices) by $p(G)$, and denote the minimal degree of a faithful representation of G by complex quasi-permutation matrices by $C(G)$, and he calculated in (4) $C(G)$ and $p(G)$ for a given finite group G by quasi-permutation matrix over Q and used the classification of finite groups of order 64 from the computer program GAP.

Let $GL(n, Q)$ be the group of invertible $n \times n$ matrices over a field Q , and $SL(n, Q)$ the special linear group is a subgroup of $GL(n, Q)$ which contains all matrices in $GL(n, Q)$ of determinant one. A homomorphism from G to $GL(n, Q)$ a rational representation of G and its corresponding character will be called a rational character of G . In this paper we calculate the $p(G)$ and $C(G)$ of $G = SL(2, q)$, $q = p^k$, p is a prime number, $k > 0$.

Preliminaries

In this section we give some concepts that we shall use latter, we can found these concepts in (5), (6) and (7).

The group $\text{SL}(n, q)$

The general linear group $\text{GL}(n, F)$ is the group of invertible $n \times n$ matrices over a field F . The determinant of these matrices is a homomorphism from $\text{GL}(n, F)$ into F^* and we denote the kernel of this homomorphism by $\text{SL}(n, F)$, the special linear group. Thus $\text{SL}(n, F)$ is the subgroup of $\text{GL}(n, F)$ which contains all matrices in $\text{GL}(n, F)$ of determinant one.

In this paper we consider the case when $n = 2$ and $F = \mathbb{F}_q$ where q is a power of a prime p ($q = p^k$), $k \in \mathbb{N}$, so we have $\text{SL}(2, q)$. Note that the order of $\text{SL}(2, p^k)$ is $p^k(p^{2k}-1)$.

Conjugacy classes of $\text{SL}(2, q)$

$G = \text{SL}(2, q)$, $q = p^k$ has exactly p^k+4 conjugacy classes [6]. For any $x \in G$, we denote (x) the conjugacy class of G containing x by the table.

Table -1: The conjugacy classes of $\text{SL}(2, q)$.

x	1	z	c	D	zc	zd	a^l	b^m
$ (x) $	1	1	$\frac{(2q-1)}{2}$	$\frac{(2q-1)}{2}$	$\frac{(2q-1)}{2}$	$\frac{(2q-1)}{2}$	$q(q+1)$	$q(q-1)$

Where $1 \leq l \leq \frac{(q-3)}{2}$, $1 \leq m \leq \frac{(q-1)}{2}$

The character table of $\text{SL}(2, q)$

Let $\varepsilon = (-1)^{(q-1)/2}$, let $\rho \in C$ be a $(q-1)$ th root of unity and $\sigma \in C$ be a $(q+1)$ th root of unity. Then the complex character table of $G = \text{SL}(2, q)$ is:

Table -2: The character table of $\text{SL}(2, q)$. [6]

	1	z	c	d	a^l	b^m
1_G	1	1	1	1	1	1
ψ	Q	0	0	0	1	-1
χ_i	$q+1$	$(-1)^l(q+1)$	1	1	$\rho^{il} + \rho^{il}$	0
θ_j	$q-1$	$(-1)^l(q+1)$	-1	-1	0	$-\sigma^{jm} - \sigma^{jm}$
ζ_1	$\frac{q+1}{2}$	$\frac{\varepsilon(q+1)}{2}$	$\frac{1+\sqrt{\varepsilon q}}{2}$	$\frac{1-\sqrt{\varepsilon q}}{2}$	$(-1)^l$	0
ζ_2	$\frac{q+1}{2}$	$\frac{\varepsilon(q+1)}{2}$	$\frac{1-\sqrt{\varepsilon q}}{2}$	$\frac{1+\sqrt{\varepsilon q}}{2}$	$(-1)^l$	0
η_1	$\frac{q-1}{2}$	$\frac{-\varepsilon(q-1)}{2}$	$\frac{-1+\sqrt{\varepsilon q}}{2}$	$\frac{-1-\sqrt{\varepsilon q}}{2}$	0	$(-1)^{m+1}$
η_2	$\frac{q-1}{2}$	$\frac{-\varepsilon(q-1)}{2}$	$\frac{-1-\sqrt{\varepsilon q}}{2}$	$\frac{-1+\sqrt{\varepsilon q}}{2}$	0	$(-1)^{m+1}$

Where $1 \leq i \leq \frac{(q-3)}{2}$, $1 \leq j \leq \frac{(q-1)}{2}$, $1 \leq l \leq \frac{(q-3)}{2}$, $1 \leq m \leq \frac{(q-1)}{2}$.

Note that the character values for zc and zd can be derived from the following relations for all irreducible character χ of $SL(2, q)$:

$$\chi(zc) = \frac{\chi(z)}{\chi(1)} \chi(c), \quad \chi(zd) = \frac{\chi(z)}{\chi(1)} \chi(d).$$

A faithful representation

A representation of G with representation space V is a homomorphism $\nu: g \rightarrow \nu(g)$ of G into $GL(V)$. $GL(V)$ is the group of all linear isomorphism of a vector space V onto itself.

From the homomorphism property we have for $g, h \in G$:

$$\nu(gh) = \nu(g)\nu(h), \quad \nu(1) = 1_V$$

for all $v \in V$, where 1_V denotes the mapping on V . An immediate consequence of (1) is $\nu(g)^{-1} = \nu(g^{-1})$ for all $v \in V$.

It should be noted that a representation does not have to be injective. If this is the case, however, the representation is said to be faithful.

A faithful character

Let χ be a character of G . Then $\ker(\chi) = \{g \in G: \chi(g) = \chi(1)\}$ and χ is called faithful if $\ker \chi = 1$.

2. THE $P(G)$ OF $G = SL(2, q)$

In this section we find $P(G)$ when $G = SL(2, q)$ and $G = PSL(n, q)$, $q = p^k$, $k > 0$, where $PSL(n, q)$ is the projective special linear group which is obtained if we factor out $SL(n, q)$ by its center. We need some definitions and notations which can we found in [8].

Lemma (2.1).(8) : Let G be a finite group with a unique minimal normal subgroup. Then $P(G)$ is the smallest index of a subgroup with trivial core (see def.in[2]) (that is containing no non-trivial normal subgroup).

Definition (2.2).(8) : Let χ be a character of G such that for all $g \in G$, $\chi(g) \in \mathbb{Q}$ and $\chi(g) \geq 0$. Then we say that χ is a non-negative rational valued character.

Theorem (2.3).(8) : Let $G = PSL(2, q)$, where $q = p^n$. Then G contains only the following subgroups:

- 1) Elementary abelian p -groups of each order dividing q .
- 2) Cyclic groups of each order I with $I \mid \frac{q \pm 1}{k}$ where $k = (q-1, 2)$.
- 3) Dihedral groups of each order $2I$ with I as in (2).

- 4) Alternating group A_4 for $p > 2$ or $p = 2$ and $n \equiv 0 \pmod{2}$.
- 5) Symmetric group S_4 for $q^2 - 1 \equiv 0 \pmod{16}$.
- 6) Alternating group A_5 for $p = 5$ or $q^2 - 1 \equiv 0 \pmod{5}$.
- 7) Semi direct products of an elementary abelian group of order p^m and a cyclic group of order t for each m , $1 \leq m \leq n$, and each t such that $t \nmid p^m - 1$ and $t \nmid q - 1$.
- 8) The groups $\text{PSL}(2, p^m)$ for any m such that m divides n and $\text{PGL}(2, p^m)$ for any m such that $2m \mid n$.

Lemma (2.4).(8) : Every proper normal subgroup of $G = \text{SL}(m, k)$ is in $Z(G)$ except when $m = 2$ and $|k| = 2$ or 3 .

Lemma (2.5).(8) : Let $G = \text{SL}(2, K)$ and $\text{char}(K) \neq 2$. Then G has a unique involution (see def.in(8)).

Corollary (2.6).(8) : Let $G = \text{SL}(2, k)$ and $\text{char}(k) \neq 2$. Then $Z(G) = \{\pm I_2\}$ and $|Z(G)| = 2$. Moreover $Z(G)$ is the unique minimal normal subgroup of G and the core of any subgroup of even order is non-trivial.

Proof: $Z(G) = \{\pm I_2\}$ by (8,p.181). Since G has a unique involution so by lemma (2.4) when $q \neq 3$ the unique minimal normal subgroup of G is $Z(G)$. Now let $q = 3$, then the order of G is 24, any non-trivial subgroup of G has order 3 or even order.

If its order is 3, then in the notation of (10,38.1) we have two different classes in which the elements have order 3 (namely c and d). Since $\langle c \rangle = \langle d \rangle$ and c and d are not conjugate, the subgroup of order 3 are not normal. When its order is even it contains an element of order two.

Since G has a unique involution and $Z(G)$ is contained in such a subgroup. Therefore $Z(G)$ is the unique minimal normal subgroup of G .

Lemma (2.7).(9) : Let $G = \text{SL}(2, q)$ where $q = p^n$ is odd. Then the odd order subgroups of G are as follows:

- 1) Cyclic subgroups of each odd order dividing $q \pm 1$.
- 2) Subgroups of odd order of $T(2, q) = \left\{ \begin{pmatrix} a & b \\ 0 & a^{-1} \end{pmatrix} : a, b \in F_q, a \neq 0 \right\}$ where F_q is the finite field of q elements, and $|T(2, q)| = (q-1)q$.

Theorem (2.8): Let $G = \text{SL}(2, q)$ where q is odd. Then

$$P(G) = (q-1)_2 (q+1).$$

Proof: By lemma (2.1) we have to find a subgroup of G with maximal order and trivial core, suppose it H . If $|H|$ be even then by corollary(2.6) its core is not trivial. So $|H|$ is odd. Conversely by corollary(2.6) every subgroup of odd order has trivial core. We will use lemma(2.7) frequently.

Let $q \equiv 3 \pmod{4}$, that is $\frac{q-1}{2} \equiv 1 \pmod{2}$. By lemma (2.7) we have $|H| = q(\frac{q-1}{2})$ and $P(G) = 2(q+1)$. Let $q \equiv 1 \pmod{4}$, that is $\frac{q-1}{2} \equiv 0 \pmod{2}$ and $\frac{q+1}{2} \equiv 1 \pmod{2}$. But $q > \frac{q+1}{2} > \frac{q-1}{2}$ (as $q \geq 3$). Thus the Sylow P-subgroup of G has order exceeding than of any odd order subgroup of type (1).
 On the other hand, if $H = \left\{ \begin{pmatrix} a & b \\ 0 & a^{-1} \end{pmatrix} : a, b \in F_q, a^q = 1 \right\}$, where $q-1 = (q-1)_2 I$, then H is of type (2) and of order qI which is maximal. Hence $P(G) = (q-1)_2(q+1)$.

Lemma (2.9).(8) : Let $G = SL(2, q)$ where $q = 2^n$. Then G is a simple group when $n \neq 1$, and when $n=1$ it has a unique minimal normal subgroup, which has order 3.

Theorem (2.10): Let $G = SL(2, q)$ where $q = 2^n$. Then $P(G) = q+1$.

Proof: We show that every proper subgroup H of G has order less than or equal to $q(q-1)$. Let $P^m = q$ and $t = q-1$. Then by theorem (2.3) a subgroup of type (7) exists whose order is equal to $q(q-1)$.

Let $n = 1$. Then $|G| = 6$ and it has a subgroup of order 2 with trivial core and a normal subgroup of order 3. So $P(G) = \frac{6}{2} = 3$. Now let $n \neq 1$. Note that

$|SL(2, 4)| = 60$ and $SL(2, 4) \cong A_5$. So subgroup of type (6) cannot be considered when $n = 2$. We will use theorem (2.3) frequently.

Subgroups of type (1), (2), (3) and (7). By theorem (2.3) part (1), (2), (3) and (7) the orders of such subgroups of G are less than or equal to q , $q \pm 1$, $2(q \pm 1)$ and $q(q-1)$ respectively. But $2(q+1) < q(q-1)$ because $q^2 - 3q - 2 > 0$ when $q \geq 4$. So among these subgroups of G the maximal order is $q(q-1)$.

Subgroup of type (4). Let $n = 2k$, that is $q = 4^k$. Then G has a subgroup of order 12 by theorem (2.3) part (4). But $q(q-1) \geq 12$ (as $k \geq 1$ and $q \geq 4$).

Subgroup of type (5). As q is a power of 2, $16 \times q^2 - 1$. So S_4 is not a subgroup of G.

Subgroup of type (6). Let $2^{2n} \equiv 1 \pmod{5}$, we may assume that $n \geq 3$. Further, if $n = 3$, $2^6 = 64 \equiv -1 \pmod{5}$ so that we may assume that $n \geq 4$. Now $2^4 = 16$ and $q(q-1) \geq 16 \times 15 > |A_5| = 60$.

Subgroup of type (8). We will consider two different cases. Let $m \nmid n$ and $2m \nmid n$, that is, $n = m(2k+1)$. Theorem (2.3) part(8) implies that $PSL(2, 2^m)$ is a subgroup of G, and $|PSL(2, 2^m)| = (2^m-1)2^m(2^m+1)$. We have

$$(2^m - 1)(2^m + 1) \leq (2^{mk} - 1)(2^{mk} - 1) = 2^{2mk} - 1 \leq 2^{m(2k+1)-1}$$

$$\text{So } (2^m - 1)(2^m + 1) \leq 2^m(2^{m(2k+1)} - 1) \leq 2^{m(2k+1)}(2^{m(2k+1)} - 1) = q(q-1)$$

Now let $2m \mid n$. Then $n = 2mk$. We know that

$$|PSL(2, 2^m)| = (2^m-1)2^m(2^m+1) \text{ and } (2^m-1)(2^m+1) \leq 2^{2mk}-1 \text{ so}$$

$$(2^m - 1)2^m(2^m + 1) \leq 2^m(2^{2mk} - 1) \leq 2^{2mk}(2^{2mk} - 1) = q(q - 1).$$

Therefore in both cases $(2^m - 1)2^m(2^m + 1) \leq q(q - 1)$. Hence $P(G) = q + 1$.

Theorem (2.11): Let $G = \text{PSL}(2, q)$ where q is odd. Then $P(G) = q + 1$ except when $q = 5, 7, 9, 11$ and in these cases $P(G) = 5, 7, 6, 11$ respectively.

Proof: When $q \geq 5$, the result follows from [8] because G is simple so that every non-trivial permutation representation is faithful.

When $q = 3$, G is isomorphic to the alternating group A_4 of degree 4 in which a Sylow 3-subgroup is core-free and of minimal index among such subgroups.

3. THE $C(G)$ OF $G = \text{SL}(2, q)$

In this section we find $C(G)$ when $G = \text{SL}(2, q)$ and $G = \text{PSL}(2, q)$, by using tables (3), (4) and (5).

Definition (3.1).(6) : Let G be a finite group. Let χ be an irreducible complex character of G . Then define:

1) $d(\chi) = |\Gamma(\chi)| \chi(1)$, $\Gamma(\chi)$ is the Galois group of $Q(\chi)$ over Q .

$$2) m(\chi) = \begin{cases} 0 & \text{if } \chi = 1_G \\ \min \left\{ \sum_{\alpha \in \Gamma(\chi)} \chi^\alpha(g) : g \in G \right\} & \text{otherwise} \end{cases}$$

3) $c(\chi) = \sum_{\alpha \in \Gamma(\chi)} \chi^\alpha + m(\chi)1_G$, where $c(\chi)$ is a non-negative rational valued character of G

Corollary (3.2).(5) : Let $\chi \in \text{Irr}(G)$. Then $\sum_{\alpha \in \Gamma(\chi)} \chi^\alpha$ is a rational valued character of G , and $c(\chi)(1) = d(\chi) + m(\chi)$

Lemma (3.3): Let G be a finite group with a unique minimal normal subgroup. Then:

$$C(G) = \min \{c(\chi)(1) : \chi \text{ is a faithful irreducible complex character of } G\}$$

Proof: See (2, corollary 3.11).

Lemma (3.4): Let $\chi \in \text{Irr}(G)$. $\chi \neq 1_G$. Then $c(\chi)(1) \geq d(\chi) + 1 \geq \chi(1) + 1$

Proof: From definition(3.1) it follows that $c(\chi)(1)$ is a non-negative rational valued character of G , so by (2, Lemma 3.2), $m(\chi) \geq 1$. Now the result follows from definition 3.1.

Lemma (3.5): Let $\chi \in \text{Irr}(G)$. Then

$$1) c(\chi)(1) \geq d(\chi) \geq \chi(1)$$

$$2) c(\chi)(1) \leq 2d(\chi)$$

Equality occurs if and only if $Z(\chi)/\ker \chi$ is of even order.

Proof: (1) Follows from the definition of $c(\chi)(1)$.

(2) See(2,Lemm 3.13) .

Theorem (3.6): If $G = SL(2, q)$ where q is odd, and if χ is a faithful irreducible character of G , then $m(\chi) = 2d(\chi)$.

It follows that $C(G) = 2\min\{d(\chi) : \chi \in \text{Irr}(G), \chi \text{ faithful}\}$

Proof: Let Z be a conjugacy class of G of order 1. As χ is faithful and $Z^2 = 1$, $\chi(Z) = -\chi(1)$. Thus $z \in Z(\chi)/\ker \chi$. Therefore $Z(\chi)/\ker \chi$ is of even order. Hence by lemma (3.5), $m(\chi) = 2d(\chi)$.

As G has a unique minimal normal subgroup by corollary (3.2) the result follows from corollary (2.6).

Lemma (3.7).(11) : Let σ be a primitive $(q+1)$ th root of unity and let $q = p^n$ where p is an odd prime. Suppose that $q \equiv 7 \pmod{8}$ and that

$j = 1, 3, \dots, \frac{q-1}{2}$. Then $\sigma^j + \sigma^{-j}$ is not rational.

Corollary (3.8): Let $G = SL(2, q)$ where q is odd. If $q \equiv 3 \pmod{8}$ then $\theta_{\frac{q+1}{4}}$ is a faithful irreducible rational valued character.

Proof: Clearly from table -2-.

Theorem (3.9): Let $G = SL(2, q)$ where $q = p^n$ is odd.

If $q \equiv 1 \pmod{4}$ then

$$C(G) = \begin{cases} (q-1) & \text{if } n \text{ is even} \\ 2(q-1) & \text{otherwise} \end{cases}$$

If $q \equiv 3 \pmod{4}$ then

$$C(G) = \begin{cases} 2(q+1) & \text{if } q \equiv 7 \pmod{8} \\ 2(q-1) & \text{if } q \equiv 3 \pmod{8} \end{cases}$$

Proof: By theorem (3.6) we need to look at each faithful irreducible character χ , and calculate $d(\chi)$. By lemma (3.5) we have $d(\chi_i) \geq q+1$.

$d(\theta_j) = |\Gamma_j| (q-1) \geq q-1$ where $\Gamma_j = \Gamma(\theta(\theta_j): \theta)$. Hence $d(\theta_j) \geq q-1$. But by lemma (3.7) we can proof this inequality when $q \equiv 7 \pmod{8}$ and

$j = 1, 3, \dots, \frac{q-1}{2}$ as $|\Gamma_j| \geq 2$. So in this case $d(\theta_j) \geq 2(q-1)$. Also, when

$q \equiv 3 \pmod{8}$, then $\frac{q+1}{4}$ is odd and $1 \leq \frac{q+1}{4} \leq \frac{q-1}{2}$. So by corollary (3.8) the character $\theta_{\frac{q+1}{4}}$ is an irreducible rational valued character. Therefore $|\Gamma_{\frac{q+1}{4}}| = 1$

and $d(\theta_{\frac{q+1}{4}}) = q-1$. $d(\zeta_1) = d(\zeta_2) = \frac{1}{2} |\Gamma_\zeta| (q+1)$ where

$\Gamma_\zeta = \Gamma(Q(\zeta_1): Q) = \Gamma(Q(\zeta_2): Q)$, $d(\eta_1) = d(\eta_2) = \frac{1}{2} |\Gamma_\eta| (q-1)$ where

$\Gamma_\eta = \Gamma(Q(\eta_1): Q) = \Gamma(Q(\eta_2): Q)$

Moreover

$$|\Gamma_\zeta| = |\Gamma_\eta| = \begin{cases} 1 & \text{if } n \text{ is even and } \varepsilon = 1 \\ 2 & \text{otherwise} \end{cases}$$

First let $q \equiv 1 \pmod{4}$. Then by (10) we have $\varepsilon = 1$. Hence the faithful irreducible characters are $\eta_1, \eta_2, \chi_1, \chi_3, \dots, \chi_{\frac{q-3}{2}}, \theta_1, \theta_3, \dots, \theta_{\frac{q-3}{2}}$.

For n even we have $d(\eta_1) = d(\eta_2) = \frac{1}{2}(q-1)$ and this is the minimal value.

For n odd we have $d(\eta_1) = d(\eta_2) = q-1$.

Next let $q \equiv 3 \pmod{4}$, then by (5) we have $\varepsilon = -1$. Hence the faithful irreducible characters are $\zeta_1, \zeta_2, \chi_1, \chi_3, \dots, \chi_{\frac{q-5}{2}}, \theta_1, \theta_3, \dots, \theta_{\frac{q-1}{2}}$. In this case

$d(\zeta_1) = d(\zeta_2) = q+1$. Finally, note that when $q \equiv 3 \pmod{8}$, $\theta_{\frac{q+1}{4}}$ is rational valued and $d(\theta_{\frac{q+1}{4}}) = q-1$, the minimal value.

When $q \equiv 7 \pmod{8}$, then by lemma (3.7), the minimal value is achieved by ζ_1 as $2(q-1) \geq q+1$.

An overall picture is provided by the table -3-, compiled using lemma (3.6) and (10).

Table -3: The minimal value for a faithful representation of $G = \text{SL}(2, p^n) \cap \text{Cz}$

q	$\equiv 1 \pmod{4}$		$\equiv 3 \pmod{4}$	
q	n even	n odd	$\equiv 3 \pmod{8}$	$\equiv 7 \pmod{8}$
$d(\chi_i)$	$\geq q+1$	$\geq q+1$	$\geq q+1$	$\geq q+1$
$d(\theta_j)$	$\geq q-1$	$\geq q-1$	$\geq q-1$	$\geq 2(q-1)$
$d(\zeta_i)$	Not faithful	Not faithful	$q+1$	$q+1$
$d(\eta_i)$	$\frac{1}{2}(q-1)$	$q-1$	Not faithful	Not faithful
$C(G)$	$q-1$	$2(q-1)$	$2(q-1)$	$2(q+1)$

Theorem (3.10): Let $G = \text{SL}(2, 2)$. Then $d(\psi) = 2$, $c(\psi)(1) = 3$, $C(G) = 3$.

Proof: From (11) the Schur index (see def.in (8)) of each irreducible character is 1. Since the only faithful irreducible character of G is ψ , the result follows.

Lemma (3.11).(1): Let $G = \text{PSL}(2, q)$ where $q = p^n$ and q is odd. Let n be odd and $q \notin C = \{3, 5, 7, 11\}$. Then $c(\theta_j)(1) \geq q+1$ for j , $0 \leq j \leq \frac{q-1}{2}$.

Theorem (3.12): Let $G = \text{PSL}(2, q)$ where $q = p^n$ is odd. Then:

$$1) C(G) = \begin{cases} \frac{1}{2}(q + \sqrt{q}) & \text{if } n \text{ is even} \\ q+1 & \text{otherwise} \end{cases}, \text{ if } q \notin \{5, 7, 11\};$$

2) $C(G) = 5, 7, 11$, if $q = 5, 7, 11$, respectively.

Proof: From (11) the Schur index of each irreducible character is 1, and ψ is an irreducible rational valued character of G . So $c(\psi)(1) = q+1$.

From lemma (3.5), for all i , $c(\chi_i)(1) \geq q+1$.

That $c(\theta_j)(1) \geq q+1$ for all j was shown in lemma (3.11).

Let $q \notin \{3, 5, 7, 11\}$. If $q \equiv 1 \pmod{4}$ then by (11)

$$c(\zeta_1)(1) = c(\zeta_2)(1) = \begin{cases} \frac{q+1}{2} + \frac{\sqrt{q}-1}{2} = \frac{q+\sqrt{q}}{2} & \text{if } n \text{ even} \\ q+3 & \text{otherwise} \end{cases}$$

If $q \equiv 3 \pmod{4}$ then $\varepsilon = -1$ and by (8)

$$c(\eta_1)(1) = c(\eta_2)(1) = q+1$$

$$\text{As } q+2 \geq \sqrt{q}, q+1 \geq \frac{q+\sqrt{q}}{2}.$$

This establishes (1) as can be seen in the summary tables which follows:

Table -4: The minimal value for afathful representation of $G = \text{PSL}(2, p^n) n \in \mathbb{Z}$

q	$\equiv 1 \pmod{4}$		$\equiv 3 \pmod{4}$	
q	n even	n odd	$\equiv 3 \pmod{8}$	$\equiv 7 \pmod{8}$
$d(\psi)$	q	q	q	q
$d(\chi_i)$	$\geq q+1$	$\geq q+1$	$\geq q+1$	$\geq q+1$
$d(\theta_j)$	$\geq q-1$	$\geq q-1$	$\geq q-1$	$\geq q-1$
$d(\zeta_i)$	$\frac{1}{2}(q+1)$	q+1	No ζ_1 exists	No ζ_1 exists
$d(\eta_i)$	No η_1 exists	No η_1 exists	q-1	q-1
$c(\psi)(1)$	q+1	q+1	q+1	q+1
$c(\chi_i)(1)$	$\geq q+1$	$\geq q+1$	$\geq q+1$	$\geq q+1$
$c(\theta_i)(1)$	$\geq q+1$	$\geq q+1$	$\geq q+1$	$\geq q+1$
$c(\zeta_i)(1)$	$\frac{q+\sqrt{q}}{2}$	q+3	No ζ_1 exists	No ζ_1 exists
$c(\eta_i)(1)$	No η_1 exists	No η_1 exists	q+1	q+1
$C(G)$	$\frac{q+\sqrt{q}}{2}$	q+1	q+1	q+1

Now let $q \in \{3, 5, 7, 11\}$. We will show that when $q \in \{5, 7, 11\}$ then $c(\theta_j)(1) = q$ and this value is minimal.

From lemma (3.5) we have:

Table -5: The minimal value for afathful representation of $G = \text{SL}(2, q) q \in \{3, 5, 7, 11\}$

q	3	5	7	11
$d(\psi)$	3	5	7	11

$d(\chi_i)$	No χ_i exists	No χ_i exists	≥ 8	≥ 12
$d(\theta_j)$	No θ_j exists	4	6	10
$d(\zeta_1)$	No ζ_1 exists	6	No ζ_1 exists	No ζ_1 exists
$d(\eta_1)$	2	No η_1 exists	6	10

Let $q = 3$. Then $\psi_1\eta_1$ and η_2 are the faithful irreducible characters of G . Note that $d(\eta_1) = d(\eta_2) = 2$ and $m(\eta_1) = m(\eta_2) = 2$. Therefore $C(G) = 4$.

Let $q = 5$. Then the irreducible characters of G are ψ , θ_2 , ζ_1 and ζ_2 . Here θ_2 is rational valued. Also $m(\theta_2) = 1$ so $c(\theta_2)(1) = 5$. Therefore $C(G) = 5$.

Let $q = 7$. Then the irreducible characters of G are ψ , χ_2 , θ_2 , η_1 and η_2 . But $m(\theta_2) = 1$ so $c(\theta_2)(1) = 7$. Also by lemma (3.4) we have $c(\eta_1)(1) = c(\eta_2)(1) \geq 7$.

Let $q = 11$. Then the irreducible characters of G are ψ , χ_1 , χ_4 , θ_2 , θ_4 , η_1 and η_2 . But $m(\theta_2) = 1$ so $c(\theta_2)(1) = 11$. Also by lemma (3.4) we have $c(\theta_4)(1) \geq 11$ and $c(\eta_1)(1) = c(\eta_2)(1) \geq 11$. Therefore $C(G) = 11$.

REFERENCES

1. Isaacs I.M., Character theory of finite groups. 1976, Academic Press, London.
2. Behraves H., Quasi-permutation representations of P -groups of class 2. J. London Math. Soc. (2) 55:241-250(2000).
3. Behraves H. & Ghafarrarzadeh G., Characters and quasi-permutation representations of 2-groups of order ≤ 32 . J. Far East J. Math. Sci. 23, (3):361-367 (2006).
4. Behraves H. and Ghafarrarzadeh G., Quasi-permutation representations of group of order 64. Turk J. Math. 31:1-6(2007).
5. Allenby R.B.J.T., Rings, fields and groups: an introduction to abstract algebra, Edward Arnold, London(1986).
6. Katrin E.G., Ordinary characters of finite special linear groups, School of Math. And Sta., Univ. of St Andrews(2002).
7. Rotman J.J., An introduction to the theory of groups, 4th ed., Springer-Verlag, New York(1995).
8. Huppert B., Endliche Gruppen I, Springer-Verlag, Berlin(1967).
9. Ghorbany M., Simple representations of some simple groups with minimal degrees. Acta Math. Acad. 24:287-296(2008).
10. Dornhoff L., Group representation theory., Marcel Dekker, New York(1971).
11. Shahabi Shojaei M. A., Schur indices of irreducible characters of $\text{SL}(2, q)$. Arch. Math. Basel 40:212-213 (1983).

Single Machine with Multicriteria Problems

¹Tariq Salih Abdul-Razaq and ²Fadia Mohammed Salman

¹Department of Mathematics, Collage of Science University of Al-Mustansiriyah

²Al-Resafa Elec. Distribution Dep, Ministry Of Electricity

الخلاصة

مجال المسألة التي أختيرت لهذا البحث تخص مشكلة جدولة الماكينة الواحدة و المقاييس التي بُحثت هي أعظم غرامة للتأخير مع أخذ الوزن بنظر الاعتبار و المجموع الوزني لأوقات الإتمام. لذا ناقشنا في هذه الرسالة مسألتين ثنائية المعايير لجدولة (n) من الأعمال على ماكينة واحدة:

1. تصغير مجموع أوقات الإتمام بشرط أن أعظم تأخير وزني يكون أمثل.
 2. تصغير حاصل جمع المجموع الوزني لأوقات الإتمام وأعظم تأخير موزون.
- فيما يخص المسألة الأولى اقترحنا خوارزمية والتي أعطت حل أمثل لهذه المسألة وهي مسألة ثنائية المعايير متتابعة. وتم برهنة الأمثلية لهذه الخوارزمية.

فيما يخص المسألة الثانية والتي عُرفت بأنها NP-hard. تم اشتقاق قيد أدنى (LB) جيد ويعتمد على تجزئة الهدف، لكي نتمكن من تصميم خوارزمية التفرع والتقييد (BAB) التي تستخدم لإيجاد الحل الأمثل لهذه المسألة. ونتيجة لصعوبة الأمثلية لأكثر من هدف سوية لذلك يقترح بأنه ليس بالإمكان دائماً إيجاد حل أمثل لهذه المسألة وبطريقة سريعة. لذلك وبدلاً من البحث عن الحل الأمثل وبذل مجهود حسابي كبير، و كبديل يمكن استخدام طرائق الحل المحلية (Local search methods) لتوليد حلول تقريبية وهي قريبة من الحل الأمثل وفي زمن حسابي أقل. طورنا طرائق الحل المحلية والتي تهدف الى إيجاد حل قريب من الحل الأمثل لهذه المسألة.

وبعد ذلك تم تطبيق بعض هذه الطرائق مثل

Descent method (DM), simulated annealing (SA), tree type heuristic method (TTHM) and genetic algorithm (GA).

كذلك قدمنا اختبارات حسابية للطرائق الحل المضبوطة والمحلية على مجموعة كبيرة من المسائل الاختبارية وكانت النتائج:

- أن خوارزمية التفرع والتقييد (BAB) كفوءة للمسائل ذات الحجم الصغير من الأعمال.
- 2. أداء طرق الحل المحلية كفوءة للمسائل ذات الحجم الكبير من الاعمال. وعند اختبار كفاءة هذه الطرائق التقريبية على مجموعة كبيرة من المسائل الاختبارية، كانت النتائج تشير إلى أن أداء طريقة (SA) هي الافضل مع وقت حسابي معقول.

ABSTRACT

The problem domain chosen for this research is the single machine scheduling problem, and the performance measures investigated are maximum weighted tardiness and total weighted completion time. Hence, the following two bicriteria scheduling problems of n jobs on a single machine are discussed:

- a) Minimizing total completion times subject to the maximum weighted tardiness is optimal.
- b) Minimizing the sum of total weighted completion times and the maximum weighted tardiness.

For the first problem, an algorithm is proposed which gives optimal solution for this hierarchical bicriteria problem. Also the optimality proof for this algorithm is given.

For the second problem which is known as NP-hard. We derive a good lower bound based on objective splitting, in order to design a branch and bound (BAB) algorithm for its solution. The NP-hardness of this second simultaneous optimization problem suggests that it is not always possible to find an optimal solution quickly. Therefore, instead of searching for an optimal solution with enormous computational effort, we may use a local search to generate approximate solutions that are close to the optimum with considerably less computational time. We develop, local search heuristics methods that aim to find near optimal solutions for this problem. We then adopted some of these local search methods such as descent method (DM), simulated

annealing (SA) method, tree type heuristic (TTH) method and genetic algorithm (GA).

We present computational experiments for the exact and local search methods on a large set of test problems, it seems that

- a) The BAB algorithm is efficient for small size problems.
 - b) The performance of these local search methods on large size problems are very effective, and the performance of (SA) method is the best and within reasonable search time.
-

INTRODUCTION

Scheduling problems in real life applications generally involve optimization of more than one criterion. These criteria are often conflicting in nature and are quite complex(1).

This research addresses the bicriteria scheduling problems involving single

machine. A practical application of this would be to minimize the cost of production or production time given the penalty for delaying the product. There are basically two approaches for multiple criteria : The hierarchical approach (or Lexicographical) , which is denoted by $Lex(f,g)$, where f and g are two performance criteria, and the simultaneous approach.

In this research we consider the problem of scheduling n jobs on a single machine for a variety of multicriteria. Our object is to find a schedule that minimize the multicriteria for the following problems:

- The total completion times subject to the constraint that the maximum weighted tardiness is optimal (i.e. $1//Lex(T_{max}^w, \sum C_j)$) problem.
- The sum of the total weighted completion times and the maximum weighted tardiness (i.e. $1//\sum w_j C_j + T_{max}^w$) problem .

For the first problem, proposed an algorithm for finding optimal solution and proved its optimality, for the second problem, two special cases are proposed and proved concerning the optimality, as well as branch and bound algorithm based on a lower bound obtained from the decomposition of objectives of $1//\sum w_j C_j + T_{max}^w$ problem.

Also heuristic approaches have been proposed for this problem: local search algorithm such as descent method, simulated annealing algorithm, tree type heuristic method, and genetic algorithm.

Formulation of the problems:

Our multiple objective problem can be described as follows:

$$V_1 = \min_{\sigma \in S} Lex(T_{\max(\sigma)}^w, \sum_{j=1}^n C_{\sigma(j)})$$

S.t.

$$(P_1) \quad \left. \begin{array}{ll} C_{\sigma(j)} \geq P_{\sigma(j)} & j = 1, \dots, n \\ C_{\sigma(j)} = C_{\sigma(j-1)} + P_{\sigma(j)} & j = 2, \dots, n \\ T_{\sigma(j)} \geq C_{\sigma(j)} - d_{\sigma(j)} & j = 1, \dots, n \\ T_{\sigma(j)} \geq 0 & j = 1, \dots, n \end{array} \right\}$$

$$T_{\max(\sigma)}^w = \min_{\sigma \in S} \left\{ \max \{w_j T_{\sigma(j)}\} \right\}$$

Where $\sigma(j)$ denotes the position of job j in the ordering σ and S denotes the set of all enumerated schedules.

$$V_2 = \min_{\sigma \in S} \left\{ \sum_{j=1}^n w_{\sigma(j)} C_{\sigma(j)} + T_{\max}^w(\sigma) \right\}$$

S.t.

$$(P_2) \quad \left. \begin{array}{ll} C_{\sigma(j)} \geq P_{\sigma(j)} & j = 1, \dots, n \\ C_{\sigma(j)} = C_{\sigma(j-1)} + P_{\sigma(j)} & j = 2, \dots, n \\ T_{\sigma(j)} \geq C_{\sigma(j)} - d_{\sigma(j)} & j = 1, \dots, n \\ T_{\sigma(j)} \geq 0 & j = 1, \dots, n \end{array} \right\}$$

Algorithm for finding an optimal value for (P1)

The following algorithms suggest a scheme for solving the $1//Lex(T_{\max}^w, \sum C_j)$ problem.

An algorithm :

Step (1): Compute T_{\max}^w by using (Lawler algorithm [2]).

Step (2): Compute $t = \sum_{j=1}^n p_j$ and set $N = \{1, \dots, n\}$, $k=n$.

Step (3): Calculate $T_j \quad \forall j \in N$ as follows:

If $t \leq d_j$ then $w_j T_j = 0$ otherwise $w_j T_j = (t - d_j)w_j$.

Find the job $j^* \in N$ with smallest $w_j T_j = (t - d_j)w_j \leq T_{\max}^w$,

then

sequence j^* in position $\sigma(k)$ if there exists a tie, choose the

job j^*

with largest P_{j^*} .

Step (4): $t = t - p_{j^*}$, $N = N - \{j^*\}$, $k=k-1$ if $k \leq 1$ go to step (3), otherwise

go to step (5).

Step (5): compute $\sum_{j=1}^n C_{\sigma(j)}$.

Step (6): Stop.

To illustrate the algorithm for the $1//Lex(T_{\max}^w, \sum C_j)$ problem, we give the following example:

Example (1): Consider the $1//Lex(T_{\max}^w, \sum C_j)$ problem with five jobs. To find the minimum $\sum C_j$, subject to T_{\max}^w is optimal.

Table -1: Data for processing times, due dates and weights.

j	1	2	3	4	5
p_j	2	3	4	5	8
d_j	12	17	10	20	13
w_j	2	5	4	3	6

By applying Lawler's algorithm (step (1)) we get a schedule $\sigma = (3, 5, 1, 2, 4)$, for this schedule σ we compute $T_{\max}^w(\sigma)$.

j	3	5	1	2	4
p_j	4	8	2	3	5
d_j	1 0	4 3	1 2	1 7	2 0
w_j	4	6	2	5	3
C_j	4	1 2	1 4	1 7	2 2
T_j	0	0	2	0	2
$w_j T_j$	0	0	4	0	6

It is clear from the table that $T_{\max}^w(\sigma) = \max_j \{w_j T_j\} = 6$. A schedule that minimizes the total completion time ($\sum C_j$) is, constructed by the above algorithm, given in the following table.

$t = \sum$	1	2	3	4	5	j^*
2 2	2 0	2 5	4 8	6	5 4	4
1 7	1 0	0	2 8	*	2 4	2
1 4	4	*	1 6	*	6	5
6	0	*	0	*	*	3
2	0	*	*	*	*	1

The entries in column j ($j=1, \dots, 5$) are respectively

- * it job j has already scheduled,
- or $w_j(t - d_j)$ weighted tardiness of job j ,
- or \bigcirc it is possible to schedule job j last.

The final schedule may be found by reading up the final column (j^*) and the minimum value of $\sum C_j$ found by the following table :

J	1	3	5	2	4
p_j	2	4	8	3	5
d_j	12	10	13	17	20
w_j	2	4	6	5	3
C_j	2	6	14	17	22
T_j	0	0	1	0	2
$w_j T_j$	0	0	6	0	6

Hence the optimal schedule is $\sigma' = (1, 3, 5, 2, 4)$, and minimum $\sum_{j=1}^n C_{\sigma'(j)} = 61$, which gives $T_{\max}^w(\sigma') = 6$.

Proposition (1):

The above algorithm gives an optimal solution for $1//Lex(T_{\max}^w, \sum C_j)$ problem.

Proof:

Since the problem $1//Lex(T_{\max}^w, \sum C_j)$ can be written as:

$$\text{Min } \sum C_j \quad \dots\dots\dots (1)$$

S.t.

$$\begin{aligned} w_j T_j = w_j (C_j - d_j) &\leq T_{\max}^w, \quad j=1, \dots, n \\ &= w_j \left(\sum_{i=1}^j p_i - d_j \right) \leq T_{\max}^w \\ &= w_j (t - d_j) \leq T_{\max}^w \quad \dots\dots\dots (2) \end{aligned}$$

First notice that any job j^* that is chosen in step (3) of the above algorithm to be scheduled last must satisfy (2) (i.e. $w_j T_j < T_{\max}^w$, this does not make the weighted tardiness of the chosen job j^* violate the maximum weighted tardiness schedule (T_{\max}^w) (which is obtained by Lawler algorithm). Second, if there exists a tie (more than one job j^*) then we choose the job j^* with largest p_j to be scheduled last which

minimizes $\sum C_j$ also. Hence, any schedule constructed by the algorithm is optimal. \square

Remark (1):

The problem $1//Lex(T_{\max}^w, \sum w_j C_j)$ cannot be solved by the above algorithm. Since the optimality with respect to the primary criterion (T_{\max}^w) yields a set of deadlines that have to be obeyed when minimizing the secondary criterion ($\sum w_j C_j$). Hence, the above $1//Lex(T_{\max}^w, \sum w_j C_j)$ problem is equivalent to the $1|\bar{d}_j|\sum w_j C_j$ problem, which is known to be NP-hard in the strong sense (3).

Remark (2):

We can modify the algorithm described in section (3) for the problem $1//Lex(T_{\max}^w, \sum w_j C_j)$ which gives good results. The modification is in step (3) of the above algorithm, when a tie exists for the choice of job j^* , then we choose the job j^* with largest ratio $\frac{p_j}{w_j}$ to be scheduled last. This job

j^* minimizes $\sum w_j C_j$, Remark (3):

It should be noted that the optimal solution for the $1//Lex(T_{\max}^w, \sum C_j)$ problem (i.e., (6, 61) in the example (1)), which is obtained by the above algorithm, is one of the efficient solutions for the $1//(\sum w_j C_j, T_{\max}^w)$ problem, which is NP-hard.

Some Special Cases for the Problem (P2) :

The aim in problem (P2) is to find a processing order of the jobs on a single machine to minimize the sum of the total weighted completion times and the maximum weighted tardiness (i.e. $1//\sum w_j C_j + T_{\max}^w$ problem). Finding special cases for scheduling problem means finding an optimal schedule directly without using mathematical programming techniques. In problem with multiple objective functions it is more difficult to find such special cases, since each condition must satisfy both of the objectives. Now two special cases are states and proved:

Case (1): If SWPT schedule gives $T_{\max}^w(SWPT) = T_{\max}^w(Lawler)$, then SWPT schedule is optimal for $\sum w_j C_j + T_{\max}^w$ problem.

Proof :

Since T_{\max}^w is minimized by Lawler's algorithm and since SWPT gives the minimum of $\sum w_j C_j$ and also gives $T_{\max}^w(SWPT) = T_{\max}^w(Lawler)$, then SWPT is optimal for $\sum w_j C_j + T_{\max}^w$ problem.

Case (2): If SWPT schedule gives $C_j \leq d_j \forall j$, then SWPT schedule is optimal for $\sum w_j C_j + T_{\max}^w$ problem.

Proof:

Since SWPT schedule gives $C_j \leq d_j \forall j$, this means that all jobs are early. Hence $T_{\max}^w = \max \{w_j T_j\} = 0$, $T_{\max}^w = \max \{w_j T_j\} = \max w_j \{C_j - d_j, 0\} \forall j$, then SWPT schedule is optimal for $\sum w_j C_j + T_{\max}^w$ problem. \square

Note this problem (P2) is decomposed in to two subproblems with a simple structure, as shown later and we state some results which help us in solving the problem (P2) by using branch and bound (BAB) method.

Decomposition of problem (P2) :

We decompose the second problem (P2) in to two subproblems with a simpler structure. The object of the second problem is

$$V_2 = \min_{\sigma \in S} \left\{ \sum_{j=1}^n w_{\sigma(j)} C_{\sigma(j)} + T_{\max}^w(\sigma) \right\}$$

This problem (P2) can be decomposed into two subproblems as follows:

$$\begin{aligned}
 N_1 &= \min_{\sigma \in S} \sum_{j=1}^n w_j C_{\sigma(j)} \\
 \text{S.t.} \quad & C_{\sigma(j)} \geq P_{\sigma(j)} \quad j = 1, \dots, n \\
 & C_{\sigma(j)} = C_{\sigma(j-1)} + P_{\sigma(j)} \quad j = 2, \dots, n \\
 N_2 &= \min \left\{ \max \left\{ w_j T_{\sigma(j)} \right\} \right\} \\
 \text{S.t.} \quad & T_{\sigma(j)} \geq C_{\sigma(j)} - d_{\sigma(j)} \quad j = 1, \dots, n \\
 & T_{\sigma(j)} \geq 0 \quad j = 1, \dots, n
 \end{aligned}
 \quad \left. \begin{array}{l} \\ \\ \\ \end{array} \right\} \begin{array}{l} (Sp_1) \\ \\ (Sp_2) \end{array}$$

Theorem (1): (4)

$N_1 + N_2 \leq V_2$ where N_1 , N_2 and V_2 are the minimum objective function values of (SP1), (SP2) and (P2) respectively \square .

Derivation of Lower Bound (LB):

The lower bound is based on decomposing (P2) into two subproblems, (SP1) and (SP2). Then calculate N_1 to be the minimum value for (SP1) and N_2 to be the minimum value for (SP2) then applying theorem (1) to obtain $LB = N_1 + N_2$.

Heuristics to Calculate Upper Bound (UB):

A simple heuristic is obtained by ordering the jobs in SWPT order, that is, sequencing the jobs j , ($j = 1, \dots, n$) in non-decreasing order of the ratio

$$\frac{p_j}{w_j} \text{ then}$$

$$UB = \sum_{j=1}^n w_{\sigma(j)} C_{\sigma(j)} + T_{\max}^w(\sigma).$$

Example (2): Consider the $1 // \sum w_j C_j + T_{\max}^w$ problem with five jobs.

Table -2: Data for processing times, due dates and weights.

j	1	2	3	4	5
p_j	10	3	9	1	4
d_j	20	14	25	29	16
w_j	4	1	8	5	2

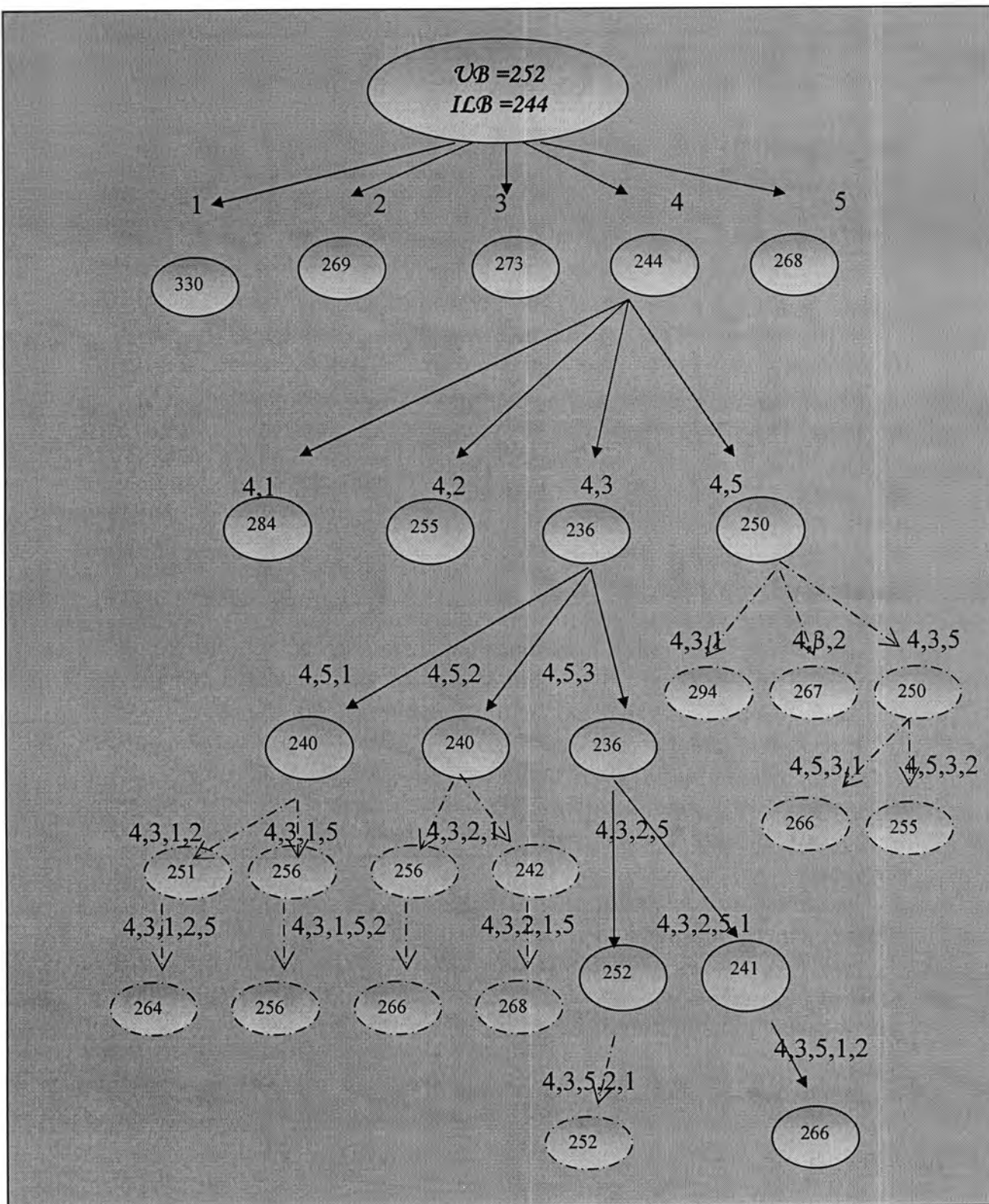


Figure -1: Solution search tree of example (2)

Now by using the lower and upper bounds (given in (6), (7)), we have a solution search tree which is shown in figure (1), with upper bound (UB=252) and initial lower bound (ILB=244), and an optimal sequence

(4,3,5,1,2), with $v_2 = \min_{\sigma \in S} \{ \sum w_{\sigma(j)} C_{\sigma(j)} + T_{\max}^w(\sigma) \}$ is 252. The lower bounds of each node in this solution search tree are written against the nodes of the tree.

Computational Experience with branch and bound algorithm:

The BAB algorithm were tested by coding it in Matlab languages, and run on Pentium IV. Test problems were generated as in (5). We list (10) problems for each value of (n), where $n \in \{5, 7, 9, 11, 13, 15, 17, 18, 19, 20\}$. We determined a condition for stopping the BAB algorithm and consider that the problem is unsolved, that the BAB algorithm is stopped after a fixed period of time, here after 1800 second (i.e. after 30 minutes). We observe that whenever the number of nodes increases, the computational time increases too as well as the number of unsolved problems. The (BAB) algorithm solves all test problems of 5, 7, 9, 11, 13 and 15 jobs. It, also, solves all test problem but 3, 4 and 8 of 10 problems for 17, 18, and 19 jobs respectively. It is clear that this problem (P2) is NP-hard, we cannot increase the size of the problem n more than 19 in BAB algorithm, consequently, it has been tackled by local search methods and genetic algorithm.

Local Search and Genetic Algorithm for the Problem (P2):

Local search is a family of methods that iteratively search through the set of solutions. Starting from an initial solution, a local search procedure moves from one feasible solution to a neighboring solution until some stopping criteria are met. (6)

1. Descent Method (DM):

This method is a simple form of local search methods. In this method, only moves that result in an improvement in the objective function value are accepted (7).

2. The Simulated Annealing (SA) Method:

In this method improving and neutral moves are always accepted. While deteriorating moves are accepted according to a given probability acceptance function(8).

3. The Genetic Algorithm (GA):

Genetic algorithms are general search and optimization methods that work on a population of feasible solutions (individuals) to a given problem (5).

Computational results and comparison

1. Test Problem for the local search:

Some examples have been constructed in special design such that these

examples (with $n = 25, 30, 35, 50, 75, 100$) satisfied the conditions given in section (4), as solvable special cases, for these examples the optimal solution is known. Hence, for every value of n ($n = 5, 10, 15, 25, 30, 35, 40, 50, 75, 100$), ten problems were generated. For all 5, 10 and 15 jobs,

we used the (BAB) algorithm to obtain the optimal solutions with reasonable limits on computation time. Also, the optimal solutions of n ($n = 25, 30, 50, 75, 100$) have been chosen as solvable special cases. For the problems that are not solved by optimality we used instead, local search method which described in section (9). In this case, best solution value found by any of the local search methods forms the basis for comparison. The efficiency of the local search methods, comparing it with the optimal solution to each test problem.

2. Computational results:

The local search algorithms (Descent method, Simulated annealing, Tree type heuristic method, and Genetic algorithm) were tested by coding them in Matlab language, and being run on Pentium IV.

Efficiency of local search algorithms:

For the test problems with $20 \leq n \leq 7500$ jobs, it is really impossible to find optimal solution by the (BAB) method in reasonable amounts of time. For such problems size we use the local search methods to find near optimal solutions. the (SA) method obtains the best results as compared with the remaining methods for most of the cases. Whereas the computational time of (SA) is approximately the same(close) to that of (DM). The computational time of (GA) is very large as compared with the remaining methods (SA, DM, TTH).

Table -3: The performance of local search methods for $n=1000$

Ex	Best	DM	SA	TTH	GA
1	9183776	9184184	9183776	9190646	*
2	8525094	8525309	8525094	8532180	*
3	8654327	8655033	8654327	8661668	*
4	7971193	7971193	7971313	7980312	*
5	8995862	8995938	8995862	9002717	*
6	8968386	8968927	8968386	8974892	*
7	8389056	8389737	8389056	8393795	*
8	8403919	8403924	8403919	8410627	*
9	8070236	8070236	8070268	8078278	*
10	8973350	8973350	8974020	8979949	*
No. best		3	7	0	0
Av. time		73.3022	69.6144	337.9339	*

Table -4: The performance of local search methods for n=5000

Ex	Best	DM	SA	TTH	GA
1	213607579	213607579	213607579	*	*
2	223192728	223192728	223192728	*	*
3	213056071	213056184	213056071	*	*
4	219241509	219243229	219241509	*	*
5	221749110	221749110	221749110	*	*
6	215101640	215101709	215101640	*	*
7	213455518	213455530	213455518	*	*
8	204990668	204990748	204990668	*	*
9	213955878	213955878	213955918	*	*
10	211403365	211403365	211403497	*	*
No. best		5	8	0	0
Av. time		330.3207	322.402	*	*

Table -5: The performance of local search methods for n=7500

Ex	Best	DM	SA	TTH	GA
1	484644882	484644922	484644882	*	*
2	490630332	490630675	490630332	*	*
3	481048256	481048256	481048256	*	*
4	491337530	491337530	491337530	*	*
5	489955371	489957711	489955371	*	*
6	486239124	486241335	486239124	*	*
7	481094305	481094315	481094305	*	*
8	484305652	484305652	484305652	*	*
9	492273891	492273891	492273891	*	*
10	470333461	470333461	470333461	*	*
No. best		5	10	0	0
Av. time		462.79494	465.6157	*	*

The results of the above tables show that the (SA) method performs very well and then comes (DM) which gives reasonable results, (SA) method has better (NO) values than (DM); the(ACT) values of both methods (DM and SA) are quite similar.

We can conclude:

The research considered two problems of scheduling jobs on a single machine for a variety of multicriteria. To the best of our knowledge, there is no published work on these two problems. We have developed optimal and near optimal solution approaches for these problems of scheduling a single machine.

For the first problem (P1), an algorithm has been proposed which gives the optimal solution, with proof of its optimality.

The second problem (P2) develops exact and approximate approaches for it. A

good lower bound has been proposed to design a branch and bound (BAB) algorithm for its optimal solution and proved two special cases which leads to optimal solutions. Because the problem (P2) is NP-hard, we used heuristic approaches. Hence, problem (P2) is solved using different local search methods: Descent method (DM), simulated annealing (SA), tree type heuristic method (TTHM), and genetic algorithm (GA). We developed efficient procedures for the problem (P2). The computational results for the problem (P2) are favorable. The approaches we developed are rather general and can be easily adapted to many other bicriteria scheduling problems.

Also, we reports the results of extensive computations tests of the following developed methods: Descent method (DM), simulated annealing (SA), tree type heuristic method (TTHM), and genetic algorithm (GA). The main conclusion to be drawn from the computation results is that (SA) method is more effective for the problem and is done with less computational effort

REFERENCES

1. Prakash, D., "Bi-criteria Scheduling Problems on Parallel Machines" Master of Science in Industrial System Engineering Blacksburg, Virginia, May, (1997).
2. French, S., Sequencing and Scheduling: An Introduction to the Mathematics of Job-Shop, Horwood, Chichester, (1982).
3. Hoogeveen, H., "Invited Review of Multicriteria Scheduling", European Journal of Operational Research 167:592–623. (2005).
4. Al-Assaf, S.S., "Solving Multiple Objectives Scheduling Problems", M.Sc. thesis University of Al-Mustansiriyah, Collage of Science, Department of Mathematics (2007).
5. Salman, F.M., "Exact and Local Search Method for Single Machine Problem" M.Sc. thesis University of Al-Mustansiriyah, Collage of Science, Department of Mathematics (2008).
6. Vredereld, T., "Combinatorial Approximation Algorithms Guaranteed Versus Experimented Performance". Ph.D. Thesis, Technische Universiteit Eindhoven, The Netherlands. (2002).
7. Chen B., Potts C.N., and Woeginger, G.J., "A review of Machine Scheduling: Complexity, Algorithms and Approximability. Handbook of Combinatorial optimization, Kluwer Academic Publishers, (1998).
8. Anderson, E.J., Glass, C.A. and Potts, C.N., "Applications of Local Search in Machine Scheduling", Preprint OR56, Faculty Of Mathematical Studies, University of Southampton, Southampton, UK. (1995).

$\Gamma(m,n)$ - $\Gamma(m,n)$ -Quasi-ASI-Injective Modules

Mehdi Sadik Abbas and Akeel Npasir Kadhim

Department of Mathematics, College of Science, Mustansiriya University

الخلاصة

لتكن R حلقة تجميعية ذات عنصر محايد غير صفري. لأجل عددين صحيحين موجبين m و n يقال لمقاس أيمن M على R أنه شبه أغماري من النمط $\Gamma(m,n)$ إذا كان كل تشاكل مقاسي من مقاس جزئي متولد من النمط Γn من M^m إلى M يمكن أن يوسع لتشاكل مقاسي من M^m إلى M . على وجه الخصوص، يقال لمقاس أيمن M على R أنه شبه أغماري من النمط Γn إذا كان M مقاس شبه أغماري من النمط $\Gamma(1,n)$. وبشكل أخص يقال لمقاس أيمن M على R أنه شبه أغماري أساسي من النمط Γ إذا كان M شبه أغماري من النمط $\Gamma(1,1)$. يُرهن أن المقاس الأيمن M على R أنه شبه أغماري من النمط $\Gamma(m,n)$ إذا وفقط إذا كان المقاس الأيمن M^m على R شبه أغماري من النمط $\Gamma(1,n)$. العديد من الخواص والتمييزات للمقاسات شبه أغمارية من النمط (m,n) (شبه أغماري من النمط $(1,n)$ و شبه أغماري أساسي على الترتيب) وسُغت على المقاسات شبه أغمارية من النمط $\Gamma(m,n)$ (شبه أغماري من النمط $\Gamma(1,n)$ و شبه أغماري أساسي من النمط Γ على الترتيب).

ABSTRACT

Let R be associative ring with non-zero identity. For two fixed positive integers m and n , a right R -module M is called $\Gamma(m,n)$ -quasi-injective, if each R -homomorphism from a Γn -generated submodule of M^m (or M_m) to M extends to one from M^m (or M_m) to M . In particular, a right R -module M is called Γn -quasi-injective, if M is $\Gamma(1,n)$ -quasi-injective. More particularly, an R -module M is called Γ principally quasi-injective if M is $\Gamma(1,1)$ -quasi-injective. It is shown that a right R -module M is $\Gamma(m,n)$ -quasi-injective if and only if the right R -module M^m is $\Gamma(1,n)$ -quasi-injective. Many properties and characterizations of (m,n) -quasi-injective (resp. n -quasi-injective and principally quasi-injective) modules are extended to $\Gamma(m,n)$ -quasi-injective (resp. Γn -quasi-injective and Γ principally quasi-injective) modules.

INTRODUCTION

Throughout this work all rings R considered are associative with unity and all modules M are unitary right R -modules. We write $N \leq M$ ($L \leq R$) to mean that N is a submodule (ideal of R) of M . For any subset X of R , $\ell(X)$ and $r(X)$ denote, respectively, the left and right annihilators of X in R . Let m and n be two fixed positive integers. For an Abelian group M , we write $M^{m \times n}$ for the set of all formal $m \times n$ matrices with entries in M , and write M^m (resp. M_m) for $M^{1 \times m}$ (resp. $M^{m \times 1}$). A^T will denote the transpose of A . Let ${}_S M_R$ be a bimodule. For $x \in M^{m \times n}$, $u \in S^{l \times m}$ and $v \in R^{n \times k}$, under the usual multiplication of matrices, ux (resp. xv) is a well defined element in $M^{l \times n}$ (resp. $M^{m \times k}$). If $X \subseteq M^{l \times n}$, $U \subseteq S^{l \times m}$ and $V \subseteq R^{n \times k}$, define

$$r_{R^{n \times k}}(X) = \{v \in R^{n \times k} \mid xv = 0, \forall x \in X\}$$

$$\ell_{S^{m \times l}}(X) = \{u \in S^{m \times l} \mid ux = 0, \forall x \in X\}$$

$$r_{M^{m \times n}}(U) = \{y \in M^{m \times n} \mid uy = 0, \forall u \in U\}$$

$$\ell_{M^{m \times n}}(V) = \{z \in M^{m \times n} \mid zv = 0, \forall v \in V\}$$

Let M be an R -module, $\Gamma(M)$ denote the set of all right ideals L of R such that L not contained in right annihilator $r_R(x)$ for each non-zero $x \in M$, i.e. $\Gamma(M) = \{L \leq R \mid L \not\subseteq r_R(x) \text{ for all } (0 \neq) x \in M\}$.

In the following remarks we consider some properties that are relevant to our work.

Remarks (1): For any R -module M . The following properties are hold for $\Gamma(M)$:

- (1) $R \in \Gamma(M)$.
- (2) If $L \in \Gamma(M)$ and $L \subseteq K$, where K is an ideal in R then $K \in \Gamma(M)$. In particular if $L \in \Gamma(M)$ then $(L + I) \in \Gamma(M)$ for each ideal I in R .
- (3) $r_R(x) \notin \Gamma(M)$ for each non-zero $x \in M$.
- (4) If $N \leq M$, then $\Gamma(M) \subseteq \Gamma(N)$ for each non-zero submodule N of M .

Proof: It is clear by definition of $\Gamma(M)$.

Examples (2) :

(1) Consider Z_2 as a Z -module, since $r_Z(\bar{1}) = 2Z$ and $nZ \subset 2Z$ for all even integer n , then $\Gamma(Z_2) = \{mZ \mid m \text{ is odd integer}\}$.

(2) Consider Z_2 which is the field of integers modulo 2, and R be the ring of all matrices of the form $\begin{pmatrix} a & b \\ 0 & c \end{pmatrix}$ with $a, b, c \in Z_2$.

The only right ideals of R are (0) , R , $\text{Rad}(R) = \begin{pmatrix} 0 & Z_2 \\ 0 & 0 \end{pmatrix}$, $\text{Soc}(R_R) = \begin{pmatrix} 0 & Z_2 \\ 0 & Z_2 \end{pmatrix}$,

$\text{Soc}({}_R R) = \begin{pmatrix} Z_2 & Z_2 \\ 0 & 0 \end{pmatrix}$, $E_k = \begin{pmatrix} 0 & k \\ 0 & 1 \end{pmatrix} R$ where $\text{Rad}(R)$, $\text{Soc}(R_R)$ and $\text{Soc}({}_R R)$ are the Jacobson radical, right (and left) Socle of R respectively [1, p. 361].

It is easy to check that $E_{\bar{0}} = \begin{pmatrix} \bar{0} & \bar{0} \\ \bar{0} & \bar{1} \end{pmatrix} R = \begin{pmatrix} 0 & 0 \\ 0 & Z_2 \end{pmatrix}$, $E_{\bar{1}} = \begin{pmatrix} \bar{0} & \bar{1} \\ \bar{0} & \bar{1} \end{pmatrix} R = \left\{ \begin{pmatrix} 0 & \bar{0} \\ 0 & \bar{0} \end{pmatrix}, \begin{pmatrix} 0 & \bar{1} \\ 0 & \bar{1} \end{pmatrix} \right\}$

and $r_R(1^*) = E_{\bar{0}}$, $r_R(2^*) = E_{\bar{1}}$, $r_R(3^*) = (0)$, $r_R(4^*) = (0)$, $r_R(5^*) = \text{Soc}({}_R R)$, $r_R(6^*) = \text{Soc}({}_R R)$, $r_R(7^*) = \text{Soc}({}_R R)$. Since $\text{Soc}({}_R R)$, $E_{\bar{0}}$ and $E_{\bar{1}}$ are annihilators

and $Rad(R) \subset Soc(R)$, then $Soc(R)$, E_0 , E_1 and $Rad(R) \notin \Gamma(R)$ (by Remarks(1)(3) and definition of $\Gamma(R)$). Hence $\Gamma(R) = \{R, Soc(R)\}$.

Recall that an R -module M is cyclic, if there exists an element x in M such that $M = xR$ [1, p.19].

As a generalization of cyclic submodule, we introduce the following:

Definition (3): Let N be a submodule of an R -module M . We say that N is Γ -cyclic, if there are an element x in M and an ideal L in $\Gamma(M)$ such that $N = xL$.

Examples and Remarks (4)

(1) It is clear that each cyclic submodule is Γ -cyclic. (In particular Z as Z -module is Γ -cyclic, and each of its submodule is Γ -cyclic).

(2) The converse of (1) is not true in general. In Example (2)(2), we saw that $Soc(R_R) \in \Gamma(R)$. Since $3^* Soc(R_R) = \begin{pmatrix} \bar{1} & \bar{1} \\ \bar{0} & \bar{1} \end{pmatrix} \begin{pmatrix} 0 & Z_2 \\ 0 & Z_2 \end{pmatrix} = \begin{pmatrix} 0 & Z_2 \\ 0 & Z_2 \end{pmatrix} = Soc(R_R)$. Then $Soc(R_R)$ is Γ -cyclic. But not cyclic [1, p. 362]

(3) Clearly, if $\Gamma(M) = \{R\}$ for any R -module M , then each Γ -cyclic submodule is cyclic.

Recall that an R -module M is principally quasi-injective (shortly; PQ-injective) if each R -homomorphism from a principal submodule of M to M can be extending to an endomorphism of M (2). The above concepts motivate us to introduce the stronger concept of it.

Definition (5): An R -module M is called Γ principally quasi-injective (shortly; Γ pq-injective), if for each R -homomorphism from Γ -cyclic submodule of M to M can be extending to an endomorphism of M .

A ring R is called Γ principally quasi-injective ring (shortly; Γ pq-injective ring), if R_R is Γ principally quasi-injective.

Examples and Remarks (6)

(1) Clearly every quasi-injective module is Γ pq-injective. In particular Q as Z -module is Γ pq-injective.

(2) The converse of (1) not true in general. For example, consider Clark example [3, p.134]. If R be a commutative ring with ideal lattice

$$0 = Rv_0 \subset Rv_1 \subset Rv_2 \subset \dots \subset V \subset \dots \subset Rp^2 \subset Rp \subset R$$

Where p and v_i , $i \geq 0$, satisfy $pv_k = v_{k-1}$ for all $k \geq 1$, and where V is the only nonprincipal ideal, then each ideal is an annihilator, in fact

$Rv_m = r(Rp^m)$ and $Rp^m = r(Rv_m)$ for all $m \geq 0$, and $r(V) = V$ [3, p.134]. Since each ideal is annihilator, then $\Gamma(R) = \{R\}$ by Remarks (6)(7). R is P -injective (3) p.133], hence R is Γpq -injective by Remark (6)(6), but R not self-injective (3) p.133].

(3) Clearly, every Γpq -injective module is PQ -injective, (since every cyclic submodule is Γ -cyclic (Remark (4) (1))).

(4) The converse of (3) is not true in general, Consider Example(2)(2) It is easy to check that R is PQ -injective and all ideals in R are Γ -cyclic, so if we suppose R is Γpq -injective, then for each R -homomorphism from Γ -cyclic ideal (i.e, from each ideals) of R to R can be extending to an endomorphism of R , this mean R is self-injective, but this is a contradiction (since the injective envelope of R not equal to

R , in fact $E(R) = \begin{pmatrix} Z_2 & Z_2 \\ Z_2 & Z_2 \end{pmatrix} \neq R$ (1) p. 362].

(5) If R is principal ideal ring, then every PQ -injective R -module is Γpq -injective. Proof: Assume M is PQ -injective R -module and let $N = xL$ is any Γ -cyclic submodule of M where $x \in M$ and $L \in \Gamma(M)$ and let $f: N \rightarrow M$ be R -homomorphism. Since R is a principal ideal ring, then $L = rR$ for some $r \in R$, therefore $N = xL = xrR = mR$ where $m = xr \in M$, hence N is principal submodule of M . But M is PQ -injective, hence f can be extending to endomorphism of M . So M is Γpq -injective module.

(6) Let M be an R -module such that $\Gamma(M) = \{R\}$. Then by Remark(4)(3) each Γ -cyclic submodule is cyclic. Hence each PQ -injective is Γpq -injective module.

(7) If every ideal L of a ring R is annihilator, then $\Gamma(M) = \{R\}$ for any R -module M , since $L \notin \Gamma(M)$ (by Remarks (1)(3)). Hence by (6) the concepts of PQ -injectivity and Γpq -injectivity coincide. In particular any module over Quasi-Frobenius ring (those rings in which all ideals are annihilator and satisfies ascending chain condition on annihilator ideals(4)Theorem 15.1].

Recall that an R -module M is called (m,n) -quasi-injective in case each R -homomorphism from an n -generated submodule of M^m to M extends to one from M^m to M (5) definition 1.1].

Firstly, we introduce the next concept as a generalization of n -generated submodule.

Definition (7): A submodule N of an R -module M is called Γn -generated submodule, if there are n -elements $x_1, \dots, x_n \in M$ and $L \in \Gamma(M)$ such that $N = x_1L + x_2L + \dots + x_nL$.

It is clear that Γ -cyclic submodules are exactly $\Gamma 1$ - generated submodules

For two fixed positive integers m and n , we introduce the following concept which is a generalization of quasi injective modules and stronger than (m,n) -quasi-injective modules.

Definition(8): An R -module M is called $\Gamma(m,n)$ -quasi-injective module (shortly; $\Gamma(m,n)$ -q-injective), if each R -homomorphism from a Γn -generated submodule of M^m (or M_m) to M extends to one from M^m (or M_m) to M .

A ring R is called $\Gamma(m,n)$ -quasi-injective ring, if R_R is $\Gamma(m,n)$ -quasi-injective module.

Definition(9): An R -module M is called Γn -quasi-injective, if it is $\Gamma(1,n)$ -quasi-injective.

Examples and Remarks(10)

- (1) M is Γpq -injective R -module if and only if M is $\Gamma(1,1)$ -quasi-injective.
- (2) M is PQ -injective R -module if and only if M is $(1,1)$ -quasi-injective(5).
- (3) Every $\Gamma(m,n)$ -quasi-injective module is (m,n) -quasi-injective.
- (4) The converse of (3) is not true in general (see example (6)(4)).
- (5) Every quasi-injective module is $\Gamma(m,n)$ -quasi-injective for all positive integers m and n (by using [6, Proposition(16.13) p.188]).
- (6) The converse of (5) is not true in general (see example (6)(2)).
- (7) If M is Γn -quasi-injective for all positive integer n then M is finitely quasi-injective.
- (8) If R_R is $\Gamma(m,n)$ -quasi-injective then (by (3)) R_R is (m,n) -quasi-injective and so R is (m,n) -injective by (5)Example (2)]

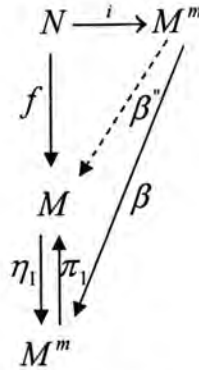
Remark(11): An R -module M is $\Gamma(m,n)$ -quasi-injective if and only if it is $\Gamma(m,k)$ -quasi-injective if and only if it is $\Gamma(l,k)$ -quasi-injective for all $1 \leq k \leq n$ and $1 \leq l \leq m$.

Proof: It is clear by definition(8)

As a characterization of $\Gamma(m,n)$ -quasi-injective modules, we have:

Theorem(12): Let M be an R -module. Then M is $\Gamma(m,n)$ -quasi-injective if and only if the R -module M^m (or M_m) is Γn -quasi-injective.

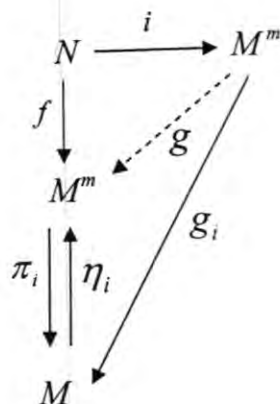
Proof: (\Leftarrow) Let N be a Γn -generated submodule of M^m and $f: N \longrightarrow M$ be an R -homomorphism, $i: N \longrightarrow M^m$ be inclusion map and $\pi_1: M^m \rightarrow M$, $\eta_1: M \longrightarrow M^m$ be projection and injection maps (resp.). Then $\eta_1 \circ f: N \longrightarrow M^m$ is R -hom.. Since M^m is Γn -q-injective, then there is an R -homomorphism $\beta: M^m \longrightarrow M^m$ such that β is an extension of $\eta_1 \circ f$. Then $\beta'' (= \pi_1 \circ \beta): M^m \longrightarrow M$ is R -homomorphism and for each $n \in N$, we have $(\beta'' i)(n) = (\pi_1 \beta)(n) = \pi_1(\beta(n)) = \pi_1((\eta_1 f)(n)) = (\pi_1 \eta_1 f)(n) = (I_M f)(n) = f(n)$, hence β'' is extension of f .



(\Rightarrow) Let N be a Γn -generated submodule of M^m and $i: N \longrightarrow M^m$ be the inclusion map, $f: N \longrightarrow M$ be an R -homomorphism and $\pi_i: M^m \rightarrow M$, $\eta_i: M \longrightarrow M^m$ be projection and injection maps (resp.) ($i=1,2,\dots,m$). Then $\pi_i \circ f: N \longrightarrow M$ ($i=1,2,\dots,m$) are R -homomorphism. Since M is $\Gamma(m,n)$ -q-injective, then there is R -homomorphism $g_i: M^m \longrightarrow M$ such that g_i is an extension of $\pi_i \circ f$ ($i=1,2,\dots,m$). Put $g (= \sum_{i=1}^m \eta_i g_i): M^m \longrightarrow M^m$. Clearly g is R -hom. and

$$(g \circ i)(n) = g(i(n)) = \sum_{i=1}^m \eta_i g_i(i(n)) = \sum_{i=1}^m \eta_i \pi_i f(n) = (\sum_{i=1}^m \eta_i \circ \pi_i)(f(n)) = I_{M^m} \circ f(n) = f(n)$$

for each $n \in N$, hence g is an extension of f .



Corollary(13): Let M be an R -module. Then M is $\Gamma(m,1)$ -quasi-injective if and only if the R -module M^m is Γ pq-injective.

Recall that a bimodule ${}_S M_R$ is left balanced in case every right R -endomorphism of M is left multiplication by an element of S (5) Definition 1.2].

Proposition(14): Let ${}_S M_R$ be a left balanced bimodule. Then M_R is $\Gamma(m,n)$ -quasi-injective if and only if for each Γ n-generated N of M^m and R -homomorphism $f: N \rightarrow M$ then there is $y \in S^m$ such that $f(n) = yn^T$ for each $n \in N$.

Proof: (\Rightarrow) Let N and f be given as above. Since M_R is $\Gamma(m,n)$ -q-injective, then there is R -homomorphism $g: M^m \rightarrow M$ such that g is an extension of f , hence $g \circ \eta_i: M \rightarrow M$ is R -endomorphism where η_i is injection maps ($i=1, \dots, m$). But ${}_S M_R$ is left balanced bimodule, then $g \circ \eta_i = y_i \cdot$ for some $y_i \in S$. Let $n = (n_1, n_2, \dots, n_m) \in N$, then

$$\begin{aligned} f(n) &= g(n) = g((n_1, 0, \dots, 0) + (0, n_2, 0, \dots, 0) + \dots + (0, 0, \dots, n_m)) \\ &= g(\eta_1(n_1) + \dots + \eta_m(n_m)) = g \circ \eta_1(n_1) + \dots + g \circ \eta_m(n_m) \\ &= y_1 n_1 + y_2 n_2 + \dots + y_m n_m = (y_1, y_2, \dots, y_m)(n_1, n_2, \dots, n_m)^T = yn^T \end{aligned}$$

(\Leftarrow) Obvious

Definition(15): An R -module M is called Γ -self-divisible if for each $m \in M$ and $L \in \Gamma(M)$, there is $\ell \in L$ such that $m = m\ell$.

Examples and Remarks(16):

(1) Z_2 as Z -module is Γ -self-divisible, since $r_z(\bar{1}) = 2Z$ so $\Gamma(Z_2) = \{nZ \mid n \text{ is odd integer}\}$. For each $nZ \in \Gamma(M)$, then $\bar{1} = \bar{1}n$ (since n is odd)

(2) (see example (2)(2)) R not Γ -self-divisible, since $2^* = \begin{pmatrix} \bar{1} & \bar{1} \\ 0 & 0 \end{pmatrix} \in R$ and

$Soc(R_R) \in \Gamma(R)$, but $2^* \neq 2^* \ell$ for all $\ell \in Soc(R_R)$.

Remark(17): Let M be an R -module and $L \in \Gamma(M^m)$, Then $\ell_{M^n}(L_n) = 0$ for each positive integer n .

Proof: By induction, for $n=1$, suppose $\ell_M(L) \neq 0$, then there is a non-zero element $w \in M$ such that $w \in \ell_M(L) \Rightarrow wh = 0 \quad \forall h \in L$, so $L \subseteq r_R(w) \subseteq r_R((w, 0, 0, \dots, 0))$, where $(0 \neq)(w, 0, 0, \dots, 0) \in M^m$ a contradiction (with $L \in \Gamma(M^m)$). Suppose true for all $k < n$. Suppose $\ell_{M^n}(L_n) \neq 0 \Rightarrow \exists (0 \neq)(m_1, m_2, \dots, m_n) \in M^n$ such that $(m_1, m_2, \dots, m_n)L_n = 0$. We can assume $m_1 \neq 0 \Rightarrow (m_1, \dots, m_n) \begin{pmatrix} L_{n-1} \\ 0 \end{pmatrix} = 0$, then $(m_1, m_2, \dots, m_{n-1})L_{n-1} = 0$, where $(m_1, m_2, \dots, m_{n-1}) \neq 0$ a contradiction \square

Notice that the condition $\ell_{M^n}(L_n) = 0$, it is always satisfied when $L=R$.

Theorem(18): Let ${}_S M_R$ be a left balanced bimodule and M^m is Γ -self-divisible. Let L be an ideal in $\Gamma(M^m)$. Then the following statements are equivalent:

- (1) M_R is $\Gamma(m,n)$ -quasi-injective.
- (2) $\ell_{M^n} r_{L_n} \{v_1, v_2, \dots, v_m\} = Sv_1 + Sv_2 + \dots + Sv_m$, for any m -elements subset $\{v_1, v_2, \dots, v_m\}$ of M^n .
- (3) $\ell_{M^n} r_{L_n}(A) = S^m A$ for all $A \in M^{m \times n}$.
- (4) If $r_{L_n}(A) \subseteq r_{L_n}(B)$ where $A, B \in M^{m \times n}$. Then $S^m B \subseteq S^m A$.
- (5) If $z \in M^n$ and $A \in M^{m \times n}$ satisfy $r_{L_n}(A) \subseteq r_{L_n}(z)$. Then $z \in S^m A$.
- (6) $\ell_{M^n}[CL_n \cap r_{L_n}(A)] = \ell_{M^n}(C) + S^m A$ for all positive integer w , $A \in M^{m \times w}$ and $C \in R^{w \times n}$.
- (6'') $\ell_{M^n}[CL_n \cap r_{L_n}(A)] = \ell_{M^n}(C) + S^m A$ for all $A \in M^{m \times n}$ and $C \in R^{n \times n}$.

Proof: (2) \Leftrightarrow (3) \Rightarrow (4) and (6) \Rightarrow (6'') \Rightarrow (3) are clear

(4) \Rightarrow (5) \Rightarrow (6). Argue as the proof of (5) theorem 1.3]

(1) \Rightarrow (2) Let $v_i = (a_{i1}, a_{i2}, \dots, a_{im}) \in M^n$ ($i=1, 2, \dots, m$). Suppose $x = (x_1, x_2, \dots, x_n) \in \ell_{M^n} r_{L_n} \{v_1, v_2, \dots, v_m\}$, where L be an ideal in $\Gamma(M^m)$. Take $w_i = (a_{i1}, a_{i2}, \dots, a_{im}) \in M^m$ ($i=1, 2, \dots, n$), we define $g: w_1 L + w_2 L + \dots + w_n L \rightarrow M$ by $g(\sum_{i=1}^n w_i t_i) = \sum_{i=1}^n x_i t_i$ for all $t_i \in L$ ($i=1, 2, \dots, n$). If $\sum_{i=1}^n w_i t_i = 0$, then $\sum_{i=1}^n a_{ij} t_i = 0$ ($j=1, 2, \dots, m$). Put $h = (t_1, t_2, \dots, t_n)^T \in L_n$, then $v_j h = 0$ ($j=1, 2, \dots, m$). Since $x = (x_1, x_2, \dots, x_n) \in \ell_{M^n} r_{L_n} \{v_1, v_2, \dots, v_m\}$, then $xh = 0$ hence $\sum_{i=1}^n x_i t_i = 0$, therefore g is well-defined. Clearly g is R -homomorphism. Since M_R is $\Gamma(m,n)$ -quasi-injective

and ${}_S M_R$ be a left balanced, then for each $k \in \sum_{i=1}^n w_i L$, $g(k) = yk^T$ for some

$y = (y_1, y_2, \dots, y_m) \in S^m$ (by Prop. 14).

For each $(t_1, t_2, \dots, t_n)^T \in L_n$ then

$$\begin{aligned} \sum_{i=1}^n x_i t_i &= g\left(\sum_{i=1}^n w_i t_i\right) = (y_1, y_2, \dots, y_m) \left(\sum_{i=1}^n w_i t_i\right)^T \\ &= (y_1, y_2, \dots, y_m) \left(\sum_{i=1}^n a_{i1} t_i, \sum_{i=1}^n a_{i2} t_i, \dots, \sum_{i=1}^n a_{im} t_i\right)^T \\ &= (y_1, y_2, \dots, y_m) ((a_{ij})_{n \times m})^T (t_1, t_2, \dots, t_n)^T \\ &= \left(\sum_{i=1}^m y_i a_{i1}, \sum_{i=1}^m y_i a_{i2}, \dots, \sum_{i=1}^m y_i a_{in}\right) (t_1, t_2, \dots, t_n)^T \\ &\Rightarrow (x_1, x_2, \dots, x_n) (t_1, t_2, \dots, t_n)^T = \left(\sum_{i=1}^m y_i a_{i1}, \sum_{i=1}^m y_i a_{i2}, \dots, \sum_{i=1}^m y_i a_{in}\right) (t_1, t_2, \dots, t_n)^T \\ &\Rightarrow [(x_1, x_2, \dots, x_n) - \left(\sum_{i=1}^m y_i a_{i1}, \sum_{i=1}^m y_i a_{i2}, \dots, \sum_{i=1}^m y_i a_{in}\right)] (t_1, t_2, \dots, t_n)^T = 0 \end{aligned}$$

Since $L \in \Gamma(M^m)$, then $\ell_{M^n}(L_n) = 0$ (by Remark (17)). So

$$(x_1, x_2, \dots, x_n) = \left(\sum_{i=1}^m y_i a_{i1}, \sum_{i=1}^m y_i a_{i2}, \dots, \sum_{i=1}^m y_i a_{in}\right)$$

$$\begin{aligned} (x_1, x_2, \dots, x_n) &= \sum_{i=1}^m (y_i a_{i1}, y_i a_{i2}, \dots, y_i a_{in}) \\ &= \sum_{i=1}^m y_i (a_{i1}, a_{i2}, \dots, a_{in}) \\ &= \sum_{i=1}^m y_i v_i = y_1 v_1 + y_2 v_2 + \dots + y_m v_m \end{aligned}$$

Then $\ell_{M^n} r_{L_n} \{v_1, v_2, \dots, v_m\} \subseteq Sv_1 + Sv_2 + \dots + Sv_m$

The other inclusion it's clear, hence $\ell_{M^n} r_{L_n} \{v_1, v_2, \dots, v_m\} = Sv_1 + Sv_2 + \dots + Sv_m$.

(2) \Rightarrow (1) Let $N = m_1 L + m_2 L + \dots + m_n L$ be a Γ n-generated submodule of M^m and $f: N \longrightarrow M$ be an R-homomorphism, write $m_i = (a_{i1}, a_{i2}, \dots, a_{im}) \in M^m$ ($i=1, 2, \dots, n$), and $v_j = (a_{1j}, a_{2j}, \dots, a_{mj}) \in M^n$ ($j=1, 2, \dots, m$). Let $u_i = f(m_i)$ ($i=1, 2, \dots, n$) (since M^m is Γ -self-divisible), and $u = (u_1, u_2, \dots, u_n)$. Then for any $h = (t_1, t_2, \dots, t_n)^T \in r_{L_n} \{v_1, v_2, \dots, v_m\}$, we have $v_j h = 0$ ($j=1, 2, \dots, m$) i.e.

$$\sum_{i=1}^n a_{ij} t_i = 0, (j=1, 2, \dots, m). \quad \text{Then} \quad \left(\sum_{i=1}^n a_{i1} t_i, \sum_{i=1}^n a_{i2} t_i, \dots, \sum_{i=1}^n a_{im} t_i\right) = 0 \quad \text{and hence}$$

$$\sum_{i=1}^n (a_{i1}, a_{i2}, \dots, a_{im}) t_i = \mathbf{0} \quad \text{i.e.} \quad \sum_{i=1}^n m_i t_i = \mathbf{0}, \quad \text{and} \quad \text{so}$$

$$uh = \sum_{i=1}^n u_i t_i = \sum_{i=1}^n f(m_i) t_i = f\left(\sum_{i=1}^n m_i t_i\right) = f(\mathbf{0}) = 0.$$

Therefore $u \in \ell_{M^n} r_{L_n} \{v_1, v_2, \dots, v_m\} \Rightarrow u \in Sv_1 + Sv_2 + \dots + Sv_m$ by assumption, let $u = (u_1, u_2, \dots, u_n) = y_1 v_1 + y_2 v_2 + \dots + y_m v_m$ for some $y_i \in S$ ($i=1, 2, \dots, m$). Then $(u_1, u_2, \dots, u_n) = (\sum_{j=1}^m y_j a_{1j}, \sum_{j=1}^m y_j a_{2j}, \dots, \sum_{j=1}^m y_j a_{nj})$. This implies $u_i = \sum_{j=1}^m y_j a_{ij} = y m_i^T$ ($i=1, 2, \dots, n$) where $y = (y_1, y_2, \dots, y_m) \in S^m$.

$$\text{Let } w = m_1 \ell_1 + m_2 \ell_2 + \dots + m_n \ell_n \in N, \quad \text{then} \quad w = \left(\sum_{i=1}^n a_{i1} \ell_i, \sum_{i=1}^n a_{i2} \ell_i, \dots, \sum_{i=1}^n a_{im} \ell_i \right)$$

$$\begin{aligned} \text{and } f(w) &= f(m_1 \ell_1 + m_2 \ell_2 + \dots + m_n \ell_n) \\ &= f(m_1) \ell_1 + f(m_2) \ell_2 + \dots + f(m_n) \ell_n \\ &= u_1 \ell_1 + u_2 \ell_2 + \dots + u_n \ell_n \\ &= y m_1^T \ell_1 + y m_2^T \ell_2 + \dots + y m_n^T \ell_n \\ &= \left(\sum_{j=1}^m y_j a_{1j} \right) \ell_1 + \left(\sum_{j=1}^m y_j a_{2j} \right) \ell_2 + \dots + \left(\sum_{j=1}^m y_j a_{nj} \right) \ell_n \\ &= \sum_{i=1}^n \sum_{j=1}^m y_j a_{ij} \ell_i = \sum_{j=1}^m \sum_{i=1}^n y_j a_{ij} \ell_i = \sum_{j=1}^m y_j \left(\sum_{i=1}^n a_{ij} \ell_i \right) = y w^T \end{aligned}$$

So M_R is $\Gamma(m,n)$ -quasi-injective (by proposition (14)).

Corollary(19): Let ${}_S M_R$ be a Γ -self-divisible left balanced bimodule, let L be an ideal in $\Gamma(M)$, Then the following statement are equivalent:

- (1) M_R is Γn -quasi-injective.
- (2) If $r_{L_n}(A) \subseteq r_{L_n}(B)$ where $A, B \in M^n$. Then $SB \subseteq SA$.
- (3) $\ell_{M^n}[CL_n \cap r_{L_n}(A)] = \ell_{M^n}(C) + SA$ for all $A \in M^n$ and $C \in R^{n \times n}$.

Corollary(20): Let ${}_S M_R$ be an Γ -self-divisible left balanced bimodule, let L be an ideal in $\Gamma(M)$, Then the following statement are equivalent:

- (1) M_R is Γpq -injective.
- (2) If $r_L(x) \subseteq r_L(y)$ where $x, y \in M$. Then $Sy \subseteq Sx$.
- (3) $\ell_M[cL \cap r_L(x)] = \ell_M(c) + Sx$, for all $x \in M$ and $c \in R$.

If $L=R$ in theorems (12) and (18) then we have the following corollary which appears in (5) theorem 1.3].

Corollary(21): Let ${}_S M_R$ be a left balanced bimodule. Then the following statements are equivalent:

- (1) M_R is (m,n)-quasi-injective,
- (2) $\ell_{M^n} r_{R_n} \{v_1, v_2, \dots, v_m\} = Sv_1 + Sv_2 + \dots + Sv_m$, for any m-elements subset $\{v_1, v_2, \dots, v_m\}$ of M^n .
- (2) $\ell_{M^n} r_{R_n} (A) = SA$ for all $A \in M^{m \times n}$.
- (3) If $r_{R_n} (A) \subseteq r_{R_n} (B)$ where $A, B \in M^{m \times n}$. Then $S^m B \subseteq S^m A$.
- (4) If $z \in M^n$ and $A \in M^{m \times n}$ satisfy $r_{R_n} (A) \subseteq r_{R_n} (z)$. Then $z \in S^m A$.
- (5) $\ell_{M^w} [CR_n \cap r_{R_n} (A)] = \ell_{M^w} (C) + S^m A$ for all positive integer w $A \in M^{m \times w}$ and $C \in R^{n \times w}$.
- (5") $\ell_{M^n} [CR_n \cap r_{R_n} (A)] = \ell_{M^n} (C) + S^m A$ for all $A \in M^{m \times n}$ and $C \in R^{n \times n}$.
- (6) The right R-module M^m is n-quasi-injective.

Theorem(22): Let M be an R-module. The following are equivalent:

- (1) M is $\Gamma(m,n)$ -quasi-injective module.
- (2) For any R-module A, any exact sequence $0 \rightarrow M \xrightarrow{\alpha} A$ splits, whenever there exists a $\beta: M^m \rightarrow A$ with $\alpha(M) + \beta(M^m) = A$ and $\beta^{-1}(\alpha(M))$ is Γn -generated submodule.

Proof: (1) \Rightarrow (2) Let $N = \beta^{-1}(\alpha(M))$; by hypothesis the homomorphism $\alpha^{-1}\beta: N \rightarrow M$ extends to a $\eta: M^m \rightarrow M$. By assumption $A = \alpha(M) + \beta(M^m)$, i.e. $\forall a \in A \quad \exists w \in M^m, x \in M$ s.t. $a = \alpha(x) + \beta(w)$, define $\lambda: A \rightarrow M$ by $\lambda(a) = x + \eta(w)$. λ is well-defined since

If $a = \alpha(x) + \beta(w) = 0 \Rightarrow \alpha(x) = \beta(-w) \Rightarrow -w \in N$ but η extends to $\alpha^{-1}\beta$ this implies $x = \alpha^{-1}\beta(-w) = \eta(-w) \Rightarrow x - \eta(w) = 0$ i.e. $\lambda(a) = 0$. It is clear λ is R-homomorphism satisfying $\lambda\alpha = I_M$ hence the sequence $0 \rightarrow M \xrightarrow{\alpha} A$ splits.

(2) \Rightarrow (1) Let N be Γn -generated submodule of M^m (i.e. $N = x_1 L + \dots + x_n L$, where $L \in \Gamma(M^m)$) and $f: N \rightarrow M$ be an R-homomorphism. Let $i: M^m \rightarrow M^m \oplus M$ and $j: M \rightarrow M^m \oplus M$ be injection maps. Define $h: N \rightarrow M^m \oplus M$ by $h(n) = (n, -f(n))$ for each $n \in N$. It is clear that h is well-defined R-homomorphism. Put $A = (M^m \oplus M) / h(N)$ and let

$\rho: (M^m \oplus M) \rightarrow (M^m \oplus M) / h(N) = A$ be the natural epimorphism. To complete the proof we need to showing that the conditions in (2) are satisfied. Put $\alpha = \rho j$ and $\beta = \rho i$, then $\alpha: M \rightarrow A$ and $\beta: M^m \rightarrow A$ are R-homomorphism.

Claim (I): $\alpha = \rho j$ is monomorphism

If $m \in \ker(\rho j) \Rightarrow \rho j(m) = h(N) \Rightarrow (0, m) + h(N) = h(N) \Rightarrow (0, m) \in h(N) \Rightarrow (0, m) = (n, -f(n))$ for some $n \in N$, and hence $m = f(n) = f(0) = 0$.

Claim (II): $\beta(M^m) + \alpha(M) = A$

Let $a \in \rho i(M^m) + \rho j(M) \Leftrightarrow a = \rho i(w) + \rho j(x)$, for some $w \in M^m, x \in M$
 $\Leftrightarrow a = \rho(w, 0) + \rho(0, x) \Leftrightarrow a = \rho((w, 0) + (0, x)) \Leftrightarrow a = \rho(w, x) \Leftrightarrow a = (w, x) + h(N) \in A$

Claim (III): $\beta^{-1}(\alpha(M))$ is Γn -generated submodule

To prove $\beta^{-1}(\alpha(M))$ is Γn -generated submodule, we claim first that $\rho j f$ can be extended to ρi .

If $n \in N$ then $\rho i(n) = \rho(n, 0) = \rho(n, -f(n) + (0, f(n))) = \rho(n, -f(n)) + \rho(0, f(n)) = \rho(h(n)) + \rho(0, f(n)) = h(N) + (0, f(n)) + h(N) = (0, f(n)) + h(N) = \rho(0, f(n)) = \rho(j(f(n))) = \rho j f(n)$.

Now $\beta^{-1}(\alpha(M)) = (\rho i)^{-1}(\rho j(M)) = \{v \in M^m \mid \rho i(v) = \rho j(x) \text{ for some } x \in M\}$
 $= \{v \in M^m \mid \rho((v, 0)) = \rho((0, x)), \text{ for some } x \in M\}$
 $= \{v \in M^m \mid (v, 0) + h(N) = (0, x) + h(N), \text{ for some } x \in M\}$
 $= \{v \in M^m \mid (v, -x) \in h(N), \text{ for some } x \in M\}$
 $= \{v \in M^m \mid (v, -x) = (n, -f(n)), \text{ for some } n \in N \text{ and } x \in M\}$
 $= \{v \in M^m \mid v = n \text{ and } x = f(n), \text{ for some } n \in N \text{ and } x \in M\}$

i.e. $\beta^{-1}(\alpha(M)) = (\rho i)^{-1}(\rho j(M)) = \{n \in N \mid \rho i(n) = \rho j(x) = \rho j(f(n))\}$, but ρi extends $\rho j f$, this implies that each element $n \in N$ satisfies $\rho i(n) = \rho j(x) = \rho j(f(n))$, hence $\beta^{-1}(\alpha(M)) = N$.

By hypothesis there exist $\varphi: A \rightarrow M$ such that $\varphi \alpha = \varphi \rho j = I_M$

Put $\gamma (= \varphi \rho i): M^m \rightarrow M$ then $\gamma(n) = \varphi \rho i(n) = \varphi \rho j f(n) = f(n)$ for all $n \in N$

This mean γ extends f , therefore M is $\Gamma(m,n)$ -quasi-injective module.

If $L=R$ in the above theorem, then we have the following corollary which gives a new characterization of (m,n) -quasi-injective modules.

Corollary(23): Let M be an R -module. The following are equivalent:

- (1) M is (m,n) -quasi-injective module.
- (2) For any R -module A , any exact sequence $0 \rightarrow M \xrightarrow{\alpha} A$ splits, whenever there exists a $\beta: M^m \rightarrow A$ with $\alpha(M) + \beta(M^m) = A$ and $\beta^{-1}(\alpha(M))$ is n -generated submodule.

If $m=n=1$ in the above corollary, then we have a new characterization of principally quasi-injective modules

Corollary(24): Let M be an R -module. The following are equivalent:

- (1) M is PQ-injective module.
- (2) For any R -module A , any exact sequence $0 \rightarrow M \xrightarrow{\alpha} A$ splits, whenever there exists a $\beta: M \rightarrow A$ with $\alpha(M) + \beta(M) = A$ and $\beta^{-1}(\alpha(M))$ is cyclic submodule.

Corollary(25): Let M be an R -module. The following are equivalent:

- (1) M is Γn -quasi-injective module.
- (2) For any R -module A , any exact sequence $0 \rightarrow M \xrightarrow{\alpha} A$ splits, whenever there exists a $\beta: M \rightarrow A$ with $\alpha(M) + \beta(M) = A$ and $\beta^{-1}(\alpha(M))$ is Γn -generated submodule.

If $L=R$ in the above corollary then we have the following corollary

Corollary(26): Let M be an R -module. The following are equivalent:

- (1) M is n -quasi-injective module.
- (2) For any R -module A , any exact sequence $0 \rightarrow M \xrightarrow{\alpha} A$ splits, whenever there exists a $\beta: M \rightarrow A$ with $\alpha(M) + \beta(M) = A$ and $\beta^{-1}(\alpha(M))$ is n -generated submodule.

The following corollary follows from the above corollary which is deduced from (7) theorem (4.1)].

Corollary(27): Let M be an R -module. The following are equivalent:

- (1) M is finitely quasi-injective module.
- (2) For any R -module A , any exact sequence $0 \rightarrow M \xrightarrow{\alpha} A$ splits, whenever there exists a $\beta: M \rightarrow A$ with $\alpha(M) + \beta(M) = A$ and $\beta^{-1}(\alpha(M))$ is finitely generated submodule.

Recall that an R -module M is called terse if every distinct submodules of M are not isomorphic (8). This is equivalent to saying that isomorphic submodules of M are equal. In the following proposition we get quasi-correspondence but for the $R^{n \times n}$ -module $M^{m \times n}$ provided the R -module M is $\Gamma(m,n)$ -quasi-injective.

Proposition(28): If M is $\Gamma(m,n)$ -quasi-injective R -module with $S = \text{End}(M)$ then $S^m H = S^m K$, for any isomorphic $R^{n \times n}$ -submodules H, K of $M^{m \times n}$.

Proof: Since $H \cong K$, then there is an $R^{n \times n}$ -isomorphism $\alpha: H \rightarrow K$. Since α is onto, then for each $k \in K$ there is $h \in H$ such that $k = \alpha(h)$. It is clear that $r_{L_n}(k) = r_{L_n}(h)$ for each $L \in \Gamma(M^m)$. Since M is $\Gamma(m,n)$ -quasi-injective, then $S^m k = S^m h$ (by theorem(18)(4)) and so $S^m k \subseteq S^m H$ for each $k \in K$, then $S^m K \subseteq S^m H$ similarly we get $S^m H \subseteq S^m K$ and so the proof is complete.

Proposition(29): If M is (m,n) -quasi-injective R -module with $S=\text{End}(M)$ then $S^m H = S^m K$, for any isomorphic $R^{m \times n}$ -submodules H, K of $M^{m \times n}$.

Proof: By using (5, theorem (1.3)) and the same way in the above proof.

Corollary(30): If M is PQ-injective R -module with $S=\text{End}(M)$ then $SH = SK$, for any isomorphic R -submodules H, K of M .

If $M=R$ in the above corollary then we have the following corollary which appears in (9).

Corollary(31): Let R be a P-injective ring and H, K be two-sided ideals of R . If $H \cong K$, as right ideals of R , then $H=K$.

Corollary(32): If M is Γ_{pq} -injective R -module and $S=\text{End}(M)$, then $SH = SK$, for any isomorphic R -submodules H, K of M .

REFERENCES

1. Kasch F.: Modules and rings, Academic press, London, 1982.
2. Nicholson W. K., Park J. K. and Yousif M. F.: Principally quasi-injective Modules, Communication in Algebra, 27(4):1683-1693 (1999)
3. Nicholson W.K.&Yousif M.F."Quasi-Frobenius Rings"Cambridge Univ.Press., (2003).
4. Lam T.Y."Lectures on Modules and Rings" Springer-Verlag New York, Inc (1999).
5. Chen J., Zhang X. and Zhu Z.: On (m,n) -quasi-injective Modules, Acta Math. Univ. Comenianae, Vol. LXXIV: 25-36(2005).
6. Anderson F. W. and Fuller K. R."Rings and Categories of Modules"Springer-Verlag New York, Inc (1992).
- 7.Ramamurthi V.S.& Rangaswamy K.M."On Finitely Injective Modules,J.Austral. Math. Soc., 16:239-248(1973).
8. Weakley W.D."Modules whose distinct submodules are not isomorphic"comm. in algebra, 15:1569-1587(1987).
- 9.Kamal M.A. & Elmanophy O.A."On P-extending modules"Acta Math.Univ. Comenianae, LXXIV, 2: 279-286(2005).

Reflection Arrangement which is neither Hypersolvable nor supersolvable

¹Michel Jambu, ²Abid A.Al-Taai and ³Rabeaa G.A.AL-Aleyawee

¹Laboratoire de Mathematiques, UMR6629 CNRS, Universite de Nantes 2, rue de la

²Houssiniere, BP 92208, 44322 Nantes cedex 3, France; Ministry of Higher Education and Scientific Research

³Al- Mustansiriya University, College of Science, Mathematics Department.

الخلاصة

في بحثنا هذا قمنا بتحليل الترتيبية الانعكاسية المركبة $A(G_{25})$ المقابلة لزمرة شيفارد G_{25} حيث قمنا بحساب معادلة بونكاريه (Poincare) وتمكننا من اشتقاق الشبكة (lattice) لـ $A(G_{25})$ والتي تتألف من (44) عنصرا واثبتنا بان هذه الترتيبية ذات الرتبة الثالثة غير قابلة للحل العلوي (hypersolvable) وكذلك غير قابلة للحل الفائق (supersolvable).

ABSTRACT

In our study research we construct the complex reflection arrangement $A(G_{25})$, corresponding to the Shephard group G_{25} , and we compute its Poincare polynomial. We found the lattice which consists of "44" elements, and we proved that $A(G_{25})$ is not a hypersolvable nor supersolvable, rank three arrangement.

INTRODUCTION

Let $V \cong C^t$ and choose coordinates for V s.t we can identify the symmetric algebra $S = S(V^*)$ with the polynomial ring $C[Z_1, \dots, Z_t]$.

A hyperplane in V is a codimension one affine space in V .

A hyperplane arrangement in V is a finite collection of hyperplanes denoted by A .

When the hyperplane of an arrangement contain the origin we say the arrangement is central.

For each $H \in A$ choose a linear polynomial $\alpha_H \in S$ s.t $H = \text{Ker } \alpha_H$. Let $Q = \prod_{H \in A} \alpha_H$ denote

the defining polynomial of the arrangement A . Through out this paper we use the following notations:-

Let L_A be the intersection lattice of A which is the set of all intersections of elements from A with the order being reverse inclusion i.e. $X \leq Y \leftrightarrow Y \subseteq X$, for each $X, Y \in L_A$. Moreover,

for $X \in L_A$, let $A_X = \{H \in A / X \subseteq H\}$, $(L_A)_X = \{Y \in L_A / Y \leq X\}$,

$(L_A)^X = \{Y \in L_A / Y \geq X\}$. Then we define the Möbius function μ on L_A by: $\mu(V) = 1$ & the

recursive formula: $\mu(X) = - \sum_{Y \in (L_A)_X} \mu(Y)$.

The rank of A is $\text{rk}(A) = \text{cod}(\bigcap_{H \in A} H)$ and the number of hyperplanes is $|A|$. We say that A

is essential if $\text{rk}(A) = \dim(V)$. The Poincare polynomial of (A) is defined by

$\pi(A, t) = \sum_{X \in L_A} \mu(X) (-t)^{\text{rk}(X)}$, (where t is an indeterminate).

SUPERSOLVABLE ARRANGEMENTS

The next definitions are standard for lattices in general, see (1, 2). We will use them for central arrangements. It simplifies notation to assume that $L = L_A$ and A is central and essential. Let $\text{rk}(A) = n$ and $T = T(A)$.

Definition (2.1)(3): Let G be a finite reflection group i.e. $G \subset O(V)(U(V))$. The set of all reflecting hyperplanes of G is called the reflection arrangement of G , and denoted by $A(G)$.

In particular, when the group G is a coxeter group, the reflection arrangement $A(G)$ is called a coxeter arrangement.

Theorem (2.2)(4): Let G be a finite reflection group ($G \subset O(V)(U(V))$), and let T be a subspace of V . Then G_T is a reflection group generated by reflections in the hyperplanes of $A(G)$ which contains T .

Proposition(2.3): Let G be a finite complex reflection group ($G \subset U(V)$). Then for any atom of $L_{A(G)}$, there exist a cyclic subgroup G_H , which fixed H pointwise.

Proof: For any hyperplane $H \in A$, $H \in L_{A(G)}$ is called an atom of L . By theorem (2.2) G_H is a reflection subgroup of $G \subset U(V)$, generated by reflections in the hyperplanes of $A(G)$ which contains H . Therefore, by theorem (2.2), $\exists g \in G$ s.t. $\text{Fix}(g) = H$ i.e. $H = \{v \in V \mid gv = v\}$. Now, for each $g \in G_H$, we have $gH = H$ and $g^2H = g(gH) = gH = H$. Therefore G_H is a cyclic reflections subgroup of G fixed H pointwise.

Examples (2.4):

1- The Braid arrangement (is the reflection arrangement corresponding to the symmetric group S_n).

2- The B_3 -arrangement which is defined by

$Q(A) = xyz(x-y)(x+y)(x-z)(x+z)(y-z)(y+z)$ is the reflection arrangement (coxeter arrangement) corresponding to the coxeter group B_3 which is generated by reflections about the symmetry planes of the cube.

Remark (2.5): Every real reflection group (coxeter group) may be viewed as a complex reflection group.

Example (The Hessian configuration) (2.6): Every non-singular cubic in \mathbb{CP}^2 is projectively equivalent to one defined by $f(x, y, z) = x^3 + y^3 + z^3 - 3axyz$ with $a^3 \neq 1$ and $a \neq \infty$. The inflection points of a cubic are the solutions of $f = 0 = H(f)$, where $H(f)$ is the Hessian determinant of second partials. Direct calculation shows that for this family of curves the

nine inflection points are independent of a . Set $\omega = e^{\frac{2\pi i}{3}}$. The projective coordinates of the nine inflection points are:

$$(0, 1, -1), (0, 1, -\omega), (0, 1, -\omega^2)$$

$$(1, 0, -1), (1, 0, -\omega), (1, 0, -\omega^2)$$

$$(1, -1, 0), (1, -\omega, 0), (1, -\omega^2, 0)$$

These "9" points lie on "12" projective lines, which are the four degenerate cubics corresponding to the parameter values $a = \infty$ and $a^3 = 1$:

$x = 0, y = 0, z = 0, x + \omega^i y + \omega^j z = 0$, where $0 \leq i, j \leq 2$. These "12" projective lines meet in "12" additional points. This configuration of "12" lines and "21" points is called the Hessian configuration. Each of the first nine points is contained in four lines, so we refer to them as quadruple points. Each of the second twelve points is contained in two lines, so we refer to them as double points.

Each line contains three quadruple points and two double points, Fig.(1). The Hessian configuration has a distinguished history. For a complete account see (5).

Its group of symmetries was determined by Jordan in 1878 as a subgroup of $PGL(2, C)$ of order 216. It is generated by projective transformations of order "3" which leave one of the "12" projective lines pointwise fixed. In addition the group contains "9" projective transformations of order "2" which fix projective lines.

This group give rise to two complex reflection groups.

One is called G_{25} in the classification of Shephard and Todd (6).

The group G_{25} has order 648 and generated by reflections of order "3" its reflection arrangement is given by:

$$Q_1 = Q(A(G_{25})) = xyz \prod_{0 \leq i, j \leq 2} (x + \omega^i y + \omega^j z).$$

The other complex reflection group is called G_{26} . It has order 1296 and contains additional reflections of order "2".

Its reflection arrangement is given by:

$$Q_2 = Q(A(G_{26})) = Q_1 (x^3 - y^3)(x^3 - z^3)(y^3 - z^3)$$

Reflection Arrangement which is neither Hypersolvable nor supersolvable

Michel, Abid and Rabeea

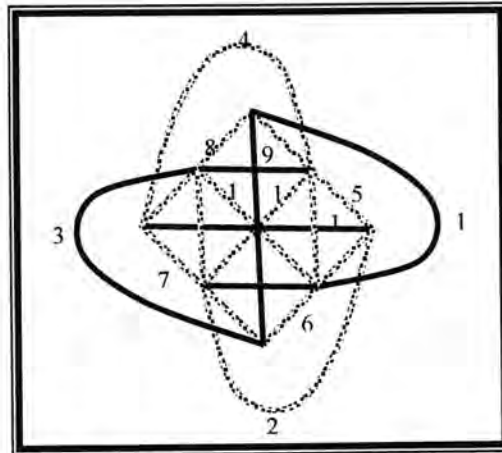


Fig -1: The Hessian

Lattice of $A(G_{25})$ (2.7): The defining polynomial of $A(G_{25})$ is $Q(A(G_{25})) = xyz \prod_{0 \leq i, j \leq 2} (x + \omega^i y + \omega^j z)$.

If we renumbered H_i where $H_i = \ker \alpha_{H_i}$, $1 \leq i \leq 12$ as follows :

- $H_1 : x = 0$
- $H_2 : y = 0$
- $H_3 : z = 0$
- $H_4 : x + y + z = 0$
- $H_5 : x + y + \omega z = 0$
- $H_6 : x + y + \omega^2 z = 0$
- $H_7 : x + \omega y + z = 0$
- $H_8 : x + \omega y + \omega z = 0$
- $H_9 : x + \omega y + \omega^2 z = 0$
- $H_{10} : x + \omega^2 y + z = 0$
- $H_{11} : x + \omega^2 y + \omega z = 0$
- $H_{12} : x + \omega^2 y + \omega^2 z = 0$

The $L_{A(G_{25})}$ consist of :-

1- (C^3) as the minimal element.
2- The rank one element set of atoms (the hyperplanes).
$H_1 : x = 0$
$H_2 : y = 0$
$H_3 : z = 0$
$H_4 : x + y + z = 0$
$H_5 : x + y + \omega z = 0$
$H_6 : x + y + \omega^2 z = 0$
$H_7 : x + \omega y + z = 0$
$H_8 : x + \omega y + \omega z = 0$
$H_9 : x + \omega y + \omega^2 z = 0$
$H_{10} : x + \omega^2 y + z = 0$
$H_{11} : x + \omega^2 y + \omega z = 0$
$H_{12} : x + \omega^2 y + \omega^2 z = 0$
3- The rank two elements :-
1) $H_1 \cap H_4 \cap H_8 \cap H_{12} : x = 0, y = -z$

2) $H_1 \cap H_5 \cap H_9 \cap H_{10}$: $x = 0$, $y = -\omega z$
3) $H_1 \cap H_6 \cap H_7 \cap H_{11}$: $x = 0$, $y = -\omega^2 z$
4) $H_2 \cap H_4 \cap H_7 \cap H_{10}$: $y = 0$, $x = -z$
5) $H_2 \cap H_5 \cap H_8 \cap H_{11}$: $y = 0$, $x = -\omega z$
6) $H_2 \cap H_6 \cap H_9 \cap H_{12}$: $y = 0$, $x = -\omega^2 z$
7) $H_3 \cap H_4 \cap H_5 \cap H_6$: $z = 0$, $x = -y$
8) $H_3 \cap H_7 \cap H_8 \cap H_9$: $z = 0$, $x = -\omega y$
9) $H_3 \cap H_{10} \cap H_{11} \cap H_{12}$: $z = 0$, $x = -\omega^2 y$
10) $H_1 \cap H_2$: $y = x = 0$
11) $H_1 \cap H_3$: $x = z = 0$
12) $H_2 \cap H_3$: $y = z = 0$
13) $H_4 \cap H_9$: $x = -\frac{\omega}{1+\omega} y = \omega z$
14) $H_4 \cap H_{11}$: $x = \omega y = \frac{-\omega}{1+\omega} z$
15) $H_5 \cap H_7$: $x = -(1+\omega) y = -(1+\omega) z$
16) $H_5 \cap H_{12}$: $x = \omega y = \frac{-\omega^2}{1+\omega} z$
17) $H_6 \cap H_8$: $x = -(1+\omega) y = -(\omega+\omega^2) z$
18) $H_6 \cap H_{10}$: $x = -(1+\omega^2) y = -(1+\omega^2) z$
19) $H_7 \cap H_{12}$: $x = \frac{-\omega^2}{1+\omega} y = \omega z$
20) $H_8 \cap H_{10}$: $x = -(\omega+\omega^2) y = -(1+\omega) z$
21) $H_9 \cap H_{11}$: $x = -(\omega+\omega^2) y = -(\omega+\omega^2) z$
4- The rank three element	
$T = \bigcap_{i=1}^{12} H_i = \{0\}$	

Finally, to compute the Poincare polynomial of $A(G_{25})$, note that if $X \in L_{A(G_{25})}$ s.t. $\text{rk}(X) = 1$, then $\mu(X) = -1$, if $\text{rk}(X) = 2$, and X is in two planes then $\mu(X) = 1$, and if $\text{rk}(X) = 2$, s.t. X is in four planes then $\mu(X) = 3$. This allows calculation of $\mu(\{0\}) = -28$. Thus

$$\begin{aligned} \pi(A(G_{25})) &= 1 + 12t + 12t^2 + 27t^2 + 28t^3 \\ &= (1+t)(1+4t)(1+7t) \end{aligned}$$

Definitions (2.8)(7): 1- The pair $(X, Y) \in L \times L$ is called modular if for all $Z \in L$ with $Z \leq Y$, $Z \vee (X \wedge Y) = (Z \vee X) \wedge Y$.]

2- An element $X \in L$ is called modular, if (X, Y) is a modular pair, for all $Y \in L$.

The following lemma appear as statement in (8) and we prove it here.

Proposition(2.9):For any central arrangement A,the elements V,T and all atoms are modular.

Proof:To prove that V is modular, let $Z, Y \in L$, such that $Z \leq Y$

$$\begin{aligned}
 \text{Since } Z \vee (V \wedge Y) &= Z \cap (V \wedge Y) \\
 &= Z \cap \{\cap\{W \in L \mid V \cup Y \subseteq W\}\} \\
 &= \cap\{Z \cap W \in L \mid Z \cap (V \cup Y) \subseteq Z \cap W\} \\
 &= \cap\{W' \in L \mid (Z \cap V) \cup (Z \cap Y) \subseteq W'\} \\
 &= \cap\{W' \in L \mid (Z \cap V) \cup Y \subseteq W'\}, \text{ since } Y \subseteq Z \\
 &= (Z \cap V) \wedge Y \\
 &= (Z \vee V) \wedge Y
 \end{aligned}$$

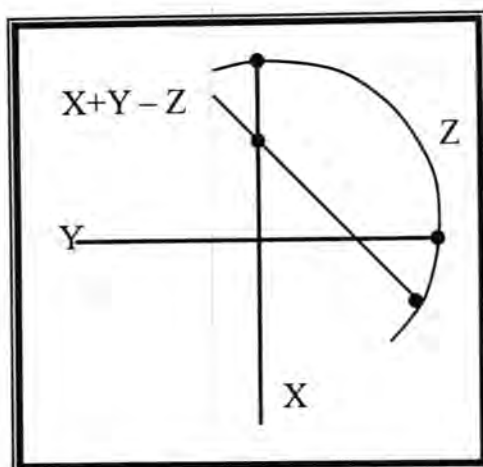
Therefore, V is modular

T is modular, since for any $Y \in L$, if $Z \leq Y$. Then:

$$\begin{aligned}
 Z \vee (T \wedge Y) &= Z \cap (T \wedge Y) \\
 &= Z \cap \{\cap\{W \in L \mid T \cup Y \subseteq W\}\} \\
 &= \cap\{Z \cap W \in L \mid Z \cap (T \cup Y) \subseteq Z \cap W\} \\
 &= \cap\{W' \in L \mid (Z \cap T) \cup (Z \cap Y) \subseteq W'\} \\
 &= \cap\{W' \in L \mid (Z \cap T) \cup Y \subseteq W'\} \\
 &= (Z \cap T) \wedge Y \\
 &= (Z \vee T) \wedge Y
 \end{aligned}$$

By the same way all atoms are modular. ■

Example (2.10): Consider $Q(A) = xyz(x + y - z)$, Fig. (2). In L_A , each atom is modular, but no element of rank two is modular

.Fig. -2: $Q(A) = xyz(x + y - z)$

An important and rather well understood class of arrangements are the supersolvable ones.

Definition (2.11)(1): Let A be an arrangement with $\text{rk}(A) = n$, and L be its lattice, then we call A supersolvable if L has a maximal chain of modular elements

$$V = X_0 < X_1 < \dots < X_n = T$$

Hereby, several examples of supersolvable arrangements.

Examples (2.12):

1. In example (2.10), A is not supersolvable, since L has no modular element of rank 2.
2. The B_3 -arrangement is supersolvable, since it has a maximal chain of modular elements:
 $V < \{x = 0\} < \{x = y = 0\} < \{0\}$
3. The Boolean arrangement is supersolvable, since every element in L is modular, so we may take any maximal chain of modular elements.
4. In the Braid arrangement, not all elements of L are modular, but there exists a maximal chain of modular elements given by:

$$V < \{x_1 = x_2\} < \{x_1 = x_2 = x_3\} < \dots < \{x_1 = x_2 = \dots = x_n\} = T$$

5. For $Q(A) = xyz(x - y)(x - z)(y - z)$, a maximal chain of modular elements is given by: $V < \{x = 0\} < \{x = y = 0\} < \{0\}$

Therefore, A is supersolvable.

Theorem (2.13)(7): If A is supersolvable arrangement, then A is free.

Furthermore, A has $\exp A = \{m_1, \dots, m_n\}$, where $m_i = |A_{x_i} - A_{x_{i-1}}|$, $1 \leq i \leq n$.

Therefore the class of free arrangements include all coxeter arrangements, complex reflection arrangements (including shepherd groups) and supersolvable arrangements.

The following example shows that the implication in theorem (2.13) can not be reversed.

Example (2.14): The reflection arrangement $A(G_{25})$, is free (9) but it is not supersolvable. Since $L_{A(G_{25})}$

has no modular element of rank "2", for example $X \in L_{A(G_{25})}$ s.t.

$X = \{H_1 \cap H_4 \cap H_8 \cap H_{12}\} = \{(x, y, z) \in C^3 \mid x = 0, y = -z\}$ is not modular since $\exists Y \in L_{A(G_{25})}$, $Y = \{H_2 \cap H_4 \cap H_7 \cap H_{10}\} = \{(x, y, z) \in C^3 \mid x = -\omega z, y = 0\}$ and $X + Y \notin L_{A(G_{25})}$.

HYPERSOLVABLE ARRANGEMENTS

Let $A = \{H_1, H_2, \dots, H_\ell\}$ be a central arrangement in the complex vector space V . Denote also by $A^p = \{\alpha_1, \alpha_2, \dots, \alpha_\ell\} \subset P(V^*)$ its set of defining equations (forms) viewed as points in the dual projective space, where $H_i = \ker \alpha_i$, $i = 1, 2, \dots, \ell$.

Definition (3.1)(10): Let $B \subset A$ be a proper non-empty sub-arrangement of A and set $B^c = A - B$. We say that (A, B) is a solvable extension if the following conditions are satisfied:

1. The extension is closed:

If no point $a \in B^c$ sits on a projective line determined

by $\alpha, \beta \in B$, i.e., $\text{rk}\{\alpha, \beta, a\} = 3$.

2. The extension is complete:

If for every $a, b \in B^c$ with $a \neq b$, there exist a point $\gamma \in B$, on the line passing through a and b , i.e., $\text{rk}\{a, b, \gamma\} = 2$.

3. For every distinct points $a, b, c \in B^c$, the three points α, β, γ determined by (a, b) , (b, c) and (a, c) respectively are either equal or collinear.

Definition (3.2)(10): The arrangement A is called hypersolvable if it has a hypersolvable composition series, i.e., an ascending chain of sub-arrangements

$A_1 \subset A_2 \subset \dots \subset A_i \subset A_{i+1} \subset \dots \subset A_k = A$, where $\text{rk } A_1 = 1$, and each (A_i, A_{i+1}) is a solvable extension.

Remarks (3.3):

1. The positive integer $k \geq 2$ is called the length of the composition series, which is denoted by $L(A)$, and depends only on A . i.e. $L(A) = k$.
2. We can decide whether it is a hypersolvable or not only from level 2, since level 2 of L_A contains only the hyperplanes from which we define the composition series.
3. The class of hypersolvable includes supersolvable and many others (11).

Now, we will give several examples of hypersolvable arrangements.

Examples (3.4):

1. Let A be the 3-arrangement in C^3 defined by:

$$Q(A) = (x+z)(x-z)(y+z)(y-z)(x+y-2z)(x+y+2z)z$$

and $\{H_1, H_2, \dots, H_7\}$ are the hyperplanes defined by the defining equation given above consequently, (see Fig.(3)). Then A is a hypersolvable arrangement since

$$\{H_7\} \subset \{H_3, H_4, H_7\} \subset \{H_3, H_4, H_5, H_6, H_7\} \subset A$$

is a hypersolvable composition series of A . Notice that $\text{rk}(A)=3$ and $L(A)=4$.

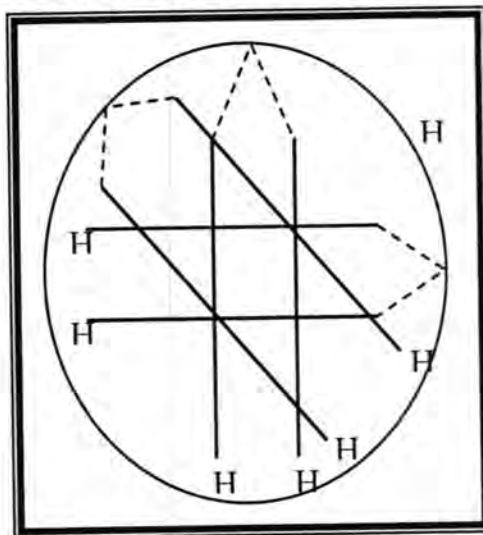


Fig. -3: $Q(A) = (x+z)(x-z)(y+z)(y-z)(x+y-2z)(x+y+2z)z$

2. Let A be the 3-arrangement Fig.(4) given in (2) as an example of non-free arrangement, but not discussed as a hypersolvable arrangement. A is a hypersolvable, since

$\{H_2\} \subset \{H_2, H_3, H_7\} \subset \{H_2, H_3, H_5, H_7\} \subset A$, is a hypersolvable composition series of A , with $L(A) = 4$.

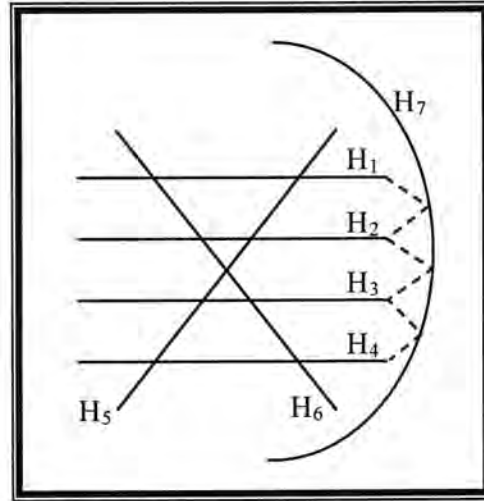


Fig. -4

4. The 3-arrangement A given in (10) Fig. (5) is a hypersolvable arrangement with $\text{rk}(A) = 3$ and $L(A) = 4$.

$\{H_6\} \subset \{H_6, H_1, H_2\} \subset \{H_6, H_1, H_2, H_3\} \subset A$.

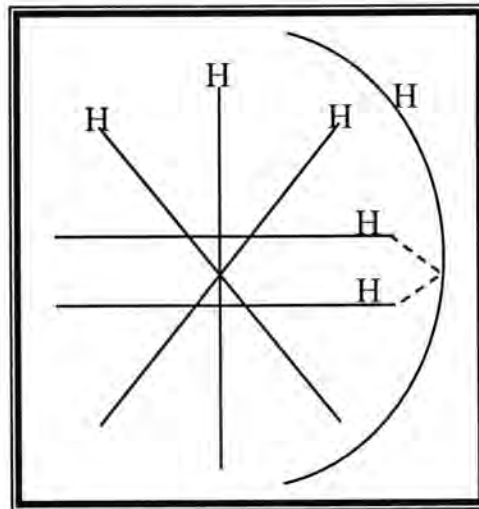


Fig. - 5

However, not all arrangements are hypersolvable, for example

Examples (3.5): The classical coxeter arrangements A of type $(D_n)_{n \geq 4}$, and the exceptional coxeter arrangements A of type E_6, E_7 and E_8 are not hypersolvable, (10).

Remark(3.6): If B is solvable in A , then for any three distinct elements $a, b, c \in B^c$, such that $\gamma_{a,b}$, $\gamma_{b,c}$ and $\gamma_{a,c}$ are distinct, then $\text{rk}\{\gamma_{a,b}, \gamma_{b,c}, \gamma_{a,c}\} = 2$, otherwise $\gamma_{a,b} = \gamma_{b,c} = \gamma_{a,c}$ and hence $\text{rk}\{\gamma_{a,b}, \gamma_{b,c}, \gamma_{a,c}\} = 1$.

Theorem (3.7)(10): Let A be a hypersolvable. Then A is supersolvable if and only if $L(A) = \text{rk}(A)$.

Notice that, theorem (3.7) provides a very simple supersolvability test. Therefore, in examples (3.4), the arrangements are not supersolvable since $\text{rk}(A) = 3$ and $L(A) = 4$.

Proposition(3.8): The reflection arrangement $A(G_{25})$ is not a hypersolvable arrangement.

Proof: By the classification of Shephard and Todd (6) G_{25} is a Shephard group and these groups are closely related to the coxeter groups, but all coxeter arrangements are not hypersolvable(10) and hence all Shephard arrangements are not hypersolvable. So $A(G_{25})$ is not hypersolvable arrangement.

REFERENCES

1. Stanley, R.P. "Modular elements of geometric Lattices" *Algebra Universalis* :214 – 217, 1 (1971).
2. Stanley, R.P., "Supersolvable lattices" *Algebra universalis*, (2) (1972).
3. Orlik, P. Solomon, L., "Arrangements defined by unitary reflection groups" *Math. Ann.* (261) :339 – 357 (1982).
4. Steinberg, R. "Invariant of finite reflection groups" *Canad. J. Math.* (12) :616–618 (1960).
5. Brieskorn, E. & Knörrer, H. "Plane Algebraic curves" Birkhauser, Boston. (1986).
6. Shephard, G.C., Todd, J.A. "Finite unitary reflection groups" *Canad. J. Math.* (6): 274–304 (1954).
7. Jambu, M., Terao, H. "Free arrangements of hyperplanes & supersolvable lattices" *Advances in Math.* (52):248–258 (1984).
8. Orlik, P., Terao, H. "Arrangements of hyperplanes" *Grundlehren, Math. Wiss.*, 300, Springer -Verlag, Berlin, (1992).
9. Terao, H. "Generalized exponents of a free arrangement of hyperplanes & shephard–Todd–Brieskorn" *Formula, Inv. Math.* (63):159–179 (1981).
10. Jambu M., Papadima S. "A generalization of fiber-type arrangements and new deformation method" *Topology*. 37:1135 -1164 (1998).
11. Jambu M., "Deformations of hypersolvable arrangements", *Topology and its applications* 118:103–111 (2002).

Exact Solution for a Spherical Symmetric Perfect Fluid Model of Embedding Class Two

¹Mahmood K. Jasim, ²Inaam A. Malloki and ³Arwa A. Abd Al-Hameed

¹Nizwa University, Nizwa, Oman.

²Mustansiriya University, Baghdad, College of Science, Dept. of Mathematics

³Mustansiriya University, Baghdad, College of Science, Dept. of Mathematics

الخلاصة

بعض نماذج التماثل الكروي للمائع التام المغمور من النمط الثاني درست بإنشاء كرة مائع تتغير فيها الضغط والكثافة طبقاً لخاصية الضغط والكثافة تتلاشى عند الحدود التي يسود فيها حل شوارزشيلد الخارجي. الحلول العامة الجديدة حصل عليها بتقديم صيغة رياضية لـ $e^{-\lambda}$ كمجموعة حدود من الدرجة الثانية، الحلول المكتسبة مقبولة فيزيائياً والمعلمة غير البعدية m/R ظهرت في الحلول حيث m تمثل الكتلة النسبية للمائع و R يمثل نصف القطر. النتائج وضحت على شكل رسوم وجداول.

ABSTRACT

Some spherical symmetric perfect fluid models of embedding class two have been investigated by constructing a fluid sphere of variable pressure and density with property that the pressure and density vanishes at the boundary beyond which Schwarzschild exterior solution prevails. New general solutions have been obtained by introducing the mathematical form of $e^{-\lambda}$ as a polynomial of degree two, the solutions so obtained are physically acceptable and the non-dimensional parameter m/R appears in the solution, where m is the relativistic mass of the fluid model and R is the radius. The results have been depicted in the form of tables and graphs.

Key words: GRG, Perfect fluid model.

INTRODUCTION

In general relativity, an exact solution is a Lorentzian manifold equipped with certain tensor fields which are taken to model states of ordinary matter, such as fluid or non-gravitational fields (electromagnetic field). These tensors obey any relevant physical law following by a standard recipe which is widely used in mathematical physics (1).

Perfect fluid distributions in general can be divided in two categories, in the 1st category we may include these class one perfect fluid conformally and non-conformally while in the 2nd category are included those perfect fluid which are characterized by non-vanishing Wyle conformal curvature tensor. Barnes, 1974 has obtained many interesting solutions of both these categories (2). Pandey and Sharma, 1980 has studied in greater details Taub's plane symmetric space-time in search of perfect fluid distributions of class one and of class two (3).

Gupta and Jasim obtained the most general exact as well as accurate solution of isentropic fluid spheres with reference to weak and strong energy conditions (4,5).

In this article some spherical symmetric perfect fluid models of embedding class two have been investigated by referring to Karmarkar condition 1948. Our main interest is in constructing spherical models of finite size with vanishing pressure and density at the interface beyond which Schwarzschild exterior solution prevails. We are guided by the form of Schwarzschild interior metric and we have obtained some perfect fluid models of class two. A general solution has been obtained by power

series method; the coefficients appearing in the polynomial have been determined by matching the interior metric tensors and its derivatives of various orders across the interface with the exterior Schwarzschild metric. The non dimensional parameter m/R appears in all these solutions, where m is the relativistic mass of the fluid model and R is the radius. In addition to that, some of these models are analyzed numerically and the results so obtained are new, physically acceptable and depicted in the form of graphs and tables.

This article is organized as follows:

Section two is devoted to mathematical formulation for spherical symmetry model, In the third section we present exact solution for some models of class two, In the fourth section we discuss the physical acceptability of the solutions presented in the second section.

MATHEMATICAL FORMULATION FOR SPHYRICAL SYMMETRIC MODEL

Einstein field equations

The static spherical symmetric line element is

$$ds^2 = -e^{\lambda(r)} dr^2 - r^2 (d\theta^2 + \sin^2 \theta d\phi^2) + e^{\mu(r)} dt^2, \quad (1)$$

where, the functions $\lambda(r)$ and $\mu(r)$ are gravitational potentials gives rise to the following expressions for the energy momentum tensor and flow-vector v^i ($i=1,2,3,4$) respectively(4)

$$T_j^i = (P + \rho) v^i v_j - P \delta_j^i, \quad (2)$$

$$g_{ij} v^i v^j = 1 \quad (3)$$

A perfect fluid distribution substituted in the Einstein's field equations can be expressed as follows:

$$8\pi P = e^{-\lambda} \left(\frac{\mu'}{r} + \frac{1}{r^2} \right) - \frac{1}{r^2}, \quad 8\pi P = e^{-\lambda} \left(\frac{\mu''}{2} - \frac{\lambda' - \mu'}{4} + \frac{\mu'^2}{4} + \frac{\mu' - \lambda'}{2r} \right),$$

$$8\pi \rho = e^{-\lambda} \left(\frac{\lambda'}{r} - \frac{1}{r^2} \right) + \frac{1}{r^2}, \quad v^i = (0, 0, 0, e^{-\mu/2}), \quad (4) - (7)$$

overhead dash denotes ordinary differentiation with respect to r .

Karmarker's Condition

The class one condition for (1), in case of a perfect fluid distribution, is expressed by Karmarker (1948) condition (6):

$$3F^2 - 8\pi F(\rho + 3P) + 64\pi^2 P\rho = 0 \quad (8)$$

where

$$F = (1/r^2)(1 - e^{-\lambda}) \quad (9)$$

The condition (8) implies that $e^{-\lambda}$ takes one of the following forms:

$$(i) \quad e^{-\lambda} = 1 - \frac{8\pi}{3} \rho r^2 \quad (ii) \quad e^{-\lambda} = 1 - 8\pi P r^2 \quad (10)$$

Karmarker, 1948 has shown that the only class one spherically symmetric static perfect fluid distribution, which is physically meaningful, is the well-known Schwarzschild interior solution and follows from (10).

EXACT SOLUTIONS FOR SOME MODELS OF CLASS TWO

In this section, we have constructed some spherical sphere models filled with a perfect fluid. These models are of class two and may be guided by the mathematical form of $e^{-\lambda}$ for Schwarzschild interior solutions.

In view of (4) and (5), the functions $\lambda(r)$ and $\mu(r)$ are related by the equation:

$$2r^2\mu'' + r^2\mu'^2 - \mu'(2r + r^2\lambda') - 2r\lambda' - 4(1 - e^\lambda) = 0 \quad (11)$$

If we set

$$x = r^2/R^2 \text{ and } y^2 = e^\mu, \quad (12)$$

where R is a constant, then the equation (11) reduces to the form:

$$\frac{d^2y}{dx^2} - \frac{1}{2} \frac{d\lambda}{dx} \frac{dy}{dx} - \frac{1}{4x} \left[\frac{d\lambda}{dx} + \frac{1 - e^\lambda}{x} \right] y = 0 \quad (13)$$

Hence any solution of (13), which does not satisfy (10), will be of class two. This is because of a spherical symmetric space-time is in general of class two.

It is evident that equation (13) is under consideration.

Consequently, we need to specify one of the variables $\lambda(r)$ or $\mu(r)$ in advance, so that a solution can be obtained.

Hence, according to Karmarker's condition above we assume that

$$e^{-\lambda} = \sum_{i=0}^N \alpha_i x^i \quad (14)$$

If $\alpha_0 = 1$ for $i \geq 1$ then (14) becomes

$$e^{-\lambda} = 1 + \sum_{i=1}^N \alpha_i x^i \quad (15)$$

This form ensures that

$$e^{-\lambda} = 1 + O(r^2) \quad (16)$$

near $r = 0$ for suitable choice of N . In fact this is a sufficient condition for a static perfect fluid sphere to be regular at the center as pointed out by Maartens and Maharaj as in (5).

Case (I) ($N=0$):

We assume the simple expression for $e^{-\lambda}$ as $e^{-\lambda} = \alpha_0$

where α_0 is a positive constant. With this choice the equation (13) will be reduced to:

$$x^2 y'' - \frac{(\alpha_0 - 1)}{4\alpha_0} y = 0 \quad (17)$$

By using Euler method the equation (17) will be:

$$\ddot{y} - \dot{y} - \frac{(\alpha_0 - 1)}{4\alpha_0} y = 0 \quad (18)$$

This is a linear second order ordinary differential equation with constant coefficients. Its characteristic equation is:

$$m^2 - m - \frac{(\alpha_0 - 1)}{4\alpha_0} = 0 \quad \text{and, } m = 0.5 \left(1 \mp \frac{\sqrt{2\alpha_0 - 1}}{\sqrt{\alpha_0}} \right)$$

Now, we have a sub cases as follows:

Sub case (I):

If $0 < \alpha_0 < \frac{1}{2}$, then

$$y(s) = e^{\frac{1}{2}s} (A \cos(\alpha s) + B \sin(\alpha s)) \quad , \quad \alpha = 0.5 \sqrt{\frac{1-2\alpha_0}{\alpha_0}}$$

and the metric will be:

$$ds^2 = -\frac{1}{\alpha_0} dr^2 - r^2 (d\theta^2 + \sin^2 \theta d\phi^2) + \left(x^{\frac{1}{2}} (A \cos(\alpha \ln x) + B \sin(\alpha \ln x)) \right)^2 dt^2$$

where A and B are arbitrary constants.

Sub case (II):

If $\alpha_0 = 0.5$, then $m_1 = m_2 = 0.5$

Hence, $y(s) = (A + Bs)e^{\frac{1}{2}s}$

This implies: $ds^2 = -\frac{1}{\alpha_0} dr^2 - r^2 (d\theta^2 + \sin^2 \theta d\phi^2) + x(A + B \ln x)^2 dt^2$

where A and B are arbitrary constants.

Sub case (III):

If $\alpha_0 > \frac{1}{2}$, then $y(s) = Ae^{m_1 s} + Be^{m_2 s}$

Hence: $ds^2 = -\frac{1}{\alpha_0} dr^2 - r^2 (d\theta^2 + \sin^2 \theta d\phi^2) + (Ax^{m_1} + Bx^{m_2})^2 dt^2$,

where A and B are arbitrary constants.

Case II (N=1):

We assume the expression for $e^{-\lambda}$ as $e^{-\lambda} = \alpha_0 + \alpha_1 x$

where α_0, α_1 are constants.

By substituting in equation (13) we have:

$$(\alpha_0 + \alpha_1 x)y'' + \frac{1}{2}\alpha_1 y' - \frac{1}{4x^2}(\alpha_0 - 1)y = 0 \quad (19)$$

To solve this equation we have two sub cases:

Sub case (I):

For singularity free model, we choose $\alpha_0 = 1$, and then equation (19) will be reduced to:

$$(1 + \alpha_1 x)y'' + \frac{1}{2}\alpha_1 y' = 0 \quad (20)$$

Let $u = y'$, then equation (20) becomes

$$2(1 + \alpha_1 x)u' + \alpha_1 u = 0, \text{ with the solution } u(x) = y'(x) = A(1 + \alpha_1 x)^{-\frac{1}{2}}$$

When $x = r^2$ then u becomes: $u(r) = y'(r) = A(1 + \alpha_1 r^2)^{-\frac{1}{2}}$

This implies, $y(r) = A\sqrt{1 + \alpha_1 r^2} + B$

$$\text{Hence: } ds^2 = -(1 + \alpha_1 r^2)^{-1} dr^2 - r^2(d\theta^2 + \sin^2(\theta)d\varphi^2) + (A\sqrt{1 + \alpha_1 r^2} + B)^2 dt^2$$

Sub case (II):

If $\alpha_0 \neq 1$, then equation (19) can be written as:

$$y'' + R(x)y' + Q(x)y = 0 \quad (21)$$

where

$$R(x) = \alpha_1 / 2(\alpha_0 + \alpha_1 x), \quad Q(x) = (\alpha_0 - 1) / 4x^2(\alpha_0 + \alpha_1 x)$$

The singular points for this equation are

$$x = 0, \quad x = -\alpha_0 / \alpha_1,$$

where $x = 0$ is regular singular point and $x = -\alpha_0 / \alpha_1$ is irregular singular point.

Here, we solve equation (21) near the regular singular point $x = 0$ by using Frobenius method, we get

$$\begin{aligned} (\alpha_0 m(m-1) - \frac{(\alpha_0 - 1)}{4})a_0 &= 0, \quad a_0 \neq 0, \\ a_n &= -\frac{[\alpha_1(m+n-1)(m+n-\frac{3}{2})]}{4\alpha_0(m+n-1)(m+n) - (\alpha_0 - 1)} a_{n-1}, \quad n \geq 1 \end{aligned} \quad (22)$$

We have two cases:

(1) If $m_1 - m_2 = 0$, then $m_1 = m_2 = 0.5$, we get:

$$a_0 \neq 0, \quad a_1 = a_2 = \dots = a_n = 0$$

$$\therefore y_1 = a_0 x^{\frac{1}{2}} \text{ and } y_2 = y_1' = \frac{1}{2} a_0 x^{-\frac{1}{2}}, \text{ Thus } y_G = a_0 A x^{\frac{1}{2}} + \frac{1}{2} a_0 B x^{-\frac{1}{2}}$$

$$\text{Hence } ds^2 = -\frac{1}{(\alpha_0 + \alpha_1 x)} dr^2 - r^2(d\theta^2 + \sin^2(\theta)d\varphi^2) + (a_0 A x^{\frac{1}{2}} + m a_0 B x^{-\frac{1}{2}})^2 dt^2$$

where A and B are arbitrary constants.

(2) If $m_1 - m_2 \neq 0$

(a) If $m_1 - m_2 = a$, where a is not integer number.

$$\begin{aligned} y_1(x) &= a_0 x^{m_1} - \frac{2\alpha_1 m_1(2m_1 - 1)}{4\alpha_0 m_1(m_1 + 1) - (\alpha_0 - 1)} a_0 x^{m_1+1} - \frac{\alpha_1(m_1 + 1)(m_1 + 1/2)}{4\alpha_0(m_1 + 1)(m_1 + 2) - (\alpha_0 - 1)} a_1 x^{m_1+2} \\ &\quad - \dots - \frac{\alpha_1(m_1 + n - 1)(m_1 + n - 3/2)}{4\alpha_0(m_1 + n - 1)(m_1 + n) - (\alpha_0 - 1)} a_{n-1} x^{m_1+n} - \dots \\ y_2(x) &= a_0 x^{m_2} - \frac{2\alpha_1 m_2(2m_2 - 1)}{4\alpha_0 m_2(m_2 + 1) - (\alpha_0 - 1)} a_0 x^{m_2+1} - \frac{\alpha_1(m_2 + 1)(m_2 + 1/2)}{4\alpha_0(m_2 + 1)(m_2 + 2) - (\alpha_0 - 1)} a_1 x^{m_2+2} \\ &\quad - \dots - \frac{\alpha_1(m_2 + n - 1)(m_2 + n - 3/2)}{4\alpha_0(m_2 + n - 1)(m_2 + n) - (\alpha_0 - 1)} a_{n-1} x^{m_2+n} - \dots \end{aligned}$$

$\therefore y_G = A y_1(x) + B y_2(x)$, where A, B are arbitrary constants.

(b) If $m_1 - m_2 = b$, where b is an integer number.

$$y_1(x) = a_0 x^{m_1} - \frac{2\alpha_1 m_1 (2m_1 - 1)}{4\alpha_0 m_1 (m_1 + 1) - (\alpha_0 - 1)} a_0 x^{m_1 + 1} - \frac{\alpha_1 (m_1 + 1)(m_1 + 1/2)}{4\alpha_0 (m_1 + 1)(m_1 + 2) - (\alpha_0 - 1)} a_1 x^{m_1 + 2} \\ - \dots - \frac{\alpha_1 (m_1 + n - 1)(m_1 + n - 3/2)}{4\alpha_0 (m_1 + n - 1)(m_1 + n) - (\alpha_0 - 1)} a_{n-1} x^{m_1 + n} - \dots$$

$$y_2(x) = \left(\frac{\partial y_1}{\partial m_1} \right)_{m_1}$$

$\therefore y_G = Ay_1(x) + By_2(x)$, where A, B are arbitrary constants.

Case (III) ($N=2$):

We assume the expression $e^{-\lambda} = \alpha_0 + \alpha_1 x + \alpha_2 x^2$

where $\alpha_0, \alpha_1, \alpha_2$ are constants.

By substituting in equation (13) we have:

$$x^2(\alpha_0 + \alpha_1 x + \alpha_2 x^2)y'' + 0.5x^2(\alpha_1 + 2\alpha_2 x)y' + 0.25\alpha_2 x^2 y - 0.25(\alpha_0 - 1)y = 0 \quad (23)$$

To solve this equation we have two sub cases:

Sub case (I):

For singularity free model, we choose $\alpha_0 = 1$, and then equation (13) will be reduced to:

$$(1 + \alpha_1 x + \alpha_2 x^2)y'' + \frac{1}{2}(\alpha_1 + 2\alpha_2 x)y' + \frac{1}{4}\alpha_2 y = 0 \quad (24)$$

We can solve this equation by power series method, we get:

$$a_0 \neq 0, a_1 \neq 0, a_2 = -\frac{(2a_1\alpha_1 + a_0\alpha_2)}{8}, a_3 = -\frac{(12a_2\alpha_1 + 5a_1\alpha_2)}{24} \\ \dots a_n = -\frac{[(4n^2 - 16n + 17)a_{n-2}\alpha_2 + (4n^2 - 10n + 6)a_{n-1}\alpha_1]}{4n(n-1)} \\ \therefore y = a_0 + a_1 x - \frac{(2a_1\alpha_1 + a_0\alpha_2)}{8}x^2 - \frac{(12a_2\alpha_1 + 5a_1\alpha_2)}{24}x^3 - \dots - \\ \frac{[(4n^2 - 16n + 17)a_{n-2}\alpha_2 + (4n^2 - 10n + 6)a_{n-1}\alpha_1]}{4n(n-1)}x^n + \dots$$

If $\alpha_1 = 0$, then equation (24) becomes: $(1 + \alpha_2 x^2)y'' + \alpha_2 xy' + 0.25\alpha_2 y = 0$, and

$$a_0 \neq 0, a_2 = \left(-\frac{\alpha_2}{4}\right)^1 \frac{1/4}{2 \times 1} a_0, a_4 = \left(-\frac{\alpha_2}{4}\right)^2 \frac{4 + (1/4)}{4 \times 3} a_2 \\ \dots a_{2k} = \left(-\frac{\alpha_2}{4}\right)^k \frac{[(2k-2)^2 + 1/4]}{(2k)(2k-1)} a_{2k-2} \\ a_1 \neq 0, a_3 = \left(-\frac{\alpha_2}{4}\right)^1 \frac{[1 + 1/4]}{3 \times 2} a_1, a_5 = \left(-\frac{\alpha_2}{4}\right)^2 \frac{[9 + 1/4]}{5 \times 4} a_3 \\ \dots a_{2k+1} = \left(-\frac{\alpha_2}{4}\right)^k \frac{[(2k-1)^2 + 1/4]}{(2k+1)(2k)} a_{2k-1}$$

Then,

$$a_{2k} = \left(-\frac{\alpha_2}{4}\right)^k \frac{\prod_{i=1}^k [(2i-2)^2 + 1/4]}{(2k)!} a_0, \quad k \geq 1 \quad (25)$$

$$a_{2k+1} = \left(-\frac{\alpha_2}{4}\right)^k \frac{\prod_{i=1}^k [(2i-1)^2 + 1/4]}{(2k+1)!} a_1, \quad k \geq 1$$

By the ratio test we can show that the two series (25) above are convergences and then

$$y = \left(1 - \left(\frac{\alpha_2}{4}\right) \frac{[1/4]}{2 \times 1}\right) x^2 + \dots + \left(-\frac{\alpha_2}{4}\right)^k \frac{\prod_{i=1}^k [(2i-2)^2 + 1/4]}{(2k)!} x^{2k} a_0$$

$$+ \left(x - \left(\frac{\alpha_2}{4}\right) \frac{[1+1/4]}{3 \times 2}\right) x^3 + \dots + \left(-\frac{\alpha_2}{4}\right)^k \frac{\prod_{i=1}^k [(2i-1)^2 + 1/4]}{(2k+1)!} x^{2k+1} a_1$$

Sub case (II):

If $\alpha_0 \neq 1$, then equation (13) can be solved by Frobeniu's method, we get:

$$(\alpha_0 m(m-1) - \frac{(\alpha_0 - 1)}{4}) a_0 = 0, \quad a_0 \neq 0, \quad a_1 = -\frac{(m(m-1) + \frac{1}{2}m) \alpha_1 a_0}{4\alpha_0 m(m+1) - (\alpha_0 - 1)} a_0 \quad (26)$$

$$\dots \quad a_n = -\frac{[(m+n-1)(m+n-\frac{3}{2}) \alpha_1 a_{n-1} + ((m+n-2)^2 + \frac{1}{4}) \alpha_2 a_{n-2}]}{4\alpha_0 (m+n-1)(m+n) - (\alpha_0 - 1)}, \quad n \geq 2$$

We have two cases:

(1) If $m_1 - m_2 = 0$, then $m_1 = m_2 = \frac{1}{2}$, and by replace in equations (26) we get:

$$a_0 \neq 0, \quad a_1 = \frac{-\alpha_1}{2(2\alpha_0 + 1)} a_0, \quad a_2 = \frac{-(3\alpha_1 a_1 + \alpha_2 a_0)}{2(14\alpha_0 + 1)}, \quad a_3 = \frac{-(10\alpha_1 a_2 + 5\alpha_2 a_1)}{2(34\alpha_0 + 1)}$$

$$\dots \quad a_n = \frac{-\left[(n-1)(n-\frac{1}{2}) \alpha_1 a_{n-1} + ((n-\frac{3}{2})^2 + \frac{1}{4}) \alpha_2 a_{n-2}\right]}{4\alpha_0 n^2 - 2\alpha_0 + 1}$$

$$\therefore y_1 = \sum_{n=0}^{\infty} a_n x^{n+\frac{1}{2}} \quad \text{and} \quad y_2 = y_1'$$

$$\therefore y_G = a_0 A x^m + m a_0 B x^{m-1}$$

$$\text{Hence, } ds^2 = -(\alpha_0 + \alpha_1 x + \alpha_2 x^2)^{-1} dr^2 - r^2 (d\theta^2 + \sin^2(\theta) d\varphi^2) + (A y_1 + B y_2)^2 dt^2$$

where A and B are arbitrary constants.

For the above result if $\alpha_1 = 0$, then $a_1 = a_2 = \dots = a_n = 0$,

$$\text{and } y_1 = a_0 x^{\frac{1}{2}} \quad \text{and} \quad y_2 = y_1' = 0.5 a_0 x^{-\frac{1}{2}}, \quad \text{thus} \quad y_G = a_0 A x^{\frac{1}{2}} + 0.5 a_0 B x^{-\frac{1}{2}}$$

where A and B are arbitrary constants.

(2) If $m_1 - m_2 \neq 0$

(a) If $m_1 - m_2 = a$, where a is not integer number

$$y_1(x) = a_0 x^{m_1} - \frac{[m_1(m_1-1) + \frac{1}{2}m_1]\alpha_1}{4\alpha_0 m_1(m_1+1) - (\alpha_0-1)} a_0 x^{m_1+1} - \frac{[(m_1+1)(m_1+2)a_1\alpha_1 + (m_1^2 + \frac{1}{4})a_0\alpha_2]}{4\alpha_0(m_1+1)(m_1+2) - (\alpha_0-1)} x^{m_1+2} \\ - \dots - \frac{[(m_1+n-1)(m_1+n-\frac{3}{2})a_{n-1}\alpha_1 + ((m_1+n-2)^2 + \frac{1}{4})a_{n-2}\alpha_2]}{4\alpha_0(m_1+n-1)(m_1+n) - (\alpha_0-1)} x^{m_1+n} - \dots$$

$$y_2(x) = a_0 x^{m_2} - \frac{[m_2(m_2-1) + \frac{1}{2}m_2]\alpha_1}{4\alpha_0 m_2(m_2+1) - (\alpha_0-1)} a_0 x^{m_2+1} - \frac{[(m_2+1)(m_2+2)a_1\alpha_1 + (m_2^2 + \frac{1}{4})a_0\alpha_2]}{4\alpha_0(m_2+1)(m_2+2) - (\alpha_0-1)} x^{m_2+2} \\ - \dots - \frac{[(m_2+n-1)(m_2+n-\frac{3}{2})a_{n-1}\alpha_1 + ((m_2+n-2)^2 + \frac{1}{4})a_{n-2}\alpha_2]}{4\alpha_0(m_2+n-1)(m_2+n) - (\alpha_0-1)} x^{m_2+n} - \dots$$

$\therefore y_G = Ay_1(x) + By_2(x)$, where A, B are arbitrary constants.

(b) If $m_1 - m_2 = b$, where b is an integer number.

$$y_1(x) = a_0 x^{m_1} - \frac{[m_1(m_1-1) + \frac{1}{2}m_1]\alpha_1}{4\alpha_0 m_1(m_1+1) - (\alpha_0-1)} a_0 x^{m_1+1} - \frac{[(m_1+1)(m_1+2)a_1\alpha_1 + (m_1^2 + \frac{1}{4})a_0\alpha_2]}{4\alpha_0(m_1+1)(m_1+2) - (\alpha_0-1)} x^{m_1+2} \\ - \dots - \frac{[(m_1+n-1)(m_1+n-\frac{3}{2})a_{n-1}\alpha_1 + ((m_1+n-2)^2 + \frac{1}{4})a_{n-2}\alpha_2]}{4\alpha_0(m_1+n-1)(m_1+n) - (\alpha_0-1)} x^{m_1+n} - \dots$$

$y_2(x) = (\frac{\partial y_1}{\partial m_1})_{m_1}$, thus $y_G = Ay_1(x) + By_2(x)$, where A, B are arbitrary constants.

PHYSICAL ANALYSIS OF THE SOLUTIONS

The physical acceptability static spherical symmetric perfect fluid solutions of Einstein field equations must comply with the following conditions (7):

(i) The matter density ρ and the fluid pressure P should be positive through out the distribution and, vanished at the boundary and equal ∞ at $r=R$.

(ii) The gradients $\frac{d\rho}{dr}, \frac{dP}{dr}$ should be negative with increasing radius.

(iii) The speed of the sound should not exceed the speed of light as implication of causality fulfillment.

(iv) The interior metric should match continuously with the Schwarzschild exterior solution

$$ds^2 = -(1 - \frac{2M}{r})^{-1} dr^2 - r^2(d\theta^2 + \sin^2(\theta)d\phi^2) + c^2(1 - \frac{2M}{r})dt^2$$

(v) In addition to that the weak energy (WE) and strong energy (SE) conditions should be positive.

Case (I): for $e^{-\lambda} = \alpha_0$

In consequence of (14) and $e^{-\lambda}$, it is found that

$$e^\mu = (Ax^{m_1} + Bx^{m_2})^2, \quad (27)$$

where $x = r^2/R^2$ and m_1, m_2 are the root of the equation $m^2 - m - \frac{1}{4}(1 - \frac{1}{\alpha_0})$, A and B

are arbitrary constants. This case is identical with the well-known model [3]

Case II: Let $e^{-\lambda} = \alpha_0 + \alpha_1 x$ (28)

Where α_0, α_1 are constants

Now, using (28) into (13), we get

$$(\alpha_0 + \alpha_1 x) \frac{d^2 y}{dx^2} + \frac{\alpha_1}{2} \frac{dy}{dx} - \frac{1 - \alpha_0}{4x^2} y = 0 \quad (29)$$

Sub case (I):

For $e^{-\lambda} = 1 + \alpha_1 x$, the continuity of $e^{-\lambda}$ and its first derivative with g_{11} of Schwarzschild exterior metric at the boundary $r=R$, gives α_1 as

$$\alpha_1 = -2m/R \quad (30)$$

Then the density of the distribution turns out to be

$$8\pi\rho R^2 = 6m/R \quad (31)$$

which is unphysical.

Sub case (II):

The continuity of $e^{-\lambda}$ and its first derivative with g_{11} of Schwarzschild exterior metric at the boundary $r=R$, gives α_0, α_1 as follows

$$\alpha_0 = 1 - 4m/R, \quad \alpha_1 = 2m/R \quad (32)$$

The density of the distribution turns out to be

$$8\pi\rho R^2 = 2m(2-x)/Rx \quad (33)$$

The pressure of the model is determined by the first order ordinary differential equation

$$\frac{dP}{dx} = \frac{1}{4x} \left[Px + \frac{3m}{R}(1-x) \right] \left[1 - e^{\lambda}(1+Px) \right] \quad (34)$$

So the physical acceptability may be fulfilled as $\frac{m}{R}$ enters in $e^{-\lambda}$, the value of

$\frac{m}{R}$ is restricted by the condition $e^{-\lambda} > 0$, this requires that

$$\begin{aligned} e^{-\lambda} &= \alpha_0 + \alpha_1 x \\ &= 1 - \frac{4m}{R} + \frac{2m}{R}x > 0, \quad 0 \leq x \leq 1 \end{aligned}$$

That is fulfilled if $m/R < 0.25$.

Again the value of m/R is restricted further by the roots of the indicial equation which requires that $\alpha_0 > 0.5$ i.e. $m/R < 0.25$. For this reason in this case we have taken the values of m/R as 0.1 and 0.15 as follows in the following tables in addition to that some other conditions weak energy condition (WEC) and strong energy condition (SEC) have been tabulated and shown it is greater than zero which is physically acceptable as will be shown in following tables and Fig (1-4) below.

Table-1: Pressure and Density when $N=1$ and $\alpha_0 \neq 1$

$\frac{m}{R}$	0.1				0.15			
x	Density	Pressure	WEC	SEC	Density	Pressure	WEC	SEC
0.1	28.704	3.664	25.040	17.712	43.057	13.348	29.709	3.013
0.2	20.160	0.743	19.417	17.931	30.240	2.480	27.760	22.800
0.3	13.506	0.254	13.255	12.744	20.258	0.798	19.460	17.864
0.4	8.505	0.104	8.401	8.193	12.758	0.312	12.446	11.849
0.5	4.922	0.045	4.877	4.787	7.383	0.131	7.252	6.990
0.6	2.520	0.020	2.500	2.460	3.780	0.055	3.725	3.615
0.7	1.063	0.008	1.055	1.039	1.595	0.022	1.573	1.529
0.8	0.315	0.003	0.312	0.306	0.472	0.007	0.465	0.451
0.9	0.039	0.001	0.038	0.036	0.059	0.001	0.058	0.056
1.0	0.000	0.000	0.000	0.000	0.000	0.000	0.000	0.000

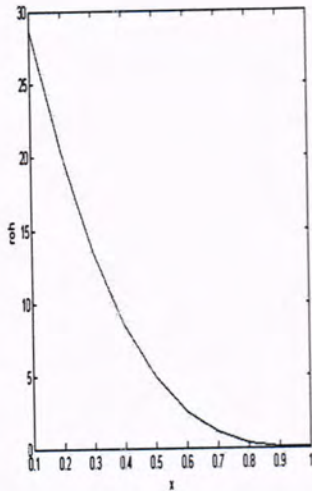


Figure-1 : Density when $\frac{m}{R} = 0.1$

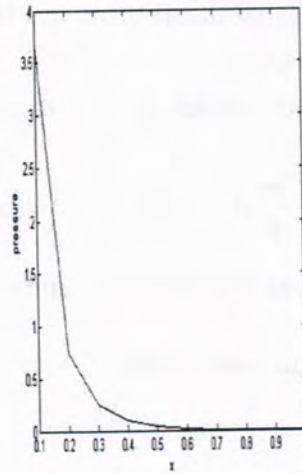
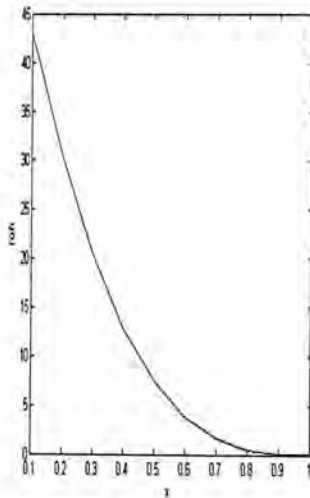
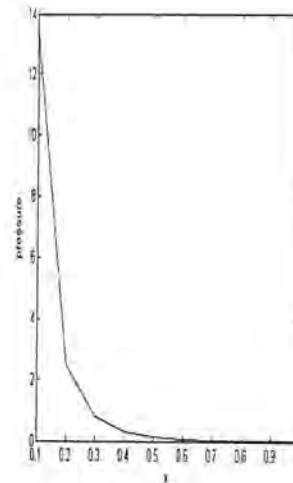


Figure-2 : Pressure when $\frac{m}{R} = 0.1$

Figure-3 : Density when $\frac{m}{R} = 0.15$ Figure-4 : Pressure when $\frac{m}{R} = 0.15$

Case III:

As we mentioned in earlier that we may guided by the assumption of $e^{-\lambda}$, the density becomes infinite at the center of the model.

Sub case (I):

In order to obtain a Singularity-free model we start with a polynomial expression

$$e^{-\lambda} = 1 + \alpha_1 x + \alpha_2 x^2 \quad (35)$$

To determine the constants α_1, α_2 , we demand the continuity of $e^{-\lambda}$ and its first derivative with g_{11} of Schwarzschild exterior metric at the boundary $r=R$, gives $\alpha_0, \alpha_1, \alpha_2$ as follows

$$1 + \alpha_1 + \alpha_2 = 1 - \frac{2m}{R} \quad (36)$$

And the continuity of the first derivative of g_{11} at $r=R$ gives

$$\alpha_1 + 2\alpha_2 = m/R \quad (37)$$

Solving (36) and (37), we get

$$\alpha_1 = -\frac{5m}{R}, \quad \alpha_2 = \frac{3m}{R} \quad (38)$$

In view of (38), (36) and (29), the density and pressure are furnished as follows

$$8\pi\rho R^2 = \frac{15m(1-x)}{R} \quad (39)$$

$$\frac{dP}{dx} = \frac{1}{4x} \left[P + \frac{15m}{R}(1-x) \right] \left[1 - e^{\lambda}(1+Px) \right] \quad (40)$$

The solutions so obtained has been tabulated numerically for some restriction to $\frac{m}{R} < 0.48$ and it has shown physically acceptable as follows in the following table and Fig (5-8).

Table-2: Pressure and Density when $N=2$ and $\alpha_0 = 1$

$\frac{m}{R}$	0.1				0.15			
x	Density	Pressure	WEC	SEC	Density	Pressure	WEC	SEC
0.1	2.870	0.095	2.775	2.585	4.306	0.252	4.054	3.550
0.2	2.061	0.088	1.973	1.797	3.024	0.235	2.789	2.319
0.3	1.351	0.078	1.273	1.117	2.026	0.204	1.822	1.414
0.4	0.851	0.063	0.788	0.662	1.276	0.168	1.108	0.772
0.5	0.492	0.048	0.444	0.348	0.738	0.128	0.610	0.354
0.6	0.252	0.033	0.219	0.153	0.378	0.087	0.291	0.117
0.7	0.106	0.019	0.087	0.049	0.160	0.053	0.107	0.001
0.8	0.032	0.009	0.023	0.005	0.067	0.022	0.045	0.001
0.9	0.014	0.002	0.012	0.008	0.016	0.005	0.011	0.001
1.0	0.000	0.000	0.000	0.000	0.000	0.000	0.000	0.000

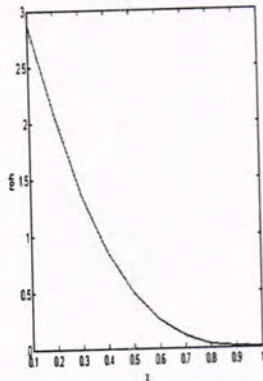


Figure-5 : Density when $\frac{m}{R} = 0.1$

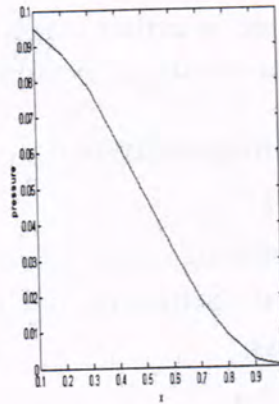


Figure-6 : Pressure when $\frac{m}{R} = 0.1$

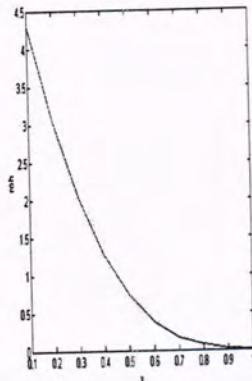


Figure-7 : Density when $\frac{m}{R} = 0.15$

Sub case (II):

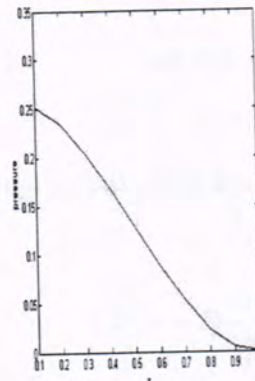


Figure-8 : Pressure when $\frac{m}{R} = 0.15$

When we start with a polynomial expression of $e^{-\lambda}$ as follows:

$$e^{-\lambda} = \alpha_0 + \alpha_1 x + \alpha_2 x^2 \quad (41)$$

To determine the constants $\alpha_0, \alpha_1, \alpha_2$, we demand the continuity of $e^{-\lambda}$ and its first derivative with g_{11} of Schwarzschild exterior metric at the boundary $r=R$, gives $\alpha_0, \alpha_1, \alpha_2$ as follows

$$\alpha_0 + \alpha_1 + \alpha_2 = 1 - 2m/R \quad (42)$$

And the continuity of the first derivative of g_{11} at $r=R$ gives

$$\alpha_1 + 2\alpha_2 = m/R \quad (43)$$

The continuity of the second derivatives of g_{11} at $r=R$ gives

$$2\alpha_2 = -2m/R \quad (44)$$

Solving (42), (43) and (44), we get:

$$\alpha_2 = -m/R, \quad \alpha_1 = 3m/R, \quad \alpha_0 = 1 - 4m/R$$

In view of (41), (42), (43) and (29), we get

$$8\pi\rho R^2 = 3m(x^2 - 3x + 3)/Rx$$

which does not vanish at boundary. Hence the solution of this sub case is unphysical.

We can conclude :

Static spherical fluid spheres have been considered for obtaining a perfect fluid distributions with pressure and density both vanishing at the boundary beyond with the Schwarzschild exterior gravitation field. The solutions so obtained are discussed and analyzed with respect to the physical acceptability as we shown in the above sections.

REFERENCES

1. Stephani, H et al, "Exact solutions of Einstein's field equation" ISBN 0521461367, 2nd edition, (2003).
2. Barnes A. "Space-Times of Embedding Class One Integral Relativity" GRG., 5, (2) :147, (1974).
3. Pandey, S.N & Sharma, S P "Insufficiency of Karmarkar's condition" GRG, 14(2) (1981).
4. Gupta Y K & Jasim M.K. "On most general exact solution for Vadya-Tikekar isentropic super dense star" published in the Astrophysics & Space Science Journal, 272:403-415, Holland, (2000).
5. Gupta Y K & Jasim M.K. "On the most general accurate solutions for Buchdal's fluid spheres" published in the Astrophysics & Space Science Journal, 283, (3) :337-346, Holland, (2003).
6. Karmarkar, K.R. "Gravitational Metric of Spherical Symmetry and Class One", Proc. Indian Acad. Sci., A27: 56, (1948).
7. Knutsen H. "The Physical Properties and Analytic Model for Relativistic Star", Astrophysics. And Space Sci., 162, :315-336, (1989).

Solving combinatorial optimization problem by using genetic algorithm

¹Tariq S. Abdull-Raza and ²Waffa Abdul-Abbas

¹University of Al-Mustansiriyah, College of Science, Dept. of mathematics,

²University Thi-Qar, College of Education, Dept. of mathematics,

الخلاصة

هناك عدة مسائل في الجدولة تمتلك الصيغة التوافقية وهذه المسائل يكون من الصعب جدا إيجاد الحل الأمثل لها خلال اوقات حسابية معقولة. وحينما يكون الحل القريب من الحل الأمثل مقبولا فأنه من المناسب استخدام الطرائق التقريبية لإيجاد ذلك الحل. تناولنا في هذا البحث مسأله جدولة n من الاعمال على ماكينة واحدة لتقليل الكلفة الكلية من تبكير, تأخير, زمن الاتمام وعدد الاعمال المتأخرة $\sum (E_j + T_j + C_j + U_j)$.

هذه المسألة من النوع المعقد لذلك فان وجود خوارزمية متعددة الحدود لإيجاد الحل الأمثل غير ممكن. في هذا البحث اقترحنا خوارزمية التفرع والتقييد (BAB) للحصول على الحل الأمثل وقد تم استخدام قواعد الهيمنة لتقليل عدد التفرعات في شجرة البحث. كذلك قمنا ببرهنة بعض الحالات الخاصة لمسائلنا والتي تقودنا الى الحل الأمثل.

كما قمنا باستخدام مجموعة من الطرائق التقريبية للحصول على حل قريب من الحل الأمثل منها (VNA, SA, GA, HGA) وعند اختبار كفاءة الطرائق على مجموعة كبيرة من المسائل الاختبارية, كانت النتائج تشير الى ان HGA هي الافضل.

ABSTRACT

Many sequencing problems have a combinatorial nature and they are very difficult to solve the optimality within acceptable computation times. When a near optimal solution is acceptable, it is appropriate to use heuristic methods.

In this work we consider the problem of scheduling n jobs on a single machine to minimize the total cost of earliness, tardiness, completion time and the number of late jobs $\sum_j (E_j + T_j + C_j + U_j)$.

This problem is NP-hard; hence the existence of a polynomial time algorithm for finding an optimal solution is unlikely. In this paper we propose a branch and bound algorithm to solve this problem. The BAB procedure uses dominance properties to reduce the number of sequences that must be considered. Also, we prove some special cases of the problem which leads to optimal solutions. We also apply some local search methods such as: Variable Neighborhood Search (VNS), Simulation Annealing (SA) algorithm, Genetic Algorithm (GA) and hybrid Genetic Algorithm (HGA). Performance of these heuristic methods is evaluated on a large set of test problems; it seems that the performance of (HGA) is the best.

Keywords

Scheduling, Branch and bound, Simulation annealing, genetic algorithm, Variable Neighborhood Search and hybrid Genetic Algorithm.

INTRODUCTION

Currently, a major thrust in scheduling research is directed towards improving performance with respect to due dates. Most of the literature on due date criteria deals with static deterministic scheduling problem. In other

words, all jobs are known in advance and are simultaneously available at time zero. Furthermore, the majority of the literature on earliness and tardiness problem has been involved with single machine problems.

The early/tardy problem has been considered by several authors, and both exact and heuristic approaches have been proposed. Among the exact approaches, branch-and-bound algorithms were presented by Abdul-Razaq and Potts (1), Li (8) and Liaw (9). The lower bounding procedure of Abdul-Razaq and Potts was based on the subgradient optimization approach and the dynamic programming state-space relaxation technique, while Li and Liaw Lagrangian relaxation and the multiplier adjustment method. Valente and Alves (12) presented an additional dispatch rule and a greedy procedure, and also considered the use of dominance rules to further improve the schedule obtained by the heuristics. A neighborhood search algorithm was also presented by Li (8).

Formulation of the problem

The problem of scheduling jobs on a single machine to minimize total cost is stated as follows. Each job of the set $N = \{1, \dots, n\}$ is to be processed without interruption on a single machine that can handle only one job at a time. Job j ($j \in N$) becomes available for processing at time zero, requires an integer processing time p_j . The objective is to find a processing order (σ) of the jobs with associated completion times C_j ($j \in N$) where $C_j = \sum_{i=1}^j P_i$ we can calculate the earliness $E_j = \text{Max}_j \{d_j - C_j, 0\}$, the tardiness

$$T_j = \text{Max}_j \{C_j - d_j, 0\} \text{ and the number of late jobs is } \sum_{j=1}^n U_j \text{ where,}$$

$$U_j = \begin{cases} 0 & \text{if } C_j \leq d_j & (\text{job } j \text{ is early}) \\ 1 & \text{otherwise} & (\text{job } j \text{ is late}) \end{cases}$$

The objective is to find a processing of the jobs on the machine, i.e. to find a schedule $\sigma = (\sigma(1), \dots, \sigma(n))$ that minimize the cost $f(\sigma)$.

Hence our problem (RR) can be written formally as:

$$\left. \begin{aligned} \text{Min}_{\sigma \in S} \{f(\sigma)\} &= \text{Min}_{\sigma \in S} \left\{ \sum_{j=1}^n (E_{\sigma(j)} + T_{\sigma(j)} + C_{\sigma(j)} + U_{\sigma(j)}) \right\} \\ \text{S.T} \\ C_{\sigma(j)} &\geq P_{\sigma(j)} & j=1, \dots, n \\ C_{\sigma(j)} &= C_{\sigma(j-1)} + P_{\sigma(j)} & j=2, \dots, n \\ E_{\sigma(j)} &\geq d_{\sigma(j)} - C_{\sigma(j)} & j=1, \dots, n \end{aligned} \right\} \quad (\text{RR})$$

$$\begin{aligned}
 E_{\sigma(j)} &\geq 0 & j=1, \dots, n \\
 T_{\sigma(j)} &\geq C_{\sigma(j)} - d_{\sigma(j)} & j=1, \dots, n \\
 T_{\sigma(j)} &\geq 0 & j=1, \dots, n \\
 U_{\sigma(j)} &= 1 \quad \text{if } C_{\sigma(j)} > d_{\sigma(j)} & j=1, \dots, n \\
 U_{\sigma(j)} &= 0 \quad \text{if } C_{\sigma(j)} \leq d_{\sigma(j)} & j=1, \dots, n
 \end{aligned}$$

where $\sigma(j)$ denote the position of job j in the ordering σ and S denoted the set of all feasible schedules.

Clearly, this problem is NP-hard, since the total tardiness problem is NP-hard(7).

Decomposition of the problem and derivation of lower bounds

Let S be the set of all feasible solutions, σ is a schedule in S . The object is to find a processing order of jobs σ , $\sigma = (\sigma(1), \dots, \sigma(n))$. (we abbreviate $\sigma(j)$ to σ_j) which minimizes the objective function of (RR) defined by

$$\begin{aligned}
 \text{Min } f(\sigma) &= \text{Min}_{\sigma \in S} \left\{ \sum_{j=1}^n (E_{\sigma_j} + T_{\sigma_j} + C_{\sigma_j} + U_{\sigma_j}) \right\} \\
 &= \text{Min}_{\sigma \in S} \sum_{j=1}^n \{ \text{Max} \{ d_{\sigma_j} - C_{\sigma_j}, 0 \} + \text{Max} \{ C_{\sigma_j} - d_{\sigma_j}, 0 \} + C_{\sigma_j} + U_{\sigma_j} \} \\
 &= \text{Min}_{\sigma \in S} \sum_{j=1}^n \{ \text{Max} \{ d_{\sigma_j} - C_{\sigma_j}, C_{\sigma_j} - d_{\sigma_j}, 0 \} + C_{\sigma_j} + U_{\sigma_j} \} \\
 &= \text{Min}_{\sigma \in S} \left\{ \sum_{j=1}^n \text{Max} \{ d_{\sigma_j}, 2C_{\sigma_j} - d_{\sigma_j} + U_{\sigma_j}, C_{\sigma_j} \} \right\} \dots \dots \dots (1)
 \end{aligned}$$

If $C_{\sigma_j} = d_{\sigma_j}$ the term C_{σ_j} is the Max in (3.1), then we can write the objective function $f(\sigma)$ by the form:-

$$\text{Min } f(\sigma) = \text{Min}_{\sigma \in S} \left\{ \sum_{j=1}^n \text{Max} \{ d_{\sigma_j}, 2C_{\sigma_j} - d_{\sigma_j} + U_{\sigma_j} \} \right\} \dots \dots \dots (2)$$

$$f(\sigma_j) = \begin{cases} d_{\sigma_j} & \text{if } C_{\sigma_j} \leq d_{\sigma_j} \\ 2C_{\sigma_j} - d_{\sigma_j} + U_{\sigma_j} & \text{otherwise} \end{cases}$$

It is clear that the problem (RR) can be decomposes into two subproblems (P_1) and (P_2) as follows:

$$Z_1 = \text{Min} \sum_{j=1}^n (E_{\sigma_j} + T_{\sigma_j} + C_{\sigma_j})$$

S.t.

$$C_{\sigma(j)} \geq P_{\sigma(j)} \quad j=1, \dots, n$$

$$\begin{aligned}
 C_{\sigma(j)} &= C_{\sigma(j-1)} + P_{\sigma(j)} & j=2, \dots, n \\
 E_{\sigma(j)} &\geq d_{\sigma(j)} - C_{\sigma(j)} & j=1, \dots, n \\
 E_{\sigma(j)} &\geq 0 & j=1, \dots, n \\
 T_{\sigma(j)} &\geq C_{\sigma(j)} - d_{\sigma(j)} & j=1, \dots, n \\
 T_{\sigma(j)} &\geq 0 & j=1, \dots, n
 \end{aligned} \tag{P_1}$$

$$\begin{aligned}
 Z_2 &= \text{Min} \sum_{j=1}^n U_{\sigma(j)} \\
 \text{S.t.} & \\
 C_{\sigma(j)} &\geq P_{\sigma(j)} & j=1, \dots, n \\
 C_{\sigma(j)} &= C_{\sigma(j-1)} + P_{\sigma(j)} & j=2, \dots, n \\
 U_{\sigma(j)} &= 1 \quad \text{if } C_{\sigma(j)} > d_{\sigma(j)} & j=1, \dots, n \\
 U_{\sigma(j)} &= 0 \quad \text{if } C_{\sigma(j)} \leq d_{\sigma(j)} & j=1, \dots, n
 \end{aligned} \tag{P_2}$$

We can find a lower bound by using the following technique.

The first two terms in Z_1 can be decomposed into two subproblems (see Li [8]),

$$\begin{aligned}
 V_1 &= \text{Min}_{\sigma \in S} \sum_{j=1}^n E_{\sigma(j)} \\
 \text{S.t.} & \\
 E_{\sigma(j)} &\geq 0 & j=1, \dots, n \\
 E_{\sigma(j)} &\geq d_{\sigma(j)} - C_{\sigma(j)} & j=1, \dots, n
 \end{aligned} \tag{P_3}$$

$$\begin{aligned}
 V_2 &= \text{Min}_{\sigma \in S} \sum_{j=1}^n T_{\sigma(j)} \\
 \text{S.t.} & \\
 T_{\sigma(j)} &\geq 0 & j=1, \dots, n \\
 T_{\sigma(j)} &\geq C_{\sigma(j)} - d_{\sigma(j)} & j=1, \dots, n
 \end{aligned} \tag{P_4}$$

Li used Lagrangian techniques to find a lower bound for (P_3) and (P_4) . Hence the sum of their lower bounds and the minimum value of $\sum C_j$ (which is obtained by Smith rule) is the lower bounds (LB_L) for our subproblem (P_1) .

Hence the first LB_1 for our problem (RR) is given by $LB_1 = LB_L + Z_2$, where (LB_L) is the lower bound of Li and Z_2 is obtained by using Moore's algorithm for the subproblem (P_2) .

A new lower bound (LB_2) for our problem (RR) is obtained as follows:

Since $\sum_{j \in T} T_j$ is minimized by EDD rule if $T_j \leq P_j$ for every job j [11], then we can find a lower bound LB_2 by relaxation $T_j = P_j$ if $T_j > P_j$.

Suppose the EDD rule gives the sequence $\sigma = (1, 2, \dots, n)$ and let $ER = \{j: j \in \sigma, C_j \leq d_j\}$ and $LT = \{j: j \in \sigma, C_j > d_j\}$ then we have:

$$\begin{aligned} \text{Min} \sum_{j \in \sigma} (E_j + T_j + C_j + U_j) &= \text{Min} \left\{ \sum_{j \in ER} (E_j + C_j) \right\} \sum_{j \in LT} (T_j + C_j + U_j) \\ &= \text{Min} \left\{ \sum_{j \in ER} d_j + \sum_{j \in LT} (T_j + C_j - d_j + d_j + U_j) \right\} \\ &= \text{Min} \left\{ \sum_{j \in ER} d_j + \sum_{j \in LT} (T_j + T_j + d_j + U_j) \right\} \\ &= \text{Min} \left\{ \sum_{j \in ER} d_j + \sum_{j \in LT} d_j + \sum_{j \in LT} (2 T_j + U_j) \right\} \\ &= \text{Min} \left\{ \sum_{j \in \sigma} d_j + 2 \sum_{j \in LT} T_j + \sum_{j \in LT} U_j \right\} \geq \sum_{j \in \sigma} d_j + 2 \text{Min} \sum_{j \in LT} T_j + \text{Min} \sum_{j \in LT} U_j \\ &= LB_2 \dots\dots(3) \end{aligned}$$

LB_2 is a lower bound for our problem (RR), since the first term is constant and $\sum T_j$ is minimized by EDD rule since we relaxed $T_j > P_j$ to $T_j = P_j$.

The last term $\sum U_j$ become a constant and equal to the number of late jobs in the set LT .

To get another lower bound (LB_3) for our problem (RR), by sequencing the jobs by SPT rule and we have from (3.1)

$$\begin{aligned} \text{Min}_{\sigma \in S} \sum_{j=1}^n \text{Max} \{ d_{\sigma j}, 2C_{\sigma j} - d_{\sigma j} + U_{\sigma j}, C_{\sigma j} \} &\geq \\ \text{Min}_{\sigma \in S} \left\{ \text{Max} \left\{ \sum_{j=1}^n d_{\sigma j}, \sum_{j=1}^n \text{Max} \{ 2C_{\sigma j} - d_{\sigma j} + U_{\sigma j}, C_{\sigma j} \} \right\} \right\} \end{aligned}$$

$$\text{Let } X_{\sigma j} = \text{Max} \{ 2C_{\sigma j} - d_{\sigma j} + U_{\sigma j}, C_{\sigma j} \}$$

To show

$$\text{Min}_{\sigma \in S} \sum_{j=1}^n \text{Max} \{ d_{\sigma j}, X_{\sigma j} \} \geq \text{Min}_{\sigma \in S} \left\{ \text{Max} \left\{ \sum_{j=1}^n d_{\sigma j}, \sum_{j=1}^n X_{\sigma j} \right\} \right\} \dots\dots$$

(4)

Since $d_{\sigma j}$ and $x_{\sigma j}$ are positive integers, hence it is clear that

$$\text{Min}_{\sigma \in S} \sum_{j=1}^n \text{Max} \{ d_{\sigma j}, 2C_{\sigma j} - d_{\sigma j} + U_{\sigma j}, C_{\sigma j} \} \geq$$

$$Min_{\sigma \in S} \left\{ \text{Max} \left\{ \sum_{j=1}^n d_{\sigma j}, \sum_{j=1}^n \text{Max} \{ 2C_{\sigma j} - d_{\sigma j} + U_{\sigma j}, C_{\sigma j} \} \right\} \right\}$$

$$LB_3 = Min_{\sigma \in S} \left\{ \text{Max} \left\{ \sum_{j=1}^n d_{\sigma j}, \sum_{j=1}^n \text{Max} \{ 2C_{\sigma j} - d_{\sigma j} + U_{\sigma j}, C_{\sigma j} \} \right\} \right\} \dots\dots\dots$$

(5)

This lower bound LB_3 is very good comparing with the others. Hence this lower bound will be used in our branch and bound (BAB) method as a lower bound to solve our problem (RR).

Special cases

There are special cases in which an optimal schedule can be found directly without using BAB method. This depends on satisfying some conditions in order to make the problem easily solved. The objective function of our problem (RR) is:

$$\text{Min } f(\sigma) = Min_{\sigma \in S} \left\{ \sum_{j=1}^n \text{Max} \{ d_{\sigma j}, 2C_{\sigma j} - d_{\sigma j} + U_{\sigma j} \} \right\}$$

Lemma (1): The SPT (short processing time) schedule is optimal for problem (RR) if $d_j + P_j < C_{j+1}$, $j=1, 2, \dots, n-1$ and if the SPT gives the minimum number of late jobs $\sum U_j$.

Proof: Let $\sigma = (1, 2, \dots, n)$ is obtained by the SPT rule

Since $d_j + P_j \leq C_{j+1}$ $j=1, 2, \dots, n-1$, hence

$$\begin{aligned} d_j &\leq C_{j+1} - P_j = C_j + P_{j+1} - P_j \\ C_j &\quad \text{if } P_j = P_{j+1} \quad j=1, 2, \dots, n-1 \\ (C_j + P_{j+1}) - P_j &= \begin{cases} C_j & \text{if } P_j = P_{j+1} \\ C_j + P & \text{if } P = P_{j+1} - P_j \end{cases} \quad j=1, 2, \dots, n-1 \end{aligned} \dots\dots\dots (6)$$

By SPT rule, we have

(a) Either $P_j = P_{j+1}$ then $C_j + P_{j+1} - P_j = C_j$

Hence from (6) we have

$$d_j \leq C_j \quad j=1, 2, \dots, n-1$$

This means that job j either on time or late

$$\begin{aligned} \therefore \sum (T_j + E_j + C_j + U_j) &= \sum (2C_j - d_j + U_j) \\ &= 2\sum C_j - \sum d_j + \sum U_j \end{aligned}$$

Since by assumption that $\sum U_j$ is minimum by SPT, $\sum d_j$ is constant, and $\sum C_j$ is minimized by SPT.

\therefore SPT schedule is optimal.

(b) Or $C_j + P_{j+1} - P_j = C_j + P$ if $P = P_{j+1} - P_j$

Hence from (6) we have

$$\begin{aligned} d_j &\leq C_j + P & P > 0 \\ d_j - C_j &\leq p & \text{for } j=1, 2, \dots, n-1 \end{aligned}$$

Hence job j is either late and SPT is optimal as in case (a) or it is early. If job j is early then we have,

$$\sum (E_j + T_j + C_j + U_j) = \sum_{j=1}^n d_j$$

Hence, $\sum_{j=1}^n d_j$ is constant

\therefore SPT schedule is optimal.

Lemma (2):

The EDD schedule is optimal for problem(RR) if $T_j \leq P_j$ for every $j=1, \dots, n$ and the number of late jobs $\sum U_j$ in the EDD schedule is equal to the minimum number of late jobs given by using Moor's algorithm (MA).

Proof :-

Let the EDD sequence $\sigma = (1, 2, \dots, n)$ it is well known that T_{\max} is minimum by EDD rule since for each job j ,

$$C_j - d_j \leq T_j \leq T_{\max} = \sum_{j=1}^k P_j - d_k \leq P_k \text{ for some job } k \text{ where}$$

$$T_{\max} = \text{Max}_j \{T_j\} = \text{Max}_j \{C_j - d_j, 0\}$$

Remember that the EDD rule gives the sequence $\sigma = (1, 2, \dots, n)$.

(1) If $T_{\max} = 0$, then $\sum_{j=1}^n (E_j + T_j + C_j + U_j) = \sum_{j \in \sigma} d_j$, hence the EDD rule is optimal since $\sum_{j \in \sigma} d_j$ is constant.

(2) If $T_{\max} > 0$, then $T_{\max} = \sum_{j=1}^k P_j - d_k \leq P_k$ for some job k ,

This means that some of the jobs are early and some of them are late in σ .

Let $ER = \{j: j \in \sigma, C_j \leq d_j\}$ and

$LT = \{j: j \in \sigma, C_j > d_j\}$

Now consider the objective

$$\begin{aligned} \sum_{j=1}^n (T_j + E_j + C_j + U_j) &= \sum_{j \in ER} (E_j + C_j) + \sum_{j \in LT} (T_j + C_j + U_j) \\ &= \sum_{j \in ER} d_j + \sum_{j \in LT} (T_j + C_j - d_j + d_j + U_j) \\ &= \sum_{j \in ER} d_j + \sum_{j \in LT} (T_j + T_j + d_j + U_j) \\ &= \sum_{j \in ER} d_j + \sum_{j \in LT} d_j + \sum (2T_j + U_j) \\ &= \sum_{j \in \sigma} d_j + \sum_{j \in LT} (2T_j + U_j) \dots\dots\dots (7) \end{aligned}$$

It is clear that $\sum T_j$ is minimized by EDD since $T_j \leq P_j$ and since

$$\sum_{j=1}^n U_j = \text{Min} \left\{ \sum U_j \right\}$$

Hence EDD schedule is optimal.

Lemma (3):

If in every schedule the jobs are early, then all the $n!$ schedules are optimal

for problem (RR) with
$$\text{Min} \sum_{j=1}^n (T_j + E_j + C_j + U_j) = \sum_{j=1}^n d_j.$$

Proof: It is clear from proof of lemma (1).

Lemma (4)

The SPT and EDD schedule are optimal for problem (RR) if $d_i \leq d_j$ and $P_i \leq P_j$, $i, j \in N$

Proof: It is clear from lemma (1) and lemma (2).

Lemma (5)

The SPT schedule is optimal for problem (RR) if d is common due date i.e. $d = d_j$ for every j .

Lemma (6)

The EDD schedule is optimal for problem (RR) if P_j is constant i.e. $P_j = P$, for every j .

Dominance rule

The Dominance rules specify a node can be discarded before its LB calculated. There are two dominance rules used in this section.

Dominance rule (1)

An attempt is made to eliminate nodes using a dominance theorem of dynamic programming (DP). This DP dominance uses an adjacent job interchange to compare the sum of $f(ij) = \sum (E_j + T_j + C_j + U_j)$ for the two jobs (i, j) must recently added to the initial partial sequence with the corresponding sum when these two jobs are interchanged in position (j, i) : if the former sum is larger than the later, then the current node is eliminated, while if both sum are the same, some convention is used to decide whether the current node should be discarded.

Dominance rule (2)

If there exist a job j such that $d_j \geq \sum P_i$, then job j is sequence last in an optimal sequence.

The branch and bound (BAB) algorithm

We now give a description of our branch and bound algorithm and its implementation. The BAB method starts by applying the special cases. If the data for the problem (RR) satisfy the conditions of the special cases, then the problem (RR) is solved.

Two heuristic methods (SPT, EDD) are applied at the root node of the search tree, the better of the two heuristic sequence is used to provide an upper bound (UB) on the cost of an optimal schedule. Also at the root node of the search tree an initial lower bound on the cost of an optimal schedule is obtained from (LB_3).

Our algorithm uses a forward sequencing branching rule for which nodes at level k of the search tree correspond to initial partial sequence in which jobs are sequenced in the first k position. If it can be shown that an optimal solution can always be generated, without branching from particular node of the search tree, then that node is dominated and can be eliminated by using dominance theorems. At each node prior to applying the branching rule at the second level of the search tree or below, the DP dominance rule is used in an attempt to reduce the number of nodes within each level of the search tree. Clearly, dominance rules are particularly useful when a node can be eliminated which has a lower bound that is less than the optimal solution.

For nodes that are not eliminated by the dominance rules, a lower bound LB_3 is computed. At any level, if the lower bound for any node is greater than or equal to the current upper bound already computed, then this node is discarded, otherwise it may be selected for our next branching. The branch and bound method continues in a similar way. Whenever a complete sequence is obtained, this sequence is evaluated and the upper bound UB is altered if the new value less than the old one. The procedure is repeated until all nodes have been considered (i.e. lower bounds of the nodes in the scheduling tree are greater than or equal to the UB), a feasible solution with this UB is an optimal solution.

Finally, the search strategy used in our algorithm is the newest active search. This selects a node from which to branch which has the smallest lower bound amongst nodes.

Local Search and Genetic Algorithms

1. Hybrid between neighborhoods

The local search start by applying the special cases in the same way as in the BAB method. Several researchers have applied hybrid between the neighborhoods. Besten et al. [3] use hybrid on iterative descent algorithms using deferent neighborhoods. In this paper we mix more than one neighborhood as (transpose, swap, insert) neighborhoods. It is an important to know the size of neighbors for each type of the hybridization, i.e. the number of neighbors for a single solution. In this section, the following types will be applied:-

- 1) (trans+insert) $N_{tra+ins}$

- 2) (trans+swap) $N_{tra+swap}$
- 3) (insert+trans) $N_{ins+tra}$
- 4) (insert+ swap) $N_{ins+swap}$
- 5) (swap+ trans) $N_{swap+tra}$
- 6) (swap+insert) $N_{swap+ins}$

The following steps describe these methods:

Step (1): Initialization

The best solution of SPT and EDD sequence can be used as an initial feasible solution $\sigma \in S$ with its objective function value $f(\sigma)$.

Step (2): Neighbor generation

In order to improve the sequence σ , the traveling between different neighborhoods gives a new sequence σ^* will be obtained with its objective function value $f(\sigma^*)$.

Step (3): Evaluation

We will accept the sequence σ^* as the current solution, if the improvement is made (i.e. $f(\sigma^*) < f(\sigma)$), otherwise σ is retain as the current solution, then repeated from step 2.

Step (4): Termination

The methods are terminated after 600 iterations at a near optimal solution.

2. Simulated Annealing (SA)

In a simulated annealing procedure, solutions which improve upon the current solution value are always accepted, while those which cause a deterioration in the objective function value are accepted according to a given probabilistic acceptance function.

The following steps describe SA:-

Step (1): Initialization

The same technique described in section (7.1) is used to choose an initial feasible solution to obtain the current solution s and compute its objective function value $f(s)$.

Step (2): Neighbor generation

A feasible neighbor of s is generated by the same procedure described in section (7.1) to obtain the neighbor s^* and compute its objective function value $f(s^*)$.

Step (3): Acceptance test

We calculate the difference value between the current initial solution $f(s)$ and the new value $f(s^*)$, $\Delta = f(s^*) - f(s)$, then evaluated it as follows:-

- a) If $(\Delta \leq 0)$: then $f(s^*)$ is accepted as the new current solution.
- b) Otherwise (i.e. $\Delta > 0$): $f(s^*)$ is accepted with $\Pr(\Delta, t) = \exp(-\Delta/t)$, let (it) denoted the number of iterations that are considered. At each iteration j , $1 \leq j \leq it$, a temperature t_j is derived from the following recursive formula [4],

$$t_j = t_{j-1} / (1 + \beta \times t_1) \quad j=2, \dots, it$$
where : $\beta = (t_1 - 1) / (it \times t_{j-1})$;

$t_1=1000$ and $it=600$

Step (4): Termination test

The algorithm is stopping at a near optimal solution after 600 iterations.

3. Genetic Algorithm (GA)

Genetic algorithms (GAs) were developed by Holland in the 70s. They are based on a direct analogy to Darwinian natural selection and mutation in biological reproduction [10]. A genetic algorithm maintains a population of solutions through the search. It initializes the population with a pool of potential solutions to the problem and seeks to produce better solutions by combining the better of the existing ones through the use of genetic operators (selection, crossover and mutation).

The following steps described structure of (GA):

Step (1): Initialization The initial population can be generated at random or can be constructed by using heuristic methods. In this paper, we start with 20 solutions two of them are obtained by using heuristic methods SPT rule and (EDD) rule and the remaining are randomly.

Step (2): New Population

Generate a new population from the current population by using the genetic operators:

a) Selection: There are various types of selection strategies [5, 6], in this paper we use to choose the parent:

* With a solution σ_{worst} satisfying $\text{cost}(\sigma_{\text{worst}}) \geq \text{cost}(\sigma)$ for all $\sigma \in P$, let $P^* = P \cup \{\sigma_{ck}\} - \{\sigma_{\text{worst}}\}$ ($k = 1, 2$).

b) Crossover

In this section we introduce new type of crossover calls homogeneous mixture crossover (HMX), which is given by the mixture of the two parents uniformly by making a set from genes M , the odd position from the first parent and the even position from the second parent. Then separate genes without repetition of the gene, since we read the set M from the left, if the gene j does not exist in the child σ_{c*} put it, otherwise, we put gene j in the second child $\sigma_{c\#}$ until M genes are exhausted. This way also gives two new children.

Parents:	Mixture:	Exchanging:
7 9 8 2 5 1 6 3 4	\Rightarrow 7 9 9 5 8 6 2 4 5 8 1 3 6 2 3 7 4 1	$\Rightarrow \sigma_{c*}: 7 9 5 8 6$
2 4 1 3		
9 5 6 4 8 3 2 7 1	**#*****##**#####	$\sigma_{c\#}: 9 5 8 6 2$
3 7 4 1		

Partially mapped crossover (PMX), legitimate (LEGX) and homogeneous mixture crossover HMX are applied on the two parent solutions to generate two new solutions (child solutions).

c) Mutation

Mutation operator is applied after crossover operator to perturb and diversify the child solutions, with the hope that one of them converge to a good quality solution.

Trans-mutation operator is applied to perturb some of these new solutions.

Step (3): Termination

The procedure stops when a fixed number of generations are executed here (600) iteration.

4. Hybrid genetic algorithm

The aim of this section is to clearly demonstrate the importance of finding a good balance between genetic search and local search in the implementation of hybrid evolutionary multicriterion optimization algorithms.

We first modify the local search part of an existing multi-objective genetic local search (MGLS) algorithm. In this MGLS algorithm, the computation time spent by local search can be decreased by applying local search to only good solutions in the current population. The local search direction for each solution was specified by the fitness function used in the selection of its parents. This means that we apply local search to only selected solutions (not all solutions) and to terminate local search before all neighbors of the current solution are examined. In this algorithm a new population is generated by local search. Then the new population is improved by genetic operations (selection, crossover and mutation). The improved population is handled as the current population in the MGLS algorithm. In this manner, the population update is iterated by local search and genetic operations until a pre-specified stopping (termination) condition is satisfied.

The following steps described structure of MGLS algorithm:-

Step (1): Initialization

The initial population can be generated by the same procedure described in section (7.3).

Step (2): Improving population:

Create an improving population by repeating the following substeps:-

(a) Selection:

Two parent solutions from a current population according to their fitness values (SPT and EDD rules among them may be selected).

(b) Neighbor generation:

Variable Neighborhood Search (VNS) and Simulation annealing (SA) described in section (7.1) and (7.2) respectively are applied on the two parent solutions to get the best two solutions.

(c) Termination:

This step is terminated after (100) iterations with the best two solutions to be used in genetic algorithm part.

Step (3): The genetic operators

We will use crossover operator on the best two solutions and the same procedure described in section (7.3) is used.

Step (4): Mutation operator

We will use the same procedure described in section (7.3).

Step (5): Termination

The procedure stops when a fixed number of iteration is executed here (600) iterations.

Computational Experience

1. Test Problems

The BAB algorithm was tested by coding it in Microsoft Fortran Power Station and the local search methods were tested by coding them in Matlab 6.5 and all runned on a Pentium IV at 2.26 GHZ, with Ram 256 MB computer.

The tested problem instances are generated as follows; for $n = 10, 15, 20, 25, 35, 50, 75, 100$ and 150 , the processing time P_j for $j \in N = \{1, 2, \dots, n\}$ is generated by randomly selecting integers from interval $[1, 10]$. It has been observed in the literature (e.g. [4]) that problem hardness is related to two parameters RDD and LF, called the relative range of due dates and the average lateness factor, respectively. In our experiment, $RDD = 0.2, 0.4, 0.6, 0.8, 1.0$, $LF = 0.2, 0.4$, are used. Corresponding to each of these $5 \times 2 = 10$ cases, one problem instance is generated by selecting integer due dates $d_j, j \in N$, from interval

$$[(1 - LF - RDD / 2) SP, (1 - LF + RDD / 2) SP], \text{ where } SP = \sum_{j \in N} p_j.$$

Since $n = 10, 20$ and 25 are the sizes that were solved to optimality by the BAB method, the other sizes should also be tested by using the local search and the genetic algorithms and hybrid genetic algorithms.

2. Comparative Computational Results

This section shows the efficiency of local search heuristics and genetic methods, comparing it with the optimal solution (obtained by our BAB algorithm) for each test problem. An optimal solution for each test problem (with $n \leq 25$) is obtained by BAB algorithm, these optimal solution values are used to asses the quality of solutions generated by the methods. The methods (Variable neighborhood search(VNS), Simulated annealing(SA), Genetic algorithms (GAs) and Hybrid genetic algorithms (HGA), We present tables of results which show the importance of each method. Since for $n > 25$ job problems the BAB algorithm can not generate optimal

solutions using reasonable limits on computation time. In this case, the best solution value found by any of the above local search and genetic methods form the basis for comparison. In our computation, we firstly, choose the best neighborhood from the VNS, which is used as a neighborhood in SA and use it as a neighborhood in a mutation in the GA. The results in table (1) show that the neighborhood (N_{tra}) gives the best times, and the best values, hence we use this N_{tra} in the SA, GA and HGA. It should be noted that in table(1) and other tables, the method are compared by listing for each value of n , the best average value and the best average time denoted by (*) and(**) respectively.

For genetic algorithms, table (2) shows that HMX gives the best values with the mutation N_{tra} , and LEGX gives the best times with the same mutation N_{tra} .

Results comparing the performances of the hybrid genetic algorithms HGV_{tra} given in table (3). It shows that HMX is the best in value, and PMX and LEGX are almost the same in case of times, Also the results of the hybrid genetic algorithms (HGSA) are given in table (4). The results show that HMX is the best in values, and LEGX is the best in times, Also results comparing the performances of hybrid genetic algorithms (HGV_{tra}) and (HGSA) are given in table (5). The results show that (HGSA) is the best in case of values and times.

The results in table(6) show that the local search methods VNS and HGSA of all heuristic method perform very well and the difference between them are quite small.

Also, it is clear from table (6) that these two methods are more effective than SA and GA. HGSA has the best values with respect to VNS, SA and GA. Also it is clear that VNS has the best times with respect to HGSA, SA and GA.

For all $n \leq 25$ job problems the optimal solutions are available by using branch and bound (BAB) algorithm. Results comparing the performances of the exact, local search and genetic algorithms are given in table (7) for 20 and 25 jobs. An optimal solution for each test problem with $n \leq 25$ is obtained by BAB algorithm, these optimal solution values are used to asses the quality of solutions generated by local search and genetic algorithm, it is clear from table (7) and for $n \leq 25$ that SA and HGSA gives the best values and (VNS) gives the best times.

Table -1: Comparative results for VNS

		N _{tra}	N _{ins}	N _{swap}	N _{tra+ins}	N _{ins+tra}	N _{ins+swap}	N _{swap+ins}	N _{tra+swap}	N _{swap+tra}
10	V _{avg}	411	408.7	408.4	409.5	407*	415.7	409.4	407.6	409.9
	T _{avg}	0.0735**	0.0953	0.0781	0.1032	0.1094	0.1047	0.0874	0.103	0.0782
15	V _{avg}	818.1*	822.4	823.3	824.9	824	826	822.6	823.3	825.4
	T _{avg}	0.0749**	0.1095	0.0813	0.1156	0.1187	0.1235	0.0859	0.1218	0.0765
20	V _{avg}	1482.4	1470.8*	1476.6	1473.3	1480.4	1471.6	1471.5	1476.6	1473.5
	T _{avg}	0.0749**	0.1218	0.0859	0.1296	0.1361	0.1326	0.086	0.1346	0.0751
25	V _{avg}	2323.5*	2333.2	2333	2332.2	2333	2332.9	2332.2	2333	2332.7
	T _{avg}	0.075**	0.1406	0.086	0.15	0.1532	0.1499	0.0843	0.1499	0.0767
35	V _{avg}	4550.1	4550.7	4561.9	4549.1	4554.9	4547.3*	4562.8	4568.9	4552.3
	T _{avg}	0.0876	0.1668	0.0923	0.172	0.1814	0.1751	0.0939	0.181	0.0796**
50	V _{avg}	9749.4*	9760.2	9765	9760.3	9760.6	9753.6	9763.5	9765	9757.3
	T _{avg}	0.0844**	0.2095	0.0938	0.222	0.2249	0.2234	0.0936	0.2203	0.0859
75	V _{avg}	20870.7*	20874.8	20884	20888.3	20874.3	20889.9	20898	20897.9	20889.8
	T _{avg}	0.086**	0.2875	0.1031	0.3015	0.3015	0.3032	0.0986	0.2938	0.0875
100	V _{avg}	37764.9	37773.1	37787.4	37771.7	37773.1	37761.4*	37786.3	37787.4	37771.7
	T _{avg}	0.092**	0.3514	0.1	0.3642	0.3703	0.3687	0.1032	0.369	0.0969
150	V _{avg}	84780.6*	84803.9	84804.7	84804	84804	84803.5	84804.7	84804.7	84804.3
	T _{avg}	0.1076**	0.4718	0.1187	0.4766	0.4844	0.4813	0.1204	0.4798	0.1077

V_{avg} : average value of objective function.T_{avg} : average time of objective function (in seconds).

Table -2: Comparative results for GA

		PMX	LEGX	HMX
10	V _{avg}	410.7*	410.9	412.4
	T _{avg}	0.3527**	0.5338	2.271
15	V _{avg}	792	795.5	788*
	T _{avg}	0.3596**	0.4622	1.6159
20	V _{avg}	1440.8	1441.3	1430.7*
	T _{avg}	0.5207**	0.5342	2.1738
25	V _{avg}	2277	2266.9*	2278.9
	T _{avg}	0.5926	0.5144**	2.6436
35	V _{avg}	4512.2*	4522.1	4512.9
	T _{avg}	0.9827	0.559**	7.0279
50	V _{avg}	9687.2	9662.2	9640.5*
	T _{avg}	1.5796	0.7929**	10.262
75	V _{avg}	20729	20727	20683*
	T _{avg}	3.6433	1.3321**	16.041
100	V _{avg}	37517	37524	37303*
	T _{avg}	7.0787	1.0878**	23.734
150	V _{avg}	84407	84458	83734*
	T _{avg}	14.445	1.291**	33.922

Table -3: Comparative results for HG_{V_{tra}}

		PMX	LEGX	HMX
10	V _{avg}	407.1*	409.1	409.3
	T _{avg}	0.3714**	0.503	1.7894
15	V _{avg}	796.9	797	788.9*
	T _{avg}	0.4257**	0.5149	1.9665
20	V _{avg}	1427.7*	1443.4	1445.9
	T _{avg}	0.5143**	0.5523	2.6759
25	V _{avg}	2270	2260.6*	2271.8
	T _{avg}	0.6375**	0.6492	3.6468
35	V _{avg}	4523.4	4525.5	4505.6*
	T _{avg}	1.2241	0.9134**	9.7137
50	V _{avg}	9688.9	9675.1	9667.2*
	T _{avg}	2.6227	1.1665**	13.505
75	V _{avg}	20741	20742	20614*
	T _{avg}	5.1493	1.476**	17.678
100	V _{avg}	37498	37522	37316*
	T _{avg}	8.9235	1.35**	29.367
150	V _{avg}	84442	84487	83722*
	T _{avg}	18.646	1.676**	47.816

T_{avg} : average times objective function (in seconds).

V_{avg} : average values objective function.

HMX : homogeneous mixture crossover.

LEGX : legitimate crossover.

PMX : partially matched crossover.

Table-4: Comparative results for HGSA

		PMX	LEGX	HMX
10	V _{avg}	408.4*	408.6	406.2*
	T _{avg}	0.379**	0.4683	2.4857
15	V _{avg}	789.5	794.5	783.1*
	T _{avg}	0.4087**	0.5471	1.6952
20	V _{avg}	1437.9	1433.5	1427.6*
	T _{avg}	0.4639**	0.538	3.079
25	V _{avg}	2284.7	2253*	2272.8
	T _{avg}	0.6318	0.5829**	4.5866
35	V _{avg}	4521.5	4514.9	4509.8*
	T _{avg}	1.1887	0.8244**	7.1597
50	V _{avg}	9679.7	9665.1	9652.2*
	T _{avg}	2.3664	1.1471**	12.359
75	V _{avg}	20742	20748	20612*
	T _{avg}	4.4835	1.3866**	22.303
100	V _{avg}	37491	37512	37324*
	T _{avg}	8.2907	1.2442**	27.581
150	V _{avg}	84386	84449	83727*
	T _{avg}	16.979	1.4705**	43.55

V_{avg}: average values objective function.
HMX: homogeneous mixture crossover.
LEGX: legitimate crossover.
seconds).
HGSA: hybrid genetic algorithms with
simulation annealing.
HGV_{tra}: hybrid genetic algorithms with
transpose.

Table-5: Comparative results between HGSA and HGV_{tra}

		HGSA		HGV _{tra}	
		LEGX	HMX	LEGX	HMX
10	V _{avg}	408.6	406.2*	409.1	409.3
	T _{avg}	0.4683**	2.4857	0.503	1.7894
15	V _{avg}	794.5	783.1*	797	788.9
	T _{avg}	0.5471	1.6952	0.5149**	1.9665
20	V _{avg}	1433.5	1427.6*	1443.4	1445.9
	T _{avg}	0.538**	3.079	0.5523	2.6759
25	V _{avg}	2253*	2272.8	2260.6	2271.8
	T _{avg}	0.5829**	4.5866	0.6492	3.6468
35	V _{avg}	4514.9	4509.8	4525.5	4505.6*
	T _{avg}	0.8244**	7.1597	0.9134	9.7137
50	V _{avg}	9665.1	9652.2*	9675.1	9667.2
	T _{avg}	1.1471**	12.359	1.1665	13.505
75	V _{avg}	20748	20612*	20742	20614
	T _{avg}	1.3866**	22.303	1.476	17.678
100	V _{avg}	37512	37324	37522	37316*
	T _{avg}	1.2442**	27.581	1.35	29.367
150	V _{avg}	84449	83727	84487	83722*
	T _{avg}	1.4705**	43.55	1.676	47.816

V_{avg}: average values objective function.
HMX: homogeneous mixture crossover.
T_{avg}: average times objective function (in
LEGX : legitimate crossover.
PMX: partially matched crossover.

Table -6: Comparison between local search methods

		VNS	SA	GA		HGSA	
		N _{tra}	N _{tra}	LEGX	HMX	LEGX	HMX
10	V _{avg}	411	406.3	410.9	412.4	408.6	406.2*
	T _{avg}	0.0735**	0.0875	0.5338	2.271	0.4683	2.4857
15	V _{avg}	818.1	794.9	795.5	788	794.5	783.1*
	T _{avg}	0.0749**	0.0875	0.4622	1.6159	0.5471	1.6952
20	V _{avg}	1482.4	1427.9	1441.3	1430.7	1433.5	1427.6*
	T _{avg}	0.0749**	0.0811	0.5342	2.1738	0.538	3.079
25	V _{avg}	2323.5	2265.3	2266.9	2278.9	2253*	2272.8
	T _{avg}	0.075**	0.0893	0.5144	2.6436	0.5829	4.5866
35	V _{avg}	4550.1	4521.3	4522.1	4512.9	4514.9	4509.8*
	T _{avg}	0.0876	0.0862**	0.559	7.0279	0.8244	7.1597
50	V _{avg}	9749.4	9694.5	9662.2	9640.5*	9665.1	9652.2
	T _{avg}	0.0844**	0.0923	0.7929	10.262	1.1471	12.359
75	V _{avg}	20870.7	20978.5	20727	20683	20748	20612*
	T _{avg}	0.086**	0.0933	1.3321	16.041	1.3866	22.303
100	V _{avg}	37764.9	37651.4	37524	37303*	37512	37324
	T _{avg}	0.092	0.0906**	1.0878	23.734	1.2442	27.581
150	V _{avg}	84780.6	84629.7	84458	83734	84449	83727*
	T _{avg}	0.1076	0.1016**	1.291	33.922	1.4705	43.55

T_{avg} : average times objective function (in seconds).

V_{avg} : average values objective function.

HMX : homogeneous mixture crossover.

LEGX : legitimate crossover.

HGSA : hybrid genetic algorithms with simulation annealing.

VNS : variable neighborhood search.

SA : simulation annealing.

GA : genetic algorithm

Table - 7: Comparison between local search methods and optimal solution.

		BAB	VNS (N_{tra})		SA (N_{tra})		GA (HMX)		HGSA	
			Values	Times	Values	Times	Values	Times	Values	Times
20	1	1230	1504	0.078**	1254*	0.078	1313	1.174	1310	3.078
	2	965	1066	0.078**	972*	0.093	972*	1.394	972*	1.751
	3	1660	1689	0.062**	1681	0.078	1688	2.315	1670*	2.623
	4	1446	1550	0.078**	1461	0.078	1468	1.025	1460*	0.675
	5	1274	1329	0.078**	1295*	0.093	1295*	2.451	1300	5.672
	6	1083	1353	0.063**	1320	0.078	1326	0.437	1313*	1.251
	7	****	2125	0.078**	2108	0.078**	2088	1.219	2076*	5.816
	8	1337	1374	0.078**	1363	0.079	1341*	1.205	1358	2.423
	9	1289	1335	0.078**	1326	0.078**	1317	4.674	1309*	1.363
	10	1441	1499*	0.078**	1499*	0.078**	1499*	5.844	1499*	6.138
25	1	2832	2889	0.078**	2845*	0.094	2888	5.827	2859	5.762
	2	****	1995	0.062**	1982	0.079	1980*	1.094	1994	6.126
	3	****	1917	0.079**	1897	0.094	1858*	3.871	1875	6.916
	4	2573	2727	0.078**	2632	0.078**	2714	4.733	2620*	1.259
	5	2462	2543	0.078**	2514	0.078**	2513	1.78	2509*	6.28
	6	****	2290	0.078**	2202	0.11	2200*	1.206	2202	3.517
	7	1822	1862	0.063**	1861	0.094	1849*	3.265	1860	1.378
	8	1920	2171	0.073**	1981	0.094	1996	2.245	1973*	2.28
	9	2561	2639	0.078**	2569*	0.094	2607	1.22	2636	4.464
	10	2130	2202	0.078**	2170*	0.078	2184	1.195	2203	7.784

BAB: Optimal solution by BAB method.

VNS (N_{tra}) : variable neighbourhood search (neighbourhood ' N_{tra} ').

SA (N_{tra}) : simulated annealing (neighbourhood ' N_{tra} ').

GA (HMX & N_{tra}) : genetic algorithm (crossover 'HMX' & mutation ' N_{tra} ').

HGSA : hybrid genetic algorithms with simulation annealing.

* : best values.

** : best times.

**** : unsolved problems.

We can conclude:

In this paper, we have developed exact and approximate solutions for the problem of scheduling n jobs on a single machine to minimize the total cost of earliness, tardiness, completion times and the number of late jobs. For this NP-hard problem, we proposed a branch and bound (BAB) algorithm to solve it. We have proved some special cases of our problem which leads to optimal solutions. A promising genetic algorithm is described for our problem. The GA representation described seems to provide reasonable with less time consuming in comparison with BAB algorithm.

This paper reports the results of extensive computational test of the following developed methods: variable neighborhood search (VNS), simulated annealing (SA), genetic algorithm (GA) and hybrid genetic algorithm (HGA). The results show that for the number of jobs $n \leq 25$, SA and (HGSA) give the best values and (VNS) gives the best times, and for $n > 25$ HGSA gives the best values and VNS gives the best times. The main conclusion to be drawn from our computation results is that genetic algorithm (GA) is a more effective method for our problem for the large problem for instance if ($n > 25$).

An interesting future research topic would involve experimentation with flow shop and job shop scheduling problems.

REFERENCES

1. Abdul-Razaq, T.S. and Potts, C.N., "Dynamic programming state-space relaxation for single-machine scheduling", *Journal of the operational Research Society*, 39:141-152, (1988).
2. Abid B.F. "Solving traveling salesman problem and machine scheduling problem using genetic algorithm," M.Sc. Thesis, College of science, Dept. of computer, Univ. of Baghdad (1998).
3. Besten, M. den, Stützle, T. and Dorigo, M., "Design of iterated local search algorithms an example application to the single machine total weighted tardiness problem", E.J.W. Boers et. al. (Eds.), *Evo Workshop, LNCS 2037*: 441-451, (2001).
4. Crauwels, H.A.J., "A comparative study of local search methods for one machine sequencing problems", Ph. D. thesis, Katholieke University, Lenuven, (1998).
5. Davis, L., "Handbook of Genetic Algorithms", Van No Stand Reinhold, New York, (1991).
6. Goldberg, D.E. "Genetic Algorithms in Search", *Optimization and Machine Learning*, (Addison-Wesley, Massachusetts), (1989).
7. Lentra J. K. and Rinnooy Kan A. H. G., "Computational Complexity of Discrete Mathematics", 4: 121-140 (1979).

8. Li, G., "Single machine earliness and tardiness scheduling", *European Journal of Operational Research*, 96:546-558, (1997).
9. Liaw, C. F. "A branch and bound algorithm for the single machine earliness and tardiness scheduling problem". *Computers & Operations Research* 20:679-693 (1999).
10. Madureira, A., Ramos C., and Silva, S. D. G, "A genetic approach to dynamic scheduling for total weighted tardiness problem", University of Braga Portugal (1999).
11. Rinnooy Kan, and A.H.G., "Machine scheduling problems classification", *Complexity and Computations*, Martinus Nyhoff, The Hague, (1979).
12. Valente, J.M.S. & Alves, R.A.F.S. "Improved heuristics for the early/tardy scheduling problem with no idle time", Working Paper 126, Faculdade de Economia do porto, Portugal, (2003).
13. Mustafa, N.R. "Some Algorithms for Machine Scheduling Problem" Ph.D. thesis, University of Al-Mustansiryah (2005). *Math. Basel* 40, 212-213 (1983).

Degree of Best Approximation of Bounded μ - Measurable Function by Means of K - Functional

Sahib K. AL- Saidy and Zainab Esa Abdul Naby
Al – Mustansiriyah University / College of Science/ Department of Mathematics

الخلاصة

في عملنا هذا قدمنا مفهوم التخمين المباشر و النظير لإيجاد أفضل درجة تقريب باستخدام دالة K - Functional للحوال المقيدة و القابلة للقياس في فضاء $L_{p,\mu}(X)$ $(1 \leq p < \infty)$.

ABSTRACT

In this work, we introduce direct and inverse estimate for the degree of best approximation of bounded μ -measurable functions by the K - Functional in the space $L_{p,\mu}(X)$, $(1 \leq p < \infty)$.

INTRODUCTION

Let $X = [a, b]$; $a, b \in R$ (the set of all real numbers) . Then we define the $L_p(X)$, $(1 \leq p < \infty)$ space of all bounded measurable functions f on X , for which (1) :

$$\|f\|_p = \left(\int_X |f(x)|^p d(x) \right)^{1/p} < \infty \dots\dots\dots(1.1)$$

Also, we denote by $L_{p,\mu}(X)$, $(1 \leq p < \infty)$ the space of all bounded μ -measurable functions f on X , for which (2) :

$$\|f\|_{p,\mu} = \left(\int_X |f(x)|^p d\mu(x) \right)^{1/p} < \infty \dots\dots\dots(1.2)$$

where μ is the non-negative measure function on a countable set .

Now ,we shall introduce what so-called average modulus of smoothness and we define the k th symmetric difference of f by (3) :

$$\Delta_h^k f(x) = \sum_{m=0}^k (-1)^{m+k} \binom{k}{m} f(x + mh) , \quad x, x + mh \in [a, b] \dots\dots(1.3)$$

The k th locally of smoothness for $f \in L_\infty$, is defined by :

$$w_k(f, \delta) = \sup_{|h| < \delta} \left\{ \left| \Delta_h^k f(x) \right| : |h| \leq \delta, x, x + kh \in [a, b] \right\} . \dots\dots(1.4)$$

Sendov B. and Popov V. A. (3) introduced the ordinary L_p - modulus of continuity which are very useful in some approximation theoretical problem and defined as :

$$w(f, \delta)_p = \sup_{|h| \leq \delta} \left\{ \|f(x+h) - f(x)\|_p : x+h, x \in X \right\}, \delta > 0 \dots\dots(1.5)$$

The k th ordinary L_p - modulus of continuity for $f \in L_p$ is defined by :

$$w_k(f, \delta)_p = \sup_{|h| \leq \delta} \left\{ \|\Delta_h^k f(x)\|_p \right\}, \delta > 0 \dots\dots\dots(1.6)$$

The k th average modulus of smoothness for $f \in L_p$ is defined by :

$$\tau_k(f, \delta)_p = \|w_k(f, \delta)\|_p \quad \delta > 0 \dots\dots\dots(1.7)$$

In [3] proved If f is a measurable bounded function on $[a, b]$, then :

$$w_k(f, \delta)_p \leq \tau_k(f, \delta)_p \leq w_k(f, \delta)(b-a)^{1/p} \dots\dots\dots(1.8)$$

From (1.8) one can introduce these concepts in the space $L_{p, \mu}$.

The k th average modulus of smoothness for $f \in L_{p, \mu}$ is defined by (2):

$$\tau_k(f, \delta)_{p, \mu} = \|w_k(f, x, \delta)\|_{p, \mu} \dots\dots\dots(1.9)$$

and the k th ordinary L_p - modulus of continuity for $f \in L_{p, \mu}$ is defined as:

$$w_k(f, \delta)_{p, \mu} = \sup_{|h| \leq \delta} \left\{ \|\Delta_h^k f(x)\|_{p, \mu} \right\}, \delta > 0 \dots\dots\dots(1.10)$$

Let X_0, X_1 be two Banach spaces, with $X_1 \subset X_0$, then for every $f_1 \in X_0, f_2 \in X_1$ one can define the K - Functional (3) :

$$K(f, \delta, X_0, X_1) = \inf_{f_1 \in X_1} \left\{ \|f_0\|_{X_0} + \delta \|f_1\|_{X_1}, f = f_0 + f_1 \right\}, \delta > 0 \dots\dots(1.11)$$

For same the space with $X_1 \subset X_0$, The K - Functional for $f \in X_0, g \in X_1$ are defined in (4) by :

$$K(f, \delta) = K(f, \delta, X_0, X_1) = \inf_{g \in X_1} \left\{ \|f - g\|_{X_0} + \delta \|g\|_{X_1} \right\}, \delta > 0 \dots\dots(1.12)$$

The inequality $K(f, \delta) < \varepsilon$ for some, $\delta > 0$, ε is a real number, implies that f has approximated with error $\|f - g\|_{X_0} < \varepsilon$ in X_0 by an element $g \in X_1$, whose norm is not too large $(\|g\|_{X_1} < \varepsilon \delta^{-1})$.

It is well known that the usual modulus of smoothness are connected with the K - Functional from (1.11). In this connection, we quote by Popov (3).

There are considerations on the interpolation of the modulus of smoothness and averaged modulus with the K - Functional, if we let, $X_0 = L_p(0, 2\pi)$ and $X_1 = W_p^r$ be the Sobolov - space (the set of all functions with an absolutely continuous $(r-1)$ th derivative and with the r th derivative in $L_p(X)$), with the semi norm $\|g\|_{W_p^r} = \|g^r\|_p$, we then consider the following :

Let $X_0 = L_p(X)$, $X_1 = W_p^r$ and $X_0 \subseteq X_1$, define the K - Functional in L_p space. Such that [4] :

$$K_r(f, \delta^r)_p = \inf_{g \in W_p^r} \left\{ \|f - g\|_p + \delta^r \|g^r\|_p, \delta > 0 \right\} \dots\dots\dots(1.13)$$

$$\text{Then,} \quad K_r(f, \delta^r)_p \approx w_r(f, \delta)_p \dots\dots\dots(1.14)$$

Let us now introduce these concepts in the space $L_{p,\mu}$:

Let $X_0 = L_{p,\mu}(X)$, $X_1 = W_{p,\mu}^k$ and $X_0 \subseteq X$, define the K - Functional in $L_{p,\mu}$ space is define as :

$$K_r(f, \delta^r)_{p,\mu} = \inf_{g \in W_{p,\mu}^k} \left\{ \|f - g\|_{p,\mu} + \delta^r \|g^r\|_{p,\mu}, \delta > 0 \right\} \dots\dots\dots(1.15)$$

Let T_n and H_n be respectively the sets of all trigonometric and algebraic polynomials of degree not greater than n , (defined on the set X). Let $P_n = T_n$ or $P_n = H_n$, then the degree of best approximations of a function $f \in L_p(X)$ space is given by :

$$E_n(f)_p = \inf \left\{ \|f(x) - Q(x)\|_p : Q \in P_n \right\} \dots\dots\dots(1.16)$$

Now we define the degree of best approximation of functions $f \in L_{p,\mu}$ spaces with polynomials from P_n in $L_{p,\mu}(X)$ spaces respectively

$$\text{as :} \quad E_n(f)_{p,\mu} = \inf \left\{ \|f(x) - Q(x)\|_{p,\mu} : Q \in P_n \right\} \dots\dots\dots(1.17)$$

A. S. Andreev, V. A. Popov [5], found the degree of best approximation of bounded measurable function in spaces $L_p(X)$ when f is a 2π - periodic bounded measurable function and $(1 \leq p \leq \infty)$, then :

$$E_n(f)_p \leq C(k) w_k(f, 1/n)_p \dots\dots\dots(1.18)$$

where $k \in \mathbb{N}$

A.H. Al-Abdullah (2) found the best approximation of bounded μ -measurable function by using the Linear positive operator in $L_{p,\mu}(X)$

spaces for $(1 \leq p < \infty)$ when f is a 2π -periodic bounded μ -measurable function then :

$$E_n(f)_{p,\mu} \leq C(p) \tau_k(f, \delta)_{p,\mu} \dots \dots \dots (1.19)$$

Now we shall give some lemmas which need in our works :

Lemma 1.1 : (2)

Let f be a bounded μ -measurable function and $1 \leq p < \infty$, then

$$\|f\|_p \leq C(p) \|f\|_{p,\mu} \dots \dots \dots (1.20)$$

where $C(p)$ is a constant depends only on p .

Lemma 1.2 : (2)

Let f be 2π -periodic bounded μ -measurable, then for $(1 \leq p < \infty)$

$$\text{then, } \tau_k(f, \delta)_{p,\mu} \leq c(p) \|f\|_{p,\mu} \dots \dots \dots (1.21)$$

Lemma 1.3 : (2)

Let f and g are two functions defined on the same domain, then for $(1 \leq p < \infty)$, then :

$$\tau_k(f, \delta)_{p,\mu} \leq \tau_k(f - g, \delta)_{p,\mu} + \tau_k(g, \delta)_{p,\mu} \dots \dots \dots (1.22)$$

Lemma 1.4 : (2)

Let $f \in L_{p,\mu}(x)$, $(1 \leq p < \infty)$, then :

$$\tau_k(f, \frac{1}{n})_{p,\mu} \leq (c_k n^{-k}) \sum_{s=0}^n (s+1)^{k-1} \tilde{E}_s(f)_{p,\mu} \dots \dots \dots (1.23)$$

where $\tilde{E}_s(\cdot)$ is standing for the degree of one-sided approximation of functions $f \in L_{p,\mu}(x)$.

Lemma 1.5 : (3)

If f is a bounded measurable function on the interval $[a, b]$, then

$$\int_a^b f(x) dx \approx \frac{b-a}{n} \sum_{i=1}^n f(x_i) \dots \dots \dots (1.24)$$

$$\text{where, } x_i = a + \frac{(b-a)(2i-1)}{2n}$$

Lemma 1.6 : (3)

The k th τ -modulus can be estimated by means of the norm of the k th derivative of the function :

$$\tau_k(f, \delta)_p \leq C(p) \delta^k \|f^k\|_p \dots\dots\dots (1.25)$$

where $C(p)$ is constant .

MAIN RESULTS

The following lemmas (2.1),(2.2),(2.3),(2.4) and theorem (2.1) are developed for proving some properties of the averaged modulus of smoothness when f is belong to $L_{p,\mu}(X)$, $1 \leq p < \infty$.

Lemma 2.1 :

Let f be a bounded μ -measurable function then for $1 \leq p < \infty$,
we have : $\|f\|_{p,\mu} \leq c(p) \|f\|_p \dots\dots\dots (2.1)$

Proof :

From (1.2), we have :

$$\|f\|_{p,\mu} = \left[\int_a^b |f(x)|^p d\mu(x) \right]^{1/p}$$

since $|f(x)|^p d\mu(x)$ is integrable , So

$$\int_a^b g(x) d(x) , \text{ is exists , } g(x) = |f(x)|^p d\mu(x)$$

Now , from (1.24) and (1.1) , we obtain:

$$\begin{aligned} \int_a^b g(x) dx &\approx \frac{b-a}{n} \sum_{c=1}^n g(x_c) ; x_c = \frac{(b-a)(2c-1)}{2n} + a \\ \|f(x)\|_{p,\mu}^p &= \int_a^b |f(x)|^p d\mu(x) \\ &= \int_a^b g(x) d(x) \\ &\leq \frac{b-a}{n} \sum_{c=1}^n g(x_c) ; x_c = \frac{(b-a)(2c-1)}{2n} + a \\ &\leq c_1(p) \sum_{c=1}^n |f(x_c)|^p d\mu(x_c) \end{aligned}$$

$$\leq c_1(p) c_2(p) \sum_{c=1}^n |f(x_c)|^p$$

By (1.24) we have

$$\begin{aligned} &\leq c_3(p) \int_a^b |f(x)|^p dx, \quad c_3(p) = c_1(p) \cdot c_2(p) \\ &= c_3(p) \|f\|_p^p, \end{aligned}$$

That is :

$$\|f\|_{p,\mu} \leq c(p) \|f\|_p$$

Lemma 2.2 :

Let $f \in L_p[a, b]$ $a, b \in R$ $1 \leq p < \infty$, we have

$$w_r(f, \delta)_p \leq c \|f\|_p \dots\dots\dots(2.2)$$

Proof :

From (1.6), (1.5)

$$\begin{aligned} w_r(f, \delta)_p &= \left\| \sup_{|h| \leq \delta} \left\{ \left| \Delta_h^k f(t) \right| : t, t+kh \in \left[x - \frac{k\delta}{2}, x + \frac{k\delta}{2} \right] \cap [a, b] \right\} \right\|_p \\ &= \left\| \sup_{|h| \leq \delta} \sum_{m=0}^k (-1)^{m+k} \binom{k}{m} f(t+mh) : t, t+mh \in [a, b] \right\|_p \end{aligned}$$

Since

$$\begin{aligned} \left| \Delta_h^k f(t) \right| &= \left| \sum_{i=0}^k (-1)^{m+k} \binom{k}{m} f(t+mh) \right| \\ &\leq \sum_{i=0}^k \binom{k}{i} \|f\|_{C_A} \end{aligned}$$

Then

$$w_r(f, \delta)_p \leq c(p) \|f\|_p$$

□

Lemma 2.3 :

Let $f \in L_p[a, b]$ $a, b \in R$ $1 \leq p < \infty$, we have

$$w_r(f, \delta)_p \leq C(p) \|f - g\|_p + \delta^r \|g^{(r)}\|_p \dots\dots\dots(2.3)$$

Proof :

From (1.5), (1.6), (2.2) and by Minkowski's inequality

$$\begin{aligned}
 w_r(f, \delta)_p &= \|w_r(f - g + g, \delta)\|_p \\
 &= \left\| \sup_{|h| < \delta} \left\{ \left| \Delta_h^k ((f - g) + g)(t) \right| : t, t + kh \in \left[x - \frac{k\delta}{2}, x + \frac{k\delta}{2} \right] \cap [a, b] \right\} \right\|_p \\
 &= \left\| \sup_{|h| < \delta} \left\{ \left| \sum_{m=0}^k (-1)^{m+k} \binom{k}{m} ((f - g) + g)(t + mh) \right| : t, t + kh \in \left[x - \frac{k\delta}{2}, x + \frac{k\delta}{2} \right] \cap [a, b] \right\} \right\|_p \\
 &\leq \left\| \sup_{|h| < \delta} \left\{ \left| \sum_{m=0}^k (-1)^{m+k} \binom{k}{m} (f - g)(t + mh) \right| \right\} \right\|_p + \\
 &\quad \left\| \sup_{|h| < \delta} \left\{ \left| \sum_{m=0}^k (-1)^{m+k} \binom{k}{m} (g)(t + mh) \right| \right\} \right\|_p \\
 &= \left\| \sup_{|h| < \delta} \left\{ \left| \Delta_h^k (f - g)(t) \right| \right\} \right\|_p + \left\| \sup_{|h| < \delta} \left\{ \left| \Delta_h^k (g)(t) \right| \right\} \right\|_p \\
 &= w_r(f - g, \delta)_p + w_r(g, \delta)_p \\
 &\leq C(p) \|f - g\|_p + \delta^r \|g^{(r)}\|_p \quad \square
 \end{aligned}$$

Lemma 2.4 :

Let f be a 2π -periodic bounded μ -measurable function then

For $1 \leq p < \infty$, we have:

$$\tau_k(f, \delta)_{p, \mu} \leq c(p) \delta^k \|f^{(k)}\|_{p, \mu} \dots \dots \dots (2.4)$$

Proof :

From (2.1), (1.25) and (1.20) we get

$$\begin{aligned}
 \tau_k(f, \delta)_{p, \mu} &\leq c_1(p) \tau_k(f, \delta)_p \\
 &\leq c_2(p) \cdot \delta^k \cdot \|f^{(k)}\|_p \\
 &\leq c_3(p) \delta^k \cdot \|f^{(k)}\|_{p, \mu} \quad \square
 \end{aligned}$$

Also , we conclude a relation between the integral modulus and the averaged modulus of smoothness when $f \in L_{p,\mu}$, $1 \leq p < \infty$:

Theorem 2.1 :

If $f \in L_{p,\mu}[a,b]$, then

$$w_k(f, \delta)_{p,\mu} \leq C(p) \tau_k(f, \delta)_{p,\mu} \dots\dots\dots(2.5)$$

where $C(p)$ is constant

Proof :

From (1.10) , (2.1) and (1.8), (1.20) we get

$$\begin{aligned} w_k(f, \delta)_{p,\mu} &= \sup_{0 \leq h \leq \delta} \left\{ \int_a^b |\Delta_h^k f(x)|^p d\mu(x) \right\}^{1/p} \\ &\leq c_1(p) \sup_{0 \leq h \leq \delta} \left\{ \int_a^b |\Delta_h^k f(x)|^p dx \right\}^{1/p} \\ &= c_1(p) w_k(f, \delta)_p \\ &\leq c_2(p) \tau_k(f, \delta)_p \\ &\leq c_3(p) \tau_k(f, \delta)_{p,\mu} \quad \square \end{aligned}$$

Now we want to introduce the relation between averaged modulus of smoothness and with the K - Functional to find the estimation of bounded μ -measurable functions in the $L_{p,\mu}(X)$, $1 \leq p < \infty$ spaces .

The following lemmas and theorems are constructed in such away to satisfy the above purpose .

Theorem 2.2 :

For $f \in L_{p,\mu}[a,b]$, $1 \leq p < \infty$ and $a, b \in R$, we have

$$K_r(f, \delta^r)_{p,\mu} \approx w_r(f, \delta)_{p,\mu} \dots\dots\dots(2.6)$$

that is

$$c_1(x) w_r(f, \delta)_{p,\mu} \leq K_r(f, \delta^r)_{p,\mu} \leq c_2(x) w_r(f, \delta)_{p,\mu}$$

Proof :

By (1.15) (2.1) , (1.20) and (1.13) , (1.14) we have

$$\begin{aligned} K_r(f, \delta^r)_{p,\mu} &= \inf_{g \in W_p^k} \left\{ \|f - g\|_{p,\mu} + \delta^r \|g^r\|_{p,\mu}, \delta > 0 \right\} \\ &\leq c_1(p) \inf_{g \in W_p^k} \left\{ \|f - g\|_p + \delta^r \|g^r\|_p, \delta > 0 \right\} \\ &= c_2(p) K_r(f, \delta^r)_p \end{aligned}$$

$$\begin{aligned} &\leq c_3(p) w_r(f, \delta)_p \\ &\leq c(p) w_r(f, \delta)_{p,\mu} \end{aligned}$$

So

$$K_r(f, \delta^r)_{p,\mu} \leq c(p) w_r(f, \delta)_{p,\mu}$$

also from (2.1), (2.3), and (1.13), (1.20) we get

$$\begin{aligned} w_r(f, \delta)_{p,\mu} &\leq c_1(p) w_r(f, \delta)_p \\ &\leq c_2(p) \|f - g\|_p + \delta^r \|g^r\|_p \\ &\leq c_3(p) K_r(f, \delta^r)_p \\ &\leq c_4(p) K_r(f, \delta^r)_{p,\mu} \end{aligned}$$

So

$$w_r(f, \delta)_{p,\mu} \leq c(p) K_r(f, \delta^r)_{p,\mu}$$

that is

$$K_r(f, \delta^r)_{p,\mu} \leq w_r(f, \delta)_{p,\mu}$$

□

Theorem 2.3 :

For $f \in L_{p,\mu}$, $1 \leq p < \infty$ and $a, b \in R$, we have

$$K_r(f, \delta^r)_{p,\mu} \approx \tau_r(f, \delta)_{p,\mu}$$

Proof :

From (1.22), and (1.21), (2.4), (1.15)

$$\begin{aligned} \tau_r(f, \delta)_{p,\mu} &\leq \tau_r(f - g, \delta)_{p,\mu} + \tau_r(g, \delta)_{p,\mu} \\ &\leq \tau_r(f - g, \delta)_{p,\mu} + \delta^r \|g^r\|_{p,\mu} \\ &\leq c(p) \|f - g\|_{p,\mu} + \delta^r \|g^r\|_{p,\mu} \\ &\leq c(p) K_r(f, \delta^r)_{p,\mu} \end{aligned}$$

So

$$\tau_r(f, \delta)_{p,\mu} \leq c(p) K_r(f, \delta^r)_{p,\mu} \dots \dots \dots (2.7)$$

also, from (1.15), (2.1), (1.13) and (1.14), (1.20), (2.5), we have that

$$\begin{aligned} K_r(f, \delta^r)_{p,\mu} &= \inf_{g \in W_p^r} \left[\|f - g\|_{p,\mu} + \delta^r \|g^r\|_{p,\mu} \right] \\ &\leq c_1(p) \inf_{g \in W_p^r} \left[\|f - g\|_p + \delta^r \|g^r\|_p \right] \\ &= c_1(p) K(f, \delta^r)_p \\ &\leq c_2(p) w_r(f, \delta)_p \\ &\leq c_3(p) w_r(f, \delta)_{p,\mu} \\ &\leq c_4(p) \tau_r(f, \delta)_{p,\mu} \end{aligned}$$

So

$$K_r(f, \delta^r)_{p, \mu} \leq c(p) \tau_r(f, \delta)_{p, \mu} \dots \dots \dots (2.8)$$

that is

$$K_r(f, \delta^r)_{p, \mu} \approx c(p) \tau_r(f, \delta)_{p, \mu} \quad \square$$

Now, we want to prove direct and inverse inequalities of best approximations of functions in the space $L_{p, \mu}$ but by means the K-Functional :

Theorem 2.4 , (Direct Theorem):

For $f \in L_{p, \mu}$, $1 \leq p < \infty$ and $a, b \in R$, we have

$$E_n(f)_{p, \mu} \leq c(p) K_r(f, \delta^r)_{p, \mu} \dots \dots \dots (2.9)$$

Proof :

From (1.17) , (2.1), (1.18) and (1.20) , (2.7)

$$\begin{aligned} E_n(f)_{p, \mu} &= \inf_{\delta > 0} \|f - g\|_{p, \mu} \\ &\leq c_1(p) \inf_{\delta > 0} \|f - g\|_p \\ &\leq c_2(p) E_n(f)_p \\ &\leq c_3(p) w_r(f, \delta)_p \\ &\leq c_4(p) \tau_r(f, \delta)_p \\ &\leq c_5(p) \tau_r(f, \delta)_{p, \mu} \\ &\leq c_6(p) K_r(f, \delta^r)_{p, \mu} \end{aligned} \quad \square$$

Theorem 2.5 , (Inverse Theorem) :

For $f \in L_{p, \mu}[a, b]$, $1 \leq p < \infty$ and $a, b \in R$, we have

$$K_r(f, \delta^r)_{p, \mu} \leq c(p) , \frac{1}{n^s} \sum_{s=0}^r (s+1)^{r-1} E_s(f)_{p, \mu} \dots \dots \dots (2.10)$$

Proof :

By (1.15), (2.1), (1.13) and (1.20) , (1.23), (2.8)

$$\begin{aligned} K_r(f, \delta^r)_{p, \mu} &= \inf_{g \in W_p^r} \left\{ \|f - g\|_{p, \mu} + \delta^r \|g^r\|_{p, \mu} \right\} \\ &\leq c_1(p) \inf_{g \in W_p^r} \left\{ \|f - g\|_p + \delta^r \|g^r\|_p \right\} \\ &= c_1(p) K_r(f, \delta)_p \\ &\leq c_2(p) K_r(f, \delta)_{p, \mu} \end{aligned}$$

$$\leq c_3(p) \tau_r(f, \delta)_{p,\mu}$$

$$\leq c_4(p) \frac{1}{n^s} \sum_{s=0}^r (s+1)^{k-1} E_s(f)_{p,\mu} \quad \square$$

Corollary :

For $f \in L_{p,\mu}[a,b]$, $1 \leq p < \infty$ and $a, b \in R$, we have :

$$E_n(f)_{p,\mu} \approx K_r(f, \delta^r)_{p,\mu}$$

We can conclude:

- 1- The relation between the modulus of smoothness and averaged modulus in $L_{p,\mu}(X)$ space have been obtained .
- 2- The equivalence between the K – functional and the averaged modulus of smoothness in $L_{p,\mu}(X)$ space have been obtained e .
- 3- The direct and inverse estimate by using the equivalence between the K – functional and the averaged modulus of smoothness in $L_{p,\mu}(X)$ space have been obtained .

REFERENCES

1. Al-Asady E.H. "A Study on the Best Approximation of Function in the Spaces $L_p(\mu)$; ($0 < p < \infty$)", M.Sc. Thesis, Baghdad University, Department of Mathematics, College of Education (Ibn Al – Haitham), (2007).
2. Al - Abdulla A.H., "On Equiapproximation of Bounded μ -Measurable Function in $L_p(\mu)$ -Spaces" Ph.D. Thesis, Baghdad University, Department of Mathematics, College of Education (Ibn Al – Haitham), (2005) .
3. Sendov B., Popov V.A. "The Averaged Moduli of Smoothness " Sofia, (1983) .
4. Kasim N.M. "On the Monotone and Comonotone Approximation" M.Sc. Thesis, Kufa University, Department of Mathematics, College of Education (2004) .
5. Andreev A. S., Popov V. A. , "Stechin's Type Theorem For One-Sided Trigonometric And Spline Approximation " Comp. Rend. Acad. Bulg. Sci., 31: 151-154 (1978) .

On Relative Pure Injective Modules*

¹Mehdi Sadik Abbas and ²Mohanad Farhan Hamid

¹Department of Mathematics /College of Science /University of Mustansiriya

²Department of Mathematics /College of Education/Misan University

الخلاصة

برهنا في هذا البحث أن المقاس M يكون شبه غامر نقى إذا وفقط إذا أي متتابعة مضبوطة (نقية) $0 \rightarrow M \rightarrow B$ منفصلة كلما وجد تشاكل $\beta: M \rightarrow B$ حيث أن $\beta^{-1}(M)$ نقى في M و $B = M + \beta(M)$. طورنا خواص أخرى للمقاسات شبه الغامرة النقية. مفهوم المقاس شبه الغامر النقي عم إلى المقاس شبه الغامر النقي حسب مفهوم فوكس، المقاس M يسمى مقاساً شبه غامر نقى حسب مفهوم فوكس إذا كان كل تشاكل α من مثالي K في R إلى M بحيث نواة α تحتوي على تالف عنصر ما m في M ، و mK نقى في M ، له توسيع إلى تشاكل من R إلى M . هذه المقاسات شخّصت، كما في المقاسات شبه الغامرة النقية، باستعمال المتتابعات المضبوطة. ميزنا بعض الحلقات بدلالة المفاهيم أعلاه. الحلقة R منتظمة إذا وفقط إذا كان كل مقاس شبه غامر نقى (شبه غامر نقى حسب مفهوم فوكس على الترتيب) مقاساً شبه غامر، وتكون R شبه بسيطة أرتينية إذا وفقط إذا كان كل مقاس شبه غامر نقى (شبه غامر نقى حسب مفهوم فوكس على الترتيب) مقاساً غامراً.

ABSTRACT

It is proved in this paper that an R -module M is quasi-pure-injective iff every (pure) exact sequence $0 \rightarrow M \rightarrow B$ splits whenever there is a homomorphism $\beta: M \rightarrow B$ with $\beta^{-1}(M)$ is pure in M and $B = M + \beta(M)$. Other properties of quasi-pure-injective modules are developed. The concept of quasi pure injectivity is generalized to that of pure-Fuchs-quasi-injectivity, an R -module M is called pure-Fuchs-quasi-injective if every homomorphism α from an ideal K of R into M , such that $\text{Ker } \alpha$ contains the annihilator of some element m in M and mK is pure in M , has an extension to a homomorphism from R into M . Such modules are characterized, like quasi pure injectives, using exact sequences. Certain types of rings are characterized by means of the above concepts. R is regular iff every quasi-pure-injective (resp. pure-Fuchs-quasi-injective) R -module is quasi-injective, and R is semi-simple artinian iff every quasi-pure-injective (resp. pure-Fuchs-quasi-injective) R -module is injective.

INTRODUCTION

Let R denote an associative ring with a non-zero identity. Unless otherwise stated, every module is a unitary right R -module. A submodule N of an R -module M is said to be a *pure submodule* (denoted $N \leq^p M$) if the mapping $N \otimes U \rightarrow M \otimes U$ induced by the inclusion map $N \rightarrow M$ is monic for any (finitely presented) left R -module U . Let M and N be two modules. M is said to be *N -pure-injective* (1) if any homomorphism α from a pure submodule of N into M has an extension to a homomorphism from N into M . M is said to be *quasi-pure-injective* if it is M -pure-injective. M is called *pure-injective* if it is N -pure-injective for any module N . Every module M can be embedded as a pure

submodule in a pure injective module (2). Finite direct sums of pure injective modules are pure injectives. A ring R is said to be (von Neumann) regular if every R -module M is regular, i.e. every submodule of M is a pure submodule (3). So over a regular ring R if a module is pure injective then it is injective, and if it is quasi-pure-injective then it is quasi-injective. The converse of the first assertion has been proved in (4), i.e. if every pure injective R -module is injective then R is regular. In section 2, we proved the converse of the second assertion, i.e. if every quasi-pure-injective R -module is quasi-injective then R is regular. Finally, $A \leq B$ (resp., $A \leq^{\oplus} B$) means that A is a submodule of B (resp., A is a direct summand of B).

RELATIVE PURE INJECTIVE MODULES

We begin by characterizing relative pure injective modules in terms of split (pure) exact sequences. The proof is adapted from (5)

Theorem (2.1): *Let A and M be R -modules. The following statements are equivalent:*

- 1) A is M -pure-injective.
- 2) Any exact sequence $0 \rightarrow A \xrightarrow{\alpha} B$ splits whenever there is an R -homomorphism $\beta: M \rightarrow B$ with $\alpha(A) + \beta(M) = B$ and $\beta^{-1}(\alpha(A)) \leq^p M$.
- 3) Any pure exact sequence $0 \rightarrow A \xrightarrow{\alpha} B$ splits whenever conditions in (2) hold.

Proof: (1) \rightarrow (2) Let $N = \beta^{-1}(\alpha(A))$. By hypothesis, the homomorphism $\alpha^{-1}\beta: N \rightarrow A$ extends to $\gamma: M \rightarrow A$. Now proceed as in (i) \rightarrow (ii) in (5, Theorem 4.1). (2) \rightarrow (3) Trivial. (3) \rightarrow (1) Let $N \leq^p M$ and $g: N \rightarrow A$ be a given R -homomorphism, and let i and j be the inclusion mappings of M and A respectively, into $M \oplus A$. Define $h: N \rightarrow M \oplus A$ by $h(n) = (n, -g(n)) \forall n \in N$. Put $B = (M \oplus A)/h(N)$ and let $p: M \oplus A \rightarrow (M \oplus A)/h(N) = B$ be the natural epimorphism.

Again proceed as in (ii) \rightarrow (i) in (5, Theorem 4.1) by putting $\alpha = pj$ and $\beta = pi$. Notice that $\beta(A) \leq^p (M \oplus A)/h(N)$. Indeed, we know that $N \leq^p M$ and $A \leq^p A$, hence $N \oplus A \leq^p M \oplus A$ (6), so by (6) $(N \oplus A)/h(N) \leq^p (M \oplus A)/h(N)$, but it is clear that $pj(A) \leq^{\oplus} (N \oplus A)/h(N)$ so $pj(A) \leq^p (M \oplus A)/h(N)$.

The above theorem gives a characterization for quasi-pure-injective modules.

A well-known characterization of pure-injective modules is now a corollary of theorem (2.1):

Corollary (2.2): *An R -module A is pure-injective iff any pure-exact sequence $0 \rightarrow A \xrightarrow{\alpha} B$ splits.*

Proof: ' \Rightarrow ' Let A be pure-injective and let $0 \rightarrow A \xrightarrow{\alpha} B$ be a pure-exact sequence. Then, in particular, A is B -pure-injective, so if we consider β of Theorem (2.1) as the identity map of B , we have $\alpha(A) + \beta(B) = \beta(B)$ and $\beta^{-1}(\alpha(A)) = \alpha(A) \leq^p B$ by assumption. So the hypotheses of Theorem (2.1) are satisfied and we must have $\alpha(A) \leq^{\oplus} B$, i.e. the given sequence splits.

' \Leftarrow ' An immediate application of Theorem (2.1).

It is well-known that a module is quasi-injective iff it is fully invariant in its injective envelope (7). On the other hand, quasi-pure-injective modules are invariant under certain elements of the endomorphism ring of their injective envelopes:

Theorem (2.3): *Let A and M be R -modules. If A is M -pure-injective, then $\alpha(M) \subseteq A \forall \alpha \in \text{Hom}(E(M), E(A))$ such that $\alpha^{-1}(A) \cap M \leq^p M$.*

Proof: Let $B = A + \alpha(A)$, and $\beta: M \rightarrow B$ be defined by:
 $\beta(m) = \alpha(m) \forall m \in M$ (i.e. β is α with domain restricted on M and codomain restricted on B).

Then

$\beta^{-1}(A) = \{m \in M \mid \beta(m) \in A\} = \{x \in E(M) \mid \alpha(m) \in A\} \cap M = \alpha^{-1}(A) \cap M \leq^p M$
 by assumption. So the hypotheses of Theorem (2.1) are satisfied and we must have $A \leq^{\oplus} A + \alpha(A)$. But $A + \alpha(A) \leq E$ and A is essential in E , hence A is essential in $A + \alpha(A)$, so $A = A + \alpha(A)$ and $\alpha(A) \subseteq A$.

We do not know whether the converse of theorem (2.3) is true. However, we have the following proposition, but first we need to introduce a definition:

Definition (2.4): Let A and M be R -modules and $T = \text{Hom}(E(M), E(A))$.

Define:

$P = P(M, A) = \{\alpha \in T \mid \alpha(K) \subseteq A \text{ for some non-zero pure submodule } K \text{ of } M\}$,

and

$Q = Q(M, A) = \{\alpha \in T \mid K \subseteq \text{Ker } \alpha \text{ for some non-zero pure submodule } K \text{ of } M\}$.

Remarks: For any R -modules A and M such that P and Q are as in definition (2.4), we have:

- a) $P \neq \emptyset$, for, $0 \in P$ and if $A = M$, then we have $1 \in P$.
- b) $Q \subseteq P$ but they may not be equal, for if $A = M$ then $1 \in P - Q$.
- c) For any $\alpha \in T$ with $\alpha^{-1}(A) \cap M \leq^p M$, we have $\alpha \in P$. Indeed, if we put $K = \alpha^{-1}(A) \cap M$, then, clearly $\alpha(K) \subseteq A$, and either $K = 0$ or $K \neq 0$. If $K \neq 0$, then the proof is complete. If $K = 0$, then $\alpha^{-1}(A) \cap M = 0$, and by essentiality of M in $E(M)$ we have $\alpha^{-1}(A) = 0$, hence $\alpha(E(M)) \cap A = 0$, so by essentiality of A in $E(A)$, we have $\alpha(E(M)) = 0$, hence $\alpha = 0 \in P$ by (a) above.

Proposition (2.5): Let A, M, T, P and Q be as given in definition (2.4), then:

A is M -pure-injective and $QM \subseteq A$ iff $PM \subseteq A$.

Proof: ' \Rightarrow ' Let $\alpha \in P$, then there is $0 \neq K \leq^p M$ such that $\alpha(K) \subseteq A$. Since A is M -pure-injective, then there is an R -homomorphism $\beta: M \rightarrow A$ such that $\beta|_K = \alpha|_K$. By injectivity of $E(A)$, $\exists \gamma \in T$ such that $\gamma|_M = \beta|_M$. Then $\gamma(M) = \beta(M) \subseteq A$. So, $(\alpha - \gamma)(K) = 0$, then $K \subseteq \text{Ker}(\alpha - \gamma)$. Then $\alpha - \gamma \in Q$, by hypothesis $(\alpha - \gamma)(M) \subseteq A$, thus for $x \in M$ we have $(\alpha - \gamma)(x) = a \in A$, hence $\alpha(x) = a + \gamma(x) \in A$. Then $\alpha(M) \subseteq A$.

' \Leftarrow ' Let $PM \subseteq A$. Since $Q \subseteq P$ we have $QM \subseteq A$. Let $K \leq^p M$ and $\alpha: K \rightarrow A$ be an R -homomorphism. Injectivity of $E(A)$ implies that there is an

R -homomorphism $\varphi: E(M) \rightarrow E(A)$ such that $\varphi(K) \subseteq A$. Thus $\varphi \in P$, so $\varphi(M) \subseteq A$, therefore $\varphi|_M: M \rightarrow A$ is an extension of α .

Clearly, if in theorem (2.4) (or in proposition (2.5)) $A = M$ and $E(A)$ is replaced by the quasi-injective envelope of A , the argument remains valid.

A GENERALIZATION: PURE-FUCHS-QUASI-INJECTIVE MODULES

L. Fuchs (8) has given an analogy between injectivity and quasi-injectivity by means of Baer Criterion. He showed that an R -module M is quasi-injective iff for every ideal K of R , every R -homomorphism $\eta: K \rightarrow M$ whose kernel contains the annihilator ideal of some $a \in M$ can be extended to an R -homomorphism $\psi: R \rightarrow M$. In this section, we study the corresponding property for quasi-pure-injective modules; we call them pure-Fuchs-quasi-injective modules, and we will seek a relation

between the two concepts. First, we introduce pure-Fuchs relative injectivity, of which pure-Fuchs-quasi-injectivity is a special case.

Definition (3.1): Let A and M be R -modules.

- 1) A is said to be *pure-Fuchs- M -injective* if for every ideal K of R and every R -homomorphism $\eta: K \rightarrow A$ such that $\text{ann}(m) \subseteq \text{Ker } \eta$ and $mK \leq^p M$ for some $m \in M$, there is an R -homomorphism $\psi: R \rightarrow M$ such that $\psi|_K = \eta$.
- 2) A is said to be *pure-Fuchs-quasi-injective* if A is pure-Fuchs- A -injective.

Proposition (3.2): Let A and M be R -modules. If A is M -pure-injective, then A is pure-Fuchs- M -injective. Hence any quasi-pure-injective module, and any (quasi-) injective module, is pure-Fuchs-quasi-injective.

Proof: Let $K \leq R$ and $\eta: K \rightarrow A$ be an R -homomorphism such that $aK \leq^p M$ and $\text{ann}(a) \subseteq \text{Ker } \eta$ for some $a \in M$. Define $\alpha: aK \rightarrow A$ by $\alpha(ak) = \eta(k) \forall ak \in aK$, if $ak = 0$, then $k \in \text{ann}(a) \subseteq \text{Ker } \eta$, so $\eta(k) = 0$. This shows that α is well defined. It is an easy matter to verify that α is an R -homomorphism. Since A is M -pure-injective, and $aK \leq^p M$, there is an R -homomorphism $\beta: M \rightarrow A$ such that $\beta|_{aK} = \alpha$. Define, now $\gamma: R \rightarrow aR$ by $\gamma(r) = ar \forall r \in R$, γ is an R -homomorphism. Let $\psi = \beta \circ \gamma: R \rightarrow A$. For each $k \in K$ we have $\psi(k) = \beta(ak) = \eta(k)$, hence ψ is the desired extension of η .

The converse of proposition 3.2 is not true in general as in the following example:

Example (3.3): Consider $A = \mathbb{Z}^{(\mathbb{N})}$ and $B = \mathbb{Z}^{\mathbb{N}}$ as modules over \mathbb{Z} . First $A \oplus B$ is not quasi-pure-injective, for if so, then A would be B -pure-injective by (1), hence there is a \mathbb{Z} -homomorphism $\alpha: B \rightarrow A$ such that $\alpha \circ i = 1_A$ and $A \leq^{\oplus} B$, which is not the case (see (6)). However, $A \oplus B$ is pure-Fuchs-quasi-injective: Let $n\mathbb{Z} \leq \mathbb{Z}$, and $x \in A \oplus B$. Suppose that $X = xn\mathbb{Z} \leq^p A \oplus B$, then $i \otimes 1: X \otimes \mathbb{Z}_n \rightarrow (A \oplus B) \otimes \mathbb{Z}_n$ is monic, but X is infinite cyclic and hence isomorphic to \mathbb{Z} , so $X \otimes \mathbb{Z}_n \cong \mathbb{Z} \otimes \mathbb{Z}_n \cong \mathbb{Z}_n \neq 0$ but $i \otimes 1(xnz \otimes \bar{1}) = xnz \otimes \bar{1} = xz \otimes \bar{n} = 0$, i.e. $i \otimes 1(X \otimes \mathbb{Z}_n) = 0$ which means that $i \otimes 1$ can be monic only in the cases that $n = 1, -1$ and 0 . In the first two cases we have $n\mathbb{Z} = \mathbb{Z}$, and when $n = 0$, we have $n\mathbb{Z} = 0$, and pure-Fuchs-quasi-injectivity of $A \oplus B$ is immediate.

Proposition (3.4): Let A and M be R -modules. Then, A is pure-Fuchs- M -injective iff A is pure-Fuchs- N -injective for every pure submodule N of M .

Proof: ' \Rightarrow ' Let $K \leq R$, $\alpha: K \rightarrow A$ be an R -homomorphism with $nK \leq^p N$ and $\text{ann}(n) \subseteq \text{Ker } \alpha$ for some $n \in N$. Then $n \in M$ and purity of N in M gives purity of nK in M , and by assumption there is an extension $\beta: R \rightarrow A$ of α .

' \Leftarrow ' Choice $N = M$ yields the result.

Proposition (3.5): Let A_1 and A_2 be R -modules. If $A_1 \oplus A_2$ is pure-Fuchs-quasi-injective, then A_i is pure-Fuchs- A_j -injective for every $i, j = 1, 2$.

Proof: $A_1 \oplus A_2$ is pure-Fuchs- A_j -injective $\forall j = 1, 2$ by proposition 3.4. Now let $K \leq R$ and $\alpha: K \rightarrow A_i$ ($i = 1, 2$) be an R -homomorphism such that $aK \leq^p A_j$ and $\text{ann}(a) \subseteq \text{Ker } \alpha$. Since $A_1 \oplus A_2$ is pure-Fuchs- A_j -injective, there is an R -homomorphism $\varphi: R \rightarrow A_1 \oplus A_2$ such that $\varphi|_K = \iota_j \circ \alpha$ where $\iota_i: A_i \rightarrow A_1 \oplus A_2$ is the inclusion mapping for each $i = 1, 2$. So $\pi_j \circ \varphi$, where π_j is the projection of $A_1 \oplus A_2$ onto A_j for each $j = 1, 2$, is the desired extension of α .

The following corollary follows immediately from proposition (3.5).

Corollary (3.6): A direct summand of a pure-Fuchs-quasi-injective module is pure-Fuchs-quasi-injective.

Direct sums of two pure-Fuchs-quasi-injective modules may not be pure-Fuchs-quasi-injective, as one may consider a regular ring which is not noetherian so it must have two (pure-Fuchs-) quasi-injective modules while their direct sum is not (9).

A characterization of pure-Fuchs relative injective modules similar to that of theorem (2.1) is given here:

Theorem (3.7): Let A and M be R -modules. The following statements are equivalent:

- 1) A is pure-Fuchs- M -injective.
- 2) Any exact sequence $0 \rightarrow A \xrightarrow{\alpha} B$ splits whenever there is an R -homomorphism $\beta: R \rightarrow B$ with $\alpha(A) + \beta(R) = B$, $m\beta^{-1}(\alpha(A)) \leq^p M$ and $\text{ann}(m) \subseteq \text{Ker } \beta$ for some $m \in M$.

Proof: The proof is similar to that of theorem 4.1 of (5), but notice for (1) \rightarrow (2), we have by assumption that $\text{ann}(m) \subseteq \text{Ker } \beta = \text{Ker } \alpha^{-1}\beta$, for α is monic and that $mN \leq^p M$ where $N = \beta^{-1}(\alpha(A))$.

We conclude this section by giving characterizations of certain types of rings by means of quasi-pure-injective and pure-Fuchs-quasi-injective modules.

Lemma (3.8): For a ring R , the following statements are equivalent:

- 1) R is regular.
- 2) Every pure-injective R -module is quasi-injective.
- 3) Every pure-injective R -module is injective.

Proof: The equivalence of (1) and (3) is given in (4). $(1) \rightarrow (2)$ is immediate.

$(2) \rightarrow (3)$ Let M be a pure-injective R -module, hence quasi-injective by assumption. To prove that M is injective, imbed R in a pure-injective module P . So $M \oplus P$ is pure-injective, hence quasi-injective. So by (10), M is P -injective. Hence M is R -injective by (10, proposition 1.4, p.2), which means that M is injective.

Since every pure injective module is quasi-pure-injective and hence pure-Fuchs-quasi-injective, the following proposition is now immediate:

Proposition (3.9): For a ring R , the following statements are equivalent:

- 1) R is regular.
- 2) Every quasi-pure-injective R -module is quasi-injective
- 3) Every pure-Fuchs-quasi-injective R -module is quasi-injective.

Recall that a ring R is called *pure-semisimple* (4, p.528) if every pure-exact sequence of R -modules splits (i.e. any pure submodule of an R -module is a direct summand), or equivalently, every R -module is pure-injective (4, p.528). And R is *semi-simple artinian* iff every exact sequence of R -modules splits, or equivalently, every R -module injective (11, corollary 8.2.2, p.196). A semi-simple ring can be characterized by the property that every R -module is quasi-injective (12). For pure-semisimple rings, we have a similar result:

Proposition (3.10): For a ring R , the following statements are equivalent:

- 1) R is pure-semisimple.
- 2) Every R -module is quasi-pure-injective.

Proof: $(1) \rightarrow (2)$ Clear. $(2) \rightarrow (1)$ Let $N_R \leq^p M_R$, then $N \oplus M$ is quasi-pure-injective by assumption. So by (1), N is M -pure-injective. Hence there is an R -homomorphism $\alpha: M \rightarrow N$ such that $\alpha \circ i = 1_N$ or $N \leq^{\oplus} M$.

Recall that a ring R is called a *QII-ring* if every quasi-injective R -module is injective (9). Over such rings the direct sum of any two quasi-injective modules is quasi-injective. For rings over which the direct sum of any two quasi-pure-injective modules is quasi-pure-injective, we have the following:

Proposition (3.11): For a ring R , the following statements are equivalent:

- 1) Every quasi-pure-injective R -module is pure-injective.

2) *The direct sum of any two quasi-pure-injective R -modules is quasi-pure-injective.*

Proof: (1) \rightarrow (2) is clear since the direct sum of any two pure-injective modules is pure-injective.

(2) \rightarrow (1) Let M_R be quasi-pure-injective. Imbed M in a pure-injective module P . Then, by assumption, $M \oplus P$ is quasi-pure-injective, and by (1) M is P -pure-injective. Hence, since $M \leq^p P$, we must have an R -homomorphism $\alpha: P \rightarrow M$ which extends the identity map of M . So $\alpha \circ \iota = 1_M$ or $M \leq^{\oplus} P$, hence M is pure-injective.

A ring R is semi-simple artinian iff every R -module is injective. In the following proposition, we show that: 'any quasi-pure-injective R -module or any pure-Fuchs-quasi-injective R -module is injective' is enough to make R semi-simple artinian.

Proposition (3.12): *For a ring R , the following statements are equivalent:*

- 1) R is semi-simple artinian.
- 2) Every pure-Fuchs-quasi-injective R -module is injective.
- 3) Every quasi-pure-injective R -module is injective.

Proof: (1) \rightarrow (2) and (2) \rightarrow (3) are clear.

(3) \rightarrow (1) Every quasi-pure-injective R -module is injective, hence quasi-injective. So R is regular by proposition (3.9). And any quasi-injective R -module is injective implies that R is QII, so it is noetherian (9). Hence R is semi-simple artinian.

REFERENCES

1. Mao, L. X. and Ding, N. Q, "Cotorsion modules and relative pure injectivity", J. Aust. Math. Soc. 81: 225-243(2006).
2. Warfield, R.J., "Purity and algebraic compactness for modules". Pacific J. Math. , 28: 699-719(1969).
3. Fieldhouse, D.J., "Pure simple and indecomposable modules" Bulletin 13 (1) (1970).
4. Wisbauer, R. W., "Foundations of Module and Ring Theory" Gordon and Breach, Philadelphia(1991).
5. Ramamurthi, V. S. and Rangaswamy, K. M , "On finitely injective modules", J. Aust. Math. Soc. 16: 239-248(1973).
6. Lam, T. Y., "Lectures on Modules and Rings" GTM 189, Springer-Verlag, New York(1999).

7. Johnson, R. E. and Wong, E. T, "Quasi-injective modules and irreducible rings" J. London Math. Soc., 36: 260-268, (1961).
8. Fuchs, L, "On quasi-injective modules", Annali. della Scuola Norm. Sup. Pisa 23: 541-546, (1969).
9. Byrd, K. A, "Rings whose quasi-injective modules are injective", Proc. Amer. Math. Soc., 33(2) (1972).
10. Mohamed, S. H. and Müller, B. J. "Continuous and Discrete Modules", Math. Soc. lecture note in Math. series, Cambridge University press, London(1990).
11. Kasch, F. "Modules and Rings", Academic press, London, (1982).
12. Faith, C. and Utumi, Y, "Quasi-injective modules and their endomorphism rings", Archiv. Math. 15:166-174 (1964).

Comparison of Approximation Algorithms for Unrelated Parallel Machines to Minimize the Weighted Makespan

¹Tariq S.Abdul-Razaq and ²Najwa Raheem Mustafa

¹Dept.of Mathematics, College of Science, Al-Mustansiriyah University

²Dept. of Mathematics, College of Science for Women, Baghdad University

الخلاصة

تمت دراسة جدولة الماكائن المتوازية غير المترابطة في هذه الحالة يجب جدولة مجموعة n من الاعمال على m من الماكائن المتوازية غير المترابطة. كل عمل متوفر للمعالجة عند الزمن صفر وكل ماكينة يمكنها معالجة عمل واحد على الاكثر في نفس الوقت وكل عمل يمكن إنجازه بواسطة ماكينة واحدة في نفس الوقت. تمت دراسة حالة تطبيقية لجدولة اعمال في ورشة قطع لتصغير زمن الانهاء الاعظم الموزون. تم اقتراح خمسة خوارزميات ودراسة ادائها.

ABSTRACT

The problem of scheduling of unrelated parallel machines is considered. In this environment, a set of n jobs has to be scheduled on m unrelated parallel machines. Each job is available for processing at time zero and each machine can process at most one job at a time and a job can be processed by at most one machine at a time. A case study is considered to schedule jobs in a cutting workshop to minimize the weighted makespan. Five algorithms are proposed and their performance is studied.

INTRODUCTION

The problem considered in this paper is the scheduling of unrelated parallel machines. In parallel machines environment there are multiple machines. In identical parallel machines environment all machines operate at the same speed, while in uniform parallel machines environment each machine has its own speed. For unrelated parallel machines; there are multiple machines with different job-related speeds, that is the processing times are unrelated. In this research environment, a set N of n jobs, $1, \dots, n$, each of which has to be scheduled on one of m machines, M_1, \dots, M_m is given. Each job j has a processing requirement p_j , weight w_j and is available for processing at time zero. Each machine can process at most one job at a time and a job can be processed by at most one machine at a time. All machines start working at time zero and process their jobs sequentially. For the unrelated parallel machines, the speed of machine M_i on job j , v_{ij} , depends on both the machine and the job; job j requires p_j / v_{ij} processing time on a machine M_i . We define $p_{ij} = p_j / v_{ij}$ (1). The notation N^i denotes the set of jobs assigned to machine M_i . Let C_j denotes the completion time of job j and CM_i denotes the completion time of the last job on machine M_i , that is:

$$CM_i = \sum_{j \in N^i} p_{ij} \quad i=1, \dots, m, j=1, \dots, n$$

The maximum completion time (makespan) C_{max} is defined by (2):

$C_{max} = \max\{C_{M_1}, \dots, C_{M_m}\}$, we can define C_{max}^w by:

$C_{max}^w = \max\{C_{M_1}, \dots, C_{M_m}\}$ with respect to some priority rules that depend on job weight; the objective is to minimize the weighted makespan C_{max}^w .

There is extensive literature describing approximation algorithms for unrelated parallel machine scheduling problems. Horwitz and Sahni (1976) proposed several exact and approximate algorithms for some special cases of the $R // C_{max}$ problem. Also, Ibarra and Kim (3), Davis and Jaffe (4) proposed several algorithms to solve the problem $R // C_{max}$. There are many papers that present an experimental comparison of approximation algorithms, some of which are based on linear programming and others based on local search heuristics. For example, Hariri and Potts (5) solve the $R // C_{max}$ problem. The Branch and bound method can also be used, as was the case with Salem, Anagnostopoulos and Rabadi [2] when solving the problem $R // C_{max}$.

Bruno, Coffman and Sethi (1974) and Lenstra et al. (1977) (6) showed that the problem of minimizing total weighted completion time on two identical parallel machines is NP-hard, thus $R // \sum w_j C_j$ is NP-hard in the strong sense (7).

If there is only one machine the problem is solved to optimality by ordering the jobs in a non-decreasing order of the ratio p_j / w_j (the SWPT rule) (Smith 1956). Hence, the problem reduces assigning the jobs appropriately to the machines and then sequencing the jobs on each machine by the SWPT rule.

Karp (1972) show that the problem of scheduling two identical parallel machines to minimize the maximum completion time is NP-hard. Clearly, the more general unrelated parallel machine problem is also NP-hard (5). Thus for the $R // C_{max}^w$ problem it seems unlikely that a polynomial time algorithm that always produce optimal solution exists.

The Problem $R // C_{max}^w$

The problem $R // C_{max}^w$ can be formulated as a linear program as follows:

Minimize $Z = C_{max}^w$.

Subject to

$$\sum_{j=1}^n x_{ij} w_j p_{ij} \leq C_{max}^w \quad i = 1, \dots, m$$

$$\sum_{i=1}^m x_{ij} = 1 \quad j = 1, \dots, n$$

$$x_{ij} \in \{0,1\} \quad i=1,\dots,m; j=1,\dots,n$$

Where x_{ij} is an assignment variable that is equal to 1 if job j is assigned to machine M_i and 0 otherwise.

The best time of the j th job, denoted by b_j , equals $\min_{1 \leq i \leq m} p_{ij}$. The efficiency of the i th machine on the j th job, denoted by ef_{ij} , equals to b_j / p_{ij} (4). The maximum efficiency is one. Using these concepts, the following algorithm is a modification of the algorithm proposed by Davis and Jaffe (4).

Algorithm 1: Algorithm WCM1

Step (1): $N = \{1, \dots, n\}$, $N^i = \phi$. For $j=1, \dots, n$, find $b_j = \min_{1 \leq i \leq m} p_{ij}$;

for $j=1, \dots, n; i=1, \dots, m$, find $ef_{ij} = b_j / p_{ij}$;

for $i=1, \dots, m$, create a list of the jobs $j=1, \dots, n$ sorted in a non-increasing order of $w_j ef_{ij}$. Set $sum_i = 0$, $CM_i = 0$ for $i=1, \dots, m$.

Designate all machines as 'available' and all jobs as 'unassigned';

Step (2): If $N = \phi$, go to step(6), else find a machine i such that sum_i is minimal among all available machines;

Step (3): Find the next unassigned job j on i 's list;

Step (4): If j does not exist or if $ef_{ij} < 1/\sqrt{m}$ then mark i as unavailable;

Step (5): Otherwise assign job j to machine i ; $N = N - \{j\}$,

$N^i = N^i \cup \{j\}$. Set $sum_i = sum_i + p_{ij}$, $CM_i = CM_i + p_{ij}$, return to step(2).

Step (6): $C_{max}^w = \max_{1 \leq i \leq m} \{CM_i\}$.

Figure -1: The WCM1 algorithm

The ratio ef_{ij} can be used to propose another algorithm that is called WCM2.

Algorithm 2: Algorithm WCM2

Algorithm WCM2 is similar to algorithm WCM1 except that in step (1) the jobs are sorted in a non-decreasing order of ef_{ij} / w_j .

Figure -2: The WCM2 algorithm

Ibarra and Kim (3) proposed several algorithms for the problem $R // C_{max}$. Some of these algorithms are modified to fit the problem $R // C_{max}^w$ as follows.

Algorithm 3: Algorithm WCM3

Step (1): $N = \{1, \dots, n\}$, $N^i = \phi$ and $sum_i = 0$ for $i=1, \dots, m$;
Step (2): If $N = \phi$, go to step (4);
Step (3): Otherwise find a job $j \in N$ such that

$$\min_{1 \leq i \leq m} \{sum_i + p_{ij}\} \leq \min_{1 \leq i' \leq m} \{sum_{i'} + p_{ij'}\} \text{ for all } j' \in N; \text{ let } i \text{ be such that}$$

$$sum_i + p_{ij} \text{ is minimum; } sum_i = sum_i + w_j p_{ij}, CM_i = CM_i + p_{ij},$$

$$N^i = N^i \cup \{j\}, N = N - \{j\}, \text{ return to step (2);}$$
Step (4): $C_{max}^w = \max_{1 \leq i \leq m} \{CM_i\}$.

Figure 3: The WCM3 algorithm

Other algorithms can be proposed by first arranging jobs according to some priority rules as in the following two algorithms.

Algorithm 4: Algorithm WCM4

Step (1): $N = \{1, \dots, n\}$, $N^i = \phi$, $sum_i = 0$, $i=1, \dots, m$;
Step (2): For each job j , find $p'_{min}(j) = \min_{1 \leq i \leq m} p_{ij} / w_j$
Step (3): Order the jobs in N according to non-decreasing order of $p'_{min}(j)$;
Step (4): If $N = \phi$, go to step(6);
Step(5): Else, find the machine i such that $sum_i + w_j p_{ij} \leq sum_k + w_j p_{kj}$ for all $k = 1, \dots, m$; set $sum_i = sum_i + w_j p_{ij}$; $N = N - \{j\}$,
 $CM_i = CM_i + p_{ij}$; $N^i = N^i \cup \{j\}$; return to step(4);
Step (6): $C_{max}^w = \max_{1 \leq i \leq m} \{CM_i\}$.

Figure-4: The WCM4 algorithm

Also the following algorithm is a modification of the LRPT-FM (Longest Remaining Processing Time on the Fastest Machine) rule.

Algorithm 5: Algorithm WCM5

Step (1): $N = \{1, \dots, n\}$, $N^i = \phi$, $sum_i = 0$, $i = 1, \dots, m$;

Step (2): For each job j , find $p'_{max}(j) = \max_{1 \leq i \leq m} p_{ij} / w_j$

Step (3): Order the jobs in N according to non-increasing order of $p'_{max}(j)$;

Step (4): If $N = \phi$, go to step(6);

Step (5): Else, find the machine i such that $sum_i + p_{ij} \leq sum_k + p_{kj}$ for all $k = 1, \dots, m$; set $sum_i = sum_i + p_{ij}$; $CM_i = CM_i + p_{ij}$,

$N = N - \{j\}$; $N^i = N^i \cup \{j\}$; return to step(4);

Step (6): $C_{max}^w = \max_{1 \leq i \leq m} \{CM_i\}$.

Figure -5: The WCM5 algorithm

Case Study

The Five algorithms : WCM1, WCM2, WCM3, WCM4 and WCM5 are applied in the cutting workshop in Al-Karama General State Company. The company has a complete engineering department for design and technology that works jointly with the planning and follow-up department and different factories to accomplish production operations within the annual plan, in addition to some specified orders for special projects. One of the divisions of the planning and follow-up department is the cutting workshop, which carries out a huge and basic part in preparing and providing production work orders the raw materials for all factories in primary measurements specified by technological procedure of these parts production.

The work of the cutting workshop is of great importance in preparing and providing raw materials in correct dimensions and required quantities within accurate times and specified types to all factories by best utilization of available self capabilities. Thus the work of the cutting workshop is a bottleneck to progress of production operation in factories and the company.

The cutting workshop environment includes the following components:

- a) Machines: There are different types of machines used in this unit. The speed of each machine depends on its own specifications and the raw materials.
- b) Raw materials: There is a wide range of metal ores and materials used in the workshop works which are divided into five kinds according to their cutting speed, these types are: Aluminium, Stainless steel, Other types of steel, Teflon and different plastics and Cooper and brass.

- c) **Work Style:** The cutting workshop receives work orders to prepare materials weekly. The company runs an annual production plan and the planning department has a monthly plan for the factories production and the cutting workshop prepares materials at least one month ahead.
- d) **Constraints:** Jobs in the cutting workshop include cutting shafts, blocks and plates ,each of these material need certain time as a loading cost. Some machines have certain constraints, for example, they cannot handle some raw materials. Raw materials are available in standard measurements.

The algorithms WCM1, WCM2, WCM3, WCM4 and WCM5 are implemented on a case study of 10 assemblies. These assemblies consist of different numbers of jobs and machines. The jobs vary in their types and raw materials, also the machines are of different types. The efficiency of the proposed algorithms is tested using programs coded in Microsoft FORTRAN Power Station version 4.0; the sketches were drawn using MATLAB 6.5. Both codes are executed on a Pentium III 1GHz personal computer with 256 MB memory.

The schedules yielding from these algorithms are compared. Table (1) presents the results obtained by these algorithms and the results are compared to the best of them using the percentage relative deviation from the best value (PRD), calculated as $\frac{H - B}{B} * 100$, where H and B represents the heuristic and best values, respectively. Also, they are compared using the deviation (DEV) of each value w.r.t. arithmetic mean of all values. The best result is presented in bold.

Table -1: Comparison of the results for C_{max}^w

ASSEMBLY	NO. OF JOBS	NO.OF MACHINES	ALGORITHM	VALUE	PRD	DEV
1	21	6	WCM1	750	79.42583	165.6
			WCM2	522	24.88038	-62.4
			WCM3	733	75.35885	148.6
			WCM4	499	19.37799	-85.4
			WCM5	418	0.000	-
2	18	6	WCM1	836	12.66846	32.8
			WCM2	742	0.000	-61.2
			WCM3	865	16.57682	61.8
			WCM4	811	9.29919	7.8
			WCM5	762	2.69542	-41.2

3	16	5	WCM1	1781	69.1358	363.8
			WCM2	1312	24.59639	-
			WCM3	1239	17.66382	-
			WCM4	1701	61.53846	283.8
			WCM5	1053	0.000	-
4	22	5	WCM1	1546	0.000	0.000
			WCM2	1546	0.000	0.000
			WCM3	1546	0.000	0.000
			WCM4	1546	0.000	0.000
			WCM5	1546	0.000	0.000
5	20	7	WCM1	1138	37.10843	118
			WCM2	1118	34.6988	98
			WCM3	995	19.87952	-25
			WCM4	1019	22.77108	-1
			WCM5	830	0.000	-190
6	16	6	WCM1	962	55.16129	133.6
			WCM2	895	44.35484	66.6
			WCM3	783	23.06452	-65.4
			WCM4	902	45.48387	73.6
			WCM5	620	0.000	-
7	14	5	WCM1	481	37.03704	-40.8
			WCM2	481	37.03704	-40.8
			WCM3	815	132.1937	293.2
			WCM4	481	37.03704	-40.8
			WCM5	351	0.000	-
8	15	5	WCM1	1786	6.05701	17
			WCM2	1786	6.05701	17
			WCM3	1753	4.09739	-16
			WCM4	1836	9.02613	67
			WCM5	1684	0.000	-85
9	17	6	WCM1	1130	9.07336	-82.8
			WCM2	1378	33.01158	165
			WCM3	1278	23.35907	65
			WCM4	1242	19.88417	29
			WCM5	1036	0.000	-
10	19	5	WCM1	1665	25.18797	95.2
			WCM2	1665	25.18797	95.2
			WCM3	1665	25.18797	95.2
			WCM4	1524	14.58647	-45.8
			WCM5	1330	0.000	-

It can be seen from table (1) that algorithm WCM5 is the best one. It generates the best solution almost for all the assemblies given (nine out of 10).

The performance of other algorithms varies radically from an assembly to another. It is interesting to see that the five algorithms perform identically on assembly (4). Except algorithm WCM5, other algorithms perform badly on some assemblies and well on others. The running time for the program of 10 assemblies is $1.500000E - 01$ seconds. The results are presented in the figure (6).

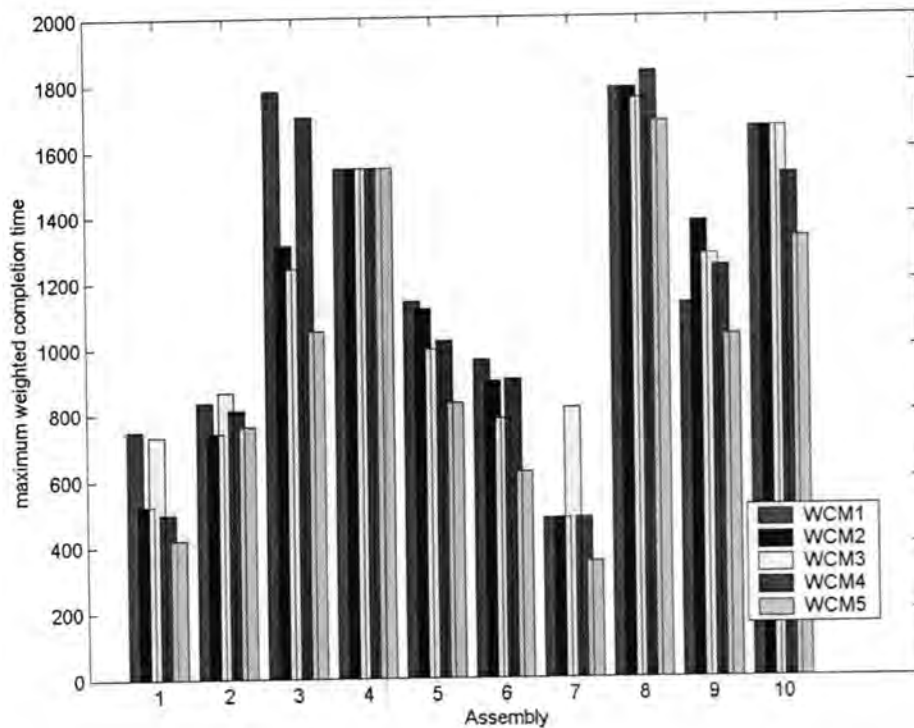


Figure-6: The performance of algorithms WCM1, WCM2, WCM3, WCM4 and WCM5

Conclusions

In this work an applied problem was studied, which is the problem of scheduling n jobs on m unrelated parallel machines. Several algorithms are proposed to minimize the maximum weighted completion time. They are applied on the work of a cutting workshop in Al-Karama general state company and their performance is analyzed hoping to suit the company demands. Algorithm WCM5 is the best one for the maximum weighted completion time problem of unrelated parallel machines. The performance of other algorithms for the problems (minimizing the maximum weighted completion time) varies between an assembly and another one. To improve the performance, one can study the preemption of jobs. Also, on-line scheduling, i.e. scheduling when jobs arrive over time, can be studied.

REFERENCES

1. Karger, D., Stein, C. and Wein, J., Scheduling Algorithms, in Atallah, M.J.(ed.) CRC Handbook on Algorithms and Theory of Computation, CRC Press, (1998).
2. Salem,A., Anagnostopoulos, G.C. and Rabadi, G, A Branch-and-Bound Algorithm for Parallel Machine Scheduling Problems, in Proceedings of Harbour, Maritime & Multimodal Logistics Modeling and Simulation Workshop, a Publication of the Society for Computer Simulation International (SCS), Petrofina, Italy:88-93, October (2000).
3. Ibarra, O.H. and Kim, C.E., Heuristic Algorithms for Scheduling Independent Tasks on Nonidentical Processors, Journal of the Association for Computing Machinery 24:280-289, (1977).
4. Davis,E.& Jaffe, J.M., Algorithms for Scheduling Tasks on Unrelated Processors, Journal of the Association for Computing Machinery 28:721-736 (1981).
5. Hariri, A.M.A. and Potts, C.N., Heuristics for Scheduling Unrelated Parallel Machines, Computers and Operations Research 18:323-331, (1991).
6. Lenstra, J.K., Rinnooy Kan, A.H.G. & Brucker,P.,Complexity of Machine Scheduling Problems, Annals of Discrete Mathematics 1:343-362(1977).
7. Valente, J.M.S. and Alves, R.A.F.S., Improved Heuristics for the Early/Tardy Scheduling Problem with no Idle Time, Computers & Operations Research 32 :557-569(2005).

Fully Stable Modeles Relative To An Ideal

Mehdi Sadik Abbas and Anaam Moter Sharky

Department of Mathematics, College of Science, Mustansiriya University

الخلاصة

في هذا البحث، نقدم مفهوم المقاسات تامة الاستقرار بالنسبة الى مثالي كتعميم الى مفهوم المقاسات تامة الاستقرار. ثم حققنا فيه بعض خواص ومبرهنات الوصف الى المقاسات تامة الاستقرار بالنسبة الى مثالي كتعميم الى المبرهنات والخواص على المقاسات تامة الاستقرار. ربطنا ذلك المفهوم مع فيصلية بير بالنسبة الى مثالي.

ABSTRACT

In this paper, we introduce the notion of fully stable modules relative to an ideal as a generalization of the notion of fully stable modules. Then we investigate some characterization, theorems, and properties of fully stable modules relative to an ideal which are generalizations of those on fully stable modules. We relate this notion with Baer's criterion relative to an ideal.

INTRODUCTION

Throughout, R is commutative ring with identity and all modules are unitary. Let M be an R -module, a submodule N of M is said to be fully invariant if $\theta(N) \subseteq N$ for each R -endomorphism θ of M . In the case that each submodule of M is fully invariant, then M is called duo module (1). Fully stable modules have been discussed in (2), an R -module M is called fully stable, if $\theta(N) \subseteq N$ for each submodule N of M and R -homomorphism θ from N into M . It is an easy matter to see that M is fully stable, if and only if $\theta(xR) \subseteq xR$ for each x in M and R -homomorphism $\theta : xR \rightarrow M$. This is equivalent to saying that for each x, y in M , $y \notin \langle x \rangle$ implies that $\text{ann}_R(x) \not\subseteq \text{ann}_R(y)$ (2). Also it is proved that, an R -module M is fully stable if and only if $\text{ann}_M(\text{ann}_R(x)) = \langle x \rangle$ for each $x \in M$ i.e each cyclic submodule satisfies the double annihilater condition (2). Our work is to introduce generalization of fully stable modules and extending these results. Where, we introduce the concepts of fully stable modules relative to an ideal and Baer's criterion relative to an ideal and we prove that an R -module M is fully stable relative to A , if and only if Baer's criterion relative to A holds for each cyclic submodule of M .

Properties Of Fully Stable Modeles Relative To an Ideal:

Definition (2.1): Let M be an R -module and A be an ideal of R . A submodule N of M is said to be stable relative to A , if $f(N) \subseteq N + MA$, for each R -homomorphism $f : N \rightarrow M$. M is said to be fully stable relative to A in case each submodule of M is stable relative to A . A ring R is fully stable relative to an ideal A of R if it is fully stable relative to A as R -module.

Notice that the concepts of fully stable module and fully stable module relative to an ideal coincide for zero ideal. Every R -module is fully stable relative to R . An ideal I of a ring R is stable if and only if I is stable relative to itself. Let M be an R -module and $\{N_i \mid i \in I\}$ be a family of stable submodule of M relative to an ideal A of R . The sum of $\{N_i \mid i \in I\}$ is stable submodule of M relative to A .

The following definition is a generalization of duo module.

Definition (2.2): Let M be an R -module and A be an ideal of R . A submodule N of M is said to be fully invariant relative to A , if $f(N) \subseteq N + MA$ for each R -homomorphism $f: M \rightarrow M$. M is called duo module relative to A if each submodule of M is fully invariant relative to A . A ring R is duo module relative to an ideal A of R if it is duo module relative to A as R -module.

Examples and Remarks (2.3):

- Every fully stable (resp. duo) R -module is a fully stable (resp. duo) R -module relative to each non-zero ideal of R . But the converse is not true. For example, the \mathbb{Z} -module \mathbb{Q} is a fully stable module relative to $m\mathbb{Z}$ for each $m(\neq 0) \in \mathbb{Z}$, while it is not fully stable module (2), also \mathbb{Q}/\mathbb{Z} as \mathbb{Z} -module.
- Recall that, for any R -module M , we define $tr(M)$ to be $\sum im(f)$, where f ranges over $M^* = Hom(M, R)$ (3). Let M be an R -module and A be an ideal of R . If $M = MA$, then M is a fully stable relative to A . In particular, if M is a projective R -module, then $M = M \cdot tr(M)$ (3, Prop. (2.40), p. 51). Thus we have that, every projective R -module is fully stable relative to $tr(M)$.
- \mathbb{Z} as \mathbb{Z} -module is not fully stable module relative to $m\mathbb{Z}$, for each $m(\neq \pm 1) \in \mathbb{Z}$. Since \mathbb{Z} as \mathbb{Z} -module is not fully stable (2), thus $\mathbb{Z}_{\mathbb{Z}}$ is not fully stable relative to zero ideal of \mathbb{Z} . Now, to show that \mathbb{Z} is not fully stable relative to each $m\mathbb{Z}$, $m(\neq 0, \pm 1)$ in \mathbb{Z} . Consider $m\mathbb{Z} \leq \mathbb{Z}$ and \mathbb{Z} -homomorphism $f: m\mathbb{Z} \rightarrow \mathbb{Z}$ defined be $f(mz) = z$, for each z in \mathbb{Z} . It is clear that f is a well-defined \mathbb{Z} -homomorphism. Since $f(m) = 1 \in f(m\mathbb{Z})$ and $1 \notin m\mathbb{Z} = m\mathbb{Z} + \mathbb{Z} \cdot m\mathbb{Z}$. Therefore \mathbb{Z} as \mathbb{Z} -module is not fully stable relative to $m\mathbb{Z}$, for each $m(\neq 0, \pm 1) \in \mathbb{Z}$. But $\mathbb{Z}_{\mathbb{Z}}$ is a fully stable relative to \mathbb{Z} by using (2).
- It is clear that every fully stable R -module relative to an ideal A of R is duo module relative to A . But the converse is not true. For example, observe every commutative ring is duo ring, hence $\mathbb{Z}_{\mathbb{Z}}$ is duo module relative to each ideal, but \mathbb{Z} is not fully stable module relative to $m\mathbb{Z}$, for each $m(\neq \pm 1) \in \mathbb{Z}$.
- Unlike for fully stable modules, the submodule of fully stable R -module relative to an ideal A of R needs not be fully stable relative to A . For example, $\mathbb{Z} \leq \mathbb{Q}$ and $\mathbb{Q}_{\mathbb{Z}}$ is fully stable relative to $m\mathbb{Z}$, for each $m(\neq 0)$ in \mathbb{Z} , while \mathbb{Z} is not fully stable relative to $m\mathbb{Z}$, for each $m(\neq \pm 1) \in \mathbb{Z}$.
- Every simple module is trivially fully stable module relative to each ideal. There is no direct relation between semi-simple modules and fully stable module relative to an ideal. For example, $\mathbb{Q}_{\mathbb{Z}}$ is fully stable relative to each

non-zero ideal of Z , while Q_Z is not semi-simple module. On the other hand, every vector space V_F of dimension $n > 1$ is not fully stable (2), hence is not fully stable relative to zero ideal of F even though it is semi-simple.

• Let R be any ring if K is direct summand of R i.e $R = K \oplus N$ for some ideal N of R , then K is stable relative to N .

• If M is fully stable R -module relative to an ideal A of R , then M is fully stable relative to B for each ideal B containing A . In particular, let $\{A_i \mid i \text{ in } I\}$ be a family of ideals of R , if M is fully stable relative to A_i for some $i \in I$, then M is a fully stable relative to $\sum_{i \in I} A_i$.

• If M is fully stable R -module relative to A , then M needs not be fully stable relative to B for some $B \subseteq A$. For example Q_Z is fully stable relative to mZ , for each $m(\neq 0)$ in Z , but it is not fully stable relative to zero ideal.

To see full stability relative to an ideal for modules it is enough to show that every cyclic submodule is stable relative to that ideal. For this we have the following and the proof is obvious.

Proposition (2.4): Let M be an R -module and A be an ideal of R . Then M is fully stable relative to A iff every cyclic submodule of M is stable relative to A . \square

Corollary (2.5): M is fully stable R -module relative to each cyclic ideal of R iff M is fully stable relative to each ideal of R . \square

The following proposition is one of the main tools for our subsequence results.

Proposition (2.6): An R -module M is fully stable relative to an ideal A of R iff for each x, y in M , $y \notin xR + MA$ implies that $\text{ann}_R(x) \not\subseteq \text{ann}_R(y)$.

Proof: Suppose that there exists two elements x, y in M with $y \notin xR + MA$ and $\text{ann}_R(x) \subseteq \text{ann}_R(y)$. Define $f: xR \rightarrow M$ be $f(xr) = yr$ for each r in R . It is easy to see that, f is well-defined R -homomorphism, then $y = f(x) = xt + w$ for some $t \in R$ & $w \in MA$. Hence, $y \in xR + MA$ which is a contradiction. Conversely, assume that there exists a cyclic submodule xR of M and R -homomorphism $f: xR \rightarrow M$ with $f(xR) \not\subseteq xR + MA$. There exists $y \in xR$ and $f(y) \notin xR + MA$, then $\text{ann}_R(x) \not\subseteq \text{ann}_R(f(y))$, which is a contradiction. \square

Notice that, in the "only if" part we did not use the commutative property of the ring in above Proposition.

From Proposition (2.6) we have the following.

Corollary (2.7): Let M be a fully stable R -module relative to an ideal A of R . Then for each two elements x and y in M , $\text{ann}_R(x) = \text{ann}_R(y)$ implies that $xR + MA = yR + MA$. \square

Recall that, an R -module M is said to multiplication module if each submodule of M is of the form MI for some ideal I of R [4]. M is said to be multiplication module iff $N=M$ [$N:M$] for each submodule N of M [5].

The following proposition gives an answer for the question: when is a fully stable module relative to ideal, fully stable?.

Proposition (2.8): Let M be a multiplication R -module. Then M is fully stable module iff M is fully stable module relative to each non-zero ideal of R .

Proof: (\Rightarrow). It is clear.

(\Leftarrow). Let N be any submodule of M and $f: N \rightarrow M$ be any R -homomorphism. If $N = (0)$, then it is clear that N is stable. Let $N \neq (0)$, and since M is a multiplication module, then $N = MK$, for some non-zero ideal K of R . By hypothesis $f(N) \subseteq N$. \square

There is no direct relation between fully stable modules relative to an ideal and multiplication modules. In fact, Z is a multiplication Z -module which is not fully stable module relative to nZ , for each $n(\neq \pm 1)$ in Z , while Q is a fully stable Z -module relative to each non-zero ideal of Z , which is not multiplication Z -module.

It is clear that, every submodule of fully stable module is a fully stable. And we show that, the submodule of fully stable module relative to an ideal need not be fully stable relative to that ideal (2.3)(5). This motivates to the following question: When the submodule of fully stable module relative to an ideal, a fully stable relative to that ideal?. For this we have the following.

Corollary (2.9): If M is a multiplication R -module and fully stable relative to each non-zero ideal of R , then each submodule of M is a fully stable relative to each ideal of R .

Proof: By Proposition (2.8). \square

Proposition (2.10): Let M be a multiplication R -module, N be any submodule of M and $[N:M]^2 = [N:M]$. Then N is a fully stable module relative to $[N:M]$.

Proof: Let $K \leq N$ and $f: K \rightarrow N$ be an R -homomorphism. Since M is multiplication, then $N = M[N:M]$, (5). Therefore, $f(K) \subseteq M[N:M]^2 = M[N:M][N:M]$, $f(K) \subseteq N[N:M] \subseteq K + N[N:M]$. \square

Recall that, an ideal I in a ring R is called pure if for each $a \in I$, there exists $b \in I$ \ni $ab = a$ (6). Thus, we have the following corollary.

Corollary (2.11): Let M be a multiplication R -module, N be a submodule of M and $[N:M]$ is pure ideal of R . Then N is a fully stable relative to $[N:M]$. \square

As we have seen every stable submodule is stable relative to each non-zero ideal, while the converse needs not be true. For example, $2Z \leq Q$ and $2Z$ is stable relative to $3Z$, but $2Z$ is not stable. For this we have the following.

Corollary (2.12): Let M be a multiplication R -module and N be any submodule of M . Then N is stable if and only if N is stable relative to $[N:M]$.

Proof: (\Rightarrow). It is clear.

(\Leftarrow). Since M is multiplication module, then $N = M[N:M]$ by (5), and this implies that N is stable. \square

For this we have the following corollary.

Corollary (2.13): Let M be a multiplication R -module. Then M is a fully stable if and only if M is a fully stable module relative to $[N:M]$, for each non-zero cyclic submodule N of M . \square

Let M be an R -module. We write the ideal $\theta(M)$ by $\theta(M) = \sum_{x \in M} [xR:M]$, it is proved in (7) that if M is multiplication, then $M = M\theta(M)$.

Corollary (2.14): Every multiplication R -module M is a fully stable module relative to $\theta(M)$. \square

We observe that, every fully stable R -module relative to an ideal A of R is a fully stable relative to each ideal contains A see (2.3)(8), while if $B \subseteq A$, for some ideal B of R , then M needs not be fully stable relative to B see (2.3)(9). However, we have the following:

Corollary (2.15): Let M be a multiplication R -module and B be an ideal of R such that B is contained in the residual of each non-zero cyclic submodule by M . Then the following statements are equivalent.

- M is fully stable module.
- M is fully stable module relative to $[\langle a \rangle : M]$, $\forall a (\neq 0) \in M$.
- M is fully stable relative to B . \square

Now, we will discuss the direct sum and the direct summand of fully stable modules relative to an ideal.

Proposition (2.16): Every direct summand of fully stable R -module relative to an ideal A of R is a fully stable module relative to A .

Proof: Let M be a fully stable R -module relative to an ideal A of R , N be a direct summand of M , K be a submodule of N and $f: K \rightarrow N$ be an R -homomorphism. Then $M = N \oplus L$, for some submodule L of M . Since M fully stable relative to A , then $f(K) \subseteq K + NA \oplus LA$. Now, $\forall k \in K$, $f(k) = k' + n + l$, for some $k' \in K, n \in NA$ & $l \in LA$, hence $l \in N \cap L$. Then $f(k) \in K + NA$. \square

Example (2.17): Recall that an R -module is free if it is isomorphic to a direct sum of copies of R . We claim that, every free R -module of rank greater than one cannot be fully stable relative to each ideal A of R (where $A \neq R$). It is enough to show that every R -module of rank two cannot be fully stable relative to A . Consider the submodule $N = R \oplus (0)$ of $F = R \oplus R$, and define $\theta: N \rightarrow F$ by $\theta((r, 0)) = (0, r)$ for each $(r, 0)$ in N . Clearly θ is a well-defined R -homomorphism. Then $\theta((1, 0)) = (0, 1) \in \theta(N)$, while $(0, 1) \notin N + (R \oplus R)A$. On the other hand, a free R -module of rank one may or may not be fully stable module relative to each ideal $A (\neq R)$. For example, every field is a fully stable ring relative to each ideal, while the ring Z fails to be fully stable relative to mZ , for each $m (\neq \pm 1) \in Z$ see (2.3)(6). Now, let R be a fully stable ring relative to an ideal $A (\neq R)$, and consider $S = R \oplus R$, then S is free R -

module of rank two. Hence S is not fully stable module relative to A . Thus we have the following proposition.

Proposition (2.18): Let $M = M_1 \oplus M_2$ where M_1 and M_2 are fully stable R -modules relative to an ideal A of R . If $\text{ann}_R(M_1) + \text{ann}_R(M_2) = R$, then M is a fully stable module relative to A .

Proof: Let K be any submodule of M . First claim that $K = N_1 \oplus N_2$ for some submodule N_1 of M_1 and N_2 of M_2 . In fact, if $k \in K$, then $k = x + y$ for some $x \in M_1$ and $y \in M_2$. Moreover, there exists elements $a \in \text{ann}_R(M_1)$ and $b \in \text{ann}_R(M_2)$ $\exists a + b = 1$. Let $N_1 = x\text{ann}_R(M_2)$ and $N_2 = y\text{ann}_R(M_1)$. Now, $x = x \cdot 1 \in M_1$ and $y = y \cdot 1 \in M_2$. Then $k \in N_1 \oplus N_2$, therefore $K \subseteq N_1 \oplus N_2$. For the other direction, let $w \in N_1 \oplus N_2$, then $w = xc + yd$ for some $c \in \text{ann}_R(M_2)$ and $d \in \text{ann}_R(M_1)$, $w = xc + yd = k(c + d) \in K$. Let $\theta: K \rightarrow M$ be any R -homomorphism, $i_1: N_1 \rightarrow N_1 \oplus N_2, i_2: N_2 \rightarrow N_1 \oplus N_2$ be inclusion mappings and, $\pi_1: M \rightarrow M_1$ and $\pi_2: M \rightarrow M_2$ be projection mappings. Put $\theta_1 = \pi_1 \circ \theta \circ i_1$ and $\theta_2 = \pi_2 \circ \theta \circ i_2$. Hence, $\theta = \theta_1 + \theta_2$, thus $\theta(K) \subseteq K + MA$. \square

Corollary (2.19): Let $M = M_1 \oplus M_2 \oplus \dots \oplus M_n$ where M_i is an R -module for each $i = 1, \dots, n$, $\text{ann}_R(M_i) + \bigcap_{j \neq i} \text{ann}_R(M_j) = R$ and A is an ideal of R . Then M is a fully stable module relative to A if and only if each M_i is a fully stable module relative to A . \square

Baer's Criterion Relative To An Ideal

We start by the following definition which is a generalization of Baer's criterion (2).

Definition (3.1): Let M be an R -module, A be an ideal of R , and N be any submodule of M . We say that N satisfies Baer's criterion relative to A if for every R -homomorphism $f: N \rightarrow M$, there exists element $r \in R$ such that $f(n) - nr \in MA$ for each $n \in N$. M is said to satisfy Baer's criterion relative to A , if each submodule of M satisfies Baer's criterion relative to A .

It is clear that, every module which satisfies Baer's criterion, satisfies Baer's criterion relative to each non-zero ideal, but the converse needs not be true. For example, Q_Z satisfies Baer's criterion relative to each non-zero ideal nZ of Z , while Q_Z does not satisfy Baer's criterion because Q_Z is not fully stable module (2).

In the following we give a new characterizations of fully stable modules relative to an ideal in terms of Baer's criterion relative to an ideal.

Theorem (3.2): The following statements are equivalent for an R -module M and an ideal A of R .

- M is a fully stable module relative to A .
- Every cyclic submodule of M is stable relative to A .
- For each x, y in M , $y \notin \langle x \rangle + MA$ implies $\text{ann}_R(x) \not\subseteq \text{ann}_R(y)$.
- M satisfies Baer's criterion relative to A for each cyclic submodule.

- For each $x \in M$, $\text{ann}_M(\text{ann}_R(x)) \subseteq \langle x \rangle + MA$.
- For each $x \in M$ and $r \in R$ $\text{ann}_M(rR \cap \text{ann}_R(x)) \subseteq \text{ann}_M(r) + xR + MA$. \square

Proof: (1) \Leftrightarrow (2). By Proposition (2.4).

(1) \Leftrightarrow (3). By Proposition (2.6).

(1) \Rightarrow (4). Let $x \in M$ and $f: xR \rightarrow M$ be an R -homomorphism. By using (1), we have $f(x) = xr + w$, for some r in R and w in MA . Therefore, $\exists r \in R \ni f(y) - yr \in MA, \forall y \in xR$.

(4) \Rightarrow (1). It is clear.

(4) \Leftrightarrow (5). It is an easy matter to see that.

(3) \Rightarrow (6). Let $x \in \text{ann}_M(rR \cap \text{ann}_R(y))$. Then $\text{ann}_R(yr) \subseteq \text{ann}_R(xr)$, by using (3), $xr = yrs + w$ for some $s \in R$ and $w \in MA$, then $(x - ys) \in \text{ann}_M(r)$ modulo MA , so $x \in yR + \text{ann}_M(r)$ modulo MA . Therefore, $x \in yR + \text{ann}_M(r) + MA$.

(6) \Rightarrow (5). By putting $r=1$, in (6). \square

Notice that, we can prove (1) \Leftrightarrow (5) without use R is commutative.

Next, we will study a certain class of fully stable modules relative to an ideal in which Baer's criterion relative to an ideal holds for all its submodules. We have the following proposition.

Proposition (3.3): Let A be an ideal of R and M be an R -module such that $\text{ann}_R(N) + \text{ann}_R(K) = R$ for every finitely generated submodules N and K of M . Then M is a fully stable relative to A if and only if M satisfies Baer's criterion relative to A for finitely generated submodules.

Proof: (\Leftarrow). By Theorem (3.2).

(\Rightarrow). Let N be a finitely generated submodule of M and R -homomorphism $f: N \rightarrow M$, $N = x_1R + x_2R + \dots + x_nR$, for some $x_1, x_2, \dots, x_n \in N$. We use induction on the number of generators of N . For, $n=1$, there is no thing to proof by using theorem (3.2). Suppose that Baer's criterion relative to A holds for all submodules generated by m elements for $m \leq n-1$, there exists two elements r, s in R such that $f(x) - xr \in MA$ for each $x \in x_1R + x_2R + \dots + x_{n-1}R$ and $f(x') - x's \in MA$ for each $x' \in x_nR$, thus exists $u \in \text{ann}_R(x_1R + x_2R + \dots + x_{n-1}R)$ & $v \in \text{ann}_R(x_nR) \ni r - s = u + v$ or $r - u = s + v = t$. For each $z \in N$, $z = \sum_{i=1}^n x_i r_i$ for some $r_i \in R$, for each $i = 1, \dots, n$. $f(z) - zt = f(\sum_{i=1}^{n-1} x_i r_i) - (\sum_{i=1}^{n-1} x_i r_i)t + f(x_n r_n) - (x_n r_n)s \in MA$. Therefore N satisfies Baer's criterion relative to A .

Corollary (3.4): Let A be an ideal of R and M be a Noetherian R -module such that $\text{ann}_R(N) + \text{ann}_R(K) = R$ for each two submodules N and K of M . Then M is a fully stable module relative to A if and only if Baer's criterion relative to A holds for each submodule of M .

Fully stable R -module M relative to an ideal A of R were characterized see Theorem (3.2) as those modules in which all cyclic submodules satisfy $\text{ann}_M(\text{ann}_R(x)) \subseteq \langle x \rangle + MA, \forall x \in M$. It is natural to characterize those modules

which satisfy $\text{ann}_M(\text{ann}_R(N)) \subseteq N + MA$ for all submodules N of M . The following lemma in this direction is needed.

Lemma (3.5): Let M be a fully stable R -module relative to an ideal A of R such that for each $x \in M$ and each ideal I of R , each R -homomorphism $\theta: xI \rightarrow M$ can be extended to an R -homomorphism $\alpha: xR \rightarrow M$. If a submodule N of M satisfies $\text{ann}_M(\text{ann}_R(N)) \subseteq N + MA$, so does $N + xR$.

Proof: Denote $\text{ann}_R(N)$ and $\text{ann}_R(x)$ by B and C respectively then by the assumption $\text{ann}_M(B) \subseteq N + MA$. Since M is fully stable relative to A , $\text{ann}_M(C) \subseteq \langle x \rangle + MA$ by Theorem (3.2). To prove that $\text{ann}_M(\text{ann}_R(N + xR)) \subseteq N + xR + MA$. It is enough to show that $\text{ann}_M(B \cap C) \subseteq N + xR + MA$. Let $y \in \text{ann}_M(B \cap C)$. Define $\theta: xB \rightarrow M$ by $\theta(xb) = yb, \forall b \in B$. θ is well-defined R -homomorphism. By hypothesis there exist extension $\alpha: xR \rightarrow M$ of θ and since M is fully stable relative to A , $\alpha(xR) \subseteq xR + MA$. Now, $\forall b \in B, \alpha(x)b = \alpha(xb) = \theta(xb) = yb$ implies that $y \in N + xR + MA$.

Proposition (3.6): Let M be an R -module such that for each x in M and each ideal I of R , each R -homomorphism $\theta: xI \rightarrow M$ can be extended to an R -homomorphism $\alpha: xR \rightarrow M$. Then the following statements are equivalent for an ideal A of R .

1. M is a fully stable module relative to A .
2. $\text{ann}_M(\text{ann}_R(N)) \subseteq N + MA$ for each finitely generated submodule N of M .

Corollary (3.7): Let M be a Noetherian R -module such that for each x in M and each ideal I of R , each R -homomorphism $\theta: xI \rightarrow M$ can be extended to an R -homomorphism $\alpha: xR \rightarrow M$. Then the following statements are equivalent for an ideal A of R .

1. M is a fully stable module relative to A .
2. $\text{ann}_M(\text{ann}_R(N)) \subseteq N + MA$ for each submodule N of M . \square

Recall that, an R -module M is called quasi-injective, if each R -homomorphism of any R -submodule N of M can be extended to an R -homomorphism of M into M (8). Observe that quasi-injective modules satisfy the condition of Prop. (3.6), hence we have the following.

Corollary (3.8): Let M be a quasi-injective R -module. Then the following statements are equivalent for an ideal A of R .

- M is a fully stable module relative to A .
- $\text{ann}_M(\text{ann}_R(N)) \subseteq N + MA$ for each finitely generated submodule N of M . \square

Corollary (3.9): Let M be a Noetherian quasi-injective R -module. Then the following statements are equivalent for an ideal A of R .

- M is a fully stable module relative to A .
- $\text{ann}_M(\text{ann}_R(N)) \subseteq N + MA$ for each submodule N of M . \square

REFERENCES

1. Nicholson, W. K., Park, J.K., Yousif, M. F. Principally quasi-injective modules, *Comm. In Algebra*, 27:1683-1693 (1999).
2. Abbas, M.S., On fully stable modules, Ph.D.thesis, Univ. of Baghdad (1990).
3. Lam, T. Y., *Lectures on Modules and rings*, Springer (1999).
4. Barnard, A., Multiplication modules, *J. of Algebra*, 71:174-178 (1981).
5. EL-Bast, Z. A., Smith, P. F., Multiplication modules, *Comm. In Algebra*, 16:755-779 (1988).
6. AL-Ezeh, H., Pure ideals in commutative reduced Gelfand rings with unity, *Arch. Math.* 53:266-269 (1989).
7. Anderson and Yousef AL-Shaniafi, D. D., Multiplication modules and the ideal $\theta(M)$, *Comm. In Algebra*, 30:3383-3390 (2002).
8. Johnson, R. E. Wong, E. T., Quasi-injective modules and irreducible rings, *J. London Math. Soc.*, 39: 260-268 (1961).

On reverse $*$ -centralizer of prime and semiprime ring with involution

Abd Al- Rahman.H.Majeed and Ali Abd Abeed.AL-Tay
Department of mathematics, college of science, University of Baghdad

الخلاصة

في هذا العمل تم تقديم دوال جمعية جديدة، مثل تمرکزات $*$ -جوردن وتمرکزات $*$ -العكسية وبعض المفاهيم الجديدة التي ترتبط بهذه الدوال، وأيضا سوف نعطي بعض الأمثلة الضرورية التي توضح هذه المفاهيم. كذلك تمت دراسة العلاقات بين هذه البنى الجبرية في الحلقات الأولية وشبه الأولية.

ABSTRACT

In this paper, new additive mappings are presented, such as Jordan $*$ -centralizers, reverse $*$ -centralizers, and some new concepts which concerning these new mappings. Also we will give some necessary examples that illustrate these concepts. And we will give a relation between Jordan $*$ -centralizer and reverse $*$ -centralizer and some results on reverse $*$ -centralizers on prime and semiprime $*$ -ring.

INTRODUCTION

Throughout, R will represent an associative ring with center $Z(R)$. A ring R is n -torsion free, if $nx = 0$, $x \in R$ implies $x = 0$, where n is a positive integer. Recall that R is prime if $aRb = (0)$ implies $a = 0$ or $b = 0$, and semiprime if $aRa = (0)$ implies $a = 0$. An additive mapping $x \rightarrow x^*$ on a ring R is called an involution if $(xy)^* = y^* x^*$ and $(x^{**}) = x$ for all $x, y \in R$. A ring equipped with an involution is called $*$ -ring (1). For example of involution the first is a complex plan, and the second is taking the transpose in a matrix ring. An element x in a $*$ -ring R is said to be hermitian if $x^* = x$ and skew-hermitian if $x^* = -x$. The sets of all hermitian and skew-hermitian elements of R will be denoted by $H(R)$ and $S(R)$, respectively. If R is 2-torsion free then every $x \in R$ can be uniquely represented in the form $2x = h + k$ where $h \in H(R)$ and $k \in S(R)$. An element $x \in R$ is called normal element if $xx^* = x^*x$, and if all the elements of R are normal then R is called a normal ring [2]. As usual the commutator $xy - yx$ will be denoted by $[x, y]$. We shall use basic commutator identities $[xy, z] = [x, z]y + x[y, z]$ and $[x, yz] = [x, y]z + y[x, z]$ for all $x, y, z \in R$, also we write $x \circ y = xy + yx$ for all $x, y \in R$ (1). An additive mapping $d: R \rightarrow R$ is called a derivation if $d(xy) = d(x)y + x d(y)$ holds for all pairs $x, y \in R$, and is called a Jordan derivation in case $d(x^2) = d(x)x + x d(x)$ is fulfilled for all $x \in R$. Every derivation is a Jordan derivation, but the converse is in general not true. A classical result of Herstein (3) asserts that every Jordan derivation on a prime ring of characteristic different from 2 is a derivation. Cusack (4) generalized

Herstein's theorem to 2-torsion free semiprime ring (see (5) for an alternative proof). An additive mapping $d: R \rightarrow R$ is called a *-derivation if $d(xy) = d(x)y^* + xd(y)$ holds for all pairs $x, y \in R$ and is called a Jordan *-derivation in case $d(x^2) = d(x)x^* + xd(x)$ is fulfilled for all $x \in R$ (6). A left (right) centralizer of R is an additive mapping $T: R \rightarrow R$ which satisfies $T(xy) = T(x)y$ ($T(xy) = xT(y)$) for all $x, y \in R$. A centralizer of R is an additive mapping which is both left and right centralizer. A left (right) Jordan centralizer of R is an additive mapping $T: R \rightarrow R$ which satisfies $T(x^2) = T(x)x$ ($T(x^2) = xT(x)$) for all $x \in R$. A Jordan centralizer of R is an additive mapping which is both left and right Jordan centralizer. Every centralizer is a Jordan centralizer. B. Zalar (7) proved the converse when R is 2-torsion free semiprime ring. Some results concerning centralizers in prime and semiprime rings can be found in (8,9). Inspired by the above definition we define. A left (right) reverse *-centralizer of a *-ring R is an additive mapping $T: R \rightarrow R$ which satisfies $T(yx) = T(x)y^*$ ($T(yx) = x^*T(y)$) for all $x, y \in R$. A reverse *-centralizer of R is an additive mapping which is both left and right reverse *-centralizer. A left (right) Jordan *-centralizer of R is an additive mapping $T: R \rightarrow R$ which satisfies $T(x^2) = T(x)x^*$ ($T(x^2) = x^*T(x)$) for all $x \in R$. A Jordan *-centralizer of R is an additive mapping which is both left and right Jordan *-centralizer. Every reverse *-centralizer is a Jordan *-centralizer. In this paper we prove the converse when R is a 2-torsion free semiprime *-ring.

EXAMPLES

The following three example explore the relation between Jordan *-centralizer and *-centralizer.

Example (2.1) Let F be a field, and $M_2(F)$ be a set of all matrices of order 2, with respect to the usual operation of addition and multiplication, and transpose involution, then $M_2(F)$ is an associative *-ring. Let $T_1, T_2: M_2(F) \rightarrow M_2(F)$ be additive mappings defined as

$$T_1 \left(\begin{bmatrix} x & y \\ z & w \end{bmatrix} \right) = \begin{bmatrix} 0 & 0 \\ y & w \end{bmatrix}, \text{ for all } x, y, z, w \in F.$$

Then T_1 is a left reverse *-centralizer

$$T_2 \left(\begin{bmatrix} x & y \\ z & w \end{bmatrix} \right) = \begin{bmatrix} 0 & z \\ 0 & w \end{bmatrix}, \text{ for all } x, y, z, w \in F.$$

Then T_2 is a right a reverse $*$ -centralizer

Example (2.2) Let F be a field, with involution $*$, and $D_2(F)$ be a set of all diagonal matrices of order 2, with respect to the usual operation of addition and multiplication, and the involution $*^1$ on $D_2(F)$ defined by

$$*^1\left(\begin{bmatrix} x & 0 \\ 0 & y \end{bmatrix}\right) = \begin{bmatrix} x^* & 0 \\ 0 & y^* \end{bmatrix}, \text{ for all } x, y \in F.$$

Then $D_2(F)$ is a commutative $*^1$ -ring. Let $T: D_2(F) \rightarrow D_2(F)$ be an additive mappings defined as

$$T\left(\begin{bmatrix} x & 0 \\ 0 & y \end{bmatrix}\right) = \begin{bmatrix} x^* & 0 \\ 0 & 0 \end{bmatrix}, \text{ for all } x, y \in F.$$

Then T is a reverse $*$ -centralizer.

Example (2.3) Let F is a field of characteristic not equal 2, and R be F -algebra of triangular matrices of the form:

$$x = \begin{pmatrix} 0 & a & c & b \\ 0 & 0 & 0 & c \\ 0 & 0 & 0 & -a \\ 0 & 0 & 0 & 0 \end{pmatrix} \quad \text{for all } a, b, c, d \in F.$$

With

$$x^* = \begin{pmatrix} 0 & a & c & -b \\ 0 & 0 & 0 & c \\ 0 & 0 & 0 & -a \\ 0 & 0 & 0 & 0 \end{pmatrix} \quad \text{for all } a, b, c, d \in F.$$

It is easy to verify that $*$ is an involution on R . Define the mapping $T: R \rightarrow R$ as follows

$$T(x) = \begin{pmatrix} 0 & 0 & 0 & b \\ 0 & 0 & 0 & 0 \\ 0 & 0 & 0 & 0 \\ 0 & 0 & 0 & 0 \end{pmatrix} \quad \text{for all } a, b, c, d \in F.$$

Then T is a Jordan *-centralizer but not reverse *-centralizer.

MAIN RESULTS

In the following theorem we will prove every Jordan *-centralizer is a reverse *-centralizers on a 2-torsion free semiprime *-ring.

Theorem (3.1) Let R be a 2-torsion free semiprime *-ring, then every left (right) Jordan *-centralizer is a left (right) reverse *-centralizer.

To prove this theorem, we need the following lemmas.

Lemma (3.2):[7] Let R be a semiprime ring and $A, B: R \times R \rightarrow R$ biadditive mappings. If $A(x, y) \circ B(x, y) = 0$ for all $x, y, w \in R$, then $A(x, y) \circ B(u, v) = 0$ for all $x, y, u, v, w \in R$.

Lemma (3.3):[7] Let R be a semiprime ring. If $a, b \in R$ are such that $axb = 0$ for all $x \in R$, then $ab = ba = 0$.

Lemma (3.4):[7] Let R be a semiprime ring, and let a be an element in R , if $a[x, y] = 0$ for all $x, y \in R$, then there exists an ideal U of R such that $a \in U \subset Z(R)$.

Lemma (3.5) Let R be 2-torsion free semiprime *-ring, and let $c \in Z(R)$, let $T: R \rightarrow R$ be a left Jordan *-centralizer then

$$G(x, c) = G(c, x) = 0.$$

Where $G(x, y) = T(xy) - T(x)y^*$ for all $x, y \in R$.

Proof: We have the relation

$$T(x^2) = T(x)x^* \quad \text{for all } x \in R. \quad (1)$$

If we replace $x+y$ for x in (1) we get

$$T(xy+yx) = T(x)y^* + T(y)x^* \quad \text{for all } x, y \in R. \quad (2)$$

By replacing y with $xy + yx$ and using (2), we arrive at

$$T(x^2y+yx^2) + 2T(xyx) = T(x)x^*y^* + 2T(x)y^*x^* + T(y)x^{*2} \quad \text{for all } x, y \in R. \quad (3)$$

Now replace x by x^2 in (2) we get

$$T(x^2y+yx^2) = T(x)x^*y^* + T(y)x^{*2} \quad \text{for all } x, y \in R. \quad (4)$$

If we Comparing (3) and (4) we get

$$T(xyx) = T(x)y^*x^* \quad \text{for all } x, y \in R. \quad (5)$$

If we linearization (5), we get

$$T(xyz + zyx) = T(x)y^*z^* + T(z)y^*x^* \quad \text{for all } x, y, z \in R. \quad (6)$$

Now we compute

$$T(xcy+ycx) = T((xc)y+y(xc)). \quad (7)$$

In two different way by using (2) and (6) and comparing the tow results we arrive at

$$G(x,c) R G(x,c)=0 \text{ for all } x \in R. \quad (8)$$

Since R is a semiprime $*$ -ring, and $G(x,c)=-G(c,x)$, we get

$$G(x,c)=G(c,x)=0 \text{ for all } x \in R. \quad (9)$$

Proof of Theorem 3.1:

Now we shall compute $j = T(xzyzx + yxzxy)$ for all $x,y,z \in R$ in two different ways. Using (5) we have

$$j = T(x) y^* z^* y^* x^* + T(y) x^* z^* x^* y^*, \quad (10)$$

Using (6), we have

$$j = T(xy) z^* x^* y^* + T(yx) z^* y^* x^*, \quad (11)$$

Then comparing (10), (11) we have

$$B(y,x) (z^* y^* x^*) + B(x,y) (z^* x^* y^*) = 0 \text{ for all } x,y,z \in R. \quad (12)$$

Where $B(x,y)$ stands for $T(xy)-T(y)x^*$. Equality (2) can be rewritten in this notation as $B(x,y) = -B(y,x)$ for all $x,y \in R$. Using this fact and equality (12), we obtain

$$B(x,y) z^* [x^*, y^*] = 0 \text{ for all } x,y,z \in R, \quad (13)$$

Using Lemma 3.2, we have

$$B(x,y) z^* [u, v] = 0 \text{ for all } x,y,z,u,v \in R. \quad (14)$$

Using Lemma 3.3.

$$B(x,y) [u, v] = 0 \text{ for all } x,y,z,u,v \in R. \quad (15)$$

Using Lemma 3.4, we have $B(x,y) \in Z(R)$.

Now let $c \in Z(R)$. Then consider the quantity

$$B(x,y) c^* = T(xy) c^* - T(y) x^* c^* \text{ for all } x,y \in R. \quad (16)$$

Since $c \in Z(R)$ by Lemma 1.1.39, Lemma 1.1.40, and the relation (16) we arrive at

$$\begin{aligned} B(x,y) c^* &= T(xyc) - T(y) c^* x^* \\ &= T(xyc) - T(y) c^* x^* \\ &= T(xyc) - T(cy) x^* \\ &= T(xyc) - T(c) y^* x^* \\ &= T(xyc) - T(c) (xy)^* = T(xyc) - T(cxy) = 0. \end{aligned}$$

Therefore,

$$B(x,y) c^* = 0 \text{ for all } x,y \in R, \text{ and } c \in Z(R). \quad (17)$$

Since $B(x,y) \in Z(R)$ by using Lemma 3.5, we get

$$B(x,y) B(x,y) = 0. \text{ for all } x,y \in R, \quad (18)$$

Right multiplication the relation (18) by r we obtain

$$B(x,y) r B(x,y) = 0. \text{ for all } x,y,r \in R, \quad (19)$$

Since R is a semiprime ring then from the relation (19) we get

$$B(x,y) = 0. \text{ for all } x \in R, \quad (20)$$

If $T(x^2) = x^*T(x)$, we obtain the assertion of the theorem with similar approach as above, the proof is complete. \square

If R is prime ring, we get the following corollary,

Corollary (3.6) Let R be a 2-torsion free prime $*$ -ring, then every left (right) Jordan $*$ -centralizer is a left (right) reverse $*$ -centralizer.

B. Zalar in (7) proved that every additive mapping $T: R \rightarrow R$ which satisfies $T(xoy) = T(x)oy = xoT(y)$ for all $x, y \in R$, is a centralizer. In the following proposition we will give a result similar to the above proposition, but in case reverse $*$ -centralizers.

Proposition (3.7) Let R is a 2-torsion free semiprime $*$ -ring, and $S: R \rightarrow R$ an additive mapping which satisfies

$$S(xoy) = S(x)oy^* = x^*oS(y) \text{ for all } x, y \in R. \quad (21)$$

Then S is a reverse $*$ -centralizer of R .

To prove this proposition, we need the following lemmas

Lemma (3.8): [7] Let R be a semiprime ring and $D: R \rightarrow R$ be a derivation, and $a \in R$ be fixed element then we have:

(1) If $D(x)D(y) = 0$ for all $x, y \in R$. Then $D = 0$.

(2) If $a - xax \in Z(R)$ for all $x \in R$. Then $a \in Z(R)$.

Lemma (3.9) Let R be a semiprime $*$ -ring and let $a \in R$ be a fixed element, and let $S(x) = ax^* + x^*a$ is satisfy (21), then $a \in Z(R)$.

Proof: We have

$$S(xoy) = S(x)oy^* = S(y)ox^* \text{ for all } x, y \in R.$$

Gives us

$$\begin{aligned} a(xy+yx)^* + (xy+yx)^*a &= (ax^* + x^*a)y^* + y^*(ax^* + x^*a), \\ ay^*x^* + x^*y^*a - x^*ay^* - y^*ax^* &= 0 = (ay^* - y^*a)x^* - x^*(ay^* - y^*a). \end{aligned}$$

Then from second part of Lemma 3.8, we get $a \in Z(R)$.

Lemma (3.10) Let R be a semiprime $*$ -ring. Then every mappings T of R satisfy (21) maps $Z(R)$ into $Z(R)$.

Proof: Let $c \in Z(R)$, and let $a = T(c)$. Then

$$2T(cx) = T(cx+xc) = T(c)x^* + x^*T(c) = ax^* + x^*a.$$

Now we will show, $S(x) = 2T(cx)$, is satisfy the relation (21),

$$\begin{aligned} S(xy+yx) &= 2(T(c(xy+yx))), \\ &= 2T((cx)y+y(cx)) = 2T((cy)x+x(cy)), \\ &= S(x)y^* + y^*S(x) = S(y)x^* + x^*S(y), \end{aligned}$$

Hence by Lemma 3.9, we get $a \in Z(R)$.

Proof of Proposition 3.7: We have

$$S(xy+yx) = S(x)y^* + y^*S(x) = S(y)x^* + x^*S(y) \text{ for all } x, y \in R.$$

Replace y by xoy , we get

$S(x) \circ (x \circ y)^* = (S(x) \circ y^*) \circ x^*$ for all $x, y \in R$.

Now it follows that $[S(x), x^*]y^* = y^*[S(x), x^*]$ holds for all $x, y \in R$ and so we get $[S(x), x^*] \in Z(R)$. The next goal is to show that $[S(x), x^*] = 0$ holds. Take any $c \in Z(R)$.

$$2S(cx) = S(cx + xc) = S(c)x^* + x^*S(c) = 2S(x)c^*$$

Using Lemma 3.10 we get

$$S(cx) = S(x)c^* = S(c)x^*$$

Therefore,

$$[S(x), x^*]c^* = S(x)x^*c^* - x^*S(x)c^* = S(c)x^{*2} - x^*S(c)x^* = 0$$

Since $[S(x), x^*]$ itself is central element, our goal is achieved.

$$2S(x^2) = S(xx + xx) = S(x)x^* + x^*S(x) = 2S(x)x^* = 2x^*S(x)$$

Theorem 3.1, now concludes the proof. \square

REFERENCES

1. I. N. Herstein "Topics in ring theory" University of Chicago Press, (1969).
2. F. J. Dyson "Quaternion determinants" *Helvetica Physica Acta*, 45:289-302 (1972).
3. I. N. Herstein "Jordan derivations in prime rings" *Proc. Amer. Math. Soc.* 8: 1104-1110 (1957).
4. J. Cusack "Jordan derivations on rings" *Proc. Amer. Math. Soc.* 53:321-324 (1975).
5. M. Brešar "Jordan derivations on semiprime rings" *Proc. Amer. Math. Soc.* 104 (4) 1003-1006 (1988).
6. M. Brešar & J. Vukman "On some additive mappings in rings with involution" *Aequationes Math.* 38: 178-185 (1989).
7. B. Zalar "On centralizers of semiprime rings" *Comment. Math. Univ. Carolinae* 32: 609-614 (1991).
8. A. H. Majeed & H. A. Shaker "Some Results on Centralizers" *Dirasat, Pure Sciences*, 35, (1):23-26 (2008).
9. J. Vukman "Centralizers in prime and semiprime rings" *Comment. Math. Univ. Carolinae* 38: 231-240 (1997).

S^* - Order continuous

Ali Hussain Battor and Falah Hasan Sarhan

University of Kufa, College of Education, Department of Mathematic

الخلاصة

في هذا البحث سلسلة من الحقائق والأفكار العامة المعروفة لنظرية الجبر البولياني والحزم المتجه (1, 2, 9), نظرية التكامل بالنسبة إلى المعايير ذات القيم في أشباه الحقول (4, 5, 7, 8). كذلك سوف نستعرض بعض التعاريف والمبرهنات التي نحتاجها في عملنا. وأخيرا برهنا بأن حزم أورليتز- S^* تكون حزم كاملة وأن المعيار- S^* يكون مستمر برتبة.

ABSTRACT

In this paper a series of known notions, notations and facts of the theory of Boolean algebra, vector lattices (1,2,9), the integration theory for measures with values in semi-field (4,5,7,8) is cited. We shall review some of the definitions and propositions which are needed in our work. Also we have proved that an S^* -Orlicz Lattice is a complete Lattice and an S^* -norm is order continuous.

INTRODUCTION

In this work a series of known notions, notations and facts of the theory of Boolean algebra, vector lattices (1,2,9), the integration theory for measures with values in semi-field (4,5,7,8) is cited. Suppose that R is the set of real numbers and E is a partially ordered set ($E \subseteq R$). The main results in this work is the following :

Theorem I: An S^* -Orlicz Lattice $(X, \|\cdot\|_F)$ is a complete Lattice and an S^* -norm $\|\cdot\|_F$ is order continuous.

Theorem II: Suppose that $(X, \|\cdot\|_F)$ is an S^* -Orlicz lattice, $0 \leq x_n \uparrow x$, $x_n, x \in X$, then $F(x_n) \uparrow F(x)$.

2. The Basic Concepts

In this section, we shall review some of the definitions and propositions which are needed in our work.

2.1. DEFINITION (5)

A vector space X equipped with a partial order " \leq " is called a vector lattice, if for each pair x, y in X :

- there is the smallest element z (denoted by $x \vee y$) for which $x \leq z$ and $y \leq z$.
- there is the largest element w (denoted by $x \wedge y$) for which $w \leq x$ and $w \leq y$.
- if $x \leq y$, then $x + z \leq y + z$ for all $x, y, z \in X$.
- if $x \leq y$ and $c \in R^+$, then $c x \leq c y$.

2.2. DEFINITION (3)

Suppose that X is a S^* -vector lattice. A mapping $F: X \rightarrow S^*$ is called an S^* -Orlicz modular if:

- $F(x) \geq 0$ for all $x \in X$ and $F(x) = 0$, if and only if, $x = 0$.
- $F(x) \leq F(y)$, if $|x| \leq |y|$ for all $x, y \in X$.

3. $F((\alpha x + (\hat{1}-\alpha) y) \leq \alpha F(x) + (\hat{1}-\alpha) F(y)$ for all $x, y \in X$, $\alpha \in S^*$ and $0 \leq \alpha \leq \hat{1}$ ($\hat{1}$ is a A Freudenthal unit).
4. $F(2x) \leq c F(x)$ for all $x \in X$ and $c > 0$.
5. $F(x + y) = F(x) + F(y)$, if $x, y \in X$ and $x \wedge y = 0$.
6. $F(e x) = e F(x)$ for all $x \in X$ and $e \in \nabla(S^*)$.

From the definition, we get that $F(x) = F(|x|)$ and $F(\alpha x) \leq \alpha F(x)$ for all $x \in X$, $\alpha \in S^*$ and $0 \leq \alpha \leq \hat{1}$.

2.3. Note (3)

Suppose that X is an S^* -Orlicz modular on a S^* -vector lattice X . For all $x \in X$, we set

$$B(x) = \{\lambda \in S_+^* : F(\lambda^{-1}x) \leq \hat{1}, \lambda \text{ is invertible}\}.$$

If $x \in X$, $\lambda = F(x) + \hat{1}$, then

$$F(\lambda^{-1}x) \leq \lambda^{-1} F(x) \leq \hat{1},$$

it means, that $B(x) \neq \emptyset$.

For each $x \in X$, we set

$$\|x\|_F = \inf \{\lambda : \lambda \in B(x)\}.$$

2.4. Proposition (6)

For a Banach S^* -vector lattice $(X, \|\cdot\|_F)$, the following conditions are equivalent:

1. X is a complete Lattice and the S^* -norm $\|\cdot\|_F$ is order continuous.
2. Every bound above the sequence of mutuality disjoint elements from X_+ , (x_n) -converges to zero ($\{x_n\}$ converges to zero in the topology t).

2.5. proposition (10)

Suppose that an N -function $M(u)$ satisfies the Δ_2 -condition with $u_0 = 0$, (i.e $M(2u) \leq k M(u)$ for all $u \geq 0$ and some $k > 0$), and suppose $x_n, x \in L_M^* = L_M$ ($L_M^* = x \in C_\infty(Q(\nabla)) : \lambda^{-1} x \in L_M$ for some number $\lambda = \lambda(x) > 0$). The following conditions are equivalent:

1. $\|x_n - x\|_M \xrightarrow{(o)} 0$ (respectively, $\|x_n - x\|_M \xrightarrow{(t)} 0$).
2. $\mu(M(x_n - x)) \xrightarrow{(o)} 0$ (respectively, $\mu(M(x_n - x)) \xrightarrow{(t)} 0$).

3. The main result

In this section, we shall prove an important proposition related to the order continuous.

3.1. THEOREM

An S^* -Orlicz Lattice $(X, \|\cdot\|_F)$ is a complete Lattice and an S^* -norm $\|\cdot\|_F$ is order continuous.

Proof. According to the proposition 2.3, we need to show that, if $\{x_n\} \subset X_+$, $x_n \wedge x_k = 0$ for all $n \neq k$, and $x_n \leq x \in X$, $n=1,2,\dots$.

Then $\|x_n\|_F \xrightarrow{(t)} 0$.

Suppose $y_n = \sum_{i=1}^n x_i = \bigvee_{i=1}^n x_i$, $1 \leq i \leq n$.

Then, we have, $0 \leq y_n \leq y_{n+1} \leq x$, $n=1,2,\dots$, and by the property (5) of the S^* -modular F , we have

$$\sum_{i=1}^n F(x_i) = F(y_n) \leq F(x).$$

Therefore,

$$F(x_n) \xrightarrow{(o)} 0.$$

By proposition 2.4, implication $2 \rightarrow 1$, we get

$$F(2^i x_n) \xrightarrow{(o)} 0.$$

From the previous assertion, the element

$$\lambda = F(x) + \hat{1} \in B(x).$$

Hence

$$\|x\|_F \leq F(x) + \hat{1} \text{ for all } x \in X.$$

Since $F(2y) \leq k F(y)$ for any $y \in C_\infty(Q(\nabla))$ [3], then

$$F(2^i(x_n)) \leq k^i F(x_n) \text{ for all } i=1,2,\dots,$$

from which, we get

$$F(2^i(x_n)) \xrightarrow{(o)} 0 \text{ as } n \rightarrow \infty \text{ for any fixed } i.$$

Thus, using Young's inequality [2], notice that, for any $y \in L_N$ with $\mu(N(y)) \leq \hat{1}$, the inequality

$$|(2^i x_n) y| \leq F(2^i x_n) + \hat{1}, \text{ take place.}$$

Hence

$$\|2^i(x_n)\|_F \leq F(2^i x_n) + \hat{1},$$

and

$$\|x_n\| \leq 2^{-i} F(2^i x_n) + 2^{-i} \hat{1}.$$

From this, we get

$$(o)- \overline{\lim} \|x_n\|_F = \bigwedge_{k=1}^{\infty} \bigvee_{n \geq k} \|x_n\|_F \leq 2^{-i} \hat{1}, \text{ for any } i=1,2,\dots$$

This means that

$$(o)- \overline{\lim} \|x_n\|_F = 0, \text{ i.e. } \|x_n\|_F \xrightarrow{(o)} 0,$$

which implies that

$$\|x_n\|_F \xrightarrow{(t)} 0.$$

Thus, X is a complete lattice and the S^* -norm $\|\cdot\|_F$ is order continuous.

3.2. Proposition

Suppose that $(X, \|\cdot\|_F)$ is an S^* -Orlicz lattice, $0 \leq x_n \uparrow x$, $x_n, x \in X$, then $F(x_n) \uparrow F(x)$.

Proof. Since $F(x_n) \leq F(x_{n+1}) \leq F(x)$, then, there exists in $C_\infty(Q(\nabla))$ [3] an element

$$y = \sup_{n \geq 1} F(x_n) \leq F(x).$$

Suppose $\lambda \in S^*$, then

$$x = (1-\lambda) x_n + \lambda (x_n + \lambda^{-1} (x - x_n)).$$

Therefore,

$$F(x) = F((1-\lambda) x_n + \lambda (x_n + \lambda^{-1} (x - x_n)))$$

$$\begin{aligned} &\leq (1-\lambda) F(x_n) + \lambda F(x_n + \lambda^{-1}(x - x_n)) \\ &\leq (1-\lambda) F(x_n) + \lambda (F(x_n) + F(\lambda^{-1}(x - x_n))) . \end{aligned}$$

Since $F(\lambda^{-1}(x - x_n)) \xrightarrow{(0)} 0$, then by theorem (3.3.9), we get
 $\|\lambda^{-1}(x - x_n)\|_F \xrightarrow{(0)} 0$.

Thus,

$$\begin{aligned} F(x) &\leq (1-\lambda) F(x_n) + \lambda F(x_n) \\ &= F(x_n) - \lambda F(x_n) + \lambda F(x_n) \\ &= F(x_n) \leq \sup_{n \geq 1} F(x_n) = y . \end{aligned}$$

Therefore, $F(x) = y = \sup_{n \geq 1} F(x_n)$, i.e. $F(x_n) \uparrow F(x)$.

REFERENCES

- 1.A.Battor" Orlicz space associated with S^* -valued measure and their measurable decompositions " Ph.D. Dissertation. Tashkent State University(1991).
- 2.A.Battor"Orlicz space for measurable function " Lecture notes(2002).
- 3.A.Battor, F. Hasan: " On The Orlicz Lattice and Modular " . MS.C thesis, University of Kufa(2008).
- 4.B.Z.Vulih; Introduction to the theory of partially ordered set. Moscow,:407 (1961).
5. C .D. Aliprantis & K.C. Border, Infinite Dimensional Analysis: A Hitchhiles's Guide, Springer-Verlag(1994).
6. D.A. Vladimirov; Boolean algebras. Moscow : Nauka, :319(1969) .
7. H.H. Schaefer Banach Lattices and positive operators, Springer –Verlag(1974).
8. J. Borwein and V. weff : " Convex function on Banach space Note containig.
9. L.L. Dornhoff (1978): " Applied Modern Algebra ". New York, London, : 265.
- 10.M. Stone; Applications of the theory of Boolean ring to general topology /Trans. Amer. Math. Soc. 41. : 375-481(1937).
11. S.L. Gubta an N. Rani " Fundamental real analysis ". Delhi(1970).

On The θ -Convergence of Net and Filter in Bitopological space

Bassam Jabbar AL-Asadi and Amer Ismael Al-Saeed
Department of Mathematics, College of Science, Al-Mustansiriya University

الخلاصة

في هذا البحث قمنا بدراسة بعض الخواص التوبولوجية للتقارب θ بالنسبة للشبكة والمرشح في الفضاء التوبولوجي الثنائي مستخدمين مفهوم المجموعات المفتوحة من النمط $ij - \theta$ وكذلك درسنا بعض خواص النقاط العنقودية من النمط $ij - \theta$ للشبكة والمرشح وكذلك قمنا بإيجاد بعض المكافئات للفضاء يورسن في الفضاء التوبولوجي الثنائي .

ABSTRACT

In this paper we introduce and study topological properties of θ -convergent of net and filter in bitopological space using the concept of $ij - \theta$ - open sets, also some properties of $ij - \theta$ - cluster points of net and filter are studies and we find some characterizations of $ij - \theta$ - Urysohn space.

Keywords and phrases: Bitopology, $ij - \theta$ -open sets, $ij - \theta$ -closed sets, $ij - \theta$ -convergent.

INTRODUCTION

The concept of bitopological space was first introduced by Kelly J.C. in 1963 in your paper "bitopological space" and in 1981 Bose, S. and Sinha, D. introduced the concept of $ij - \theta$ -continuous map in your paper "almost open, almost closed, θ -continuous and almost quasi compact mappings in bitopological spaces"

We recall that a bitopological space is a triple (X, τ_1, τ_2) , where X is a nonempty set and τ_1 and τ_2 are two topologies on X . Ever since Kelly (1) introduced them, bitopological spaces have been subject of intensive investigation of many topologists.

We use $ij - \theta$ to certain properties with respect to topology τ_i and τ_j , where $i, j \in \{1, 2\}$ and $i \neq j$. By $i - \text{int}(A)$, $i - \text{cl}(A)$, we will mean the interior and the closure of subset A of X with respect to topology τ_i . If $x \in X$, O_x is the set of all open subsets of X with respect to topology τ_i which contains x and N_x is the set of all neighborhoods of x with respect to topology τ_i . The $ij - \theta$ - closure of A (2), denoted by $ij - \text{cl}_\theta(A)$, is the set of all $x \in X$ for which every closure (with respect to τ_i) of every open neighborhood of

x (with respect to τ_i , we denoted by N_x) intersects A nontrivially. A set A is called ij - θ -closed if $A = ij-cl_\theta(A)$. The ij - θ -interior of A (2), denoted by $ij-int_\theta(A)$, is the set of all $x \in X$ for which A contains j -closure of open neighborhood of x (with respect to τ_i). A set A is said to be ij - θ -open provided that $A = ij-int_\theta(A)$. Furthermore, the complement of an ij - θ -open set is ij - θ -closed and the complement of a ij - θ -closed set is ij - θ -open. Clearly that every ij - θ -open (ij - θ -closed) is i -open (i -closed).

A map $f: (X, \tau_1, \tau_2) \longrightarrow (Y, \sigma_1, \sigma_2)$ is said to be ij - θ -continuous at $x \in X$ if for each $V \in \sigma_i$, $f(x) \in V$ there exist $U \in \tau_i$, $x \in U$, such that $f(j-cl(U)) \subseteq j-cl(V)$. If this condition is satisfied at each $x \in X$, then f is said to be ij - θ -continuous.

ij - θ -Convergent of net

Definition 1.1[3]. Let (X, τ_1, τ_2) be a bitopological space. A net $(x_\alpha)_{\alpha \in \Lambda}$ in X is said to be i -converge to a point x (or x is an i -limit point of $(x_\alpha)_{\alpha \in \Lambda}$) if for each $U \in \tau_i$, $x \in U$, $\exists \alpha_0 \in \Lambda$, $\forall \alpha \geq \alpha_0$, $x_\alpha \in U$.

Definition 1.2 Let (X, τ_1, τ_2) be a bitopological space. A net $(x_\alpha)_{\alpha \in \Lambda}$ in X is said to be ij - θ -convergent to a point $x \in X$ iff $\forall U \in \tau_i$ s.t. $x \in U$, $\exists \alpha_0 \in \Lambda$, $\forall \alpha \geq \alpha_0$, $x_\alpha \in j-cl(U)$, and denoted by $x_\alpha \xrightarrow{ij\theta} x$ and x is called ij - θ -limit point, and $x \in X$ is called ij - θ -cluster point of the net $(x_\alpha)_{\alpha \in \Lambda}$ in X iff $\forall U \in \tau_i$ s.t. $x \in U$ and $\forall \alpha_0 \in \Lambda$, $\exists \alpha \in \Lambda$, $\forall \alpha \geq \alpha_0$, $x_\alpha \in j-cl(U)$ and is

denoted by $x_\alpha \overset{ij\theta}{\propto} x$.

Remark 1.3. Let (X, τ_1, τ_2) be a bitopological space and $(x_\alpha)_{\alpha \in \Lambda}$ be a net in X and $x \in X$, then

- 1- If $(x_\alpha)_{\alpha \in \Lambda}$ i -convergent to a point x , then $(x_\alpha)_{\alpha \in \Lambda}$ ij - θ -convergent to x .
- 2- If $(x_\alpha)_{\alpha \in \Lambda}$ is ij - θ -convergent to x , then x is ij - θ -cluster point to $(x_\alpha)_{\alpha \in \Lambda}$.

The converses of (1 and 2) in remark (1.3) are not true in general. To show that we give the following examples:

Examples 1.4.

- 1- Let (R, T_0, T_{ind}) be the bitopological space where R be the set of all real numbers, $T_0 = \{A \subseteq R : 0 \in A\} \cup \{\emptyset\}$ and T_{ind} is indiscrete topology then the net

$\left(\frac{1}{n}\right)_{n \in \mathbb{N}}$ is 12 - θ -convergent to 0 , since

$\forall U \in T_0 \quad j-cl(U) = R$, and $\frac{1}{n} \in j-cl(U) \forall n \in N$ but $(\frac{1}{n})_{n \in N}$ does not 1-convergent to 0 since $\{0\} \in T_0$ and $\frac{1}{n} \notin \{0\} \forall n \in N$.

2- Let (R, T_u, T_d) be a bitopological space, where T_u is the usual topology and T_d is the discrete topology, then the net $s_n = (n + (-1)^n n)_{n \in N}$ in R has 0 as θ -cluster point but not θ -limit point,

Theorem 1.5. Let $(x_\alpha)_{\alpha \in \Lambda}$ be a net in a bitopological spaces (X, τ_1, τ_2) , then

i- $x_\alpha \xrightarrow{ij\theta} x$ iff every subnet of $(x_\alpha)_{\alpha \in \Lambda}$ is $ij-\theta$ -convergent to x .

ii- If every subnet of $(x_\alpha)_{\alpha \in \Lambda}$ has a subnet $ij-\theta$ -convergent to x , then $x_\alpha \xrightarrow{ij\theta} x$

proof: i) suppose that $x_\alpha \xrightarrow{ij\theta} x$ and let $(x_{\alpha_\mu})_{\mu \in M}$ be a subnet of the net $(x_\alpha)_{\alpha \in \Lambda}$ that is $M \xrightarrow{\varphi} \Lambda \xrightarrow{j} X$ where φ is increasing cofinal function, and let $U \in N_x$, since $x_\alpha \xrightarrow{ij\theta} x$ then there is $\alpha_0 \in \Lambda$ such that $x_{\alpha_0} \in j-cl(U)$ $\forall \alpha \geq \alpha_0$ and since φ is cofinal, then there is $\mu_0 \in M$ such that $\alpha_0 \leq \varphi(\mu_0)$, and since φ is increasing, then $\forall \mu \geq \mu_0$ hence $\varphi(\mu) \geq \varphi(\mu_0)$ therefore $\varphi(\mu) \geq \alpha_0$ that is $P(\varphi(\mu)) \in j-cl(U) \quad \forall \mu \geq \mu_0$ which is mean $x_{\alpha_\mu} \in j-cl(U) \quad \forall \mu \geq \mu_0$ so $x_{\alpha_\mu} \xrightarrow{ij\theta} x$

Conversely: it is clear since every net in X is a subnet of itself.

ii) suppose that x_α is not $ij-\theta$ -converge to x , then by (i) there is a subnet of $(x_\alpha)_{\alpha \in \Lambda}$ s.t. no subnet of which is $ij-\theta$ -converge to x .

Now since x_α is not $ij-\theta$ -converge to x , then there is $U \in \tau_1$ s.t. there is no $\alpha_0 \in \Lambda$ s.t. $x_\alpha \in j-cl(U) \forall \alpha \geq \alpha_0$. Now let $M = \{k \in \Lambda : x_k \notin j-cl(U)\}$, then M is a directed set, and define $\varphi: M \rightarrow \Lambda$ to be the identity map, then $p \circ \varphi$ (where $p: \Lambda \rightarrow X$ be the net $(x_\alpha)_{\alpha \in \Lambda}$ in X) and there is no subnet of the net $p \circ \varphi$ which is $ij-\theta$ -converge to x

Theorem 1.6. Let (X, τ_1, τ_2) be a bitopological space and $A \subseteq X$, then

i- if A is $ij-\theta$ -open, then no net in $X \setminus j-cl(A)$ can $ij-\theta$ -convergent to a point in A .

ii- if A is $ij-\theta$ -closed, then no net in $j-int(A)$ can $ij-\theta$ -convergent to a point in $X \setminus A$.

Proof: i- let A be $ij-\theta$ -open, and suppose there is a net $(x_\alpha)_{\alpha \in \Lambda}$ in $X \setminus j-cl(A)$ can $ij-\theta$ -convergent to a point in A say y since A is

ij - θ -open then A is i -open then $x_\alpha \xrightarrow{ij\theta} y$ hence there is $\alpha_0 \in \Lambda$ such that $x_\alpha \in j-cl(A) \quad \forall \alpha \geq \alpha_0$, therefore $x_\alpha \in j-cl(A) \cap (X \setminus j-cl(A))$ but that is contradiction hence no net in $X \setminus j-cl(A)$ can ij - θ -convergent to a point in A .

ii-Since A is ij - θ -closed, then X/A is ij - θ -open, from (i) no net in $X \setminus j-cl(X/A) = j-int(A)$, hence no net in $j-int(A)$ can ij - θ -convergent to a point in $X \setminus A$.

The following example show that the converse of (1.6,i) is not true in general.

Example 1.7. Let (R, T_{co}, T_{ind}) be a bitopological space where T_{co} is the co-finite topology and T_{ind} is the indiscrete topology, let $A = R \setminus \{0\} \subseteq R$, then there is no net in $R \setminus j-cl(A)$ which is ij - θ -converge to a point in A but A is not θ - ij -open.

Theorem 1.8. Let (X, τ_1, τ_2) be a bitopological space and $A \subseteq X$, if there is no net in $X \setminus A$ can ij - θ -convergent to a point in A , then A is ij - θ -open.

Proof: Suppose A is not ij - θ -open, then $\exists x \in A$ and $\forall U \in \tau_i$ such

that $x \in U \quad j-cl(U) \not\subseteq A$, thus $j-cl(U) \cap (X \setminus A) \neq \emptyset$, pick $x_{j-cl(U)} \in j-cl(U) \cap (X \setminus A)$, let

$cl(O_x) = \{j-cl(U) : U \in \tau_i, x \in U\}$, then $cl(O_x)$ is directed by the inclusion relation

, then $(x_{j-cl(U)})_{j-cl(U) \in cl(O_x)}$ is net in $X \setminus A$ and it is ij - θ -convergent to x , but that is contradiction, hence A is ij - θ -open.

Theorem 1.9. Let (X, τ_1, τ_2) be a bitopological space and $A \subseteq X$, then $x \in ij-cl_\theta(A)$ iff there exists a net $(x_\alpha)_{\alpha \in \Lambda}$ in A such that $(x_\alpha)_{\alpha \in \Lambda}$ is ij - θ -convergent to x .

Proof: Suppose $x \in ij-cl_\theta(A)$, then $\forall U \in \tau_i$ and $x \in U$, then $j-cl(U) \cap A \neq \emptyset$,

pick

$x_{j-cl(U)} \in j-cl(U) \cap A$, then $cl(O_x)$ is directed by inclusion relation \subseteq and, so $(x_{j-cl(U)})_{j-cl(U) \in cl(O_x)}$ is a net in A . Now let $V \in \tau_i$ and $x \in V$ then $j-cl(V) \in$

$cl(O_x)$ and $x_{j-cl(U)} \in j-cl(V) \quad \forall \quad j-cl(U) \geq j-cl(V)$ (i.e. $j-cl(U) \subseteq j-cl(V)$)

that is $(x_{j-cl(U)})_{j-cl(U)} \in cl(O_x)$ is $ij-\theta$ -convergent to x .

Conversely; Let $(x_\alpha)_{\alpha \in \Lambda}$ be a net in A such that $(x_\alpha)_{\alpha \in \Lambda}$ is $ij-\theta$ -convergent to x , and let $U \in \tau_i$, such that $x \in U$ then $\exists \alpha_0 \in \Lambda, \exists x_\alpha \in j-cl(U) \forall \alpha \geq \alpha_0$,

but $x_\alpha \in A \forall \alpha \in \Lambda$, then $j-cl(U) \cap A \neq \emptyset$, hence $x \in ij-cl_\theta(A)$.

Theorem 1.10. Let f be a function from a bitopological space (X, τ_1, τ_2) in to a bitopological space (Y, σ_1, σ_2) , and $(x_\alpha)_{\alpha \in \Lambda}$ be a net in X , then f is $ij-\theta$ -continuous at $x \in X$ iff $f(x_\alpha) \xrightarrow{ij\theta} f(x)$ in Y whenever the net $(x_\alpha)_{\alpha \in \Lambda} \xrightarrow{ij\theta} x$ in X .

Proof: Let f be a $ij-\theta$ -continuous at x and $(x_\alpha)_{\alpha \in \Lambda} \xrightarrow{ij\theta} x$, let $V \in \tau_i$ such that $f(x) \in V$, since f is $ij-\theta$ -continuous, then $\exists U \in \tau_i, x \in U$ s.t. $f(j-cl(U)) \subseteq j-cl(V)$, but $x_\alpha \xrightarrow{ij\theta} x$, then

$\exists \alpha_0 \in \Lambda \quad \exists x_\alpha \in j-cl(U) \quad \forall \alpha \geq \alpha_0$, then

$f(x_\alpha) \in f(j-cl(U)) \subseteq j-cl(V) \quad \forall \alpha \geq \alpha_0$ thus $f(x_\alpha) \xrightarrow{ij\theta} f(x)$.

Conversely; suppose f is not $ij-\theta$ -continuous at x i.e. $\exists V \in \tau_i, f(x) \in V$ such that $\forall U \in \tau_i, x \in U$, then $f(j-cl(U)) \not\subseteq j-cl(V)$, so

pick $x_{j-cl(U)} \in j-cl(U) \quad \exists \quad f(x_{j-cl(U)}) \notin j-cl(V)$, then $(x_{j-cl(U)})_{j-cl(U) \in cl(O_x)}$ is net in

X and $x_{j-cl(U)} \xrightarrow{ij\theta} x$ and thus $f(x_{j-cl(U)}) \xrightarrow{ij\theta} f(x)$ then $f(x_{j-cl(U)}) \in j-cl(V) \quad \forall \quad j-cl(U) \geq j-cl(U_0)$ for some $j-cl(U_0) \in cl(O_x)$ but

that is contradiction, hence f is $ij-\theta$ -continuous at x .

Lemma.1.11 Let $(\prod_{\alpha \in \Lambda} X_\alpha, \tau_1, \tau_2)$ (where $\tau_i, i \in \{1, 2\}, i \neq j$ is the product topology) be product bitopological space then pr_α (the projection map) is $ij-\theta$ -continues map for any $\alpha \in \Lambda$

Proof : Let $U_\lambda \in \tau_{i,\lambda}$, then $pr_\lambda^{-1}(U_\lambda) = \prod_{\lambda \neq \alpha} X_\alpha \times U_\lambda$ and

$$j-cl(pr_\lambda^{-1}(U_\lambda)) = j-cl(\prod_{\lambda \neq \alpha} X_\alpha \times U_\lambda) = \prod_{\lambda \neq \alpha} j-cl(X_\alpha) \times j-cl(U_\lambda)$$

$$= \prod_{\lambda \neq \alpha} X_\alpha \times j-cl(U_\lambda)$$

$pr_\lambda(j-cl(pr_\lambda^{-1}(U_\lambda))) = pr_\lambda(\prod_{\lambda \neq \alpha} X_\alpha \times j-cl(U_\lambda)) = j-cl(U_\lambda)$, hence pr_α is $ij-\theta$ -continues map for any $\alpha \in \Lambda$.

Theorem 1.12. A net $(x_\alpha)_{\alpha \in \Lambda}$ in a product bitopological space $X = \prod_{\alpha \in \Lambda} X_\alpha$ is $ij-\theta$ -convergent to a point $x \in X$ iff for each $\alpha \in \Lambda$, $Pr_\lambda(x_\alpha) \xrightarrow{ij\theta} Pr_\lambda(x)$ in X_λ .

Proof: If $x_\alpha \xrightarrow{ij\theta} x$ in X , and by lemma (1.11) pr_λ is $ij-\theta$ -continuous, then $pr_\lambda(x_\alpha) \xrightarrow{ij\theta} pr_\lambda(x)$ by (1.10.), for each $\lambda \in \Lambda$.

Conversely; suppose that $pr_\lambda(x_\alpha) \xrightarrow{ij\theta} pr_\lambda(x)$ for each $\lambda \in \Lambda$. now let $U = \prod_{\lambda \in \Lambda} U_\lambda$ be an i basic open neighborhood of x in the product bitopological space where $U_\lambda = X_\lambda$ for all but finite say $U_{\lambda_i} \subset X_{\lambda_i}$ $i = 1, \dots, n$ there is α_i

such that whenever $\alpha \geq \alpha_i$, $pr_{\lambda_i}(x_\alpha) \in j-cl(U_{\lambda_i})$, thus if α_0 is picked greater than all of $\alpha_1, \dots, \alpha_n$, we have that $pr_{\lambda_i}(x_\alpha) \in j-cl(U_{\lambda_i})$ for all $\alpha \geq \alpha_i$ it follows that $x_\alpha \in \prod_{\lambda \in \Lambda} j-cl(U_\lambda) = j-cl(\prod_{\lambda \in \Lambda} U_\lambda) = j-cl(U)$ for all $\alpha \geq \alpha_i$ and hence that

$x_\alpha \xrightarrow{ij\theta} x$ in the product bitopological space X .

$ij--\theta$ -Convergent of filter

Definition 2.1.[4] Let (X, τ_1, τ_2) be a bitopological space. A filter \mathfrak{F} in X is said to be $ij-\theta$ -convergent to a point $x \in X$ iff $\forall U \in N_x$ $j-cl(U) \in \mathfrak{F}$ and written as $\mathfrak{F} \xrightarrow{ij\theta} x$, and x is said to be $ij-\theta$ -cluster point of a filter \mathfrak{F} iff $\forall U \in N_x, j-cl(U) \cap F \neq \emptyset \quad \forall F \in \mathfrak{F}$ and written as $\mathfrak{F} \overset{ij\theta}{\propto} x$.

Clearly that every i -limit point of a filter is $ij-\theta$ -limit point of that filter and every i cluster point of a filter is $ij-\theta$ -cluster of that filter but not conversely as it is shown in the next examples:

Examples.2.2

1- Let (R, T_{co}, T_{md}) be a bitopological space and $\mathfrak{F} = \{R\}$ be filter on R , then $\mathfrak{F} \xrightarrow{ij\theta} 0$ but \mathfrak{F} is not $i-\theta$ -converge to 0 with respect to T_{co} since $R \setminus \{1\} \in N_{10}$ but $R \setminus \{1\} \notin \mathfrak{F}$.

2- Let (R, T_0, T_{md}) be a topological space where R is the set of all real numbers and $T_0 = \{A \subseteq R : 0 \in A\} \cup \{\emptyset\}$, let $A = \{1\}$ and $\mathfrak{F} = \{B \subseteq X : A \subseteq B\}$ filter

on R , then $\mathfrak{F} \overset{ij\theta}{\propto} 0$. Since $\forall U \in N_{j_0} (j-cl(U) = R) \cap B \neq \emptyset \quad \forall B \in \mathfrak{F}$ but 0 is

not i -cluster point to \mathfrak{F} since $\{0\} \cap A = \emptyset$ and $\{0\} \in N_0$.

Remark 2.3. Let (X, τ_1, τ_2) , (Y, σ_1, σ_2) be bitopological spaces, \mathfrak{F} be a filter in X and $x \in X$:

- 1- If $\mathfrak{F} \overset{ij\theta}{\longrightarrow} x$, then $\mathfrak{F} \overset{ij\theta}{\propto} x$.
- 2- $\mathfrak{F} \overset{ij\theta}{\propto} x$ iff $x \in ij-cl_\theta(M), \forall M \in \mathfrak{F}$.
- 3- If $\mathfrak{F} \overset{ij\theta}{\longrightarrow} x$, then every filter finer than \mathfrak{F} also $ij-\theta$ -convergent to x .
- 4- Let ψ be the set of all filters in X , which are $ij-\theta$ -convergent to some point x , then $\cap \{\mathfrak{F} : \mathfrak{F} \in \psi\}$ is $ij-\theta$ -convergent to x .
- 5- If \mathfrak{F} is filter in X and $f: X \longrightarrow Y$ be a function, then

$$f(\mathfrak{F}) \overset{ij\theta}{\longrightarrow} y (y \in Y) \quad \text{iff} \quad \forall V \in N_y, \exists M \in \mathfrak{F} \ni f(M) \subseteq j-cl(V) \quad \text{iff} \quad f^{-1}(j-cl(V)) \in \mathfrak{F}.$$
- 6- Let (X, τ_1, τ_2) be a bitopological space and \mathfrak{F} be a filter in X , then \mathfrak{F} has x as an $ij-\theta$ -cluster point iff there is a filter \wp in X which is finer than \mathfrak{F} and which is $ij-\theta$ -convergent to x .

Theorem 2.4. Let (X, τ_1, τ_2) be a topological space and $A \subseteq X$, then $x \in ij-cl_\theta(A)$ iff there is a filter \mathfrak{F} in X such that $A \in \mathfrak{F}$ and $\mathfrak{F} \overset{ij\theta}{\longrightarrow} x$

Proof: Let $x \in ij-cl_\theta(A)$, $\forall U \in N_x, j-cl(U) \cap A \neq \emptyset$ and $\mathfrak{F}_x = \{j-cl(U) \cap A : U \in N_x\}$ is a filter base, since if $j-cl(U_1) \cap A, j-cl(U_2) \cap A \in \mathfrak{F}_x$, $U_1 \cap U_2 \in N_x$ and $j-cl(U_1 \cap U_2) \cap A \neq \emptyset$, then $j-cl(U_1 \cap U_2) \cap A \subseteq (j-cl(U_1) \cap A) \cap (j-cl(U_2) \cap A)$, then \mathfrak{F}_x is filter base to a filter $\mathfrak{F} = \{B \subseteq X : \exists U \in N_x \ni (j-cl(U) \cap A) \subseteq B\}$, since $\forall U \in N_x, j-cl(U) \cap A \in \mathfrak{F}_x$ then $j-cl(U) \cap A \in \mathfrak{F}$ and since $j-cl(U) \cap A \subseteq A$, then $A \in \mathfrak{F}$ and $j-cl(U) \cap A \subseteq j-cl(U)$, then $j-cl(U) \in \mathfrak{F}$, that is $\mathfrak{F} \overset{ij\theta}{\longrightarrow} x$.
 Conversely:- Let $U \in N_x$, since $\mathfrak{F} \overset{ij\theta}{\longrightarrow} x$, then $j-cl(U) \in \mathfrak{F}$ and since $A \in \mathfrak{F}$, then $j-cl(U) \cap A \neq \emptyset$ hence $x \in ij-cl_\theta(A)$

Remark 2.5. Let (X, τ_1, τ_2) , (Y, σ_1, σ_2) be bitopological spaces, $f: X \rightarrow Y$ be a function and \mathfrak{F} be a filter on X , then $f(\mathfrak{F})$ is filter on Y generated by the filter base $\{f(F), F \in \mathfrak{F}\}$. that is $f(\mathfrak{F}) = \{F \subseteq Y : \exists F_0 \in \mathfrak{F} \wedge f(F_0) \subseteq F\}$

Theorem 2.6 Let (X, τ_1, τ_2) , (Y, σ_1, σ_2) be bitopological spaces and \mathfrak{F} be a filter in X , then $f: X \rightarrow Y$ is an $ij-\theta$ -continuous at $x \in X$ iff $f(\mathfrak{F}) \overset{ij\theta}{\longrightarrow} f(x)$ whenever $\mathfrak{F} \overset{ij\theta}{\longrightarrow} x$.

Proof: Let $V \in N_{if(x)}$, that is $f(x) \in V$, then there is $W \in \sigma_i$ such that $f(x) \in W$ and $W \subseteq V$, since f is ij - θ -continuous at x , there is $U \in \tau_i, x \in U$ such that $f(j-cl(U)) \subseteq j-cl(W)$ and since $\mathfrak{F} \xrightarrow{ij\theta} x$, then $f(j-cl(U)) \in f(\mathfrak{F})$ then $j-cl(W) \in f(\mathfrak{F})$ hence $j-cl(W) \subseteq j-cl(V) \in f(\mathfrak{F})$ therefore $f(\mathfrak{F}) \xrightarrow{ij\theta} f(x)$.

Conversely : Suppose that for any filter \mathfrak{F} on X such that $\mathfrak{F} \xrightarrow{ij\theta} x$, $f(\mathfrak{F}) \xrightarrow{ij\theta} f(x)$, let $\mathfrak{F}_0 = \{j-cl(U) : U \in N_{ix}\}$, then \mathfrak{F}_0 is filter base and let \mathfrak{F} be the filter generated by \mathfrak{F}_0 , then $f(\mathfrak{F}) \xrightarrow{ij\theta} f(x)$, (since $\mathfrak{F} \xrightarrow{ij\theta} x$). Now let $V \in \sigma_i$ such that $f(x) \in V$, then $j-cl(V) \in f(\mathfrak{F})$ hence there is $F \in \mathfrak{F}$ such that $f(F) \subseteq j-cl(V)$, and there is $W \in N_{ix}$ such that $j-cl(W) \subseteq F$

Theorem 2.7. A filter \mathfrak{F} is ij - θ -convergence to x_0 in $(\prod_{\alpha \in \Lambda} X_\alpha, \tau_1, \tau_2)$ iff $pr_\alpha(\mathfrak{F}) \xrightarrow{ij\theta} pr_\alpha(x_0)$ in $(X_\alpha, \tau_{1\alpha}, \tau_{2\alpha})$ for each $\alpha \in \Lambda$.

Proof : If $\mathfrak{F} \xrightarrow{ij\theta} x_0$ in $\prod_{\alpha \in \Lambda} X_\alpha$ since pr_α is ij - θ -continuous for each $\alpha \in \Lambda$

(by lemma (1.11)), then $pr_\alpha(\mathfrak{F}) \xrightarrow{ij\theta} pr_\alpha(x_0)$ in X_α for each $\alpha \in \Lambda$ (2.6).

Conversely; suppose $pr_\alpha(\mathfrak{F}) \xrightarrow{ij\theta} pr_\alpha(x_0)$ for each $\alpha \in \Lambda$. Let $U = \prod_{\alpha \in \Lambda} U_\alpha$ be an i -basic open neighborhood of x_0 in $\prod_{\alpha \in \Lambda} X_\alpha$, then $U_\alpha = X_\alpha$ for all but finite say $U_{\alpha_i} \subset X_{\alpha_i}$, where U_{α_i} i -open neighborhood contain $pr_{\alpha_i}(x_0)$, for each $k = 1, \dots, n$.

So, $j-cl(U_{\alpha_{i_k}}) \in pr_{\alpha_{i_k}}(\mathfrak{F})$, for each $k = 1, \dots, n$, and hence $pr_{\alpha_i}(F) \subseteq j-cl(U_{\alpha_i})$

for some $F_k \in \mathfrak{F}$ then $\bigcap_{k=1}^n F_k \in \mathfrak{F}$ and $\bigcap_{k=1}^n F_k \in \prod_{\alpha \in \Lambda} j-cl(U_\alpha)$, so $j-cl(U) \in \mathfrak{F}$, thus

$\mathfrak{F} \xrightarrow{ij\theta} x_0$.

Definition 2.8. [5]

i-If $(x_\alpha)_{\alpha \in \Lambda}$ is a net in X , the filter generated by the filter base \mathfrak{F} , consisting of the sets $B_{\alpha_0} = \{x_\alpha : \alpha \geq \alpha_0\}, \alpha_0 \in \Lambda$ is called the filter generated

by $(x_\alpha)_{\alpha \in \Lambda}$.

ii-If \mathfrak{F} is a filter on X , let $\Lambda_{\mathfrak{F}} = \{(x, F) : x \in F \in \mathfrak{F}\}$. Then $\Lambda_{\mathfrak{F}}$ is directed by the

relation $(x_1, F_1) \leq (x_2, F_2)$ iff $F_2 \subseteq F_1$, so the map $P : \Lambda_{\mathfrak{F}} \rightarrow X$ defined by

$P(x, F) = x$ is a net in X . It is called the net based on \mathfrak{F} .

Theorem 2.9. Let (X, τ_1, τ_2) be a bitopological space

i-If \mathfrak{F} is a filter in X , then $\mathfrak{F} \xrightarrow{ij\theta} x_0$ iff the net based on \mathfrak{F} is ij - θ -convergent to x_0 .

ii-If \mathfrak{F} is the filter generated by a net $(x_\alpha)_{\alpha \in \Lambda}$, then $x_\alpha \xrightarrow{ij\theta} x_0$ iff $\mathfrak{F} \xrightarrow{ij\theta} x_0$.

Proof:

i-Let $U \in N_{x_0}$, then $j-cl(U) \in \mathfrak{F}$, pick, $p \in j-cl(U)$, $(p, cl(U)) \in \Lambda_{\mathfrak{F}}$, and if $(q, j-cl(F)) \geq (p, j-cl(U))$, then $q \in cl(F) \subseteq cl(U)$. Thus the net based on \mathfrak{F} convergent to x_0 .

Conversely; suppose the net based on \mathfrak{F} ij - θ -convergent to x . Let $U \in N_{x_0}$, $\exists (x^*, F^*) \in \Lambda_{\mathfrak{F}} \exists x_{(x^*, F^*)} \in j-cl(U), \forall (x_0, F) \geq (x^*, F^*)$, then $x_0 \in F \subseteq F^*$. Now

$F^* \subseteq j-cl(U)$ or $F^* \not\subseteq j-cl(U)$. If $F^* \not\subseteq j-cl(U)$, then $\exists p \in F^*, p \notin j-cl(U)$, that is $(p, F^*) \in \Lambda_{\mathfrak{F}}$ and $(p, F^*) \geq (x^*, F^*)$ but

$x_{(p, F^*)} \notin j-cl(U)$, then F^* must be belong to $j-cl(U)$ therefore $j-cl(U) \in \mathfrak{F}$, hence $\mathfrak{F} \xrightarrow{ij\theta} x_0$.

ii- Let $x_\alpha \xrightarrow{\theta} x_0$ and $U \in N_{x_0}$, then $\exists \alpha_0 \in \Lambda$ s.t. $x_\alpha \in j-cl(U) \forall \alpha \geq \alpha_0$,

then $j-cl(U) \in \mathfrak{F}$ that is $\mathfrak{F} \xrightarrow{ij\theta} x_0$.

Conversely; let $\mathfrak{F} \xrightarrow{ij\theta} x_0$, to prove that $x_\alpha \xrightarrow{ij\theta} x_0$, let $U \in N_{x_0} \Rightarrow j-cl(U) \in \mathfrak{F}$, then $\exists B_{\alpha_0} \in \mathfrak{F} \exists B_{\alpha_0} \subseteq j-cl(U)$ (where \mathfrak{F} is the filter base of

\mathfrak{F}) then $x_\alpha \in j-cl(U) \forall \alpha \geq \alpha_0$, hence $x_\alpha \xrightarrow{ij\theta} x_0$.

Theorem 2.10.

i-A net $(x_\alpha)_{\alpha \in \Lambda}$ has x as a ij - θ -cluster point iff the filter generated by $(x_\alpha)_{\alpha \in \Lambda}$ has x as a ij - θ -cluster point.

ii- A filter \mathfrak{F} has x as a ij - θ -cluster point iff any net based on \mathfrak{F} has x as a

ij - θ -cluster point.

Proof: (i) Suppose $x_\alpha \overset{ij\theta}{\propto} x$. Let $U \in N_x$ and $B_{\alpha_0} \in \mathcal{B}$, $\exists \alpha \in \Lambda$, $\exists x_\alpha \in j-cl(U)$

whenever $\alpha \geq \alpha_0$, but $x_\alpha \in B_{\alpha_0}$, thus $j-cl(U) \cap B_{\alpha_0} \neq \emptyset$. Therefore $\mathcal{B} \overset{ij\theta}{\propto} x$.

Conversely; Suppose $\mathcal{B} \overset{ij\theta}{\propto} x$. Let $U \in N_x$ and $\alpha_0 \in \Lambda$, then $j-cl(U) \cap B_{\alpha_0} \neq \emptyset$,

i.e. $\exists x_\alpha \in j-cl(U)$ and B_{α_0} ($\alpha \geq \alpha_0$). Thus $x_\alpha \overset{ij\theta}{\propto} x$.

ii- Suppose $\mathfrak{F} \overset{ij\theta}{\propto} x$. Let $U \in N_x$ and $\lambda_0 = (x_0, F_0) \in \Lambda_{\mathfrak{F}}$, then $j-cl(U) \cap F_0 \neq \emptyset$.

Pick $x' \in j-cl(U) \cap F_0$, then $\lambda = (x', F_0) \in \Lambda_{\mathfrak{F}}$, $\lambda \geq \lambda_0$ and $x'_\lambda \in j-cl(U)$, thus the net based on \mathfrak{F} has x as a ij - θ -cluster point.

Conversely; Suppose the net based on \mathfrak{F} has x as a ij - θ -cluster point. Let

$U \in N_x$, $F \in \mathfrak{F}$ and $\lambda_0 = (x_0, F_0) \in \Lambda_{\mathfrak{F}}$, for some $x_0 \in F_0$, then $\exists \lambda = (x, F) \in \Lambda_{\mathfrak{F}}$, $\exists x \in j-cl(U)$, whenever $\lambda \geq \lambda_0$ but $x \in F_0$, thus $x \in j-cl(U) \cap F_0$. Therefore, the result is satisfied.

Definition 2.11. A bitopological space (X, τ_1, τ_2) is called ij -Urysohn space iff for every $x, y \in X$ s.t. $x \neq y$ there are $U \in N_x$, $V \in N_y$ such that $j-cl(U) \cap j-cl(V) = \emptyset$

Examples:-The treble (R, T_u, T_d) is ij -Urysohn space where R is the set of all real number, U is usual topological space and D is discrete topological space but the treble (R, T_u, T_{co}) is not ij -Urysohn space where T_{co} is cofinite topological space

The following theorem is a useful characterization of ij -Urysohn space.

Theorem 2.12. Let (X, τ_1, τ_2) be a bitopological space, then the following statements are equivalent:

- 1) X is ij -Urysohn space.
- 2) Every ij - θ -convergent filter in X has a unique ij - θ limit.
- 3) The diagonal $\Delta = \{(x, x) : x \in X\}$ is ij - θ -closed in $X \times X$.

Proof: (1 \Rightarrow 2) Let X be ij -Urysohn space and let \mathfrak{F} be a filter in X ij - θ -convergent to two distinct points x and y , then $j-cl(U) \subseteq \mathfrak{F}$, $j-cl(V) \subseteq \mathfrak{F} \forall U \in N_x$ and $V \in N_y$, since X is ij -Urysohn space, then there exist i -open neighborhood M of x and i -open

neighborhood N of y , such that $j-cl(M) \cap j-cl(N) = \emptyset$ that is contradiction since $j-cl(M), j-cl(N) \in \mathfrak{I}$, hence \mathfrak{I} has a unique $ij-\theta$ -limit point.

(2 \Rightarrow 3) Suppose Δ is not $ij-\theta$ -closed, hence by (1.8), there exists a net $((x_\alpha, x_\alpha))$ in $X \setminus j-cl(X \setminus \Delta) \subseteq \Delta$ which is $ij-\theta$ -convergent to (x, y) in $(X \times X) \setminus \Delta$ i.e. $x \neq y$ and the net (x_α) is a net in X $ij-\theta$ -converge to both x and y , which impossible hence Δ is $ij-\theta$ -closed.

(3 \Rightarrow 1) Suppose Δ is $ij-\theta$ -closed. If $x \neq y$ in X , then $(x, y) \notin \Delta$, and hence there is an i -basic neighborhood $U \times V$ in $X \times X$ such that $j-cl(U \times V) \cap \Delta = \emptyset$. But then $j-cl(U)$ and $j-cl(V)$ are disjoint neighborhoods of x and y , thus X is ij -Urysohn space.

REFERENCES

1. Kelly J.C., Bitopological spaces, Proc. London Math. Soc., 3, (13):71-89 (1963).
2. Karioflis, C.G., On pair wise almost compactness. Ann. Soc. Sci. Bruxelles 100 :129-137 (1986).
3. Shafe M.E. El "Pairwise weakly Hausdorff space" Archivam Mathematicam (BRNO) Tomus, 41 : (281-287) (2005).
4. Sen S.K. Mukherjee M.N. "On extension of certain map from a topological space to a bitopological space" Indian J. Pure appl. Math. 25, (5):507-511 may (1994).
5. Willard, S., "General Topology" Addison - Wesley, Inc., Mass. (1970).

Coincidence Points of Two Maps In Banach Spaces

Zena Hussein Mabeed

Baghdad University/College of Education Ibn-Al-Haitham/Department of Mathematics

الخلاصة

الغرض الاساسي لهذا البحث هو لتوسيع النتائج في (1) الذي تضمن بعض النتائج في حالة مجموعة starshaped الجزئية لفضاء بناخ. الجزئية لفضاء بناخ لضمان الوجود للنقاط المتطابقة والصامدة في حالة مجموعة غير star-shaped الجزئية لفضاء بناخ.

ABSTRACT

The main purpose of this paper is to extend the results in (1) which include some results in the case of starshaped subset of Banach space to guarantee the existence of coincidence and fixed points in the case of non-starshaped subset of Banach space.

INTRODUCTION

Let X be a Banach space, M be a closed subset of X and $CB(M)$ is the collection of all nonempty bounded closed subset of X .

If $T:M \rightarrow CB(M)$ and $f:M \rightarrow X$ be maps. Then the map T is said to be f -nonexpansive (2) if

$$H(Tx, T(y)) \leq \|fx - fy\|.$$

Where H denotes the Hausdorff metric on $CB(X)$.

Definition (1.1)(2)

The two maps f and g on X are said to be *commute* if $fg_x = gf_x$ for all x .

Definition (1.2)(1)

Let X be a linear space. A p -norm on X is a real valued function $\|\cdot\|_p$ on X with $0 < p \leq 1$, satisfying the following conditions:

$$1- \|x\|_p \geq 0 \text{ and } \|x\|_p = 0 \Leftrightarrow x = 0.$$

$$2- \|\alpha x\|_p = |\alpha|^p \cdot \|x\|_p$$

$$3- \|x + y\|_p \leq \|x\|_p + \|y\|_p$$

for all $x, y \in X$. The pair $(X, \|\cdot\|_p)$ is called a p -normed.

Definition (1.3): (4)

Let f be a single valued mapping on a p -normed space, $0 < p \leq 1$ and $T:X \rightarrow 2^X$ is a multivalued mapping. A point $x \in X$ is called *coincidence point* of f and T if $f(x) \in T(x)$, where the collection 2^X is of all non-empty subset of X , we denote the set of all coincidence points of T and f by $C(f \cap T)$.

Definition (1.4): (1)

Let the maps f and T as define above. Then they are said to be ***R-subcommuting*** if there exists a positive number R such that

$$H(T(f(x)) - f(T(x))) \leq \frac{R}{k} \|kT(x) + (1-k)q - fx\|$$

for all $x \in M$ and $k \in (0, 1]$, where $f(q) = q$.

Two maps T and f are said to be ***R-weakly commuting*** if there exists a positive constant R such that, for each $x \in M$

$$H(T(f(x)) - f(T(x))) \leq R \|fx - Tx\|$$

Definition (1.5): (4)

Let M be a subset of a p -normed X , $0 < p \leq 1$, M is called ***star-shaped*** with respect to a point $q \in M$ if

$$(1-k)q + kx \in M \text{ for each } x \in M, 0 \leq k \leq 1.$$

Definition (1.6):

Let X be a p -normed space, $0 < p \leq 1$ and $M \subseteq X$, $T: X \rightarrow X$ be a mapping we say that M has property (A) if

i. $T: M \rightarrow M$,

ii. $(1-k_n)q + k_n Tx \in M$,

for some $q \in M$ and a fixed real sequence $\langle k_n \rangle$ ($0 < k_n < 1$) converging to 1 and for each $x \in M$.

Definition (1.7): (5)

A self mapping of a linear space X is said to be affine if for al x, y in X and for any λ , $0 \leq \lambda \leq 1$, $f(\lambda x + (1-\lambda)y) = \lambda f(x) + (1-\lambda)f(y)$.

Now, illustrate that every star-shaped set has property (A) but the converse is not necessarily true, we give the following example (special case):

Example (1.1):

Consider $X = \mathbb{R}^2$ with p -norm $\|(x, y)\|_p = |x| + |y|$, $0 < p \leq 1$ and $M = A \cup B$

$\cup \{(1, 0)\}$, where

$$A = \{(0, y) : y \in [-1, 1]\}$$

$$B = \{(1 - \frac{1}{n+1}, 0) : n \in \mathbb{N}\}$$

$$\forall q \in M, (1-\lambda)q + \lambda x \notin M.$$

$T: M \rightarrow M$ as define

$$T(x, y) = \begin{cases} (0, -y) & ; (x, y) \in A \\ (0, 1 - \frac{1}{n+1}) & ; (x, y) \in B \\ (0, 1) & ; (x, y) = (0, 1) \end{cases}$$

if $q = (0, 0)$, then

$$k_n = 1 - \frac{1}{n+1} < 1 \text{ and } k_n \longrightarrow 1 \text{ as } n \longrightarrow \infty, \forall (x, y) \in C$$

$$(1 - k_n)(0, 0) + k_n T(x, y) = k_n T(x, y) \subset M$$

Thus property (A) satisfies but not star-shaped.

Theorem (1.1): (6)

Let X complete metric space and T, f be R -weakly commutative, $T(X) \subseteq f(X)$ and T is f -contraction. If T or f continuous. Then $F(T) \cap F(f) \neq \emptyset$.

2.MAIN RESULTS

The theorems from [1] to be generalized are the following:

Theorem (2.1): (1)

Let X be a Banach space, M be a closed subset of X which is star-shaped with respect to a point $q \in M$ such that $f(M) = M$ and $f(q) = q$. Let $T: M \longrightarrow CB(M)$ be an f -nonexpansive map which R -subcommutes with f such that $(f-T)M$ is closed and $T(M)$ is bounded. If f is a continuous affine map, then $C(f \cap T) \neq \emptyset$.

Theorem (2.2): (1)

Suppose that M, f, T and q satisfy the assumptions of theorem (2.1) and that $f(x) \in T(x)$ implies that $\lim_{n \rightarrow \infty} f^{(n)}(x)$ exists.

...(2.1)

Then T and f have a common fixed point in M .

Our first result is the following:-

Theorem (2.3):

Let X be a Banach space, M be a closed subset of X which has property A with respect to a point $q \in M$ such that $f(M) = M$ and $f(q) = q$. Let $T: M \longrightarrow CB(M)$ be an f -nonexpansive map which R -subcommutes with f such that $(f-T)M$ is closed and $T(M)$ is bounded. If f is a continuous affine map, then $C(f \cap T) \neq \emptyset$.

Proof:

Define the multivalued map J_n by $(J_n: M \longrightarrow CB(M))$
 $J_n(x) = (1 - k_n)q + k_n T(x)$.

Then, for each $n \geq 1$, J_n maps M into $CB(M)$ and $J_n(M) \subset f(M)$.

$$\begin{aligned} H(J_n(fx), fJ_n(x)) &= H((1-k_n)q + k_n T(fx), (1-k_n)q + k_n fT(x)) \\ &= k_n H(T(fx), fT(x)) \\ &\leq k_n \frac{R}{k_n} \|k_n T(x) + (1-k_n)q - fx\| \\ &= R \|J_n(x) - fx\|, \end{aligned}$$

and J_n and f are R -weakly commutative. Weakly commutative maps commute at coincidence points, and are therefore weakly compatible. For each $y \in M$

$$\begin{aligned} H(J_n(x), J_n(y)) &= k_n H(T(x), T(y)) \\ &\leq k_n \|fx - fy\|. \end{aligned}$$

Hence, T_n is f -contraction and $T_n(M) \subseteq M = f(M)$ by theorem (1.1), T_n, f has a fixed point, $\forall n \in \mathbb{N}$. Then $\forall n \exists x_n = f(x_n) \in Tx_n$. By definition of $T_n(x_n)$, $\exists y_n \in Tx_n$ such that

$$\begin{aligned} f(x_n) &= (1-k_n)q + k_n y_n \\ f(x_n) - y_n &= (1-k_n)q - (1-k_n)y_n \\ &= \left(\frac{1}{k_n} - 1\right)(q - y_n) \\ &= \left(\frac{1}{k_n} - 1\right)(q - f(x_n)). \end{aligned}$$

Since $T(M) \subseteq M$, $T(M)$ is bounded and $f(x_n) \in T_n x_n \in M$.

We have $\|f(x_n)\|$ bounded.

By $k_n \rightarrow 1$, we have $\|f(x_n) - y_n\| = \left(\frac{1}{k_n} - 1\right)(q - f(x_n))$ goes to 0 as $n \rightarrow \infty$.

Now as $f(x_n) - y_n \in (f-T)x_n$ and $(f-T)M$ is closed, we have $0 \in (f-T)M$, hence $\exists z \in M \exists f(z) \in T(z)$. Then $C(f \cap T) \neq \emptyset$. ■

Theorem (2.4):

Suppose that M, f, T and q satisfy the assumptions of theorem (2.3) and (2.1). Then T and f have a common fixed point in M .

Proof:

From theorem (2.1), there exists a point $x_0 \in M$ with $fx_0 \in T(x_0)$. Since f is f -nonexpansive, and f is continuous and so is T . Since f and T are R -subcommuting, they are compatible. The continuity of f and T implies that they commute at coincidence points. Therefore, we have

$$f^n x_0 = f^{n-1}(fx_0) \in f^{n-1}(T(x_0)) = T(f^{n-1}x_0).$$

Taking the limit of the above inclusion yields, from (2.1) that

$$p = \lim_{n \rightarrow \infty} f^n x_0 \in T(p)$$

But, since f is continuous,

$$\lim_{n \rightarrow \infty} f^n x_0 = \lim_{n \rightarrow \infty} f(f^{n-1}x_0) = f(p),$$

and p is a common fixed point of f and T . ■

Clearly commuting map implies R-subcommuting, which implies R-weakly commuting. We now show that these implications are proper.

To show that there exists R-subcommuting operators which are not commutative, consider the following example.

Example (2.1):

Let $X=[0,1]$ with the norm the absolute value, $Ix=bx$, $0 < b < 1$. Define T on X s.t. $Tx = \frac{b}{2}x^2$. Then I and T do not commute since $TIx = \frac{b^3}{2}x^2$ and $ITx = \frac{b^2}{2}x^2$.

We will now show that I and T are R-subcommuting. For $x \in X$, since $0 \in F(I)$,

$$|TIx - ITx| = \frac{b^2x^2}{2}(1-b)$$

$$\begin{aligned} |kTx + (1-k)p - Ix| &= \left| k \frac{b}{2}x^2 + 0 - bx \right| \\ &= \frac{bx}{2}(2-kx) \end{aligned}$$

Therefore we need to find a positive number R such that

$$\frac{b^2x^2}{2}(1-b) \leq \left(\frac{R}{k}\right) \frac{bx}{2}(2-kx)$$

The above inequality is trivially true for $x=0$.

For $x > 0$, it is equivalent to

$$kbx(1-b) \leq R(2-kx)$$

This inequality will certainly be satisfied for all $0 < x, k \leq 1$ if $b(1-b) \leq R$.

The following is an example of a pair of maps which are R-weakly commuting, but not R-subcommuting:

Example (2.2):

Let $X=[1,\infty]$ with the norm the absolute value, $Tx = x^2$ and $Ix=2x-1$. Then $|TIx - ITx| = 2(x-1)^2$ and $|Tx - Ix| = (x-1)^2$.

Consider

$$\begin{aligned} |TIx - ITx| &\leq R|Tx - Ix|, \text{ i.e.,} \\ 2(x-1)^2 &\leq R(x-1)^2 \end{aligned}$$

This is true for any $R \geq 2$, and T and I are R-weakly commuting.

Now, consider

$$|TIx - ITx| \leq \frac{R}{k} |kTx + (1-k)p - Ix|, \text{ i.e.,}$$

$$\begin{aligned} 2(x-1)^2 &\leq \frac{R}{k} |kx^2 + (1-k)(1) - 2x + 1| \\ &= \frac{R}{k} |kx^2 - 2x + 2 - k| \end{aligned}$$

The right hand side vanishes whenever

$$kx^2 - 2x + 2 - k = 0, \text{ i.e.,}$$

$$\text{for } x = \frac{2-k}{k}, \text{ or } x = 1.$$

For any $k < 1$, $x = \frac{2-k}{k} > 1$, the inequality is violated. Therefore T and I are not

R-subcommuting, and the inclusions between commutative, R-subcommuting, and R-weakly commutative are proper.

REFERENCES

1. Rhoades, B.E., On Multivalued f -Nonexpansive Maps, Department of Mathematics, Indiana University, Bloomington, 19:89-92(2000).
2. Latif, A., , A Result on Best Approximation in p -Normed Spaces, Arch. Math. (Brno), 37:71-75(2001).
3. Bano, A., Khan, A.R., Latif, A., Coincidence Points and Best Approximations in p -Normed Spaces, Rad. Math., 12 :27-36 (2003).
4. Song, Y., Common Fixed Points and Invariant Approximations for Generalized (f,g) -Nonexpansive Mappings, Heran Normal University, P.R.Chain, 2(2) :17-26 (2007).
5. Zeidler, E., (1986), "Non Linear Functional Analysis and Applications, I.Fixed Point Theorems", Springer Verlage, New York, Inc.
6. Pant, R.P., Common Fixed Points of Non-Commuting Mappings, J.Math. Anal. Appli., 188 (2) :436-440(1994).

The Escape Time Dimension of the Filled Julia Set

¹Adil Mahmood Ahmed, ²Abdul Al-Samee Al-Janabi and ²Arkan Jassim Mohammed

¹University of Taiz-College Of Science- Yemen

²Al-Mustansiriah University - College of Science- Department of Mathematics-Iraq

الخلاصة

هدفنا في هذا البحث هو تقديم طريقة جديدة لحساب بعد الكسوريات المتكونة بواسطة خوارزمية تسمى خوارزمية زمن الهروب (Escape Time Algorithm) وذلك بنشر النقاط داخل النافذة المقترحة وقد سمينا هذا البعد D_E ببعد زمن الهروب (Escape Time Dimension) لكسوريات زمن الهروب (Escape Time Fractals) وقد وجدنا بعد زمن الهروب لمجموعة جوليا المملوءة F_c (Filled Julia Set) المتحققة مع الدالة $f_c: C \rightarrow C$ المعرفة بـ: $f_c(z) = z^2 + c$ وكذلك وجدنا بعد زمن الهروب الى $F_c(f_c^{[n]})$ ولكل التكرارات n . وقد وجدنا أن $D_E(F_c(f_c)) = D_E(F_c(f_c^{[n]}))$

ABSTRACT

Our objective in this paper is to invent a new method for counting the dimension of fractals constructed by the Escape Time Algorithm using the method of spreading the points inside the proposed window and we call this dimension the Escape Time dimension of the Escape Time fractals. We find the Escape Time dimension of the filled Julia set F_c (which has not been evaluated before) associated with the function $f_c: C \rightarrow C$ defined by: $f_c(z) = z^2 + c$, where $c \in C$. And we also find the Escape Time

dimension of filled Julia set $(F_c(f_c^{[n]}))$ associated with $f_c^{[n]}$, for each iteration n . And we find that $D_E(F_c(f_c)) = D_E(F_c(f_c^{[n]}))$.

KEYWORDS: Fractal geometry, Fractal dimension, Julia sets, filled Julia set.

INTRODUCTION

An algorithm called the Escape Time Algorithm will be introduced and the fractals (images) produced by this algorithm, are coined as the Escape Time Fractals because the colored contours indicate the time required for the orbit to escape from the region.

The Escape Time Algorithm can be applied to any dynamical system of the form $\{R^2; f\}$, $\{C; f\}$, or $\{\hat{C}; f\}$. We need only to specify a viewing window W and a region V , to which orbits of points in W might escape. The result will be a "picture" of W , wherein the pixel corresponding to the point z is colored according to the smallest value of the positive integer n , such that $f^{[n]}(z) \in V$, where $f^{[n]}$ be the forward iterates transformations of f defined by :

$$f^{[0]}(z) = z, f^{[1]}(z) = f(z), \dots, f^{[n+1]}(z) = f \circ f^{[n]}(z) = f(f^{[n]}(z)), \text{ for } n = 0, 1, \dots$$

A special color, such as black, may be reserved to represent points whose orbits do not reach V before $(\text{numits} + 1)$ iterations. The Escape Time Algorithm, which is a numerical, computer graphical experiment to compare the number of iterations required for the orbits of different points to escape from a ball of large radius, centered at the origin.

Consider \mathbb{R}^m ; $m = 1, 2, 3$ and take as an example when $m = 2$. Let (a, b) and (c, d) , respectively, denote the coordinates of the lower left corner and the upper right corner of a closed, filled rectangle $W \subset \mathbb{R}^2$. Let M be a positive integer, and define an array of points in W by:

$$x_{p,q} = \left(a + p \frac{(c-a)}{M}, b + q \frac{(d-b)}{M} \right), \text{ for } p, q = 0, 1, \dots, M.$$

These points will be represented by pixels on a computer graphics display device. We compare the orbits $\{f^{[n]}(x_{p,q})\}_{n=0}^{\infty}$, for $p, q = 0, 1, \dots, M$. Let R be a positive number, sufficiently large that the ball with center at the origin and radius R contains both the fractal set and W .

Define: $V = \{(x, y) \in \mathbb{R}^2 : x^2 + y^2 > R\}$. Let numits denote a positive integer. We compute a finite set of points: $\{x_{p,q}, f(x_{p,q}), f^{[2]}(x_{p,q}), \dots, f^{[n]}(x_{p,q})\}$ belonging to the orbit of $x_{p,q} \in W$, for each $p, q = 1, 2, \dots, M$. The total number of points computed on an orbit is at most numits . If the set of computed points of the orbit $x_{p,q}$ does not include a point in V when $n = \text{numits}$, then the pixel corresponding to $x_{p,q}$ will be black color, and the computation passes to the next value of (p, q) . Otherwise the pixel corresponding to $x_{p,q}$ is assigned a color indexed by the first integer n , such that $f^{[n]}(x_{p,q}) \in V$, and then the computation passes to the next value of (p, q) .

In our work, we will consider all colors except the black to be a white color, that is, if $f^{[n]}(x_{p,q}) \in V$, for some $n \leq \text{numits}$, then the point $x_{p,q}$ will be colored white, and if $f^{[n]}(x_{p,q}) \notin V$, for all $n \leq \text{numits}$, then the point $x_{p,q}$ is colored black. So, we have a closed subset A of W constructed by the Escape Time Algorithm, defined by:

$$\begin{aligned} A &= \{x_{p,q} \in W, \text{ such that } f^{[n]}(x_{p,q}) \notin V, \text{ for all } n \leq \text{numits}\} \\ &= \{x_{p,q} \in W, \text{ such that } x_{p,q} \text{ is black point}\}. \end{aligned}$$

The set A is called the Escape Time Fractal. (1)

PRELIMINARIES

Definition 1 : Let (X, d) be a complete metric space. Then $H(X)$ denotes the set whose points are the non empty compact subsets of X . (2)

Definition 2: Let $A \in H(\mathbb{R}^m)$ and let $N(A, \varepsilon)$ be the smallest number of m -dimensional boxes of side length ε , required to cover A . Then the box-counting dimensions of A is defined to be $D(A) = \lim_{\varepsilon \rightarrow 0} \left\{ \frac{\ln(N(A, \varepsilon))}{\ln(1/\varepsilon)} \right\}$.

We will use the notation $D = D(A)$ and we will say “ A has box dimension D ”.(3)

Theorem 1:(Box Counting Theorem): Let $A \in H(\mathbb{R}^m)$, where the Euclidean metric is used. Cover \mathbb{R}^m by closed square boxes of side length $(1/2^n)$. Let $N_n(A)$ denote the number of boxes of side length $(1/2^n)$ which intersect the attractor.

If $D(A) = \lim_{n \rightarrow \infty} \left\{ \frac{\ln(N_n(A))}{\ln(2^n)} \right\}$, then A has box dimension D .(3)

FILLED JULIA SET AND JULIA SET

Definition 3: Let c be any complex number and f is the complex function defined by: $f_c(z) = z^2 + c$. The smallest closed set in the complex plane that contains all repelling periodic points of f_c is called the Julia set of f_c , and is denoted by J_c , that is

$J_c = \text{cl} \{ z \in \mathbb{C} : |(f_c^{[n]})'(z)| > 1, \text{ and } f_c^{[n]}(z) = z, n = 1, 2, \dots \}$. We mean by cl , the closure of the set. (4)

Theorem 2: If $|z| > |c| + 1$, then the orbit of z for f_c is unbounded. (4)

Definition 4: The filled Julia set for $f_c(z) = z^2 + c$, where c is a complex parameter is the collection of complex numbers z , whose orbit under f_c is bounded, and denoted by F_c . That is: $F_c = \{ z \in \mathbb{C} : \lim_{n \rightarrow \infty} f_c^{[n]}(z) \not\rightarrow \infty \}$. F_c is a closed set in the complex plane, and $F_c \supseteq J_c$, that is, J_c is the boundary of F_c .(2)

Definition 5: Let $f_c(z) = z^2 + c$, where c is a complex constant and $r(c) = \max\{|c|, 2\}$. Then, $r(c)$ is called the threshold radius of f_c . (3).

From above theorem, we observe that if for any $z \in \mathbb{C}$, $|f_c^{[n]}(z)| > r(c)$ for some positive integer n , then the orbit of z escape to ∞ and consequently $z \notin F_c$. Based on the above remark, we now introduce escape time algorithm to generate F_c . As in introduction, picture a square grid centered at the origin

with the side of length $r(c)$. We fix the maximum number of allowed iterations to be N . Then, for each z in the grid,

1. If $|f_c^{[n]}(z)| > r(c)$, for some $n \leq N$, color the point z white.
2. If $|f_c^{[n]}(z)| \leq r(c)$, for all $n \leq N$, color the point z black.

The black points provide approximation of the filled Julia set F_c , that is,

$$F_c = \{z \in \mathbb{C} : \left\{ |f_c^{[n]}(z)| \right\}_{n=0}^{\infty} \text{ is bounded} \}. \text{ See figure -1}$$



Figure -1: The filled Julia set F_c , $c = -0.1 + 0.8i$.

By (ETA.BAS) computer program listed in appendix, we can generate the filled Julia sets.

Theorem 3: Let $f_c: \hat{\mathbb{C}} \rightarrow \hat{\mathbb{C}}$ denote a polynomial of degree greater than 1. Let F_c denote the filled Julia set of f_c . Then F_c is a nonempty compact subset of \mathbb{C} ; that is, $F_c \in H(\mathbb{C})$. Moreover, $f(F_c) = F_c = f^{-1}(F_c)$. (1).

Example 1: Let the function $f_{c=1.1}: \mathbb{C} \rightarrow \mathbb{C}$, be given by the formula:

$$f_{c=1.1}(x, y) = (x^2 - y^2 - 1.1, 2xy), \text{ for all } (x, y) \in \mathbb{C}.$$

Define V by choosing $R = 4$, and let $W = \{(x, y) : -2 \leq x \leq 2, -2 \leq y \leq 2\}$.

The result of running the Escape Time Algorithm, with V , W and f , thus defined, is

shown in figure -2 The black object represents the filled Julia set $F_{c=1.1}$.

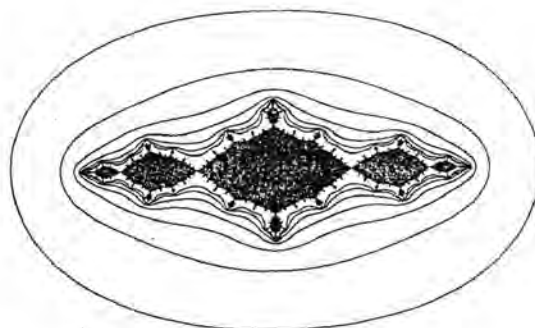


Figure -2: The black object represents the filled Julia set $F_{c=1.1}$.

THE ESCAPE TIME DIMENSION

Now, we invent a new technique for counting the dimension of some fractals that are constructed by the Escape Time Algorithm. We call this dimension the Escape Time dimension.

Consider a function $f: \mathbb{R}^2 \rightarrow \mathbb{R}^2$, and let A be the Escape Time Fractal (set formed by the Escape Time Algorithm) with parameters (a, b) , (c, d) , R and a numits = N determined by the function f as defined in the introduction.

In order to find the dimension of the Escape Time Fractal A . First, we divide by taking $\varepsilon > 0$, such that $\varepsilon = \frac{c-a}{M_1} = \frac{d-b}{M_2}$, where $M_1, M_2 \in \mathbb{N}$.

By using the Escape Time Algorithm to count $N(A, \varepsilon)$, which is the number of squares in this grid that meet A , and by definition (1), we find

$$D_{\varepsilon_1}(A) = \frac{\ln(N(A, \varepsilon_1))}{\ln(1/\varepsilon_1)},$$

if we increase both M_1, M_2 (that is, to decrease ε_1) and we use again the Escape Time Algorithm to count the new $N(A, \varepsilon_2)$ and we find

$$D_{\varepsilon_2}(A) = \frac{\ln(N(A, \varepsilon_2))}{\ln(1/\varepsilon_2)}.$$

This will form a sequence $\{D_{\varepsilon_n}(A) : n \in \mathbb{N}\}$. If

$\lim_{n \rightarrow \infty} D_{\varepsilon_n}(A) = D$, this is box counting dimension of the Escape Time Fractal

A . As an example, suppose we try to approximate the box-dimension of the He'non attractor A_H , say, with the grid shown in figure -3.

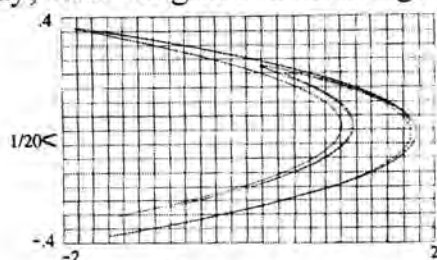


Figure -3:

We notice that the number of squares that intersect A_H is approximately 100. If we let ε equal the height of each squares, then $\varepsilon = 1/20$, so that

$$\frac{\ln(\mathcal{N}(A_H, \varepsilon))}{\ln(1/\varepsilon)} \approx \frac{\ln 100}{\ln 20} \approx 1.58. \text{ However, it is known that } D(A_H) \approx 1.58.$$

In this method, a sequential scanning is made to all points in the window W by using the Escape Time Algorithm, and when we changed ε , we have a new partition and we neglect the last partitions. So, we invent a new technique to find the Escape Time dimension of the Escape Time fractals. In this method, a separate scanning to a point inside the window W is used, starting from the center of the window and separate this point to the whole region W . This method is better than the box counting dimension method in its time speed, efficiency and without neglecting the previous steps .

ESCAPE TIME DIMENSION ALGORITM

- (i) Standardize the coordinates, such that the window
 $W = \{(x, y) \in \mathbb{R}^2 : -2 \leq x \leq 2, -2 \leq y \leq 2\}.$
- (ii) Using double binary tree method in the Euclidian plane to find the coordinates of the points in the window W , such that each binary tree will form a coordinate in one dimension by taking $\varepsilon_n = \frac{1}{2^n}$, $n = 0, 1, \dots$.

Then, each point (x_i, y_i) in the window W with the following coordinates:

$$\begin{aligned} &(-1, 1), (-1, -1), (1, 1), (1, -1), \left(-\frac{3}{2}, -\frac{3}{2}\right), \left(-\frac{3}{2}, -\frac{1}{2}\right), \left(-\frac{3}{2}, \frac{1}{2}\right), \left(-\frac{3}{2}, \frac{3}{2}\right), \\ &\left(-\frac{1}{2}, -\frac{3}{2}\right), \left(-\frac{1}{2}, -\frac{1}{2}\right), \left(-\frac{1}{2}, \frac{1}{2}\right), \left(-\frac{1}{2}, \frac{3}{2}\right), \left(\frac{1}{2}, -\frac{3}{2}\right), \left(\frac{1}{2}, -\frac{1}{2}\right), \left(\frac{1}{2}, \frac{1}{2}\right), \left(\frac{1}{2}, \frac{3}{2}\right), \\ &\left(\frac{3}{2}, -\frac{3}{2}\right), \left(\frac{3}{2}, -\frac{1}{2}\right), \left(\frac{3}{2}, \frac{1}{2}\right), \left(\frac{3}{2}, \frac{3}{2}\right), \left(-\frac{7}{4}, -\frac{7}{4}\right), \left(-\frac{7}{4}, -\frac{5}{4}\right), \left(-\frac{7}{4}, -\frac{3}{4}\right), \left(-\frac{7}{4}, -\frac{1}{4}\right), \\ &\left(-\frac{7}{4}, \frac{1}{4}\right), \left(-\frac{7}{4}, \frac{3}{4}\right), \left(-\frac{7}{4}, \frac{5}{4}\right), \left(-\frac{7}{4}, \frac{7}{4}\right), \left(-\frac{5}{4}, -\frac{7}{4}\right), \left(-\frac{5}{4}, -\frac{5}{4}\right), \left(-\frac{5}{4}, -\frac{3}{4}\right), \\ &\left(-\frac{5}{4}, -\frac{1}{4}\right), \left(-\frac{5}{4}, \frac{1}{4}\right), \left(-\frac{5}{4}, \frac{3}{4}\right), \left(-\frac{5}{4}, \frac{5}{4}\right), \left(-\frac{5}{4}, \frac{7}{4}\right), \left(-\frac{3}{4}, -\frac{7}{4}\right), \left(-\frac{3}{4}, -\frac{5}{4}\right), \\ &\left(-\frac{3}{4}, -\frac{3}{4}\right), \left(-\frac{3}{4}, -\frac{1}{4}\right), \left(-\frac{3}{4}, \frac{1}{4}\right), \left(-\frac{3}{4}, \frac{3}{4}\right), \left(-\frac{3}{4}, \frac{5}{4}\right), \left(-\frac{3}{4}, \frac{7}{4}\right), \left(-\frac{1}{4}, -\frac{7}{4}\right), \end{aligned}$$

$$\begin{aligned} & \left(-\frac{1}{4}, -\frac{5}{4}\right), \left(-\frac{1}{4}, -\frac{3}{4}\right), \left(-\frac{1}{4}, -\frac{1}{4}\right), \left(-\frac{1}{4}, \frac{1}{4}\right), \left(-\frac{1}{4}, \frac{3}{4}\right), \left(-\frac{1}{4}, \frac{5}{4}\right), \left(-\frac{1}{4}, \frac{7}{4}\right), \\ & \left(\frac{1}{4}, -\frac{7}{4}\right), \left(\frac{1}{4}, -\frac{5}{4}\right), \left(\frac{1}{4}, -\frac{3}{4}\right), \left(\frac{1}{4}, -\frac{1}{4}\right), \left(\frac{1}{4}, \frac{1}{4}\right), \left(\frac{1}{4}, \frac{3}{4}\right), \left(\frac{1}{4}, \frac{5}{4}\right), \left(\frac{1}{4}, \frac{7}{4}\right), \\ & \left(\frac{3}{4}, -\frac{7}{4}\right), \left(\frac{3}{4}, -\frac{5}{4}\right), \left(\frac{3}{4}, -\frac{3}{4}\right), \left(\frac{3}{4}, -\frac{1}{4}\right), \left(\frac{3}{4}, \frac{1}{4}\right), \left(\frac{3}{4}, \frac{3}{4}\right), \left(\frac{3}{4}, \frac{5}{4}\right), \left(\frac{3}{4}, \frac{7}{4}\right), \\ & \left(\frac{5}{4}, -\frac{7}{4}\right), \left(\frac{5}{4}, -\frac{5}{4}\right), \left(\frac{5}{4}, -\frac{3}{4}\right), \left(\frac{5}{4}, -\frac{1}{4}\right), \left(\frac{5}{4}, \frac{1}{4}\right), \left(\frac{5}{4}, \frac{3}{4}\right), \left(\frac{5}{4}, \frac{5}{4}\right), \left(\frac{5}{4}, \frac{7}{4}\right), \left(\frac{7}{4}, -\frac{7}{4}\right), \\ & \left(\frac{7}{4}, -\frac{5}{4}\right), \left(\frac{7}{4}, -\frac{3}{4}\right), \left(\frac{7}{4}, -\frac{1}{4}\right), \left(\frac{7}{4}, \frac{1}{4}\right), \left(\frac{7}{4}, \frac{3}{4}\right), \left(\frac{7}{4}, \frac{5}{4}\right), \left(\frac{7}{4}, \frac{7}{4}\right), \dots \end{aligned}$$

and so on which will form a new window, denoted by $W_0 \subseteq W$.

To find the formula for the sequence of these points, we will use the sum in the following way for the program:

$$\pm 1 \pm \frac{1}{2} \pm \frac{1}{(2)^2} \pm \frac{1}{(2)^3} \pm \frac{1}{(2)^4} \pm \dots \pm \frac{1}{(2)^n} \pm \dots$$

- (iii) By using the Escape Time Algorithm on this set of points in these window (not all) will form a set B defined by: $B = \{(x, y) \in W_0 : f^{(n)}(x, y) \notin V, \text{ for all } n \leq N\}$.

This set B is a subset of $A = \{(x, y) \in W : f^{(n)}(x, y) \notin V, \text{ for all } n \leq N\}$, where A is a fractal set constructed by the Escape Time Algorithm. Moreover, when N is large enough ($N \rightarrow \infty$), then $\bar{B} = A$ (B is dense in A). Therefore, dimension of

$B \cong$ dimension of A . Since by box counting theorem (2), $D(A) = \lim_{n \rightarrow \infty} \frac{\ln(\mathcal{N}_n(A))}{\ln(2^n)}$.

Hence: $D_{E_n}(B) = \frac{\ln(\mathcal{N}_n(B))}{\ln(2^n)}$. Where $N_n(B)$ is the number of black points. This

approximation depends on the tolerance (tol) that we choose.

Now, if $|D_{E_n}(B) - D_{E_{n-1}}(B)| < \text{tol}$

Then, the Escape Time Dimension of the Escape Time fractal B equals to $D_{E_n}(B)$, which is denoted by $D_E(B)$.

Example 2 : Let $f_c : C \rightarrow C$ defined by: $f_c(z) = z^2 - c$, $c \in C$.

If $z = x + iy$ and $c = a + ib$, where $x, y, a, b \in \mathbb{R}$, then $f(x, y) = (x^2 - y^2 - a, 2xy - b)$.

In this example, we want to find the Escape Time Dimension of the Escape Time fractal filled Julia set F_c associated with f_c , that is constructed before

(example 1)First, we will define the window W and the region V for the Escape Time Algorithm. Let $W \subseteq \mathbb{R}^2$, which is define by: $W = \{(x, y) \in \mathbb{R}^2 : -2 \leq x \leq 2, -2 \leq y \leq y\}$ and let $R = \left(0.5 + \sqrt{0.25 + \sqrt{a^2 + b^2}}\right)^2$ and define $V = \{(x, y) \in \mathbb{R}^2 \mid \sqrt{x^2 + y^2} > R\}$

In this paper, a computer program (ETDFG.BAS) have been written for finding the Escape Time dimension for the filled Julia sets F_c for each $c \in \mathbb{C}$, which is listed in the Appendix. By applying this program for different types of c , we have

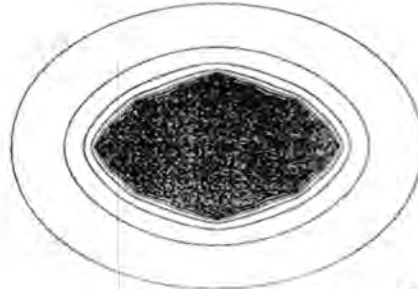


Figure -4:The filled Julia set of a quadratic $f_c(z) = z^2 + c$, $c = 0.3$, $D_E(F_c) = 2$.

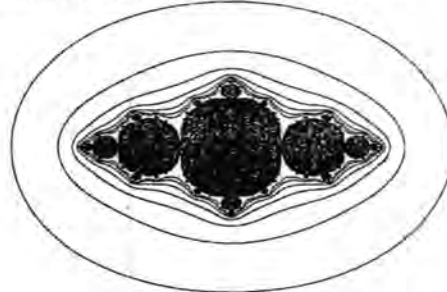


Figure -5:The filled Julia set of a quadratic $f_c(z) = z^2 + c$, $c = 1$, $D_E(F_c) = 1.7861474675$.

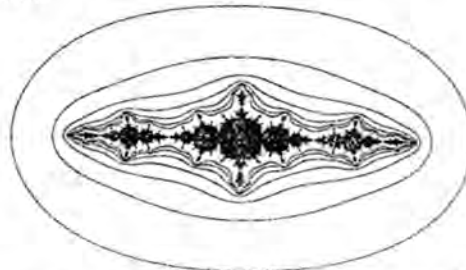


Figure -6:The filled Julia set of a quadratic $f_c(z) = z^2 + c$, $c = 1.3$, $D_E(F_c) = 1.6816862309950$.

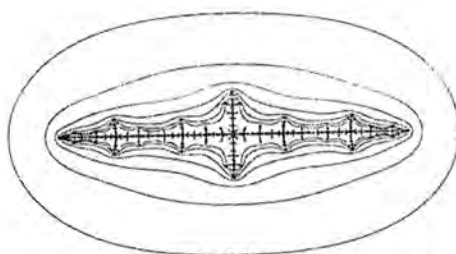


Figure -7: The filled Julia set of a quadratic $f_c(z) = z^2 + c$, $c = 1.6$, $D_E(F_c) = 1.4748523328$.



Figure -8: The filled Julia set of a quadratic $f_c(z) = z^2 + c$, $c = 0.281 - 0.53i$, $D_E(F_c) = 1.93235561951$.



Figure -9: The filled Julia set of a quadratic $f_c(z) = z^2 + c$, $c = -0.1 + 0.6557i$, $D_E(F_c) = 1.7360406917$.



Figure -10: The filled Julia set of a quadratic $f_c(z) = z^2 + c$, $c = -0.12 + 0.81i$, $D_E(F_c) = 1.43798566291$.

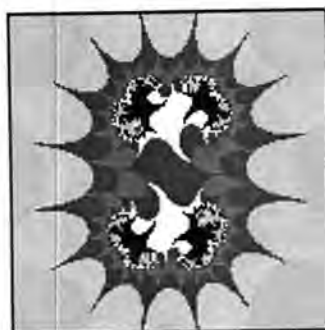


Figure -11: The filled Julia set of a quadratic $f_c(z) = z^2 + c$, $c = 0.6 - 0.1i$, $D_E(F_c) = 1.9285613794$.

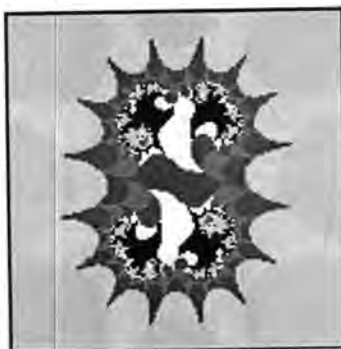


Figure -12: The filled Julia set of a quadratic $f_c(z) = z^2 + c$, $c = 0.53 - 0.1i$, $D_E(F_c) = 1.9285613794$.

The Escape Time dimension of the filled Julia set given in figure-1 is $D_E(F_c) = 1.4904874919$, and the Escape Time dimension of the filled Julia set given in figure (2) is $D_E(F_c) = 1.63089048$.

Now, we will show that we can find the Escape Time dimension of the filled Julia sets $F_c(f_c^{[n]})$ associated with $f_c^{[n]}$, for each positive integer n , but before that, we need the following theorem.

Theorem 4: If f_c is a polynomial, then $F_c(f_c) = F_c(f_c^{[n]})$ for every positive integer n . (1).

According to theorem (4), we can find the Escape Time dimension of the filled Julia sets $F_c(f_c^{[n]})$ for each positive integer n . That is, if $f_c(z) = z^2 - c$, where $c = (-0.2, 0.7)$ and applying the computer program (ETDFJ.BAS) for f_c , we obtain the Escape Time dimension of $F_c(f_c) = 1.520262505$. Then, the Escape Time dimension of $F_c(f_c^{[n]}) = 1.5202625$, for each positive integer n . That is, when we apply our program on $F_c(f_c^{[n]})$, the Escape Time dimension of the Escape Time fractals formed by f_c is evaluated. So that:

$$D_E(F_{(-0.2, 0.7)}(f_c^{[2]})) = 1.520262505$$

$$D_E(F_{(-0.2, 0.7)}(f_c^{[3]})) = 1.520262505$$

$D_E(F_{(-0.2, 0.7)}(f_c^{[4]})) = 1.520262505$
and so on for each positive integer n.

APPENDIX

COMPUTER PROGRAMS

1- THE ETDFJ.BAS PROGRAM

```

REM *****
REM ** Computer program for evaluating the **
REM ** Escape Time Dimension for filled Julia set **
REM *****
INPUT a, b, tol
r = (.5 + SQR(.25 + SQR(a * a + b * b))) ^ 2
sum = 0: w = 100: n = -1
40 n = n + 1: PRINT "n="; n
m = 2 ^ n: k = 2 * m - 1
FOR i = -k TO k STEP 2
FOR j = -k TO k STEP 2
x = i / m: y = j / m
FOR p = 1 TO 20
u = x * x - y * y - a: v = 2 * x * y - b
IF u * u + v * v > r THEN GOTO 150
x = u: y = v
NEXT p
sum = sum + 1
PSET (500 * (x + 2) + 10, 500 * (y + 2) + 10)
150 NEXT j
NEXT i
IF n = 0 THEN GOTO 40
IF sum = 0 THEN GOTO 40
z = LOG(sum) / (n * LOG(2))
IF ABS(z - w) < tol THEN GOTO 220
w = z
GOTO 40
220 'text4.textz
END
2- ETA.BAS PROGRAM:

```

```

REM **** The Escape Time Algorithm ****
numits = 20: a = 0: b = 0: c = 1: d = 1: m = 100
r = 200

```

```

SCREEN 9: CLS
FOR p = 1 TO m
FOR q = 1 TO m
 $x = a + (c - a) * p / m$ :  $y = b + (d - b) * q / m$ 
FOR n = 1 TO numits
IF y > .5 THEN
     $x = 2 * x$ :  $y = 2 * y - 1$ 
ELSEIF x > .5 THEN
     $x = 2 * x - 1$ :  $y = 2 * y$ 
ELSE
     $x = 2 * x$ :  $y = 2 * y$ 
END IF
IF  $x * x + y * y > r$  THEN PSET (p, q), n: n = numits
NEXT n
NEXT q
NEXT p.
    
```

REFERENCES

1. Barnsley, M. F. "Fractals Every Where" Academic Press, Inc. New York (1993).
2. Emerson, N. D. "Dynamics of Polynomials with Disconnected Julia Sets" Discrete and Continuous Dynamical Systems, 9, (4) : 801-834, July (2003).
3. Gulick, D., "Encounters with Chaos" McGraw-Hill, Inc., (1992).
4. Gupta, S. and Iyer, P. L., "Julia Sets; Properties and Plot" A Project for PHY 306 (Order and Chaos in Nature), April, (2003).

Some Topological Properties of $I(X)$ -Spaces

Amal Ibrahim Al-Attar and Habeeb Kareem Abdullah

Department of mathematics, College of Science, AL-Mustansiriyah University

Department of mathematics, College of Education for women, Kufa University

الخلاصة

إن مجموعة كل الدوال المتقايسة (المتساوية القياس) على فضاء مترى X تكون زمرة تسمى بزمرة الدوال المتقايسة والتي يرمز لها بالرمز $I(X)$. في بحثنا هذا استطعنا توضيح أن $I(X)$ زمرة تحويل توبولوجي مع توبولوجيا التقارب النقطي، كذلك درسنا العلاقة بين $I(X)$ و X إذا كان احدهما متراسا. من الأهداف الرئيسية للبحث هو البحث عن شرط ضروري لجعل تلك الزمرة $I(X)$ مرصوصة محلياً، وحصلنا عندما تكون مجموعة الغاية (limit set) خالية لعنصر ما، شرط ضروري لجعل تلك الزمرة مرصوصة محلياً، لذلك درسنا تلك المجموعات بشكل واسع وبحثنا متى تكون مغلقة.

ABSTRACT

The set of all isometries on a metric space X with the usual composition of functions forms a group and it is called the group of isometries and is denoted by $I(X)$. In this work we illustrate that this group forms a topological transformation group with pointwise convergence topology. We also give relationships between the compactness of X and $I(X)$. From the main goals of our work is searching about a necessary condition which make the group of isometries locally compact. We find that the limit sets have active situation for suggestion, so we study the closeness of limit sets.

INTRODUCTION

If (X, d) and (Y, ρ) are metric spaces and f is a function of X onto Y , then f is called an isometry if $d(x, y) = \rho(f(x), f(y))$ for all points x and y of X . Every isometry is a one-to-one continuous open function. The composition of two isometries is again an isometry and the inverse of an isometry is also an isometry. Then the set of all isometries on a metric space (X, d) is a group and it is denoted by $I(X)$, (5).

In §1, we prove that for any metric space (X, d) , $(I(X), X, \theta)$ is a topological transformation group (with out using compactness of X which was used in the classical proof of this theorem) where θ is the action defined by $\theta(f, x) = f(x)$ with pointwise convergence topology, Th.1.2. Also we have the orbit space $X/I(X)$ is a T_2 -space iff each orbit of an element of X is closed in X , Th.1.3.

We shall study in §2 the relationship between X and $I(X)$ if one of them is compact and we find that if X is compact then $I(X)$ is compact, Th.2.3 and the converse is not true in general.

Key words and phrases: Isometry, Group of Isometrics $I(X)$, point wise convergence topology, limit sets, locally compact $I(X)$ -spaces.

Section three is important to the next section which concludes the generalization of the concepts of a limit sets and a prolongational limit set of a point, from dynamic system into $I(X)$ -space. We found these limits equal in an $I(X)$ -space, Th.3.2 and this is not true in general. Also in this section we study closedness of the limit sets, Th.3.5 and Th.3.7, and here we show that not all elements of a limit set of x , $\Lambda(x)$, are images under some elements of a group, so

we define subsets of $\Lambda(x)$ which are denoted by $k(x)$ and $d(x)$, Def.3.9, and which can be used to answer our question for the closedness of $\Lambda(x)$, Prop.3.10, and Th.3.11.

Manoussos and Stranzalos gave a necessary condition for the local compactness of $I(X)$, (6), (7). Similarly, in §4 we give but with different condition for the necessary of local compactness of $I(X)$, we find that if there exists $x \in X$ such that the limit set $\Lambda(x) = \phi$, then $I(X)$ is locally compact and closed, Th. 4.4, and we prove some important equivalent statements for this condition, Th.4.5. As an application of this theorem, $I(R)$ is locally compact (where R is the usual metric space). In this section also we recall the concept of proper action and we prove if an $I(X)$ -space is proper then $I(X)$ is locally compact and closed, Cor.4.12, and the converse is false in general, Example 4.13.

§1. Some results on $I(X)$ -spaces .

A topological transformation group is a triple (G, X, θ) where G is topological group, X is a topological space and $\theta: G \times X \rightarrow X$ is a continuous function such that ,

- (i) $\theta(g, \theta(h, x)) = \theta(gh, x)$ for all $g, h \in G$ and $x \in X$.
 - (ii) $\theta(e, x) = x$, for all $x \in X$, where e is the identity element of G .
- The map θ is called an action of G on X and the space X together with a given action θ of G is called a G -space (or, more precisely, a left G -space), (3). We shall often use the notation $g.x$ for $\theta(g, x)$.

We are now ready to prove that the group of isometries $I(X)$ acts on a metric space (X, d) with pointwise convergence topology. For this step we will need the following important lemma.

1.1 Lemma: Let (X, d) be a metric space and $\{x_\alpha\}_{\alpha \in D}$ be a net in X . Then $x_\alpha \rightarrow x$ in X iff $d(x_\alpha, x) \rightarrow 0$.

Proof: \rightarrow). Let $x_\alpha \rightarrow x$ in X and $\varepsilon > 0$, then there is $\beta \in D$ such that $x_\alpha \in B(x, \varepsilon)$ for every $\alpha \geq \beta$. Thus $d(x_\alpha, x) < \varepsilon$ for every $\alpha \geq \beta$ so $d(x_\alpha, x) \in B(0, \varepsilon)$ for every $\alpha \geq \beta$ where $B(0, \varepsilon)$ is a ball in the Euclidean metric space with center 0 and radius ε . Hence $d(x_\alpha, x) \rightarrow 0$.

\leftarrow). Given $d(x_\alpha, x) \rightarrow 0$, let $\varepsilon > 0$, then there exists $\beta \in D$ such that $d(x_\alpha, x) < \varepsilon$ for every $\alpha \geq \beta$ that is $x_\alpha \in B(x, \varepsilon)$ for every $\alpha \geq \beta$. Thus $x_\alpha \rightarrow x$.

1.2 Theorem: Let $I(X)$ be the group of isometries of a metric space (X, d) . If $\theta: I(X) \times X \rightarrow X$ is defined by $\theta(f, x) = f(x)$ for every $f \in I(X)$ and $x \in X$ then $(I(X), X, \theta)$ is a topological transformation group with the pointwise convergence topology on $I(X)$.

Proof:- First we want to prove that the multiplication function $\mu: I(X) \times I(X) \rightarrow I(X)$, defined by $\mu(f,g)=g \circ f$ is continuous. Let $f, g \in I(X)$ and $\{(f_\alpha, g_\alpha)\}$ be a net in $I(X) \times I(X)$ such that $(f_\alpha, g_\alpha) \rightarrow (f, g)$. Thus $f_\alpha \rightarrow f$ and $g_\alpha \rightarrow g$ then by Lemma 1.1, $d(f_\alpha(x), f(x)) \rightarrow 0$ and $d(g_\alpha(x), g(x)) \rightarrow 0$ for every $x \in X$. Now, by the isometry of f_α we have,

$$\begin{aligned} d((g_\alpha \circ f_\alpha)(x), (g \circ f)(x)) &= d(g_\alpha(f_\alpha(x)), f(g(x))) \\ &\leq d(g_\alpha(f_\alpha(x)), g_\alpha(f(x))) + d(g_\alpha(f(x)), g(f(x))) \\ &= d(f_\alpha(x), f(x)) + d(g_\alpha(f(x)), g(f(x))) \end{aligned}$$

But $d(f_\alpha(x), f(x)) \rightarrow 0$ and $d(g_\alpha(f(x)), g(f(x))) \rightarrow 0$ for every $x \in X$. Then $d((g_\alpha \circ f_\alpha)(x), (g \circ f)(x)) \rightarrow 0$ for every $x \in X$. Thus by Lemma 1.1, $(g_\alpha \circ f_\alpha)(x) \rightarrow (g \circ f)(x)$ for every $x \in X$. So by [8,Th.42.2] $g_\alpha \circ f_\alpha \rightarrow g \circ f$. Hence μ is continuous. Also we must prove that the inversion function $v: I(X) \rightarrow I(X)$ where $v(f) = f^{-1}$ is continuous. Let $f \in I(X)$ and $\{f_\alpha\}$ be a net in $I(X)$ such that $f_\alpha \rightarrow f$. Now, for any $x \in X$

$$\begin{aligned} d(f_\alpha^{-1}(x), f^{-1}(x)) &= d(x, f_\alpha(f^{-1}(x))) \\ &= d(f_\alpha(f^{-1}(x)), f(f^{-1}(x))) \dots (1) \text{ (Since } f_\alpha^{-1} \text{ is an isometry)} \end{aligned}$$

Since $f_\alpha \rightarrow f$, then by [8,Th.42.2] and Lemma 1.1 $d(f_\alpha(f^{-1}(x)), f(f^{-1}(x))) \rightarrow 0$ for every $x \in X$. Thus from (1) we get $d(f_\alpha^{-1}(x), f^{-1}(x)) \rightarrow 0$ for every $x \in X$. So $f_\alpha^{-1} \rightarrow f^{-1}$.

Second we want to prove that θ is continuous. Let $(f, x) \in I(X) \times X$ and $\{(f_\alpha, x_\alpha)\}$ be a net in $I(X) \times X$ such that $(f_\alpha, x_\alpha) \rightarrow (f, x)$. Thus $f_\alpha \rightarrow f$ and $x_\alpha \rightarrow x$. Now,

$$\begin{aligned} d(f_\alpha(x_\alpha), f(x)) &= d(x_\alpha, f_\alpha^{-1}(f(x))) \\ &\leq d(x_\alpha, x) + d(x, f_\alpha^{-1}(f(x))) \quad \text{(Since } f_\alpha \text{ is an isometry)} \\ &= d(x_\alpha, x) + d(f_\alpha(x), f(x)) \end{aligned}$$

Since $f_\alpha \rightarrow f$ and $x_\alpha \rightarrow x$ then by Lemma 1.1 and [8,Th.42.2], $d(f_\alpha(x), f(x)) \rightarrow 0$ and $d(x_\alpha, x) \rightarrow 0$, so $d(f_\alpha(x_\alpha), f(x)) \rightarrow 0$.

Then by Lemma 1.1 $f_\alpha(x_\alpha) \rightarrow f(x)$, thus θ is continuous.

Also θ satisfied, $\theta(\text{id}, x) = \text{id}(x) = x$ (where id the identity element of $I(X)$) and $\theta(f, \theta(g, x)) = \theta(f, g(x)) = (f \circ g)(x)$ for every $f, g \in I(X)$ and $x \in X$, so $(I(X), X, \theta)$ is a topological transformation group.

From now on, by $I(X)$ -space (X, d) we mean the topological transformation group $(I(X), X, \theta)$ which is described in the above theorem.

Let X be a G -space and $x \in X$ then the subspace $G(x) = \{g.x / g \in G\}$ is called the orbit (trajectory) of x under G . These subspaces form a partition on X and the sets of all orbits in X is denoted by X / G . Let $\pi: X \rightarrow X / G$ denote the canonical map taking x into its orbit $G(x)$. Then X/G endowed with the quotient topology ($U \subseteq X / G$ is open if $\pi^{-1}(U)$ is open in X) is called the orbit space of X (with respect to G), (3).

We shall now give a useful characterization of Hausdorff orbit space of $I(X)$ -space.

1.3 Theorem: Let (X, d) be an $I(X)$ -space. Then the orbit space $X/I(X)$ is a T_2 -space iff each orbit of an element of X is closed in X .

Proof: \rightarrow). Clear.

\leftarrow). Denote $I(X)$ by G . Let the orbit $G(x)$ of x be closed for every $x \in X$. We want to prove that the graph of the action $\theta: G \times X \rightarrow X$ is closed. Let R be the graph of θ and let (x, y) be a limit point of R . Then there exist a net $\{(x_\alpha, f_\alpha(x_\alpha))\}$ in R such that $(x_\alpha, f_\alpha(x_\alpha)) \rightarrow (x, y)$. Thus $x_\alpha \rightarrow x$ and $f_\alpha(x_\alpha) \rightarrow y$. Now,

$$d(f_\alpha(x), y) \leq d(f_\alpha(x), f_\alpha(x_\alpha)) + d(f_\alpha(x_\alpha), y).$$

Since f_α is an isometry then $d(f_\alpha(x), y) \leq d(x, x_\alpha) + d(f_\alpha(x_\alpha), y)$ and since $x_\alpha \rightarrow x$ and $f_\alpha(x_\alpha) \rightarrow y$, then by Lemma 1.1, $d(f_\alpha(x), y) \rightarrow 0$. Thus $f_\alpha(x) \rightarrow y$.

Since the orbit $G(x)$ of x is closed (by hypothesis), then $y \in G(x)$. So there exist $f \in G$ such that $y = f(x)$. Then $(x, f(x)) = (x, y) \in R$ that is R is closed. Thus the diagonal set of X/G is closed in $X/G \times X/G$, so X/G is T_2 .

Let (X, G, θ) be a topological transformation group. A point $x \in X$ is called critical (fixed) if $G(x) = \{x\}$, where $G(x)$ is the orbit of x , (1).

1.4 Lemma: Let (X, d) be an $I(X)$ -space and $x \in X$. Then x is critical iff every neighborhood of x contains an orbit.

Proof: \rightarrow). Let $x \in X$ be a critical point and U be a neighborhood of x . Since the orbit of x is $\{x\}$. Thus U contains an orbit.

\leftarrow). Suppose that x is not critical. Then there exists $f \in I(X)$ such that $x \neq f(x)$ put $\varepsilon = \frac{1}{2} d(x, f(x))$. Then we have $B(x, \varepsilon) \cap B(f(x), \varepsilon) = \emptyset$. Since f is an isometry then $f(B(x, \varepsilon)) = B(f(x), \varepsilon)$. Thus if $y \in B(x, \varepsilon)$, then $f(y) \notin B(x, \varepsilon)$. So there exists a neighborhood $B(x, \varepsilon)$ of x that cannot contain an orbit. This completes the proof.

1.5 Proposition: The set of all critical points in any $I(X)$ -space is closed.

Proof: Let A be the set of all critical points in X and x be a limit point of A . Then there exists a net $\{x_\alpha\}_{\alpha \in D}$ in A such that $x_\alpha \rightarrow x$, thus for every $\varepsilon > 0$, there exists $\beta \in D$ such that $x_\alpha \in B(x, \varepsilon)$ for every $\alpha \geq \beta$. Since x_α is critical then the orbit of x_α is $\{x_\alpha\}$, thus for every neighborhood of x contains an orbit. So by Lemma 1.4, x is critical. Hence A is closed.

§ 2. Compact $I(X)$ -spaces.

In this section we study the relationship between X and $I(X)$ if one of them is compact.

2.1 Proposition: Let (X, d) be an $I(X)$ -space and $\{f_\alpha\}$ be a net in $I(X)$ such that $f_\alpha \rightarrow f$, for some $f \in X^X$. Then f preserves d .

Proof: Let $x, y \in X$. Since $f_\alpha \rightarrow f$ then $f_\alpha(x) \rightarrow f(x)$ and $f_\alpha(y) \rightarrow f(y)$. Let n be a positive integer, then there are α_0 and α_1 such that $f_\alpha(x) \in B(f(x), 1/n)$ for every $\alpha \geq \alpha_0$ and $f_\alpha(y) \in B(f(y), 1/n)$ for every $\alpha \geq \alpha_1$. Since $\{f_\alpha\}$ is a net then there exists β_n such that $\beta_n \geq \alpha_0$ and $\beta_n \geq \alpha_1$. Thus $f_\alpha(x) \in B(f(x), 1/n)$ and $f_\alpha(y) \in B(f(y), 1/n)$ for every $\alpha \geq \beta_n$. Now,

$$d(f(x), f(y)) \leq d(f(x), f_\alpha(x)) + d(f_\alpha(x), f_\alpha(y)) + d(f_\alpha(y), f(y))$$

$$< \frac{1}{n} + d(x, y) + \frac{1}{n} = \frac{2}{n} + d(x, y)$$

For every $\alpha \geq \beta_n$. Thus $d(f(x), f(y)) \leq d(x, y) \dots\dots\dots(1)$

Since f_α is an isometry then

$$\begin{aligned} d(x, y) &= d(f_\alpha(x), f_\alpha(y)) \\ &\leq d(f_\alpha(x), f(x)) + d(f(x), f(y)) + d(f(y), f_\alpha(y)) \\ &< \frac{2}{n} + d(f(x), f(y)) \end{aligned}$$

For every $\alpha \geq \beta_n$. So $d(x, y) \leq d(f(x), f(y)) \dots\dots\dots(2)$

Then from (1) and (2) we have $d(f(x), f(y)) = d(x, y)$, thus f preserves d .

2.2 Proposition: Let (X, d) be a compact $I(X)$ -space. Then $I(X)$ is a closed subset of the Tychonof space X^X .

Proof: Let f be a limit point of $I(X)$. Then there exists a net $\{f_\alpha\}$ in $I(X)$ such that $f_\alpha \rightarrow f$. So we have only to prove that f is onto, let $y \in X$. Since f_α is bijective, for every α then $\{f_\alpha^{-1}(y)\}$ is a net in X . Since X is compact, then there are $x \in X$ and subnet $\{f_\beta^{-1}(y)\}$ of $\{f_\alpha^{-1}(y)\}$ such that $f_\beta^{-1}(y) \rightarrow x$. Since f_β^{-1} is an isometry for each β then $d(f_\beta(x), y) = d(f_\beta^{-1}(y), x)$. Thus by Lemma 1.1,

$f_\beta(x) \rightarrow y$. But $f_\beta(x) \rightarrow f(x)$ and X is a T_2 -space, then $y = f(x)$ that is f is onto. So by Prop.2.1 $f \in I(X)$. Hence $I(X)$ is a closed subset of X^X .

2.3 Theorem: Let (X,d) be an $I(X)$ -space. If X is compact then $I(X)$ is compact.

Proof: Let X be a compact space, then the Tychonof space X^X is compact [8,Th.17.8]. Since X is a Hausdorff space, then X^X is Hausdorff, and since $I(X)$ is a closed subset of X^X (by Prop. 2.2), then $I(X)$ is compact.

The converse of Th.2.3 is not true in general, since if $X = (0,1)$ and d be the usual metric on X , then X is not compact, but $I(X) = \{f,g\}$ is compact, where $f(t) = t$ and $g(t) = 1 - t$, for every $t \in X$.

§3. Limit Sets.

Dydo (4) generalized the concepts of limit sets from a dynamic system to a G -space. Let X be a G -space. For any $x \in X$, define $\Lambda(x) = \{y \in X \mid \text{there exist a net } \{g_\alpha\} \text{ in } G \text{ with } g_\alpha \rightarrow \infty \text{ such that } g_\alpha x \rightarrow y\}$,

$J(x) = \{y \in X \mid \text{there are a net } \{g_\alpha\} \text{ in } G \text{ any }, \text{ d a net } \{x_\alpha\} \text{ in } X \text{ with } g_\alpha \rightarrow \infty \text{ and } x_\alpha \rightarrow x \text{ such that } g_\alpha x_\alpha \rightarrow y\}$.

$\Lambda(x)$ is called the limit set of x and $J(x)$ is called the prolongational limit set of x .

A subset A of a G -space X is called invariant under G if $ga \in A$ for every $g \in G$ and $a \in A$, (3).

The proof of the following proposition is straight-forward and hence is omitted.

3.1 Proposition: Let X be a G -space and $x, y \in X$. Then,

- (i) $\Lambda(x) \subseteq J(x)$.
- (ii) $\Lambda(x)$ and $J(x)$ are invariant under G .
- (iii) $\overline{G(x)} = G(x) \cup \Lambda(x)$.

Let (R,d) be the usual metric space. Define $\theta : R \setminus \{0\} \times R \rightarrow R$ by $\theta(r,t) = rt$. Then $(R \setminus \{0\}, R, \theta)$ is a topological transformation group with respect to the Euclidian metric. Notice that $\Lambda(0) = \{0\}$ and $J(0) = R$ thus $\Lambda(0) \neq J(0)$. Then a limit set and a prolongational limit set of a point are not equal in general. But in an $I(X)$ -space X , $\Lambda(x) = J(x)$, for each $x \in X$ as it is shown by the following theorem.

3.2 Theorem: Let (X,d) be an $I(X)$ -space. Then $\Lambda(x) = J(x)$, for every $x \in X$.

Proof: Let $x \in X$. By Prop.(3.1), $\Lambda(x) \subseteq J(x)$. Let $y \in J(x)$, then there are two nets $\{f_\alpha\}$ in $I(X)$ and $\{x_\alpha\}$ in X with $f_\alpha \rightarrow \infty$ and $x_\alpha \rightarrow x$ such that $f_\alpha(x_\alpha) \rightarrow y$. Now, by the isometry of f_α^{-1} we have

$$\begin{aligned}
 d(f_\alpha(x), y) &= d(x, f_\alpha^{-1}(y)) \\
 &\leq d(x, x_\alpha) + d(x_\alpha, f_\alpha^{-1}(y)) \\
 &= d(x_\alpha, x) + d(f_\alpha(x_\alpha), y)
 \end{aligned}$$

By Lemma 1.1 $d(x_\alpha, x) \rightarrow 0$ and $d(f_\alpha(x_\alpha), y) \rightarrow 0$. Thus $d(f_\alpha(x), y) \rightarrow 0$ therefore by Lemma 1.1, $f_\alpha(x) \rightarrow y$. But $f_\alpha \rightarrow \infty$, so $y \in \Lambda(x)$.

Now we will discuss the question "is $\Lambda(x)$ closed?". In general $\Lambda(x)$ is not closed.

Let R be the set of all real numbers and Q be the set of all rational numbers. Take the topological group $(Q, +)$ with the Euclidian metric. Define $\theta: Q \times R \rightarrow R$, by $\theta(q, r) = q + r$. Thus (Q, R, θ) is a topological transformation group with the Euclidian metric. Notice that,

$\Lambda(\sqrt{2}) = R \setminus \{q + \sqrt{2} / q \in Q\}$, so it is not closed in R .

3.3 Proposition: Let X be a G -space and $x \in X$. If $x \in \Lambda(x)$, then $\Lambda(x)$ is closed.

Proof: Since $\Lambda(x)$ is invariant (by Prop.(3.1)), then the orbit $G(x)$ of x is a subset of $\Lambda(x)$. But $\overline{G(x)} = G(x) \cup \Lambda(x)$, thus $\Lambda(x) = \overline{G(x)}$, so $\Lambda(x)$ is closed.

The converse of Proposition 3.3 is not true in general. Define $\theta: R \setminus \{0\} \times R \rightarrow R$ by $\theta(r, t) = t/r$. Then θ is the action of R on $R \setminus \{0\}$ with the Euclidian metric space. Since for every sequence $\{t_n\}$ in $R \setminus \{0\}$ such that $t_n \rightarrow \infty$, then $1/t_n \rightarrow 0$. So $\Lambda(1) = \{0\}$. Hence $\Lambda(1)$ is closed but $1 \notin \Lambda(1)$.

While the converse of Prop.3.3 is true in any $I(X)$ -space if $\Lambda(x) \neq \emptyset$.

3.4 Proposition: Let (X, d) be an $I(X)$ -space and $x \in X$ such that $\Lambda(x) \neq \emptyset$. If $\Lambda(x)$ is closed, then $x \in \Lambda(x)$.

Proof: Let $\Lambda(x)$ be closed. Since $\Lambda(x) \neq \emptyset$, then there are $y \in X$ and a net $\{f_\alpha\}$ in $I(X)$ with $f_\alpha \rightarrow \infty$ such that $f_\alpha(x) \rightarrow y$. Now,

$$d(f_\alpha^{-1}(y), x) = d(y, f_\alpha(x)) \text{ (Since } f_\alpha \text{ is an isometry).}$$

Then by Lemma 1.1 we have $f_\alpha^{-1}(y) \rightarrow x$. Since $\Lambda(x)$ is invariant (by Prop. 3.1, ii) and $y \in \Lambda(x)$ then $f_\alpha^{-1}(y) \in \Lambda(x)$ for every α . Then we have a net $\{f_\alpha^{-1}(y)\}$ in $\Lambda(x)$ converges to x . Thus $x \in \Lambda(x)$ (since $\Lambda(x)$ is closed).

It follows from Prop.3.3 and Prop.3.4, that:-

3.5 Theorem: Let (X, d) be an $I(X)$ -space and $x \in X$. If $\Lambda(x) \neq \emptyset$, then $\Lambda(x)$ is closed iff $x \in \Lambda(x)$.

In fact without the condition $\Lambda(x)$ is closed we get,

3.6 Lemma: Let (X, d) be an $I(X)$ -space and $x \in X$. If $\Lambda(x) \neq \emptyset$, then $x \in \overline{\Lambda(x)}$.

Proof: Let $\Lambda(x) \neq \emptyset$, then there are $y \in X$ and a net $\{f_\alpha\}$ in $I(X)$ with $f_\alpha \rightarrow \infty$ such that $f_\alpha(x) \rightarrow y$. Since $\Lambda(x) \subseteq \overline{\Lambda(x)}$, then $y \in \overline{\Lambda(x)}$, but $\overline{\Lambda(x)}$ is invariant then $f_\alpha^{-1}(y) \in \overline{\Lambda(x)}$ for every α . Notice that $f_\alpha^{-1}(y) \rightarrow x$ and $\overline{\Lambda(x)}$ is closed, then $x \in \overline{\Lambda(x)}$.

In fact Lemma 3.6 is not true for a G -space. In the above example $\Lambda(1) \neq \emptyset$, but $1 \notin \overline{\Lambda(1)}$.

3.7 Theorem: Let (X, d) be an $I(X)$ -space and $x \in X$. Then the following statement are equivalent,

- (i) $\Lambda(x) \neq \emptyset$.
- (ii) $x \in \overline{\Lambda(x)}$.
- (iii) $\overline{\Lambda(x)} = \overline{G(x)}$, (where $G = I(X)$ and $G(x)$ is the orbit of x).

Proof: i \rightarrow ii). By Lemma 3.6.

ii \rightarrow iii). Let $x \in \overline{\Lambda(x)}$. Since $\overline{\Lambda(x)}$ is invariant then $\overline{G(x)} \subseteq \overline{\Lambda(x)}$.

But $\overline{G(x)} = G(x) \cup \Lambda(x)$, thus $\overline{\Lambda(x)} = \overline{G(x)}$.

iii \rightarrow i). Let $\overline{\Lambda(x)} = \overline{G(x)}$. Since $x \in \overline{G(x)}$ then $x \in \overline{\Lambda(x)}$.

Thus $\Lambda(x) \neq \emptyset$.

In fact not all elements of $\Lambda(x)$ are images of x under some element of G . See the following example.

3.8 Example: Let (\mathbb{R}, d) be the Euclidian metric space and Q be the set of all rational numbers. Define $\theta : Q \setminus \{0\} \times \mathbb{R} \rightarrow \mathbb{R}$ by $\theta(q, r) = r/q$. Then it is clear that $(Q \setminus \{0\}, \mathbb{R}, \theta)$ is a topological transformation group with the Euclidian metric. Notice that the elements of the set $\mathbb{R} \setminus \{q\sqrt{2} / q \in Q \setminus \{0\}\}$ are not images of $\sqrt{2}$ but they are belong to $\Lambda(\sqrt{2})$.

So let us define subsets of $\Lambda(x)$ which will be denoted by $k(x)$ and $d(x)$ and which can be used to answer our question for the closedness of $\Lambda(x)$.

3.9 Definition: Let X be a G -space. For each $x \in X$ define,

$k(x) = \{y \in \Lambda(x) / \text{there exist } g \in G \text{ such that } y = gx\}$,

$d(x) = \Lambda(x) \setminus k(x)$, that is $d(x) = \{y \in \Lambda(x) / y \neq gx \text{ for every } g \in G\}$.

We are now ready to prove some properties of $k(x)$ and $d(x)$.

3.10 Proposition: Let X be a G -space and $x \in X$. Then,

- (i) $k(x)$ and $d(x)$ are partitions of $\Lambda(x)$.
- (ii) $d(x)$ and $k(x)$ are invariant.
- (iii) If $k(x) \neq \emptyset$ then $x \in k(x)$.

- (iv) $x \notin d(x)$.
- (v) $G(x) \cap d(x) = \phi$, where $G(x)$ is the orbit of x .
- (vi) $\overline{G(x)} = G(x) \cup d(x)$.
- (vii) $G(x)$ is closed iff $d(x) = \phi$.
- (viii) If $\Lambda(x) = k(x)$ then $\Lambda(x)$ is closed.

Proof: i). By Definition 3.9.

ii). Let $y \in d(x)$ and $g \in G$. Then $y \in \Lambda(x)$ and $y \neq hx$ for every $h \in G$. Since $\Lambda(x)$ is invariant, then $gy \in \Lambda(x)$. Since $y \neq hx, \forall h \in G$ then also $gy \neq hx \forall h \in G$ (otherwise $y = g^{-1}hx$ for some $h \in G$), then $gy \in d(x)$. Hence $d(x)$ is invariant. In the same way, $k(x)$ is invariant.

iii). Let $k(x) \neq \phi$, then there exist $y \in k(x)$ and there exist $g \in G$ such that $y = gx$. Since $k(x)$ is invariant, then $x \in k(x)$.

iv). Clear.

v). Since $x \notin d(x)$ and $d(x)$ is invariant, then $G(x) \cap d(x) = \phi$.

vi). Clear.

vii). By v and vi.

viii). Let $\Lambda(x) = k(x)$. If $k(x) = \phi$, then $\Lambda(x)$ is closed. If $k(x) \neq \phi$, then by (iii), $x \in k(x)$, thus $x \in \Lambda(x)$. So by Prop. 3.3, $\Lambda(x)$ is closed.

If we replace a G -space by an $I(X)$ -space then we get the following theorem.

3.11 Theorem: Let (X, d) be an $I(X)$ -space and $x \in X$ such that $\Lambda(x) \neq \phi$. Then,

- (i) If $d(x)$ is closed, then $d(x) = \phi$.
- (ii) $\Lambda(x)$ is closed iff $k(x) \neq \phi$.
- (iii) If $k(x) \neq \phi$ and $k(x)$ is open then $d(x) = \phi$.

Proof:

i) Let $d(x)$ be a closed set. Suppose that $d(x) \neq \phi$, then there are $y \in d(x)$ and a net $\{f_\alpha\}$ in $I(X)$ with $f_\alpha \rightarrow \infty$ and $f_\alpha(x) \rightarrow y$. From Lemma 1.1 and $d(f_\alpha^{-1}(y), x) = d(y, f_\alpha(x))$ (since f_α is an isometry), we have $f_\alpha^{-1}(y) \rightarrow x$. Since $d(x)$ is invariant and $y \in d(x)$, then $f_\alpha^{-1}(y) \in d(x)$, for every α and since $d(x)$ is closed then $x \in d(x)$, a contradiction (see Prop. 3.10, iii). This completes the proof.

ii) \rightarrow . Let $\Lambda(x)$ be closed. Since $\Lambda(x) \neq \phi$ then by Th. 3.5 $x \in \Lambda(x)$. But $x \notin d(x)$ (by Prop. 3.10, iii) and $\Lambda(x) = k(x) \cup d(x)$, then $x \in k(x)$, thus $k(x) \neq \phi$.

\leftarrow . Let $k(x) \neq \phi$ then by Prop. 3.10, ii, $x \in k(x)$. So $x \in \Lambda(x)$ and by Th. 3.5, $\Lambda(x)$ is closed.

- iii) Let $k(x) \neq \emptyset$ and $k(x)$ is an open set. We want to prove that $\Lambda(x) \subseteq k(x)$. Let $y \in \Lambda(x)$, then there exists a net $\{f_\alpha\}$ in $I(X)$ with $f_\alpha \rightarrow \infty$ such that $f_\alpha(x) \rightarrow y$. Since $d(f_\alpha^{-1}(y), x) = d(f_\alpha(x), y)$ (f_α is an isometry) then by Lemma 1.1, $f_\alpha^{-1}(y) \rightarrow x$. But $x \in k(x)$ (by Prop.3.2, ii) and $k(x)$ is open, so there exists a β such that $f_\alpha^{-1}(y) \in k(x)$ for every $\alpha \geq \beta$. Since $k(x)$ is invariant (by Prop.3.2, i), then $y \in k(x)$. Thus $\Lambda(x) \subseteq k(x)$. This completes the proof.

3.12 Corollary: Let (X, d) be an $I(X)$ -space and $x \in X$ such that $\Lambda(x) \neq \emptyset$. If $\Lambda(x)$ is compact. Then the closure of the orbit of x is compact.

Proof: Let $\Lambda(x)$ be a compact. Since X is a Hausdorff space, then $\Lambda(x)$ is closed. Then by Th.3.11, we have $x \in \Lambda(x)$. Since $\Lambda(x)$ is invariant, then the orbit of x is a subset of $\Lambda(x)$, i.e. $G(x) \subseteq \Lambda(x)$ (where $G = I(X)$). Since $\Lambda(x)$ is closed then $\overline{G(x)} \subseteq \Lambda(x)$ and since $\Lambda(x) \subseteq \overline{G(x)}$ (by Prop. (3.1), iii) then $\overline{G(x)}$ is compact.

The converse of Cor.3.12 is true whenever $\Lambda(x)$ is closed,

3.13 Proposition: Let (X, d) be an $I(X)$ -space such that $I(X)$ is noncompact. If there exist $x \in X$ such that the closure of the orbit of x is compact, then,

- (i) $\Lambda(x) \neq \emptyset$.
- (ii) $\overline{\Lambda(x)}$ is compact.
- (iii) If $\Lambda(x)$ is closed, then $\Lambda(x)$ is compact.

Proof:

- (i) We denote $I(X)$ by G . Let $x \in X$ such that the closure of the orbit of x , $\overline{G(x)}$ is compact. Since G is noncompact, then there exists a net $\{f_\alpha\}$ in G which has no convergence subnet, then $\{f_\alpha(x)\}$ is a net in a compact set $\overline{G(x)}$, so $\Lambda(x) \neq \emptyset$.
- (ii) By (i), $\Lambda(x) \neq \emptyset$, then by Th.3.7, $\overline{\Lambda(x)} = \overline{G(x)}$ thus $\overline{\Lambda(x)}$ is compact.
- (iii) By (ii), $\overline{\Lambda(x)}$ is compact. So $\Lambda(x)$ is a closed subset of a compact space which is compact.

§ 4. Locally Compact $I(X)$ -spaces.

In this section we study the question of locally compactness of $I(X)$.

The following examples show that there exists a locally compact metric space (X, d) for which $I(X)$ is not locally compact, and also there exists a metric space (X, d) such that X is not locally compact, but $I(X)$ is locally compact.

4.1 Example: Let N be the set of all positive integers and (N, d) be the discrete metric space. Then N is locally compact but $I(N)$ is not locally compact.

4.2 Example: Let Q be the set of all rational numbers and let $X = Q \setminus \{0\}$. Take the Euclidian metric d on X . Then (X, d) is not locally compact but

$I(X) = \{f, g\}$ is locally compact, where $f(t) = t$ and $g(t) = -t$.

Let A and B be subsets of a G -space X , then the set $\{g \in G / gA \cap B \neq \emptyset\}$ is denoted by $((A, B))$.

4.3 Proposition: Let (X, d) be a locally compact $I(X)$ -space and $x \in X$. If $\Lambda(x) = \emptyset$, then:

- There exists $\varepsilon > 0$ such that $((x, B(x, \varepsilon)))$ is a relatively compact subset of $I(X)$.
- There exists $\varepsilon > 0$ such that $((B(x, \varepsilon), B(x, \varepsilon)))$ is a relatively compact subset of $I(X)$.
- For every $y \in X$, there is $\varepsilon > 0$ such that $((x, B(y, \varepsilon)))$ is a relatively compact subset of $I(X)$.

Proof:

- Since $x \in X$ and X is locally compact space, then there exists $\varepsilon > 0$ such that the ball $B(x, 2\varepsilon)$ is a relatively compact neighborhood of x . We want to prove that $((x, \overline{B(x, \varepsilon)}))$ is compact. Let $\{f_\alpha\}$ be a net in $((x, \overline{B(x, \varepsilon)}))$, then $f_\alpha(x) \in \overline{B(x, \varepsilon)} \subseteq B(x, 2\varepsilon)$, for every α . Since $B(x, 2\varepsilon)$ is relatively compact then there exists $y \in X$ and a subnet $\{f_\beta\}$ of $\{f_\alpha\}$ such that $f_\beta(x) \rightarrow y$. Since $\Lambda(x) = \emptyset$, then the net $\{f_\alpha\}$ has a convergent subnet. Thus $((x, \overline{B(x, \varepsilon)}))$ is a compact set. Now we show that $((x, \overline{B(x, \varepsilon)})) \subseteq ((x, \overline{B(x, \varepsilon)}))$. Let $h \in ((x, \overline{B(x, \varepsilon)}))$, then there exists a net $\{h_\alpha\}$ in $((x, B(x, \varepsilon)))$ such that $h_\alpha \rightarrow h$, so $h_\alpha(x) \rightarrow h(x)$. Since $h_\alpha(x) \in B(x, \varepsilon)$ for every α , then $h(x) \in \overline{B(x, \varepsilon)}$. Thus $h \in ((x, \overline{B(x, \varepsilon)}))$. So $((x, \overline{B(x, \varepsilon)})) \subseteq ((x, \overline{B(x, \varepsilon)}))$. Since $((x, \overline{B(x, \varepsilon)}))$ is compact then $((x, B(x, \varepsilon)))$ is relatively compact.

- Since $x \in X$ and X is locally compact space, then there exists $\varepsilon > 0$ such that the ball $B(x, 5\varepsilon)$ is a relatively compact neighborhood of x . We will show that $((B(x, \varepsilon), B(x, \varepsilon)))$ is relatively compact. Let $\{f_\alpha\}$ be a net in $((\overline{B(x, \varepsilon)}, \overline{B(x, \varepsilon)}))$. Then $f_\alpha(\overline{B(x, \varepsilon)}) \cap \overline{B(x, \varepsilon)} \neq \emptyset$, for every α .

Thus $f_\alpha(B(x, 2\varepsilon)) \cap B(x, 2\varepsilon) \neq \emptyset$ for every α (since $\overline{B(x, \varepsilon)} \subseteq B(x, 2\varepsilon)$).

Since f_α is an isometry then, $B(f_\alpha(x), 2\varepsilon) \cap B(x, 2\varepsilon) \neq \emptyset$ for every α .

Thus for every α there exists $z_\alpha \in B(x, 2\varepsilon)$ such that $d(f_\alpha(x), z_\alpha) < 2\varepsilon$.

Since $d(z_\alpha, x) < 2\varepsilon$ then,

$$d(f_\alpha(x), x) \leq d(f_\alpha(x), z_\alpha) + d(z_\alpha, x) < 2\varepsilon + 2\varepsilon = 4\varepsilon.$$

So $f_\alpha(x) \in B(x, 5\varepsilon)$, for every α . Since $B(x, 5\varepsilon)$ is relatively compact then there are $y \in X$ and a subnet $\{f_\beta\}$ of $\{f_\alpha\}$ such that $f_\beta(x) \rightarrow y$. But $\Lambda(x) = \phi$. Then the net $\{f_\alpha\}$ has a convergent subnet. Thus $((B(x, \varepsilon), B(x, \varepsilon)))$ is relatively compact.

- iii) Let $y \in X$ since X is a locally compact space. Then there exist $\varepsilon > 0$ such that $B(y, 2\varepsilon)$ is a relatively compact neighborhood of y . Let $\{f_\alpha\}$ be a net in $\overline{((x, B(y, \varepsilon)))} \subseteq \overline{((x, B(y, \varepsilon)))}$. Then $f_\alpha(x) \in \overline{B(y, \varepsilon)} \subseteq B(y, 2\varepsilon)$ for every α . Since $B(y, 2\varepsilon)$ is relatively compact then $\{f_\alpha(x)\}$ has a convergent subnet and since $\Lambda(x) = \phi$, So $((x, B(y, \varepsilon)))$ is relatively compact.

4.4 Theorem: Let (X, d) be a locally compact $I(X)$ -space and $\Lambda(x) = \phi$, for some $x \in X$. Then:

- (i) $I(X)$ is a locally compact space.
- (ii) $I(X)$ is a closed subset of X^X .

Proof:

- i) Since X is a locally compact space and $\Lambda(x) = \phi$. Then by Prop. 4.3, i, there exists $\varepsilon > 0$ such that $((x, B(x, \varepsilon)))$ is a relatively compact neighborhood of the identity element of $I(X)$, thus by the left translation we have $I(X)$ is locally compact.
- ii) Let f be a limit point of $I(X)$. Then there exists a net $\{f_\alpha\}$ in $I(X)$ such that $f_\alpha \rightarrow f$. Thus $f_\alpha(x) \rightarrow f(x)$. Since $\Lambda(x) = \phi$, then the net $\{f_\alpha\}$ has a convergent subnet in $I(X)$, that is there exists $g \in I(X)$ and a subnet $\{f_\beta\}$ of $\{f_\alpha\}$ such that $f_\beta \rightarrow g$. Since $f_\alpha \rightarrow f$ then $f_\beta \rightarrow f$. But $I(X)$ is a T_2 -space then $f = g$. Thus $f \in I(X)$, so $I(X)$ is closed.

The following theorem gives a useful characterization of $\Lambda(x) = \phi$.

4.5 Theorem: Let (X, d) be a locally compact $I(X)$ -space and $x \in X$. Then the following statements are equivalent:-

- (i) $\Lambda(x) = \phi$.
- (ii) For every $y \in X$ there exist $\varepsilon > 0$ such that $((B(x, \varepsilon), B(y, \varepsilon)))$ is relatively compact in $I(X)$.
- (iii) For every $y \in X$ there exist $\varepsilon > 0$ such that $((x, B(y, \varepsilon)))$ is relatively compact in $I(X)$.

Proof: i \rightarrow ii). Let $y \in X$ since X is a locally compact space then there exists $\varepsilon > 0$ such that $B(y, 3\varepsilon)$ is a relatively compact neighborhood of y . Let $f \in \overline{((B(x, \varepsilon), B(y, \varepsilon)))}$. Then there exists a net $\{f_\alpha\}$ in $((B(x, \varepsilon), B(y, \varepsilon)))$ such that $f_\alpha \rightarrow f$. Thus $f_\alpha(B(x, \varepsilon)) \cap B(y, \varepsilon) \neq \phi$, for every α . Since f_α is an isometry then $B(f_\alpha(x), \varepsilon) \cap B(y, \varepsilon) \neq \phi$ for every α , so $d(f_\alpha(x), y) < 2\varepsilon$ for

every α . Then $f_\alpha(x) \in B(y, 3\varepsilon)$. Since $\overline{B(y, 2\varepsilon)}$ is closed, then $f(x) \in \overline{B(y, 2\varepsilon)}$, thus $f(x) \in B(y, 2\varepsilon)$. Now we prove that $((B(x, \varepsilon), B(y, \varepsilon)))$ is relatively compact. Let $\{g_\alpha\}$ be any net in $((B(x, \varepsilon), B(y, \varepsilon)))$. Then it is clear that $g_\alpha(x) \in B(y, 3\varepsilon)$. Since $B(y, 3\varepsilon)$ is relatively compact then the net $\{g_\alpha(x)\}$ has a convergent subnet. But $\Lambda(x) = \emptyset$, then the net $\{g_\alpha\}$ has a convergent subnet. Thus $((B(x, \varepsilon), B(y, \varepsilon)))$ is relatively compact.

ii \rightarrow iii) Let $y \in X$. Then by (ii) there exists $\varepsilon > 0$ such that $((B(x, \varepsilon), B(y, \varepsilon)))$ is relatively compact. Now, if $f \in ((x, B(y, \varepsilon)))$ then $f(x) \in B(y, \varepsilon)$. Thus $B(f(x), \varepsilon) \cap B(y, \varepsilon) \neq \emptyset$. Since f is an isometry, then $f(B(x, \varepsilon)) \cap B(y, \varepsilon) \neq \emptyset$.

Thus $f \in ((B(x, \varepsilon), B(y, \varepsilon)))$, so $((x, B(y, \varepsilon))) \subseteq ((B(x, \varepsilon), B(y, \varepsilon)))$. Hence $((x, B(y, \varepsilon)))$ is relatively compact.

(iii \rightarrow i) Let $\Lambda(x) \neq \emptyset$. Then there exists $y \in X$ and a net $\{f_\alpha\}$ in $I(X)$ with $f_\alpha \rightarrow \infty$ such that $f_\alpha(x) \rightarrow y$. Thus for every $\varepsilon > 0$ there exists β such that $f_\alpha(x) \in B(y, \varepsilon)$ for every $\alpha \geq \beta$; therefore $f_\alpha \in ((x, B(y, \varepsilon)))$ for every $\alpha \geq \beta$. But $f_\alpha \rightarrow \infty$, so $((x, B(y, \varepsilon)))$ is not relatively compact, for every $\varepsilon > 0$. This completes the proof.

4.6 Corollary: Let (X, d) be a locally compact $I(X)$ -space and $x \in X$ such that $\Lambda(x)$ is closed. Then the following statements are equivalent:

(i) $\Lambda(x) = \emptyset$.

(ii) There exists $\varepsilon > 0$ such that $((x, B(x, \varepsilon)))$ is relatively compact.

Proof: i \rightarrow ii) By Th.4.5.

ii \rightarrow i) Let $\Lambda(x) \neq \emptyset$. Since $\Lambda(x)$ is closed then it follows from Th.3.5, $x \in \Lambda(x)$. So there exists a net $\{f_\alpha\}$ in $I(X)$ with $f_\alpha \rightarrow \infty$ such that $f_\alpha(x) \rightarrow x$. Thus for every $\varepsilon > 0$ there exists β such that $f_\alpha(x) \in B(x, \varepsilon)$, for every $\alpha \geq \beta$. Then $f_\alpha \in ((x, B(x, \varepsilon)))$ for every $\alpha \geq \beta$. But $f_\alpha \rightarrow \infty$ then $((x, B(x, \varepsilon)))$ is not relatively compact for every $\varepsilon > 0$. This completes the proof.

4.7 Corollary: Let (R, d) be the usual metric space. Then $I(R)$ is locally compact.

Proof: First we will calculate $I(R)$. Let $f \in I(R)$ and $r \in R$ such that $r > 0$. Since f is an isometry then $|f(r) - f(0)| = |r - 0| = r$, so either $f(r) = r + f(0)$ or $f(r) = -r + f(0)$. Take $f(r) = r + f(0)$. Now, let $s \in R$ such that $s \neq 0$. Since f is an isometry then $|f(r) - f(s)| = |r - s|$. Also $|f(s) - f(0)| = |s|$. Notice that if $f(s) = -s + f(0)$, then we have $|r - s| = |r + s|$, thus either $r = 0$ or $s = 0$ and this contradicts that $r \neq 0$ and $s \neq 0$. So $f(s) = s + f(0)$. Similarly if $f(r) = -r + f(0)$, we have $f(s) = -s + f(0)$ for every $s \in R$ such that $s \neq 0$. So if $r < 0$ then $-r > 0$. Thus also we have $f(s) = s + f(0)$ and $f(s) = -s + f(0)$ for

every $s \neq 0$. Thus $I(R)$ is the set of all translations and reflections that is followed by translations. Let $y \in R$, we want to prove that $((0, B(y, 1)))$ is a relatively compact. Notice that,

$$\begin{aligned} ((0, B(y, 1))) &= \{f \in I(R) / f(0) \in B(y, 1)\} \\ &= \{f \in I(R) / |f(0) - y| < 1\} \\ &= \{f \in I(R) / y - 1 < f(0) < 1 + y\} \end{aligned}$$

Let $\{f_\alpha\}$ be any net in $((0, \overline{B(y, 1)}))$. Thus $y - 1 \leq f_\alpha(0) \leq 1 + y$ for every α . Since $[y - 1, 1 + y]$ is a compact set in R , then there exists $t \in [y - 1, 1 + y]$ and a subnet $\{f_\beta\}$ of $\{f_\alpha\}$ such that $f_\beta(0) \rightarrow t$. We can choose a subnet $\{f_\gamma\}$ of $\{f_\beta\}$ such that either $f_\gamma(r) = r + f_\gamma(0)$ for every γ or $f_\gamma(r) = -r + f_\gamma(0)$ for every γ . Take $f_\gamma(r) = r + f_\gamma(0)$ for every γ . Thus for every $x \in R$, $f_\gamma(x) = x + f_\gamma(0) \rightarrow x + t$ (since $f_\gamma(0) \rightarrow t$), here we define $f: R \rightarrow R$ by $f(x) = x + t$ for every $x \in R$, thus $f \in I(R)$ and $f_\gamma \rightarrow f$. So a net $\{f_\alpha\}$ has a convergent subnet. Thus $((0, \overline{B(y, 1)}))$ is compact. But $((0, \overline{B(y, 1)})) \subseteq ((0, \overline{B(y, 1)}))$, then $((0, B(y, 1)))$ is relatively compact for every $y \in R$. Thus by Th.4.5, $\Lambda(0) = \phi$. Hence by Th.4.4,i, $I(R)$ is locally compact.

Also in this section we study the relation between proper $I(X)$ -space and local compactness. We now introduce the definition of proper G -space.

Let f be a function from a topological space X into a topological space Y , f is said to be proper if f is continuous and the function $f \times i_Z: X \times Z \rightarrow Y \times Z$ is closed for every topological space Z , and if X is a G -space then X is said to be proper G -space if the function $\theta: G \times X \rightarrow X \times X$ define by $\theta(g, x) = (x, gx)$ is proper, (2).

4.8 Lemma ,(9): Let X be a G -space. Then X is a proper G -space if and only if $J(x) = \phi$ for every $x \in X$, (where X and G are Hausdorff spaces).

Since for $I(X)$ -space, $\Lambda(x) = J(x)$ for every $x \in X$, Th.3.2, then we get:-

4.9 Proposition: Let (X, d) be an $I(X)$ -space. Then X is proper iff $\Lambda(x) = \phi$ for every $x \in X$.

4.10 Corollary: Let (X, d) be a discrete $I(X)$ -space. Then X is proper iff there exists $x \in X$ such that $\Lambda(x) = \phi$.

Proof: \rightarrow). By Prop.4.9.

\leftarrow). Let there exist $x \in X$ such that $\Lambda(x) = \phi$. Suppose that there exists $y \in X$ such that $\Lambda(y) \neq \phi$. Since X is a discrete space, then $\Lambda(y)$ is closed, so by Th.3.5, $y \in \Lambda(y)$. Thus there exists a net $\{f_\alpha\}$ in $I(X)$ with $f_\alpha \rightarrow \infty$.

and $f_\alpha(y) \rightarrow y$. Define $f: X \rightarrow X$, by $f(t) = t$ for every t distinct from x , y and $f(x) = y$, $f(y) = x$. Thus it is clear that $f \in I(X)$. Since f_α is an isometry for every α , then

$$\begin{aligned} d(f_\alpha(y), y) &= d(y, f_\alpha^{-1}(y)) \\ &= d(f(x), f_\alpha^{-1}(y)) \quad (\text{Since } y = f(x)) \\ &= d(f_\alpha(f(x)), y) \end{aligned}$$

Since $f_\alpha(y) \rightarrow y$ then by Lemma 1.1, $(f_\alpha \circ f)(x) \rightarrow y$. But we have $f_\alpha \rightarrow \infty$, so $y \in \Lambda(x)$, a contradiction. Then X is proper.

4.11 Corollary: Let (R, d) be the usual metric space. Then R is a proper $I(R)$ -space.

Proof: From the proof of Cor.4.7, we have $\Lambda(0) = \emptyset$. We want to prove $\Lambda(x) = \emptyset$ for every $x \in R$. Suppose that there exist $x \in R$ such that $\Lambda(x) \neq \emptyset$. Thus there exists $y \in \Lambda(x)$ and a net $\{f_\alpha\}$ with $f_\alpha \rightarrow \infty$ such that $f_\alpha(x) \rightarrow y$. Define $f: R \rightarrow R$ by $f(t) = -t + y$. Thus it is clear that $f \in I(R)$. Notice that $f(y) = 0$. Since $f_\alpha(x) \rightarrow y$, then by Lemma 1.1 and f is an isometry, $(f \circ f_\alpha)(x) \rightarrow 0$. Since $f \circ f_\alpha$ is an isometry for every α then $x \in \Lambda(0)$ which is contradiction. Thus $\Lambda(x) = \emptyset$ for every $x \in R$. So by Prop.4.9, R is a proper $I(R)$ -space.

4.12 Corollary: Let (X, d) be a locally compact $I(X)$ -space. If X is a proper $I(X)$ -space then:

- (i) $I(X)$ is locally compact.
- (ii) $I(X)$ is closed in X^X .

Proof: By Prop.4.9 and Th.4.4.

The converse of Cor.4.12 is not true in general, see the following example.

4.13 Example: Let R be the set of all real numbers and let $X = Y \cup \{(1, 0)\}$, where $Y = \{(0, y) / y \in R\}$ and $d = \min\{1, \delta\}$, where δ denotes the Euclidian metric. Then $I(X)$ is locally compact and closed but X is not proper.

Solution: Since $(0, y) \in Y$, then

$$\overline{B((0, y), 1/2)} = \{(0, x) \in X / |x - y| \leq 1/2\} = \{(0, x) \in X / y - 1/2 \leq x \leq y + 1/2\}$$

Notice that $(1, 0) \notin \overline{B((0, y), 1/2)}$, thus $((0, 0), \overline{B((0, y), 1/2)})$ is relatively compact for every $(0, y) \in Y$ (see the proof of Cor.4.6). It is clear that $f(1, 0) = (1, 0)$ for every $f \in I(X)$. Thus $((0, 0), \overline{B((1, 0), 1/2)}) = \emptyset$. Then we have $((0, 0), \overline{B(z, 1/2)})$ is relatively compact, for every $z \in X$. Thus by Th.4.5, $\Lambda((0, 0)) = \emptyset$. So by Th.4.4, $I(X)$ is closed and locally compact in X^X . We show that X is not proper. For every positive integer n , define $f_n: X \rightarrow X$,

by $f_n((0, y)) = (0, y + n)$, and $f_n((1, 0)) = (1, 0)$. Notice that $f_n \in I(X)$, for every n and $f_n \rightarrow \infty$. Then $(1, 0) \in \Lambda((1, 0))$ (since $f_n((1, 0)) \rightarrow (1, 0)$), thus by Prop.4.9, X is not proper.

REFERENCES

1. BHATIA, N.P., & G.P, SZEGO, Stability theory of dynamical system, Springer-verlag New York –Heidelberg .Berlin (1970).
2. BOURBAKI, N, Elementary of mathematics, General topology, chapter 1-4, Springer-Verlag Berlin Heidelberg New York, (1989).
3. BREDON, G.E, introduction to compact transformation groups, Academic press, N, Y, (1972).
4. DYDO, W, Proper G-spaces, J.Diff. Geometry, 9:565-569(1974).
5. KELLEY, J.L, General topology, Van No strand, Princeton, (1955).
6. MANOUSSOS, A., STRANZALOS, P, On the groups of isometrics on a locally compact metric space, Journal of lie Theory, 13:7-12(2003).
7. MANOUSSOS, A, STRANZALOS, P, The role of connectedness in the structure and the action of group of isometrics of locally compact metric space, arXive: math.GN/0010083 v19 Oct,(2000).
8. WILLARD, S., general topology, Addition-Wesley publishing company, Inc ,(1970).
9. STRANZALOS, P., Action by isometries, Transformation groups, proceedings of a conference ,Osaka ,Japan , Dec :16-21: 319-325(1987).

On Prime and Semiprime Rings With Derivations

Mehsin Jabel Atteya

AL-Mustansiriya University/College of Education/Department of Mathematics

الخلاصة

ان الغرض الرئيسي من هذا البحث هو اعطاء نتائج جديدة حول الحلقات الاولى وشبه الاولى
الحلقات الاولى وشبه الاولى R عندما تسمح للاشتقاق الغير صفري d بتحقيق شروط جديدة على المثالي غير
الصفري في الحلقات

ABSTRACT

The main purpose of the paper is to give some new results on prim and semiprime ring R admitting aderivation d satisfying new conditions on non-zero ideal of R .

Key words: Prime ring, semiprime ring, derivation, central ideal, commutative.

AMS Mathematics Subject Classification 2000: 16W25, 16U80, 16N60, 16U80.

INTRODUCTION

Various authors studied commutativity in prime and semiprime rings admitting aderivations which are centralizing or commuting on a appropriate subsets of these rings. We have shown, H. E. Bell and M. N. Daif (1) proved that, let R be prime ring and U anon-zero right ideal. If R admits a non-zero U^* -dervation d , then either R is commutative or $d^2(U) = d(U)d(U) = \{0\}$. If d is aderivation on R such that $d(x)d(y) + d(xy) = d(y)d(x) + d(yx)$ for all $x, y \in U$, we say that d is a U^* -derivation; and if $d(x)d(y) + d(yx) = d(y)d(x) + d(xy)$ for all $x, y \in U$, we say that d is a U^{**} -derivation. Herstein (2) proved that if R is a prime ring of characteristic not 2 which admits a non-zero derivation such that $d(x)d(y) = d(y)d(x)$ for all $x, y \in R$, then R is commutative. H. E. Bell and W. S. Martindale (3) proved that, let R be a prime ring and U a non-zero right ideal. If R admits a non-zero derivation d such that $[x, d(x)]$ is central for all $x \in U$, then R is commutative. M. N. Daif (4) proved that, let R be a semiprime ring and d a derivation of R with $d^3 \neq 0$. If $[d(x), d(y)] = 0$ for all $x, y \in R$, then R contains a non-zero central ideal. M. N. Daif and H. E. Bell (5) proved that, let R be a semiprime ring a dmitting a derivation d for which either $xy + d(xy) = yx + d(yx)$ for all $x, y \in R$ or $xy - d(xy) = yx - d(yx)$ for all $x, y \in R$. Then R is commutative. A. H. Majeed (6) proved that, let R be a prime ring and U a non-zero right ideal of R . If R admits a non-zero derivations d and g on U , such that $d(xy) = g(yx)$ for all $x, y \in U$. Then either R is commutative, or $d^2(U) = g^2(U) = d(U)d(U) = g(U)g(U) = d(U)g(U) = g(U)d(U) = 0$. Borut Zalar (7) proved that, let R be a semiprime ring, d a derivation of R and $a \in R$ some fixed element, $d(x)d(y) = 0$ for all $x, y \in R$ implies $d = 0$. Mehsein Jabel (8) proved that, let R be a 2-torsion free semi- prime ring and U a non-zero ideal of R . If R admits a non-zero U^{d^2} -derivation d , then R contains a non-zero central

ideal. We say that d is U^{d^2} -derivation, R is a semiprime and U a non-zero ideal of R . If d is a non-zero derivation on R such that $[d(x), d(y)] = [x, y]$ for all $x, y \in U$. In the present paper, we shall study a prime and semiprime rings admitting a derivation d to satisfying new conditions.

Preliminaries:

Throughout this paper, R will represent an associative ring with center $Z(R)$, R denoted a semiprime ring if $aRa = (0)$, with $a \in R$ implies $a = 0$, and called a prime ring if $aRb = (0)$, $a, b \in R$ implies that $a = 0$ or $b = 0$. A prime ring is semiprime but the converse is not true in general. A ring R is said to be n -torsion free, where $n \neq 0$ is an integer, if whenever $nx = 0$, with $x \in R$ then $x = 0$. If U is a non empty subset of R , then the centralizer of U in R , denoted by $C_R(U)$, is defined by: $C_R(U) = \{ a \in R \mid ax = xa \text{ for all } x \in U \}$. If $a \in C_R(U)$ we say that a centralizes U . An additive map d from R to R is called a derivation if $d(xy) = d(x)y + xd(y)$ for all $x, y \in R$, and we say a derivation d acts as a homomorphism if $d(xy) = d(x)d(y)$ for all $x, y \in U$, U a non-zero ideal of R . A map $d: R \rightarrow R$ is said to centralizing on U (resp. commuting on U) if $[x, d(x)] \in Z(R)$ for all $x \in U$ (resp. $[x, d(x)] = 0$ for all $x \in U$) and let n be a positive integer, d is said to be n -centralizing on U (resp. n -commuting on U), if $[x^n, d(x)] \in Z(R)$ for all $x \in U$ (resp. $[x^n, d(x)] = 0$ for all $x \in U$). We write $[x, y] = xy - yx$ and $xoy = xy + yx$. Note that important identities $[x, yz] = y[x, z] + [x, y]z$ and $[xy, z] = x[y, z] + [x, z]y$. Moreover, we shall require the following known results,

Lemma 1 (9)

Let n be a fixed integer, let R be $n!$ -torsion free semiprime ring and U be a non-zero left ideal of R . If R admits a derivation d which is non-zero on U and n -centralizing on U , then R contains a non-zero central ideal.

Lemma 2 (10)

Let R be a prime ring and U is a non-zero left ideal of R . If R admits a derivation d with $d(U) \neq \{0\}$, satisfies one of the following conditions:

- (i) d is centralizing on U .
- (ii) d is skew-centralizing on U . Then R is commutative.

Lemma 3 [5 : Lemma 1]

Let R be a semiprime ring and U be a non-zero ideal of R . If z in R centralizes the set $[U, U]$, then z centralizes U .

Lemma 4 [11 : Lemma 3]

If the prime ring R contains a commutative non-zero right ideal U , then R is commutative.

Lemma 5 [12: Main Theorem]

Let R be a semiprime ring, d a non-zero derivation of R , and U a non-zero left ideal of R . If for some positive integers t_0, t_1, \dots, t_n and all $x \in U$, the identity $[[\dots[[d(x^{t_0}), x^{t_1}], x^{t_2}], \dots], x^{t_n}] = 0$ holds, then either $d(U) = 0$ or else $d(U)$ and $d(R) \cap U$ are contained in a non-zero central ideal of R . In particular when R is a prime ring, R is commutative.

Lemma 6 (10)

Let R be a prime ring with center $Z(R)$, and let U be a non-zero ideal of R . If U is a commutative ideal, then R is commutative.

Lemma 7 [13: Lemma 3.1]

Let R be a semiprime ring and $a \in R$ some fixed element. If $a[x, y] = 0$ for all $x, y \in R$, then there exists an ideal U of R such that $a \in U \subseteq Z(R)$ holds.

The Main Results:**Theorem 1**

Let R be a 2-torsion free semiprime ring and U a non-zero ideal of R . If R admitting a non-zero derivation d satisfying $yx \pm d([x, y]) = xy \pm d([y, x])$ for all $x, y \in U$. Then $d(U)$ centralizes $[U, U]$.

Proof:

We suppose that first when $d \neq 0$, then

$$yx - d([x, y]) = xy - d([y, x]) \text{ for all } x, y \in U. \text{ Then we can be rewritten as}$$

$$[y, x] = 2 d([x, y]) \text{ for all } x, y \in U. \quad (1)$$

Replacing y by z and x by $[x, y]$, we obtain

$$z[x, y] - d([x, y], z) = [x, y]z - d([z, [x, y]]). \text{ Then}$$

$$z[x, y] - d([x, y]z) + d(z[x, y]) = [x, y]z - d(z[x, y]) + d([x, y]z).$$

Thus we get

$$z[x, y] - 2 d([x, y])z - 2 [x, y]d(z) + 2z d([x, y]) - [x, y]z + 2 d(z)[x, y] = 0$$

for all $x, y, z \in U$. Now according to (1), we have.

$$2 d(z)[x, y] - 2[x, y]d(z) = 0 \text{ for all } x, y, z \in U. \quad (2)$$

Since R is 2-torsion free, we obtain $[d(z), [x, y]] = 0$ for all $x, y, z \in U$.

Thus $d(U)$ centralizes $[U, U]$.

We obtain same result when $yx + d([x, y]) = xy + d([y, x])$ for all $x, y \in U$.

Corollary 1

Let R be a prime ring with $\text{char} \neq 2$ and U an ideal of R . If R admitting a derivation d satisfying $yx \pm d([x, y]) = xy \pm d([y, x])$ for all $x, y \in U$, then R is commutative.

Proof:

When we have $d \neq 0$, then

$yx - d([x,y]) = xy - d([y,x])$ for all $x,y \in U$. Then

$[y,x] = 2 d([x,y])$ for all $x,y \in U$.

(3)

Replacing y by xy , we obtain

$x[y,x] = 2 d(x[x,y])$ for all $x,y \in U$. Then

$x[y,x] = 2 d(x)[x,y] + 2 xd([x,y])$ for all $x,y \in R$.

$x[y,x] = 2 d(x)[x,y] + x[y,x]$ for all $x,y \in U$.

According to (3), the above calculation reduces to

$2 d(x)[x,y] = 0$ for all $x,y \in U$. Since $\text{char.} R \neq 2$, we get

$d(x)[x,y] = 0$ for all $x,y \in U$. By Lemma (7), we obtain

$d(x) \in U \subset Z(R)$, for all $x \in U$. By Lemma (6), we get

R is commutative. Similarly when $d = 0$.

We obtain same result when $yx + d([x,y]) = xy + d([x,y])$ for all $x,y \in U$.

Remark 1

In Theorem 1, when $d = 0$, then U is non central ideal.

The following example illustrate this remark.

Example1

Let $R = \left\{ \begin{pmatrix} g & h \\ 0 & 0 \end{pmatrix} \mid g, h \in F \right\}$ be a ring over a field F ;

and $U = \left\{ \begin{pmatrix} a & 0 \\ 0 & 0 \end{pmatrix} \mid a \in F \right\}$ be one-sided ideal of R . Then U is commutative ideal but non central ideal.

Theorem 2

Let R be a 2-torsion free semiprime ring and U a non-zero ideal of R . If R admits a non-zero derivation d such that

$yx \pm d([x,y]) = xy \pm d([y,x])$ for all $x,y \in U$. Then R contains a non-zero central ideal.

Proof:

From Theorem 1, we obtain $d(U)$ centralizes $[U,U]$, then by Lemma (3), $d(U)$ centralizes U . Then by Lemma (1) R contains a non-zero central ideal.

Theorem 3

Let R be a 2-torsion free semiprime ring and U a non-zero ideal of R . If R admitting a non-zero derivation d satisfying $d(y) - d(x) = d([x,y])$ for all $x,y \in U$. Then R contains a non-zero central ideal.

Proof:

We have $d(y) - d(x) = d([x,y])$ for all $x,y \in U$. Then

$d(y) - d(x) = d(x)y + xd(y) - d(y)x - yd(x)$ for all $x,y \in U$. Thus

$$d(y) - d(x) = [d(x), y] + [x, d(y)] \text{ for all } x, y \in U. \quad (4)$$

Replacing xy for y , we get

$$d(xy) - d(x) = [d(x), xy] + [x, d(xy)] \text{ for all } x, y \in U. \text{ Then}$$

$$d(x)y + xd(y) - d(x) = x[d(x), y] + [d(x), x]y + [x, d(x)y] + [x, xd(y)] \text{ for all } x, y \in U.$$

$$d(x)y + xd(y) - d(x) = x[d(x), y] + [d(x), x]y + d(x)[x, y] + [x, d(x)]y + x[x, d(y)] \text{ for all } x, y \in U.$$

Since we have $[d(x), x]y + [x, d(x)]y = 0$ for all $x, y \in U$. Therefore, the above calculation reduces to

$$d(x)y + xd(y) - d(x) = x([d(x), y] + [x, d(y)]) + d(x)[x, y] \text{ for all } x, y \in U.$$

According to (4) we obtain

$$d(x)[x, y] = d(x)y + xd(x) - d(x) \text{ for all } x, y \in U. \quad (5)$$

Replacing y by x , we obtain

$$d(x)x + xd(x) - d(x) = 0 \text{ for all } x \in U. \quad (6)$$

Then

$$d(x^2) = d(x) \text{ for all } x \in U. \quad (7)$$

Multiplying (7) from left by y , we obtain

$$yd(x^2) = yd(x) \text{ for all } x, y \in U. \quad (8)$$

Multiplying (7) from right by y , we obtain

$$d(x^2)y = d(x)y \text{ for all } x, y \in U. \quad (9)$$

By subtracting (8) from (9) gives

$$[d(x^2), y] - [d(x), y] = 0 \text{ for all } x, y \in U. \quad (10)$$

Replacing x by $-x$, we get

$$[d(x^2), y] + [d(x), y] = 0 \text{ for all } x, y \in U. \quad (11)$$

From (10) and (11), we obtain

$$2[d(x^2), y] = 0 \text{ for all } x, y \in U. \quad (12)$$

Since R is 2-torsion free, we have

$$[d(x^2), y] = 0 \text{ for all } x, y \in U. \quad (13)$$

Now replacing y by x and using Lemma (1), we obtain R contains a non-zero central ideal.

Corollary 2

Let R be a prime ring with $\text{char.} \neq 2$ and U a non-zero ideal of R . If R admitting a non-zero derivation d satisfying $d(y) - d(x) = d([x, y])$ for all $x, y \in U$. Then R is commutative.

Proof:

From (13) in Theorem 3, we have $[d(x^2), y] = 0$ for all $x, y \in U$. By using (4) in same theorem, we get $[d(x), y] = 0$ for all $x, y \in U$. Replacing y by x and using Lemma (2(i)) we have R is commutative.

Theorem 4

Let R be a prime ring and U a non-zero ideal of R . If R admitting a non-zero derivation d satisfying $d([x, y], z) = 0$ for all $x, y, z \in U$ with $d([U, U]) \neq 0$. Then R is commutative.

Proof:

First we have $d([x,y],z) = 0$ for all $x,y,z \in U$.

Then $d([x,y]z) - d(z[x,y]) = 0$ for all $x,y,z \in U$.

Now we have,

$$d([x,y])z + [x,y]d(z) - d(z)[x,y] - zd([x,y]) = 0 \text{ for all } x,y,z \in U. \text{ Thus} \\ [d([x,y]),z] + [[x,y],d(z)] = 0 \text{ for all } x,y,z \in U. \quad (14)$$

Replacing z by $z[x,y]$, we obtain

$$[d([x,y]),z[x,y]] + [[x,y],d(z)[x,y] + zd([x,y])] = 0 \text{ for all } x,y,z \in U. \\ z[d([x,y]),[x,y]] + [d([x,y]),z][x,y] + [[x,y],d(z)[x,y]] + [[x,y],zd([x,y])] = 0 \\ \text{for all } x,y,z \in U. \text{ Then}$$

$$z[d([x,y]),[x,y]] + [d([x,y]),z][x,y] + [[x,y],d(z)[x,y]] + z[[x,y],d([x,y])] + \\ [[x,y],z]d([x,y]) = 0 \text{ for all } x,y,z \in U.$$

Then

$$z([d([x,y]),[x,y]] + [[x,y],d([x,y])]) + ([d([x,y]),z] + [[x,y],d(z)])[x,y] + \\ [[x,y],z]d([x,y]) = 0 \text{ for all } x,y,z \in U. \text{ Then since we have} \\ [d([x,y]),[x,y]] + [[x,y],d([x,y])] = 0 \text{ and according to (14), we obtain} \\ [[x,y],z]d([x,y]) = 0, x,y,z \in U. \quad (15)$$

Replacing z by rz , $r \in R$, we obtain

$$r[[x,y],z]d([x,y]) + [[x,y],r]z d([x,y]) = 0 \text{ for all } x,y,z \in U, r \in R. \text{ According} \\ \text{to (15), we obtain}$$

$$[[x,y],r] U d([x,y]) = 0 \text{ for all } x,y \in U, r \in R. \quad (16)$$

Then

$$[[x,y],r] U R d([x,y]) = 0 \text{ for all } x,y \in U, r \in R. \quad (17)$$

Since R is a prime ring and $d([U,U]) \neq 0$, we obtain

$$[[x,y],r] U = 0 \text{ for all } x,y \in U, r \in R. \text{ Then}$$

$[[x,y],r] R U = 0$ for all $x,y \in U, r \in R$. Since R is prime ring and U a non-zero ideal of R , then we have

$[[x,y],r] = 0$ for all $x,y \in U, r \in R$. Then by Lemma (3), U is commutative, therefore, by Lemma (4), R is commutative.

Theorem 5

Let R be a semiprime ring and U a non-zero ideal of R . If R admits a non-zero derivation d such that $d([x,y]) = xy$ for all $x,y \in U$. Then R contains a non-zero central ideal.

Proof:

First we have $d([x,y]) = xy$ for all $x,y \in U$.

Now, for all $x,y,z \in U$. We have

$$d([x,y],z) = [x,y]z. \text{ Then}$$

$$d([x,y])z + [x,y]d(z) - d(z)[x,y] - zd([x,y]) = [x,y]z. \text{ Then}$$

according the relation $d([x,y]) = xy$, we obtain

$$xyz + [x,y]d(z) - d(z)[x,y] - zxy = xyz - yxz. \text{ Thus}$$

$$[x,y]d(z) - d(z)[x,y] + yxz - zxy = 0 \text{ for all } x,y,z \in U.$$

Replacing y by x , we obtain

$[z, x^2] = 0$ for all $x, z \in U$. $z[d(x), x^2] + [z, x^2]dx = 0$ for all $x, z \in U$ since we have $[z, x^2] = 0$, therefore we get $z[d(x), x^2] = 0$ for all $x, z \in U$. Replacing z by $zd(x)$, we get

$zr[d(x), x^2] = 0$ for all $x, z \in U, r \in R$. Replacing z by $d(x)x$ and r by xr , we obtain

$d(x)x^2r[d(x), x^2] = 0$ for all $x \in U, r \in R$. Again replacing z by x^2 and r by $d(x)r$, we get

$x^2d(x)r[d(x), x^2] = 0$ for all $x \in U, r \in R$. Subtracting our equations, we obtain

$[d(x), x^2]r[d(x), x^2] = 0$ for all $x \in U, r \in R$. Since R is semiprime with using Lemma (1), we obtain R contains a non-zero central ideal.

By depend on Theorem 5 we can easy to proof the following corollary.

Corollary 3

Let R be a prime ring and U a non-zero ideal of R . If R admits a non-zero derivation d such that $d([x, y]) = xy$ for all $x, y \in U$. Then R is commutative.

Theorem 6

Let R be a prime ring and U a non-zero right ideal of R . If R admits a non-zero U^* - or U^{**} -derivation d with $d^2(U) + d(U) \neq 0$. Then R is commutative.

Proof:

Since d is a U^* -derivation, we have $[d(x), d(y)] = -d([x, y])$ for all $x, y \in U$. Then

$$[d(x), d(y)] = [d(y), x] + [y, d(x)] \text{ for all } x, y \in U. \quad (18)$$

Then by substituting xy for y , we get

$$[d(x), x]d(y) + d(x)[d(x), y] + x[d(x), d(y)] = d(x)[y, x] + ([d(x), x] + [x, d(x)])y + x([d(y), x] + d(x)) \text{ for all } x, y \in U.$$

According to (18), we have

$$d(x)[y, x] = [d(x), x]d(y) + d(x)[d(x), y] \text{ for all } x, y \in U. \quad (19)$$

Replacing y by yx and using (19), we have

$$[d(x), x]yd(x) + d(x)y[d(x), x] = 0 \text{ for all } x, y \in U. \quad (20)$$

In (19), we substitute $yd(x)$ for y , we obtain

$$\begin{aligned} d(x)y[d(x), x] - [d(x), x]yd^2(x) &= [d(x), x]d(y)d(x) + d(x)[d(x), y]d(x) - \\ &= ([d(x), x]d(y) + d(x)[d(x), y])d(x) - d(x)[y, x]d(x) \text{ for all } x, y \in U. \end{aligned}$$

Now according to (19), we obtain

$$d(x)y[d(x), x] - [d(x), x]yd^2(x) = 0 \text{ for all } x, y \in U. \quad (21)$$

From (20) and (21), we get

$$[d(x), x]y(d^2(x) + d(x)) = 0 \text{ for all } x, y \in U. \quad (22)$$

Thus from (22) we have

$$[d(x), x] UR(d^2(x) + d(x)) = 0 \text{ for all } x \in U. \quad (23)$$

Since R is prime ring and $d^2(U) + d(U) \neq 0$, we obtain

$[d(x), x] RU = 0$ for all $x \in U$. Also since R is prime ring and $U \neq \{0\}$, then we get $[d(x), x] = 0$ for all $x \in U$.

Thus by Lemma (2(i)), R is commutative.

We obtain same result for U^{**} -derivation.

Corollary 4

Let R be a prime ring and U a non-zero right ideal of R . If R admits a non-zero U^* - or U^{**} -derivation d with $d^2(U) = d(U)$, then R is commutative.

Proof:

In (23) of Theorem 6, since R is prime ring and $d^2(U) = d(U)$, we obtain $[d(x), x] RU = 0$ for all $x \in U$.

We complete the proof by same method in Theorem 6.

The next result, we assume that a derivation d acts as a homomorphism.

Theorem 7

Let R be a semiprime ring and U a non-zero ideal of R . If R admits a non-zero U^* - or U^{**} -derivation d . If d acts as a homomorphism, then R contains a non-zero central ideal.

Proof:

Since d a U^* -derivation. We have $[d(x), d(y)] = -d([x, y])$ for all $x, y \in U$.

Replacing x by x^2 , we obtain

$$[d(x)x, d(y)] + [xd(x), d(y)] = -d([x^2, y]) \text{ for all } x, y \in U.$$

Then

$$d(x)[x, d(y)] + [d(x), d(y)]x + x[d(x), d(y)] + [x, d(y)]d(x) = -d([x^2, y]) \text{ for all } x, y \in U.$$

Replacing y by x , we obtain $[x, d(x)^2] = 0$ for all $x \in U$.

Since d acts as a homomorphism, then $[x, d(x^2)] = 0$ for all $x \in U$.

By Lemma (5), R contains a non-zero central ideal.

We obtain same result for U^{**} -derivation.

Acknowledgments. The author would like to thank the referee for her/his useful comments.

REFERENCES

1. H. E. Bell and M. N. Daif. "On derivations and commutativity in prime rings", *Acta Math. Hungar.*, 66(4): 337-343(1995).
2. I.N. Herstein, "A note on derivations" *Canad. Math. Bull.* 21:369-370 (1978).
3. H. E. Bell and W. S. Martindale III, "Centralizing mappings of semiprime rings", *Canad. Math. Bull.*, 30: 92-101(1987).

4. M. N. Daif, "Commutativity results for semiprime rings with derivations", *Internat. J. Math. and Math. Sci.* 21, (3):471- 474(1998).
5. M.N.Daif and H.B.Bell, "Remarks on derivations on semiprime rings", *Internat. J. Math. and Math. Sci.* 15: 205-206(1992).
6. A. H. Majeed, "Derivations on prime and semiprime rings", Ph. D. Thesis, Jilin University, China (1999).
7. Borut Zalar, "On centralizers of semiprime rings", *comment. Math. Univ. Carolinae* 32, 4 :609-614(1991).
8. Mehsin Jabel, "Derivations on semiprime rings", M. Sc. Thesis, Univ. of AL-Mustansiriyah (2004).
9. Q.Deng and H. E. Bell, "On derivations and commutativity on semiprime rings", *Comm. Algebra*, 32: 3703-3713(1995).
10. M. Breser, "Centralizing mappings and derivations in prime rings", *J. Algebra*, 156:385-394(1993).
11. Joseph H. Mayne, "Centralizing mappings of prime rings", *Canad. Math. Bull.* 27 (1)(1984).
12. C. Lanski, "An Engel condition with derivation for left ideals", *Proc. Amer-Math. Soc.* 125 (2) :339-345(1997),.
13. C.A.Muhammad and S.,S.Mohammed, "Generalized inverses of centralizer of semiprime rings", *Aequations Mathematicae*, 71:1-7 (2006).

Approximately Projective Models and The Endomorphism Ring of Approximately Projective Models

Mehdi Sadik Abbas and Maha Abdulazeez Ali

Department of Mathematics, University of Mustansiriyah, Baghdad, Iraq

الخلاصة

نقدم في هذا البحث مفهوم المقاسات الإسقاطية تقريباً كإعصام لمفهوم المقاسات الإسقاطية و كذلك نعطي عدداً من التشخيصات لهذا المفهوم ونناقش بعضاً من خواصه. في هذا البحث ندرس حلقة التشاكلات للمقاسات الإسقاطية تقريباً وكذلك نقدم مفهوم المقاسات الجزئية الصغيرة تقريباً ودراسة بعض خواص هذا المفهوم.

ABSTRACT

As a generalization to the concept of projective modules, we introduce the concept of approximately projective modules. We also give characterization of this concept and discuss some properties of this type of modules. In this paper we study the endomorphism ring of approximately projective and some results. We introduce the concept of approximately-small submodules of an R -module M and some properties of this concept.

INTRODUCTION

Throughout this paper R will denote a commutative ring with identity and all modules are left R -module. The Jacobson radical of R is denoted by $J(R)$ which is the intersection of all maximal ideals in R . Recall that an R -module P is nearly projective, if for each R -epimorphism $f: M \rightarrow N$ (where M and N are R -modules), and every R -homomorphism $g: P \rightarrow N$, there exists an R -homomorphism $h: P \rightarrow M$ such that $(f \circ h)(a) - g(a) \in J(N)$, $\forall a \in P$ [1]. We call an R -module M is approximately-projective module (for short AP-projective module), if for each R -epimorphism $\alpha: A \rightarrow B$ (where A and B are R -modules) and every R -homomorphism $f: M \rightarrow B$, there exists an R -homomorphism $g: M \rightarrow A$ such that $(\alpha \circ g)(a) - f(a) \in J(R)B$, $\forall a \in M$. Clearly every projective module is AP-projective, but the converse is not true. In general, with $J(R) = 0$, then the converse is true. Recall that, a ring R which satisfies $J(P) = J(R)P$ for every module ${}_R P$ is called a good ring [2]. We see that every AP-projective module is nearly projective, but the converse is not true. In general, with R is a good ring, then the converse is true. Finally we have approximate projectivity is an intermediate between projectivity and near projectivity. As a generalization of a pure submodule, we introduced the concept of approximately-pure (for short AP-pure).

In section 2, we study this class of modules which is an intermediate between the class of projective modules and the class of nearly projective modules and satisfies some properties similar to that of projective modules,

for examples we prove that the tensor product of two AP-projective modules is AP-projective and

if $M = \bigoplus_{\alpha \in \Lambda} M_{\alpha}$, then M is AP-projective module iff each M_{α} is AP-projective module.

In section 3, we study the endomorphism ring of AP-projective modules. We introduce the concept of approximately-dense subring of $S = \text{End}_R(M)$ and we prove that $\Delta = \{f \in S \mid \text{Im}(f) \text{ is AP-small in } M\}$ is AP-dense in S where M is AP-projective R -module.

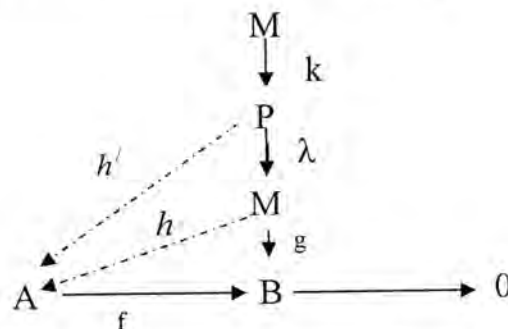
AP-PROJECTIVE MODULES

Recall that R -modules A and B are epi-equivalent, if there exist an R -epimorphism $f: A \rightarrow B$ and an R -epimorphism $g: B \rightarrow A$. We denote it by $A \equiv B$ [3].

We call an R -module M is approximately epi-equivalent to an R -module X , if there exist an R -epimorphism $f: M \rightarrow X$ and an R -homomorphism $g: X \rightarrow M$ such that $(g \circ f)(m) - m \in J(R)M \forall m \in M$. It is clear that epi-equivalent implies that approximately epi-equivalent.

Proposition (2.1): Let P be a projective R -module and M be approximately epi-equivalent to P , then M is AP-projective.

Proof: Let M be an R -module which is approximately epi-equivalent to the projective R -module P . Consider the following diagram:



where $f: A \rightarrow B$ is an R -epimorphism (where A and B are R -modules) and $\lambda: P \rightarrow M$ is an R -epimorphism. Since P is projective, then there exists an R -homomorphism $h': P \rightarrow A$ such that $g \circ \lambda = f \circ h'$. Since M is approximately epi-equivalent to P , then there exists an R -homomorphism $k: M \rightarrow P$ s.t.

$(\lambda \circ k)(m) - m \in J(R)M \forall m \in M$. Defined $h = h' \circ k$.

Hence $g((\lambda \circ k)(m) - m) \in J(R)B \forall m \in M$.

So $(g \circ \lambda \circ k)(m) - g(m) \in J(R)B \forall m \in M$.

Then $(f \circ h' \circ k)(m) - g(m) \in J(R)B \forall m \in M$.

So $(f \circ h)(m) - g(m) \in J(R)B \forall m \in M$. Then M is AP-projective.

Corollary (2.2): Let P be a projective R -module and M be epi-equivalent to P , then M is AP-projective.

Examples (2.3):

(1) $\forall n \in \mathbb{Z}$, Z_n as a \mathbb{Z} -module is not AP-projective. Suppose that Z_n as a \mathbb{Z} -module is AP-projective and let $f: \mathbb{Z} \rightarrow Z_n$ be an epimorphism and consider the following diagram:

$$\begin{array}{ccccc} & & Z_n & & \\ & g \nearrow & \downarrow I_{Z_n} & \searrow & \\ Z & \xrightarrow{f} & Z_n & \xrightarrow{\quad} & 0 \end{array}$$

Let $(\bar{0}) \neq \bar{x} \in Z_n$, then there exists a homomorphism $g: Z_n \rightarrow \mathbb{Z}$ such that $(f \circ g)(\bar{x}) - \bar{x} \in J(\mathbb{Z})Z_n$, but $J(\mathbb{Z})=0$ i.e. $f(g(\bar{x})) = \bar{x} \neq \bar{0} \Rightarrow g(\bar{x}) \neq \bar{0}$, which is a contradiction since $\text{Hom}_{\mathbb{Z}}(Z_n, \mathbb{Z})=0$, so Z_n as a \mathbb{Z} -module is not AP-projective.

(2) In the following example, we shall see that there exists a nearly projective module which is not AP-projective.

The Z_{p^∞} as a \mathbb{Z} -module is nearly projective; it is known that every proper

submodule of Z_{p^∞} is cyclic of the form $(\frac{1}{pn} + \mathbb{Z})$, where $n \in \mathbb{Z}^+$ and p is a prime number, and the submodules in Z_{p^∞} contains a unique ascending chain $0 \subset (\frac{1}{p} + \mathbb{Z}) \subset (\frac{1}{p^2} + \mathbb{Z}) \subset \dots$. It is clear that every submodule of Z_{p^∞} is small, thus $J(Z_{p^\infty}) = Z_{p^\infty}$, i.e. Z_{p^∞} has no maximal submodule, and every module which has no maximal submodule is nearly projective (1). So Z_{p^∞} as a \mathbb{Z} -module is nearly projective, but it is not AP-projective since $J(\mathbb{Z})=0$, and Z_{p^∞} is not a projective \mathbb{Z} -module.

The following theorem gives a characterization of AP-projective modules.

Theorem (2.4): Let M be an R -module. Then M is AP-projective if and only if for each exact sequence $0 \rightarrow K \xrightarrow{i} F \xrightarrow{\pi} M \rightarrow 0$ with F is a free R -module and $K = \text{Ker}(\pi)$, there exists an R -homomorphism $\theta \in \text{End}_R(F)$ that satisfies :

- (1) $\pi \circ \theta(x) - \pi(x) \in J(R)M$ for each x in F .
- (2) $\text{Ker}(\pi) \subseteq \text{Ker}(\theta)$.

Proof: (\Rightarrow) See (1).

(\Leftarrow) Let $f:A \rightarrow B$ be an R -epimorphism (where A and B are R -modules), and $g:M \rightarrow B$ be an R -homomorphism. Let $\{m_\alpha\}_{\alpha \in \Lambda}$ be a generated set of M and

F be a free R -module with basis $\{x_\alpha\}_{\alpha \in \Lambda}$. Define $\pi:F \rightarrow M$ as follows:

$\pi(w) = \sum_{i=1}^n r_{\alpha_i} m_{\alpha_i}$, for each $w \in F$. In particular, $\pi(x_\alpha) = m_\alpha, \forall \alpha \in \Lambda$. It is clear

that π is an R -epimorphism. Then by hypothesis, there exists an R -homomorphism $\theta \in \text{End}_R(F)$ such that

(a) $(\pi \circ \theta)(x) - \pi(x) \in J(R)M \quad \forall x \in F$.

(b) $\text{Ker}(\pi) \subseteq \text{Ker}(\theta)$.

Define $\psi:M \rightarrow F$ as follows:

$$\psi(m) = \psi\left(\sum_{j=1}^k s_j m_{\beta_j}\right) = \sum_{j=1}^k s_j \theta(x_{\beta_j}) = \theta\left(\sum_{j=1}^k s_j x_{\beta_j}\right)$$

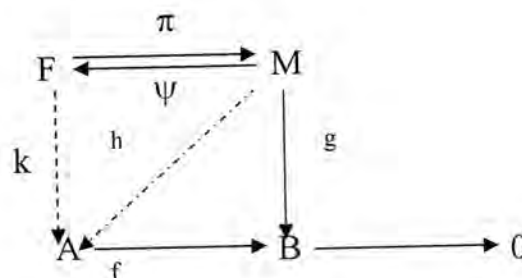
where $m \in M, m = \sum_{j=1}^k s_j m_{\beta_j}$. In particular $\psi(m_\alpha) = \theta(x_\alpha) \quad \forall \alpha \in \Lambda \dots$ (c)

To show that ψ is well defined. Let $\sum_{j=1}^k s_j m_{\beta_j} = \sum_{t=1}^n r_t m_{\delta_t}$. Then

$\sum_{j=1}^k s_j \pi(x_{\beta_j}) = \sum_{t=1}^n r_t \pi(x_{\delta_t})$ which implies that $\pi\left(\sum_{j=1}^k s_j x_{\beta_j} - \sum_{t=1}^n r_t x_{\delta_t}\right) = 0$, thus

$\left(\sum_{j=1}^k s_j x_{\beta_j} - \sum_{t=1}^n r_t x_{\delta_t}\right) \in \text{Ker}(\pi)$. But $\text{Ker}(\pi) \subseteq \text{Ker}(\theta)$ by (b).

Hence $\psi\left(\sum_{j=1}^k s_j m_{\beta_j}\right) = \psi\left(\sum_{t=1}^n r_t m_{\delta_t}\right)$. Now for the following diagram:



Since F is free, then there exists an R -homomorphism $k:F \rightarrow A$ such that $f \circ k = g \circ \pi$. Define $h:M \rightarrow A$ as follows: $h = k \circ \psi$. Now for each element $m_{\alpha_0} \in \{m_\alpha\}_{\alpha \in \Lambda}$. We have:

$(f \circ h)(m_{\alpha_0}) - g(m_{\alpha_0}) = (f \circ k \circ \psi)(m_{\alpha_0}) - g(m_{\alpha_0})$, and by (c) we have
 $(f \circ k)(\psi(m_{\alpha_0})) - g(m_{\alpha_0}) = (g \circ \pi)(\theta(x_{\alpha_0})) - g(\pi(x_{\alpha_0})) = g((\pi \circ \theta)(x_{\alpha_0}) - \pi(x_{\alpha_0}))$ and
 since $(\pi \circ \theta)(x_{\alpha_0}) - \pi(x_{\alpha_0}) \in J(R)M$, then
 $g((\pi \circ \theta)(x_{\alpha_0}) - \pi(x_{\alpha_0})) \in J(R)B$, thus M is AP-projective R -module.

We call an R -homomorphism $\alpha: A \rightarrow B$ approximately-split (for short AP-split), if there exists an R -homomorphism $\beta: B \rightarrow A$ such that $(\alpha \circ \beta)(b) - b \in J(R)B$, for each b in B . In the following theorem, we give several characterizations of AP-projective modules by splitting homomorphisms:

Theorem (2.5): Let M be an R -module. Then the following statements are equivalent:

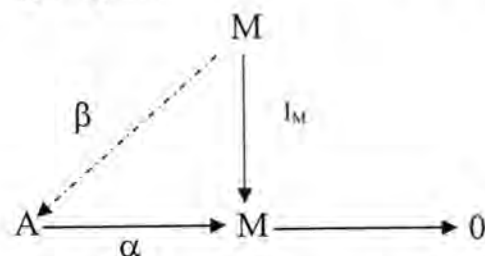
- (1) M is AP-projective.
- (2) Every R -epimorphism $\alpha: A \rightarrow M$ is AP-split for each R -module A .
- (3) Every R -epimorphism $\alpha: F \rightarrow M$ is AP-split for each free R -module F .
- (4) For every family $\{x_i\}_{i \in I}$ of generators of M , there exists a family

$\{f_i\}_{i \in I}$, $f_i \in M^*$ with for each m in M .

(a) $f_i(m) \neq 0$ only for finitely many $i \in I$.

(b) $\sum_{i \in I} f_i(m)x_i - m \in J(R)M$.

Proof: (1) \Rightarrow (2). Let A be an R -module and $\alpha: A \rightarrow M$ be an R -epimorphism and consider the following diagram:



Since M is AP-projective, then there exists an R -homomorphism $\beta: M \rightarrow A$ such that $(\alpha \circ \beta)(m) - m \in J(R)M$. Thus α is AP-split.

(2) \Rightarrow (3). Trivial.

(3) \Rightarrow (4). Let $\{m_i\}_{i \in I}$ be a generated set for M and F be a free R -module over M with basis $\{x_i\}_{i \in I}$ and define $\psi: F \rightarrow M$ as follows:

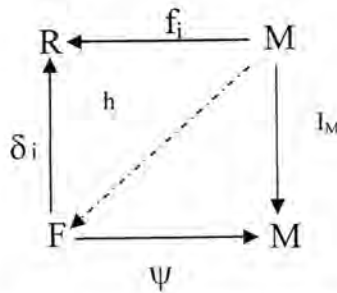
$\psi(y) = \psi(\sum_{i=1}^t r_i x_i) = \sum_{i=1}^t r_i m_i \forall y \in F$. In particular $\psi(x_i) = m_i \forall i \in I$. It is clear that ψ is a well-defined R -epimorphism. Then by hypothesis ψ is AP-split. i.e. there exists an R -homomorphism $h: M \rightarrow F$ such that $(\psi \circ h)(m) - m \in J(R)M$.

Now define a homomorphism $\delta_i: F \rightarrow R$ as follows:

$$\delta_i(x_j) = \begin{cases} 1 & \text{if } i = j \\ 0 & \text{if } i \neq j \end{cases}$$

For each $y \in F$, then $y = \sum_{i=1}^t r_i x_i = \sum_{i=1}^t \delta_i(y) x_i$, and for each $i \in I$

Define $f_i: M \rightarrow R$ as follows: $f_i = \delta_i \circ h$. Consider the following diagram:



Let $a \in M$, then $a = \sum_{j=1}^k s_j m_j, s_j \in R$, it is clear that $f_i(a) = (\delta_i \circ h)(a) \neq 0$ for only

finitely many $i \in I$. Now notice that,

$$\sum_{i \in I} f_i(a) m_i - a = \sum_{i \in I} (\delta_i \circ h)(a) m_i - a = \sum_{i \in I} \delta_i(h(a) \psi(x_i)) - a = \psi \left(\sum_{i \in I} \delta_i(x_i) (h(a)) \right) - a = \psi(h(a)) - a = (\psi \circ h)(a) - a$$

But $(\psi \circ h)(a) - a \in J(R)M$. Then $\sum_{i \in I} f_i(a) m_i - a \in J(R)M$.

(4) \Rightarrow (1). Let $\{x_i\}_{i \in I}$ be a generated set of M . Then there exists a family

$\{f_i\}_{i \in I}$ such that $\forall m \in M$

(a) $f_i(m) \neq 0$ only for finitely many $i \in I$.

(b) $\sum_{i \in I} f_i(m) x_i - m \in J(R)M$.

Let F be a free R -module over M with basis $\{y_i\}_{i \in I}$ and $\pi: F \rightarrow M$ be an epimorphism defined as follows: $\pi(y_i) = x_i, \forall i \in I$. Now define $\theta: F \rightarrow F$ as

follows: let $x \in F$ and since π is an epimorphism, then there exists $a \in M$ such that $\pi(x) = a$. Then $\sum_{i \in I} f_i(a) x_i - a \in J(R)M$ i.e., $a = \sum_{i \in I} f_i(a) x_i + t$ where

$t \in J(R)M$.

Now put $\theta(x) = \sum_{i \in I} f_i(a) y_i$. Notice that

$$(\pi \circ \theta)(x) - \pi(x) = \pi \left(\sum_{i \in I} f_i(a) y_i \right) - \pi(x) = \sum_{i \in I} f_i(a) \pi(y_i) = \sum_{i \in I} f_i(a) x_i - a = t.$$

Thus $(\pi \circ \theta)(x) - \pi(x) \in J(R)M$. Now let $y \in \text{Ker}(\pi)$, then $\pi(y) = 0$, i.e.,

$\theta(y) = \sum_{i \in I} f_i(0)y_i = 0$, then $y \in \text{Ker}(\theta)$, then $\text{Ker}(\pi) \subseteq \text{Ker}(\theta)$. Then by theorem

(2.3), M is AP-projective.

We call statement (4) in the above theorem the Dual-Basis Lemma for AP-projective modules.

Proposition (2.6): If M is AP-projective R -module, then $J(M) = J(R)M$.

Proof: It is clear that $J(R)M \subseteq J(M)$. Now let $m \in J(M)$, then $m \in M$ and by Dual-Basis Lemma of AP-projective modules, then there exist $\{x_i\}_{i \in I}, x_i \in M$, and $\{\varphi_i\}_{i \in I}, \varphi_i \in R^*$ s.t. $\sum_{i \in I} \varphi_i(m)x_i - m \in J(R)M$ and since $m \in J(M)$, then $\varphi_i(m) \in J(R)$. Then $m \in J(R)M$, so $J(M) \subseteq J(R)M$. Then $J(M) = J(R)M$.

It is known that $M = \bigoplus_{i \in I} M_i$ is projective iff only M_i is projective for each

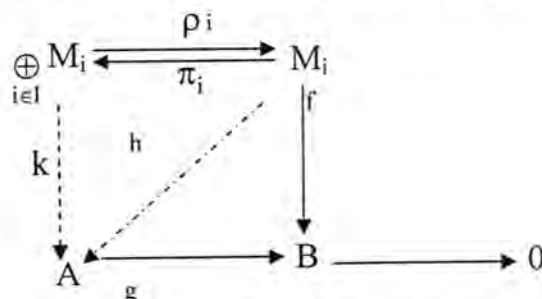
$i \in I$ [2]. A similar result holds for AP-projective R -modules.

Proposition (2.7): Let $M = \bigoplus_{i \in I} M_i$ be a direct sum of R -modules M_i . Then M

is AP-projective if and only if M_i is AP-projective for each $i \in I$.

Proof: Suppose that M is AP-projective, and let $g: A \rightarrow B$ be an R -epimorphism

(where A and B are R -modules). Consider the following diagram:



where $\rho_i: \bigoplus M_i \rightarrow M_i$ is the projection defined by $\rho_i(\varphi) = \varphi(i) \forall i \in I$ and

$\forall \varphi \in M$ i.e. $\varphi: I \rightarrow \bigcup M_i$ s.t. $\varphi(i) \neq 0$ only for finitely many $i \in I$ and

$\pi_i: M_i \rightarrow M$ is defined by: $\pi_i(x_i) = (0, 0, \dots, x_i, 0, 0, \dots)$.

It is clear that $\rho_i \circ \pi_i = I_{M_i}$. Since M is AP-projective, then there exists an

R -homomorphism $k: M \rightarrow A$ s.t. $(g \circ k - f \circ \rho_i)(\varphi) \in J(R)B \forall \varphi \in M$.

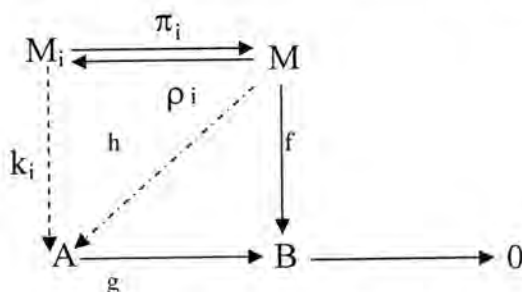
Define $h: M_i \rightarrow A$ as follows: $h = k \circ \pi_i$. Then for each a_i in M_i we have:

$(g \circ h - f)(a_i) = (g \circ k \circ \pi_i - f)(a_i) = (g \circ k)(\pi_i(a_i)) - (f \circ \rho_i)(\pi_i(a_i)) \in J(R)B$ Thus

M_i is AP-projective R -module, $\forall i \in I$.

Conversely, suppose that $\forall i \in I$, M_i is AP-projective R-module and let $g: A \rightarrow B$ be an R-epimorphism (where A and B are R-modules) and $f: M \rightarrow B$ be an R-homomorphism and ρ_i, π_i are defined as above. Since M_i is AP-projective, for each $i \in I$, then there exists an R-homomorphism $k_i: M_i \rightarrow A$ such that

$(g \circ k_i - f \circ \pi_i)(x_i) \in J(R)B$, for each $x_i \in M_i$. Consider the following diagram



Let $\varphi \in M$ i.e. $\varphi: I \rightarrow \cup M_i$ s.t. $\varphi(i) \neq 0$ only for finitely many $i \in I$.

Define $h: M \rightarrow A$ as follows: $h(\varphi) = \sum_{i \in I} (k_i \circ \rho_i)(\varphi) \forall \varphi \in M$. Now for each φ

in M, we have,

$$(g \circ h - f)(\varphi) = (g \circ h)(\varphi) - f(\varphi) = g\left(\sum_{i \in I} (k_i \circ \rho_i)(\varphi)\right) - f\left(\sum_{i \in I} (\pi_i \circ \rho_i)(\varphi)\right) =$$

$$\sum_{i \in I} (g \circ k_i)(\varphi(i)) - \sum_{i \in I} (f \circ \pi_i)(\varphi(i)) \in J(R)B$$

Thus M is AP-projective.

It is known if both M and N are projective R-modules, then so is $M \otimes N$ [2]. In AP-projective R-modules, we see the following proposition:

Proposition (2.8): If both M and N are AP-projective R-modules, then so is $M \otimes N$.

Proof: Since M is AP-projective, then there exist families

$$\{x_i\}_{i \in I}, x_i \in M, \text{ and } \{\varphi_i\}_{i \in I}, \varphi_i \in M^* \text{ s.t. } \sum_{i \in I} \varphi_i(m)x_i - m \in J(R)M$$

$\forall m \in M$ and since N is AP-projective, then there exist

$$\text{families } \{y_j\}_{j \in J}, y_j \in N, \text{ and } \{\delta_j\}_{j \in J}, \delta_j \in N^* \text{ such}$$

that $\sum_{j \in J} \delta_j(n)y_j - n \in J(R)N \forall n \in N$. Now claim that $\{x_i \otimes y_j\}_{i \in I, j \in J}$ and

$$\left\{ \eta \circ (\varphi_i \otimes \delta_j) \right\}_{i \in I, j \in J} \text{ satisfies condition (4) of theorem (2.5) such that}$$

$\eta: R \otimes R \rightarrow R$ defined by $\eta(r_1 \otimes r_2) = r_1 r_2 \quad \forall r_1, r_2 \in R$. Now let $m \otimes n \in M \otimes N$. Then

$$(m - \sum_{i \in I} \varphi_i(m)x_i) \otimes (\sum_{j \in J} \delta_j(n)y_j) + m \otimes (n - \sum_{j \in J} \delta_j(n)y_j) \in J(R) M \otimes N$$

$$(m \otimes \sum_{j \in J} \delta_j(n)y_j) - (\sum_{i \in I} \varphi_i(m)x_i) \otimes (\sum_{j \in J} \delta_j(n)y_j) + m \otimes n - (m \otimes (\sum_{j \in J} \delta_j(n)y_j)) \in J(R) M \otimes N.$$

Thus

$$m \otimes n - (\sum_{i \in I} \varphi_i(m)x_i) \otimes (\sum_{j \in J} \delta_j(n)y_j) \in J(R) M \otimes N$$

Notice that $\eta(\varphi_i(m) \otimes \delta_j(n)) = \varphi_i(m)\delta_j(n)$.

Now

$$\sum_{j \in J} \sum_{i \in I} \varphi_i(m)x_i \otimes \delta_j(n)y_j = \sum_{i \in I} \sum_{j \in J} \varphi_i(m)\delta_j(n)(x_i \otimes y_j) = \sum_{i \in I} \sum_{j \in J} (\eta \circ (\varphi_i \otimes \delta_j))(m \otimes n)(x_i \otimes y_j)$$

$$\text{Then } m \otimes n - (\sum_{i \in I} \sum_{j \in J} (\eta \circ (\varphi_i \otimes \delta_j))(m \otimes n)(x_i \otimes y_j)) \in J(R) M \otimes N$$

Thus $M \otimes N$ is AP-projective R-module.

Recall that a submodule P of an R -module M is said to be pure submodule, if $P \cap IM = IP$ for each ideal I in R . An ideal K of a ring R is a pure ideal in R , if it is a pure submodule of R considered as R -module [4]. As a generalization of a pure submodule, we introduce the following concept:

Defintion (2.9): A submodule N of an R -module M is called approximately-pure submodule (for short AP-pure), if $N \cap IM = IN + J(R)M \cap (N \cap IM)$, for each ideal I of R .

Now, we characterize AP-pure submodule in terms of equation form.

Proposition (2.10): A submodule N of an R -module M is AP-pure if and

only if for every finite subsets $\{m_i\}_{i=1}^n, m_i \in M$, and $\{n_j\}_{j=1}^k, n_j \in N$, and $\{r_{ij}\}_{i,j}, r_{ij} \in R$ s.t. $n_j = \sum_{i=1}^n r_{ij} m_i, \forall j, 1 \leq j \leq k$,

There exist b_i in N , $1 \leq i \leq n$ such that $\sum_{i=1}^n r_{ij} b_i - n_j \in J(R)M \cap N$
 $\forall j, 1 \leq j \leq k$.

Proof: Assume that N is AP-pure submodule of M and I be the ideal of R generated by the elements $\{r_{ij}\}_{i,j}$. Then $N \cap IM = IN + J(R)M \cap (N \cap IM)$.

Now if $n_j \in N \cap IM$, then $n_j \in IN + J(R)M \cap (N \cap IM)$. Hence there exist $b_i \in N, 1 \leq i \leq n$ such that $\sum_{i=1}^n r_{ij} b_i - n_j \in J(R)M \cap N, \forall j, 1 \leq j \leq k$.

Conversely, let I be an ideal of R and $n_j \in N \cap IM, \forall j, 1 \leq j \leq k$. Then

$n_j = \sum_{i=1}^n r_i m_i, r_i \in R$ and $m_i \in M, \forall j, 1 \leq j \leq k$. By the hypothesis, there exist

$b_i \in N, 1 \leq i \leq n$ s.t. $\sum_{i=1}^n r_i b_i - n_j \in J(R)M \cap N, \forall j, 1 \leq j \leq k$. But $\sum_{i=1}^n r_i b_i - n_j$

$\in IM, \forall j, 1 \leq j \leq k$. Hence $\sum_{i=1}^n r_i b_i - n_j \in IM, \forall j, 1 \leq j \leq k$. Thus

$N \cap IM \subseteq IN + J(R)M \cap (N \cap IM)$. The other inclusion is clear. Hence N is AP-pure submodule.

The following corollary is an immediate consequence of the above proposition.

Corollary (2.11): A submodule N of an R -module M is AP-pure if and only if, for each n in N , if $n = \sum_{i=1}^t r_i m_i, r_i \in R$, and $m_i \in M$, then there exist

$b_i \in N$ s.t. $\sum_{i=1}^t r_i b_i - n \in J(R)M \cap N$.

Proposition (2.12): Let M be AP-projective R -module. If N is AP-pure submodule of M and $J(R)M \cap N \subseteq J(R)N$, then N is AP-projective.

Proof: Let M be AP-projective and N be AP-pure submodule of M . If $a \in N$, then $a \in M$ and since M is AP-projective, then exist families $\{x_i\}_{i \in I}, x_i \in M$, and $\{f_i\}_{i \in I}, f_i \in M^*$ s.t. $\sum_{i \in I} f_i(a)x_i - a \in J(R)M$ for each $a \in M$, and since N is AP-pure submodule, then by proposition (2.10), there exist b_i in N , such that $\sum_{i=1}^n f_i(a)b_i - a \in J(R)M \cap N$. Let $\phi_i = f_i|_N$ be the restriction of f_i to N . Then $\sum_{i=1}^n \phi_i(a)b_i - a \in J(R)M \cap N \subseteq J(R)N$. Hence by

Dual-Basis Lemma of AP-projective modules, N is AP-projective.

Corollary (2.13): Let M be AP-projective module over a good ring R . If N is AP-pure submodule of M , then N is AP-projective.

Corollary (2.14): Let M be AP-projective R -module. If N is pure-submodule of M , then N is AP-projective module.

Corollary (2.15): Let M be a projective R -module. If N is pure of M , and $J(R)M \cap N \subseteq J(R)N$, then N is AP-projective.

If M is an R -module, then the trace of M , denoted by T , is defined by $T = \sum_{f \in M^*} f(M)$. (3). Recall that if M is a projective R -module and

$T = \text{trace}(M)$, then $M = TM$ and $T = T^2$ and $\text{ann}_R(M) = \text{ann}_R(T)$ (5). For AP-projective R -modules, we have the following:

Proposition (2.16): Let M be AP-projective R -module.

Then

$$(1) M = TM + J(R)M.$$

$$(2) T = T^2 + J(R) \cap T.$$

$$(3) \text{ann}_R(M) = \text{ann}_R(T) \cap \text{ann}_R(J(R)M).$$

Proof: (1) It is clear that $TM + J(R)M \subseteq M$. Let $m \in M$, then by Dual-Basis Lemma of AP-projective modules, there exist families $\{x_i\}_{i=1}^n, x_i \in M$ and

$$\{\varphi_i\}_{i=1}^n, \varphi_i \in M^* \text{ s.t. } \sum_{i=1}^n \varphi_i(m)x_i - m \in J(R)M. \text{ It is clear that } m \in TM + J(R)M,$$

thus $M \subseteq TM + J(R)M$, then $M = TM + J(R)M$.

(2) It is clear that $T^2 + J(R) \cap T \subseteq T$, and since M is AP-projective, then by Dual-Basis Lemma of A-projective modules, for each m in M there exist families $\{m_i\}_{i=1}^n, m_i \in M$ and $\{f_i\}_{i=1}^n, f_i \in M^* \text{ s.t. } \sum_{i=1}^n f_i(m)m_i - m \in J(R)M.$

Hence $m = \sum_{i=1}^n f_i(m)m_i + k$, where $k \in J(R)M$. Thus, for each $g \in M^*$, we have

$$g(m) \in T \text{ and } g(m) = \sum_{i=1}^n f_i(m)g(m_i) + g(k) \in T^2 + T \cap J(R). \text{ Hence } T \subseteq T^2 + T \cap J$$

(R) . Thus $T = T^2 \cap J(R)$.

(3) let $r \in \text{ann}_R(M)$, thus $rM = 0$, let $t \in T$, $t = \sum_{i=1}^n \varphi_i(m_i)$, where $m_i \in M$

and $\varphi_i \in M^* \forall i, 1 \leq i \leq n$. $rt = r(\sum_{i=1}^n \varphi_i(m_i)) = \sum_{i=1}^n \varphi_i(rm_i) = 0$. Hence $r \in$

$\text{ann}_R(T)$, this implies that $\text{ann}_R(M) \subseteq \text{ann}_R(T)$ and since $J(R)M \subseteq M$, then

$\text{ann}_R(M) \subseteq \text{ann}_R(J(R)M)$. Thus $\text{ann}_R(M) \subseteq \text{ann}_R(T) \cap \text{ann}_R(J(R)M)$. Now let $s \in$

$\text{ann}_R(T) \cap \text{ann}_R(J(R)M)$. Then $sT = 0$ and $s(J(R)M) = 0$. Since M is APP-projective, then by Dual-Basis Lemma of AP-projective modules, $\forall a \in M$

there exist families $\{x_i\}_{i=1}^n, x_i \in M$ and $\{\delta_i\}_{i=1}^n, \delta_i \in M^* \text{ s.t. } \sum_{i=1}^n \delta_i(a)x_i -$

$a \in J(R)M$. So $a = \sum_{i=1}^n \delta_i(a)x_i + k$, where $k \in J(R)M$. Then we have

$$sa = s(\sum_{i=1}^n \delta_i(a)x_i + k) = \sum_{i=1}^n s\delta_i(a)x_i + sk, \text{ thus } s \in \text{ann}_R(M) \text{ which implies that}$$

$\text{ann}_R(T) \cap \text{ann}_R(J(R)M) \subseteq \text{ann}_R(M)$, thus $\text{ann}_R(M) = \text{ann}_R(T) \cap \text{ann}_R(J(R)M)$.

The Endomorphism Ring of Approximately Projective Models

Let M be an R -module and let $S = \text{End}_R(M)$ be the ring of endomorphism of M , we denote the center of ring S by $C(S)$. It is known that if M is a projective R -module, then for each g in $C(S)$, there exists r in R such that $g(m) = rm$ for each $m \in M$ (6).

Proposition (3.1): Let M be AP-projective R -module. Then for each $g \in C(S)$, there exists $r \in R$ such that $g(m) - rm \in J(R)M$ for each m in M .

Proof: Since M is AP-projective, then by Dual-Basis Lemma of AP-projective

modules there exist families $\{m_i\}_{i \in I}$, $m_i \in M$ and $\{f_i\}_{i \in I}$, $f_i \in M^*$ s.t.

$$\sum_{i \in I} f_i(m) m_i - m \in J(R)M. \text{ Hence } m = \sum_{i \in I} f_i(m) m_i + t,$$

where $t \in J(R)M$. Now for each $I \in M^*$ and $a \in M$. We can define $I_a : M \rightarrow M$ by $I_a(x) = I(x)a$, for each x in M . It is clear that $I_a \in S$ and

$$m = \sum_{i \in I} I_{m_i}(m) + t. \text{ Thus for each } g \in C(S) \text{ we have,}$$

$$g(m) = \sum_{i \in I} g(I_{m_i}(m)) + g(t) = \sum_{i \in I} I_{m_i}(g(m)) + g(t) =$$

$$\sum_{i \in I} I_i(g(m_i))m + g(t)$$

$$\text{and } g(t) \in J(R)M. \text{ Put } r = \sum_{i \in I} I_{m_i}(g(m_i)) \in R. \text{ Then } g(m) = rm + g(t)$$

$$\text{Thus } g(m) - rm \in J(R)M.$$

Definition (3.2): A submodule N of R -module M is said to be approximately-small in M (for short AP-small), if whenever $N + K = M$, then $K + J(R)M = M$, for any submodule K of M .

Remarks (3.3):

1. Let M be an R -module. Then, it is clear that every small submodule of M is AP-small.
2. If $J(R)M$ is small in M , then every AP-small submodule of M is small.
3. Let $U \subseteq N \subseteq M$. If N is AP-small in M , then U is AP-small in M .
4. If A_i is AP-small in M , $i = 1, 2, \dots, n$. Then $\sum_{i=1}^n A_i$ is AP-small in M .

Proposition (3.4): Let M be AP-projective R -module and $S = \text{End}_R(M)$ and

$$\Delta = \{f \in S \mid \text{Im}(f) \text{ is AP-small in } M\}. \text{ Then}$$

$$(1) J(S) \subseteq \Delta.$$

$$(2) J(S) \subseteq \text{Hom}_R(M, J(R)M).$$

Proof: (1) Let $f \in J(S)$, and suppose that $\text{Im}(f) + K = M$, where K any submodule of M . Let $\pi: M \rightarrow M/K$ be a natural map.

Then $\text{Im}(f) + K = M$ implies that $\pi \circ f: M \rightarrow M/K$ is an epimorphism and consider the following diagram:

$$\begin{array}{ccccc}
 & & M & & \\
 & \nearrow g & \downarrow \pi & & \\
 M & \xrightarrow{f} & M & \xrightarrow{\pi} & M/K \longrightarrow 0
 \end{array}$$

Since M is AP-projective, then there exists an R -homomorphism $g: M \rightarrow M$ s.t. $(\pi \circ f \circ g)(m) - \pi(m) \in J(R)(M/K) \subseteq (J(R)M)/K \quad \forall m \in M$. Hence $(\pi \circ f \circ g)(m) - \pi(m) \in (J(R)M)/K \quad \forall m \in M$.

Then there exists $t \in J(R)M$ such that $\text{Im} \pi(f \circ g - I)(m) = t + K$. But $I - f \circ g$ is invertible. In particular $I - f \circ g$ is an isomorphism. Hence $\text{Im} \pi(f \circ g - I) = M$. Thus $M \subseteq J(R)M + K$. Then $M = J(R)M + K$.

(2) Let $f \in J(S)$ i.e. $f: M \rightarrow M$, then by (1) we have $\text{Im}(f)$ is AP-small in M . i.e. whenever $\text{Im}(f) + K = M$, for any submodule K of M , then $K + J(R)M = M$. Now $(I - f)(M) + f(M) = M$. But $\text{Im}(f)$ is AP-small. Then $(I - f)(M) + J(R)M = M$

$$\Rightarrow (I - f)(M) - M \in -(J(R)M) \Rightarrow I(M) - f(M) - M \in -(J(R)M)$$

$$\Rightarrow M - f(M) - M \in -(J(R)M) \Rightarrow f(M) \in (J(R)M). \text{ So } f \in \text{Hom}_R(M, J(R)M).$$

$$\text{Then } J(S) \subseteq \text{Hom}_R(M, J(R)M).$$

In the above proposition if $J(R)M$ is small submodule of M , then

$$1. J(S) = \Delta.$$

$$2. J(S) = \text{Hom}_R(M, J(R)M).$$

Let M be an R -module. Then for each element r in R , there exists a ring homomorphism $\phi: R \rightarrow S$ defined by: $\phi(r) = \phi_r$ where $\phi_r(m) = rm$, for each m in M . Now define $[\cdot]: M \times M^* \rightarrow S$ by $[m, f] = f_m$; for each f in M^* and m in M , where $f_m(a) = f(a).m$; for each a in M . We denote by ∇ the ideal generated by the image of $[\cdot]$. See (7).

Let M be an R -module, a subring J of S is said to be dense in S , if $\forall f \in S$ and $\forall m_1, \dots, m_k \in M$, there exists $g \in J$ such that $g(m_i) = f(m_i) \quad \forall i, 1 \leq i \leq k$ see (8). In the following we introduce the concept of approximately-dense subring.

Definition (3.5): Let M be an R -module. A subring J of S is said to be approximately-dense in S (for short AP-dense), if $\forall f \in S$ and $\forall m_1, \dots, m_k \in M$, there exists $g \in J$ such that $g(m_i) - f(m_i) \in J(R)M, \quad \forall i, 1 \leq i \leq n$.

Proposition (3.6): Let M be AP-projective R -module. Then ∇ is AP-dense in S .

Proof: Let $f \in S = \text{End}_R(M)$ and let $\{m_1, \dots, m_k\}$ be a finite subset of M and by Dual-Basis Lemma of AP-projective modules, there exist families $\{x_i\}_{i=1}^n, x_i \in M$, and $\{\varphi_i\}_{i=1}^n, \varphi_i \in M^*$ s.t. $\sum_{i=1}^n \varphi_i(m_j) x_i = m_j \in J(R)M \quad \forall j, 1 \leq j \leq k$. Now $\sum_{i=1}^n \varphi_i(m_j) f(x_i) - f(m_j) \in J(R)M \quad \forall j, 1 \leq j \leq k$. So $\sum_{i=1}^n [f(x_i), \varphi_i](m_j) - f(m_j) \in J(R)M$, put $g = \sum_{i=1}^n [f(x_i), \varphi_i]$, then $g(m_j) - f(m_j) \in J(R)M$, thus ∇ is AP-dense in S .

Let M and N be R -modules, and let $f \in \text{Hom}_R(M, N)$. Then f is said to be nearly compact homomorphism if $f(M)$ is contained in a finitely generated submodule of N . We denote $C_o(H)$ the set of all nearly compact R -homomorphism of $\text{Hom}_R(M, N)$. See (9) i.e. $C_o(H) = \{f \in \text{Hom}_R(M, N) \mid f \text{ is nearly compact}\}$. And $T(M, N) = \sum f(M)$, for each $f \in \text{Hom}_R(M, N)$, then $T(M, N)$ is called the trace of M on N [9]. Now define $\Phi: N \times M^* \rightarrow \text{Hom}_R(M, N)$ by $\Phi(n, f) = f_n$ for each n in N and f in M^* , where $f_n(a) = f(a) \cdot n, \forall a \in M$. Let $F(H)$ be the submodule of $T(M, N)$ generated by $\text{Im}(\Phi)$, and we denote $F(M)$ for $F(H)$ and $C_o(M)$ for $C_o(H)$ [9]. We have the following proposition:

Proposition (3.7): Let M be an R -module and N be AP-projective R -module. Then

(1) $C_o(H) \subseteq F(H) + J(R)N$.

(2) $F(H)$ is AP-dense in $\text{Hom}_R(M, N)$.

Proof:

(1) Let $f \in C_o(H)$, then there exists a finitely generated submodule P of N s.t. $f(M) \subseteq P$, P generated by $\{n_i\}_{i=1}^t$. Now let $a \in M, f(a) = \sum_{i=1}^t r_i n_i, r_i \in R$. Since N is AP-projective, then by Dual-Basis Lemma of AP-projective modules there exist families $\{x_j\}_{j=1}^k, x_j \in N$ and $\{\varphi_j\}_{j=1}^k, \varphi_j \in N^*$ s.t. $\sum_{j=1}^k \varphi_j(n_i) x_j = n_i \in J(R)N, \forall i, 1 \leq i \leq t$. Then $n_i = \sum_{j=1}^k \varphi_j(n_i) x_j + s_i \quad \forall i, 1 \leq i \leq t, s_i$

$$\in J(R)N. \text{ So } f(a) = \sum_{i=1}^t r_i n_i = \sum_{i=1}^t r_i \left(\sum_{j=1}^k \varphi_j(n_i) x_j + s_i \right) = \sum_{j=1}^k \varphi_j \left(\sum_{i=1}^t r_i n_i \right) x_j + \sum_{i=1}^t r_i s_i$$

$$\text{i.e. } f(a) = \sum_{j=1}^k (\varphi_j \circ f)(a) x_j + s \text{ s.t. } s = \sum_{i=1}^t r_i s_i, \text{ put } \psi_j = \varphi_j \circ f \forall j, 1 \leq j \leq k,$$

$$\text{then } f(a) = \sum_{j=1}^k \psi_j(a) x_j + s. \text{ By using definition of } \Phi, \text{ we have } f(a) - \sum_{j=1}^k$$

$$\Phi(x_j, \psi_j)(a) \in J(R)N. \text{ It is clear that } \sum_{j=1}^k \Phi(x_j, \psi_j) \in F(H).$$

(2) let $f \in \text{Hom}_R(M, N)$ and A be a finitely generated submodule of M , generated by $\{a_1, \dots, a_n\}$, then $f(A)$ is a finitely generated submodule of N , and $f(A) = \langle \{Z_1, \dots, Z_s\} \rangle$, $f(a_i) \in N$, $\forall i, 1 \leq i \leq n$, then there exist families

$$\left\{ x_j \right\}_{j=1}^k, x_j \in N \text{ and } \left\{ \varphi_j \right\}_{j=1}^k, \varphi_j \in N^* \text{ such that } \sum_{j=1}^k \varphi_j(f(a_i)) x_j - f(a_i) \in J(R)N, \forall i, 1 \leq i \leq n. \text{ i.e. } \sum_{j=1}^k \Phi(x_j, \varphi_j \circ f)(a_i) - f(a_i) \in J(R)N. \text{ Put}$$

$$g = \sum_{j=1}^k \Phi(x_j, \varphi_j \circ f). \text{ It is clear that } g \in F(H). \text{ Then } g(a_i) - f(a_i) \in J(R)N. \text{ So}$$

$F(H)$ is AP-dense in $\text{Hom}_R(M, N)$.

Corollary (3.8): Let M be AP-projective R -module. Then

(1) $C_o(M) \subseteq F(M) + J(R)M$.

(2) $F(M)$ is AP-dense in $S = \text{Hom}_R(M, M)$.

Proof:

(1) Let $f \in C_o(H)$, then there exists a finitely generated submodule P of M s.t.

$f(M) \subseteq P$, P generated by $\{m_i\}_{i=1}^t$. Now let $a \in M$, $f(a) = \sum_{i=1}^t r_i m_i$, $r_i \in R$. Since

M is AP-projective, then by Dual-Basis Lemma of AP-projective modules

there exist families $\left\{ x_j \right\}_{j=1}^k$, $x_j \in M$ and $\left\{ \varphi_j \right\}_{j=1}^k$, $\varphi_j \in M^*$ s.t. $\sum_{j=1}^k \varphi_j(m_i)$

$$x_j - m_i \in J(R)M, \forall i, 1 \leq i \leq t. \text{ Then } m_i = \sum_{j=1}^k \varphi_j(m_i) x_j + s_i \forall i, 1 \leq i \leq t, s_i$$

$$\in J(R)M. \text{ So } f(a) = \sum_{i=1}^t r_i m_i = \sum_{i=1}^t r_i \left(\sum_{j=1}^k \varphi_j(m_i) x_j + s_i \right) = \sum_{j=1}^k \varphi_j \left(\sum_{i=1}^t r_i m_i \right) x_j + \sum_{i=1}^t r_i s_i$$

$$x_j + \sum_{i=1}^t r_i s_i$$

i.e. $f(a) = \sum_{j=1}^k (\varphi_j \circ f)(a)x_j + s$ s.t. $s = \sum_{i=1}^l r_i s_i$, put $\psi_j = \varphi_j \circ f \forall j, 1 \leq j \leq k$,
then $f(a) = \sum_{j=1}^k \psi_j(a)x_j + s$. By using definition of Φ , we have $f(a) - \sum_{j=1}^k$

$\Phi(x_j, \psi_j)(a) \in J(R)M$. It is clear that $\sum_{j=1}^k \Phi(x_j, \psi_j) \in F(H)$.

(2) let $f \in S = \text{Hom}_R(M, M)$ and A be a finitely generated submodule of M , generated by $\{a_1, \dots, a_n\}$, then $f(A)$ is a finitely generated submodule of M , and $f(A) = \langle \{Z_1, \dots, Z_s\} \rangle$, $f(a_i) \in M, \forall i, 1 \leq i \leq n$, then there exist families

$\{x_j\}_{j=1}^k, x_j \in M$ and $\{\varphi_j\}_{j=1}^k, \varphi_j \in M^*$ such that $\sum_{j=1}^k \varphi_j(f(a_i))x_j -$

$f(a_i) \in J(R)M, \forall i, 1 \leq i \leq n$. i.e. $\sum_{j=1}^k \Phi(x_j, \varphi_j \circ f)(a_i) - f(a_i) \in J(R)M$. Put

$g = \sum_{j=1}^k \Phi(x_j, \varphi_j \circ f)$. It is clear that $g \in F(H)$. Then $g(a_i) - f(a_i) \in J(R)M$. So

$F(H)$ is AP-dense in $S = \text{Hom}_R(M, M)$.

REFERENCES

1. Naoum A.G. & AL-Mothafer N.S: Nearly Projective Module, to appear. Iraqi J. Sci.
2. Kasch. F: Modules and Rings, Academic Press, London (1982).
3. Bierkenmeier G.F: "Modules Which are epi-equivalent to Projective Modules" Acta. Univ. Caroline Math, 24: 9-16 (1983).
4. Fieldhous D. J: Pure Theories, Math. Ann. 184:1-18 (1969).
5. Jondrup S and Trosbory P.J: "A Remark on Pure and Projective Modules" J. Scand: 16-20 (1974).
6. Naoum A. G and AL-Mathafar N. S: "A Note on Z-regular Modules, Dirasat" 22b: 25-33 (1995).
7. Zimmermann-Huisgen. B: Pure Submodules of Direct Products of Free Modules, Math. Ann. 224:233-245 (1976).
8. Willard E.R: "Properties of Projective Generators, Math. Ann. 158:352-364 (1956).
9. Naoum A.G. & Kider J.R: "On the Module of Homomorphism in to Projective Modules and Multiplication Modules" Periodica Mathematica Hungarica, 33 :55-63 (1996).

Special Injective Modules and Their Endomorphism Ring

Mehdi Sadik Abbas and Shaimaa Noori Abd-alridha
Department of Mathematics, University of Mustansiriyah, Baghdad, Iraq

الخلاصة

في هذا البحث قمنا بتعميم مفهوم المقاسات الغامرة (المقاسات الغامرة النسبية) الى المقاسات الغامرة الخاصة (المقاسات الغامرة النسبية الخاصة) كثير من الحقائق و التشخيصات للمقاسات الغامرة تم توسيعها على هذا النوع المعمم من المقاسات . تمت دراسة حلقات التشاكلات الذاتية للمقاسات الغامرة النسبية الخاصة.

ABSTRACT

In this paper we introduce the concept of special injective (special relative injective) modules as a generalization of injective (relative injective) modules. And we study some properties of these concepts. The endomorphism ring of special injective modules are studies.

INTRODUCTION

Let R be a commutative ring with 1, and M be a unitary left R -module. An R -module M is injective if for any R -monomorphism f from A to B (where A and B are arbitrary R -modules) each R -homomorphism $g:A \rightarrow M$ is a restriction of an R -homomorphism $h:B \rightarrow M$, that is $h \circ f = g$ (1). In other words, the following diagram is commutative.

$$\begin{array}{ccccc}
 & & A & \xrightarrow{f} & B \\
 & & \downarrow g & & \searrow h \\
 & & & & M
 \end{array}$$

The concept of injective modules was generalized by many authors. In this work we introduced a generalization of injective modules such that the above diagram is commutative modulo the prime radical of module where the prime radical of an R -module M is defined to be the intersections of all prime submodule of M . We call such generalization as special injective modules. It shows that these modules are closed under arbitrary direct product, finite direct sum and direct summand. We introduced special direct summand and then prove that an R -module M is special injective if and only if, it is a special direct summand of every extension of itself. The endomorphism ring of this concept is studied by using the concept of special kernel of R -homomorphism.

SPECIAL RELATIVE INJECTIVE MODULES

Definition (2.1):- Let M , N and K be R -modules. M is called special injective relative to N (or special N -injective) if for each R -monomorphism $f:K \rightarrow N$ and each R -homomorphism $g:K \rightarrow M$ there is an R -homomorphism $h:N \rightarrow M$ such that $h \circ f(x) = g(x) \in L(M)$ for each x in K . An R -module M is called special injective if M is special injective relative to all R -modules.

$$\begin{array}{ccccc}
 0 & \longrightarrow & K & \xrightarrow{f} & N \\
 & & \downarrow g & & \searrow h \\
 & & M & &
 \end{array}$$

Examples and Remarks 2.2:

1) It is clear that every injective (relative injective) is special injective (special relative injective)

2) Every R -module M which has no prime submodule (i.e. $L(M)=M$) is a special injective. In fact, if we consider the following diagram with exact row (where K and N are R -modules)

$$\begin{array}{ccccc}
 0 & \longrightarrow & K & \xrightarrow{f} & N \\
 & & \downarrow g & & \searrow h \\
 & & M & &
 \end{array}$$

Let $h:N \rightarrow M$ be the trivial homomorphism. It is clear that for all b in K . Thus special injective (resp. special injective) modules may not be injective (resp. relative injective). $(h \circ f)(b) - g(b) \in L(M)$

3) It is clear that, in the class of modules with zero prime radical, the concept of injective (resp. relative injective) is equivalent to that of special injective (resp. special relative injective). In particular, the \mathbb{Z} -modules \mathbb{Z} and \mathbb{Z}_p where p is a prime number (are not special injective).

4) If M is a special N -injective R -module and M is isomorphism to M_1 (resp. N is isomorphism to N_1). Then M_1 is a special N -injective (resp. M is a special N_1 -injective).

5) Let N and M be R -module. Then the following statements are equivalent:

a) M is special N -injective.

b) For any diagram, where A is a submodule of an R -module N and i is the inclusion mapping,

$$\begin{array}{ccccc}
 0 & \longrightarrow & A & \xrightarrow{i} & N \\
 & & \downarrow g & & \searrow h \\
 & & M & &
 \end{array}$$

There exists an R -homomorphism $h : N \rightarrow M$ s.t. $(h \circ i)(a) - g(a) \in L(M)$, for all a in A .

6) Let N be an R -module. Then an R -module M is special N -injective if, and only if, for each essential sub module X of N and each R -homomorphism

$f: X \rightarrow M$, there is an R -homomorphism $g: N \rightarrow M$ s.t. $g \circ i(x) - f(x) \in L(M)$ for each x in X .

Proof: (\Rightarrow) . It is direct from examples and remarks ((2.2), 5).

(\Leftarrow) . Let K be any submodule of N and f be any R -homomorphism $f: K \rightarrow M$.

$$\begin{array}{ccccc} 0 & \longrightarrow & K & \xrightarrow{i} & N \\ & & \downarrow f & & \downarrow \\ & & M & & \end{array} \quad (\text{diagram (1)})$$

Let K^c be any complement submodule of K in N . By [2], we have $K \oplus K^c \leq^e N$. Define $g: K \oplus K^c \rightarrow M$ By $g(k + k_1) = f(k)$ for all $k \in K$ and $k_1 \in K^c$. It clear that g is a well-defined R -homomorphism. Therefore we have the diagram (2).

$$\begin{array}{ccccc} 0 & \longrightarrow & K \oplus K^c & \xrightarrow{i} & N \\ & & \downarrow g & & \downarrow h \\ & & M & & \end{array} \quad (\text{Diagram (2)})$$

By hypothesis there exists an R -homomorphism $h: N \rightarrow M$ such that $h \circ i(x) - g(x) \in L(M)$ for all x in $K \oplus K^c$ for diagram (1). We have that $(h \circ i)(k) - f(k) = (h \circ i)(k) - g(k) \in L(M)$. Therefore M is a special N -injective R -module, by examples and remarks ((2.2), 5).

7) Recall that a submodule N of an R -module M is J -stable if $\alpha(N) \subseteq N + J(M)$ for all $\alpha: N \rightarrow M$. The R -module M is called fully J -stable if each submodule of M is J -stable [3].

Let $R = Z_2[x, y] / \langle x^2, y^2, xy \rangle$ the polynomial ring in two indeterminates x and Y over Z_2 modulo the ideal $\langle x^2, y^2, xy \rangle$. It is easy to see that $L(R) = J(R) = (\bar{x}, \bar{y})$. We claim that R is special R -injective.

For this, let I be any ideal of R and $f: I \rightarrow R$ be any R -homomorphism if $I = R$, then put $g = f$. Now if $I \neq R$,

it is proved in [3], that R is fully J -stable ring, thus $f(I) \subseteq I + L(R)$.

Since $(\bar{0}), (\bar{x}), (\bar{y}), (\bar{x}, \bar{y})$ and R are the only ideals in R , thus $I \subseteq L(R)$ for all

ideal $I \neq R$ and this implies that $f(I) \subseteq L(R)$. Define $g: R \rightarrow R$ by $g(r) = r\bar{x}$ for all r

in R in. It is clear that g is R -homomorphism. Since $\bar{x} \in L(R)$, thus $g(r) \in L(R)$

for all r in R . Therefore $g(r) - f(r) \in L(M)$ for all r in I . Hence R is special R -injective

ring. Since R is not fully stable ring (4), thus R is not self injective i.e. R is not R -injective.

In this part of this paper we are studies the direct product and direct sum of special relative injective modules. Let $\{N_\lambda\}_{\lambda \in \Lambda}$ be a family of R-modules. It is well-know that $\prod_{\lambda \in \Lambda} N_\lambda$ is A-injective (where A is an R-module) if, and only if, each N_λ is A-injective (5) proposition (1.11), p.6].

The following result show that this result it true in case of special relative injective.

Proposition 2.3: Let $\{N_\lambda\}_{\lambda \in \Lambda}$ be a family of R-modules. Then $\prod_{\lambda \in \Lambda} N_\lambda$ is a special A-injective (where A is an R-module) if, and only if, each N_λ is a special A-injective.

Proof: (\Rightarrow). Put $N = \prod_{\lambda \in \Lambda} N_\lambda$, let $i_\lambda: N_\lambda \rightarrow N$ and $p_\lambda: N \rightarrow N_\lambda$ denoted the injections and projections associated with this direct product respectively. Assume that N is a special A-injective, to prove that N_λ is a special A-injective for each $\lambda \in \Lambda$. Consider the following diagram with exact row, (where X is a submodule of A) and α_λ be an R-homomorphism.

$$\begin{array}{ccccc}
 0 & \longrightarrow & X & \xrightarrow{i} & A \\
 & & \alpha_\lambda \downarrow & & \downarrow g \\
 & & N_\lambda & \xleftarrow{h} & A \\
 & & i_\lambda \downarrow & & \downarrow p_\lambda \\
 & & N & &
 \end{array}$$

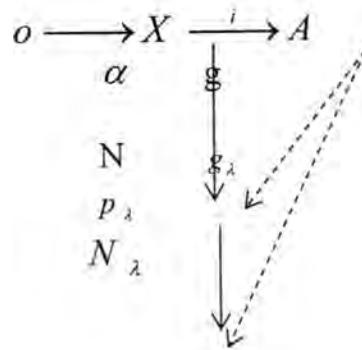
Since N is a special A-injective, thus there exists an R-homomorphism $h: A \rightarrow N$ s.t.

$(h \circ i)(x) - (i_\lambda \circ \alpha_\lambda)(x) \in L(M)$ for all x in X. Put $g_\lambda: p_\lambda \circ h: A \rightarrow N_\lambda$, for every x in X we have

$$\begin{aligned}
 (g_\lambda \circ i)(x) - \alpha_\lambda(x) &= g_\lambda(x) - \alpha_\lambda(x) = (p_\lambda \circ h)(x) - \alpha_\lambda(x) \\
 &= (p_\lambda \circ h)(x) - ((p_\lambda \circ i_\lambda) \circ \alpha_\lambda)(x) = (p_\lambda \circ h)(x) - (p_\lambda \circ (i_\lambda \circ \alpha_\lambda))(x) \\
 p_\lambda(h(x) - (i_\lambda \circ \alpha_\lambda)(x)) &\in L(N_\lambda)
 \end{aligned}$$

By [6] $g_\lambda(x) - \alpha_\lambda(x) \in L(N_\lambda)$, for each $\lambda \in \Lambda$ and for every $x \in X$. Therefore N_λ is a special A-injective for each $\lambda \in \Lambda$.

(\Leftarrow). Consider the following diagram with exact row.



For each $\lambda \in \wedge$, define projection R-homomorphism $p_\lambda : N \rightarrow N_\lambda$. Since each N_λ is a special A-injective, thus there exists an R-homomorphism $g_\lambda : A \rightarrow N_\lambda$, for each $\lambda \in \wedge$ such that $(g_\lambda \circ i)(x) - (p_\lambda \circ \alpha)(x) \in L(N_\lambda)$, for every x in X .

Define $g : A \rightarrow N$ by $g(x) = \{g_\lambda(x)\}_{\lambda \in \wedge}$, for every x in A . It is clear that g is an R-homomorphism. For every x in X , we have that

$$(g \circ i)(x) - f(x) = \{g_\lambda(i(x))\}_{\lambda \in \wedge} - \{(p_\lambda \circ \alpha)(x)\}_{\lambda \in \wedge} = \{(g_\lambda \circ i)(x) - (p_\lambda \circ \alpha)(x)\}_{\lambda \in \wedge} \in \prod_{\lambda \in \wedge} (L(N_\lambda))$$

Since $\prod_{\lambda \in \wedge} (L(N_\lambda)) = L(\prod_{\lambda \in \wedge} N_\lambda)$ by [7], thus $(g \circ i)(x) - \alpha(x) \in L(N)$ for every x in X . Therefore N is a special A-injective.

Let $\{N_\lambda\}_{\lambda \in \wedge}$ be a family of R-modules. It is well-known that if $\bigoplus_{\lambda \in \wedge} N_\lambda$ is an A-injective R-module, then each N_λ is an A-injective. Also the converse is true, if \wedge is finite set by [5, proposition (1.11), p.6]. The following shows that this result is true in case of special relative injective modules.

Corollary 2.4: Let $\{N_\lambda\}_{\lambda \in \wedge}$ be a family of R-modules and let $N = \bigoplus_{\lambda \in \wedge} N_\lambda$

- 1) If N is special A-injective, then each N_λ is a special A-injective.
- 2) If \wedge is a finite set, then the converse of (1) is true.

Proof: The same proof of proposition (2.3) by replacing $\prod_{\lambda \in \wedge} N_\lambda$ of $\bigoplus_{\lambda \in \wedge} N_\lambda$.

Examples 2.5:

- a) The converse of (1) in corollary (2.4) is not true in general. For example, let \wedge be an infinite countable index set and let $T_\lambda = \mathbb{Q}$ for all $\lambda \in \wedge$ (where \mathbb{Q} is the field of rational numbers). Then $R = \prod_{\lambda \in \wedge} T_\lambda$ is a ring, called the ring product of the family $\{T_\lambda / \lambda \in \wedge\}$. It is easy to prove that R is a regular ring. For $k \in \wedge$ denote by e_k that element of R whose k th - component is 1 and whose remaining

components are 0. Let $A = \bigoplus_{\lambda \in \Lambda} Re_{\lambda}$, it is clear that A is an R -submodule of the R -module R . A is a direct sum of injective R -modules, but A is not injective R -module [8, p.140]. Since every injective R -module is a special injective, thus A is a direct sum of special injective R -modules. But A is not special injective, in fact if A is a special injective since R is a regular ring, thus $L(A)=0$ (since $L(A) \subseteq J(A)=0$) and this implies that A is injective R -module by ((2.2),3), and this contradiction. Therefore A is a direct sum of special injective, but it is not special injective.

b) $N = Q \oplus Z$ is not special Z -injective as Z -module. In fact, if N is a special Z -injective then corollary (2.4) implies that Z is special Z -injective and this is not true (see examples and Remarks ((2.2), 3)).

Recall that a submodule N of an R -module M is a direct summand of M if there exists an R -submodule K of M such that $M = N \oplus K$, (i.e.) $M = N + K$ and $N \cap K = 0$ this is equivalent to saying that, for every commutative diagram with exact rows,

$$\begin{array}{ccccccc} 0 & \longrightarrow & A & \xrightarrow{\alpha} & B & & \\ & & f & & h & \searrow & g \\ & & & & & \downarrow & \downarrow \\ & & & & & & \\ 0 & \longrightarrow & N & \xrightarrow{\beta} & M & & \end{array}$$

(where A and B be two R -modules), there exists an R -homomorphism $h : B \rightarrow N$ such that $f = h \circ \alpha$ (9). It is well-known that an R -module M is injective if and only if, M is a direct summand of every extension of it self (1) Theorem. (2.15), p.39]

We call a qasubmodule N of an R -module M is called special direct summand of M if for every commutative diagram with exact rows.

$$\begin{array}{ccccccc} 0 & \longrightarrow & A & \xrightarrow{\alpha} & B & & \\ & & f & & h & \searrow & g \\ & & & & & \downarrow & \downarrow \\ & & & & & & \\ 0 & \longrightarrow & N & \xrightarrow{\beta} & M & & \end{array}$$

(Where A and B be two R -modules), there exists an R -homomorphism $h : B \rightarrow N$ such that $(h \circ \alpha)(a) - f(a) \in L(N)$, for all a in A .

Proposition 2.6: Let M be an R -module and N be a submodule of M then the following statements are equivalent:-

- 1) N is a special direct summand of M .
- 2) For each diagram with exact row,

$$\begin{array}{ccccc} 0 & \longrightarrow & N & \xrightarrow{\alpha} & M \\ & & \downarrow I_N & \searrow h & \downarrow \\ & & & & N \end{array}$$

There exists an R -homomorphism $h: M \rightarrow N$ such that $(h \circ \alpha)(a) - a \in L(N)$, for all a in N (where I_N is the identity map of N).

Proof: (1) \Rightarrow (2). Assume that N is a special direct summand of M . Consider the diagram (1) with exact row.

$$\begin{array}{ccccc} 0 & \longrightarrow & N & \xrightarrow{\alpha} & M \\ & & \downarrow I_N & & \downarrow \\ & & & & N \end{array} \quad \text{(Diagram (1))}$$

Therefore we have the commutation diagram (2) with exact rows.

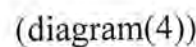
$$\begin{array}{ccccc} 0 & \longrightarrow & N & \xrightarrow{\alpha} & M \\ & & \downarrow I_N & \searrow h & \downarrow I_M \\ & & & & N \end{array} \quad \text{(Diagram (2))}$$

By (our assumption), there exists an R -homomorphism $h: M \rightarrow N$ such that $(h \circ \alpha)(a) - I_N(a) \in L(N)$, for all a in N . Hence $(h \circ \alpha)(a) - a \in L(N)$, for all a in N .

(2) \Rightarrow (1). Consider the commutative diagram (3) with exact rows.

$$\begin{array}{ccccc} 0 & \longrightarrow & A & \xrightarrow{\alpha} & B \\ & & \downarrow f & & \downarrow g \\ 0 & \longrightarrow & N & \xrightarrow{\beta} & M \end{array} \quad \text{(diagram (3))}$$

Thus we have the diagram (4).


$$\begin{aligned} (h_1 \circ \alpha)(a) - f(a) &= ((h \circ g) \circ \alpha)(a) - f(a) = (h \circ (g \circ \alpha))(a) - f(a) \\ &= (h \circ (\beta \circ f))(a) - f(a) = (h \circ \beta)(f(a)) - f(a) \in L(N) \end{aligned}$$

The following theorem gives another characterization of special relative injective modules.

- 1) M is a special A -injective.
- 2) M is a special direct summand of every extension of itself.
- 3) M is a special direct summand of every A -injective extension of itself.
- 4) M is a special direct summand of at least, one A -injective extension of itself.

$$\begin{array}{ccccc}
 0 & \longrightarrow & B & \xrightarrow{g} & A \\
 & & \alpha \downarrow & & \downarrow \beta \\
 & & M & \xrightarrow{h} & M_1
 \end{array}$$

(2) \Rightarrow (3) and (3) \Rightarrow (4) are obvious.

(4) \Rightarrow (1). Assume that M is special direct summand of at least, one A -injective extension R -module of M . Thus there exists an A -injective extension R -module of M , say M_1 , such that M is a special direct summand of M_1 , to prove that M is a special relative injective. Given diagram (1) with exact row (where B be an R -module) and $\beta : B \rightarrow M$ be an R -homomorphism.

$$\begin{array}{ccccc} 0 & \longrightarrow & B & \xrightarrow{\alpha} & A \\ & & \beta \downarrow & & \downarrow \\ & & & & M \end{array} \quad \text{(diagram (1))}$$

Since M_1 is an extension of M , thus there is an R -monomorphism say $f : M \rightarrow M_1$. Therefore we have the diagram (2).

$$\begin{array}{ccccc} 0 & \longrightarrow & B & \xrightarrow{\alpha} & A \\ & & \beta \downarrow & & \downarrow \\ & & & & M \\ & & f \downarrow & & \nearrow g \\ & & & & M_1 \end{array} \quad \text{(diagram (2))}$$

Since M_1 is an A -injective R -module, thus there exists an R -homomorphism $g : A \rightarrow M_1$ such that $g \circ \alpha(b) = f \circ \beta(b)$ for all b in B . thus we have the commutative diagram (3) with exact rows.

$$\begin{array}{ccccc} 0 & \longrightarrow & B & \xrightarrow{\alpha} & A \\ & & \beta \downarrow & & \downarrow h \\ & & & & M \\ & & & & \downarrow f \\ & & & & M_1 \end{array} \quad \begin{array}{c} \nearrow g \\ \downarrow \end{array} \quad \text{(diagram (3))}$$

Since M is a special direct summand of M_1 , thus there exists an R -homomorphism $h : A \rightarrow M$ such that $h \circ \alpha(b) - \beta(b) \in L(M)$, for all b in B .

Therefore the diagram (1), we get an R -homomorphism $h : A \rightarrow M$ such that $h \circ \alpha(b) - \beta(b) \in L(M)$, for all b in B . Hence M is a special A -injective.

Recall that an R -homomorphism $\alpha : A \rightarrow B$ (where A and B are R -modules) is split if there exists an R -homomorphism $\beta : B \rightarrow A$ such that $\beta \circ \alpha = I_A$ [8].

It is well-known that an R -module M is A -injective (where A is an R -module) then any R -monomorphism $\alpha: M \rightarrow A$ splits. For special relative injective we introduce the following concept.

We call an R -homomorphism $f: A \rightarrow B$ (where A and B be two R -modules) is said to be special split, if there exists an R -homomorphism $g: B \rightarrow A$ such that $(g \circ f)(a) - a \in L(A)$ for all a in A .

Theorem 2.8: Let M and A be two R -modules. If M is special A -injective, then any monomorphism $\alpha: M \rightarrow A$ is special split.

Proof: Let α be any R -monomorphism such that $\alpha: M \rightarrow A$. Consider the following diagram:

$$\begin{array}{ccccc} 0 & \longrightarrow & M & \xrightarrow{\alpha} & A \\ & & \downarrow I_m & \searrow h & \\ & & M & & \end{array}$$

Since M is a special, A -injective then there exists an R -homomorphism $h: A \rightarrow M$ such that $h \circ \alpha(a) - a \in L(M)$ for all a in M . Therefore α is a special split.

In the following proposition, we give a relation between special split and special direct summand.

Proposition 2.9: For $\alpha: A \rightarrow B$, the following statements are equivalent:

- α is a special split monomorphism.
- $\text{Im}(\alpha)$ is a special direct summand in B .

Proof: $(a) \Rightarrow (b)$. Since α is a special split monomorphism. Then there exists an R -homomorphism $\beta: B \rightarrow A$ such that $\beta \circ \alpha(a) - I_A(a) \in L(A)$ for all a in A . Consider the following diagram with exact rows, where g and f be an R -homomorphism and α_1 be an R -homomorphism $\alpha_1: A \rightarrow \text{Im}(\alpha)$ such that $\alpha_1(a) = \alpha(a)$ for all a in A .

$$\begin{array}{ccccc} 0 & \longrightarrow & A & \xrightarrow{\alpha} & B \\ & & \downarrow \alpha_1 & \searrow h & \downarrow \\ & & \text{Im}(\alpha) & \xrightarrow{f} & B \end{array}$$

α_1 is an isomorphism. Put $h : \alpha \circ \beta : B \longrightarrow \text{Im}(\alpha)$ be an R-homomorphism $h \circ \alpha(a) - \alpha_1(a) = (\alpha_1 \circ \beta) \circ \alpha(a) - \alpha_1(a) = \alpha_1(\beta \circ \alpha(a) - a)$ and by [6]

$\alpha_1(\beta \circ \alpha(a) - a) \in L(\text{Im}(\alpha))$. Then $h \circ \alpha(a) - \alpha_1(a) \in L(\text{Im}(\alpha))$

For all a in A . Thus $\text{Im}(\alpha)$ is a special direct summand in B .

(b) \Rightarrow (a). Since $\text{Im}(\alpha)$ is a special direct summand in B , then in commutative diagram with exact rows,

$$\begin{array}{ccccccc} 0 & \longrightarrow & A & \xrightarrow{\alpha} & B & & \\ & & \alpha_1 \downarrow & \searrow h & \downarrow g & & \\ & & \text{Im}(\alpha) & \xrightarrow{\sigma} & B & & \end{array}$$

there exists an R-homomorphism $h : B \longrightarrow \text{Im}(\alpha)$ such that

$h \circ \alpha(a) - \alpha_1(a) \in L(\text{Im}(\alpha))$. Since α_1 is an isomorphism, then $\alpha_1^{-1} : \text{Im}(\alpha) \longrightarrow A$ is

exists. Let $f : \alpha_1^{-1} \circ h : B \longrightarrow A$,

$f \circ \alpha(a) - I_A(a) = \alpha_1^{-1} \circ h \circ \alpha(a) - a = \alpha_1^{-1} \circ h \circ \alpha(a) - \alpha_1^{-1} \circ \alpha_1(a) = \alpha_1^{-1}(h \circ \alpha(a) - \alpha_1(a))$ Since

α_1^{-1} is an R-homomorphism. Then by [6], $\alpha_1^{-1}(h \circ \alpha(a) - \alpha_1(a)) \in L(A)$ For all a in A , then monomorphism. $f \circ \alpha(a) - I_A(a) \in L(A)$ for all a in A . Thus α is a special split.

Theorem 2.10: Let A be an R-module, then the following statements are equivalent for an R-module M .

- 1) M is a special A-injective.
- 2) Each R-monomorphism $\alpha : M \longrightarrow A$ is a special split.
- 3) If A is injective, then each R-monomorphism $\alpha : M \longrightarrow A$ is a special split.
- 4) Each R-monomorphism $\alpha : M \longrightarrow E(M)$ is a special split. (where $E(M)$ is injective envelope of M).

Proof: (1) \Rightarrow (2) by theorem (2.8)

(2) \Rightarrow (3) and (3) \Rightarrow (4) are obvious.

(4) \Rightarrow (1) Assume that each R-monomorphism $\alpha : M \longrightarrow E(M)$ is a special split (where $E(M)$ is the injective envelope of M).

To prove that M is a special A-injective. Give a diagram (1) with exact row. Where B is an R-module and $g : B \longrightarrow M$ be an R-homomorphism.

$$\begin{array}{ccccc}
 0 & \longrightarrow & B & \xrightarrow{f} & A \\
 & & \downarrow g & & \\
 & & M & &
 \end{array}
 \quad (\text{diagram (1)})$$

Since $E(M)$ is an extension of M by $[1]$, thus there is an R -monomorphism says $\alpha: M \rightarrow E(M)$ thus we have the diagram (2) with exact row

$$\begin{array}{ccccccc}
 0 & \longrightarrow & B & \xrightarrow{f} & A & & \\
 & & \downarrow g & & \downarrow h & & \\
 & & M & & & & \\
 & & \downarrow \alpha & & \downarrow \beta & & \\
 & & & & E(M) & &
 \end{array}
 \quad (\text{diagram (2)})$$

By injectivity of $E(M)$, there exists an R -homomorphism $h_1: A \rightarrow E(M)$ such that $(h_1 \circ f)(b) = (\alpha \circ g)(b)$, for all b in B by (our assumption) we have $\alpha: M \rightarrow E(M)$ is a special split. Therefore there exists an R -homomorphism $\beta: E(M) \rightarrow M$ s.t. $(\beta \circ \alpha)(a) - a \in L(M)$, for all a in M . Put $h = \beta \circ h_1$, it is clear that h is an R -homomorphism for each b in B , we have that:

$$(h \circ f)(b) - g(b) = ((\beta \circ h_1) \circ f)(b) - g(b) = (\beta \circ (h_1 \circ f))(b) - g(b)$$

$$= (\beta \circ (\alpha \circ g))(b) - g(b) = (\beta \circ \alpha)(g(b)) - g(b) \in L(M)$$

Thus $(h \circ f)(b) - g(b) \in L(M)$, for all b in B . Therefore M is a special A -injective

Endomorphism ring of Space Special Relative Injective Modules

Let M be an R -module and $S = \text{End}_R(M)$. It well-known that $\Delta = \{f \in S / \text{Ker}(f) \leq^e M\}$ is a two-sided ideal of S [10] also if M is an injective R -module, then S/Δ is regular ring [2] if $\Delta = 0$, then S is a right self-injective ring(2).

For analogous results for special relative injective modules we consider the special kernel of f , let M and N be two R -modules and $f: M \rightarrow N$ be an R -

homomorphism we call the set $f^{-1}L(N) = \{x \in M / f(x) \in L(N)\}$ a special kernel of f and denoted by $\text{Sker}(f)$.

Proposition 3.1: Let M be an R -module and $S = \text{End}_R(M)$. Define $S\Delta = \{f \in S \mid \text{Sker}(f) \leq^e M\}$, then $S\Delta$ is a two-sided ideal of S .

Proof: It is clear that $S\Delta$ is a non-empty set since the zero function belong to $S\Delta$ such that $\text{Sker}(\text{zero function}) = M$ and $M \leq^e M$. Let $f, g \in S\Delta$, $\text{Sker}(f) \leq^e M$ and $\text{Sker}(g) \leq^e M$. By [8, Lemma (5.1.5), p.109], then $\text{Sker}(f) \cap \text{Sker}(g) \leq^e M$. But $\text{Sker}(f) \cap \text{Sker}(g) \leq \text{Sker}(f - g)$, since for each $x \in \text{Sker}(f) \cap \text{Sker}(g)$, then $f(x), g(x) \in L(M)$, thus $(f - g)(x) \in L(M)$, hence $x \in \text{Sker}(f - g)$. Therefore $\text{Sker}(f - g) \leq^e M$ by [8, Lemma (5.1.5), p.109], hence $f - g \in S\Delta$. Let $f \in S\Delta$ and $h \in S$. $\text{Sker}(f) \leq \text{Sker}(h \circ f)$, since for each x in $\text{Sker}(f)$, $f(x) \in L(M)$, then [6] implies that $h(f(x)) \in L(M)$. Thus $(h \circ f)(x) \in L(M)$ and hence $x \in \text{Sker}(h \circ f)$, therefore $\text{Sker}(h \circ f) \leq^e M$ by [8, Lemma (5.1.5), p.109]. Now we want to prove that $f \circ h \in S\Delta$, since $f \in S\Delta$ thus $\text{Sker}(f) \leq^e M$, [2, Lemma (3.3) p. 46] implies that $h^{-1}(\text{Sker}(f)) \leq^e M$ but $h^{-1}(\text{Sker}(f)) \leq \text{Sker}(f \circ h)$, therefore $\text{Sker}(f \circ h) \leq^e M$, by [8, Lemma (5.1.5), p.109] then $f \circ h \in S\Delta$ and hence $S\Delta$ is a two-sided ideal of S .

□

As $\ker(f) \leq \text{Sker}(f)$ we have $\Delta \subseteq S\Delta$.

Now, we are ready to consider the main result of this section, (compare with analogous result for injective modules in [2]).

Theorem 3.2: Let M and A be two R -modules. If M is a special A -injective and $S = \text{End}_R(M)$, then

- 1) $S/S\Delta$ is a regular ring.
- 2) If $S\Delta = 0$, then S is a right self-injective ring.

Proof: Let $\lambda + S\Delta \in S/S\Delta$, hence $\lambda \in S$ put $K = \text{Ker}(\lambda)$ let L be a relative complement of K in M . Define $\alpha: \lambda(L) \rightarrow M$ by $\alpha(\lambda((x))) = x \quad \forall x \in L$. α is well-defined, since if $\lambda(x) = \lambda(y)$ for some $x, y \in L$, thus $x - y \in K$ and hence $x - y \in K \cap L = 0$, thus $x = y$. α is an R -homomorphism since

- 1) $\alpha(\lambda(x) + \lambda(y)) = \alpha(\lambda(x+y)) = x+y = \alpha(\lambda(x)) + \alpha(\lambda(y))$
 2) $\alpha(r\lambda(x)) = \alpha(\lambda(rx)) = rx = r \cdot \alpha(\lambda(x))$ for some $r \in R$ thus consider the following diagram with exact row, where $g: \lambda(L) \rightarrow A$ be any R -monomorphism

$$\begin{array}{ccc} 0 & \xrightarrow{\quad} & \lambda(L) \xrightarrow{g} A \\ & \searrow \alpha & \downarrow h \\ & & M \end{array}$$

Special A -injective of M implies that, there exists an R -homomorphism $h: A \rightarrow M$ such that $(h \circ g)(\lambda(x)) - \alpha(\lambda(x)) \in L(M)$ for each $x \in L$, $h(g(\lambda)) = \alpha(\lambda(x)) + l$, for some $l \in L(M)$. Let $u \in K \oplus L$, hence $u = x + y$ where $x \in K, y \in L$. Put $f = hog: \lambda(L) \rightarrow M$ and for each $x \in L$
 $f(\lambda(x)) = \alpha(\lambda(x)) + l$ For some $l \in L(M)$.

$(\lambda - \lambda f \lambda)(u) = (\lambda - \lambda f \lambda)(x + y) = \lambda(x) - \lambda f(\lambda(x)) + \lambda(y) - \lambda f(\lambda(y))$
 $= 0 - 0 - \lambda(y) - \lambda(\alpha(\lambda(y)) + l) = \lambda(y) - \lambda(y + l) = \lambda(y) - \lambda(y) + \lambda(l) \in L(M)$
 by [6], thus $u \in \text{Sker}(\lambda - \lambda f \lambda)$. Hence for each $u \in K \oplus L$, then $u \in \text{Sker}(\lambda - \lambda f \lambda)$ and this implies that $K \oplus L \leq \text{Sker}(\lambda - \lambda f \lambda)$ since $K \oplus L \leq^e M$ by [11], thus [8] implies that $\text{Sker}(\lambda - \lambda f \lambda) \leq^e M$. Hence $\lambda - \lambda f \lambda \in S\Delta$, thus $\lambda + S\Delta = (\lambda f \lambda) + S\Delta$. Therefore $S/S\Delta$ is a regular.

(2) Assume that $S\Delta = 0$, then by (1), S is a regular ring. Let $f: I \rightarrow S$ be any S -homomorphism of a right ideal I of S into S . Consider the following diagram:

$$\begin{array}{ccc} 0 & \xrightarrow{\quad} & I \xrightarrow{i} S \\ & \searrow f & \downarrow \\ & & S \end{array}$$

By IM we mean an R -submodule of M generated by $\{\lambda m \mid \lambda \in I, m \in M\}$, it follows that if $x \in IM$, then there exists $\lambda_1, \lambda_2, \dots, \lambda_n \in I$ and $m_1, m_2, \dots, m_n \in M$ where $n \in \mathbb{Z}^+$ such that $x = \sum_{i=1}^n \lambda_i m_i$. Define $h: IM \rightarrow M$ as follows, for each $x = \sum_{i=1}^n \lambda_i m_i \in IM$, put $h(x) = h(\sum_{i=1}^n \lambda_i m_i) = \sum_{i=1}^n f(\lambda_i)(m_i)$. For each $x, y \in IM$,

we have that $x = \sum_{i=1}^n \lambda_i m_i$ and $y = \sum_{j=1}^t \alpha_j m'_j$, where $\lambda_i, \alpha_j \in I$ and $m_i, m'_j \in M$, for all $i = 1, \dots, n$ and $j = 1, \dots, t$ where $n, t \in \mathbb{Z}^+$. Since S is a regular ring, thus by [2, proposition (4.14), p.42] each finitely generated right ideal of S which is generated by an idempotent, thus the right ideal of S which is generated by $\lambda_1, \dots, \lambda_n, \alpha_1, \dots, \alpha_t$ has the form eS where $e = e^2 \in I$. Since λ_i, α_j belong to the right ideal of S which is generated by $\lambda_1, \dots, \lambda_n, \alpha_1, \dots, \alpha_t$ for all $i = 1, \dots, n, j = 1, \dots, t$ thus $\lambda_i, \alpha_j \in eS$ for all $i = 1, \dots, n, j = 1, \dots, t$ and this implies that $\lambda_i = es_i$ and $\alpha_j = es'_j$ for some $s_i, s'_j \in S$ and for all $i = 1, \dots, n, j = 1, \dots, t$. Hence $e\lambda_i = e(es_i) = e^2 s_i = es_i = \lambda_i$, for all $i = 1, \dots, n$ and

$e\alpha_j = e(es'_j) = e^2 s'_j = es'_j = \alpha_j$ for all $j = 1, \dots, t$. Therefore $f(\lambda_i) = f(e)\lambda_i$ and $f(\alpha_j) = f(e)\alpha_j$ for all $i = 1, \dots, n$ and $j = 1, \dots, t$ thus

$$h(x) = h(\sum_{i=1}^n \lambda_i m_i) = \sum_{i=1}^n f(\lambda_i)(m_i) = \sum_{i=1}^n f(e)\lambda_i m_i = f(e) \sum_{i=1}^n \lambda_i m_i = f(e)x$$

and similarly we have $h(y) = f(e)y$. h is well-defined, since for all $x, y \in IM$, if $x = y$, we have just proved that $h(x) = f(e)x$ and $h(y) = f(e)y$, hence $h(x) = h(y)$.

For each $x, y \in IM$ and for all $r \in R$ we have that $h(x+y) = f(e)(x+y) = f(e)x + f(e)y = h(x) + h(y)$ & $h(rx) = f(e)(rx) = r(f(e)x) = rf(x)$.

Therefore h is well-defined R -homomorphism of the R -submodule IM into M . Thus we have the following diagram (where i is the inclusion mapping and g is any R -homomorphism) with exact row.

$$\begin{array}{ccccccc} 0 & \longrightarrow & IM & \xrightarrow{i} & M & \xrightarrow{g} & A \\ & & \downarrow h & \searrow \varphi & & \nearrow \alpha & \\ & & M & & & & \end{array}$$

Since M is a special A -injective, thus there exists an R -homomorphism $\alpha: A \rightarrow M$ s.t. $(\alpha \circ g)(x) - h(x) \in L(M)$ for all x in IM .

Put $\varphi = \alpha \circ g : M \rightarrow M$. φ is an R -homomorphism since

$$\begin{aligned}\varphi(x+y) &= (\alpha \circ g)(x+y) = \alpha(g(x+y)) = \alpha(g(x) + g(y)) = \alpha \circ g(x) + \\ &\alpha \circ g(y) = \varphi(x) + \varphi(y)\end{aligned}$$

for all $x, y \in M$. $\varphi(rx) = \alpha \circ g(rx) = \alpha(g(rx)) = \alpha(rg(x)) = r\alpha \circ g(x) = r\varphi(x)$ for all $r \in R$ and $\varphi(x) - h(x) = (\alpha \circ g)(x) - h(x) \in L(M)$ for all $x \in IM$. For each $m \in M$, if $\lambda \in I$, then $(\varphi\lambda)(m) = \varphi(\lambda m) = h(\lambda m) + l$, for some $l \in L(M)$. Hence $(\varphi\lambda - f(\lambda))(m) \in L(M)$, and this implies that $m \in \text{Sker}(\varphi\lambda - f(\lambda))$, hence $M = \text{Sker}(\varphi\lambda - f(\lambda))$ for each $\lambda \in I$. Therefore $\text{Sker}(\varphi\lambda - f(\lambda)) \leq^e M$, for all $\lambda \in I$ and thus $\varphi\lambda - f(\lambda) \in S\Delta$ for all $\lambda \in I$. The hypothesis implies that $f(\lambda) = \varphi\lambda$, for all $\lambda \in I$. Thus S satisfied Baer's condition and hence S is a right self-injective ring by (2) Theorem (1.6), P.5].

In the following we shall consider the analogous result for special injective modules. First we introduce the following

Let M be an R -module. Consider the set $SZ(M) = \{m \in M \mid [L(M):m]_R \text{ is an essential ideal in } R\}$.

Lemma 3.3: Let M be an R -module and $S = \text{End}_R(M)$. Then $[L(M):\lambda(x)]_R = [\text{Sker}(\lambda):x]_R$, for each $\lambda \in S$ and for each $x \in M$.

Proof: Let $r \in [L(M):\lambda(x)]$, thus $r\lambda(x) \in L(M)$ and so $\lambda(rx) \in L(M)$

and this implies that $rx \in \text{Sker}(\lambda)$, hence $r \in [\text{Sker}(\lambda):x]_R$, therefore

$[L(M):\lambda(x)]_R \leq [\text{Sker}(\lambda):x]_R$. By the same method we prove

$[\text{Sker}(\lambda):x]_R \leq [L(M):\lambda(x)]_R$. Hence $[L(M):\lambda(x)]_R = [\text{Sker}(\lambda):x]_R$. \square

Now, we are ready to prove the analogous proposition of the Osofsky's statement (12).

Proposition 3.4: Let M be an R -module and $S = \text{End}_R(M)$. If $SZ(M) = (0)$, then $S\Delta = (0)$.

Proof: Let $\lambda \in S\Delta$, thus $\text{Sker}(\lambda) \leq^e M$ by [2, Lemma (3), P.46] implies that $[\text{Sker}(\lambda):x]_R \leq^e R$ for each x in M . Since $[L(M):\lambda(x)]_R = [\text{Sker}(\lambda):x]_R$ by above Lemma, thus $[L(M):\lambda(x)]_R \leq^e R$ and this implies that $\lambda(x) \in \text{SZ}(M) = 0$ therefore $\lambda(x) = 0$, for all x in M (i.e. $\lambda = 0$) and hence $S\Delta = (0)$. \square

The following corollary (for special injective modules) is analogous of the statement for injective modules (2).

Corollary 3.5: Let M be a special A -injective (where A be an R -module) and $S = \text{End}_R(M)$. If $\text{SZ}(M) = (0)$, then S is a right self-injective regular ring.

Proof: Assume that M be a special A -injective with $\text{SZ}(M) = (0)$, proposition (3.4) implies that $S\Delta = (0)$, therefore S is a right self-injective regular ring, by Theorem (3.2). \square

It is known, if R is a ring and x is an element in R , then $x_L: R \rightarrow R$ which is defined by $x_L(a) = ax$, for all a in R is an R -homomorphism, also $\text{End}_R(R) = \{x_L \mid x \in R\}$ (2)p.47].

Lemma 3.6: Let R be a ring and $S = \text{End}_R(R)$.

Define $f: R/\text{SZ}(R) \rightarrow S/S\Delta$: as follows

$f(x + \text{SZ}(R)) = x_L + S\Delta$ for each x in R , then f is an R -isomorphism.

Proof: f is well-defined, since for each $x + \text{SZ}(R), y + \text{SZ}(R) \in R/\text{SZ}(R)$ if $x + \text{SZ}(R) = y + \text{SZ}(R)$, thus $x - y \in \text{SZ}(R)$ and hence $[L(R):x - y] \leq^e R$.

But $\text{Sker}(x_L - y_L) = \{r \in R \mid (x - y)_L(r) \in L(R)\}$

$= \{r \in R \mid r(x - y) \in L(R)\} = [L(R):(x - y)]_R$,

thus $\text{Sker}(x_L - y_L) \leq^e R$ and so $x_L - y_L \in S\Delta$, therefore $x_L + S\Delta = y_L + S\Delta$, thus

$f(x + \text{SZ}(R)) = f(y + \text{SZ}(R))$ for all $x + \text{SZ}(R), y + \text{SZ}(R) \in R/\text{SZ}(R)$ and for all $r \in R$, then

$f((x + \text{SZ}(R)) + (y + \text{SZ}(R))) = f((x + y) + \text{SZ}(R)) = (x + y)_L + S\Delta$
 $(x_L + y_L) + S\Delta = (x_L + S\Delta) + (y_L + S\Delta) = f(x + \text{SZ}(R)) + f(y + \text{SZ}(R))$

And

$$f(r(x + SZ(R))) = f(rx + SZ(R)) = (rx)_L + S\Delta = rx_L + S\Delta = r(x_L + S\Delta) = rf(x + SZ(R))$$

therefore f is well-defined R -homomorphism. It is clear that f is an epimorphism.

Since $\forall x_L + S\Delta \in S/S\Delta$ there exists $x + SZ(R) \in R/SZ(R)$ such that $f(x + SZ(R)) = x_L + S\Delta$. Thus f is an epimorphism. Now we want to prove that f is a monomorphism, let $x + SZ(R), y + SZ(R) \in R/SZ(R)$ such that $f(x + SZ(R)) = f(y + SZ(R))$ thus $x_L + S\Delta = y_L + S\Delta$ and hence $x_L - y_L = (x - y)_L \in S\Delta$ therefore $\text{Sker}((x - y)_L) \leq^e R$. But

$$\begin{aligned} \text{Sker}((x - y)_L) &= \{r \in R / (x - y)_L(r) \in L(R)\} \\ &= \{r \in R / r(x - y) \in L(R)\} = [L(R) : (x - y)]_R \end{aligned}$$

hence $[L(R) : (x - y)]_R \leq^e R$ and this implies $x - y \in SZ(R)$ and so $x + SZ(R) = y + SZ(R)$, thus f is a monomorphism. Hence f is an R -isomorphism. \square

Now, we are ready to prove the following proposition for self-special injective rings which is analogous of statement for self-injective rings (3).

Proposition 3.7: Let A be an R -module. If R is special A -injective ring. Then $R/SZ(R)$ is a regular ring.

Proof: Let $f: R/SZ(R) \rightarrow S/S\Delta$ be the R -isomorphism as in Lemma (3.6), where $S = \text{End}_R(R)$. Let $x + SZ(R) \in R/SZ(R)$, thus

$f(x + SZ(R)) = x_L + S\Delta \in S/S\Delta$. Since R is a self-special A -injective ring, thus $S/S\Delta$ is a regular ring, by theorem (3.2) and this implies that there exists an element $y_L + S\Delta \in S/S\Delta$ such that $x_L + S\Delta = x_L y_L x_L + S\Delta = (xyx)_L + S\Delta$.

Since f is an R -isomorphism, thus f^{-1} exists and

$$\begin{aligned} f^{-1}(x_L + S\Delta) &= f^{-1}((xyx)_L + S\Delta), \text{ hence} \\ x + SZ(R) &= xyx + SZ(R) = (x + SZ(R)) \cdot (y + SZ(R)) \cdot (x + SZ(R)). \end{aligned}$$

Since $f^{-1}(y_L + SA) = y + SZ(R) \in R/SZ(R)$, therefore we get an element $y + SZ(R) \in R/SZ(R)$ s.t.

$$x + SZ(R) = (x + SZ(R)) \cdot (y + SZ(R)) \cdot (x + SZ(R))$$

Hence $R/SZ(R)$ is a regular ring. \square

Corollary 3.8: Let A be an R -module. If R is a special A -injective ring and $SZ(R) = 0$, then R is a regular ring

.Proof: Assume that R is a special A -injective ring, hence by proposition (3.7) $R/SZ(R)$ is a regular ring. Since $SZ(R) = 0$, thus R is a regular ring.

REFERENCES

1. Sharpe W., Vámos D.P. "Injective Modules" Cambridge Univ. press, London, (1972).
2. Faith C. "Lectures On Injective Modules And Quotient Rings" Springer- verlag, Berlin, Heidelberg, New York, (49) (1967).
3. Abbas M.S. "Semi-regular modules and fully J-stable modules, Iraqi J.Sci. 41D(1) (2000).
4. Abbas M.S. "On fully stable modules" Ph.D. thesis, Univ. of Baghdad (1991).
5. Smith, P.F. "Injective modules and their Generations, University of Glasgow Department of Math. , preprint series : 97-07 (1997).
6. Saeed A.B. "L-Regular Modules" Mcs. thesis, Univ. of Al-Mustansiriyah (2000).
7. James Jenkins & Smith, P.F. "On the Prime Radical of a Module Over a Commutative Ring" comm. In Algebra, 20(12):3593-3602 (1992).
8. Kasch F. "Modules and Rings" Academic press, London, New York (1982).
9. Naude C.G. & Pectorius, L.M. "Equation Characterizations of Relative Injectives, comm. In Algebra" 14(1): 39-48 (1988).
10. Hussain A.H. "Ker-injective and L-injective modules" Mcs. Thesis University of Baghdad (1993).
11. Hungerford T.W. "Algebra, Springer-verlag" New York Heidelberg, Berlin (1974).
12. Losofsky B. "Endomorphisms rings of quasi-injective modules" Canadian J. Math. 20: 895-903 (1968).
13. Utumi Y. "On continuous rings and self-injective rings" Trans. Of Amer. Math. Soc. 138: 505-512 (1969).

Using Genetic Algorithm and Local Search to Solve Flow shop NP - complete

¹Tariq S. Abdul-Razaq and ²Lika Z. Hummady

¹Mathematics Department / Al-Mustansiriyah University

²Geology Department/ Baghdad University

الخلاصة

هناك عدة مسائل في الجدولة تمتلك الصيغة التوافقية وهذه المسائل يكون من الصعب إيجاد الحل الأمثل لها ولذلك نلجأ إلى الطرق التقريبية لإيجاد الحل الأمثل أو حلول مقبولة قريبة من الحل الأمثل. لقد تناولنا في هذا البحث مسألة جدولة النتائج على ماكنتين لتصغير دالة الهدف المركبة وهي (أكبر وقت اتمام وأكبر تأخير لا سالب) وفي بحثنا هذا قمنا باستعراض وتطبيق بعض الطرق التقريبية وهي Adjacent pairwise interchange method (APIM), Descent method (DA), Simulated annealing method (SAM) كما قمنا بتطوير طريقة Genetic Algorithm (GA) ولقد تم تقييم كفاءة هذه الطرق على مجموعة كبيرة من مسائل اختيارية. كما قمنا بإيجاد طريقة تقريبية جديدة (New heuristic method (NHM)) وعند مقارنة النتائج لهذه الطريقة مع الطرق السابقة وجدت أنها الأفضل من حيث الكفاءة.

ABSTRACT

There are a lot of scheduling problems that have a combinatorial manner and these problems are difficult to be solved. For these scheduling problems, local search methods are used to find the optimal solution or near optimal solutions.

In this paper we consider the scheduling problem on two machine flow Shop to find the minimum maximum completion time and maximum of tardiness to be compared with some of the local search methods namely (Descent method (DM), Adjacent pairwise interchange method (APIM) and Simulated annealing method (SAM)). We developed the Genetic Algorithm (GA) by using a large number of experimental problems, we proposed a new heuristic method (NHM) and when comparing the results of this method with the preceding methods we found that it is the best in case of qualification.

INTRODUCTION

The general flow shop problem, indicated by $Fm // C_{max}$, can be stated as follows. There are n jobs numbered $1, \dots, n$, each of which is to be processed on machines $1, \dots, m$ in that order. Each job i ($i=1, \dots, n$) has a processing time P_{ik} on machine k ($k=1, \dots, m$). Each machine can process not more than one job at a time and each job can be processed by not more than one machine at a time. The order in which jobs are processed need not be the same on all machines. The objective is to find a processing order on each machine which minimizes C_{max} , the maximum completion time of all the jobs. For $Fm // C_{max}$ problem, Conway *et al.* (1) observe that there exists an optimal schedule with the same processing order of jobs on the first pair of machines and the same order on the last pair of machines. It is also well known that for $m=2$, the resulting flow shop problem (*i.e.* $F2 // C_{max}$), can be solved using Johnson's algorithm (2) in which job i is sequenced before job j if $\min\{P_{i1},$

$P_{j2} \leq \min\{P_{i2}, P_{j1}\}$. Note that using other criteria usually leads to NP-hard problems for example $F2 // L_{\max}$ (Lenstra et al.(3)). That leads to use local search methods, which tend toward but do not guarantee the finding of optimal solution for any instance of an optimization problem.

Recently, there has been considerable excitement about the success of a new family of algorithms in attacking notoriously difficult (NP-hard) computational problems such as traveling salesman and resource-constrained scheduling.(4). These are so-called "genetic algorithms" (GA,s) use concepts drawn from the theory of evolution to "breed" progressively better solutions to problems with very large solution spaces.

Problem Formulation

To state our scheduling problem more precisely, we are given n jobs which are numbered $1, \dots, n$. All jobs are available for processing at time zero and are to be processed on machines **A** and **B** in that order during uninterrupted processing times a_i and b_i respectively. The objective is to find a processing order of the jobs that minimizes the composition objective function (maximum of completion time and maximum of tardiness on the second machine), this objective function is denoted by $(C_{\max} + T_{\max})$. Using the three field classification suggested by Graham et al.(5), this problem denoted as $F2 // C_{\max} + T_{\max}$. The problem under investigation is known to be NP-complete,

since $F2 // T_{\max}$ is NP-complete (Lenstra et al.(3)). Given any sequence $\pi = (\pi(1), \dots, \pi(n))$, the minimum completion times $C_{\pi(1)}^A$ and $C_{\pi(1)}$ of the first job $\pi(1)$ in the sequence on the first and second machines are equal to $a_{\pi(1)}$ and $a_{\pi(1)} + b_{\pi(1)}$ respectively. The minimum completion times of any other job $\pi(i)$, ($i=2, \dots, n$) on the first and second machines are given by

$$C_{\pi(i)}^A = C_{\pi(i-1)}^A + a_{\pi(i)} \text{ and } C_{\pi(i)} = \max \{ C_{\pi(i)}^A, C_{\pi(i-1)} \} + b_{\pi(i)}$$

respectively, hence the tardiness for each job $\pi(i)$, $i=1, \dots, n$ on the second machine is given by $T_{\pi(i)} = \max \{ C_{\pi(i)} - d_{\pi(i)}, 0 \}$ where the $d_{\pi(i)}$ is the due date of job $\pi(i)$. The objective is to find a schedule σ ($\sigma(1), \dots, \sigma(n)$) of the jobs that minimize the total cost $Z(\sigma)$. Our problem (P) can formally be stated as

$$\min_{\sigma \in S} \{ Z(\sigma) \} = \min \{ C_{\max} + T_{\max} \}$$

$$\text{s.t. } C_{\sigma(1)} = C_{\sigma(1)}^A + b_{\sigma(1)}$$

$$C_{\sigma(i)} = \max \{ C_{\sigma(i)}^A, C_{\sigma(i-1)} \} + b_{\sigma(i)} \quad i=2, \dots, n$$

$$C_{\max} = C_{\sigma(n)}$$

(P)

$$T_{\sigma(i)} \geq C_{\sigma(i)} - d_{\sigma(i)} \quad i=1, \dots, n$$

$$T_{\max} = \max \{T_{\sigma(i)}\}$$

Where $\sigma(i)$ denotes the position of job i in the ordering σ and S denotes the set of all sequences.

The following special cases yields optimal solutions for our problem (P).

Case (1): The sequence which is obtained by Johnson's rule is optimal for $F2 // C_{\max} + T_{\max}$ problem if $T_i = 0$ for each job $i (i=1, \dots, n)$.

Proof : Since all jobs are early or completed on time this mean that there are no tardiness (i.e. $T_i = 0$ for each i) and hence $T_{\max} = 0$, and our problem $F2 // C_{\max} + T_{\max}$ is reduced to $F2 // C_{\max}$ which can be solved by Johnson's rule (J.R)(2).

Case (2): The sequence which is obtained by Johnson's rule is optimal for $F2 // C_{\max} + T_{\max}$ problem If $d_i = d$ for each $i (i=1, \dots, n)$.

Proof: Let $\sigma = (1, \dots, n)$ be the sequence obtained by Johnson's rule (J.R) and the minimum C_{\max} is given by: $C_{\max} = \max \{C_{n-1}, C_n^d\} + b_n$ where C_{n-1} is the completion time of job $n-1$ on machine B, C_n^d is the completion time of job n on machine A, b_n is the processing time of the last job n on machine B. For each job $i \in \sigma$, $T_i = \max\{C_i - d, 0\}$ and hence the maximum tardiness $T_{\max} = C_{\max} - d$, which is less than or equal to the maximum tardiness given by any other sequence $\pi \neq \sigma$. Hence σ is optimal for $F2 // C_{\max} + T_{\max}$.

Drived the Upper and Lower bounds for the problem(P)

Consider the two machine flow-shop problem to minimize the composition objective function the maximum of completion time and maximum of tardiness ($C_{\max} + T_{\max}$). This problem is clearly NP-hard since the simpler version $F2 // T_{\max}$ is already NP-hard (6). It is well known that computation can be reduced by using a heuristic to find a good solution to act as an upper bound(UB). Also a simple techniques is used to obtain a lower bound (LB) for our problem (P).

1. Upper bound (UB)

We can find upper bound (UB) for our problem (p) by using Johnson's rule (J.R), since Johnson's rule gives the optimal solution to the important part C_{\max} of this problem.

2. Lower bound (LB)

Decomposition of the problem and derivation of lower bound (LB). Now consider again the formulation of the problem(P), we decompose the problem into two subproblems with a simpler structure. Then the lower bound (LB) of

the problem (P) is the sum of the minimum value of the subproblem (P₁) and the lower bound of the subproblem (P₂).

$$Z_1 = \min_{\sigma \in S} \{C_{\max}\}$$

s.t.

$$C_{\sigma(1)} = C_{\sigma(1)}^d + b_{\sigma(1)}$$

$$C_{\sigma(i)} = \text{Max} \{ C_{\sigma(i)}^d, C_{\sigma(i-1)} \} + b_{\sigma(i)} \quad i=2, \dots, n$$

$$C_{\max} = C_{\sigma(n)}$$

(P₁)

And

$$Z_2 = \min T_{\max}$$

s.t.

$$T_{\sigma(i)} \geq C_{\sigma(i)} - d_{\sigma(i)} \quad i=1, \dots, n$$

$$T_{\max} = \text{Max} \{ T_{\sigma(i)} \}$$

$$T_{\sigma(i)} \geq 0$$

(P₂)

It is clear from the decomposition that (P₁) and (P₂) have simpler structures than (P), and thus appear easily to solve optimality for (P₁) (i.e. (P₁) is solved by Johnson's rule), and a lower bound can be obtained for (P₂) by using the relaxation techniques. The lower bound for (P₂) is obtained as follows. Let $b_i = 0$ for each job i and the resulting problem is $1 // T_{\max}$ which is solved by EDD rule (the job i is sequenced before job j if $d_i \leq d_j$ ($i, j=1, \dots, n$)), let $LBT = \min \{ T_{\max} \}$ for (P₂). Hence $LB = Z_1 + LBT$.

An optimal solution for each test problem (with $n < 30$) is obtained by branch and bounds (BAB) method were applied to scheduling problems by Ignall and Schrage (7) and Lomnicki(8). The branch and bound finds s^* by implicit enumeration all $s \in S$ through examination of smaller subsets of the set of feasible solutions S . These subsets can be treated as sets of solutions of corresponding subproblems of the original problem.

This method is determined by the following procedures:

I-The branching procedure: This describes the method to partition a subset of possible solution. These subsets can be treated as a set of solutions of corresponding subproblems of the original problem.

II-The bounding procedure: This indicates how to calculate a lower bound(LB) on the optimal solution value for each subproblem generated in the branching process.

III-The search strategy: This strategy describes the method of choosing a node of the search tree to branch from it, we usually branch from a node with the smallest lower bound (LB) among the recently created nodes.

The New Heuristic Method(NHM)

It is well known that the complete enumeration methods generate one by one all the possible feasible solutions searching for an optimal solution and eliminate the non-optimal solutions. Suppose we are given n jobs to be process on m machines, in this case, there exists $(n!)^m$ possible ordering of the jobs. Clearly, using this method searching for an optimal schedule is not suitable even for small n and m . Thus, we introduce a new heuristic for the two machine flow shop problem where the objective is to minimize the maximum completion time and maximum tardiness of jobs. An improved heuristic method for complete enumeration methods has been constructed. The method appears to be difficult to give through extensive empirical runs failed to generate even a single counter example which has not optimal or near optimal solution. This leads to an interesting observation, that the developed heuristic method, will yield optimal solutions in most instances of the extensive empirical runs performed by us. We expect that this new heuristic would produce optimal solutions for most of other instances too. In the following we shall give the outline of this heuristic:

Step 1: Start with counter =0

Step 2: Find the initial solution s .

Step3: Calculate the values of UB and LB (such that the initial solutions for UB).

Step4: Find the neighborhoods (Using subalgorithm) and compute costs for the neighborhoods.

Step 5: If all costs $> UB$ then go to step (4).

Step 6: Register costs in the result file .

Step7: If costs $\leq (UB+LB)/2$ then register costs in Quick file and let counter = counter +1 . Otherwise (i.e. Cost $> (UB+LB)/2$, go to step (10).

Step 8: If counter =5 then go to step (11).

Step9: Go to step (4).

Step10: Choose minimum of result file and go to step (12).

Step11: Chose minimum of Quick file.

Step12: End.

Where in this heuristic,

Cost : The value of the objective function($C_{\max} + T_{\max}$).

Result: A file for results with cost less than UB.

Quik : A file for results with cost less than $(UB+LB)/2$.

Counter: A counter for good solutions in Quick file.

Neighborhoods Subalgorithm

Setp1 : for $i= 1$ to 25

Step2 : Exchange single job.

Step3: Exchange each job with the last one.

Step4: Exchange adjacent jobs.

Step 5:Exchange the first with the last one .

Step6: Exchange each job with the first one.

Step7: Next.

The Genetic Algorithm (GA):

Genetic algorithm (GA) was firstly introduced by Holand , as a highly robust strategy. It may be viewed as population based algorithm, that constructs solutions by combining others. It is based on genetic process of biological organisms. In contrast to the single current solution in neighborhood search, a genetic algorithm works with a population of solutions, where each solution may not be selected and others may appear several times. Solutions are chosen from the mating pool according to fitness values, where better quality solutions are assigned a higher fitness. The following steps describe structure of GA:

Step 1: Initialization

Generate random initial population of m individuals (solutions) and evaluate fitness values for each of them. In this paper, we start with different values of m . The initial population can be generated at random or can be constructed by using heuristic methods.

Step 2: New Population:

Create a new population by repeating the following steps untill the new population is completed:

a) Selection

The selection of parents to create the next generation is based on the fitness of individual. The probability of selection of any individuals is proportional to its fitness, thus, the better fitness individuals are more likely to be selected for reproduction. The reproduction operator uses the fitness values for the selection of solutions. Solutions with higher fitness values tend to have more of their copies at the next generation. When the objective is to minimize a function, objective function value can not be directly used for the fitness values. One way to overcome this problem is to transform the objective function value (Z_i) to fitness value (f_i). A classic method for transformation is subtracting the objective function value from an arbitrary large constant,(determine this large constant as the largest objective function value in the current population).

The selection operator may be implemented in an algorithmic form in a number of ways. In this study, we have used roulette wheel selection which

assigns a probability to each individual (solution), it is computed as the proportion:

$$Fi = \frac{fi}{\sum_{j=1}^N fi}, i=1,2,\dots,n \text{ ----- (1)}$$

Once the fitness value (f_i) are calculated, the survival of the fittest principle can be implemented by roulette wheel selection, each solution is given a space on this wheel proportional to its fitness. The probability to select a solution s is given by (1).

Clearly, fitter sequences (solutions) stand a better chance of passing through it, but it is important to note that even sequences with a very low initial fitness have some chance of getting through. This ensures that each has some chance of developing into a better sequence by subsequent breeding. Suppose a sample population of sequences has fitness function

Example-1 : The problem of 4 jobs with the following data :-

value f_i as shown in the following table (1), where $\bar{F} = \frac{\sum_{i=1}^n fi}{n}$, $[\frac{Fi}{\bar{F}}]$ the integer number represent the number of times that the sequence appear.

i	1	2	3	4
a _i	3	7	5	3
b _i	2	4	8	6
d _i	6	20	15	22

Table -1: Description of the sequences which appear in the new population

i	Sequence s	$Z_i(s)$	$fi = Z_{\max} - Z_i$	$Fi = \frac{fi}{\sum_{i=1}^N fi}$	$\frac{Fi}{\bar{F}}$	$[\frac{Fi}{\bar{F}}]$	Sequence appear in new population
1	(3,4,1,2)	40	10	0.25	1	1	(3,4,1,2)
2	(3,1,2,4)	34	16	0.40	1.6	2	(3,1,2,4)
3	(2,3,4,1)	50	0	0	0	0	(3,1,2,4)
4	(4,3,1,2)	36	14	0.35	1.4	1	(4,3,1,2)
Sum		160	40	1			
Average		40	10	0.25			

i : number

Z_i : The objective function ($C_{\max} + T_{\max}$) value

In fitness- proportionate selection, sequence(3 ,1 ,2 ,4) is given probability of 40 % of being selected for each of the four positions in the new population. Thus, we expect that sequence (3 , 1 ,2 ,4) will occupy two of the

four positions in the new population, while sequence (3,4, 1 ,2) will occupy one of the four positions in the new population.

The corresponding weighted roulette wheel for this generation reproduction is shown in fig (1).

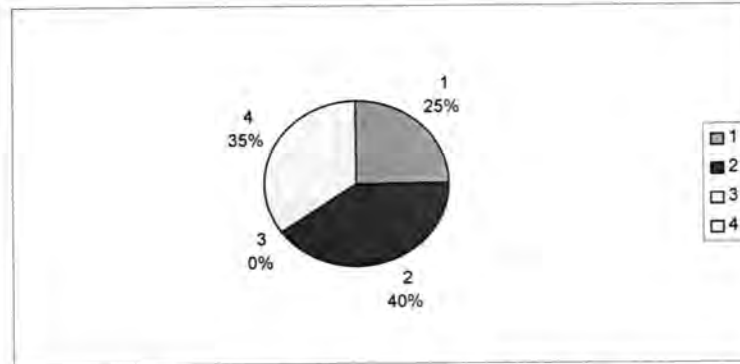


Figure -1: Sample wheel is sized for the example of table(1)

b) Crossover rate

These three different crossover rates are ($XRT > 0.5$, $XRT = 0.5$, $XRT < 0.5$). Results comparing the performances of the different crossover rates are given in table (2). It is clear from table (2) and Fig.(2) that $XRT > 0.5$ is the best one. Where the * indicate that the problem has the best solution in Table (2).

Table -2: Comparative computational results of the different crossover rate and for some value of n

n	Crossover Rate of GA		
	$XRT < 0.5$	$XRT = 0.5$	$XRT > 0.5$
10	68	66	58*
20	142	138	136*
30	227	222	221*
40	316	311	310*
50	399	393*	393*
60	491	489*	489*
70	595	595	593*
80	705	702*	703
90	793	791*	791*
100	877	873*	874

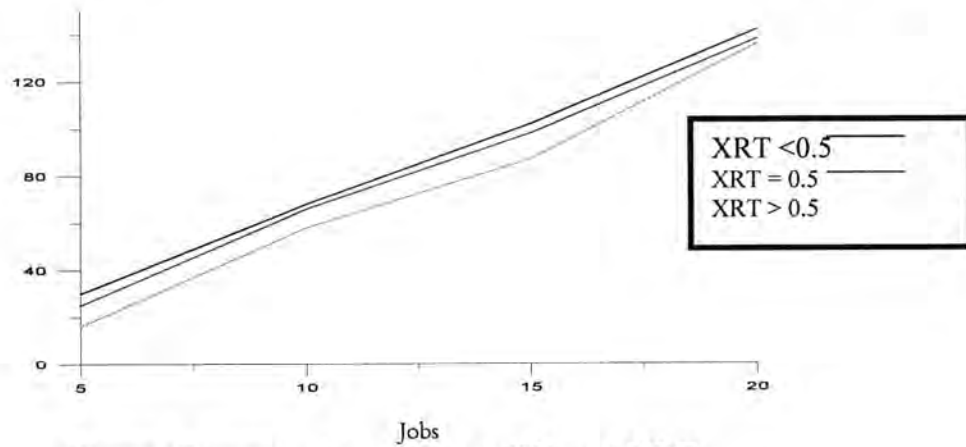
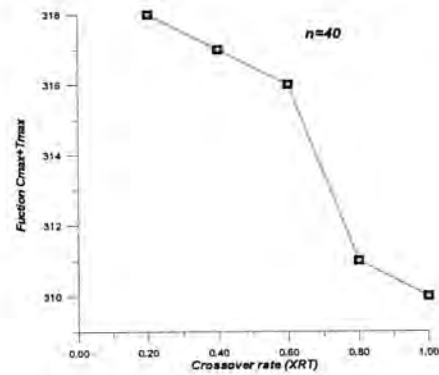
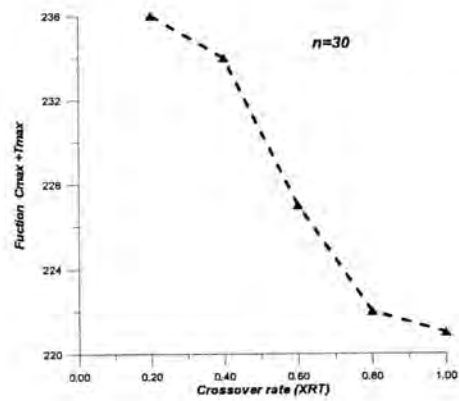
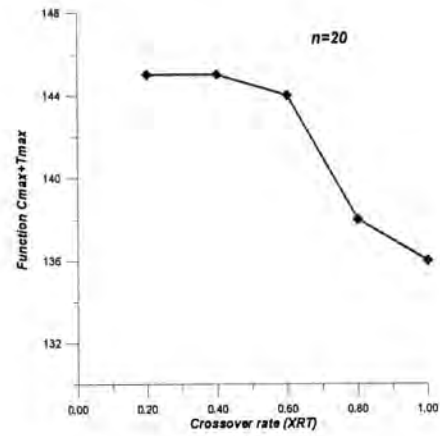
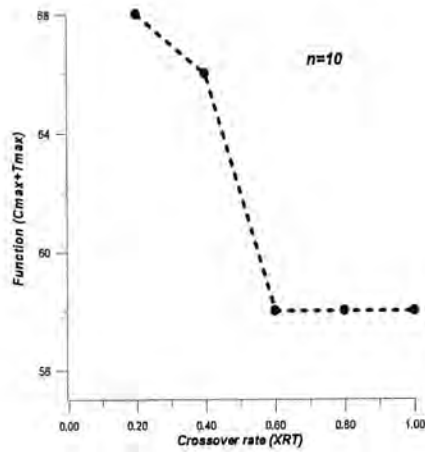


Figure -2: comparison of three different XRT,



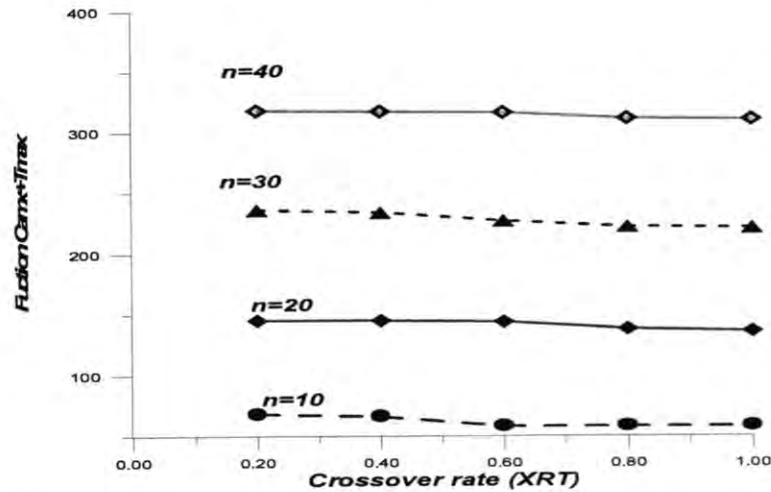


Figure -3: Description of the crossover rates for some values of n .

Figure (2) shows the difference between the crossover rates (XRT) such that crossover rate ($XRT > 0.5$) gives the best sequence (gen) for most of the time of the cases. Figure (3) shows that crossover rate (XRT) works for some values of n , ($n=10$, $n=20$, $n=30$ and $n=40$). The results show that when a crossover rate gives the best sequence (gen) then all the rates after this rate give the same sequence.

c) PBX crossover operator

In this step we used position based crossover (PBX) to generate the new population, to find the optimal solution or near optimal solution. Table (3) shows the results for (PBX) for example (1).

Example (2): Consider again the problem of 4 jobs with data given in example (1).

Table -3: Description of the processes of GA for finding solutions

Sequence appear in new population	PBX	Objective value $Z(s)$	$fi = Z_{\max} - Zi$	$Fi = \frac{fi}{\sum_{i=1}^N fi}$	$\frac{Fi}{F}$	$[\frac{Fi}{F}]$
(3,4,1,2)	(3,4,1,2)	40	0	0	0	0
(3,1,2,4)	(4,1,3,2)	28	12	0.63	2.52	3
(3,1,2,4)	(4,1,2,3)	37	3	0.16	0.63	1
(4,3,1,2)	(4,3,1,2)	36	4	0.21	0.84	1
Sum		141	19	1		
Average		35.25	4.75	0.25		
minimum		28				

d) Mutation Operator:

This operator should alter a solution (sequence) only slightly. The mutation operator is applied to perturb some of these new solutions. Hence it is clear that a small modification in the solution will result in a small deviation of its fitness value only.

Step 3 : Termination

The GA procedure stops when a fixed number of generations (or iterations) are executed here 1000 iterations. This means that the GA procedure continues until the population is converged to a good, if not optimal solution to our problem (P).

Local Search methods

Local search is a family of methods that iteratively search through the set of solutions. Starting from initial solution, a local search procedure moves from one feasible solution to a neighboring solution until some stopping criteria are met the choice of a suitable neighborhood functions has an important influence on the performance of local search.

Adjacent Pairwise Interchange Method (APIM)

This (APIM) depends on interchange elements (jobs) at positions (i) and (i+1) of a given sequence , (i=1,.....,n-1) (9). The following steps describe this method:

1-Initialization:

To obtain an initial current solution jobs are ordered according to Johnson rule (J.R),by sequencing job i with ($a_i \leq b_i$) first in non-decreasing order of a_i followed by the remaining jobs i with ($a_i > b_i$) sequenced in non- increasing order of b_i (i= 1,....,n) to obtain the current

sequence $\sigma = (\sigma(1), \dots, \sigma(n))$, with its objective function value (UB), where $UB = C_{\max} + T_{\max}$.

2-Neighbor Generation :

In order to improve the sequence σ , the position of two adjacent jobs $\sigma(i)$, $\sigma(i+1)$, $(1 \leq i \leq n-1)$ are transposed. Hence a new sequence σ' is obtained with its objective function $UB' = C_{\max} + T_{\max}$.

3-Evaluation :

If the improvement is made (i.e. $UB' < UB$) then, the two jobs are left in their new positions. On the other hand, the two jobs are replaced in their original positions. The procedure is then repeated from step (2) and other possibilities are considered in a similar way.

4-Termination Step:

The method is terminated when all possibilities are considered for adjacent jobs $\sigma(i)$, $\sigma(i+1)$, $(i=1, \dots, n-1)$, without making any improvement.

Descent Method (DM)

This method is a simple form of local search methods. It can be executed as follows:

1- Initialization:

In this step, the feasible solution $\sigma = (\sigma(1), \dots, \sigma(n))$ obtained from Johnson rule (J.R), is chosen to be the initial current solution for descent method, with its objective function value (IUB).

2- Neighbor Generation:

In this step, a feasible neighbor $\sigma' = (\sigma'(1), \dots, \sigma'(n))$ of the current solution is generated by choosing randomly two jobs from σ in the first time, (not necessarily adjacent) and transpose their positions, and a feasible neighbor is also generated by choosing randomly a block of jobs from σ at the second time, and transpose their positions, for each case calculate the function values and the minimum value is denoted by (CUB).

3- Acceptance Test:

Now consider the test whether to accept the move from σ to σ' or not, as follows:

(a) If $CUB < IUB$: then σ' replace σ as the current solution and we set $IUB = CUB$, and go to step (2) (Neighbor generation).

(b) Other wise (i.e. $IUB \leq CUB$): σ is retained as the current solution, and go to step 2.

4-Termination Test: Repeat step (2), and other possibilities are considered in a similar way. The DM terminates if no neighbor provides an improved objective function value, in which case the current solution IUB is a local minimum.

The Simulated Annealing Method(SAM):

It is well known that in SAM, improving and neutral moves are always accepted, while deteriorating moves are accepted by a controlled probability (10).

The following steps describe SAM.

1-Initialization:

The same technique described in DM is used to obtain an initial current solution $\sigma = (\sigma(1), \dots, \sigma(n))$ and IUB.

2-Neighbour Generation:

A feasible neighbor of the current solution σ is generated by choosing randomly two jobs $\sigma(i), \sigma(j)$ such that $(1 \leq i < n) (1 \leq j \leq n)$ not necessary adjacent and transpose their positions and compute the function value for this neighbor to be (CUB).

3-Acceptance Test:

In this step, the difference value between the current initial solution IUB and the new value CUB, $\Delta = \text{CUB} - \text{IUB}$ is calculated, then evaluated as follows:

a) If $(\Delta < 0)$: then (CUB) is accepted as the new current solution, and set $\text{IUB} = \text{CUB}$ and go to step 2

b) If $(\Delta > 0)$: (CUB) is accepted with $P(\Delta) = \exp(-\Delta/t)$, which is the probability of accepting a move, which results in an increase of Δ in the objective function value, where t is a parameter known as the temperature and is usually set to large (i.e. the probability of accepting a worse solution is high) in the beginning of the search, and gradually decreases as the search proceeds.(11)

Let (it) denotes the number of iterations that are considered. Where at each iteration i , $1 \leq i \leq it$ a temperature t_i is derived from the following recursive formula, described by Anderson *et al.* (12).

$$t_i = t_{i-1} / (1 + B * t_{i-1}) \quad i=2, \dots, it$$

Where: $B=(t_1-1)/(it*t_{i-1})$; $t_1=10$ and $it=1000$

4-Termination Test:

After one thousand iterations the algorithm terminates at a feasible solution (SUB).

Test problems

In selecting test problems, one important goal is to create problem instances that are representatives of the general problem class. We generated the test problems with value of n (10,20,30,40,50,60,70,80,90,100,150,200). When comparing the performance of algorithms, it is important to test them on a range of problem instances. The main characteristic of an instance of our scheduling problem is its size, as measured by numbers of jobs n . Our test problems were generated as follows: (13). The processing times a_i and b_i in the test problems were randomly sampled from a uniform distribution on the integers defined on (1,10), and due dates were generated from the uniform distribution on $[(1-TF-RDD/2) sp, (1-TF+RDD/2) sp]$ such that

$$sp = \sum_{i=1}^n C_i \text{ where } C_i = (a_i + b_i)/2, TF = 0.2, 0.4, RDD = 0.2, 0.4, 0.6, 0.8, 1$$

Five test problem were created for some contributions of TF and RDD.

1. Initial Solutions

The sequence which is obtained by using Johnson's rule (J.R) can be used as an initial solution for adjacent pairwise interchange method (APIM), descent method (DM) and simulation annealing method (SAM) as well as in the new heuristic method (NHM). But in genetic algorithm we generate old population randomly. Also J.R. is used to generate upper bound (UB) on the optimal solution for our problem.

If such constructive methods can produce initial solutions of sufficiently high quality, then the need for local search methods, with their heavier computational requirements, is reduced.

2. Comparison between the optimal (BAB) solution and the new heuristic method (NHM)

This section shows the efficiency of the new heuristic method given in section (4) and compares it with optimal solution obtained by BAB algorithm for each test problem.

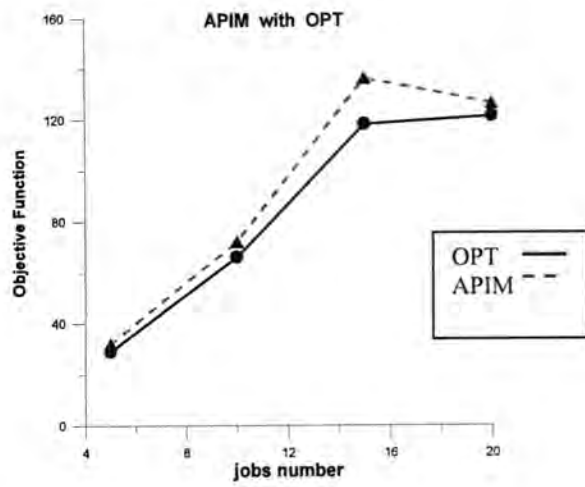
An optimal solution for each test problem (with $n \leq 30$) is obtained by BAB algorithm, these optimal solution values are used to assess the quality of solutions generated by the new heuristic methods. For our BAB algorithm, whenever a problem was not solved within a time of 6000 second, computation was bounded for that problem (11). Since the BAB algorithm can not generate optimal solutions using reasonable limits on computation time for test problems (with $n > 30$). In this case, the new heuristic method (NHM) is used to obtain the best solution value and forms the basis for comparison. It should be noted that this (NHM) for $n=80$ and $n=100$, also sometimes a large amount

of time is needed to give good solutions. Table (4) gives the results of comparison between BAB and the new heuristic method (NHM). Also table (4) shows the results for lower and upper bounds for our problem. It is clear from table (4) that the results show that the new heuristic method NHM have the exact value of the optimal for 18 of the 20 test problems.

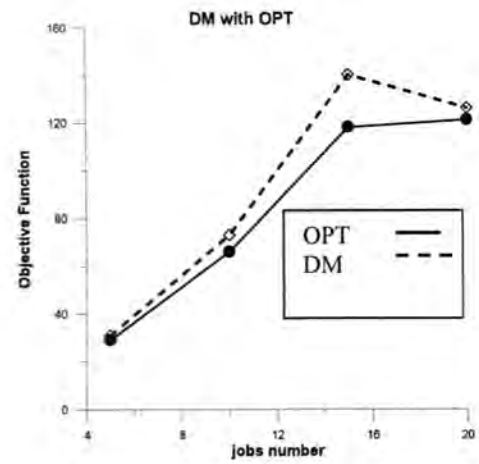
Table -4: Comparative Computational Results

n	No	UB	LB	BAB	NHM	CT of NHM
5	1	35	24	29	29	0.3
	2	31	21	27	27	0.21
	3	31	20	28	28	0.13
	4	40	26	35	35	1.2
	5	56	37	43	43	0.3
10	1	60	49	50	50	1.33
	2	81	64	69	69	1.50
	3	77	60	67	67	1.54
	4	102	66	73	73	1.65
	5	73	58	66	66	1.23
15	1	110	91	91	91	3.25
	2	142	113	118	118	5.13
	3	128	92	97	97	5.2
	4	149	114	123	123	3.25
	5	104	79	89	89	4.25
20	1	126	112	121	121	15.3
	2	159	118	124	126	12.3
	3	193	132	143	143	14.42
	4	176	128	128	128	15.33
	5	190	132	148	152	11.22

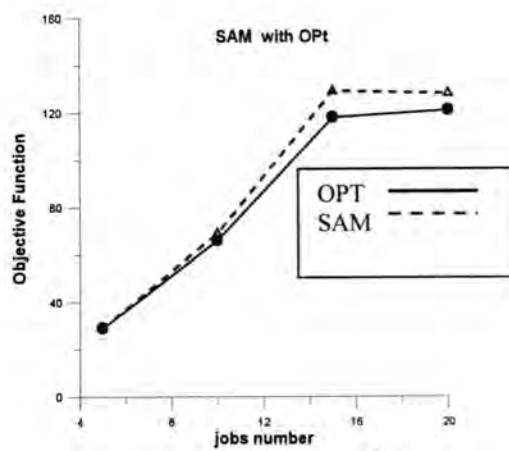
No: test problem number , n : Number of jobs
 UB:Upper bound , LB: Lower bound
 BAB: Branch and bound algorithm , NHM: New heuristic method
 CT: computation time (in seconds)



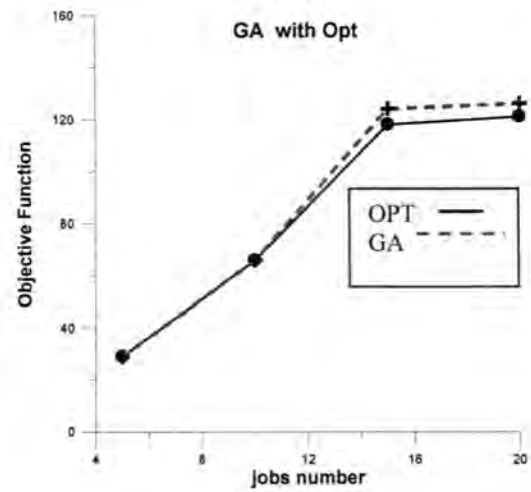
(a)



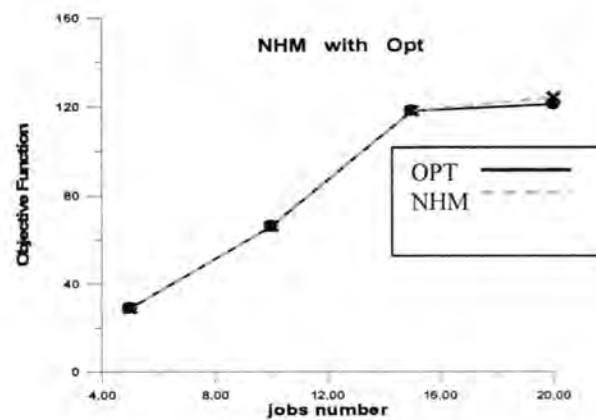
(b)



(c)



(d)



(e)

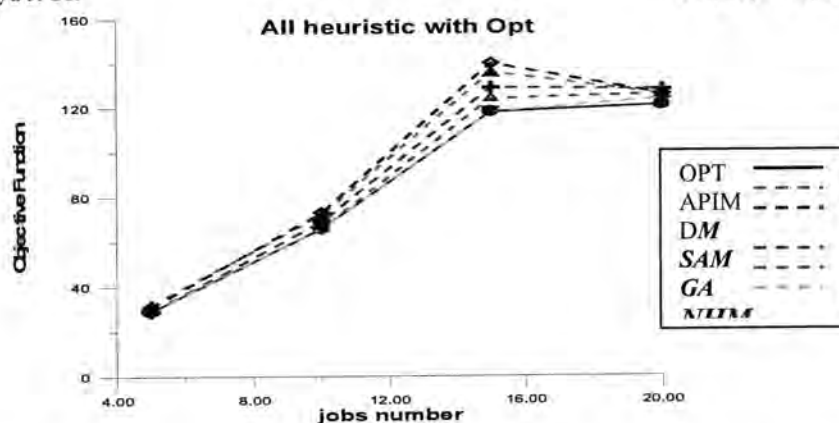


Figure -4:for (a, b, c, d and e) shows each local search heuristic , Optimal and comparing between them

3. Comparative Computational Results

In this section, we shall report on the computational experience with different local search heuristic methods. For the methods (adjacent pairwise interchange method (APIM), descent method (DM), simulated annealing method (SAM), genetic algorithm (GA) and the new heuristic method (NHM) that have been described in this paper, we present a table of results which shows the importance of each method. Table (5) shows that the (NHM) gives the best results than all the other heuristic methods but with longer time, while, the genetic algorithm GA gives the second better value after (NHM) with shorter time. Table (5) describes the comparison between the local search heuristic methods, the upper and lower bounds. Table (5) Compares the computational results.

Table -5: Comparative Computational Results

Number of jobs	Upper bound	Lower bound	API	DM	SAM	GA	NHM
10	70	52	66	68	62	58	58
20	156	129	150	140	142	136	135
30	238	211	231	226	226	221	220
40	325	289	317	316	313	310	301
50	411	379	407	396	396	393	390
60	505	471	501	494	491	489	485
70	613	570	602	598	597	593	592
80	719	633	712	706	707	703	700
90	803	758	800	794	795	791	788
100	885	849	879	877	877	874	870
125	1122	1076	1115	1119	1115	1106	---
150	1363	1311	1349	1353	1350	1346	---
175	1616	1539	1601	1613	1599	1596	---
200	1833	1778	1819	1823	1822	1817	---

REFERENCES

1. Conway , R.W. Maxwell W.L. and Miller L.W. " Theory of Scheduling Addison Wesley, Reading, MA, (1967).
2. Johnson S.M." Optimal two and three stage production schedules with set-up times included". *Naral Res. Logist Quart* 1:61-68(1954).
3. Lenstra J.K., Rinnooy Kan A.H.G., and Brucker P., " Complexity of Machine Scheduling Problems". *Ann. Of Discrete Mathematics* ,1:343-362(1977).
4. Robert A.J. Matthews "The Us of Genetic Algorithm In Cryptanalysis *Cryptologia* . XVII (2)Apil (1993).
5. Graham R.L., Lawler E.L., Lenstra J.K., and Rinnooy kan A.H.G., " Optimization and approximation in deterministic sequencing and scheduling theory : a survey ", *Discrete math.* 5, :287-326(1979).
6. Karp R.M., Reducibility among combinatorial problems. In *complexity of computer computations*, Miller R.E and Thatcher J.W.Eds. plenum press , New York:95-103 (1972).
7. Ignall E., Schrage L.E., "Application of the branch and bound technique to some flow shop scheduling problem", *Oper.Res.* 13:400-412 (1965).
8. Lominickiz. A., "A branch and bound algorithm for the exact solution of three- machine scheduling problem", *Oper. Res. Quart* 16, :89-100(1965).
9. Chen B., A better heuristic for preemptive parallel machine scheduling with batch set-up time. *SIAM Jornal on computing* 22:1303-1318 (1993).
10. Caruwels H.A.J., A comparative study of local search methods for one machine sequencing problems, Ph.D. thesis, Katholike University Leuren (1998).
11. Reeves C.R., " modern heuristic techniques for combinatorial problems", John Wiley and sons. Inc., New York (1993).
12. Anderson E.J., Glass C.A. and Potts C.N., " local search in combinatorial optimization, edited by E.H.L. Aarts and J.K. Lenstra, wiley (1997).
13. Anderson E.J., Glass C.A. and Potts C.N., "Application of local search in machine scheduling", March (1995).

مجلة علوم المستنصرية

تصدر عن كلية العلوم الجامعة المستنصرية

عدد خاص

بحوث المؤتمر العلمي السادس
لكلية العلوم - الجامعة المستنصرية
للفترة 9-10 شباط لسنة 2010

رئيس التحرير

أ. د. رضا ابراهيم البياتي

مدير التحرير

أ.م.د. اقبال خضر الجوفي

هيئة التحرير

أ. م. د. ايمان طارق محمد العلوي

أ. م. د. رمزي رشيد علي العاني

أ. م. د. انعام عبد الرحمن حسن

أ. م. د. عوني ادوار عبد الاحد

أ. م. د. ماجد محمد محمود

أ. م. د. سعد نجم باشخ

أ. م. د. حسين كريم سليمان الوندائي

الهيئة الاستشارية

أ. م. د. كاظم حسن حسين الموسوي

أ. د. طارق صالح عبد الرزاق

أ. د. مهدي صادق عباس

أ. م. د. عبد الله احمد رشيد

أ. م. د. حسين اسماعيل عبد الله

أ. م. د. مهند محمد نوري

أ. م. د. منعم حكيم خلف

أ. م. د. عامر صديق الملاح

أ. م. د. طارق سهيل نجم

أ. م. د. يوسف كاظم عبد الامير

عضوا
عضوا
عضوا
عضوا
عضوا
عضوا

رئيسا
عضوا
عضوا
عضوا
عضوا
عضوا
عضوا
عضوا
عضوا
عضوا

المحتويات

الموضوع	رقم الصفحة
تأثير إضاءة القاعة الدراسية على وضوحية النصوص الملونة على سبورة بيضاء	8-1
رشا عواد عبطان	
دراسة الخصائص الاحصائية للشدات المسجلة بواسطة متحسسات الويب كاميرا enet لصورة اختبارية بيضاء	16-9
اسماء محمد روؤف و فرح جواد كاظم و شيما حسين عبد مسلم و علي عبد داود الزكي	
دراسة خصائص I-V في تنفيق غشاء السوبر	20-17
سوزان ملك شاقولي	
دراسة فجوة الطاقة للبولي ستايرين (PS) المشوب بثاني كلوريد الحديد (FeCl ₂)	25-21
محمد حميد عبد الله و عبدة عامر عبد الحسين و داد هنو عباس	
تأثير الإضاءة غير المنتظمة على وضوحية النصوص باختلاف المسافة	36-26
علي عبد داود الزكي و رشا عواد عبطان و عدي عواد عبطان	
دراسة الخصائص الاحصائية لكاميرا الهاتف النقال نوع (Nokia7610) تحت شروط إضاءة مختلفة	58-37
هاله نصير كاظم و علي عبد داود الزكي و كاظم جواد الشجيري	
المعاملة بطريقة الفرن الحراري وتقنية الليزر وتأثير اضافة الزنك على بعض الخواص الميكانيكية لسبيكة حشوة الاسنان	66-59
حليمه جابر محمد و جعفر هاشم محسن و اقبال فاضل و اطياف خالد و سندس كريم	
تحضير وتشخيص معقدات بعض العناصر الانتقالية مع مشتقات 2،1،4- ثيادايازول	82-67
نجاه جواد العبيدي و سنان مدحت البياتي	
تقديرات طيفية امتصاصية جزيئية واخرى ذرية للمضادات الحياتية: الامبيسيلين والاموكسيسلين والسيفالكسين والسيفترايكسون والسيفوتاكسيم في بعض المستحضرات الصيدلانية	101-83
فاضل جاسم محمد و منى محمود خضير و انتظار ناصر حسون	
تخليق ودراسة طيفية وثرموديناميكية لبعض معقدات البورفيرينات- الفلزية مع بعض المانحات الاليكترونية	117-102
مؤيد حسن محمد و ناجي علي عبود	
تحضير اقطاب انتقائية للمادة الدوائية Diclofenac sodium ومقارنتها طيفيا	123-118
محمد خليل محمد علي و عدي احمد عبد الستار و لمياء حسين كاظم و ابتسام عبد الحسين	
دراسة تأثير التراكيز المختلفة للمواد الفعالة المستخلصة من النباتات الطبية على التغيرات الكروموسومية	130-124
إقبال فاضل علوان و عصام فاضل الجميلي و علي عبيس و حسين علي محمد و حليلة جابر	

136-131	دراسة تأثير التلوث بالكروم على فيتامينات مضادات التأكسد حنان فاضل عباس وجعفر هاشم محسن وحليمة جابر محمد واسماء سوري محمد ومحمد خليل محمد وعدنان عبدالله حسين واسيل عبد الحسين عبيد
145-137	تأثير المستخلصات المائية والكحولية لنبات الهيل <i>Elettaria</i> <i>cardamomum</i> في نمو بعض البكتريا المعزولة من التهابات الأذن الوسطى زيد شاكر ناجي محمود و محمد عبد الجليل خليل
152-146	المكونات الكيميائية لبذور الحلبة المحلية - <i>Trigonella foenum</i> <i>graecum</i> وتأثير مستخلصها على بعض الاحياء المجهرية الممرضة. رامي علي تقي وامنة نعمة الثويني وصفاء عبد لطيف المعيني
161-153	تنشيط النطف البربخية في الفئران باستخدام مصل دم النساء الفاعل المضاف الى اوساط زرعية مختلفة خالد سهيل عيود العزاوي
167-162	التحري عن سم الباتوليين في ثمار التفاح المتعفن في السوق المحلية خالد نصيف جاسم
173-168	إلكتار الدقيق لنباتات الأناناس <i>Ananas sativas</i> باستخدام تقنية زراعة الأنسجة زينب عبد الجبار حسين الحسيني و عبد الجاسم محسن الجبوري و هاشم كاظم محمد العبيدي و محمد خزعل حميد
184-174	تحديد المتغيرات في وزن أنسجة وطول الحبل السري وأبعاد الاوردة والشرايين مع دراسة نسيجية مرضية للمريضات المصابات بداء المقوسات <i>Toxoplasmosis</i> بدر محمد العزاوي وسالم رشيد العبيدي وآمال خضير عباس وشذى خضير عباس
195-185	مقاومة الانسولين <i>Insulin resistance</i> لدى مرضى قصور الدرقية <i>Hypothyroid patients</i> شيماء رزاق إبراهيم وصباح ناصر العلوجي وخالد إبراهيم اللهيبي
206-196	تأثير مستخلصي عرق السوس وثمار الكاكي في تثبيط الأنحرفات الكروموسومية المستحثة بمادة كبريتيت الصوديوم في خلايا الفأر الأبيض رحيم فاضل مرهون وعبد الأمير ناصر غلوب ومؤيد صبري شوكت
212-207	تشخيص الفطريات الجلدية الخيطية المعزولة من المرضى المصابين بسعفة الرأس <i>tinea capitis</i> في بغداد عبد الرضا طه سرحان ورسول عبد السادة كريم
221-213	إنتاج البروتينيز القاعدي من بكتريا <i>B. stearotheophilus</i> AEAL2 بوساطة تخمرات الحالة الصلبة واختبار كفاءته في بعض التطبيقات الصناعية عصام فاضل علوان الجميلي واسماء وليد داود

225-222	الكشف عن بكتريا <i>Pseudomonas aeruginosa</i> المنتجة لأنزيم البييتالاكتاميز المعدني (IMP1) والمعزولة من المرضى في محافظة النجف محمد فرج المرجاني وأنتصار علي مزعل وميسون حميد اسماعيل
236-226	استخدام بعض المطفرات على بكتريا حامض اللاكتيك لتحسين الفعالية التنبؤية ضد البكتريا المرضية والتألفة للأغذية عبد الواحد باقر ونبراس نزار محمود وسمير فتح الله سمعان
245-237	قابلية تأثر بكتريا الـ <i>Salmonella enterica serovar typhi</i> لبعض عوامل المضادات الجرثومية ودراسة العوامل المؤثرة على امراضيتها نهاد خلاوي تكتوك
253-246	دراسة القابلية التطفيرية والمضادة للتطهير للمستخلص الفلافوني المنقى جزئياً لنبات الميرمية <i>Salvia officinalis</i> باستخدام نظام بكتيري علي حافظ عباس و عصام فاضل علوان
270-254	مقارنة لبعض الطرائق الحصينة لتقدير معلمة القياس لبعض التوزيعات الاحتمالية نادية هاشم النور
273-271	دراسة تأثير زاوية ميل واتجاه السطح في قياس الإشعاع الشمسي الكلي احمد أنور القيسي
282-274	الموارد المائية وأهميتها البيئية في منخفض الكعرة (صحراء العراق الغربية) عقيل عباس احمد الزبيدي

تأثير إضاءة القاعة الدراسية على وضوحية النصوص الملونة على سبورة بيضاء

رشا عواد عبطان

الجامعة المستنصرية/كلية التربية الأساسية / قسم الرياضيات

الخلاصة

أن توزيع شدة الإضاءة بشكل متجانس على النصوص الملونة المكتوبة على السبورة (Whiteboard) ينتج فرق ثابت تقريباً في قيم التباين للنصوص الملونة أي للمركبات اللونية الثلاث RGB لأن هذه النصوص سوف تستلم نفس المقادير من قيم شدة الإضاءة مهما غيرنا شدة الإضاءة زيادة أو نقصان ، لكن في حالة شدة الإضاءة بشكل انتقائي وغير متجانس بين تلك النصوص ، فإن كل نص قيم تباينه سوف يختلف عن النص الآخر بسبب اختلاف توزيع شدة الأضاءة بينها . لذا توجهنا إلى دراسة تباين النصوص الملونة على اللوحة البيضاء باختلاف المسافات وبإضاءة تامة (قليلة) داخل القاعة الدراسية (قاعة عتمة) . إذا تبين أن بزيادة المسافة نلاحظ انخفاض قيم التباين للنصوص المكتوبة على اللوحة ولجميع الألوان المعتمدة في كتابة النص، إضافة إلى انخفاض وضوحية هذه النصوص للمركبات اللونية الثلاث RGB ولمركبة الإضاءة L.

Abstract

That the distribution of light intensity uniformly colored texts written on the blackboard (Whiteboard) almost invariably result in a difference in the values of variation of the text color for any of the three RGB color vehicles because these texts will receive the same amounts from the values of others, no matter how light intensity light intensity increases or decreases, but in the case of light intensity selectively and inconsistently with those texts, all the text values of variability will differ from the other text because of the different distribution of light intensity between them. So we went to study texts contrast color on the whiteboard in different spaces and lighting complete (a few) within the classroom (Hall of darkness). If it turns out that the increase of the distance note down the values of variation of the texts written on the board and all the colors approved in writing the text, as well as reduced and Douhip these texts of the three RGB color vehicles and vehicle lighting L.

المقدمة

اللون هو الصفة المرئية لكل الأشكال والهيئات وهو من الناحية العلمية الفيزيائية يعتبر صفة للضوء وهو واحد من أشكال الطاقة الإشعاعية ويأخذ أسمه من الإحساس الناتج عن إثارة العين بطاقة إشعاعية معينه أو بضوء ذي طول موجي معين وتستطيع عين الإنسان أن ترى مزيجاً لعدد من الأطوال الموجية للضوء المرئي التي تبدأ بأطولها الأحمر وتنتهي بأقصرها وهو البنفسجي وهذه الأطوال الموجية تحمل معلوماتها إلى النظام المرئي للإنسان حيث تغزو الألوان إلى الأجسام التي تظهرها وباقتراانها مع أنواع أخرى من المعلومات كالهئية والحجم وغيرها ينتج الإحساس الذي يفسره العقل باللون (1) . أن تحسس الإنسان للألوان يعتمد على طبيعة الضوء المنعكس عن الجسم . فالجسم الذي يعكس كل الأطوال الموجية في النطاق المرئي بنفس الدرجة نراه أبيضاً بينما الجسم الذي يمتص معظم تلك الأطوال ويعكس الأطوال الخاصة باللون الأخضر مثلاً يظهر باللون الأخضر . أما اللون الخالي من الألوان فيدعى بالضوء الأحادي اللون Monochromatic or Achromatic وتعد الشدة هي الخاصية الوحيدة لهذا الضوء (2).

وتشير البحوث إلى إن استجابة الإنسان هي استجابة موضوعية وذاتية فالعين تعمل تكيفات عندما تستقبل موجات الضوء الأحمر والتي تركز خلف الشبكية ولذلك فإن عدسة العين تتحدب بشكل كبير للتركيز على اللون الأحمر وتسقط موجاتها إلى الأمام وهذا يخلق نوعاً من الخداع البصري للسطوح الحمراء حيث تبدو أقرب وأكبر مما هي عليه في الحقيقة . أما اللون الأزرق فيتصرف بعكس الأحمر بالضبط فهو يسبب تسطح عدسة العين وبذلك يجعل السطح الأزرق يتراجع في البعد البؤري ويبدو كأنه

يصغر في الحجم . بينما الضوء الأخضر تتركز أمواجه مباشرة على الشبكية ولهذا السبب فإن الأخضر هو الأكثر راحة للبصر(3).

هنالك العديد من الدراسات السابقة التي اهتمت بدراسة تباين الصور الملونة من خلال تحسين الإضاءة ودراسة تأثير الإضاءة على جودة الصورة وفيما يلي إيجاز أهم هذه الدراسات :-

- عام 1990 اقترح Johnson استخدام طريقة التباين للكشف عن الحافات الموجودة في الصورة ذات الإضاءة غير المتساوية أو الضعيفة حيث أن هذه الطريقة لا تعتمد على القيمة المطلقة للإضاءة Absolute Brightness كما استخدم الباحث نوافذ حيزيه 5×5 ذات عوامل التدرج للكشف عن الحافات إذ تعد طريقة التباين مناسبة للصور المرئية والصور بالأشعة تحت الحمراء حيث يمكن اعتماد هذه الطريقة في تطبيقات الإنسان الآلي التي لا يمكن فيها السيطرة على الإضاءة (4).

- عام 1996 اجري الباحث Peli Eli دراسة حول تأثير الإضاءة والتردد المكاني على تحسس التباين ما فوق العتبة واستعمال أنماط اختباريه مختلفة للإضاءة والتردد المكاني لغرض مقارنة التباين ، ففي حالة العتبة كان انخفاض الإضاءة اقل ما يمكن من التأثير على تحسس التباين فوق العتبة عند الترددات الواطنة . إن نتائج هذه الدراسة مهمة للنماذج البصرية المستخدمة في تحليل جودة الصورة (5) .

- عام 1997 قدم Curlander بحثاً يهدف إلى تحسين الجودة العالية للصورة الرقمية من خلال استخدام المرشحات المحسنة لاسترجاع الحافات وتحسين معالم الصورة حيث قام الباحث ببناء برنامج حاسوبي لزيادة حدة الحافات sharpening edges عن طريق حساب القيمة العليا المثلى فوق الإضاءة العالية over shoot كدالة للسطوع والتباين إذ توصل إلى أن القيمة العليا المثلى فوق الإضاءة العالية تزداد مع زيادة كلا من السطوع والتباين حيث تأخذ شكل الزيادة فيها شكل الدالة الأسية بالنسبة لدالة السطوع في حين تزداد بصورة غير خطية عند الحافات ذات التباين وتتسطح عند قيم التباين الأكثر من 20 (6) .

- اقترح الباحثون Pingxue , Kaiyu and Leiwang سنة 2001 طريقة لتحسين الصور الناتجة من التشاكة البصري Optical Coherence Tomography(OCT) ، في هذه الطريقة تم استخدام ثلاث طرائق للتكميم وهي أقل تشويه minimum distortions ، توسيع المعلومات information expansion والانتروبي الأعظم maximum entropy . إن نتائج التكميم باستخدام هذه الطرق مقارنة مع الطرائق المعتمدة على اللوغاريتم أظهرت زيادة في التباين وزيادة نسبة الإشارة إلى الضوضاء بالإضافة إلى تقليل خطأ التكميم (7) .

- اقترح الباحثون William Thompson. 2003 خوارزمية معالجة لتحسين الصور للمناظر الليلية، حيث تمكنت هذه الخوارزمية من جعل الصور المأخوذة في ضوء النهار وكأنها مأخوذة ليلاً حيث تقوم بتقليل التباين وتقليل اضاءة الصورة. وجعل الصور بإضاءة زرقاء، وشملت دراستهم المناظر الحقيقية المشاهدة ليلاً والضوضاء المرافقة لها ومقدار التشوه الحاصل فيها(8).

الرؤية الملونة

هي القابلية التي يتم التفريق بين مختلف الألوان حسب التحسس للأطوال الموجية . أن استيعاب اللون هو من وظيفة المخاريط في العين وهذا يحدث فقط في حالة Photonic Vision أي في الإضاءة العالية أو المتوسطة أو إلى حد ما عند تكيف الشبكية للضوء القليل .

هنالك ثلاث أنواع من المخاريط التي تتحسس ألوان الطيف الضوئي (RGB) ، أما الضوء الأبيض فيتم أدراكه عن طريق ألوان الطيف الضوئي وتسمى (Trichromatic) وهي أساسيات نظرية لرؤية ألوان الطيف الضوئي (9) .

أهم الظواهر المؤثرة في الرؤية اللونية

ظاهرة بور كنجي Purkinge Phenomenon

هو التغير الذي يطرأ على الدرجة القصوى من اللعان في الطيف الضوئي المرئي اللوني ، انطلاقاً من اللون الأصفر نحو اللون الأخضر ، فالألوان ذات الأمواج الطويلة كالأحمر تفقد لمعانها لدى تقليل الضوء المسلط عليها أكثر مما يفقده من لمعان الألوان ذات الأمواج القصيرة كالأزرق وذلك لان الشبكية تفقد

حساسيتها للون الأحمر أولاً ، وعند تقليل الإضاءة بالتدريج تفقد حساسيتها للونين الأخضر والأزرق ، فاللون الأحمر يبدو فاقعاً أكثر من الأزرق بالإضاءة الساطعة بينما الأزرق أكثر لمعاناً في النور القاتم وقد سميت هذه الظاهرة باسم مكتشفها العالم (بور كنجي) (10) .

● ظاهرة مابعد الصورة After Image Phenomena

تعرف على أنها الصورة الحسية في الذاكرة والذهن بعد زوال المنبه الخارجي . فإذا ما تكيفت العين على لون معين من خلال التحديق به لبعض الوقت ثم إزاحة النظر باتجاه سطح أبيض أو رصاصي على لون معين فإن اللون المكمل سوف يظهر على هذا السطح . فاللون الأبيض سوف يظهر أخضر فاتح إذا ما حددت بعامل أو محفز ذي لون أحمر وهذه الظاهرة تسمى بالظاهرة مابعد الصورة وتفهم هذه الظاهرة نتيجة للإجهاد البصري .

فعندما تتكيف الشبكية على لون معين ولنقل اللون الأحمر حيث المتحسسات للون الأحمر الموجود فيها تعاني من أجهاد مؤقت ، وعند استبدال العامل المحفز الأحمر باللون الأبيض فإن استجابة هذه المتحسسات تكون أكثر قوة في تحسسها للأشعة الكلية المنعكسة من السطح وفي نفس الوقت تكون متحسسة باتجاه اللون الأخضر تعمل بكامل كفاءتها(11).

● التباين المتزامن Estimation Contrast

قلما ترى في الحقل البصري لونا منفرداً ومنعزلاً حيث غالباً ما يلاحظ وجود ألوان مختلفة بشكل متزامن وأنى . وهذا يخلق تأثيراً بصرياً يرتبط بقوة بالظاهرة البعدية فالعين تولد اللون المكمل للون المرئي وتسقطه باتجاه اللون المجاور أو تفرضه عليه . ويمكن ملاحظة ظاهرة التباين المتزامن بين لونين متكاملين أو غير متكاملين من خلال تجربة بسيطة وذلك بأخذ مربع رصاصي حيادي محاط بخلفية حمراء اللون فنلاحظ أن اللون الرصاصي أصبح تشويهاً مسحة من اللون الأخضر (اللون المكمل للون الأحمر) (11).

الإدراك اللوني

لأدراك اللون متطلبات يجب توفرها هي :-

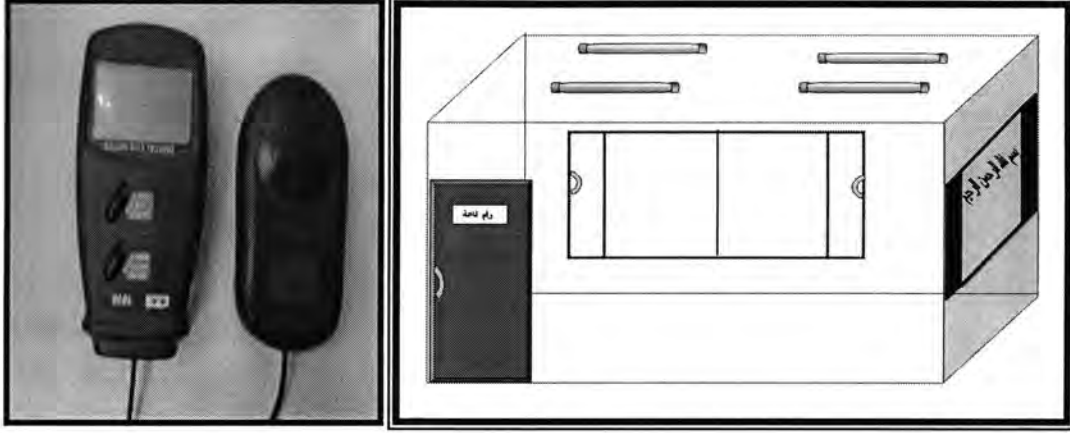
1. يجب أن يكون هنالك تباين أو اختلافات في طول الموجات الضوئية التي تستلمها العين في المحيط المرئي.
2. يجب أن يكون هنالك تباين في الانعكاسات الضوئية للسطوح .
3. يجب أن يكون هنالك اثنان أو أكثر من المتسلّمات (Receptors) يختلفان في تأثيرهما بالأطوال الموجية التي تولف الضوء المرئي .

وهكذا فإن اللون لا يخلق انطباعات ذاتية وموضوعية بل يؤثر في تقييمنا و إدراكنا للزمن والحجم والوزن والحرارة والضوضاء ، إذا أن تحقيق الرؤيا الجيدة وأبصار الألوان على حقيقتها يتم بالاعتماد على الإضاءة النهارية (11).

منظومة العمل

دراسة تأثير الإضاءة على النصوص المكتوبة على السبورة في قاعة دراسية .

إن النصوص المكتوبة على اللوحة البيضاء (White board) تبدو أقل قيمة ضوئية بالنسبة للطالب الجالس على مسافة بعيدة مقارنة بالطالب الجالس على مسافة قريبة من اللوحة إذا كان هنالك تساوي في شدة إضاءة قاعة الدرس إضاءة منتظمة حيث تؤثر مسافة النظر على قيم التباين للنص المكتوب على اللوحة والسبب في ذلك لأن المسافات البعيدة تقلل من قيمة التباين للنصوص فتؤثر في وضوحيتها من حيث التفاصيل أو الحدود الفاصلة بين النصوص المكتوبة على اللوحة ويعود السبب في ذلك إلى الهواء الذي يفصل بين العين والنص المكتوب الذي يزداد غشاوة في النص كلما زادت المسافة الفاصلة . لذا اعتمدنا في هذه الدراسة على كتابة نص باستخدام ألوان قلم بورد مختلفة نوع Dry – Erase ولمسافات مختلفة cm (100 , 200 , 300) ، حيث تمت عملية التصوير في صباح الساعة العاشرة من يوم 14 / 4 / 2009 داخل قاعة دراسية موضحة موقع الإضاءة الصناعية العمودية من السقف وموقع الشباك (الإضاءة الطبيعية) بالنسبة للوحة البيضاء (Whiteboard) كما مبين بالشكل (1) حيث استخدم جهاز قياس شدة الإضاءة (Lux meter) الموضح في الشكل (2) لقياس شدة الإضاءة في مختلف الاتجاهات للقاعة الدراسية .



شكل 1- القاعة الدراسية المستخدمة في عملية التصوير شكل 2- جهاز قياس شدة الإضاءة

حيث تم التقاط صور بواسطة الكاميرا الرقمية Sony - Digital Camera المكتوب على اللوحة وبإضاءة منتظمة وقليلة (عتمة) أي فقط الإضاءة الداخلة من الشباك (الإضاءة الطبيعية) والشكل (3) و (4) يوضح الصور الناتجة من منظومة العمل باختلاف المسافة والكاميرا الرقمية المستخدمة في عملية التصوير .



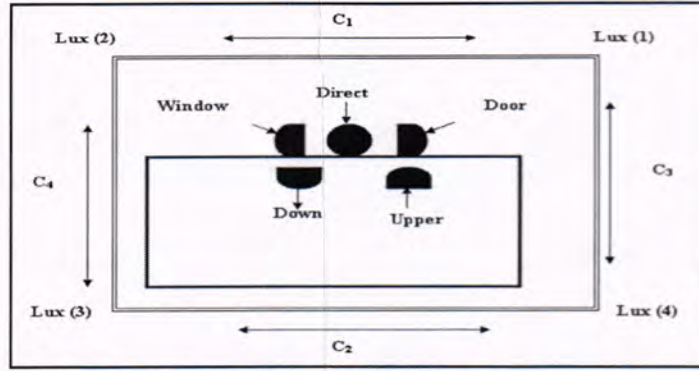
شكل 4- يوضح الكاميرا الرقمية المستخدمة في عملية التصوير

شكل 3- يوضح الصور الناتجة من عملية التصوير باختلاف المسافة

تقنيات حساب التباين للنص
تم حساب التباين للنص المكتوب على اللوحة البيضاء (Whiteboard) بالاعتماد على نقاط الحافات فقط من اعتماد المعادلة التالية (12) :

$$C = \frac{I_{\max} - I_{\min}}{I_{\max} + I_{\min}} \quad (1)$$

I_{\min} و I_{\max} تمثل أعلى وأقل شدة ضمن نافذه 3×3 حول كل نقطة حافة كما تم حساب التباين من العلاقة (1) بالاعتماد على قراءات جهاز قياس شدة الإضاءة لتمثل هنا قيمة I_{\min} و I_{\max} أعظم وأصغر شدة في الاتجاهات المتعكسة عند قياس الأضاءة بواسطة جهاز Lux meter كما موضح في الشكل (5) ، أذ تم استخدام مؤثر سوبل للكشف الحافي للحزم اللونية RGB وحزمة الإضاءة L ، حيث تم اقتراح عدة تقنيات مختلفة لحساب التباين بين لون النص المكتوب على اللوحة ولون الخلفية (White Board) وهي كالآتي :

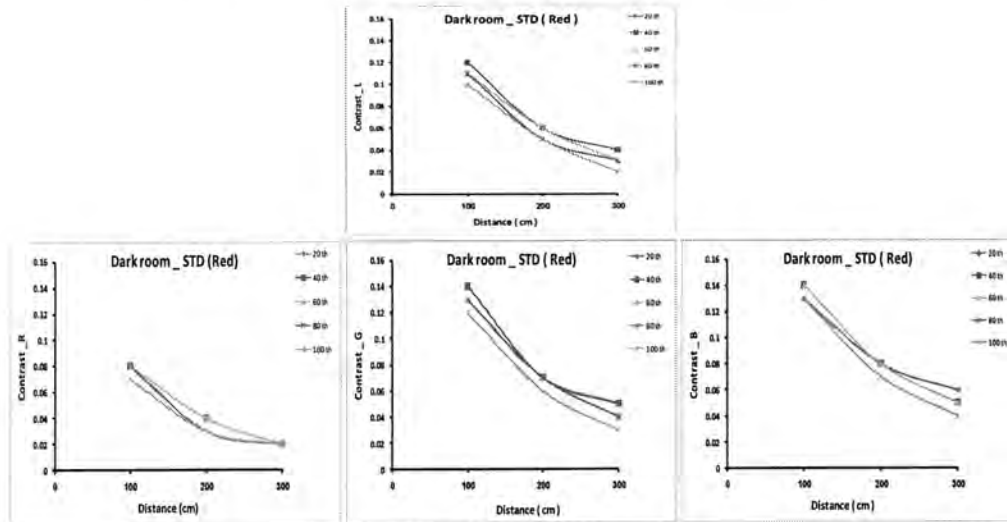


شكل -5: اتجاهات شدة الإضاءة داخل القاعة الدراسية

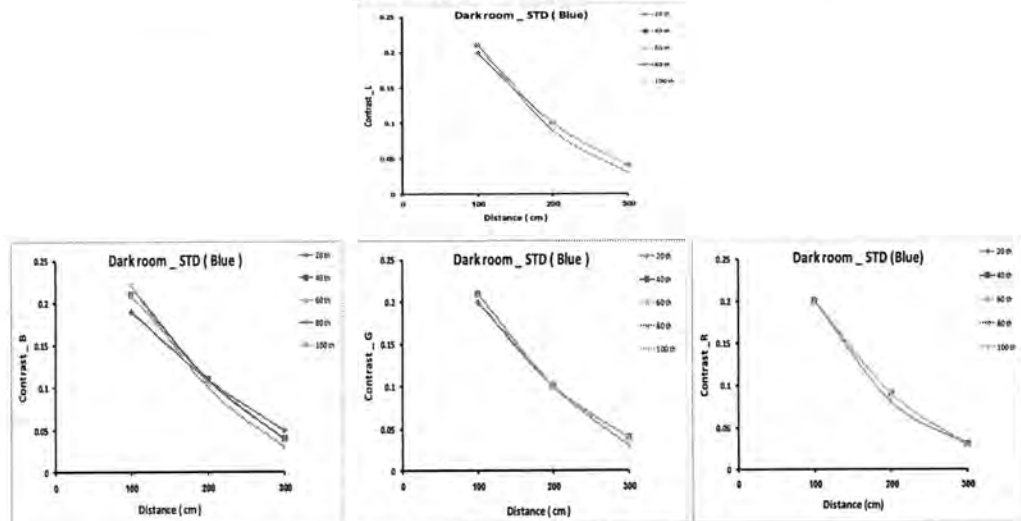
❖ تقنية التباين بالاعتماد على الخصائص الإحصائية أظهرت هذه التقنية كفاءة في حساب قيمة التباين للنص المكتوب على اللوحة لمسافات مختلفة وبإضاءة منتظمة قليلة (عتمة) حيث تعتمد هذه التقنية على قيمة المعدل Mean والانحراف المعياري Standard Deviation لعناصر الحافات للحزم اللونية الثلاث ومركبة الإضاءة، وتم حساب التباين ولعبارات مختلفة لمؤثر سوبل (20, 40, 60, 80, 100) ولمسافات مختلفة عن اللوحة البيضاء.

❖ تقنية التباين العمودي تم في هذه التقنية حساب التباين لنقاط الحافات فقط وأساس عمل هذه التقنية هي تكوين نافذة ثلاثية (3 × 3) حول عنصر الحافة ثم إيجاد مجموع عناصر العمود الأول ومجموع عناصر العمود الثالث ثم يتم تحديد أكبر مجموع I_{max} وأصغر مجموع I_{min} فيما بينهم أي العمود الأول والعمود الثالث وتطبيقها في معادلة التباين (1) للحصول على التباين.

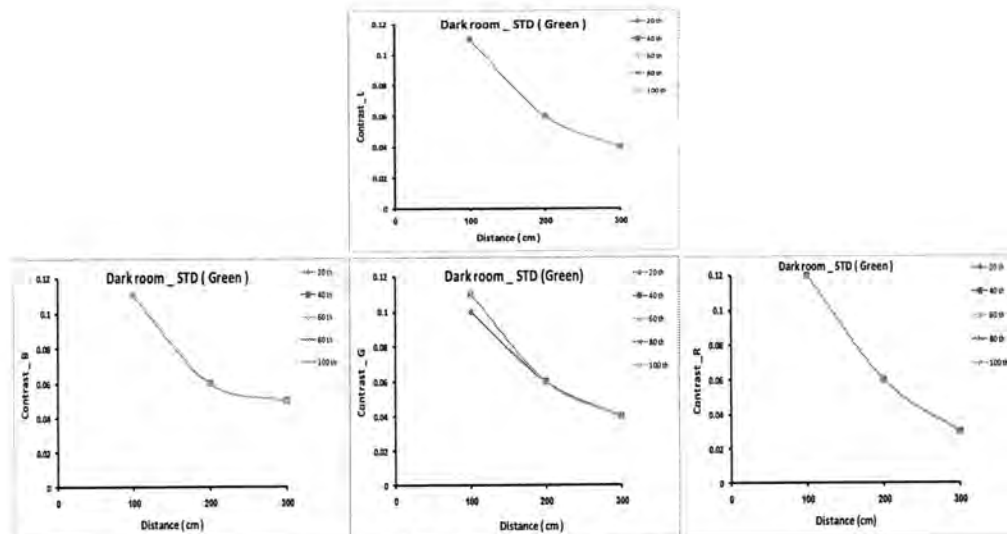
نتائج دراسة تأثير الإضاءة على تباين النصوص باختلاف المسافة أن نتائج دراسة التباين للنصوص المكتوبة بألوان مختلفة على اللوحة البيضاء (Whiteboard) للمركبات اللونية الثلاث (Red, Green, Blue) ولمركبة الإضاءة L في حالة الإضاءة بصورة منتظمة (قليلة) والمعتمدة فقط على الإضاءة الواصلة من الشباك (الإضاءة الطبيعية) للنصوص المكتوبة على اللوحة البيضاء (Whiteboard) بالألوان (الأحمر، الأخضر، الأزرق) ولمسافات مختلفة عن اللوحة موضحة بالشكل (6) لتقنية التباين الإحصائي الذي يوضح العلاقة بين التباين الإحصائي والمسافة بين لوحة النصوص وكاميرا التصوير، إذا يلاحظ انخفاض واضح في قيم التباين كلما زادت المسافة مما يدل على قلة وضوح النص مع الابتعاد عن السبورة ويلاحظ أن هذا الانخفاض لا يمثل علاقة خطية. والشكل (7) يبين العلاقة بين التباين العمودي مع المسافة بين الكاميرا والسبورة ويلاحظ هنا أيضاً انخفاض واضح في قيم التباين للألوان المختلفة مع زيادة المسافة. إذا يلاحظ وجود تقارب في النتائج للتباين الإحصائي والتباين العمودي رغم أن الأسلوب الإحصائي لكل منهما مختلف عن الآخر.



النص المكتوب باللون الأحمر

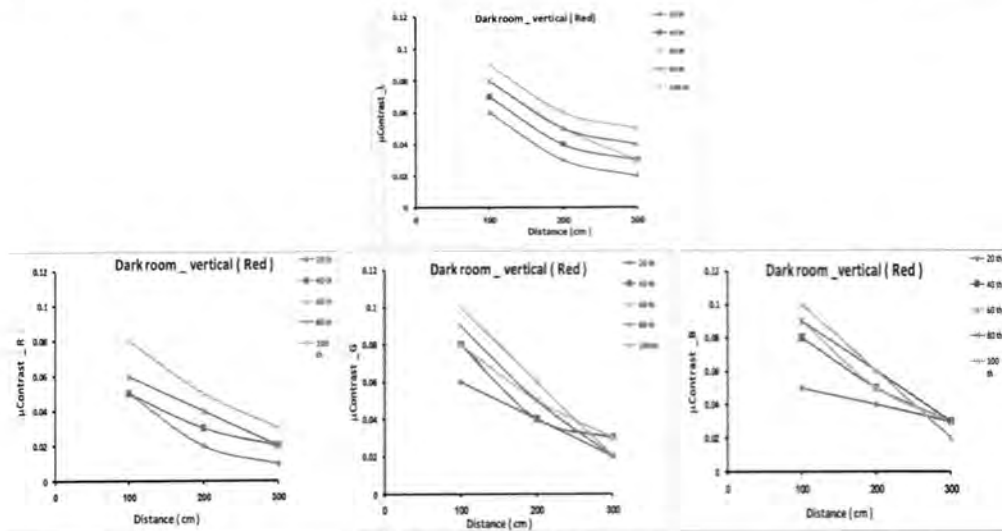


النص المكتوب باللون الأزرق

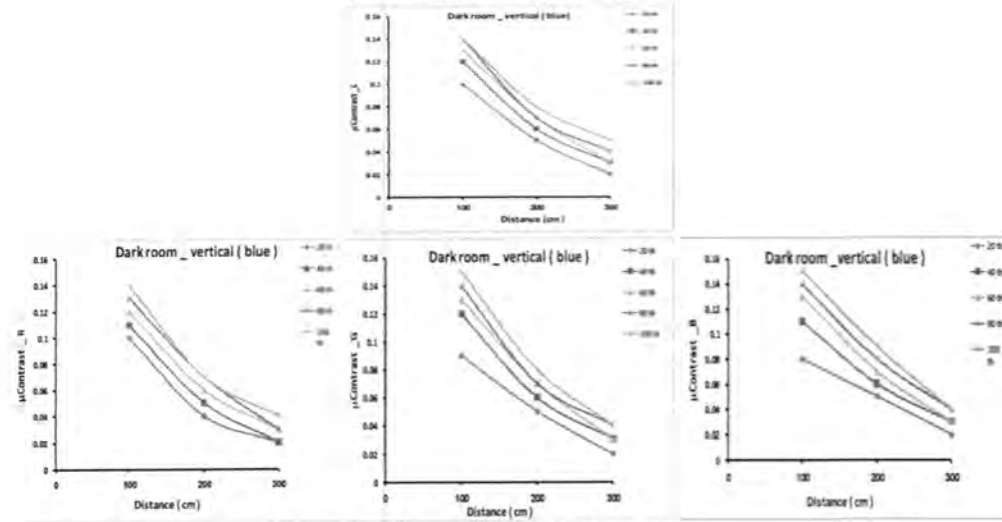


النص المكتوب باللون الأزرق

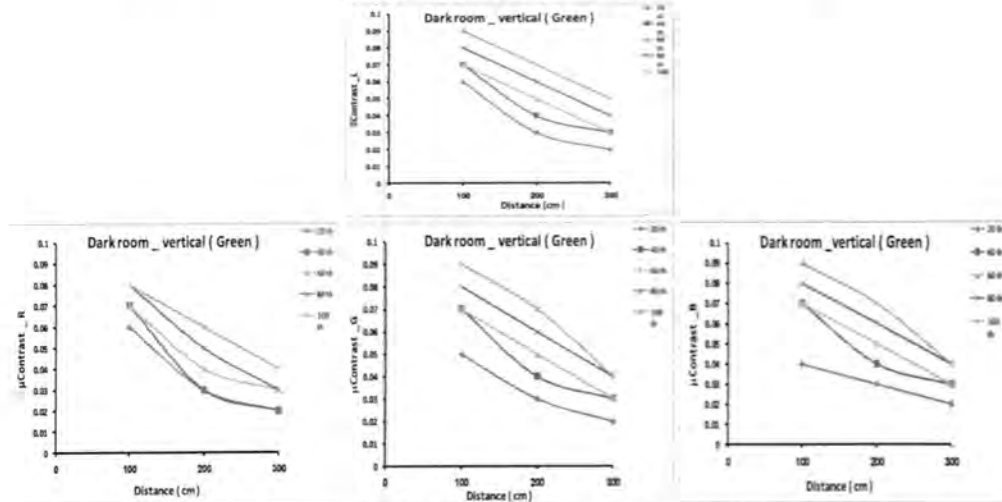
شكل - 6 : التباين الإحصائي للحزم اللونية RGB ولمسافات المختلفة



النص المكتوب باللون الأحمر



النص المكتوب باللون الأزرق



النص المكتوب باللون الأخضر

شكل 7- : التباين العمودي للحزم اللونية RGB ولمسافات مختلفة

ومن خلال ذلك يمكن ان نستنتج :

1. من خلال المقارنة بين نتائج التباين لمناطق الحافات للنصوص المكتوبة بالألوان على اللوحة البيضاء (Whiteboard) ، أن تقنية التباين بالاعتماد على الخصائص الإحصائية كانت الأفضل في إبراز قيم التباين للمركبات اللونية الثلاث (RGB) ولمركبة الإضاءة L .
2. أن قيم التباين الإحصائي أعلى مقارنة بقيم التباين العمودي لان التباين الإحصائي يعتمد على قيم المعدل والانحراف المعياري لنقاط الحافات للنصوص الملونة RGB .
3. تكون النصوص المكتوبة على اللوحة البيضاء أقل وضوحية كلما ابتعدنا عن اللوحة ، إذ أن زيادة المسافة تقلل من قيم التباين وبالتالي تزيد من غشاوة النص المكتوب على اللوحة للمركبات اللونية الثلاث RGB ولمركبة الإضاءة L .
4. أن قيم التباين للنص المكتوب باللون الأزرق أعلى من القيم التباين للنصوص المكتوبة باللون الأحمر والأخضر ولكلا تقنيتي التباين (الأحصائي والعمودي) .

المصادر

1. شبر ، ندى ماجد ، " التصميم الداخلي في الحركات المعمارية الحديثة " ، رسالة ماجستير ، كلية الهندسة ، جامعة بغداد ، (1988).
2. Ian.T. , Jonj G. , Lucas J. , " Fundamentals of Image Processing "(1995)
3. Michel , Lou , " Light, The Shape of Space , Desinning With Space and Light " , John Willey and Sons , Inc , (1996).
4. Jonhson R .P ., " Contrast Based on Edge Detection " , pattern Recongition , 23, (3/2) (1990).
5. Eli Peli , Lawrence Arend , Angrla T.Labiance , " Contrast Perception a Cross Change in Luminance and spatial frequency "Optical Society America ,(1996) .
6. Curlander , R .J., " Image Enhancement Using Digital Adaptive Filtering " , M.Sc – Thesis , Department Electrical Engineering , University of Colorado , (1997).
7. Kai – Yu and Liang Ji , " How to Optimize Optical Coherent Tomography OCT Image " , Department of Automation ,Tsinghua University , (2001) .
8. William.B .Thompson , peter. Shirly , and J.A. Ferwerdo , " A spatial Post Processing Alogrithum for Images of Night Scences " , Auther Address : Unive of Utah and Cornellh Unive. , (2003).
9. Cook .,S.,J.,and Smith , E. L., " Frontier in Visual Scientific " (1977).
10. صالح ، قاسم حسين " سايكولوجية أدراك اللون والشكل " دار الرشيد ، بغداد ، العراق : 164 (1982).
11. Mahnke Frank H. and Mahnke , Rudolf H . "Color and Light in man –mad ,Environments ,New York: 28 -29 (1987).
12. Antoshchuk S.,” The automatized systems with the visual information processing design” , International Conference volume , Issue , 24-28 Feb. : 268 (2004) .

دراسة الخصائص الاحصائية للشدات المسجلة بواسطة متحسسات الويب كاميرا enet لصورة اختبارية بيضاء

اسماء محمد روؤف و فرح جواد كاظم و شيماء حسين عبد مسلم و علي عبد داود الزكي
الجامعة المستنصرية – كلية العلوم – قسم الفيزياء

ABSTRACT

This study aimed to determine the quality of enet web- camera in capturing images for homogenous target (white test image) under different fluorescent illumination. where we compute the mean (\bar{x}) and standard deviation (σ), for the color RGB-bands and L-component, of the test white images. Also, we build algorithms to study relation between the mean and standard deviation.

From the result we find that there are no large differences between the RGB-color bands, and L-component, where the distributions of RGB-lightness are very similar to each other, because the fluorescent light represent white light (i.e. give same values for RGB-bands). The statistical study for the white image show that the stationary in high power (high lightness). While at low powers fluorescent the relation between the mean (\bar{x}) and standard deviation (σ) that represent linear function.

الخلاصة

تهدف الدراسة الى تحديد جودة الويب كاميرا نوع enet Web Camera في التسجيل المتجانس لصور ملقطة لصورة اختبارية بيضاء تحت شروط اضاءة فلورسنت مختلفة. حيث تم حساب الانحراف المعياري σ والمعدل μ للحزم اللونية RGB والمركبة L لقيم الشدات المسجلة بواسطة الكاميرا للصورة الاختبارية التي تم تصويرها. وتم دراسة العلاقة بين المعدل والانحراف المعياري وتم بناء خوارزميات لذلك ومنها تم الحصول على انه لم نجد هنالك فروق كبيرة بين الحزم اللونية الثلاثة RGB ومركبة الأضاءة L، حيث كانت قيم توزيع شدة الأضاءة متقاربة جداً من بعضها وتسلق نفس السلوك بسبب طبيعة ضوء الفلورسنت الأبيض الذي يعطي شدات متساوية تقريباً. وأن دراسة الخصائص الاحصائية للصورة البيضاء تبين بأن قيم المعدل تكون مستقرة عند القدرات العالية (أضاءة عالية)، أما عند القدرات المختلفة الأخرى فتكون العلاقة بين المعدل والانحراف المعياري علاقة خطية لمصدر الأضاءة الفلورسنت.

مقدمة

ان منظومات التصوير لا تعطي صوراً تامة ومثالية، وانما غالباً ما تعطي صوراً "بوضوحيات محددة اي لا تعطي صوراً" بحافات حادة مثالية وانما حافات عريضة نوعاً ما فيها شيء من الغشاوة وسبب ذلك يعزى الى ظاهرة الحيود للضوء والزيوغ والتشوهات البصرية في المنظومة البصرية. الصورة هي وصف لكيفية تغير معامل التحسس البصري على سطح معين، والصورة عادة ما تنتج من تغير الشدة الضوئية عبر مستوي ثنائي البعد، اذ ان أي منظومة تصوير تعطي تحسناً صورياً قد يكون مألوفاً لعين الإنسان مثل المناظر والمشاهد أو قد تعطي صوراً يتم تحسسها بتحويل الشدة المتحسنة الى شدة ضوئية بحيث يمكن أن تتحسسها عين الإنسان مثل الصور الراديوية Radio Image وصور الأشعة السينية X-Ray Image. ونظراً للكم الهائل من المعلومات التي تحويها الصورة برزت الحاجة الماسة الى تمثيل الصور حاسوبياً وذلك بتحويلها من الصيغة التماثلية (Analogue Form) الى الصيغة الرقمية (Digital Form) لغرض تسهيل عملية تداولها واستنساخها واستخلاص المعلومات الحاسوبية منها. ترسم الصورة على شاشة الحاسوب بواسطة إشارة كهربائية تقوم بعملية مسح خط افقي واحد عبر الشاشة في لحظة زمنية معينة ثم يتكرر هذا المسح للخطوط التي تليها حتى يشمل كل اجزاء الصورة، ان اصغر فرق في الشدة الضوئية ممكن تحسسه بين عنصرين متجاورين في الصورة يدعى وضوحية التباين (Contrast resolution) لذا يمكن قياس هذا التباين بأخذ الفروق في الشدة الضوئية لعناصر الصورة المتجاورة وهذا يعتبر مقياساً لقياس جودة الصورة كمياً (1).

2-الضوء:

الضوء هو نوع خاص من الطاقة يعرف بالطاقة الكهرومغناطيسية وهو شكل للطاقة المرئية التي قد تكون صادرة من مصدر او منعكسة من جسم ما مثل الشمس او اللهب او المصباح الكهربائي (2). والضوء الابيض هو في الحقيقة مزيج من الطاقة الاشعاعية لاطول موجية مختلفة وبنسب متساوية تقريبا". واي موجة تنفصل من المزيج تشير الى لون معين وبهذا فان كل من الضوء واللون متلازمين , هناك نوعين من مصادر الاضاءة (3) :

- 1.مصادر الاضاءة الطبيعية : يعرف الضوء الطبيعي وهو الضوء الذي تنتجته الشمس والذي يصل الى الارض من الشمس بشكل مباشر او يصل جزء منه جراء التشتت والاستطارة .
- 2.مصادر الاضاءة الصناعية :الضوء الصناعي هو ضوء ناجم من فعل الاثارة الناتجة عن التيار الكهربائي او التقنيات الاخرى مثل ضوء المصابيح الكهربائية مثل الفلورسنت .
- 3-الصورة الرقمية

الصورة عبارة عن تمثيل بصري للجسام المسلط عليها شدة اشعاعية قد تكون موجات كهرومغناطيسية وتمثيلها بصيغة رقمية ، والصيغة المستخدمة في المعالجة الحاسوبية هي الصيغة الرقمية اذ تمثل الصورة بدالة ثنائية البعد بواسطة مجموعة من المتغيرات الحيزية المجزئة والدالة العددية $f(x,y)$ ممكن ان تستخدم لتمثيل شدة الضوء في المحاور الحيزية في النقطة (x,y) . كما يمكن تصنيف الصور الى اربعة انواع رئيسية(4,5) : 1.الصورة الثنائية

2.الصور ذات التدرج الرمادي

3.الصورة الملونة

4.الصور المتعددة الاطراف

4-الكاميرا:

بصورة عامة تعرف الكاميرا بانها جهاز التقاط الصور والذي يتمكن من التقاط صور لمنظر ثلاثي الابعاد وتحويله الى الصور ثنائية البعد . مبدأ عمل الكاميرا مشابه تماما" لعمل عين الانسان في الرؤية (6).

تعد الكاميرا الرقمية (digital cameras) والماسحات الضوئية (light scanner) من أهم أجهزة لادخال الشائعة لتسجيل الصور الرقمية في الوقت الحاضر . اذ تقوم هذه الاجهزة بوظيفة رئيسة هي عملية الرقمنة Digitization والتي تقوم بتحويل الصورة الاصلية الى تمثيل رقمي ملائم للخرن والمعالجة باستخدام الحاسوب (7,8) . اهم العيوب التي تصيب الصور الرقمية هي الضوضاء التي قد تلطخها وتصيبها وتقلل وضوحيتها, وتجعل عملية تحليلها واستخلاص المعلومات منها عملية معقدة وصعبة .

5- الضوضاء :

وتعرف الضوضاء بصورة عامة بانها البيانات المعلوماتية غير المرغوب فيها مسببة تشوية الصورة وعدم وضوحيتها وهي ناتجة بسبب تداخلات في اشارات الصورة او اشارات المؤثرات الخارجية مثل اشارات ناتجة من تغيرات البيئة او تغيرات في حاسبة الكاشف Sensitivity of (Detecor) وكذلك بسبب الاخطاء الحاصلة اثناء النقل والترقيم. ويمكن تصنيف انواع الضوضاء رياضيا" كما يلي(9,10) :

1.الضوضاء الجمعية (Additive Noise)

2.الضوضاء الضربية (Multicative noise)

3.ضوضاء الملح والبهار (Salt and pepper noise)

الضوضاء الجمعية (المضافة) (Additive noise):

تكون هذه الضوضاء عشوائية ولا تعتمد على الإشارة وتتميز بالصفات الاتية :

ا- ضوضاء بيضاء(White noise) وتكون كثافة طيفها (Spectral density) ثابتة .

ب- خطية الاضافة (Additive linear) وتكون الصورة المشوية ناتجة من الصورة الاصلية

$R(x,y)$ النقية مضاف لها قيم الضوضاء وذلك كما في المعادلة التالية(11,12) .

$$f(x,y)=R(x,y)+n(x,y) \quad (1)$$

حيث ان $n(x,y)$ تمثل الضوضاء المضافة غير المعتمدة على الإشارة معدلها عادة يساوي صفر ($n(x,y)=0$).

$f(x,y)$ تمثل الصورة المشوبة (المشاهدة) ، $R(x,y)$ تمثل الصورة الأصلية الخالية من الضوضاء. الضوضاء الضريبية (المضاعفة) (Multiplicative noise):

تختلف الخصائص الاحصائية لهذا النوع من الضوضاء عن الضوضاء المضاعفة وهي ضوضاء عشوائية معتمدة على الإشارة اي ان المناطق ذات الشدة العالية في الصورة تكون ذات ضوضاء عالية حيث كلما قلت شدة الاضاءة قلت الضوضاء معها وهذا يدل على ان هناك علاقة بين مقدار الضوضاء والشدة للإشارة وهذه العلاقة هي علاقة تتناسب طرديا. ويكون التعبير عنها رياضيا كما يلي (13,14):

$$f(x,y)=R(x,y).k(x,y) \quad (2)$$

حيث ان $f(x,y)$ تمثل الصورة المشوبة (المشاهدة) ، $R(x,y)$ تمثل الصورة الأصلية الخالية من الضوضاء.

$k(x,y)$ تمثل متغير عشوائي ضوضائي (غير معتمد على الإشارة وعادة يكون معدل $k=1$).

6- أحصائيات الصورة الرقمية

أن أحصائيات الصورة الرقمية Digital Image Statistics تكون أساسية في أغلب عمليات معالجة الصورة الرقمية. تعتبر في كثير من الأحيان هذه الأحصائيات واصفة لطبيعة الصور وكيفية توزيع المعلومات فيها. والأحصائيات تكون مرتبطة بمبدأ احتمالية توزيع المعلومات للصورة حيث يمكن أن تعرف دالة احتمالية توزيع الأضائية Brightness Probability Density Function بأنها دالة كثافة الاحتمالية للأضياء وهذه الخواص للصورة $f(x,y)$ هي (15) :

(a) دالة احتمالية التوزيع PDF

يعبر عن دالة احتمالية التوزيع بالصيغة $P(I)$ وهي تمثل احتمالية توزيع الأضياء $f(x,y)$ في الصورة حيث أن

$$0 < f(x,y) < L-1 \quad (3)$$

حيث أن L تمثل عدد مستويات الشدة في الصورة $f(x,y)$.

وأن الاحتمالية لظهور الشدات $f(x,y)$ في الصورة تكون محدده بالاحتمالية

$$0 \leq P(f) \leq 1 \quad (4)$$

حيث مجموع الاحتماليات الكلي مساوي للواحد ويدعى رسم توزيع الاحتمالية عادة بالمخطط التكراري لعناصر الشدة في الصورة وعادة ما تكون قيم الشدات محدده ضمن المدى [0-255].

(b) المعدل (μ)

معدل الشدات في الصورة ويعرف بأنه معدل الشدة في الصورة ويحسب المعدل μ من العلاقة الآتية (15):

$$\mu = \frac{1}{MN} \sum_{x=1}^M \sum_{y=1}^N f(x,y) \quad (5)$$

(c) الانحراف المعياري (σ)

يعرف الانحراف المعياري بأنه مقدار انحراف القيم للإشارة عن المعدل ويحسب الانحراف المعياري (σ) من العلاقة (15):

$$\sigma = \sqrt{\frac{1}{MN} \sum_{x=1}^M \sum_{y=1}^N (f(x,y) - \mu)^2} \quad (6)$$

كذلك من الممكن حسابه كمايلي (15):

نحسب معدل مربع الشدة لعناصر الصورة وذلك باستخدام إحدى المعادلتين الآتيتين :

$$avs = \frac{1}{MN} \sum_{x=1}^M \sum_{y=1}^N f^2(x,y) \quad (7)$$

ثم يحسب الانحراف المعياري من العلاقة :

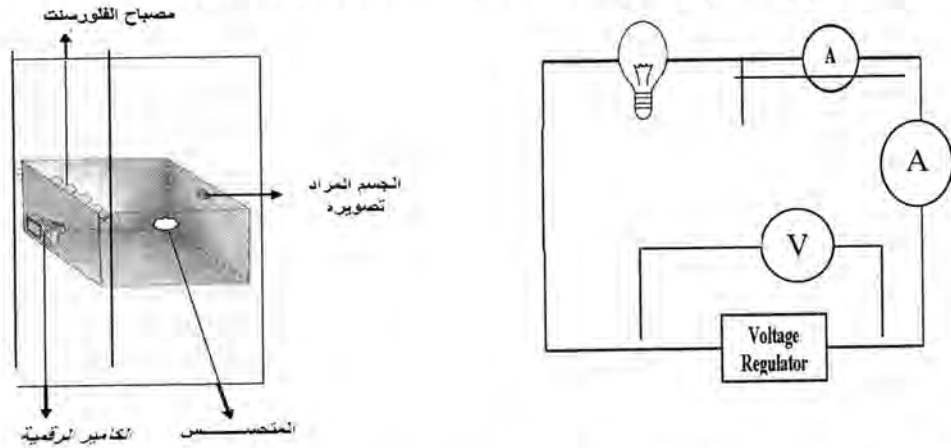
$$\sigma = \sqrt{(avs - \mu^2)} \quad (8)$$

ويعتبر هذا المقياس من المعايير المهمة في تحديد مقدار التفاصيل في الصورة .

7- منظومة العمل

اجريت هذه الدراسة باستخدام المنظومة المبينة في الشكل (1), ومكونات المنظومة البصرية هي كالآتي:-

1. صندوق مظلم ذا أبعاد (61 × 74 × 120) cm بحيث تكون المسافة بين الجسم ومصدر الإضاءة (مصباح الفلورسنت) 120cm , وعلى نفس جانب مصدر الإضاءة توجد فتحة للتصوير توضع عليها الكاميرا الرقمية مرتبطة بالحاسوب لخزن الصور الملتقطة , وتحت شروط إضاءة مختلفة حيث يتم التحكم بشدة الإضاءة باستخدام الدائرة الالكترونية الموضحة في الشكل (2) كما يوجد في الجانب المقابل للكاميرا متحسس , لتسحب شدة الضوء



الشكل 2: يوضح الدائرة الالكترونية

شكل 1- : المنظومة البصرية باستخدام مصباح الفلورسنت لمنظومة التصوير

2. الترانزستور الضوئي الكاشف

أن المتحسس المستخدم في منظومة العمل هو الترانزستور الكاشف الضوئي Photo Transistor Detector وهو عبارة عن شريحة من مادة شبة موصلة من السيلكون نوع-NPN-PP [103] (16).

3. الويب كاميرا أن نوع الكاميرا الرقمية المستخدمة في الدراسة هي , (enet Web Camera model E6-6.High quality CMOS sensor)

4. الحاسبة وتكون مربوطة مع الكاميرا.

5. المصابيح في هذه الدراسة تم استخدام مصباح الفلورسنت يحتاج الى جهد تشغيل قليل حيث أن مصباح الفلورسنت يعمل على فرق جهد منخفض فالضوء المنبعث من الفلورسنت يبدو أبيض في معظم الحالات أي أن اللون الأبيض (مشابه لضوء الشمس) يحتوي على كل ألوان الطيف المرئي ولكنه أيضاً يعطي أطوال موجية تختلف في نسب الأطوال الموجية للضوء , أن مصباح الفلورسنت يعمل بقدرة (18)W وفولتية التشغيل له (80 – 220) volt , ويبعث هذا المصباح طيف مستمر من الأطوال الموجية ضمن المنطقة المرئية .

6. جهاز الفولتميتر والاميتر تم استخدام جهاز الفولتميتر لقياس الفولتية المسلطة على المصابيح وجهاز الاميتر لقياس التيار المار بالمصابيح وذلك لغرض إيجاد القدرة الكهربائية المصروفة عند كل شدة إضاءة مستخدمة .

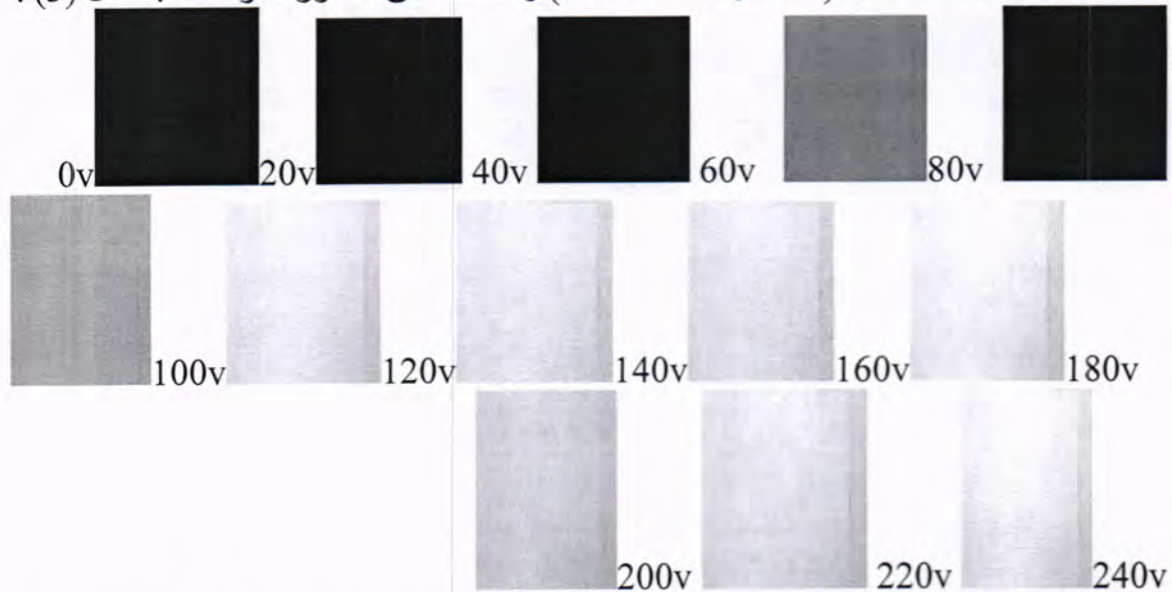
7. منظم الفولتية يستخدم منظم الفولتية لكي يتم التحكم بالتيار المار في المنظومة وبالتالي يمكن التحكم بشدة ضوء مصباح الفلورسنت داخل الصندوق.

8.

النتائج والمناقشة

تم دراسة تأثير تغير شدة اضاءة مصباح الفلورسنت على قابلية الويب كاميرا نوع enet web camera في التحسس والتسجيل للصور لورقة بيضاء A_4 الموضوع في صندوق الذي يحتوي على منظومة اضاءة الفلورسنت الممكن التحكم بها كهربائيا".

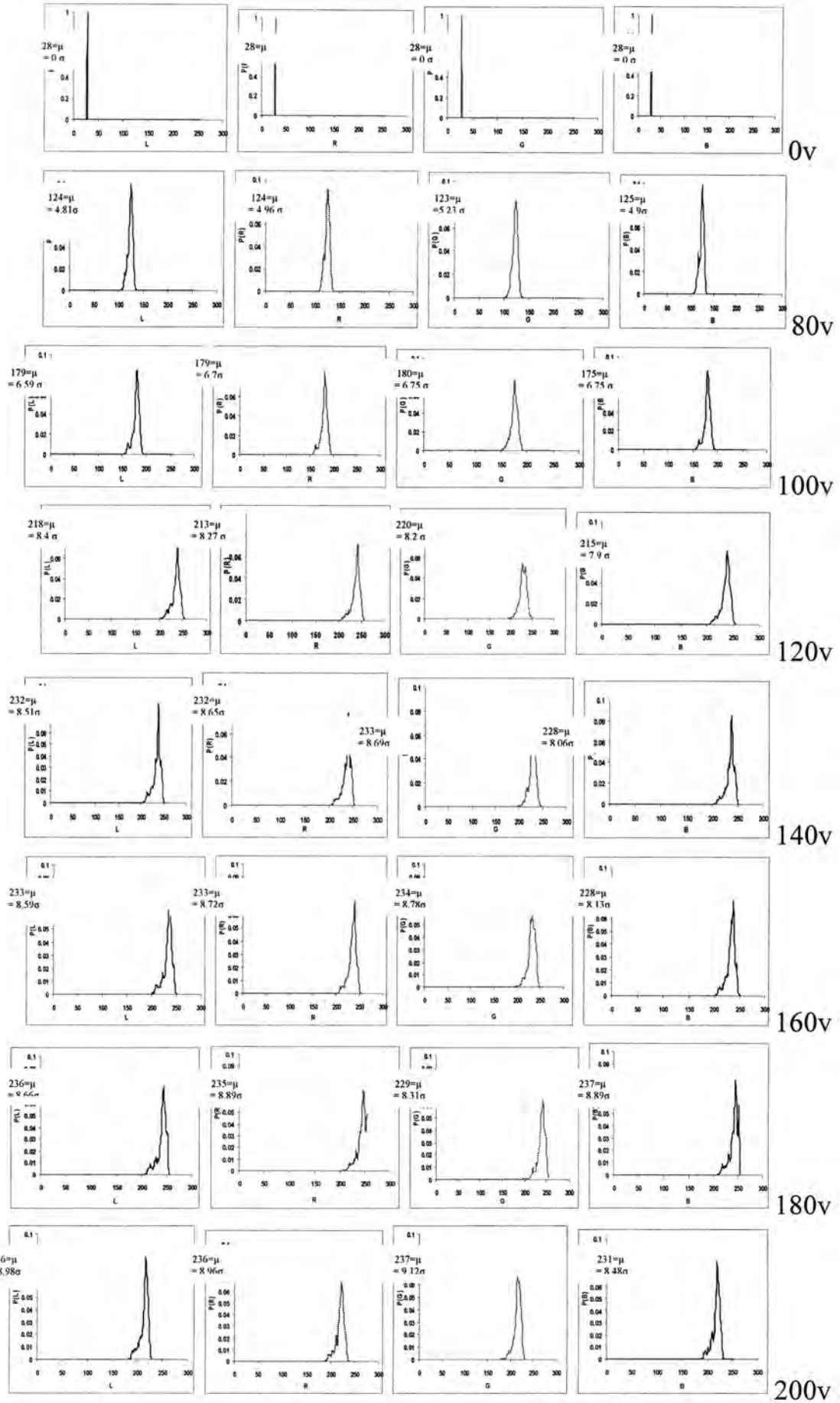
ان الصورة وخصائصها تعتمد على شدة الإضاءة وطبيعة الضوء المستخدم وان شدة الإضاءة تعتمد على القدرة الكهربائية المجهزة لمنظومة الاضاءة حيث تم استخدام مصباح الفلورسنت تم التحكم بشدة الاضاءة له بواسطة الفولتية المسلطة عليه , تم في هذه الدراسة تحليل نتائج تصوير صورة اختبارية بيضاء (ورقة A_4) بواسطة الويب كاميرا نوع enet web camera , حيث تم تصوير الورقة البيضاء في الصندوق الذي يمكن التحكم بأضاءته بمصباح الفلورسنت وتم التقاط مجموعة من الصور المختلفة عند شدة الاضاءة المختلفة (عند الفولتيات المختلفة) وحصلنا على الصور الموضحة بالشكل (3) .

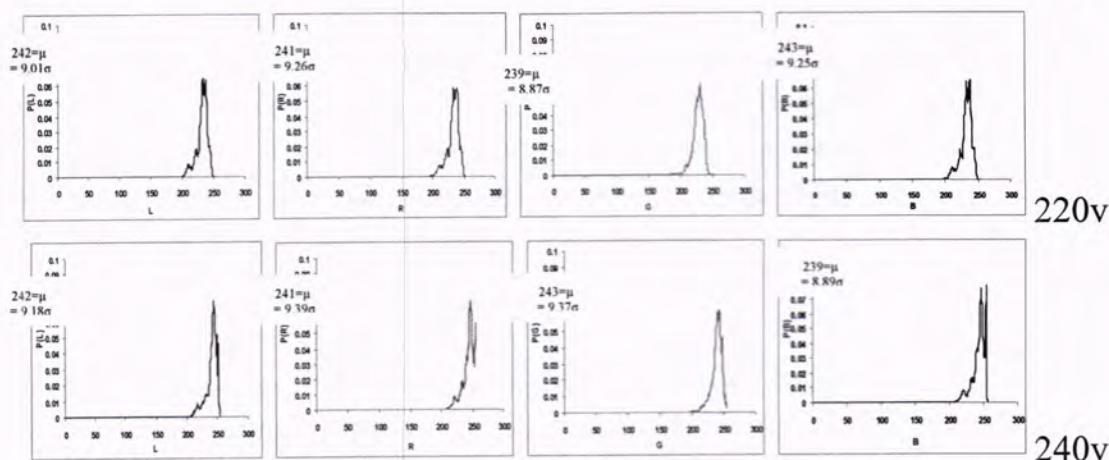


شكل -3: يوضح الصور الملتقطة للصورة الاختبارية البيضاء عند فولتيات اضاءة مختلفة لمنظومة مصباح الفلورسنت

حيث تم دراسة الخصائص الإحصائية لكل من الحزم اللونية الثلاثة RGB ومركبة الإضاءة L , ودرسنا توزيع الاضاءة في مستوي الصورة برسم المخطط التكراري لكل صورة وهذه الرسوم موضحة بالشكل (4) , ولاحظنا حصول انخفاض في احتمالية التوزيع لمنحنيات المركبات اللونية الثلاثة RGB ومركبة الإضاءة L أي يحصل إتساع في قاعدة القمم وانخفاض ارتفاعها مع المحافظة على تساوي المساحة تحت المنحني في بعض الحالات . كما نلاحظ تطابق في ارتفاع وموقع القمة لحزمة الإضاءة L مع انخفاض الحزمة الخضراء G والمحافظة على ارتفاع المنحنيات RGB والمركبة L كما نلاحظ زيادة تدريجية في اللمعان من خلال الزحف التدريجي لمواقع قمم هذه المنحنيات (زيادة المعدل μ) نحو المستويات العالية بالشدة بسبب زيادة شدة الاضاءة في داخل الصندوق . كما ان زيادة اتساع المنحني اي زيادة الانحراف المعياري σ هو السبب الرئيسي في نقصان ارتفاع القمة المركزية للمخطط التكراري لجميع الحزم RGB والمركبة L . كما ويلاحظ ان شكل المنحنيات متناظرة عند الفولتيات الواطئة ثم يأخذ شكل غير متناظر عند الفولتيات العالية (الاضائية العالية) لوجود امتداد للمنحني باتجاه القيم الواطئة للشدة RGBL .

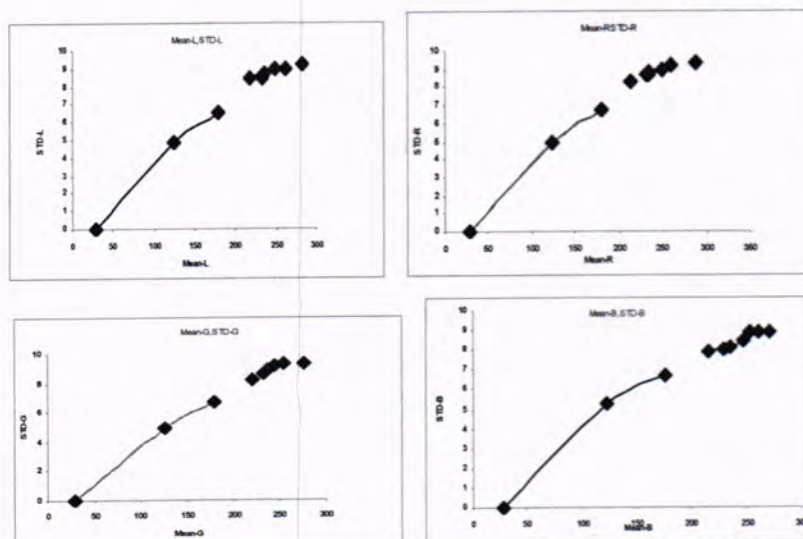
دراسة الخصائص الاحصائية للشدات المسجلة بواسطة متحسسات الويب كاميرا enet لصورة اختبارية بيضاء
اسماء و فراح و شيماء وعلي





شكل 4- يوضح المخططات التكرارية للشدات اللونية RGB والمركبة L للصور الملتقطة للصورة الاختبارية البيضاء عند شدات اضاءة مختلفة

ولقد درسنا هذه الصور ودرسنا خصائصها كدالة لكفاءة التحسس للويب كاميرا المستخدمة , كما درس التغير في تذبذب اشارة المتحسسات الضوئية للكاميرا وذلك بدراسة العلاقة بين معدل الشدة للحزم اللونية RGB ومركبة الإضاءة L مع الانحراف المعياري في منظومة الاضاءة انظر الشكل (5), نلاحظ أن العلاقة بين المعدل μ والانحراف المعياري σ للصور الملتقطة بأضائيات الفلورسنت المختلفة علاقة خطية ومتقاربة في قيم المركبات اللونية RGB والأضائية L لقيم المعدل المحددة من (0-200Watt) والتي تقابل قدرة مصباح الفلورسنت (0 – 10 Watt) ، بينما نلاحظ انخفاض بصورة غير منتظمة لقيم المعدل والانحراف المعياري في توزيع شدة الأضاءة عندما تكون القدرة (6-8 Watt) والتي تقابل قيم المعدل (150- 170) كما موضح بالشكل (7). أن قيم شدة الأضاءة للمركبات اللونية RGB ولمركبة الأضائية L تكون متقاربة في القيم بسبب أن المصدر الضوئي (مصباح الفلورسنت) يعتمد على تأين الغاز بالإضافة الى أن مصباح الفلورسنت أبيض أي أن جميع الحزم اللونية لها نفس الشدة.



شكل 5- يوضح العلاقة بين المعدل والانحراف المعياري

ومن ذلك يمكن ان نستنتج :

- عند دراسة أنظام توزيع شدة الأضاءة للصورة الاختبارية البيضاء A4 باستخدام المصدر الضوئي (مصباح الفلورسنت) لم نجد هنالك فروق كبيرة بين الحزم اللونية الثلاثة RGB

ومركبة الأضاءة L , حيث كانت قيم توزيع شدة الأضاءة متقاربة جداً من بعضها وتسلق نفس السلوك بسبب طبيعة ضوء الفلورسنت الأبيض الذي يعطي شدات متساوية تقريباً.

• أن دراسة الخصائص الإحصائية الصورة البيضاء تبين بأن قيم المعدل تكون مستقرة عند القدرات العالية (أضاءة عالية) ، أما عند القدرات المختلفة الأخرى فتكون العلاقة بين المعدل والانحراف المعياري علاقة خطية لمصدر الأضاءة الفلورسنت.

المصادر

1. قاسم حسين صالح "سايكولوجية إدراك اللون والشكل" دار الرشيد للنشر (1982).
2. Ziemer R.E.&Tranter W.H"principles of communication" Houhton misslin (1985).
3. Christopher C.Yang&Jeffery J.Rodriguez,"Efficient Luminance and Saturation Processing Techniques for Bypassing Color Coordinate Transformations", Dept. of Electrical and Computer Engineering, the University of Arizona, Tucson, Arizona. ,<http://www.christopher.c.yang-ResearchIndex.document.query.htm>, (1997)
4. Suha, H.I "Physical Study for the Noise in Digital Images" M.Sc. Thesis, physics Dept., College of Science Al-Mustansiriya University (2003) .
5. Jain, K., "Fundamentals of Digital Image Processing" Prentice Hall, India (2000).
6. Marshall R., "Computer Graphic in Application" Prentice Hall, (1987).
7. Garari, E.M. & Wechsler, H., "On the Difficulties Involved in the Segmentation of picture" IEEE Tran. Patt. Anal. Mach. Int, PAMI-4(3):304-306, May, (1982).
8. Hussain Z. "Digital Image Processing Practical Applications of Parallel Processing Techniques" ELL is Harwood, England, (1991).
9. Huda, S.k, "Quantum analysis of noise in photonic system" M.Sc. thesis, physics Dept., College of Education for Women, Baghdad University (2001) .
10. Rabbani, M., "Bayesian Filtering of Poisson Noise Using Local Statistics" IEEE, Trans. (36) : 933-936, (1988).
11. AL-Lihebi, A.A., "Linear Digital Restoration Filters" M.Sc thesis Baghdad University, College of Education for Women (1998).
12. Lee, J.S, "Refined Filtering of Image Noise Using Local Statistics" Computer Graphics and Image Processing, 15:380-389 (1981) .
13. Nowak, R.D. "Wavelet - Domain Filtering for photo Image Systems" IEEE Transactions on image processing, (1997).
14. Lopes, A., Touzi, R., & Nezey, E., "Adaptive Speckle Filter and Scene Heterogeneity" Computer Trans, GE- 28, (6) : 992-1000, (1990).
15. I.T. Young, J. Gerbrands & L.J. Van Vliet , "Fundamental of Image Processing" , Printed in Netherlands at Delf Univ. of Technology, ISBN 90-75691:10-7, NUGI 841 , (1998).
16. Hopkinson, R.G, Kay, J.D, "The Lighting of Buildings" Faber and Faber, London (1972).

دراسة خصائص $I-V$ في تنفيق غشاء السوبر

سوزان ملك شاقولي

الجامعة المستنصرية / كلية التربية / قسم الفيزياء

ABSTRACT

In this search we study $I - V$ characteristic for device consist of super - insulter - super. With zero and non - zero voltage .

And their effect on super energy states and on movement cooper pairs which responsible of tunneling current in super .

الخلاصة

في هذا البحث ندرس خصائص $I - V$ لنبيطة مكونة من غشاء سوبر - عازل - سوبر في غياب فولتية المجال وبوجود الفولتية وتأثيرهما على مستويات طاقة السوبر وعلى حركة حاملات الشحنة (ازواج كوبر) المسؤولة عن تيار الانتفاق في السوبر.

المقدمة

مفاهيم اساسية

عند وضع حاجز عازل بين غشائين من مادة السوبر سمك كل منها يحدد بحدود (1A)، الأزواج تنتفق من جانب الى اخر عبر الحاجز، وهناك اختلاف مهم بين الالكترونات الغير مزدوجة في المعدن وازواج كوبر، اذ تكون ممانعة الأزواج مساوية للصفر، بينما الالكترونات غير المزدوجة تواجه مقاومة بسبب التصادم مع المادة كما ان التفاعل بين الالكترونات في مادة المعدن يكون مهماً، بينما تفاعلات الأزواج المترابطة في مادة السوبر تكون ذو اهمية كبيرة في عملية التوصيل (1,2,3). السوبر وازواج كوبر يتواجدان اذا افترضنا تحرك الالكترون خلال شبكة من الايونات الموجبة فان المجال السالب للالكترون يستقطب ويشوه شبكية الايونات الموجبة ليكون منطقة فائضة من الايونات الموجبة وفي المقابل تجذب الالكترون ثاني وينتج تفاعل جذب فعال بين الالكترونين (4، 5)، فاذا كان تفاعل الجذب بين الالكترونين اكبر من تنافر كولوم فان السوبر يتولد، والشكل (1) يوضح تفاعل الالكترون مع الشبيكة المشوهة. الأزواج المتولدة تمتلك نفس كمية التحرك وكثافتها منظمة وبالتالي فان التيار الناتج من ازواج كوبر المار عبر المفارق العازل يكون معتمد على حجم المفارق وعلى مادة السوبر وعلى درجة الحرارة، والشكل (1) يوضح تفاعل الالكترون مع الشبيكة المشوهة (2)، والشكل (2) يوضح مفارق متكون من حاجز عازل يفصل بين غشائين من مادة سوبر (5) البناء النظري

عند تسليط جهد كهربائي على نبيطة من سوبر - عازل - سوبر يمر تيار مكون من الأزواج عبر العازل بعملية (انتفاق ميكانيك الكم) والتيار يعتمد على كثافة الحالات الفارغة في احد الغشائين وكثافة الحالات المشغولة للغشاء الاخر.

الفولتية المطبقة تخلق مجال كهربائي ينفذ عبر العازل مؤثراً على غشاء السوبر والعازل يمثل قناة لمرور التيار فيؤثر على مستويات طاقة ازواج كوبر فتعمل على تهيج الالكترونات (ازواج كوبر)، اما الفولتية السالبة فيكون تأثيرها على التيار قليل اذ يقيد الحاملات (ازواج كوبر) ويقلل من طاقتها ويعمل على خلق شحنة فراغ موجبة (6، 7).

ولتوضيح خصائص $I=V$ بالتفصيل الشكل (3) يوضح نبيطة مربوطة الى مصدر كهربائي. عند غياب الجهد الكهربائي $VF=0$ فان مستويات طاقة الغشائين يكونان بنفس المستوى فيكون التيار المار من الغشاء (2) الى الغشاء (1) مساوي للتيار المار من غشاء (1) الى (2) وبالنتيجة لا يمر تيار في الدائرة.

وعند تطبيق فولتية مجال على النبيطة، وعندما يكون الغشاء (1) مربوط الى القطب الموجب والغشاء (2) مربوط الى القطب السالب فان مستويات طاقة الغشاء (1) تهبط نسبتة للغشاء (2) بمقدار (ev) وصافي تنفيق الالكترونات سيكون من (2 الى 1). وذلك لان ازواج كوبر في الطرف (1) لا تملك مستويات فارغة في الطرف (2) بينما ازواج كوبر في غشاء (2) تكون قادرة على التنفق الى الغشاء (1) تحت قعر الحالات. ولهذا يزداد التيار لغاية كل مستويات الطاقة الفارغة في الغشاء (1) تشغل. وعند

ازدياد فولتية المجال فان التيار يبقى ثابت ولا تستطيع أزواج كوبر في غشاء (1) التنفيق اما في الغشاء (2) يستطيع التنفيق وعندما تقترب الفولتية من $V = \frac{2\Delta}{e}$ حيث 2Δ تمثل فجوة طاقة السوبر يحدث انشطار أزواج كوبر (7، 8، 9)، اذ تنفق احد الالكترونات الى غشاء (1) لكي تشغل الحالات الواطئة وتكون مرتبطة بفقدان طاقة مقدارها Δ أما الالكترون الثاني يخسر الجزء الاخر من الطاقة فيشغل حالات متهيجة واطئة في غشاء (2) لاكتسابها طاقة مقدارها Δ .

وبعد فولتية $V = \frac{2\Delta}{e}$ تفقد المادة سوبريتها، والشكل (3) يوضح تيار جوزفين الاعظم عند وجود فولتية وفي غيابها. ولايجاد شدة المجال الكهربائي المتولد نتيجة للفولتية المسلطة نطبق صيغة كاوس

$$\nabla E = \frac{\rho_1}{\epsilon_1} + \frac{\rho_2}{\epsilon_2} \dots \dots \dots 1$$

حيث

$$\rho_2 = qN_2, \rho_1 = qN_1$$

ρ_1, ρ_2 كثافة الشحنة لغشاء سوبر (2 و 1) على التوالي N_1 و N_2 كثافة الحالات لمستويات طاقة السوبر (2، 1) (ϵ_1, ϵ_2) سماحية الكهربائية لكل من غشائين (1، 2) وبتعويض (ρ_1, ρ_2) في علاقة (1) وبأجراء التكامل لصيغة كاوس

$$\int \frac{dE}{dx} = \frac{qN_1}{\epsilon_1} + \frac{qN_2}{\epsilon_2}$$

$$\int_0^E dE = \left(\frac{qN_1}{\epsilon_1} + \frac{qN_2}{\epsilon_2} \right) \int_0^{d_{ins}} dx$$

اذ d_{ins} سمك الغشاء العازل

$$E = q \left(\frac{N_1}{\epsilon_1} + \frac{N_2}{\epsilon_2} \right) d_{ins} \dots \dots \dots 2$$

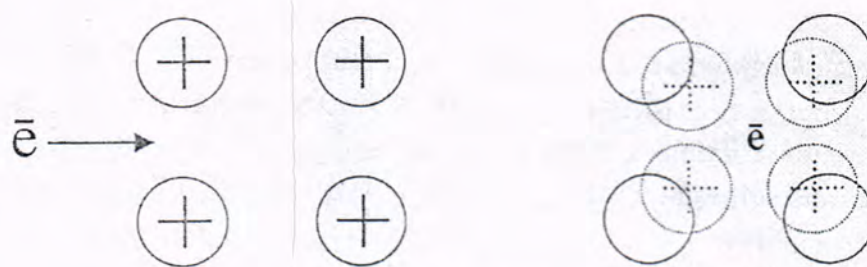
العلاقة (2) تمثل علاقة سمك العازل مع شدة المجال الكهربائي المتولد.

النتائج والمناقشة

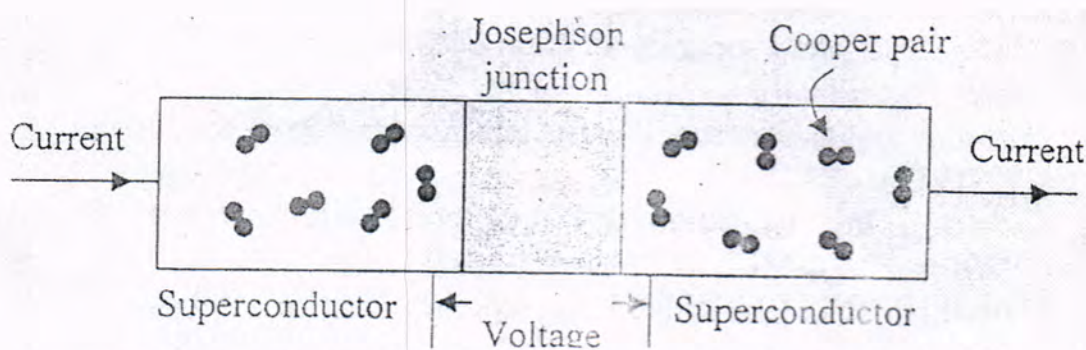
1. التنفيق بين مادتي سوبر من نفس النوع.
2. التنفيق بين مادتي بفجوات طاقة مختلفة.
3. كلما كان سمك العازل صغير يزداد شدة المجال الكهربائي فتزداد معدل جرف الا زواج بين مادتين بعملية التنفيق Tunneling

ومن ذلك يمكن ان نستنتج ان :

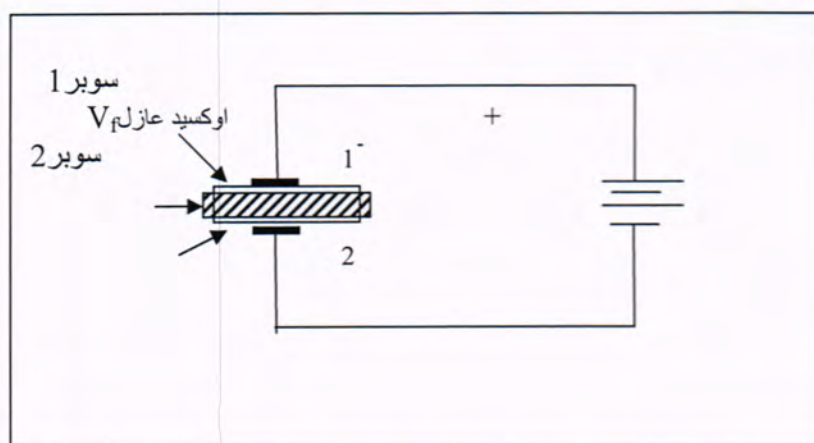
نستنتج ان النبيلة تعمل على متسعة مكونة من صفيحتين من غشاء مادة سوبر تفصلهما مادة عازلة سعة المتسعة تعتمد على سمك العازل بين المادتين وكلما كان سمك العازل صغير ومساحة الغشاء كبير تزداد شدة المجال الكهربائي فتزداد معدل جرف الا زواج بين المادتين بعملية التنفيق للازواج ويكون هذا ضمن فولتية مجال اقل من $\frac{2\Delta}{e}$ ، اذ تفرغ الحالات في احدى جانبي الغشاء وتملأ في الجانب الاخر حسب نوع الفولتية المطبقة.



شكل 1- تفاعل الإلكترون مع الشبكة المشوهة (b)



شكل 2- مفرق جوزفين متكون من حاجز عازل يفصل بين غشائي مادة السوبر



شكل 3- يوضح نبيلة مربوطة الى مصدر كهربائي



شكل 4- يوضح تيار جوزيف الاكظم عند وجود فولتية المجال في غيابها

المصادر

1. J. Axnas, L. Bryntse, L. Safanova and Rapp: phys B. V. 284-288. : 1010(2000).
2. T. Watanabe, K. Tokiwa, S. Ito, N. Urite. S. Mikusu, H. Okumoto, Y. Hashinaka A. Iyo, and Y. Tanaks, Phys C:Superconductivity, V.388-389: 353-354 (2003).
3. D. M. Baastidas, S. Pinol, J. Ploin, T. Puig and X. Obradors. Phys C. V. 403, PP. 132-138(2004).
4. I. Hase, N. Hamada & Y. Tanaks : Phys C: V. superconductivity V.412-414(1) : 246-249 (2004).
5. H. Mukuda, M. Abe Y. Arki, Y. Kitaoka, K. Tokiwa, T. Watanab A. Lyo, H. Kito and Y. Tadaka : Phys Rrey Lett , V. 96. : 087001 (2006).
6. H.change Chinese,J.Phys:34,(2-11)(1996).Su " Fabrication and Characterization of Mercurocuprate super conduction on Silver Substrates " , Ph. D. Floria State University . (2004) .
7. A Barone and G. Paterno, Physics and Application of the Juephs a Effect . Wiley NY. (1982).
8. Tirlham , Intr oducation to Super conductivity. Robert E. Krieger Punlit (1985).
9. EUROPHYSICS LETTERS Europhys. Lett. 59 (4). : 590-605 (2002).

دراسة فجوة الطاقة للبولى ستايرين (PS) المشوب بثاني كلوريد الحديد (FeCl_2)

¹ محمد حميد عبد الله و ² عبدة عامر عبد الحسين و ² وداد هنو عباس

¹ جامعة ديالى - كلية العلوم - قسم الفيزياء

² الجامعة المستنصرية - كلية التربية - قسم الفيزياء

² الجامعة المستنصرية - كلية التربية الأساسية - قسم العلوم

ABSTRACT

Films of pure polystyrene (PS) and doped by (FeCl_2) with percentages(2%) prepared by using casting technique in room temperature , the absorption and transmission spectra has been recorded in the wavelength rang (300-900) nm . We calculate the absorption coefficient and energy gap of the indirect, allowed, forbidden transition.

الخلاصة

تم تحضير أغشية من البولى ستايرين (PS) النقية والمشوبة بثاني كلوريد الحديد (FeCl_2) بنسبة (2%) بطريقة الصب وفي درجة حرارة الغرفة، وتم تسجيل طيفي الامتصاص والنفاذية لأغشية البوليمر النقي والمشوب ولمدى من الأطوال الموجية (300 - 900)nm. وحساب معامل الامتصاص و فجوة الطاقة للانتقال غير المباشر المسموح والممنوع.

المقدمة

يعتبر البولى ستايرين من البوليمرات غير المكلفة الشائعة الاستخدام ولها تطبيقات تقليدية كثيرة منها في التغليف، وكصفائح شفافة، وفي لعب الاطفال، اغشية الكمبيوتر (2,1)، ولكن في الاونة الاخيرة بدأت هذه التطبيقات تتخذ منحى جديد فقد استخدم البولى ستايرين بعد تعريضه للبكتريا والتي تتجه نحو سطح هذا البوليمر ذو السمك 100-120 مايكرون لان البيانات تشير الى ان خصائص البولى ستايرين تتغير بوجود البكتريا لتصبح اكثر ملائمة للتطبيقات الصناعية (3)، تستخدم كصفحة عزل مفرغة (vacuum insulator panel) والتي تمتلك توصيلية حرارية واطنة تكون مناسبة للكثير من تطبيقات حفظ الحرارة على سبيل المثال العازل الذي يستخدم في الثلاجات (4).

يهدف هذا البحث الى دراسة الانتقالات الالكترونية لاغشية البولى ستايرين المشوبة بثاني كلوريد الحديد.

المواد وطرائق العمل

لقد استخدمت طريقة الصب لتحضير غشاء البولى ستايرين (PS) وذلك لعدم احتياج تحضيرها إلى تقنيات متقدمة وأجهزة معقدة، ويمكن بواسطتها تحضير نماذج ذات مساحة كبيرة نسبيا وذات سمك متساوي تقريبا . تم تحضير النماذج على شكل أفلام مكونة من خليط من البوليمر النقي المجهز من قبل شركة (Dentaurum) الألمانية وملح ثاني كلوريد الحديد المجهز من قبل شركة (General Purpose reagent BDH-Limited Poole England) وبنقاوة (99.99%) عن طريق إذابة البولى ستايرين (PS) في الكلورفورم ثم صب الخليط في أحواض زجاجية للحصول على أغشية بوليمرية بسمك 20 مايكرون وبنسب شائبة مقدارها (2%) علما بان قطر حبيبية الشائبة (FeCl_2) كان 18 مايكرون .

قيس سمك النماذج المحضرة باستخدام جهاز (indicating micrometer 0.25nm) ذي المدى (0-100µm) ، سجل طيفي النفاذية والامتصاصية باستخدام مطياف من نوع (UV-160A UV-VIS Recording Spectrophotometer) المصنع من قبل شركة

شيمادزو اليابانية ولمدى من الأطوال الموجية يتراوح بين (200-900) nm وقد سجلت جميع القياسات في درجة حرارة الغرفة.

النتائج والمناقشة

تم حساب معامل الامتصاص (α) في منطقة الامتصاص الأساسية وفق العلاقة الآتية (6,5):

$$\alpha = 2.303 \frac{A}{d} \quad \text{----- (1)}$$

حيث أن: A الامتصاصية, d سمك الغشاء.

يوضح الشكل (1) العلاقة بين معامل الامتصاص وطاقة الفوتون الساقط لغشاء البولي ستايرين النقي والمشوب ونلاحظ من الشكل بأن تغير معامل الامتصاص في الطاقات الواطئة يكون قليل وعليه فإن احتمالية الانتقالات الإلكترونية قليلة أما في الطاقات العالية فإن تغير معامل الامتصاص يكون كبيراً ويدل ذلك على احتمالية كبيرة للانتقالات الإلكترونية قرب منطقة حافة الامتصاص.

أن معامل الامتصاص يساعد على استنتاج طبيعة الانتقالات الإلكترونية فعندما تكون قيم معامل الامتصاص عالية ($\alpha > 10^4 \text{ cm}^{-1}$) عند الطاقات الفوتونية العالية يتوقع حدوث انتقالات الكترونية مباشرة وتكون طاقة وزخم الإلكترون والفوتون محفوظتين، أما عندما تكون قيم معامل الامتصاص واطئة ($\alpha < 10^4 \text{ cm}^{-1}$) عند الطاقات الفوتونية الواطئة في هذا الحالة يتوقع حدوث انتقالات الكترونية غير مباشرة وفيها يحفظ زخم الإلكترون والفوتون بمساعدة الفونون (7,6).

أن النتائج أظهرت أن قيم معامل الامتصاص للبوليمر النقي والمشوب أقل من 10^4 cm^{-1} مما يرجح حدوث الانتقال الإلكتروني غير المباشر كما في الشكل (1). تم حساب طاقة الفجوة الممنوعة في الانتقال غير المباشر بنوعية المسموح والممنوع وفقاً للعلاقة (8,7):

$$\alpha hf = B(hf - E_g \pm E_p)^r \quad \text{----- (2)}$$

حيث أن: (hf): طاقة الفوتون (eV), (B): ثابت التناسب, (E_g): فجوة الطاقة الممنوعة للانتقال غير المباشر (eV), (E_p): طاقة الفونون المصاحب (eV), (+): امتصاص فونون, (-): امتصاص فونون.

إذا كان ($r = 2$) يكون الانتقال غير المباشر مسموحاً فتكون المعادلة (2) على الصورة الآتية (8,7):-

$$(\alpha hf)^{1/2} = B^2 (hf - E_g \pm E_p) \quad \text{----- (3)}$$

الشكل (2) يمثل العلاقة بين $(\alpha hf)^{1/2} (\text{cm}^{-1} \cdot \text{eV})^{1/2}$ وطاقة الفوتون للبولي ستايرين (PS) النقي، وبأخذ امتداد الجزء المستقيم من المنحني ليقطع محور طاقة الفوتون عند النقطة $(\alpha hf)^{1/2} = 0$ سوف نحصل على قيمة فجوة الطاقة الممنوعة للانتقال غير المباشر المسموح والذي تساوي (4.6 eV)، أما الشكل (3) فيمثل نفس العلاقة السابقة لكن للبولي ستايرين (PS) المشوب بنفس الطريقة السابقة يمكن الحصول على قيمة فجوة الطاقة الممنوعة للانتقال غير المباشر المسموح والذي تساوي (4.5 eV)، إذ نلاحظ بأن قيمة فجوة الطاقة قلت بعد التشويب مما يؤكد حدوث تحلل تسبب في زيادة الجذور الحرة.

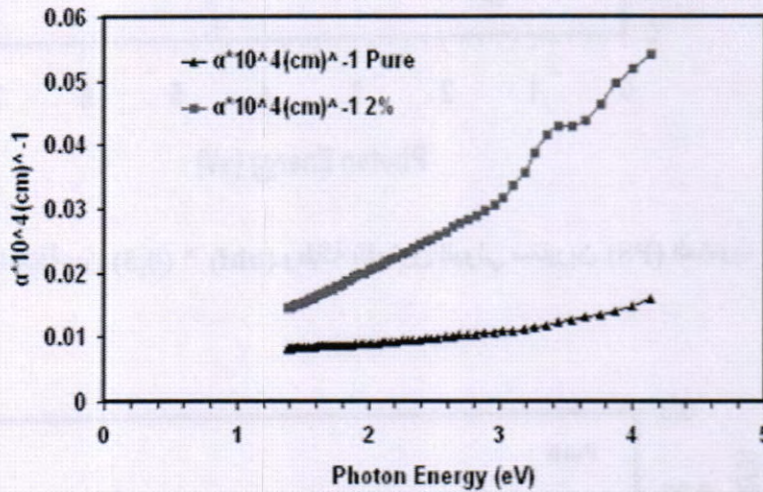
أما إذا كان ($r = 3$) فيكون الانتقال غير مباشر ممنوع فتكون المعادلة (2) على الشكل الآتي (8,7):-

$$(\alpha hf)^{1/3} = B^3 (hf - E_g \pm E_p) \quad \text{----- (4)}$$

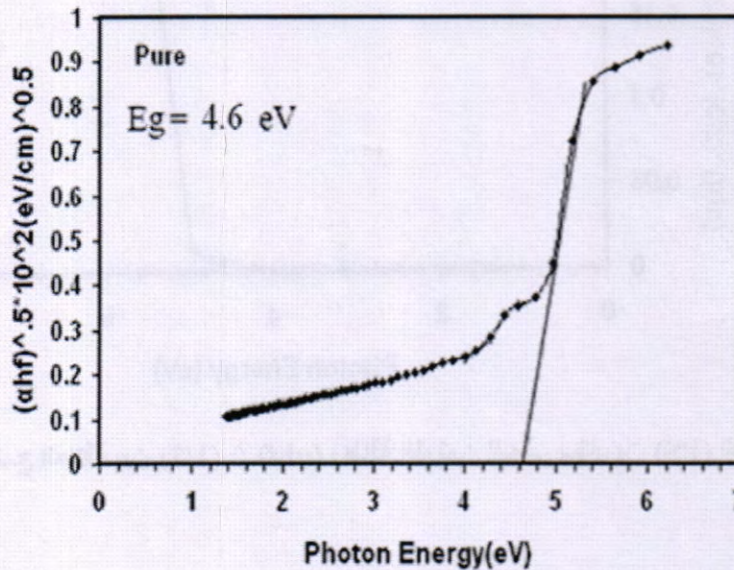
الشكل (4) يمثل العلاقة بين $(\alpha hf)^{1/3} (\text{cm}^{-1} \cdot \text{eV})^{1/3}$ وطاقة الفوتون للبولي ستايرين (PS) النقي، وبنفس الطريقة السابقة يتم الحصول على فجوة الطاقة الممنوعة للانتقال غير المباشر

الممنوع والذي تساوي (4.37eV)، أما الشكل (5) فيمثل نفس العلاقة السابقة لكن للبولي ستايرين (PS) المشوب، وب نفس الطريقة السابقة يمكن الحصول على قيمة فجوة الطاقة الممنوعة للانتقال غير المباشر الممنوع والذي تساوي (4.32eV)، اذ نلاحظ بان قيمة فجوة الطاقة قلت بعد التشويب.

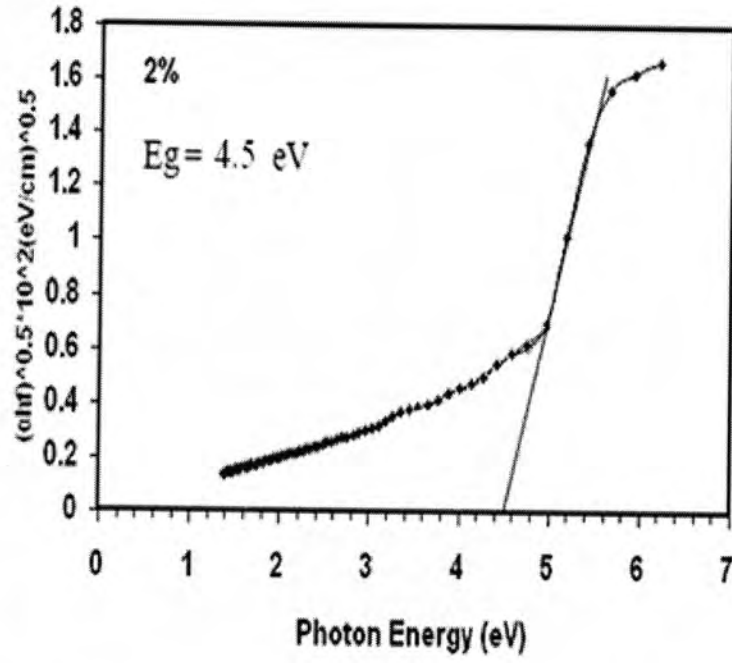
- 1- أن التشويب أدى إلى زيادة معامل الامتصاص.
- 2- أظهرت النتائج أن معامل الامتصاص اقل من (10^4 cm^{-1}) وهذا يعني حدوث انتقالات الكترونية غير مباشرة مسموحة وممنوعة.
- 3- لم يغير التشويب من طبيعة الانتقالات الالكترونية لأغشية البولي ستايرين (PS) بل حافظ على طبيعة انتقاله غير المباشرة.
- 4- أن التشويب أدى إلى تقليل فجوة الطاقة.



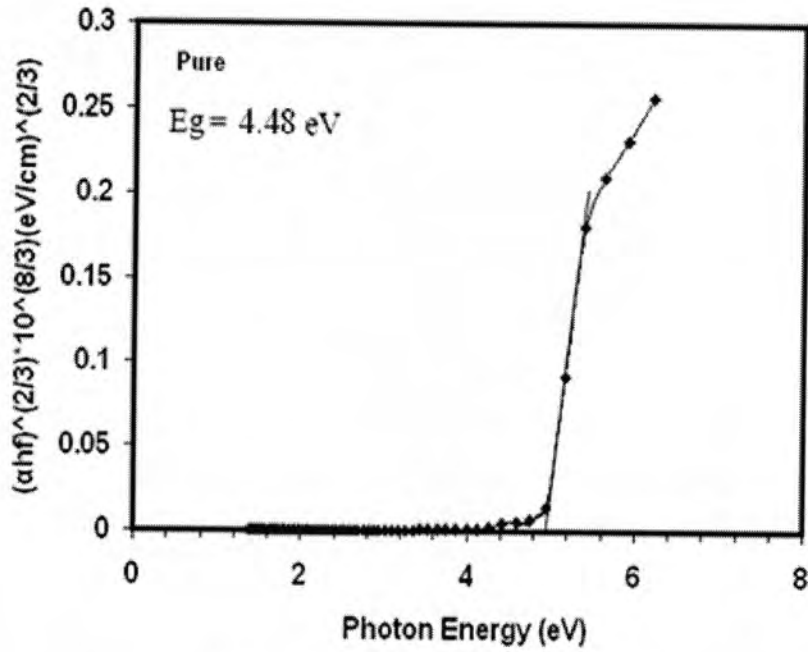
شكل 1: يوضح العلاقة بين معامل الامتصاص مع طاقة الفوتون للبولي ستايرين (PS) النقي والمشوب



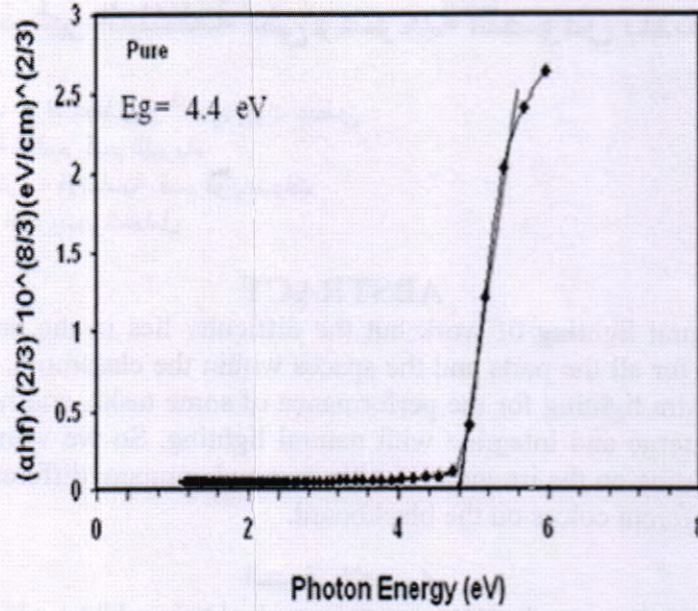
شكل 2: يوضح العلاقة بين $(\alpha hf)^{0.5}$ وطاقة الفوتون للبولي ستايرين (PS) النقي



شكل 3- يوضح العلاقة بين $(\alpha hf)^{0.5}$ وطاقة الفوتون للبولي ستايرين (PS) المشوب



شكل 4- يوضح العلاقة بين $(\alpha hf)^{1/3}$ وطاقة الفوتون للبولي ستايرين (PS) النقي



شكل 5- يوضح العلاقة بين $(\alpha hf)^{1/2}$ وطاقة الفوتون للبولي ستايرين (PS) المشوب

المصادر

1. Sheu M. S., Hudson D. M., Loh and loh I. H., Encyclopedie Handbook of Biomaterials and Bio – Eng Part A, Marcel Dekker, New York, (1995).
2. Chan C. M., Ko T. M. and Hiroka H., Polymer Surface Modification by Plasms And Photons , Surf Sci, Rep., 24 (1):12 (1996).
3. Pawde S. M. and Parab S. S., Spectroscopic and Antibactenal Stucies of Poystyrene Films Under Air Plasma and He-Ne Laser Treatment, Indian Journal Academy of Sciences, 70 (5):935(2008).
4. Tseng P. C., Chu H. S., The Effects of Pe Additives on The Performance of Polystyerne Vacuum Insulation Panels, International Jonral of Heat And Mass Transfer, 52:3084, (2009).
5. Harman F. M., Encyclopedia of Polymer Science and Engineering, 2nd Ed, 15 :377-397(1976).
6. Ballato J., Novelpolymric optical fibers amplifiers and lasers, National textile center research Briefs-Materials competency, (2003).
7. Sinth Archeic P., Materials Research Society Symp., 629(2002).
8. Mujdat Caglar, Saliha Ilcan, Yasemin Caglar, Structural Morpho - logical and Optical Properties of CuAlS₂ Films Deposited by Spray Pyrolysis Method, Optics Communications, 281:1615–1624, (2008).

تأثير الإضاءة غير المنتظمة على وضوحية النصوص باختلاف المسافة

¹ علي عبد داود الزكي و ²رشا عواد عبطان و ³عدي عواد عبطان

¹ الجامعة المستنصرية / كلية العلوم قسم الفيزياء

² الجامعة المستنصرية / كلية التربية الأساسية قسم الرياضيات

³ الجامعة التكنولوجية / مركز التدريب والمعامل

ABSTRACT

People prefer the natural lighting of work but the difficulty lies in the provision of appropriate levels of natural light for all the parts and the spaces within the classroom. " If that areas near the windows may need extra lighting for the performance of some tasks, and here are the need to use artificial lighting to merge and integrate with natural lighting. So we went in this research is to study the effect of lighting on the irregular Douhip text and compare different distance variation of the texts written in different colors on the blackboard.

الخلاصة

يفضل الأشخاص العمل بالإضاءة الطبيعية إلا أن الصعوبة تكمن في توفير المستويات الملائمة للإضاءة الطبيعية لجميع الأجزاء والمسافات في داخل القاعة الدراسية. إذا أن المساحات القريبة من الشبابيك قد تحتاج إلى إضاءة إضافية لأداء بعض المهام، وهنا تكون الحاجة لاستخدام الإضاءة الصناعية لتندمج وتتكامل مع الإضاءة الطبيعية. لذا توجهنا في هذا البحث إلى دراسة تأثير الإضاءة الغير منتظمة على وضوحية النص باختلاف المسافة و مقارنة التباين للنصوص المكتوبة بألوان مختلفة على السبورة.

المقدمة

الضوء هو شكل من أشكال الطاقة الذي له خواص تستطيع تحفيز الأجهزة المستقبلية في العين البشرية ليحدث فعل الرؤية، ويمكن للضوء أن ينتقل دون الحاجة إلى وسط مادي من المصدر الضوئي في خطوط مستقيمة وفي جميع الاتجاهات (1).

يمكن التعرف على سلوك الإشعاع من خلال خصائصه الموجية. فالموجات الضوئية ذات طبيعة الكتر ومغناطيسية تشغل حيزاً ضيقاً من طيف الموجات الكهرومغناطيسية بين 380 - 670 نانومتر وبالتفريق بين هذه الأطوال الموجية من قبل العين البشرية يتم الإحساس بالألوان.

أن مصطلح الوهج يعني كمية الضوء المستقبل من قبل العين. وتبدو الأجسام متوهجة أما لكونها مصدراً بذاتها مثل الشمس والشمعة أو من جراء عكسها للأشعة الضوئية الساقطة على سطحها. وتقاس طاقة الإشعاع المرئي بمعدل تأثيرها على العين البشرية بما يسمى باللومين (Lumen) وعند انتشار الضوء على سطح معين نطلق على هذه العملية تسمية الاستنارة E أو القيمة الانارية (Illuminance) وتقاس بلومين / وحدة المساحة أو بال (لوكس Lux).

تسمى خواص المصدر الذي يبعث الضوء باتجاه معين بالشدة المنيرة للمصدر (Luminance- Intensity) وهي كمية الضوء الساقطة عمودياً في الثانية الواحدة على وحدة السطوح وتقاس (بالشمعة Candela / وحدة المساحة) (2).

أن الدفق المنير المنتشر على سطح جسم ما لايسبب فعل الرؤية بل إن قابلية السطح على عكس الدفق الضوئي إلى العين (Brightness) هي السبب في فعل الرؤية، فلو لم يملك السطح أمكانية عكس الضوء (سطح أسود مثلاً) فإن العين سوف لن تدركه. ينعكس الضوء على السطوح المختلفة بنسب تتباين مع نوعية المادة ملمسها ولونها و اشراقيتها إذ تقل نسب الانعكاسية Reflection كلما كانت المادة التي تعكس الضوء ذات قابلية عالية للنفذية

إن قابلية الضوء على عكس الأشعة الضوئية تسمى بالانعكاسية ويمكن قياسها نسبة الاضائية الواصلة من الجسم إلى الإضاءة الكلية الأصلية الساقطة عليه (3).

هنالك العديد من الدراسات السابقة التي اهتمت بدراسة تباين الصور الملونة من خلال تحسين الإضاءة ودراسة تأثير الإضاءة على جودة الصورة وفيما يلي إيجاز أهم هذه الدراسات :-

- عام 1990 اقترح Johnson استخدام طريقة التباين للكشف عن الحافات الموجودة في الصورة ذات الإضاءة غير المتساوية أو الضعيفة حيث أن هذه الطريقة لا تعتمد على القيمة المطلقة للإضاءة Absolute Brightness كما أستخدم الباحث نوافذ حيزيه 5×5 ذات عوامل التدرج للكشف عن الحافات إذ تعد طريقة التباين مناسبة للصور المرئية والصور بالأشعة تحت الحمراء حيث يمكن اعتماد هذه الطريقة في تطبيقات الإنسان الآلي التي لا يمكن فيها السيطرة على الإضاءة (4).
- قدم الباحثان Scharff و Ahumada عام 2003 بحثاً بإمكانية قياس التباين للنصوص وإمكانية قراءتها ، حيث وجدوا بأن إمكانية تمييز الكلمة وتصنيفها تتأثر بشكل كبير بالخلفية لها (5).
- اقترح الباحث Thompson et al. عام 2003 خوارزمية لتحسين الصور للمناظر الليلية ، حيث تمكنت هذه الخوارزمية من جعل الصور المأخوذة في ضوء النهار وكأنها مأخوذة ليلاً حيث تقوم بتقليل التباين اضافية الصورة وجعل الصور بازاحة زرقاء ، وشملت دراستهم المناظر الحقيقية المشاهدة ليلاً والوضوءاء المرافقة لها ومقدار التشوه الحاصل فيها (6) .
- الباحثان Aditi Majumder و Sandy Irani عام 2005 اقترحا تقنية لتحسين تباين الصورة باستخدام حساسية التباين البشري حيث يتم تحسين التباين الصورة الموقعي بوساطة التحكم بميل الصورة الموقعي اعتماداً على الدراسة التي اثبتت ان حساسية تباين العين البشرية في تمييز التباين تخضع لقانون ويبر (Weber) لمستويات ما فوق العتبة وان هذه الطريقة تقوم بتحسين التباين دون تقسيم الصورة سواء في المجال المكاني أو المجال الترددي (7) .
- اقترح الباحثان Yehya و Norio عام 2006 تقنية جديدة لتحسين التباين للنموذج المشوش ومعتم للصورة ضمن منطقة معينة وفي هذه التقنية يتم تحسين النوعية البصرية للصورة. إن هذه التقنية طبقت على الصورة الحقيقية التي من الصعب ان تتباين بواسطة التقنيات التقليدية (8) .

السطوع (الانارية Luminance)

تؤثر كمية الضوء المنبعثة من الجسم ذي مساحة سطحية معينة على مظهره ، والسطوع هو قابلية مساحة ضوئية معينة من المصدر الضوئي أو السطح العاكس للضوء لعمل فعل الإحساس بالسطوع فلو كان هنالك سطحين مختلفين المساحة ولهما نفس شدة السطوع باتجاه معين فان السطح الأقل مساحة يكون له سطوع اكبر. فالسطوح المضيئة تكون على نوعين ، مصادر متألقة بذاتها أو سطوح عاكسة للضوء ويمكن أن تحسب الانارية لسطح معين فيزيائياً بحاصل ضرب الاستنارة في معامل الانعكاس . ويمكن أن تطلق عليه الوهج (Brightness) عند التعامل معه كتأثير بصري على العين البشرية (3) .

الدفق المنير Luminous Flux

يعبر بواسطة الدفق المنير عن معدل جريان الطاقة الضوئية (الكهرومغناطيسية) أو يعبر عنه بمفهوم القوة ، ووحدته اللومن (Lumen) (9) .

الاستنارة E- illuminance

يضاء سطح معين بسقوط الدفق المنير ويسمى الاستنارة ويعبر عن مفهوم الاستنارة عن كثافة الدفق المنير الواصل إلى السطح ووحدته Lux $(\text{Lumen} / \text{m}^2)$ (9) .

قوانين السيطرة على الأشعة الضوئية وتوزيعها

• الانعكاسية Reflection

عند سقوط الأشعة الضوئية على سطح جسم له القابلية على عكس تلك الأشعة ، فان الجزء الأكبر من الأشعة الضوئية سوف ينعكس عن ذلك السطح وجزء منه قد يمتص أو ينفذ . إن نسبه كميته الأشعة الضوئية المنعكسة إلى كمية الأشعة الضوئية الساقطة أصلاً على سطح الجسم يسمى بمعامل الانعكاس وهذه النسبة تتغير من 92% للفضة الملمعة إلى 0% للون الأسود . وأشعة الضوء الساقطة على سطح ما يمكن ان تنعكس بعدة طرق تعتمد على طبيعة ذلك السطح (10) .

- انعكاس مباشر Specular Reflection
هو انعكاس مباشر باتجاه واحد من سطح صقيل وزاوية سقوط الأشعة الضوئية على السطح تساوي زاوية انعكاسها عنه.
- انعكاس مشتت Diffuse Reflection
هو انعكاس تشتتت فيه الأشعة الضوئية الساقطة على سطح متعرج الملمس إلى مختلف الاتجاهات ، حيث يبدو كل السطح متوهجاً من أي زاوية نظر إليه .
- انعكاس مميز Preferential Reflection
هو انعكاس مشتت يكون فيه الإشعاع الضوئي الأقوى باتجاه واحد مثل الانعكاس المباشر . أي مجموعة من صفات الانعكاسين السابقين .

● النفاذية Transmission

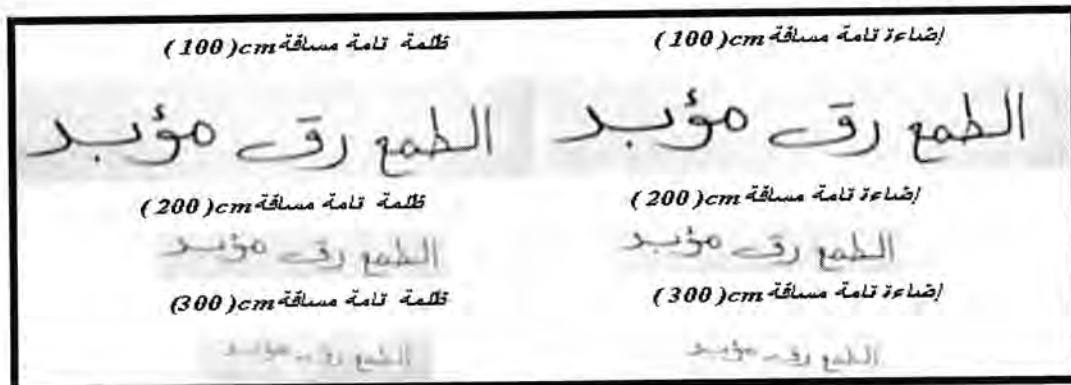
عند سقوط أشعة الضوء على سطح جسم ما فإنه قد ينعكس منه أو خلاله داخل مادة السطح ثم ينفذ إلى الخارج بما يسمى بالنفاذية . أن نسبة كمية الأشعة الضوئية النافذة من الجسم ما إلى كمية الأشعة الضوئية الساقطة أصلاً عليه تسمى بمعامل النفاذية . وتتراوح المواد بين مواد ذات معامل نفاذية عالية تصل إلى 92% مثل الكريستال الشفاف إلى مواد ذات معامل نفاذية قليل يصل إلى الصفر للمواد المعتمة . وتكون النفاذية بنوعين فهي ، إما تكون (مباشرة) في حال خروج الأشعة الضوئية الساقطة على الجسم وبنفس صفاتها الأصلية لحظة دخولها إلى الجسم أو مشتتة إذا انتشرت الأشعة الضوئية عند خروجها من الجسم . ووفق قوانين محددة بنفس مبدأ تصرف موجات الماء عند سقوط حجر في بركة سوف تتعرض الأشعة الضوئية خلال عبورها من وسط إلى الآخر إلى الانحناء الذي يسمى بالانكسار (Reflection) . إن الأشعة الضوئية تنكسر بزوايا انكسار أقل من زاوية السقوط إن كان الوسط الجديد أكثر كثافة من الوسط الأصلي والعكس صحيح وعلى هذا الأساس تبقى الأشعة الضوئية محافظة على اتجاهها حين اختراقها لمادة الزجاج لكن الذي سيتغير موقع الأشعة (10) .

● الامتصاص Absorption

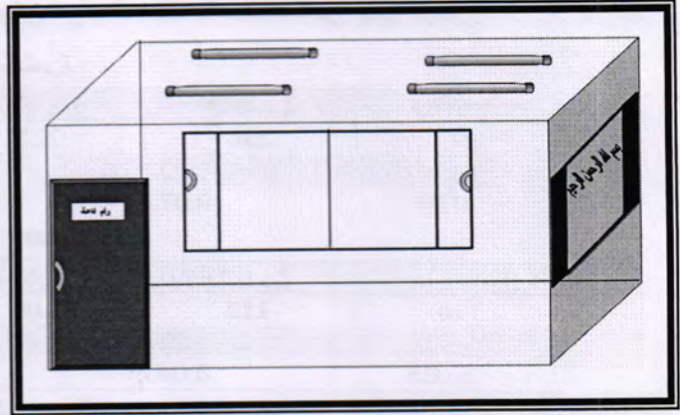
بعض من الأشعة الضوئية الساقطة على الجسم ما قد يتم امتصاصها من قبل مادة الجسم نفسها . ومعامل الامتصاص هو نفسه كمية الأشعة الضوئية الممتصة من قبل مادة الجسم إلى كمية الأشعة الضوئية الساقطة أصلاً على الجسم . إن مجموع قيم معامل الانعكاس ومعامل النفاذية والامتصاصية لجسم ما يجب إن تكون 100% من قيمة الطاقة الضوئية الساقطة عليه أصلاً (10) .

منظومة العمل لدراسة تأثير الإضاءة على وضوحية النص باختلاف المسافة

اعتمدنا في هذه الدراسة على كتابة نص بشكل أفقي باستخدام ألوان قلم بورد مختلفة نوع - Dry Erase لبيان وضوحية النص المكتوب على السبورة في القاعة الدراسية . حيث تمت عملية التصوير في القاعة الدراسية كما موضح بالشكل (1) في صباح الساعة العاشرة من يوم 2009 / 4 / 14 باستخدام الكاميرا الرقمية Sony - Digital Camera كما موضح بالشكل (2) ، والشكل (3) يوضح صور النصوص المكتوبة على السبورة ولمسافات مختلفة .



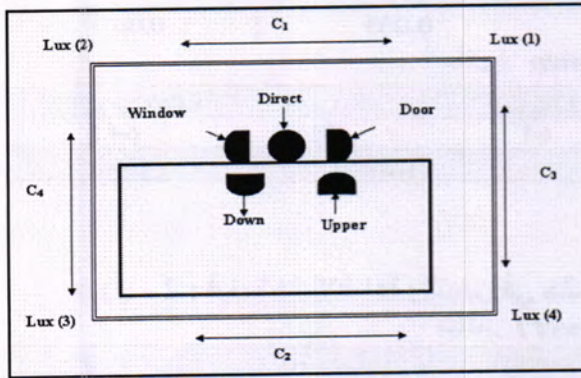
شكل -3: يوضح الصور الناتجة من عملية التصوير باختلاف المسافة



شكل -1: القاعة الدراسية المستخدمة في عملية التصوير

شكل -2: يوضح الكاميرا الرقمية المستخدمة في عملية التصوير

تم إضاءة القاعة الدراسية بإضاءة مختلفة وذلك بتشغيل المصابيح من جهة الشباك وغلقها من جهة الباب وبالعكس ، حيث تم قياس شدة الإضاءة Luxmeter الموضح بالشكل (4) لقياس شدة الإضاءة بالاتجاهات المختلفة داخل القاعة الدراسية، والشكل (5) يوضح الاتجاهات التي تم فيها قياس شدة الإضاءة .



شكل -5: اتجاهات شدة الإضاءة داخل القاعة الدراسية



شكل -4: جهاز قياس شدة الإضاءة

التباين Contrast

هو الاختلاف في الخصائص البصرية التي تجعل عناصر الصورة قابلة للتمييز بين العناصر المختلفة أو الخلفية أي انه النسبة بين إضاءة الجسم Object وإضاءة الخلفية Background التي تحيط بالجسم كما موضح بالعلاقة الآتية (11) :

$$C = \frac{I_{\max} - I_{\min}}{I_{\max} + I_{\min}} \quad \dots\dots\dots(1)$$

إن النظام البصري البشري هو أكثر حساسية للتباين من الإضاءة فلهذا يمكننا تحسس الضوء على نفس النحو بغض النظر عن التغيرات الكبيرة في الإضاءة على مدى اليوم .

تقنيات حساب التباين للنص المكتوب على السبورة

يتم حساب التباين للنص المكتوب على اللوحة البيضاء (Whiteboard) بالاعتماد على نقاط الحافات ، حيث تم تطبيق العلاقة السابقة لإيجاد التباين من خلال قراءة جهاز قياس شدة الإضاءة حسب اتجاه الكاشف وكما موضح في الجدولين (1) و(2) للإضاءة من اليمين واليسار على التتابع .

جدول - 1 : قيم شدة الإضاءة والتباين في حالة القاعة مضاءة من جهة اليمين

مباشرة

Lux (1)	Lux(2)	Lux(3)	Lux(4)	Lux(average)
197	236	222	192	211.75
C1	C2	C3	C4	
0.09	0.072	0.012	0.03	

(Window) شباك

Lux (1)	Lux(2)	Lux(3)	Lux(4)	Lux(average)
116	122	118	130	121.5
C1	C2	C3	C4	
0.025	0.048	0.056	0.016	

(Door) باب

Lux (1)	Lux(2)	Lux(3)	Lux(4)	Lux(average)
270	300	272	254	274
C1	C2	C3	C4	
0.052	0.034	0.03	0.048	

(Upper) أعلى

Lux (1)	Lux(2)	Lux(3)	Lux(4)	Lux(average)
218	257	261	233	242.25
C1	C2	C3	C4	
0.082	0.056	0.033	0.007	

(Down) أسفل

Lux (1)	Lux(2)	Lux(3)	Lux(4)	Lux(average)
63	73	64	58	64.5
C1	C2	C3	C4	

جدول - 2 : قيم شدة الإضاءة والتباين في حالة القاعة مضاءة من جهة اليسار

مباشر (Direct)

Lux (1)	Lux(2)	Lux(3)	Lux(4)	Lux(average)
234	226	207	232	224.75
C1	C2	C3	C4	
0.0173	0.056	0.004	0.043	

(Window) شباك

Lux (1)	Lux(2)	Lux(3)	Lux(4)	Lux(average)
161	171	182	168	170.5
C1	C2	C3	C4	
0.03	0.04	0.02	0.03	

(Door) الباب

Lux (1)	Lux(2)	Lux(3)	Lux(4)	Lux(average)
154	162	199	165	170
C1	C2	C3	C4	
0.025	0.093	0.034	0.1	

(Upper) الأعلى

Lux (1)	Lux(2)	Lux(3)	Lux(4)	Lux(average)
273	261	243	255	258
C1	C2	C3	C4	
0.022	0.024	0.034	0.035	

(Down) الأسفل

Lux (1)	Lux(2)	Lux(3)	Lux(4)	Lux(average)
89	100	87	80	89
C1	C2	C3	C4	
0.058	0.04	0.053	0.069	

علي ورشاو عدي

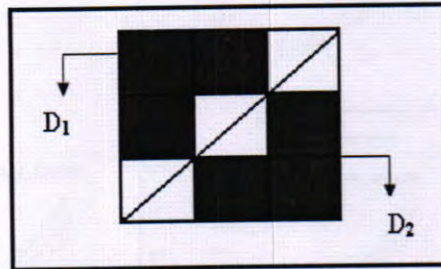
في هذه الدراسة تم اقتراح عدة تقنيات تعتمد على مناطق الحافات بين مناطق الصورة المختلفة لحساب التباين بين لون النص المكتوب على اللوحة ولون الخلفية (White Board) لمركبة الإضاءة L وللمركبات اللونية RGB ومن هذه التقنيات :

❖ تقنية التباين المباشر

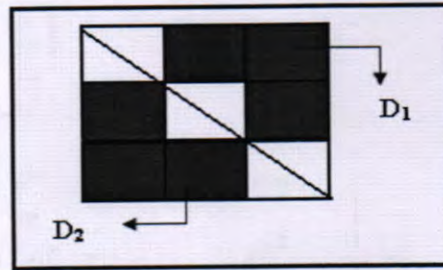
في هذه التقنية يتم حساب التباين من العلاقة (1) بالاعتماد على أكبر واصغر شدة من نقاط الحافات للحزم اللونية ومركبة الإضاءة L ، ويتم ذلك بأخذ نافذة ثلاثية حول نقطة الحافات في الصورة (cimg) والبحث على أوطأ وأعلى قيمة في الشدة لعناصر الصورة التابعة للحافات حيث استخدم مؤثر سوبل في تحديد نقاط الحافات في الصورة .

❖ تقنية التباين القطري الرئيسي

إن أساس عمل هذه التقنية يعتمد على تكوين نافذة ثلاثية حول العنصر (cimg) الذي يمثل حافة ثم إيجاد مجموع العناصر فوق وأسفل القطر الأول ومن ثم يحسب منهما التباين اعتماداً على معادلة التباين (1) حيث I_{max} يساوي أكبر قيمة لمجموع عناصر فوق أو أسفل القطر الأول و I_{min} يساوي اصغر قيمة لمجموع عناصر فوق أو أسفل القطر الأول وكما موضح بالشكلين (6) و (7).



شكل 7- نافذة عناصر القطر الثاني لحساب D_1 و D_2



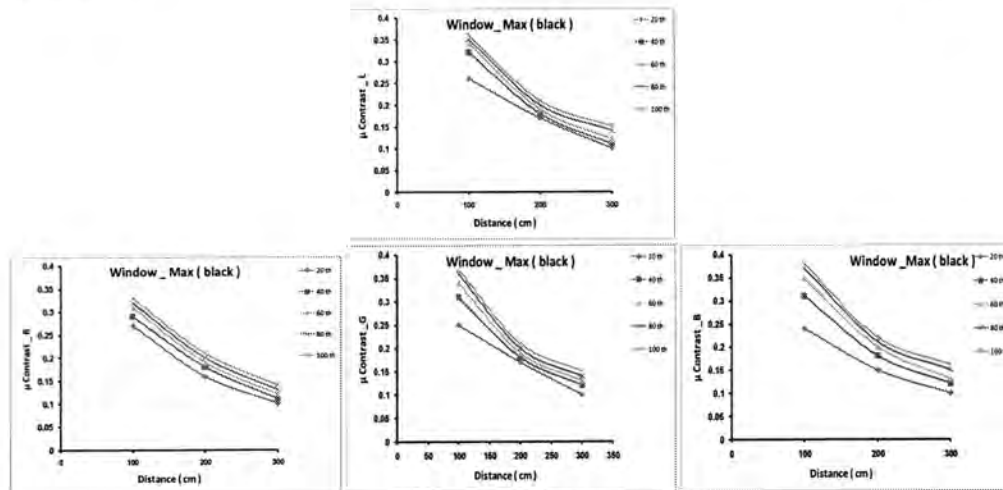
شكل 6- نافذة عناصر القطر الأول لحساب D_1 و D_2

نتائج دراسة تأثير الإضاءة على وضوحية النص باختلاف المسافة

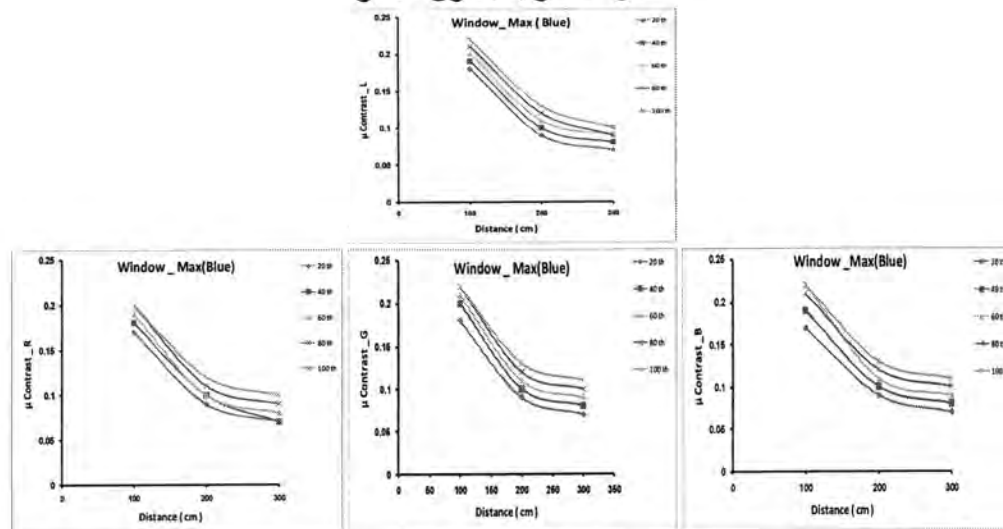
أن نتائج دراسة التباين للنصوص المكتوبة بالألوان على اللوحة موضحة بالشكل (8a,8b) لتقنية التباين المباشر في حالة الإضاءة من جهة اليمين واليسار بالتتابع ، إذا نلاحظ أن قيم التباين للنص المكتوب باللون الأسود أعلى من قيم تباين النصوص المكتوبة باللون الأحمر والأزرق في حالة الإضاءة من جهة اليسار عن جهة اليمين مما يؤدي الى زيادة وضوحية النص . أما نتائج تقنية التباين القطري في حالة الإضاءة من جهة اليمين واليسار فنلاحظ انخفاض في قيم التباين للألوان المختلفة مقارنة بتقنية التباين المباشر ويلاحظ أن هذا الانخفاض لا يمثل علاقة خطية ، إذا نلاحظ التقارب في قيم التباين لكلا حالتي الإضاءة من جهة اليمين واليسار كما موضح بالشكل (9a,9b) بالتتابع .

ومن ذلك يمكن ان نستنتج:

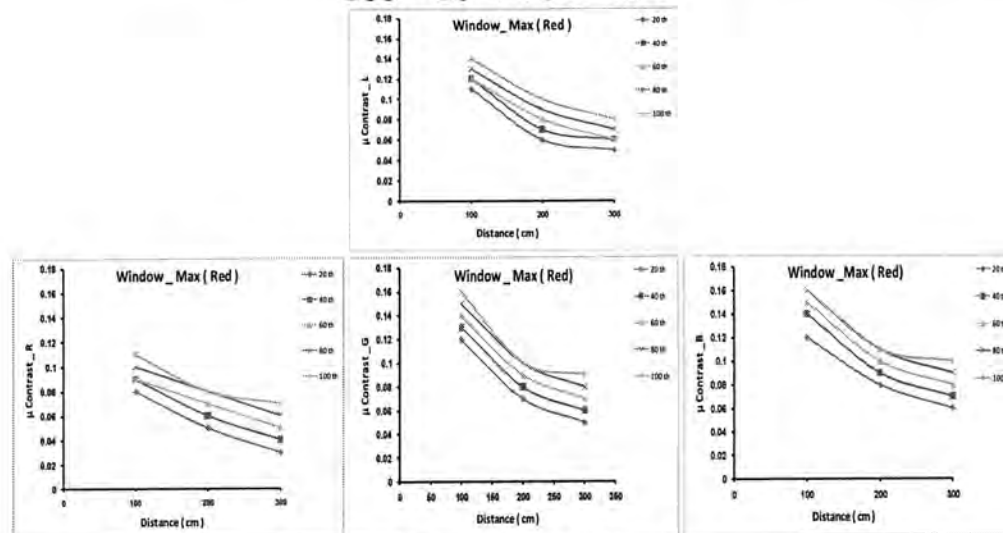
- تكون النصوص المكتوبة على اللوحة البيضاء أقل وضوحية كلما ابتعدنا عن اللوحة للمركبات اللونية الثلاث RGB ولمركبة الإضاءة L ، والسبب في ذلك لان المسافات البعيدة تقلل من قيمة التباين للنصوص فتؤثر في وضوحيتها من حيث التفاصيل أو الحدود الفاصلة بين النصوص المكتوبة على اللوحة ، إضافة إلى الهواء الذي يفصل بين العين والنص المكتوب الذي يزداد غشاوة في النص كلما زادت المسافة الفاصلة .
- إن نتائج المقارنة بين تباين ألوان النص المكتوب على السبورة تبين أن اللون الأسود أعطى أعلى قيم للتباين من اللونين الأزرق والأحمر وخاصة في حالة الإضاءة من جهة اليسار .
- أن نتائج قيم شدة الإضاءة تبين أن شدة الإضاءة من جهة اليسار أفضل من جهة اليمين وهذا راجع إلى الإضاءة (الطبيعية) الواصلة من الشبائيك إضافة الى الإضاءة الصناعية المكملة داخل القاعة الدراسية .



النص المكتوب باللون الأسود



النص المكتوب باللون الأزرق

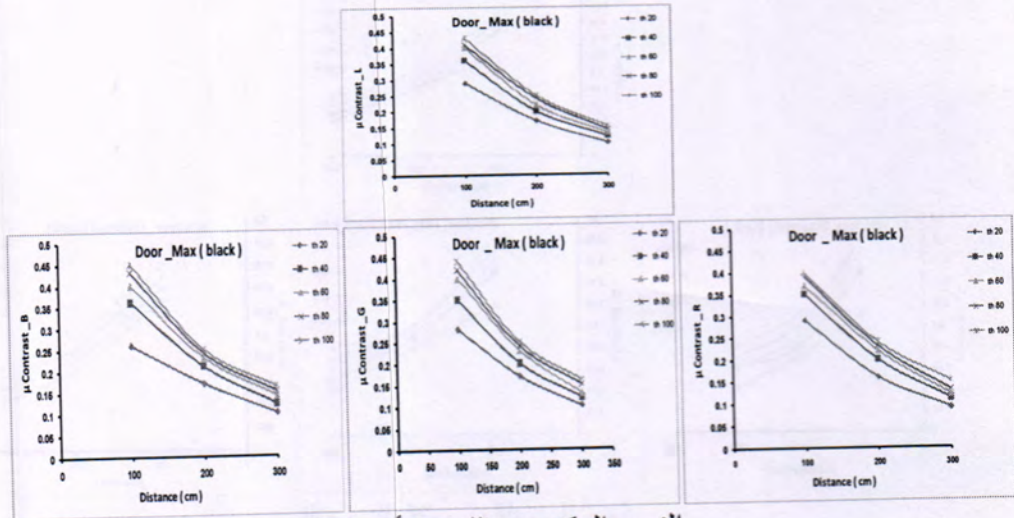


النص المكتوب باللون الأحمر

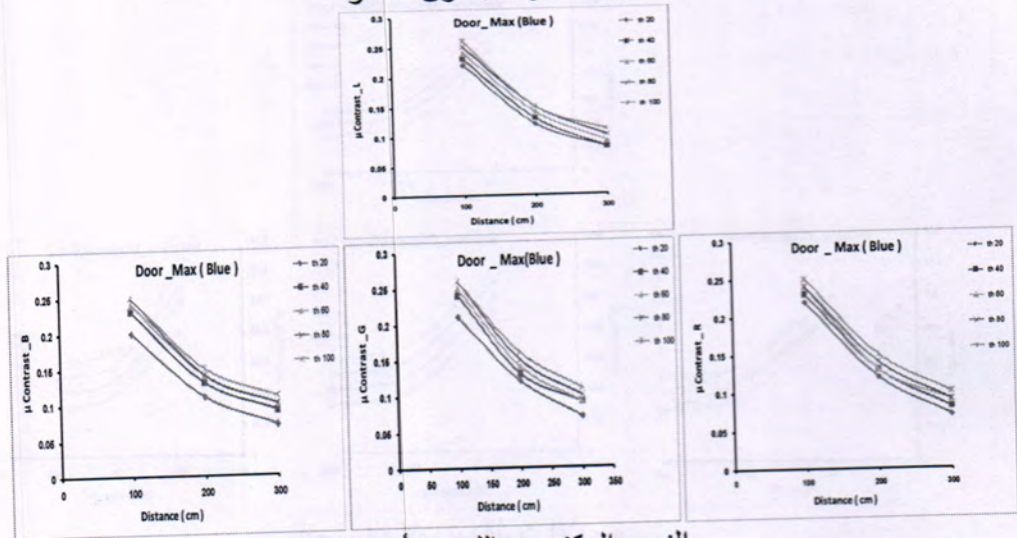
شكل - 8a: التباين المباشر لقاعة الدرس المضاءة يميناً (إضاءة غير منتظمة) للحزم اللونية ومركبة الإضاءة RGB,L

تأثير الإضاءة غير المنتظمة على وضوحية النصوص باختلاف المسافة

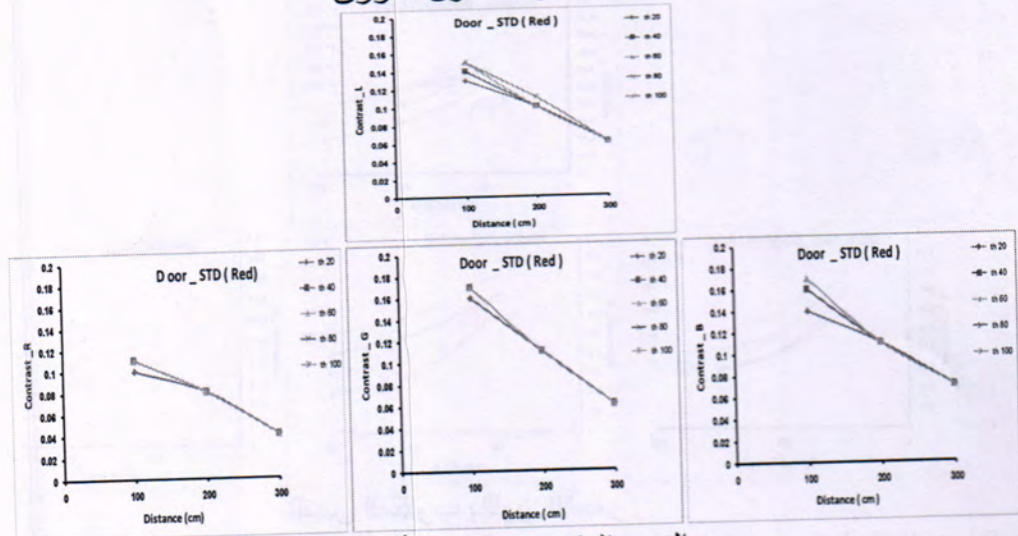
علي ورشا و عدي



النص المكتوب باللون الأسود

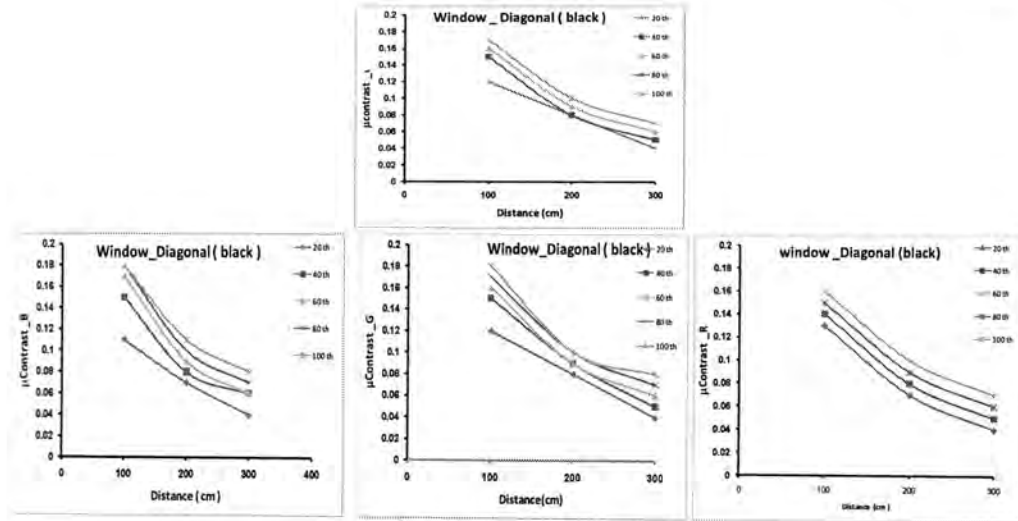


النص المكتوب باللون الأزرق

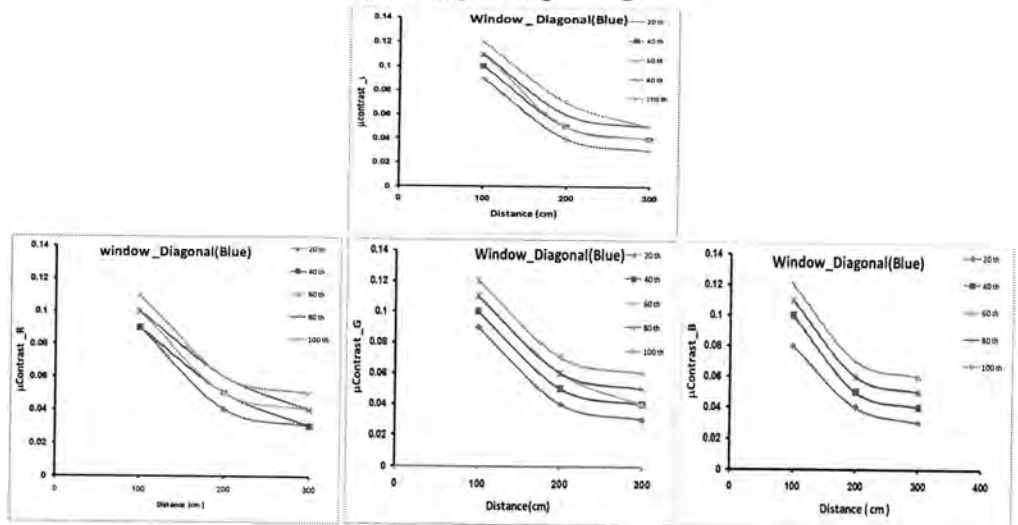


النص المكتوب باللون الأحمر

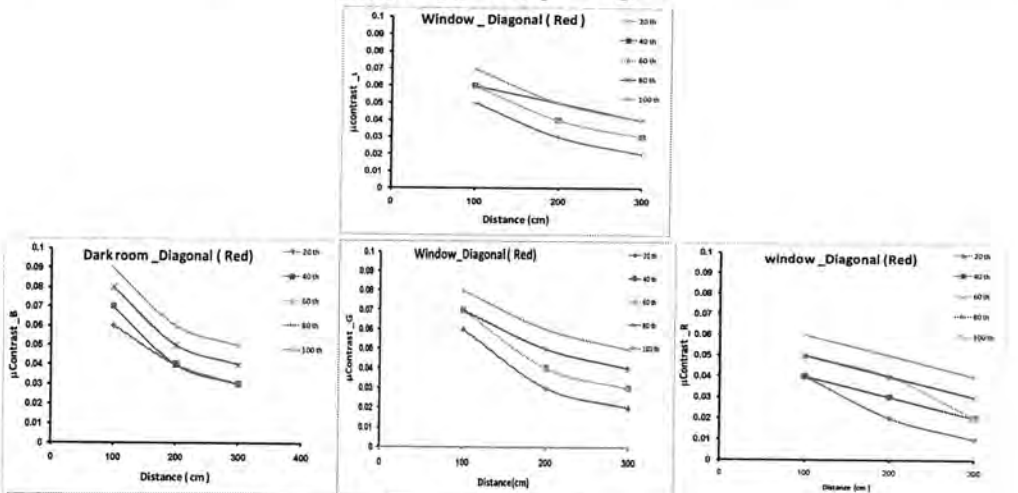
شكل - 8b : التباين المباشر لقاعة الدرس المضاءة يسارا (إضاءة غير منتظمة) للحزم اللونية ومركبة الإضاءة RGB,L



النص المكتوب باللون الأسود

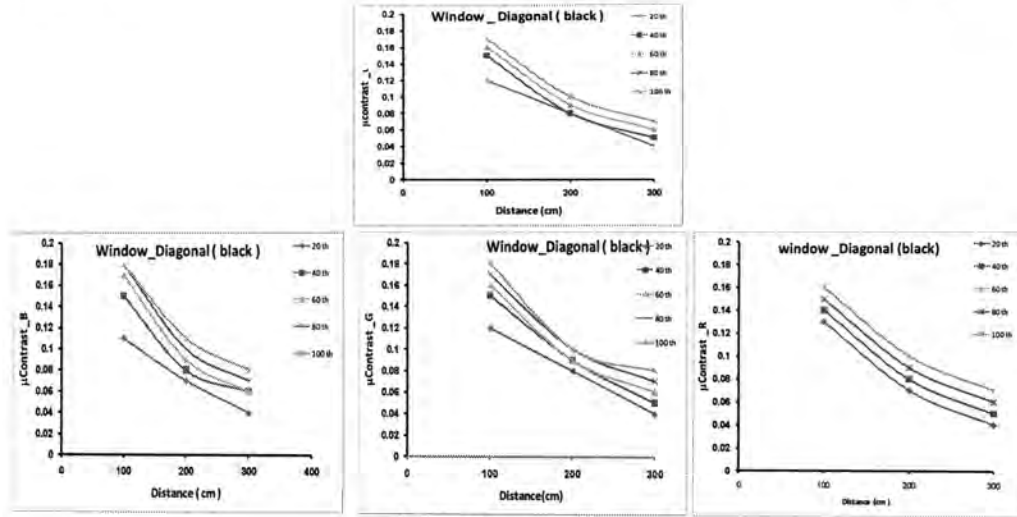


النص المكتوب باللون الأزرق

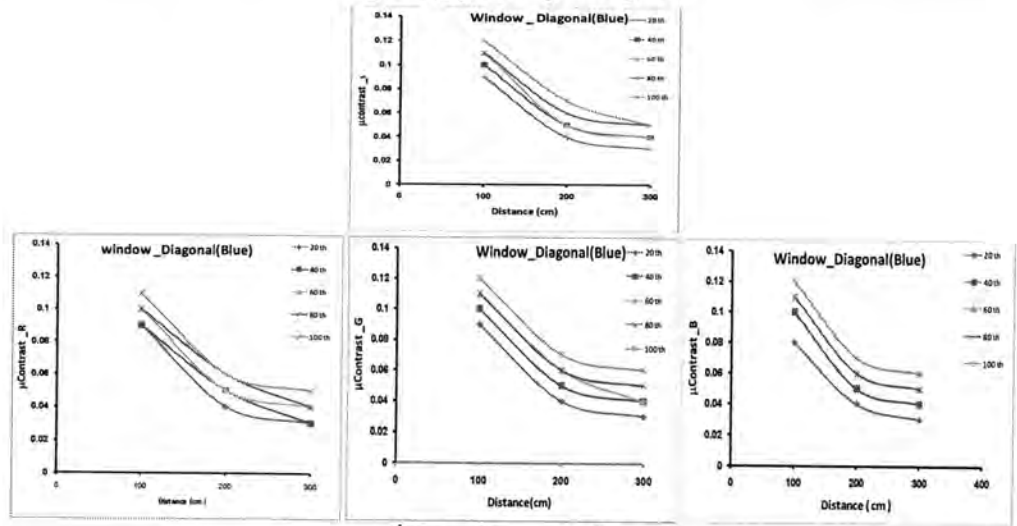


النص المكتوب باللون الأحمر

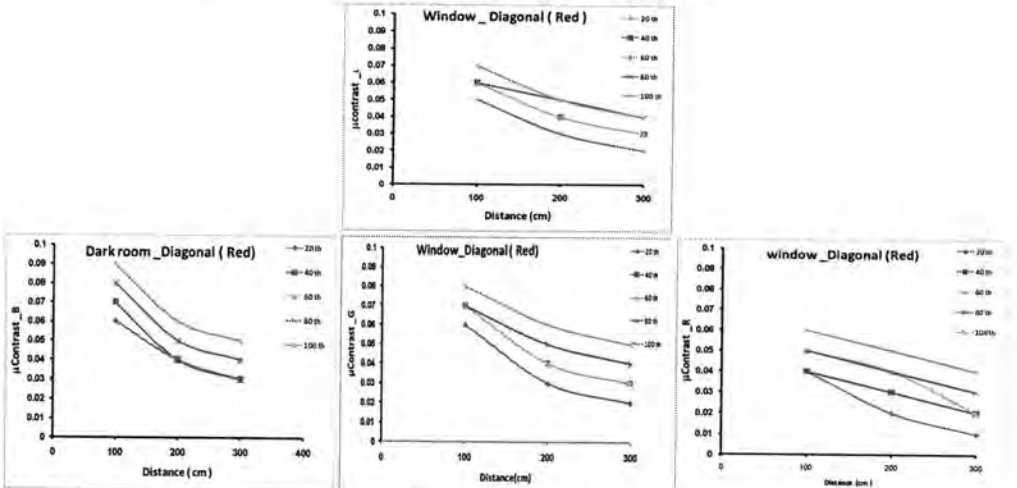
شكل - 9a : التباين القطري الرئيسي لقاعة الدرس المضاءة يمينا (إضاءة غير منتظمة) للحزم اللونية
ومركبة الإضاءة RGB,L



النص المكتوب باللون الأسود



النص المكتوب باللون الأزرق

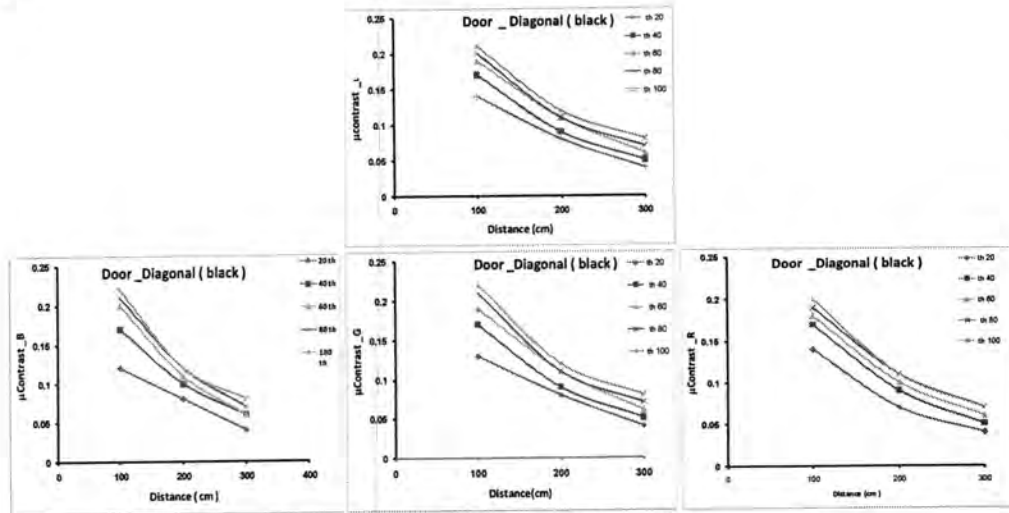


النص المكتوب باللون الأحمر

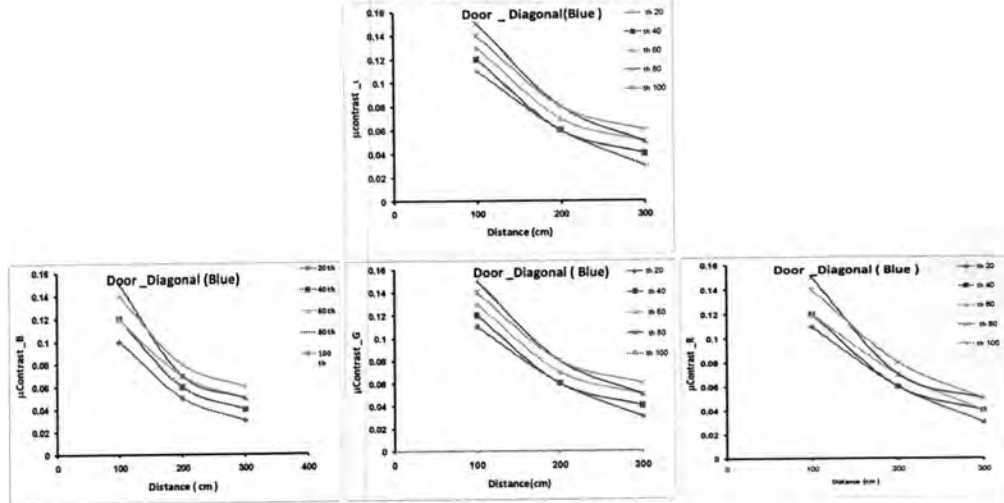
شكل - 9a : التباين القطري الرئيسي لقاعة الدرس المضاءة يمينا (إضاءة غير منتظمة) للحزم اللونية ومركبة الإضاءة RGB,L

تأثير الإضاءة غير المنتظمة على وضوح النصوص باختلاف المسافة

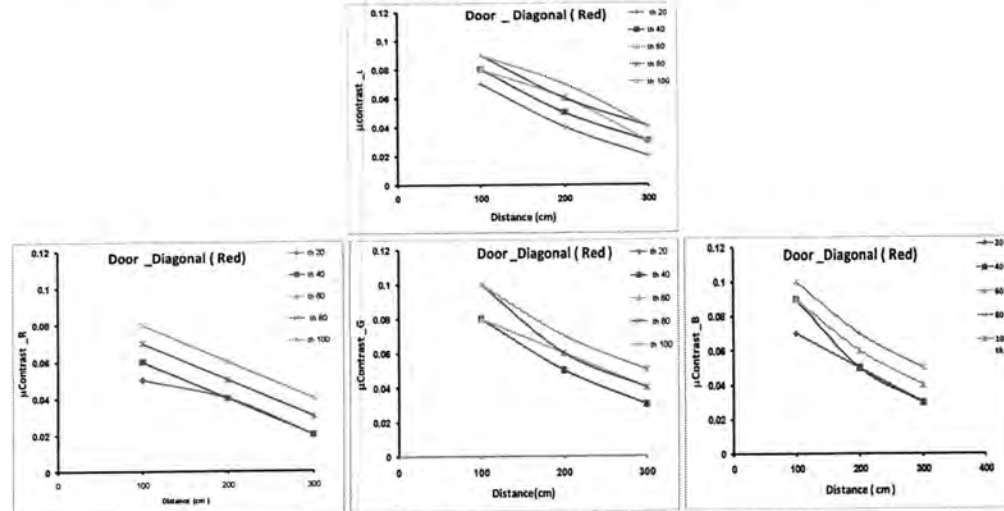
علي ورشاو عدي



النص المكتوب باللون الأسود



النص المكتوب باللون الأزرق



النص المكتوب باللون الأحمر

الشكل - 9b : التباين القطري الرئيسي لقاعة الدرس المضاءة يسارا (إضاءة غير منتظمة) للحزم اللونية RGB,L ومركبة الإضاءة

المصادر

1. Turner ,Jaret. , " An Introduction To Light, Lighting and Light Use ", B.T Bats Ford Ltd London , (1994).
2. Kurtich ,John and Eakin , Garrel ., " Interior Architecture ", Van Nostrand Reinhold , New York ,(1993).
3. حماد . رزق نمر شعبان . الاضاءة النهارية والصناعية في العمارة . الاردن ، عمان : المركز العربي للخدمات الطلابية . 1996 .
4. Jonhson R .P ., "Contrast Based on Edge Detection " , pattern Recongition , 23 , (3/2) (1990).
5. Scharff L. & Ahumada A., "Contrast Measure For Predicting text readability " Airspace operation systems (AOS) project of Nasa's Airspace systems program (2003) .
6. Thompson W. and Shirly P. and Ferwerda J., " A spatial Post Processing algorithm for Images of Night Scenes " , Anthers Address : University . of Utah and Cornell University (2003) .
7. Aditi Majumder , Sandy Irani , "contrast Enhancement of Image Using Human Contrast Sensitivity " , Computer Science Department , University of California , Irvine 2005 .
8. Yehya N. , Norio A ., "Contrast Enhancement Technique of dark Blurred Image " , International Journal of Computer Science and Network Security , 6 (2A) February (2006) .
9. عبد الله . موفق عبد الغني .قيم الإضاءة الطبيعية والعمارة في المناطق الحارة الجافة. هندسة معماري . جامعة بغداد . (1996).
10. Julian , Warner G .” Lighting : an Urgent case for a major Research Effect in Architectural Science “ Building and Environment . 22 (3) (1987).
11. Antoshchuk S . , ” The automatized systems with the visual information processing design” International Conference ,Issue, 24-28 Feb.: 268 (2004) .

دراسة الخصائص الاحصائية لكاميرا الهاتف النقال نوع (Nokia7610) تحت شروط إضاءة مختلفة

هاله نصير كاظم وعلي عبد داود الزكي و كاظم جواد الشجيري
الجامعة المستنصرية /كلية العلوم/قسم الفيزياء

ABSTRACT

In the latest decades increase importance of digital image capturing, and increase the communicate the information news especially after large development in computer technology. So, we have been developing a digital camera sensor to get high digital images at low costs. While the different digital camera types are so varying in image capturing quality. This gives different qualities for different conditions.

In this study, we analyzed the captured images by cell phone Nokia 7610 camera. Where we captured several images under different lightness conditions, with different resolutions. Then we study the statistical RGB distribution for the homogeneous regions. Then compute the statistical properties for RGB distributions by computing the mean and standard deviation of these distributions.

The results shown that the captured image under sunlight give high RGB-means comparing with other lightness conditions, also give low RGB standard deviation for all homogeneous regions. Also, we find the yellow, Green, and Blue targets have only Red histograms for all lightness intensities.

الخلاصة

ازدادت أهمية التصوير الرقمي خلال العقود الأخيرة، وتزايدت الحاجة إلى توفير المعلومات الخيرية بشكل كبير و خصوصاً مع هذا التطور الهائل لأنظمة الحاسوب. لذلك تم تطوير متحسسات التصوير الرقمية لغرض الحصول على صورة عالية الجودة، وبتكلفة قليلة. إلا أن كفاءات الأنواع المختلفة للكاميرات الرقمية متباينة، وقد تختلف باختلاف ظروف التصوير.

تم في هذه الدراسة، دراسة وتحليل الصور الملتقطة بواسطة كاميرا الهاتف النقال نوع (Nokia7610). حيث تم التقاط مجموعة من الصور ضمن شروط إضاءة مختلفة، وبوضوحات كاميرا مختلفة. وتمت دراسة التوزيع الاحصائي لمناطق متجانسة من الصور، وشملت هذه الخصائص حساب المعدل μ ، الانحراف المعياري σ ، والمخطط التكراري. ولقد لوحظ أن الصور التي تم التقاطها بضوء الشمس تمتلك معدل أعلى من الصور التي تم التقاطها بالاضاءات الأخرى، وانحراف معياري أقل، وعند تحليل المناطق اللونية المتجانسة في الصورة، نجد أن كل من المنطقة الصفراء والخضراء والزرقاء في الصورة تمتلك مخطط تكراري فقط عند الحزمة الحمراء، لجميع شدة الاضاءة المستخدمة.

المقدمة

طورت الكاميرا الرقمية بشكل كبير خلال العقود الأخيرة، وبدأت أنظمة التصوير الرقمية تحل بدلاً من التقنيات القديمة في مختلف المجالات، وذلك لمرونته وإمكاناته العالية خصوصاً في ثبات جودة الصورة بغض النظر عن طول فترة التخزين وإمكانية المعالجة بالحاسوب. ومن الأمثلة المهمة لذلك، استخدامها في مجال الطب، وإنتاج الأفلام والفيديو، وفي التصوير الفوتوغرافي، والتحسس عن بعد، والمراقبة الأمنية، والسيطرة العملية وأنظمة الإنسان الآلي. إن هذه المجالات وغيرها كثيرة، تقوم بإنتاج كميات هائلة من بيانات الصور الرقمية يومياً بحيث أصبح من الصعب إحصائها (1).

غالباً ما يعتمد عمل الكاميرا الرقمية بالدرجة الأولى على المتحسسات الالكترونية، والتي تتحسس شدة الضوء واللون المستلم لتكوين الصورة. إن الفكرة الأساسية لعمل المتحسس هي تحويل الطاقة التي يتحسسها إلى إشارة كهربائية بواسطة الدائرة الالكترونية لمنظومة التصوير والتي عادة تحتوي على متحسس يتأثر بدرجة الإضاءة ويمكن بعد ذلك تحويل الإشارة التماثلية إلى إشارة رقمية.

هاله وعلي و كاظم

فالمتحسسات التي تحول طاقة الإضاءة الى صورة رقمية تكون على انواع ومساحات مختلفة سيتم ايضاحها لاحقا، وبالتالي تتباين كفاءة هذه الحساسات (2). لذلك توجهنا الى تحليل جودة الصور الملتقطة بواسطة كاميرا الهاتف النقال نوع (Nokia7610) والتي تم التقاطها تحت شروط إضاءة مختلفة واستنتاج خصائص هذه الكاميرا.

دراسة كفاءة المنظومات البصرية تعتمد بشكل اساسي على دراسة وضوحية التمييز المكاني وتمييز الشدة واللون، وهناك العديد من الدراسات السابقة في هذا المجال وهي كما يلي:

- عام 1996 أجرى الباحث Eli peli دراسة حول تأثير الإضاءة والتردد المكاني على تحسس التباين ما فوق العتبة باستعمال أنماط اختبارية مختلفة الإضاءة والتردد المكاني لغرض مقارنة التباين، حيث ان معدل الإضاءة للأنماط الاختيارية كان ضمن المدى $(0.5 - 5) \text{ cd/m}^2$ وذو تردد مكاني $(1 - 16) \text{ cycles / degree}$ ، لكل مجموعة من التجارب كان التردد المكاني لنمط الاختياري يتغير بشكل عشوائي (ثلاثة تكرارات عند كل تردد لكل مجموعة) بينما تكون الإضاءة ثابتة (3).
- اقترح العالم William B. Thompos عام 2003 خوارزمية لتحسين الصور للمناظر الليلية وذلك من خلال تقنية جعل الصورة المأخوذة في النهار وكأنها صور ليلية من خلال تقليل التباين والسطوع لكل الصورة وإضافة تشوه للصورة وإعطاء الصورة الليلية التي تكون ذات غشاوة عالية Blur، وذات خسارة في الحدة البصرية ومقدار التشوه الحاصل فيها (4).
- الباحثان Martin Cadik , Pavel Slavik عام 2004 قدما دراسة لتقييم جودة الصورة بالاعتماد على الخواص البصرية للتحسس البشري حيث استخدموا في هذه الدراسة صور مضغوطة بشكل منتظم وصور مضغوطة بشكل غير منتظم ثم تمت مناقشة أداء النموذجين بالاعتماد على أوجه التشابه والاختلاف (5).
- الباحث Mukul V-Shirvaikar عام 2004 وضع مقياس إحصائي مثالي لتقييم جودة الصورة في المنظومات البصرية المستخدمة في الفحص الصناعي والتصوير الفوتوغرافي والمجهر الالكتروني وهذا المقياس الإحصائي يعتمد على الانحراف المعياري Standard Deviation والمعدل Mean، والانتروبي Entropy، والنسبة المئوية لعنصر الصورة في مدى المستويات الرمادية Percentage of Pixels in the Gray Level، والقيمة المطلقة للعزم المركزي (ACM) Absolute Central Moment (6).

2- الكاميرا الرقمية

ان التطور الهائل في تقنية الحاسوب، والتقدم الكبير في مجال التسجيل الرقمي للصور ساعد على ظهور الاجهزة التي تسمح بالحصول على الصورة بدون معالجة كيميائية، وهي الكاميرات الرقمية الالكترونية. عند استعمال الكاميرات العادية (غير الرقمية) فإن الصورة في هذه الحالة ناتجة من تحسس الإشارة الضوئية بواسطة متحسسات كيميائية (الفيلم) الذي يتكون من بلورات هاليدات الفضة. بينما الكاميرات الرقمية تحوي غالبا بدلا من الفيلم على متحسسات ضوئية، حيث تتركز الصورة على بلورة شبه موصلة حساسة للضوء تسمى جهاز الشحن المزدوج charge coupled device ويرمز لها اختصارا CCD. او هناك تقنية اخرى للكاميرات الرقمية وهي complementary metal oxide semiconductor ويرمز لها CMOS وفي كلتا الحالتين فإن CCD, CMOS تقومان بتحويل الفوتونات الى إلكترونات، (7,8). وان المتحسسات التي تحول طاقة الإضاءة الى صورة رقمية تكون على ثلاثة أنواع هي كالآتي (2) :-

أ- المتحسس الوحيد

يعرف هذا النوع بالمتحسس Photo Diode الذي يتكون من مادة السيليكون التي يتناسب الجهد الخارج منها مع الضوء الساقط عليها، ويلاحظ أن استخدام مرشح أمام المتحسس يحسن انتقائيته Selectivity و للحصول على صورة ذات بعدين باستخدام متحسس وحيد فلا بد من تحريكه في اتجاهين وذلك على المشهد المراد تصويره.

ب- المتحسسات على شكل خط

للحصول على صورة يتم في هذه الطريقة تجميع مجموعة من المتحسسات على شكل خط مستقيم و يمكن الحصول على عدد من عناصر الصورة المراد الحصول عليها في أحد الإحداثيات وليكن x ، بعد ذلك يتم تحريك هذه المجموعة في اتجاه عمودي للحصول على باقي عناصر الصورة في الإحداثي y وتستخدم هذه الطريقة عادة في التصوير بالطائرات.

ج- المتحسسات على شكل مصفوفة

للحصول على صورة يتم في هذه الطريقة توجيه الأشعة المنعكسة من الجسم المراد تصويره عن طريق العدسة الى مجموعة من المتحسسات المرتبة على شكل مصفوفة $N \times M$ من العناصر المتحسسة حيث أن خروج الإشارة الكهربائية من كل عنصر حساس يمثل نقطة من نقاط الصورة. وتتكون الكاميرا الرقمية من الأجزاء التالية (9,10) :-

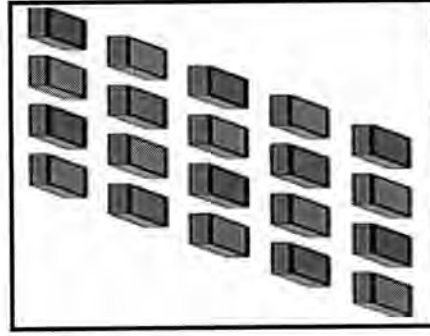
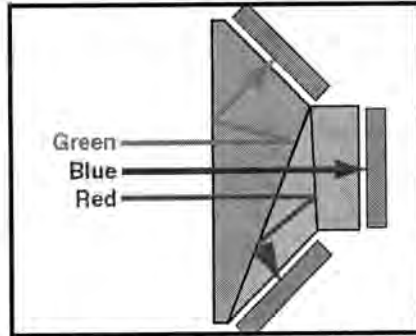
1. وحدة الكاميرا التي تحتوي على شريحة CCD، والنظام البصري المكون من العدسات المستخدمة للتقريب والتباعد والتبوير والتحكم بفتحة العدسة.
2. شاشة العرض (Liquid Crystal Display) واختصارا يرمز لها LCD .
3. الوحدة التي تحول الإشارة التماثلية الى إشارة رقمية Analog to Digital Signal Converter(ADC)

3- تقنية النقاط الكاميرا الرقمية للألوان

تعتبر المتحسسات الضوئية في الكاميرا الرقمية غير مدركة للألوان ولا تميزها وذلك لان فكرة عمل هذه المتحسسات هو قياس شدة الضوء وتحويله الى شحنة كهربائية ولكي يتم التقاط الصورة بكامل ألوانها فلا بد من استخدام مرشحات للضوء بحيث يكون لكل لون من الألوان الأساسية مرشح خاص به فمثل المرشح الأحمر هو عبارة عن شريحة زجاجية ذات لون احمر تسمح بدخول اللون الأحمر وتمنع دخول باقي الألوان ونفس الشيء بالنسبة للون الأزرق والأخضر فبمجرد التقاط الكاميرا الصورة لأي مشهد فانه يتم تحليل ألوان هذا المشهد الى الألوان الأساسية الثلاث (الأخضر، الأزرق، الأحمر) ومن ثم يتم تجميعها للحصول على المشهد بكافة ألوانه. هنالك طرق مختلفة لالتقاط الألوان الأساسية في الكاميرا الرقمية، فالكاميرات الرقمية عالية الجودة تستخدم ثلاثة وحدات من الرقائق CCD منفصلة ومثبت فوق كل رقاقة CCD مرشح لوني حتى تتخصص كل رقاقة برصد اللون الأساسي الخاص بها، عندما يتم تركيز الضوء المنعكس من الجسم الى داخل الكاميرا بواسطة عدستها فان الضوء يتم تجزئته باستخدام مجزئ ليسقط على المرشح اللوني ثم الى CCD، يتم تجميع الإشارة الصادرة من الثلاث رقائق CCD بواسطة المعالج لتكوين الصورة الملونة بالكامل كما في الشكل (1) من مميزات هذه الطريقة ان الكاميرات تلتقط كل لون من الألوان الثلاثة الأساسية على نفس الموضع المخصص لعنصر الصورة على CCD، والطريقة الأخرى في تجزئة الألوان هي تدوير قرص يحتوي على المرشحات الثلاثة امام رقاقة CCD واحدة، ويقوم CCD بتسجيل ثلاثة لقطات منفصلة في عملية سريعة هذه العملية تزودنا أيضا بكل لون في الموضع المخصص

هاله وعلي و كاظم

لعنصر الصورة. ولأن اللقطات الثلاث لا تؤخذ في نفس الزمن فإنه يتوجب على الكاميرا والمشهد المراد تصويره البقاء ساكنين للحظة حتى يتم اخذ القراءات الثلاث مما يجعل هذه الطريقة غير عملية ولا بد من تثبيت الكاميرا على حامل وان يكون المشهد المراد تصويره ثابت. اما الطريقة العملية والمستخدم في التقاط الألوان الأساسية تتمثل في تثبيت مرشح يسمى بمصفوفة مرشح الألوان Color Filtering Array على رقاقة CCD وأكثر أنواع مصفوفات المرشحات استخداما نموذج مرشح باير Bayer Filter pattern كما في الشكل (2) ويتكون من عمودين متبادلين احدهما مكون من مرشح للون الأخضر والأزرق والعمود الآخر مرشح للون الأخضر والأحمر ونلاحظ وجود الكثير من العناصر الخضراء مقارنة بالأزرق والأحمر وذلك لان العين البشرية لا تكون حساسيتها متساوية بالنسبة للألوان الثلاثة الأساسية، من محاسن هذه الطريقة إنها تحتاج لرقاقة CCD واحدة ويتم التقاط الألوان RGB في نفس اللحظة (11,12).



شكل 1- رقائق CCD مع مرشح (11)

شكل 2- نموذج مرشح باير

(Bayer filter) (11)

4- وضوحية الصورة

تعرف الوضوحية بأنها قدرة منظومة التصوير على تسجيل التفاصيل الدقيقة عن طريق التمييز بين إشارتين متقاربتين مكانيا او طيفيا او متقاربتين في الشدة او متقاربة زمنيا، وتصف التفاصيل التي تحملها الصورة الرقمية، فكلما كانت الوضوحية عالية كانت تفاصيل الصورة اكثر. يمكن التعبير عن وضوحية الصورة الرقمية بعدة طرق مختلفة هي (13) :

أ. الوضوحية الطيفية Spectral Resolution

تشير الى عدد الحزم الطيفية من الطيف الكهرومغناطيسي التي يمكن للمتحمس ان يتحسسها فمثلا صور الرسم الحراري (TM) Thematic Mapper الذي يعتمد على سبع حزم طيفية في عملية التصوير، تكون كل حزمة تحمل كما من المعلومات فكلما زاد عدد الحزم زادت المعلومات المحتواة في الصور متعددة الطيف وهذه الصور تمتلك وضوحية طيفية عالي (14,15).

ب. الوضوحية الإشعاعية Radiometric Resolution

تعرف بأنها حساسية الكاشف (المتحمس) للتمييز بين الإشارة المسجلة عن الإشعاع المنعكس او المنبعث من الجسم . وبمعنى اخر فان الحساسية الإشعاعية تشير الى عدد المستويات الرقمية المستعملة لتمثيل البيانات التي تمثل الإشارة المتحمسة ويعبر عنها بعدد البتات (الارقام الثنائية) المطلوبة لخرن اقصى مستوى فمثلا بيانات صور الراسم الحراري TM تمثل 256 مستويا او ما يعادل ($L=2^8$) ، الوضوحية الإشعاعية العالية تعني استخدام عدد مستويات رمادية عالية لتمثيل الشدة في عناصر الصورة ، وزيادة عدد المستويات تعني زيادة التفاصيل

المحتواة في الصورة ، اما من الناحية العملية تحدد الوضوحية الاشعاعية بمستوى الضوضاء بدلا من ان تحدد بعدد البتات (15,16) .

ج- الوضوحية المكانية Spatial Resolution

تعرف الوضوحية المكانية لمنظومات التصوير من خلال معايير مختلفة فهي تعتبر الخواص الهندسية لمنظومة التصوير في مجال الرؤية للجسم او المشهد والمتحسس الذي يسجل المشهد ويمكن ان نعرف التحليلية بانها ابعاد مساقط المشهد على منظومة المتحسس وذلك خلال زمن النقاط الصورة او التعرض للفلم وهذه التحليلية يمكن ان تقاس باحدى الطريقتين بتحديد الزاوية او المسافة على الارض للمشهد المصور ، ابعاد المساقط للمشهد تعتمد على الارتفاع وعلى زاوية الرؤية للكاميرا ، او هي قابلية المنظومة على التمييز بين الأجسام المحددة مشابه لصورة فحص البصر او مخططات الفحص لأجهزة العرض التلفزيوني او بتعبير اخر فان الوضوحية المكانية تشير الى اصغر انفصال زاوي او خطي بين جسمين مختلفين يمكن ان يحللها المتحسس ، وتعتمد الوضوحية المكانية على خواص المنظومة البصرية وليس على وضوحية عنصر الصورة بوحدات Pixels Per Inch (PPI) حيث تتأثر الوضوحية المكانية بعدة عوامل قد تسبب الغواشية في الصورة مثل التبئير غير الجيدة . وعوامل الاستطارة في الهواء بين الجسم المراد تصويره والكاميرا او حركة الكاميرا او حركة الهدف وحيود الضوء . ان الوضوحية المكانية العالية للصورة تشير الى ان عناصر الصورة عددها كبير وإحجامها صغيرة والتفاصيل الدقيقة ممكن ان تشاهد في هذه الصورة بوضوح بينما الوضوحية المكانية الواطئة تشير الى ان عناصر الصورة قليلة وحجم البكسل كبيرة . ان التحليلية المكانية العالية تعطي اعظم تحليلية لمنظومة التصوير (16,17,2)

د- الوضوحية الزمانية Temporal Resolution

تشير الوضوحية الزمانية في منظومة التصوير الى عدد مرات تسجيل الصور في منطقة معينة، فمثلا يمكن للقمر الصناعي (CARTOSAT - 1) ان يلتقط صور لمنطقة من الكرة الارضية نفسها كل 5 ايام، بينما يلتقط القمر الصناعي (LISSIII) صورا لهذه المنطقة كل 24 يوم. ان للوضوحية الزمانية لمتحسس القمر الصناعي فائدة كبيرة في كشف التغيرات. ان تحليل الصور متعددة التواريخ توفر معلومات حول كيفية تغير المتغيرات بمرور الزمن، اما التصوير التلفزيوني فانه يعطي بحدود 30 صورة بالثانية مما يولد المشاهد المتحركة (18).

5- تعطي خصائص الصورة الاحصائية وفقا للمقاييس التالية:-

أ- دالة احتمالية التوزيع Probability Density Function

دالة احتمالية التوزيع يعبر عنها بالصيغة $P(f)$ وهي تمثل احتمالية توزيع الشدة f في الصورة حيث ان $0 \leq f(x,y) \leq L - 1$ وان الاحتمالية لظهور الشدات تكون محدودة بالعلاقة $0 \leq P(f) \leq 1$ ، حيث ان مجموع الاحتماليات الكلي يساوي واحد ، ورسم العلاقة بين توزيع الاحتمالية $P(f)$ وقيم $f(x,y)$ يدعى بالمخطط التكراري لعناصر الشدة في الصورة وتكون قيم الشدة محصورة ضمن المدى (0 - 255) ، حيث ان الاحتمالية مساوية لتكرار العنصر $oc(f)$ مقسوما على عدد عناصر الصورة . علما بان الاحتمالية مساوية لتكرار العنصر $oc(f)$ مقسوما على عدد عناصر الصورة. (19,20,→)

ب- المعدل Mean

معدل الإضاءة في الصورة يعرف بأنه معدل الإضاءة لعناصر هذه الصورة ويحسب المعدل μ من العلاقة (21, 6) :-

$$\mu = \frac{1}{MN} \sum_{x=1}^M \sum_{y=1}^N f(x, y) \quad \dots \dots \dots (1)$$

حيث ان N,M طول وعرض الصورة على التوالي وحاصل ضربهما يساوي عدد عناصر الصورة

ج- الانحراف المعياري Standard Deviation

يعرف بأنه مقدار انحراف القيم للإشارة عن المعدل ويحسب الانحراف المعياري σ من العلاقة الآتية (20, 6) :

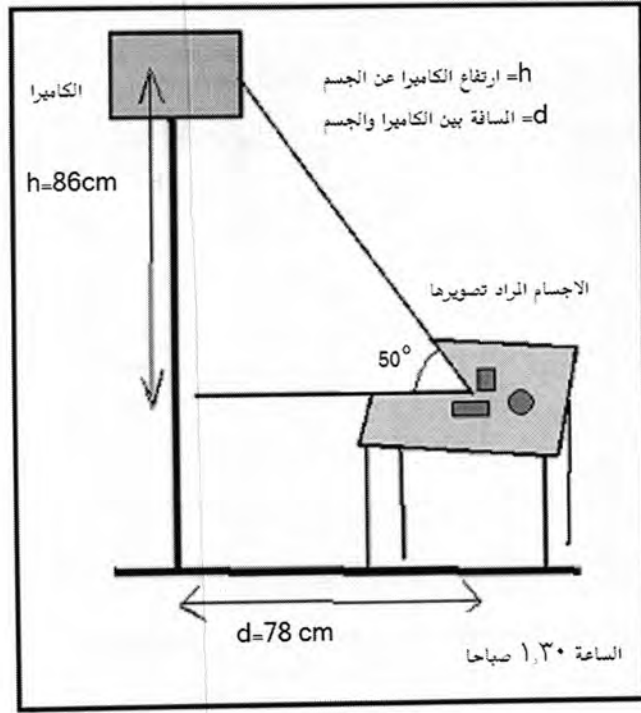
$$\sigma = \sqrt{\frac{1}{MN} \sum_{x=1}^M \sum_{y=1}^N (f(x, y) - \mu)^2} \quad \dots \dots \dots (2)$$

6- منظومة التصوير

اعتمدت الدراسة على مجموعة من الصور تم التقاطها بواسطة الكاميرا الرقمية للهاتف النقال نوع (nokia7610) , وتم استخدام ثلاث جودات مختلفة موجودة ضمن نظام الهاتف النقال وهي :

- 1- High quality with image resolution = 1152*864
- 2- Normal quality with image resolution = 1152*864
- 3-Basic quality with image resolution = 640*480

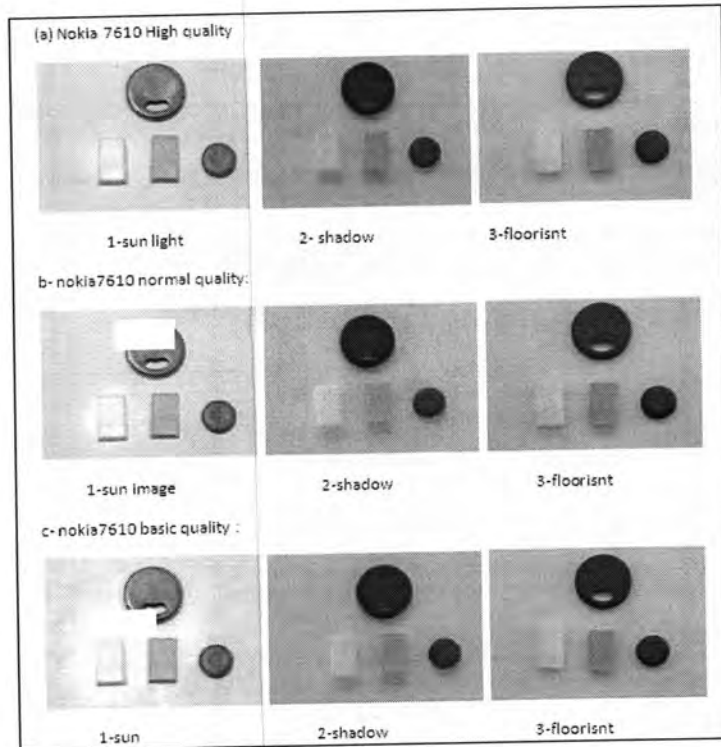
واعتمدت الدراسة على ظروف الإضاءة المختلفة حيث تم تصوير أربعة اجسام مختلفة الألوان بثلاث حالات إضاءة وهي ضوء الشمس المباشر, ظل الشمس او ضوء الشمس غير المباشر, وضوء الفلورسنت داخل الغرفة. تتم عملية التسجيل على شكل صور رقمية تسجل في الحاسوب بعد عملية نقل الصور الى الحاسبة و تخزينها بصيغة Bit map يتم استخلاص خصائصها العامة من المعدل, والانحراف المعياري, والمخطط التكراري باستخدام خوارزميات طبقت على الحاسوب بلغة Visual Basic. ثم بعد ذلك يتم استقطاع عدد معين من البلوكات من كل جسم داخل الصورة واستخلاص خصائصه لغرض دراستها على حدة. اي تم دراسة خصائص كل منطقة لونية من الصورة و تم مقارنة النتائج للحالات المختلفة. والشكل (3) يمثل رسم توضيحي لمنظومة التصوير المستخدمة.



شكل 3: المخطط التوضيحي لعملية التصوير

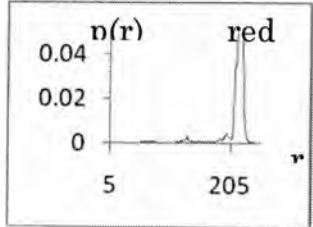
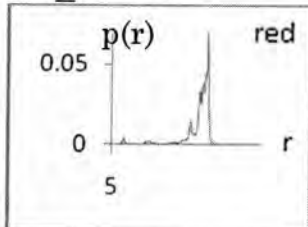
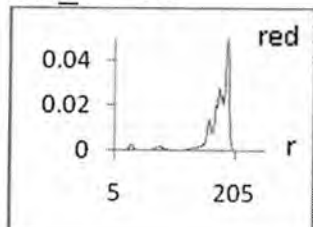
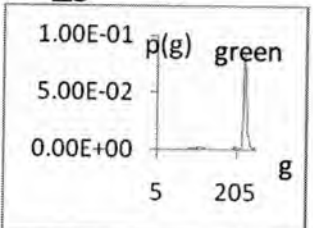
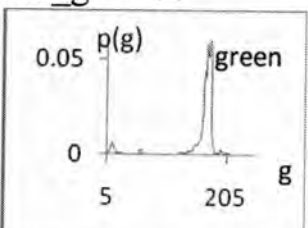
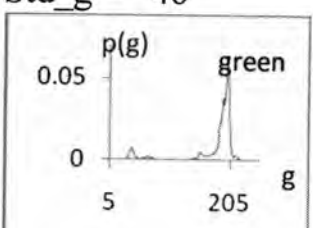
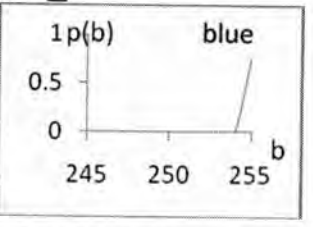
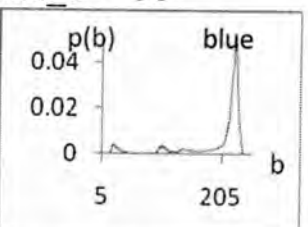
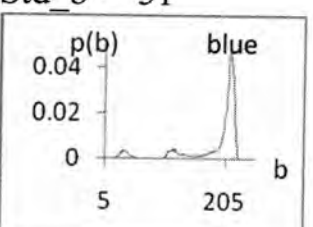
7- النتائج والاستنتاجات

الشكل (4) يمثل الصور الملتقطة بالاضاءات الثلاث ولجودات الهاتف النقال الثلاثة المذكورة اعلاه. حيث يلاحظ ان الصور الملتقطة بالجودة العالية تحتوي على اقل تباين للاجسام فيها ويقل التباين ووضوح الالوان كلما قلت الجودة.

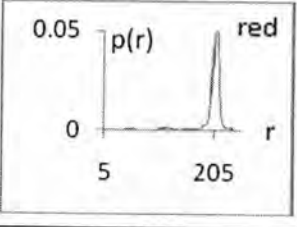
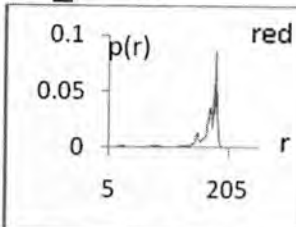
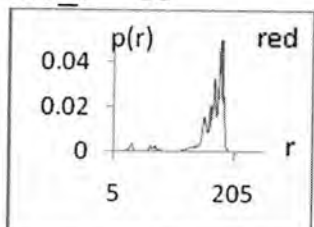


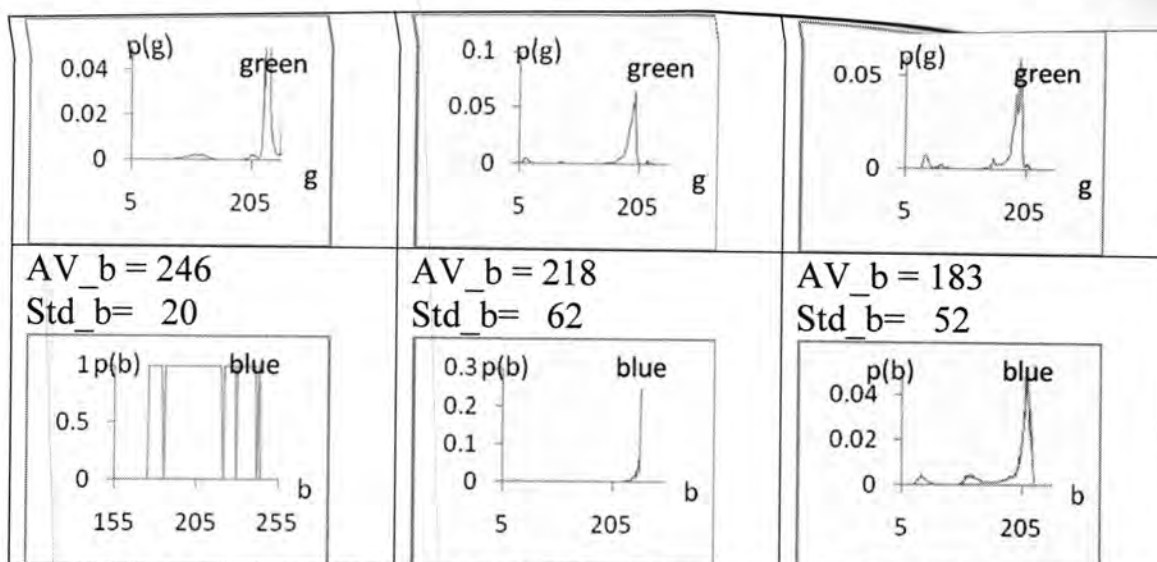
شكل 4: الصور للحالات المختلفة التي تمت الدراسة عليها.

هاله وعلي و كاظم

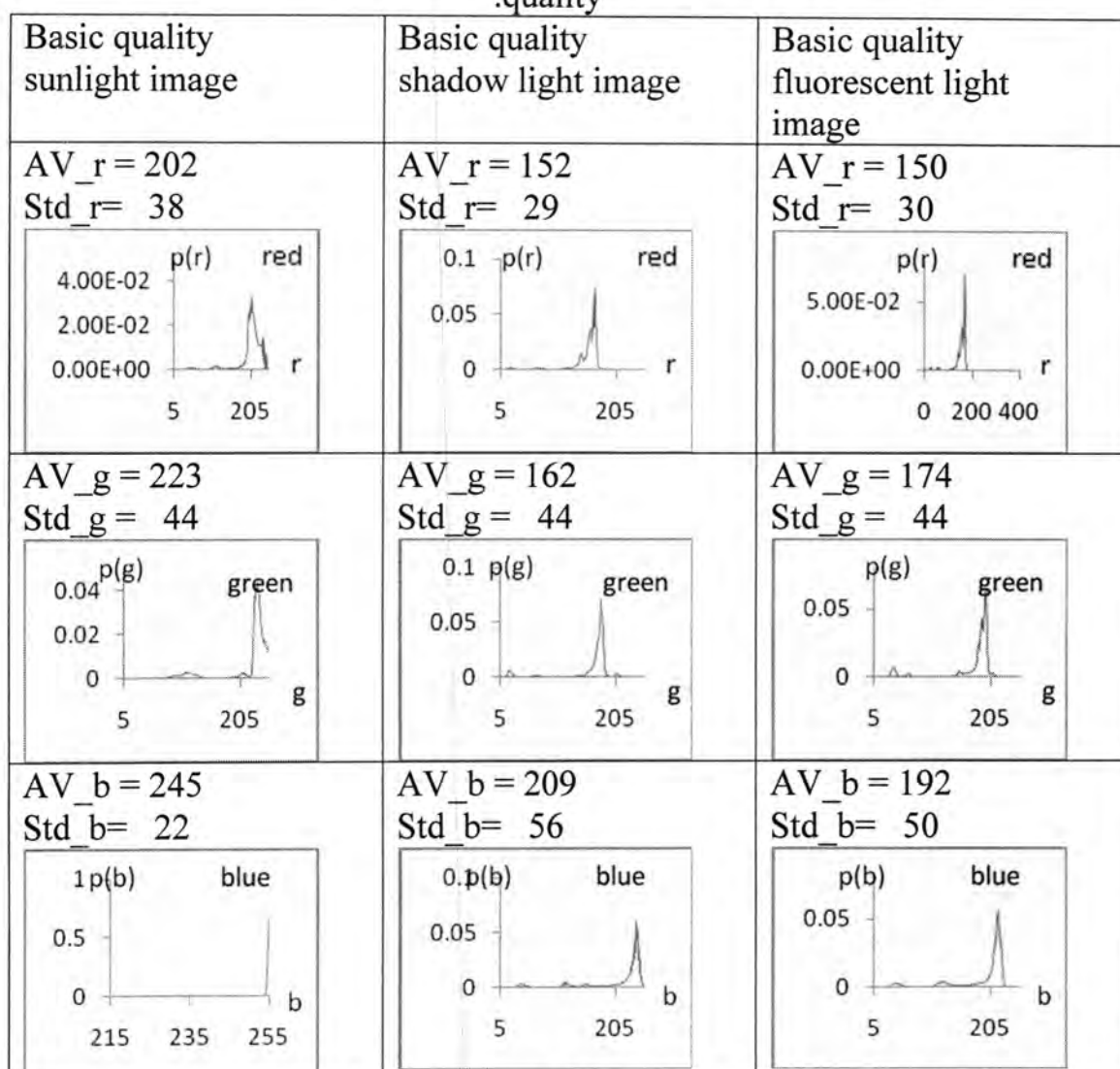
<p>Nokia7610 high q sun light image</p> <p>AV_r = 208 Std_r = 34</p> 	<p>Nokia7610 high q shadow light image</p> <p>AV_r = 149 Std_r = 28</p> 	<p>Nokia7610 high q floorisnt light image</p> <p>AV_r = 172 Std_r = 33</p> 
<p>AV_g = 211 Std_g = 42</p> 	<p>AV_g = 157 Std_g = 44</p> 	<p>AV_g = 177 Std_g = 46</p> 
<p>AV_b = 240 Std_b = 31</p> 	<p>AV_b = 197 Std_b = 56</p> 	<p>AV_b = 185 Std_b = 51</p> 

شكل 5: المخططات التكرارية العامة (لاحتمالية العناصر) للحزم الثلاثة للصور الملتقطة باضائيات مختلفة: ضوء الشمس , ظل الشمس , ضوء الفلورسنت لوضوحية الهاتف النقال: high quality.

<p>Normal quality sun light image</p> <p>AV_r = 197 Std_r = 34</p> 	<p>Normal quality shadow light image</p> <p>AV_r = 167 Std_r = 31</p> 	<p>Normal quality fluorescent light image</p> <p>AV_r = 164 Std_r = 33</p> 
<p>AV_g = 216 Std_g = 42</p>	<p>AV_g = 175 Std_g = 49</p>	<p>AV_g = 171 Std_g = 46</p>



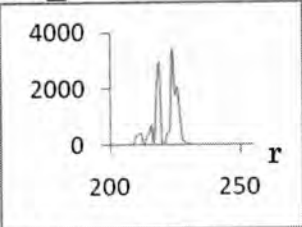
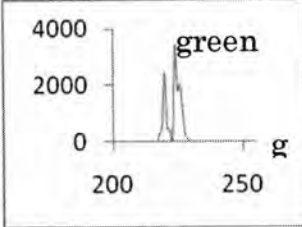
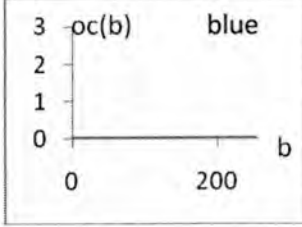
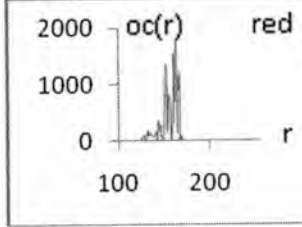
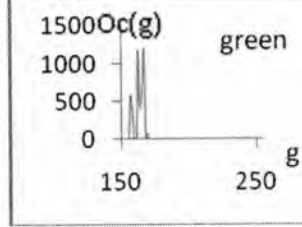
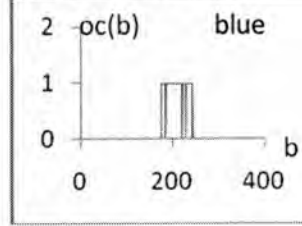
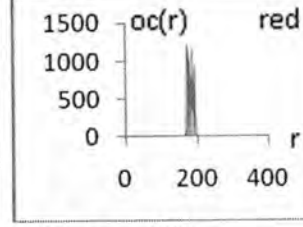
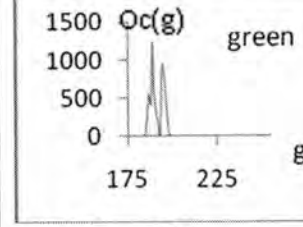
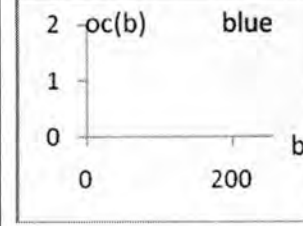
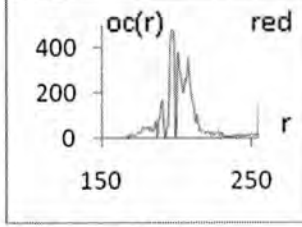
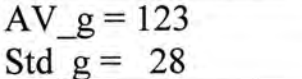
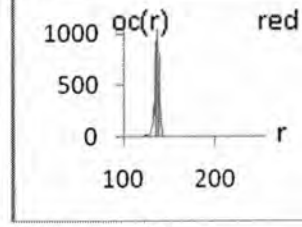
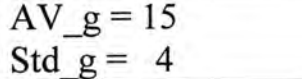
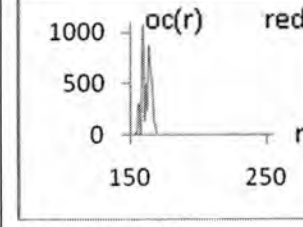
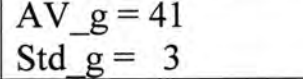
شكل-6: المخططات التكرارية العامة (لاحتمالية العناصر) للحزم الثلاثة للصور الملتقطة باضائيات مختلفة: ضوء الشمس، ظل الشمس، ضوء الفلورسنت لوضوحية الهاتف النقال: normal quality.

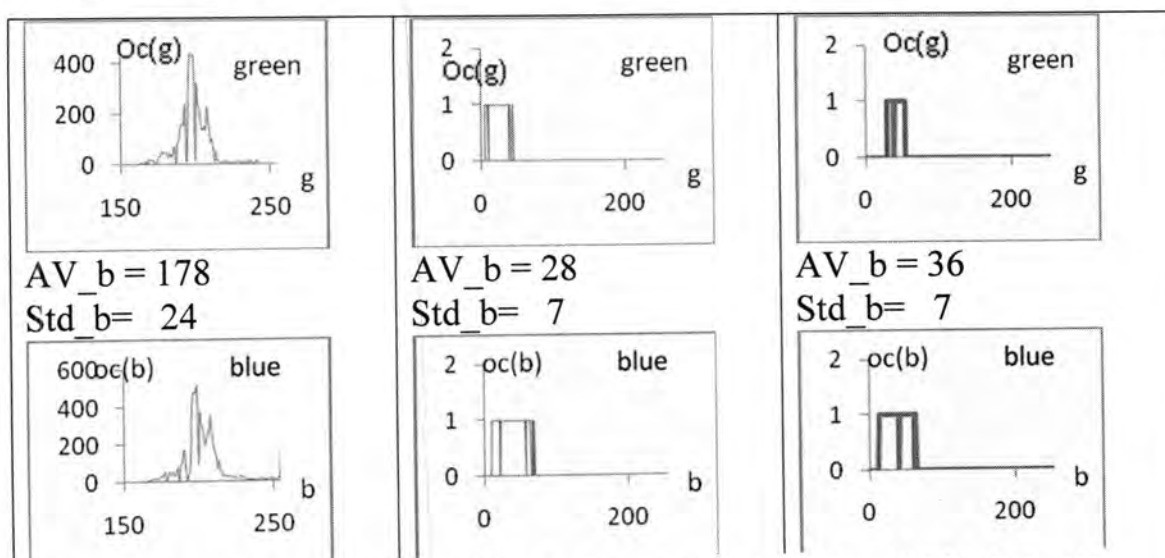


شكل-7: المخططات التكرارية العامة (لاحتمالية العناصر) للحزم الثلاثة للصور الملتقطة باضائيات مختلفة: ضوء الشمس، ظل الشمس، ضوء الفلورسنت لوضوحية الهاتف النقال: basic quality. نلاحظ في الشكل (5)(6)(7) لجميع وضوحيات الكاميرا ان الصور الملتقطة بضوء الشمس تسجل اعلى معدل واقل انحراف معياري من الازضاءات الاخرى، اما المخطط التكراري لها فإنه يسجل

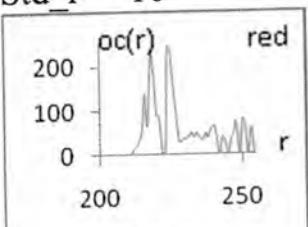
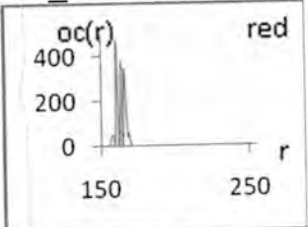
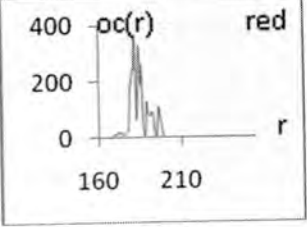
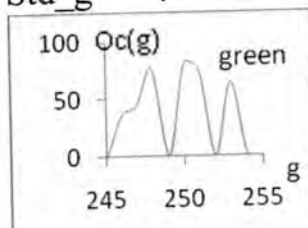
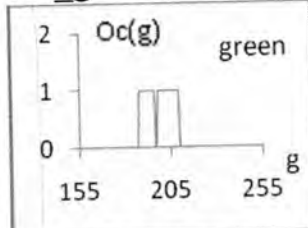
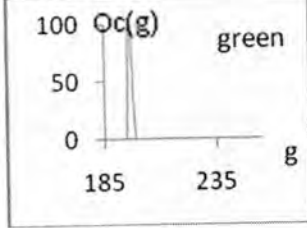
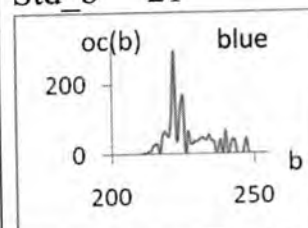
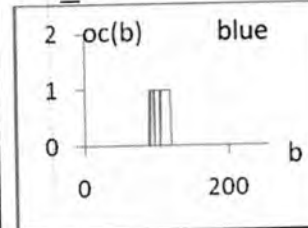
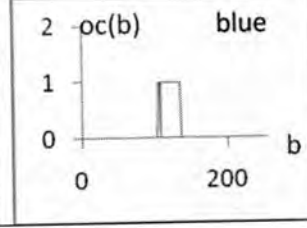
هاله وعلي و كاظم

اعلى منحني عند الحزمة الزرقاء, اعلى من الحزمتين الحمراء والخضراء. الصور الملتقطة بالاضاءات الاخرى يكون مخططها التكراري متقارب للحزم الثلاثة.

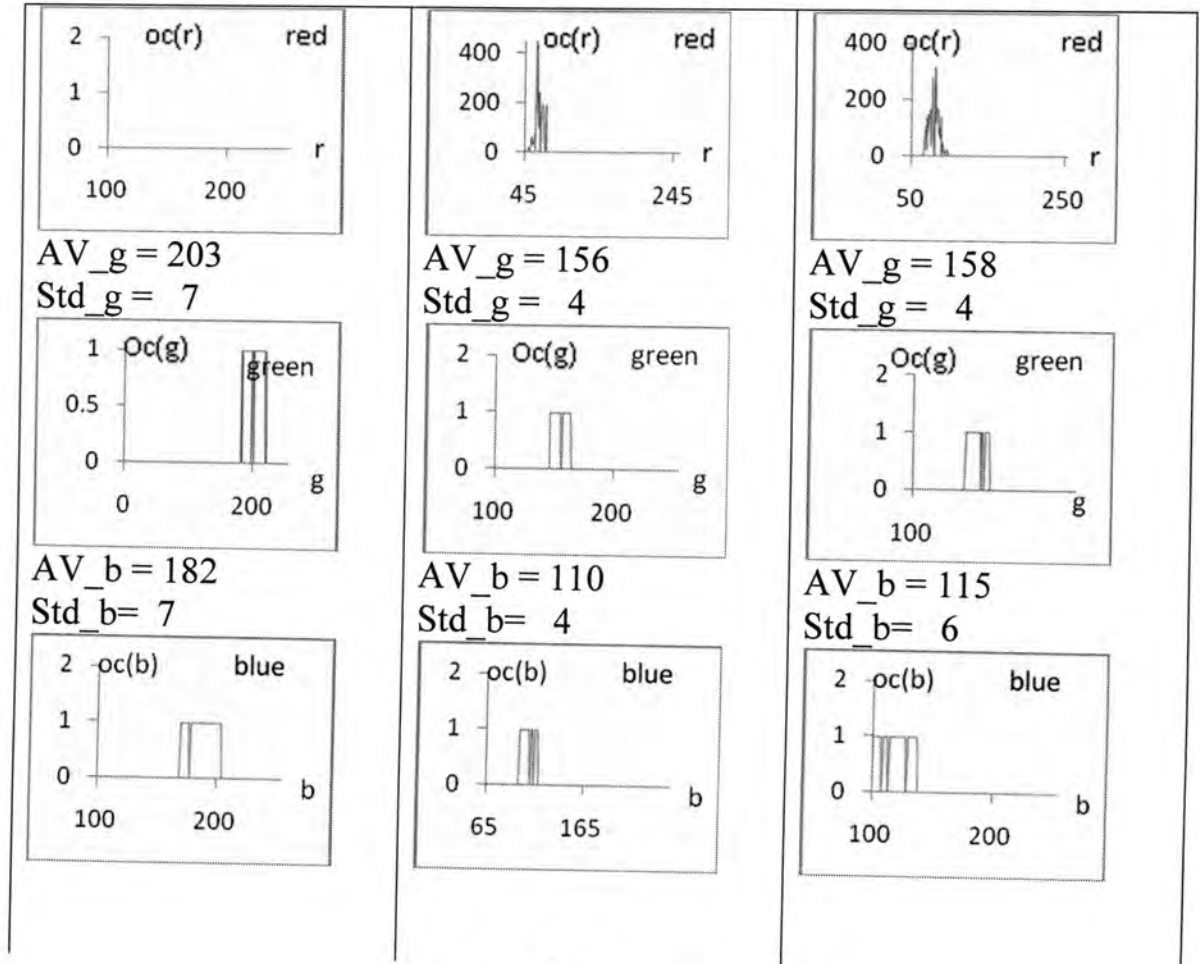
1-sunlight image	2-shadow light image	3-floorisnt light image
White region AV_r = 221 Std_r = 4  AV_g = 228 Std_g = 4  AV_b = 255 Std_b = 0 	White region AV_r = 157 Std_r = 8  AV_g = 173 Std_g = 5  AV_b = 223 Std_b = 10 	White region AV_r = 186 Std_r = 8  AV_g = 198 Std_g = 5  AV_b = 213 Std_b = 6 
Red region AV_r = 203 Std_r = 16  AV_g = 123 Std_g = 28 	Red region AV_r = 136 Std_r = 3  AV_g = 15 Std_g = 4 	Red region AV_r = 162 Std_r = 3  AV_g = 41 Std_g = 3 



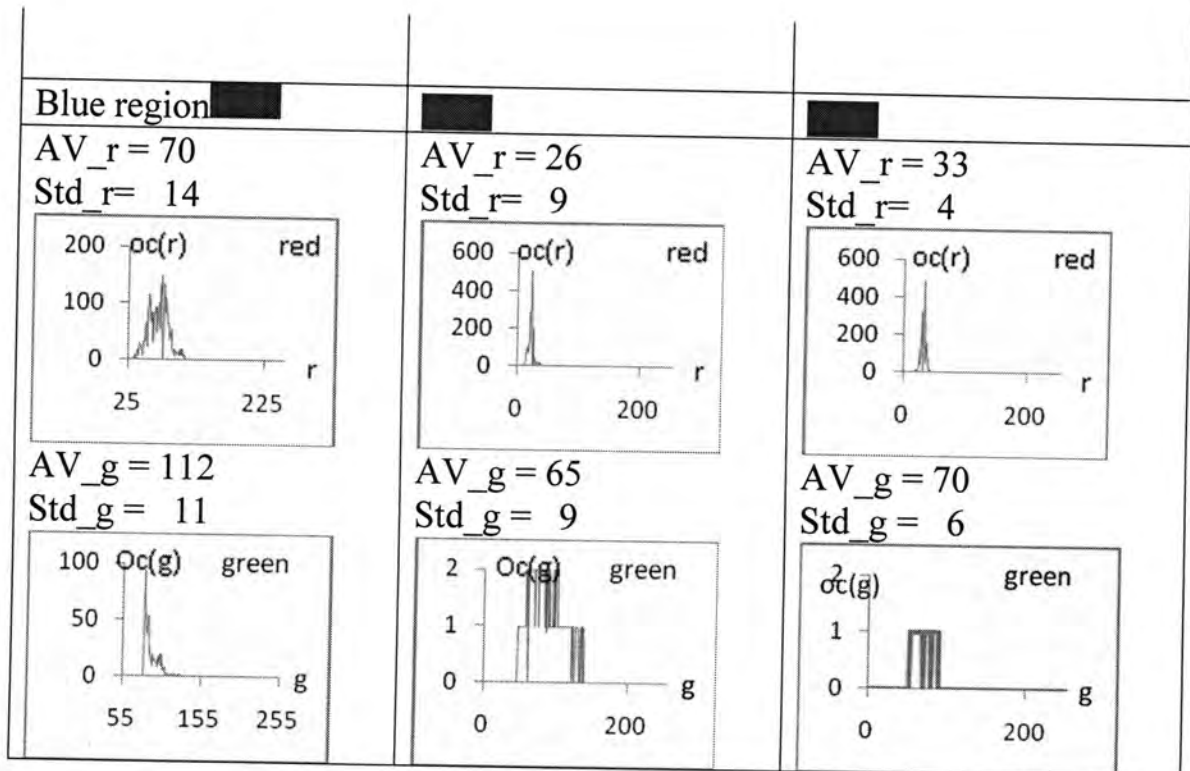
شكل 8: المخطط التكراري (تكرار العناصر) والخصائص لكل منطقة لونية متجانسة للحزم الثلاثة، للصور الملتقطة بالوضوحية: high quality.

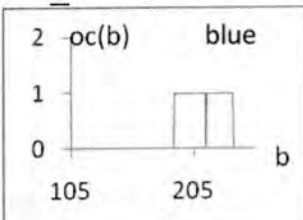
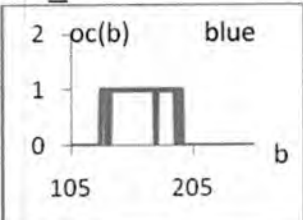
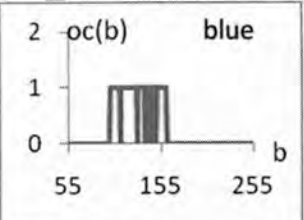
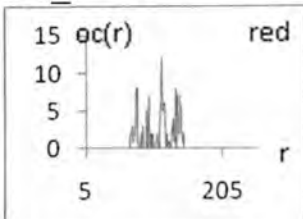
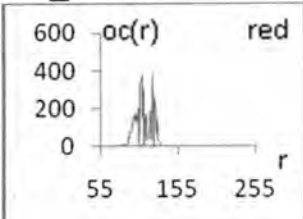
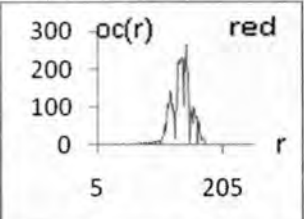
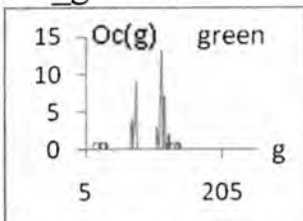
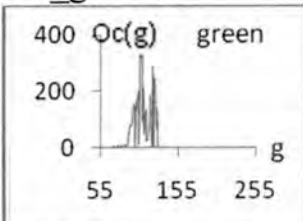
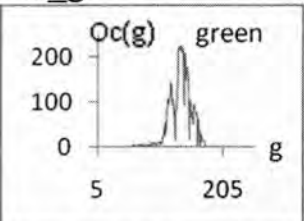
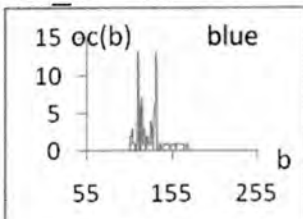
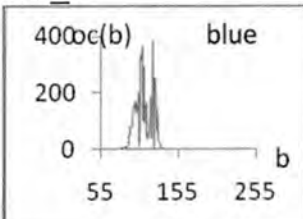
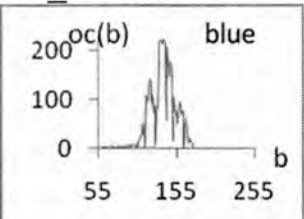
Yellow region		
AV_r = 227 Std_r = 10 	AV_r = 163 Std_r = 3 	AV_r = 186 Std_r = 5 
AV_g = 251 Std_g = 4 	AV_g = 197 Std_g = 4 	AV_g = 212 Std_g = 6 
AV_b = 196 Std_b = 21 	AV_b = 104 Std_b = 3 	AV_b = 120 Std_b = 5 
Green region		
AV_r = 131 Std_r = 9	AV_r = 65 Std_r = 5	AV_r = 80 Std_r = 6

هاله وعلي و كاظم

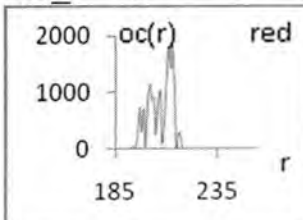
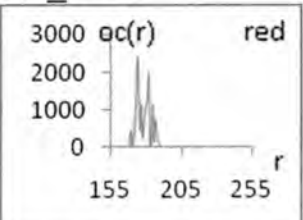
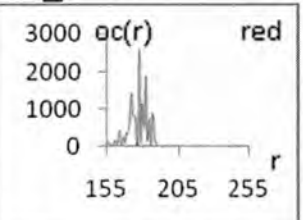


تابع للشكل (8)

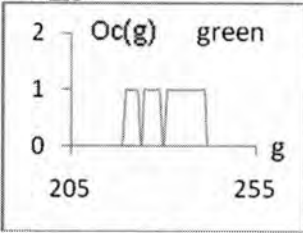
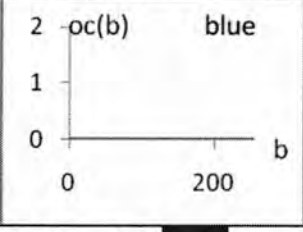
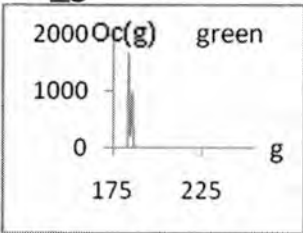
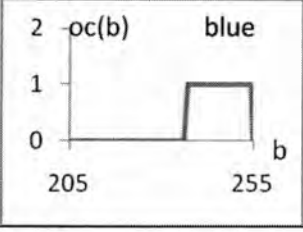
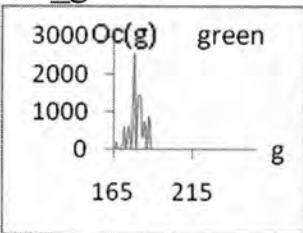
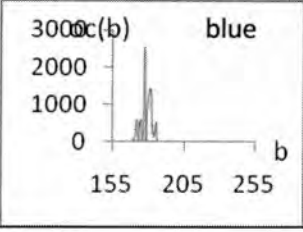
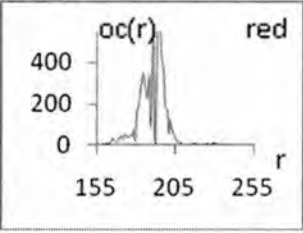
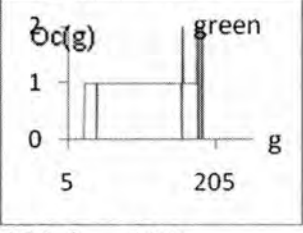
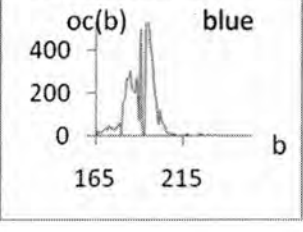
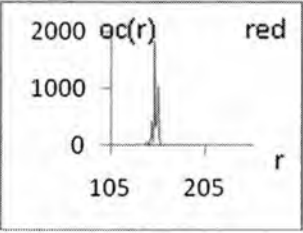
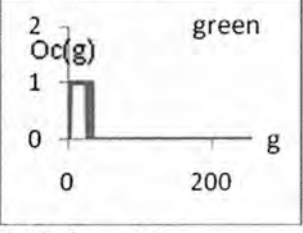
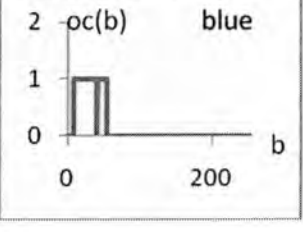
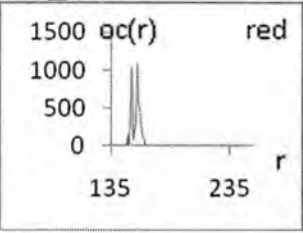
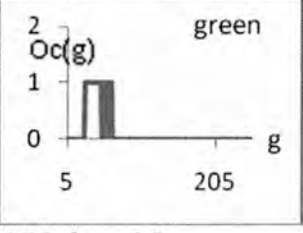
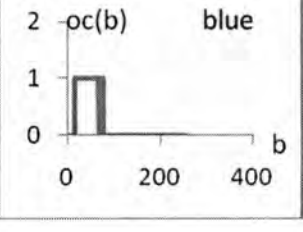


<p>AV_b = 208 Std_b = 8</p> 	<p>AV_b = 146 Std_b = 9</p> 	<p>AV_b = 135 Std_b = 10</p> 
Shadow region		
<p>AV_r = 115 Std_r = 24</p> 	<p>AV_r = 113 Std_r = 11</p> 	<p>AV_r = 138 Std_r = 18</p> 
<p>AV_g = 88 Std_g = 45</p> 	<p>AV_g = 129 Std_g = 16</p> 	<p>AV_g = 145 Std_g = 23</p> 
<p>AV_b = 147 Std_b = 18</p> 	<p>AV_b = 139 Std_b = 17</p> 	<p>AV_b = 147 Std_b = 26</p> 

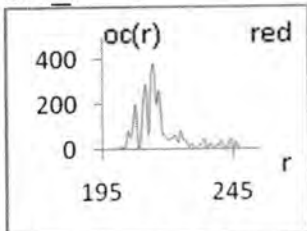
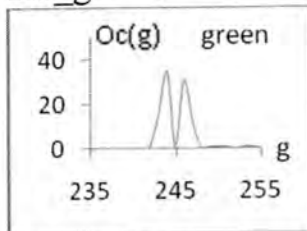
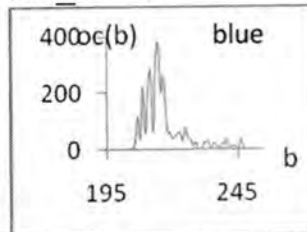
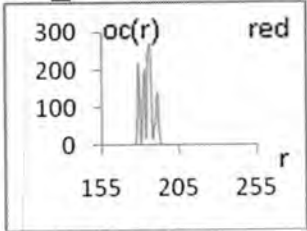
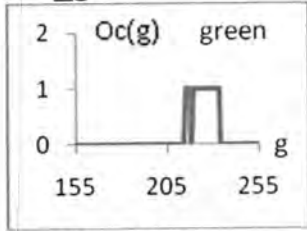
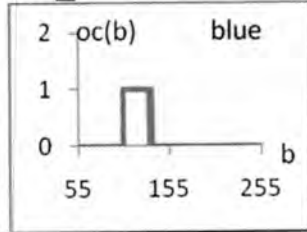
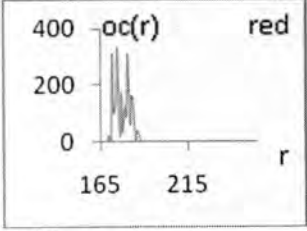
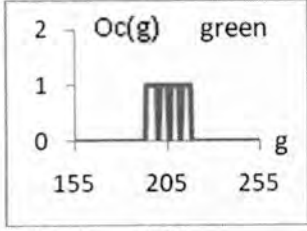
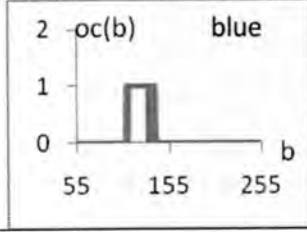
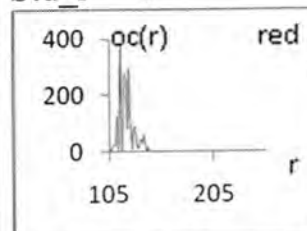
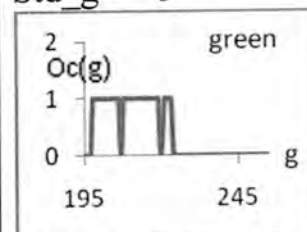
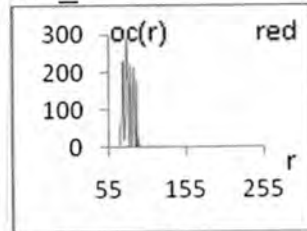
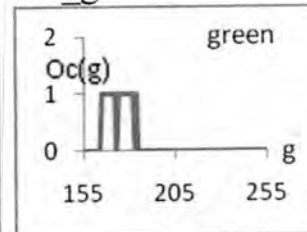
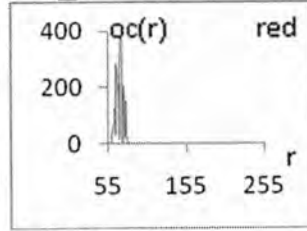
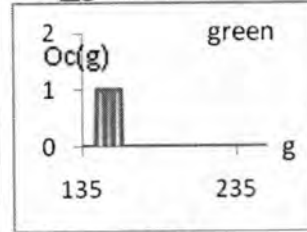
تابع للشكل (8)

1-sunlight image	2-shadow light image	3-floorisnt light image
White region		
<p>AV_r = 207 Std_r = 5</p> 	<p>AV_r = 180 Std_r = 5</p> 	<p>AV_r = 178 Std_r = 9</p> 
<p>AV_g = 231</p>	<p>AV_g = 195</p>	<p>AV_g = 193</p>

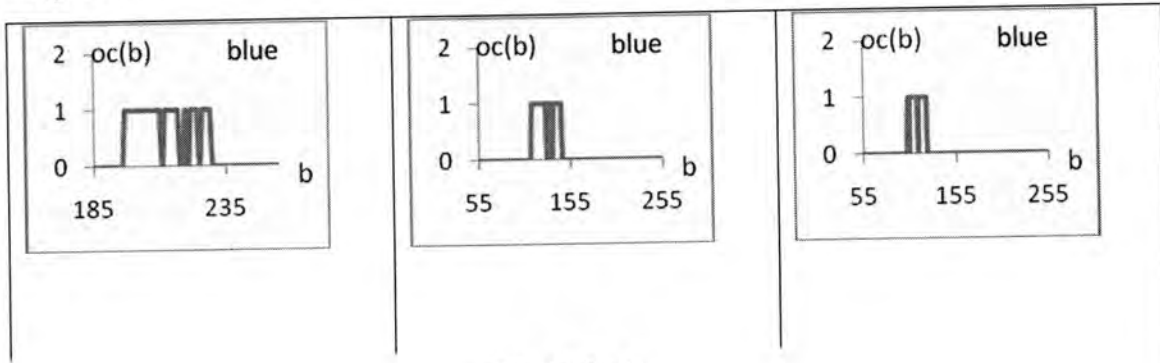
هاله وعلي و كاظم

<p>Std_g = 4</p>  <p>AV_b = 255 Std_b = 0</p> 	<p>Std_g = 4</p>  <p>AV_b = 253 Std_b = 3</p> 	<p>Std_g = 6</p>  <p>AV_b = 211 Std_b = 9</p> 
<p>Red region</p> <p>AV_r = 190 Std_r = 11</p>  <p>AV_g = 113 Std_g = 21</p>  <p>AV_b = 192 Std_b = 16</p> 	<p>AV_r = 152 Std_r = 3</p>  <p>AV_g = 17 Std_g = 4</p>  <p>AV_b = 29 Std_b = 7</p> 	<p>AV_r = 155 Std_r = 3</p>  <p>AV_g = 38 Std_g = 3</p>  <p>AV_b = 38 Std_b = 8</p> 

شكل 9- يمثل المخطط التكراري (لتكرار العناصر) والخصائص لكل منطقة لونية متجانسة للحزم الثلاثة للصور الملتقطة بالوضوحية: normal quality.

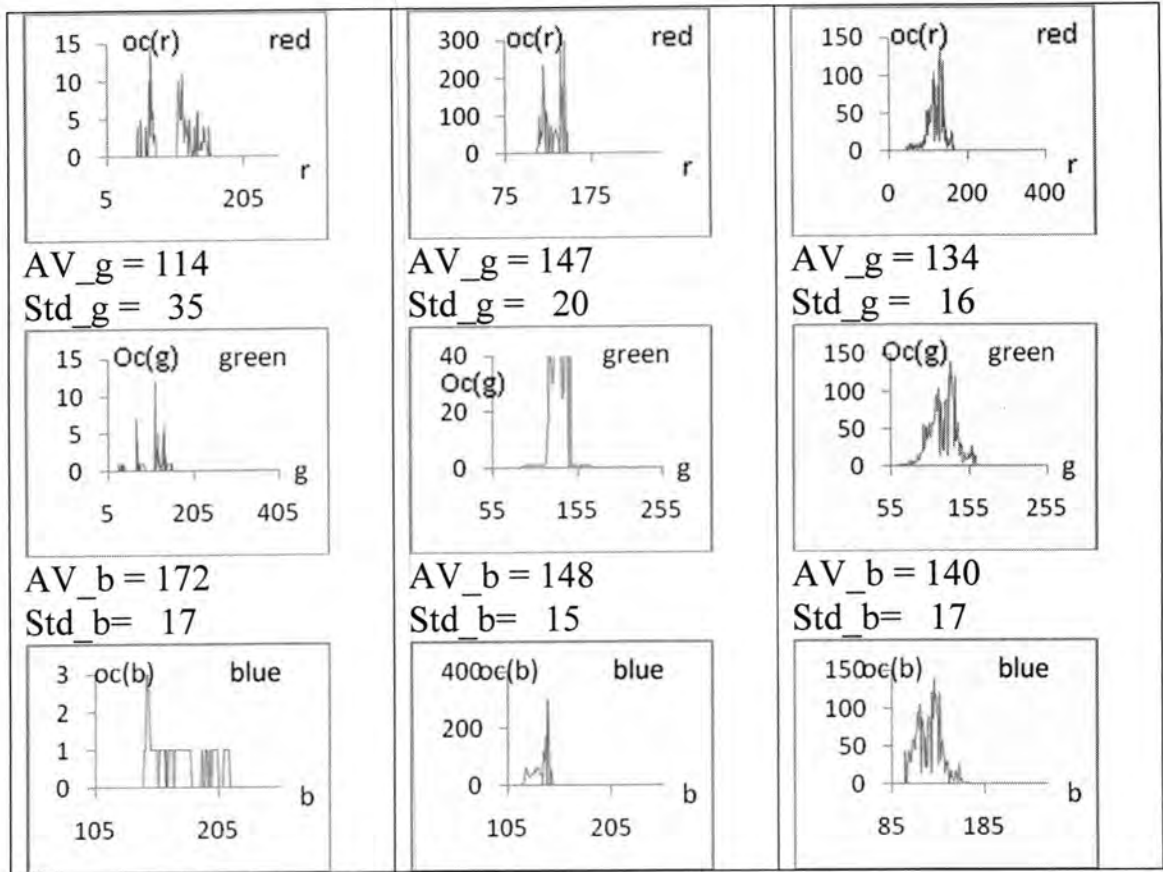
Yellow region		
<p>AV_r = 216 Std_r = 9</p>  <p>AV_g = 255 Std_g = 1</p>  <p>AV_b = 228 Std_b = 14</p> 	<p>AV_r = 183 Std_r = 3</p>  <p>AV_g = 222 Std_g = 4</p>  <p>AV_b = 115 Std_b = 5</p> 	<p>AV_r = 177 Std_r = 4</p>  <p>AV_g = 207 Std_g = 5</p>  <p>AV_b = 121 Std_b = 5</p> 
Green region		
<p>AV_r = 121 Std_r = 7</p>  <p>AV_g = 210 Std_g = 5</p>  <p>AV_b = 211 Std_b = 7</p>	<p>AV_r = 82 Std_r = 6</p>  <p>AV_g = 175 Std_g = 4</p>  <p>AV_b = 127 Std_b = 5</p>	<p>AV_r = 71 Std_r = 5</p>  <p>AV_g = 153 Std_g = 3</p>  <p>AV_b = 113 Std_b = 4</p>

هاله وعلي و كاظم

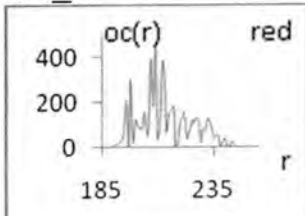
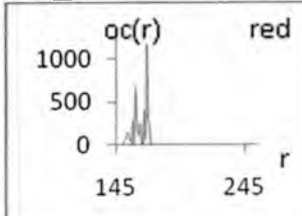
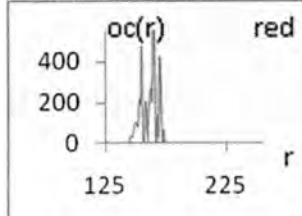
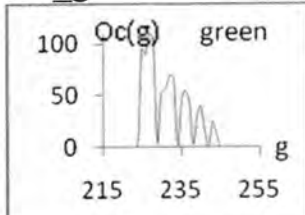
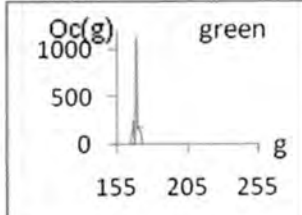
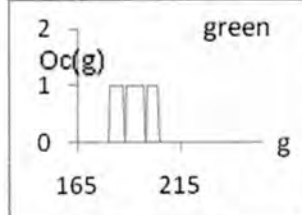


تابع للشكل (9)

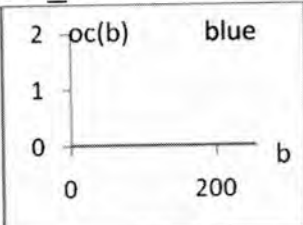
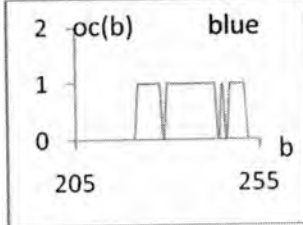
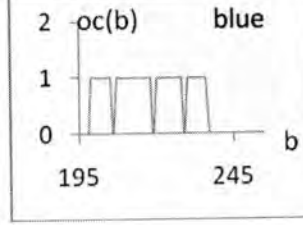
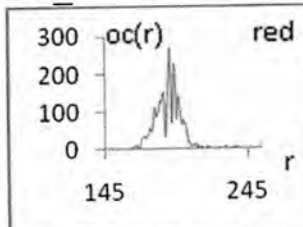
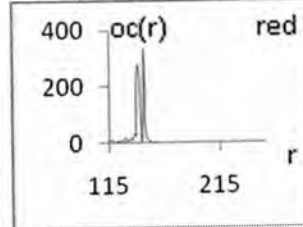
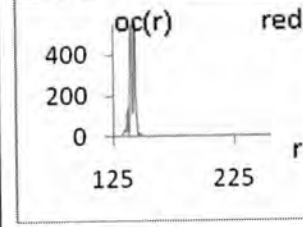
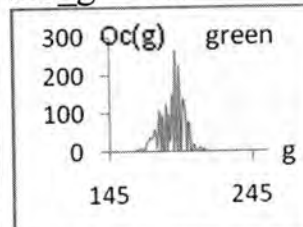
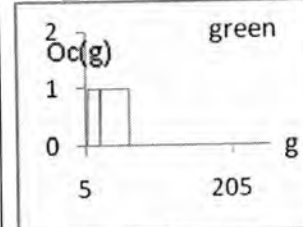
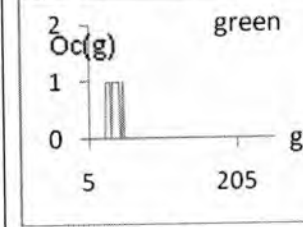
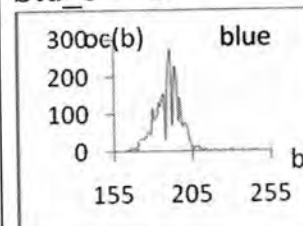
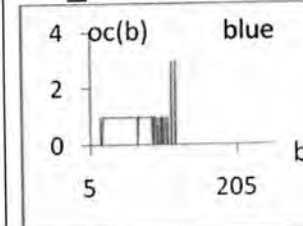
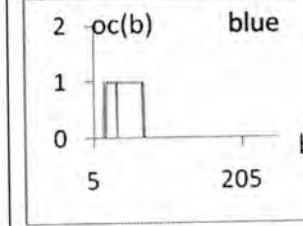
Blue region		
<p>AV_r = 56 Std_r = 14</p> <p>AV_g = 113 Std_g = 10</p> <p>AV_b = 234 Std_b = 9</p>	<p>AV_r = 25 Std_r = 3</p> <p>AV_g = 74 Std_g = 4</p> <p>AV_b = 163 Std_b = 5</p>	<p>AV_r = 32 Std_r = 4</p> <p>AV_g = 67 Std_g = 6</p> <p>AV_b = 135 Std_b = 10</p>
Shadow region		
<p>AV_r = 107 Std_r = 29</p>	<p>AV_r = 134 Std_r = 11</p>	<p>AV_r = 120 Std_r = 21</p>



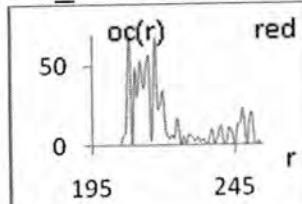
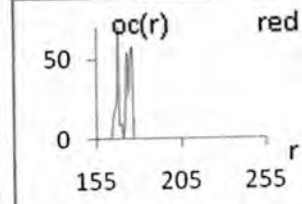
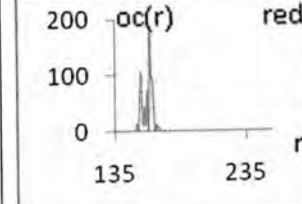
تابع للشكل (9)

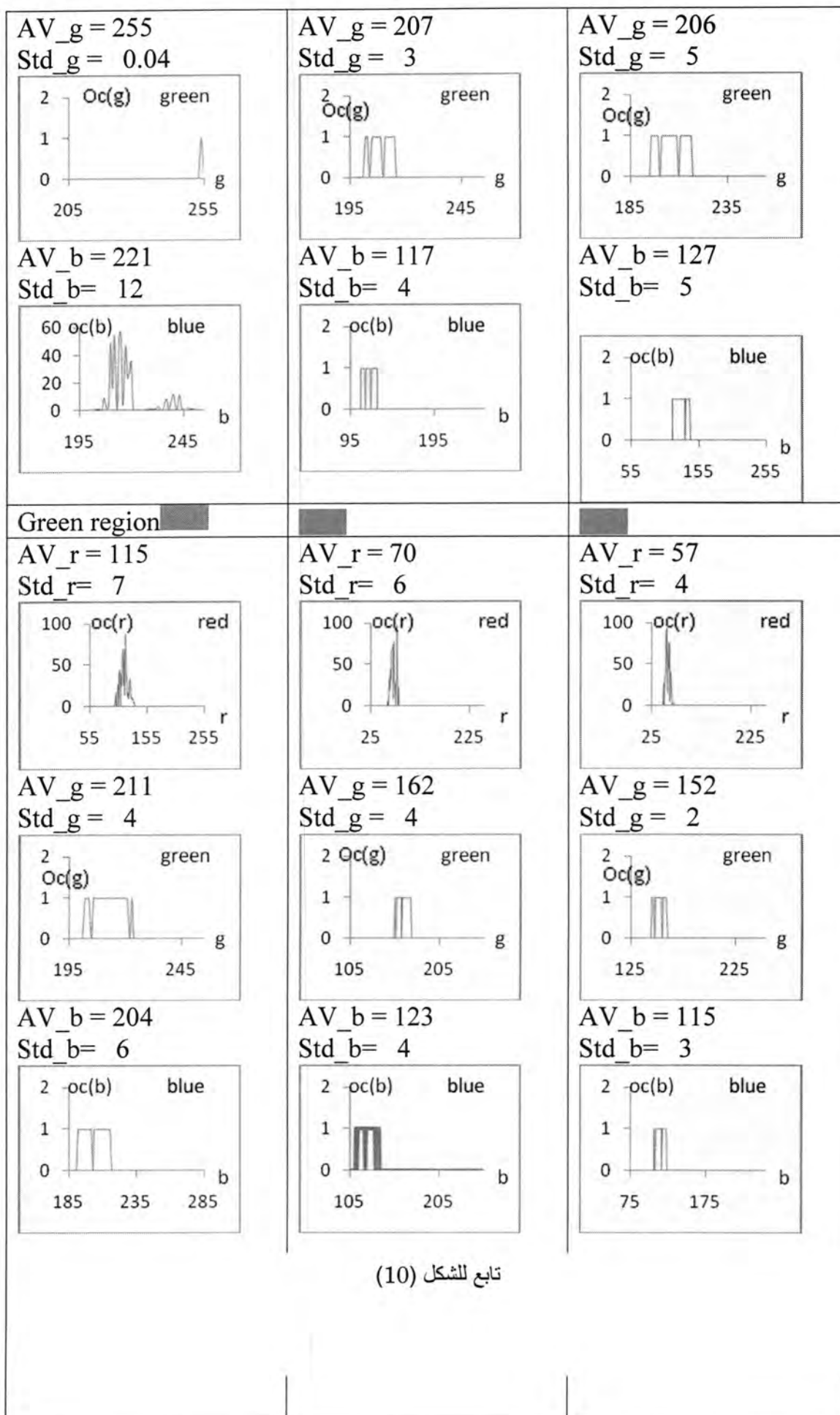
1-sunlight image	2-shadow light image	3-floorisnt light image
White region		
AV_r = 213 Std_r = 11 	AV_r = 164 Std_r = 5 	AV_r = 163 Std_r = 6 
AV_g = 239 Std_g = 8 	AV_g = 180 Std_g = 4 	AV_g = 194 Std_g = 4 

هاله وعلي و كاظم

<p>AV_b = 255 Std_b = 0</p> 	<p>AV_b = 241 Std_b = 5</p> 	<p>AV_b = 219 Std_b = 5</p> 
<p>Red region</p> <p>AV_r = 191 Std_r = 12</p> 	<p>AV_r = 143 Std_r = 4</p> 	<p>AV_r = 141 Std_r = 3</p> 
<p>AV_g = 116 Std_g = 20</p> 	<p>AV_g = 23 Std_g = 8</p> 	<p>AV_g = 38 Std_g = 3</p> 
<p>AV_b = 187 Std_b = 14</p> 	<p>AV_b = 45 Std_b = 12</p> 	<p>AV_b = 42 Std_b = 7</p> 

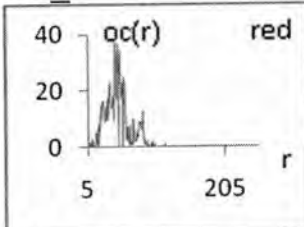
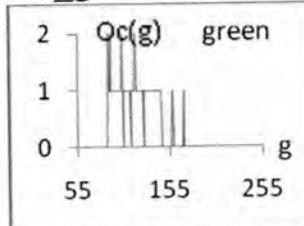
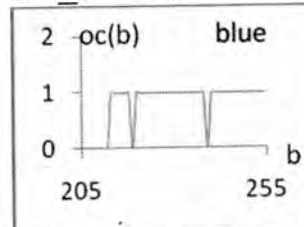
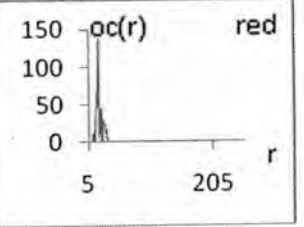
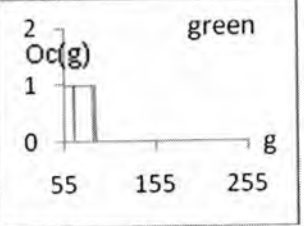
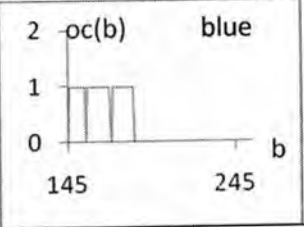
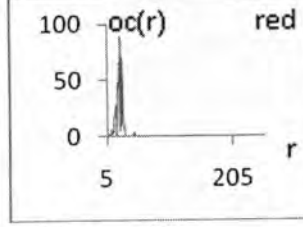
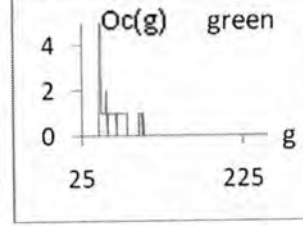
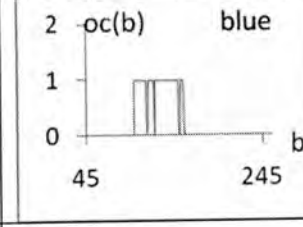
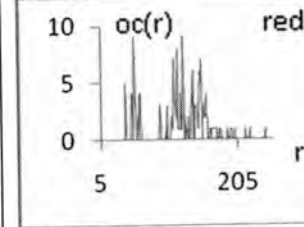
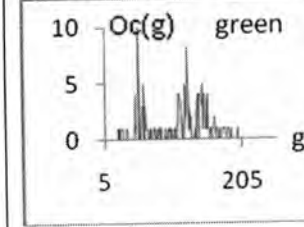
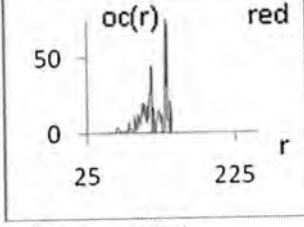
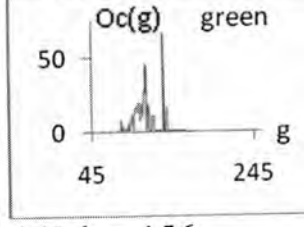
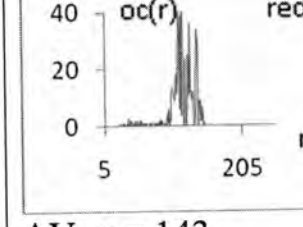
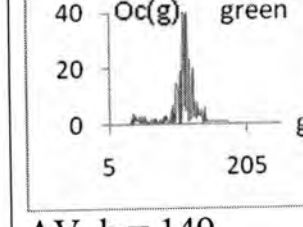
شكل 10- يمثل المخطط التكراري (لتكرار العناصر) والخصائص لكل منطقة لونية متجانسة للحزم الثلاثة للصور الملتقطة بالوضوحية : basic quality.

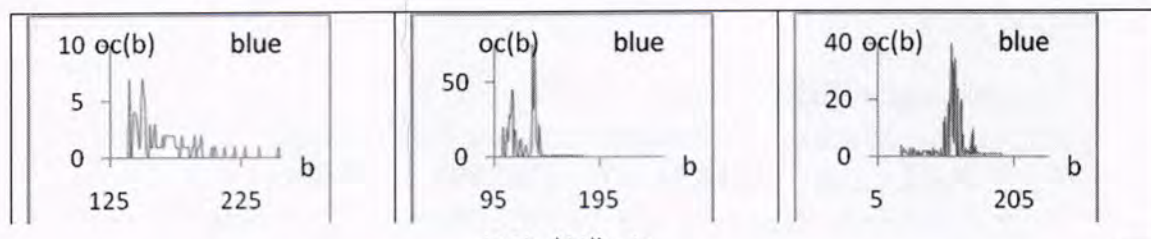
<p>Yellow region</p> <p>AV_r = 220 Std_r = 13</p> 	<p>AV_r = 171 Std_r = 2</p> 	<p>AV_r = 160 Std_r = 4</p> 
---	---	---



تابع للشكل (10)

هاله وعلي و كاظم

Blue region		
<p>AV_r = 49 Std_r = 17</p>  <p>AV_g = 113 Std_g = 12</p>  <p>AV_b = 228 Std_b = 10</p> 	<p>AV_r = 23 Std_r = 5</p>  <p>AV_g = 69 Std_g = 6</p>  <p>AV_b = 160 Std_b = 8</p> 	<p>AV_r = 25 Std_r = 5</p>  <p>AV_g = 65 Std_g = 5</p>  <p>AV_b = 135 Std_b = 10</p> 
Shadow region		
<p>AV_r = 115 Std_r = 42</p>  <p>AV_g = 126 Std_g = 41</p>  <p>AV_b = 166 Std_b = 16</p>	<p>AV_r = 117 Std_r = 16</p>  <p>AV_g = 134 Std_g = 18</p>  <p>AV_b = 156 Std_b = 12</p>	<p>AV_r = 119 Std_r = 18</p>  <p>AV_g = 143 Std_g = 29</p>  <p>AV_b = 149 Std_b = 28</p>



تابع للشكل (10)

نلاحظ من الشكل (8)(9)(10) عند دراسة المناطق اللونية المتجانسة للحزم الثلاثة و لجميع الصور الملتقطة بوضوحيات مختلفة , وجد ان اعلى معدل لجميع المناطق اللونية يسجل للصور الملتقطة بضوء الشمس . ثم تليه الصور الملتقطة بإضاءة الفلورسنت , ثم ظل الشمس . وعند ملاحظة الخططات التكرارية للحزم الثلاثة في الشكل , نجد ان كل من المنطقة الصفراء والخضراء والزرقاء في الصورة تمتلك مخطط تكراري اعلى عند الحزمة الحمراء , وذلك لجميع شدات الاضاءة المستخدمة.

REFERENCES

1. T. seemann , "Digital image processing using local segmentation" information technology , Monash university , Australia , (2002).
2. R.Gonzalez , R. E. wood , " Digital Image Processing " , (1992).
3. E. Peli , L. Arend , A. T. Labianca , " Contrast Perception a Cross Changes in Luminance and Spatial Frequency " , Optical Society America , (1996) .
4. W. B. Thompson and P. Shirley , " A spatial Post Processing algorithm for Images of Night Scenes " , Cornell and Utan University , (2003) .
5. W.F.Schreiber , " Fundamental of Electronic Imaging Systems " , Springer – Verlag , Berlin , (1998) .
6. M. V. Shirvaikar , " An Optimal Measure for Camera focus and Exposure " , electrical engineering Department , University of Texas at Tyler , Proceeding of IEEE (2004) .
7. T. Acharya and A. K. Ray , " Image processing principles and applications " , (2005).
8. S.S. salman , " A Study of test image as function of the luminance " department of physics , college of science , Al-Mustansiriyah university , (2008).
9. S.W. Smith " The Scientist and Engineers Guide to Digital Signal Processing " , California Publishing ISBN O – 966176 – 33 (1997) .
10. J. C. Russ , " The Image Processing Hand Book " , 3rd edition , Materials Science and engineering , Department North Carolina State University , ISBN : 0849325323 , (1998) .
11. J. C. Russ , " Image Processing Hand Book " , 5th edition , Materials Science and Engineering Department , North Carolina State , University , (2006) .
12. W.G. Kropatsch and H. Bischof " Digital Image analysis Selected Techniques and Application " Vienna University of Technology , (2001) .
13. Fried, David " Optical Resolution Through a Randomly in Homogeneous medium for very long and very short exposure " J.opt.Soc.Amer 56:1372– 9 (1966).
14. Gaskill , Jack , " Linear System , Fourier Transform and Optics " , Wiley

هاله وعلي و كاظم

- interscience ISBNO – 471 – 29288 – 5 , (1978) .
- 15.Smith , Warrenj , " Modern Optical Engineering " , 3rd edition , MC Graw Hill Profession , ISBNO – 07 – 136360 – 2 , (2000).
- 16.Roggemann , Michael and Welsh , Byron , " Imaging Through Turbulence" CRC press ISBNO – 8493 – 3787 – 9 , (1996) .
- 17.Robin, Michal and Poulin , " Digital Television Fundamentals " 2nd edition , MC Graw – Hill Profession ISBNO – 07 – 135581 – 2 ,(2000) .
- 18.Accetta , J.S. and Shumaker , D.L. , " The Infrared and Electro - Optical System Hand Book " , SPIE , IERIMISBNO – 8194 – 1072 – 1(1993) .
- 19.S.E. Umbaugh, "Computer vision and Image processing",
- 20.Prentice Hall ,PTR , Upper Saddle River, USA, (1998).
- 21.J.B. Compbell, "Introduction to remote sensing", The Guilford press, (1996).

المعاملة بطريقة الفرن الحراري وتقنية الليزر وتأثير إضافة الزنك على بعض الخواص الميكانيكية لسبيكة حشوة الاسنان

حليمه جابر محمد و جعفر هاشم محسن و اقبال فاضل واطيف خالد وسندس كريم
وزارة العلوم والتكنولوجيا

ABSTRACT

Spictin been prepared for the type of dental filling (low copper) of the raw materials according to specific ratios by thermal oven first alloy composed of silver, copper, tin. The second alloy of silver, copper, tin, zinc, and ran the process of thermal treatment technology laser both, were analyzed X-ray diffraction (XRD) of the alloys prepared and the appointment of oddball phenomenon and compared with standard tables (ASTM), the result of the analysis showed that stage (γ - Ag_3Sn) is the basis of the proportion of output ways, as is the case in the standard alloy, and the results of each elements involved in this process and the disappearance of X-ray analysis of the process of the alloy γ laser treatment completely, and the disappearance of tin in such a manner prepared for the oven temperature alloy or alloy II first shows all of the elements involved and the disappearance of tin and zinc. The results of the study to increase a harder alloy containing zinc, and through this been a substantial increase in the amount of hardness and resistance to corrosion and clear through the rates of low solubility of the elements in the test solutions.

الخلاصة

تم تحضير سبيكتين لحشوة الاسنان نوع (واطنة النحاس) من موادها الاولى وحسب نسب محدده بواسطة الفرن الحراري تتكون السبيكة الاولى من الفضة، النحاس، القصدير اما السبيكة الثانية من الفضة، النحاس، القصدير والزنك. اجريت عملية المعاملة الحرارية بتقنية الليزر لكليهما باعتماد تحليل حيود الاشعة السينية (XRD) للسبائك المحضرة وتعيين الاطوار الظاهره بمقارنه مع الجداول القياسية (ASTM)، اظهرت نتيجة التحليل الى ان طور (γ - Ag_3Sn) يشكل نسبة الاساس في ناتج الطريقتين وكما هو الحال في السبيكة القياسية، كما بينت نتائج التحاليل ظهور لكل العناصر الداخلة في هذه العملية كما اظهرت تحليلات الاشعة السينية اختفاء طور كما من السبيكة المعاملة بالليزر كليا، واختفاء القصدير في تلك المحضرة بطريقة الفرن الحراري للسبيكة الاولى اما السبيكة الثانية تظهر كل العناصر الداخلة واختفاء القصدير والزنك. اوضحت نتائج الدراسة زيادة صلادة السبيكة المتضمنه عنصر الزنك ومن خلالها ذلك تم الحصول على زيادة كبيرة في مقدار الصلادة ومقاومة لتآكل واضحه من خلال معدلات الذوبانية للواظنه للعناصر في محاليل الاختبار.

المقدمة

استخدم أطباء الأسنان سبائك ذهبية في صنع حشوات الأسنان لأكثر من 4000 سنة. حيث إستعمل الباحثين Etruscans, Phoenicians السلك الذهبي في ربط الاسنان ، ثم قام الرومان بجعل جسور ثابتة من شريط الذهب (1). اما في القرن العشرون فقد ظهرت تشكيلة واسعة من المواد الجديدة وتقنيات حديثة قدمت إلى طب الأسنان من خلال استخدام سبائك المعادن النبيلة (2) حيث استخدمت حشوات الأسنان لعدة سنوات وبإنجاح كبير كمادة لترميم الاسنان لما لهذه المادة من خصائص تجعلها تتكيف داخل تجويف السن (3)، حيث تتكون الحشوات من مزج معدنيين او اكثر من عناصر الفضة، النحاس، القصدير، بعض الاحيان تحتوي على الزنك، البلاديوم و الانديوم، وتسمى عملية المزج بين الزئبق وهذه السبيكة (بالملمغ) بالتفاعل يؤدي الى تكوين ماده صلبه بترميم فجوات السن وتكون ذات مظهر رمادي - فضي (4). فتركيب حبيبات مسحوق الحشوة يتغاير من منتج الى اخر وان كميات الفضة والقصدير الداخلة في تركيب حشوة الاسنان تضمن تكوين طور Ag_3Sn المعروف بطور γ لنظام فضة قصدير والذي له دور مهم اذ يتفاعل مع الزئبق بسهولة لتكوين مادة الحشوة (5)

وتصنف السبائك المحضرة للملمغ الى نوعين هما :

أولاً: السبائك عالية النحاس: وهي تتضمن السبائك الامتزاجية والسبائك احادية التركيب وسبائك تحتوي على جزئين من السبائك الامتزاجية وجزء واحد من السبيكة التقليدية

ثانياً: السبائك الواطئة النحاس. ان الاختلاف الرئيسي بين مختلف السبائك التقليدية يكون في حجم السبائك وشكلها (6,7)

كما كان لاكتشاف الليزر اثر كبير لفتح افاق علمية جديدة في مختلف المجالات العلمية ذات التطبيقات المختلفة، حيث بحث (Sindo kov) (8) تأثيرات الليزر على التحولات الطورية والصلادة السطحية. اوجد الباحث (Hick) (9) المعاملة الحرارية السريعة للسطوح، وجرى الباحث (Gillener) (10) دراسة حول الانصهار السطحي باشعة الليزر على التغيرات التركيب المجهرية والصلادة المايكروية للمعادن، في عام 1991 تم معالجة حراريه لمغم حشوة الاسنان بواسطة CO2 النبضي والمستمر وكذلك تم استخدام ليزر Nd-YAG (11)

كما تمكن الباحث (Lilinan Sandu) وجماعته من اجراء عملية اللحام لسبائك الاسنان في بيئة (غاز خامل) مما أدى الى تحسينات كبيره مقارنة الى الطرق التقليدية (12)

المواد وطرائق العمل

1- تحضير السبيكة :

ان عملية تحضير السبيكة الداخلة في اعداد حشوة الاسنان يتطلب استخدام الافران الحرارية والاختيار الحذر لدرجة الحرارة والزمن اللازم لاجداث التفاعل بين المعادن، بعد خلط النسب الوزنية المشار اليها في الجدول (1). وضعت المعادن في بودقة من الكوارتز تستوعب 100gm داخل خلية مفرغة لتكون معزولة عن الهواء داخل الفرن الحراري من نوع Carbolite tube furnace انتاج شركة (D-6450 Hanau)، في درجه C (1100) ولمدة 8 ساعات، بعدها تترك حتى تبرد.

وضعت السبيكة في خلية فراغ (10^{-3} torr) لعزلها عن التأثيرات الجوية واستخدم ليزر نبضي من نوع Nd-YAG الطول موجي $1.06 \mu m$ ، ويمكن لهذا الليزر ان يجهز طاقة مقدارها J (1.5) وكان امد نبضة الليزر (2-10 msec) والمسافة (5 cm)، وباستخدام عدسة بعدها البؤري 8 أمكن تركيز حزمة الليزر في مساحة صغيرة .

2_ تحضير عينات الحشوة للفحوصات

بعد اخراج السبيكة المحضرة جرى العمل بطحن السبيكة باستخدام مطحنة من انتاج Shimadzu ذات حاويات طحن من كاربيد التنكستن للحصول على الحجم المطلوب بعدها ينخل المسحوق الدقيق بواسطة منخل دقيق Mesh قطر فتحاته $45 \mu m$ ثم ينخل المتبقي بواسطة منخل اخر فتحاته اكبر من $45 \mu m$ ثم ينخل بواسطة منخل اخر قطر فتحاته $75 \mu m$ ، (وقد ثبتنا في هذه الدراسة ان احسن قيمه تاخذ $45 \mu m$) عند القياس ولغرض تخليص السبيكة من الاجهادات نتيجة الطحن توضع هذه السبيكة المطحونه في بودقة داخل فرن حراري عند درجة تتراوح بين C (50-100) عندها تصبح مساحيق السبيكة جاهزة للفحص الاشعة السينية .

ولغرض تحضير العينات للفحص الصلاده، تم تثبيتها في قالب من مادة (Epoxy-resin)، وتسمى هذه العملية بالتثبيت على البارد ثم تركت العينات لمدة (24h) لتجف. اجريت عملية التنعيم واثناء ذلك تكون عملية الترطيب بالماء مستمرة لمنع ارتفاع درجة الحرارة للعينات، وبعد الانتهاء من عملية التنعيم اجريت عملية الصقل polishing باستخدام ورقة التنعيم 4000 لازالة الخدوش الناتجة خلال عملية التنعيم. ثم يتم التنظيف بالماء المقطر ثم الكحول المثيلي وبعدها تجفف فتصبح جاهزة للفحص .

3- مقاومة التآكل:

لغرض اختبار مقاومة العينات للتآكل علقت العينات المحضرة في انايبب الاختبار، بواسطة سلك بلاستيكي بحيث تحتوي كل انبوبة على (30ml) من محلول التآكل، وتم تغطية فوهة الانايبب بقطعة من

البلاستيك الرقيقة لمنع تبخر المحلول، ووضعت هذه العينات داخل فرن حراري عند درجة حرارة . (37)C لمدة شهرين وبعد ذلك تم تنظيفها بالماء المقطر والكحول، وقيست ذوبانية العناصر (Ag,Cu,Sn,Zn) في محاليلها باستخدام مطياف الامتصاص الذري.

النتائج والمناقشة

1- نتائج حيود الأشعة السينية :

تم استخدام جهاز حيود الأشعة السينية (XRD) نوع (Philips PW 1840) الذي يولد أشعة سينية بطول موجي ($\lambda = 1.5417 \text{ \AA}$) لمصدر (Cu) باستخدام مرشح من النيكل ولمدى من الزوايا ($2\theta = 20^\circ - 90^\circ$) وباستخدام قانون براك Bragg's Low [13] ويمكن حساب المسافة (d) بين المستويات من العلاقة المبينة رقم (1)

$$n\lambda = 2d \sin \theta \text{-----} (1)$$

إذ أن n = رتبة الحيود وهي عدد صحيح ويساوي (1).

d = المسافة البينية .

λ = الطول الموجي للأشعة السينية.

θ = زاوية حيود الأشعة السينية.

من خلال دراسة انماط حيود الأشعة السينية (XRD) الموضحة في الاشكال (1,2,3,4) يتم تحديد اطوار السبائك المنتجة بحساب قيم المسافات البينية للمستويات الذرية (d-spacing) لمسحوق السبيكة ومطابقته مع القيم المقاسة للاطوار (γ, η, λ) الواردة في الجداول القياسية (ASTM).

يبين الشكل (1) انماط حيود الأشعة السينية للسبيكة (A)، حيث يظهر فيها طور ($\gamma\text{-Ag}_3\text{Sn}$). وهذا متوقع من خلال مخطط اطوار الفضة -قصدير الذي يعطي اعظم نمو لطور ($\gamma\text{-Ag}_3\text{Sn}$) عند تراكيز الفضة القصدير المستعملة في هذه السبيكة (14) فضلا عن ظهور العناصر الفضة والنحاس الموضحة بالجدول (2).

يبين الشكل (2) انماط حيود الأشعة السينية للسبيكة (A1)، بعد معاملتها بالليزر حيث يظهر فيها طور ($\gamma\text{-Ag}_3\text{Sn}$) من خلال مخطط اطوار الفضة -قصدير الذي يعطي اعظم نمو لطور ($\gamma\text{-Ag}_3\text{Sn}$) عند التراكيز الفضة القصدير المستعملة في هذه السبيكة ظهور العناصر الفضة والنحاس الموضحة بالجدول (2).

يبين الشكل (3) انماط حيود الأشعة السينية للسبيكة (B)، حيث يظهر فيها طور ($\gamma\text{-Ag}_3\text{Sn}$). من خلال مخطط اطوار الفضة -قصدير الذي يعطي اعظم نمو لطور ($\gamma\text{-Ag}_3\text{Sn}$) عند التراكيز الفضة القصدير المستعملة في هذه السبيكة ظهور العناصر الفضة، النحاس والقصدير.

يبين الشكل (4) انماط حيود الأشعة السينية للسبيكة (B1)، بعد المعاملة بالليزر حيث يظهر فيها طور ($\gamma\text{-Ag}_3\text{Sn}$). في مخطط اطوار الفضة -قصدير الذي يعطي اعظم نمو لطور ($\gamma\text{-Ag}_3\text{Sn}$) عند التراكيز الفضة القصدير المستعملة في هذه السبيكة (14)، ظهور كل العناصر الفضة، النحاس، القصدير والزنك

ومن خلال دراسة الاشكال والجداول للحالتين يبين لنا فقدان القصدير والزنك في حالة استخدام الفرن الحراري وذلك ما يؤدي الى تدني نوعية السبيكة الناتجة.

2_ نتائج فحص الصلادة

جرى فحص فيكرز للصلادة (Viker hardness test) العينات المحضرة باستخدام جهاز (Viker) حيث كان الحمل المسلط عند القياس (50gm) ولزمن قدره (15sec) وقد جرى القياس لاربعة اركان من العينة وعند مسافة (50μm) من كل حافة ومن مقدار المعدل الحسابي لهذه القياسات يتم حساب عدد فيكرز للصلادة (HVN), [15] وبموجب العلاقة الرياضية الخاصة رقم (2)

$$HVN = (2F \sin \phi) / D^2 \text{ -----(2)}$$

حيث تمثل : HVN : عدد فيكرز للصلادة .

F: الحمل المسلط (Kg/mm^2) .

ϕ : الزاوية الراسية بين الوجهين المتقابلين للقاعدة الرباعية للهرم وتساوي (136/2) .

: المعدل الحسابي لقطري المضلع الرباعي (mm) ،

يوضح الجدول (3) قيم عدد فيكرز. حيث ظهرت السبيكة (B) صلادة اعلى من السبيكة (A) المعاملة بالفرن وكذلك السبيكة (B1) صلادة اعلى من صلادة (A1) ومن خلال العمل لوحظ ان اضافة الزنك الى هذه السبيكة له تأثير كبير على الصلادة فكلما ازدادت نسبة الزنك زادت من الصلادة المادة وحسب النسب المحدده التي عمل بها اثناء العمل حيث ثبتت احسن قيمة للصلادة عند ذلك الوزن في هذه الدراسة كما مبين في الجدول (1) ،

اما المعاملة بالليزر فان الطاقة والمسافة هما العاملان المهمان لهما تأثيران كبيران فزيادة طاقة الليزر المستخدمة تزداد كمية الحرارة الممتصة من قبل المعدن او السبيكة وبالتالي تؤدي ارتفاع درجة حرارته وبزمن كبير جدا ونتيجة للتبريد السريع سوف يتولد انحدار حراري مولدا اجهادات داخلية وهذه الاجهادات تزداد بزيادة سرعة التسخين والتبريد للمعدن او السبيكة مؤديا بذلك الى زيادة في قيمة الصلادة المايكروية للمعدن او السبيكة والمسافة بين العينة وعدسة منظومة الليزر المستخدم تأثير كبير على تجانس المنطقة المتأثرة بالليزر وبالتالي على قيمة الصلادة المايكروية ، حيث يحدث نقصان في قيمة الصلادة المايكروية بزيادة المسافة بين العينة وعدسة منظومة الليزر . لان زيادة المسافة سوف تؤدي الى اتساع مساحة الضربة (نقصان بكثافة الطاقة) وبالتالي لا تسمح بحصول التحولات الطورية بشكل كامل والذي يعتقد بانها المسؤولة عن الزيادة في قيمة الصلادة المايكروية (16).

3 _ نتائج مقاومة التآكل

يبين الجدول (4) معدل ذوبانية العناصر المكونه للحشوة الذي يظهر هيمنة القصدير على المعادن المتحرره في محلول الاختبار خلال شهرين من التغطيس في محلول (NaCl) فتظهر امتلاك السبيكة B,B1 ذوبانية عالية للقصدير بموجب التآكل الذي يحدث في الطور اما السبيكة A,A1 تملك ذوبانية قليلة للقصدير اما ذوبانية الفضة فتظهر تحرر كمية ضئيلة منها .

ومن ذلك يمكن ان نستنتج:

يتبين من خلال النتائج ان اضافة عنصر الزنك له تأثير على زيادة الصلادة للعينة وكذلك ان استخدام تقنية الليزر بالمقارنه مع الجداول القياسية (ASTM)، يكون سببا في الحصول على مواصفات افضل من ماهو عليه في حالة استخدام طريقة الفرن الحراري وذلك بسبب فاعلية الليزر في التسخين السريع لاحداث التفاعلات المطلوبة وعدم فقدان المكونات الاساسية كما هو الحال في حالة الفرن الحراري

جدول -1: يبين نسبة الخلط لسبائك الحشوة

Type	Low copper	Ag	Sn	Cu	Zn
	A	69.5	26	4.5	
	B	68	26	4.5	1.5

A: السبيكة الاولى

B: السبيكة الثانية

جدول -2: يوضح قيم تحليلات حيود الاشعة السينية

ت	نوع السبيكة	D(standard) القياسية وفق جداول (ASTM)	D عمليا	2θ زاوية الطور	الطور والعنصر
1	سبيكة A	2.28	2.272	38.4	-Ag ₃ Snγ
		2.36	2.380	36.4	Ag
		2.92	----	-----	Sn
		2.09	2.084	34 24.9	Cu
2	سبيكة A1 المعاملة بالليزر	2.28	2.278	38.2	-Ag ₃ Snγ
		2.36	2.358	36.9	Ag
		2.92	2.87	30	Sn
		2.09	2.086	33.5 42.2	Cu
3	سبيكة B	2.28	2.267	39.6	-Ag ₃ Snγ
		2.36	2.385	37.9	Ag
		2.92	----	-----	Sn
		2.09	2.085	43.5 34.9	Cu
		2.19	-----	-----	Zn
4	سبيكة B1 المعاملة بالليزر	2.28	2.278	39.7	γ-Ag ₃ Sn
		2.36	2.379	37.8	Ag
		2.92	2.891	31	Sn
		2.09	2.088	43.6 35.7	Cu
		2.19	2.16	33.2	Zn

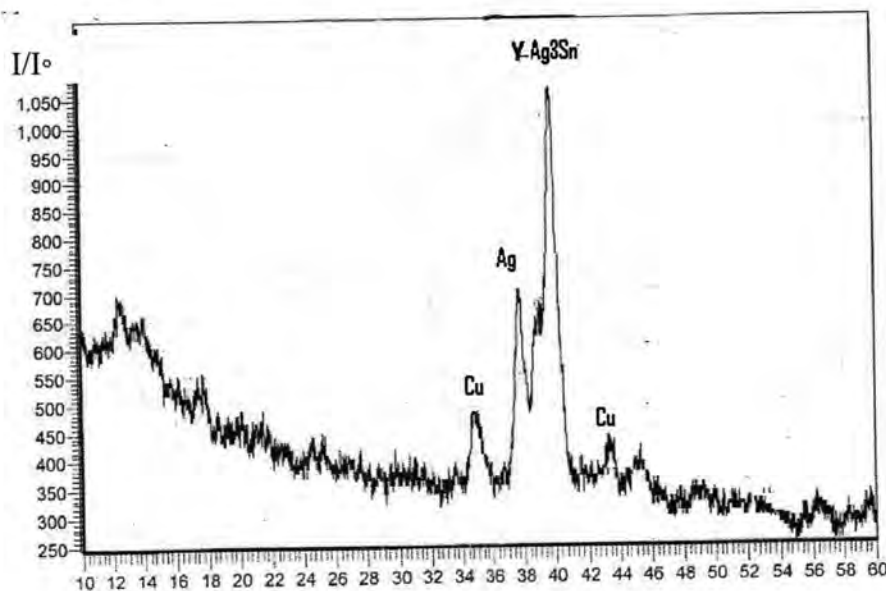
جدول-3: نتائج الصلادة الدقيقة لسبيكة (A) و (B)

الصلادة H.V	السبيكة
201.3	سبيكة A
231	سبيكة A1
239.2	سبيكة B
253.01	سبيكة B1

جدول -4: يبين معدل قيم الذوبانية

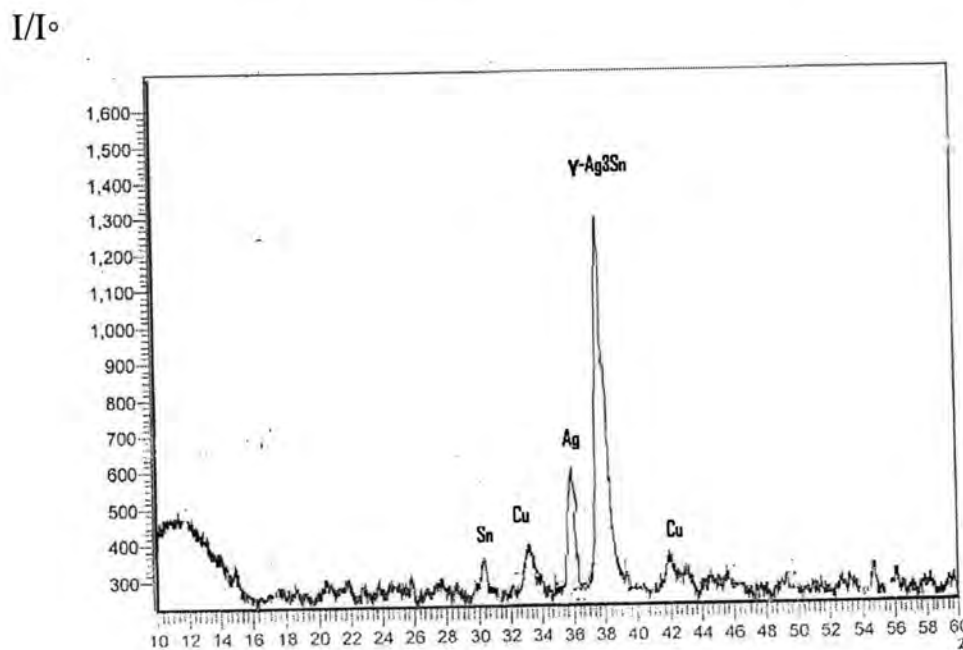
السبائك	الفضة	القصدير	النحاس	الزنك
سبيكة A	أقل من 0.02	18.5	0.00	
سبيكة A1	أقل من 0.03	8	0.00	
سبيكة B	أقل من 0.02	10,4	0.00	0.00
سبيكة B1	أقل من 0.02	4.03	0.00	0.00

المعاملة بطريقة الفرن الحراري وتقنية الليزر وتأثير إضافة الزنك على بعض الخواص الميكانيكية لسبيكة حشوة الاسنان
حليمه و جعفر و اقبال واطيف وسندس



20

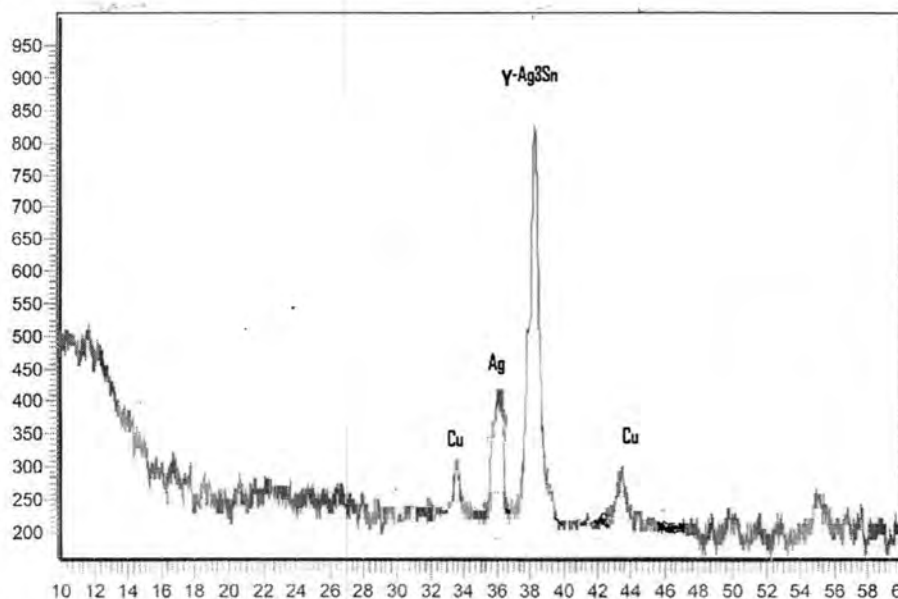
شكل 1- حيود الأشعة السينية لسبيكة حشوة الاسنان (A)



20

شكل 2- حيود الأشعة السينية لسبيكة حشوة الاسنان (A1)

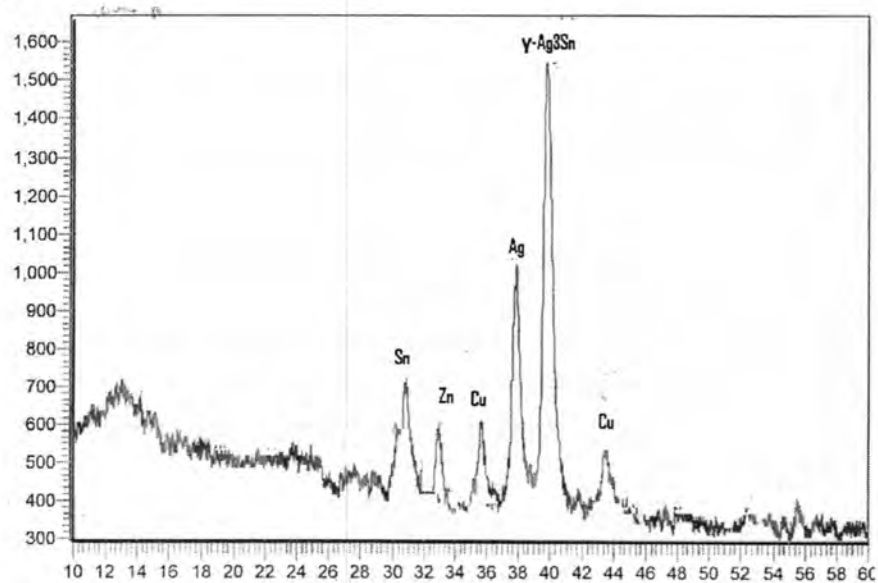
I/I_0



2θ

شكل 3: حيود الاشعة السينية لسبيكة حشوة الاسنان (B)

I/I_0



2θ

شكل 4: حيود الاشعة السينية لسبيكة حشوة الاسنان (B1)

المصادر

1. Helmut Knosp, Richard J Holliday, Christopher W. Corti, Gold in Dentistry: Alloys, Uses and Performance, Gold Bulletin , 36/3(2003).
2. Mark J. Jackson and Waqar Ahmed. Surface Engineered Surgical Tools and Medical Devices, 201-239, Friday, August 03, Springer US(2007)
3. M. Fathi PhD, V. Mortazavi DDS, A Review on Dental Amalgam Corrosion and Its Consequences. Journal of Research in Medical Sciences 1: 42-51. (2004).
4. سلام داود سلمان القيسي, ضياء حسين ابراهيم الدوري "المعادن والسبائك المستعملة في طب الاسنان" وزارة التعليم العالي والبحث العلمي هيئة المعاهد الفنية (1996)
5. N H Abu Kassim, N A Yahya, Z Radzi, W J Basirun, A A Ghani, Silverfil: Its Physical Characterization, Biomed 06, IFMBE Proceedings 15:134-136, (2007)
6. Karl-Johan M.S. derholm, Define the terms amalgam, amalgamation, dental amalgam alloys, low copper amalgams, high copper amalgams, lathe-cut powder, atomized powder, trituration, and condensation. C. Dental Amalgam, (1999)
7. P.J. Knibbs, C.G. Plant, D.S. Shovelton P.A. Jones, An evaluation of a lathe-cut high-copper amalgam alloy, Journal of Oral Rehabilitation. me 14:465 – 47. 8 Jun (2007).
8. J A.J I lick "Rapid surface heat treatment a Review of laser and electron beam hardening "Heat treatment of metal, 1 ,(1983).
9. Sindo.kov "fundamental study of laser transformation" Metallurgical transaction ,14 April, (1983) .
10. A.Gillénier. laser surface melting of cast iron processing structures hardness laser treatment of material England, (1987)
11. John, White Man Roy, 12 point on Mercury Toxicity Germany paper, (2001).
12. Lilinan Sandu, Valontin Birdeanu, Cristina Bortun, Florin Topala, Sorin Porojan, Laser welding optimizations for practical use in dental technology, 58:3 – 4 . 212 TMJ , (2008).
13. عبد الهادي يحيى الصائغ، فيصل عبد المجيد الكفيشي، زكي عبد الجبار الجبوري، علم البلورات (1981).
14. Robert G. Graig "Restorative Dentar Materials "tenth" Edition ,(1989).
15. R.G.Grai "Dental Material properties and Manipulation" 6th ed, book.inc.USA, (1996).
16. Awasumi H.K. "Metal surface Hardening with CO₂ laser" 6,(11) (1983).

تحضير وتشخيص معقدات بعض العناصر الانتقالية مع مشتقات 4،2،1-ثيادايازول

نجاة جواد العبيدي و سنان منحت البياتي

مختبرات قسم الكيمياء / كيمياء لاعضوية / كلية العلوم / الجامعة المستنصرية

الخلاصة

تتضمن هذه الدراسة ثلاث فصول الفصل الاول يتم فيه استعراض الادبيات الخاصة بالمركب 4،2،1-ثيادايازول ومشتقاته واهميته، ويتضمن الفصل الثاني تحضير الليكاندين (L_2, L_1) ومعقداتها مع الايونات الفلزية $[Cr(III), Mn(II), Co(II), Ni(II), Cu(II), Zn(II), Cd(II), Hg(II)]$ ، اما الفصل الثالث فاختص باستعراض نتائج تحضير الليكاندين (L_2, L_1) ومعقداتها واثبات صيغتها التركيبية بواسطة مطيافية ما تحت الحمراء، التحليل الدقيق للعناصر ومطيافية الأشعة فوق البنفسجية - المرئية وقياس درجة الانصهار وتحليل الفلزات بواسطة تقنية الامتصاص الذري وقياس العزم المغناطيسية والتوصيلية المولارية وقد بينت النتائج بان معقدات الليكاند (L_1) لها النسبة (1:1) باستثناء ($Ni(II), Co(II)$) حيث كانت النسبة (2:1) واطهرت ان معقدات ($Co(II), Mn(II), Cr(III)$) تأخذ شكل ثماني السطوح ومعقد ($Cu(II)$) أخذ شكل ثماني السطوح المشوه بشكل دايمر ومعقد ($Ni(II)$) أخذ شكل مربع مستوي في حين ان شكل رباعي السطوح قد اقترح لمعقدات ($Cd(II), Zn(II), Hg(II)$) اما معقدات (L_2) فان نسبة (1:1) لكل من ($Cu(II), Zn(II), Cd(II), Cr(III)$) ونسبة (2:1) لكل من ($Ni(II), Hg(II)$) بينما اخذت معقدات ($Co(II), Mn(II), Cr(II)$) شكل ثماني السطوح واخذ معقد ($Cu(II)$) شكل ثماني السطوح المشوه دايمر والمعقد ($Ni(II)$) أخذ شكل المربع المستوي واتخذت المعقدات ($Hg(II), Cd(II), Zn(II)$) شكل رباعي السطوح.

ABSTRACT

This study contain three paragraphs, the first one is introduction in which we reviewed the literature of 1,2,4- thiadiazole and its derivatives , the second part contain synthesis of two ligand (L_2, L_1) and their complexes with metal ions ($Cr(III), Mn(II), Co(II), Ni(II), Cu(II), Zn(II), Cd(II), Hg(II),$) and the third part deals with results and prepared of this ligand (L_2, L_1) and their complexes and proved their structure by the element analysis infra red, electronic spectral data and measurement of melting point , magnetic moment . These result explain that complexes of ligand (L_1) have molar ratio (1:1)(L:M) with exception of $Co(II), Ni(II)$ complexes which have (2:1)(L:M), also appeared that complexes of $Cr(II), Mn(II), Co(II)$ have octahedral structures and $Cu(II)$, have taken octahedral (dimmer) and complexes of ion $Ni(II)$ have taken square planner structure while the complexes of $Zn(II), Cd(II), Hg(II)$ have taken tetra hedral structure, the complexes of ligand (L_2) have molar ratio (1:1) (L:M) with complexes $Cr(III), Cu(II), Cd(II), Zn(II)$ and (2:1)(L:M) for $Mn(II), Co(II), Ni(II), Hg(II)$ the result of analysis appeared that complexes of ions ($Cr(II), Mn(II), Co(II)$) have taken octahedral structure and ($Cu(II)$) have taken octahedral (dimmer) and ($Ni(II)$) have taken square planner and tetrahedral structure suggested for ($Zn(II), Cd(II), Hg(II)$) complexes.

المقدمة

ان لاكتشافات ادوية السلفا الاثر الكبير في تخليق واكتشاف مشتقات جديدة للثيادايازولات كواحدة من المركبات الحلقية الغير متجانسة والمهمة بايولوجياً، يدعى الايزومر 4،2،1- ثيادايازول ازوسلفات امينات (1) او بيرثايوسيانات تحتوي هذه الحلقة في تركيبها على ذرة كبريت في موقع رقم واحد وذرتي نايتروجين في موقعين اثنان واربعة فضلاً على انها مركبات اروماتية تعاني تفاعلات تعويض الكتروليفية ونيوكوفيلية.

حُضر المشتق 3-اريل -5- مركبتو -4،2،1- ثيادايازول لأول مرة من قبل الباحث بيتر (2) باستخدام الاميدواوكسيم وذلك بتكثيفه مع (CS_2) او مع زيادة من ازوثايوسيانات البنزين المعوض

ويأتي السياق العام لتحضير هذا اللايزومر امكا بالغلق الحلقي الذاتي لمشتقات 4،2- ثنائي ثايوبايوريت (4،3) او بالغلق الحلقي الجزيئي متشابهين بالاكسدة لمشتقات او معوضات الايزوسيانات او الثايوبوريا بوجود عامل مؤكسد مثل بيروكسيد الهيدروجين او حامض النتروز (6،5) او بالغلق الحلقي لكبريتيدات النتريل باستخدام (tetra cyano ethylene) قات جديدة لهذا الايزومر هذا وقد اجريت دراسة بايولوجية موسعة لتحضير مركبات حلقة تاجية (9) لها فعالية ضد انواع مختلفة من البكتريا ناتجة من تكثيف -المشتق 5،3- ثنائي امينو 2،1،4- ثايدايازول مع المشتق ازواندولين والمركبات الحلقية التاجية التي تدخل من تفاعلات البايوكيميائية (10) كمضيف مرافق لجزيئات الاحماض الامينية والتي لها القدرة على التناسق مع الفلزات ذي الحجوم الذرية الكبيرة وتم تحضير قواعد شيف (11) كواحدة من المشتقات 1،4،2- ثايدايازول والمهمة بايولوجياً وجميع المشتقات التي تم تحضيرها للايزومر المذكور لها القدرة العالية على التناسق وتكوين معقدات مستقرة نظراً لامتلاك حلقة 1،2،4- ثايدايازول ذرتي نتروجين وذرة كبريت وهي مواقع مهمة للتأخر التناسقي خصوصاً عند وجود مجاميع معوضة على الحلقة في المواقع 3،5- قادرة على منح مزدوجات الكترونية الى فلزات العناصر الانتقالية وتكوين حلقات خماسية او سداسية مستقرة.

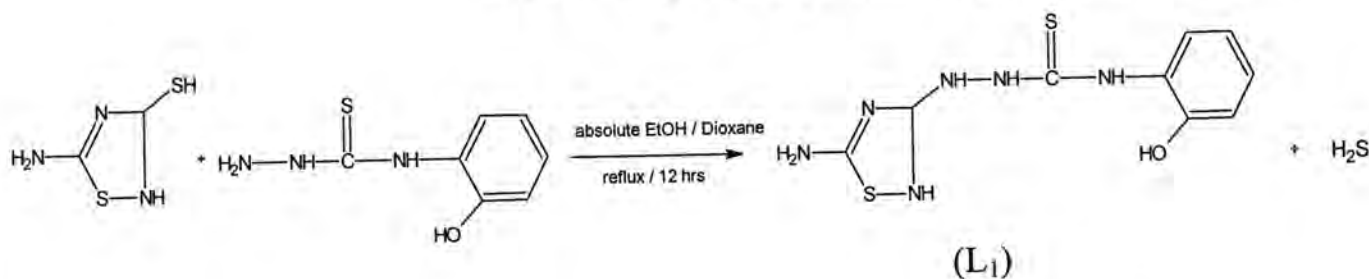
المواد وطرائق العمل

تحضير الليكاندات :

تحضير الليكاند الاول (L₁):

5-amino-3-[4'-O-hydroxy phenyl-thio semi carbazido-1, 2, 4- thiadiazole

يوزن (0.01mole, 1.33g) من 5-امينو-3-مركبتو-4،2،1- ثايدايازول ويذاب في (25ml) من الايثانول المطلق ويحرك المزيج بدرجة (70C°) لحين اكمال الذوبان ، ثم يضاف اليه (0.01mole, 1.83g) من (ortho - hydroxyphenylThiosemicarbazide) المذاب في مزيج من (15ml Ethanol absolute + 5ml Dioxane) ويجري التصعيد العكسي (Reflux) لمدة (12hrs.) ، وبعدها يبخر الى نصف الحجم الاصلي ويبرد في حمام ثلجي مع التحريك المستمر الى ان تتكون مادة زيتية تعاد بلورتها بالايثانول المطلق وتجفيفها لنحصل على راسب اصفر بمنتوج (1.94g ، 70%) والمبينة في المعادلة ادناه:



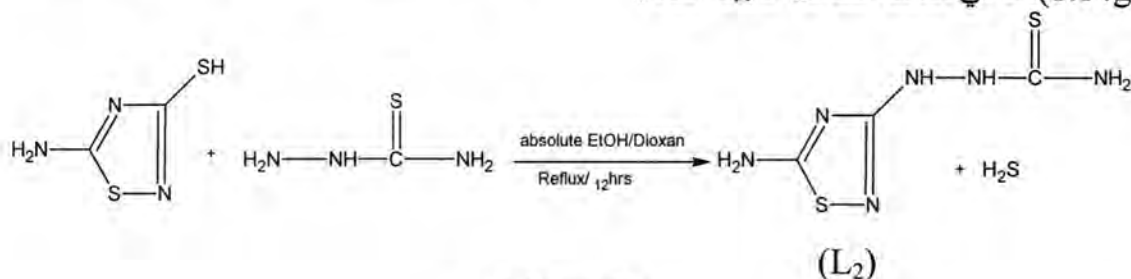
Scheme(1)

تحضير الليكاند الثاني L₂:

5-amino-3[4',Thiosemicarbazido]-1,2,4-thiadiazole

يوزن (0.01mole, 1.33g) من 5-امينو-3-مركبتو-4،2،1- ثايدايازول يذاب في (15ml) من الايثانول المطلق بدرجة (70C°) الى حين اتمام الاذابة ثم يضاف الثايوسيميكاربازيد (0.01mole, 1.2g) المذاب في

(15ml absolute EtOH + 5ml Dioxan) ويجري التصعيد العكسي لمدة (12hrs). يرشح الراسب ويغسل عدة مرات بالكلوروفورم فنحصل على راسب ابيض بلوري بمنتوج (60%, 1.14g) كما في معادلة التفاعل المبينة ادناه :



Scheme(2)

جدول -1: الخواص الفيزيائية للليكاندين المحضرين (L₁,L₂)

الصيغة الجزيئية	الوزن الجزيئي غم /مول	المنتوج % الوزن العملي (g)	درجة الانصهار C°	اللون	التحليل الدقيق للعناصر النظري (العملي)			
					C%	H%	N%	S%
C ₉ H ₁₀ N ₆ S ₂ O L ₁	282	70 (1.9)	(258-256)	اصفر	38.29 (37.39)	3.546 (3.28)	29.78 (28.82)	22.7 (22.4)
C ₃ H ₆ N ₆ S ₂ L ₂	190	60 (1.14)	(178-176)	ابيض	18.447 (18.50)	3.1579 (2.75)	44.2 (43.7)	33.68 (32.9)

تحضير المعقدات الفلزية:

1- تحضير معقدات (الكروم(III)، المنغنيز(II)، النحاس(II) والخاصين(II) والكاديوم(II) والزنك(II)

يضاف (0.38g,0.32,0.2g,0.14,0.197g,0.26g) من كلوريدات الايونات الفلزية المذابة في (10 مل) من الايثانول المطلق ((Cr(II),Mn(II),Cu(II),Zn(II),Cd(II),Hg(II)) على التوالي الى (1mmole,0.282g) من (L₁) او (1mmole,0.190g) من (L₂) المذاب في 15 مل من الايثانول المطلق يحرك المزيج لمدة ساعتين مع اجراء عملية التصعيد العكسي و تغيير الدالة الحامضية بالنسبة الى معقدي (Cr(III)) الى (pH=7.80) باضافة قطرات من الامونيا (10%) والى (pH=6.7) بالنسبة الى معقد (Mn(II)) بعدها يرشح الراسب لكل معقد ويخفف وتعاد بلورته بالايثانول المطلق .

2- تحضير معقدات كل من (Co(II),(Ni(II)) مع الليكانين (L₁) و (L₂) :

يضاف (1mmole,0.47g-0.627g) من كلوريد كل من (Co(II),(Ni(II)) على التوالي المذاب - 10 مل من الايثانول المطلق الى (2mmole-0.564g) من (L₁) او (2mmole,0.38g) من (L₂) المذابة ب 15 مل من الايثانول المطلق يحرك المزيج وتجرى له التصعيد العكسي لمدة ساعة ونصف بعدها تجفف الرواسب وتعاد بلورتها بالايثانول المطلق.

جدول رقم 2: الخواص الفيزيائية ونسب التحليل الدقيق للفلز في معقدات [L₁].

الصيغة الجزيئية	درجة الانصهار	Yield% الوزن العملي (g)	اللون	النسبة المئوية للفلز (M%)
C ₉ H ₁₀ N ₆ S ₂ O	258-256	70 (1.9)	اصفر	—
[Cr(C ₉ H ₁₀ N ₆ S ₂ O)(H ₂ O) ₂ Cl ₂]Cl	218 -220 d*	63 (0.3)	اخضر فاتح	10.9 (11.39)
[Mn(C ₉ H ₁₀ N ₆ S ₂ O)(H ₂ O) ₂ Cl ₂]	206-208 d*	56 (0.25)	اصفر خردلي فاتح	12.3 (14.5)
[Co(C ₉ H ₁₀ N ₆ S ₂ O) ₂ (H ₂ O) ₂]Cl ₂	224 -226d*	62 (0.627)	اخضر	8.48 (6.97)
[Ni(C ₉ H ₁₀ N ₆ S ₂ O) ₂]Cl ₂	210 -212 d*	59.6 (0.47)	برتقالي	8.46 (6.82)
[Cu ₂ (C ₉ H ₁₀ N ₆ S ₂ O) ₂ (H ₂ O) ₄ Cl ₂]Cl ₂	214 -216d*	45 (0.41)	بني غامق	14.04 (15.25)
[Zn(C ₉ H ₁₀ N ₆ S ₂ O)Cl ₂]	228-230 d*	48 (0.2)	اخضر فاتح جداً	15.62 (16.32)
[Cd(C ₉ H ₁₀ N ₆ S ₂ O)Cl ₂]	279-281 d*	66 (0.32)	اصفر فاتح جداً	24.15 (24.38)
[Hg(C ₉ H ₁₀ N ₆ S ₂ O)Cl ₂]	246-248 d*	52 (0.38)	اصفر فاتح جداً	36.23 (40.39)

جدول رقم 3: الخواص الفيزيائية ونسب التحليل الدقيق للفلزات في معقدات [L₂].

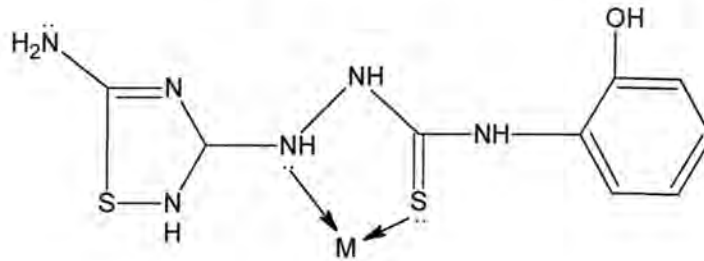
الصيغة الجزيئية	درجة الانصهار M.P.C°	اللون	المنتج % الوزن العملي (g)	النسبة المئوية للفلز M% العملي
C ₃ H ₆ N ₆ S ₂	(176-178)	ابيض لماع	60 (1.14)	—
[Cr(C ₃ H ₆ N ₆ S ₂)(H ₂ O) ₂ Cl ₂]Cl	(244-246)d*	اخضر	71 (0.274)	13.52 (13.7)
[Mn(C ₃ H ₆ N ₆ S ₂) ₂ (H ₂ O) ₂]Cl ₂	(258-260)d*	اخضر فاتح جداً	54.5 (0.29)	10.85 (8.01)
[Co(C ₃ H ₆ N ₆ S ₂) ₂ (H ₂ O) ₂]Cl ₃	(184-186)d*	رصاصي غامق	50 (0.274)	10.8 (11.02)
[Ni(C ₃ H ₆ N ₆ S ₂) ₂]Cl ₂	(280-282)d*	رصاصي مخضر	65 (0.34)	11.6 (12.37)
[Cu ₂ (C ₃ H ₆ N ₆ S ₂) ₂ (H ₂ O) ₄ Cl ₂]Cl ₂	(206-208)d*	بني فاتح	50.7 (0.33)	18.06 (16.99)
[Zn(C ₃ H ₆ N ₆ S ₂)Cl ₂]	(128-130)d*	ابيض	61 (0.2)	20.03 (21.38)
[Cd(C ₃ H ₆ N ₆ S ₂)Cl ₂]	(178-180)d*	اصفر فاتح جداً	67 (0.25)	30.1 (30.04)
[Hg(C ₃ H ₆ N ₆ S ₂) ₂]Cl ₂	(218-220)d*	رصاصي فاتح جداً	69 (0.45)	30.7 (31.5)

d*=decomposition

النتائج والمناقشة

أ- دراسة طيف الأشعة تحت الحمراء لليكاند الأول (L_1) ومعقداته :

يظهر جدول (4) امتصاصات غير متماثلة عند المنطقة ($3111-3157\text{cm}^{-1}$) والتي تشير الى مجموعة ($-\text{NH}_2$) الحرة عند موقع رقم 5 والتي لم تشهد اي انحراف فب المعقدات المحضرة وعدم مشاركة ذرة النتروجين مجموعة الامينو في التناسق اضافة الى ان الحزم العريضة السائدة ضمن المدى ($3150-3330\text{cm}^{-1}$) في المعقدات والتي تشير الى التأصر الهيدروجيني الحلقي الخماسي بين ذرة (H) لمجموعة ($-\text{NH}$) مجموعة الثايسيميكاربازون في موقع 4 مع اوكسجين مجموعة ($-\text{OH}$) حلقة الفينيل ، اما التغيرات الملحوظة في ترددات الاواصر ($\text{C}=\text{S}$) عند الموقع (1107cm^{-1}) عند الليكاند الحر والازاحة نحو التردد الواطي بمدى ($7-20\text{cm}^{-1}$) في المعقدات اي نقصان رتبة الاصرة هو دليل على دخول ذرة كبريت مجموعة ($\text{C}=\text{S}$) في التناسق مع الايونات الفلزية كذلك التغيرات التي تشهدها مجموعة (NH) لمجموعة الثايسيميكاربازون المرتبطة بحلقة الثايداديازول فقد شهدت ازاحة حمراء من (1363cm^{-1}) في الليكاند الحر الى ($1400-1373\text{cm}^{-1}$) في المعقدات المحضرة وزيادة رتبة الاصرة يدل على دخول هذه المجموعة في التناسق وتكوين حلقة كلايية خماسية مستقرة (12) كذلك ظهور حزم امتصاص جديدة عائدة للترددات الامتطاطية للاصرة ($\text{M}-\text{N}$) و ($\text{M}-\text{S}$) والتي تقع ضمن المديات المحددة في البحوث المنشورة (13) هو دليل اخر على ان التناسق يكون من ذرة كبريت مجموعة ($\text{C}=\text{S}$) وذرة (N) مجموعة ($-\text{NH}$) المرتبطة بحلقة الثايداديازول (نموذج a) اضافة الى حزم الترددات الواطية لمجموعة ($\text{M}-\text{Cl}$) والتي يتفق موقعها مع الادبيات المنشورة (14) لمعقدات كل من ($\text{Cr(III)Mn(II), Cu(II), Zn(II), Cd(II), Hg(II)}$) وكذلك جزيئات الماء المتناسقة مع الايون الفلزي المركزي والحزم العريضة التي تظهر عند المدى ($3500-3400\text{cm}^{-1}$) لمعقدات كل من ($\text{Mn(II), Cu(II), Co(II), Mn(II), Cr(III)}$) الاشكال (3-6).



نموذج (a)

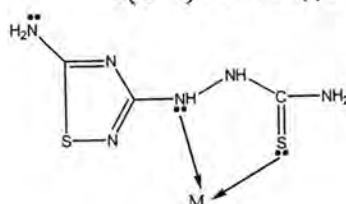
جدول 4-:- قيم الامتصاصات المميزة لطيف (IR) (vcm^{-1}) لليكاند (L_1) ومعدناته.

الصيغ الجزيئية	ν NH	ν C-N	ν C=S	ν C=N	ν M-N	ν M-S	ν M-Cl	ν -OH
$C_9H_{10}N_6S_2O$	3250	1363 (m)	1107 (m)	1537 (s)	—	—	—	3450 (s)
$[Cr(C_9H_{10}N_6S_2O)(H_2O)_2Cl_2]Cl$	3230	1400(s)	1080(w)	1543(s)	532	400	330	3450 (br.)
$[Mn(C_9H_{10}N_6S_2O)(H_2O)_2Cl_2]$	3221	1400 (m)	1090 (w)	1550 (s)	560	450	300	3425 (br.)
$[Co(C_9H_{10}N_6S_2O)_2(H_2O)_2]Cl_2$	3200	1400 (m)	1050 (w)	1525 (s)	590	420	—	3400 (br.)
$[Ni(C_9H_{10}N_6S_2O)_2]Cl_2$	3227	1380 (m)	1100 (w)	1550 (s)	574	470	—	3491 (br.)
$[Cu_2(C_9H_{10}N_6S_2O)_2(H_2O)_4Cl_2]Cl_2$	3226	1373 (m)	1090 (w)	1540 (s)	530	460	210	3400 (s)
$[Zn(C_9H_{10}N_6S_2O)Cl_2]$	3230	1380 (m)	1086 (w)	1545 (s)	510	430	310	3437 (br.)
$[Cd(C_9H_{10}N_6S_2O)Cl_2]$	3296	1386 (s)	1076 (w)	1533 (s)	570	450	300	3425 (br.)
$[Hg(C_9H_{10}N_6S_2O)Cl_2]$	3281	1375 (m)	1090(w)	1546 (s)	560	410	330	3433 (m)

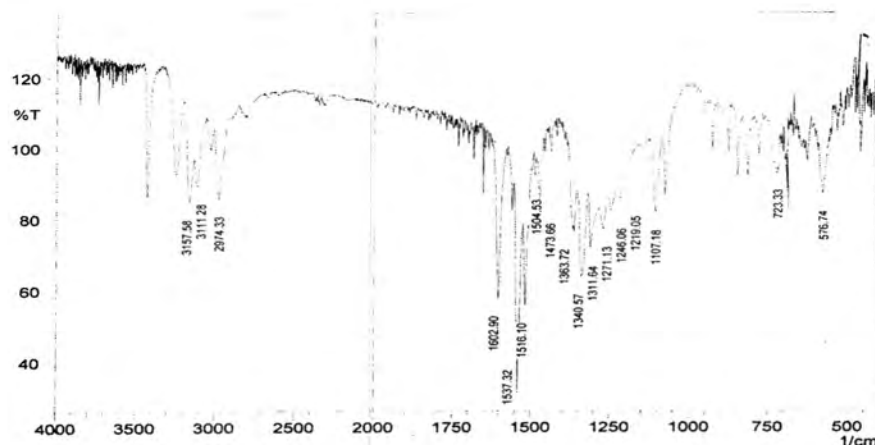
s=strong. m=medium. w = weak. br=broad.

2- دراسة طيف الاشعة تحت الحمراء لليكاند الثاني (L_2) ومعداته :

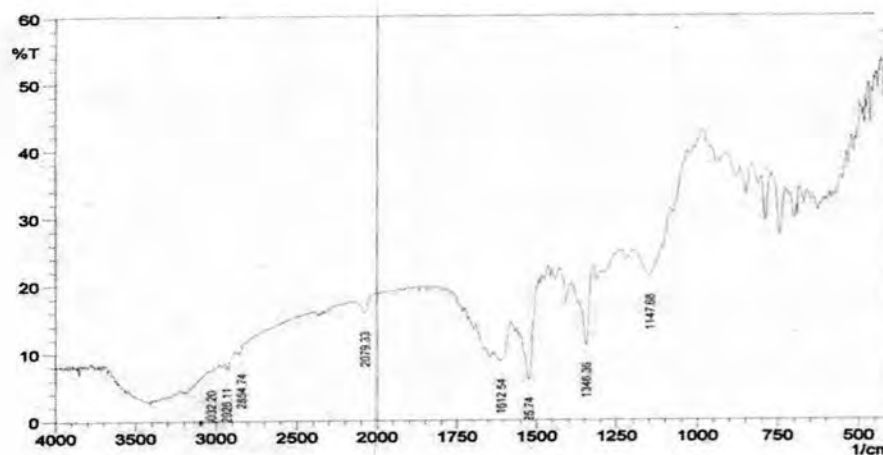
يوضح جدول (5) حزم الامتصاص المميزة لليكاند الحر (L_2) ومعقداته حيث يبدو جلياً ان الترددات الرئيسية عند ($1317-1284\text{cm}^{-1}$) لمجموعة ($\nu\text{C-N}$) و ($1645-1533\text{cm}^{-1}$) لمجموعة ($\nu\text{C=N}$) و (3265cm^{-1}) لمجموعة ($-\text{NH}$) و (1000cm^{-1}) لمجموعة ($\nu\text{C=S}$) حصل فيها انحرافات واضحة في المعقدات المحضرة عما كانت في الليكاند الحر يشير الى ان التناسق حصل بين ذرة كبريت مجموعة (C=S) والتي شهدت انخفاضاً في تردداتها في المعقدات المحضرة وبين ذرة نتروجين مجموعة ($-\text{NH}$) المرتبطة بحلقة الثايدايازول وتكوين النظام الكليتي الخماسي المستقر (12) (نموذج (b) اضافة الى الترددات الجديدة للاواصر التناسقية (M-N) ، (M-S) يؤكد هذا التناسق (13) هذا بالاضافة الى امتطاطات ضعيفة الشدة ضمن المدى ($330-310\text{cm}^{-1}$) والتي تشير الى ارتباطات (M-Cl) لمعقدات كل من (Cr(III)). و ($\text{Cd(II)}, \text{Zn(II)}, \text{Cu(II)}$) والحزم العريضة عند الموقع ($3340-3390\text{cm}^{-1}$) يوضح دخول جزيئات الماء في التناسق (14) مع الايونات الفلزية للمعقدات ($\text{Cu(II)}, \text{Co(II)}, \text{Mn(II)}, \text{Cr(III)}$) الاشكال (4-6).



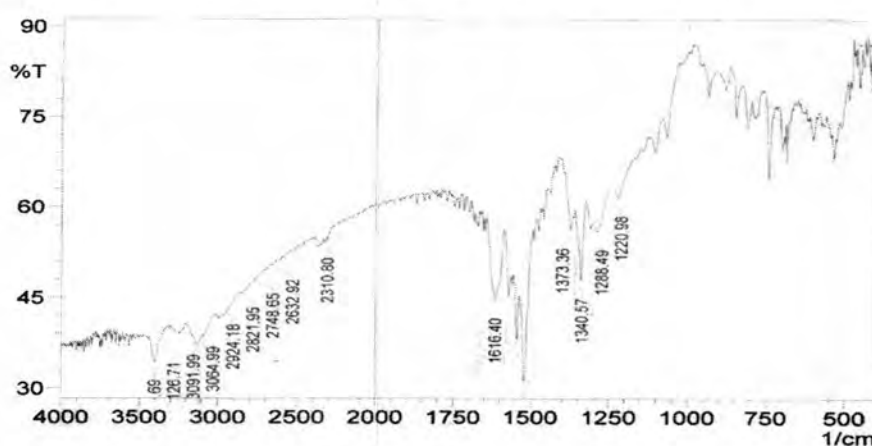
نموذج (b)



شكل-1: طيف الاشعة تحت الحمراء لـ $(C_9H_{10}N_6S_2O) L_1$ باستخدام أقراص KBr .



شكل -2: طيف الاشعة تحت الحمراء للمعقد $[Co(C_9H_{10}N_6S_2O)_2(H_2O)_2]Cl_2$ باستخدام أقراص CsI .

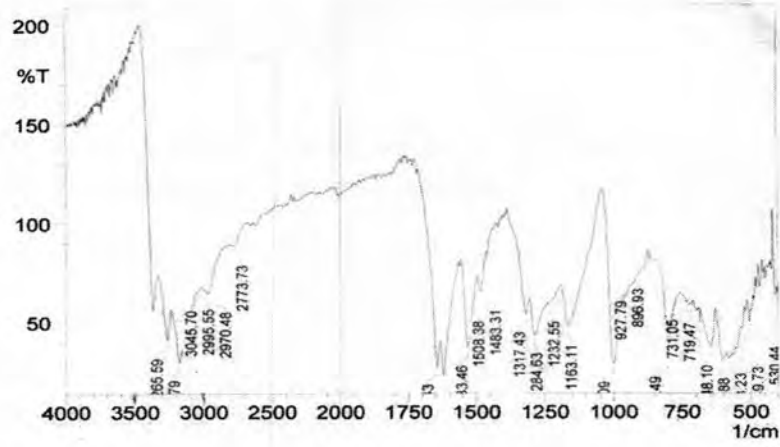


شكل-3: طيف الاشعة تحت الحمراء للمعقد $[Cu_2(C_9H_{10}N_6S_2O)_2(H_2O)_4]Cl_2$ باستخدام أقراص CsI

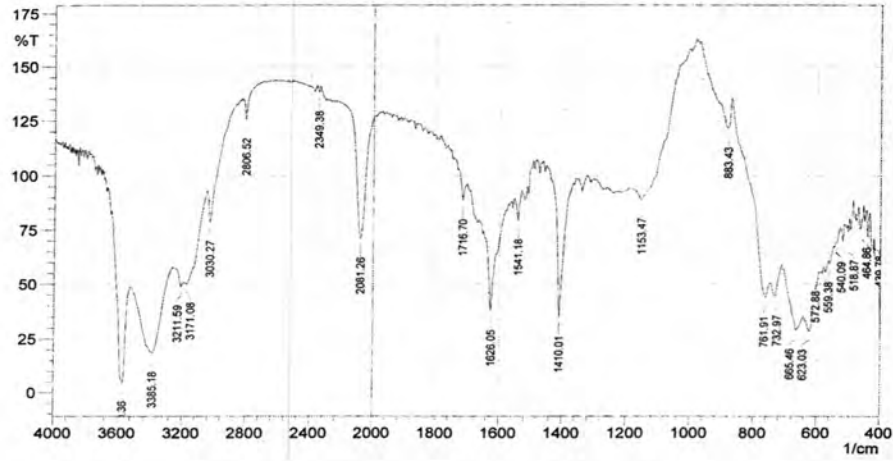
جدول 5- قيم الامتصاصات المميزة لطيف (IR) (vcm^{-1}) للبيكاند (L_2) ومعقداته.

الصيغ الجزيئية	νNH	$\nu (\text{C-N})$	$\nu (\text{C=S})$	$\nu (\text{C=N})$	$\nu (\text{M-N})$	$\nu (\text{M-S})$	$\nu (\text{M-Cl})$	νOH
$\text{C}_3\text{H}_6\text{N}_6\text{S}_2$	3265	1284-1317 (s)	1000 (s)	1533-1646 S	—	—	—	—
$[\text{Cr}(\text{C}_3\text{H}_6\text{N}_6\text{S}_2)(\text{H}_2\text{O})_2\text{Cl}_2]\text{Cl}$	3281	1398-1435 (s)	879 (w)	1556-1650 br.	698	430	327	3390 br
$[\text{Mn}(\text{C}_3\text{H}_6\text{N}_6\text{S}_2)_2(\text{H}_2\text{O})_2]\text{Cl}_2$	3385	1410 (vs)	883	1626 Vs	623	464	—	3600
$[\text{Co}(\text{C}_3\text{H}_6\text{N}_6\text{S}_2)_2(\text{H}_2\text{O})_2]\text{Cl}_3$	3281	1398-1406 (m)	887 (w)	1650 br	696	430	—	3037-3281 (br)
$[\text{Ni}(\text{C}_3\text{H}_6\text{N}_6\text{S}_2)_2]\text{Cl}_2$	3252	1381-1438 (m)	887 (w)	1608-1637 S	590	440	—	—
$[\text{Cu}_2(\text{C}_3\text{H}_6\text{N}_6\text{S}_2)_2(\text{H}_2\text{O})_4]\text{Cl}_2\text{Cl}_2$	3250	1360-1400 (vs)	980 (w)	1604-1631 Vs	600	450	310	3400
$[\text{Zn}(\text{C}_3\text{H}_6\text{N}_6\text{S}_2)\text{Cl}_2]$	3285	1390 (s)	890 (w)	1550-1600 S	540	400	310	—
$[\text{Cd}(\text{C}_3\text{H}_6\text{N}_6\text{S}_2)\text{Cl}_2]$	3260	1400 (s)	960 (w)	1650 S	563	410	330	—
$[\text{Hg}(\text{C}_3\text{H}_6\text{N}_6\text{S}_2)_2]\text{Cl}_2$	3218	1398 (m)	880 (m)	1598-1608 s	530	430	—	—

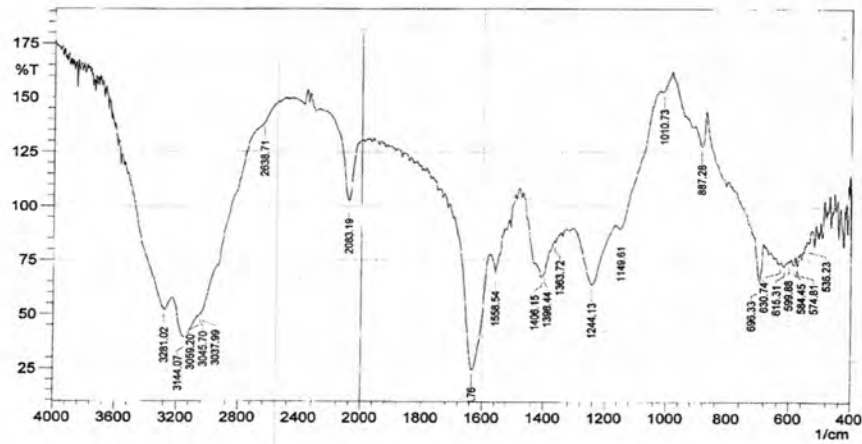
vs= very strong , s= strong , m= medium, br= broad.



شكل (4) طيف الاشعة تحت الحمراء ($C_3H_6N_6S_2$) باستخدام أقراص KBr .



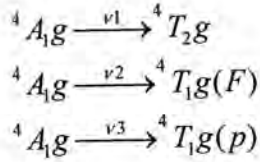
شكل 5: طيف الاشعة تحت الحمراء للمعقد $[Mn(C_3H_6N_6S_2)_2(H_2O)_2]Cl_2$ باستخدام أقراص CsI .



شكل 6: طيف الاشعة تحت الحمراء للمعقد $[Co(C_3H_6N_6S_2)_2(H_2O)_2]Cl_2$ باستخدام أقراص CsI .

الاطياف الالكترونية لمعقدات الليكاندين (L_1) و (L_2) 1- معقدات الكروم الثلاثي التكافؤ :

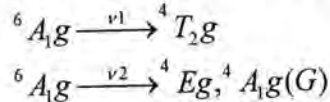
اظهر الطيف الالكتروني لكل من معقدي الكروم الثلاثي التكافؤ للليكانين (L_1) و (L_2) ثلاث حزم امتصاص موضح قيمتها بالجدولين (6،7) تعود الى الانتقالات:



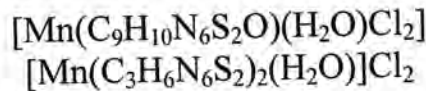
وهذه الانتقالات تقع ضمن مجال ثماني السطوح (16) اما قيم العزوم المغناطيسية فقد كان قيمة (μ_{eff}) للليكاند الاول مع ($Cr(III)$) مقداره (3.3BM) اما الليكاند الثاني شكل (12) فكانت (3.809BM) وهذه القيم تقع ضمن معقدات ثماني السطوح عالي البرم (17)،(18)،(19) ومن قيم التوصيلية المولارية والتي تؤكد ان المعقدين الكتروليتين وباستكمال هذه النتائج يمكن اقتراح الصيغة التالية للمعقدين $[Cr(C_9H_{10}N_6S_2O(H_2O)Cl_2)]Cl$ و $[Cr(C_3H_6N_6S_2)(H_2O)_2Cl_2]Cl$.

2- معقدات المنغنيز الثنائي التكافؤ:

اظهر الطيف الالكتروني لمعقدي المنغنيز الثنائي التكافؤ مع (L_1) و (L_2) حزمتي امتصاص موضح قيمتها في جدولين (6،7) هذه لحزمتين تابعة للانتقالين الاتيين:

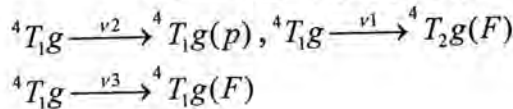


وبذلك فان المعقدين يأخذان شكل ثماني السطوح وهذا يتفق مع ما هو منشور في الادبيات (17)،(20) اما قيم العزوم المغناطيسية فتكون للمعقد الليكاند الاول مع ($Mn(II)$) ذات قيمة ($\mu_{eff}=2.5B.M$) فيكون هذا المعقد واطى البرم وتوجد مساهمة اوربيتالية (21)،(22). اما معقد الليكاند الثاني مع ($Mn(II)$) شكل (11) فان قيمته ($\mu_{eff}=5.304B.M$) وبذلك هو معقد عالي البرم اما قيم التوصيل المولاري فقد اظهرت النتائج في الجدولين (6،7) ان معقد (L_2Mn) غير الكتروليتي بينما يكون (L_1Mn) ايوني وبذلك وبعد استكمال النتائج امكن اقتراح الصيغة لكل منهما :

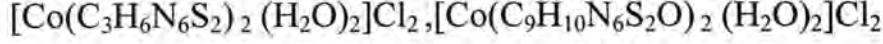


3- معقدات الكوبلت الثنائي التكافؤ:

يبين الطيف الالكتروني لمعقدات الكوبلت الثنائي التكافؤ مع الليكاندين (L_1) و (L_2) ظهر ثلاث حزم امتصاص قيمتها مبين في الجدولين (6،7) والتي تعزى الى الانتقالات

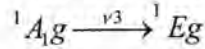
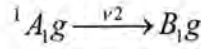
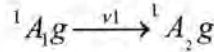


والتي تعزى الى ان المعقدات تأخذ شكل ثماني السطوح (23) اما قيم العزوم المغناطيسية فقد اظهر معقد (L_1Co) عزماً قدره ($\mu_{eff}=5.9B.M$) وهي قيمة عالية بسبب المساهمة الاوربيتالية كذلك تؤكد ان المعقد ذات شكل ثماني السطوح عالي اليرم (24)،(25) شكل (8) اما معقد (L_2Co) فان قيمة العزم المغناطيسي ($\mu_{eff}=3.58B.M$) اما قيم التوصيلية المولارية تؤكد ان المعقدين الكتروليتين وبذلك تكون الصيغة المقترحة لها كما يلي:

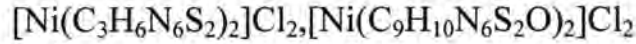


4- معقدات النيكل ثنائي التكافؤ:

أظهرت الاطياف الالكترونية لهذه المعقدات ثلاث حزم امتصاص موضحة في جدولين (6،7) والتي تعود الى الانتقالات شكل (9) :

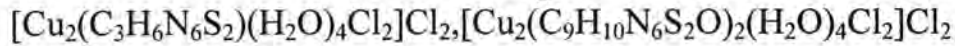


هذه الانتقالات تؤكد ان المعقدين تتخذ اشكال المربع المستوي (26) تدعمها قيم العزوم المغناطيسية المساوية للصفر هذا بالاضافة الى ان قيم التوصيل المولاري الذي تؤكد ان المعقدين الكتروليتين وبذلك وحسب هذه النتائج تكون الصيغة المقترحة:



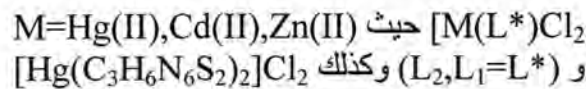
5- معقدات النحاس ثنائية التكافؤ:

تتخذ معقدات النحاس مع الليكاند الاول والثاني شكل ثماني السطوح المشوه (27) ذات حزمة امتصاص عريضة واحدة تعود الى الانتقال $^2Eg \rightarrow ^2T_2g$ اما قيم العزوم فانها تساوي ($\mu_{eff}=0.00$) وبذلك فان هذه المعقدات تكون بشكل دائري هذا بالاضافة الى انها معقدات الكتروليتية استنتاجاً من قيم التوصيلية المولارية وبذلك لها الصيغ المقترحة الآتية:



6- معقدات الزنك والكادميوم والزنابق الثنائية التكافؤ:

تتخذ معقدات كل من ($Hg(II)$) و ($Cd(II)$) ، ($Zn(II)$) شكل الرباعي السطوح وهو التناسق المشاع لهذه المعقدات ولا تمتلك اطياف الكترونية وقيم (μ_{eff}) لانها مشبعة وجميعها غير الكتروليتية بالاعتماد على قيم التوصيل المولاري ما عدا (L_2Hg) فانه الكتروليتي وبذلك نأخذ الصيغة المقترحة:

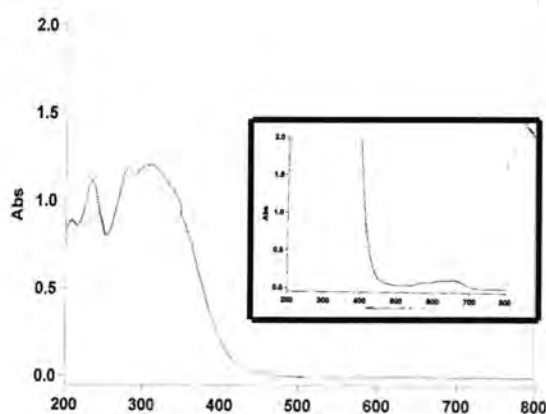


جدول 6- :- الاطياف الالكترونية لمعقدات الليكاند [L₁] في مذيب الايثانول المطلق

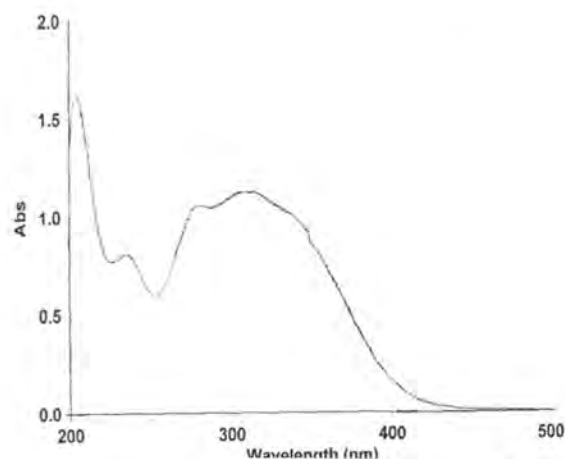
الصيغة الجزيئية	حزم الامتصاص (cm ⁻¹)	تشخيص الانتقال	μ _{eff} (B.M)	الشكل المقترح	Λ _m ohm ⁻¹ .cm ² .ml ⁻¹
C ₉ H ₁₀ N ₆ S ₂ O	32258 49019	n→π* π→π*	—	—	—
[Cr(C ₉ H ₁₀ N ₆ S ₂ O)(H ₂ O) ₂ Cl ₂]Cl	15625 28735 34364	${}^4A_{2g}(F) \xrightarrow{\nu_1} {}^4T_{2g}(F)$ ${}^4A_{2g}(F) \xrightarrow{\nu_2} {}^4T_{1g}(F)$ ${}^4A_{2g}(F) \xrightarrow{\nu_3} {}^4T_{1g}(P)$	3.308	O.h	38.6
[Mn(C ₉ H ₁₀ N ₆ S ₂ O)(H ₂ O) ₂ Cl ₂]	14306 23584	${}^6A_{1g} \xrightarrow{\nu_1} {}^4T_{2g}$ ${}^6A_{1g} \rightarrow {}^4E_g, {}^4A_{1g}(G)$	2.54	Oh.	12
[Co(C ₉ H ₁₀ N ₆ S ₂ O) ₂ (H ₂ O) ₂]Cl ₂	15337 26109 27174	${}^4T_{1g}(F) \xrightarrow{\nu_1} {}^4T_{2g}(F)$ ${}^4T_{1g}(F) \xrightarrow{\nu_2} {}^4T_{1g}(P)$ ${}^4T_{1g}(F) \xrightarrow{\nu_3} {}^4A_{2g}(F)$	5.9	Oh.	70
[Ni(C ₉ H ₁₀ N ₆ S ₂ O) ₂]Cl ₂	12870 24570 27173	${}^1A_{1g} \xrightarrow{\nu_1} {}^1A_{2g}$ ${}^1A_{1g} \xrightarrow{\nu_2} {}^1B_{1g}$ ${}^1A_{1g} \xrightarrow{\nu_3} {}^1E_g$	0.84	S.P	80
[Cu ₂ (C ₉ H ₁₀ N ₆ S ₂ O) ₂ (H ₂ O) ₄ Cl ₂]Cl ₂	11358	${}^2E_g \rightarrow {}^2T_{2g}$	0.00	Oh.	90

جدول 7- : الاطياف الالكترونية لمعقدات الليكاند [L₂] في مذيب (DMSO)

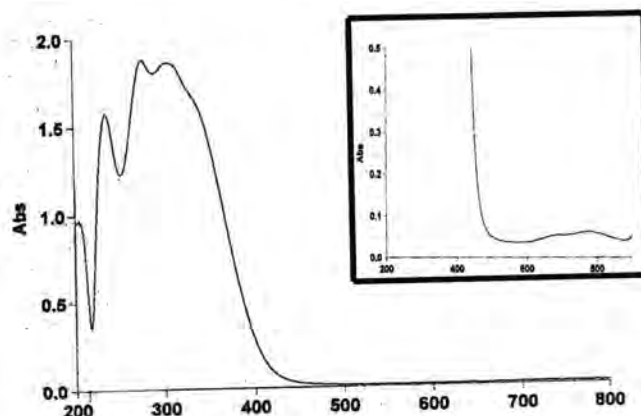
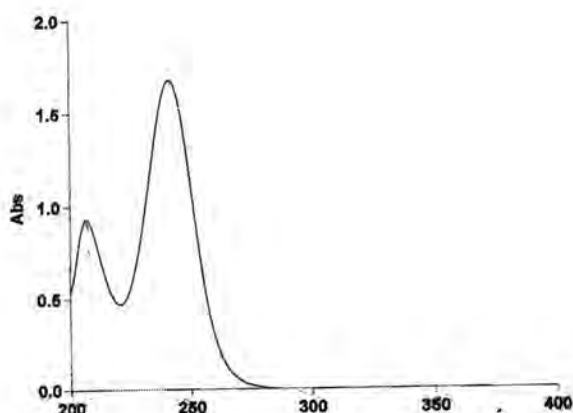
الصيغة الجزيئية	حزم الامتصاص (cm ⁻¹)	تشخيص الانتقال	μ_{eff} (B.M)	الشكل المقترح	Λ_m ohm ⁻¹ .cm ² .ml ⁻¹
C ₃ H ₆ N ₆ S ₂	41493 48309	$n \rightarrow \pi^*$ $\pi \rightarrow \pi^*$	—	—	—
[Cr(C ₃ H ₆ N ₆ S ₂)(H ₂ O) ₂ Cl ₂]Cl	16155 21978 25000 36496	${}^4A_{2g} \rightarrow {}^4T_{2g}$ ${}^4A_{2g} \rightarrow {}^4T_{1g}(F)$ ${}^4A_{2g} \rightarrow {}^4T_{1g}(P)$ Charge transfer	3.809	O.h high	40
[Mn(C ₃ H ₆ N ₆ S ₂) ₂ (H ₂ O) ₂]Cl ₂	18167 22624	${}^6A_{1g} \rightarrow {}^4T_{2g}$ ${}^6A_{1g} \rightarrow {}^4E_g, {}^4A_{1g}(G)$	5.304	O.h high	63
[Co(C ₃ H ₆ N ₆ S ₂) ₂ (H ₂ O) ₂]Cl ₂	14492 18518 23809	${}^4T_{1g} \xrightarrow{v_1} {}^4T_{2g}(F)$ ${}^4T_{1g} \xrightarrow{v_2} {}^4T_{1g}(P)$ ${}^4T_{2g} \xrightarrow{v_3} {}^4A_{1g}(F)$	3.558	O.h high	74
[Ni(C ₃ H ₆ N ₆ S ₂) ₂]Cl ₂	11764 21978 25706	${}^4A_{1g} \rightarrow {}^4A_{2g}$ ${}^1A_{1g} \rightarrow {}^1B_{1g}$ ${}^1A_{1g} \rightarrow {}^1E_g$	0.00	S.P	78
[Cu(C ₃ H ₆ N ₆ S ₂) ₂ (H ₂ O) ₄ Cl ₂]Cl ₂		${}^2E_g \rightarrow {}^2T_{2g}$	0.00	O.h	93



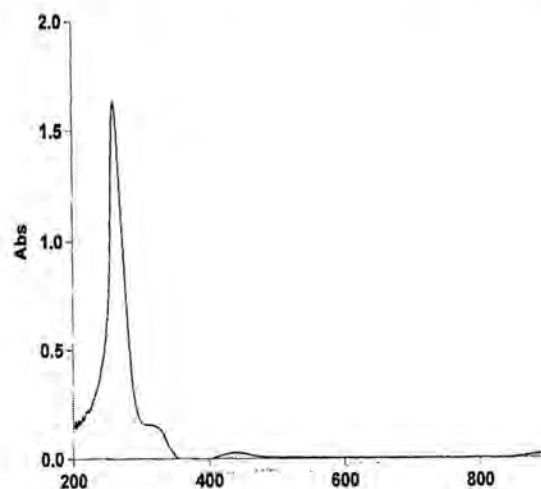
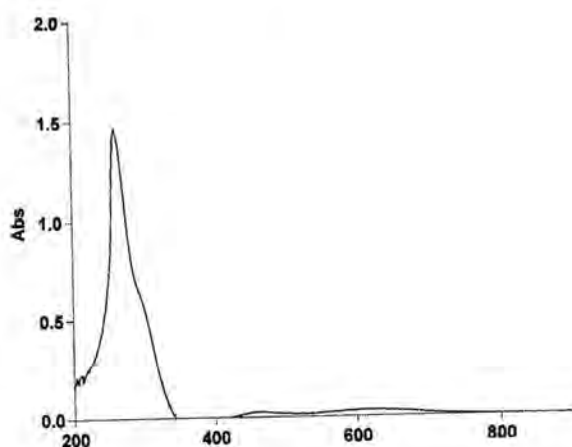
شكل-8: طيفم الأشعة فوق البنفسجية - المرئية للمعقد
[Co(C₉H₁₀N₆S₂O)₂(H₂O)₂]Cl₂



شكل-7: طيفم الأشعة فوق البنفسجية - المرئية للـ
(C₉H₁₀N₆S₂O)(L₁)



شكل 9- طيف الأشعة فوق البنفسجية - المرئية للـ $[\text{Ni}(\text{C}_9\text{H}_{10}\text{N}_6\text{S}_2\text{O})_2]\text{Cl}_2$ شكل 10- طيف الأشعة فوق البنفسجية - المرئية للـ $(\text{C}_3\text{H}_6\text{N}_6\text{S}_2)(\text{L}_2)$



شكل 25- طيف الأشعة فوق البنفسجية - المرئية للمعقد $[\text{Cr}(\text{C}_3\text{H}_6\text{N}_6\text{S}_2)_2(\text{H}_2\text{O})_2\text{Cl}_2] \text{Cl}$

شكل 11- طيف الأشعة فوق البنفسجية - المرئية للمعقد $[\text{Mn}(\text{C}_3\text{H}_6\text{N}_6\text{S}_2)_2(\text{H}_2\text{O})_2]\text{Cl}_2$

المصادر

1. W.Sherman . "Heterocyclic compounds"(R.C.Elderfield Ed.),7,:558 Ed Seq. Wiley, New York (1961)
2. Birr .E.J. Germanpatent,950,537;"Chemistry Abstract",53, 17737 (1959).
3. J.E.Franz, O.P.Dginga"Comprehensive Heterocyclic Chemistry" Wily,6,463(1984).
4. D.J.Wilkins,P.A.Bradley"Comprehensive Heterocyclic Chemistry"4,307 (1996).

5. N.S.Cho.,J.H.Moon and S.K.Kang"Synthetic and spectroscopic study of 5- Amino-2-acyl-1,2,4-thiadiazole-3-ones" J.Heterocyclic Chem.,35,1435 (1998).
6. J.Goerder,H.Groshopp and U.Sommerland,Chem.Ber.,90182(1952).
7. John,E.F.,Robert,K.H. and Helen,K.P., "Periselectine of Nitrile Sulfides, Nitrile Oxides, and Di phenyl diazomethane to tetracyano ethylene" J.Org.Chem.,.41,(4)(1976).
8. J.E.Franz,R.K.Howe and H.K.Pearl" Periselective Addition of Nitrile Sulfides, Nitrile Oxides, and diphenyl diazomethane to Tetracyanoethylene" J.Org..Chem.,41(4)(1976).
9. A.Smirnov,V.Aleksand and B.Tomchin,J.Heterocyclic Chem.47,1718(2002).
- 10.N.S.Cho.,Y.H.Kim and C.H.Lee" Converrgent synthesis of Macrocycles composed of 5-amino-2H-1,2,4-thiadiazole-3-one or 5-amino-2H-1,2,4-thiadiazole-3-thione and 1,3-benzene dimethane thiol" Bull.KoreanChem.Soc.25,10(2004).
- 11.M.N.Al-Jubouri and N.J.Al-Obaidi " Synthesis and Characterization of New Derivative of 1,2,4-thiadiazole and their transition Metal Complexes of Expected Biological Activity Ph.D. of Sci. in Chem.Ph.D thesis , Al-Mustansirya University(2003).
- 12.K.Nakamoto,"Infrared of Inorganic and Coordination Compounds" 6th Ed.,John-Wiely,Inc.,New York,London,(1997).
- 13.K.Nakamoto,"Infrared and Raman Spectra of Inorganic and Coordination Compounds" 4th Ed.,Wiely,Inc.,New York(1986).
- 14.R.M.Silver Stein,G.C.Bassler and T.G.Morrill,"Spectrometric Identification of Organic Compounds", 4th Ed.,John-Wiely and Sons , Inc.New York, London,(1981).
- 15.N.N.Green Wood and A.Earnshaw"Chemistry of Element" 2nd .Ed.Preyamon Press(1998).
- 16.A.B.P.Lever"Inorganic Electronic Spectroscopy":274-281,New York (1968).
- 17.D.Sutton,"Electronic spectra of transition metal complexes" 1st Ed., Mc.Graw-Hill Publishing,London(1968).
- 18.B.N.Figgis"Introduction to Ligand Fields" John-wiely and sons,Inc.,New York,(1966).
19. N.B.J "Inorganic Nucluer Chemistry"41: 1384-1385(1979).
- 20.K.Burger"Coordination Chemistry , Experimental Methods" London Bult/Worths and Co.Publishers,Ltd.(1978).
- 21.C.K.Jorgenson"Absorption Spectra and Chemical Bonding in Complexes" Perganmon Press (1964).

- 22.D.Nicholis"Complexes and First Row Transition Elements" Translated by Wissam.Ibrahim(1983).
- 23.T.Sarojini and A.Ramachandraiah," Synthesis and Characterization of Cobalt(II),Copper(II),Nickel ,Iron(II) and OxoVanadium(IV) Chelates of New Pair of Schiff base Ligands derived from 1,3-bis(amino methyl) Cyclohexane"J.Indian od Chem.,35A,940-945(1996).
- 24.Konig E."Structure and bonding ", :175(1971).
- 25.N.N.Freen Wood and A.Earn Chaw,"Chemistry of the Elements",2nd .,Pergaman Press,(1998).
- 26.A.Antipas and M.Gouterman"Electronic States of Co(II),Ni(II),Rh(II) and Pd(II) Complexes J.Am.,Chem.Soc.,105(23),(1983).
- 27.D.Nicholls"Complexes and 1st. Raw Transition Elements",2st .Ed. London and Basing stoke(1974).

تقديرات طيفية امتصاصية جزيئية واخرى ذرية للمضادات الحيوية: الامبيسيلين والاموكسيسلين والسيفالكسين والسيفترايكون والسيفوتاكسيم في بعض المستحضرات الصيدلانية

¹ فاضل جاسم محمد و ² منى محمود خضير و ³ انتظار ناصر حسون

¹ قسم الكيمياء/كلية العلوم/جامعة بغداد

² دائرة بحوث الكيمياء والصناعات البتروكيمياوية/وزارة العلوم والتكنولوجيا

³ دائرة بحوث الكيمياء والصناعات البتروكيمياوية / وزارة العلوم والتكنولوجيا

ABSTRACT

This research aims to develop new chemical reaction to determine some of beta lactam antibiotics which include Ampicillin, Amoxycillin, Cephalexin, Ceftriaxone and Cefotaxime in some pharmaceuticals using indirect Flame Atomic Absorption and Molecular Absorption . This include the preparation of new chelate complexes by reaction of drugs Ampicillin, Amoxycillin, Cephalexin, Ceftriaxone and Cefotaxime with palladium ion and using them for the UV-Vis determination at $\lambda_{max}=390$ nm. Benzyl alcohol proved to be the best organic solvent for extraction of the complexes without interference .

The analytical figures of merits obtained on applying the developed procedure for Ampicillin, Amoxycillin, Cephalexin, Ceftriaxone and Cefotaxime determination resp. was:-

Linear dynamic range [(5-50),(5-50),(3-50),(3-100),(3-65)] $\mu\text{g.ml}^{-1}$

LOD(0.3407, 0.4683, 0.2426, 0.3930, 0.1792) $\mu\text{g.ml}^{-1}$.

Erel% (1.4660%, 1.5833%, 2.0833%, 1.9160%, 3.1666%).

Recovery% (101.46%, 101.58%, 102.08%, 101.91%, 103.16%).

The structures of the metal-chelate complex for the five drugs were found to be 1:1 ;M:L,the stability constants of the five complexes are(10.49×10^5 , 1.16×10^5 , 1.16×10^5 , 0.51×10^5 , 10.69×10^5) M^{-1} resp.

The developed procedures have been applied to the determination of drugs Ampicillin, Amoxycillin, Cephalexin, Ceftriaxone, and Cefotaxime in pharmaceutical preparations Pesillin, Pulmoxyl, Cephalexin, Gramocof, and Sefotak using direct and standard addition methods. The analytical results match well with the drug contents as indicated by the recovery percent had : (90.71%, 104.03%, 96.86%, 95.63%, 97.86%).

A new FAAS has been established for the determination of Ampicillin, Amoxycillin , Cephalexin, Ceftriaxone and Cefotaxime in pharmaceutical preparations: Pesillin, Pulmoxyl, Cephalexin, Gramocof, and Sefotak these complexes were extracted with benzyl alcohol. The analytical figures of merits obtained on applying the developed procedure for Ampicillin, Amoxycillin , Cephalexin, Ceftriaxone and Cefotaxime resp. was:-

Linear dynamic range (1.5-17), (1.5-17), (3-17), (3-33), (3-22) $\mu\text{g.ml}^{-1}$.

LOD (0.6474, 0.4968, 0.8674, 1.0098, 1.1413) $\mu\text{g.ml}^{-1}$.

Erel% (1.8883%, 4.2565%, 4.2565%, 2.7520%, 3.9060%).

Recovery% (101.88%, 104.25%, 102.75%, 103.90%, 103.42%).

The optimal experimental conditions concentration of pd ion was (5) $\mu\text{g.ml}^{-1}$ The developed procedures have been applied to determination of drugs Ampicillin, Amoxycillin , Cephalexin, Ceftriaxone and Cefotaxime in pharmaceutical preparations: Pesillin, Pulmoxyl, Cephalexin, Gramocof, and Sefotak using direct and standerd addition methods the analytical results mach well with the drug content as indicated by the recovery percent had: (92.42%, 99.34%, 96.43%, 94.05%, 98.28%).

الخلاصة

يتضمن البحث استحداث تفاعل كيميائي لتقدير بعض المركبات الدوائية المضادة للبكتريا وهي الامبيسيلين والاموكسيسلين والسيفالكسين والسيفترايكون والسيفوتاكسيم اللتي تنتمي الى عائلة مضادات البيتا لاکتام باستعمال طرائق تحليلية مختلفة منها طريقة الامتصاص الذري اللهبى غير المباشر وطريقة امتصاص الاشعة فوق البنفسجية والمرئية. اذ تم

فاضل و منى و انتظار

تحضير معقدات مخلبية من تفاعل الادوية المذكورة مع ايون البلاديوم الثنائي وتقديرها بمطيافية امتصاص الاشعة فوق البنفسجية والمرئية بهيئة معقدات مخلبية تقاس ممتصيتها عند الطول الموجي (390) نانوم بعد استخلاصها بمذيب عضوي مناسب هو كحول البنزول ودراسة الظروف التجريبية المثلى للتفاعل وبلغت مديات خطية التراكيز التي تطيع قانون بيرفي تقدير الامبيسلين (5-50) مايكروغرام.مل⁻¹ والاموكسيسلين (5-50) مايكروغرام.مل⁻¹ والسيفالكسين (3-50) مايكروغرام.مل⁻¹ و السيفترايكسون (3-100) مايكروغرام.مل⁻¹ والسيفوتاكسيم (3-65) مايكروغرام.مل⁻¹ اما حدود الكشف بلغت (0.3407، 0.1792، 0.3930، 0.2426، 0.4683) مايكروغرام.مل⁻¹ للادوية الخمسة على التوالي. وبلغ الخطأ النسبي المنوي (1.4660% و 1.5833% و 2.0833% و 1.9160% و 3.1666%) ، أما الاستردادية فكانت (101.46% و 101.58% و 102.08% و 101.91% و 103.16%) للادوية الخمسة على التوالي. وكذلك تم تقدير الادوية الامبيسلين والاموكسيسلين والسيفالكسين والسيفترايكسيم بتفاعلها مع ايون البلاديوم الثنائي وتكوين معقدات مخلبية مستقرة لايام عدة باستعمال مطيافية الامتصاص الذري اللهبى بعد دراسة الظروف العملية المثلى في التقدير ، إذ وجد ان افضل تركيز لأيون البلاديوم الثنائي هو (5) مايكروغرام.مل⁻¹ للادوية الخمسة. وبلغت مديات التركيز في تعيين الادوية (17-1.5)، (17-3)، (33-3)، (22-3) مايكروغرام.مل⁻¹ للادوية الخمسة على التوالي. في حين بلغت حدود الكشف (0.6474، 0.4968، 0.8674، 1.0098، 1.1413) مايكروغرام.مل⁻¹ للادوية الخمسة على التوالي. وبلغ الخطأ النسبي المنوي (1.8883% و 4.2565% و 2.7520% و 3.9060% و 3.4296%) ، أما الاستردادية فكانت (101.88% و 104.25% و 102.75% و 103.90% و 103.42%) للادوية الخمسة على التوالي. تم تعيين الادوية الامبيسلين والاموكسيسلين والسيفالكسين والسيفترايكسون والسيفوتاكسيم في المستحضرات الصيدلانية الآتية Pulmoxyl، Pesillin، Sefotak، Gramocef، Cephalixin على التوالي بالطريقة المستحدثة وبأسلوب منحني المعايرة المباشرة وأسلوب اضافات القياس بمطيافية الامتصاص الجزيئي والذري.

المقدمة

المضادات الحيوية مواد كيميائية تنتج من الاحياء المجهرية والانسجة الحية الاخرى ، لها القابلية على تثبيط نمو البكتريا والاحياء المجهرية حتى وان كانت بتركيز قليلة ، تتميز المضادات الحيوية بصفتين اساسيتين هما فعاليتها الحياتية العالية داخل جسم الكائن الحي والسمية القليلة مما يجعلها تستعمل لعلاج الامراض المعدية (1، 2) وتختلف المضادات الحيوية بالتراكيب الكيميائية ومدى الاوزان الجزيئية اذ تتراوح من (100 - 13000) غم/مول لكن اغلبها تكون مدى اوزانها الجزيئية من (300 - 800) غم/مول.

تنتج المضادات الحيوية من احياء مجهرية عديدة مثل Algae, Bacteria, Fungi, Antinomycetes ، تعمل المضادات الحيوية بميكانيكيات مختلفة (3) اذ يقوم عدد كبير منها بتثبيط تكوين جدار خلية البكتريا وبعضها يقوم بتثبيط تكوين البروتين والقسم الاخر يقوم بتثبيط عمل الغشاء السايوتوبلازمي ، اما الصنف الاخير فيتضمن تثبيط تكوين الاحماض النووية RNA, DNA.

تتميز البكتريا (4) بامتلاكها جدار خلية خلافا للخلايا السرطانية مما يجعل المضادات الحيوية من نوع بيتا لاكتام فعالة جدا تجاه الخلايا البكتيرية ، اما المضادات الحيوية التي تعمل على تثبيط تكوين الاحماض النووية Adriamycin فلها تأثير سمي كبير في الخلايا السرطانية اذ تكون اكثر فاعلية في تثبيط نمو الخلايا السرطانية مقارنة مع الخلايا البكتيرية ، لذلك يكون المضاد الحيوي Adriamycin فعالاً جداً لعلاج امراض كثيرة ومن ابرزها السرطان.

تتمتع المضادات الحيوية (5) باستعمالات واسعة منها ما يأتي :-

- 1- علاج الالتهابات الناتجة عن البكتريا.
 - 2- علاج الاورام السرطانية.
 - 3- علاج السل والجذام.
 - 4- علاج الامراض الناتجة عن الفطريات.
 - 5- علاج الامراض الناتجة عن الفيروسات.
 - 6- لها استعمالات واسعة ومتنوعة مثل مضافات لأطعمة الحيوانات لغرض زيادة نموها وكما تستعمل في القضاء على الطفيليات المعوية الموجودة في الانسان والحيوان.
- تعد مضادات (5) البيتا لاكتام من اهم اصناف المضادات الحيوية المستعملة لعلاج الامراض المعدية وتشمل عدداً كبيراً من المركبات الحاوية على حلقة بيتا لاكتام الرباعية الذرات ، تعمل هذه المضادات على

تنشيط تكوين جدار خلية البكتريا ان فعالية مضادات البيتا لاكتام (6-8) تعتمد على الاسيلة الانتقائية التي تؤدي الى تثبيط عمل انزيم انتقال السلسلة الببتيدية الضروري لتكوين جدار الخلية البكتيرية.

وتعد البنسيلينات (9) واحدة من عائلة المضادات الحيوية التي تمتلك تراكيب كيميائية متشابهة وسلوكاً حياتياً متشابهاً وبخاصة ضد بكتريا Gram-positive. وتحتوي نواة جزيئة البنسيلين على نظام ثنائي الحلقة الذي يضم حلقة البيتا لاكتام β -lactam ملتحمة مع حلقة ثيازولدين Thiazolidine Ring، تختلف البنسيلينات عن بعضها بطبيعة المجاميع المعوضة في السلسلة الجانبية المرتبطة بالنظام ثنائي الحلقة. توالى التطورات (9) للعمل على هذا الصنف من المضادات الحيوية من جوانب عديدة منها طرائق التحضير والعمل على زيادة نسبة المنتج وتقليل الشوائب غير المرغوب فيها للحصول على مادة ذات نقاوة عالية.

وتمثل السيفالوسبورينات (5) مجموعة كبيرة من مضادات البيتا لاكتام الحاوية على حلقة بيتا لاكتام الرباعية الذرات الملتحمة من خلال ذرتي النتروجين والكربون الى حلقة سداسية غير متجانسة مكونة حلقة تسمى Dihydrothiazine، من الملامح الاساسية الشائعة لدى السيفالوسبورينات وجود مجموعة الكربوكسيل على حلقة Dihydrothiazene على الكربون القريبة من نتروجين الحلقة ووجود مجموعة الامين الفعالة على كربون رقم 7، تشبه السيفالوسبورينات مضادات البيتا لاكتام من حيث ميكانيكية العمل اذ تقوم بتثبيط تكوين جدار خلية البكتريا مما يجعلها تستعمل لعلاج الامراض الناتجة عن البكتريا، تتميز السيفالوسبورينات بالفعالية العالية والسمية القليلة.

ويوجد اكثر من خمسين مركباً من مشتقات السيفالوسبورينات التي لها تطبيقات طبية واسعة، يمكن تصنيف السيفالوسبورينات على وفق التركيب الكيميائي او المدى الطيفي او الاستعمال الصيدلاني وغيرها لكن التصنيف المهم الذي يعتمد عليه هو مدى التضادية لأنواع البكتريا (10). وهناك عدد كبير من الطرق الطيفية (11-15) والكهربائية (16، 17) التي تستعمل لتقدير بعض البنسيلينات والسيفالوسبورينات. ولقد استعملت طرق الفصل الكروموتوغرافية (18-20) لفصل وتقدير بعض مضادات البيتا لاكتام وفي البحث الحالي تم استعمال البلايدوم في تقدير بعض مضادات البيتا لاكتام مثل الاميسيلين والاموكسيسلين والسيفالكسين والسفترايكسون والسيفوتاكسيم في ظروف معينة كما سيتم توضيحها لاحقاً.

المستحضرات الصيدلانية

1- المستحضر الصيدلاني Ampicillin

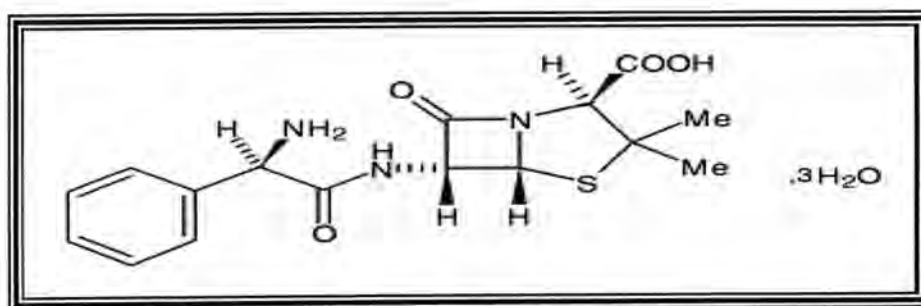
ان الاسم الكيميائي لهذا الدواء هو (21):-

(2S,5R,6R)-6-[(R)-2-amino-2-phenylacetamido]-3,3-dimethyl-7-oxo-4-thia-1-azabicyclo[3.2.0]heptane-2-carboxylic acid

اما اسماءه التجارية فعدة ومنها مايتي:-

Amcill (Parke, Davis), Ampilag(Lagap), Ampilar(Lagap), Alpen(Lederle Amblosin).

ان التركيب الكيميائي للدواء هو كما يأتي:



الاميسيلين (22) عبارة عن بلورات بيضاء اللون، له وزن جزيئي (349.41) غم/مول ونقطة انصهار تتراوح من (199 - 202) م° يمتاز بذوبانية ضعيفة في الماء له زاوية دوران نوعي (287.9+).

تقديرات طيفية امتصاصية جزيئية واخرى ذرية للمضادات الحيوية: الامبيسلين والاموكسسلين والسيفالكسين والسيفترايكون والسيفوتاكسيم في بعض المستحضرات الصيدلانية

فاضل و منى و انتظار

يؤخذ الدواء عن طريق الفم ويمتص منه اقل من نصف الجرعة ويقل الامتصاص بوجود الطعام، يطرح الدواء خلال البول وعصارة الصفراء.

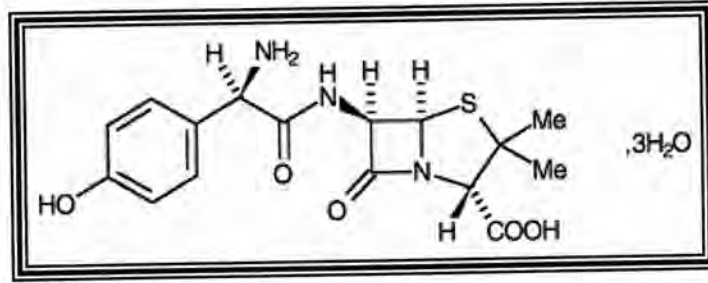
2- المستحضر الصيدلاني Amoxycillin

ان الصيغة الجزيئية للدواء هي $C_{16}H_{19}N_3O_5S$ والاسم الكيميائي لهذا الدواء هو (21):-
(2S,5R,6R) -6- {[(R)-2-amino-2- (4-hydroxyphenyl) acetyl] amino}-3,3-dimethyl-7-oxo-4-thia-1-azabicyclo[3.2.0]heptane-2-carboxylic acid.

وللدواء اسماء تجارية عديدة ومنها كالآتي:-

Agram(Inava), Alfamox(Alfa), Amodan(Berk), Amoxcilline(Inpharzam), Amodex(Bo u chare).

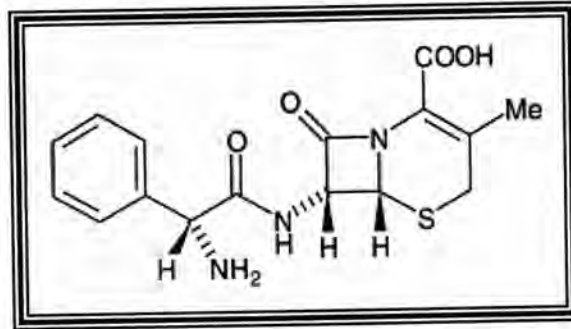
اما التركيب الكيميائي للدواء فهو كالآتي:-



الاموكسسلين (22) عبارة عن مسحوق بلوري مائل الى الاصفرار ،له زاوية دوران نوعي مساوية الى (246+)، يذوب الاموكسسلين في الماء والميثانول والايثانول، ولا يذوب في الهكسان والبنزين وخلات الاثيل والاسيتونايترايل. يؤخذ الدواء عن طريق الفم ويعطي تركيز عالي في البلازما والانسجة ولايتاثر الامتصاص بوجود الطعام في المعدة.

3- المستحضر الصيدلاني Cephalixin

الجزيئية للدواء هي $C_{16}H_{17}N_3O_4S$ والاسم الكيميائي لهذا الدواء هو (21):-
(6R,7R)-7[(R)-2-amino-2-phenylacetamido]-3-methyl-8-oxo-5-thia-1-azabicyclo[4.2.0]oct-2-ene-2-carboxylic acid. ان الصيغة
اما التركيب الكيميائي للدواء فهو كالآتي:-

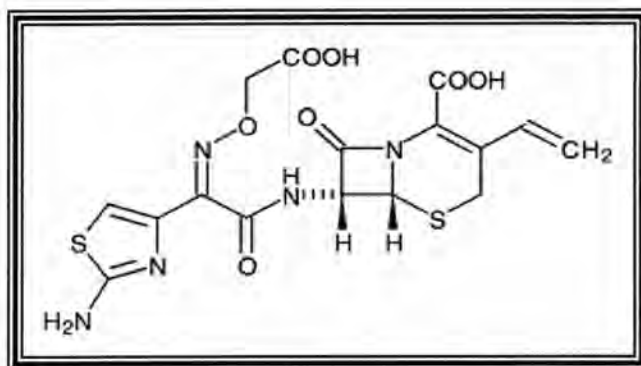


السيفالكسين (22) عبارة عن مسحوق بلوري ابيض اللون ذو وزن جزيئي (365.4) غم/مول وله زاوية الدوران النوعي مساوية الى (149+ _ 158). يذوب الدواء في الماء ولا يذوب في الكحول والايثر، يتراوح الرقم الهيدروجيني لمحلول الدواء من (4-5.5).

4- المستحضر الصيدلاني Ceftriaxone

ان الصيغة الجزيئية للسفترايكسون هي $C_{18}H_{16}N_8Na_2O_7S_3$ والاسم الكيميائي له هو (21):-
Disodium (Z)- (6R,7R)-7- [2- (2-amino-1, 3-thiazol-4- yl)-2- (methoxy- imino)acetamido] -8-oxo-3-[(2,5-dihydro-2-methyl -6-oxido-5-oxo-1,2,4-triazin - 3- yl) thiomethyl]- 5-thia - 1- azabicyclo [4. 2. 0] oct - 2- ene -2-carboxylate.

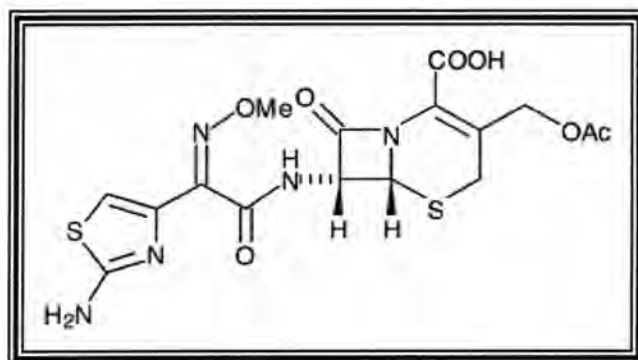
اما تركيبه الكيميائي فهو كالآتي:-



الدواء (22) عبارة عن مسحوق بلوري ابيض اللون او اصفر ذو وزن جزيئي (662) غم/مول وزاوية الدوران النوعي تتراوح (+155 - 170). يذوب الدواء بدرجة كبيرة في الماء ويذوب بشكل قليل في الميثانول، يتراوح الرقم الهيدروجيني للمحلول المائي للدواء من (6 - 8).

5- المستحضر الصيدلاني Cefotaxime

ان الصيغة الجزيئية للدواء هي $C_{16}H_{16}N_5NaO_7S_2$ والاسم الكيميائي (21) له هو:-
sodium(6R,7R)-3- [(acet-yloxy) methyl]-7-[(Z)-2-(2-aminothiazol-4-yl)-2- (methoxyimino)acetyl]-8-oxo-5-thia-1-azabicyclo[4.2.0]oct-2-ene-2 carboxylate
 اما التركيب الكيميائي فهو كالآتي:



السيفتاكسيم (22) عبارة عن مسحوق ابيض او مائل الى الاصفرار له وزن جزيئي (477.4) غم/مول، وتتراوح زاوية الدوران النوعي (+58 - 64). يذوب الدواء بدرجة كبيرة في الماء وقليل الاذابة في الميثانول لكنه لا يذوب في الايثر، يبلغ الرقم الهيدروجيني للمحلول المائي للدواء من (4.5 - 6.5).

المواد وطرائق العمل**1- الاجهزة والمواد الكيميائية**

تم استعمال مقياس طيف الامتصاص الذري اللهب Flame Atomic Absorption Spectrometer (GBC (q 32 plus)) المزود بمصباح الكاثود المجوف (H.C.L.) للحصول على شعاع رنين البلاديوم ومصباح تصحيح الخلفية ومردة من نوع خرزة الارثيطام ولهيب (Air-Acetylene) وكانت

تقديرات طيفية امتصاصية جزيئية وأخرى ذرية للمضادات الحيوية: الامبيسيلين والاموكسيسلين والسيفالكسين والسيفترايكسون والسيفوتاكسيم في بعض المستحضرات الصيدلانية

فاضل و منى و انتظار

سرعة الوقود المستعملة (2) لتر بالدقيقة وسرعة جريان المؤكسد (10) لتر بالدقيقة، وكذلك مطياف الأشعة فوق البنفسجية-المرئية من النوع (Shimadzu) UV-Visible Spectrophotometer المزود بخلايا مصنوعة من السليكا بطول 2 سم ومقياس الرقم الهيدروجيني من النوع pH Meter (Philips, PW 9420)، ويمثل الجدول (1) المواد الكيميائية المستخدمة.

جدول 1- المواد الكيميائية ومواصفاتها والجهة المصنعة لها

الجهة المصنعة	أسم المادة ومواصفاتها	التسلسل
BDH	Palladium Chloride, $\text{PdCl}_2 \cdot 2\text{H}_2\text{O}$,	1
BDH	Benzyl Alcohol, $\text{C}_6\text{H}_5\text{CH}_2\text{OH}$, Analar	2
SDI	Ampicillin, ST.Material,	3
India	Pesillin, (500)mg Ampicillin	4
SDI	Amoxycillin, ST.Material	5
India	Pulmoxy, (500)mg Amoxycillin	6
SDI	Cephalexin ST.Material	7
Iraq	Cephalexin, (250)mg Cephalexin	8
SDI	Ceftriaxone ST.Material	9
India	Gramocel, (1000)mg Ceftriaxone	10
SDI	Cefotaxime ST.Material,	11
Turkey	Sefotak, (1000)mg Cefotaxime	12

2- طريقة العمل

نقلت حجوم تتراوح بين (0.25-2.5) مل من الامبيسيلين والاموكسيسلين والسيفالكسين ذوات التركيز (100) جزء بالمليون، (0.06-2.5) مل من السيفترايكسون ذي التركيز (200) جزء بالمليون، و(0.15-3.2) مل من السيفوتاكسيم ذي التركيز (200) جزء بالمليون إلى دوارق حجمية سعة (5) مل ثم أضيف إلى كل منها (0.75) مل من محلول أيون البلاديوم الثنائي ذي التركيز (100) جزء بالمليون وضبطت الظروف العملية الأخرى وأكمل الحجم بالماء، وأستخلص المعقد المتكون بحجم (1) مل من كحول البنزول وقيست الممتصيات بمطيافية الامتصاص الأشعة فوق البنفسجية والمرئية.

تمت دراسة الظروف المثلى (Optimum Conditions) لتقدير الامبيسيلين والاموكسيسلين والسيفالكسين والسيفترايكسون والسيفوتاكسيم وهي تركيز أيون البلاديوم، الرقم الهيدروجيني، نسبة الطور كفاءة الاستخلاص، زمن التفاعل، زمن الاستخلاص، المذيبات العضوية، إيجاد نسبة الدواء إلى الفلز في المعقد Drug-Pd (II) بطريقة النسب المولية.

ونقلت حجوم تتراوح من (0.15-1.7) مل من الامبيسيلين، والاموكسيسلين، والسيفالكسين، (0.3-3.3) مل من السيفترايكسون، و(0.3-3.3) مل من السيفوتاكسيم ذوات التركيز (50) جزء بالمليون إلى دوارق حجمية سعة كل منها (5) مل ثم أضيف إلى كل منها (0.5) مل من محلول أيون البلاديوم الثنائي ذي التركيز (50) جزء بالمليون وضبطت الظروف العملية الأخرى وأكمل الحجم بالماء، وأستخلص المعقد المتكون بحجم (1) مل من كحول البنزول وقيست الممتصيات بمطيافية الامتصاص الذري وتم دراسة تأثير تركيز أيون البلاديوم الثنائي.

النتائج والمناقشة

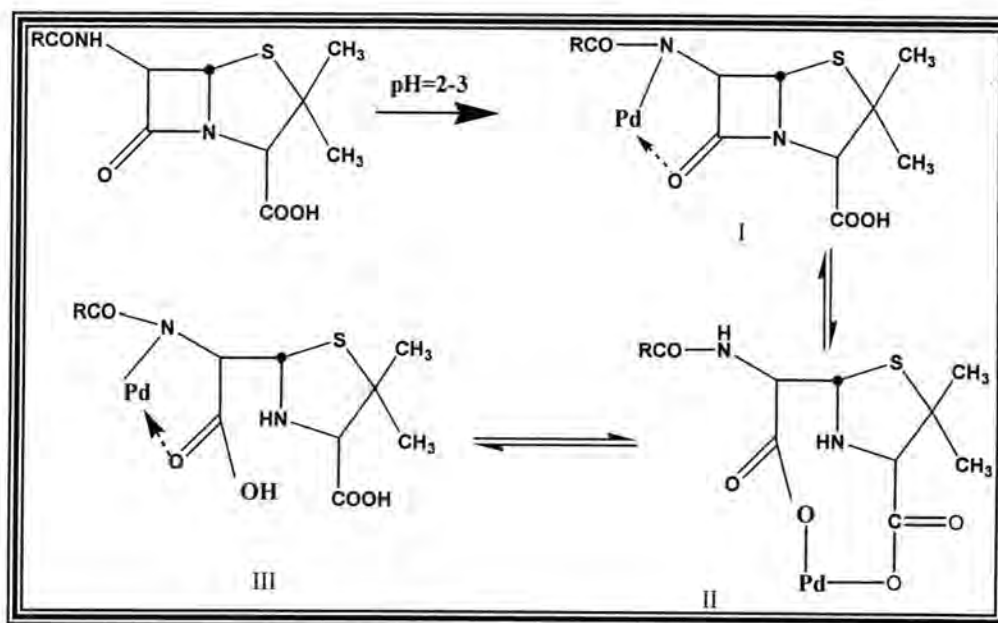
تم في هذا البحث تقدير الأدوية الأمبيسيلين والأموكسيسلين والسيفالكسين والسيفترايكسون والسيفوتاكسيم بأسلوب غير مباشر وذلك بتفاعلها مع أيون البلاديوم الثنائي في الوسط الحامضي باستعمال مطيافية الامتصاص الذري اللهبى ومطيافية الامتصاص الجزيئي.

تم اختيار أيون البلاديوم في تقدير هذه الأدوية وذلك للاستجابة القوية للتفاعل واللون المميز للنتائج، ومن خلال مراجعة الأدبيات لم يتم العثور على تفاعل هذه الأدوية الأمبيسيلين والأموكسيسلين والسيفالكسين والسيفترايكسون والسيفوتاكسيم مع أيون البلاديوم وعليه تعد هذه المعقدات الجديدة محضرة لأول مرة في العمل الحالي بالإضافة الى تقدير الأدوية.

إن استعمال الاوساط الحامضية في مثل هذه التفاعلات له فوائد عديدة منها:-

الاولى:- منع ترسيب هيدروكسيد الفلز غير المرغوب فيه الذي يتكون عند استعمال الاوساط القاعدية.
الثانية:- يعمل الوسط الحامضي على تحلل حلقة البيتا لاكتام التي ترتبط بسهولة مع أيون الفلز المستعمل.
الثالثة:- إمكانية استخلاص المعقدات المخيلية المتكونة بمذيبات عضوية ملائمة، وفي دراستنا هذه تم استعمال كحول البنزيل كمذيب عضوي ملائم في عملية استخلاص المعقدات المحضرة.

وهناك احتمالات (23، 24) عديدة لموقع ارتباط أيون البلاديوم مع الأدوية ومن هذه الاحتمالات المقترحة ما يأتي:-

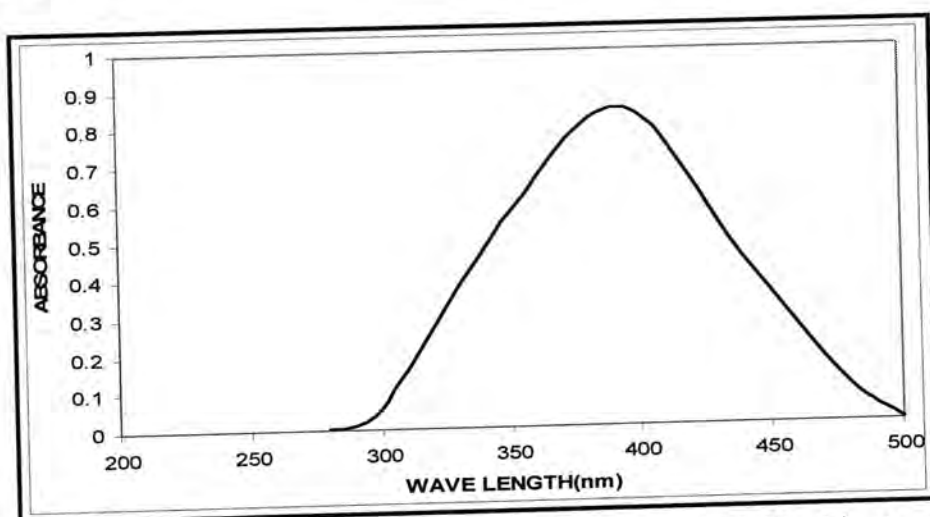


1- استعمال مطيافية الامتصاص الاشعة فوق البنفسجية والمرئية

بين الشكل (1) طيف معقدات الأدوية الأمبيسيلين والأموكسيسلين والسيفالكسين والسيفترايكسون والسيفوتاكسيم مقابل المذيب العضوي كمحلول خلب. ويتضح من الشكل أن أيون البلاديوم يكون معقدات صفراء اللون مع الأدوية ذلك لظهور قمة امتصاص عظمى جديدة غير موجودة في طيف امتصاص الدواء وهذه القمة يمكن ملاحظتها عند الطول الموجي (390) نانوم.

تقديرات طيفية امتصاصية جزيئية وأخرى ذرية للمضادات الحيوية: الأمبيسلين والأموكسيسيلين والسيفالكسين والسيفترايكون والسيفوتاكسيم في بعض المستحضرات الصيدلانية

فاضل و منى و انتظار



شكل 1: طيف الامتصاص الاشعة فوق البنفسجية والمرئية للمعد الناتج

تمت دراسة الظروف التجريبية المثلى للتفاعل و كانت الرقم الهيدروجيني (2 - 3) ، تركيز ايون البلاديوم الثنائي (15) مايكروغرام.مل⁻¹، نسبة الطور المائي الى الطور العضوي (1:5) للادوية الخمسة جميعها، زمن التفاعل (5) دقائق لكل من الامبيسيلين والسيفالكسين والسيفترايكون والسيفوتاكسيم و (3) دقائق للاموكسيسيلين، زمن الاستخلاص (3) دقائق لكل من الامبيسيلين والاموكسيسيلين (5) دقائق لكل من السيفالكسين والسيفترايكون والسيفوتاكسيم ولمرة واحدة ويبين الجدول (2) مدى التراكيز الذي تطيع قانون بير على وفق منحني المعايرة المباشرة وحد الكشف لتعيين الادوية الأمبيسيلين والأموكسيسيلين والسيفالكسين والسيفترايكون والسيفوتاكسيم بعد تكوين معقدات مخلبية مع أيون البلاديوم الثنائي.

جدول 2-خطية التراكيز وحد الكشف النظري والعملية والانحراف القياسي وحدود الثقة لكل دواء

Name of drug	Linear-ity (µg/ml)	D.L. (µg/ml)	D.L.T. (µg/ml)	S (µg/ml)	Conf.L-imit.Co-nce. (µg/ml) 95%.C.I	Conf.L-imit.Abs. 95%.C.I	ε (l.mol ⁻¹ cm ⁻¹) ×10 ³
Amp.	5-50	0.34 076	2.23 304	0.09 24	24.2171 ±0.1918	0.2497 ±0.0020	3.7806
Amox.	5-50	0.46 832	0.97 825	0.10 24	25.7567 ±0.2885	0.2445 ±0.0032	3.5622
Ceph.	3-50	0.24 264	1.97 985	0.10 45	24.6225 ±0.2259	0.2480 ±0.0022	3.4956
Ceft.	3-100	0.39 304	3.24 599	0.09 96	49.8771 ±0.2922	0.5557 ±0.0032	6.6420
Cefo.	3-65	0.17 923	1.06 746	0.06 21	30.2860 ±0.6136	0.4887 ±0.0066	7.6861

ويبين الجدول (3) معادلة الخط المستقيم ومعامل الارتباط والفحص t- ذي الجانبين وحدود الثقة للميل ونقطة التقاطع عند مستوى ثقة 95%.

جدول 3- معادلة الخط المستقيم ومعامل الارتباط (R) والفحص (t-) ذي الجانبين وحدود الثقة للميل ونقطة التقاطع عند حدود ثقة 95%

Name of drug	Regr.eq. Y=Bx+A	Corr. coef. (R)	t-test statistic	Tabu-lated t-test two tailed %95 C.I.	Conf. for the slope $b \pm t_{s_b} \text{ limit}$	Conf. for the intercept $a \pm t_{s_a} \text{ limit}$
Amp.	$Y=0.1044x - 0.0030$	0.999 0	67.031 7	2.262	0.1044 ± 0.0003	-0.0030 ± 0.0099
Amox.	$Y=0.0095x - 0.0004$	0.999 8	149.98 49	2.262	0.0095 ± 0.0001	-0.0004 ± 0.0039
Ceph.	$Y=0.0099x - 0.0027$	0.999 3	84.468 3	2.228	0.0099 ± 0.0002	0.0027 ± 0.0073
Ceft.	$Y=0.0112x - 0.0040$	0.999 5	99.962 4	2.228	0.0112 ± 0.0002	-0.0040 ± 0.0134
Cefo.	$Y=0.0161x - 0.0010$	0.999 8	165.80 63	2.201	0.0161 ± 0.0001	-0.0010 ± 0.0061

ومن ملاحظة قيم (t-) المحسوبة ومقارنتها مع القيمة المجدولة في الجدول السابق نجد أن المحسوبة أعلى قيمة وهذا يشير إلى وجود علاقة بين المتغيرين X,Y.

وبيين الجدول (4) الانحراف القياسي المئوي (%RSD) والخطأ النسبي المئوي (%Erel) والإستردادية (%Rec) لتعيين الأدوية الأميسيلين والأموكسيسلين والسيفالكسين والسيفترايكسون والسيفوتاكسيم بعد مفاعلتها مع أيون البلاديوم الثنائي.

جدول 4- الانحراف القياسي المئوي والإستردادية والخطأ النسبي المئوي للأدوية

Name of drug	Amou-nt (taken(g/ml)	Amount found (µg/ml)	%Re- cov.	%Erel .	%RSD (n=3)	Mean %Rec-ov.	Mean %Erel.
Ampicillin							
	10	10.1300	101.30	1.3000	2.2023	101.46 ± 0.8400	+1.4660
	20	20.4600	102.30	2.3000	1.2032		
	40	40.3200	100.80	0.8000	0.9321		
Amoxycillin							
	10	10.2000	102.00	2.0000	0.7235	101.58 ± 0.4167	+1.5833
	20	20.3000	101.50	1.5000	0.9372		
	40	40.5000	101.25	1.2500	1.1321		
Cephalexin							
	10	10.3000	103.00	3.0000	2.2531	102.08 ± 0.9167	+2.0833
	20	20.4000	102.00	2.0000	1.9738		
	40	40.5000	101.25	1.2500	0.8878		
Ceftriaxone							
	20	20.4000	102.00	2.0000	0.7210	101.916 ± 0.5834	+1.9166
	40	40.5000	101.25	1.2500	0.9321		
	80	82.0000	102.50	2.5000	1.2321		
Cefotaxime							
	15	15.6000	104.00	4.0000	0.6321	103.16 ± 0.8334	3.1666+
	30	31.5000	103.50	3.5000	0.9455		
	50	51.0000	102.00	2.0000	1.4927		

تقديرات طيفية امتصاصية جزيئية وأخرى ذرية للمضادات الحيوية: الأمبيسلين والأموكسيسيلين والسيفالكسين والسيفترايكون والسيفوتاكسيم في بعض المستحضرات الصيدلانية

فاضل و منى و انتظار

تعيين الأدوية الأمبيسلين والأموكسيسيلين والسيفالكسين والسيفترايكون والسيفوتاكسيم في بعض مستحضراتها الصيدلانية بمطيافية الامتصاص الاشعة فوق البنفسجية والمرئية

تم اتباع أسلوبين لتعيين الأدوية الأمبيسلين والأموكسيسيلين والسيفالكسين والسيفترايكون والسيفوتاكسيم في بعض مستحضراتها الصيدلانية، يتضمن الأسلوب الأول قياس الامتصاصية للمحلول المستخلص للمعدن المخلي بتركيز عدة من المستحضر واستخراج التركيز من منحنى المعايرة المباشرة. أما الأسلوب الآخر فهو إضافات القياس يتضمن قياس الامتصاصية للمعدن المخلي بتركيز عديدة من الدواء بعد إضافة تركيز معين من المستحضر واستخراج التركيز.

يبين الجدول (5) نتائج تعيين الأدوية طيفياً في مستحضراتها الصيدلانية باستعمال أيون البلاديوم الثنائي بالأسلوب المباشر وإضافات القياس .

جدول 5- نتائج تعيين الأدوية طيفياً في مستحضراتها الصيدلانية باستعمال أيون البلاديوم الثنائي بالأسلوب المباشر وإضافات القياس

Name of drugs	State of Drug	Stated concentration (mg per unit)	Found direct calb (mg per unit)	%Erel.	Found st.add. calb. (mg per unit)	%Erel
Amp.	tablet	500	507.3300	1.4660+	453.5675	9.2865-
Amox.	tablet	500	507.9165	1.5833+	520.1940	4.0388+
Ceph.	tablet	250	255.2082	2.0833+	242.1622	3.1351-
Ceftr.	vial	1000	1019.1666	1.9166+	956.3470	4.3653-
Cefo.	vial	1000	1031.6666	3.1666+	978.6920	2.1308-

حسبت معادلة الخط المستقيم لمنحنى إضافات القياس والميل ونقطة التقاطع والفحص (t-) ذي الجانبين وقيمة التركيز المحسوب بطريقة إضافات القياس (XE) عند حدود ثقة 95% كما موضح في الجدول (6) اللاحق:-

الجدول (6) معادلة الخط المستقيم ومعامل الارتباط (r) والفحص (t-) ذي الجانبين وقيمة التركيز (XE) المحسوب بطريقة إضافات القياس عند حدود ثقة (95%) عند الطول الموجي (390) نانوم للمستحضرات الصيدلانية

Name of drug	Regr.eq. Y=Bx+A	Corr. Coef. (r)	t-test stati-stic	Tabulat ed t-test two tailed %95 C.I.	Conf. for x-value X _E ± ts X _E	%Rec.	%Eer.
Amp.	Y=0.0108 +0.0979	0.9996	115.4343	2.306	9.0707 ±0.5395	90.7074	9.2925
Amox.	Y=0.0093 x+0.0968	0.9990	66.6000	2.306	10.4086 ±1.0935	104.0860	4.086060000
Ceph.	Y=0.0099 x+0.0960	0.9997	141.3930	2.306	9.6874 ± 0.4078	96.8741	3.1258
Ceft.	Y=0.0112 x+0.2155	0.9994	94.8327	2.262	19.1299 ±1.4646	95.6496	4.3504
Cefo.	Y=0.0161 x+0.2378	0.9994	94.8327	2.262	14.6768 ± 0.9727	97.8457	2.1550

ويلحظ أن ميل منحني إضافات القياس للأدوية مواز لمنحني المعايرة المباشرة وهذه إشارة إلى عدم وجود تداخلات منشأ. أما الجدول (7) فيوضح الانحراف القياسي المنوي النسبي (%RSD) ونسبة الاسترداد المنوي (%Reco) والخطأ النسبي المنوي (%Erel) لتعيين المستحضرات الصيدلانية بطريقة إضافات القياس.

جدول 7- الانحراف القياسي النسبي المنوي والإستردادية والخطأ النسبي المنوي لتعيين الأدوية في مستحضراتها الصيدلانية طيفيا وعند الطول الموجي (390) نانوم بطريقة إضافات القياس

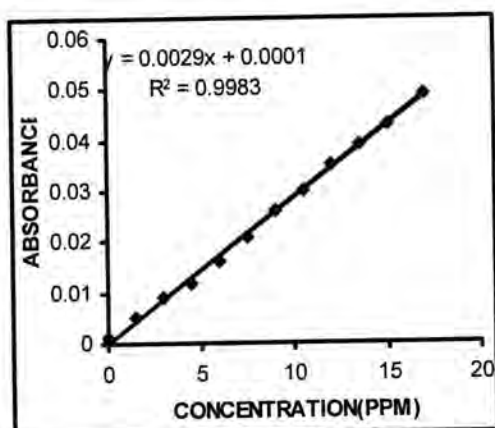
Name of drug	Amount taken $\mu\text{g/ml}$ (Amount found $\mu\text{g/ml}$ (%Re-cov.	%Erel.	%R.S. D. n=3)(Mean %Recov.	Mean %Erel.
Ampicillin							
	10	9.0707	90.70	9.2925	1.3279	90.7136 \pm 0.2115	9.2864-
	20	18.1862	90.90	9.0688	1.0781		
	40	36.2008	90.50	9.4979	0.7321		
Amoxycillin							
	10	10.4086	104.08	4.0860	0.9371	104.0388 \pm 0.4715	4.0388+
	20	20.7040	103.52	3.5201	0.4521		
	40	41.8041	104.51	4.5103	0.6128		
Cephalexin							
	10	9.6874	.8796	3.1258	0.5545	96.8649 \pm 0.8564	-3.1351
	20	19.1998	95.99	4.0008	0.9321		
	40	39.0885	97.72	2.2787	1.5321		
Ceftriaxone							
	20	19.1299	95.64	4.3504	2.1032	95.6346 \pm 0.7925	4.3653-
	40	37.9308	94.82	5.1728	1.1203		
	80	77.1416	96.42	3.5729	0.6329		
Cefotaxime							
	15	14.6768	97.84	2.1550	0.4872	97.8691 \pm 0.6202	-2.1308
	30	29.1819	97.27	2.7268	0.9327		
	50	49.2446	98.48	1.5107	1.2379		

2- استعمال مطيافية الامتصاص الذري

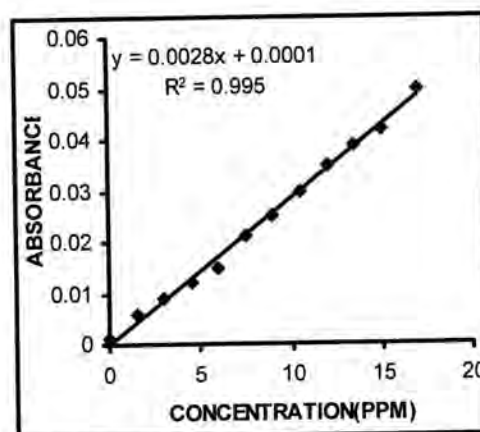
تبين الأشكال (2)، (3)، (4)، (5)، (6) منحنيات المعايرة المباشرة لكل من الأمبيسيلين والأموكسيسيلين والسيفالكسين والسيفترايكون والسيفوتاكسيم مع أيون البلاديوم الثنائي على التوالي، رسمت المنحنيات بأخذ الممتصة الذرية للبلاديوم مقابل تركيز الدواء ووجد أن أقصى تركيز يطيع قانون بيير هو (17) مايكروغرام.مل⁻¹ لكل من الأمبيسيلين والأموكسيسيلين والسيفالكسين و(33) مايكروغرام.مل⁻¹ للسيفترايكون و(22) مايكروغرام.مل⁻¹ للسيفوتاكسيم وبعد هذه التراكيز (لم تظهر في الأشكال) تبدأ المنحنيات بالانحراف تجاه إحداثي التركيز ويعود سبب ذلك إلى نقصان تركيز الذرات الحرة الطليقة من فلز البلاديوم في الحجم التحليلي ضمن مسار شعاع الرنين وهذا دليل واضح على أن المذيب العضوي لا يستخلص الزيادة من أيون البلاديوم الثنائي وبالنتيجة فإن المذيب يستخلص المعقد فقط.

تقديرات طيفية امتصاصية جزيئية وأخرى ذرية للمضادات الحيوية: الأموكسيسيلين والسيفالوكسين والسيفترياكسون والسيفوتاكسيم في بعض المستحضرات الصيدلانية

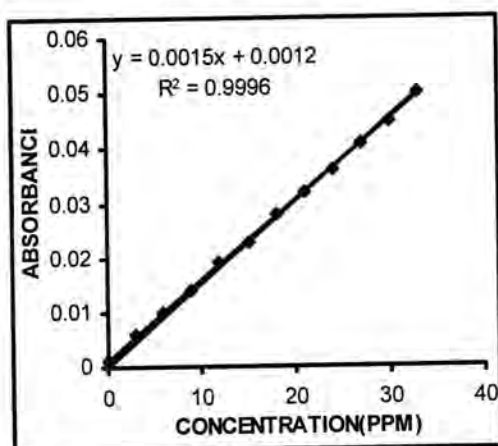
فاضل ومنى و انتظار



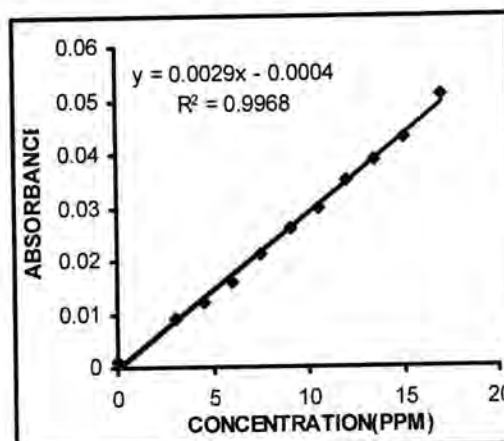
شكل-3: منحنى المعايرة المباشر لتقدير
Amoxycillin بهيئة Amoxycillin-Pd(II)
بطريقة (FAAS)



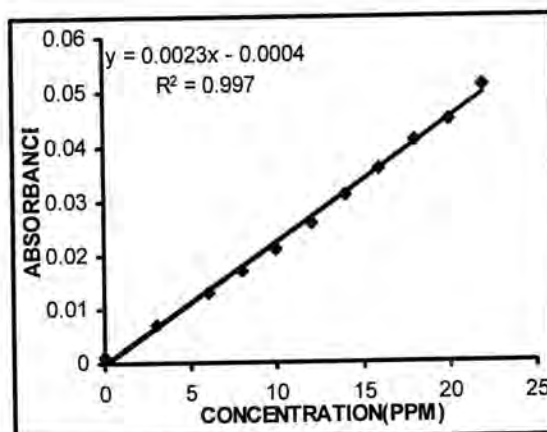
شكل-2: منحنى المعايرة المباشرة لتقدير
Ampicillin بهيئة Ampicillin-Pd(II)
بطريقة (FAAS)



شكل-5: منحنى المعايرة المباشرة لتقدير
Ceftriaxone بهيئة Ceftriaxone-Pd(II)
بطريقة (FAAS)



شكل-4: منحنى المعايرة المباشرة لتقدير
Cephalixin بهيئة Cephalixin-Pd(II)
بطريقة (FAAS)



شكل-6: منحنى المعايرة المباشرة لتقدير
Cefotaxime بهيئة Cefotaxime-Pd(II)
بطريقة (FAAS)

يبين الجدول (8) مدى التراكيز التي تطيع قانون بيير على وفق منحني المعايرة المباشرة وحد الكشف لتعيين الأدوية الأمبيسيلين، الأموكسيسلين، السيفالكسين، السيفترايكسون، والسيفوتاكسيم بعد تكوين معقدات مخلبية مع أيون البلاديوم الثنائي.

جدول-8: خطية التراكيز وحدود الكشفين النظري والعملي

Name of drug	Linearity (µg/ml)	D.L. (µg/ml)	D.L.T. (µg/ml)
Ampicillin	1.5-17	0.6474	1.2411
Amoxycillin	1.5-17	0.4968	1.1312
Cephalexin	3-17	0.8674	0.9122
Ceftriaxone	3-33	1.0098	0.9310
Cefotaxime	3-22	1.1413	1.5640

ويبين الجدول (9) معادلة الخط المستقيم ومعامل الارتباط والفحص t- ذي الجانبين وحدود الثقة للميل ونقطة التقاطع عند مستوى ثقة 95%.

جدول -9: معادلة الخط المستقيم ومعامل الارتباط (R) والفحص (t-) ذي الجانبين وحدود الثقة للميل ونقطة التقاطع

Name of drug	Regr.eq. Y=Bx+A	Corr. coef. (R)	t-test statistic	Tabu-lated t-test two tailed %95 C.I.	Conf. for the slope $b \pm t_{s_b}$ (limit)	Conf. for the intercept $(a \pm t_{s_a})$ limit
Amp.	$Y=0.0029x - 0.0002$	0.9974	44.6050	2.2280	0.0029 ± 0.0001	-0.0002 ± 0.0014
Amox.	$Y=0.0030x - 0.0012$	0.9991	74.4852	2.2280	0.0030 ± 0.0001	-0.0012 ± 0.0013
Ceph.	$Y=0.0029x - 0.0001$	0.9982	51.3569	2.2620	0.0029 ± 0.0001	-0.0001 ± 0.0012
Ceft.	$Y=0.0015x + 0.0006$	0.9989	67.3460	2.2280	0.0015 ± 0.00002	0.0006 ± 0.0005
Cefo.	$Y=0.0022x + 0.0008$	0.9983	51.3704	2.2620	0.0022 ± 0.0001	0.0008 ± 0.0015

ومن ملاحظة قيم (t-) المحسوبة ومقارنتها مع القيمة المجدولة في الجدول السابق نجد أن المحسوبة أعلى قيمة وهذا يشير إلى وجود علاقة بين المتغيرين X,Y. يبين الجدول (10) الانحراف القياسي المئوي (%RSD) والخطأ النسبي المئوي (%Erel) والإستردادية (%Rec) لتعيين الأدوية الأمبيسيلين والأموكسيسلين والسيفالكسين والسيفترايكسون والسيفوتاكسيم بعد مفاعلتهما مع أيون البلاديوم الثنائي.

فاضل ومنى و انتظار

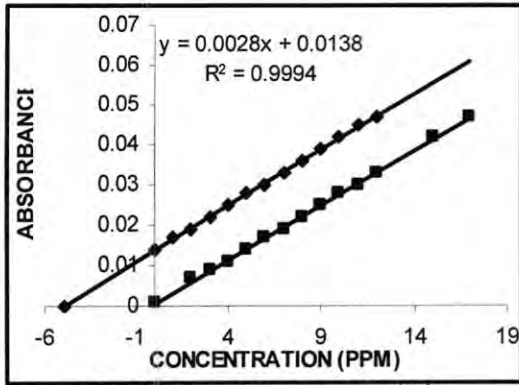
جدول-10: الانحراف القياسي النسبي المنوي والإستردادية للأدوية

Name of drug	Amount taken $\mu\text{g/ml}$	Amount found $\mu\text{g/ml}$	%Re-cov.	%Erel.	%R.S. D. n=3	Mean %Recov.	Mean %Erel.
Ampicillin							
	5	5.0660	101.32	1.3210	0.6711	101.8883	1.8883+
	8	8.1625	102.03	2.0320	1.9908	± 0.4237	
	12	12.2774	102.31	2.3120	2.2594		
Amoxycillin							
	5	5.2158	104.31	4.3160	0.3000	104.2	+4.2565
	8	8.2985	103.73	3.7320	1.7482	563 \pm 0	
	12	12.5665	104.72	4.7210	1.1600	.4647	
Cephalexin							
	5	5.1182	102.36	2.3650	0.5320	102.7	+2.7520
	8	8.3031	103.78	3.7890	1.5310	520 \pm 1	
	12	12.2522	102.10	2.1020	1.2369	.0370	
Ceftriaxone							
	9	9.3168	103.52	3.5210	0.7489	103.9	+3.9060
	12	12.5185	104.32	4.3210	1.3167	060 \pm 0	
	24	24.9302	103.87	3.8760	1.5259	.4150	
Cefotaxime							
	4	4.0928	102.32	2.3210	1.6676	103.4	+3.4296
	8	8.3616	104.52	4.5200	1.2723	226 \pm 1	
	14	14.4827	103.44	3.4480	0.5789	.0904	

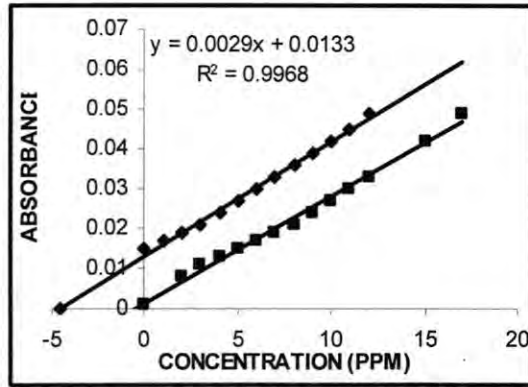
تعيين الأدوية الأمبيسيلين والأموكسيسيلين والسيفالكسين والسيفترايكسون والسيفوتاكسيم في بعض مستحضراتها الصيدلانية بمطيافية الامتصاص الذري

وتم تعيين الأدوية الأمبيسيلين والأموكسيسيلين والسيفالكسين والسيفترايكسون والسيفوتاكسيم في بعض مستحضراتها الصيدلانية تم اتباع أسلوبين لتعيين الأدوية الأمبيسيلين والأموكسيسيلين والسيفالكسين والسيفترايكسون والسيفوتاكسيم في بعض مستحضراتها الصيدلانية، يتضمن الأسلوب الأول قياس الامتصاصية الذرية للبلاديوم باستعمال تراكيز عدة من المستحضر واستخراج التركيز من منحنى المعايرة المباشرة. أما الأسلوب الآخر فهو إضافات القياس ويتضمن قياس الامتصاصية الذرية للبلاديوم باستعمال تراكيز عديدة من الدواء بعد إضافة تركيز معين من المستحضر واستخراج التركيز.

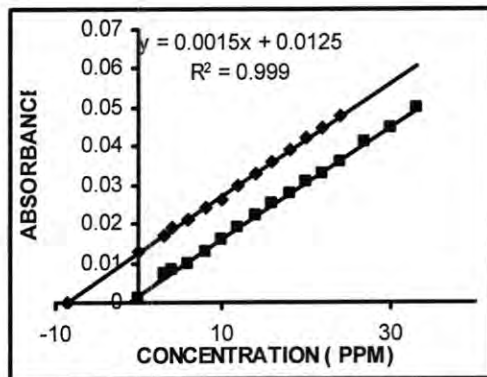
وتبين الأشكال (7)، (8)، (9)، (10)، (11) منحنيات المعايرة لتقدير الأدوية الأمبيسيلين والأموكسيسيلين والسيفالكسين والسيفترايكسون والسيفوتاكسيم في بعض مستحضراتها الصيدلانية بالطريقة المباشرة وبطريقة إضافات القياس بعد تفاعلها مع أيون البلاديوم الثنائي بمطيافية الامتصاص الذري.



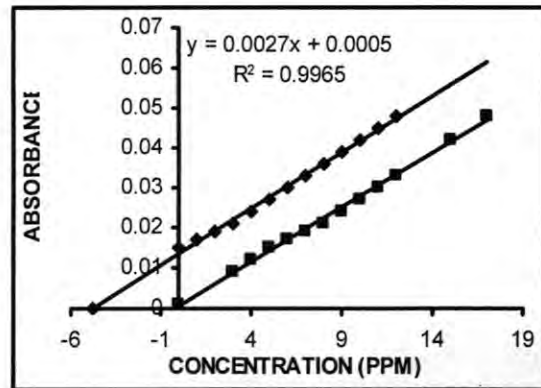
شكل-8: تعيين Amoxicillin في المستحضر الصيدلاني Pulmoxyل بطريقة إضافات القياس بتقنية (FAAS)



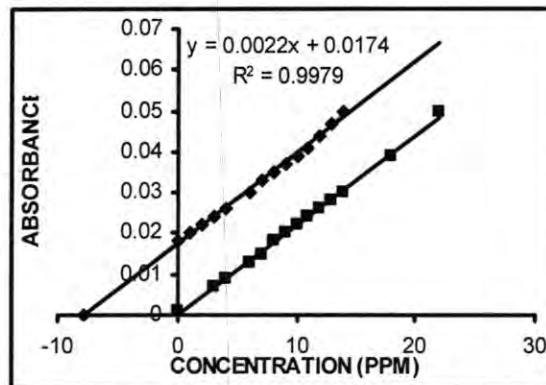
شكل-7: تعيين Ampicillin في المستحضر الصيدلاني Pesillin بطريقة إضافات القياس بتقنية (FAAS)



شكل-10: تعيين Ceftriaxone في المستحضر الصيدلاني Gramocéf بطريقة إضافات القياس بتقنية (FAAS)



شكل-9: تعيين Cephalixin في المستحضر الصيدلاني Cephalixin بطريقة إضافات القياس بتقنية (FAAS)



شكل-11: تعيين Cefotaxime في المستحضر الصيدلاني Sefotak بطريقة إضافات القياس بتقنية (FAAS)

يبين الجدول (11) نتائج تعيين الأدوية بمطيافية الامتصاص الذري في مستحضراتها الصيدلانية باستعمال أيون البلاديوم الثنائي بالأسلوب المباشر وإضافات القياس .

تقديرات طيفية امتصاصية جزيئية وأخرى ذرية للمضادات الحيوية: الأمبيسيلين والاموكسيسيلين والسيفالكسين والسيفترايكسون والسيفوتاكسيم في بعض المستحضرات الصيدلانية

فاضل و منى و انتظار

جدول -11: نتائج تعيين الأدوية بمطيافية الامتصاص الذري في مستحضراتها الصيدلانية باستعمال أيون البلاديوم الثنائي بالأسلوب المباشر وإضافات القياس

Name of drug	Type of preparation	Stated concentration (mg per unit)	Found direct-calb.(mg per unit)	%Eer	Found st.add. cal. (mg per unit)	%Erel
Ampicillin	tablet	500	509.4415	+1.8883	462.1190	-7.5762
Amoxycillin	tablet	500	521.2815	+4.2563	496.7305	-0.6539
Cephalexin	tablet	250	256.8800	+2.7520	241.0775	-3.5690
Ceftriaxone	vial	1000	1039.0600	+3.9060	940.5990	-5.9401
Cefotaxime	vial	1000	1034.2960	+3.4296	982.8410	-1.7159

حسبت معادلة الخط المستقيم لمنحنى إضافات القياس والميل ونقطة التقاطع والفحص (t-) ذي الجانبين وقيمة التركيز المحسوب بطريقة إضافات القياس (XE) عند حدود ثقة 95% كما موضح في الجدول (12).

جدول -12: معادلة الخط المستقيم ومعامل الارتباط (R) والفحص (t-) ذي الجانبين وقيمة التركيز (XE) المحسوب بطريقة إضافات القياس عند حدود ثقة 95% للمستحضرات الصيدلانية باستخدام مطيافية الامتصاص الذري

Name of drug	Regr.eq. Y=Bx+A	Corr. Coef. (R)	t-test statistic	Tabulated t-test two tailed %95 C.I.	Conf. for x- value $X_E \pm ts$ X_E	%Rec	%Eer
Amp.	Y=0.0029X +0.0134	0.9974	46.7822	2.201	4.6206 ±0.5494	92.4137	7.5862
Amox.	Y=0.0027X +0.0138	0.9995	104.8416	2.201	4.9685 ±0.2152	99.3701	0.6298
Ceph.	Y=0.0028X +0.0135	0.9980	53.6952	2.201	4.8214 ±0.4971	96.4285	3.5714
Ceft.	Y=0.0015X +0.0127	0.9996	125.3065	2.201	8.4666 ±0.9677	94.0740	5.9259
Cefo.	Y=0.0022X +0.0173	0.9980	58.3729	2.160	7.8636 ±0.6488	98.2954	1.7045

يلحظ في الجدول (12) أن ميل منحنى إضافات القياس للأدوية مواز لمنحنى المعايرة المباشرة وهذه إشارة إلى عدم وجود تداخلات منشأ. أما الجدول (13) فيوضح الانحراف القياسي المئوي النسبي (%RSD) ونسبة الاسترداد المئوي (%Reco) والخطأ النسبي المئوي (%Erel) لتعيين المستحضرات الصيدلانية بطريقة إضافات القياس.

جدول -13: الانحراف القياسي النسبي المنوي والإستردادية للأدوية

Name of drug	Amou-nt (taken µg/ml)	Amount found (µg/ml)	%Re-cov.	%Erel.	%RSD (n=3)	Mean %Recov.	Mean %Erel.
Ampicillin							
	5	4.6206	92.41	7.5862	2.1642	92.4238± 1.1996	7.5762-
	8	7.2987	91.23	8.7658	0.3055		
	12	11.2348	93.63	6.3766	0.8900		
Amoxycillin							
	5	4.9685	99.37	0.6298	1.2972	99.3464± 0.5143	0.6535-
	8	7.9065	98.83	1.1679	0.9727		
	12	11.9804	99.83	0.1630	1.3575		
Cephalexin							
	5	4.8214	96.42	3.5714	0.9721	96.4309± 0.4012	-3.5690
	8	7.7465	96.83	3.1679	0.4572		
	12	11.5238	96.03	3.9679	0.9989		
Ceftriaxone							
	9	8.4666	94.07	5.9259	1.3271	94.0599± 0.7870	5.9401-
	12	11.3799	94.83	5.1673	1.1029		
	24	22.3854	93.27	6.7271	0.7321		
Cefotaxime							
	4	3.9489	98.72	1.2755	0.9721	98.2840± 0.4519	1.7159-
	8	7.8636	98.29	1.7045	0.8501		
	14	13.6964	97.83	2.1676	1.2876		

ومن ذلك يمكن ان نستنتج:

- 1- استحداث طرائق تحليلية جديدة لتقدير الأدوية الأمبيسيلين والأموكسيسلين والسيفالكسين والسيفترايكون والسيفوتاكسيم تتصف بالدقة والحساسية والسرعة والحدود الكشفية الواطئة بمطابقة الامتصاص الجزيئي والامتصاص الذري.
- 2- أظهرت بعض مضادات البيتا لاكمات استجابة عالية لتكوين معقدات مخلبية جديدة مع أيون البلاذ يوم الثنائي إذ لم يظهر في الأدبيات ما يشير إلى وجود مثل هذه المعقدات.
- 3- تمت مقارنة نتائج طريقة الامتصاص الذري اللهبى مع طريقة الامتصاص الاشعة فوق البنفسجية والمرئية المستحدثتين في تقدير الأدوية المشار إليها سابقاً وأظهرت النتائج تقارباً من حيث الدقة ولكن تعد تقنية AAS أكثر حساسية وأقل خطية من طريقة UV-Vis وأدنى حدوداً كشفية أيضاً.

المصادر

1. DeVoe S.E., Storms M., and Haraki K. "Antibiotics Properties and Structures Data Base", Maintained at the Medical Research Division American Cyanamid Co., Pearl River (1990).
2. Highton A.A. and Roberts A.D. "Dictionary of Antibiotics and Related Substances" Chapman and Hall, New York (1988)
3. Gale E.F., Cundliffe E., Reynolds P.E., Richmond M.H., and Waring J., "The Molecular Bases of Antibiotic Action", 2nd ed., John Wiley & Sons, Inc., New York (1981).
4. Haskell C.M. and co-workers "Cancer Treatment", 3rd ed., W. B. Saunders Co., Philadelphia, chap. 4 (1990).

فاضل و منى و انتظار

- 5.Krik and Othmer, "Encyclopedia of Chemical Technology" , 2nd ed., John Wiley & Sons Inc., New York , 3 : 1-250(1992).
- 6.Richmond M.,Salton M.and Shockman G.D."β-Lactam Antibiotics", Press,New York, : 261-274(1981).
- 7.Medeiros A.A. ,Jacoby G.A. , Queener S.F. ,Webber J.A.,and Queener S.W. , "Clinical Pharmacology 4,β -Lactam Antibiotics for Clinical Use" ,Marcel Dekker Inc., New York, :49-84 (1986).
- 8.Georgopapadakou N.H. and Sykes R.B."Antibiotics Containing the β -Lactam Structure", part 2, Springer-Verlag, New York :1-78 (1983).
- 9.Krik and Othmer "Encyclopedia of Chemical Technology" , 2nd ed., John Wiley & Sons Inc., New York , 16(1986).
- 10.Mandell G.L.,Douglas R.G.and Bennett J.E. "Anti- infective Therapy", John Wiley & Sons,Inc.,New York,:76(1985).
- 11.Buhl F.and Szpikowska-Sroka, Spectrophotometric determination of cephalosporins with leuco crystal violet , Chem.Anal., 48(1):145-149 (2003).
- 12.Fernandez-Gonzalez, Badia R., and Diaz-Garcia, Micelle – mediated spectrofluorimetric determination of ampicillin based on metal ion-catalysed hydrolysis ,Anal.Chim. Acta,484(2):223-231(2003).
- 13.Farajzadeh M.&Mardani A."Analysis of residual solvents in ampicillin powder by headspace spectrophotometric methods",Anal.Sci.,18(2):171-175(2002).
- 14.Saleh G.A., Askal H.F.,Radwan M.F.,and Omer M.A., Use of charge- transfer complexation in the spectrophotometric analysis of certain cephalosporins", Talanta ,54(6):1205-1215(2001).
- 15.Bobrowska-Grzesik E."Determination of amox and clavulanic acid in some pharmaceutical preparation by derivative spectrophotometry"Mikrochim.Acta, 136(1-2):31-34,2001.
- 16.Prasad B.B. and Arora B.,"Application of polymer-modified hanging mercury drop electrode in the indirect determination of certain beta-lactam antibiotics by differential pulse ion-exchange voltammetry", Electroanalysis,15(14):1212-1218 (2003).
- 17.Basaez L.,Peric I.,Aguirre C.,&Vanysek P.,"Electrochemical study of amoxicillin antibiotic across liquid-liquid interface",Bol.Soc.Chilena Quim.46(2):203-208 (2001).
- 18.Storms M.and Stewart J.,"Development of reversed-phase liquid chromatography method for analysis of amoxicillin ,metronidazole and pantoprazole in human plasma using solid phase extraction",J.Liq.Chromatogr. Relat.Technol., 25(16):2433-2443(2002).
- 19.De Baere S.,Charlet M.Baert K.De Backer P."Quantitative analysis of amoxicillin and its major metabolites in animal tissues by liquid chromatography combined with electrospray ionization tandem mass spectrometry" ,Chromatographia,53 (7-8) :367-371(2001).

20. Gamba V. and Dusi G., "Liquid chromatography with fluorescence detection of amoxicillin & ampicillin in feeds using pre-column derivatization, Anal. Chim. Acta, 483(1-2):69-72(2003).
21. "The Merk Index on CD-Ram" 12th ed., copyright by Merk Co., Inc., Whiteho. (2000).
22. "British Pharmacopoeia on CD-Ram": 1-2(2002).
23. Anaconda J.R. "Synthesis and antibacterial activity of some metal complexes of beta-lactamic antibiotics", J. Coord. Chem., 54(3-4):355-365(2001).
24. Lopez R. and Sordo T.L., "A Det Study of Sites of Complexation of Cu(2) with Penicillins".

تخليق ودراسة طيفية وثرموديناميكية لبعض معقدات البورفيرينات- الفلزية مع بعض المانحات الالكترونية

¹ مؤيد حسن محمد و² ناجي علي عبود

¹ قسم الكيمياء البيئية البحرية- مركز علوم البحار - جامعة البصرة

² قسم الكيمياء - كلية التربية - جامعة البصرة

ABSTRACT

Some porphyrins were prepared from the reaction between Pyrrole and some aromatic aldehydes (Benzaldehyd and Anisaldehyd). Six organo – metallic complexes were also prepared. They were :

ZnTPP Zn(p-OCH₃)TPP
NiTPP Ni(p-OCH₃)TPP
MgTPP Mg(p-OCH₃)TPP

The prepared compounds were specified by C H N analysis, Infrared and Visible spectra. The visible spectra of the prepared compounds , some electronic donors and molecular complexes in benzene were measured. The molar ratio of the complexes were determined. The equilibrium constant of the resultant complexes with molar ratios 1:1, 1:2 were calculated. The thermodynamic function ($\Delta H, \Delta G, \Delta S$) of all studied interactions were also calculated. The interaction between the electronic acceptor (metalloporphtrin complexes) and the electronic donors (Nitrogen , Phosphorus , Oxygen and Sulfur bases) was studied. The result indicated that the strongest interaction is with Nitrogen electronic donor. On addition, the study showed that the central atom in the core of porphyrin affects the interaction, and it was found that the strongest interaction is with the case of zinc atom..However, the solvent used affect the interaction and the thermodynamic parameters. The complex Zn(p-OCH₃)TPP was found to be favouring the polar solvent in accordance with following order :

Chloroform > Benzene > Carbon tetrachloride

The effect of the substituent group (methoxy group -OCH₃) in porphyrin upon the interaction between the donor and the acceptor and upon the thermodynamic functions of some interaction were studied .

الخلاصة

تم تحضير بعض البورفيرينات من تفاعل البيروول مع بعض الالدهيدات الاروماتية (البنزالدهيد والانسالدهيد) وتم تحضير ستة معقدات عضوية فلزية هي :

ZnTPP Zn(p-OCH₃)TPP
NiTPP Ni(p-OCH₃)TPP
MgTPP Mg(p-OCH₃)TPP

وشخصت المركبات المحضرة عن طريق التحليل الدقيق للعناصر وأطياف الأشعة تحت الحمراء وأطياف الأشعة المرئية. ودرست أطياف الأشعة المرئية للمركبات المحضرة في مذيب واحد هو البنزين مع بعض الواهبات الالكترونية وعينت النسب المولية للليكاندات في المعقدات وتم حساب ثابت الاتزان للمعقدات المتكونة التي دلت الحسابات أنها حصلت بنسب مولارية 1:1 و 2:1. وحسبت الدوال الثرموديناميكية ($\Delta S, \Delta G, \Delta H$) لجميع التداخلات المدروسة. و درس التداخل (interaction) بين المستقبل الالكتروني (معقد بور فرين- فلز) والمانح الالكتروني (قواعد نيتروجينية وفسفورية واوكسجينية وكبريتية) وظهر أن أقوى تداخل هو مع المانح الالكتروني النيتروجيني. وظهر أن الذرة المركزية في قلب البورفيرين تؤثر في التداخل ووجد أن أقوى تداخل يحصل مع ذرة الخارصين. كما أن المذيب المستخدم يؤثر في التداخل وفي الدوال الثرموديناميكية ووجد أن المعقد Zn(p-OCH₃)TPP يفضل المذيب القطبي وحسب الترتيب التالي:

Chloroform > Benzene > Carbon tetrachloride

كما درس تأثير المجموعة المعوضة (مجموعة الميثوكسي -OCH₃) في البورفيرين على التداخل الحاصل وعلى الدوال الثرموديناميكية.

المقدمة

البورفيرينات (Porphyrins) والكورينات (Corrins) يشكلان جزءا مهما من المجاميع التخليقية المستخدمة في تشكيلة كبيرة ومتنوعة من النواتج الطبيعية الحيوية المهمة مثل الهيموغلوبين (1) والمايوغلوبين (2). ونتيجة للاهتمام المكثف بالتركيب والوظيفة والوصف الميكانيكي للأنظمة البايولوجية المحتوية على البورفيرينات والكورينات فإن كامل مجال الدراسة قد تطور ونمي وشمل طرقا بالغة التطور وخصوصا في السنوات الأخيرة. كذلك الفثالوسينانينات التي اكتشفت أصلا عن طريق الصدفة والتي ليس لها أهمية بايولوجية في أشكالها الملونة، ومع ذلك، ثبت أنها يمكن أن تكون أصباغا مهمة جدا وحتى يومنا هذا فإنها تستخدم وبكميات ضخمة في التجارة (3). إن الكثير من مظاهر الحياة على الكرة الأرضية تكون متصلة بصورة مباشرة أو غير مباشرة بوظيفة التخليق الضوئي في النباتات والتخليق الضوئي المتضمن البورفيرينات الفلزية (Metalloporphyrins). إن شرح جوهر عملية التخليق الضوئي غير ممكن بدون تعيين دور البورفيرينات الفلزية في هذه العملية البايولوجية المهمة. وعليه فقد أصبح ضروريا أن يتركز العمل على عدد من معقدات البورفيرينات الأسهل تركيبا من الكلوروفيل. إن كروموفور البورفيرين والكلورين (الكلوروفيل) والى حد بعيد هما الأكثر وجودا في المركبات الطبيعية وهو المسؤول عن اللون الأحمر للدم وكذلك المسؤول عن جميع الألوان الخضراء الحقيقية في النبات. كذلك الهيم (معقد الحديد II للبروتوبورفيرين) هو وحدة البناء في الهيموكلوبينات، المايوغلوبيينات، السايتركرومات وغيرها. وأيضا البورفيريا S-411 (4) توجد في العقي (meconium) الذي يعرف بأنه مادة داكنة تخرج من بطن المولود بعيد ولادته بهدف البحث إلى تخليق مجموعة جديدة من معقدات البورفيرينات ودراسة الدوال الثرموديناميكية للتداخلات التي تحصل بين المانح والمتقبل الالكتروني ودراسة تأثير نوع المانح الالكتروني في التداخل ودراسة تأثير الذرة المركزية في قلب البورفيرين على التداخل وكذلك دراسة تأثير المذيب على تلك التداخلات ودراسة تأثير المجموعة المعوضة في البورفيرين (مجموعة الميثوكسي $-OCH_3$) على التداخل الحاصل وعلى الدوال الثرموديناميكية للتداخل.

المواد وطرائق العمل

1- المواد الكيميائية:

استخدمت في هذه الدراسة مواد كيميائية جهزت من مصادر مختلفة وهي :
 الايثانول والميثانول ونترات النيكل من شركة BDH .
 البنزالدهيد والانسالدهيد والاثير والبيريدين ون- بيوتيل امين وثلاثي كلوريد الفسفور وثنائي مثيل سلفايد وكبريتات الصوديوم اللامائية من شركة Fluka .
 الفيوران من شركة Burrough Wellcome Co. .
 البيرول من شركة Hopkin and Williams LTD .
 البيوتانول وبيوتيل امين الثانوي وكلوريد الخارصين من شركة Merck .
 البيريدين والثايوفين و N,N - ثنائي مثيل اسيت اميد وثنائي مثيل سلفوكسايد وحامض البروبيونيك من شركة Reidel - De Haen AG .
 كلوريد الكالسيوم من شركة Aldrich .

2- الأجهزة Instruments :

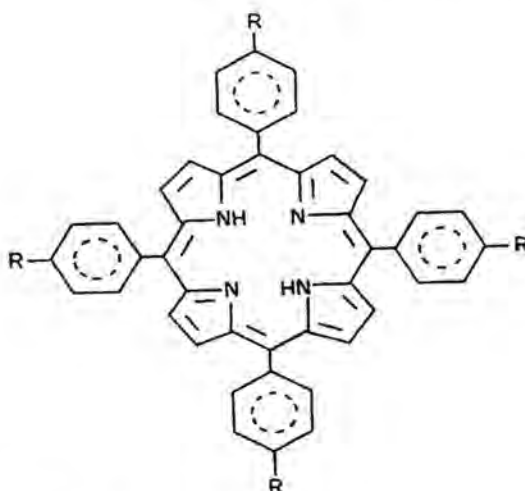
- جهاز تحليل العناصر: استخدم جهاز تحليل العناصر من نوع CHN, O-EA 1108-Element Analyzer في مختبرات كلية العلوم- جامعة النهرين- بغداد .
 - جهاز قياس أطيايف الأشعة تحت الحمراء : استخدم جهاز الأشعة تحت الحمراء من نوع Shimadzu IR-408 وبدرجة حرارة المختبر باستخدام تقنية أقراص بروميد البوتاسيوم KBr .

- جهاز قياس الأشعة المرئية : تم تسجيل الأطياف الأليكترونية للمعقدات المحضرة وليكانداتها باستخدام جهاز من نوع Ultraspace II Uv/Vis Spectrophotometer موديل 4050 . وقد استخدمت خلية من الكوارتز طول مسار الضوء فيها 1 سم باستخدام البنزين كمرجع في القياسات.

- جهاز التنقية بالتسامي : أجريت طريقة التنقية بالتسامي لتنقية المركبات المحضرة باستخدام جهاز الإصبع البارد (Cold finger apparatus) .

3- طرق التحضير Procedures :

تمتلك المركبات المحضرة في هذه الدراسة التركيب العام التالي:

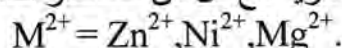


حيث:

R = H, meso- Tetraphenyl Porphin, TPP.

R = -OCH₃, meso Tetra(p-methoxyphenyl) Porphin, (p-OCH₃)TPP .

وقد استخدم المركبين أعلاه في تحضير معقدات عضوية - فلزية مع كل من العناصر التالية :



أ - تحضير البورفيرينات (p-OCH₃)TPP, TPP :

استخدمت طريقة Adler وجماعته⁽⁵⁾ لتحضير البورفيرينات المدروسة من خلال التقطير الارتجاعي ل (0.8 مول , 2.8 مل) من البيروول المقطر أنيا لمرة مع (0.8 مول) من احد الالدهيدات (4 مل من البنزالدهيد أو 4.5 مل من الانسالدريد) في وسط من حامض البروبيونيك (150 مل) في دورق تفاعل كروي سعة (250 مل) لمدة نصف ساعة . وتمت عملية مراقبة سير التفاعل باستخدام تقنية كروماتوغرافيا الطبقة الرقيقة TLC . برد مزيج التفاعل الى درجة حرارة المختبر ورشح المزيج وغسل الراسب بالميثانول ثم بالماء المقطر الساخن فتجبت بلورات أرجوانية اللون تركت مدة ساعة لتجف . وجفت البلورات الناتجة تحت الضغط المخلخل لإزالة الحامض الممتز . وكانت الحصيلة هي 1.25 غم (20%) من البورفيرين.

ب- تحضير المعقدات فلز- بورفيرين:

ZnTPP	Zn(p-OCH ₃)TPP
NiTPP	Ni(p-OCH ₃)TPP
MgTPP	Mg(p-OCH ₃)TPP

استخدمت طريقة Adler وجماعته⁽⁶⁾ في التحضير بوضع (100 مل) من N,N'-ثنائي ميثيل اسيتاميد في دورق تفاعل كروي (سعة 250 مل) ثم اضيف إليه غرام واحد من احد البورفيرينات المعنية [(p-OCH₃)TPP, TPP] ورج المزيج لمدة دقيقة واحدة لإكمال إذابة البورفيرين ثم اضيف إليه (0.3 غرام) من احد الأملاح المعنية (كلوريد الخارصين , نترات النيكل , نترات المغنيسيوم) الى دورق

التفاعل للحصول على المعقد (فلز - بورفرين) المعين وأجريت عملية التقطير الارجاعي لخليط التفاعل لمدة (20 دقيقة لمعقد الخارصين , 30 دقيقة لمعقد النيكل , 210 دقيقة لمعقد المغنيسيوم) ثم برد دورق التفاعل الكروي في حمام ثلجي لمدة (15) دقيقة واضيفت (100 مل) من الماء المقطر الى محتويات دورق التفاعل فتكونت بلورات . رشحت البلورات الناتجة باستخدام قمع بخنر أعقبها عملية غسل بالماء المقطر . تركت البلورات المتكونة لتجف فترة ساعة واحدة . كانت الحصيلة 0.9 غم من المعقد المعين .

ج- تحضير المركب ثلاثي بيوتيل الفوسفيت(7):

وضعت 7.4 غم (9.1 مل , 0.1 مول) من 1- بيوتانول و 7.9 غم (8.1 مل , 0.1 مول) من البيريدين و 25 مل من الايثر الجاف في دورق تفاعل (سعة 100 مل) ذو ثلاث فتحات مزود بمحرك ميكانيكي ومكثف إرجاع وقمع تقطير يحتوي على 4.6 غم (2.9 مل , 0.033 مول) من ثلاثي كلوريد الفسفوروز PCl_3 , و 3 مل من الايثر الجاف وسدت فتحة القمع بأنبوبة تحتوي على كلوريد الكالسيوم . برد دورق التفاعل في حمام ثلجي ثم اضيف اليه محلول PCl_3 ببطء مع التحريك وحفظت درجة حرارة مزيج التفاعل عند حوالي صفر مئوي . استمرت عملية تحريك المزيج لمدة 15 دقيقة بعد إكمال إذابة PCl_3 . رشح كلوريد البيريدين المتكون بواسطة قمع بخنر . غسل الرايب بواسطة الايثر . جفف الراشح بواسطة كبريتات الصوديوم اللامائية . بخر الايثر بواسطة المبخر الدوار وقطر السائل المتبقي تحت الضغط المخلخل وجمع ثلاثي بيوتيل الفوسفيت عند 122°C / 12 تور . وكانت الحصيلة 90% .

النتائج والمناقشة

1- تحليل العناصر:

تم تقدير نسب عناصر كل من الكربون والهيدروجين والنيتروجين في المركبات المحضرة بعد اجراء عملية التنقية لها بالتسامي ويظهر من الجدول (1) ان نتائج التحليل قريبة من القيم المحسوبة نظريا مما يبين ملائمة طرق تحضيرها وتنقيتها وثباتها عند التسامي.

جدول -1: نتائج تحليل العناصر للمركبات المحضرة

Symbol	Calculated / (found)		
	%C	%H	%N
TPP $C_{44}H_{30}N_4$	85.99 (85.26)	4.88 (4.99)	9.12 (8.91)
(p-OCH ₃)TPP $C_{48}H_{38}N_4$	85.97 (86.03)	5.67 (5.69)	8.35 (7.66)

2- أطياف الأشعة تحت الحمراء : Infrared Spectra

سجلت أطياف الأشعة تحت الحمراء للمركبات المحضرة في هذه الدراسة ويبين الجدول (2) أهم الامتصاصات المميزة لمختلف المجاميع الفعالة في كل مركب ونوع الحزمة التي ظهرت. تتميز هذه الأطياف بحزم عند حوالي (1350, 3400) سم^{-1} والتي تعود الى التذبذب الاتساعي لمجموعة N-H المتأصرة هيدروجينيا والتذبذب الاتساعي للأصرة $C=N$ على التوالي . أما الامتصاصات عند حوالي (1500, 1600) سم^{-1} فتنشأ من الحلقات الاروماتية . وعند مقارنة طيف اليورفرين الحر (المركبات 1 و 2 في الجدول) مع طيف فلز - بورفرين (المركبات 3-8 في الجدول) يتضح ان أيون الفلز يتأصر من خلال ذرة النيتروجين بإزاحة الهيدروجين (8,7). وعند المقارنة مع طيف البيرو لوحده (9) الذي يتميز بحزمة قوية عند حوالي 3125 سم^{-1} العائدة الى التذبذب الاتساعي للأصرة C-H ، وحزم عند حوالي (1430, 1665) سم^{-1} العائدة الى التذبذب الاتساعي للأصرة $C=C$. يتميز الطيف بحزم قوية عند حوالي (3225-3450) سم^{-1} تعود الى التذبذب الاتساعي لمجموعة N-H ,

يتضح الاختلاف أو الفرق بين البورفرين والبيروك ومعد فلز- بورفرين (9,8)، حيث عانت هذه الحزم العائدة للبيروك من ازاحات نحو عدد موجي أقل كما أن الحزم العائدة للتذبذب الاتساعي لمجموعة N-H اختفت في حالة معد فلز - بورفرين (9). ويتضح في النهاية أن أطيف المركبات المدروسة تتفق إلى حد بعيد مع الأدبيات والأطيف المتوقعة (10-13).

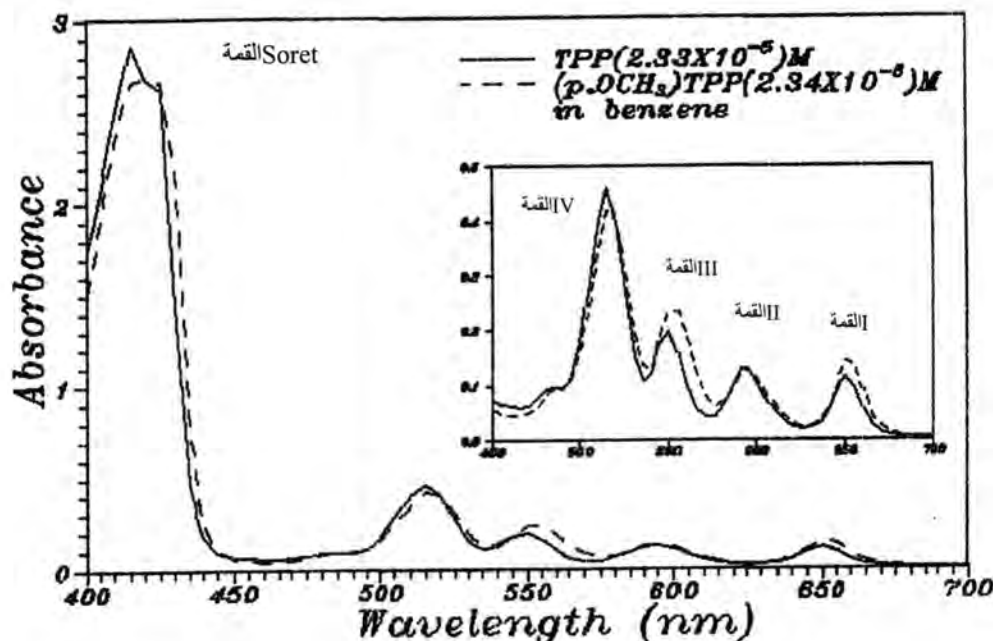
الجدول 2: نتائج قياسات الأشعة تحت الحمراء للمركبات المدروسة سم⁻¹

1 TPP	2 (p-OCH ₃)TPP	3 ZnTPP	4 NiTPP	5 MgTPP	6 Zn(p-OCH ₃)TPP	7 Ni(p-OCH ₃)TPP	8 Mg(p-OCH ₃)TPP	Assignment
3360 w	3375 w							N-H.....N stretch
3053 w 2925 w 2875 w	3030 w 2985wbr	3007 w	3050 m 3000 w 2900wsh	2900 m 2800 m	2900 w 2800 w	2900 w 2800 w	2900 w 2800 w	C-H stretch
1597 m 1570 m 1550 m 1540wsh	1600 m 1575 m 1560wsh 1545wsh	1600 w	1599 m	1600 s	1600 m	1600 m	1600 m	C=C stretch
1500 m 1490 w 1475 m	1500 m 1465 m 1452wsh	1500 w	1500 w 1480 w	1515 s	1500 m 1460 m	1500 m 1460 m	1505 m 1460 m	C=C phenyl
1445 m 1409 w	1440 m 1404wbr	1437 w 1425 w	1435 w	1465 m 1440 m	1400 w	1400 w	1435 w	C-H bend
		1343 w	1345 s	1350 s	1345 m	1350 m	1345 m	C=N stretch
	1243 s 1215wsh				1243 s	1245 s	1245 s	C-O stretch
1187 m 1175 m	1172 m	1210 w	1170 s	1190 s 1163 m	1170 s	1170 s	1170 s	C ₆ H ₆ subs OCH ₃
1067 m 1055 m 1030 w	1030 m	1070 w	1070 m	1060 w	1100 w	1103 w	1100 w	C-H bend in plane
900 m 975 m 963 s	987 w 978 m 935 s	992 w 982 w 962 m	1005 s 978 sh 963 m	980 w 965 m 945 s	1030 m 995 w 962 w	1030 m 1000 w 960 m	1030 m 980 w	C-H rock (Pyrrole)
723 s	735 m	722 w 700 m	740 m	740 m 710 sh	735 m	730 w	735 m	C-H bend out of plane

حيث: حيث: s = قوية , m = وسط , w = ضعيفة , sh = كتف , br = عريضة.

3- أطيف الأشعة المرئية Visible Spectra :

لقد تم تحضير ليكاندين هما (p-OCH₃)TPP, TPP وتم تحضير معقداتهما العضوية الفلزية مع الفلزات : الخارصين والنيكل والمغنيسيوم . يبين الشكل (1) طيف امتصاص الأشعة المرئية للمركبين السابقين في مذيب البنزين ويظهر جليا من خلال هذا الطيف القيم الخمسة المميزة للبورفيرينات.



شكل 1- طيف الأشعة المرئية لكل من المركبين TPP و (P-OCH₃)TPP في البنزين .

ويوضح الجدول (3) بيانات الاشعة المرئية العائدة للمركبين السابقين.

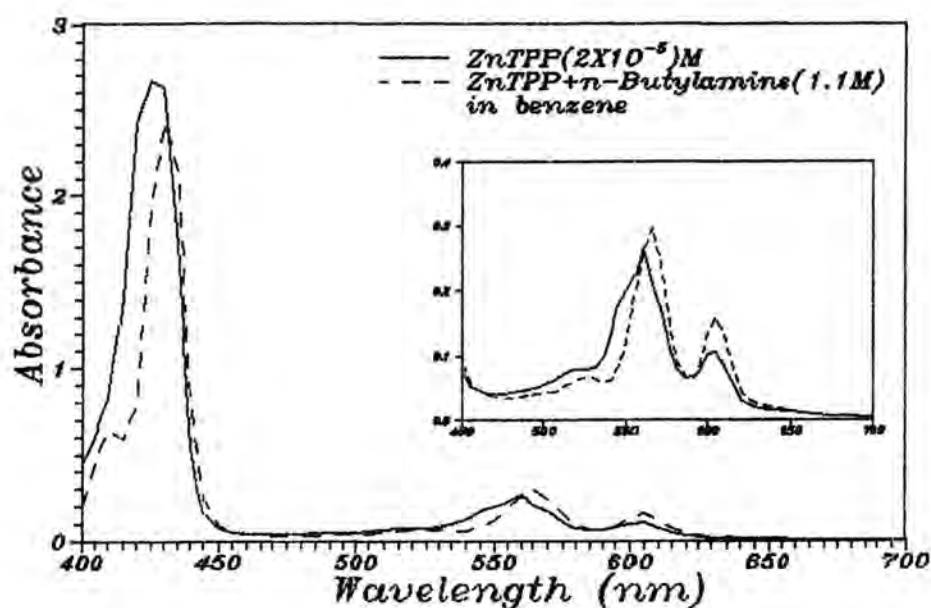
جدول 3- نتائج قياسات الاشعة المرئية للمركبين TPP, (p-OCH₃)TPP في مذيب البنزين

Symbol	$\lambda_{max} \text{ nm } (\epsilon \text{ L cm}^{-1} \cdot \text{mol}^{-1})$				
	القمة Soret	القمة IV	القمة III	القمة II	القمة I
TPP	415 (115321)	515 (19742)	550 (8412)	595 (5579)	650 (4978)
(p-OCH ₃)TPP	420 (114487)	515 (17948)	555 (9957)	595 (5590)	650 (6196)

ان القمة Soret تعود الى طريق التعاقب الكبير في النظام الاروماتي الضخم في الجزيئة الحلقية الكبيرة (4). بينما القمم الأربع الأخرى فتعزى الى الانتقالات الالكترونية من نوع ($\pi - \pi^*$) (14-16). ان إدخال ايون الفلز في قلب البورفيرين يسبب زحف قمم الامتصاص نحو طول موجي أطول (إزاحة حمراء) بحدود 10 نانوميتر وفي كلا المركبين . كما يؤدي الى زيادة شدة هذه القمم في حالة المركب TPP ونقصان في شدة القمم في حالة المركب (p-OCH₃)TPP . كما ان إدخال الايون الفلزي (وخصوصا Zn) يؤدي الى اختفاء بعض القمم من الطيف ويؤدي الى زيادة شدة قمم أخرى في نفس الطيف (14).

4- التداخل بين المتقبل والمانح الاليكتروني :

يبين الشكل (2) طيف الامتصاص الكلي لمعقد بورفرين - فلز (Acceptor) لوحده بدون إضافة أي مانح اليكتروني له (Donor)، وكذلك يبين طيف الامتصاص الكلي بعد إضافة المانح الاليكتروني



شكل 2- طيف الأشعة المرئية للتداخل بين ZnTPP و N- بيوتيل أمين في البنزين

المعينة. و الطيف هنا يخص المركب ZnTPP والمانح الاليكتروني هو N- بيوتيل امين في البنزين كمذيب.

ويلاحظ من خلال هذا الشكل تأثير المانح الاليكتروني في قمم امتصاص البورفرين كما يوضح التداخل الحاصل بين الواهب والمتقبل الاليكتروني. يمكن التعبير عن هذا التداخل بالمعادلة التالية (17):



حيث ان P_{Zn} يمثل ZnTPP .

ولغرض دراسة التداخل الحاصل يجب ان نجد المولية للليكاندات (المانحات الاليكترونية) في التداخل ومن ثم نطبق المعادلة الخاصة بحساب ثابت الاتزان . يمكن حساب قيمة n (التي تمثل عدد مولات المانح في المعقد النهائي) بتطبيق المعادلة التالية (18):

$$\log (D-D_0)/(D_{\infty}-D) = \log K + n \log C_L \dots \dots \dots (2)$$

حيث ان :

D = امتصاص مزيج التوازن (معقد بورفرين - فلز مع المانح الاليكتروني).

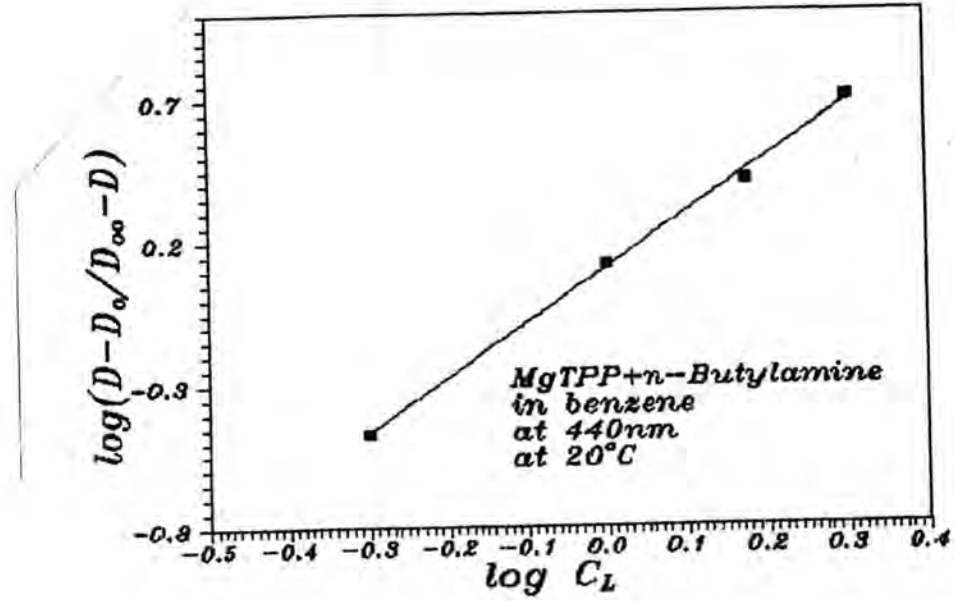
D_{∞} = امتصاص مزيج التوازن عند أعظم تركيز للمانح الاليكتروني.

D_0 = امتصاص محلول بورفرين - فلز وحده .

C_L = تركيز المانح الاليكتروني عند كل إضافة .

K = ثابت الاتزان .

ويمثل الشكل (3) تطبيق المعادلة السابقة لتحديد قيمة n بالنسبة للتداخل بين MgTPP و n- Butylamine .



شكل-3: حساب عدد مولات المانح الاليكتروني في حالة التداخل بين MgTPP و n-Butylamine

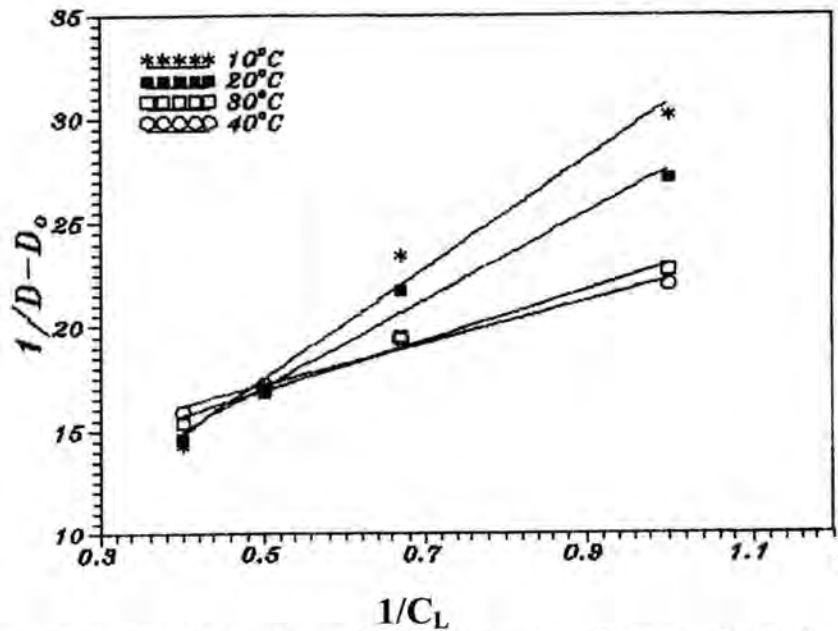
ان المعقدات النهائية التي يحصل فيها التداخل بنسبة 1:2 تكون قيم تركيز المانح الاليكتروني فيها كبيرة جدا عند مقارنتها مع تركيز المتقبل الاليكتروني (معقد بورفيرين - فلز) وبعد تحديد قيمة n يتم تطبيق المعادلة المناسبة بكل تداخل . ففي حالة حصول التداخل بنسبة 1:1 تطبق المعادلة التالية (19,18):

$$K_1 = fc / (1 - fc) \cdot C_L \quad \text{where } fc = (D - D_0) / (D_\infty - D_0) \quad \dots\dots\dots(3)$$

أما عند حصول التداخل بنسبة 1:2 فتطبق المعادلة التالية (19,18):

$$1/K_2 = 1 / [(D - D_0) \cdot C_L] + 1 / (D_\infty - D_0) \quad \dots\dots\dots(4)$$

ويمثل الشكل (4) رسم المعادلة اعلاه للتداخل بين MgTPP و n-Butylamine في اربع درجات حرارية.



شكل-4: حساب ثابت الاتزان K₂ للتداخل بين MgTPP و n-Butylamine في اربع درجات حرارية

لقد أظهرت معقدات بورفرين - مغنيسيوم بشكل عام تداخلا من نوع 1:2 . ويبين الجدول (4) القيم المحسوبة لعدد مولات المانح الاليكتروني وقيم ثابت الاتزان K_2 في أربع درجات حرارية.

جدول -4: قيم عدد مولات المانح الاليكتروني (n) وقيم ثابت الاتزان K_2 بالنسبة للتدخلات التي حصلت بنسبة 1:2 في مذيب البنزين

Acceptor	Donor	Slope n	Equilibrium Constant K_2			
			283k	293k	303k	313k
MgTPP	n-Butylamine	1.9	0.2260	0.1515	0.0910	0.0820
MgTPP	Sec-Butylamine	2.0	1.7330	2.4030	1.3550	0.8590
Mg(p-OCH ₃)TPP	n-Butylamine	2.0	21.7390	2.4390	1.2870	0.8510
Mg(p-OCH ₃)TPP	Sec-Butylamine	1.7	2.9410	0.8580	0.2740	0.2710

في حين أظهرت معقدات بورفرين - نيكل وبورفرين - خارصين تداخلا من نوع 1:1. وبالنسبة لعنصر خارصين فقد أظهرت بعض دراسات علم البلورات بان ايون خارصين Zn^{+2} يقع خارج مستوى هيكل البورفرين ولذلك يفضل هذا الايون تناسق المربع الهرمي (20). وعليه فان عنصر خارصين يكون تداخلا بنسبة 1:1 . ويبين الجدول (5) القيم المحسوبة لثوابت الاتزان بالنسبة للتدخلات التي حصلت بنسبة 1:1 في مذيب البنزين.

جدول -5: ثوابت الاتزان للتدخلات التي حصلت بنسبة 1:1 في مذيب البنزين

Acceptor	Donor	Equilibrium Constant K_1			
		283k	293k	303k	313k
ZnTPP	n-Butylamine	11347	9662.4	6575.5	5545.7
ZnTPP	Sec-Butylamine	12442.2	10993.6	9077	7486.5
Zn(p-OCH ₃)TP	Piperidine	8399.5	6512.4	5692.8	4757.2
Zn(p-OCH ₃)TP	Pyridine	7686.8	6046.8	5388.5	4655.5
NiTPP	n-Butylamine	5.482	4.024	3.020	2.237
NiTPP	Sec-Butylamine	6.125	5.412	3.901	2.642
Ni(p-OCH ₃)TPP	n-Butylamine	5.072	2.688	1.861	1.025
Ni(p-OCH ₃)TPP	Sec-Butylamine	1.681	1.224	1.000	0.540

ان التداخل الحاصل يعتمد بصورة أساسية على طبيعة الذرة المركزية الموجودة في قلب البورفرين (21). حيث يتضح من الجدولين السابقين (4, 5) ان قيم ثابت الاتزان لمعقدات خارصين تكون قيما عالية جدا عند مقارنتها مع مثيلاتها من القيم التابعة لمعقدات النيكل والمغنيسيوم. ان معقدات المنح والاكتساب تكون غير ثابتة غالبا وتبقى في حالة توازن في المحلول مع المركبات الأخرى وبالإمكان تعيينها بواسطة الامتصاص الطيفي.

5- حساب الدوال الثرموديناميكية ($\Delta S, \Delta G, \Delta H$) للتدخلات :

وبعد الحصول على قيم ثوابت الاتزان K_2, K_1 في درجات حرارية مختلفة تم احتساب المحتوى الحراري للتدخلات المدروسة (ΔH Enthalpy) بتطبيق معادلة فان- هوف (22):

$$\ln K = (\Delta S / R) - [\Delta H / (R.T)] \dots \dots \dots (5)$$

وتم احتساب كل من الطاقة الحرة ΔG (free- energy) والتغير في العشوائية ΔS (Entropy) طبقاً للمعادلتين التاليتين :

$$\Delta G = - R.T.\ln K \dots \dots \dots (6)$$

$$\Delta G = \Delta H - (T.\Delta S) \dots \dots \dots (7)$$

وبين الجدول (6) الدوال الثرموديناميكية لجميع التداخلات المدروسة.

جدول 6- الدوال الثرموديناميكية لجميع التداخلات المدروسة في مذيّب البنزين

Acceptor	Donor	$-\Delta H$ Kcal.mol ⁻¹	ΔG Kcal.mol ⁻¹	$-\Delta S$ cal.mol ⁻¹ .K ⁻¹
ZnTPP	n-Butylamin	4.45	5.342	33.4
ZnTPP	Sec-Butylamine	3.000	5.417	28.7
Zn(p-OCH ₃)TPP	Piperidine	3.24	5.112	28.5
Zn(p-OCH ₃)TPP	Pyridine	2.86	5.069	27.0
NiTPP	n-Butylamin	5.23	-0.164	17.2
NiTPP	Sec-Butylamine	5.01	0.161	17.2
Ni(p-OCH ₃)TPP	n-Butylamin	9.08	0.575	32.9
Ni(p-OCH ₃)TPP	Sec-Butylamine	6.30	0.117	21.9
MgTPP	n-Butylamin	0.92	-1.098	+0.6
MgTPP	Sec-Butylamine	14.53	0.504(289.5)	51.9(298.5)
Mg(p-OCH ₃)TPP	n-Butylamin	15.35	0.519	51.3
Mg(p-OCH ₃)TPP	Sec-Butylamine	5.71	-0.089	19.1

عند زيادة درجة الحرارة لم تحصل ازاحات في الطيف وإنما حصل التغير فقط في قيم الامتصاص في طول موجي معين . كما لوحظ ان امتصاص المعقد يعتمد على درجة الحرارة فهو ينخفض بارتفاع درجة الحرارة ويعزى ذلك الى تكسر بعض جزيئات المعقد بسبب ازدياد درجة الحرارة مما يؤدي الى قلة تركيز المعقد. وتنطبق هذه الحالة على المعقدات المدروسة كافة وقم تم حساب ثابت الاتزان عند الدرجات الحرارية المختلفة. يتضح من الجداول السابقة ان قيم K للمعقدات كافة تتأثر بدرجة الحرارة فهي تقل بازدياد درجة الحرارة وعند رسم العلاقة بين $\ln K$ ضد مقلوب الحرارة تم الحصول على خطوط مستقيمة للتداخلات المدروسة كافة ومن خلال هذه الخطوط تم حساب قيم التغير في المحتوى الحراري ΔH لجميع التداخلات وكانت القيمة سالبة وهذا يعني ان التداخل باعث للحرارة (exothermic). أما قيمة الطاقة الحرة ΔG فهي موجبة (ماعدا حالات ثلاث) وتعني ان التداخل لا تلقائي.

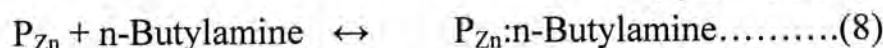
6- تأثير الذرة الواهبة في المانح الاليكتروني في التداخل :

لغرض معرفة تأثير الذرة المسؤولة عن الوهب الاليكتروني فان الجدول (7) يبين القيم المحسوبة لثوابت الاتزان والدوال الثرموديناميكية للتداخل بين البورفرين الفلزي $Zn(p-OCH_3)TPP$ مع أربع واهبات اليكترونية هي : ن- بيوتيل امين وثلاثي بيوتيل الفوسفيت (المحضر أنيا) والفيوران والثايوفين في البنزين كمذيب.

جدول 7- ثوابت الاتزان والدوال الثرموديناميكية للتداخل بين البورفرين $Zn(p-OCH_3)TPP$ مع أربع واهبات اليكترونية في مذيب البنزين

Acceptor	Donor	Donor Atom	Equilibrium Constant K				-ΔH Kcal. mol ⁻¹	ΔG 298k Kcal. mol ⁻¹	-ΔS 298k cal.mol ⁻¹ .K ⁻¹
			283k	293k	303k	313k			
Zn(p-OCH ₃)TPP	n-Butylamine	N ₂	1132 6.5	907 1.3	772 3.1	573 8.5	3.85	5.305	31.2
	Tributylphosphite	P	1109 0.5	842 5.6	733 1.9	637 2.7	3.18	5.262	28.0
	Furan	O ₂	1325. 5	105 1.8	782. 2	686. 9	3.99	4.051	27.4
	Thiophene	S	588.3	416. 1	363. 5	246. 4	4.82	3.511	28.4

يعبر عن هذه التداخلات أعلاه بالمعادلات التالية:

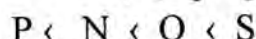


ومن خلال الجدول السابق يتضح بان التداخل الحاصل بين البورفرين الفلزي والمانحات الأربعة يتبع التسلسل التالي من حيث زيادة قيم ثابت الاتزان المحسوبة عمليا وحسب الذرة الواهبة:



ان هذا الترتيب يثبت بان الواهبات النيتروجينية تكون اشد تداخلا من بقية الواهبات وعلى العكس من ذلك تكون الواهبات الكبريتية هي الأقل شدة في التداخل ويعزى السبب الى الذرة المسؤولة عن التداخل (الذرة التي تمتلك المزدوجات الاليكترونية).

كما نلاحظ وجود فروقات بين قيم الدوال الثرموديناميكية لنفس التداخلات ومنها الترتيب التالي في قيم الانتالبية حيث تم الترتيب اعتمادا على الذرة الواهبة :



ان هذا الترتيب مفيد جدا في تصنيف البورفرين الفلزي وجعله ضمن صنف معين من المتقبلات الاليكترونية (أحماض لويس) اعتمادا على بعض الثوابت (23).

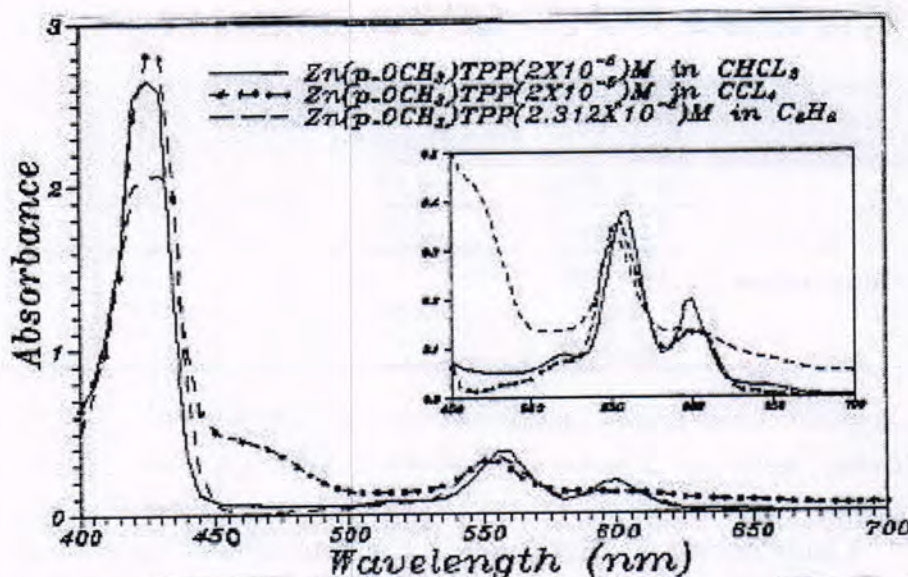
7- تأثير الذرة المركزية في قلب البورفرين على التداخل والدوال الثرموديناميكية:

بملاحظة الجداول (4-6) نستطيع ان نرى التأثير الواضح للذرة المركزية في قلب البورفرين على التداخل. فالتداخل بين المانح الاليكتروني بيوتيل أمين الثانوي مع البورفرينات الفلزية الثلاثة $Mg(p-OCH_3)TPP$, $Ni(p-OCH_3)TPP$, $Zn(p-OCH_3)TPP$ يكون ثابت الاتزان K كبيرا مع

الخاصين كذرة مركزية وصغيرا مع المغنيسيوم والنيكل كذلك تداخلها مع نفس المانح. وهناك الكثير من الأبحاث التي تناولت العديد من الصعوبات العملية في تقدير ثوابت الاتزان في معقدات الجزيئات الضعيفة (24-28) ومن ضمن هذه الصعوبات هي معرفة الحدود العليا والدنيا لإضافة المانح الالكتروني عند الطول الموجي المحدد. إن الاختلاف في التداخل بين المانح والمتقبل الالكتروني في حالة كون الذرة المركزية في قلب البورفيرين هي Mg, Ni, Zn قد يعود سببه الى حجم الذرة المركزية والى الألفة الالكترونية لتلك الذرة. (29)

8- تأثير المذيب في الدوال الثرموديناميكية:

يوضح الشكل (3) طيف امتصاص المعقد $Zn(p-OCH_3)TPP$ في ثلاث مذيبات عضوية هي البنزين والكلوروفورم ورباعي كلوريد الكربون.



شكل 3- طيف امتصاص الأشعة المرئية للمعقد $Zn(p-OCH_3)TPP$ في ثلاثة مذيبات عضوية وبيين الجدول (7) بيانات الأشعة المرئية العائدة للمركب أعلاه.

جدول 7- بيانات الأشعة المرئية للمركب $Zn(p-OCH_3)TPP$ في ثلاثة مذيبات.

Complex	Solvent	$\lambda_{max} \text{ nm } (\epsilon \text{ L.cm}^{-1}.\text{mol}^{-1})$		
		Soret القيمة		
$Zn(p-OCH_3)TPP$	Benzene	430 (89705)	555 (15354)	603 (5666)
	Chloroform	425 (133200)	560 (18850)	600 (10000)
	Carbon tetrachloride	425 (140650)	550 (15900)	

يظهر جليا" من الشكل (3) ان طيف الامتصاص بالنسبة للمعقد المدروس يكون متشابهة في كل من البنزين والكلوروفورم (مذيب قطبي) ومختلفا في رباعي كلوريد الكربون (مذيب غير قطبي). ان تغيير المذيب قد يؤدي الى ازاحة طيف المادة الماصة نحو اطوال موجي اطول (ازاحة حمراء) وتكون هذه الازاحات عالية (مقارنة الى الطيف في الفراغ) في مذيبات ذات ثابت عزل (dielectric constant) عال وذلك لان ازاحة الشحنة (charge displacement) الى حالة الطاقة العالية يحتاج الى طاقة اقل في مذيب ذي عزل عنه في الفراغ. ولهذا نلاحظ ان طيف المعقد المدروس اظهر

قما أقل في المذيب غير القطبي (CCl_4) عما هي عليه في المذيب القطبي ($\text{C}_6\text{H}_6, \text{CHCl}_3$). وبسبب وجود تجاذب الكترستاتيكي بين المذيبات القطبية والكروموفورات القطبية فإن هذه المذيبات تعمل على زيادة استقرار كل من الحالات الاليكترونية الواطئة غير المرتبطة وحالات π^* المثارة. وهذا بسبب انتقالات $n - \pi^*$ (ان وجدت) التي تحدث عادة عند طاقات أقل من انتقالات $\pi - \pi^*$ الى طاقات أعلى وتزيح انتقالات $\pi - \pi^*$ الى طاقة أقل. وهكذا فإن امتصاصات $\pi - \pi^*$ و $n - \pi^*$ للكروموفورات القطبية تتحرك قريبة من بعضها عند زيادة قطبية المذيب (30).

ويبين الجدول (8) الدوال الترموديناميكية المحسوبة للتداخل التالي:

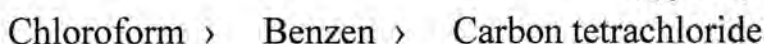


حيث ان PZn يمثل المعقد $\text{Zn}(\text{p-OCH}_3)\text{TPP}$ والتداخل مدروس في ثلاثة مذيبات عضوية هي البنزين والكلوروفورم ورباعي كلوريد الكربون.

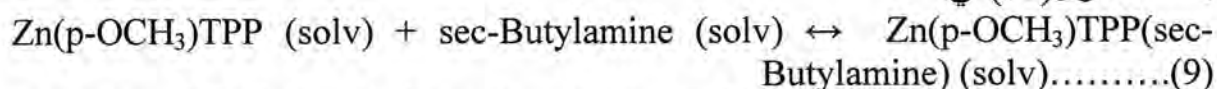
جدول 8- الدوال الترموديناميكية للتداخل بين $\text{Zn}(\text{p-OCH}_3)\text{TPP}$ مع بيوتيل امين الثانوي في ثلاثة مذيبات عضوية

Acceptor	Donor	Solvent	$-\Delta H$ K.cal.mol^{-1}	ΔG 293K K.cal.mol^{-1}	$-\Delta S$ 293K $\text{Cal.mol}^{-1}.\text{K}^{-1}$
$\text{Zn}(\text{p-OCH}_3)\text{TPP}$	Sec-Butylamine	Chloroform	4.49	5.413	33.7
		Benzene	3.06	5.380	28.8
		Carbon tetra chloride	2.92	5.260	27.9

يظهر جليا من الجدول اعلاه الفروقات الواضحة للتداخل بين المانح والمتقبل الاليكتروني عند الانتقال من مذيب قطبي الى مذيب غير قطبي او بالعكس حيث يتضح ان قيم انثالبية التداخل المدروس تتبع التسلسل التالي وحسب المذيب:



وكذلك الحال في قيم كل من الطاقة الحرة والعشوائية لنفس التداخل. ويبدو من خلال هذا الترتيب ان التداخل المدروس يفضل المذيب القطبي على المذيب غير القطبي. ويمكن التعبير عن التداخل السابق بمعادلة اخرى (31) هي:



ان تغييرات الطاقة الحرة لايعول عليها كثيرا في دراسات ومقارنات لما هو حاصل بالفعل حيث انها مع تغييرات العشوائية غالبا ماتتغير وباتجاهات مختلفة عند تغيير المذيب فضلا عن اهمية هذه التغيرات غير مسرود سابقا (24). ولتسليط الضوء على تغيرات الانثالبية يمكن الاخذ بنظر الاعتبار لبعض تداخلات مذاب - مذيب الممكنة (Solute - Solvent interaction) التي يمكن ان تقترح في حالات من هذا النوع (32):

- 1- معقدات π - complex .
- 2- معقدات انتقال الشحنة Charge - Transfer Complex .
- 3- Hydrophobic interaction .
- 4- توجيه القوى ثنائية الأقطاب Dipole Orientation Forcess .
- 5- قوى التشتت Dispersion Forcess .
- 6- الأواصر الهيدروجينية H-Bonding .

ان التداخلات من نوع 1 الى 4 من الناحية الكمية تكون اقل اهمية من بقية التداخلات وان كلا من هذه التداخلات او المؤثرات يعتمد على المذيب وكما يلي :

أولاً: الكلوروفورم CHCl_3 :

من الاحتمالات الستة المدرجة أعلاه فان التأصر الهيدروجيني سيكون الأكثر أهمية. فالتأصر الهيدروجيني أقوى احتمالاً بين نيتروجين الحلقات غير المتجانسة والكلوروفورم. إذا ارتبط الكلوروفورم مع المعقد $\text{Zn(p-OCH}_3\text{)TPP}$ بهذه الطريقة فانه من الواضح أن الليكاند الموجود لا يستطيع الارتباط مع الذرة المركزية بسبب قرب متقبلات البروتون (H-accepter) التي هي ذرات نيتروجين البيرول في البورفيرين.

التداخل بين بروتون الكلوروفورم ونظام بورفيرين – (الواضح مع ذرات نيتروجين البيرول) مرشح للحصول أيضاً ولكن عند الرجوع إلى القيم المنشورة لطاقات تداخلات شبيهة يصبح هذا التداخل ذو أهمية قليلة ولا يعول عليه (33-35).

ثانياً: البنزين C_6H_6 :

ان ميكانيكية ارتباط البنزين يجب ان تكون مختلفة عما هي عليه بالنسبة للكلوروفورم. فمن المعروف ان قوى التشنت قد تعمل بين المستويات الاروماتية (Aromatic planes) لتسبب درجة هامة من حزمة مشبكة عمودية (Vertical Stacking) للمركبات الحلقية غير المتجانسة في المذيبات غير القطبية (36). قيمة موريل وغيل (36) للانثالبية المرافقة لكل من البيريميدين والتولوين هي $(102 \pm 0.4) \text{ k cal.mol}^{-1}$ ويمكن اعتبارها كمرشد او دليل للانثالبية المتوقعة في نظام (metalloporphyrin- C_6H_6 system). ان سطح (surface) البورفيرين-الفلزي يحتاج لان يكون مشغولاً تماماً بارتباط جزيئات البنزين. طاقات اخرى ضمننت في دراسات سابقة للجهود بين الجزيئات (intermolecular potential) في البلورات الاروماتية. حيث وجد كريغ وجماعته (37) ان اسهام قوى التشنت في طاقة الشبكة (lattice energy) في البنزين حوالي 6 k cal.mol^{-1} بقرب الصفر المئوي. وثمة ملاحظة اخرى على التمدوب في البنزين لجزيئات عديدة محتوية على حلقات اروماتية هي انه ليس من المفاجئ عندما نجد جزيئات البنزين في تبلور البلورات (38-39).

ثالثاً: رباعي كلوريد الكربون CCl_4 :

ان تداخل رباعي كلوريد الكربون كمذيب يتوقع ان يكون قليلاً قد لا يصل الى الصفر وقد ثبت بواسطة قياسات موركون وترافرز (40) لحرارات محلول الكوينولين ومختلف البيريدينات في هذا المذيب ان القيم كانت صغيرة وسالبة تتراوح بحدود $-0.6 \text{ k cal.mol}^{-1}$ للمركب 3,5-dimethylptrydine وفي التداخل المعبر عنه بالمعادلة (9)، تغير العشوائية الكلي يمكن ان يتبع مايلي:

- 1- مساهمة سالبة للعشوائية تعزى الى فقدان في العشوائية الانتقالية والدورانية بسبب جزيئات الليكاند.
- 2- زيادة طفيفة في العشوائية تعزى الى زيادة الوزن الجزيئي للمعقد الكلي اعلى من الوزن الجزيئي للمعقد بورفيرين-فلز لوحده.
- 3- نقصان في العشوائية بسبب تقييد الدوران حوا آصرة فلز- نيتروجين بواسطة π .
- 4- زيادة في العشوائية لأن جزيئات المذيب المتصلة بالليكاند سوف تحرر.
- 5- مساهمة سالبة (او موجبة) في عشوائية التداخل لأن المعقد النهائي يكون اكثر (أو أقل) تمذوبا" منه في حالة المعقد بورفيرين- فلز لوحده.

9- تأثير مجموعة الميثوكسي المعوضة في البورفيرين على التداخل :

يبين الجدول (7) البيانات الخاصة بالتداخل بين N- بيوتيل امين مع ZnTPP و $\text{Zn(p-OCH}_3\text{)TPP}$ والتداخل بين بيوتيل امين الثانوي مع NiTPP و $\text{Ni(p-OCH}_3\text{)TPP}$ في البنزين كمذيب.

جدول 7- تأثير مجموعة الميثوكسي في التداخل بين البورفيرين الفلزي والمانح الاليكتروني

Acceptor	Donor	Equilibrium Constant K_1				$-\Delta H$ kcal. mol^{-1}	ΔG 293k Kcal. mol^{-1}	$-\Delta S$ 293k cal.mo $\text{l}^{-1} \cdot \text{K}^{-1}$
		283k	293k	303k	313k			
ZnTPP	n-Butylamine	11347. 0	9662.4	6575.4	5545.7	4.45	5.39 2	33.4
Zn(p-OCH ₃)TPP	n-Butylamine	11326. 5	9071.3	7723.1	5738.5	3.85	5.30 5	31.2
NiTPP	Sec-Butylamine	2.096	1.320	0.755	0.419	5.01	0.16 1	17.6
Ni(p-OCH ₃)TPP	Sec-Butylamine	1.681	1.224	1.000	0.540	6.3	0.11 7	21.9

ومن ملاحظة هذا الجدول يتضح تأثير المجموعة المعوضة (مجموعة الميثوكسي -OCH₃) في قيم ثابت الاتزان والدوال الترموديناميكية فالتداخل الذي يحصل بين المانح الاليكتروني N-بيوتيل امين مع كل من المتقبل الاليكتروني ZnTPP و Zn(p-OCH₃)TPP يكون بالنسبة للمتقبل الاول اكبر بمقدار 1.001 مرة منه الى المتقبل الثاني في قيمة ثابت الاتزان. ويعزى سبب كون التداخل بهذه الصورة الى التأثير الميزوميري الدافع لمجموعة الميثوكسي (23)(-OCH₃). ان زيادة في الكثافة الاليكترونية عند ذرات النيتروجين بسبب هذا التأثير قد يكون هو سبب ضعف الترابط مع المانح الاليكتروني N-بيوتيل امين (19,41). ونفس هذا التأثير يلاحظ في حالة التداخل الثاني في ذات الجدول.

المصادر

- 1.M.H.Mohammed&N.A.Abood,J.Al-Qadisiya For Pure Science(seasonal),13 (1):512-525 (2008).
- 2.T.Ohya and M.Sato,Bull.Chem.Soc.JPn.,69,3201(1996).
- 3.R.P>Listead,J.Chem.Soc.,1016(1934).
- 4.A.R.Katritzky&C.W.Rees'Comprehensive Heterocyclic Chemistry"4,Pergamon Press,Oxford(1984).
- 5.A.D.Adler,F.R.Longo,J.D.Finareli,J.Goldmacher,J.Assoar and I.Korsakoff, J. Org. Chem.,32,476(1967).
- 6.A.D.Adler,F.R.Longo,E.Kampas & J.Kim,J.Inor.Nucl.Chem.,32,2443(1970).
- 7.A.Vogel"Textbook of Practical Organic Chemistry"4thEd.Longman,Lodon:405 (1978).
- 8.C.H.Bedel-Cloutour,C.Barois-Gacheriew & A.Marchand, Spectrochimica Acta, 44, 567 (1988).
- 9.C.J.Pouchert,"The Aldrich Library of Infrared Spectra", Edition III, Aldrich Chemical Company,INC.,(1981).
- 10.I.L.Firer,"Organic Chemistry",2,6th Ed.,Longman,London,(1977).
- 11.D.W.Thoomas and A.E.Martel,J.Am.Chem.Soc.,78,1335(1965).
- 12.N.Datta-Gupta and T.J.Bardos,J.Heterocycl.Chem.,3,495(1966).
- 13.S.F.Mason,J.Chem.Soc.,976(1958).
- 14.M.Gouterman,J.Mol.Spectroscop,6,138(1961).
- 15.W.T.Simpson,J.Chem.Phys.,7,1218(1949).

16. M.Gouterman, J.Chem.Phys., 30, 1139 (1959).
17. M.D.Glick, G.H.Cohen and J.L.Hoard, J.Am.Chem.Soc., 89, 1996 (1967).
18. S.F.Ginburg, L.P.Brivina, G.U.Panomarev & V.V.Kharpov, S.J.Coord. Chem. (Translated from Russian), 3, 1394 (1977).
19. O.I.Koifman, T.A.Koroleva & B.D.Berezin, S.J.Coord.Chem. (Translated from Russian), 31, 1420 (1977).
20. D.M.Collins and J.L.Hoard, J.Am.Chem.Soc., 92, 3761 (1970).
21. J.R.Miller and G.D.Dorough, J.Am.Chem.Soc., 74, 3977 (1952).
22. P.W.Atkins. "Physical Chemistry", 6th Ed. Oxford University Press, Italy, :225 (2001).
23. J.March. "Advanced Organic Chemistry, Reactions, Mechanisms, and Structure" 2nd Ed., McGraw-Hill Kogakusha, LTD., Tokyo, :215 (1977).
24. D.A.Deranleau, J.Am.Chem.Soc., 91, 4044 (1969).
25. R.Foster and I.Horman, J.Chem.Soc., B, 171 (1966).
26. S.Carter, J.N.Murrell and E.J.Rosch, J.Chem.Soc., 2048 (1965).
27. W.B.Person, J.Am.Chem.Soc., 87, 167 (1965).
28. S.D.Rass, J.Am.Chem.Soc., 87, 3032 (1965).
29. F.A.Cotton & G.Wilkinson, "Advanced Inorganic Chemistry" 4th Ed., John Wiley and Sons, New York, (1980).
30. F.Scheinmann, "An Introduction to Spectroscopic methods for Identification of Organic Compounds" Pergamon Press, Oxford: 178 (1973).
31. S.J.Cole, G.C.Curthoys & E.A.Magnusson, J.Am.Chem.Soc., 93, 2153 (1971).
32. M.G.Reinecke, H.W.Johnson, Jr., and J.F.Sebastian, J.Am.Chem.Soc., 91, 3817 (1969).
33. T.Schaffer and W.G.Schneider, J.Chem.Phys., 32, 1218 (1960).
34. A.A.Bothner-By and R.E.Glick, J.Chem.Phys., 26, 165 (1957).
35. L.W.Reeves and W.G.Schneider, Can.J.Chem., 35, 251 (1957).
36. J.N.Murrell and V.M.S.Gil, Trans.Faraday Soc., 61, 402 (1965).
37. D.P.Craig, P.A.Dobsh, R.Mason and D.P.Santry, Discuss.Faraday Soc., 40, 110 (1965).
38. N.C.Payne and J.A.Ibers, Inorg.Chem., 8, 2714 (1969).
39. L.H.Vogt, Jr, A.Zalkin and D.H.Templeton, Inorg.Chem., 6, 1725 (1967).
40. K.W.Morcon and T.D.Travers, Trans.Faraday Soc., 62, 2063 (1966).
41. D.Monti, S.Nardis, M.Stefanelli, R.Paolesse, C.Di Natali and A.D'Amico, J. Sensors, 2009, 1155 (2009).

تحضير اقطاب انتقائية للمادة الدوائية Diclofenac sodium ومقارنتها طيفيا

محمد خليل محمد علي و عدي احمد عبد الستار و لمياء حسين كاظم و ابتسام عبد الحسين
وزارة العلوم والتكنولوجيا - دائرة بحوث الكيمياء

ABSTRACT

The research aims to prepared a membrane for liquid selective electrode pharmaceutical material Diclofenac sodium used as a drug analgesic pain in pharmaceutical material.

The membrane was prepared from material our laboratory with used plasticizers DBP, DBPH through the use phosphotungestic acid for a complex with pharmaceutical material.

The calibration curve is obtained in the extent of concentration (1×10^{-5} - 1×10^{-1}) molar diclofenac sodium, characterizing the electrode prepared and found the linear is equal 0.9945 assimilated Nernst responses by using the plasticizers DBPH and 0.9383 by using the plasticizers DBP.

By comparison spectrophotometric method with potentiometric electrode techniques, and found that the best wavelength at 275.8 nm for standard diclofenac sodium and we obtained the linearity is equal to 0.9987.

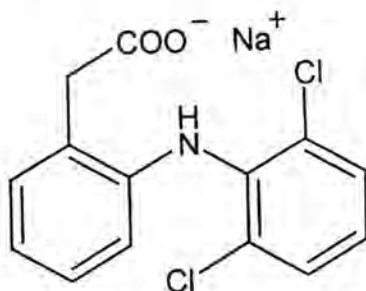
الخلاصة

يهدف البحث الى تحضير غشاء لقطب انتقائي سائل للمادة الدوائية Diclofenac sodium المستخدمة كمادة دوائية كمسكن للألم في المستحضرات الصيدلانية
تم تحضير غشاء مرّن من المادة الدوائية مع مواد ملدنة DBP, DBPH من خلال استخدام مادة Phosphotungestic Acid للحصول على معقد مع المادة الدوائية.
تم الحصول على منحنى معايرة في مدى تراكيز (1×10^{-5} - 1×10^{-1}) molar من المادة الدوائية Diclofenac sodium وتحديد خواص القطب المحضر والحصول على انحدار خطي مساوي 0.9945 مقارب للميل النيرنستي عند استخدام المادة الملدنة DBPH و 0.9383 عند المادة الملدنة DBP.
تم مقارنة الطريقة الطيفية مع تقنية الاقطاب الجهدية ووجد ان احسن طول موجي عند 275.8 nm للمسح الطيفي للمادة القياسية وحصولنا على منحنى معايرة مساوي 0.9987.

Key word : Drug, ion selective electrode , spectrophotometric

المقدمة

المادة الدوائية Diclofenac sodium هي مادة بيضاء اللون مائلة للاصفرار ذات وزن جزيئي 318.13 وصيغتها الكيميائية $C_{14}H_{10}Cl_2NNaO_2$ وذات تركيبة (1) كما موضح في الشكل رقم (1)



شكل-1 : الصيغة التركيبية لمادة Diclofenac sodium

تستخدم المادة الدوائية Diclofenac sodium كمادة خافضة للالام (2-3) ويشاع في الاسواق المحلية بأسم الفولتارين واستعمالها كبير في خفض الالام الناتج عن التشنج العضلي الخارجي والداخلي في جسم الكائن الحي .

تمكن الباحثين من مختلف الدول من تشخيص وتقدير المجاميع الفعالة للمادة الدوائية الحاوية على مجموعة الكربوكسيل الحرة Free Acid وبمختلف التقنيات التحليلية المتوفرة .

حيث تم تقدير تراكيز المادة بتقنية المطياف الجزيئي UV-Vis (4) وبواسطة الكاشف اللوني Methyl Blue وعند دالة حامضية تتراوح ما بين 9.2-9.4 وبمديات تراكيز (0.8-6.4 ug/ml) .
الباحثة Natalia وجماعته(5) قد استخدمت تقنية الكروماتوغرافيا السائل العالي الاداء HPLC وللمعومود C₁₈ وباستخدام الطور المتحرك (Acetonitril + Water) الحاوي على مادة 0.1% TriFluoro acetic Acid والكاشف UV-Vis تمكنوا من الحصول على منحنى معايرة ذو انحدار خطي 100 mg L⁻¹ وحد تحسس وصل الى 0.1 mg/L.

اما الباحث Vora وجماعته(6) فقد شخصوا المادة الدوائية وقدروا تراكيزها باستخدام HPLC بتغيير الطور المتحرك (Methanol + Water) وسرعة جريان السائل 1.25 ml/min. وكاشف UV-Vis وعند الطول الموجي 284 nm .

كما تمكن الباحث Wenrui وجماعته (7) من تحليل وتشخيص المادة الدوائية بواسطة تقنية Electrophoresis بتركيز يصل الى 4.9x10⁻³ mol/L مع فوسفات الصوديوم وتركيز 3x10⁻³ mol/L مع ثنائي هيدروجين فوسفات الصوديوم وعند الدالة الحامضية 7.0 وحد التحسس يصل الى 2.5x10⁻⁶ mol/L .

واخيرا استخدم الباحث Schender وجماعته (8) تقنية الكروماتوغرافيا الغاز GC لتشخيص وتعيين تراكيز المادة لدوائية وعبر اعمدة شعرية وكاشف الكتروني.

المواد وطرائق العمل

(1) الاجهزة المستخدمة :-

- (أ) جهاز المطياف الجزيئي UV-Vis 1650PC Shimadzu -Japan
- (ب) جهاز قياس الجهد Orion 940 USA
- (ت) ميزان حساس Mettler

(2) المواد الكيميائية :-

- (أ) المادة القياسية من شركة سامراء Diclofenac Sodium
- (ب) مواد ملدنة DBP(Dibutyl phosphate),DBPH(Dibutyl phthalate)
- (ت) مادة PVC عالي الكثافة .
- (ث) مذيب عضوي Tetahydrofuran THF
- (ج) كحولات 99% Methanol, Ethanol
- (ح) مستحضر صيدلاني Diclofenac Tablet 100 mg Made in INDIA
- Code : MH/Drugs/AD/217 BNo.AN0067AMfg:01/2007 Exp: 12/2008

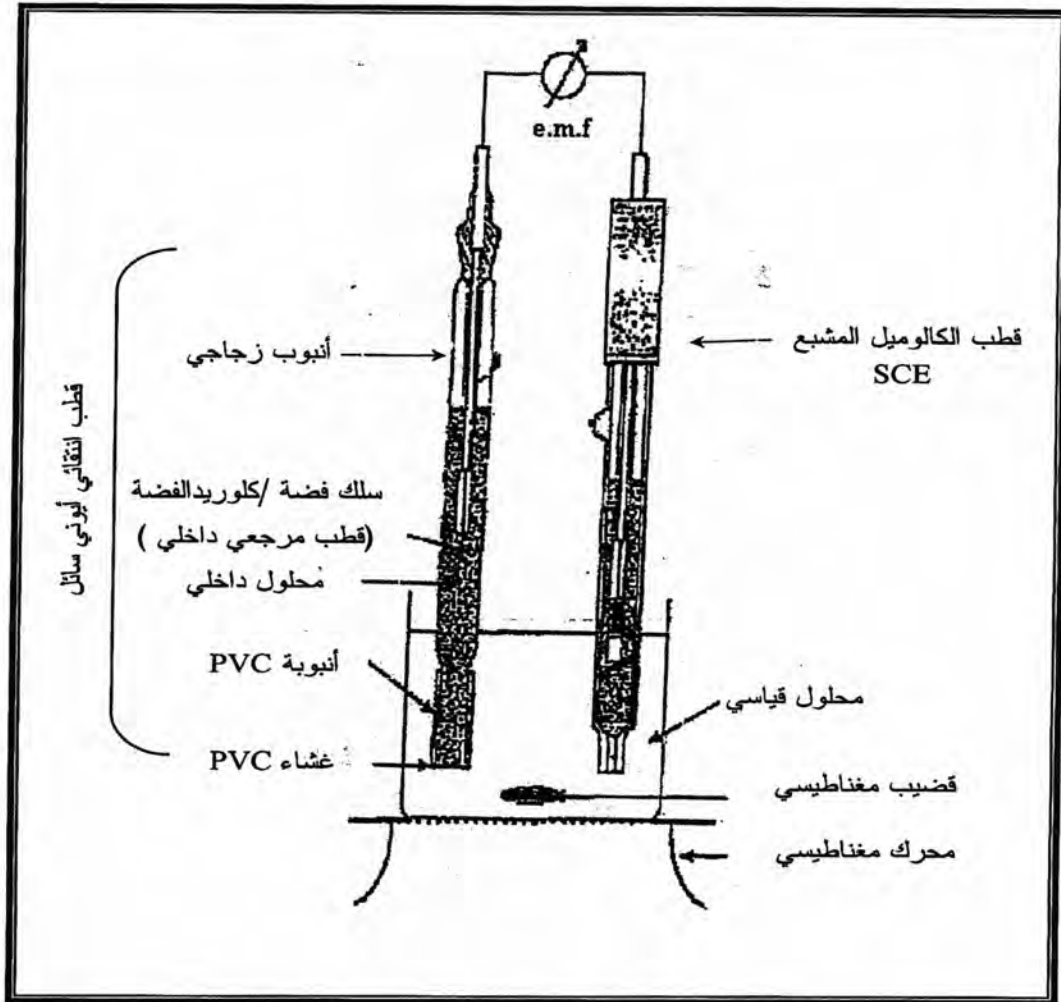
(3) تحضير المحاليل القياسية :-

- (أ) تحضير Stock solution من المادة الدوائية القياسية :
وزن 0.01 gm من المادة القياسية واذابتها بالماء المقطر اللانيوني الى حد 100 ml .
- (ب) تحضير مادة Phosphotungestic acid (PTA) :
وزن 7.2 gm من المادة PTA واذابتها بالماء المقطر الى حد 25 ml .
- (ج) تحضير المعقد الدوائي :

يمزج بنسب متساوية من الحجوم من المادة الدوائية القياسية ومادة PTA حيث سيتكون راسب نتيجة التفاعل ويخلط جيدا ثم يرشح بواسطة ورق ترشيح ويغسل عدة مرات بالماء المقطر ويترك ليجف في درجة حرارة الغرفة .
(د) تحضير الغشاء المرن :

إذابة 0.03 gm من المعقد المترسب الجاف مع 0.2 gm من PVC عالي الكثافة في محلول مكون من 0.25 ml من المادة الملدنة مع 6-7 ml من المذيب Tetrahydrofuran (THF) ثم يصب في وعاء زجاجي دائري Petrydish ذو سعة 5 ml ليغف في درجة حرارة الغرفة ثم يقطع الغشاء بمقدار قطر الأنبوب البلاستيكي للقطب المحضر .
(هـ) صنع القطب وخلية القياس :

بعد تقطيع الغشاء ولصقه بالانبوب البلاستيكي الملحق بالانبوب الزجاجي وهو جسم القطب يملأ القطب بالمحلول الداخلي وغمره بالسلك الفضة /كلوريد الفضة الموصل بجهاز قياس الجهد وكما مبين في الشكل (2) للخلية .



شكل 2- : خلية القياس الجهدية موضحة القطب العامل والقطب المساعد

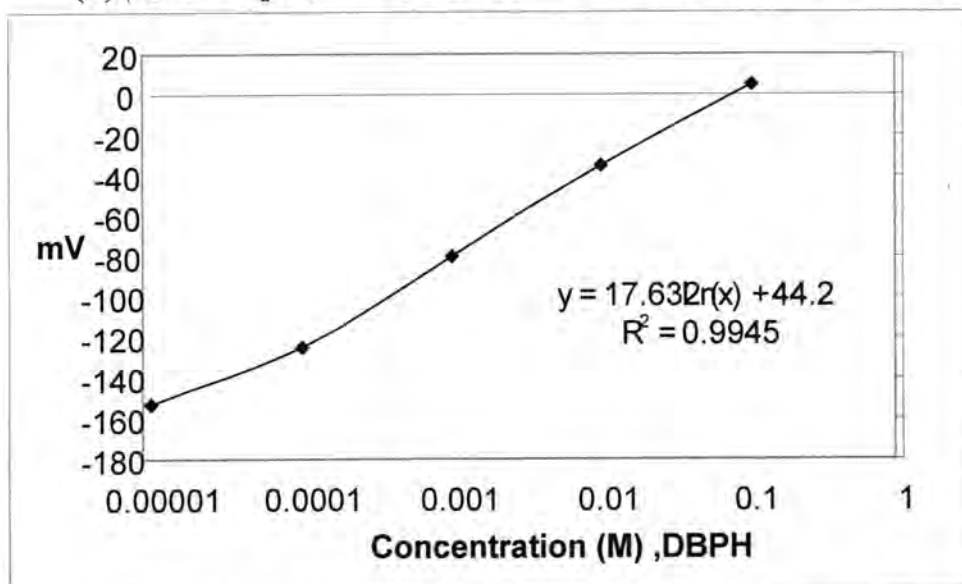
النتائج والمناقشة

لتحضير غشاء مرن من المادة القياسية Diclofenac sodium الناتج من خلط معقد PTA والمواد الملدنة المختلفة DBP, DBPH كلا على حدة مع المذيب العضوي تتراهيدروفيوران THF يجب ان تكون نسبة المزج مابين المكونات المختلفة جيدة وحسب التجربة العملية ولعدد من المحاولات

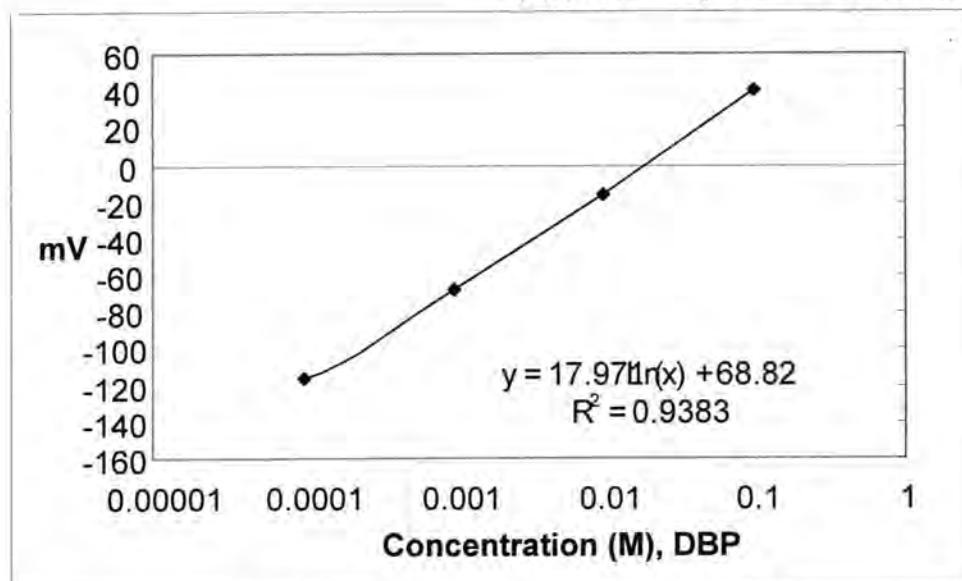
للوصول الى النسبة الصحيحة للحصول على غشاء مرن مناسب ذو مواصفات جيدة من السمك والشفافية والليونة ونفاذية المادة اثناء التطبيق في القطب .

ان هكذا دقة في عمل الغشاء يساعدنا كثيرا في التخلص من مشاكل عديدة اثناء تطبيق الغشاء على القطب واجراء القياسات الجهدية ويوفر الوقت الكثير في انجاز التحاليل الجهدية وبالتالي يمكننا من الحصول على ميل نرنيستي وخواص للقطب يمكن الاعتماد عليها في التحاليل الجهدية وتعيين تراكيز المادة الدوائية والمستحضر الصيدلاني .

بعد الحصول على الغشاء المناسب للمادة الدوائية وباستخدام مادتين ملدنيتين هما DBP و DBPH, حضر عدد من التراكيز القياسية للمادة الدوائية القياسية وبمدى تراكيز مولارية ما بين (1×10^{-5}) molar و قراءة الجهد mV لها تم رسم منحنى معايرة فكان الانحدار الخطي له قد وصل الى 0.9945 عند الغشاء المحضر للمادة الملدنة DBPH وكما مبين في الشكل رقم (3)



شكل 3- : منحنى المعايرة للقطب المحضر باستخدام المادة الملدنة DBPH
اما الغشاء المحضر مع المادة الملدنة DBP فقد حصلنا على منحنى معايرة ذو انحدار خطي يصل الى 0.9383 وكما مبين في الشكل رقم (4) .



شكل 4- : منحنى المعايرة للقطب المحضر باستخدام المادة الملدنة DBP

من خلال المعطيات السابقة الذكر يبين ان الغشاء المحضر للمادة الملدنة DBPH هي الاحسن من الغشاء المحضر للمادة الملدنة DBP من حيث قيمة الانحدار الخطي وكذلك المواصفات الاخرى من سمك الغشاء واللينة والنفاذية ، اما حد التحسس والخطأ النسبي فقد احتسب في الجدول (1)

جدول-1: حساب التراكيز والخطأ النسبي للاقطاب باستخدام عدة مواد ملدنة

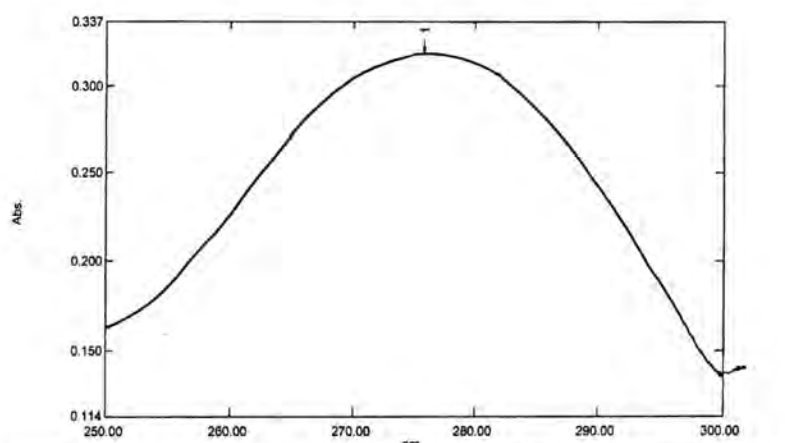
القطب المحضر بإستخدام المادة الملدنة	التركيز المأخوذ M	التركيز المحسوب M	Ex%	Rec. %
DBP	1×10^{-4}	0.95×10^{-4}	-5	95
DBPH	1×10^{-4}	1.07×10^{-4}	+7	107

وعند التطرق الى تقنية المطياف الجزيئي والحصول على الطول الموجي المناسب للمادة الدوائية القياسية Diclofenac sodium المذابة بالماء المقطر اللايوني تم الحصول على مسح طيفي وقمة ممتصية واحدة عند الطول الموجي 275.8nm وكما مبين في الشكل رقم (5).

Spectrum Peak Pick Report

12/11/20 05:11:20 a

Data Set: Storage 112906 0 - RawData - F:\cipro\D10.spc



Measurement Properties
Wavelength Range (nm): 250.00 to 300.00
Scan Speed: Fast
Sampling Interval: 0.1
Auto Sampling Interval: Enabled

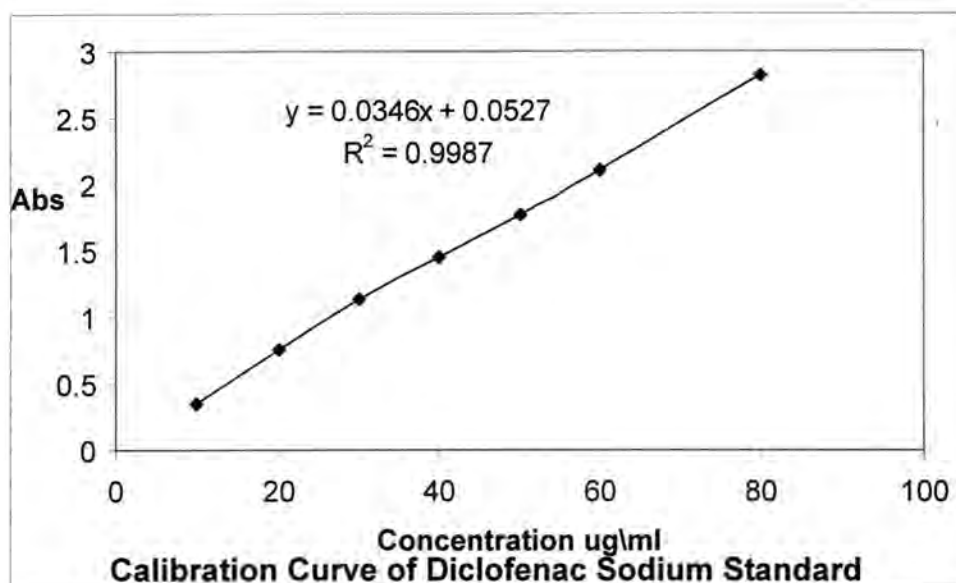
No.	P/V	Wavelength	Abs.	Description
1	⊗	275.80	0.318	

شكل-5: المسح الطيفي للمادة الدوائية القياسية Diclofenac sodium وباعتماد الطول الموجي 275.8 nm كطول موجي مناسب حضرت عدة تراكيز مختلفة من المادة القياسية وبمدى (1-80) ug/ml تم الحصول على امتصاصية مختلفة مع تغير التركيز وكما في الجدول (2)

جدول-2: مقادير الامتصاصية لعدة تراكيز للمادة الدوائية عند الطول الموجي 275.8 nm

No.	Conc. Of Diclofenac sodium ppm	Abs.(A)
1	10	0.350
2	20	0.763
3	30	1.133
4	40	1.450
5	50	1.780
6	60	2.100
7	80	2.815

وبعد رسم منحني المعايرة تمكنا من الحصول على انحدار خطي 0.9987 وحد للتحسس 1 mg/L وكما مبين في الشكل رقم (6).



شكل 6- منحنى المعايرة للمادة الدوائية القياسية Diclofenac Sodium

ومن ذلك يمكن ان نستنتج:

من الملاحظ ان المادة القياسية Diclofenac sodium التي تم تقييسها في الطريقتين الجهدية والطيفية لها واعطت منحنيات جيدة وذات انحدارات خطية متقاربة مما سمح لنا باعتماد الطريقتين في هذا الدواء .

المصادر

1. Merck&Co.,Inc., Whitehouse station.NJ,USA (1999).
2. De.Micalzzi.Y.C.; Pappano.N.B.;Debattista.N.B.;" First and second order derivative spectrophotometric determination of benzyl alcohol and diclofenac in pharmaceutical forms" .Talanta, 47 (3): 525-530(1998) .
3. M.Tubino,R.Leandro deSouza;" Determination of diclofenac sodium pharmaceutical prepration" Talanta,68(3-15): 776-780(2006).
4. J.C.Botello;G.Perez Caballero;" Spectrometry determination of diclofenac with methylene blue" .Talanta,42(1): 105-108 (1995).
5. Natalia,Novas,Rocio Urena and Luis Fermin aptain-Vallary " Determination Gelecoxib ,Rofecotib,sodium diclofenac and niflumic acid in human serum samples by HPLC with DAD detection " J.Chromatographia .,67(1-2):55-61(2008) .
6. Vora,Asfak,Danle.Mrinalini,Bhat Leena and Godge RahnL.," Diclofenac sodium and Rabeprazed Na in Buk and pharmaceutical dosage form by LC" . J.Chromatographia ,66(11),941-943(2007).
7. Wenrui.Jin and Jie Zhang," Determination of diclofenac sodium by capillaryzone electrophoresis with electrochemical detection " J.Chromagrapia A,868(1):101-107(2000).
8. W.Schender and P.H.Degan ," Simutaneous determination of diclofenac sodium and it hexroxy metabolities by capillary column gas chromatography with electron capture detection " J.Chromatography, A.,217: 263-271(1981).

دراسة تأثير التراكيز المختلفة للمواد الفعالة المستخلصة من النباتات الطبية على التغيرات الكروموسومية

¹ إقبال فاضل علوان و ² عصام فاضل الجميلي و ² علي عبيس و ¹ حسين علي محمد و ¹ حليلة جابر
وزارة العلوم و التكنولوجيا / دائرة بحوث الكيمياء
² فرع التقنية الإحيائية – معهد الهندسة الوراثية و التقنية الإحيائية للدراسات العليا – جامعة بغداد.

ABSTRACT

Extensively for their ability to protect organisms and cells from oxidative damage many researchers on Ellagic acid and grape seed , green tea , and the tail of the horse appear to be effective against the process of oxidation.

The work of a combination drug, containing 40mg of the extract alcohol Ellagic acid, 100mg of alcohol extract of grape seeds, 100mg of alcohol extract green tea and 10mg alcohol extracts of the plant a horses tail .

Having examined the toxic effects of three different concentrations of (0.75, 3.75, 18.75mg/ ml) on laboratory mice by the dosage by mouth during the month of the experiment.

Survey results showed that no changes in the chromosomal gene , which shows the effectiveness and efficiency of these extracts and the absence of significant differences compared with the control sample, indicating the possible use in the treatment of cancer.

الخلاصة

درست موانع الأكسدة على نطاق واسع لقدرتها على حماية الكائنات الحية و الخلايا من ضرر الأكسدة عند الكثير من الباحثين ذكر حامض اللاجيك وبذور العنب والشاي الأخضر و ذيل الحصان لأنها تمتلك فعالية ضد عملية الأكسدة .

تم عمل توليفة دوائية ، تحتوي على 40 ملغم من المستخلص الكحولي لحامض اللاجيك ، 100 ملغم من مستخلص الكحولي لبذور العنب ، 100 ملغم من مستخلص الكحولي لشاي الأخضر و 10 ملغم من مستخلص الكحولي لنبات ذيل الحصان .

وقد درست التأثيرات السمية لثلاثة تراكيز مختلفة منها (0.75، 3.75، 18.75 ملغم / مليلتر) على الفئران المختبرية من خلال التجريب عن طريق الفم خلال شهر من إجراء التجربة .

أظهرت نتائج الدراسة عدم حدوث تغيرات كروموسومية في الجينات الوراثية ، مما يدل على فعالية و كفاءة هذه المستخلصات وعدم وجود فروقات معنوية بالمقارنة مع عينة السيطرة مما يدل على إمكانية استخدام في علاج الأورام السرطانية .

المقدمة

مؤخراً أصبح تنوع المركبات التي تمتلك ملكية ضد عمليات التطهير واسعة و اكتشفت في الخضار و التوابل و الشاي الأخضر ، بدليل أجمع الباحثين بأن كمية الغذاء تخفض أو تقلل من خطر السرطان و الأمراض الخبيثة الأخرى في الإنسان (1) . مركبات مانع الأكسدة خصوصاً مركبات الفينولات موجودة في مصادر غذائية عديدة منها حامض كالك ، تأنين ، الكركم ، حامض اللاجيك و أجيونول لذا كان الاهتمام الكبير بأن الغذاء هو مانع تأكسدي إضافي (2) . أن المستخلصات الكحولية للشاي الأخضر و شحم الرمان ، بذور العنب هي من مجموعة المركبات المضادة للأكسدة و تقلل من مستوى الجذور الحرة و يمنع تكون الخلايا متعدد البروتين أي انه على إيقاف نمو الخلايا السرطانية في الجسم . و تستعمل بانتظام كمادة فعالة داخل الجسم ضد السرطان و تعتبر مشابهة لعمل بعض المركبات الكيماوية خلال علاج الأمراض السرطانية (3) . المبدأ لتنشيط مركبات البولي فينول بأنها تستعمل أيضاً في مستحضرات التجميل ولها تشكيلة واسعة تعرف كموانع تأكسد ضد المواد المطفرة و المسرطنة.

دراسة تأثير التراكيز المختلفة للمواد الفعالة المستخلصة من النباتات الطبية على التغيرات الكروموسومية
إقبال و عصام و علي و حسين و حليلة

مركبات المستخلصات الكحولية لها ملكية علاجية أيضاً لبعض الأمراض التي تصيب الإنسان (4). إن مركبات فينولية تستعمل بشكل دوري في علاج السرطان و كذلك يعمل كمثبط للأمراض السرطانية وبعض الأمراض المزمنة في التجارب الوراثة المتنوعة . وهناك أيضاً اهتمام للتحقيق من تأثير السمية على العوامل الوراثة من خلال دراسة الجذور الحرة التي تنتج و تجند العوامل ضد أكسدة و دمج الـ DNA (5) .

هدف الدراسة الحالية هو تحري عمل مانعات التأكسد في المستخلصات الكحولية لنباتات الدراسة لدمج

ألكروموسومات من قبل عامل الأكسدة هي مركبات الفينولية وذلك تقيم تأثيرهم على تردد الانحرافات ألكروموسومية التي تحدث في نخاع العظم الحيوانات المختبرية .

المواد وطرائق العمل

المواد المستخدمة

- 1- دارىء الفوسفات الفسلجي PBC Fluka
- 2 - الكوسجين 0.1 ملغم / 0.1 مل Fluka
- 3- كلوريد البوتاسيوم (0.075M) BDH
- 4- محلول التثبيت BDH
- 5- صبغة لشمان BDH
- 6- صبغة كمزا : Giemsa Fisher
- 7- محلول بيكرينات الصوديوم (0.75%) BDH

يتم تحضير المستخلص الكحولي لغرض إعطاه إلى الحيوان كما يلي
الحيوانات المختبرية :-

استخدم (16) فأر ذكر من نوع Balb بعمر (5 - 8) أسبوع و بوزن تقريـب (20-25) غم وزعت عشوائياً إلى أربعة مجاميع متساوية منفصلة ووضعت في أقفاص بلاستيكية . تم تغذيتها بالإضافة إلى العلف المركز و الماء على تراكيز مختلفة من التوليفة لمستخلصات النباتية وهي (0.75 و 3.75 و 18.75 ملغم / 0.1 مليلتر) يومياً و لمدة 4 أسابيع بعدها تم قتل الحيوانات وأخذ نخاع العظم لإجراء الاختبارات عليه .

إذابة محتويات الكبسولة للأجل الحصول على تراكيز التالية

يتم وزن معدل 3 كبسولة من المستخلصات و هي كمية الجرعة اليومية المحسوبة حيث يتم إذابة 7.5 ملغم / 1 مل ثم يضاعف إلى خمس مرات و يكون التركيز هو إذابة 37.5 ملغم / 1 مل وكذلك تم أخذ خمس أضعاف هذا الوزن 187.5 ملغم / 1 مل من محتويات الكبسولة لغرض تجريع الحيوانات حيث تم إعطاء الحيوانات التي قسمت إلى أربع مجاميع كل مجموعة 4 حيوانات عن طريق الفم تم قتل المجاميع الأولى خلال 2 أسبوع والمجموعة الثانية بعد مرور شهر على عملية التجريع .

1- 0.75 ملغم / مليلتر

2- 3.75 ملغم / مليلتر

3- 18.75 ملغم / مليلتر

الاختبارات الوراثة :

طريقة الحصول على كروموسومات الخلايا الجسمية لإجراء الاختبارات الوراثة إتباع طريقة Allen و جماعته 1977 و كما يلي :

- حقن الحيوان (0.25 مل) من محلول الكولجسين بتركيز 0.6 ملغم لكل 1 كغم من وزن الجسم وذلك عن طريق غشاء الخلب بعدها يترك الحيوان لمدة ساعتين .
- يقتل الحيوان بعد ساعتين و ذلك عن طريق فصل الفقرات العنقية ويثبت الفأر على جهة الظهرية فوق طبق التشريح ، يقص الجلد من فوق منطقة الفخذ و يقص عظم الفخذ من

- ارتباطه بمفصلي الحوض و الركبة . ينظف العظم خارج جسم الحيوان من بقايا العضلات و يوضع في أنبوبة اختبار و يحقن بـ (5مل) من محلول (PBC) وذلك لغسل العظم و أنزال كل النقي بحيث يصبح لونه ابيض .
- توضع الأنابيب الحاوية على نقي العظم في النبد المركزي بسرعة 2000 دورة / دقيقة لمدة 10 دقائق . أزيل الرائق و أضيف إلى الراسب (5مل) من محلول كلوريد البوتاسيوم واطى التركيز و تركت الأنابيب لمدة 30 دقيقة في الحمام المائي بدرجة 37م و ثم ترج الأنابيب بين فترة و أخرى .
- أزيل الرائق و أضيف إلى الراسب المحلول المثبت Fixative solution على شكل قطرات تم أنزالها على الجدار الداخلي للأنبوبة مع الرج المستمر ، ثم أكمل الحجم المثبت المضاف ليصل إلى (5مل) ورجت المحتويات جيدا .
- وضعت الأنابيب بدرجة حرارة (4م°) لمدة نصف ساعة و ذلك لغرض تثبيت الخلايا .
- تم إسقاط قطرات من محتويات الأنبوبة على شريحة زجاجية نظيفة و بمعدل (4-5) قطرات و بصورة عمودية على الشريحة من مسافة (3) أقدام تقريبا و ذلك لإتاحة الفرصة للكر و موسومات بالانتشار بشكل جيد ثم جففت الشرائح على صفيحة ساخنة بدرجة (50) درجة مئوية لمدة دقيقة واحدة .
- صبغة الشرائح بصبغة كمزا و تترك لمدة (20دقيقة) ثم تغسل بالماء المقطر .

اختبار معامل الانقسام الخيطي : Mitotic index Assay

تم فحص الشرائح باستخدام قوة تكبير (600) مرة (العدسة العينية $\times 15$ و العدسة الشيئية $\times 40$) و تم حساب (1000) خلية منقسمة و غير منقسمة و من ثم تم حساب النسبة المئوية للانقسام الحاصل في تلك الخلايا وفقاً للمعادلة التالية :

عدد الخلايا المنقسمة

$$\text{معامل الانقسام الخيطي MI} = \frac{100 \times \text{عدد الخلايا المنقسمة}}{\text{العدد الكلي للخلايا}} \quad (\text{King et al. 1982})$$

العدد الكلي للخلايا

اختبار التغيرات الكروموسومية

تم فحص الشرائح المحضرة باستخدام العدسة الزيتية حيث تم فحص 100 خلية منقسمة لكل حيوان و واضحة في الطور الاستوائي من الانقسام الخيطي حيث تكون الكروموسومات منتشرة بشكل جيد لغرض تحديد التشوهات الكروموسومية و حساب النسبة المئوية لها .

اخضعت نتائج الى تحليل التباين باستخدام برنامج الاحصائي الجاهز (SAS 2001) لمعرفة اصغر فرق معنوي بين معدلات المجاميع تم استخدام تحليل Least Significant difference / LSD عند مستوى احتمالية ($p < 0.05$) لمعرفة الفروق المعنوية بين مستويات المعاملات المختلفة .

النتائج والمناقشة

التأثيرات الوراثية لجرع متعددة من المستخلص الكحولي للنباتات الطبية :

1- اختبار معامل الانقسام الخيطي :

يبين كل من الجدولين رقم (1) التجريع لمدة أسبوعين و رقم (2) لمدة شهر واحد بأنه لا يوجد هناك أي انخفاض أو تغير على نسبة معامل الانقسام الخيطي باستخدام التراكيز المختلفة (0.75، 3.75، 18.75 ملغم/مل) مقارنة مع عينة السيطرة الموجبة و بمستوى معنوي ($P > 0.05$) و اما نسبة المعامل الانقسام الخيطي فكانت (6.78، 6.68، 6.78 %) مقارنة بالسيطرة الموجبة (6.63%) .

2- اختبار التغيرات الكروموسومية :

يوضح جدول رقم (3) نتائج حالة التجريع للتراكيز المختلفة لمدة أسبوعين و جدول رقم (4) يوضح نتائج التجريع للتراكيز المختلفة لمدة شهر واحد ، و التراكيز هي (0.75، 3.75، 18.75 ملغم / مل) و حيث كانت النسب هي (1.83، 1.84، 1.85 %) لهذه التراكيز مقارنة بعينة السيطرة الموجبة و التي هي (1.8 %) من هنا يتم ملاحظة عدم وجود فروقات معنوية لنسبة التغيرات الكروموسومية واضحة المستوى و التي هي ($P > 0.01$) بالمقارنة مع عينة السيطرة الموجبة و كذلك شكل رقم (1) يوضح هيئة الكروموسومات الطبيعية للسيطرة لموجبة ، شكل رقم (2) يوضح الكسر الكروماتيدي ، و شكل رقم (3) يوضح الكسر الكروموسومي . إن الاختبارات الوراثية التي تمت دراستها هي (معامل الانقسام الخيطي و التغيرات الكروموسومية) . وقد أشارت نتائج التجارب في جدول رقم (1,2) بأن النسبة المئوية لمعامل الانقسام الخيطي ليس لها تأثير ولم تسجل بذلك أية فروقات معنوية ($p < 0.01$) بالمقارنة مع السيطرة الموجبة و قد يعزى سبب الانخفاض في نسبة معامل الانقسام الخيطي و الارتفاع في نسبة التغيرات الكروموسومية إلى أن هذه النباتات تحتوي على العديد من الفيتامينات مثل (A,E,C,) بالإضافة إلى مواد بولي فينولية بسيطة (6) و كل هذه المواد تظهر مضادة للتطهير (7) لكن هذه الفعالية لم تتحول من حالة ايجابية إلى حالة سلبية أي لم تصبح للمواد خاصية سمية وراثية وهذه الخاصية لم تظهر بازدياد تركيز المستخلص الكحولي بالإضافة إلى ذلك فإن أي خلل في الموازنة بين المواد التي تمتلك صفه السمية لجزيئية إلى DNA و المواد التي تمتلك فعل مضاد للتطهير يؤدي إلى حصول تلف وراثي (Genetic damage) في خلايا الحيوانات المعالجة بمستخلصات هذه النباتات و بصوره عامه لم تظهر جميع المواد الموجودة في النباتات الطبيعية المختلفة خاصيتها السلبية عند التراكيز العالية وكل حسب نوعه (8) .

جدول 1- تأثير تراكيز المختلفة من المستخلص في الاختبارات الوراثية للفأر الأبيض لمدة أسبوعين

التركيز ملغم / مليلتر لحيوان المعاملة	نسبة معامل الانقسام الخيطي
السيطرة أو الاختبار	6.64
تركيز 0.75 ملغم / مليلتر	6.65
تركيز 3.75 ملغم / مليلتر	6.65
تركيز 18.75 ملغم / مليلتر	6.66

جدول 2- تأثير تراكيز المختلفة من المستخلص في اختبار معامل الانقسام الخيطي للفأر الأبيض لمدة 4 أسابيع .

التراكيز ملغم / مليلتر / حيوان المعاملة	نسبة معامل الانقسام الخيطي
السيطرة أو حيوانات الاختبار	6.70
تركيز 0.75 ملغم / مليلتر	6.71
تركيز 3.75 ملغم / مليلتر	6.71
تركيز 18.75 ملغم / مليلتر	6.71

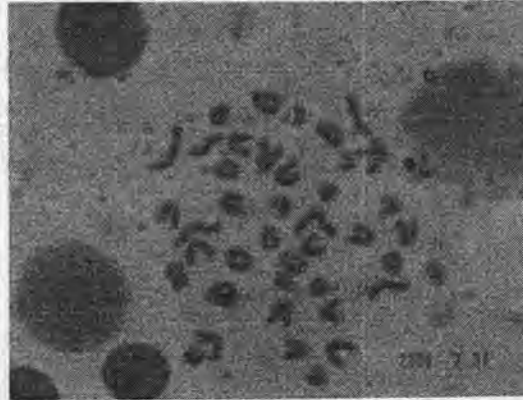
كل تجربة أربع حيوانات

من ناحيه اخرى فان الفينولات النباتية تلعب دورا مهما في تقليل الأثر السمي الوراثي لعدد من المركبات المطفرة وجد بان إعطاء آل Catchiness (أحد المركبات الفينولية الموجودة في

الشاي) بعد استخدامه يؤدي إلى التقليل من نسبة الطفرة (4)، فضلا عن ذلك فقد وجد بان المركبات البوليفينولية polyphenolic compounds تثبيط من عملية تكسر احد خيطي الـ DNA و DNA single-strand cleavage بالإضافة الى تثبيطها . إن الفينولات النباتية تظهر الخاصية المضادة للتطهير من خلال عملها على غلق مسار التنشيط الأيضي للمطفرات وإزالة الجذور الحرة المتولدة من تأييض هذه المطفرات . بالإضافة إلى ذلك فإن قسم من الفينولات تمنع من تكوين الـ (DNA adduct) من خلال ارتباطها بالمواقع الموجودة على جزئية الـ DNA والتي تكون مستهدفة من قبل المطفر (5). أن الفلافونيدات أثبتت الدراسة امتلاكها فعالية مضادة للتطهير (9) أن الفلافونيدات المستخلصة لها دور في تنشيط المركبات الكيميائية و كما وجد بان للفلافونيدات قدره في تقليل الكسور في أشرطة الـ DNA (10).

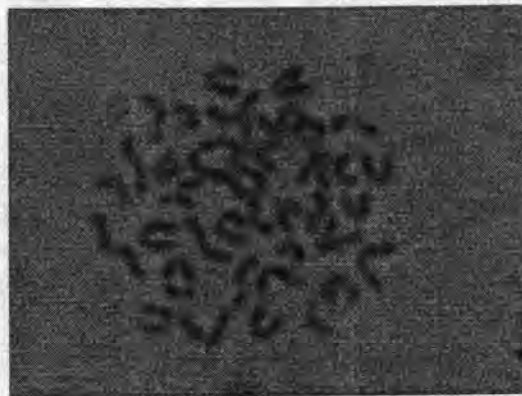
أظهرت النتائج أن المستخلصات النباتية إلي تحتوي على الفينولات التي تظهر صفة مضادة للتطهير من خلال قدرتها على غلق التنشيط التأيضي للمطفرات و كسح الجذور الحرة المتولدة من تأييض المطفرات فضلا عن الصفة المضادة لتأكسد , كما تعمل بعض الفينولات على تقليل من تكوين (DNA- Adduct) من خلال ارتباطها بمواقع الـ DNA المستهدفة من قبل المطفر (11).

وشكل رقم (1) يبين عدد الكروموسومات لخلايا نقي العظم المحضرة لفئران السيطرة الموجبة إذ يلاحظ من الشكل ان عدد كروموسومات الخلايا الجسدية و ($2n=40$) كروموسوما .



شكل -1: يوضح العدد الطبيعي الكروموسومات لخلايا نقي العظم .

أما بشأن الشكلان رقم (2) و (3) يوضحان الزيغ الكروموسومي وعند التداخل بين المستخلصات النباتية ، التغيرات المحسوبة (على الكسور الكروموسومية و الكروموماتيدية) وقد اختلفت تأثير هذه التغيرات باختلاف النبات و نوعية كل نبات والمستخلص الكحولي .



شكل -2: يبين الزيغ الكروموسومي لخلايا نقي العظم كسر الكروماتيدي



Fig. 17: Metaphase of the bone marrow cells showing the 'gape' chromatid

شكل -3: يبين الزيج الكروموسومي لخلايا نقي العظم كسر الكروموسومي .

أن المستخلص الكحولي ليس له تأثير على الزيج الكروموسومي لذلك لا يكون هناك تأثير على نسبة الكسور الكروموسومية و كذلك نسبة الكسور الكروماتيديه كما جاء في جدول (رقم 3) وكذلك جدول (رقم 4).

جدول -3: تأثير تراكيز مختلفة من المستخلص الكحولي على تغير الكروموسومي لمدة 2 أسبوع

المعامل التراكيز ملغم/ملييلتر للحيوان التجربة	تغير معامل الكروموسومي	كسر الكروماتيد	كسر كروموسومي
السيطره الموجبه	1.8	0.3	0.3
مجموع تركيز 0.75 ملغم / ملييلتر	1.81	0.301	0.305
مجموع تركيز 3.75 ملغم / ملييلتر	1.81	0.302	0.3050
مجموع تركيز 18.75 ملغم / ملييلتر	1.81	0.302	0.3050

جدول -4: تأثير تراكيز مختلفه للمستخلص الكحولي على التغيرات الكروموسومات الوراثيه
لفأر ألابيض لمدة 4 أسابيع .

المعامله التراكيز ملغم / ملييلتر	تغير معامل الكروموسومي	كسر الكروماتيد	كسر كروموسومي
السيطره الموجبه للحيوان	1.80	0.3	0.3
مجموع تركيز 0.75 ملغم/ ملييلتر	1.81	0.301	0.301
مجموع تركيز 3.75 ملغم/ ملييلتر	1.81	0.301	0.301
مجموع تركيز 18.75 ملغم/ ملييلتر	1.81	0.302	0.302

وتعتبر خلايا نقي العظم أكثر الخلايا الجسمية نشاطا حيث تتميز بانقسامها السريع ولتعدد
ليعطى أنواع كثيرة ومختلفة من خلايا الدم وفي مراحل مختلفة ، وأن تأثير معامل الانقسام
الخيطي بالمواد الكيميائية أو الفيزيائية يعتمد على الجرعة المعطاة وعلى طريقه التجريب حيث
أن تلك المواد غالبا ما تؤثر على معامل الانقسام الخيطي .

ويمكن من ذلك ان نستنتج :

يتضح من نتائج الدراسة أن المستخلصات النباتية الكحولية خالية من التأثيرات السمية بالجرعة المستخدمة و هذا ما أستنبط من نتائج معامل الانقسام الخيطي و التغيرات الكروموسومية لخلايا نقي العظام .

المصادر

1. World Health Organization . Reaearch Guide lines for Evaluation the safety and effieancy of Herbal Medicines (1993).
2. Grabaly,S. and Thierick,R.;Drug discovery from nature, :5(2003).
3. Aroea,R.B.;Hamadarol Pharmacopia of Estern Medicine,:422-448 (1998).
4. Kuroda, Y.; Hara, Y. , Antimutagenecity of tea polyphenols Mutat. Res. 436: 69-97(2003).
5. Padam,S.K.,Grover,I.S.&Singh,M.,Antimutagenic effect of polyphenols isolated from Terminala bellerica myroblan in Salmonella lyphimurium, Indin, J.of experimaental biology, 34:98-102 , (1999).
6. Shubber, E.K.; Juma, A.S.M. , Cytogenetic effects of herabel medicinal plant , 19 :3 (2002) .
7. Kojima, H., Konishi, H. and Kuroda, Y.,Effect of L-ascorpi acid on the mutagenecity of ethylmethano- sulfonate in cultured mammaliam cells, Mutat. Res., 266: 85-91,(1999).
8. Tyler,Brady,pharmacegnosy,9thEditors,Iea and Febiger Philadelphia (1998).
9. Samejima, K.; Kanazawa, K., Ashida, H. and Danna , G. ; J. Agric, Food, chem.,43: 410-414(1999).
10. Misiki, M. ; Ulubele, A. and Mabry, T. J., 6- Hydroxyl flavones from Thymbra spicata, photochemistry , 24: 2193-2194(1998).
11. Raj, A. S.; Heddle, J.A.. New mark, H.L. and Katz, M., caffeic acid as an inhibitor of DMBA induced chromosomal breakage in mice assessed by bone marrow micronucleus test, Mutat. Res.,124:247-253 (2004).

دراسة تأثير التلوث بالكروم على فيتامينات مضادات التأكسد

حنان فاضل عباس وجعفر هاشم محسن وحليمه جابر محمد واسماء سوري محمد ومحمد خليل محمد وعدنان عبد الله حسين و
اسيل عبد الحسين عبيد
وزارة العلوم والتكنولوجيا

الخلاصة

اهتمت هذه الدراسة بإلقاء الضوء على العلاقات المحتملة بين الدليل الكيميائي الحيوي لعملية الأكسدة الفوقية للدهون (المالون ثنائي الألدهايد MDA) وتأثير التلوث بالكروم في مصل دم (40) عاملاً لدى العمال المعرضين للكروم نتيجة اشتغالهم، وقد قسمت مجاميع العمال إلى مجموعتين حسب فترات اشتغالهم. أما المجموعة الثالث فقد كانت من المتطوعين الأصحاء غير المعرضين للكروم. وقد أظهرت نتائج الدراسة إن نسبة الكروم تزداد في مصل دم العاملين بازدياد فترة تعرضهم، كذلك تم قياس معدل الأكسدة الفوقية للدهون بمقدار ما يتكون من المالون ثنائي الألدهايد ولوحظ ارتفاع في مستوى الـ (MDA) لمجاميع العمال مقارنة مع مجموعة السيطرة وأيضاً تم قياس تركيز فيتامينات (A,C,E) وأظهرت الدراسة إن نقصاً واضحاً في تركيز فيتامينات (A,C,E) لدى العاملين مقارنة مع مجموعة السيطرة. نوقشت النتائج على ضوء النظريات العلمية الحديثة والتي تفسر تكون هذه النواتج الثانوية للأكسدة الفوقية للدهون

ABSTRACT

In this study we attempted to shed alight on the possible relation ships between lipid peroxidation marker, serum malondialdehyde (MDA) with the effect of Chromium exposure Using serum samples obtained from (40) Chromium exposed workers due to their occupation.

The workers were divided in two groups according to their occupational period. The third group consists of healthy volunteers that were working out side the Chromium factories as a control group.

Our results showed that Chromium levels increased with the increasing of their occupation period, The level of (MDA) was elevated in the workers

Some serum antioxidants such as vitamins (A,C,E) were evaluated and were found to be lower in all workers compared to the control group.

المقدمة

يعد الكروم أحد العناصر الثقيلة التراكمية ذات السمية العالية، ويتواجد بحالات تأكسدية من +2 إلى +6، ويعد الكروم السداسي التكافؤ هو الأكثر سمية. ولكون استخداماته كثيرة في الصناعات المختلفة على سبيل المثال في صناعة الأصباغ فضلاً عن كونه متواجد في المناطق الصناعية حيث ينتج الكروم السداسي التكافؤ السام من جراء فعاليات الإنسان حيث يشق من أكسدة المصانع للكروم المستخرج من المناجم ومن احتراق الوقود الحجري و السائل، الخشب والأوراق... الخ، وهذا ماينتج عنه زيادة في تراكيزه في البيئة مما ينتج عنه أضرار سمية على نسج وأعضاء الجسم المختلفة في جميع الكائنات الحية.

كما يعتبر من العناصر الضرورية للإنسان والحيوان وهو يدخل في الأيض الطبيعي للكربوهيدرات (1). ولكن عند وجوده بتركز عالية يصبح ساماً (2) لاسيما الكروم السداسي التكافؤ ويدخل الكروم إلى البيئة عن طريق الفضلات التي تطرح من معامل دباعة الجلود و صناعة الأصباغ والطلاء الكهربائي ومعامل النسيج ومبيدات الفطريات فضلاً عن حجر الكرومايت (3، 4)

يعد التلوث البيئي من أهم العوامل التي تؤثر في صحة الإنسان، ويعرف التلوث البيئي بأنه تغيير في واحد أو أكثر من الخواص الفيزيائية أو الكيميائية أو الحيوية لكل أو بعض مكونات الغلاف الحيوي مثل الماء والهواء والتربة وذلك بواسطة المواد التي تطلق في الجو نتيجة نشاط الإنسان وغالباً ما يؤدي هذا التغيير إلى حدوث آثار ضارة في صحة الإنسان والحيوان والنبات (5).

يمتص الكروم في الأمعاء الدقيقة بمقدار 1-0.5% وتقدر كمياته المفرزة مع الإدرار حوالي 10 مايكروغرام يوميا، كما وجد بأن معدل تركيز الكروم في مصل دم الإنسان الطبيعي يتراوح بين 4.5-008 مايكروغرام / 100 مليلتر (6). وتختلف تراكيز الكروم في الإدرار باختلاف مكونات الإدرار (المادة الأساس) كما تعتمد هذه القيم على كميات الكروم المأخوذة يوميا من الطعام وتقل كميات الكروم التي تفرز مع الإدرار مع مرور

السنين وذلك بسبب اختزاله من قبل المواد الموجودة في الادرار لتصل الى 1.0 مايكروكروم يوميا (7) . كما تقدر كميات الكروم المفقودة على شكل عرق بحوالي 20% من كمياته المفترزة مع الادرار (8) . كما وجد بان كميات الكروم تقل في انسجة الجسم مع تقدم العمر (9) . يحدث التعرض الشخصي للكروم من خلال استنشاق غباره المتصاعد خلال العمليات الصناعية المختلفة (10) . حيث يسبب امراضا مثل الحساسية وتقرح الانف والقرحة والتهابات الجلد , واما التعرض المزمن له فينتج عنه اعراض امراض المعدة وسرطان الرئة (11) . ولوحظ ان مركبات ان مركبات الكروم السداسية تخرق الجلد من خلال الغدد العابية ثم تختزل الكروم السداسي الى ثلاثي والاخير يتفاعل مع بروتين الجلد مكونا معقدات مستقرة وبذلك تتضح كيفية حدوث الضرر الذي تصاب به الغدد للعابية عند الاشخاص المتعرضين لكميات قليلة من الكروم مسببا لهم الحساسية (12) .

المواد وطرائق العمل

طريقة تقدير مستوى الاكسدة في مصل الدم بمقدار مايتكون من MDA ان المألون ثنائي الالدهايد هو من النواتج الثانوية للاكسدة الفوقية للدهون فان قياس هذه المادة يعطي انطبعا عن مستوى الاكسدة واستخدمت طريقة لونية تعتمد على التفاعل بين مركب حامض الثايو بار بتيورك والمألون ثنائي الالدهايد ليغطي مركبا لونيا على امتصاصية له في 532 nm (13) ر-2 قياس فيتامين (A, C, E) في مصل الدم بتقنية HPLC تم قياس فيتامين E باستخدام الطريقة المحورة من (Deleen heer) حيث تم تحضير محلول مانع الاكسدة والمحلول القياسي باستخدام طور متحرك (99%) ميثانول (1%) ماء مقطر بطول موجي 287 nm , نوع العمود (C-18 ODS) (14) اما فيتامين C ف استخدم الطور المتحرك باذابة صوديوم اسيتيت و (EDTA) في الماء المقطر وبضبط pH عند 6 وثبت الطول الموجي عند 254 nm وباستخدام نفس العمود (15) كذلك فيتامين A استخدم الطور المتحرك (99%) ميثانول (1%) ماء مقطر بطول موجي 330 nm وبنفس العمود (16) .

النتائج والمناقشة

نلاحظ من الجدول رقم (1) الزيادة في معدل مستوى الكروم لمجاميع العمال مقارنة بمجموعة السيطرة وان هذه الزيادة تتناسب طرديا مع طول الفترة الزمنية تتعرض لملوثات الكروم . كذلك نلاحظ من جدول رقم (2) الزيادة في معدل مستويات الاكسدة الفوقية للدهون لمجاميع العمال مقارنة بمجموعة السيطرة حيث نلاحظ هذه الزيادة مع الفترة الزمنية للتعرض . اذ استطاع الباحثون تفسير ميكانيكية الزيادة في معدل الاكسدة الفوقية بسبب ارتفاع مستويات (ROS) وهي مولدات للجذور الحرة وسوف يحصل زيادة في التلف الحاصل في الخلايا ويسرع من عملية انتقال الالكترونات والاكسدة الفوقية للدهون في الانسجة البيولوجية داخل الخلية الحية وان هذه النتائج تتفق مع بحوث اخرى وعند زيادة هذه الاكسدة فان الجذور الحرة المتولدة والمتزايدة تؤدي الى التلف لكثير من الاغشية الخلوية والنهايات العصبية في الدماغ (17,18) يبين جدول رقم (3) انخفاض في مستوى تركيز فيتامين (A) بالنسبة الى العاملين مقارنة مع قيم السيطرة مع طول مدة التعرض .

يعد فيتامين A من مركبات الكاروتينات التي لها فعالية كمضادة للاكسدة (19,20) وان فعاليته الكيميائية تأتي من السلسلة الطويلة الحاوية على اواصر مزدوجة متعاقبة التي تكون معوضة بمختلف المجاميع ان ال ROS التي يمكن ان يكتسبها فيتامين A هي O₂ وجذر البيروكسي (peroxy radical) (21) . ولفيتامين A عدة وظائف منها المشاركة في عملية الابصار بالتفاعل مع بروتين (opsin) مكونا الارجوان البصري كما يعد ضروريا في تكوين الكربوهيدرات المخاطية المكونة لمادة مخاطية لافراز الطبقة الطلائية التي توفر الحماية للقنوات الجسمية مثل القنوات التنفسية والبولية والتناسلية وكذلك ملتحمة العين والقرنية والثة.

كذلك للفيتامين دور في تكوين عدد من الهرمونات مثل الكورتيزون (cortisone) والذي تفرزه غدة الادرنايين والتي لها دور في تمثيل الدهون والكربوهيدرات و (vit. A) اهمية في تقليل مستوى الاكسدة ويعد من الفيتامينات المضادة للاكسدة

كما يوصي بتناول فيتامين (A) لما له أهمية في الحفاظ على شبكة العين وماتحمة العين والقرنية من الاضرار التي تلحق بالعين وكذلك لفيتامين (A) دور في رفع مستوى (apo-A) ومن ثم رفع (HDL) في الدم (22). يبين لنا الجدول رقم (4) النقص الحاصل في معدل فيتامين (E) عند مجاميع العمال مقارنة بمجموعة السيطرة وذلك لأن (Vit-E) هو أحد مضادات الأكسدة الذائبة في الدهون ويعمل على حماية الدهون الموجودة في الأغشية الخلوية من التلف التأكسدي وكذلك فإن فيتامين (E) له تأثير على الاستجابة المناعية الخلوية (Cellular Immune Response) حيث يعمل على تقوية الحالة المناعية⁽²¹⁾ وإن القلة الملحوظة في (Vit-E) نتيجة التلف الحاصل فيه وتقليل الاستجابة المناعية للعاملين⁽²³⁾ كما إن تأثير فيتامين (E) يمثل في تحفيز الخلايا المفاوية التائية المساعدة (T. Helper Lymphocytes) والتي تعمل على تحويل إنتاج الأجسام المضادة من نوع (IgM) إلى نوع (IgG) (24) إن النتائج التي توصلنا إليها في بحثنا هذا تتفق مع ما جاء في نتائج الباحثين.

يبين جدول رقم (5) انخفاض في مستوى تركيز فيتامين (C) بالنسبة الى العاملين مقارنة مع قيم السيطرة مع طول مدة التعرض.

على الرغم من ان فيتامين (C) من الفيتامينات الذائبة في الماء فاهميته تأتي من ناحية الحفاظ على فيتامين (E) بشكله الفعال المختزل (26) كما وجد بعض الباحثين الذين درسوا التركيز والحالة التأكسدية للاسكوربيت ان قيمته اقل بكثير عند المرضى منه في الاصحاء لان معظم الاسكوربيت وجد على شكل مؤكسد (26).

جدول رقم-1: يحدد الانحراف القياسي والمعدل ومستوى الدلالة للكروم عند مجموعة السيطرة ومجاميع العمال.

المجاميع	العدد	Mean \pm S.D	($\mu\text{g/dL}$) Cr	T
Control C	30	6.5	20.1	---
A	20	8.4	149.2	P<0.001
B	20	18.3	200.2	P<0.001

جدول-2: يحدد معدل الانحراف القياسي والمعدل ومستوى الدلالة (MDA) عند مجموعة السيطرة ومجاميع العمال.

المجاميع	العدد	Mean \pm S.D	(n mol/dL) (MDA)	T
Control C	30	5.6	26.5	---
A	20	3.1	86.8	P<0.05
B	20	7.8	120.2	P<0.001

A = مجموعة العمال (من سنة إلى 10 سنوات).

B = مجموعة العمال (من 11 سنة فما فوق).

C = مجموعة السيطرة.

جدول-3: يحدد معدل الانحراف القياسي والمعدل ومستوى الدلالة لتركيز فيتامين (A) عند مجموعة السيطرة ومجاميع العمال.

المجاميع	العدد	Mean \pm S.D (mg/dL) (Vit-A)	T
Control C	30	10.2	---
A	20	14.1	P<0.05
B	20	16.5	P<0.001

A = مجموعة العمال (من سنة إلى 10 سنوات).

B = مجموعة العمال (من 11 سنة فما فوق).

C = مجموعة السيطرة.

جدول رقم 4- يحدد معدل الانحراف القياسي والمعدل ومستوى الدلالة لتركيز فيتامين (E) عند مجموعة السيطرة ومجاميع العمال.

المجاميع	العدد	Mean \pm S.D (mg/dL) (Vit-E)	T
Control C	30	0.16	---
A	20	0.21	P<0.05
B	20	0.38	P<0.001

A = مجموعة العمال (من سنة إلى 10 سنوات).

B = مجموعة العمال (من 11 سنة فما فوق).

C = مجموعة السيطرة.

جدول رقم 5- يحدد معدل الانحراف القياسي والمعدل ومستوى الدلالة لتركيز فيتامين (C) عند مجموعة السيطرة ومجاميع العمال.

المجاميع	العدد	Mean \pm S.D (mg/dL) (Vit-C)	T
Control C	30	0.98	---
A	20	0.14	P<0.05
B	20	0.22	P<0.001

A = مجموعة العمال (من سنة إلى 10 سنوات).

B = مجموعة العمال (من 11 سنة فما فوق).

C = مجموعة السيطرة.

المصادر

1. Zahid,Z.R.;Al-Hakkak Z.S.; Kadhim A.H.; Elias E.A. & Al-Jmaily I. S. Comparative effects of Trivalent and hexavalent chromium on spermatogenesis of the mouse.Toxicological and Environmental Chemistry,25:131-136 (1989).
2. Ramo,J.Del.;Diaz-Mayans,J.;Torreblanca,A.&Nunez,A Effects of Temperature on the acute toxicity of heavy metals (Cr, Cd and Hg) to the fresh – water Crayfish, *Procambarus clarkii* (Girard) Bull. Environ. Contam.Toxicol.38 : 736 – 741. (1987).
3. Klaassen,C.D. ; Amdur,M.O. & Doull,M.D.J.(Ed.) Toxicology; the basic science of poisons. 3rd (ed.) : 596 – 598(1986).
4. WHO Guidelines for drinking-water, 2nd (ed.) 2. Health criteria and other supporting information Geneva, World Health Organization:206-215,(1996).
5. Elton,C.S, Ecology of Invasions by animals and plants 2nd (ed.), N. Y. John Wiley and Sons Inc. : 181(1986).
6. Versieck, j. and Cornelis , R, "Normal levels of trace elements in human blood plasma and serum", Anal .Chim . Acta, 116 :217-254. .(1981)
7. Veillon,c. ;patterson,k.y.and Bryden N.A., "Direct determinations of chromium in human urine by electro thermal atomic absorption spectrometry", Anal . Chim . Acta, 136 : 233-241. (1982b)
8. Doisy, R.J.; Streeten , D.H.P. and Freiberg J.M., "Chromium metabolism in man and biochemical effects" , In: Trace elements in human health and disease , 2,A.S.Prased Ed . New York , Academic Press.:79-104. (1976)
9. Harvey , B. and Crockford , J, "Chromium", In:Hand book of occupational hygiene, Vol.1,Croner Publication Limited,Britain,:1,2:7-17(1987)
10. Sax , N.I, "Dangerous properties of industrial material", Report 1,(1), New York, VanNostrand and reinhold co. (1980)
11. Sitting ,m. "chromium" In :hand book of toxic and hazardous chemical and carcinogens, 2nd ed., noyes, publications, park ridge, new jersey U.S. , :243-284. (1985),
12. Stupar, J.;vrtovec , M. and Ganter, A., "Chromium status of tannery workers in relation to metabolic disorders", J.Appl.Toxicol.,19(6),pp.437-446. (1999)
13. Fong,K.L.,Mc Cay,P.B.&poyer,J.L J.Biol.Chem.,248 : 7792. ,(1973).
14. Burtis,C.A.&Ashwood, E.R., "Fundamentals of Clinical Chemistry" 4ed., Philadelphia:341-9 20pk'S (1996)
15. Chow,F. and Omaye,S. Lipids.]:837.
16. Rose,R.&Nohiwold,D.(1981) Anal.Biochem.114:140-145.(1983)
17. McClean, S.R., Ruddel, M.and Gross,E. Gun. Chern. 28:693-696(1982)
18. Strubelet,O.;Kremer,J.;Tilse,A.;Keogh,J. and Younes, M.J.Toxical Environ,1-1ealth .,Feb:47(3):267-283. (1996)
19. Richard S.Brunoa,Maret G. Traber,13, Issue 3:143-149 August (2006)
20. Fong,K.L.,Mc Cay,P.B.&poyer,J.L.,J.Biol.Chem.,248:7792(1973)
21. Parknay,M.,Ed The use of recovery factors in trace analysis ,Royal Society of chemistry, .(1996)

22. Polozza, P. & Krinsky, N. I., Methods in Enzymology., 268: 127 (1992)
23. Mandel, N. & Chon, V. The pharmacological basis of therapeutics Afr. J. Med. Sci., 27:169 (1998)
24. Restek-Samar Zija, N., Momcilvic, B., Trosic, I., Piasek, M. & Samarzija, M., Am. J. Bio Chem., 47:8 (1996)
25. Comstock, G. W., Burke, A. E., Hoffman, S. C., Helzlsouer, K. J., BenDich, A., Masi, A. T., Norkns, E. P., Malamet, R. L. & Gershwin, M. E., Ann. Rheum. Dis., 56:323. (1997)
26. Bain C, Feskanich D, Speizer FE, Thun M, Hertzmark E, Rosner BA, Colditz GA: Lung cancer rates in men and women with comparable histories of smoking J Natl Cancer Inst, 96:826-834. (2004)

تأثير المستخلصات المائية والكحولية لنبات الهيل *Elettaria cardamomum* في نمو بعض البكتيريا المعزولة من التهابات الأذن الوسطى

زيد شاكر ناجي محمود و محمد عبد الجليل خليل
قسم علوم الحياة – كلية العلوم / الجامعة المستنصرية

Abstract

This study was done to determine the effect of watery and alcoholic extracts of *Elettaria cardamomum* on growth of bacteria isolated from Otitis media Infections which are : *Pseudomonas aeruginosa* , *Staphylococcus aureus* and *Klebsilla spp.*

The biochemical analysis revealed that watery extracts of *Elettaria cardamomum* contains: Glycosides, Alkaloids, Saponines, Tannins, and Volatile oils, (This compound Soluble in water) , while the alcoholic extracts contains : (in addition to the above mentioned compounds) Phenols , Resins , Flavonids and Coumarins. (This compound Soluble in organic solutions).

To study the effect of watery and alcoholic extracts of *Elettaria cardamomum* on growth of bacteria isolated from Otitis media Infections we make Four extracts (cold watery extract , hot watery extract , cold alcoholic extract and hot alcoholic extract.

The study shows that (hot alcoholic extract) were more effective than the other extracts, by using agar diffusion method (wells).

The study also showed that *staphylococcus aureus* (gram positive) bacteria is most sensitive to plant extract's than the gram negative bacteria , while *Pseudomonas aeruginosa* were most resistant to plant extracts than the others.

الخلاصة

أجريت هذه الدراسة لمعرفة تأثير المستخلصات المائية والكحولية لبذور الهيل *Elettaria cardamomum* في نمو البكتيريا المعزولة من التهابات الأذن الوسطى وهي : *Staphylococcus aureus* و *Klebsilla spp.* و *Pseudomonas aeruginosa*.

تم الكشف عن المركبات الفعالة الموجودة في مستخلص بذور الهيل إذ تبين نتائج الكشف الكيمائية إن المستخلصات المائية تحتوي على الكلايكوسيدات و القلويدات والصابونيات والتانينات والزيوت الطيارة . وان هذه المركبات لها القابلية على الذوبان في الماء , أما المستخلصات الكحولية فتحتوي (بالإضافة إلى ما ذكر) على مركبات راتنجية وكومارينات وفلافونيات وفينولات . وهذه المركبات لا تذوب بالماء , ولكنها تذوب بالمذيبات العضوية. لدراسة تأثير مستخلصات بذور الهيل في نمو البكتيريا المعزولة من التهابات الأذن الوسطى , تم تحضير أربعة أنواع من المستخلصات وهي : المستخلص المائي البارد , المستخلص المائي الحار , المستخلص الكحولي البارد و المستخلص الكحولي الحار.

أظهرت النتائج ان المستخلص الكحولي الحار كان اكثر كفاءة من باقي المستخلصات ثم يليه المستخلص الكحولي البارد ثم المستخلص المائي الحار واخيرا المستخلص المائي البارد وذلك باستخدام طريقة الانتشار عبر الحفر. كانت البكتيريا *Staphylococcus aureus* (الموجبة لصبغة كرام) أكثر الأنواع البكتيرية تحسناً لفعل المستخلصات النباتية مقارنة مع الأنواع الأخرى السالبة لصبغة كرام , وكانت البكتيريا *Pseudomonas aeruginosa* أكثر الأنواع البكتيرية مقاومة لفعل المستخلصات النباتية.

المقدمة

تعد النباتات عموماً أحد المكونات الأساسية للجزء الحي في النظام البيئي , ولدورها الرئيس في تجهيز هذا النظام بالطاقة أطلقوا عليها وظيفياً الكائنات المنتجة (Producer Organisms) واستغلت من قبل الإنسان للتداوي والعلاج فضلاً عن الغذاء والكساء (1).

حيث زاد الاهتمام بالعلاج بالأعشاب الطبية وذلك لأنها ذات تأثيرات جانبية اقل بكثير من الادوية الصناعية , كما وان هذه النباتات غالباً ماتتمتع بتأثير افضل من المركبات الصناعية وذلك لاحتوائها على مواد نشطة بايولوجيا والتي تعد من المواد الخام لكثير من المواد الصيدلانية (2), ويعد

تأثير المستخلصات المائية والكحولية لنبات الهيل *Elettaria cardamomum* في نمو بعض البكتريا المعزولة من التهابات الأذن الوسطى
زيد و محمد

نبات الهيل من النباتات الطبية الواسعة الانتشار , نبات الهيل نبات عشبي معمر يعود الى عائلة الزنجبيلية (Zingeraceae) , اما ثماره عبارة عن ثمار علييات لها ثلاث فلقات تحتوي على عدد كبير من البذور الصغيرة السمرء , وثمره الهيل صغيرة يتراوح طولها ما بين 8-20 ملم وعرضه 10 ملم , ومخطط تخطيطاً طويلاً ولونه اخضر يصفر مع التخزين (3) .

تحتوي ثمار الهيل على زيوت طيارة ومن اهم مركباته هي (سينيل 26 - 40%) , (ليمونين 2-14%) , (اسيتيت 28-34%) و (ساينين 3-5%) (4) .

ويعد نبات الهيل من النباتات التي استخدمت لعلاج الكثير من الالتهابات ولقابليته على قتل الأحياء المجهرية (5) و (6) .

- ولكون العلاج بالمضادات الحياتية ذا تأثيرات جانبية عديدة , لذا فقد جاء الهدف من البحث:
- أ- تحضير بعض المستخلصات النباتية لثمار الهيل (المستخلصات المائية والكحولية) , والكشف عن بعض المكونات الكيميائية الفعالة له .
 - ب- دراسة تأثير مستخلصات ثمار الهيل وعند تراكيز مختلفة في تثبيط نمو البكتريا المعزولة من التهابات الأذن الوسطى والمقاومة لبعض المضادات الحيوية .
 - ج- المقارنة بين تأثير المستخلصات المحضرة للنبات أعلاه في نمو بعض البكتريا المعزولة من التهابات الأذن الوسطى .

المواد و طرائق العمل

1- جمع العينات النباتية وتهيئتها للاستخلاص.
تم الحصول على الهيل من الأسواق المحلية , ولإجراء عمليات التهيئة تم طحنها طحناً خشناً بواسطة جهاز طحن (طاحونة) ثم حفظت الأجزاء المطحونة في حاويات بلاستيكية نظيفة بعيداً عن الضوء والحرارة والرطوبة لحين الاستعمال.

2- طرائق تحضير المستخلصات النباتية
تم تحضير أربعة أنواع من مستخلصات وابتاع طريقة (7) وطريقة (8) وهي :-

- أ- المستخلصات المائية الباردة
- ب- المستخلصات المائية الحارة
- ج- المستخلصات الكحولية الباردة
- د- المستخلصات الكحولية الحارة

3- تقدير الرقم الهيدروجيني للمستخلص (pH)
أضيفت (10) غم من المسحوق النباتي الجاف الى (50) مليلتر من الماء المقطر مع الرج اليدوي المستمر , وضع المزيج على خلاط المغناطيسي (Magnetic stirrer) لمدة (10) دقائق , رشح الخليط وقدرت قيمة pH باستعمال أوراق زهرة الشمس وبجهاز الـ (pH meter) (9) .

4- الكشف الكيميائي لبعض المركبات الفعالة في ثمار الهيل
تم تطبيق بعض الكشوفات على المستخلصات النباتية وكالاتي :-

- أ- الكشف عن الكلايكوسيدات (Glycosides)
تم إجراء الفحص بإضافة (2) مليلتر من كاشف بندكت إلى (1) مليلتر من المستخلص النباتي الموضوع في أنبوبة اختبار ثم رج المحلول جيداً ووضع في حمام مائي مغلي لمدة (5) دقائق , ثم تركت الأنبوبة لتبرد . دل ظهور راسب أحمر على وجود الكلايكوسيدات (10) .

ب- الكشف عن الفينولات (Phenols)

تم الكشف عنها باستخدام محلول كلوريد الحديدك (Ferric chloride) والذي حضر بإذابة ملح كلوريد الحديدك في الماء المقطر ونسبة (1%) . يعطي هذا الكاشف لونا أخضر أو أزرق عند إضافته إلى كمية المستخلص الموجودة في زجاجة الساعة الحاوية على المركبات الفينولية (11) .

ج- الكشف عن القلويدات (Alkaloids)

لإجراء هذا الكشف تم استخدام طريقتين وبعدها تم المقارنة بالنتائج :-

1. كاشف ماركيز الذي يعطي اللون الرمادي المحبب دليلاً على وجود القلويدات .
2. كاشف ماير الذي يعطي راسباً أبيضاً دليلاً أيضاً على القلويدات (11) .

د- الكشف عن التربينات (Terpenes) والسترويدات (Steroids)

أضيف قليل من الكلوروفورم إلى (1) مليلتر من المستخلص بعدها أضيفت إليه قطرة من الاستايل اللامائي (Acetic anhydrate) ، وقطرة من حامض الكبريتيك المركز ، ظهر لون بني دليل على احتواء المستخلص على تربين وإذا ترك المزيج لفترة وظهر لون أزرق داكن دل ذلك على أن المستخلص النباتي حاوي على السترويدات (12) .

هـ- الكشف عن الراتنجات (Resins)

اتبعت الطريقة الواردة في (13) الكشف عن الراتنجات.

تم أخذ (10) مليلتر من كل مستخلص وأضيف له (20) مليلتر ماء مقطر محمض بحامض الهيدروكلوريك HCl (4%) ، قرأت النتيجة الموجبة من خلال ظهور العكورة (Turbidity) .

و- الكشف عن الصابونينات (Saponines)

اتبعت الطريقة الواردة في (13) وكلائي :

1. حضر محلول مائي للمسحوق النباتي (غرام واحد من النبات الجاف إلى 10 مليلتر ماء مقطر) في أنبوبة اختبار ثم رج بشدة ، لحين ظهور رغوة كثيفة تبقى لعدة دقائق دلالة على وجود الصابونين .
2. بإضافة (1 - 3) مليلتر من محلول كلوريد الزنبيق $HgCl_2$ بتركيز (1%) إلى (5) مليلتر من المستخلص النباتي، ويعد ظهور راسب أبيض دليل على ايجابية الفحص.

ز- الكشف عن التانينات (Tannins)

اتبعت الطريقة الواردة في (14) للكشف عن التانينات.

تم الكشف بغلي (10) غم من المسحوق النباتي في (50) مليلتر من الماء المقطر ثم رشح المحلول وترك ليبرد ، بعدها قسم الراشح إلى قسمين أضيف للقسم الأول محلول (1%) خلات الرصاص Lead acetate للاستدلال على وجود التانينات بظهور راسب أبيض هلامي القوام . بينما أضيف للقسم الثاني محلول (1%) كلوريد الحديدك Ferric Chloride حيث يدل ظهور اللون الأخضر المزرق على وجود التانينات.

ح- الكشف عن الفلافونات (Flavones)

اعتمدت الطريقة الواردة في (15) للكشف عن الفلافونات ، فقد تم تحضير محلول الكشف بإضافة (10) مليلتر من الكحول الإيثيلي وبتركيز (50%) إلى (10) مليلتر من محلول هيدروكسيد البوتاسيوم (KOH) وبتركيز (50%) أيضاً ، وعند مزج كميات متساوية من هذا المحلول و المستخلص النباتي ، يدل ظهور اللون الأصفر على وجود الفلافونات.

ط- الكشف عن الكومارينات (Coumarines)

اعتمدت طريقة (16) للكشف عن الكومارين وكلائي .

وضع قليل من المستخلص النباتي لكل من المستخلصات المذكورة سابقاً في أنابيب اختبار (غرام واحد من النبات الجاف إلى 10 مليلتر ماء مقطر) وغطيت الأنابيب بأوراق ترشيح مرطبة بمحلول هيدروكسيد الصوديوم (NaOH) المخفف ووضعت الأنابيب في حمام مائي (Water bath) مغلي ليضع دقائق ثم بعد ذلك عرضت أوراق الترشيح إلى مصدر للأشعة فوق البنفسجية ، إذ يدل ظهور لون أصفر مخضر براق على وجود الكومارين .

ي- الكشف عن الزيوت الطيارة (Volatile oils) .

اعتمدت طريقة الكشف عن الزيوت الأساسية كما ورد في (17) , إذ تم اخذ (10) مليلتر من كل من المستخلصين النباتيين ورشحت بعد ذلك شبتت بها أوراق ترشيح وعرضت إلى مصدر للأشعة فوق البنفسجية , دل ظهور اللون الوردي البراق على وجود الزيوت الطيارة.

5- العزل والتشخيص البكتريا المعزولة من التهابات الأذن الوسطى

تم جمع 15 مسحة من المرضى المراجعين للعيادة الخارجية لشعبة الأنف والأذن والحنجرة والذين يعانون من التهابات الأذن وتحت إشراف الأطباء المختصين في مستشفى بغداد العام في (مدينة الطب) , استنبت المسحات القطنية مباشرة بعد جمعها على الأوساط الزرعية المتضمنة وسط أكار الدم ووسط أكار الماكونكي , ثم حضنت الإطباق في (37م) لمدة (24) ساعة وشخصت العزلات البكتيرية مبدئياً وحسب الصفات المظهرية لشكل المستعمرات وقوامها ولونها واستكملت لها الفحوصات التشخيصية الأخرى.

6- التشخيص البكتريولوجي

تؤخذ مستعمرة واحدة نقية من كل نمو الموجود على الأوساط الزرعية وشخصت مبدئياً اعتماداً على الصفات الشكلية التي تضمنت حجم وشكل ولون وقوام المستعمرات ثم فحصت مجهرياً لأجل وصف شكل الخلايا من خلال صبغها بصبغة كرام .

7- الاختبارات البايوكيميائية

أخضعت العزلات البكتيرية إلى عدة اختبارات (18) و (19) وكما يلي :
اختبار إنتاج أنزيم الكاتاليز Catalase Test , اختبار إنتاج أنزيم الاوكسيداز Oxidase Test , الكشف عن إنتاج الاندول (Indole Production Test) , اختبار المثل الأحمر (Methyl-Red Test) , اختبار فوكاس – بروسكاور (Voges-Proskauer Test) , فحص قابلية البكتريا على استغلال الستريت كمصدر وحيد للكربون , اختبار قابلية النمو بدرجات الحرارة (4 م° و 42 م°) و اختبار إنتاج أنزيم التجلط Coagulase Test

8- اختبار فعالية المستخلصات النباتية لنبات الهيل في نمو البكتريا المعزولة الأذن الوسطى

تم تحضير محلول الخزين Stock solution من المستخلصات النباتية بإذابة (5) غم من المسحوق النباتي المجفف في (10) مليلتر من الماء المقطر للحصول على تركيز (500) ملغم / مليلتر بعدها رشح المحلول الخزين لغرض التعقيم بمرشحات خاصة Whatman membrane filter (0.22) مايكرومتر , بعدها تم الحصول على التراكيز (30 , 60 , 120 , 240 , 480) ملغم /مليلتر بمزج حجم معين من المحلول الخزين مع الماء المقطر المعقم وحسب القانون الآتي :

$$C_1 V_1 = C_2 V_2$$

إذ يمثل $C_1 V_1$ حجم وتركيز المحلول الخزين أما $C_2 V_2$ فيمثل حجم وتركيز المحلول المراد تحضيره .

9- اختبار حساسية البكتريا لمضادات الحياة :

استخدمت طريقة الواردة في (20) القياسية لاختبار حساسية العزلات لمضادات الحياة باستخدام اكار مولر هنتون , وكالآتي :

- حضرت المزارع البكتيرية بنقل مستعمرة واحدة إلى (5) مليلتر من وسط المرق المغذي وحضنت بدرجة (37) م° ولمدة (18-24) ساعة .
- قورنت عكرة النمو مع عكرة محلول ثابت العكورة القياسي (McFarland) والذي يعطي عدداً تقريبياً للخلايا (1.5×10^8) خلية / مل.
- نشر (0.1) مليلتر من المزروع أنفاً على وسط مولر – هنتون بواسطة المسحة المعقمة (Sterile Swab) , ترك ليحجف بدرجة حرارة الغرفة لمدة (10 – 15) دقيقة.

- نقلت بعدها أقراص مضادات الحياة بملقط إلى الأطباق بواقع (5-6) أقراص للطبق الواحد , حضنت الأطباق بدرجة (37) م° ولمدة (24) ساعة.
- تمت قراءة النتائج بقياس مناطق التثبيط حول أقراص مضادات الحياة وفسرت النتائج حسب ما ورد في (NCCLS) (21) .

النتائج والمناقشة

1- الكشف الكيميائي عن المركبات الفعالة في مستخلصات نبات الهيل *Elettaria cardamomum* بينت نتائج الكشوفات الكيميائية للمركبات الفعالة الموجودة في المستخلصات النباتية الخام احتواء بذور نبات الهيل على عدد من المركبات الفعالة والتي تعد منتجات أبيض ثانوي (Secondary Metabolism) وكما مبين في الجدول (1) . حيث يحتوي النبات على مركبات القلويدات و التانينات والزيوت طيارة و الصابونيات و التربينات و الفلافونات و الكومارينات والتي تعد من المواد المضادة للبكتريا

2- عزل وتشخيص العزلات البكتيرية أجريت الفحوصات المجهرية و الكيموحياتية على العزلات البكتيرية , وتم عزل وتشخيص البكتريا المعزولة من التهابات الأذن الوسطى وهي : *Staph. aureus* , *Ps. aeruginosa* و *Klebsiella spp* . وذلك بأخذ 15 مسحة من المرضى المراجعين للعيادة الخارجية لشعبة الأنف والأذن والحنجرة والذين يعانون من التهابات الأذن وتحت إشراف الأطباء المختصين في مستشفى بغداد العام في (مدينة الطب) . ثم زرعت على الأوساط الزرعية المتضمنة وسط أكار الدم ووسط أكار الماكونكي , ثم حضنت الأطباق في (37م°) لمدة (24) ساعة وشخصت العزلات البكتيرية مبدئياً وحسب الصفات المظهرية لشكل المستعمرات وقوامها ولونها واستكملت لها الفحوصات التشخيصية الأخرى.

3- فحص حساسية البكتريا للمضادات الحيوية تم اختبار قابلية العزلات البكتيرية المشخصة والمعزولة من التهابات الأذن الوسطى في هذه الدراسة لثمانية مضادات حيوية مختلفة والتي لها طيف واسع على البكتريا الموجبة والسالبة لصبغة كرام وتم تحديد مقاومتها للمضادات اعتماداً على قياس منطقة التثبيط (بالمليمتر) ووفقاً لما ورد من قياسات عالمية في (NCCLS) (21) , جدول (2) .

4- تأثير المستخلصات النباتية في نمو البكتريا المعزولة من التهابات الأذن الوسطى أجريت دراسة تأثير المستخلصين النباتيين المائية والكحولية لنبات الهيل *Elettaria cardamomum* في الأنواع البكتيرية المعزولة من التهابات الأذن الوسطى هي : *Ps. aeruginosa* , *Staph. aureus* و *Klebsiella spp* بطريقة الانتشار في الحفر والتي تمتاز بسهولة إجرائها وكفاءتها.

تعود الفعالية التثبيطية إلى طبيعة المواد التي يحويها النبات , جدول (1) إذ ان وجود مركبات القلويدات و التانينات و الزيوت طيارة و الصابونيات و التربينات و الفلافونات و الكومارينات والتي تعد من المواد المضادة للبكتريا , فكان لها الأثر في تثبيط نمو البكتريا , فالقلويات تمتاز بقدرتها على اقتحام الخلية البكتيرية والتداخل مع الحامض النووي DNA , فيما تعمل التانينات على تثبيط الأنزيمات والبروتينات الناقلة الموجودة في غشاء الخلية (22) .

إما الصابونيات فتعمل على خفض السكر داخل البكتريا والتي تؤدي إلى موت الخلية وكذلك بالنسبة إلى الكلايكوسيدات التي لها تأثير مماثل ولكن بدرجة أقل (23) .

اما الفينولات إذ إن هذه المركبات لها القدرة على تكوين معقدات مع مجموعة السلفاهيدريل (Sulphydryl groups) مؤدية إلى الأضرار بجدار الخلية البكتيرية (24) .

في المستخلصات المائية فقد بينت النتائج بأن (المستخلص المائي الحار) كان اكفاً من (المستخلص المائي البارد) بتأثيره في نمو البكتريا *Staph. aureus* , *Ps. aeruginosa* و *Klebsiella spp* بتركيز (480 ملغم / مليلتر) جدول (3) , حيث يلاحظ من معدلات أقطار

تأثير المستخلصات المائية والكحولية لنبات الهيل *Elettaria cardamomum* في نمو بعض البكتريا المعزولة من التهابات الأذن الوسطى
زيد و محمد

مناطق التثبيط (11.5, 18, 18) ملم وعلى التوالي مقارنة مع معدلات أقطار مناطق التثبيط للمستخلص المائي البارد ولنفس التركيز (11, 14, 12) ملم وعلى التوالي وهذا يعود الى ان عامل الحرارة ساعد على اذابة اكبر كمية من المواد الفعالة الموجودة في النبات وهذا يتفق على مجاء كل من (25) و (26). اذ ان المستخلصات الحارة كانت اكفاً من المستخلصات الباردة في تأثيرها على البكتريا .

اما المستخلصات الكحولية فكان (المستخلص الكحولي الحار) اكفاً من (المستخلص الكحولي البارد) بتأثيره في نمو البكتريا *Staph.aureus*, *Ps.aeruginosa* و *Klebsiella spp.* بتركيز (480 ملغم / مليلتر) جدول (4) , حيث يلاحظ من معدلات أقطار مناطق التثبيط (17, 20, 27) ملم وعلى التوالي مقارنة مع معدلات أقطار مناطق التثبيط للمستخلص المائي البارد ولنفس التركيز (12, 15, 23) ملم وعلى التوالي وهذا يتفق على مجاء به (27) و (28) بأن المستخلصات الكحولية الحارة كانت افضل من بقية المستخلصات وذلك لوجود عاملين هما الحرارة والمذيب .

استجابت البكتريا *S. aureus* (الموجبة لصبغة كرام) لتأثير المستخلصات بصورة عامة أكثر من باقي الأنواع الأخرى من البكتريا السالبة لصبغة كرام وقد يرجع سبب ذلك إلى التركيب البنائي للجدار البكتيري إذ تفتقر البكتريا الموجبة لصبغة كرام إلى طبقة من الأغشية الخارجية تجعل نفاذية المواد لداخل الخلية اكبر مقارنة بالبكتريا السالبة لصبغة كرام (29), تليها بكتريا *Klebsiella spp.* , ثم بكتريا *Ps. aeruginosa* التي لم تتأثر بالتركيز (60 ملغم / مليلتر) في المستخلصات المائية , وقد يعزى ذلك إلى امتلاكها المحفظة Capsule خارج الجدار الخلوي والتي تتكون من مادة متعددة السكريد الشحمي والتي تكسب البكتريا صفة الأمراض ومقاومة العوامل ضد الميكروبية . وهذا يتفق مع ما توصلت إليه (30) إذ أن بكتريا *Ps. aeruginosa* كانت اقل تأثيراً من باقي أنواع البكتريا للمستخلص الكحولي لنبات ثمار القطب *Tribulus terrestris* , ويتفق أيضاً مع (31) إذ أن بكتريا *Ps. aeruginosa* كانت من أكثر البكتريا مقاومة إلى مستخلصات نبات اليوكالبتوس *Eucalyptus camaldulensis* و نبات النعناع *Mentha viridis* .

يتضح مما تقدم أن المستخلص الكحولي الحار كان افضل المستخلصات النباتية الاخرى تأثيراً في نمو البكتريا *Staph. aureus*, *Ps. aeruginosa* و *Klebsiella spp.* ثم يليه المستخلص الكحولي البارد ثم المستخلص المائي الحار واخيراً المستخلص المائي البارد , شكل (1) , وايضا يتضح بان التراكيز العالية (240 , 480) ملغم/مليلتر كانت أفضل بكثير من التراكيز الواطئة (60 , 30) ملغم/مليلتر والذي يمكن الاستدلال من خلاله على أن التراكيز العالية هي الأفضل في التطبيق العملي وذلك للحصول على نتائج أفضل .

جدول - 1 : نتائج الكشف الكيمائية للمركبات الفعالة في المستخلصات النباتية

المركبات الفعالة أنواع المستخلصات	Glycosides الكلايكوسيدات	Phenols الفينولات	Alkaloids القلويدات	Terpenes التربينات	Steroids الستيرويدات	Resins الراتجات	Saponins الصابونيات	Tannins التانينات	Flavonoids الفلافونيات	Coumarins الكومارينات	Volatile oils الزيوت الطيارة
المائي البارد	+	-	+	-	-	-	+	+	-	-	+
المائي الحار	+	-	+	-	-	-	+	+	-	-	+
الكحولي البارد	+	+	+	-	-	-	+	+	-	-	+
الكحولي الحار	+	+	+	-	-	-	+	+	+	+	+

+ وجود المركب الفعال - عدم وجود المركب الفعال

جدول - 2 : مقاومة البكتريا المعزولة من التهابات الأذن الوسطى للمضادات الحيوية

اسم المضاد (الرمز) انواع البكتريا	Aztreona m (ATM)	Ciprofloxacin (CIP)	Erythromycin (E)	Cefoxitin (FOX)	Gentamicin (GN)	Cephalothin (KF)	Carbenicillin (PY)	Vancomycin (VA)
<i>Ps. aeruginosa</i>	S	S	R	R	S	R	R	R
<i>Staph. aureus</i>	S	S	S	S	S	R	R	S
<i>Klebsiella spp</i>	S	S	R	S	S	R	R	R

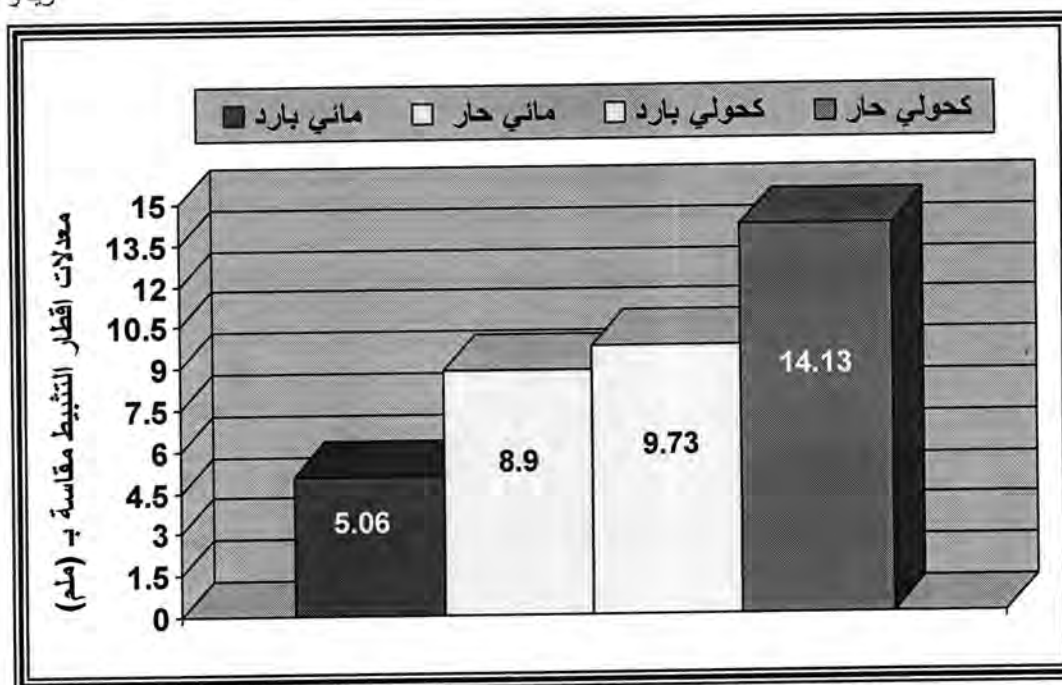
R = البكتريا مقاومة للمضاد S = البكتريا حساسة للمضاد

جدول - 3 : معدلات اقطار التثبيط بـ(مللتر) لبعض العزلات البكتيرية المعاملة بالمستخلصات المائية الخام لثمرة الهيل

الانواع البكتيرية		معدلات تثبيط النمو البكتيري مقاسه بـ (ملم)				
		480	240	120	60	30
<i>Ps. aeruginosa</i>	بارد	11	10	0	0	0
	حار	11.5	10	9	0	0
<i>S. aureus</i>	بارد	14	11	9	0	0
	حار	18	11	10	9	0
<i>Klebsiella spp.</i>	بارد	12	9	0	0	0
	حار	18	15	12	10	0

جدول - 4 : معدلات اقطار التثبيط بـ(مللتر) لبعض العزلات البكتيرية المعاملة بالمستخلصات الكحولية الخام لثمرة الهيل

الانواع البكتيرية		معدلات تثبيط النمو البكتيري مقاسه بـ (ملم)				
		480	240	120	60	30
<i>Ps. aeruginosa</i>	بارد	12	11	9	0	0
	حار	20	19	16	11	9
<i>S. aureus</i>	بارد	23	20	16	11	9
	حار	27	22	18	12	9
<i>Klebsiella spp.</i>	بارد	15	11	9	0	0
	حار	17	13	10	9	0



شكل - 1 : توزيع معدلات اقطار تثبيط النمو لأنواع البكتريا المعزولة من التهابات الأذن الوسطى تبعاً للمستخلصات (المائية والكحولية) لنبات الهيل

المصادر

1. الشحات ، نصر ابو زيد. النباتات والأعشاب الطبية - دار البحار - بيروت: 25-30 (1986).
2. قطب، فوزي طه، النباتات الطبية وزراعتها ومكوناتها. دار المريخ للنشر، الرياض: 35-40 (1981).
3. القبسي، حسان. معجم الاعشاب والنباتات الطبية. دار الكتب العلمية، بيروت. الطبعة السادسة (2004).
4. موسى، جابر. الهيل ملك التوابل وعطر الموائد. قسم العقاقير، جامعة الملك سعود. مقالة انترنت (2008).
5. مجيد ، سامي هاشم ؛ مهند ، جميل محمود . النباتات والأعشاب العراقية بين الطب الشعبي والبحث العلمي . مجلس البحث العلمي . مركز بحوث علوم الحياة قسم العقاقير وتقييم الأدوية (1988) .
6. Watt, John Mitchell,; Maria Gerdina and Breyer, Brand Wijk. Medicinal and poisonous plant of southern and Eastern Africa, second Edition, E and S. Livingstone, LTD. Edinburgh and London (1962).
7. Anesini, C. and Perez, C., Screening of plant used in Argentine folk medicine for antimicrobial activity. J. Ethnopharmacol., 39 (2): 119-128 (1993).
8. Deshmuk, S.D. and Borle, M.N., Studies on the insecticidal properties of indigenous plant products S. Indian. J. Enthnopharmacol., 37(1): 11-18 (1975).
9. Shihata, I.M., A pharmlological study of Anagallis arvensis. M.D. Vet. Thesis, Cairo University (1951).
10. الشبخلي، محمد عبد الستار ؛ العزاوي ، فريال حسن وفياض، حسن، الكيمياء التحليلية، الجامعة المستنصرية : 320-323 (1993) .
11. Harbone, J., Phytochemical methods. Chapman and Hall. London (1973).
12. Al-Abid, M.R., Zurrzusamme mse turungder Abschla B membrane in *Phoenix dactylifera*. Wurzburg University. Wurzburg, F.R. of Germany: 153-140 (1985).
13. الشامي ، سامي اغا. دراسة بعض الصفات الوراثية والسمية لازهار القيصوم . رسالة ماجستير - كلية الطب البيطري - جامعة بغداد (1982).
14. Harbone, J. B., Phytochemical methods. A guide to modern techniques of plant analysis. 2nd ed., Chapman and Hall. London.: 288 (1984).

15. Jaffer, H.J.; Mahmood, M.J. Jawad; A.M.; Naj, A. and Al Naib, A. phytochemical & Biological screening of some Iraqi plant. *Fitoterapia* Lix 299 (1983).
16. Geisman, T. A., Chemistry of Havonoids compounds. Macmillan Co. New York.: 90-101(1962).
17. Handa, Sukhder S.; Decpak Mundkinajeddu, G.V. R. Joseph; Shecla J. and Gajendra N. Indian Herbal pharmacopoeia Vol. II, Ajoint publication of Regional Research Laboratory and Indian Drug Manufacturers Association. India.:137-145 (1999).
18. Collee, J. G. ; fraser, A. G. ; Marmion, B. P. & Simmons, A. Mackie & Mc Cartney Practical Medical Microbiology, 14th ed. USA(1996).
19. Baron, E.J. and Finegold, S.M. Diagnostic Microbiology, 9th ed. Baily and Scotts (1994).
20. Baur, A. M. and Kirby, W. M. Antibiotics susceptibility testing by astandarised single disc method. *Am. J. Clin – pathol.* 45: 493-496(1966).
21. NCCLS (National Committee for Laboratory Standards) Methods for dilution antimicrobial susceptibility tests for bacteria that grow aerobically. Approved standard M7-A5, 5th ed., NCCLS, Pennsylvania(2002).
22. Phillipson, J.D. and Neill, M. G. New leads to the treatment of protozoal infections based on natural product molecules(1987).
23. Hassein, Fawzy, T.K. Medical plants in Libya. Arab Encyclopedia House, Libya (1985).
24. Rhauha, J.P. The search for biological activity in finish plant extracts containing phenolic compounds. Academic dissertation, Faculty of Science, Helsinki University (2001).
25. الربيعي, زيد شاكر ناجي. تأثير المستخلصات المائية والكحولية لنباتي الحنظل *Citrullus colocynthis* وعنب الذيب *Solanum nigrum* في نمو بعض البكتريا المعزولة من اخماج الحروق. رسالة ماجستير. كلية العلوم / الجامعة المستنصرية (2008).
26. مزعل, شيماء نعيمش, دراسة تأثير مستخلص اوراق نبات الاس *Myrtus communis* على انواع من البكتريا المعزولة (2008).
27. Sebastián P.; Fernández ; Cristina Wasowski ; Leonardo M. ; Loscalzo ; Renee E. Granger; Graham A.R. Johnston; Alejandro C. Paladini and Mariel Marder. Central nervous system depressant action of flavonoid glycosides . *European Journal of Pharmacology* Volume 539, Issue 3, :168-176(2006)
28. Suker, D.K.; Al-Mallak, M. K. and Al-Toma, M.L. The effect of tow therapeutic doses of saponin on organs. *Basrah J. Sci.*, 18(2): 51-56(2000).
29. Myrvick, N. and Weiser, S. Fundamentals of Medical Bacteriology and Mycology . 2nd ed. Lea and Febiger. Philadelphia(1988).
30. الزهيري, انعام فؤاد حسين. دراسة بعض الجوانب البايولوجية والكيميائية لنباتي القطب *Tribulus terrestris* وحشيشة الافعى *Galium aparine* وتأثير مستخلصاتهما في نمو بعض مسببات اخماج المجاري البولية, رسالة ماجستير, كلية العلوم, الجامعة المستنصرية (2005).
31. الخفاجي, الاء على مطرود, تأثير مستخلصات نبات اليوكالبتوس *Eucalyptus camaldulensis* ونبات النعناع *Mentha viridis* على بعض البكتريا المصاحبة لبعض التهابات الجهاز التنفسي العلوي في الأطفال, رسالة ماجستير, كلية العلوم, الجامعة المستنصرية (2005).

المكونات الكيميائية لبذور الحلبة المحلية - *Trigonella foenum-graecum* وتأثير مستخلصها على بعض الاحياء المجهرية الممرضة.

رامي علي تقى وامنة نعمة الثويني وصفاء عبد لطيف المعيني
معهد الهندسة الوراثية والتقنيات الاحيائية للدراسات العليا-جامعة بغداد

ABSTRACT

This study aimed to detect the chemical constituents and active ingredient of *Trigonella foenum-graecum* seed and to test the inhibitory effect of seed extracts on the growth of some pathogenic microorganism.

Different chemical reagents were used to investigate the chemical composition of these seed, the results revealed the presence of Alkaloids, Tannins, Resins, Saponins, Flavones and Coumarins, beside (9.4%) Humidity, (25.6%) Proteins, (4%) Saponins, (3.2%) Ash, (48.7%) Carbohydrates, (9%) Fixed oil and (0.1%) volatile oil. The inhibitory activity of extracts was verified on some pathogenic microorganism growth like *Escherichia coli*, *Salmonella typhi*, *Proteus mirabilis*, *Klebsiella* spp., *Serratia* spp., *Pseudomonas aeruginosa*, *Staphylococcus aureus* and *Candida albicans* by using the agar well diffusion method. The result showed that the methyl alcohol extract (80%) has an inhibitory effect on growth of *Staph. aureus* which more effective than other extracts, the inhibition zone about (32mm) and ethyl alcohol extract (20mm). The determination of the minimum inhibition concentration (MIC) and minimum bacteriocidal concentration (MBC) of methyl alcohol (80%) extract on growth of *Staph. aureus* was accomplished also which reached to (12.5) and (25) mg/ml respectively.

الخلاصة

هدفت الدراسة الى التعرف على ما تحويه بذور الحلبة من مكونات كيميائية ومركبات فعالة واختبار مستخلصات هذه البذور في تثبيط نمو بعض الاحياء المجهرية الممرضة، استخدم عدد من الكواشف الكيميائية والتي اعطت ناتجا ايجابيا لمحتوى البذور من القلويدات والتانينات والراتنجات والصابونيات والفلافونات والكومارينات. كذلك وجد انها تحتوي على (9.4%) رطوبة و (25.6%) بروتين و (4%) صابونين و (3.2%) رماد و (48.7%) كاربوهيدرات و (9%) زيت ثابت و (0.1%) زيت طيار. قيمت الفعالية البيولوجية للمستخلصات على بعض البكتيريا المرضية *Escherichia coli* و *Salmonella typhi* و *Proteus mirabilis* و *Klebsiella* spp و *Serratia* spp و *Pseudomonas aeruginosa* و *Staphylococcus aureus* و *Candida albicans* باستخدام طريقة الحفر على الاطباق، وتبين ان هناك تأثير واضح للمستخلصات المختلفة لبذور الحلبة على بكتيريا *Staphylococcus aureus* الموجبة لصبغة كرام وكان لمستخلص الكحول المثلي تأثيرا كبيرا على هذه البكتيريا مقارنة بالمستخلصات الاخرى اذ وصل القطر التثبيطي الى (32) ملمتر يليه مستخلص الكحول الايثيلي والذي بلغ (20) ملمتر. قدر التركيز المثبط الادنى (MIC) والتركيز القاتل الادنى (MBC) لمستخلص الكحول المثلي على بكتيريا *Staph. aureus* والذي بلغ (12.5) و (25) ملغم/مليتر على التوالي.

المقدمة

ان الطيبات هي خيرات الارض التي تشمل ما في بطونها وعلى وجهها وان نعم الله ظاهرة فما علينا الا ان نستعمل عقلنا الذي وهبنا الله وجمله بالصحة والعافية ولنبحث عن هذه الخيرات ثم نستفيد منها الفائدة الكاملة والكافية. والنباتات هي احدى هذه الخيرات، وقد استخدمها الانسان غذاء وملبسا ودواء، وان حكمة الخالق عز وجل ارادت ان تجعل النبات الواحد يحوي العديد من المركبات الفعالة التي تتشارك معا في معالجة المرض، اذ تمتلك معظم النباتات المعروفة للانسان المزروعة او البرية منها صفات علاجية ووقائية من الامراض التي تصيب الانسان او الحيوان. وقد اطلق مصطلح النباتات الطبية على العديد من هذه النباتات بسبب احتوائها على مركبات ذات خصائص علاجية ومنها نباتات الداتورة بانواعها والدارسين وحبّة البركة وغيرها (1، 2) والحلبة - *Trigonella foenum-graecum* هي احدى النباتات المهمة والشائعة الاستعمال في الطب منذ القدم وتستعمل اليوم على

نطاق واسع في معظم دول العالم، نباتاته عشبية وحولية، يصل ارتفاعها الى (80) سم وهي غزيرة التفرع القاعدي المنبسط او القائم، الاوراق مركبة ثلاثية الوريقات وهي معنقة متبادلة الوضع على السوق. الازهار صغيرة جدا وتخرج في صور عنقودية ذات الوان مختلفة والثمار اما طويلة على هيئة قرون صغيرة الجراب او بشكل كروي محتو بداخله على بذور صغيرة الحجم لونها بني مصفر او رمادي مصفر (3، 4). أكدت الدراسات الحديثة احتواء بذور الحلبة على الكثير من المركبات الفعالة والصيدلانية منها البروتينات والدهون والكاربوهيدرات والمعادن والفيتامينات وغيرها وبسبب وجود هذه المكونات تعددت فوائده الغذائية والطبية، اذ يستعمل كمحصول خضار في بعض المناطق تؤكل اوراقه او القرنات او البذور المستنبطة طازجة او مطبوخة او تضاف الى السلطات، ويستعمل مغلي البذور الجافة او البذور المحمصة مشروبات منعشة ومنشطة او بديلا لمشروبي القهوة والشاي (5، 6).

المواد وطرائق العمل

1- جمع العينات وتصنيفها:

أ- تم شراء كمية من بذور الحلبة من الاسواق المحلية، صنف النبات استاذ علم تصنيف النبات الدكتور علي الموسوي في قسم علوم الحياة/كلية العلوم/جامعة بغداد، الذي أكد ان جنسه ونوعه هو *Trigonella foenum-graecum*.

ب- زرع (250) غم من هذه البذور في لوح مساحته 2×3 مترات في حديقة المنزل في حي العدل، في منتصف شهر تشرين الثاني لغرض التأكد من النوع، ثم جمعت البذور الناضجة من هذه النباتات في نهاية شهر شباط، وغرلت من جميع التربة والاساخ، وحفظت في عبوة زجاجية داخل المختبر بعد تدوين علامة باسم النبات وتاريخ الجمع والمصدر.

ج- نظفت وغسلت البذور من العالق بها، ثم جففت تجفيفا طبيعيا بدرجة حرارة المختبر اذ تركت في الظل معرضة للهواء الطلق.

2- الكشف عن المركبات الفعالة في بذور نبات الحلبة:

تم الكشف عن المركبات الفعالة الموجودة في البذور حسب الطريقة التي ذكرها (7، 8، 8).

3- تقدير بعض المكونات الرئيسية لبذور الحلبة:

تم تقدير المكونات الرئيسية الموجودة في بذور الحلبة حسب الطريقة التي ذكرها (10، 11، 12).

4- تحضير مستخلصات بذور الحلبة:

حضرت المستخلصات الخام لبذور الحلبة بعدة طرق منها:

أ- تحضير المستخلص المائي والكحولي بنوعيه المثيلي والاثيلي.

حضر المستخلص المائي و المستخلص الكحولي حسب ما ذكره (13).

ب- تحضير المستخلص بواسطة الكلوروفورم:

استخدمت طريقة (14) لتحضير مستخلص الكلوروفورم.

ج- الاستخلاص بطريقة الايثر النفطي (PE) *Petroleum Ether Extract*

تم تحضير مستخلص الايثر النفطي حسب ما جاء في (15).

5- دراسة الفعالية التثبيطية لمستخلصات بذور الحلبة في الاحياء المجهرية الاختبارية.

أ- سلالات الاختبار

تم الحصول على السلالات البكتيرية والخميرة المشخصة قيد الدراسة من مختبرات صحة بغداد والتي تم عزلها من حالات التهاب المجاري البولية.

1- *Escherichia coli*

2- *Salmonella typhi*

3- *Proteus mirabli*

4- *Klebsiella spp*

5- *Serratia spp*

6- *Pseudomonas aeruginosa*

7- *Staphylococcus aureus*8- *Candida albicans*

ب- الاوساط الزرعية المستخدمة:

- وسط الاكار المغذي (Difco) Nutrient Agar/NA
- استعمل هذا الوسط لغرض تنمية الجراثيم، وفي حفظ السلالات.
- وسط المرق المغذي (Difco) Nutrient Broth/NB
- استعمل لغرض تنمية وتنشيط الجراثيم وتحضير العوائل الجرثومية المختلفة.
- وسط الاكار سابورود دكستروز (Difco) Sabouraud Dextrose Agar/SDA
- استخدم في تنمية وحفظ عزلة خميرة الـ *Candida albicans*
- وسط مرق سابورود دكستروز (Difco) Sabouraud Dextrose Broth/SDB
- استعمل لغرض تنشيط خميرة الـ *Candida albicans*
- حضرت الاوساط الزرعية الآتية الذكر بحسب تعليمات الشركة المصنعة المثبتة على العبوات وضبط الرقم الهيدروجيني ثم عقمت بالمؤسدة بدرجة حرارة (121)م وضغط (1.5) باوند/انج² لمدة 15 دقيقة، صبت في الاطباق وحضنت في درجة حرارة (37)م لمدة 24 ساعة للتأكد من عدم تلوثها.
- ج- تحضير الاطباق الزرعية لاختبار مستخلصات الحلبة:
- استخدمت طريقة الانتشار بالحفر (The agar well diffusion method) وفق ما جاء في (16)
- لملاحظة تأثير المستخلصات النباتية على نمو البكتريا المستخدمة قيد الدراسة.
- 6- تقدير التركيز المثبط الأدنى MIC والتركيز القاتل الأدنى MBC لمستخلص كحول الميثانول تجاه بكتريا *Staph. Aureus*
- حضرت سلسلة من التخفيف النصفية من تركيز المستخلص الكحولي المركز (80%) في انابيب اختبار معقمة وبتركيز (3.1 و 6.2 و 12.5 و 25 و 50 و 100) ملغرام/مليتر. حدد قيمة التركيز المثبط الأدنى (MIC) والتركيز القاتل الأدنى (MBC) حسب طريقة (17).

النتائج والمناقشة

وجد من نتائج الكشف الكيميائي للمكونات الفعالة لبذور الحلبة احتوائها على الكثير من هذه المكونات مثل الراتنجات والتانينات والصابونيات والقلويدات والكومارينات والفلافونات وخلوها من الكلايكوسيدات، كذلك وجد ان مستخلصها المائي حامضي التفاعل ذو رقم هيدروجيني (pH) يساوي (6.3) (جدول 1).

جدول 1: الكشف الكيميائي عن المركبات العقاقيرية الفعالة في بذور الحلبة المحلية.

النتيجة	الكاشف المستخدم	دليل الكشف	المركب
+	أخلات الرصاص 1%	راسب ابيض هلامي	التانينات Tannins
+	ب-كلوريد الحديد 1%	ظهور لون ازرق مخضر	
+	أرج المستخلص المائي	ظهور رغوة لمدة طويلة	الصابونيات Saponins
+	ب-كلوريد الزنبيق	راسب ابيض	
-	أ-كاشف فهلنك	عدم ظهور راسب احمر	الكلايكوسيدات Glycosides
-	ب-كاشف بندكت	عدم ظهور راسب احمر	
+	أ-كاشف واكنر	راسب بني	القلويدات Alkaloids
+	ب-كاشف دراجندروف	راسب برتقالي	
+	ج-كاشف ماير	راسب ابيض	
+	كحول ايثيلي ← غليان ← ماء مقطر	ظهور عكارة Turbidity	الراتنجات Resins
+	NaOH ورق ترشيح U.V	ظهور لون اصفر مخضر-براق	الكومارينات Coumarins
+	كحول ايثيلي ← NaOH	ظهور لون اصفر	الفلافونات Flavones
حامضي	pH meter	6.3	الرقم الهيدروجيني pH

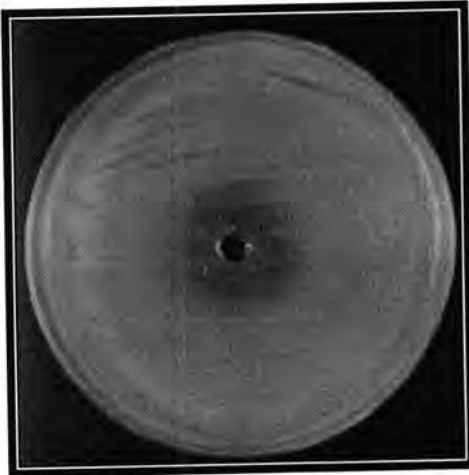
اظهرت نتائج تحليل المكونات الاساسية لبذور الحلبة احتوائها على نسبة من الرطوبة والبروتين والزيت الثابت والكربوهيدرات الكلية والصابونين والرماد والزيت الطيار (جدول 2).

المكونات الكيميائية لبذور الحلبة المحلية *Trigonella foenum-graecum* وتأثير مستخلصها على بعض الاحياء المجهرية الممرضة. رامي وامنة وصفاء

جدول -2: النسب المئوية للمكونات الاساسية لبذور الحلبة.

المكون الاساسي	النسبة المئوية %
البروتين	25.6
الزيت الثابت	9
الكاربوهيدرات الكلية	48.7
الصابونين	4
الرماد	3.2
الزيت الطيار	0.1
المجموع	%100

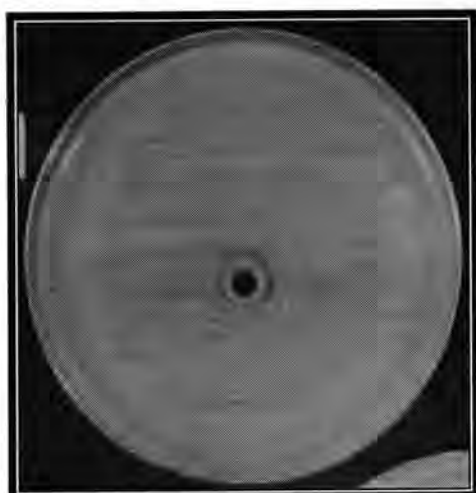
9- الفعالية التثبيطية لمستخلصات بذور الحلبة المحلية على بعض الاحياء المجهرية الممرضة: درست الفعالية التثبيطية للمستخلصات النباتية لبذور الحلبة ضد بعض الاحياء المجهرية الممرضة والمسببة لالتهاب المجاري البولية. وقد استخدمت في هذه الدراسة سبعة انواع من البكتريا الاختبارية واحدة موجبة لصبغة كرام وهي *Staph. aureus* وستة سالبة لصبغة كرام وهي *E. coli* و *Sal. typhi* و *Ps. aeruginosa* و *Kleb. spp* و *Proteus spp* و *Serratia spp* فضلا عن خميرة الـ *C. albicans*.



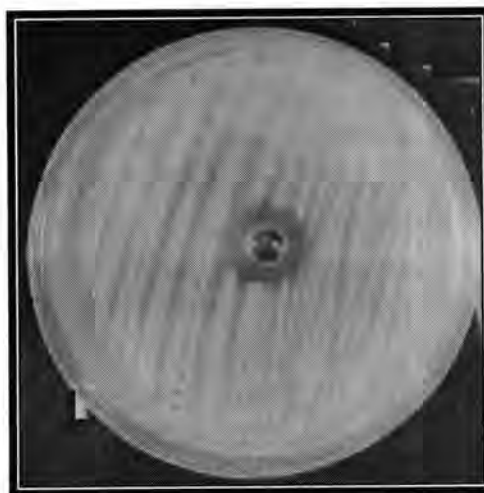
شكل -2: تأثير مستخلص الايثانول لبذور الحلبة على بكتريا *Staph. aureus*



شكل -1: تأثير مستخلص الميثانول لبذور الحلبة على بكتريا *Staph. aureus*



شكل 4- تأثير مستخلص الميثانول لبذور الحلبة على بكتريا *Sal. typhi*



شكل 3- تأثير المستخلص المائي لبذور الحلبة على بكتريا *Staph. aureus*

اقتصرت تأثير المستخلصات بشكل واضح على بكتريا *Staph. aureus* وبشكل طفيف جدا على بكتريا *Sal. typhi* (جدول 3). وجاءت نتائج مستخلص الكحول الميثيلي (80%) في الصدارة اذ اعطت افضل قطر تثبيط على بكتريا *Staph. aureus* الذي بلغ (32) ملليمتر (شكل 1). بينما كان قطر التثبيط اقل بكثير حول بكتريا *Sal. typhi* والذي بلغ (4) ملليمتر فقط (شكل 4). كذلك كان مستخلص الكحول الايثيلي (80%) ذا تأثير واضح على بكتريا *Staph. aureus* فقط وقد وصل القطر التثبيطي لنمو هذه البكتريا (20) ملليمتر (شكل 2) بينما كان تأثير المستخلص المائي على البكتريا نفسها طفيفا اذ وصل قطر التثبيط الى (9) ملليمتر (شكل 3). ولم تظهر الانواع البكتيرية الاخرى وكذلك خميرة *C. albicans* اي استجابة تذكر مع المستخلصات المستخدمة في هذه الدراسة. يعزى التفاوت في درجة تأثير المستخلص على البكتريا المختلفة الى نوع هذه البكتريا ونوع المواد الفعالة الموجودة في المستخلص نفسه (18).

جدول 3- تأثير استخدام ثلاثة انواع من المستخلصات الخام ضد بكتريا *Staph. aureus*

متوسط التثبيط		المستخلص المستخدم
<i>Sal. typhi</i>	<i>Staph. aureus</i>	
-	20 ملليمتر	كحول الايثانول 80%
4 ملليمتر	32 ملليمتر	كحول الميثانول 80%
-	9 ملليمتر	مستخلص مائي

واعتمادا على هذه النتيجة نستطيع القول ان مستخلص البذور بكحول الميثانول اكثر قدرة تثبيطية لبكتريا *Staph. aureus* من المستخلص بكحول الايثانول وهذا يعود الى طبيعة الكحولين المستخدمين وقد يكون دليلا على سعة مدى الاستخلاص لكحول الميثانول للمركبات الفعالة المضادة بالرغم من تقارب قطبيته مع قطبية كحول الايثانول علما ان قطبية كحول الاول هي (32.6) وقطبية كحول الثاني (24.3) (15). ويبدو من الواضح ان هذه المستخلصات قد أثرت بشكل جلي على بكتريا *Staph. aureus* دون البكتريا الاخرى او خميرة *C. albicans* والمعروف ان هذه البكتريا هي موجبة لصبغة كرام وان تركيب جدارها يختلف عن جدار البكتريا السالبة لصبغة كرام اذ يتميز بسمك طبقة الببتيدوكلايكان (Peptidoglycan) (19) وقد يكون لهذا دور في تأثير هذه المستخلصات على بكتريا *Staph. aureus* دون غيرها.

المكونات الكيميائية لبذور الحبة المحلية *Trigonella foenum-graecum* وتأثير مستخلصها على بعض الاحياء المجهرية الممرضة. رامي وامنة وصفاء

كذلك تم التعرف على التركيز المثبط الأدنى (MIC) والتركيز القاتل (MBC) للمستخلص الذي اعطى افضل تأثير على بكتريا *Staph. aureus* الا وهو مستخلص الكحول الميثيلي. وكان مقدار التركيز المثبط الأدنى لهذا المستخلص هو (12.5) ملغرام/مليتر والتركيز القاتل الأدنى هو 25 وكما مبين في جدول (4).

جدول 4: قيمة MIC وقيمة MBC للمستخلص الكحولي بالميثيلي (ملغرام/مليتر)

التركيز المختلف لمستخلص الكحول الميثيلي (ملغرام/مليتر)	100	50	25	12.5	6.2	3.1
نوع البكتريا						
<i>Staph. aureus</i>	-	-	-	+	+	+

+ وجود نمو

- عدم وجود نمو

المصادر

1. Morozumi, S.. Isolation, purification, and antibiotic activity of O-Methoxy cinnam aldehyde from cinnamon. Appl. And Envivoment. Micribiol. 36(4): 577-583(1978).
2. الثويني، امنة نعمة والعالمي، زينة والسما، ميثم. دراسة تأثير بعض المستخلصات النباتية في علاج الاصابات الجلدية بخمائر *C. albicans* المعزولة من الحيوانات والاشخاص العاملين على تربيتها في الزجاج والحيوانات المختبرية. مقبولة للنشر في المجلة العراقية لبحوث المناطق الحارة، 2، (2)(2005).
3. الشحات، نصر ابو زيد. النباتات والاعشاب الطبية. دار البحار، بيروت(1986).
4. Rajagopalan, M.S. FounGreek-what can this herb offer. Food and food. Ingredients Journal of Japan, 181: (300-305) (1998).
5. Newall, C.A.; Anderson, L.A. and Phillipson, J.D. Herbal medicines: A guide for health care professional. 2nd ed. London: The pharmaceutical Press; : 117-118(1998).
6. الوائلي، الحاج احمد. الادوية وصحة البدن. الطبعة الاولى، منشورات الهدى، ايران، قم، ياساز قدس، الطابق الثاني، رقم 57(2003).
7. Shihata, I.M. A pharmancolological study of anayallis arvensis. M.B. Vet. Thesis. Cairo University(1951).
8. Fahmy, I.R. Constituents of plant crude drugs. 1st ed. Paul Barbey. Cairo(1933).
9. Jaffer, H.J.; Mahmod, M.J.; Jawad, A.M.; Naji, A. and Al-Naib, A. Phytochemical and biological screening of some Iraqi plant. Fitoterupia, LIX. 299(1983).
10. Association of Official Analytical Chemists (AOAC). Official Methods of Analysis, 3rd ed. Washington D.C(1980).
11. Drum, T.D.J.; Ian, Gray, J. and Hosfield, G.L. Variability in the saccharide, protein, phenolic acid and saponin contents of four market classes of elible dry beans. J. Sci. Food Agric. 51: 285-297(1990).
12. العاني، اوس هلال. دراسة مكونات الحبة السوداء المحلية وتأثير مستخلصاتها على بعض الاحياء المجهرية. رسالة ماجستير، كلية العلوم، الجامعة المستنصرية(1998).

13. Harbone, J.B. Phytochemical methods. A guide to modern techniques of plants analysis. 2nd ed. London, New York, Chapman and Hall(1984).
14. Harbone, J.B. Phytochemical methods. A guide to modern techniques of plants analysis. Champman and hall, London, New York(1973)..
15. الجبوري، علي عواد والراوي، محمد عبد الله. علم الادوي الطبية، مستقبل النباتات الطبية في الصناعات الدوائية والطب. بغداد-العراق(1993).
16. Vignolo, G.M.; Suriani, F.; Holgado, A.P. and Oliver, G. Antibacterial activity of lacto bacillus strains isolated from dryfermented sansnges. J. App. Bac., 75: 344-349(1993).
17. Baron, E.J.; Peterson, L.R. and Finegold, S.M. Bailey and scotts diagnostic microbiology. 9th ed. Mosby Year Booking(1994).
18. Mitscher, I.A.; Len, R.P.; Bathala, M.S.; Wu, W.A. and Beal, J.L. Antimicrobiol agenst from higher plant. 1 lioyid, 35(2): 157-166(1972).
19. Jawetz, E.; Melnich, J.L. and Adelberg, E.A. Medical microbiology. Ed. Appleton and Lang(1998).

تنشيط النطف البربخية في الفئران باستخدام مصل دم النساء الفاعل المضاف الى اوساط زرعية مختلفة

خالد سهيل عبود العزاوي
قسم فسلجة التناسل السريري / معهد ابحاث الاجنة وعلاج العقم / جامعة النهرين

ABSTRACT

The objective of this research work was to induce in vitro activation of Epididymal Spermatozoa in adult fertile male Mice (*Mus musculus*) by using different culture media to compare between them by studying:

1. The effect of Fresh Blood Serum of Women with different concentration (20%, 50%) on Sperm Parameters in in vitro activation.
2. The effect of two different culture media on in vitro activation of Epididymal Sperm & determine the best one between them.

The adult fertile male Mice (*Mus musculus*) used in this research. Modified Earle's Medium (Baghdad Culture Medium) (BCM) & Dextrose Medium (5%) supplement with either 20% or 50% Women Mid – Cycle Serum was used as culture medium. Simple Layer in vitro sperm activation Method submitted in this research.

The use of 20% fresh women serum in (BCM) gave significantly ($P < 0.05$) highest sperm activation compared with 50% fresh women serum in Dextrose (5%). Sperm motility and grade activity significantly increased ($P < 0.05$) in (BCM) compared with Dextrose (5%) medium.

It concluded from the results of this study that the use of Simple Layer in vitro sperm activation method with (BCM) supplemented with 20% fresh women serum resulted in significant improvement in Epididymal sperm motility and grade activity.

الخلاصة

تهدف هذه الدراسة إلى تنشيط النطف البربخية المأخوذة من ذكور الفئران البيض البالغة (*Mus musculus*) باستخدام اوساط زرعية مختلفة للمقارنة بينها من خلال دراسة:

- 1- تأثير مصل دم النساء الفاعل بتركيز (20% و 50%) على تنشيط معالم النطف (Sperm Parameters) في الزجاج (in vitro).
- 2- دراسة تأثير وسطين إستخداما لتنشيط النطف البربخية في الزجاج واختيار أفضل هذين الوسطين لعملية تنشيط النطف في الزجاج.

تم استخدام ذكور الفئران البيض البالغة (*Mus musculus*) في هذه الدراسة كما تم استخدام وسطين زرعين مختلفين لتحديد افضلهما في عملية التنشيط كما تم أيضا استخدام طريقة التقنية الطبقيّة البسيطة في عملية فصل وتنشيط النطف المستخلصة من الفئران السليمة.

أثبتت هذه الدراسة إن استخدام طريقة التقنية الطبقيّة البسيطة (Simple Layer Method) أظهرت تحسنا معنويا ($P < 0.05$) ملحوظا في تنشيط النطف البربخية في الزجاج المستخلصة من الفئران المختبرية بالنسبة إلى جميع معالم النطف. بينت الدراسة ان تركيز المصل الفاعل للنساء بتركيز (20%) المستخدم مع وسط إيرل المحور (Modified Earle's Medium) (وسط بغداد) أفضل من المصل الفاعل للنساء بتركيز (50%) المستخدم مع وسط الديكستروز (5%) في تنشيط معالم النطف البربخية في الزجاج في الفئران المختبرية.

أثبتت الدراسة ان وسط بغداد المضاف اليه مصل دم النساء الفاعل بتركيز (20%) أفضل من محلول الديكستروز (5%) المضاف اليه مصل دم النساء الفاعل بتركيز (50%) في تنشيط النطف البربخية في الزجاج باستخدام طريقة التقنية الطبقيّة البسيطة (Simple Layer Method) التي اعطت تحسنا معنويا في تنشيط النطف البربخية المستخلصة من ذكور الفئران البيض البالغة.

المقدمة

أشار العالمان هيرست وولاك في دراسة اجريها حول عامل العقم غير المعروف أو غير المفسر (Unexplained Infertility) تضمنت طرائق لعلاج هذا العامل واحداث الحمل في النساء اللاتي يعانين أو ازواجهن من هذا العامل. إذ أوضحنا ان استخدام طريقة فرط الاباضة (Super

(Ovulation) مع طريقة التلقيح داخل الرحم (IUI) (IntraUterine Insemination) أظهرت سرعة في حدوث الحمل في المرضى الذين يعانون من حالة العقم غير المعروف، تطرقا كذلك إلى طريقة تدعى بنقل الكميات إلى داخل انبواب فالوب (Gamete IntraFallopian Transfer) (GIFT) لعلاج مرضى العقم الذين يكونون ذوي اجهزة تكاثرية سليمة من الناحية التشريحية. (1) أيضا عرضا طريقة تجمع أفضل مميزات طريقتي (IVF) و (GIFT) وتدعى بطريقة نقل البويضة المخصبة إلى داخل انبواب فالوب (ZIFT) (Zygote IntraFallopian Transfer) حيث يتم الاخصاب في الزجاجة ثم ينقل الجنين الى مكانه الطبيعي داخل جسم الام. (1)

استخدم العالم فله وجماعته ثلاث طرق لفصل وتنشيط النطف في الزجاجة من نماذج السائل المنوي في الرجال المصابين بالعقم اذ تم استخدام طريقة التقنية الطبقيّة البسيطة (Simple Layer Method) أو تسمى طريقة السباحة إلى أعلى (Swim-Up Procedure) وطريقة تدرجات بيركول (Percoll Gradients) وطريقة تدرجات بيركول المصغرة (Mini-Percoll) ولقد كان الغرض من هذه الطرق هو لتهيئة النطف لأجل عملية الاخصاب في الزجاجة (IVF) إذ لاحظوا ان استخدام طريقة بيركول المصغرة والتي تتبع مباشرة بطريقة التقنية الطبقيّة البسيطة لها نتائج افضل بكثير من طريقة تدرجات بيركول وافضل من طريقة التقنية الطبقيّة البسيطة لوحدها. (2)

حيث استهدف هذا البحث دراسة امكانية تنشيط النطف البربخية باستخدام وسط ايرل الزرع المحور (وسط بغداد) واستخدام وسط الديكستروز (5%) المضاف الى كل منهما مصل دم النساء بتركيز (20% و 50%). تم ايضا في هذه الدراسة استخدام التقنية الطبقيّة البسيطة (Simple Layer Method) لغرض تنشيط النطف البربخية في الزجاجة (In Vitro). اشارت دراسة اجريت حول استخدام التقنية الطبقيّة البسيطة بوجود مصل دم النساء (Serum Swim-up) اعطت نسبة حمل وصلت الى (62%) بينما اعطت طرق نسبة حمل وصلت الى (38%) في دراسة اخرى بينت ان للتقنية الطبقيّة البسيطة علاقة بالقابلية الاخصابية للنطف في الزجاجة حيث لاحظت الدراسة ان هذه الطريقة تعطي مجاميع غنية بالنطف المتحركة التي تمتلك قابلية اخصابية عالية في الحجوم الصغيرة المطلوبة لاجراء عمليات التخصيب في النساء ولها فائدة اخرى انها تزيل كافة مكونات السائل المنوي غير المرغوب فيها وبالاخص الجراثيم والخلايا الالتهابية لذلك يمكن اعتبار هذه الطريقة كاختبار للتنبؤ بالقابلية الاخصابية للنطف في الزجاجة. (3)

المواد وطرائق العمل

1. الحيوانات المختبرية:
استخدم في هذه الدراسة (34) ذكر خصب بالغ من ذكور الفئران البيض (Mus musculus) تم الحصول عليها من مركز الحيوانات المختبرية التابع إلى كلية العلوم الجامعة المستنصرية إذ وضعت في اقصاف مناسبة وتم توفير البيئة الملائمة لها. كان عدد الحيوانات المستخدمة في كل تجربة ما بين (7-10) حيوانات.
2. جمع النطف البربخية:
تم جمع النطف البربخية في هذه الدراسة حسب الخطوات التالية:
• تم قتل الحيوان بطريقة خلع العنق (Cervical Dislocation) ثم تشريح الحيوان من منطقة الصفن لاستخراج البربخين الايمن واليسر.
• وضع (1 مل) من محلول السلاين (Normal Saline) الدافئ في طبق بتري صغير الحجم.
• نقل كلا البربخين إلى طبق بتري الصغير الحاوي على محلول السلاين الدافئ ثم بواسطة مقص خاص تبدأ عملية تقطيع البربخين إلى قطع صغيرة على الأقل (200 مرة) وذلك لتحرير النطف الموجودة في كليهما. (3,4)
• تم وضع قطرة واحدة من المزيج (النطف البربخية + محلول السلاين) بواسطة ماصة باستور على شريحة زجاجية نظيفة وجافة ثم تغطيته بواسطة الغطاء الزجاجي الصغير (Cover Slip).
• سجلت النتائج لمعالم النطف (Sperm Parameter) قبل اجراء عملية التنشيط وبعدها.

3. الفحص المجهرى:

تم اجراء الفحص المجهرى على العينة وتم التركيز على معالم النطف الرئيسية التالية:

1. حساب العدد الكلي للنطف وتركيزها: Total Sperm Count & Concentration
2. شكلية النطف: Sperm Morphology
3. حركة النطف ودرجة الحركة الفاعلة: Sperm Motility & Grade Activity
4. حيوية النطف (3, 5): Sperm Viability

تحضير مصل دم النساء الفاعل:

جهزت الاوساط الزرعية المستخدمة في تنشيط النطف البربخية في الفئران بمصل دم النساء اثناء مرورهن بفترة الدورة الشهرية إذ جمعت نماذج الدم من الطالبات المتبرعات في قسم علوم الحياة في كلية العلوم / الجامعة المستنصرية في اليومين (12 و 13) من الدورة الشهرية وضعت في انابيب اختبار وتركت لفترة لحين حصول عملية تخثر الدم (Clotting) وبعد ذلك تم إزالة الخثرة بعد مرور (20 دقيقة). تم تنبيذ النماذج مركزيا لمدة (10 دقائق) في جهاز الطرد المركزي على سرعة (3000 RPM) ثم فصل المصل بواسطة ماصة باستور وحفظ في انابيب صغيرة (المصل الفاعل). حفظت جميع النماذج (المصل الفاعل) في التجميد تحت درجة حرارة (-20م°) لحين الاستعمال وتم تحضير تراكيز مختلفة من كلا المصلين لكي تضاف إلى الأوساط الزرعية المستخدمة في عملية تنشيط النطف في الزجاج (In Vitro). (3)

تحضير الأوساط الزرعية:

أستخدم في هذه الدراسة نوعين من الأوساط لتنشيط النطف في الزجاج و الأوساط هي:

1. محلول الديكستروز (5%) المضاف له (50%) من المصل الفاعل.
 2. وسط إيرل المحور (وسط بغداد): Modified Earls Medium
- تم تحضير (100 مل) من وسط بغداد كما ذكر من قبل (3).

تنشيط النطف في الزجاج:

يتم فحص معالم النطف قبل وبعد حصول عملية التنشيط باستخدام الأوساط الزرعية المعدة لهذا الغرض والمزودة بالمصل الفاعل بتراكيز مختلفة واستخدمت في هذه الدراسة التقنية الطبقيّة البسيطة لاجراء عملية التنشيط. كما ذكر من قبل (3,6).

التحليل الإحصائي:

استخدم لتحليل نتائج هذه الدراسة إحصائيا اختبار (T-Test) كذلك تم استخدام الطرق القياسية الإحصائية لتحديد الوسط الحسابي (Mean) والانحراف المعياري (Standard Deviation). (7)

النتائج والمناقشة

أوضحت النتائج التي تم الحصول عليها قبل وبعد التنشيط للنطف في الزجاج باستخدام مصل دم النساء الفاعل بتركيز (20%) مع وسط بغداد ان هناك فرق معنوي ($P < 0.05$) في تركيز النطف قبل التنشيط وبعد التنشيط في الزجاج حيث كانت النتائج على التوالي ($10^6 \times 32$) قبل التنشيط واصبحت ($10^6 \times 15$ و $10^6 \times 25$) لفترتي حضانة (15 و 30 دقيقة) في الزجاج. اظهرت النتائج ايضا ان هناك زيادة معنوية ($P < 0.05$) بالنسبة لحركة النطف ودرجة الحركة الفاعلة للنطف والنسبة المئوية لحيوية النطف بعد اجراء عملية التنشيط في الزجاج حيث أنها ازدادت زيادة معنوية ملحوظة مقارنة بنتائج ما قبل التنشيط خلال فترتي الحضانة (15 و 30) دقيقة في الزجاج.

اوضحت النتائج ان شكلية النطف غير الطبيعية اظهرت فرق معنوي ($P<0.05$) حيث انخفضت بعد اجراء عملية التنشيط في الزواج عما كانت عليه قبل اجراء عملية التنشيط خلال فترتي الحضانة (15 و 30 دقيقة في الزواج). كما هو موضح في جدول رقم (1).
بينت النتائج التي تم الحصول عليها قبل وبعد اجراء عملية التنشيط خلال فترتي الحضانة (15 و 30 دقيقة في الزواج ان هناك فرق معنوي ($P<0.05$) حيث أدى استخدام تركيز (50%) من مصل دم النساء الفاعل المضاف الى وسط الديكستروز (5%) الى حدوث انخفاض معنوي في جميع نتائج معالم النطف (تركيز النطف والنسبة المئوية لحركة النطف ودرجة الحركة الفاعلة والنسبة المئوية لشكلية النطف والنسبة المئوية لحيوية النطف) كما هو موضح في جدول رقم (2).
دلت النتائج ان وسط بغداد هو أفضل من وسط الديكستروز (5%) المستخدمان في تنشيط النطف البربخية في الزواج وذلك من خلال مقارنة النتائج التي تم الحصول عليها بعد اجراء عملية التنشيط في الزواج بالنسبة الى جميع معالم النطف لفترتي حضانة (15 و 30 دقيقة كما هو مبين في الأشكال رقم (1) و (2).

جدول-1: تأثير مصل دم النساء الفاعل بتركيز (20%) المضاف إلى وسط بغداد على معالم النطف البربخية المنشطة في الزواج في الفئران السليمة لفترتي حضانة (15 , 30 دقيقة).

معالم النطف	قبل التنشيط	بعد التنشيط	
		15 دقيقة	30 دقيقة
تركيز النطف ($\times 10^6$ / مل)	$6.60 \pm 32.5^*$	8.20 ± 15.4	8.61 ± 25.30
(%) لحركة النطف	$8.92 \pm 52^*$	6.95 ± 60	6.33 ± 68.40
درجة الحركة الفاعلة للنطف	$0.3 \pm 2.40^*$	0.38 ± 3.25	0.56 ± 3.65
(%) للشكلية غير الطبيعية	$4.60 \pm 38.34^*$	4.20 ± 30.50	4.28 ± 24.41
(%) لحيوية النطف	$9.70 \pm 62.61^*$	6.25 ± 70.34	5.86 ± 78

عدد الحيوانات في كل تجربة = 7 حيوانات
* وجود علاقة ذات دلالة إحصائية معنوية ($P<0.05$)

جدول-2: تأثير مصل دم النساء الفاعل بتركيز (50%) المضاف إلى وسط بغداد على معالم النطف البربخية المنشطة في الزجاج في الفرن السليمة لفترتي حضانة (15 , 30 دقيقة).

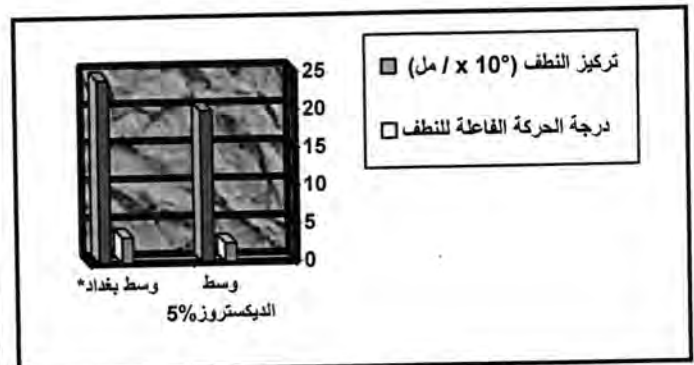
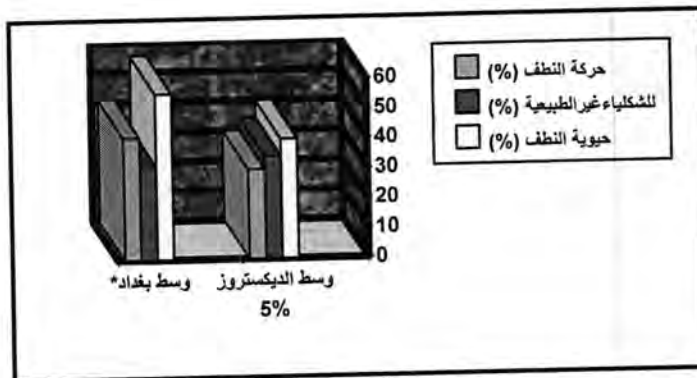
معاليم النطف	قبل التنشيط	بعد التنشيط	
		15 دقيقة	30 دقيقة
تركيز النطف ($\times 10^6$ / مل)	* 6.50±44.50	6.02±24.20	5.42±28.31
(%) لحركة النطف	* 8.90±56.80	8.92±41	7.65±30
درجة الحركة الفاعلة للنطف	** 0.20±3.30	** 0.32±3.40	0.22±2.75
(%) للشكليات غير الطبيعية	* 7.83±32.64	7.30±31.40	7.41±29.82
(%) لحيوية النطف	* 7.83±74.80	7.10±55.54	8.38±40.20

عدد الحيوانات = 7 حيوانات

* وجود علاقة ذات دلالة إحصائية معنوية ($P < 0.05$)

** عدم وجود علاقة ذات دلالة إحصائية معنوية ($P > 0.05$)

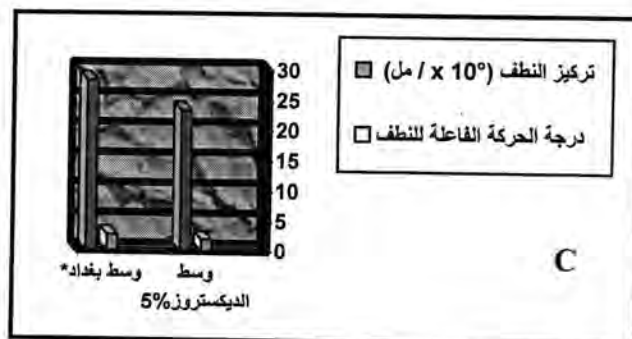
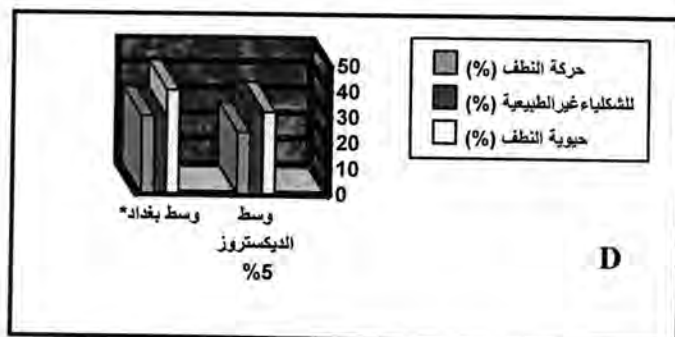
شكل-1: تأثير مصل دم النساء الفاعل بتركيز (50%) المضاف إلى كل من وسط بغداد ووسط الديكستروز (5%) على تنشيط النطف البربخية بعد فترة حضانة (15) دقيقة في الزجاج. (A) تركيز النطف ودرجة الحركة الفاعلة. (B) حركة وشكليات وحيوية النطف.



عدد الحيوانات = 7

* وجود علاقة ذات دلالة إحصائية معنوية ($P < 0.05$)

شكل-2: تأثير مصل دم النساء الفاعل بتركيز (50%) المضاف الى كل من وسط بغداد ووسط الديكستروز (5%) على تنشيط النطف البربخية بعد فترة حضانة (30) دقيقة في الزجاج. (C) تركيز النطف ودرجة الحركة الفاعلة. (D) حركة وشكليات وحيوية النطف.



عدد الحيوانات=7

* وجود علاقة ذات دلالة إحصائية معنوية ($P<0.05$)

أوضحت نتائج الدراسة الحالية بان استخدام مصل دم النساء الفاعل بتركيز (20%) المضاف الى وسط بغداد يؤدي الى زيادة معنوية ($P<0.05$) في النسبة المئوية لحركة النطف الفئران ودرجة الحركة الفاعلة للنطف (Sperm Grade Activity) بعد اجراء عملية التنشيط في الزجاج (8,9). ان مكونات المصل الفاعل تسهل عملية تاهيل النطف (Capacitation) ومعدل الاخصاب (Fertilization rate) (في داخل تجويف قناة البيض (10) تعكس هذه المكونات ببساطة التأثير النافع للمصل الفاعل على نشاط النطف وعلى الاخصاب للبيوض في الزجاج (IVF) (11,12) لوحظ ايضا ان ظاهرة التنشيط العالي (Hypercativation) باستخدام تقنية SLM يؤثر على معدلات الاخصاب فقد وجد ان هذه الظاهرة تزيد من حركة النطف وبالتالي فان عدد كبير منها سيصبح له القدرة لاحداث الاخصاب (13).

بينت نتائج تنشيط النطف البربخية في الزجاج باستخدام مصل دم النساء الفاعل بتركيز (50%) المضاف الى وسط الديكستروز (5%) الى حدوث انخفاض معنوي ($P<0.05$) في النسبة المئوية لحركة النطف ودرجة الحركة الفاعلة للنطف بسبب التركيز العالي لمصل دم النساء الفاعل المستخدم في تنشيطها ان وجود جملة المتممة في المصل الفاعل يعيق عملية تنشيط النطف من خلال عملها على مستضدات النطف (Sperm Antigens) (9,14).

تم في هذه الدراسة استخدام تقنية واحدة لتنشيط النطف البربخية في الفئران هي التقنية التطبيقية البسيطة وقد اعطت هذه التقنية نتائج جيدة في تنشيط واستخلاص النطف المتحركة وفصلها عن بقية مكونات السائل المنوي غير المرغوب فيها (15,16). تعد هذه التقنية أفضل من تقنية غسل النطف باستخدام جهاز التنبيذ المركزي (Centrifugation Method) في تحسين حركة النطف ومعالم السائل المنوي غير الطبيعي. (18,17) كما لوحظ ان النسبة المئوية للحركة تحسنت من (35.5%) الى (72.7%) باستخدام هذه التقنية (19) ان تنشيط النطف البربخية باستخدام تقنية SLM يؤدي الى انخفاض تركيز النطف بعد اجراء عملية التنشيط في جميع النتائج التي تم الحصول عليها مع تحسن في حركة النطف بنسبة (25%) وانخفاض أعداد النطف بنسبة (75%). (20) وذلك بسبب ان هذه التقنية وغيرها من التقنيات الأخرى المستخدمة في فصل وتنشيط النطف في الزجاج تؤدي إلى إزالة النطف الميتة والحية غير القادرة على الحركة أو السباحة في أوساط التنشيط (21,22).

أوضحت هذه الدراسة ان استخدام وسط بغداد في عملية التنشيط هو افضل من محلول الديكستروز (5%) في اجراء عملية تنشيط النطف في الزجاج (9) ويعود السبب في ذلك الى ان وسط بغداد يحتوي

على كل ماتحتاجه النطف للبقاء حية وما تتطلبه عملية التنشيط يحتوي على ايونات لاعضوية والبايروفيت الذي يضاف كمصدر للطاقة بالإضافة الى المواد الموجودة في مصل دم النساء مثل البروتينات والادينوسين الحلقي أحادي الفوسفات (Cyclic Adenosine MonoPhosphate) (cAMP) والكالسيوم (Ca^{+2}) والفيتامينات المختلفة وهرمونات مختلفة مثل الهرمون المحفز للجريبيات (FSH) و الهرمون المحفز للجسم الاصفر (LH) والبرجسترون والاستروجين إضافة الى الدهون (23).

أشارت نتائج هذه الدراسة الى ان النسبة المئوية للشكليات الطبيعية للنطف كانت معنويا أعلى ($P < 0.05$) بعد التنشيط في الزجاج من نسبتها قبل التنشيط . وقد بلغت الشكليات الطبيعية للنطف (80%) السبب في ذلك انتقائية وسط بغداد الجيدة التي تسمح للشكليات الطبيعية للنطف من السباحة الى الأعلى وهذه الانتقائية تماثل في عملها عمل المادة المخاطية لعنق الرحم التي تسمح فقط للشكليات الطبيعية من الهجرة أو السباحة الى أعلى باتجاه موقع الاخصاب (24) . يمكن لهذه النتائج ان تفسر التأثير الايجابي لتقنية (SLM) في كيفية استخلاص النطف النشطة الناضجة ذات الشكليات الطبيعية المأخوذة من منطقة البربخ وقد لوحظ ان منطقة البربخ وبالأخص منطقة ذيل البربخ (Caudal region) تحدث فيها أهم مراحل عملية نضج النطف (Sperm Maturation) فلقد لوحظ ان كل المتطلبات الفسلجية لعملية تاهيل النطف (Sperm Capacitation) وتفاعل الجسم الطرفي (Acrosome reaction) إضافة الى عملية خزن النطف تحدث في هذه المنطقة (25) وان ذيل البربخ يتقلص ويطلق مخزونه من النطف اثناء عملية قذف السائل المنوي (26).

ان السبب وراء استخدام تقنية (SLM) دون غيرها من الطرق التي ذكرت في مقدمة البحث ان هناك دراسة اجريت للمقارنة بين طريقة تدرجات بيركول وتقنية (SLM) وملاحظة تأثير كل منهما على شكليات النطف المفصولة والمنشطة باستخدام كلا الطريقتين حيث تبين ان طريقة بيركول ادت الى انخفاض في شكليات النطف الطبيعية (اي ازدياد الشكليات غير الطبيعية للنطف) على عكس تقنية (SLM) وذلك لسببين:

1. السرعة العالية المستخدمة في عملية التنبيد المركزي التي تتطلبها طريقة بيركول.
 2. حصول تغيرات كبيرة وشاملة في اغشية النطف المنشطة والمفصولة بهذه الطريقة.
- خلصت الدراسة الى ان طريقة بيركول تعطي نسبة عالية من النطف المتحركة ولكن لها تأثير ضار على شكليات النطف والتي تعتبر من المعايير المهمة التي تاخذ بنظر الاعتبار في عمليات الاخصاب في الزجاج (IVF) لذلك فان تقنية (SLM) هي المفضلة على طريقة بيركول لانها تعطي نسبة عالية من الشكليات الطبيعية بالإضافة الى ان العدد الكلي للنطف المتحركة يكون اكثر منه في طريقة بيركول. (27)

يستنتج من الدراسة الحالية مايلي:

1. ان استخدام طريقة التقنية الطبقيّة البسيطة (Simple Layer Method) أظهرت تحسناً معنوياً ($P < 0.05$) ملحوظاً في تنشيط النطف البربخية في الزجاج (in vitro) في الفئران بالنسبة الى جميع معالم النطف (Sperm Parameters).
2. بينت الدراسة ان مصل دم النساء الفاعل بتركيز (20%) افضل من المصل الفاعل بتركيز (50%) المستخدم في تنشيط معالم النطف البربخية في الزجاج.
3. أوضحت الدراسة ان وسط بغداد افضل من محلول الديكستروز (5%) في تنشيط النطف البربخية في الزجاج.

الإكثار الدقيق لنباتات الأناناس *Ananas sativas* باستخدام تقنية زراعة الأنسجة

زينب عبد الجبار حسين الحسيني¹، عبد الجاسم محيسن الجبوري²، هاشم كاظم محمد العبيدي³، محمد خزعل حميد¹
¹وزارة العلوم والتكنولوجيا، دائرة البحوث الزراعية وتكنولوجيا الغذاء
²مركز بحوث التقنيات الإحيائية - جامعة النهرين - بغداد.
³كلية العلوم / الجامعة المستنصرية - بغداد

ABSTRACT

Lateral buds of *Ananas sativas* were extracted and cultured on MS medium after sterilized. All cultures were incubated at $25 \pm 2^\circ\text{C}$ with 16hr/day (1000 Lux) for 60 days. Data of leaves, roots, shoots per plant, their length, fresh, dry weights and percent of rooting were investigated.

The results revealed that addition of BA at concentrations (0.24, 0.5, 1) mg/L caused significant increasing in branches per plant and fresh weight. Concentration at 1g/L showed higher mean of branches per plant (5.6) as compared with control (2.4), While 0.5 mg/L showed higher mean in leaves per plant (9.4) as compared with control which gave higher mean in length (3.78cm).

Rooting results showed that adding NAA to medium effected significantly on percentage and roots per plant, fresh and dry weights. Concentrations at 0.5, 1, 1.5 NAA showed higher rooting percent (100%) after 4 weeks.

Results of Acclimazation showed that petmose gave higher success percentage (100%) after two months, this percent was decreased according to the petmose percent.

الخلاصة

استؤصلت البراعم الجانبية لنباتات الأناناس *Ananas sativas* وزرعت على الوسط MS بعد تعقيمها وحضنت الزروعات على درجة حرارة $25 \pm 2^\circ\text{C}$ وشدة إضاءة 1000 لوكس لمدة 16 ساعة /يوم. أخذت الملاحظات بعد شهرين من الزراعة عن متوسط عدد الأفرع لكل نبات وأطوالها وعدد الأوراق /نبات والوزن الطري والجاف /نبات وعدد الجذور /نبات وأطوالها والنسبة المئوية للتجذير.

أظهرت النتائج إن إضافة Benzyl Adenine (BA) بالتركيز 0.25, 0.5, 1 ملغم/لتر إلى الوسط الغذائي قد سببت زيادة معنوية في متوسط عدد التفرعات ومتوسط الوزن الطري للنبات بلغ أعلى متوسط للأفرع 5.6 فرع /برعم عند التركيز 1 ملغم/لتر مقارنة بالمحايد الذي أعطى متوسط بلغ 2.4 فرع /نبات. أما معدل عدد الأوراق فقد ازداد معنوياً عند التركيز 0.5 ملغم/لتر BA وبلغ 9.4 ورقة/نبات مقارنة بالمحايد الذي أعطى أعلى معدل طول أفرع بلغ 3.78 سم ولم يختلف معنوياً عن التركيز 1.5 ملغم/لتر وأظهرت النتائج عدم وجود فروقات معنوية في الوزن الجاف ولجميع مستويات الـ BA.

بينت نتائج التجذير إن إضافة تراكيز مختلفة من Naphthalene acetic acid (NAA) إلى الوسط الغذائي قد أثرت معنوياً في نسب التجذير ومعدل عدد الجذور ووزنها الطري والجاف. وبلغت نسبة التجذير 100% عند الأوساط الغذائية الحاوية 0.5, 1, 1.5 ملغم/لتر NAA بعد أربعة أسابيع من الزراعة. أما نتائج تجارب الأقلمة والنقل إلى التربة فقد وجد إن أفضل الأوساط الزرعوية هو وسط البتموس فقط والذي أعطى نسبة نجاح بلغت 100% بعد شهرين من الزراعة في ظروف مسيطر عليها وانخفضت نسبة نجاح النباتات المتأقلمة بانخفاض نسبة البتموس في الوسط الزرعوي.

الكلمات المفتاحية: الأناناس، تضاعف خضري، تجذير، أقلمة

المقدمة

ينتمي الأناناس Pine apple إلى العائلة Bromeliaceae التي تضم أجناس عديدة وغالبية أفراد هذه العائلة نشأت بين خطي عرض 15-29° شمال وجنوب خط الاستواء. ومن المتفق عليه إن الموطن الأصلي للأناناس هو المنطقة المحصورة بين البرازيل والأرجنتين وبركواي ولقد انتشر الأناناس بسرعة إلى أجزاء كبيرة من العالم. تحتوي ثمار الأناناس على 80-85% ماء، 12-15% سكر، 0.6% حامض عضوي، كما تحتوي على كميات متفاوتة من البروتين والفيتامينات وخصوصاً فيتامين C تتراوح كميته 8-30 ملغم/100 غم. تكثر الأصناف التجارية للأناناس بواسطة طرق التكاثر الخضري (السرطانات Suckers والأفراخ Slips) أو

باستعمال الساق Stem إذ يقطع إلى عدة أجزاء لتزرع هذه الأجزاء وتكون نباتات جديدة (الخفاجي وآخرون، 1990).

إن استخدام تقنية زراعة الأنسجة في برنامج الإكثار الخضري أثبتت نجاحها في الأناناس شأنها في ذلك شأن بقية الأنواع النباتية فقد استخدمت في إكثار الشليك من قبل Boxus و Quoirin (1974) والجواري (2005) و Hammer Shelag (1982) في إكثار صنف الخوخ Redhaven و Sanhigh وتمكن Reaveni وآخرون (1990) في إكثار الباباظ Carcica papaya وتمكن Singh وآخرون (1994) في إكثار اللانكي *Citrus reticulat* والليمون *Citrus limon* وتمكن الباحث More وآخرون (1992) في إكثار الأناناس وتمكن الجبوري وآخرون (1997) والحسيني وآخرون (2002) في إكثار الكمثرى *Pyrus communis* كما استخدمت في إكثار أصلي الحمضيات *Troyer citrange* و *Carrizo citrange* من قبل العبيدي، (1999).

فباستخدام تقنية زراعة الأنسجة يمكن إنتاج أعداد كبيرة من النباتات في مدة زمنية قصيرة نسبياً مقارنة بالطرق التقليدية فضلاً عن إنتاج هذه النباتات على مدار السنة وفي مساحات أقل بكثير من تلك اللازمة للإكثار بالطرق التقليدية وعلى هذا الأساس فإن البحث يهدف إلى توظيف تقنية زراعة الأنسجة في الإكثار الخضري الواسع السريع لهذا المحصول وإيجاد أفضل الأوساط الغذائية الملائمة للنمو والتضاعف والتجذير ومن ثم الأقلصة ونقل النباتات إلى التربة.

المواد وطرق العمل

1- الأجزاء النباتية المستخدمة :

أخذت سيقان نباتات الأناناس وأزيلت منها الأوراق واستناداً إلى Moore وآخرون (1992) فقد عقت بمحلول هايبو كلورات الصوديوم 2% مدة 20 دقيقة مع إضافة 2-3 قطرة محلول Tween-20 ثم غسلت بالماء المقطر ثلاث مرات وبعدها فصلت البراعم الجانبية وعقت بنفس المحلول مدة 10 دقائق ثم غسلت بالماء المقطر المعقم ثلاث مرات لإزالة تأثير المادة المعقمة بعدها قصرت البراعم الجانبية لتكون جاهزة للزراعة على الوسط الغذائي زرعت البراعم الجانبية على الوسط الغذائي الخاص بإنشاء الزروعات وحضنت بدرجة حرارة 25 ± 2 م° وشدة إضاءة 1000 لوكس مدة 16 ساعة يومياً.

2- الوسط الغذائي المستخدم

استخدم الوسط الغذائي (MS) Murashige و Skoog (1962) وأضيف إليه السكروز والفيتامينات ومنظمات النمو الأخرى وكما مبين في الجدول (1) وزع الوسط الغذائي في قناني الزراعة (28.26 × 9 سم) وبواقع 30 مل. وأغلقت القناني بأغطية بلاستيكية مقاومة للحرارة وعقت بجهاز التعقيم بدرجة حرارة 121 م° وضغط 1.04 كغم/سم² مدة 20 دقيقة.

جدول-1: الوسط الغذائي المستخدم في إنشاء الزروعات

ت	المادة	التركيز (ملغم/لتر)
1	أملاح MS	قوة كاملة
2	NAA	0.1
3	BA	0.25
4	Glycine	0.4
5	Pyridoxine-Hcl	1.0
6	Nicotinic acid	0.1
7	Inositol	100
8	Thiamine-Hcl	0.2
9	Sucrose	30000
10	Agar	8000

3- تجارب التضاعف الخضري :

أخذت النباتات التي تم الحصول عليها من مرحلة إنشاء الزر وعات لإدخالها في تجارب التضاعف الخضري استخدم نفس الوسط السابق السائل بدون إضافة الاكر مع تغيير تراكيز الـ Benzyle Adenine (BA) استخدمت التراكيز (0.0, 0.25, 0.5, 1.0, 1.5) ملغم/لتر من BA.

استخدمت 5 قناني لكل تركيز وبواقع 2 نبات /قنينة. حضنت الزروع بنفس الظروف السابقة وأخذت النتائج عن عدد التفرعات وأطوالها وعدد الأوراق والوزن الطري والجاف بعد ثمانية أسابيع من الزراعة.

4- تجارب التجذير :

اختيرت النباتات الجيدة والمتجانسة قدر الإمكان لإجراء تجارب التجذير واستخدم الوسط الغذائي المبين في الجدول (1) استبعد الـ BA و أضيف الـ NAA بالتراكيز (0.0, 0.5, 1.0, 1.5, 2.0) ملغم/لتر مع إضافة الـ Agar بمقدار 9 غم/لتر. استخدمت 5 قناني لكل تركيز وبواقع 2 نبات /قنينة. حضنت بنفس الظروف السابقة وأخذت النتائج أسبوعيا عن نسبة التجذير لمدة 4 أسابيع من الزراعة أما معدل عدد الجذور والوزن الطري والجاف للجذور فقد أخذت بعد 8 أسابيع من الزراعة.

5- تجارب الأقلمة :

أخذت النباتات الجيدة والمتجانسة قدر الإمكان لإجراء الأقلمة عليها. وقد حضرت 4 أوساط زرعيه وهي (بتموس فقط، 1 حجم بتموس: 1/2 حجم رمل، 1 حجم بتموس: 1 حجم رمل ورمل فقط) وضعت في اصص وزرعت بـ 10 مكررات / وسط زرعى وبمعدل نبات واحد / سندانة بلاستيكية. غطيت النباتات المزروعة بأقداح بلاستيكية شفافة للمحافظة على الرطوبة وحضنت بنفس الظروف السابقة. تم رفع الغطاء تدريجيا مع مراعاة السقي وإضافة البنية حسب الحاجة بمقدار 1 غم /لتر مع ماء السقي. حسب النتائج عن النباتات الناجحة المتأقلمة بعد شهر من الزراعة، ثم بعد شهرين من الزراعة داخل السنادين.

6- نفذت التجارب باستخدام التصميم العشوائي الكامل C.R.D وتم تحليل التجارب ومقارنتها إحصائيا بموجب اختبار L.S.D وعلى مستوى احتمال 0.05 (الراوي وعبد العزيز، 1980).

النتائج والمناقشة

1- التضاعف الخضري

أظهرت النتائج في الجدول (2) إن إضافة الـ BA إلى الوسط الغذائي سبب زيادة معنوية في عدد التفرعات بالتراكيز 0.25, 0.5, 1.0 ملغم /لتر BA مقارنة بالمحايد لكنها لم تختلف معنويا فيما بينها إذ بلغ معدل عدد التفرعات عند هذه التراكيز 5.2, 5.4, 5.6 فرع /نبات على التوالي في حين كان معدل عدد التفرعات في معاملة المقارنة 2.4 فرع /نبات. كذلك وجد إن زيادة تركيز الـ BA إلى 1.5 ملغم /لتر أدى إلى انخفاض معدل عدد التفرعات معنويا عن بقية المستويات ولم يختلف معنويا عن معاملة المقارنة إذ بلغ 2.4 فرع /نبات.

أما معدل أطوال الأفرع فإن النتائج في الجدول نفسه تشير إلى إن معاملة المحايد تفوقت معنويا في هذه الصفة بلغ معدل أطوال الأفرع 3.78 سم لهذه المعاملة وانخفض المعدل بزيادة تراكيز الـ BA بشكل عام وتشير نتائج الجدول نفسه إلى إن معدل عدد الأوراق قد تأثر معنويا عند إضافة الـ BA بتركيز 0.5 ملغم/لتر إذ أعطى معدلا بلغ 69.4 ورقة /نبات أما بقية التراكيز فلم تختلف معنويا عن المحايد.

وبخصوص معدل الوزن الطري أوضحت النتائج في الجدول أعلاه إن إضافة تراكيز الـ BA أدى إلى زيادة معدل الوزن الطري معنويا بالتراكيز 0.25, 0.5, 1.0 ملغم /لتر BA والتي اختلفت معنويا عن المحايد لكنها لم تختلف معنويا فيما بينها إذ بلغ المعدل 1750, 1820, 1780 ملغم على

التوالي في حين انخفض المعدل بزيادة تراكيز الـ BA إلى 1.5 ملغم/لتر وبلغ 750 ملغم ولم يختلف معنويا عن المحاييد .

أما معدل الوزن الجاف فإن النتائج في الجدول نفسه تشير إلى عدم ظهور فروقات معنوية عن المحاييد في هذه الصفة إلا إن معدلات الوزن الجاف ازدادت بشكل عام عند إضافة الـ BA. إن استخدام الـ BA بتركيز 0.5 ملغم/لتر قد أثر في تحفيز نمو البراعم الجانبية وكسر السيادة القمية لذا نجد إن معدل أطوال الأفرع قد تناسبت تناسباً عكسياً بزيادة تراكيز الـ BA إذ وجد Lane وجماعته (1982)، إن هناك علاقة طردية بين معدل النمو والتضاعف وبين تراكيز الـ BA في الوسط الغذائي، أما معدل أطوال الأفرع فيقل بزيادة تراكيز الـ BA في الوسط الغذائي. أما تأثير الـ BA على الأوراق والوزن الطري والجاف فهو نتيجة طبيعية لزيادة عدد التفرعات، إن مثل هذه النتائج ذكرت من قبل عدد من الباحثين مثل Skirvin وآخرون (1986) في الكمثرى و Chevreau وآخرون (1989) في الخوخ.

جدول 2: تأثير إضافة الـ BA إلى الوسط الغذائي في صفات المجموع الخضري للأناناس

تركيز الـ BA ملغم/لتر	الصفات المدروسة				
	عدد الأفرع فرع / نبات	طول الأفرع (سم)	عدد الأوراق ورقة / نبات	الوزن الطري ملغم / نبات	الوزن الجاف ملغم / نبات
0.0	2.4	3.78	33.8	510	50
0.25	5.2	2.60	47.4	1750	620
0.50	5.4	2.48	69.4	1820	900
1.00	5.6	2.44	55.0	1780	980
1.50	2.4	3.25	36.0	750	260
ا.ق.م 0.05 = عدد الأفرع = 1.83 طول الأفرع = 0.90 عدد الأوراق = 23.93 الوزن الطري = 1.02 الوزن الجاف = غ.م					

التجذير

أ- تأثير NAA في تجذير النباتات

تشير النتائج في الجدول (3) إلى إن نسبة التجذير ازدادت بزيادة تراكيز الـ NAA المضافة إلى الوسط الغذائي وبزيادة مدة التحضين بصورة عامة. وقد تميزت المعاملة 0.5 ملغم/لتر NAA بارتفاع نسبة التجذير عن بقية المعاملات في الأسبوع الثالث من الزراعة حيث بلغت 83.3 % في حين بلغت نسبة التجذير 100% بعد أربعة أسابيع من الزراعة في الأوساط الغذائية الحاوية على 0.5، 1، 1.5 ملغم/لتر NAA.

جدول 3: تأثير إضافة الـ NAA إلى الوسط الغذائي في تجذير النباتات

تركيز الـ NAA ملغم/لتر	نسبة التجذير أسبوعياً %			
	1	2	3	4
0.0	16.6	33.3	50.0	66.6
0.5	33.3	50.0	83.3	100.0
1.0	16.6	33.3	66.6	100.0
1.5	33.3	50.0	66.6	100.0
2.0	0.0	16.6	33.3	33.3

تأثير الـ NAA في صفات المجموع الجذري

تشير النتائج في الجدول (4) إلى أن معدل عدد الجذور قد ارتفع معنوياً عن المحاييد عند إضافة تراكيز مختلفة من الـ NAA إلا إنها لم تختلف معنوياً فيما بينها، أما معدل أطوال الجذور فلم تظهر فروقات معنوية عن المحاييد عند إضافة تراكيز الـ NAA في حين ارتفع معدل الوزن الطري معنوياً عن المحاييد وبلغ أعلى معدل للوزن الطري 260 ملغم عند التركيز 2 ملغم/لتر NAA. أما معدل الوزن الجاف قد ارتفع معنوياً عند إضافة تراكيز مختلفة من الـ NAA مقارنة بالمحاييد بلغ أعلى معدل للوزن الجاف 34.8 ملغم عند التركيز 0.5 ملغم/لتر NAA. أن إضافة منظّمات النمو إلى الوسط الغذائي تلعب دوراً في تشجيع النباتات لتكوين الجذور و نموها إضافة إلى أن استخدام الـ NAA شائع في تجذير نباتات الأناناس المكثرة بزراعة الأنسجة (Moore وآخرون ، 1992) .

جدول 4- تأثير إضافة الـ NAA إلى الوسط الغذائي في صفات المجموع الجذري للأناناس

تركيز الـ NAA ملغم/لتر	الصفات المدروسة			
	عدد الجذور جذر/نبات	طول الجذور (سم)	الوزن الطري ملغم / نبات	الوزن الجاف ملغم / نبات
0.0	2.4	1.6	9.2	3.44
0.5	18.4	2.0	233.4	34.8
1.00	13.2	1.26	182.6	22.0
1.50	19.8	1.36	213.0	24.8
2.0	19.8	1.62	260.0	32.6
إ.ف.م. عدد الجذور = 7.99 طول الجذور = غ.م. الوزن الطري = 96.84 الوزن الجاف = 11.82				

ج - الأقلمة والنقل إلى التربة

أوضحت تجارب الأقلمة أن تغطية النباتات بأغطية بلاستيكية شفافة كان له دور فعال في المحافظة على جو رطب يحيط بالنباتات وأن رفعه بصورة تدريجية يعد أمراً ضرورياً كي لا تتعرض النباتات إلى الجفاف والموت في حالة رفع الغطاء بصورة كلية وهذا ما أكدته الجبوري وآخرون (1997) في الكمثرى و غزال (1997) في التفاح .
إما تأثير نوعية التربة في أقلمة النبتات المزروعة في سنا دين وتحت ظروف مسيطر عليها فقد بينت النتائج في الجدول (5) أن نسبة النجاح للنباتات المنقولة إلى الأوساط الزراعية (التربة) كانت 100% بعد شهر في جميع الأوساط الزراعية المستخدمة إلا أن نسبة النجاح انخفضت بعد شهرين من النقل إلى الأصص عدا وسط البتموس لوحدة إذ بقيت نسبة نجاح النباتات المنقولة 100% وقد يعود السبب إلى أن وسط البتموس يحتوي على تهوية جيدة وقابلية على الاحتفاظ بالرطوبة بنسبة عالية وهذه النتائج مع ما وجدته العبيدي (1999) في أقلمة أصول الحمضيات .

جدول 5: تأثير نوع التربة على نقل وأقلمة النباتات الناتجة من الزراعة خارج الجسم الحي .

الفترة الزمنية	نسبة النجاح % في الأوساط الزراعية			
	بتموس فقط	1بتموس: 0.5 رمل	1بتموس: 1 رمل	رمل فقط
بعد شهر	100	100	100	100
بعد شهرين	100	80	80	70

نستنتج من هذا البحث إمكانية استخدام تقنية زراعة الأنسجة النباتية في إكثار نباتات الأناناس خضرياً وبإعداد كبيرة وإنتاج نباتات خالية من الأمراض وعلى مدار السنة .

المصادر

1. الجبوري، عبد الجاسم محيسن جاسم، حميد، محمد خزعل، الصالحي، علي عبد الأمير مهدي. اكثار اصول الكمثرى باستخدام تقنية زراعة الانسجة. مجلة العلوم الزراعية العراقية 2: 68-82 (1997).
2. الحسيني، زينب عبد الجبار، الجبوري، عبد الجاسم، الجلبي، سامي كريم محمد. الاكثار الخضري الدقيق لطعوم واصول اشجار الكمثرى. المجلة العراقية للعلوم والتكنولوجيا. المجلد 1 العدد 1: 43-51 (2004).
3. الخفاجي، مكي علوان وسهيل عليوي عطا وعلاء عبد الرزاق محمد. الفاكهة المستديمة الخضرة - جامعة بغداد - العراق (1990).
4. الراوي، خاشع محمود وعبد العزيز، محمد خلف. تصميم وتحليل التجارب الزراعية - جامعة بغداد - العراق (1980).
5. العبيدي، هاشم كاظم محمد. مقارنة اكثار اصلين من اصول الحمضيات باستخدام تقنية زراعة الانسجة النباتية. رسالة ماجستير. كلية الزراعة. جامعة بغداد - العراق (1999).
6. غزال، محمد عبد النبي. اكثار بغض اصول التفاح خضريا باستخدام تقنية زراعة الانسجة النباتية. رسالة دكتوراة. كلية الزراعة. جامعة بغداد. العراق (1997).
7. Chevreau, E.R.M.; Abu Qauda, H.A.; Korban, S.S and Sullivan.,J.G.. Adventitious shoot regeneration from leaf tissue of three Pear (*Pyrus sp.*) cultivars in vitro Plant cell ., Rept ., 7:688-691(1989).
8. Boxus, ph and M.,Quoirin .La culture de Meristemes apicuxde quelaues especes de prunus . Bull .Soc .R. Bot . Belg . 107 : 91-101(1974) .
9. Lane, W.D and Mc Dougald. Shoot tissue culture of apple comparative response of five cultures to cytokinin and auxin Can., j ., plant ., SCI . 62: 689- 694(1982).
10. Murashige, Tand Skoog, F. Arevised medium for rapid growth and bioassaya with tobacco tissue cultures. Physiol. Plant., 15 :473-497 (1962).
11. Skirvin, R.M.; M.Kouider; H.Joung S.S., Korban. Apple (*Malus domestica* Borkh.) : 183-198 . In : Y.P.S. Bajaj (ed.) Biotechnology in agriculture and Forestry , 1 : trees 1, Springer, Berlin(1986).
12. Skirvin, R.M.; Kouider, M.; Jourg, H and Korbau, S.S. Apple (*Malus domestica* Burklo) In: Bajaj. Y.P.S.(ed) Biotechnology in Agriculture and Forestry, Vol .1, Trees, Springer, Berline, Ny:183-198(1986).
13. Singh, S.; Ray, B.K.; Bahttacharryya, S. and Deka, P.C. in vitro propagation of *Citrus reticulate* Blanco and *Citrus lemon* Burn F. Hort science . 29(3) : 214-216(1994).
14. Hammerschlage, F. A. Factors influencing in vitro establishment and growth of Peach Shoots in vitro. Hort science 17: 85-86(1982).

تحديد المتغيرات في وزن انسجة وطول الحبل السري وابعاد الاوردة والشرابين مع دراسة نسيجية مرضية للمريضات المصابات بداء المقوسات Toxoplasmosis

¹بدر محمد العزاوي و²سالم رشيد العبيدي و¹آمال خضير عباس و¹اشدى خضير عباس
¹الجامعة المستنصرية / كلية العلوم/ قسم علوم الحياة
²جامعة بغداد / كلية العلوم/ قسم علوم الحياة

ABSTRACT

Our study includes immunological, histopathological and biochemical changes accompanied the pregnancies women twenty five infection with Toxoplasmosis. In comparison with the results of 10 normally delivered pregnancies. The results of present study summarized as follows:

- Various histopathological changes were observed in the placenta of Toxoplasmosis women such as necrosis, calcification, hydropic degeneration, fibrinoid deposition, congestion and thrombosis.
- Decrease in the weight of placenta for all patient groups (545.2 gm) in compared with control group (614.6 gm) also decrease significantly the length of umbilical cord of patient groups (22.2 cm) in compared with control groups (59.9 cm).
- There was significant decrease in diameter of arteries and significant increase in thick wall for all patients groups (3.88 mm)(4.55 mm) as in compared with control groups (5.26 mm) and (3.30 mm), also there was significant decrease in diameter of veins and increase in thickness (6.24 mm and 4.83 mm) in compared with control groups (6.87 mm)(3.78mm); but there was significant decrease in diameter of capillaries for all patient groups (0.914 mm) in compared with control groups (1.004 mm).
- An increase in the levels of Placental, glucose (149 mg/dl) while a significant decrease ($p<0.005$) of glucose in serum (4.69 mmol/L) respectively in comparison with the control groups (133.2 mg/dl) and 5.09 mmol/L Respectively.
- Total protein levels in both blood and placenta was not significantly changed. A significant increase ($p<0.005$) in levels of placenta total protein and in serum (824 mg/dl) and 84.24 g/L respectively. In comparison with control groups women 788.1 mg/dl and 73.6 g/L Respectively.

الخلاصة

اجريت هذه الدراسة لمعرفة بعض المتغيرات الفسلجية المرضية والنسجية والكيميائية الحياتية المرافقة لحالات الاصابة بداء المقوسات اثناء الحمل حيث تم اختيار (25) سيدة حامل مصابة بداء المقوسات اجريت المقارنة مع (10) نساء غير مصابات ذات حمل طبيعي انتهى حملهن بولادة طبيعية، بينت نتائج الدراسة المعطيات الاتية:-
-اظهرت تغيرات فسلجية مرضية متنوعة في مستخلص مشاييم المصابات شملت التخر والتكس والاستقاء المائي والترسب الليفياني والاحتقان الدموي والتخثر.
-اظهرت النتائج انخفاضاً في اوزان المشاييم لدى المصابات gm545.2 مقارنة بنساء السيطرة البالغ gm614 وانخفاضاً معنوياً في طول الحبل السري للمريضات 22.2 cm مقارنة بنساء السيطرة 59.4 cm.
-اظهرت النتائج انخفاضاً معنوياً في اقطار الاوعية الدموية الشعرية في المصابات 0.914 μm مقارنة بنساء السيطرة 1.004mm وهناك انخفاضاً في اقطار الشرايين وارتفاعاً في سمك جدارها (3.88mm و 4.55mm) مقارنة بالسيطرة (6.26mm و 3.30mm) . وانخفاضاً غير معنوياً في اقطار الاوردة في المصابات 6.24mm مقارنة بالسيطرة 6.87mm وارتفاعاً معنوياً في سمك جدارها 4.93mm مقارنة بالسيطرة 3.78mm.
-أن هناك ارتفاعاً في مستويات الكلوكوز في مستخلص المشاييم وانخفاضاً في مصل دم النساء المصابات بداء المقوسات (149mgldl±6.6) و (4.69mmol/l±0.15) على التوالي مقارنة بنساء السيطرة (133.2mgldl±6.6) و (5.09mmol/l±0.12).
-حدث اضطراب في مستوى البروتين في مصل الدم وفي مستخلص المشاييم للنساء المصابات اذا ارتفع معنوياً ($p<0.005$) في مشاييم ومصل النساء المصابات اذ بلغ (827mgldl±24.7) و (84.24mg/dl±24.7) مقارنة بنساء السيطرة (788.1mgldl±21.6) و (73.69g/L ±0.41).

المقدمة

اكتشف الطفيلي من قبل العالمين (Nicole & Menacaeux) في عام 1908 في كبد و طحال احد القوارض البرية (*Ctnodactylus gondii*) شمال أفريقيا و في ذلك الوقت كان له انتشار كبير في الطيور و جميع

اللبائن من ضمنها الإنسان (1). اشتق اسم الطفيلي (المقوسات) من شكله الهلالي (مقوس) حيث تعني (Toxon=Arc) وكلمة plasma=form بمعنى الشكل أما اسم النوع كوندوي (gondii) فقد اشتقت من اسم القارض الذي اكتشف في الطفيلي لأول مرة. وفي عام 1939 أقام العلماء (2) بتحديد العلامات السريرية و المرضية لها فضلاً عن عزل الطفيلي كما قام كل من (3) من تحديد الإصابة المكتسبة لداء المقوسات. وفي عام 1948 اكتشف (4) أول طريقة مصلية لتشخيص المرض وهي ما تعرف بطريقة الصبغة (Dye test). هنالك علاقة بين زيادة معدلات الإجهاض وداء السكر (DM) diabetes mellitus (5). جاءت تلك الدراسة مؤكدة لما ذكره الباحثان (6) عند قيامهما بإجراء دراسة لـ 164 حامل لديهم داء السكر المعتمد على الأنسولين الذي يشكل خطورة كبيرة لحدوث الإجهاض العفوي.

تحدث تغيرات مهمة قبل وفي بداية الحمل على بطانة الرحم حيث تتراكم المواد الأولية و الأساسية و يزداد سمك بطانة الرحم و يصبح مهيناً لأنغراس البويضة المخصبة إذ تتحول خلايا السدى stroma cells فيه إلى خلايا كبيرة الحجم ممتلئة تحوي كميات كبيرة من البروتينات و الكلايوجين و الدهون و حتى بعض المعادن الضرورية لتنمية ناتج الحمل conceptus و تعرف عند ذاك بالخلايا الساقطة، إذ تعد تلك المواد المخزونة فيها من اللبائن الأساسية لبناء و نمو جسم الجنين لاسيما خلال الثمانية أسابيع الأولى من الحمل (7).

المواد وطرائق العمل

تم اختيار 35 عينة، 25 عينة مصابة بداء المقوسات Toxoplasma gondii و 10 عينات سيطرة لم يصب بداء المقوسات. أجريت اختبارات كاملة لـ 35 عينة من عينات دم ومشاييم و حبل سري تلك النساء و تلك الاختبارات تراوحت أعمارهن (16-42) سنة. جمعت العينات من محافظة بغداد فقط و من مستشفى الحبيبية للنسائية و التوليد و مستشفى ابن البلدي للولادة و مستشفى بغداد التعليمي في مدينة الطب و للفترة من شهر نيسان إلى شهر تشرين الأول سنة 2003. و قد اجري استبيان دقيق و مفصل عن التاريخ العائلي و السريري لكل حالة من تلك النسوة كما مبين في ملحق (1). أن هؤلاء النسوة لا يشكين أي أعراض مرضية ظاهرة وأن المستوى المعاشي متقارب لنساء الاختبار و السيطرة.

أجري الاختبار على عينات النساء اللاتي أكملن مدة الحمل و تم تحضير مقاطع نسيجية للمشاييم و الحبل السري لغرض دراستها. كما تم قياس أوزان المشاييم و طول الحبل السري للمصابات و السيطرة و باستخدام مسطرة القياس في العدسة العينية و الشريحة المدرجة للمجهر الضوئي ثم قياس أقطار الأوعية الدموية الشعرية Capillaries و ملاحظة التغيرات الحاصلة فيها في أنسجة المشاييم للمريضات و مقارنتها بالسيطرة و كذلك أقطار الأوردة و الشرايين في الحبل السري للمصابات و مقارنتها بالسيطرة 12.

فحص داء المقوسات Toxoplasmosis Test

استخدم في هذا الفحص عدة جاهزة (Toxoplasmosis Kit) و الذي اجري بمزج قطرة من المصل مع قطرة من مادة الفحص على شريحة زجاجية أرضيتها سوداء (خاصة موجودة مع العدة)، ثم وضعت الشريحة على هزاز أفقي لمدة دقيقتين و من ثم ملاحظة فيما إذا كان هنالك تلازن (الفحص موجب) أو عدم وجوده (الفحص سالب).

جمع عينات المشاييم Placental Samples Collection

جمعت عينات المشاييم من النساء اللاتي تعرضن للإصابة بداء المقوسات و أكملن الشهر الأخير من الحمل كذلك مشاييم نساء السيطرة غير المصابات بداء المقوسات، غسلت و اخذ منها مقاطع و وضعت في حاوية زجاجية معقمة و نقلت إلى المختبر بسرعة تحت ظروف مبردة لغرض إجراء الفحوصات المختبرية. كذلك اخذ الحبل السري و قيس طوله و أخذت منه مقاطع وضعت في حاوية معقمة أيضاً و نقلت إلى المختبر تحت ظروف مبردة.

الدراسة الكيميائية الحيوية

قياس مستويات سكر الكلوكوز في المصل

تم تعيين مستوى سكر الكلوكوز في مصل الدم بإتباع الطريقة اللونية Enzymatic colorimetric method (8) (GoD-POD).

تعيين مستوى سكر الكلوكوز في مستخلص عينات المشاييم

مبدأ الاختبار The Principle of the Test

تم تعيين مستوى سكر الكلوكوز المستخلص من عينات المشايم بإتباع طريقة (9) و هي طريقة لونية كمية تعتمد على استخدام الفينول بوجود حامض الكبريتيك المركز، و يكون اللون الناتج عن التفاعل اصفر برتقالي متباين الشدة، يقاس طيف الامتصاص له باستخدام جهاز المطياف عن طوله الموجي (490 nm).

قياس مستويات البروتين الكلي في المصل Determination of Total Protein Levels in Serum

تم استخدام العدة الخاصة لقياس تركيز البروتين الكلي في المصل (Total protein kit) (Biuret method) (10).

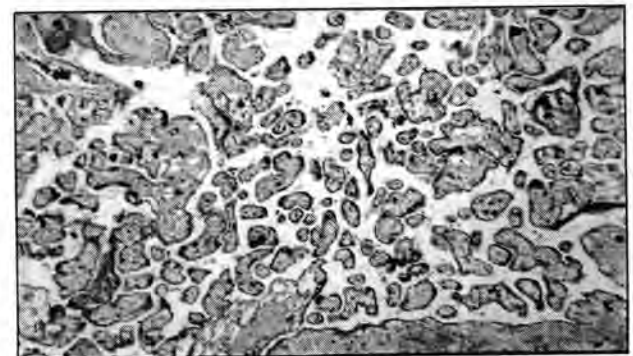
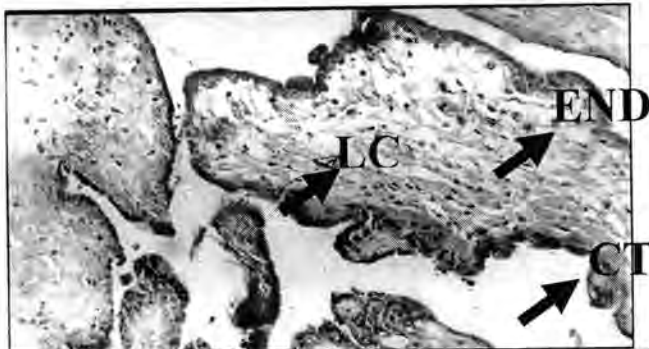
التحري عن وجود البروتين الكلي في مستخلص عينات مشايم النساء تعتمد طريقة العمل في التحري عن وجود البروتين الكلي في مستخلص المشايم على تفاعل الأواصر الببتيدية و التي تدل على وجود البروتين في العينة مع كبريتات النحاس في وسط قاعدي و إعطاء اللون البنفسجي باستخدام كاشف فولن فينول (11).

النتائج والمناقشة

الدراسة النسيجية للمشايم

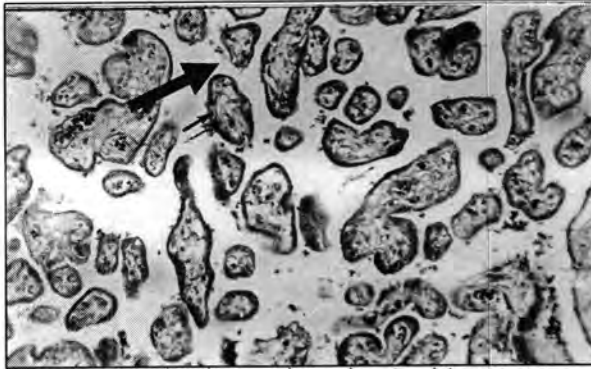
أظهرت نتائج الدراسة الحالية للمقاطع النسيجية للمشايم الطبيعية التي جمعت بعد الولادة مباشرة و التي استخدمت فيها صبغات خاصة مختلفة كصبغة Trichrom و صبغة كاشف شف الدوري Periodic Acid Schiff (PAS) بالمقارنة مع صبغتي الهيماتوكسيلين و الايوسين Hematoxylin and Eosin (H&E) وجود الزغابة المشيمية villus of placenta باعتبارها الوحدة الأساسية للمشيمة مطمورة بمادة السدى stroma و التي تتكون من نسيج ضام مفك loose connective tissue (صورة 1) حيث تحاط الزغابة بصف واحد من خلايا الأرومة الغذائية Trophoblast cell ذات شكل شبه مكعب تحتوي على نواة كروية مركزية الموقع غامقة الصبغة، يكون لب الزغابة من نسيج ضام مفك يحتوي على خلايا الأرومة الليفية Fibroblast cells ذات شكل نجمي و نواة بيضوية اصغر حجماً من نواة الأرومة الغذائية (صورة 2) (صورة 3). من المكونات الأخرى في لب الزغابة هو وجود الأوعية الدموية الجنينية fetal blood vessels تحاط ببطانة ظهارية Endothelium، كما لوحظ في الزغابة وجود خلايا ذات انوية كبيرة الحجم غامقة الصبغة و سايتوبلازم باهت الصبغة أو التي تسمى بخلايا هوف بير Hofbaure cells إذ يحتمل أن تمثل هذه الخلايا خلايا ملتهمة macrophages.

كذلك ظهرت الدراسة الوعاء الدموي (الشريان) حيث يظهر التركيب الطبيعي للوعاء الدموي (الصورة 4) و كذلك مقطع في الوريد الجنيني يظهر التركيب الطبيعي للوعاء الدموي (5). أما (صورة 6) يوضح مقطع في الزغابات المشيمية للنساء المصابات يظهر التنكس في الأرومة الزغابية مع ترسب ليغيانى على جدار الزغابة وتنخر في النسيج الزغابي وبأستخدام صبغة IF & E تظهر الزغابات المشيمية للمصابات ليظهر بداية التنخر والتنكس في الزغابات المشيمية وفي الصورة (8) مقطع في الزغابات المشيمية للنساء المصابات يظهر ترسب المادة الليفي على سطح وفي داخل الزغابة وفي الصورة (10) مقطع للشريان السري للمصابات يوضح صغر القطر وزيادة المسك وفي الصورة (11) أكبر لنفس الصورة السابقة وفي (12) صورة للوريد السري للنساء المصابات ويظهر زيادة في سمك الوعاء مع قلة التجويف .

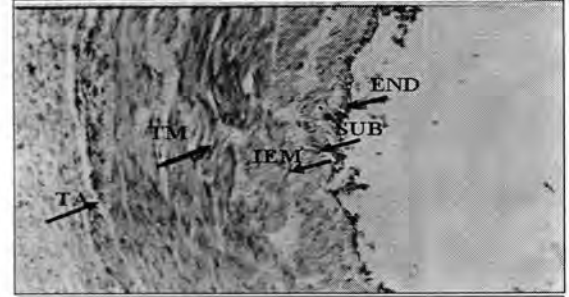


صورة-1 : مقطع مستعرض في زغابة مشيمة طبيعية بعد الولادة (9 أشهر من الحمل) المبطننة للزغابة مع وجود Loose Connective Tissue وتظهر طبقة الأرومة الغذائية (TR) Cytotrophoblast والنسيج الظهاري (Trichrom 1000X) Endothelium Tissue

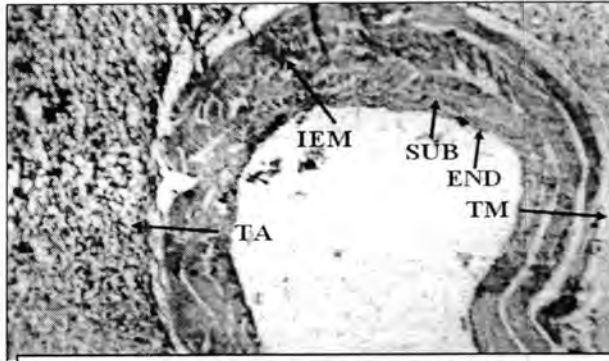
صورة-2 : مقطع مشيمة في الزغابات الطبيعية للمشيمة يظهر الشكل الطبيعي في الزغابة و المحاطة بالأرومة (400×) (Trichrom).



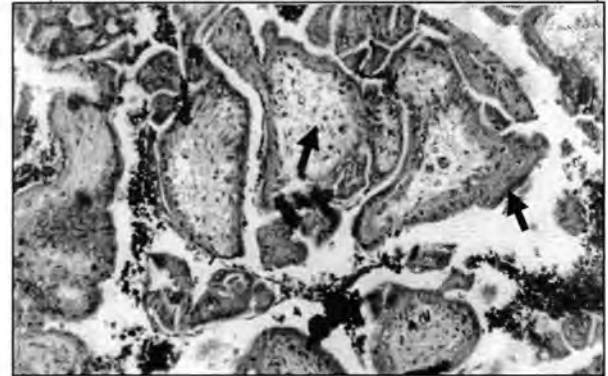
صورة-3 : مقطع اكبر لنفس الصورة السابقة يوضح الخلايا الارومية المحيطة بالزغابة $1000\times$ Trichrom.



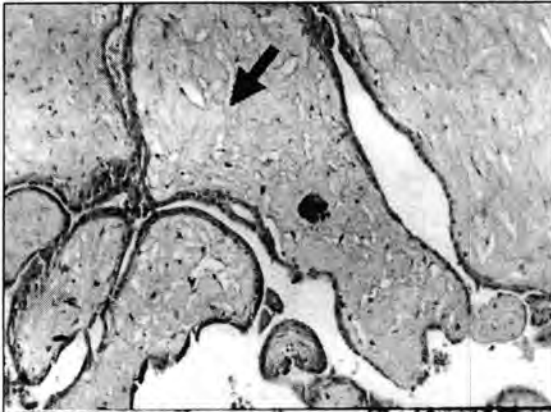
صورة-4: مقطع في الشريان السري الموجود في داخل الحبل السري الطبيعي (400x) صبغة Trichrom توضح طبقات جدار الحبل السري كالآتي :
1. Tunica interna. وتتكون من Subendothelium, Endothelium
2. Tunica Media عضلية ملساء
3. Tunica adventitia.



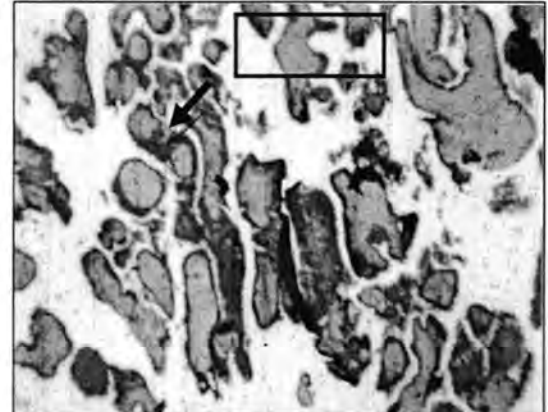
صورة-5: مقطع في الوعاء السري (الوريد) يظهر التركيب الطبيعي للوعاء السري (1000x) صبغة Trichrom توضح طبقات جدار الوريد كالآتي :
1. Tunica interna. وتتكون من Subendothelium, Endothelium و Internal / Elastic Membrane
2. Tunica Media عضلية ملساء
3. Tunica adventitia



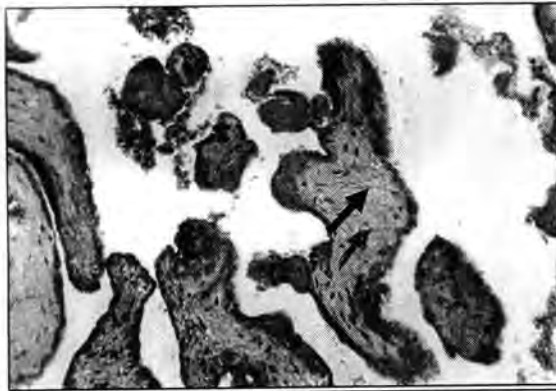
صورة-6 : مقطع في الزغابات المشيمية لنساء مصابات يظهر تنكس في الأرومة الغاذية مع ترسب ليفياني على جدار الزغابة و تنخر في النسيج الزغابي $400\times$ Trichrom



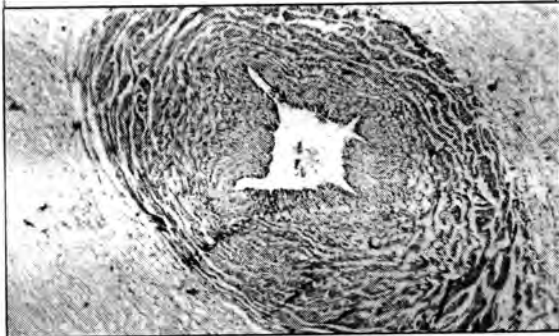
صورة-7 : مقطع في الزغابات المشيمية لنساء مصابات يظهر بداية ظهور التنخر و التنكس (↗) في الزغابات المشيمية $1000\times$ صبغة H&E



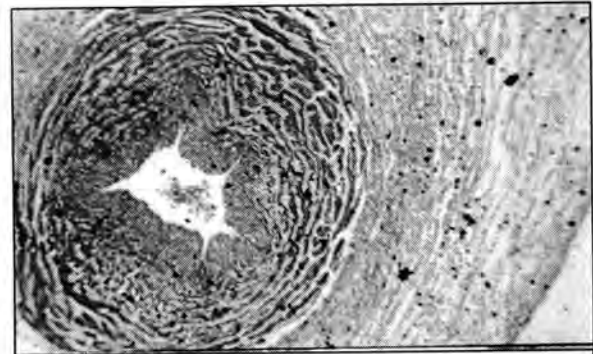
صورة-8 : مقطع في الزغابات المشيمية لنساء مصابات يظهر ترسب المادة الليفية على سطح و في داخل الزغابة (↗) $400\times$ صبغة H&E



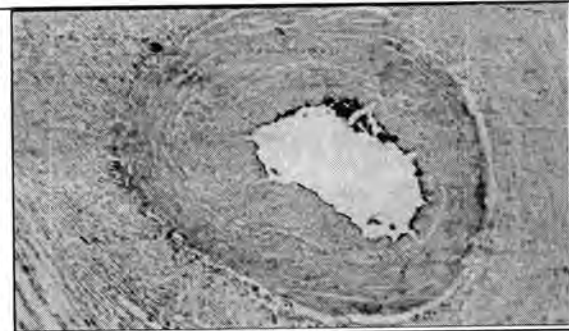
صورة 9- : مقطع اكبر لنفس الصورة السابقة كما في المربع يظهر هذا الترسيب الليفياني مع زيادة في ترسيب المادة الليفية (Fibrosis) (1000× صبغة ايو سين)



صورة 11- : مقطع اكبر لنفس الصورة السابقة في وعاء دموي (شريان) سري لنساء مصابات يظهر صغر قطر التجويف مع زيادة في سمك حدار الوعاء صبغة PAS (1000×)



صورة 10- : مقطع في وعاء دموي (شريان) للحبل السري لنساء مصابات يظهر صغر قطر التجويف مع زيادة في سمك جدار الوعاء صبغة PAS 400×



صورة 12- : مقطع في وعاء دموي (وريد) سري لنساء مصابات يظهر زيادة في سمك الوعاء الدموي مع في التجويف صبغة Trichrom 1000×



صورة 13- : طفل مصاب بأستقاء الدماغ Hy Drocephaly كبر الرأس وصغر في الجسم وضمور في القدمين وتقرح في وسط الظهر حيث يبين انفتاح في الحبل الشوكي مما يؤدي الى وفاة المولود

- أقطار الأوعية الدموية الشعرية

شملت الدراسة للأوعية الجنينية Fetal capillaries في النساء المصابات بداء المقوسات الزغابة الجنينية الوعائية fetal villous vessels ومقارنتها مع النساء الحوامل غير مصابات كانت 0.914 MM انخفاضاً معنوياً عن نساء السيطرة 1.004 MM وذلك ربما يرجع إلى تنخر وتضخم في عدد كبير من الخلايا الاندوثيلية Endothelial cells المبطننة إلى تلك الأوعية الصغيرة تتنخن و تتضخم مسببة قلة في حجم التجويف مما يؤدي إلى تضيق الـ Lumen (12).

أوزان المشايم Placenta weight

إن الأوعية الأموية maternal vascular تزود المشيمة و تؤثر على عملها و نمو الجنين (13). إن نقص وصول الأوكسجين إلى أنسجة داخل الزغابة و الذي يأتي من دوران الدم سيؤثر علي تغذية الجنين (14). إن نتيجة البحث أوضحت قلة حجم و وزن المشايم للنساء المصابات و هذا يسبب صغر حجم الاطفال

المولودين لدى تلك النساء و الذي أوضحه العالم (15)، وقد وجدوا نقص في حجم الوليد في حالة اضطراب الدوران في المشيمة و المزود بالدم من الأم بمقدار (14%).
قطر و سمك الأوعية:

سبب هذا الاختلاف هو التناكس الليفياني التي أشار إليها العالم (16) إلى أن التناكس الليفياني يعود إلى عدم التوازن في دم الأم و حدوث النزف في الفسح بين الزغابية و الاحتقان الدموي داخل الأوعية الدموية كل هذه الأمور تؤدي إلى زيادة في تكوين و ترسب مادة الليفياني لاحظ صورة (6).
من خلال دراسة الفحص النسيجي لحالات المصابات بالمقوسات Toxoplasmosis لوحظ مما سبق وصفه ان الزغابة المشيمية كانت ذات تغيرات نسيجية مرضية متنوعة و متبانية الشدة و هذا يمكن أن يؤدي إلى تعطيل وظيفة الزغابة أكثر من الاعتيادي من خلال استعمالنا لمختلف الصبغات و التي أظهرت ايجابية لصبغة Trichrome و قد اتفقت نتائج هذه الدراسة مع نتائج الباحثان (17) اللذان استخدمتا في دارستهما عدد من الصبغات الخاصة لإظهار تلك التغيرات النسيجية المرضية و التي من ضمنها صبغة (PAS) و (H & E) و Trichrome.

طول الحبل السري:

إن الحبل السري الأقصر من (20 cm) هو دليل على وقوع نقص أو تشوه في الجهاز العصبي للجنين (18) و إن الحبل بهذا الطول ربما يرجع إلى أسباب وراثية، أما طول الحبل السري ($= 32\text{ cm}$) ربما يزيد من احتمال إجهاض المشيمة و لا توجد علاقة بين الوليد الميت و الحبل القصير و قد بين الباحث (18) بأن الحبل بطول (32 cm) هو الحد الأدنى للجنين المولود حديثاً، أما الحبل السري الطويل (80 cm - 70 cm) ربما يعود إلى سبب زيادة في تضخم الحبل أو زيادة في نموه (18).

مستوى الكلوكوز في مستخلص المشيمة وفي مصل الدم

أكد عدد من الباحثين (19; 20; 21; 22) الذين أشاروا إلى أن ارتفاع مستوى الكلوكوز في مصل النساء خلال مراحل الحمل يصاحبه زيادة في نسبة فقدان الجنيني و بالتالي حدوث الإجهاض الذاتي . إن ارتفاع مستويات الكلوكوز خلال المراحل المبكرة من الحمل يسبب تشوهات جنينية و أن التشوهات في أجنة النساء ذوات الداء السكري غير المعتمد على الأنسولين يؤثر على أعضاء الجنين كافة بنفس تأثير النوع (المعتمد على الأنسولين) (19) لذا فإن ارتفاع الكلوكوز في المصل و على الأخص خلال المرحلة المبكرة من الحمل يعد عامل خطورة لحدوث الإجهاض (20).

إن ارتفاع مستوى الكلوكوز في مستخلص المشايم يعزى إلى الايض غير الطبيعي للكربوهيدرات خلال مرحلة الحمل (21). و إن الإصابة بالسكري خلال مرحلة الحمل و الذي يسمى بسكري الحمل (gestational diabetes mellitus) إذ يظهر هذا النوع خلال مراحل الحمل و يختفي بعد الحمل حيث يكون من الصعوبة في هذه الحالة معرفة فيما إذا كانت الأم الحامل مصابة بسكري الحمل مسبقاً أم لا (23). أو قد يحصل الارتفاع في مستويات الكلوكوز في المشايم بسبب حدوث نقص غير طبيعي لهرمون الأنسولين أو حدوث خلل في وظيفة المشيمة و قلة كفاءتها حيث يمكن تفسير ذلك الارتفاع بالاستناد إلى نتائج الباحثين (24) اللذان درسوا وجود انزيم Glucose-6-phosphatase في الخلايا الساقطة و الارومة الغاذية.

مستوى البروتين الكلي في مستخلص المشيمة وفي مصل الدم

لقد كان مستوى البروتين الكلي في مصل الدم ($84.2 \pm 2.7\text{ g/L}$) مقارنة بنساء السيطرة ($73.6 \pm 0.41\text{ g/L}$) و هذا ما يتفق مع الباحثين (25, 26) الذين وضحوا حدوث ارتفاع تدريجي في مستوى البروتين الكلي في مرحلة الحمل و قد فسرت النتائج تبعاً لتنوع الجزيئات البروتينية في مصل الدم خلال مرحلة الحمل و حسب الحاجة إليها لكل مرحلة من مراحل كبناء الهرمونات و الانظيمات و الغلوبينات المناعية و الالبومين الضرورية لإدامة منتوج الحمل (27).

و قد بين الباحث (28) أن الاضطراب في أيض البروتينات في دم الأم الحامل يتسبب في حدوث تباين في مستويات البروتين الكلي لديها و يؤدي بالتالي إما إلى إعاقة التكوين الجنيني داخل الرحم أو موت الأجنة أو حدوث حالات الإجهاض العفوي و ذلك لحاجة الجسم إلى البروتين لبناء الهرمونات و الالبومين الضرورية لإدامة الحمل و الغلوبينات المناعية و الانزيمات (27).

أكد الباحثون (29) على أهمية قياس مستوى البروتين كدليل على عدم كفاءة المشيمة خلال الحمل لاسيما المرحلة المبكرة منه.

أوزان المشايم

جدول 1- : يبين معدل أوزان المشيمة (gm) لنساء السيطرة و المصابات بداء المقوسات.

أوزان المشيمة (gm)			
المجموعة	العدد	المعدل	الخطأ القياسي
السيطرة	10	614.6 ± a	3.2
الاصابة	25	545.2 ± b	6.9

الحروف المتشابهة تعني عدم وجود فروق معنوية و الحروف المختلفة تعني وجود فروق معنوية عند مستوى احتمالية $0.05 >$.

جدول 2- : يبين أطوال الحبل السري (cm) بين نساء السيطرة و النساء المصابات بداء المقوسات.

أطوال الحبل السري cm			
المجموعة	العدد	المعدل	الخطأ القياسي
السيطرة	10	59.4 ± a	0.06
الاصابة	25	22.2 ± b	0.30

الحروف المتشابهة تعني عدم وجود فروق معنوية و الحروف المختلفة تعني وجود فروق معنوية عند مستوى احتمالية $0.05 >$.

أقطار الأوعية الدموية الشعرية

جدول 3- : يوضح أقطار الأوعية الشعرية (capillaries diameter μm) بين نساء مجموعة السيطرة و مجموعة النساء المصابات بداء المقوسات.

أقطار الأوعية الدموية الشعرية (μm) لمشايم النساء			
المجموعة	العدد	المعدل	الخطأ القياسي
السيطرة	10	1.004 ± a	0.0009
الاصابة	25	0.914 ± b	0.0113

الحروف المتشابهة تعني عدم وجود فروق معنوية و الحروف المختلفة تعني وجود فروق معنوية عند مستوى احتمالية $0.05 >$.

أقطار الأوردة الجنينية و سمكها

جدول 4- : يبين أقطار و سمك الأوردة (mm) بين نساء السيطرة و النساء المصابات بداء المقوسات.

سمك الوريد (مم)		قطر الوريد (مم)	
المجموعة	العدد	المعدل ± الخطأ القياسي	المعدل ± الخطأ القياسي
السيطرة	10	3.3 ± 6.87 a	2.3 ± 3.78 a
الاصابة	25	4.4 ± 6.24 a	1.8 ± 4.93 b

الحروف المتشابهة تعني عدم وجود فروق معنوية و الحروف المختلفة تعني وجود فروق معنوية عند مستوى احتمالية $0.05 >$.

المقالة I. أقطار الشرايين الجنينية و سمكها

جدول 5- : يبين أقطار و سمك الشرايين (mm) بين النساء المصابات بداء المقوسات و نساء السيطرة.

قطر الشريان (مم)		سمك الشريان (مم)	
المجموعة	العدد	المعدل ± الخطأ القياسي	المعدل ± الخطأ القياسي
السيطرة	10	1.7 ± 5.26 a	0.81 ± 3.30 a

الاصابة	25	b 1.2 ± 3.88	b 1.6 ± 4.55
---------	----	--------------	--------------

الحروف المتشابهة تعنى عدم وجود فروق معنوية و الحروف المختلفة تعني وجود فروق معنوية عند مستوى احتمالية > 0.05 .

جدول -6 : مستوى الكلوكوز في مستخلص المشيمة و في مصل الدم.

مستوى الكلوكوز mg/dl المستخلص من المشيمة					
أعلى قيمة	أقل قيمة	الخطأ الكلي	المعدل	العدد	
176	111	± 6.6	a 133.2	10	السيطرة
226	116	± 6.6	a 149	25	الاصابة

الحروف المتشابهة تعنى عدم وجود فروق معنوية و الحروف المختلفة تعني وجود فروق معنوية عند مستوى احتمالي > 0.05 .

مستوى الكلوكوز في مصل الدم و في مستخلص مشايم النساء

مستوى الكلوكوز في مصل الدم

جدول -7 : مستوى الكلوكوز في مصل الدم لمجموعة نساء السيطرة و النساء المصابات.

مستوى الكلوكوز mm01/L في مصل الدم					
المجموعة	العدد	المعدل	الخطأ القياسي	أعلى قيمة	أقل قيمة
السيطرة	10	a 5.09	± 0.121	5.8	4.7
الإصابة	25	a 4.69	± 0.152	5.6	2.7

الحروف المتشابهة تعنى عدم وجود فروق معنوية و الحروف المختلفة تعني وجود فروق معنوية عند مستوى احتمالي > 0.05 .

مستوى البروتين الكلي في مصل الدم وفي مستخلص المشايم

جدول -8 : مستوى البروتين الكلي المستخلص من مشايم مجموعة نساء السيطرة و مجموعة النساء المصابات بداء المقوسات

مستوى البروتين الكلي mg/dl المستخلص من المشايم					
المجموعة	العدد	المعدل	الخطأ القياسي	أعلى قيمة	أقل قيمة
السيطرة	10	a 788.1	± 21.62	887	679
الإصابة	25	a 827	± 24.7	990	630

الحروف المتشابهة تعنى عدم وجود فروق معنوية و الحروف المختلفة تعني وجود فروق معنوية عند مستوى احتمالي > 0.05 .

مستوى البروتين التلي في مصل الدم و في مستخلص المشايم

جدول-9: مستوى البروتين الكلي في مصل الدم لمجموعة نساء السيطرة و مجموعة النساء المصابات بداء المقوسات

مستوى البروتين الكلي g/L في مصل الدم					
المجموعة	العدد	المعدل	الخطأ القياسي	أعلى قيمة	أقل قيمة
السيطرة	10	a 73.64	± 0.41	75	71.5
الإصابة	25	+b 84.24	± 2.78	98	25

الحروف المتشابهة تعنى عدم وجود فروق معنوية و الحروف المختلفة تعني وجود فروق معنوية عند مستوى احتمالي > 0.05 .

ملحق -1 :

- 1- اسم المريض :
 - 2- تاريخ التولد : الشهر
 - 3- العمل :
- اليوم

- ## REFERENCES

- 182

7. Trnkas, V.; ReJner & Dolezal, A., The protein spectrum of cervical secretions during the course of pregnancy. *Am.J. Obstet & Gynecol*, 89(2): 215-219. (1964).
8. Braham, D. Trinder, P., Determination of glucose in blood using glucose oxidase analyst, 97;142. (1972).
9. Doubis, M.K.Gilles,K.A.Haneilton, J.K.,Colorvaetric method for determination of sugars and related substance *Anal. Chem.* 28:350-356. (1956).
10. Henry,R.W.;Cannon,D.C.;Winkelman,J.W.;Clinical chemistry principles and techniques. (1974).
11. Gornall, A.G.; Bardawi II, G.J.; David, M.M., The Enzyme *J. Biol. Chem.* 177: 751 cited by Wharton C.D. & McCarty, R.E. (1972). *Experiments and Methodes in biochemistry.* Macmillan Co. Newyork. (1949).
12. Jones, G.J.P. and Fox, H., An ultrastructural and ultrahistochemical study of the human placenta in maternal Essential hypertension, *Placenta*, 2: 193-204. (1981).
13. Gruenwald, P., Introduction the supply line of the fetus definitions relating to the fetal growth in Gruenwald, The placental and its maternal supply line, University Park press, Baltimore 1-17 Benirschke and Gnille 1977. (1975).
14. Benirschke,K.Gille,J.,Placental pathology&Asphyxia;in Gluck in trauterine asphyxia & the developing fetal brain(Yearbook Medical Publishers)Cbi Cago:117-136. (1977).
15. Carcia, A.G.P.; Romose H.L.B.; fonseca, M.E.F. et al., Placental morphology of low birth weight infants born at term *contr. Gynec. Obstet* 9:100-112. (1982).
16. Delia, L.E., *Obstetrics and gynecology placental and fetal development* 6th Ed. J. R. Lippincott Co., Philadelphia London, Syndney. (1990).
17. Gray, J.D. & Halifax, N.S., The problem of spontaneous abortion, H. changes in the placental villi, *Am. Obstete & Gynecol.*, 72(3): 615-621. (1981).
18. Richard, M. Pauli, M. D. Ph.D, The umbilical cord and stillbirth *J, Pediat* p 3:1-8. (2005).
19. Schaefer-Graf, Utem, Buchanana, T.A. Xiang, A., Patterns of congenital anomalies and relationship to initial maternal fasting glucose levels in pregnancies complicated by type 2 and gestational diabetes, *Am.J. Obstet &Gynecol*,182(2):313-320. (2000).
20. Bartha, S.L.; Martin eZ-Del-Fresno.P. & Comillo-Delgalo, R., Gestational diabetes mellitus diagnosed during early pregnancy. *Am. J. Obstet and Gynecol*, 182(2): 346-350. (2000).
21. Spellacy, W.N.; Coetz, F.G.; Greenberg B.Z.; Ells, J., The human placental gradient for plasma insulin and blood glucose. *An.J.Obstet & Gynecol*, 90(6): 753-257. (1962).
22. Samnal, S.C. & Yen, M.D., Abnormal carbohydrate metabolism and pregnancy *Am.J. Obstet & Gynecol*, 90(4): 468-473. (1964).
23. Chamberlain, G.V., *Obstetrics by ten teachers.* 6th Ed Edward Arnold, London. (1996).

24. Petri, M; Golbus, M. Anerson, R., ANA, LA and ACA in women with idiopathic habitual abortion *Arthritis & Rheumatism*, 30(6): 601-606. (1987).
25. Kock, H.; Kessel, H.V. & Stolte, L., Protein-bound iodine and abortion, *Am. J. Obstet & Gynecol*; 95(7): 897-901. (1966).
26. Plotz, E.J.; Kabara, J.J.; Davism, E., Studies on the synthesis of cholesterol in the brain of the human fetus. *Am.J.Obstet & Gynecol*; 101(4): 534-538. (1968).
27. Smith,K.E.;Alvare Z.R.R.; Forsanders J.;Wash, S.,Serum protein lipid & Lipoprotien fractions in normal human pregnancy.*Am.J. Obstet & Gynecol*; 77 (2) :326-334 (1959).
28. Langman,J.,Medical Embryology Williams&Wilkins Co.Baltimore, London. (1995).
29. Green, J.W.; Duhring. J. L. & Smith, K., Placental function tests *Am.J. Obstet & Gynecol.*, 92 (7): 1030-1051. (1965).

مقاومة الانسولين Insulin resistance لدى مرضى قصور الدرقية Hypothyroid patients

أشياء رزاق إبراهيم¹ وصباح ناصر العلوجي² وخالد إبراهيم الهبيبي³

¹جامعة بغداد / كلية العلوم / قسم التقنيات الاحيائية

²جامعة بغداد // كلية العلوم / قسم علوم الحياة

³وزارة الصحة/ مركز الغدد الصم والسكري

ABSTRACT

Hypothyroidism is a condition in which thyroid hormones levels decreased in the blood. These hormones are necessary for energy production and body viability. In many occasions this condition is accompanied or followed by different metabolic disorders. The current study is conducted in the "Specialized center for endocrinology and diabetes" and carried on 70 hypothyroid patients and 60 randomly chosen individuals with normal thyroid function. Both groups were submitted to laboratory tests to evaluate thyroid hormones (T3, T4).

The study involved evaluation of the relationship between hypothyroidism and insulin resistance (IR). Health problem related to many diseases became common lately.

The current study show that both conditions (hypothyroidism and insulin resistance) are associated and common in women, old and overweight individuals.

Insulin resistance incidence is increased in hypothyroid patients, the results show that 18.6% of hypothyroid patients have DIR compared with less percentage 3.3% in healthy individuals, and about 38.6% hypothyroid patients have PIR compared with 2.5% in healthy individuals.

Hypothyroid patients with DIR show impaired glucose tolerance (IGT) and high level of fasting glucose reaching 5.77 ± 1.24 mM/l, high level of CP reaching 5.39 ± 1.71 ng/ml and high level of HbA1c reaching $5.86\% \pm 0.84$. The values of these parameters in this group are higher when compared with other groups and control. About 10% of hypothyroid patients with PIR have high level of CP and 28.6% have IGT.

In general, PIR hypothyroid patients show a significant ($P < 0.01$) increase in F.G reaching 5.63 ± 1.97 mM/l, significant ($P < 0.01$) increase in CP level reaching 3.83 ± 2.82 ng/ml, and significant increase in HbA1c reaching $6.21\% \pm 1.62$.

الخلاصة

يمتاز مرض قصور الدرقية بانخفاض مستوى هرمونات T3 و T4 الضرورية لعمليات إنتاج الطاقة و حيوية الجسم ؛ لذلك ترافق هذه الحالة إضطرابات في عمليات الأيض المختلفة في الجسم . أجريت الدراسة في المركز التخصصي للغدد الصم و السكري في بغداد ، و شملت 70 مريضاً من مرضى قصور الدرقية ، تم تشخيص الحالة لديهم عن طريق قياس مستويات الهرمونات (T4, T3) . كما و شملت 60 شخصاً أختيروا بشكل عشوائي من غير مرضى الغدة ، و قد تم التأكد من سلامة الغدة وعدم وجود قصور في وظيفتها لديهم. تضمنت الدراسة الكشف عن نسبة حدوث مقاومة الأنسولين لدى مرضى الغدة و مقارنتها مع نسبة حدوثها لدى الأفراد الأصحاء الغدة. تشير نتائج الدراسة الحالية الى أن كلتا الحالتين المرضيتين (القصور الدرقي و مقاومة الأنسولين) مترافقتان و شائعتان لدى النساء و كبار السن و كذلك لدى الأفراد من فئة المفرطي الوزن ($BMI = 25-29.9 \text{ kg/m}^2$) و البدناء ($BMI > 30 \text{ kg/m}^2$) . و قد وجد أن 18.6% منهم لديه مقاومة مؤكدة للأنسولين ، في حين كانت النسبة أقل بلغت 3.3% لدى الأفراد الأصحاء الغدة . و بلغت نسبة المرضى الذين لديهم مقاومة ممكنة للأنسولين 38.6% بالمقارنة مع نسبة 2.5% للأفراد الأصحاء . و هي نسبة مرتفعة تؤكد دور قصور وظيفة الغدة الدرقية في نشوء مقاومة الأنسولين.

أظهر مرضى قصور الدرقية الذين لديهم مقاومة مؤكدة للأنسولين (DIR) Definite تحملاً ضعيفاً للكلوكوز Impaired glucose tolerance (IGT) ، و كذلك ارتفاعاً في مستوى الكلوكوز في حالة الصيام بلغ 5.77 ± 1.24 مليمول/لتر ، و ارتفاع مستوى الببتيد سي C-peptide (CP) بلغ 5.39 ± 1.71 نانوغرام/ملييلتر ، و ارتفاع معنوي في مستوى HbA1c و البالغ $0.84 \pm 5.86\%$ ، و قد كان مستوى هذه المؤشرات لدى هذه المجموعة أعلى من مستوياتها لدى مجموعة المرضى الممكنة المقاومة للانسولين (PIR) Possible و المجموعة غير المقاومة (NIR) None و بالمقارنة مع السيطرة .

شملت مجموعة مرضى قصور الدرقية الممكنة المقاومة للأنسولين 10% لديهم مستوى مرتفع لـ CP و 28.6% لديهم تحملاً للكلوكوز ضعيف (IGT) ، و بشكل عام أظهرت هذه المجموعة ارتفاعاً معنوياً عالياً في مستوى الكلوكوز في حالة الصيام بلغ 5.63 ± 1.97 مليمول/لتر و ارتفاعاً معنوياً عالياً ($P < 0.01$) في مستوى CP ، إذ بلغ 3.83 ± 2.82 نانوغرام/ملييلتر ، و ارتفاعاً معنوياً عالياً ($P < 0.01$) في مستوى HbA1c و البالغ $6.21\% \pm 1.62$.

المقدمة

تعد الغدة الدرقية من أهم الغدد الصم في الجسم ، إذ إن لهرموناتها (T4,T3) دوراً مهماً في تنظيم عمليات الأيض المختلفة في الجسم و توليد الحرارة (1) ، ومنها عمليات أيض الدهون عن طريق تحفيز تحلل الدهون و إنتاج الأحماض الشحمية بوصفها مصدراً للطاقة (2) ولها دور في أيض الكلوكوز. لذا فإن أي اختلال في وظيفة الغدة الدرقية له تأثير في جوانب عديدة لعمليات الأيض في الجسم مسبباً حالات مرضية عديدة و أكثرها شيوعاً قصور الدرقية (Hypothyroidism)، وتتضمن انخفاض مستوى هرمونات (T4,T3) و ارتفاع مستوى هرمون TSH . و العوامل المسببة للمرض تتراوح ما بين بيئية (Environmental) أو مناعية (Immunological) أو وراثية (Congenital) (3).

تتصف حالات قصور الدرقية المتقدمة باختزال في إستجابة الخلايا لهرمون الأنسولين الذي يتراكم في الدم مؤدياً الى فرط الأنسولين (Hyperinsulinemia) وهي من عوارض مقاومة الأنسولين Insulin resistance (IR) (4) ، التي تعرف على انها فشل الاعضاء و الانسجة في الاستجابة بشكل طبيعي لفعالية الأنسولين (5) ، مما يؤدي الى افراز تعويضي زائد للأنسولين.

من ناحية أخرى وجد في كثير من الدراسات إن انخفاض مستوى هرمونات الدرقية يؤدي الى انخفاض إستجابة الخلايا الدهنية لهرمون الأنسولين واختزال في عمليات إنتقال الكلوكوز التي يتوسطها هرمون الأنسولين الى داخل الخلايا و اختزال في عمليات الفسفرة الخلوية وتحلل السكريات (Glycolysis) في الخلايا العضلية (6). كذلك يعاني مرضى قصور الدرقية من عدم تحمل للكلوكوز (Glucose intolerance) (7) .

تعد مقاومة الأنسولين من المشاكل الصحية الأساسية في الوقت الحالي ، فقد أشارت العديد من الدراسات إلى أهمية تشخيص مقاومة الأنسولين لكونها من المؤشرات التي تؤدي إلى مخاطر الإصابة بالنوع الثاني من داء السكري (8). كما وترتبط بالعديد من الحالات المرضية مثل: البدانة ، و اضطرابات الدهون ، و تصلب الشرايين ، و ارتفاع الضغط ، و النوع الثاني من داء السكري ، وقد وجد في بعض الدراسات الاحصائية إن واحد من بين ثلاثة الى أربعة أفراد بالغين لديه مقاومة للأنسولين ، وإن حوالي 90% من مرضى السكري لديه مقاومة للأنسولين (9) . لذلك فقد هدف هذا البحث الى تقييم حالات مقاومة الانسولين لدى مرضى قصور الدرقية ودراسة بعض المؤشرات الكيموحيوية المرتبطة بهذه الحالة .

المواد و طرائق العمل:

العينات :

تم تصميم هذه الدراسة المقطعية العشوائية لتحديد حجم مقاومة الانسولين بين مرضى قصور الدرقية الذين يترددون بشكل منتظم على مركز الغدد الصم و السكري . شملت الدراسة (70) عينة دم من مرضى قصور الدرقية ومن كلا الجنسين ويمثلون المجموعة (A) ، فضلاً عن مجموعة السيطرة التي تضمنت (60) شخصاً ومن كلا الجنسين (لا يعانون من داء السكري وليس لديهم قصور أو خلل في الغدة الدرقية) ويمثلون المجموعة (B) . تم سحب 5 مليلتر من الدم الوريدي Veinal blood لكل من المرضى و مجموعة السيطرة باستخدام محقنة نبيذة Disposable Syringe، أخذ (1) مليلتر من الدم و وضع في أنابيب خاصة لقياس مستوى الهيموغلوبين السكري (HbA1c)، إذ ترج العينة بشكل جيد و تحفظ بالثلاجة بدرجة (4) °م لمدة (7) أيام قبل إجراء الاختبار ، الجزء المتبقي من الدم وضع في أنبوب خالٍ من مادة مانعة للتخثر و ترك بدرجة حرارة المختبر لحين تكون الخثرة التي يتم فصلها بجهاز النبذ المركزي بسرعة (3000) دورة بالدقيقة لمدة (5) دقائق ، يتم بعدها سحب مصل الدم و توزيعه على أنابيب أبندروف ، و يتم ترقيم كل نموذج و كتابة اسم الشخص و تاريخ السحب لكل من مجموعة المرضى ومجموعة السيطرة، و النماذج حفظت في مجمدة بدرجة حرارة (-20) °م لحين إجراء الفحوصات اللاحقة .

تحديد دليل كتلة الجسم (Body mass index (BMI)

تم تحديد دليل كتلة الجسم (BMI) من تقسيم وزن الجسم بالكيلو غرام على مربع طول الشخص بالمتر و ذلك بتطبيق المعادلة الآتية :

$$BMI = \frac{\text{Weight (kg)}}{\text{Square of height (m)}^2}$$

و تم تصنيف كل شخص حسب دليل كتلة الجسم BMI إلى أحد الفئات الآتية :

BMI	Below 18.5	18.5-24.9	25-29.9	30 and above
Weight status	Under weight	Normal weight	Over weight	Obese

قياس تراكيز الهرمونات محفز الدرقية (TSH, T4, T3) :

تم قياس تركيز هرمون محفز الدرقية TSH في مصل دم المرضى و السيطرة في مختبر الهرمونات لمركز الغدد الصم و السكري و ذلك باتباع الخطوات المرافقة مع عدة الفحص الخاصة بهذه الهرمونات و المجهزة من شركة BioMérieux .

قياس تركيز الببتيد الرابط (CP) Connecting peptide :

أستعملت طريقة الاختبار القياسي المناعي الإشعاعي المتري (IRMA) Immunoradiometric assay لقياس مستوى الببتيد الرابط CP وباستخدام العدة المستوردة من شركة Isotop . يراعى أخذ العينة في حالة الصيام Fasting .

قياس مستوى الهيموغلوبين السكري (Glycated haemoglobin A1c (HbA1c) :

تم قياس مستوى HbA1c بوساطة جهاز Variant المستورد من شركة (Bio-Rad) ، حيث يشغل الجهاز بوساطة برنامج خاص بـ HbA1c (Variant HbA1c program) . يعمل هذا الجهاز على فصل الـ HbA1c بالاعتماد على طريقة كروماتوغرافيا السائل عالي الأداء High performance liquid chromatography (HPLC) .

قياس تركيز الكلوكوز Glucose :

أتبعت التعليمات المرفقة مع عدة الفحص الخاصة بقياس تركيز سكر الكلوكوز في أمصال كل من المرضى والسيطرة و المجهزة من شركة Randox .

إختبار تحمل الكلوكوز (GTT) Glucose tolerance test :

و يتم الاتفاق مع كل شخص على يوم آخر يكون فيه صائماً لغرض إجراء اختبار التحمل للسكر ، حيث تؤخذ عينة دم (5) مل صباحاً (0 hr) ، يتناول الشخص بعدها الكلوكوز بمقدار (75) غم مذاباً بـ (300) مليلتر ماء و بعد 2 ساعة تؤخذ عينة دم أخرى (2 hr) و تؤخذ عينة ثالثة بعد ساعة أخرى (3 hr) (10) .
تشخيص مقاومة الانسولين :

تم تصنيف أفراد الدراسة الى 3 مجاميع اعتماداً على حالة مقاومة الأنسولين لديهم والتي تم التحري عنها عن طريق إجراء اختبار التحمل للكلوكوز Glucose tolerance test وقياس مستوى الببتيد سي (CP) وتضمنت هذه المجاميع ما يأتي:

A. المجموعة المؤكدة المقاومة للأنسولين (Definite Insulin Resistance (DIR)

شمل مجموعة الأشخاص الذين لديهم نسبة تحمل ضعيف للكلوكوز، إذ تجاوز مستوى الكلوكوز في المصل لديهم النسبة الطبيعية (6.7-10) مليمول (2 ساعة في اختبار OGTT) وفي الوقت نفسه لديهم ارتفاع في مستوى الببتيد سي (CP) ، وقد شكلوا نسبة 18.6% في المجموعة A ، ونسبة 3.3% في المجموعة B .

B. المجموعة الممكنة المقاومة للأنسولين (Possible Insulin Resistance (PIR)

شمل مجموعة الأشخاص الذين لديهم نسبة تحمل للكلوكوز طبيعية في حين كانت نسبة الببتيد سي (CP) لديهم أعلى من النسبة الطبيعية أو بالعكس ، وقد شكلوا نسبة 38.6% في مجموعة المرضى (A) ، ونسبة 25% في المجموعة B.

C. المجموعة غير المقاومة للأنسولين (Non Insulin Resistance (NIR)

شمل مجموعة الأشخاص الذين لديهم تحمل طبيعي للكلوكوز وكذلك مستوى طبيعي للببتيد سي (CP) ، وقد شكلوا نسبة 42.8% في المجموعة A ، ونسبة 71.7% في المجموعة B.

النتائج و المناقشة:**تشخيص مقاومة الأنسولين:**

بلغت نسبة الذين لديهم مقاومة للأنسولين (مؤكدة وممكنة) ضمن مجموعة مرضى قصور الدرقية A 57.2% و كانت أعلى من نسبتها لدى مجموعة السيطرة B و البالغة 28.3% ، و يلاحظ من (جدول 1) إن 18.6% من مجموع مرضى قصور الدرقية (A) الكلي لديه مقاومة مؤكدة للأنسولين DIR ، في حين كانت النسبة أقل بلغت 3.3% من مجموع الأفراد الأصحاء الغدة الكلي (B). و بلغت نسبة المرضى الذين لديهم مقاومة ممكنة للأنسولين 38.6% لدى مجموعة (A) بالمقارنة مع نسبة 25% للأفراد الأصحاء (B) .

تشير هذه النتائج الى ارتفاع نسبة حدوث مقاومة الأنسولين (IR) Insulin resistance لدى مرضى قصور الدرقية .

جدول-1: النسب المئوية لمجاميع مقاومة الأنسولين ضمن مجموعتي مرضى قصور الدرقية (A) ومجموعة الأصحاء (B).

مجاميع مقاومة الأنسولين Insulin Resistance (IR) groups		الاختبارات		مجاميع الدراسة	
		OGTT**	CP*	مجموعة A	مجموعة B
مؤكدة المقاومة للأنسولين	DIR	مضطرب***	مضطرب***	18.6 % (13)	3.3 % (2)
ممكنة المقاومة للأنسولين	PIR	طبيعي	مضطرب	10 % (7)	8.3 % (5)
المجموع الكلي لحالات المقاومة الممكنة للأنسولين		مضطرب	طبيعي	28.6 % (20)	16.7 % (10)
المجموع الكلي للمقاومتين (المؤكدة و الممكنة)				38.6 % (27)	25 % (15)
غير المقاومة للأنسولين	NIR	طبيعي	طبيعي	57.2 % (40)	28.3 % (17)
المجموع				42.8 % (30)	71.7 % (43)
المعنوية ضمن كل مجموعة (A و B)				100 % (70)	100 % (60)
المعنوية بين المجموعتين مجموعة (A و B)				0.029 S	0.00 HS
				0.00 HS	

CP * : الببتيد سي C-peptide

OGTT ** : إختبار تحمل الكلوكوز الفموي Oral glucose tolerance test

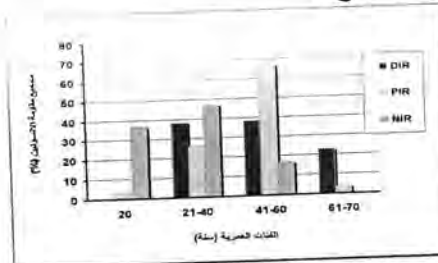
*** نتيجة الإختبار غير طبيعية

نتائج توزيع الفئات العمرية و الجنس لدى مجاميع مقاومة الأنسولين الثلاثة (NIR,PIR,DIR) ضمن مجموعة مرضى قصور الدرقية وبالمقارنة مع مجموعة السيطرة:

أظهرت النتائج أن أكثر الفئات العمرية تكراراً ضمن مجموعة مرضى قصور الدرقية كانت الفئة العمرية 41-60 سنة تلتها مجموعة الأفراد الذين تراوحت أعمارهم بين 21-40 سنة ، وهما الفئتان العمريتان اللتان حازتا على أعلى نسبة للأفراد الذين لديهم مقاومة للأنسولين مؤكدة أو ممكنة ، كذلك يلاحظ إن أفراد الفئة العمرية 61-80 سنة جميعهم لديهم مقاومة للأنسولين مؤكدة أو ممكنة .

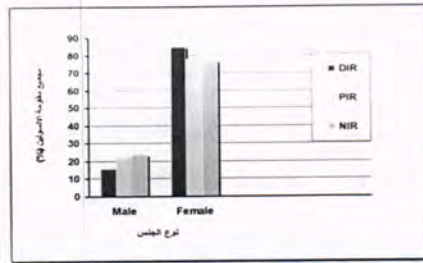
شكلت الفئة الأكثر تكراراً وهي فئة 41-60 سنة نسبة 40% وضممت : 38.6% لديهم DIR ، و 66.7% لديهم PIR ، و 16.7% ليس لديهم مقاومة للأنسولين (NIR) : أما الفئة العمرية 21-40 سنة فقد شكلت نسبة 37.1% ، وجاءت في المرتبة الثانية من ناحية التكرار . ضمت هذه الفئة 38.4% لديهم DIR ، و 25.9% لديهم PIR ، و 46.7% ليس لديهم مقاومة للأنسولين.

الفئة العمرية 1-20 سنة جاءت في المرتبة الثالثة من ناحية التكرار وقد شكلت نسبة 17.1% من مجموع مرضى قصور الدرقية وقد ضمت فرداً واحداً فقط 3.7% لديه PIR ، و 36.7% ليس لديهم مقاومة للأنسولين فقد شكلت نسبة 37.1% ، وجاءت في المرتبة الثانية من ناحية التكرار . المجموعة الأخيرة من ناحية التكرار هي فئة 61-80 سنة وقد شكلت نسبة 5.7% وضممت 23% لديهم DIR ، و 3.7% لديهم PIR ، (الشكل 1). أظهرت الدراسة الإحصائية وجود فرق معنوي عالٍ ($P < 0.01$) عند المقارنة ما بين تكرار حالات مقاومة الأنسولين الثلاثة ضمن الفئات العمرية الأربع .



شكل 1-1: توزيع مجاميع المقاومة للأنسولين (IR) حسب الفئات العمرية المدروسة.

يلاحظ من الدراسة أن غالبية مرضى قصور الدرقية كانوا من الإناث ، وقد شكلوا نسبة مقدارها 78.6% بالمقارنة مع نسبة أقل للذكور 21.4% . يلاحظ أيضاً أن مجموعة المرضى الذين لديهم DIR تضمنت نسبة أكثر للإناث وقد ضممت 84.6% بالمقارنة مع نسبة الذكور 15.4% . وكذلك الحال في مجموعة المرضى الذين لديهم PIR ، كانت نسبة الإناث أكثر ضممت 77.8% بالمقارنة مع نسبة الذكور التي ضمت 22.2% . أظهرت الدراسة الإحصائية عدم وجود فرق معنوي ($P < 0.05$) عند المقارنة ما بين تكرار حالات مقاومة الأنسولين الثلاث ضمن مجموعتي الذكور والإناث ، (الشكل 2) .



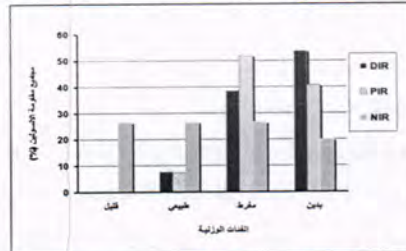
شكل-2: توزيع مجاميع المقاومة للأنسولين (IR) حسب نوع الجنس.

يعد مرض قصور الدرقية السريري من الحالات المرضية الشائعة وقد وجد أن نسبة حدوثه لدى النساء البالغات أعلى من نسبة حدوثه لدى الرجال البالغين . وهذا ما لوحظ في دراستنا فقد وجد أن نسبة الإناث (78.6%) أعلى من نسبة الذكور (21.4%) من مجموع المرضى ، كما أظهرت دراستنا أن نسبة حدوث المرض كانت أكثر لدى الفئة العمرية 41-60 سنة . وقد توافقت هذه النتيجة مع العديد من الدراسات الإحصائية التي أهرت أن نسبة حدوث مرض قصور الدرقية يزداد مع تقدم السن فقد وجد أن نسبة كبيرة من المرضى هم من البالغين الذين أعمارهم أكثر من 60 سنة بالمقارنة مع الأفراد الأصغر سناً (11). وقد أعزى ذلك إلى الزيادة في نسبة تكوّن الأجسام المضادة للدرقية Antithyroid peroxidase antibodies و Antithyroglobulin antibodies مع الارتفاع في مستوى تركيز TSH (12)، كما أن معدل هرمون TRH أيضاً يتزايد مع تقدم السن وخاصة لدى النساء . ومن أسباب كون مرض قصور الدرقية أكثر شيوعاً لدى النساء هو بسبب حصول اضطرابات في هرمونات التكاثر ولا سيما هرمون Progesterone و Estrogen نتيجة الإعياء أو الشد العصبي أو خلال مراحل الحمل أو الدورة الحياتية ، كما أن الاستروجين يحفز الجهاز المناعي مسبباً زيادة إنتاج الأجسام المضادة للدرقية (13) .

إن نسبة كبيرة من مرضى قصور الدرقية هم ممن تتراوح أعمارهم بين 40-60 سنة وكان أغلبهم ممن لديهم مقاومة ممكنة للأنسولين PIR ومقاومة مؤكدة للأنسولين DIR ، 66.7% و 38.6% على التوالي ، (الشكل 1) . أن نسبة حدوث مقاومة الأنسولين لدى كبار السن أكثر من حدوثها لدى الأفراد الأصغر سناً والمتقاربين بالوزن ونسبة الشحوم في الجسم ، وأعزى ذلك إلى هبوط في فعالية وظيفة المايوتوكونديريا نتيجة إختزال في عمليات أكسدة المايوتوكونديريا وإختزال فعالية عمليات الفسفرة Phosphorylation مع تقدم السن . كما ذكر أن معدل تناول الكلوكوز المحفز بالأنسولين لدى الأفراد الذين لديهم مقاومة للأنسولين كان تقريباً أقل بحوالي 60% بالمقارنة مع نسبته لدى الأفراد الأصحاء ، وذكر أن هذا الإنخفاض له علاقة بزيادة محتوى الدهون داخل الخلايا ، إذ تزداد نسبتها بمقدار 80% لدى الأفراد المقاومين للأنسولين (14) .

نتائج توزيع دليل كتلة الجسم (Body mass index (BMI) لمجاميع المرضى بالمقارنة السيطرة:

يلاحظ أن غالبية مرضى قصور الدرقية الذين لديهم مقاومة للأنسولين مؤكدة أو ممكنة كانوا من فئة المفرطي الوزن أو البدناء . ففي حالة مجموعة المرضى الذين لديهم DIR التي شملت (18.6%) من مجموع مرضى قصور الدرقية وكانت الفئة الأكثر تكراراً هي فئة البدناء (53.8%) ، تلتها فئة المفرطي الوزن (38.5%) ، كذلك الحال في مجموعة المرضى الذين لديهم PIR التي شكلت نسبة (38.6%) من مجموع مرضى قصور الدرقية ، وكان من بينهم (51.9%) من فئة المفرطي الوزن و (40.7%) من فئة البدناء . أما مجموعة NIR فقد شملت الفئات الوزنية جميعاً بنسب متقاربة تراوحت بين (20-26.7%) للفئات جميعاً ، وقد أظهرت الدراسة الإحصائية وجود فرق معنوي عالٍ ($P < 0.01$) بين مجاميع المقاومة للأنسولين ضمن الفئات الوزنية الأربعة ، (الشكل 3) .

شكل-3: توزيع مجاميع المقاومة للأنسولين (IR) حسب مجاميع دليل كتلة الجسم ($\text{BMI (Kg/m}^2\text{)}$).

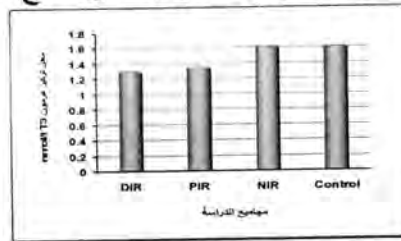
وجد من خلال الدراسات أن الأشخاص المفرطي الوزن كانوا أكثر عرضة لفقدان القدرة على تحمل الكلوكوز الطبيعي ، وكلما كان مستوى تراكيز الكلوكوز أو الأنسولين في البلازما مرتفعاً لدى هؤلاء الأفراد كلما كانوا أكثر مقاومة للأنسولين (15). وقد أشير إلى أن مقاومة الأنسولين أكثر شيوعاً لدى الأفراد المفرطي الوزن

ولها علاقة بخطورة الإصابة بالنوع الثاني من داء السكري ، وأمراض القلب الوعائية (CVD) (15) ، كما أن العديد من الدراسات أكدت الارتباط بين مقاومة الأنسولين (IR) والسمنة Obesity التي تعد من أهم عوامل الخطورة المسؤولة عن نشوء مقاومة الأنسولين ومتلازمة الأيض ، فضلاً عن أن مكونات السمنة مثل كمية الدهون الكلية وتوزيع النسيج الدهني ومخزون الأحشاء من الدهون جميعها عوامل تسهم في حث حالة مقاومة الأنسولين (17).

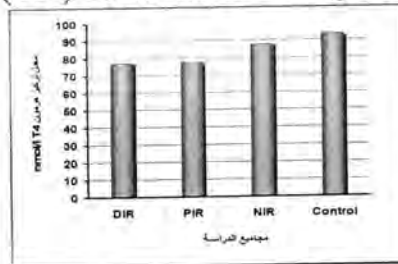
تعد وظيفة الغدة الدرقية حتى عندما يكون مستوى الهرمونات ضمن المدى الطبيعي واحدة من عوامل عديدة تعمل بالتناسق مع بعضها لتحديد وزن الجسم ، حتى إن ارتفاع ضئيل في مستوى هرمون TSH قد يكون محفزاً على حدوث السمنة ، وقد لوحظ وجود ارتباط معنوي إيجابي بين BMI ومستوى هرمون TSH في مصل الدم ، أي كلما ارتفع مستوى هرمون TSH كلما زاد وزن الجسم ، في حين أن علاقة الارتباط معنوية سالبة بين مستوى هرمون T4 و BMI (18).

نتائج اختبارات وظيفة الغدة الدرقية (TSH, T4, T3) لمجاميع المرضى وبالمقارنة السيطرة:

بلغ أقل معدل لتركيز هرمون T3 0.29 ± 1.30 نانومول/لتر لدى مجموعة المرضى الذين لديهم مقاومة للأنسولين مؤكدة ، تلتها مجموعة المرضى الذين لديهم مقاومة للأنسولين ممكنة ، إذ بلغ معدل تركيز الهرمون 0.3 ± 1.35 نانومول/لتر ، أما مجموعة المرضى الذين ليس لديهم مقاومة للأنسولين ، فقد بلغ معدل تركيز الهرمون لديهم 0.58 ± 1.61 نانومول/لتر وكان أعلى من المجموعتين الأخريين . أظهرت الدراسة الإحصائية عدم وجود فروق معنوية ($P > 0.05$) في معدل تركيز هرمون T3 بين مجاميع مقاومة الأنسولين الثلاثة بالمقارنة مع مجموعة السيطرة التي بلغ فيها معدل تركيز الهرمون 0.49 ± 1.61 نانومول/لتر ، (الشكل 4) . في حين كانت الفروق معنوية عالية ($P < 0.01$) في معدل تركيز هرمون T4 بين مجاميع مقاومة الأنسولين DIR و PIR ضمن مرضى قصور الدرقية و البالغ 21.33 ± 77.37 نانومول/لتر و 27.75 ± 77.87 نانومول/لتر على التوالي بالمقارنة بمجموعة السيطرة التي بلغ فيها معدل تركيز الهرمون 14.31 ± 93.29 نانومول/لتر ، (الشكل 5) ، كذلك يلاحظ عدم وجود فرق معنوي في معدل تركيز هرمون T4 لدى مجموع المرضى ممن ليس لديهم مقاومة للأنسولين (NIR) و البالغ 23.5 ± 87.7 نانومول/لتر بالمقارنة مع مجموعة السيطرة .



شكل 4- : توزيع معدل تركيز هرمون (T3) حسب مجاميع الدراسة .



شكل 5- : توزيع معدل تركيز هرمون (T4) حسب مجاميع الدراسة .

لوحظ أيضاً إن أقل معدل لتركيز هرمون T4 كان لدى مجموعة DIR ، تلتها مجموعة PIR ثم مجموعة NIR . يمثل هرمون T3 الشكل الفعال للهرمونات الدرقية وذلك لسهولة انفصاله عن البروتينات الناقلة وإتحاده بالمستقبلات الموجودة في خلايا الأعضاء الهدف ؛ أما هرمون T4 فيعد الهرمون الأقل فعالية من الناحية البايولوجية من هرمون T3 ، ويمثل هرمون T4 المخزون الاحتياطي في الدم (18) ، وهذا ما قد يفسر وجود فرق معنوي في مستوى هرمون T3 بين المجاميع المرضية بالمقارنة مع مجموعة السيطرة ، لأنه في حالة استهلاك مستمرة . أما في حالة هرمون T4 فيلاحظ وجود فرق معنوي في معدل تركيزه بين مجموعتي DIR و PIR بالمقارنة مع مجموعة السيطرة .

تعزز هرمونات الغدة الدرقية (T4, T3) عمليات أيض الكربوهيدرات في العضلات الهيكلية والنسيج الدهني وتعمل على زيادة هدم البروتينات وإستهلاك الدهون ، وهذه الفعاليات جميعها تتداخل مع فعالية هرمون الأنسولين

(20). لذلك يعد هرمون الأنسولين من العوامل المهمة التي تتداخل مع وظيفة الغدة الدرقية ، و قد لوحظ في دراسة أن مرضى قصور الدرقية يعانون من تحمل ضعيف للكلوكوز (IGT) ، إذ وجد أنه عند حقن مجموعة من المتطوعين من مرضى قصور الدرقية غير المعالجين ومجموعة أخرى من المرضى تحت العلاج ومجموعة من الأصحاء ، بمادة الأنسولين الصناعي (0.1 وحدة / كيلوغرام من وزن الجسم) أن معدل تركيز الكلوكوز ينخفض في البلازما لدى المجاميع جميعاً ، ويستمر بالإنخفاض الى حد معين بإستثناء مجموعة مرضى قصور الدرقية غير المعالجين ، إذ ينخفض معدل تركيز الكلوكوز في هذه المجموعة ثم يرتفع ويستمر بالارتفاع ، وذكر الباحث أيضاً إن عدم تحمل الكلوكوز هو ليس سمة ناتجة من إنخفاض هرمونات الدرقية وإنما ناتجة من مقاومة الأنسولين (21). وقد لاحظ عدد من الباحثين ارتفاع مستوى هرمون TSH لدى الأفراد البدناء الذين لديهم مقاومة للأنسولين (21) ، كما لوحظ وجود ارتباط إيجابي بين مستوى هرمون TSH ومستوى هرمون الأنسولين ؛ فكلما زاد تركيز TSH رافقه زيادة في تركيز هرمون الأنسولين وبالعكس. وقد وجد ارتباط ما بين وظيفة الغدة الدرقية وجميع مؤشرات مقاومة الأنسولين ، وقد أشير الى العديد من العوامل التي يمكن أن ترافق مقاومة الأنسولين وتؤثر في وظيفة الغدة الدرقية (20) .

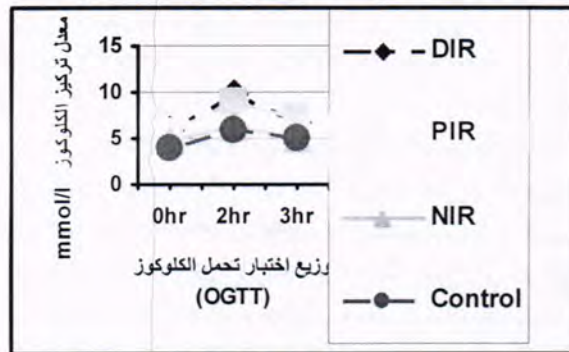
إن فقدان هرمون T3 داخل الخلايا يؤدي الى زيادة مستوى هرمون TSH واختزال فعالية مستقبلات الأنسولين GLUT-4 في الأنسجة الحساسة للأنسولين مثل : العضلات الهيكلية ، والنسيج الدهني مساهماً بذلك في حث مقاومة الأنسولين وهي حالة ملاحظة بنسبة عالية لدى الأفراد البدناء (23) .

نتائج اختبار السكر واختبار تحمل السكر لمجاميع المرضى بالمقارنة مع السيطرة:

بلغ أعلى معدل لتركيز سكر الكلوكوز في حالة الصيام 1.24 ± 5.77 مليمول/ لتر لدى المجموعة المؤكدة المقاومة للأنسولين DIR ، يليه المجموعة الممكنة المقاومة للأنسولين PIR والبالغ 1.97 ± 5.63 مليمول/ لتر ، وقد أظهرت الدراسة الإحصائية وجود فرق معنوي عالٍ ($P < 0.01$) في معدل تركيز الكلوكوز في كلا المجموعتين بالمقارنة مع مجموعة السيطرة التي بلغ فيها معدل تركيز الكلوكوز 0.75 ± 3.94 مليمول/ لتر. في حين لوحظ عدم وجود فرق معنوي بين معدل تركيز الكلوكوز لدى مجموعة NIR والبالغ 4.62 ± 4.72 مليمول/ لتر بالمقارنة مع مجموعة السيطرة .

بعد ساعتين من تناول محلول الكلوكوز وجد أن معدل تركيز الكلوكوز في المصل بلغ أعلى معدل له لدى مجموعة DIR والبالغ 1.78 ± 9.8 مليمول/ لتر، تليها مجموعة PIR وبلغ فيها معدل تركيز الكلوكوز 3.06 ± 8.97 مليمول/ لتر، وقد أظهرت الدراسة الإحصائية وجود فرق معنوي عالٍ ($P < 0.01$) بين هاتين المجموعتين و بالمقارنة مع مجموعة السيطرة التي بلغ فيها معدل تركيز الكلوكوز 1.23 ± 5.94 مليمول/ لتر. كذلك لم يظهر فرق معنوي في معدل تركيز الكلوكوز لدى مجموعة NIR والبالغ 3.73 ± 6.31 مليمول/ لتر بالمقارنة مع مجموعة السيطرة .

بعد ثلاث ساعات من تناول المحلول السكري حدث هبوط في معدل تركيز الكلوكوز وبشكل عام بلغ أعلى معدل له في مجموعة PIR والبالغ 2.78 ± 7.2 مليمول/ لتر ، و مجموعة DIR والبالغ 1.7 ± 6.71 مليمول/ لتر ، وقد وجد فرق معنوي عالٍ ($P < 0.01$) بين هاتين المجموعتين و مجموعة السيطرة . في حين لا يوجد فرق معنوي في معدل تركيز الكلوكوز بين مجموعة NIR والبالغ 2.48 ± 5.02 مليمول/ لتر و بالمقارنة مع مجموعة السيطرة التي بلغ فيها معدل تركيز الكلوكوز 0.98 ± 4.93 مليمول/ لتر ، (الشكل 6) .



شكل-6 : توزيع معدل فحص تحمل السكر (OGTT) حسب مجاميع الدراسة .

يلاحظ من الشكل ارتفاع مستوى الكلوكوز لدى مجموعة DIR و PIR بالمقارنة مع مجموعة NIR و مجموعة السيطرة ؛ مما يشير الى تعرض هاتين المجموعتين الى زيادة تدريجية في مستوى الكلوكوز و بالنتيجة

ارتفاع مستوى هرمون الأنسولين. وقد أظهرت العديد من الدراسات الإحصائية إلى إن ارتفاع مستوى الأنسولين يرتبط مع الزيادة في حدوث اضطرابات الأيض وأمراض القلب الوعائية (24).

وجد إن تعرض الخلايا الدهنية لارتفاع في مستوى الكلوكوز لبضع ساعات تجعلها تظهر خصائص مقاومة شديدة للأنسولين ، وقد بينت الدراسة الجزيئية لهذه الخلايا حدوث تغيرات في بعض بروتينات المايتوكوندريا ، وزيادة جهد الغشاء ، وإنتاج لأشكال الأوكسجين الفعالة (Reactive oxygen species (ROS) (25).

تؤكد العديد من الدراسات والبحوث على الارتباط بين الاختلالات الأيضية للكلوكوز وحالة الإلتهاب ، إذ وجد أن تحمل الكلوكوز الضعيف (IGT) وحالات النوع الثاني من داء السكري أو السكري غير المعتمد على الأنسولين (NIDDM) وغير المشخصة شائعة لدى مرضى إحتشاء العضلة القلبية الإلتهابي وذكر الباحث إن هذه الاختلالات في أيض الكلوكوز لها دور في حث مقاومة الأنسولين والإلتهاب (26).

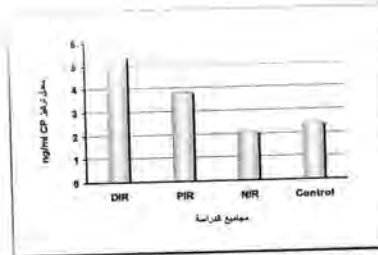
وفي دراسة وجد إن الأفراد الذين لديهم تحمل ضعيف للكلوكوز (IGT) يعانون من مضاعفات تتمثل بإنحدار في حساسية الجسم لهرمون الأنسولين ونلاحظ هذه الحالة عندما ينتقل المريض من مرحلة تحمل الكلوكوز الطبيعي (NGT) إلى مرحلة تحمل الكلوكوز الضعيف (IGT) وتصبح أكيدة عندما يفقد المريض تحمل الكلوكوز (IGF) ، عندها يصبح الشخص مقاوم للأنسولين بشكل مؤكد ، وقد تظهر عليه خصائص أخرى للمتلازمة الأيضية مثل اضطرابات الدهون (27).

كذلك وجد أن الكلوكوز يحدث تغيرات إلتهابية تتضمن إنتاج بروتين منشط Activating Protein 1 وكذلك Matrix Metalloproteinase وعوامل نسجية أخرى تعمل على تنظيم العمليات المسؤولة عن نشوء السداة الصلبة Atherosclerotic Plaque وحدث التخثر Thrombosis (28).

وظهر أيضاً أن الأفراد المفرطي الوزن يكونون أكثر عرضة على فقدان القدرة على تحمل الكلوكوز Glucose intolerance ، كذلك فكلما كان مستوى تراكيز الكلوكوز أو الأنسولين في البلازما مرتفعاً في الأفراد من غير مرضى داء السكري Non diabetic ، كلما كان هؤلاء أكثر مقاومة للأنسولين (15).

نتائج إختبار الببتيد الرابط C-Peptide (CP) لمجاميع المرضى بالمقارنة مع السيطرة:

أظهر (الشكل 7) أن أعلى معدل لتركيز الببتيد الرابط (CP) الذي بلغ 1.71 ± 5.39 نانوغرام/مليتر كان لدى مجموعة DIR. تلتها مجموعة PIR التي بلغ فيها معدل تركيز CP 2.82 ± 3.83 نانوغرام/مليتر. وقد أظهرت الدراسة الإحصائية وجود فرق معنوي عالٍ ($P < 0.001$) بين كل من هاتين المجموعتين وبالمقارنة مع مجموعة السيطرة التي بلغ فيها معدل تركيز CP 0.48 ± 2.42 نانوغرام/مليتر ، في حين لا يوجد فرق معنوي ($P > 0.05$) في معدل تركيز CP بين مجموعة NIR التي بلغ فيها معدل تركيز CP 0.81 ± 2.08 نانوغرام/مليتر ومجموعة السيطرة.



شكل-7: توزيع معدل تركيز C-peptide حسب مجاميع الدراسة.

تستخدم مستويات CP في الدم بوصفه مؤشراً على إنتاج الأنسولين ، إذ إن ارتفاع مستوى CP يعبر عن حالة فرط الأنسولين ويعد مؤشراً على فعالية خلايا البنكرياس ويستخدم أيضاً كوسيلة إضافية لتقييم تحمل الكلوكوز (29). ولهذه الأسباب جميعاً أختير إختبار CP فضلاً عن إختبارات أخرى لأجل التعبير عن مقاومة الأنسولين وفعالية خلايا بيتا وفرط الأنسولين ، وهي من خصائص مقاومة الأنسولين في الجسم. فقد وجد إن الأفراد الذين لديهم مقاومة للأنسولين يعانون من ارتفاع في مستوى CP مشيراً بذلك إلى زيادة إفراز الأنسولين التي تؤدي إلى إستجابة الجسم للتعويض عن خضوع الجسم لمقاومة الأنسولين. وقد لاحظ الباحث أنه من بين 146 شخصاً من غير المصابين بداء السكري ، كان 15 منهم قد أصيبوا بالنوع الثاني من داء السكري بعد 30 شهراً. وتميز هؤلاء المرضى بكونهم الأكبر سناً في المجموعة وكان لديهم ارتفاع في مستوى الكلوكوز في الساعة الثانية من إختبار OGTT (75 غرام) ؛ أي أن لديهم تحمل ضعيف للكلوكوز (IGT) وارتفاع في مستوى CP وزيادة نسبة الشحوم

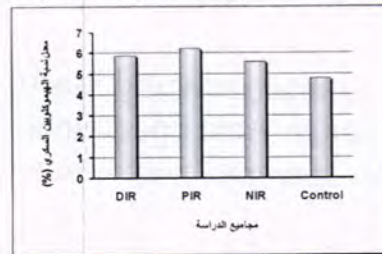
في منطقة البطن. ولاحظ الباحث أيضاً أن مستوى CP يستمر بالارتفاع حتى بعد تعديل مستوى الكلوكوز في البلازما إلى المستوى الطبيعي (30).

وفي دراسة أخرى لوحظ إن تركيز الأنسولين و CP يزداد مع الارتفاع التدريجي في مستوى الكلوكوز في الدم وأن نسبة المتغيرات الثلاث وهي: (الأنسولين ، و CP ، و الكلوكوز) كانت أكثر لدى النساء البدينات منها لدى النساء غير البدينات. كما وأشار نفس البحث إلى أن السمنة ترتبط مع مقاومة الأنسولين وإن الأخيرة ترتبط ارتباطاً إيجابياً مع معدل إفراز الأنسولين ، بمعنى آخر كلما زاد إفراز الأنسولين كلما زادت فرصة حدوث مقاومة الأنسولين (31).

على وفق إختبارات خاصة بتحمل الكلوكوز وفعالية وظيفة خلايا بيتا البنكرياسية (CP, OGTT, أنسولين) أجريت على 420 مريضاً تايلندياً ، صنف هؤلاء المرضى إلى أربع مجاميع: الأولى: مجموعة (NGT) من الذين لديهم تحمل طبيعي للكلوكوز ، والثانية: مجموعة (IFG) من الذين لديهم ارتفاع في مستوى الكلوكوز في حالة الصيام ، الثالثة: مجموعة (IGT) من الذين لديهم تحمل للكلوكوز ضعيف والرابعة: مجموعة مرضى NIDDM . وقد لوحظ إن أعلى نسبة للبدانة كانت ضمن المجموعة الأخيرة . أما مستوى الأنسولين و CP فكانت تزداد مع تقدم المرض ؛ أي أن مستواه كان أكثر لدى مجموعة NIDDM وأعلى من مستواه لدى مجموعة IFG ؛ وهذا بدوره أعلى من مستواه لدى IGT. كذلك وجد أن مقاومة الأنسولين تزداد مع تقدم المرض (32).

نتائج إختبار الهيموغلوبين السكري (Glycosylated hemoglobin (HbA1c) لمجاميع المرضى وبالمقارنة مع السيطرة:

بلغت أعلى نسبة للهيموغلوبين السكري $1.62 \pm 6.21\%$ لدى مجموعة PIR ، وقد أظهرت الدراسة الإحصائية وجود فرق عالي المعنوية ($P < 0.01$) في نسبة الهيموغلوبين السكري لدى هذه المجموعة و بالمقارنة مع مجموعة السيطرة التي بلغت فيها نسبة الهيموغلوبين السكري $0.73 \pm 4.76\%$ ، تلتها مجموعة DIR و NIR ، وقد بلغت فيها النسبة $0.84 \pm 5.86\%$ و $2.03 \pm 5.58\%$ على التوالي . وأظهرت الدراسة الإحصائية وجود فرق معنوي ($P < 0.05$) عند المقارنة بين هاتين المجموعتين ومجموعة السيطرة ، (الشكل 8) .



شكل-8: توزيع معدل نسبة الهيموغلوبين السكري HbA1c حسب مجاميع الدراسة .

يستخدم قياس نسبة الهيموغلوبين السكري وسيلة لتحديد مدى فعالية السيطرة على مستويات السكر في الجسم ، إذ يعد مقياساً لفرط السكر المزمن Chronic hyperglycemia ، وهو دليل عالي الحساسية عن وجود إعاقة في أيض الكلوكوز (33).

يلاحظ من الشكل ارتفاع نسبة الهيموغلوبين السكري HbA1c لدى المرضى الذين لديهم مقاومة للأنسولين ممكنة ، وقد أظهرت دراسة إنه كلما ازداد مستوى HbA1c كلما زادت فرصة تعرض الأفراد لخطر الإصابة بإضطرابات أيضية قد تؤدي إلى الإصابة بالنوع الثاني من داء السكري ، وقد قسمت هذه الدراسة الأفراد من غير المصابين بداء السكري على ثلاث مجاميع اعتماداً على نسبة HbA1c التي تراوحت ما بين (3.3-6.4) % . وشملت المجموعة الأولى الأفراد الذين تراوحت نسبة HbA1c لديهم بين (3.3-4.8) % ، والثانية بين (4.8-5.6) % (4.9) ، والثالثة بين (5.7-6.4) % . حيث لوحظ أن أفراد الفئة الثالثة يعانون من زيادة في وزن الجسم ، وارتفاع مستوى الكلوكوز ، و CP ، والأنسولين ، وكانت حساسية الجسم للأنسولين Insulin sensitivity أقل لدى أفراد هذه المجموعة بالمقارنة مع المجموعتين الأخريين كما كانت مقاومة الأنسولين أعلى لديهم أيضاً (34).

المصادر

1. Silva, J.E. The thermogenic effect of thyroid hormone and its clinical implications. Ann. Intern. Med.; 139: 205-213, (2003).
2. Oppenheimer, J.H.; Schwartz, H.L.; Lane, J.T. & Thompson, M.P. Functional relationship of thyroid hormone-induced lipogenesis, lipolysis, & thermogenesis in the rat. J. Clin. Invest. 87: 125-132. (1991).

3. Wu, P. Thyroid disease and diabetes. Clin. Diab. 18: 23-25. (2000).
4. Cettour-Rose, P. Theander-Carrillo, C. Asensio, C. Klein, M. Visser, T. J. Burger, A. G. Meier, C. A. & Rohner-Jeanrenaud, F. Hypothyroidism in rats decreases peripheral glucose utilization, a defect partially corrected by central leptin infusion. Diabetologia; 48: 624-633 (2005).
5. Pittas, A. G.; Joseph, N. A. & Greenberg, A. S. Adipocytokines and Insulin resistance. J. Clin. Endocrinol. Metab.; 89: 447-452. (2004).
6. Dimitriadis, G. D.; Leighton, B.; Parry-Billings, M.; West, D. and Newsholme, E. A. Effects of hypothyroidism on the sensitivity of glycolysis and glycogen synthesis to insulin in the soleus muscle of the rat. Biochem. J.; 257: 369-373. (1989).
7. Andreani, D.; Menzinger, G.; Falluca, F.; Aliberti, G.; Tamburrano, G. and Cassano, C. Insulin levels in thyrotoxicosis and primary myxedema: response to intravenous glucose and glucagon. Diabetologia; 6: 1-7 (1970).
8. Martin, B. C.; Warran, J. H.; Rosner, B.; Rich, J. S.; Soeldner, J. S. & Krilewski, A. S. Familial clustering of insulin sensitivity. Diabetes; 41: 850-554 (1992).
9. Ten, S. & McLaren, N. Insulin resistance syndrome in children. J. Clin. Endocrinol. Metab. 89: 2526-2539. (2004).
10. WHO technical report series (646) (*Diabetes mellitus*): Report of a WHO expert committee. (1980).
11. Wiersinga, W. M. Subclinical hypothyroidism and Hyperthyroidism. I. prevalence and clinical relevance. Neth. J. Med.; 46: 197-204. (1995).
12. Yamada, T. Naka, M. Komiya, L. Ichikawa, K. Aizawa, T. Hashizume, K. Takasu, N. & Watanabe, T. Age-related alteration of pituitary-thyroid function in normal female subjects and in female patients with simple goiter. Acta Endocrinol. 107: 346-351. (1984).
13. Baha, M. Estrogen replacement therapy may exacerbate hypothyroidism. N. Engl. J. Med. ; 344: 1743-1749. (2001)
14. Petersen K. F. Dufour, S. Befroy D. Garcia, R. & Shulman, G. I. Impaired mitochondrial activity in the insulin-resistant offspring of patients with type 2 diabetes N. Engl. J. Med. 350 : 664-671 (2004).
15. Reaven, G. M.; Chen, Y. D. Hollenbeck, C. B. Sheu, W. H. Ostrega, D. & Polonsky, K. S. Plasma insulin, C-peptide & proinsulin concentrations in obese and nonobese individuals with varying degrees of glucose tolerance. J. Clin. Endocrinol. Metab. 76: 44-48 (1993).
16. McLaughlin, T. Abbasi, F. Cheal, K. Chu, J. Lamendola, C. & Reaven, G. Use of metabolic markers to identify overweight individuals who are insulin resistant, Ann. Intern. Med.; 139: 802-809 (2003).
17. Pittas, A. G.; Joseph, N. A. and Greenberg, A. S. Adipocytokines and Insulin resistance. J. Clin. Endocrinol. Metab. ; 89: 447-452. (2004).
18. Knudsen, N.; Lauberg, P. Rasmussen, L. B.; Bulow, I. Perrild, H.; Ovesen, L. and Jorgensen, T. Small differences in thyroid function may be important for body mass index and the occurrence of obesity in the population. J. Clin. Endocrinol. Metab.; 10: 2004-2225. (2005).
19. Al-Wachi, S. N. Physiology. Dar al-Fekir, Amman, Jordan, (2002).
20. Fernandez-Real, J.; Lopez-Bermejo, A.; Castro, A.; Casamitjana, R. & Ricart, W. Thyroid function is intrinsically linked to insulin sensitivity and endothelium-Dependent vasodilation in healthy euthyroid subjects. J. Clin. Endocrinol. Metab. 91: 3337-3343 (2006).

21. Shah, J.H.; Motto, G.S.; Papagianes, E. and Williams, G.A. Insulin Metabolism in hypothyroidism. *Diabetes*;24:922-925(Abs)(1975).
22. Michalaki, M.A.; Vagenakis, A.G.; Leonardou, A.S.; Argentou, M.N.; Habeos, I.G.; Makri, M.G.; Psyrogiannis, A.L.; Kalfarentzos, F.E. and Kgriazopoulou, V.E. Thyroid function in humans with morbid obesity. *Thyroid* .16: 73-78(2006).
23. Mentuccia, D.; Proietti-Ponunzi, L.; Tanner, K.; Bacci, V.; Pollin, T.L.; Poehlmen, E.T.; Shuldiner, A.R. and Celi, F.S. Association between a novel variant of the human's type 2 deiodinase gene Thr92Ala and insulin resistance. *Diabetes*. 51: 880-883. (2002).
24. Haffner, S.M. and Mietten, H. Insulin resistance implications for type II *Diabetes mellitus* and coronary heart disease *Am.J.Med.* 103: 152-162(1997).
25. Lin, Y.; Berg, A.H.; Iyengar, P.; Lam, K.T.; Gracca, A.; Combs, T.P.; Rajala, M.W.; Du, X.; Rollman, B.; Li, W.; Hawkins, M.; Barzilai, W.; Rhodes, C.J.; Fantus, G.; Brownlee, M. & Scherer, P.E. The hyperglycemia induced inflammatory response in adipocytes: The role of reactive oxygen species. *J. Biol. Chem.*;280:4617-4626 (2005).
26. Choi, K.M.; Lee, K.W.; Kim, S.G.; Kim, N.H.; Park, G.G.; Seo, H.S.; Oh, D.J.; Choi, D.S. and Baik, S.H. Inflammation, Insulin resistance, and glucose intolerant without a previous diagnosis of *Diabetes mellitus*. *J. Clin. Endocrinol. Metab.* 90: 175-180(2005).
27. Tripathy, D.; Carlsson, M.; Almgren, P.; Isomaa, B.; Taskinen, M.; Tuomi, T. & Groop, L. Insulin secretion & insulin sensitivity in relation to glucose tolerance. *Diabetes*;49:975-980(2000).
28. Aljada, A.; Ghanim, H.; Mohanty, P.; Syed, T.; Bandyopadhyay, A. & Dandona, P. Glucose intake induces an increase in activator protein 1 and early growth response 1 binding activities in the expression of tissue factor & matrix metalloproteinase in mononuclear cells & in plasma tissue factor & matrix metalloproteinase concentration. *Am. J. Clin. Nutr.* 80: 51-57 (2004).
29. Banser, A. & Garcia-Webb, P. C-peptide measurement: Methods & clinical utility. (CRC) *Crit. Rev. Clin. Lab. Sci.*;19:297-352(1984).
30. Bergstrom, R.W.; Newell-Morris, L.L.; Leonetti, D.L.; Shuman, W.P.; Wahl, P.W. & Fujimoto, W.Y. Association of elevated fasting C-peptide level and increased intra-abdominal fat distribution with development of NIDDM in Japanese-American men. *Diabetes*;39: 104-111(1990).
31. Jones, C.O.; Abbasi, F.; Carantoni, M.; Polonsky, K.S. and Reaven, G.M. Roles of insulin resistance and obesity in regulation of plasma insulin concentrations. *Am. J. Physiol. Endocrinol. Metab.* 278: 501-508(2000).
32. Chailurkit, L.; Jongiaroenprasert, W.; Chanprasertyotin, S. & Ongphiphadhanakul, B. Insulin and C-peptide levels, pancreatic beta cell function, and insulin resistance across glucose tolerance status in Thais. *J. Clin. Lab. Anal.*; 21: 85-90(2007).
33. Park, S.; Barrett-Connor, E.; Wingard, D.L.; Shan, J. & Edelstein, S. GHb is a better predictor of cardiovascular disease than fasting or post challenge plasma glucose in women without diabetes. The rancho Bernardo study. *Diabetes Care*. 19:450-456(1996).
34. Osei, K.; Rhinesmith, S.; Gaillard, T. & Schuster, D. Glycosylated hemoglobin A1c as surrogate for metabolic syndrome in nondiabetic, First-Degree relative of African-American patients with type 2 diabetes? *J. Clin. Endocrinol. Metab.* 88: 4596-4601(2003).

تأثير مستخلصي عرق السوس وثمار الكاكي في تثبيط الانحرافات الكروموسومية المستحثة بمادة كبريتيت الصوديوم في خلايا الفأر الأبيض

أ. رحيمة فاضل مرهون² وعبد الأمير ناصر غلوب³ ومؤيد صبري شوكت¹

¹ جامعة واسط / كلية العلوم / قسم علوم الحياة

² الجامعة المستنصرية / كلية العلوم / قسم علوم الحياة

³ جامعة بغداد / كلية العلوم / قسم التقنية الاحيائية

ABSTRACT

Active compounds in Glycyrrhiza glabra and Diospyros kaki fruit were detected. chemical detection revealed that extracts of G.glabra contains glycosides, tannins, alkaloids, saponine, terpins, sterols, flavonoid, and coumarins. While extract of D.kaki contains tannins, saponins, phenols, resins, terpins, sterols and flavonoids.

White mice infected with chromosomal aberration induced by sodium sulphate at concentration of 100 mg/kg, injected with extracts at concentrations of 2, 5, 8 mg/kg through intreprenonally.

Results showed that all concentrations of the extracts have inhibitory effects on chromosomal aberrations. Inhibition increased at 8 mg/kg which reached 1.6% for chromosome Breaks and 2.0% for chromatid breaks in sexual cells, and reached 2.3% for chromosome Breaks and 4.1% for chromatid breaks in bone marrow cells for G.glabra extracts. percentages of inhibition using D.kaki fruit extract were 1.0% for chromosome Breaks and 1.8% for chromatid breaks in sexual cells while in bone marrow cells were 2.0% for chromosome Breaks and 3.3% for chromatid breaks. The differences were significant when the results compared with positive control. interaction between the two extracts showed inhibitory effects which increased at concentration 8 mg/kg.

الخلاصة

حددت المركبات الفعالة في مستخلصي عرق السوس Glycyrrhiza glabra وثمار الكاكي Diospyros kaki اذ أظهر الكشف الكيميائي عن احتواء مستخلص عرق السوس على الكلايكوسيدات والتانينات والقلويدات والصابونين والتربين والستيرويدات والفلافونيدات والكومارين. في حين احتوى مستخلص ثمار الكاكي على التانينات والصابونين والفينولات والراتنجات والتربين والستيرويدات والفلافونيدات.

جرعت الفئران البيضاء والمصابة بالتشوهات الكروموسومية المستحثة بفعل كبريتيت الصوديوم بتركيز 100 ملغم/كغم بالتركيز 2، 5، 8 ملغم/كغم للمستخلصين عن طريق غشاء الخلب وقد أظهرت النتائج امتلاك جميع تراكيز مستخلصي عرق السوس وثمار الكاكي (2، 5، 8 ملغم/كغم) الفعالية لتثبيط التشوهات الكروموسومية والتي ازدادت فعاليتها التثبيطية عند التركيز 8 ملغم/كغم والذي بلغ 1.6% للكسر الكروموسومي و 2.0% للكسر الكروماتيدي في الخلايا الجنسية و 2.3% للكسر الكروموسومي و 4.1% للكسر الكروماتيدي في خلايا نقي العظم لمستخلص عرق السوس و 1.0% للكسر الكروموسومي و 1.8% للكسر الكروماتيدي في الخلايا الجنسية و 2.0% للكسر الكروموسومي و 3.3% للكسر الكروماتيدي لخلايا نقي العظم لمستخلص ثمار الكاكي. وكانت الفوارق معنوية مقارنة بالسيطرة الموجبة. كما أظهرت النتائج فعالية تثبيطية للتركيز ذاتها عند دراسة التأثير المتداخل للمستخلصين وبلغت أقصاها عند التركيز 8 ملغم/كغم.

المقدمة

يعد علم النباتات الطبية من العلوم المزدهرة قديماً بسبب فعالية النباتات في علاج كثير من الامراض نتيجة احتواء تلك النباتات على مركبات فعالة استخدمت كعلاجات لكثير من الامراض. فضلاً عن قلة الاضرار الجانبية لهذه النباتات وقد استخدمت المركبات الطبيعية المشتقة من النبات كعلاجات بديلة لعلاجات طبية اخرى لكثير من الامراض كان ذا فعالية عالية في علاج تلك الامراض وقد اظهرت النتائج الايجابية فعالية هذه العلاجات لأحتواءها العديد من العوامل المضادة للأكسدة ومضادات للالتهابات ومضادات للسرطان ومضادات للأجسام المايكروبية (4,5). استخدم عرق السوس منذ القدم ولأول مرة من قبل الرومان والاعريق اذ استخدموه بصورة واسعة في الكثير من العلاجات المرضية عن صحة هذه الروايات وتمكن العالم الشهير هيبوقراط (377 - 466) ق م من استخدام هذا النبات Glycyrrhiza glabra في علاج بعض الامراض لامكانية استخدام نبات عرق السوس من الناحيتين الطبية والعلاجية (6).

نبات عرق السوس :

تأثير مستخلصي عرق السوس وثمار الكاكي في تثبيط الانحرافات الكروموسومية المستحثة بمادة كبريتيت الصوديوم في خلايا الفار الأبيض
رحيم وعبد الأمير ومزيد

صنف هذا النبات لأول مرة من قبل الاغريق اذ ذكروا انه ينتمي الى جنس *Glycyrrhiza* والذي يقسم الى النواعيات الاتية(7) :

1- *Glycyrrhiza glabra typi c*

2- *Glycyrrhiza glabra glandulife*

3- *Glycyrrhiza glabra Uiolece*

4- *Glycyrrhiza pallida*

يحتوي عرق السوس على العديد من المركبات الفعالة منها حامض الكليسيرايديك (*Glycyrrhiza*) ($C_{24}H_{42}O_{16}$) كما يحتوي عرق السوس على مركبات اخرى وهي الصابونيين ثلاثي التربينويد فضلا عن الازوفلافونز والستيرويدات ثلاثية التربين (*Triterpene sterols*) والكومورينيزات وزيتوت طيارة(8). لمستخلص عرق السوس اهمية طبية لكونه ذو فعالية استروجينية ويستخدم في علاج الكثير من الامراض الاخرى مثل مرض السعال وايقاف اوجاع الصدر والخراج(9) وانه ذو تأثير مثبط للاصابة بفايروس الايدز (HIV) عند الاشخاص المصابين به. كما ان له القابلية على تثبيط الاورام الخبيثة بفعل هذه المركبات القلويدية التي تحتويها *Vincristin* و *Gzoch & Mordski Vinblastine* (10) (1983) وان المركب الفعال في عرق السوس وهو حامض الكليسيرايديك والكافانين لهما تأثيرا مثبطا (*inhibitor effect*) لفعالية محفز سرطانات الجلد في الفئران اذ يعمل حامض الكليسيرايديك على تثبيط مادة *Tetradecanoyl phorbol 13 Acetate (TPA)* 0 - 12 الحاشة لتكوين سرطان الجلد في الفئران وتكوين اورام اخرى والتي تبدا عملها بتأثيرها على مادة 7,12-(DMBA) *Dimethylbenz{a}anthranen* (11)

ثمار الكاكي :

يعد نبات الكاكي من النباتات المهمة المستخدمة في النطاق التجاري والطبي اذ استخدمت ثماره في علاج كثير من الامراض. ومن اهم المركبات الموجودة في ثمرة نبات الكاكي هما مركبي (*Isodiospyrin*) (*Diospyrin*) اذ كلا المركبين يمتاز بأنهما ذو فعالية علاجية طبية لعلاج كثير من الامراض (12) كما تحتوي ثمار الكاكي على مركبات اخرى وهي التربينويد (*Terpinoid*)، الستيرويدات (*Steroids*) ، الفيتامينات A,B,C ، السكريات والنشا (13) اما الاهمية الطبية فتتمثل بكونه ذو فعالية عالية في تثبيط نمو البكتريا السالبة والموجبة لملون كرام لأحتواءه على مركب *Plumbagin* (14) والقابلية على تثبيط الاصابة بفايروس الايدز عند الاشخاص المصابين بالايديز وله فعالية عالية في منع حدوث او علاج السرطانات اللمفاوية والجلدية بفعل المركبات الفعالة مركب *Betulin* اذ يمتاز بكونه ذو فعالية تثبيطية عالية لمرض *Walker carcinoma* وان للمركب الفعال *Naphthoquinone* و *Isodiospyrin* المتواجد كثيرا في ثمار الكاكي يمتاز بأنه ذو فعالية عالية ضد خط الخلايا الورمية *Lymphomacyte P338* وسرطان الجلد اذ يعد هذا المركب ذو الفة تثبيطية لأنزيم *Topo 1* عند الاشخاص المصابين بالأورام فأنها تثبط نمو هذه السرطانات من خلال التداخل مع البروتينات المسؤولة عن عملية الانقسام الخلوي (15)

لذا اقترحت هذه الدراسة المعتمدة على التحليلات الوراثية الخلوية (*Cytogenetic analysis*) في تقييم العوامل الكيميائية المختلفة من ضمنها (كبريتيت الصوديوم) في احداث الاضرار الوراثية لكونها من العوامل التي تشكل خطورة على صحة الانسان بسبب قدرتها على استحداث السرطان والتشوهات الخلوية ومتابعة تأثير مستخلص عرق السوس وثمار الكاكي في تثبيط التشوهات الكروموسومية المتمثلة بالكسور الكروماتيدية والكسور الكروموسومية.

تأثير التلوث بالكبريت :

يعد الكبريت من العناصر الواسعة الانتشار في بحوالي 140 غم وهذا فضلا عن وجوده في كل خلية من خلايا الجسم علاوة على وجوده في الاغذية الطبيعية.(32)

يبلغ تركيز الكبريت في الاماكن غير الملوثة لكن من الصعب الاحتفاظ بهذا التركيز في الاماكن الصناعية , اذ يزداد عن هذا التركيز في الاماكن عالية التلوث وتصبح هذه الاماكن من الاماكن الملوثة(33)

اما تأثيرات الكبريت على الاحياء فقد لوحظ ان النباتات تكون حساسة بصورة عالية اكثر من الحيوانات ويمثل هذا التحسس بالتأثير المباشر لأكاسيد الكبريت في اوراق النباتات مسبب حدوث تبقع لأوراق النباتات فضلا عن انخفاض الغلة الزراعية بسبب الامطار الحامضية الناتجة من ذوبان اكاسيد الكبريت في بخار الماء(16).

اما تأثيره في الحيوانات فقد لوحظ ان التعرض المزمن لأكاسيد الكبريت يسبب تثخن الطبقة المخاطية للقصبات الهوائية وتضخم الغدد المخاطية والتحسس العالي للكبريت من قبل الخلايا الجلدية كما انه يؤدي الى حدوث انحرافات كروموسومية في خلايا نخاع العظم والخلايا المولدة للحيامن تمثلت بكسور كروموسومية وكروماتيدية وانخفاض معدل الانقسام فضلا عن حدوث تشوهات في رؤوس الحيامن (29) فضلا عن حدوث تغيرات فسلجية منها تغير غازات الدم وزيادة سرعة الجريان (17) كما لوحظ انخفاض ملحوظا في كريات الدم الحمر في الاسبوع الاول والثاني بسبب التأثير المباشر على مادة الهيموغلوبين وارتفاع عدد كريات الدم الحمر في الاسبوع الستة (18)

تحت الكثير من العوامل الملوثة الداخلية والخارجية على تكوين انواع مختلفة من الاضرار الوراثية مما يؤدي الى حدوث خلل وراثي فضلا عن ان الاخلال في وظيفة المادة النووية يسبب امراض وراثية كثيرة في الانسان والنبات والحيوان . اذ تتعرض الكائنات الحية لكثير من العوامل الملوثة المنتشرة في الطبيعة مثل المواد الكيماوية الصناعية والسموم المنبعثة من غازات المصانع اذ تكون هذه الملوثات ذات تأثير بيولوجي عالي يؤدي الى الاضرار بصحة الكائنات الحية المختلفة (1)

ونظرا لأهمية هذه الملوثات في التداخل مع كثير من اشكال الحياة فقد تناولت العديد من الدراسات اظهار آثار هذه الملوثات على صحة الكائنات الحية وخصوصا الانسان . استخدمت المؤشرات المرضية وخصوصا المؤشرات الوراثية الخلوية في السنوات الاخيرة منها (التشوهات الكروموسومية , التبادل الكروماتيدي الشقيق , دورة الخلية ومعامل الانقسام) لكون هذه المؤشرات تعكس المخاطر المستقبلية فضلا عن استخدام كائنات اخرى لاختبار قدرة هذه الملوثات في التأثير في الكائنات الحية (2)

يعد التلوث بالكبريت من اهم الموضوعات التي تناولتها الدراسات لايضاح مدى تأثيره على صحة الانسان كون العنصر يدخل في تركيب بعض المركبات في جسم الانسان والواسع الانتشار في الطبيعة . فضلا عن دخوله في كثير من الصناعات وانبعاثه من مخلفات المصانع علاوة على الامطار الحامضية والتي تعد كلها عوامل تسبب زيادة التأثيرات الوراثية خصوصا على الانسان . وظهرت امراض وراثية نتيجة هذه الملوثات وبهدف علاج هذه الامراض فشلت عدد من العلاجات في درء الامراض الوراثية الناجمة عن هذه الملوثات(علاوة على ان بعض هذه العلاجات تعد احد العوامل المسببة للأمراض الوراثية) لذلك التجأ العلم الحديث الى استخدام المركبات الطبيعية المفردة من الكائنات الحية وبالأخص النباتات الى استخدامها كعلاج للأمراض الوراثية وخصوصا الأمراض السرطانية (3)

المواد وطرائق العمل

استخدمت ذكور فئران بيضاء بعمر 8-10 أسابيع تم الحصول عليها من البيت الحيواني لمركز بحوث السرطان وامراض الدم التابع الى وزارة الصحة , تم ايواءها في البيت الحيواني -مركز بحوث التقنيات الاحيائية بجامعة النهرين لتحديد التشوهات الكروموسومية داخل الجسم الحي بطرق مختبرية مثلى -24م واضاءة وظلام متعاقبين 12 : 12 اذ وزعت هذه الحيوانات الى 5 مجاميع وأطعمت بالعليقة المحلية المتكونة من بروتين خام 22% ودهون بنسبة 4.5% وكاربوهيدرات بنسبة 51.5% ومركبات أخرى ضمن عليقة هذه الحيوانات وشربت ماء الحنفية عن طريق تقنية مخصصة للشرب في الاقفاص.

طرائق العمل :

1- تحضير المستخلصات النباتية :

تم الحصول على عرق السوس من حدائق جامعة بغداد (الجادرية) , اما ثمار الكاكي فقد تم الحصول عليها من الاسواق التجارية كثمار جاهزة وحضرت مستخلصات هذه النباتات بعد تجفيف العينات وطحنها , وزن

تأثير مستخلصي عرق السوس وثمار الكاكي في تثبيط الانحرافات الكروموسومية المستحثة بمادة كبريتيت الصوديوم في خلايا الفار الأبيض
رحيم و عبد الأمير و موبد

50 غم من مسحوق النبات ثم مزجت بمذيب الميثانول بنسبة 1:5 (5 غم من مسحوق النبات الى 5 مللتر من المذيب) ثم أستخلصت بجهاز السوكسلت. ركزت المستخلصات بواسطة جهاز التبخير ثم وضعت المستخلصات في قناني محكمة الغلق وحفظت بدرجة حرارة -20م لحين الأستعمال(19)

الكشف عن الكلايكوسيدات:

استخدم كاشف بندكت للكشف عن الكلايكوسيدات , دل ظهور راسب احمر على ايجابية الفحص(20).

الكشف عن المواد الفينولية :

استخدم محلول كلوريد الحديدك 1% للكشف عن المواد الفينولية واستدل على النتيجة بتكون لون اخضر او ازرق عند مزجه مع المحاليل الحاوية على المركبات الفينولية(21).

الكشف عن القلويدات :

استخدم كاشف ماركيز Marquis reagent للتأكد من احتواء المستخلص على القلويدات اذ استدل على النتيجة من خلال تكون لون رصاصي محبب(21).

الكشف عن التربين Steroid والستيرويد Terpene :

كشف عن التربينات اعتمادا اعتمادا على الطريقة الموضوعة في (22) اذ يدل تكون لون بني فاتح دلالة على ايجابية فحص التربين اما تكون لون ازرق داكن بعد ترك المزيج فإنه دلالة على وجود الستيرويد.

الكشف عن الراتنجات Resins:

اتبعت طريقة (22) ويستدل على ايجابية الفحص للراتنجات بظهور عكورة في المحلول الحاوي على المستخلص النباتي المعامل بالكحول الايثيلي والماء المحمض.

الكشف عن الصابونين Saponin:

كشف عن الصابونين استنادا الى الطريقة المتبعة في (22) اذ يعد تكون رغوة كثيفة تبقى لفترة طويلة بعد رج الانبوبة بشدة دلالة على ايجابية الكشف .

الكشف عن التانينات Tannins :

يستدل عن وجود التانينات في المستخلص بظهور راسب ابيض هلامي القوام , كما يعد ظهور لون اخضر مزرق بعد المعاملة بكلوريد الحديدك 1% على ايجابية الفحص (22).

الكشف عن الكومارينات Coumarins :

كشف عن الكومارينات بتعريض ورقة الترشيح المغمورة في المستخلص الى الأشعة فوق البنفسجية ودل ظهور لون أصفر مخضر بالورقة على ايجابية الفحص (23).

الكشف عن الفلافونات Flavonoids :

عد ظهور لون اصفر في المزيج الحاوي على المستخلص النباتي ومحلول KOH نتيجة موجبة لوجود الفلافونات في المستخلص النباتي (23).

تركيز مادة كبريتيت الصوديوم المطهرة المستخدمة بالدراسة :

حضر محلول من كبريتيت الصوديوم بتركيز 100 ملغم / كغم , ليتم استخدام 0.1 مل لتجريع الفئران في غشاء الخلب لمدة 3 ايام.

دراسة التأثيرات السمية الوراثية الخلوية لخلايا نقي العظم والخلايا المولدة للحيامن في الفئران المعاملة بكبريتيت الصوديوم بوجود مستخلص عرق السوس:

الحيوانات المختبرة قسمت الى خمسة مجاميع تمثلت ب:

1- المجموعة CI حقنت بالماء المقطر وعدت كسيطرة سالبة

2 - المجموعة CII حقنت ب(0.1) من محلول كبريتيت الصوديوم المحضر بتركيز (100) ملغم/كغم بواقع جرعة واحدة يوميا ولمدة 4 ايام وعدت كسيطرة موجبة

3- اما المجموعة CIII فقد قُسمت الى ثلاثة مجاميع (A,B,C) كل مجموعة مؤلفة من (5) فئران حقنت هذه المجاميع الثلاثة (A,B,C) بالتركيز ذاته من كبريتيت الصوديوم للوصول الى تركيز 100 ملغم/كغم ولمدة اربعة ايام. ثم بعد ذلك حقنت كل مجموعة من هذه الثلاثة مجاميع (A,B,C) بـ 0.1 مللتر من مستخلص عرق السوس للحصول على تركيز نهائي 8,5,2 مايكروغرام /كغم على التوالي لمدة (7) ايام وبواقع جرعة واحدة في اليوم.

كما استخدمت خمسة مجاميع اخرى من الفئران لتجربتها بالظروف ذاتها باستخدام مستخلص ثمار الكاكي للحصول على تركيز نهائي 8,5,2 مايكروغرام/كغم من وزن الفئران ولمدة (7) ايام وبواقع جرعة واحدة/يوم. ثم شرحت الفئران بعد انتهاء مدة التجريب واستخلص منها نقي العظم والخلايا المولدة للحيامن لدراسة التشوهات الكروموسومية.

تحضير كروموسومات خلايا نقي العظم:

بعد انتهاء مدة تجريب الحيوانات بالمستخلصات النباتية استخلصت كروموسومات خلايا نقي العظم لدراسة الانحرافات الكروموسومية فيها اعتمادا على الطريقة الموصوفة في (24) وكالاتي:

حقن كل فأر بـ (0.25) مللتر من الكولجسين المحضر بتركيز (10) ملغم/كغم من وزن الجسم للحصول على تركيز في غشاء الخلب قبل 2 ساعة من التشريح واستخلصت الكروموسومات بالخطوات الاتية:

1- ثبت الحيوان على جهته الظهرية وقص الجلد فوق منطقة الفخذ ثم ازيلت العضلات حول العظم وقطع ارتباطه بمفصلي الحوضين والركبة.

2- بعد ان تم قص عظم الفخذ وغسله قصت نهايته وحقن بـ (5) مل من داريء الفوسفات الملحي الدافيء (37)م

3- نبذت الانابيب الحاوية على خلايا نخاع العظم مركزيا بسرعة (1500) دورة/دقيقة ولمدة (10) دقائق ثم تم التخلص من الراشح ومزج الراسب جيدا وأضيف (5) مللتر من محلول KCL الدافيء

4- بعد انتهاء فترة الحضان تم نبذ الانابيب مركزيا لمدة (10) دقائق بسرعة (1500) دورة/دقيقة، أهمل الراشح ورج الراسب جيدا (عالق الخلايا) بأضافة قطرات من المحلول المثبت البارد المحضر ميثانول:حامض الخليك (1:3) على جدران الانبوبة مع الرج المستمر حتى اكمل الحجم الى (5) مللتر

5- وضعت الانابيب الحاوية على الخلايا بدرجة حرارة (4)م لمدة ساعة للتثبيت، ونبذت الانابيب مركزيا بسرعة (1500) دورة/دقيقة ولمدة (10) دقائق، ثم اعيدت عملية الغسل مرتين بالمحلول المثبت ذاته وعلقت الخلايا بـ (2) مللتر من المحلول المثبت.

6- مزج العالق جيدا باستخدام ماصة باستور وقطر منه (4-5) قطرات على شرائح زجاجية رطبة وباردة، تركت لتجف ثم صبغت بصبغة كمزا المخففة بداريء سورنسن (4:1) ولمدة دقيقتان ثم غسلت بالداريء نفسه وفحصت تحت المجهر الضوئي بقوة تكبير 100X لغرض دراسة التشوهات الكروموسومية.

تحضير كروموسومات الخلايا الجنسية:

تم الحصول على الخلايا المولدة للحيامن من الفئران المعاملة مع المستخلص النباتي والمواد المطفرة اعتمادا على الطريقة الموصوفة في (25)، بعد فتح التجويف البطني استأصلت خصيتي كل فأر ثم أزيل الغلاف الخارجي لهما ووضعتا في طبق بتري حاوي على (5) مللتر من محلول سترات الصوديوم الثلاثية تركيزه () لمدة (20) دقيقة ثم فك نسيج كل خصيتين باستخدام ملقطين دقيقين ومقص اذ تم الحصول على محلول او عالق خلوي ووضع في انبوبة اختبار تلاها نبذ الانابيب مركزيا لمدة (10) دقائق وبسرعة (1500) دورة/دقيقة ثم ازيل الراشح ومزج الراسب جيدا مع محلول KCL (وبمولارية 0.075) وحضنت الانابيب بالظروف ذاتها المذكورة في طريقة تحضير خلايا نقي العظم.

التحليل الإحصائي Statistical Analysis

لتحليل النتائج احصائيا تم استخدام برنامج الحقيبة الإحصائية للعلوم الاجتماعية Statistical Package for Social Sciences (SPSS) بتطبيق تحليل التباين أحادي الاتجاه (ANOVA) وبأستخدام المقارنات المتعددة (Multiple Comparison) وعدت قيم P بين المعاملات المساوية او التي تقل عن 0.05 ذات معنوية احصائية.

تأثير مستخلصي عرق السوس وثمار الكاكي في تثبيط الانحرافات الكروموسومية المستحثة بمادة كبريتيت الصوديوم في خلايا الفأر الأبيض
رحيم و عبد الأمير و مويد

النتائج والمناقشة

الكشف عن المواد الفعالة في المستخلصات النباتية:

اثبت الكشف الكيميائي للمركبات الفعالة احتواء اغلب المستخلصات على أكثر من مركب تمثلت بالمركبات الآتية (جدول -1):

جدول -1: المركبات الفعالة في المستخلصات النباتية

المركب	الكاشف	دليل الكشف	نبات السوس	نبات الكاكي
الكلايكوسيدات	بندكت	راسب أحمر	+	-
التانينات	خلات الرصاص خلات الحديدك	راسب أبيض اخضر مزرق	+	+
القلويدات	كاشف ماركيز	لون رصاصي	+	-
الصابونين	الرج الشديد للمستخلص كلوريد الزئبق	رغوة كثيفة راسب أبيض	+	+
الفينولات	كلوريد الحديدك	اخضر	-	+
الراتنجات	ايتانول 95% ماء محمض	عكورة	-	+
التربين والستيرويدات	كلوروفورم +حامض	لون بني لون ازرق	+	+
الفلافونات	الخليك اللاماني ايتانول+هيدروكسيد البوتاسيوم	لون اصفر	+	+
الكومارين	ورق الترشيح مرطب بهيدروكسيد الصوديوم+اشعة فوق البنفسجية	تألق لون أصفر	+	-

تأثير كبريتيت الصوديوم في استحثاث التشوهات الكروموسومية:

تظهر النتائج المبينة في الجدول (2) حدوث التشوهات الكروموسومية لخلايا نقي العظم والخلايا الجنسية المعاملة بتركيز 100 ملغم/كغم كبريتيت الصوديوم ولكلا النوعين من الخلايا اذ بلغ حالة الكسر الكروماتيدي لخلايا نقي العظم لمجموعة السيطرة السالبة 0.375% بينما نسبة الكسر الكروماتيدي للحيوانات المعاملة بتركيز كبريتيت الصوديوم (100) ملغم/كغم 18.3% وكانت ذات فروق معنوية قياسا بمجموعة السيطرة السالبة باحتمالية ($p < 0.05$).

اما في حالة الكسر الكروموسومي فقد بلغ 0.062 في مجموعة السيطرة السالبة مقارنة بنسبة 8.3% في المجموعة المعاملة بكبريتيت الصوديوم وكانت كذلك ذات فرق معنوي عند احتمالية $p < 0.05$.

كما يظهر الجدول (2) حدوث تشوهات كروموسومية للخلايا الجنسية متمثلة بالكسر الكروموسومي والكروماتيدي في مجموعة الحيوانات المعاملة بكبريتيت الصوديوم بلغ 7.4% و 11.7% على التوالي كما ان 0.062 % في الخلايا الجنسية للسيطرة السالبة وهي ذات معنوية عند احتمالية $p < 0.05$.

ويتبين من نتائج دراسة تأثير كبريتيت الصوديوم استحثاث التشوهات الكروموسومية في خلايا نقي العظم والخلايا الجنسية وهذا قد يعود الى امكانية الكبريت على استحثاث التشوهات الكروموسومية واحداث الكسور والفجوات والتبدلات الكروموسومية، وقد اشارت الدراسة (26) الى تأثير زيادة المحتوى الكبريتي بالفحم في زيادة التشوهات الكروموسومية اذ يعتقد ان المسلك الشائع لكثير من العوامل المطفرة ربما يكون في امكانيتها على تدمير الاجسام الحالة مع تحرر الانزيمات المحللة للـ DNA التي لها القابلية على احداث الكسور الكروموسومية والكروماتيدي او ربما يرجع الى التفاعل المباشر مع اشربة الـ DNA مما يسبب حدوث التشوهات (27) في حين يؤكد البعض الآخر الى ان امكانية المواد المطفرة قد يعود الى تفاعلها المباشر مع الـ DNA اذ ان المبيدات الفوسفورية تمتلك مجاميع مؤكسدة لها القابلية على احداث الضرر في الـ DNA (28).

كما لوحظ ان غاز SO_2 القابلية على استحثاث التشوهات الكروموسومية في خلايا نخاع عظم الفئران عند تعرضها لهذا الغاز لمدة اسبوع وبواقع حال أربع ساعات يوميا اذ ظهرت تشوهات كروموسومية في نخاع

العظم تمثلت بتبدلات كروماتيدية وكسور مفردة ومضاعفة تزامنت مع التعرض الى تراكيز عالية من الغاز (29).

تأثير مستخلص عرق السوس في تثبيط التشوهات الكروموسومية المستحثة بفعل كبريتيت الصوديوم:
تبين النتائج في الجدول (2) انخفاض التشوهات الكروموسومية لخلايا نقي العظم والخلايا الجنسية الناشئة عن المعاملة بكبريتيت الصوديوم والمعاملة لاحقا بمستخلص عرق السوس اذ سجلت اعلى نسبة للكسر الكروماتيدي في السيطرة الموجبة %18.3 وبلغت نسبة الكسور الكروماتيدية (8.3 و 6.3 و 4.1) % في خلايا نقي عظم الفئران المعاملة لاحقا بمستخلص عرق السوس وتركيز (2 و 5 و 8) ملغم/كغم على التوالي وقد اظهرت التراكيز الثلاثة اختلافا معنويا عن مجموعة السيطرة الموجبة وباحتمالية $p < 0.05$ فضلا عن ان التركيز الثالث اظهر فرقا معنويا عن التركيزين الاول والثاني في حين لم تكن الفروق معنوية بين التركيزين الاول والثاني. كما انخفضت نسبة الكسر الكروموسومي لخلايا نقي العظم في الحيوانات المعاملة لاحقا بمستخلص عرق السوس بتراكيز (2 و 5 و 8) ملغم/كغم لتصل الى (3.9 و 3.1 و 2.3) % على التوالي قياسا بمجموعة السيطرة الموجبة البالغة 8.3%.

كما اظهرت الخلايا الجنسية النوعين من التشوهات الكروموسومية بفعل المعاملة بكبريتيت الصوديوم، فقد انخفضت نسبتها بزيادة تركيز مستخلص عرق السوس اذ كانت نسبة الكسر الكروماتيدي %11.7 في السيطرة الموجبة وانخفضت تلك النسب الى (4.7 و 3.8 و 2.0) % عند معاملة الحيوانات لاحقا بمستخلص عرق السوس بالتراكيز (2 و 5 و 8) ملغم/كغم على التوالي اذ اظهرت التراكيز الثلاثة فرقا معنويا قياسا بمجموعة السيطرة الموجبة عند احتمالية $p < 0.05$ في الوقت الذي اظهر التركيز الثالث فرقا معنويا عن التركيزين الاول والثاني في حين لم يلاحظ فرقا معنويا بين التركيزين الاول والثاني.

والحال ذاته في ظهور الكسر الكروموسومي للخلايا الجنسية فقد كانت في السيطرة الموجبة %7.4 وانخفض الى (3.3 و 2.4 و 1.6) % في الحيوانات المعاملة لاحقا بمستخلص عرق السوس بتراكيز (2 و 5 و 8) ملغم/كغم على التوالي اذ كانت الفروق معنوية بين التراكيز الثلاث والسيطرة الموجبة فضلا عن ان التركيز الثالث اعطى فرقا معنويا عن التركيز الاول في حين لم يلاحظ فروقا معنوية بين التركيزين الاول والثاني وكذلك بين التركيزين الثاني والثالث.

دلت نتائج الدراسة الى حدوث انخفاض في التشوهات الكروموسومية لخلايا نقي العظم والخلايا الجنسية بمعاملتها بمستخلص عرق السوس كما ان هذا الانخفاض يتناسب طرديا مع تركيز المستخلص النباتي بسبب احتوائه على مركبات فعالة عدة تمتاز بقابليتها العالية للعمل كمواد مضادة للسرطان والتشوهات الكروموسومية منها حامض الكليسيرايك ومركبت اخرى منها المستيرولات ثلاثية التربين والكلابروتين ومركبات قلويدية مثل الفنركرستين والفنيلاستين، اذ اشارت الدراسات الى ان هذين المركبين الموجودين في نبات الـ *catharanthus sp.* ونباتات اخرى مثل عرق السوس لها القابلية على تثبيط التشوهات الكروموسومية الناتجة عن المطفرات (30) اشارت دراسة تضمنت تعريض الفئران الى تراكيز وجرع مختلفة من عرق السوس الى قابلية هذه المستخلصات في تثبيط الاورام السرطانية وخصوصا سرطان الدم في تلك الحيوانات فضلا عن تثبيط الورم السرطاني الجلدي والتشوهات الكروموسومية في خلايا نقي العظم (11) ان التغذية القوية للكليسيرايك تؤدي الى تثبيط سرطان البشرة الناتج عن بعض انواع المسرطنات علاوة على ان المادة الفعالة الكليسيرايك ذات تأثير مثبط لكثير من الاورام السرطانية كما في سرطان الكبد (31) وان للمركبات الفعالة Vincristin, Vinblastin دور في تثبيط الاورام السرطانية يكون عن طريق الارتباط ببروتينات النيبات الدقيقة خلال عملية الانقسام الخلوي فضلا عن تأثيرها على عمليات تخليق الـ RNA اما تأثير مركب الكليسيرايك على الخلايا المسرطنة تتضمن ان هذا المركب الفعال يعمل على تثبيط ايض المواد المسرطنة مما يشير الى ان الكليسيرايك ذو فعالية مضادة للاورام وقد يحمي الانسان من بعض الانواع السرطانية (32).

وفيما يتعلق بنتائج تأثير كبريتيت الصوديوم على الخلايا الجنسية بوجود مستخلص عرق السوس فقد اتضح ان نسبة التشوهات الكروموسومية قد انخفضت بزيادة تركيز الجرعة كما جاء في نتائج دراسة تضمنت تعريض خلايا سليفات النطف الى تراكيز مختلفة من عرق السوس ادت الى تثبيط التشوهات الكروموسومية الناتجة من بعض انواع المطفرات في تلك الخلايا (32).

تأثير مستخلص نبات الكاكي في تثبيط التشوهات الكروموسومية المستحثة بفعل كبريتيت الصوديوم:
توضح البيانات في الجدول (3) نوعين من التشوهات الكروموسومية فقد بلغت نسبة الكسر الكروماتيدي لخلايا نقي العظم في السيطرة الموجبة 18.3%، وانخفضت تلك النسبة في خلايا الحيوانات المعاملة بمستخلص ثمار الكاكي بالتركيز (2، و5، و8) ملغم/كغم لتبلغ (6.8، 5.6 و3.3) وعلى التوالي. وقد اظهر التركيز الاول والثاني والثالث فرقا معنويا عن مجموعة السيطرة الموجبة بحتمالية $p < 0.05$ فضلا عن ان التركيز الثالث اظهر فرقا معنويا عن التركيزين الاول والثاني بينما لم يظهر التركيزين الاول والثاني اختلافا معنويا فيما بينهما. وكانت نسبة الكسر الكروموسومي لخلايا نقي العظم في السيطرة الموجبة 8.3% في حين كانت (3.3، و2.7، و2.0) في خلايا الحيوانات المعاملة لاحقا بمستخلص ثمار الكاكي (2، و5، و8) على التوالي. كما سجلت الخلايا الجنسية لحيوانات السيطرة الموجبة نوعين من التشوهات الكروموسومية، اذ بلغت نسبة الكسر الكروماتيدي 11.7% وانخفضت نسبتها بزيادة تركيز مستخلص ثمار الكاكي (2 و5 و8) ملغم/كغم لتكون (3.7، و2.7، و1.8) على التوالي فقد اظهر التركيز الاول والثاني والثالث فروقا معنوية عن مجموعة السيطرة الموجبة عند احتمالية $p < 0.05$ اما التركيز الثالث فقد اظهر فرقا معنويا عن التركيز الاول بينما لم يظهر التركيزين الاول والثاني فروقا معنوية فيما بينهما وكذلك الحال في التركيزين الثاني والثالث بينما بلغت نسبة الكسر الكروموسومي للخلايا الجنسية للسيطرة الموجبة 7.4% وكانت (2.2، و1.5، و1.0) في خلايا الحيوانات المعاملة لاحقا بمستخلص ثمار الكاكي وبالتركيز (2، و5، و8) على التوالي. فقد اظهر التركيز الاول والثاني والثالث فرقا معنويا عن مجموعة السيطرة الموجبة بحتمالية $p < 0.05$. بينما اظهر التركيز الثالث فرقا معنويا عن التركيز الاول بينما لم يظهر التركيزين الاول والثاني فرقا معنويا فيما بينهما وكذلك بالنسبة للتركيزين الثاني والثالث.

يتضح من نتائج المعاملة بمستخلص ثمار الكاكي لخلايا نقي العظم المتأثرة بفعل كبريتيت الصوديوم امكانية المستخلص في تثبيط الانحرافات الكروموسومية بزيادة تركيز مستخلص ثمار الكاكي وكان التأثير معنويا لكلا النوعين من خلايا نقي العظم والخلايا الجنسية اذ جاء في نتائج الدراسة (1) التي اشارت الى امكانية مستخلص ثمار الكاكي من تقليل الكسور الكروموسومية والتبدلات الكروماتيدية لخلايا نقي عظم الفئران محثة بمطفرات وازدادت عمليات تثبيط الانحرافات الكروموسومية بزيادة تركيز المستخلص و عدد الجرعات. كما ذكر (32) ان لمستخلص ثمار الكاكي القابلية على تثبيط سرطان الجلد المستحث بمادة (TPA) في الفئران.

جدول -2: النسبة المئوية للتشوهات الكروموسومية في خلايا نقي العظم و الخلايا الجنسية في ذكور الفئران المعاملة بكبريتيت الصوديوم و مستخلصي عرق السوس و ثمار الكاكي.

المادة	خلايا جنسية % S.E±Means كسر كروموسومي	خلايا نقي العظم % S.E±Means كسر كروموسومي	الجرعة ملغم/كغم	المجاميع المعاملة
D.W بطرة سائلة	0.2d ±0.062	0.2d±0.062	100	CI
كبريتيت الصوديوم	0.54c±7.4	1.08b±8.3	100	CH
عرق السوس	0.55bs±3.3	0.34a±3.9	2	A
	0.3ab±2.4	0.5a±3.1	5	B
	0.16a±1.6	0.3a±2.3	8	C
ثمار الكاكي	0.32h±2.2	0.55a±3.3	2	A
	0.26ab±1.5	0.36a±2.7	5	B
	0.29a±1.0	0.29a±2.0	8	C

CI تمثل مجموعة السيطرة السالبة
CII تمثل مجموعة السيطرة الموجبة
CIII تمثل الثلاثة مجاميع (A,B,C) المعاملة مع المادة المطفرة و مستخلص عرق السوس
الحروف المختلفة (a,b,c,d) تعبر عن اختلاف معنوي باحتمال ($p \leq 0.05$)

تأثير التداخل بين مستخلص عرق السوس وثمار الكاكي في تثبيط التشوهات الكروموسومية المستحثة بفعل كبريتيت الصوديوم:

يظهر من نتائج الجدول (3) ان معدل التشوهات الكروموسومية قد انخفضت نسبتها بزيادة تركيز التداخل بين المستخلص في خلايا نقي العظم للفئران المعاملة والمتمثلة بنسبة الكسور الكروماتيدية الظاهرة في السيطرة

الموجبة والبالغة 18.3% لتصل الى (6.1، 13.6، 3.1)% عند تداخل المستخلصين بتركيز (2، 5، و 8) ملغم/كغم على التوالي. فقد أظهر التركيز الاول فرقا معنويا مع السيطرة الموجبة وكذلك التركيز الثاني والثالث في حين أظهر التركيز الاول فرقا معنويا مع التركيزين الثاني والثالث بينما لم يظهر التركيزين الثاني والثالث اختلافا معنويا فيما بينهما .

وكانت نسبة الكسر الكروموسومي للسيطرة الموجبة 8.3% بينما كانت نسبتها (3.3، 3.2، و 3.1)% للتركيز (2، 5، و 8) ملغم/كغم على التوالي ، وقد أظهرت التراكيز الثلاثة فروقا معنوية مع السيطرة الموجبة عند احتمالية $p < 0.05$ بينما لم تظهر التراكيز الثلاثة فروقا معنوية فيما بينها .
واما معدل التشوهات الكروموسومية المتمثلة بالكسور الكروماتيدية للخلايا الجنسية فقد بلغت السيطرة الموجبة 11.7% وانخفضت نسبتها لتبلغ (3.6، 2.5، و 1.4)% بازدياد التراكيز الى (2، 5، و 8) ملغم/كغم على التوالي . وظهرت فروقا معنوية مع السيطرة الموجبة بآتمالية $p < 0.05$ بينما لم تظهر التراكيز الثلاثة فروقا معنوية فيما بينها .

كما بلغت نسبة الكسور الكروموسومية للخلايا الجنسية في السيطرة الموجبة 7.4%، بينما بلغت نسبتها (1.7، 1.2، و 0.8)% عند تداخل المستخلص بالتركيز (2، 5، و 8) ملغم/كغم على التوالي وظهرت التراكيز الثلاثة فروقا معنوية مع السيطرة الموجبة ولم تلاحظ هذه الفروق فيما بين التراكيز الثلاثة.

من النتائج اعلاه نلاحظ حدوث عمليات تثبيط في التشوهات الكروموسومية نتيجة استخدام المستخلصات النباتية اذ توصل (33) الى ان مزيج المستخلص الكحولي لبعض انواع النباتات لها القابلية في تثبيط التشوهات الكروموسومية في خلايا نقي العظم والخلايا الجنسية فضلا عن تثبيط التشوهات الكروموسومية الناتجة من بعض انواع المطفرات الكيميائية والعقارات المستخدمة في العلاج الطبي وأشار الباحث الى انه السبب في التثبيط هو وجود المركبات الفعالة في المستخلص الكحولي لهذه النباتات وهي المركبات التربينويدية، الكومارين، الفلافونين والتانينات التي تعمل كمضاد للتطفير اذ تتواجد هذه المركبات في عرق السوس وثمار الكاكي.

كما جاء في نتائج الدراسة المذكورة من قبل (34) التي تضمنت تعريض الفئران الى المادة MMC كمعامل مطفر ثم تعريض الفئران لمزيج من مستخلصات الشيح وعرق السوس أدت المعاملة الى تثبيط التشوهات الكروموسومية في خلايا نقي العظم للفئران والسبب يعود الى امتلاك عرق السوس الى مركبات الQuinines والتي لها الدور الفعال في حماية المادة الوراثية من المطفرات فضلا عن تواجد هذا المركب الفعال في ثمار الكاكي اذ تتمثل فعالية هذا المركب من خلال ازاحته للجذور الحرة التي تسبب تحطيم المادة النووية .

جدول -3: النسبة المئوية للتشوهات الكروموسومية في خلايا نقي العظم و الخلايا الجنسية لذكور الفئران المعاملة بكبريتيت الصوديوم و تأثير تداخل مستخلصي عرق السوس و ثمار الكاكي.

المادة	خلايا جنسية % S.E±Means كسر كروموسومي	خلايا نقي العظم % S.E±Means كسر كروموسومي	الجرعة ملغم/كغم	المجـ المعاملة
D.W يطرة سالبة	0.2d ±0.062	0.2d±0.062	100	CI
كبريتيت الصوديوم	0.54c±7.4	1.08b±8.3	100	CII
تداخل	0.4a±1.7	0.55a±3.3	2	A
مستخلصي	0.3a±1.2	0.88a±3.2	5	B
عرق السوس و ثمار الكاكي	0.13a±0.8	0.27a±3.1	8	C

CI تمثل مجموعة السيطرة السالبة

CII تمثل مجموعة السيطرة الموجبة

CIII تمثل الثلاثة مجاميع (A,B,C) المعاملة مع المادة المطفرة و مستخلصي عرق السوس و ثمار الكاكي الحروف المختلفة (a,b,c,d) تعبر عن إختلاف معنوي بإآتمال ($p \leq 0.05$)

المصادر

1. Urkan,A.and Rena,G. The inhibition of the genetoxic effect oenvironmental pollution and the aging processes by plant antimutagenes. Traditional Biology.23:135-142(1999).
2. دراسة كروموسومات وصحة التكاثر للعاملين في حقول كبريت المشراق. الركابي, عبد الأمير ناصر غلوب. رسالة ماجستير.كلية العلوم/جامعة الموصل(1990).
3. Al-Berikdar,Z.T.H. Evaluting some Immuological,Antimutagenic and Hepato-protectiv properties of oregano leaves extracts (Origanum vulgare) CCL₄ - induce acute hepatic injury in albino male mice.An Msc thesis.College of science .Al-nahrain University(2007).
4. DeRocha,A.B.;Lopes.R.M.and Schwartamann,G. Natural production in anticancer therapy.Curr.Opin.Pharmacol. 1:364-369(2001).
5. Frasworth,N.R.;Akerele,O.;Bingle,A-S.Soijarto,D.D.andGoz,Z.(1985).
6. Medicinal plant in therapy. Bull.World Health Organ.63:956-981. Arber,A.A. The application of Liquorices roots. J. Nutrition. 56:230-236(1983).
7. وزارة الزراعة و الأصلاح الزراعي،الموسوعة النباتية العراقية،(3):449-445(1974).
8. Suzuki,F.;David,A;Schimitt,H.;Utsunomiya,T. and Pollard,R.B. Stimulation of host resistance against tumor by glycyrrhizin,an active component of licorice root.In Vivo.6:589-569(1992).
9. Newall,C.A.;Anderson,I.A. and Phillipsson,J.D. Herbal Medicine A guide for Health - aCare professional.The Pharmaceuttical. Press , London.England Gzoch,W. and Mordaski.R.(Transformation of Xinobiotic Acad .Pres. 61:315-3221983) (1996).
- 10.Ken,Y.;Takido,M.M.;Takeuchi,M. and Nakagawa,S. Inhibitory effect of the glycyrrhizic acid cafein on two stage carcinogenesis in mice. Biological Abstract.86:11207(1988).
- 11.Chun,Y.;Chia,T.H.;Hasiny,T.H.;Jin,S.S.;Tzong.T.C.;Woan,Y.T.;Yao,H.K. Jacqueline,W.P.;Leory,F.L and Jaualang,H. Isodiospyrin as anoval human top -oisomerase 1 inhibitor.Biochmical.Pharmacol.66:1981-1991(2003).
- 12.Mallavadhani,V.V.Anita,K.P. and Rao,Y.R. Pharmacology and Chemotaxy - nomy of Diossypyros.Phytochemistry..49:901 -951(1998).
- 13.Singh,G.B.;Singh,S and Bani,S. The inhibition effect by D.kaki for G +ve/G- ve bactria.Drug Futuer. 19:450-459(1994).
- 14.Madhushree,D.S.;Ring,G.;Amerendar,P. and Bana,H. Synthesis and antiproli - ferative activiy of some novel derivative of diospyrin aplant derived Naphthoquinone. Bioorganic Meeeeedical chem., 15:3672-3677(2007).
15. الكاطع,جاسم محمد وحمادي,صالح عبد.واقع التلوث الناجم من الصناعات الكيماوية.ندوة حماية البيئة من التلوث الصناعي(1985).
16. الميالي,أشواق عبد جبير.تأثير تداخل كبريتيت الصوديوم وأوكسيد الخارصين على بعض مؤشرات الوراثة الخلوية في الفأر الأبيض. رسالة ماجستير. كلية التربية/جامعة القادسية(2000).
- 17.Al-Azaw,T.S.SThe Influncs of Sodium thiosulphate water contamination on Hematological picture in laying has. The Veterinarian. 1:77-83(1998)..

18. Nadir, M.T.; Salih, F.M.; Dahir, A.J.; Nori, M. and Hussain, A.M. Antimicrobial activity of *Salvia* species indigenous to Iraqi. *J. Biological Sci. Res.* 17:109-117 (1986).
19. الشيخلي, محمد عبد الستار؛ العزاوي, فريال حسن فياض, المركبات الطبيعية في النبات. دار الكتب للطباعة والنشر, الموصل : 224-221 (1993).
20. Haribon, I. *Phytochemistry method of components*. Hall. London.: 89-100. (1973).
21. Shibata, R. Antitumor promoting and anti-inflammatory of licorice principles and their modified compound. *Acs. Amer. Chemical Society*. 574:308-321 (1994).
22. Geisman, T. *Chemistry of flavonoid compound*. MacMillan. Com. New York (1962).
23. Allen, J.; Shubber, C. and Latt, S.A. A simplified technique for in vivo analysis of SCE using 5-BrdU tablet. *Cytogenet. Cell Genet.* 18:231-234 (1977).
24. Evans, E.; Breckon, G. and Ford, G. An air drying method for meiotic preparation from mammalian testes. *Cytogenetics*. 3:289-294. (1964).
25. Stahl, R.G.; Frances, J.R.; Arrigani, E.; Thomas, S.; Matey, S.; Gary, S. Bernard, S. and Johaston, D.A. Mutagenic and cytogenic analysis of organic extract of stimulated runoffs from model coal. *Cytogenet. Cell Genet.* 9:18-24 (1984).
26. أحمد حسن, مفيد قائد, استخدام بعض المستخلصات النباتية لتثبيط الأثر السمي الوراثي لبعض العقاقير المضادة للسرطان في الفأر. اطروحة دكتوراه/كلية العلوم. جامعة بابل (2002).
27. Dzwonkowska, A. and Hibner, H. Induction of chromosomal aberration in Syrian hamster by insecticides in vivo. *Arch. Toxicol.* 58:152-156 (1986).
28. Ziqiang, M. & Bo, Z. Induction effect of sulfur dioxide inhalation on chromosome aberration in mouse bone marrow cells. *Mutagenesis*. 17:215-217 (2002).
29. Gzoch, W. & Mordaski, R. Transformation of *Xinobiotic* Acad. Pres. 61:315-322 (1983).
30. Shihata, I.M. *Apharmalogical study of angllis arsisis*. PhD. Thesis cairo University (1951).
31. Agamall, R. Wang, Z. Y. and Muktar, H. Inhibition of Mouse skin tumor-intiation activity by chronic oral feeding of glycyrrhizin I drinking water. *Nutrition and cancer*. 15:189-193 (1999).
32. الجنابي, عباس عبد الله محمود. تأثير مبيد القوارض (فوسفيد الخارصين والبروديفاكوم) على الهيئة الكروموسومية ومؤشر الأنقسام والنطف في الفئران الحقلية والمختبرية. اطروحة دكتوراه. كلية التربية (ابن الهيثم)/جامعة بغداد (1997).
33. Daba, M. and AbdelRahman, M. Hepatoprotective activity of TQ in isolated rat hepatocyte. *Toxicol. Lett.* 95:23-29 (1998).

تشخيص الفطريات الجلدية الخيطية المعزولة من المرضى المصابين بسعفة الرأس tinea capitis في بغداد

عبد الرضا طه سرحان و رسول عبد السادة كريم
قسم علوم الحياة / كلية مدينة العلم / جامعة بغداد.
مستشفى بغداد التعليمي / مجمع مدينة الطب / بغداد

ABSTRACT

This research was conducted to identify the dermatophytes isolated from patients infected with tinea capitis in Baghdad. A total of 146 clinical specimens were collected from dermatophytoses of patients in consultant of dermatology in Baghdad Teaching Hospital, Medicine City, Baghdad during the period from October 2008 to May 2009. The results of laboratory cultures and microscopical examination showed that 51 specimens (34.9 %) were recorded as tinea capitis. The number of male patients were 33 (64.7 %), while the number of female patients were 18 (35 %). Seven fungal species were isolated belong to two genera : *Microsporum* and *Trichophyton*. The species *M. audouinii* was the most frequent ones (33.3 %). Also, the research revealed that the highest percentage of tinea capitis (41.2 %) was appeared in patients aged (6 – 10) years. Tinea capitis infection recorded high frequency during warm months and the highest percentage (19.7 %) was at May.

الخلاصة

تضمن البحث تشخيص الفطريات الجلدية الخيطية المعزولة من المرضى المصابين بسعفة الرأس في مدينة بغداد. جمعت (146) عينة سريرية من المرضى المراجعين إلى العيادة الاستشارية للأمراض الجلدية في مستشفى بغداد التعليمي / مدينة الطب / بغداد ، مصابين بالفطريات الجلدية الخيطية للفترة من تشرين الأول 2008 ولغاية مايس 2009 . أظهرت نتائج الزرع المختبري والفحص المجهرى أن (51) عينة منها سجلت كحالات إصابة بسعفة الرأس tinea capitis وبنسبة 34.9% من المجموع الكلي للإصابات، وكان عدد إصابات الذكور 33 (64.7 %) وعدد إصابات الإناث 18 (35.3 %)، وقد تم عزل وتشخيص سبعة أنواع فطرية تعود لجنسين من الفطريات الجلدية الخيطية هما: *Microsporum* و *Trichophyton*، وكان أكثر الأنواع تكراراً هو *M. audouinii* إذ شكل نسبة 33.3 % . كما ظهر من النتائج أن أكثر الفئات العمرية إصابة بسعفة الرأس هي ما بين 6 – 10 سنوات (41.2 %)، ولوحظ أيضاً أن الإصابة تستهدف الذكور بشكل رئيسي وبنسبة أكثر من الإناث . ووجد أن الإصابة بسعفة الرأس كانت عالية في الأشهر الحارة، حيث سجلت نسبة إصابة (19.7 %) في شهر مايس بينما سجلت الأشهر الأخرى نسب إصابة أقل .

المقدمة

تشكل الإصابة بالفطريات الجلدية الخيطية نسبة عالية من الأمراض الجلدية ، وعلى الرغم من أنها تسبب إزعاجاً كبيراً فإنها لا تشكل خطراً كبيراً على حياة العائل (1) ، والإصابة الفطرية الجلدية تكون سطحية للأنسجة الكيراتينية في البشرة والشعر والأظافر وتسببها أنواع من الفطريات الجلدية الخيطية المحبة للكيراتين والتي تعود إلى ثلاثة أجناس هي :

Epidermophyton ، *Microsporum* و *Trichophyton* (2) . تعد الإصابة بسعفة الرأس مشكلة واسعة الانتشار تصيب فروة الرأس وهي بشكل رئيسي مرض الأطفال الصغار أكثر من البالغين (3)، وتسببها عدة أنواع تعود للجنسين *Microsporum* و *Trichophyton* (4)، إذ لوحظ أنه من الصعب الحد أو القضاء على أمراض سعفة الرأس وخصوصاً الناتجة عن الفطريات الجلدية المشتركة بين الإنسان والحيوان حيث يعتبر الحيوان مضيف ابتدائي لها قبل وصولها إلى الإنسان (5) . سعفة الرأس من الأمراض الفطرية الجلدية الشائعة في البلدان الحارة، وتنتشر من خلال التماس مع أشخاص مصابين أو من حوائجهم مثل غطاء الرأس أو ملابس السباحة والرياضة أو من أدواتهم الملوثة مثل المشط أو فرشاة الشعر وغيرها، إضافة إلى التماس مع الحيوانات المصابة مثل القطط والكلاب والمواشي (6) . تختلف الأعراض السريرية لسعفة الرأس باختلاف الفطر الجلدي المسبب للمرض ، فان بعض الأنواع تسبب أعراضاً التهابات شديدة بينما تسبب أنواع أخرى إصابات مزمنة وأحياناً قد تكون الصورة السريرية غير واضحة ولا يمكن تشخيصها بسهولة إلا من خلال الفحص المجهرى (7) .

المواد وطرائق العمل

جمع العينات

جمعت (146) عينة سريرية من المرضى المراجعين إلى العيادة الاستشارية للأمراض الجلدية في مستشفى بغداد التعليمي / مدينة الطب / بغداد مصابين بالفطريات الجلدية الخيطية بأعمار مختلفة ولكلا الجنسين للفترة من تشرين الأول 2008 ولغاية مايس 2009. الفطريات الجلدية الخيطية تصيب مناطق مختلفة من الجسم والمظاهر السريرية تختلف باختلاف تلك المواقع، لذلك صنفت الإصابات وفقاً إلى موقع الإصابة سريرياً، فق تم عزل (51) عينة تعود للمرضى المصابين بسعفة الرأس من خلال الزرع المختبري والفحص المجهرى إضافة إلى الأعراض السريرية.

الفحص المجهرى المباشر للعينات

أخذت العينات من جلد المرضى المصابين بسعفة الرأس من الحواف النشطة لمنطقة الإصابة بواسطة مشرط أو شفرة وملقط معقمين، الشعر المصاب يجب نزع من جذوره خاصة في حالات القرع Favus. توضع العينة على شريحة زجاجية مع قطرة من (30 % KOH) وتغطى بغطاء الشريحة ثم تسخن بلطف لكي تصبح طرية (يجب الحذر من تسخين العينة كثيراً لكي لا تغلي وبالتالي قد تؤدي إلى نتيجة سلبية بسبب تبلور هيدروكسيد البوتاسيوم)، تفحص الشرائح الزجاجية مجهرياً بالقوة الصغرى وبدون تلوين، النتيجة الايجابية تظهر خيوط فطرية مفصولة ومنفرعة إضافة إلى الكونيدات.

زرع العينات

بعد الانتهاء من الفحص المجهرى للعينات تمت عملية زرع الفطريات بأخذ جزء من العينة وزرعها في أطباق بتري أو في أنابيب اختبار تحتوي وسط سابورود دكستروز أكار SDA مضافاً إليه كلورامفينيكول (0.05 غم/لتر) وذلك لتنشيط البكتريا والفطريات الرمية، والذي حضر وفقاً لما ورد في (8)، ثم حضنت عند درجة حرارة 26 - 30 °م لمدة أسبوع أو أسبوعين، النتيجة الايجابية تعطي العديد من المستعمرات التي بالإمكان التفريق بينها وبالتالي تحديد أنواع الفطريات المسببة للإصابة وتشخيصها شكلياً ومجهرياً بالاستعانة بالمصادر المتخصصة (7,9,10,11).

التحليل الإحصائي

حلت النتائج إحصائياً وقورنت المعدلات اعتماداً على اختبار أقل فرق معنوي LSD عند مستوى احتمال 5 %.

النتائج والمناقشة

تختلف الأعراض التي تسببها الفطريات الجلدية الخيطية باختلاف نوع الفطر الممرض والمنطقة التي يستهدفها، وغالباً ما تكون الأعراض السريرية واضحة، وقد شكلت الإصابة بسعفة الرأس أعلى نسبة 34.9% من مجمل الإصابات الفطرية الخيطية (جدول 1) وهذه النتيجة تتفق مع ما حصل عليه (12)، وكان الذكور أكثر إصابة بسعفة الرأس (64.7 %) من الإناث (35.3 %)، وقد يكون سبب ذلك يعود إلى قصر الشعر لدى الذكور الذي يوفر فرصة لسهولة وصول الأبواغ الفطرية إلى فروة الرأس (13)، وهذا يتفق مع ما ذكره (14) الذي أكد بأن سعفة الرأس شائعة بين الذكور أكثر من الإناث. يوضح جدول (2) أنواع الفطريات الجلدية الخيطية المعزولة من سعفة الرأس ويظهر أن الإصابة الأودونية التي يسببها الفطر *M. audouinii* قد سجلت أعلى نسبة إصابة (33.3 %) من الفطريات الأخرى وهي أشيع الأنواع إحداثاً لسعفة الرأس يليه الفطر *M. canis* (21.6 %) الذي ينتقل من الحيوانات، ثم الفطر *T. tonsurans* (15.7 %) الذي يسبب إصابات وأعراض سريرية تسمى بالبقع السوداء Black dots، أما الأنواع الأخرى فق سجلت نسب إصابة أقل كما في النوع *T. verrucosum* (9.8 %) الذي يسبب النوع الملتهب أو ما يسمى بالشهادة Kerion، والنوع *T. mentagrophyte* (7.8 %) الذي يسبب سعفة الرأس شديدة الالتهاب، والنوع *T. schoenleinii* (5.9 %) الذي يسبب ما يسمى بالقرع Favus، والنوع *T. violaceum* (5.9 %) الذي يسبب التهاباً مزمناً، وهذا يتفق مع ما ذكره (15)

وأظهرت النتائج أن سعة الرأس هي إصابة فطرية واسعة الانتشار تصيب فروة الرأس وهي بشكل رئيسي مرض الأطفال الصغار (16) ، الذكور أكثر عرضة للإصابة من الإناث (جدول 3) ، و نادرا " ما يصاب البالغين بهذا المرض (17) ، ويعتقد أن سبب ذلك هو فرط تكوين الحوامض الدسمة في الفروة التي تشكل مركبا " مثبتا " للفطريات الجلدية، وقد أثبتت البحوث والدراسات بأن بعض الحوامض الدسمة المشبعة في شعر البالغين (التي تشتق من الزهم Sebum) هي مواد مثبطة للفطريات الجلدية (18) ، ولذلك فإن الميل للشفاء من هذا المرض في سن البلوغ يعزى إلى التغيير في تركيب الدهون في هذه الأعمار البالغة. وهو من الأمراض المعدية التي تظهر بين أطفال المدارس أو في الأماكن المزدحمة ذات العناية الصحية القليلة ومن الممكن أن تحدث على نطاق واسع، والمرض قد يكون مستوطنا " أو فرديا " (19).

ويوضح جدول (4) أنواع الإعراض السريرية لسعة الرأس، حيث لوحظ أن النوع الجاف التقرشي الأحمراري هو أكثر الأنواع السريرية لإصابة سعة رأس الذي شكل نسبة 52.9 % ، وهي إصابة جافة ومتقشرة تشبه قشرة الفروة، يليه النوع الملتهب أو ما يسمى بالشهدة الذي سجل نسبة إصابة 25.5 % ، وقد تكون أكثر التهابا " فتظهر تورما " ونزا " وتقشرا " في شكل التهاب انتفاخي في فروة الرأس ولذلك تسمى الشهدة، وتسبب أحيانا " التباسا " في تشخيصها وتعالج على أنها خراج في فروة الرأس، وقد يحصل ضياع الشعر وصلع دائم في المنطقة المصابة. أما البقع السوداء فقد شكلت نسبة إصابة بلغت 15.7 % ، وعادة ما تكون الإصابة فيها جافة والشعر مقطوع من الجذور وأسس الأشعار المصابة موجودة وتظهر المنطقة المصابة خالية من الشعر الطويل الذي يبدو كأنه مقصوص على مستوى سطح الجلد وكنقاط على سطح فروة الرأس، وتوجد درجات مختلفة من الاحمرار مع حكة وتقشر. وسجل القرع أقل نسبة إصابة 5.9 % ، والتي تتميز بقشور صلبة تتشكل فوق المنطقة المصابة وقد تنتشر لتغطي كل فروة الرأس وتسبب أحيانا " رائحة كريهة جدا " للفروة وقد تنتهي بصلع دائم (20).

أما جدول (5) يبين نسبة الإصابة بسعة الرأس خلال الأشهر المختلفة من السنة، حيث بينت النتائج أن الإصابة كانت مرتفعة في الأشهر الحارة فسجلت أعلى نسبة لها في شهر مايس (19.3 %) ويليهما الإصابة في تشرين الأول (17.6 %) ، وهذا يتفق مع ما ذكره (21) من أن معدلات الإصابة ترتفع في المناطق الحارة لتوفر الظروف المناسبة من رطوبة وحرارة ، بينما سجلت الأشهر الأقل حرارة نسب أقل للإصابة فسجل شهر كانون الثاني أدنى نسبة إصابة بسعة الرأس مما يؤكد بأنها تمثل مشكلة في البلدان الحارة.

جدول -1: التشخيص السريري لأنواع الإصابات الفطرية الجلدية الخيطية حسب الفئة العمرية والجنس

نوع الإصابة	الفئة العمرية (سنة) / الجنس												المجموع	نسبة الإصابة (%)
	شهر - 10		20 - 11		30 - 21		40 - 31		50 - 41		60 - 51			
	أ	ذ	أ	ذ	أ	ذ	أ	ذ	أ	ذ	أ	ذ		
سعفة الرأس*	23	16	9	2	1	-	-	-	-	-	-	-	51	34.9
سعفة الجسم	5	3	6	2	9	4	5	1	3	1	-	-	39	26.7
سعفة القدم	2	1	5	-	4	-	3	2	3	1	1	-	21	14.4
سعفة الفخذ	-	-	3	1	3	2	2	1	1	-	1	-	14	9.6
سعفة الوجه	4	3	2	1	1	-	-	-	-	-	-	-	11	7.5
سعفة الذقن	-	-	-	-	2	-	4	-	1	-	-	-	7	4.8
سعفة الأظافر	-	-	-	1	-	1	-	1	-	-	-	-	3	2.1
المجموع	34	23	25	7	20	7	14	5	8	1	2	-	146	100

* نسبة إصابة الذكور بسعة الرأس = 64.7 % ونسبة إصابة الإناث بسعة الرأس = 35.3 %
 ** أقل فرق معنوي عند احتمال 5 % بين نوع الإصابة = 3.27 ، بين جنس المريض = 1.44 ، بين الفئة العمرية = 2.65

جدول- 2: أنواع الفطريات الجلدية الخيطية المعزولة من سعة الرأس والنسبة المئوية لكل منها

نوع الفطر	عدد العزلات	النسبة المئوية (%)
-----------	-------------	----------------------

تشخيص الفطريات الجلدية الخيطية المعزولة من المرضى المصابين بسعفة الرأس tinea capitis في بغداد

عبد الرضا و رسول

33.3	17	<i>Microsporum audouinii</i>
21.6	11	<i>M. canis</i>
15.7	8	<i>Trichophyton tonsurans</i>
9.8	5	<i>T. verrucosum</i>
7.8	4	<i>T. mentagrophyte</i>
5.9	3	<i>T. schoenleinii</i>
5.9	3	<i>T. violaceum</i>
100	51	المجموع

جدول- 3 : عدد المرضى المصابين بسعفة الرأس موزعين حسب الفئة العمرية والجنس

الفئة العمرية (سنة) / الجنس												نوع الفطر
مجموع العزلات	50 - 41		40 - 31		30 - 21		20 - 11		شهر - 10			
	أ	ذ	أ	ذ	أ	ذ	أ	ذ	أ	ذ		
17	-	-	-	1	1	3	2	7	1	2	<i>Microsporum audouinii</i>	
11	-	-	-	1	1	1	1	5	1	1	<i>M. canis</i>	
8	-	1	-	1	-	1	-	2	1	2	<i>Trichophyton tonsurans</i>	
5	-	-	-	1	-	1	-	1	-	2	<i>T. verrucosum</i>	
4	-	-	-	-	-	1	-	1	1	1	<i>T. mentagrophyte</i>	
3	-	-	-	-	-	1	-	1	-	1	<i>T. schoenleinii</i>	
3	-	-	-	1	-	1	-	1	-	-	<i>T. violaceum</i>	
51	-	1	-	5	2	9	3	18	4	9	المجموع	
100	1.9		9.8		11.7		41.2		25.4		النسبة المئوية / الفئة العمرية	

* أقل فرق معنوي عند احتمال 5 % بين الفطريات = 0.72 ، بين جنس المريض = 0.44 ، بين الفئة العمرية = 1.15

جدول- 4 : أنواع الأعراض السريرية لسعفة الرأس التي تسببها أنواع الفطريات الجلدية الخيطية

مجموع العزلات	أنواع الأعراض السريرية				نوع الفطر
	القرع	النوع الملتهب (الشبهة)	التقشر الأحمراري (النوع الجاف)	البقع السوداء	
17	-	6	11	-	<i>Microsporum audouinii</i>
11	-	3	8	-	<i>M. canis</i>
8	-	-	-	8	<i>Trichophyton tonsurans</i>
5	-	1	4	-	<i>T. verrucosum</i>
4	-	1	3	-	<i>T. mentagrophyte</i>
3	3	-	-	-	<i>T. schoenleinii</i>
3	-	2	1	-	<i>T. violaceum</i>
51	3	13	27	8	المجموع
100	5.9	25.5	52.9	15.7	النسبة المئوية / نوع الأعراض

جدول- 5: عدد الإصابات والنسبة المئوية للإصابة بسعفة الرأس حسب أشهر السنة

الشهر	عدد الإصابات	نسبة الإصابة (%)
تشرين أول / 2008	9	17.6
تشرين ثاني / 2008	6	11.7
كانون أول / 2008	5	9.8
كانون ثاني / 2009	3	5.9
شباط / 2009	4	7.8
آذار / 2009	6	11.7
نيسان / 2009	8	15.6
مايس / 2009	10	19.7
المجموع	51	100

المصادر

1. Jawetz, E., Melnich, J.L. and Adelberg, E.A. Medical Microbiology. Middle East edition . Librairie du Liban Appleton & Lange. 45:584–610 (1998).
2. Weitzman, I. and Kane, J. Dermatophytes and agent of superficial mycoses. Manual of Clinical-Microbiology. 5th. ed. :606- -616 (1991).
3. Capesius-Dupin,C.Benailly,N.,Hennequin,C.and De-Prost,Y.Dermatomycoses in pediatrics.Journal de Mycologie Medicale. 5(1) :40–45(1995).
4. Degreef, H. Clinical forms of dermatophytosis (ringworm infection). Mycopathology.166 (5– 6): 257 – 265 (2008).
5. Tanka, S.,Summerbell, R. C. , Tsuboi, R. Kaaman, T. , Sohnle,P., Matsumoto, T. and Ray, T.L Advances in dermatophytes and dermatophytosis. J. Med. & Vet. Mycol. 30 Suppl. 1: 29 – 39 (1992).
6. Al-Rubaiy,K.Q. and Abid Al–Salam ,S.The pattern of skin disease in Basrah province. Review of 9252 patients. The Med.J.of Basrah Univ.13 :183–190 (1995).
7. Elmer,W.and Glermn,D.R.Practical Laboratory Mycology.3rd.ed.Williams& Wilkins, Baltimore , USA: 211 (1985).
8. Emmons, C.W. , Bin ford, C.H. and Utz J .P. Medical Mycology 2nd ed.Lea & Febiger. Philadelphia: 428 (1974).
9. Beneke,E.S.&Roquers,A.L.Medical mycology manual with human mycoses monograph.Burgess Publ. Comp. Minneapolis Minnesota.5: 59–86(1985).
- 10.Forbes,A.B.,Saham,D.F.and Weissfeld,A.S. Diagnostic Microbiology 10th ed. Baily&Scotts Mosby Com.:422(1998).
- 11.Kilic,H. and Sahin,F.U. Identification of the dermatophytes in patients clinically and microbiologically diagnosed as dermatophytosis Mikrobiologi. Bullten.27(3):196–202(1993).
12. محمود ، وجدان رضا . مسح للإصابات الفطرية الجلدية في محافظة بابل، رسالة ماجستير ، كلية العلوم، جامعة بابل (2000).
13. الحسنی ، مثال كريم . دراسة بيئية للفطريات الجلدية والانتهازية الممرضة للإنسان في محافظة القادسية. رسالة ماجستير، كلية التربية ، جامعة القادسية (2002).
- 14.Richardson, M. Fungal Infection: Diagonsis and Management. Cambridge, MA:Blackwell Publishers. ISBN 1578-5 (2003).
- 15.Seebacher, C., Bouchara, J.P. and Mignon,B. Updates on the epidemiology of dermatophyte infections.Mycopath.166(5-6):335-352(2008).

16. Ali, S., Graham, T. A. and Forgie, S. E. The assessment and management of tinea capitis in children. *Pediatric Emerg. Ca.* 23(9):662-665 (2007).
17. Teska, J., Kaimba, C., Geagers, A. and Delmond, V. Clinical Infectious diseases. *Annals of Saudi Medicine.* 14:871-874 (1992).
18. Cremer, G. Boumerias, T., Vandemeleubrouck, E., Horn, R. and Revus, J. Tinea capitis in adults; misdiagnosis or re-appearance, *Dermatology.* 149(1):8-11 (1997).
19. Arnold, H. L., Odom, R. B. and James, W. D. Andrews diseases of skin. W. S. Saunders Com. Philadelphia, London, Toronto, Montreal, Sydney, Tokyo: 286 (1990).
20. Andrews, M. D. & Burns, M. Common tinea capitis in children. *Am. Fam. Physician.* 77:1415-1420 (2008).
21. Ali, T. M. A study of tinea capitis in Baghdad (Iraq). M. Sc. thesis, College of Medicine. University of Baghdad. (1990).

إنتاج البروتياز القاعدي من بكتريا *B. stearothermophilus* AEAL2 بواسطة تخمرات الحالة الصلبة واختبار كفاءته في بعض التطبيقات الصناعية

عصام فاضل علوان الجميلي وأسماء وليد داود
معهد الهندسة الوراثية والتقنية الاحيائية للدراسات العليا - جامعة بغداد

ABSTRACT

Local isolates (40) of the genus *Bacillus*, the thermophilic bacteria, were screened for production of alkaline protease (EC. 3.4). (The isolate *B. stearothermophilus* AEAL2) was selected based on its high production of enzymes in solid and submerged cultures and used in the present study.

The optimum conditions for the production of alkaline protease by solid-state fermentation systems were determined and they included the use of fermentation media consisted of wheat bran, moistened with 0.2M phosphate (pH 9.0). The hydration ration was 1:5(V:W), and the initial pH was 9.0. The optimum inoculums size was 10^6 spore/10g solid materials, and incubation period was 48 hours at 60°C.

The protease II (1% solution) removed blood spots from cloth after 20min., furthermore, the enzyme was quite efficient in the preparation of soluble protein hydrolysis's from cat fish by products as indicated by releasing 36 –38% soluble protein during 90-120 min. of incubation.

The enzyme was immobilized by entrapment in calcium alginate beads. The enzyme retained 50% of its original activity after 30 days of storage at 4°C.

الخلاصة

تم اختبار 40 عزلة محلية من بكتريا الـ *Bacillus* المحبة للحرارة حول انتاجها للبروتياز القاعدي وظهرت سلالة *B. stearothermophilus* AEAL2 اعلى انتاجية للبروتياز القاعدي باستخدام اسلوب تخمر الحالة الصلبة فظهر ان وسط نخالة الحنطة يعطي اعلى انتاج للانزيم ، وان محلول فوسفات البوتاسيوم الدارئ بتركيز 0.2 مولار ورقم هيدروجيني 9 هو المحلول الانسب للترطيب وان افضل نسبة للترطيب هي 1:5 (حجم : وزن) والرقم الهيدروجيني الابتدائي الامثل للانتاج 9 . وعندما لقيح الوسط باعداد مختلفة من الابواغ وجد ان العدد 10^6 بوغ / 10 غرام مادة صلبة يعطي اعلى انتاج للانزيم وكانت درجة الحرارة المثلى للانتاج 60 م ولمدة حضن مثلى 48 ساعة .
اختبرت قابلية البروتياز القاعدي 11 في عملية تنظيف الملابس من بقع المواد البروتينية ف لوحظ زوال نسبة كبيرة من بقع الدم عند نقع الاقمشة الملوثة بالبقع بمحلول 1% انزيم لمدة 20 دقيقة ، كما اختبرت كفاءة الانزيم في انتاج المتحللات البروتينية الذائبة وذلك باستخدام مسحوق جلد سمك الجري وسطا للانتاج وبعد معاملته بالانزيم ظهرت زيادة في نسبة البروتين الذائب 36-38% عند 90-120 دقيقة بعد اضافة الانزيم .
كذلك تم تقيد الانزيم بطريقة الاقتناص باستخدام الجينات الكالسيوم إذ دلت النتائج على احتفاظ الانزيم بما يقارب 50% من فعاليته بعد 30 يوم بدرجة 4 م .

المقدمة

تعد البروتياز (EC.3.4) من الانزيمات المنتشرة أنتشاراً واسعاً في الطبيعة إذ تتواجد في خلايا الحيوانات والنباتات والاحياء المجهرية ، وتحفز البروتياز التحلل المائي للاصرة الببتيدية التي تربط الاحماض الامينية في تركيب البروتين الذي يعد الركيزة لهذه الانزيمات .
تحتل البروتياز أهمية صناعية كبيرة وتشكل نسبة 60% من الاستخدامات الصناعية للانزيمات المختلفة إذ يبلغ أنتاج البروتياز من المصادر المايكروبية مئات الاطنان المستخلصة من بكتريا الـ *Bacillus* ، وعشرات الاطنان من البروتياز البكتيري والفطري ، ويأتي اختيار البروتياز القاعدي لما لهذا الانزيم من تطبيقات واسعة في المجال الصناعي إذ يشكل نسبة 25% من الانزيمات المسوقة تجارياً على المستوى العالمي (1) .

طبقت تقنية تخمرات الحالة الصلبة من قبل (2) لانتاج البروتياز والاميليز من بكتريا *B. subtilis* و *Aspergillus oryzae* W215 وفطر *Endomycopsis fibuligera* S.B.5 وخميرة *B. 73*

باستخدام وسط فول الصويا ولقد بين ان استخدام خليط من مزارع هذه الاحياء يعطي انتاجية عالية للانزيمات بالمقارنة من استخدام كل مزرعة من هذه الكائنات المجهرية على حدة . وكما تمكن (3) من انتاج البروتييز من بكتريا *B. licheniformis* باستخدام وسط كسبة بذور القطن بوصفه وسطاً تخميراً صلباً ووجد أنه افضل وسط في انتاج البروتييز بالمقارنة مع كسبة فول الصويا ، ولقد تم اثبات ارجحية استخدام تخمرات الحالة الصلبة في انتاج انزيم البروتييز على غيرها من التخمرات إذ بلغت فعالية البروتييز المنتج *Streptomyces* باستخدام تقنية تخمرات الحالة الصلبة 26.7 وحدة / مليلتر من المادة في حين بلغت الفعالية 17.4 وحدة / مليلتر في الوسط السائل (4) .

كما أثبت (5) أن انتاج الانفريتيز من ثلاث سلالات من فطر *A. niger* باستخدام تخمرات الحالة الصلبة أفضل من التخمرات السائلة لذا يفضل في حالات كثير استخدام أسلوب التخمرات الصلبة للانتاج على التخمرات السائلة.

أما في مجال الصناعة فتستخدم البروتييزات في دباغة الجلود ، ويقصد بالدباغة هو معاملة الجلد الخام عدة معاملات كيميائية وانزيمية لجعلها طرية ومقاومة للتلف المايكروبي وهذه المعاملات تشمل التفتيح Soaking وازالة الشعر Dehairing والتطرية Bating والدباغة Tanning ويستعمل في بعض هذه المراحل البروتييز القاعدي الحيواني او المايكروبية ومن ابرز هذه المراحل هي ازالة الشعر والتطرية (6,7)، كما يستعمل البروتييز القاعدي في صناعة المنظفات إذ تشكل حوالي 25% من المبيعات الكلية في الاسواق (8). يسهم البروتييز المختلفة في الاستفادة من مخلفات المجازر ومعامل الاسماك والمواد البروتينية الرخيصة لانتاج متحللات بروتينية ذات قيمة غذائية عالية يمكن اضافتها الى اعلاف الحيوانات لتحسين خواصها الوظيفية (9).

تشير الدراسات الى ان معظم انزيمات التنظيف التجارية هو البروتييز القاعدي المنتجة من سلالة الـ *Bacillus* واكثر هذه الانزيمات استخداما هو انزيم Alcalase ويعمل هذا الانزيم بنحو جيدة عند درجة حرارة المنخفضة خلال النقع ويتحمل درجة حرارة تصل 60 °م ، كما ان هذا الانزيم يمكن ان يقوم بنشاطه في مدى متسع من الرقم الهيدروجيني (5.8-9) وقد يصل لاكثر من 10 (10) ومن الامثلة الاخرى هو البروتييز القاعدي المنتج من *Conidiobolus coronatus* والذي يستخدم ايضاً في المنظفات التجارية في الهند (11). تهدف الدراسة الحالية الى انتاج البروتييز القاعدي بطريقة الحالة الصلبة من عزلة محلية واستخدامه في بعض التطبيقات الصناعية المهمة التي يدخل فيها ومنها صناعة المنظفات .

المواد وطرائق العمل

تم انتاج الانزيم من العزلة *B. stearothermophilus* AEAL2 باستخدام اسلوب تخمر المواد الصلبة ، إذ استخدم الوسط نخالة الحنطة و المرطبه بمحلول فوسفات البوتاسيوم الدارئ بتركيز 0.2 مولار ورقم هيدروجيني 9 و بنسبة للتطبيب 1:5 (حجم : وزن) . ولقح الوسط بالعدد 10^6 بوغ / 10 غرام مادة صلبة وكانت درجة الحرارة المثلى للانتاج 60 °م ولمدة حضن 48 ساعة وفق الطريقة الموصوفة من قبل (12)

تقدير فعالية أنزيم البروتييز

اتبعت طريقة (13) في تقدير فعالية أنزيم البروتييز وذلك باضافة 0.1 مليلتر من محلول الانزيم الى 1 مليلتر من محلول التفاعل وحضن في حمام مائي بدرجة حرارة 60 °م لمدة 10 دقائق ثم اوقف التفاعل باضافة 2 مليلتر من محلول ثلاثي كلوروحامض الخليك ويترك المحلول لمدة نصف ساعة بدرجة حرارة الغرفة . تم تقدير تركيز البروتين بالطريقة الواردة من قبل (14).

تعريف الوحدة الانزيمية : كمية الانزيم التي تسبب زيادة في الامتصاص الضوئي على الطول الموجي 280 نانوميتر مقدارها 0.001 في الدقيقة تحت الظروف القياسية ، اما الفعالية النوعية Specific Activity فانها تعبر عن وحدات الفعالية لكل ملغرام بروتين .

أختبار كفاءة الانزيم في تنظيف الاقمشة

نقعت قطع من الاقمشة القطنية البيضاء الملوثة ببقع الدم في 25 مليلتر من الماء الاعتيادي المذاب فيه 0.25 غرام من الانزيم الخام المجفف (مايعادل 1000 وحدة) ، كما نقعت قطعة قماش اخرى بالماء الاعتيادي الخالي من الانزيم وحضنت بدرجة حرارة 60 ° م لمدة 20 دقيقة مع الرج المستمر بعدها غسلت الاقمشة بالماء الاعتيادي وجففت .

أختبار كفاءة الانزيم في تحليل بروتينات مخلفات الاسماك

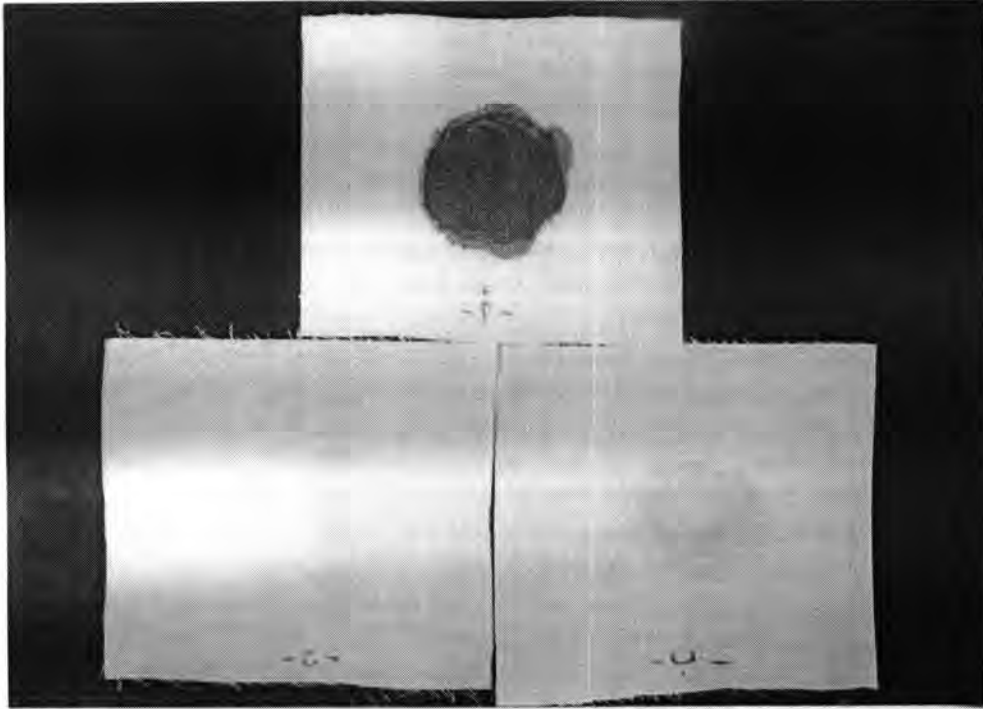
جفف جلد سمك الجري في فرن بدرجة حرارة 60 ° م ثم طحن واضيف الهكسان الى مسحوق بنسبة 5:1 (وزن : حجم) وترك لمدة ساعة مع الرج المستمر ثم رشح وغسل الراسب بالهكسان وترك ليحفظ في جو الغرفة . أخذ (1) غرام من مسحوق جلد الجري واضيف له (100) مليلتر من محلول منظم الترسيب برقم هيدروجيني 9 وحضن في حمام مائي بدرجة حرارة 60 ° م لمدة 10 دقائق ، أضيف (1) غرام من الانزيم الخام المجفف لكل 100 مليلتر من عالق جلد السمك المحضر واستمر حضنها بدرجة حرارة 60 ° م لمدة 5 ساعات سحبت خلالها نماذج من العالق بحجم (2) مليلتر في اوقات معينة واضيف لها 3 مليلتر من محلول ثلاثي كلورو حامض الخليك 5% ونبذ بسرعة 2500xg لمدة 20 دقيقة وقدر البروتين في المحلول الرائق (البروتين الذائب) بالطريقة الموصوفة من قبل (14) ، واذيب الراسب في محلول هيدروكسيد الصوديوم بتركيز 0.05 مولار وتم تقدير البروتين في المحلول (البروتين غير الذائب) .

تقييد انزيم البروتيز القاعدي:

استخدم طريقة التغليف الرقيق (Entrapment) باستخدام الجينات الكالسيوم في تقدير انزيم البروتيز القاعدي المنقى تبعاً للطريقة الموصوفة من قبل (15) إذ تم اضافة 2 مليلتر من مستخلص الانزيم المنقى المحتوي على 100 وحدة / مليلتر الى محلول الجينات الصوديوم ومزج جيداً بالتحريك المستمر لمدة 10 دقائق ، وبعد ذلك سحب الخليط بواسطة محقنة طبية معقمة وتم اضافة المزيج على شكل قطرات في اناء يحتوي على محلول كلوريد الكالسيوم البارد لتكوين حبيبات بقطر 3 ملم ، وترك الحبيبات لتتصلب وبعدها غسلت عدة مرات بمحلول كلوريد الكالسيوم لازالة بقايا الانزيم غير المرتبط وبعدها تم تقدير الفعالية الانزيمية للانزيم المقيد وعلى مدد زمنية مختلفة تضمنت 60 يوم إذ اضيف 0.1 غرام من الانزيم المقيد الى 1 مليلتر من محلول 0.8% كازين برقم هيدروجيني 9 وحضنت الخليط في حمام المائي بدرجة حرارة 60 ° م لمدة 10 دقائق وبعدها تم اضافة 2 مليلتر من محلول 10% ثلاثي كلور حامض الخليك وقدرت الفعالية الانزيمية في المحلول الرائق بعد عملية النبذ .

النتائج والمناقشة

تم انتاج البروتيز القاعدي من العزلة المحلية *B. stearothermophilus* AEAL2 في الوسط الصلب وبلغت الفعالية النوعية 789 وحدة / ملغم بروتين بعد مرور 48 ساعة ، وقد وجد كل من (16) بان افضلية استخدام تخمرات المواد الصلبة في انتاج البروتيز إذ بلغت الفعالية الانزيمية للبروتيز المنتج من بكتريا *Streptomyces rimosus* باستخدام التخمرات الحالة الصلبة 26.7 وحدة / مليلتر . أبدى أنزيم البروتيز القاعدي المنتج من العزلة المحلية *B. stearothermophilus* AEAL2 كفاءة جيدة في ازالة بقع الدم من الاقمشة القطنية البيضاء عند نقعها بمحلول الانزيم خلال 20 دقيقة بدرجة حرارة 60 ° م مقارنة بالقماش الذي تم نقعه بماء الحنفية (الشكل 1) ، وأن أنزيمات البروتيز الموجودة في المنظفات تعمل على ازالة الصبغات المرئية (هيموغلوبين الدم)



شكل-1 : كفاءة أنزيم البروتين القاعدي في إزالة بقع الدم من قطع القماش المعاملة بانزيم. أ-معاملة السيطرة

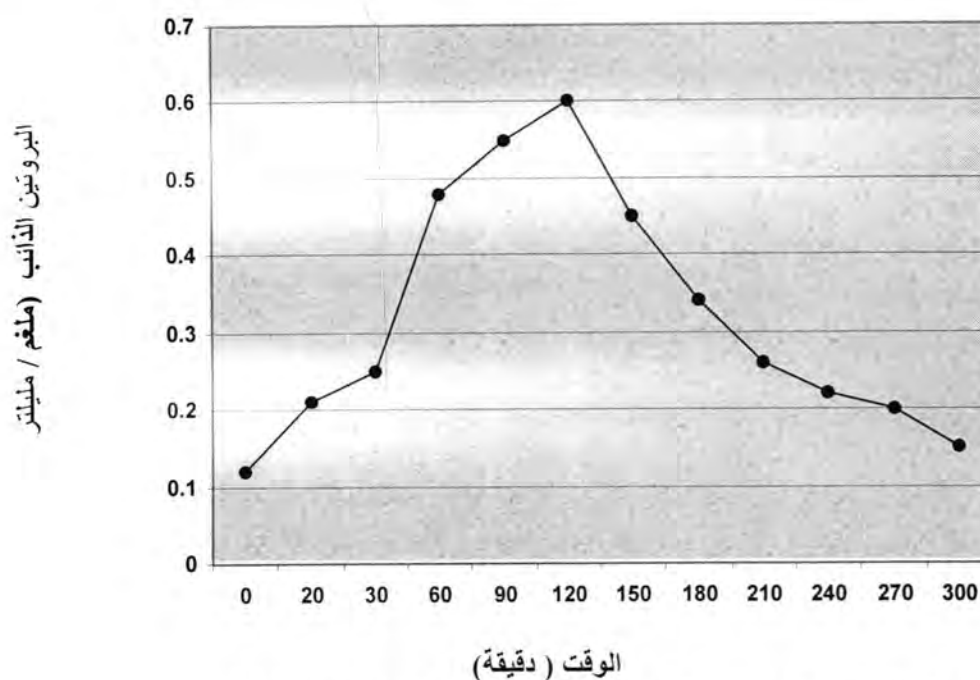
ب- المعاملة بالماء المقطر فقط

ج- معاملة بالماء المقطر + أنزيم البروتين القاعدي

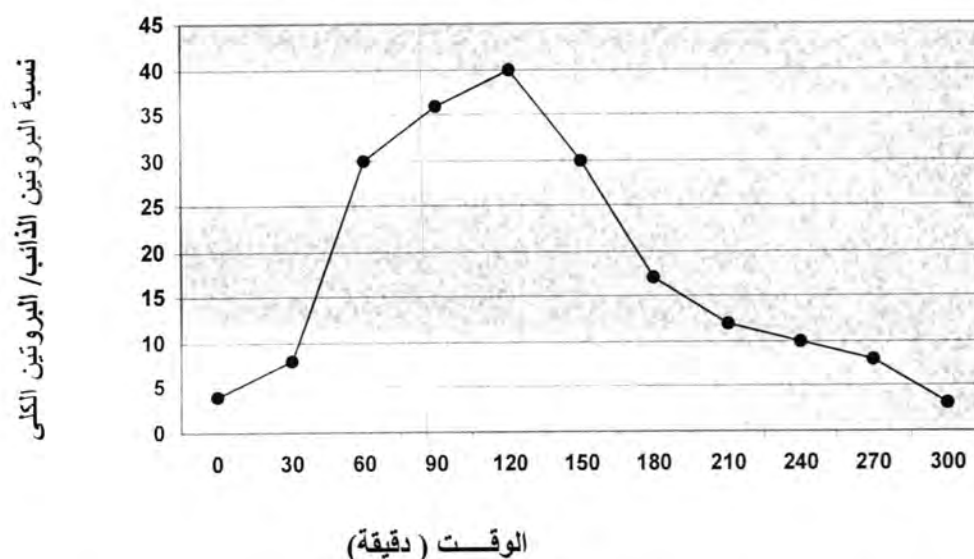
وكذلك تزيل البروتينات غير المرئية في الملابس كالبروتينات التي تأتي من بقايا المواد الغذائية كالحليب والبيض واللحم وتعمل هذه البروتينات الى تكتل المواد المختلفة على القماش اثناء مرحلة الغسل إذ تتحد البروتينات المترسبة مع التراب مما يؤدي الى صعوبة ازالتها وظهورها بلون رمادي وتبدو الملابس كأنها غير نظيفة بعد عدة غسلات ،وقد اشير الى ان عملية النقع هو الاسلوب الامثل لتنظيف الملابس إذ ثبت انها تساعد في عمل ونشاط الانزيمات وبناء على ذلك فقد اصبح استخدام الانزيمات في اجهزة الغسيل والتنظيف المنزلي وسيلة مؤكدة وناجحة (17).

ومن الصفات التي يجب ان تتصف بها البروتين المضافة الى مواد الغسيل هي مقاومتها للارقام الهيدروجينية المرتفعة لهذه المواد وأن تتحمل درجات حرارة عالية وظروف الغسل الاخرى (10) . لقد توجه الاهتمام الى البروتين القاعدي المايكروبي سواء المنتجة من البكتريا أو الاعفان لما تتميز به من صفات تؤهلها للاستخدام في مواد التنظيف (18) . إذ تمكن (19) من انتاج البروتين القاعدي ذي الرقم الهيدروجيني الامثل 10.5 من بكتريا *B. sphaericus* ومن أستخدامه في المنظفات إذ تم خلط هذا الانزيم مع ثلاثة انواع من المنظفات التجارية واطهر الانزيم ثباتية عالية في إحدى هذه المنظفات التجارية الاخرى المستخدمة.

أستخدم البروتين القاعدي المنتج من العزلة المحلية *B. stearothermophilus* AEAL2 في تحليل بروتينات جلد سمك الجري ، إذ يلاحظ من (الشكل 2) زيادة في تركيز المواد البروتينية الذائبة بزيادة الوقت إذ بلغت نسبتها عند درجة 60 °م لمدة 90 دقيقة 0.55 ملغرام بروتين / مليلتر ولوحظ عند زيادة المدة الزمنية الى 120 دقيقة حصلت زيادة طفيفة في تركيز المواد البروتينية الذائبة إذ بلغت 0.57 ملغرام بروتين / مليلتر . كذلك درست العلاقة بين المدة الزمنية ونسبة التحلل للبروتين الذائب / البروتين الكلي (الشكل 3) إذ وجد أن هذه النسبة تزداد بزيادة المدة الزمنية إذ بلغت 36-38% بعد مرور 90-120 دقيقة.



شكل 2: استخدام انزيم البروتيز القاعدي في إنتاج المتحللات البروتينية .



شكل 3: استخدام البروتيز القاعدي المنتج من العزلة المحلية *B. steurothermophilus* AEAL2 في إنتاج المتحللات البروتينية .

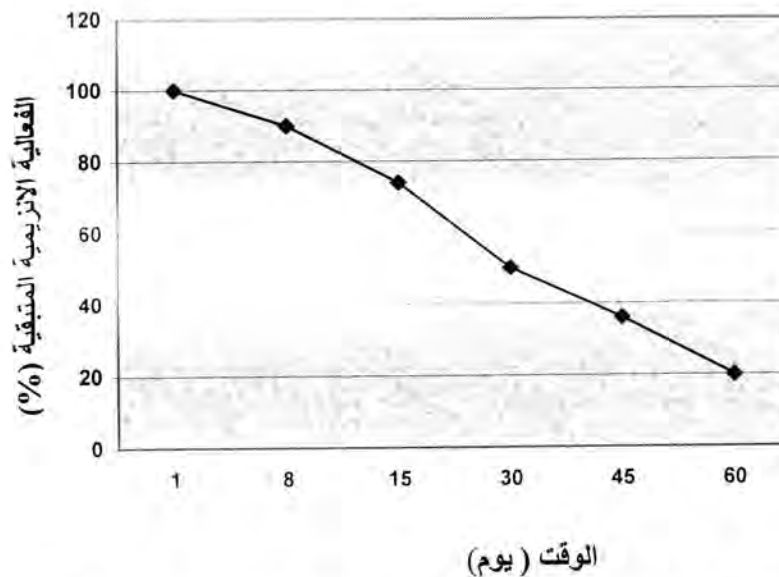
ويتبين من هذه النتائج أن نشاط الانزيم في زيادة إذابة بروتين السمك يصل أقصاه خلال ساعتين إذ يقوم الانزيم خلالها بتكسير الاواصر الببتيدية لبروتينات السمك وتحرير مخلفات الاحماض الامينية والبيبتيدات الصغيرة الذائبة في الوسط ويعزى تناقص تركيز البروتين الذائب ونسبة التحلل بعد ذلك الى الدور الاخر الذي يقوم به الانزيم وهو اعادة ربط البيبتيدات المتحررة (Transpeptidation) عشوائياً ويطلق على هذا مصطلح البلاستين . واستنتج المختصون بدراسة البروتينات ان البلاستين يمثل عكس عملية التحلل التي تقوم بها أنزيمات البروتيز .

أستخدم البروتيز القاعدي المنتج من بكتريا *B. licheniformis* والذي يطلق عليه اسماً تجارياً وهو (Alcalase) في إنتاج المتحللات البروتينية من سمك يعود الى جنس السردين (Herring) إذ أمتاز هذا الانزيم باعطاء نسبة عالية من البروتينات الذائبة إذ تم ملاحظة زيادة في نسبة التحلل بزيادة

المدة الزمنية أذ بلغت اقصاها 36% بعد 60 دقيقة (20) . وقد تم الاستفادة من قدرة البروتيناز على إنتاج المتحللات البروتينية في تطبيقات عديدة فالتحللات البروتينية تعطي دعماً تغذوياً للأعلاف الحيوانية والاعذية الفقيرة أذ وجد أن المتحللات البروتينية المنتجة من لحم سمك القد المعامل بالبروتيناز تحتوي على نسبة عالية من البروتين الذائب تصل الى 63% ودلت نتائج تحليل الحوامض الامينية وجود نسبة عالية من الحوامض الامينية الاساسية، واثبت الفحص الحيوي كفاءة هذه المستحضرات في تغذية الفران إذ ازداد وزنها عند اطعامها الاعذية الحاوية على المتحللات كالحنطة والذرة الصفراء والرز مقارنة بالاعذية الخالية منها (21)

ولقد استخدم (22) المركبات البروتينية المعاملة بأنزيم الببسين في تغذية أفراخ دجاج اللحم أذ أعطى متوسط استهلاك العلف الاسبوعي للافراخ اعلى معدل مقارنة مع المركز البروتيني السمكي المحلي والمركز البروتيني الاجنبي المستوردة .

في ما تقدم من التطبيقات تم استخدام الانزيم الحر وقد يكون من الانسب في بعضها استخدام الانزيم المقيد لما في ذلك من مميزات مفيدة سبق الاشارة اليها في استعراض المراجع. لذا اجريت معاملة لتقييد أنزيم البروتيناز القاعدي المنتج من العزلة المحلية *B. stearothermophilus* AEAL2 بالطريقة الموصوفة من قبل (23) إذ تضمنت استخدام الجينات الصوديوم في تقييد هذا الانزيم ، والشكل (4) يوضح نتائج خزن الانزيم المقيد لمدة 60 يوماً في درجة حرارة 4 °م أذ أشارت النتائج التي تم الحصول عليها الى ان الفعالية الانزيمية بدأت تتناقص من 100% في اليوم الاول من الخزن الى 50% بعد مرور 30 يوماً . لم يرد في الدراسات التي أهتمت بتقييد البروتيناز استخدام الجينات الصوديوم ولكن هنالك دراسات عديدة اثبتت كفاءة استخدام الجينات الصوديوم في تقييد الانزيمات أو الخلايا لما تمتاز به هذه الطريقة من صفات جعلتها ملائمة للاستخدام على المستوى الصناعي أذ تكون هذه الطريقة بسيطة وسهلة وغير مكلفة ولا تحتاج الى أجهزة أو معدات معقدة وقلة تأثرها بالتغيرات البيئية في وسط الإنتاج (24) .



شكل 4- : تأثير فترة الخزن على ثابت البروتيناز القاعدي المقيد المنتج من العزلة المحلية *B. stearothermophilus* AEAL2 .

لقد تم تقييد العديد من الانزيمات منها الكراتينيز (Keratinase) (وهو احد أنواع انزيمات البروتيناز) المنتج من بكتريا *B. licheniformis* PWD-1 باستخدام كرات من الزجاج وأمتاز الانزيم المقيد بثبات عالٍ تجاه الحرارة العالية والارقام الهيدروجينية المتطرفة كما أحتفظ الانزيم بـ 40% من

الفعالية الاصلية بعد سبعة أيام عند درجة حرارة 50 مئوية (24). وتستخدم طرائق أخرى للتقييد منها مواد سائدة كالطين وقشور البيض وغيرها والتي تعتمد على تكوين روابط تساهمية مما تزيد من حماية وثبات الانزيمات كما في تقييد البروتينات المنتج من *Thermomonospora fusco* YX تساهمياً باستخدام السيفاروز Sepharose 4B المنشط بمادة Cyanogen bromide واثبت أن عملية التقييد عملت على حماية الانزيم من التحلل الذاتي autolysis عند درجة حرارة عالية 85 °م ورقم هيدروجيني 8.5 ، أزدادت ثباتية الانزيم بعد التقييد كما تم ملاحظة احتفاظ الانزيم بفعاليته إذ عمل على تحليل كل من الالبومين البقري وبيتا لاكتوكلوبولين (25). وكذلك تمكن (26) من تقييد البروتينات المنتج من بكتريا *Pseudomonas aeruginosa* بواسطة الارتباط التساهمي باستخدام Hydroxyproupyl methyl cellulose acetate succinate إذ أظهرت النتائج احتفاظ الانزيم المقيد عند خزنه بدرجة حرارة 4 °م بـ 50% من فعالية الاصلية بعد 12 يوماً للانزيم المقيد و 8 أيام للانزيم الحر. ومن الدراسات التي اثبتت كفاءة استخدام الجينات الكالسيوم في التقييد إذ تم تقييد الالفـ الاميليز (α-amylase) المنتج من بكتريا *B. stearothermophilus* MAG3 بطريقة الاقتناص باستخدام الجينات الكالسيوم إذا احتفظ الانزيم بما يقارب 50% من فعاليته بعد شهر من خزنه بدرجة حرارة 4 °م (27). كما قام (28) بتقييد الكاتينيز (Chitinase) المنتج من بكتريا *Bacillus sp.* BG-11 باستخدام الجينات الكالسيوم إذ احتفظ الانزيم 50% من فعالية الاصلية بعد 8 أسابيع عند خزنه بدرجة حرارة 4 °م كما اصبح الانزيم مقاوماً للبروتينات التي تعمل على تحليله في حالة كون الانزيم غير مقيد.

يمكن الاستنتاج من خلال هذه البحث بان البروتينات القاعدي المنتج من العزلة المحلية يمتلك مواصفات جيدة تجعله ملائماً للعديد من التطبيقات الصناعية وخصوصاً في صناعة المنظفات كذلك امكن من قييد الانزيم باستخدام الجينات الصوديوم مما أدى الى زيادة ثباتية الخزنية بالمقارنة مع الانزيم الحر .

المصادر

1. Joshi, G.K. ; Kumar, S. and Sharma, V. Production of moderately halotolerant , SDS stable alkaline protease from *Bacillus cereus* MTCC 6840 isolated from lake nainital, utteranchal state , India. Brazilian J. of Microbiology. 38 . (4) : 1590-1602.(2007).
2. Settakana, P. Solid-state fermentation for water soluble protein enrichment of soybean using mixed cultures Bangkok (Thailand). 190 leaves (Abstract). (1992)
3. Krathumkett, N. Study on potentiality of *Bacillus* fermentation on nutritional value of cotton seed meal Bangkok (Thailand) . 126 leaves. (Abstract). (1987)
4. Yang, S. and Wang, J. Protease and amylase production of *Streptomyces rimosus* in submerged and solid state cultivations. Bot. Bull. Acad. Sin. 40: 259-265(1999).
5. Romero-Gomez, S.J.; Augur, C. and Viniegra-Gonzalez, G.. Invertase production by *A. niger* in submerged and solid-state fermentation. Lett.22: 1255-1258.(2000).
6. Al-Jumaily, E.A, Hibibi, K.A. and Kadhum ,S.E.. Optium conditions for the production of neutral protease from local strain *Aspergillus* Um-samla J. vol.5. (4) :472-481 ((2008).
7. Godfrey, T. and Reichelt, J., Leather. In: Industrial Enzymology (eds. Godfrey, T. and Reichelt, J.) : 437-449, The Nature Press.(1983).

8. samal,B.B.; Karan,B. and Stabinsky,Y. Stability of two novel serine proteinases in commercial laundry detergent formulations. *Biotechnol. Bioeng.*35: 650-652(1990)..
9. Kumar, D.;Bhalla, T.C. Purification and characterization of a small size protease from *Bacillus sp.* APR-4 . *Ind. J.Exp. Biol.* 42: 515-521(2004)..
- 10.Rao,M.B.Tanksale,AM.; Ghatge,M.S. and Deshpande,V.V. Molecular and Biotechnology aspects of microbial.Proteases.*Microbiol. Molecul. Biol. Rev.* 62(3):597-635(1998).
11. Phadatare, S.U.; Srinivasan, M.C. and Deshpande, V.V. High activity alkaline protease from *Conidiobolus coronatus*: enzyme production and compatibility with commercial detergents. *Enzyme Microb. Technol.* 15: 72-76. (1993).
12. **Al-Jumaily**, E.F. ; Daweed, A.W. and Nadir, M.I. Production of Alkaline protease from local *Bacilus stearothermophilus* AEAL2 by soil state fermentation. *Iraqi J. Biotech.*,3, (1): 137-155(2004).
13. Brock, F.M.; Forsberg,C.W. and Buchanan, J.G. Proteolytic activity of remen microorganisms and effects of proteinase inhibitors. *Appl. Environ. Mircobiol.*44:561-569(1982).
14. Whitaker, J.R. and Granum, P.E. An absolute method for protein determination based on difference in adsorbance at 235 and 280 nm. *Analytical Biochem.*109: 156-159(1980).
15. **Guo**, Y.; Lou, F.; Peng,Z.; Yuan, Z. and Korus, R.A. Kinetics of growth and -amylase production of immobilized *B. subtilis* in an air lift bioreator. *Biot. Bioeng.* 35: 99-102(1990).
- 16.Yang,S. And Wang,J. Protease and amylase production of *Streptomyces rimosus* in submerged and soil state cultivations. *Bot. Bull. Acad.Sin.* 40:259-265(1999).
17. Barfoed, H.C. Detergents . In: *Industrial enzymology.* (Eds. Godfrey, T.and Reichelt, T.) : 284-293. The Nature Press. New York. (1983).
18. Becker, M.D. *Industrial biotechnology.* Antenat (2001).
- 19.Singh, J.; Vohra, R.M. and Sahoo, P.K. Alkaline protease from a new obligate alkalophilic isolate of *B.sphaericus*.*Biotechnol.Lett.*21:921-924.(1999).
20. Liceaga-Gesualdo, A.M. and Li-Chan, E.C.Y. Functional properties of fish protein hydrolysate from Herring (*Clupea harengus*).*J.Food Sci.*64(6):1000-1004 (1999).
21. Yanez, E.; Ballester, D. and Monckeberg, F. Enzymatic fish protein hydrolyzate : Chemical composition, Nutritive value and use as a supplement to cereal protein . *J.Food Sci.* 41: 1289-1292(1976).
22. **الخالدي** ، محمد رفيق . استغلال مخلفات المجازر والاسماك في انتاج المركبات البروتينية واختبار كفاءتها . رسالة ماجستير . كلية العلوم . جامعة بغداد . (1998) .
23. Cheetham, P.S,J, Production of isomatulose using immobilized microbial cells. In: *Methods in Enzymology.*(ed. Mosbach, K.)136: part C. :432-454. Academic press. INC.(1987).

24. Lin, X.; Shih, J.C.H. and Swaisgood, H.E. Hydrolysis of feathers keratin by immobilized keratinase . Appl. Environ. Microbol. 62(11): 4273-4275.(1996).
25. Johnson, R.D.; Gusek, T.W. & Kinsella, J.E. Immobilization of the serine protease from *Thermomonospora fusca* YX. J. Agric. Food Chem. 38: 918-922(1990)
26. Oh, Y.; Shih, I.; Tzeng, Y. and Wang, S. Protease produced by *Pseudomonas aeruginosa* K-187 and its application in the deproteinization of shrimp and crabshell wastes. Enzyme Microbial Technol. 27: 3-10.(2000).
27. الصفار ، منتهى عبد الكريم . إنتاج أنزيم ألفا- اميليز من *B. Stearothermophilus* MAG3 بواسطة تخمرات الحالة الصلبة وتنقيته . رسالة ماجستير . كلية العلوم . جامعة بغداد . (1998).
28. Bhushan, B. Production and characterization of a thermostable chitinase from a new alkalophilic *Bacillus* sp. BCII. J. Appl. Microbiol. 88(5):800-808. (2000).

الكشف عن بكتريا *Pseudomonas aeruginosa* المنتجة لأنزيم البييتالاكتاميز المعدني (IMP1) والمعزولة من المرضى في محافظة النجف

محمد فرج المرجاني وأنتصار علي مزعل وميسون حميد اسماعيل
قسم علوم الحياة / كلية العلوم / الجامعة المستنصرية

ABSTRACT

One hundred isolates of *Pseudomonas aeruginosa* were collected from patients in Najaf hospitals for detect IMP-1 Metallo- β -Lactamase production .

The results showed that 66.6% of isolates were resistant to Aztreoname and 5% of these isolates were resistant to Imipenem, and these isolates were selected to detect the ability to Metallo β -lactamases production (MBLs) . Four isolates were able to produce MBLs ,and these isolates were tested to bla_{IMP-1} by using polymerase chain reaction(PCR) and using Primer :

(F) 5- ACC GCA GCA GAG TCT TTG CC – 3

(R) 5-ACA ACC AGT TTT GCC TTA CC _ 3

None of isolates appeared to carry bla_{IMP-1} gene after electrophoresis of the results on 1.2 % agarose .

الخلاصة

تم عزل 100 عزلة تعود لبكتريا *Pseudomonas aeruginosa* من أصابات مختلفة من مرضى من محافظة النجف لغرض الكشف عن انتشار الأنزيم IMP1 وهو من انزيمات البييتالاكتاميز المعدنية Metallo β - lactamases (MBLs) والذي يمنح البكتريا المنتجة له قابلية مقاومة مضادات Carbapenems . أظهرت 66.6 % من العزلات مقاومتها لمضاد Aztreoname و 5% منها كانت مقاومة لمضاد Imipenem وقد اختبرت لغرض الكشف عن انتاج انزيم IMP1 , كان لأربع عزلات القابلية على انتاج هذه الانزيمات , وقد انتخبت للكشف عن الجين bla_{IMP-1} المشفر لأنزيمات MBLs باستخدام تقنية التفاعل التضاعفي لسلسلة الدنا (PCR) واعتماد البادئ :

(F) 5- ACC GCA GCA GAG TCT TTG CC – 3

(R) 5-ACA ACC AGT TTT GCC TTA CC _ 3

وبعد ترحيل الناتج على هلام الأكاروز بتركيز 1.2 % لوحظ عدم ظهور أي حزمة ناتجة عن عملية التضاعف في إشارة الى عدم ارتباط البادئ مع التسلسل المكمل له في دنا القالب .

المقدمة

يعد إنتاج أنزيمات البييتالاكتاميز أحد اهم وسائل مقاومة البكتريا للمضادات الحيوية (1) , وقد ازدادت خطورة هذه الانزيمات بعد ظهور أصناف جديدة وأكثر خطورة منها مثل انزيمات البييتالاكتاميز الواسعة الطيف Extended – Spectrum β -lactamases (ESBLs) وأنزيمات البييتالاكتاميز المعدنية Metallo β - lactamases (MBLs) , ان انتاج انزيمات MBLs يعد تطورا بمقاومة المضادات الحيوية في بكتريا *Pseudomonas aeruginosa* وبقية البكتريا السالبة لصيغة كرام (2) فهي تمنح البكتريا المنتجة لها صفة مقاومة مضادات البييتالاكتام وواسعة الطيف ومن ضمنها مجموعة الكاربينيم Carbapenems ومثاله مضاد Imipenem , وهناك اربعة انواع رئيسية لأنزيمات MBLs هي IMP وVIM وSPM وGIM (3) , اكتشف انزيم IMP اولا في اليابان سنة 1990 (4) , ثم في اوربا بعد سنة 1990 (5) وفي سنة 1997 تم عزل البكتريا المنتجة لأنواع VIM-1 في ايطاليا (6) والمنتجة ل SPM في البرازيل في نفس السنة (7) , ثم اكتشفت بعد ذلك الانواع البقية من انزيمات MBLs في مناطق مختلفة من العالم .

درست في العراق انزيمات البييتالاكتاميز بشكل عام , لكن الدراسات حول أنزيمات البييتالاكتاميز المعدنية MBLs تعد قليلة رغم أهميتها من الناحية الطبية , لذا جاءت هذه الدراسة لتهدف الى دراسة انتشار الأنزيم IMP1 المنتج من بكتريا *Pseudomonas aeruginosa* والكشف عن الجين المشفر له باستخدام تقنية التفاعل التضاعفي لسلسلة الدنا PCR .

المواد وطرائق العمل

1- العزلات البكتيرية : تم الحصول على 100 عزلة تعود لبكتريا *Pseudomonas aeruginosa* من اصابات مختلفة من مرضى في محافظة النجف وتم تشخيص العزلات اعتمادا على الفحوصات المظهرية والكيموحيوية التي وردت في (8) .

2- اختبار حساسية العزلات للمضادات الحيوية :

(أ) اختبرت حساسية العزلات للمضادات الحيوية التالية بطريقة الاقراص باستخدام وسط اكار مولر هنتون :-

Co- trimoxazole , Imipenem , Cefoxitin , Nalidix acid , Pipracillin, Ampicillin , Amoxycillin , Cephalexin , Cefixime , Gentamicin , Amikacin and Aztreoname .

(ب) تم تحديد التركيز المثبط الأدنى لمضادي الأمينيم والأز تريونام بطريقة التخفيف المتضاعفة المتسلسلة في اكار مولر هنتون.

3- اختبار قابلية العزلات على انتاج انزيمات البيتا لكتاميز المعدنية :-

اعتمدت طريقة Yong وجماعته (9) لأختبار قابلية العزلات المقاومة لمضادات السيفوتاكسيم و السفتازديم والامينيم على أنتاج انزيمات البيتا لكتاميز المعدنية حيث تم تحضير عالق بكتيري (10⁶ خلية/مل) لكل عزلة تحت الاختبار ثم فرشت على وسط مولر هنتون الصلب، بعدها وضع قرصين لمضاد الامينيم (10 مايكروغرام/قرص) على سطح الاكار . وبعد تحضير 0.5 مولر EDTA ، نقل (10) مايكرو ليتر من محلول EDTA لأحد القرصين المذكورين أعلاه (قرصي مضاد الامينيم) ، وبعد الحضانة ب 37 °م لمدة 18 ساعة تم مقارنة مناطق التثبيط حول قرص الامينيم لوحده و الامينيم مع EDTA .

4- دراسة المحتوى البلازميدي :

درس المحتوى البلازميدي للعزلات المنتجة لأنزيمات البتا لكتاميز المعدنية حسب طريقة (10).

5- الكشف عن الجين bla_{IMP-1} باستعمال تقنية PCR :-

تم اختيار العزلات التي اظهرت مقاومة لمضادات الامينيم والاز تريونام والتي كان لها القابلية على انتاج انزيمات البيتا لكتاميز المعدنية لغرض الكشف عن وجود الجين bla_{IMP-1} باستعمال تفاعل PCR وحسب طريقة (11) باستعمال البادئ :

(F) 5- ACC GCA GCA GAG TCT TTG CC – 3

(R) 5-ACA ACC AGT TTT GCC TTA CC – 3

6- الاقتران البكتيري :-

أجريت تجارب الاقتران البكتيري بين العزلات المنتجة لأنزيمات البيتا لكتاميز المعدنية كعزلات واهبة والعزلة القياسية E.coli MM 294 كعزله مستلمة لاختبار قابلية انتقال صفة انتاج هذه الانزيمات الى العزله المستلمة بالاقتران البكتيري ، واجريت تجارب الاقتران حسب طريقة (12).

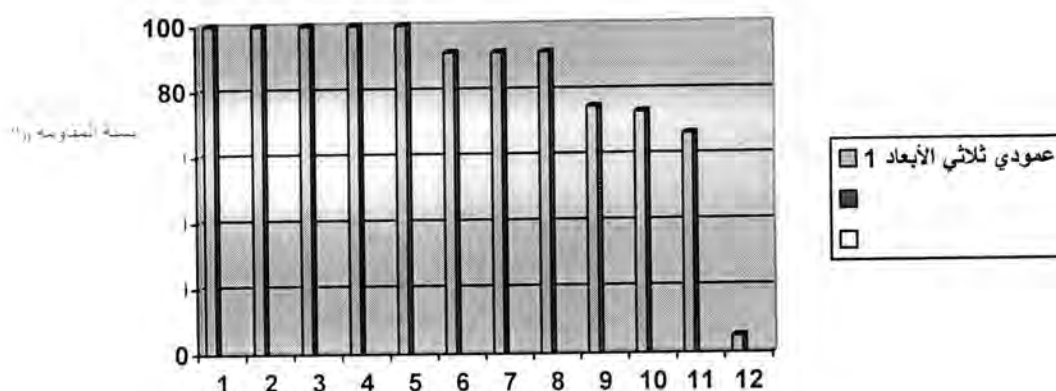
النتائج والمناقشة

يعد مضاد الامينيم من المضادات الفعالة للاصابات المتعلقة بالمستشفيات وهو عال الثبات بوجود انزيمات البيتا لكتاميز ومن صفاته المهمة كونه جزيئة صغيرة قادرة على عبور قنوات Porins في الغشاء الخارجي للبكتريا (13) ، يعد أنتاج أنزيمات البيتا لكتاميز أحد اهم وسائل مقاومة البكتريا للمضادات الحيوية خاصة أنزيمات النوع IMP1 β -lactamases ، في دراستنا الحالية اختبرت حساسية عزلات بكتريا *Pseudomonas aeruginosa* لعدد من المضادات الحيوية لغرض انتخاب العزلات المقاومة لمضادات البيتا لكتام لأختبار قابليتها على انتاج انزيمات البيتا لكتاميز المعدنية (MBLs) .

اظهرت النتائج (شكل 1) وجود مقاومة عالية بين العزلات لمضادات Ampicillin و Cefoxitin و Amoxycillin و Cefixime و Cephalexin ، حيث بلغت نسبة المقاومة 100% لهذه المضادات ، وكانت المقاومة عالية كذلك لمضادات Co- trimoxazole و Nalidix acid و Gentamicin حيث بلغت 91.6% لهذه المضادات وبلغت نسبة المقاومة بين العزلات 75% لمضاد pipracillin و 66.6% لمضاد Aztreoname و كانت اقل نسبة مقاومة هي لمضاد الامينيم وبلغت 5% .

أزدادت خطوره أنزيمات البيتا لكتاميز بعد حصول طفرات وراثية في الجينات التركيبية المشفرة لأنزيمات البيتا لكتاميز الاساسيه من عائلته TEM و SHV ، مما أدى الى ظهور أصناف جديدة وأكثر خطوره من

هذه الانزيمات مثل انزيمات البييتالاكتاميز واسعه الطيف Extended-Spectrum β -Lactamases (ESBLs) وأنزيمات البييتالاكتاميز المعدنية Metallo β -lactamases (MBLs) التي لها القابلية على تحطيم مضادات البييتالاكتام واسعه الطيف مثل Imipenem و Meropenem أضافه الى المضادات الاخرى (2).



المضادات الحيوية

شكل -1: نسبة المقاومة بين عزلات بكتريا *Pseudomonas aeruginosa*.

(1) Cefoxitin , (2) Ampicillin , (3) Amoxycillin , (4) Cephalexin , (5) Cefixime , (6) Co- trimoxazole , (7) Nalidix acid , (8) Gentamicin , (9) Pipracillin , (10) Amikacin (11) Aztreoname (12) Imipenem

اجري اختبار الكشف عن قابلية العزلات على انتاج انزيمات البييتالاكتاميز المعدنية (MBLs) بين العزلات التي اظهرت مقاومة لمضادات الازتريونام والامينيم باستخدام EDTA كمثبطات لانزيمات البييتالاكتاميز المعدنية , ذكر (14) ان استعمال مثبطات انزيمات البييتالاكتاميز المعدنية مثل CuCl_2 و FeCl_2 و EDTA ومركبات thiol مثل mercaptoacetic acid و mercaptoethanol و 2- mercaptopropionic acid يعطي نتيجة جيدة للكشف عن انزيمات IMP-1 .

اظهرت النتائج قابلية اربعة عزلات على انتاج هذه الانزيمات وقد اختيرت للكشف عن وجود الجين $\text{bla}_{\text{IMP-1}}$ المشفر لانزيمات IMP1 باستخدام تقنية PCR ، وبعد ترحيل الناتج على هلام الأكاروز بتركيز 1.2 % لوحظ عدم ظهور اي حزمة ناتجة عن عملية التضاعف في اشارة الى عدم ارتباط البادئ مع التسلسل المكمل له في دنا القالب.

من جانب اخر لم نلاحظ انتقال صفة انتاج انزيمات البييتالاكتاميز المعدنية الى السلالة المستلمة . هذا يتفق مع (4) الذي وجد ان الجينات المسؤولة عن انزيمات البييتالاكتاميز المعدنية نوع IMP-13 التي درسها الباحث لا تنتقل بالاقتران وتكون محمولة على الكروموسوم . كذلك ذكر (15) ان البلازميد pVA758 الذي يحمل جين $\text{bla}_{\text{IMP-12}}$ لم ينتقل بالاقتران بين عزلات *Pseudomonas putida* و *E. coli*.

المصادر

- 1.Prescott J.F.;Baggot,J.D.& Walker,R.D"Antimicrobial Therapy in Veterinary Epidemiology, 3rd ed. Iowa State University Press.(2000).
- 2.Nordmann,P.,&Poirel,L.Emerging carbapenemases in gram-negative aerobes. Clin. Microbiol.Infect. 8:321-331(2002)
- 3.Shibata,N.;Doi,Y.;Yamane,K.;Yagi,T.;Kurokawa,T.;Shibayama,K.;Kato,H.Kai, K.&Arakawa,Y.PCR Typing of Genetic Determinants for Metallo- β -Lactamases and Integrases Carried by Gram-Negative Bacteria Isolated in Japan, with Focus on the Class 3 Integron.J.of Clinic. Microb.,41(12):5407-5413.(2003).

- 4.Osana,E.;Arakawa,Y.;Wacharo,R.;Ohata,M.&Kato,N.Molecular characterization of an enterobacterial metallo- β -lactamase found in a clinical isolate of *Serratia marcescens* that shows imipenem resistance .Antimicrob. Agent. Chemother.38:71-78(1994)..
- 5.Toleman,M.A.;Biedenbach,D.;Bennett,R.N.;Jones,N.&Walsh,T.R.Genetic characterization of a novel metallo- β -lactamase gene, bla_{IMP-13}, harboured by a novel Tn5051-type transposon disseminating carbapenemase genes in Europe: report from the SENTRY worldwide antimicrobial surveillance programme.J. Antimicrob. Chemother. 52:583-590(2003).
- 6.Laurettil, L.; Riccio, M. L. ; Mazzariol, G. ;Cornaglia, G.; Amicosante, R. Fontana, G. and Rossolini,M. Cloning and characterization of bla_{VIM}, a new integron-borne metallo- β -lactamase gene from a *Pseudomonas aeruginosa* clinical isolate. Antimicrob. Agents Chemother. 43:1584-1590(1999).
- 7.Toleman, M. A.; Simm, T. A.; Murphy, A. C. ; Biedenbach, R. N. Jones, and Walsh,T.R. Molecular characterization of SPM-1, a novel metallo- β -lactamase isolated in Latin America: report from the SENTRY antimicrobial surveillance programme. J. Antimicrob. Chemother. 50:673-679(2002).
- 8.Greenwood,D.;Slack,R.C.and Peutherer,J.F.Medical Microbiology. (Sixteenth ed.). Churchill Livingstone(2002).
- 9.Yong, D.; Lee, K.; Yum, K.; Shin, H.; Rossolini, G. and Chong Y. Imipenem-EDTA Disk Method for Differentiation of Metallo- β -Lactamase-Producing Clinical Isolates of *Pseudomonas* spp. and *Acinetobacter* spp. J. of Clinic. Microbiol., 40(10) :3798-3801(2002).
10. Sambrook,J.; Fritsch,E.F. and Maniatis,E ., Molecular Cloning .2nd ed. Cold Spring Harbor Laboratory Press,N.Y. (1998).
- 11.Johann D.D.;Pitout,D.;Daniel,B.;Gregson,B.;Poirel,L.;Jo-Ann McClure, Le,P. and Church ,D.L. Detection of *Pseudomonas aeruginosa* Producing Metallo- β -Lactamases in a Large Centralized Laboratory J.of Clinic.Microbiol.,43(7):3129-3135.(2005).
- 12.Pagani,L.;Colinon,C.;Migliavacca,R.;Labonia,R.;Docquier,J.Nucleo,E.;Spalla, M.; Bergoli, M. and Rossolini ,G. Nosocomial Outbreak Caused by Multidrug-Resistant *Pseudomonas aeruginosa* Producing IMP-13 Metallo- β -Lactamase J. of Clinic. Microbiol.,43(8): 3824-3828(2005).
- 13.Chen,H.P.;Chen,T.L.;Lai,C.H.;Wong,W.W.;Yu,K.W.and Lia,C.,X. Predictors of mortality in *Acinetobacter baumani* bacteremia.J.Microb.Immunol.Infect.38 (2):127-36.(2005).
- 14.Arakawa,Y.;Shibata,N.;Shibayama,H.;Kurokawa,K.;Yagi,T.;Fujiwara,H.&Goto , M.Convenient test for screening metallo- β -lactamase-producing gram-negative bacteria by using thiol compounds. J. Clin. Microbiol. 38:40-43(2000).
- 15.Docquier, J.; Riccio, M.; Mugnaioli, C.; Luzzaro, F. Endimiani, A. ; Toniolo, A.;Amicosante,A.and Rossolini,G.IMP-12,a New Plasmid-Encoded Metallo - β -Lactamase from a *Pseudomonas putida* Clinical Isolate.J. Antimicrob. Agents and Chemother., 47(5) : 1522-1528(2003).

استخدام بعض المطفرات على بكتريا حامض اللاكتيك لتحسين الفعالية التثبيطية ضد البكتريا المرضية والتألفة للأغذية

¹ عبد الواحد باقر، ² نبراس نزار محمود، ² سمير فتح الله سمعان

¹ قسم التقنية الاحيائية - كلية العلوم - جامعة النهرين

² قسم علوم الحياة - كلية العلوم - الجامعة المستنصرية

ABSTRACT

Susceptibility of four LAB isolates, who possessed inhibitory activity against test bacteria, were examined toward (13) common antibiotics. All of them resistant to Streptomycin, Gentamicin, Cephotoxime, Ciprofloxacin, Pencilline – G and Co – Triamoxazole. While they differed in their susceptibility for other antibiotics.

Plasmids of the tow isolates (*Lb. fermentum* and *Lc. raffinolactis*) were isolated and cured to investigate whether properties of bacteriocin production and inhibitor activity were on plasmids. Results Showed that property of the inhibitory activity were located on their plasmids. After the two isolates were mutated by Ultra Violet radiation, their inhibitory activity was increased against the test bacteria, especially after subjecting *Lc. raffinolactis* for (5) sec. and the isolated *Lb. fermentum* for (20) sec. (wave length 254 nanometer) When *Lc. raffinolactis* isolate was subjected to N₂-laser (weave length 337.1 nanometer) with the orange acridine for (5) min and 6 pulses/sec., its inhibitory activity was increased after grown in MRS broth compared to that mutated by orange acridine alone.

الخلاصة

لدى اختبار حساسية أربع عزلات من بكتريا حامض اللاكتيك (*Lactococcus lactis*, *Lactobacillus fermentum*, *Lactobacillus plantarum*, *Lactococcus raffinolactis*) والتي أعطت فعالية تثبيطية ضد بكتريا الإختبار تجاه (13) مضاداً حيويًا، كانت جميعها مقاومة لمضادات الستربتومايسين وجنتاميسين وسيفوتاكسيم وسبروفلوكاسين وبنسليين – ج و كوتراي موكسازول، فيما تباينت حساسيتها لبقية المضادات المستعملة. تم عزل بلازميدات العزلتين *Lc. raffinolactis* و *Lb. fermentum* كونهما أعطتا أفضل فعالية تثبيطية، وتمت دراسة تحييد بلازميداتها للتحري عن كون صفة انتاج البكتريوسين أو الفعالية التثبيطية محمولة عليها. أظهرت النتائج أن صفة التثبيط كانت محمولة على البلازميدات. كما وأخضعت العزلتين للتطهير بالأشعة فوق البنفسجية حيث أدى إلى زيادة الفعالية التثبيطية تجاه بكتريا الإختبار ولا سيما بعد تعريض *Lc. raffinolactis* لمدة (5) ثوان والعزلة *Lb. fermentum* لمدة (20) ثانية (بطول موجي 254 نانوميتر). فيما أخضعت العزلة *Lc. raffinolactis* للتطهير بأشعة الليزر – نتروجين بطول موجي (337.1) نانوميتر مع مادة الاكردين البرتقالي ولمدة تعرض (5) دقائق وبمعدل 6 نبضة/ثانية إلى زيادة الفعالية التثبيطية في وسط MRS (De Man Rogosa Sharpe) السائل مقارنة بتلك المعاملة بمادة الاكردين البرتقالي فقط.

المقدمة

شهدت السنوات الأخيرة اهتماماً كبيراً وملحوظاً للتوسع في مجال تصنيع واستهلاك العديد من منتجات الألبان والأغذية الحاوية على الأحياء المجهرية ذات الفائدة العلاجية، لاسيما تلك المستخدمة في تدعيم أغذية الأطفال الرضع، فضلاً عن استخدامها كمستحضرات طبية لعلاج بعض الحالات المرضية، ومن أهم هذه الأحياء المجهرية هي بكتريا حامض اللاكتيك التي لعبت منذ القدم دوراً أساسياً في إنتاج وحفظ معظم الأغذية المخمرة، وإكسابها النكهة المرغوبة كاللبن الرائب والحليب والفواكه والخضراوات من خلال قدرتها على إنتاج مواد مثبطة لنمو الأحياء المجهرية الملوثة لهذه الأغذية (1,2). وتتصف أغلب هذه الأنواع بكونها أحياء مجهرية تعايشية مما يعزز إمكانية استهلاكها من قبل الإنسان بصورة آمنة وصحيحة، كما وانتشرت الأغذية المخمرة ببكتريا حامض اللاكتيك

انتشاراً واسعاً كونها سهلة الهضم وذات قيمة غذائية عالية (4,3) تتحكم بإنتاج البكتريوسين من قبل البكتريا الموجبة لصبغة غرام بمحددات وراثية محمولة على البلازميدات (5). وتحمل أكثر أنواع *Lactobacillus* عادة واحداً أو أكثر من البلازميدات التي تكون متغايرة بالحجم، ولهذه البلازميدات وظائف عدة أهمها أيض اللاكتوز وإنتاج البكتريوسين (6). وتعدّ بكتريا *Lb.fermentum* من أكثر أنواع بكتريا حامض اللاكتيك شيوعاً في القناة الهضمية للإنسان والحيوان، وتحتوي على بلازميد يعرف PLEM3 بحجم 7.5 كيلو روج قاعدة (7) أما بكتريا *Lactococcus* فقد أشار Stiles و Hastings (8) إلى أن صفة إنتاج البكتريوسين قد تكون محمولة على بلازميد أو كرموسوم هذه البكتريا. للأشعة فوق البنفسجية تأثيرات مختلفة في خلايا البكتريا المستخدمة إذ تؤدي هذه التأثيرات إلى حدوث طفرات أو تأثيرات قاتلة للبكتريا المعرضة لها (9). لكنها تعتمد على عدة عوامل أهمها الطول الموجي ومدة التعرض لها. يعدّ استخدام الليزر في مجالات علوم الحياة من المواضيع التي لاقت اهتماماً كبيراً من الباحثين ومهدت الطريق باتجاه إنجاز عدد من البحوث المتميزة التي فسحت المجال أمام استخدام الليزر في التطبيقات التي شملت فروع علوم الحياة المختلفة (10). كما يؤدي الليزر دوراً مهماً في تحديد كمية فيتامين النياسين (Niacin) اللازم لنمو بكتريا *Lb.plantarum*. وتتم دراسة تأثير دور الليزر من خلال قياس النمو الميكروبي عن طريق ضوء الليزر المشتت بواسطة خلايا البكتريا الذي يتناسب مع نسبة فيتامين النياسين (Niacin) المراد قياسها (11).

جاءت هذه الدراسة لتهدف إلى دراسة المحتوى البلازميدي لعزلات بكتريا حامض اللاكتيك ذات الفعالية التثبيطية وتحديد البلازميدات لمعرفة تأثير ذلك في الفعالية التثبيطية، وتطهير بعض عزلات بكتريا حامض اللاكتيك فيزيائياً وكيميائياً لزيادة فعاليتها التثبيطية ضد بعض البكتريا المسببة لتسمم وتلف الأغذية.

المواد وطرائق العمل

- حساسية عزلات اللاكتيك للمضادات الحيوية

تم نشر (0.1) مل من مزرعة عزلة بكتريا حامض اللاكتيك المنشطة مسبقاً على سطح وسط أكار MRS وباستخدام الناشر الزجاجي وبصورة متجانسة، وبعد ترك الاطباق لتجف بدرجة حرارة الغرفة لمدة (15-20) دقيقة، وضعت أقراص المضادات الحيوية

[Streptomycin, Gentamicin, Chloramphenicol, Co-Triamoxazole, Erythromycin, Tetracycline, Cephotaxime, Amoxicillin, Pencilline-G, Cloxacillin, Ciprofloxacin, Rifampicin, Lincomycin]

وحضنت بحرارة (37) °م ولمدة (24) ساعة بعدها تم قياس أقطار مناطق التثبيط بالمليمتر (12)

- عزل الدنا البلازميدي

أتبعت طريقة Anderson and McKay (13) لعزل بلازميدات بكتريا حامض اللاكتيك، إذ تم التحري عن البلازميدات بالترحيل الكهربائي باستخدام هلام الاكاروز (14).

- تحييد البلازميدات

استخدمت صبغة الاكردين البرتقالية (Acridine orange) وبتراكيز (10, 20, 30, 40, 50) مايكروغرام/مليلتر، إضافة إلى معاملة السيطرة بوصفه عاملاً كيميائياً للتحييد (15)، وأتبع طريقة Tomoeda وجماعته (16) في تحييد البلازميدات باستخدام مادة SDS وبتراكيز (50, 100, 150) (5, 10, 15, 20, 25) مايكروغرام/مليلتر بالإضافة إلى معاملة السيطرة.

- تطهير بكتريا حامض اللاكتيك بالأشعة فوق البنفسجية

استخدمت الطريقة الموصوفة في (3) وذلك بتعريض الخلايا البكتيرية للأشعة فوق البنفسجية ولمدد تعرض (5, 10, 15, 20, 25) ثانية. واستخدمت طريقة عد الاطباق لحساب العدد الحي على وسط أكار MRS، ثم حسبت بالأطباق نسبة التثبيط المئوية على وفق المعادلة الآتية الواردة في (17)

نسبة التثبيط % = (عدد الخلايا/ مل في معاملة السيطرة - عدد الخلايا/ مل بعد التطهير) / (عدد الخلايا / مل في معاملة السيطرة $\times 100$)

ملاحظة:

(عدت نسبة البقاء 100% في معاملة السيطرة)

نُقل كل من النماذج المشعة ونموذج السيطرة والمحلل المنتظم بدون تشجيع إلى أنابيب اختبار احتوى كل منها على وسط MRS السائل. وبعد أن رجت الأنابيب جيداً حضنت بحرارة (37) °م ولمدة (18-24) ساعة ثم اختبرت الفعالية التثبيطية لكل معاملة تعرض.

- تطهير العزلات باستعمال الليزر

لحق وسط MRS السائل في كل من أنابيب الاختبار ببكتريا *Lc. raffinolactis* بنسبة (1%) ثم حضنت الأنابيب لا هوائياً بحرارة (37) °م ولمدة (24) ساعة بعدها رسبت الخلايا بالطرد المركزي (3000 دورة/ دقيقة) ولمدة (15) دقيقة، أهمل الراشح وأخذ الراشب الذي هو عبارة عن الخلايا المترسبة والتي تم غسلها ثلاث مرات بمحلول ملحي (0.85 %) ذو أس هيدروجيني (7)، ثم علقت الخلايا بمحلول Tris- HCl ذو أس هيدروجيني (6)، نقل بعدها (1) مل من المحلول المعلق إلى أنبوبة ابندروف، تم تعريض النموذج إلى أشعة الليزر بمعدل (6) نبضة/ ثانية وبوقت تعريض بلغ (20) دقيقة، ثم أعيدت التجربة بإضافة صبغة الاكردين البرتقالية بتركيز (20) مايكروغرام/ مل (18). ثم عرضت أنابيب ابندروف إلى أوقات تعريض مختلفة (15, 20, 1, 3, 5, 10 دقيقة) وبمعدل (6) نبضة/ ثانية. بعدها رسبت الخلايا المعرضة وغسلت ثلاث مرات بمحلول الفوسفات المنتظم لإزالة تأثير المادة المطهرة، ثم أضيف (5) مل من وسط MRS السائل المعقم للخلايا المترسبة المعاملة والمغسولة. وبعد الحضان بحرارة (37) °م ولمدة (24) ساعة، تم قياس نسبة التثبيط. كما وتم نقل المستعمرات الحية بعد كل تعريض إلى وسط MRS السائل لتحضن بحرارة (37) °م ولمدة (24) ساعة حيث اختبرت فعاليتها التثبيطية.

لمقارنة النتائج مع تلك التي تم الحصول عليها من التطهير بصبغة الاكردين البرتقالية فقط وبدون استخدام أشعة الليزر تمت معاملة الخلايا المترسبة والمغسولة بهذه الصبغة بنفس التركيز السابق وأوقات التعريض ولكن دون تعريضها لأشعة الليزر.

- تحليل النتائج إحصائياً

تم تطبيق تحليل التباين الأحادي (ANOVA) One Way Analysis of Variance للمقارنة بين المعالجات جميعاً واختبار معنوية الفرق فيما بينها.

النتائج والمناقشة

- حساسية عزلات اللاكتيك للمضادات الحيوية.

يتضح من الجدول (1) أن جميع العزلات المستخدمة في هذا الاختبار كانت مقاومة للمضادات Co- ,Pencillin-G, Ciprofloxacin, Cephotaxime, Streptomycin, Gentamicin Triamoxazole كما كانت مقاومة أيضاً للـ *Gloxacilline* و *Lincomycin* باستثناء العزلة *Lc. lactis* إذ بلغ قطر منطقتي التثبيط لها (17, 20) ملم وعلى التوالي. لكن هذه العزلات كانت حساسة لمضاد *Chloramphenicol*، عندما أدى إلى تثبيط بلغت أقطاره (20) ملم للعزلة *Lb. plantarum* و (19) ملم لـ *Lc. lactis* و (15) ملم لـ *Lc. raffinolactis* باستثناء العزلة *Lb. fermentum* التي كان تأثيرها ضعيفاً بهذا المضاد بقطر تثبيط بلغ (10) ملم فقط. أما بالنسبة لمضاد *Rifampicin* فقد كان تأثير العزلتين *Lb. plantarum* و *Lb. fermentum* ضعيفاً إذ لم يبلغ معدلاً قطري منطقة التثبيط لكلا العزلتين سوى (9, 10) ملم على التوالي. وتباين تأثير العزلتين بمضاد *Erythromycin* حيث بلغ معدل قطر منطقة التثبيط (15, 17) على التوالي.

استخدام بعض المطفرات على بكتريا حامض اللاكتيك لتحسين الفعالية التثبيطية ضد البكتريا المرضية والتألفة للأغذية
عبد الواحد ونبراس وسمير

جدول 1- حساسية عزلات بكتريا حامض اللاكتيك لعدد من المضادات الحيوية

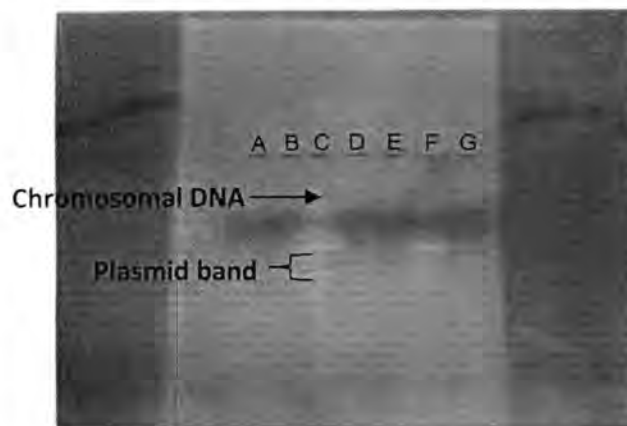
قطر منطقة التثبيط (مليمتر)													المضاد الحيوي
Lincomycin	Erythromycin	Co- Triamoxazole	Pencilline G	Cloxacilline	Ciprofloxacine	Rifampicin	Tetracycline	Cephataxime	Amoxicillin	Streptomycin	Gentamicin	Chloramphenicol	العزلة
20	9	R	R	17	R	R	21	R	22	R	R	19	<i>Lc. lactis</i>
R	11	R	R	R	R	R	R	R	20	R	R	15	<i>Lc. raffinolactis</i>
R	17	R	R	R	R	9	25	R	23	R	R	20	<i>Lb. plantarum</i>
R	15	R	R	R	R	10	22	R	22	R	R	10	<i>Lb. fermentum</i>

R = المقاومة للمضاد، الأرقام = الحساسية للمضاد

أشار Givers وجماعته (12) إلى أن بكتريا *Lactobacillus* المعزولة من أنواع مختلفة من الصوصج المتخمّر كانت مقاومة لمضادات *Pencilline-G*, *Erythromycin*, *Tetracycline*, *Rifampicin*, أكدت المراجع العلمية على دراسة حساسية بكتريا حامض اللاكتيك تجاه المضادات الحيوية بغية التأكيد على ضرورة امتلاك الأنواع المستعملة كمواد لصفة مقاومتها لأكثر عدد ممكن من المضادات الحيوية، كذلك اللجوء عند الضرورة إلى المنتجات اللبنية الحاوية على أنواع من بكتريا (LAB) العلاجية المقاومة للمضادات الحيوية بهدف إعادة توطينها وتوازنها داخل الأمعاء (19).

- عزل الدنا البلازمي

بإستخدام طريقة (1983) Anderson and Mackay كانت العزلتين المستخدمتين حاملة للبلازميد حيث أظهرت النتائج أن بكتريا *Lb. fermentum* كانت تحمل حزمة بلازميدية واحدة لكن العزلة *Lc. raffinolactis* احتوت على حزمتين من البلازميدات، فيما لم تحمل العزلة القياسية (*E. coli* MM 294) أي دنا بلازميدي وكما في الشكل (1).



شكل 1- المحتوى البلازميدي للعزلتين *Lc. raffinolactis* و *Lb. fermentum* وتحديد البلازميدات.

A: بلازميدات العزلة *Lc. raffinolactis* المحيطة بـ SDS, B: بلازميدات العزلة *Lc. raffinolactis* المحيطة بمادة الاكردين البرتقالي, C: بلازميدات العزلة *Lb. fermentum* المحيطة بـ SDS, D: بلازميدات العزلة *Lb. fermentum* المحيطة بمادة الاكردين البرتقالي, E: بلازميدات العزلة *E. coli* MM 294, F: بلازميدات العزلة *Lb. fermentum*, G: بلازميدات العزلة *Lc. raffinolactis*.

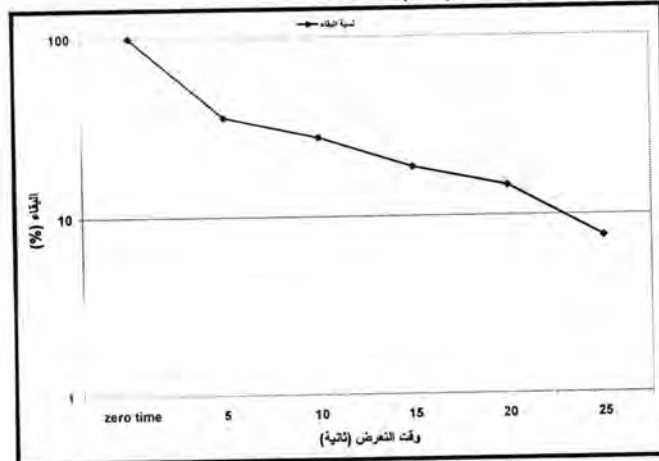
وبأتباع نفس الطريقة المذكورة أعلاه تمكن Givers وجماعته (12) عزل البلازميدات من بكتريا *Lactobacillus* المعزولة من المنتجات المخمرة. فيما وجد Totter وجماعته (20) أن بكتريا *Lactococcus lactis* تحمل بلازميداً واحداً مسنولاً عن إنتاج البكتريوسين. كما وتمكن Alfred Alpert وجماعته (6) من استخلاص بلازميد بكتريا *Lactobacillus sakei* حين وجدها تحمل بلازميداً واحداً.

- تحييد البلازميد

استخدمت صبغة الاكردين البرتقالية على عزلي بكتريا حامض اللاكتيك (*Lc.* *raffinolactis* و *Lb. fermentum*) التي سبق وأن أظهرتا فعالية تثبيطية ضد بكتريا الاختبار المرضية المستخدمة. فقد أظهرت النتائج الموضحة في الشكل (1) أن هاتان العزلتان فقدتا قابليتهما على تثبيط بكتريا الاختبار جميعها بعد إجراء تحييد لبلازميداهما بطريقة الانتشار في الحفر. فقد أشارت النتائج التي تم الحصول عليها إلى أن صفة إنتاج الفعالية التثبيطية يمكن أن تحمل على حزم بلازميدية وأن استخدام التحييد مع العوامل الكيميائية قادت إلى فقدان صفة إنتاج الفعالية التثبيطية. كذلك تمت دراسة تحييد البلازميدات باستخدام مادة SDS، حيث أكدت النتائج فقدان العزلتان قابليتهما التثبيطية تجاه بكتريا الاختبار وأصبحتا حساستين لمضاد Streptomycin و Gentamicin بعد أن كانتا مقاومتين لهما. وبهذا الخصوص فقد ذكر Trevors (21) أن مادة SDS لها تأثير العامل المحيد أكثر من استخدام درجات الحرارة المرتفعة أو المعامل بمادة الايثديوم برومايد. من هذا يمكن الاستنتاج بأن تجارب التحييد على العزلات المحلية لبكتريا حامض اللاكتيك التي تمتلك فعالية تثبيطية يمكن أن تفقدها هذه الفعالية تجاه بكتريا الاختبار. وهذا مما قد يشير إلى وجود علاقة تربط بين وجود البلازميد وإنتاج الفعالية التثبيطية تجاه بكتريا الاختبار كما في الشكل (1). وكان Nowroozi وجماعته (22) قد وجدوا نتائج مشابهة في دراستهم.

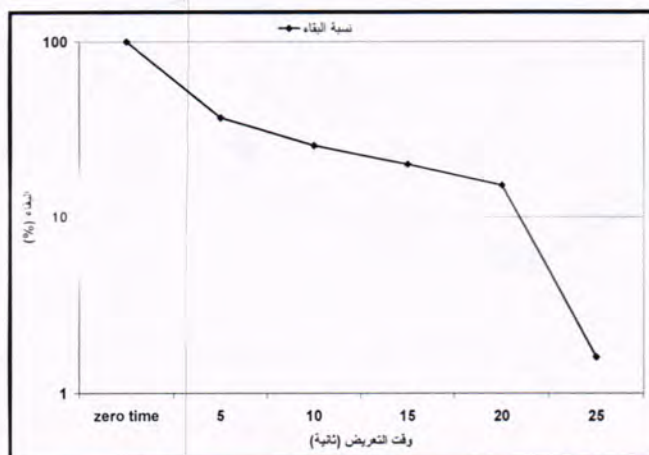
- تطهير عزلات اللاكتيك بالأشعة فوق البنفسجية

يعد استخدام الأشعة فوق البنفسجية بطول موجي (254) نانوميتر لمعاملة بكتريا *Lc.* *raffinolactis* و *Lb. fermentum* ولمدد زمنية مختلفة. تم في البداية تحديد منحنى البقاء (Survival curve) لهذه العزلات حية بعد تعريضها للأشعة بمعدل (10×17) خلية/مل من بكتريا *Lc. raffinolactis* و (10×12.5) خلية/مل من بكتريا *Lb. fermentum* ولمدد زمنية مختلفة، يعد هذا العدد من الخلايا مناسباً لمثل هذه الدراسات (23). يتضح من الشكل (2) انخفاض أعداد البكتريا للعزلة *Lc. raffinolactis* لأكثر من النصف بعد التعرض للأشعة لمدة (5) ثوان، حيث تنخفض أعدادها كلما زادت مدة التعرض وصولاً إلى نسبة البقاء بلغت 7.64% بعد التعرض لمدة (25) ثانية.



شكل-2: المنحنى البياني لبقاء بكتريا *Lc. raffinolactis* حية بعد تعرضها للأشعة فوق البنفسجية بطول موجي (254) نانوميتر ولمدد زمنية مختلفة

أما أعداد البكتريا الحية بالنسبة للعزلة *Lb. fermentum* فقد انخفضت لأكثر من النصف وذلك عندما وصلت نسبة البقاء 20% بعد التعرض للأشعة فوق البنفسجية لمدة (15) ثانية، واستمرت الأعداد بالانخفاض وصولاً إلى نسبة البقاء 1.6% بعد مدة تعرض (25) ثانية كما في الشكل (3).



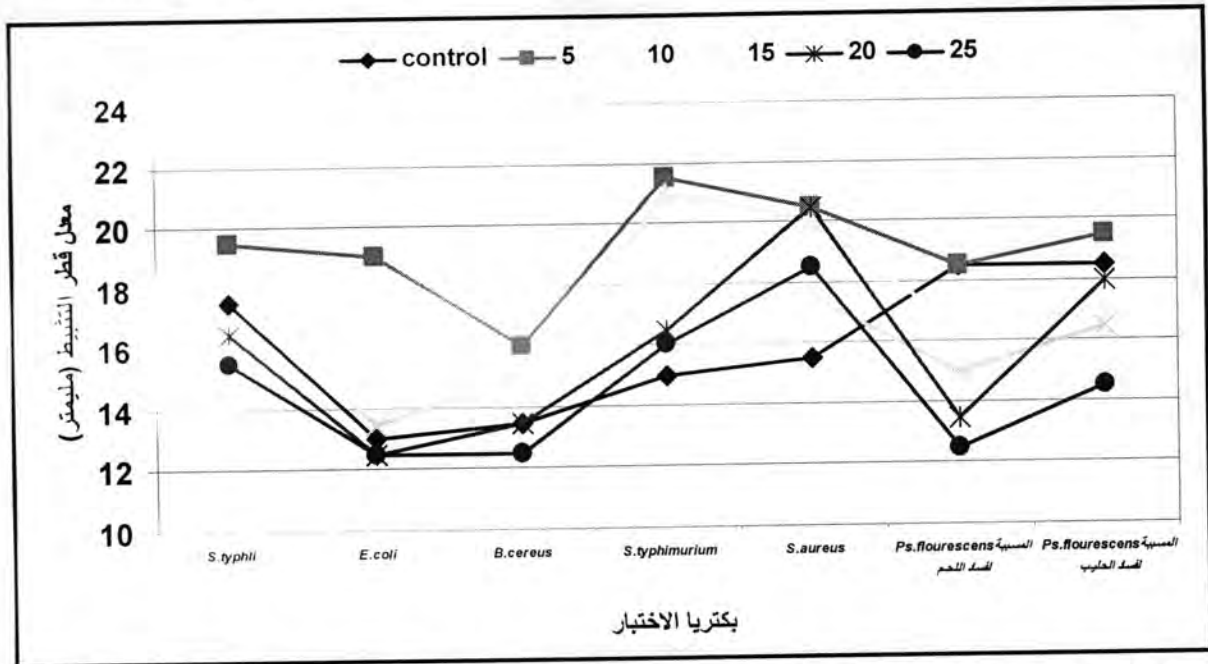
شكل-3: المنحنى البياني لبقاء بكتريا *Lb. fermentum* حية بعد تعرضها للأشعة فوق البنفسجية بطول موجي (254) نانومتر ولمدد زمنية مختلفة

بيّنت نتائج التحليل الإحصائي وجود فروق معنوية في الفعالية التثبيطية للعزلتين بمستوى معنوية ($P < 0.05$) وذلك عندما بلغت معدلات أقطار التثبيط (16, 19, 19.5) ملم تجاه بكتريا: (*S. typhi*) و (*E. coli* و *B. cereus*) على التوالي.

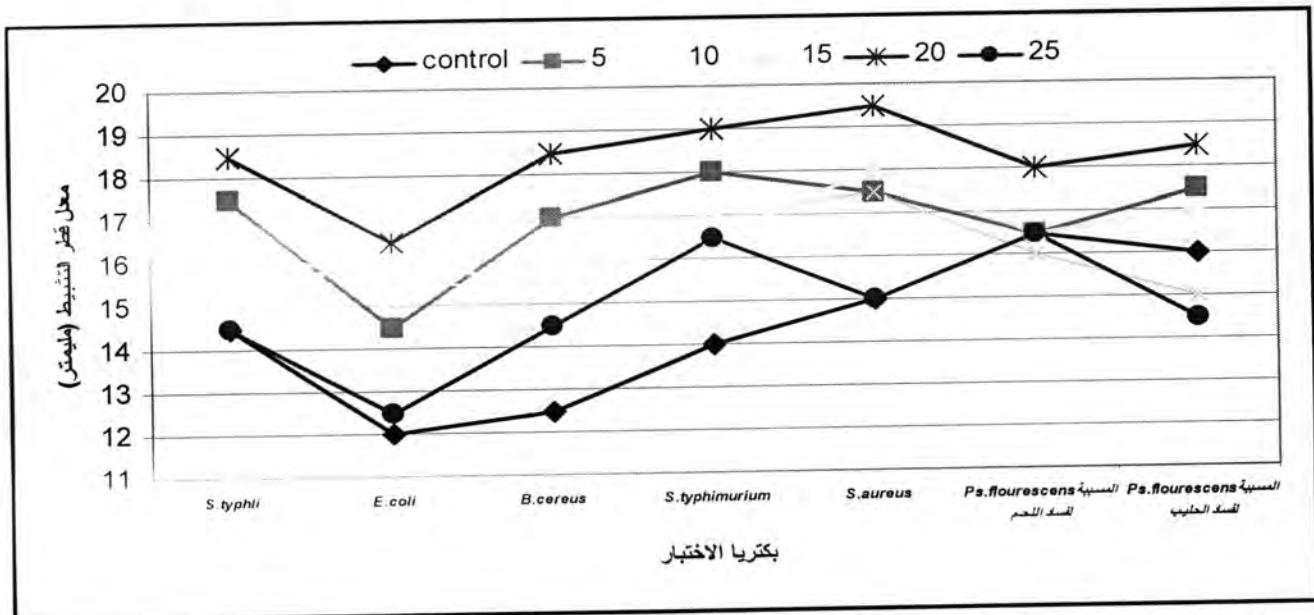
كما لوحظ وجود فروق معنوية كبيرة تجاه بكتريا اختبار *S. typhimurum* و *Staph. aureus* حيث بلغت معدلات أقطارهما (20.5 و 21.5) ملم على التوالي بعد مدة تعرض (5) ثوان تجاه جميع العزلات لبكتريا الاختبار المذكورة آنفاً للعزلة *Lc. raffinolactis*. فيما لم تظهر فروق معنوية تجاه بكتريا الاختبار لعزلات *Ps. fluorescens* المسببة لفساد الحليب و *Ps. fluorescens* المسببة لفساد اللحم بعد مدة تعرض (5) ثوان أيضاً مقارنة بمعاملة السيطرة وكما في الشكل (4).

فيما يخص العزلة *Lb. fermentum* فقد أظهرت النتائج أن أفضل مدة تعرض هي (20) ثانية إذ أعطت أعلى فعالية تثبيطية تجاه أكثر أنواع بكتريا الاختبار وكما في الشكل (5)، حيث سجلت أعلى معدلات أقطار مناطق التثبيط تجاه بكتريا الاختبار *S. typhimurum* و *Staph. aureus* بلغت 19.5, 19 ملم على التوالي مقارنة بمعاملة السيطرة. ولم يلاحظ وجود فروق معنوية في الفعالية التثبيطية تجاه بكتريا الاختبار *Ps. fluorescens* المسببتين لفساد الحليب واللحم مقارنة بمعاملة السيطرة. ذكر Nester وجماعته (24) أن تأثير العوامل المطفرة قد يكون مباشراً (مثل استعمال NTG) أو غير مباشر (مثل الأشعة فوق البنفسجية).

ولاحظ Ogunbanwo وجماعته (25) أن الأشعة فوق البنفسجية و Mitomycin C لا تؤثران في فعالية إنتاج البكتريوسين من قبل العزلتين *Lb. plantarum* F1 و *Lb. brevis* G1 فيما حصلت الشبخلي (26) في دراستها على طفرات بكتريا حامض اللاكتيك باستعمال الأشعة فوق البنفسجية احتفظت بقابليتها على إنتاج البكتريوسين وإنتاج الحموضة مقارنة بالعزلة الأم.

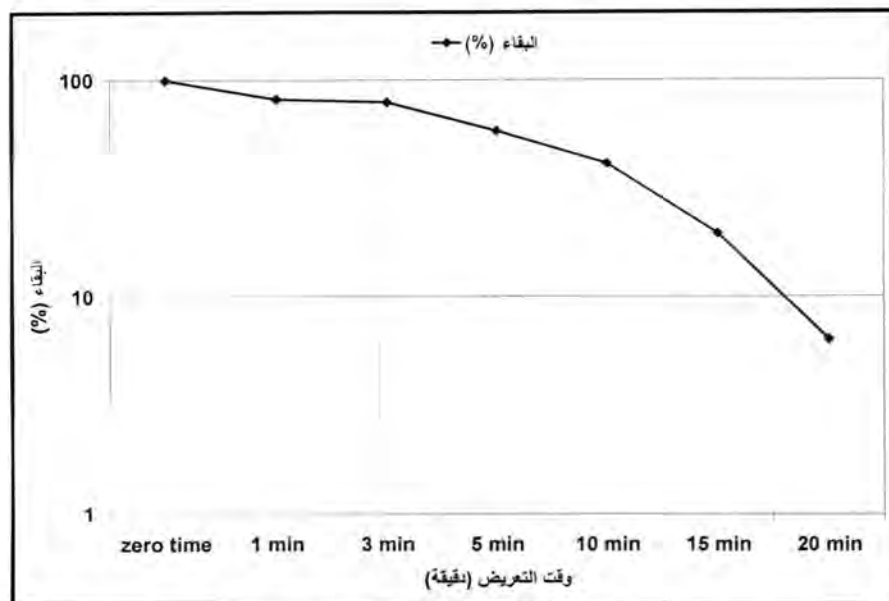


شكل 4-: الفعالية التثبيطية للعزلة *Lc. raffinolactis* بعد تعرضها للأشعة فوق البنفسجية بطول موجي (254) نانومتر ولمدد زمنية مختلفة (5, 10, 15, 20, 25) ثانية تجاه بكتريا الاختبار



شكل 5-: الفعالية التثبيطية للعزلة *Lb. fermentum* بعد تعرضها للأشعة فوق البنفسجية بطول موجي (254) نانومتر ولمدد زمنية مختلفة (5, 10, 15, 20, 25) ثانية تجاه بكتريا الاختبار

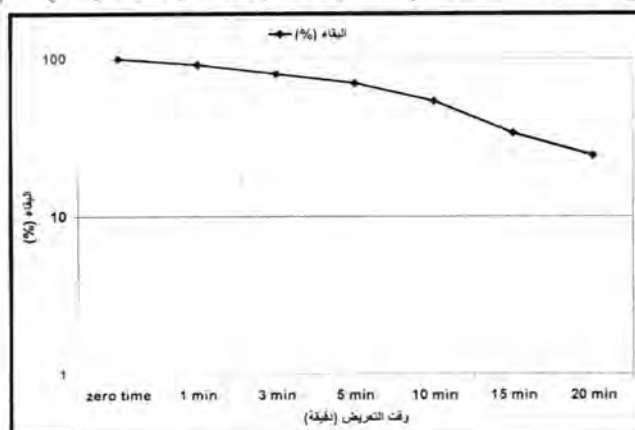
اختبرت بكتريا *Lc. raffinolactis* في تجربة التطهير بأشعة الليزر لكونها أعطت نتائج إيجابية وبفروق معنوية في تجربة التطهير بالأشعة فوق البنفسجية. بعد إضافة صبغة الاكردين البرتقالية بتركيز (20) مايكوغرام/ مل، تم تحديد منحني البقاء للعزلة *Lc. raffinolactis* بعد تعريض (10×18.9) خلية/ مل من هذه البكتريا وكما في الشكل (6). ثم عرضت لأشعة الليزر بطول موجي (337.1) نانومتر ولأوقات تعريض مختلفة وبعد 6 نبضه/ ثانية.



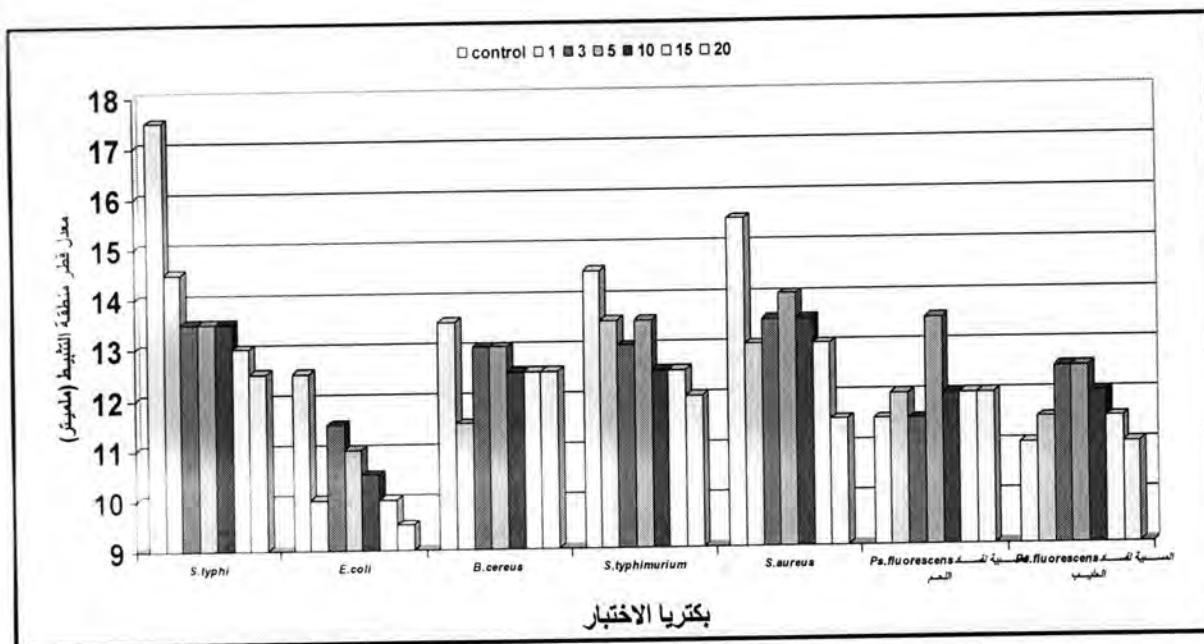
شكل 6: المنحنى البياني لبقاء بكتريا *Lc. raffinolactis* حية بعد تعرضها لمادة الاكردين البرتقالي ولمدد زمنية مختلفة

بعد تقدير معدلات مناطق التثبيط تجاه بكتريا الاختبار قورنت النتائج هذه مع تلك المعاملة بصيغة الاكردين البرتقالية فقط (بدون تشيع بالليزر). وأكدت النتائج ايجابية المعاملة بالاكردين البرتقالي وأشعة الليزر ولاسيما بوقت التعريض (5) دقائق، عندما وجد أن هنالك فروقا معنوية تجاه بكتريا *B.cereus* وكذلك تجاه بكتريا *S.typhimurum* و *Staph. aureus* فقد كانت عند معاملة السيطرة (التطهير بالاكردين البرتقالي فقط) (11.5 و 13 و 12.5) ملم وأصبحت بعد التعريض (14.5, 15.5) (13 ملم على التوالي). من هذا يتضح أن أفضل وقت للتطهير هو (5) دقائق وهذا ما اكدته نتائج التشيع بالليزر مع تلك التي تم الحصول عليها من تجربة التعريض للاكردين البرتقالي فقط (بدون تشيع بالليزر) وكما موضحة في منحنى البقاء شكل (7).

وأدى تعريض العزلة *Lc. raffinolactis* لصيغة الأكردين البرتقالية (لوحدها) لمدد تعرض مختلفة إلى انخفاض فعاليتها وبفروق معنوية وكما في الشكل (8)، حيث لم يؤدي تعريض العزلة لصيغة الاكردين البرتقالية إلى تطور الفعالية التثبيطية بصورة ملحوظة وذلك عندما بلغت معدلات اقطار مناطق التثبيط وبعد مدة تعرض (5) دقائق (11, 13, 13.5, 14, 12.5) ملم تجاه بكتريا *E.coli*, *Ps.fluorescens*, *Staph.aurens*, *S.typhimurium*, *B.cereus*, الحليب بعد أن كانت في معاملة السيطرة (11, 15.5, 14.5, 13.5, 12.5) ملم على التوالي.



شكل 7: المنحنى البياني لبقاء بكتريا *Lc. raffinolactis* حية بعد تعرضها لمادة الاكردين البرتقالي فقط ولمدد زمنية مختلفة تجاه بكتريا الاختبار



شكل 8: الفعالية التثبيطية للعزلة *Lc.raffinolactis* بعد تعرضها لمادة الاكردين البرتقالي فقط ولمدد زمنية مختلفة (20, 15, 10, 5, 3, 1) دقيقة تجاه بكتريا الاختبار

تم اختيار صبغة الاكردين البرتقالية المحبة للماء لأنها تعدّ متحسناً ضوئياً (photosensitizer) يمكنها النفاذ إلى الخلية وهي صبغة تتفاعل مع الحمضين النوويين RNA, DNA في الخلايا الحية (27)، كما أنها تعدّ تفريقية للشريط المفرد والمزدوج للحمض النووي (28). كما وأن طيف الامصاص للاكردين البرتقالي يكون عند طول موجي منبعث من ليزر النتروجين (337.1) نانومتر يمكن أن يسبب ليزر النتروجين تأثيراً محفزاً لإثارة جزيئه NADH التي تؤدي إلى زيادة في تفاعلات الاكسدة والاختزال، ويمكن أن تحدث طاقة عالية من سيل الالكترونات خلال السلسلة التنفسية مودية إلى إنتاج طاقة عالية بواسطة جزيئات ATP وبذلك تزيد مثل هذه النتيجة من فعالية الخلية (29). وبهذا الخصوص فقد حصل Alkarakolly (30) على عزلات من بكتريا حامض اللاكتيك اتصفت بكونها ذات كفاءة عالية في إنتاج حامض اللاكتيك مقارنة بالعزلات الأم بعد معاملتها بطاقة قليلة من أشعة الليزر - نتروجين.

المصادر

- Galvez, A.; Abriouel, H.; Lopez, R. L. and Ben Omar, N. Bacteriocin-based strategies for food biopreservation. Int. J. Food Microbiol. 120(1-2): 51-70 (2007).
- Settanni, L. and Corsetti, A. Application of bacteriocins in vegetable food biopreservation. Int. J. food Microbiol. 121(2): 123-138 (2008).
- Martirani, L.; Varcamonti, M.; Naclerio, G. and Defelice, M. Purification and partial characterization of bacillocin 490, a novel bacteriocin produced by a thermophilic strain of *Bacillus licheniformis*. Microbial cell factories. 1(2002).
- Soomro, A. H.; Masud, T. and Anwaar, K. Role of lactic Acid Bacteria (LAB) in food preservation and Human Health. A Review. Pakistan Journal of Nutrition, 1(1): 20-24 (2002).
- Tagg, J. R., Dajain, A. S. and Wannamaker, L. W. Bacteriocins of gram positive bacteria. Bacteriol. Rev., 40(3): 722 (1976).

6. Alfred Alpert, C.; Le Coq, A.M. C.; Malleret, C. and Zagorec, M. Characterization of theta type plasmid from *Lactobacillus sakei*: apotential basis for low copy- number vectors in Lactobacilli. Appl. Environ Microbiol. 69(9):5574-5584(2003).
7. Fons. M.; Hege, T.; Ladire, M.; Raibaud, P.; Ducluzean, R. and Maguin, E. Isolation and characterization of a plasmid from *Lactobacillus fermentum* conferring erythromycin resistance plasmid, 37(3):199-203. (Abst.) (1997)
8. Stiles, M.E. and Hastings, J.W. Bacteriocins production by lactic acid bacteria, Potential for use in meat preservation. Trends in food science and Technology. 2(10):247-251(1991).
9. Glass. R. Gene function: *E.coli* and its heritable element, croom. Hcttm, London. (1982).
10. Goldman, L. Applications of Laser. 2nd ed. CRC. Press. Inc.: 155-172. Robert E. Krieger publishing company Malabar, Florida. (1982).
11. Anderson, E.M.; Angyal, G.N, Weaver, C.N. Felkner, I.C.; Wolf, W.F and Worthy, B.E Potential application of laser/ Microbioassay technology for determining water soluble vitamins in food. J.AOAC.Int, 76(3):682-690. (1993).
12. Givers, D.; Danielson, M.; Hugs, G. and Savings, J. Molecular characterize - ation for tet (M.) genes in *Lactobacillus* isolates from different types of fermented dry sasage. Appl. Environ. Microbiol. 69(2):1270-1275. (2003)
13. Anderson, D.G. and McKay, L.L. Simple and Rapid method for isolating larg plasmid DNA from lactic streptococci Appl. Environ. Microbiol. 46(3): 549-552(1983).
14. Maniatis, T.; Fritsch, E.F. and Sambrook, J. Molecular cloning alabrotary manual. Cold spring labootae, New York. (1982).
15. Khalid, F.; Siddiqi, R. and Mojgani, N. Detection and characterization of a heat stable bacteriocin (Lactocin LC-Oq) produced by a clinical isolate lactobacilli. Med. J. Islam. Acad. Science, 12(3)(1999).
16. Tomoeda, M.; Inuzuka, M.; Kubo, N. and Nakamura, S. Effective Elimination of Drug Resistance and sex factors in *Escherichia coli* by Sodium Dodecyl Sulfate. J.Bacteriol. 95(3): 1078-1089(1968).
17. Suskovis, J.; Brick, B.; Matosic, S. and Maric, V. *Lactobacillus acidophilus* M92 as potential probiotics strain. J.Milchwissen Schaft., 52(8): 430-435(1997).
18. Muriana, P.M. and Klaenhammetr, T.R. Conjugal trausfer of plasmid encoded determinants for bacteriocin production and immunity in *Lactobacillus acidophilus* 88. Appl. Envioron. Microbiol., 52:553-560. (1987).
19. Sullivan, A. and Nord, C.E. Probiotics in human infections. Journal of Antimicrobial chemotherapy. 50:625-627. (2002).

20. Trotter, M.; McAuliffe, O.E; Fitzgerald, G.F.; Hill, C. Paul Ross, R. and Coffey, A. Variable bacteriocin production in the commercial starter *Lactococcus lactis* DPC 4275 is linked to the formation of cointegrate plasmid PMR CO₂. Appl. Environ. Microbiol. 70(1):34-42 (2004).
21. Trevors, J.T. Plasmid curing in bacteria. FEMS Microbiology Reviews. 32:149-157(1986).
22. Nowroozi, J. and Mirzaii, M. A study of the characteristics of *Lactobacillus plantarum* isolated from sausage in Iran. Rogan institute. Org/ Yakhteh/Y20-6 fullhtm-32K(2004).
23. Singh, J. and Chopra, A.K. Accelerated fermentation of milk by nitrosoguanidine induced mutants of lactobacilli. J. Food Sci., 47: 1027-1029(1982).
24. Nester, E.W.; Anderson, D.G.; Roberts, G.E.; Pearsall, N.N. and Nester, M.T. Microbiology 3rd ed. McGraw-Hill. New York.(2001).
25. Ogunbanwo, S.T.; Sanni, A.I. and Onilude, A.A. Characterization of bacteriocin produced by *Lactobacillus plantarum* F1 and *Lactobacillus brevis* OG1. African Journal of Biotechnology 2(8):219-227(2003).
26. الشخيلي، ضمياء محمود إبراهيم. دراسة البكتريوسينات المنتجة من قبل بكتريا حامض اللاكتيك. أطروحة دكتوراه. كلية العلوم- الجامعة المستنصرية. (1999)
27. Kobayashi, K. and Ito, T. Wavelength dependence of single oxygen mechanism in Acridine orange sensitized Photodynamic action in yeast cells, Experiments With 470nm. Photochem. Photobiol. 25:585-588 (1977).
28. Kusuzaki, K. Binuclear cells induced by acridine orange in giant cells tumor of bone. Anticancer Research. 20(54):3013-3017(2000).
29. Jeevan, A. and Kripke, M. Alteration of the immune response to *Mycobacterium bovis* in mice exposed to low doses of UV radiation. Cell Immunology. 130:32-41(1990).
30. Al-Karakolly, Z.N.H. A study of N₂-Laser effect on lactic acid production by *Lactobacillus bulgaricus* and *Streptococcus thermophilus*, M.Sc. Thesis, Institute of Laser and Plasma for post graduate studies, University of Baghdad. (2001).

قابلية تأثر بكتريا الـ *Salmonella enterica serovar typhi* لبعض عوامل المضادات الجرثومية و دراسة العوامل المؤثرة على امراضيتها

نهاد خلاوي تكتوك
كلية التقنيات الطبية والتقنية

ABSTRACT

The research include general survey of *Salmonella enterica serovar Typhi* which causing typhoid fever and study the factors which help to increasing the typhoid fever and its source in this population, as well as its prevalence among the population of Baghdad city (Al- Aubaide, Al-Kammalia, Al- Fadhelia), the direction examination by widal test (Widal testing was done by using the Sanofi qualitative agglutination test kits (Bio-Rad) agglutination was visible, the results were considered positive (37.5 %), and culture sample (fecal and urine), The mean age of our patients was 25 years old who presented with typhoid fever, between June to September 2008 collected sample were eligible for enrollment. all sample was transported on the day of collection to kidy hospital for diagnostic, The over all rate of infection was (37.5 %), infect in male more than female (66.5, 33.5) % respectively and the highest percentage was recorded among young (49%). The most common resistances among *S. Typhi* isolates were to tetracycline (98%), none of the *S. Typhi* isolates tested were resistant to ciprofloxacin and cefotaxime.

الخلاصة

تضمنت الدراسة عزل وتشخيص بكتريا الـ *Salmonella enterica serovar Typhi* المسببة لحمى التيفوئيد والتحري عن العوامل المساعدة و المؤدية لانتشار حمى التيفوئيد ومصدر العدوى بين سكان بعض نواحي بغداد وسبل الحد والوقاية من المرض.

تضمن البحث اختيار ثلاث مناطق من نواحي بغداد (العبيدي، الكماليه، الفضيليه) للتقصي عن بكتريا الـ *Salmonella enterica serovar Typhi* المسببة لحمى التيفوئيد المنتشرة بين سكان هذه المناطق وذلك بالاعتماد على الفحص السريري من قبل طبيب اختصاص ثم التشخيص البكتريولوجي من خلال زرع عينات من ادرار وخروج المريض اضافة الى اجراء فحص الـ widal test للدم بطريقة التلازن، كانت النتيجة الايجابية لهذا الفحص 37.5 % وقد كان متوسط الاعمار لمرضى يعانون من حمى التيفوئيد هو 25 سنة، جمعت عينات الدراسة من الفترة حزيران 2008- ايلول 2008، واجريت عليها الفحوصات في مستشفى الكندي التعليمي، وقد تم تسجيل معدل الاصابه الكلية (37.5%) وكانت نسبة الخمج بين ذكور هذه المناطق اعلى من اناثها (66.5, 33.5 %) على التوالي، وقد سجلت اعلى نسبة للاصابه في الفئة العمرية الثانية (49 %) وان عصيات التيفوئيد في الزرع الايجابي للخروج كانت بنسبة (29.1 %) مقارنة عما كانت في الزرع الايجابي للادرار (8.3 %). وقد تبين ايضا ان 11.4 % من مرضى حمى التيفوئيد من الزرع الايجابي للخروج كان لديهم تاريخ عائلي بالاصابة مقارنة بـ 88.5 % ليس لديهم تاريخ عائلي في حين الزرع الايجابي للادرار كان 10 % لديهم تاريخ عائلي مقارنة بـ 90 % ليس لديهم تاريخ عائلي للاصابة بحمى التيفوئيد. اظهرت بكتريا الـ *Salmonella enterica serovar Typhi* مقاومتها العاليه لمضاد الـ tetracycline (98%)، وفي حين اظهرت حساسيتها العالية (100%) تجاه مضادي الـ ciprofloxacin, cefotaxime. وقد ظهر ان رداءة الصرف الصحي وعدم توفر المياه الصالحة للشرب والانقطاع المستمر للتيار الكهربائي مع استخدام مضخة الماء اضافة لعدم العلاج الصحيح وسوء استخدامه وتناول الطعام من الباعة المتجولين كلها عوامل تعمل على انتشار حمى التيفوئيد في منطقة الدراسة.

المقدمة

تعرف حمى التيفوئيد بانها واحدة من اكثر انواع الامراض الحميه شيوعا خصوصا في فصل الصيف حيث يصيب الميكروب الامعاء مسببا حمى قوية تصعب معالجتها حتى انها قد تؤدي بحياة المريض اذا لم تعالج في الوقت المناسب (1,2). تبدأ الحمى تدريجيا خلال هذه الاثناء يصاب المريض بتقرحات في جدار الامعاء الداخلي والسبب وراء الاصابة بهذا المرض هو نوع من انواع البكتريا عصوية الشكل تعرف باسم السالمونيلا (3)، وقد أثبتت الدراسات على المتطوعين بان العدد المطلوب لحدوث الاصابة

قابلية تأثر بكتريا الـ *Salmonella enterica serovar typhi* لبعض عوامل المضادات الجرثومية و دراسة العوامل المؤثرة على امراضيتها نهاد

بحمى التاييفويد حوالي عشرة ملايين جرثومة لكي يصاب 50% من المتطوعين الاصحاء اما اقل من هذا العدد فمناعة جسم الانسان كفيطة بالقضاء عليها ومنع حدوث العدوى كذلك فان عدد الجراثيم المبتلعة يؤثر على فترة الحضانة (وهي المدة من دخول الجراثيم للجسم لحين ظهور الاعراض) ففترات الحضانة القصيرة على العموم مرتبطة بالاعداد الكبيرة . حيث تعتبر البكتيريا النافعة الموجودة في الجهاز الهضمي العلوي ذات آلية حماية مهمة ضد هجوم بكتيريا السالمونيلا (4). ويمكن أن تحدث منه حالات خفيفة تمر دون الحاجة إلى علاج بالأخص في المناطق التي يتوطن فيها المرض (5)، أما الباراتيفويد فهو يؤدي إلى نفس الأعراض أعلاه ولكن بصورة خفيفة مع اختلاف نوع البكتيريا المسببة له تبدأ الحمى بصورة تدريجية بحيث لا يشكو المريض من علة تذكر في الايام الاولى من الإصابة مما يتيح المجال امام البكتيريا لتدمير انسجة الامعاء الداخلية (6, 7)، بعد ذلك يبدأ المريض بالشعور بالصداع والتعب وعدم الراحة يصاحبها ارق وارتفاع درجة حرارة الجسم خصوصا في الليل (8). تحتوي عصيات التاييفويد بداخلها على مواد كيميائية سمية تؤدي الى حدوث حمى وانخفاض في عدد كريات الدم البيضاء وانخفاض في عدد الصفائح الدموية المسؤولة عن تخثر الدم وتضخم في خلايا الكبد والطحال. اما كيس الصفراء والاقنية الصفراوية فغالبا ما يصاب بالعدوى خلال الإصابة بالمرض وتكون غير مصحوبة باعراض بالرغم من انه قد تتطور العدوى الى التهاب المرارة الحاد احيانا وقد بينوا (9) في دراستهم ان حمى التاييفويد تصيب حوالي 21 مليون شخص سنويا وتؤدي بحياة 200000 في انحاء العالم (9). أن المصدر الأساسي للعدوى هم الاشخاص الحاملين لجراثيم المرض والذين لا تظهر عليهم اعراضه (الحاملين المزمنين chronic carriers) والانسان يعتبر الحاضن الوحيد لهذه البكتيريا في الطبيعة حيث تدخل عن طريق الفم بعد تناول طعام او شراب ملوث بها فيفرز الاشخاص المصابون بالعدوى الملايين من هذه البكتيريا في برازهم والذي يعتبر المصدر المعتاد لتلوث الطعام والشراب (6,10)، وأيضا تطرح في افرازات الجهاز التنفسي وفي القي وفي سوائل الجسم الأخرى (11).

يلعب الذباب دورا فعالا في نقلها من الفضلات البشرية والمواد الملوثة الى الطعام والشراب مما يؤدي الى حدوث وباء بين فترة وأخرى (6,12). وحقيقة كون هذه البكتيريا تقاوم التجميد والتجفيف وتبقى حية يزيد من احتمالية انتشار العدوى بواسطة المثلجات والمطابخ الملوثة والاطعمة المجمدة الملوثة وبالبغبار وبشبكة المجاري (13).

ان لارتفاع حرارة الجو في فصل الصيف دور في تسريع تكاثر البكتيريا المسببة للمرض مما يؤدي الى ارتفاع عدد الاصابات صيفا (13). ولا توجد لضربة الشمس اي علاقة بحمى التاييفويد لانها حالة اختلال في درجة حرارة الجسم واضطراب في ضغط الدم مع فقدان لسوائل الجسم (11).

تهدف الدراسة في هذا البحث الى عزل و تشخيص بكتريا الـ *Salmonella enterica serovar Typhi* المسببة لحمى التاييفويد وحساسيتها لبعض المضادات الجرثومية مع التحري عن العوامل المساعدة و المؤدية لانتشار حمى التاييفويد ومصدر العدوى بين سكان بعض نواحي بغداد.

المواد وطرائق العمل

تناولت هذه الدراسة جمع 120 عينة ادرار وخروج ودم بعد الفحص السريري من قبل طبيب باطنية اختصاص ثم التشخيص البكتريولوجي من خلال زرع هذه العينات على وسط الـ tetrathionat broth المضاف اليه قطره من الايودين ويوضع في الحاضنه لمدة 24 ساعة ثم يزرع عينه منة على وسطي الـ Blood agar, Macconky agar ويترك في الحاضنه لمدة 24 ساعة (14)، ثم أجريت فحوصات الـ (biochemical test (oxidase, urea test, H₂S production, citrate test) وقد اجري فحص الحساسية لعزلات بكتريا الـ *Salmonella enterica serovar Typhi* للمضادات الحيوية cefotaxime بالاعتماد على قياس قطر منطقة تثبيط النمو (Inhibition zone) بالملمتر حول اقراص (30µg), ciprofloxacin (30µg), chloramphenicol (30µg), ampiclox (30µg)

المضادات المستخدمة وحسب طريقة (15)، بالإضافة إلى الفحص السيرولوجي للدم (فحص الويدال widal test وبالاعتماد على طريقة التلازن) (15) وقد كانت مدى القيم المعتمدة لهذا الفحص (من 1/160 – من 1/640 المعدل 1/320) .
وقد كانت متوسط الاعمار في عينة الدراسة 25 سنة (المدى 10 – 40 سنة) النسبة الذكور الى الاناث كانت 1.5 : 1.

النتائج والمناقشة

في جدول (1) تراوحت أعمار المرضى المشمولين بهذه الدراسة 10-35 عاماً من كلا الجنسين ذكراً وإناثاً مقسمين إلى ثلاث فئات عمرية، الفئة الأولى تضمنت الأعمار 10-25 عاماً والفئة الثانية من 25-35 والأخيرة أكبر أو تساوي 35 عاماً .
تظهر النتائج من خلال هذا الجدول ان الفئة العمرية الثانية (35-25 سنة) كانت الأكثر إصابة بحمى التايفوئيد حيث بلغت نسبتها 49% وتليها الفئة العمرية الثالثة (35 سنة) ونسبة 33.3% والفئة العمرية الاولى (25-10) بنسبة 17.7% وقد فاقت نسبة الإصابة في الذكور 66.5% عما هو في الاناث 33.5% اي نسبة الذكور الى الاناث كانت 2 : 1 تظهر عصابات التايفوئيد في الزرع الايجابي للخروج بنسبة (29.1%) اما في الادرار فقد كانت نسبة الزرع الايجابي له (8.3%) مما يتبين ان نسبة حاملي المرض بالخروج الى الادرار كانت 3.5 : 1

جدول-1: توزيع المرضى المصابين والمشكوك باصابتهم بحمى التايفوئيد حسب العمر والجنس.

حالات حمى التايفوئيد	عينات الخروج		عينات الادرار		مجموع		الحالات السلبية	
	عدد	%	عدد	%	عدد	%	عدد	%
العمر (سنة)	(35)	(29.1)	(10)	(8.3)	(45)	(37.5)	(75)	(62.5)
10-25	8	22.8	0	0	8	17.7	10	13.4
25-35	17	48.2	5	50	22	49	30	40
≥35	10	28	5	50	15	33.3	35	46.6
الجنس								
ذكر	23	65.8	7	70	30	66.5	40	53
أنثى	12	34.2	3	30	15	33.5	35	47

يظهر من خلال هذه الدراسة ان المصابين بحمى التايفوئيد بالنسبة لزرعي الخروج والبول الايجابي كان اغلبهم يستخدمون الماء الذي يسحب عن طريق مضخة الماء الكهربائية ونسبة (43 , 50) % على التوالي في حين المستخدمين لماء البئر وماء الحنفية كانوا بنسبة (28.7) % بالنسبة لزرع الخروج الايجابي اما للزرع الايجابي للبول فقد كان (20 , 30) % على التوالي ، اما مصدر الطعام فقد كان معظم المصابين بالحمى ولكلا الزرعين الخروج والبول الايجابي يتناولون وجباتهم خارج المنزل (من المطاعم والباعة المتجولين) بنسبة (60,57) % على التوالي مقارنة بأولئك الذين يتناولون وجباتهم من داخل المنزل ونسبة (43 , 40) % على التوالي لزرعي الخروج والإدرار الايجابي.

جدول-2: حالات الاصابة بحمى التايفوئيد حسب مصدر مياه الشرب والطعام

حالات حمى التايفوئيد		عينات الخروج		عينات الادرار		الحالات السلبية	
عدد	%	عدد	%	عدد	%	عدد	%
(35)	(29.1)	(10)	(8.3)	(75)	(62.5)		
مصدر الماء							
10	28.5	2	20	10	13		
10	28.5	3	30	25	33		
15	43	5	50	40	53		
مصدر وجبات الغذاء							
15	43	4	40	25	33		
20	57	6	60	50	67		

من جدول (3) يظهر 11.4 % من مرضى حمى التايفوئيد من الزرع الايجابي للخروج لديهم تاريخ عائلي بالاصابة مقارنة بـ 88.5 % ليس لديه تاريخ عائلي في حين الزرع الايجابي للادرار كان 10 % لديهم تاريخ عائلي مقارنة بـ 90 % ليس لديهم تاريخ عائلي للاصابة بحمى التايفوئيد.

جدول-3: التاريخ العائلي * للاصابة بحمى التايفوئيد بالنسبة لمجموعة الدراسة

التاريخ العائلي لمرضى حمى التايفوئيد		له تاريخ عائلي *		ليس له تاريخ عائلي	
عدد	%	عدد	%	عدد	%
4	11.4	31	88.5		
1	10	9	90		
5	11.1	40	89.9		

يتضح من الجدول اعلا مقاومة بكتريا الـ *Salmonella enterica serovar Typhi* كانت عليه لمضاد الـ وبنسبة 98% اما لمضاد الـ ampiclox, chloramphenicol فقد كانت (50,58)% على التوالي في حين وصلت نسبة مقاومه 28% للـ ampicillin بينما اظهرت البكتريا حساسيتها العاليه (100%) على التوالي لكل من الـ cefotaxime, ciprofloxacin.

جدول-4: نسبة مقاومة بكتريا الـ *salmonella typhi* لبعض المضادات الحيوية

اسم المضاد الحيوي	نسبة المقاومة (%)
tetracycline	98
Chloramphenicol	58
ampiclox	50
ampicillin	28
Ciprofloxacin	0
cefotaxime	0

*يقصد بالتاريخ العائلي هو احد أفراد عائلة المصاب بمن هم على تماس بالمريض مصاب حالياً" أو سابقاً" أو حامل للمرض.

إن الإصابات البكتيرية أو الفايروسية وغيرها تزداد بتقدم العمر نتيجة لضعف عوامل المقاومة (ضعف الجهاز المناعي) غير انه هذه الدراسة بينت ان الإصابة بالتيفوئيد تكون في اوجها لدى الفئة العمرية الثانية (49%) والتي تمثل فئة الشباب، حيث بين (11) أن هذه الفئة التي تمثل الفئة العمرية العاملة يكون معظم أوقاتهم خارج المنزل مما يؤدي ذلك الى تناول وجباتهم الغذائية خارجاً" وتنقل بذلك الإصابة بسبب الطعام والشراب الملوثين بعصيات التيفوئيد وقد جاء هذا متفقاً مع (16، 17) أما (18) فقد اظهر من خلال دراسته ان هذا المرض ينتقل بواسطة نادل المطعم.

ان عامل المطاعم ربما يكونوا حاملي للمرض لكن لا تظهر عليهم الأعراض (21). أما سبب ارتفاع الإصابة بحمى التيفوئيد بالذكور عن الإناث (66.5, 33.5%) على التوالي فقد جاء نتيجة لتناول معظم وجباتهم خارج المنزل فقد بين (19) في دراسته أن الذكور أكثر إصابة بالتيفوئيد من الإناث وبنسبة (56, 44) % على التوالي، وهذا ما جاء متوافقاً مع (20, 8) وهذا يناقض دراسة (12) حيث بينت نتائجها ان نسبة التيفوئيد في اناث الهند (20%) اعلى مما هي في ذكورهم (13.3 %).

وان الحاملين المزمنين للمرض نسبتهم اعلى في الإناث بثلاثة اضعاف وكذلك من كبار السن اي ان 88% من الحاملين المزمنين تتعدى اعمارهم الخمسين سنة.

ان تناول المتلجبات والمرطبات والأطعمة المجمدة الملوثة وامتلاك بكتريا السالمونيلا صفة مقاومه للتجميد والتجفيف مايزيد من احتمالية انتشار العدوى هنا لاسيما في مناطق الدراسة (العبيدي، الكمالية، الفضيلية).

وقد جاءت ظهور حالات حمى التيفوئيد في منطقة الدراسة (العبيدي، الكمالية، الفضيلية) نتيجة التلوث الكبير الحاصل في ماء الشرب فقد اوضحت الدراسة زيادة نسبة المصابين بالحمى لاسيما الذين يستخدمون المضخة الكهربائية لسحب الماء مما يؤدي الى شطف المياه الاسنة وبسبب تشقق وقدم انابيب المجاري في المنطقة له الدور الكبير في سحب كميات كبيرة من مياه المجاري بواسطة هذه المضخات وبالتالي تتسبب في حصول التلوث وهذا يتفق تماماً مع (13, 18).

تنتقل عصيات التيفوئيد بواسطة الأطعمة الملوثة و يعتبر الذباب هنا الناقل للميكروب لذا نجد في هذه الدراسة ان المصابين (عينات الخروج والإدراج) اغلبهم من الذين يتناولون وجباتهم في المطاعم (60, 57) % مقارنة مع المصابين الذين يتناولون وجباتهم داخل المنزل لـ (40, 43) % على التوالي.

وهذا يتفق مع (11) الذي أوعز في دراسته الى سبب انتشار التيفوئيد هو نتيجة للطعام والشراب الملوثين خارج المنزل.

إما ظهور النسب العالية من حالات الإصابة للذين يتناولون وجباتهم داخل المنزل فقد جاء نتيجة لتلوث الطعام إضافة لانقطاع المستمر والمتكرر للتيار الكهربائي في منطقة الدراسة حيث ذوبان الأطعمة المجمدة وتلوثها مرة أخرى بالميكروب إضافة إلى تناول الكثير منهم المتلجبات والمرطبات الملوثة (21). هذا وان لارتفاع درجة حرارة الجو في فصل الصيف له دور في تسريع في تكاثر عصيات التيفوئيد في المنطقة مما يجعلها عرضة للكثير من الامراض لاسيما التيفوئيد.

أن تلوث مياه الشرب المياه الاسنة والمجاري تجعلها مصدراً حيوياً للأمراض الانتقالية كالتيفوئيد وهذا ما يتفق مع (17) أما في دراسة أجريت في الفيوم فقد بينت ان سبب انتشار حمى التيفوئيد تكون ناجمة عن تناول الآيس كريم، بسبب تلوث معظم الألبان المجففة المستخدمة في إنتاجه ببكتيريا تؤدي إلى الإصابة باضطرابات معوية قد تصل إلى التسمم الغذائي، كما قد تنجم عن تناول الاسماك المتفسخ (الفسخ) الذي يقبل المصريون على تناوله فهو يحتوي على كميات كبيرة من بكتريا السالمونيلا وكذلك بكتيريا "E.coli" المعروفة باسم بكتريا التعفن والمسببة للتسمم الغذائي القاتل (22).

أن الإصابة بحمى التيفوئيد لاحد افراد العائلة يزيد من احتمالية الإصابة لدى افرادها الآخرين حيث مخالطة المصاب واستخدام ادواته يتيح الفرصة لانتشار الامراض الانتقالية لاسيما التيفوئيد مع توفر الظروف المساعدة الاخرى كالطعام والشراب الملوثين. فقد أوضح (23) من خلال دراسة اجراها في مدينة سوهاج في جمهورية مصر العربية ان 34.5% من مرضى حمى التيفوئيد من الزرع الايجابي للخروج لديهم تاريخ عائلي بالإصابة مقارنة بـ 14.7% من الزرع الايجابي للادراج كان لديهم تاريخ

قابلية تأثر بكتريا الـ *Salmonella enterica serovar typhi* لبعض عوامل المضادات الجرثومية ودراسة العوامل المؤثرة على مر صيد نهاد

عائلي للإصابة. في حين أوضح (18) في دراسة أجراها في سانتياكو أن الناقلين المزمنين في بعض العوامل تزيد من خطر انتشار الإصابة لبقية أفراد العائلة وكذلك الأفراد الحاملين للمرض لكن لا تظهر عليهم أعراض.

أن مضاد التتراسايكلين يعتبر من المضادات المثبطة للنمو bacteriostatic وذلك حيث يدخل إلى الكائن الحي بواسطة الانتشار السلبي passive diffusion بصورة جزئية وبواسطة عملية معتمدة على الطاقة بالنقل الفعال transport active يتركز داخل الخلايا الحساسة ليرتبط في الوحدة الثانوية S30 من راببوسومات البكتريا بصورة انعكاسية، ليمنع ارتباط acyl-tRNA amino إلى الموضع المقبول من راببوسوم mRNA، هذه العملية ستمنع إضافة حوامض أمينية إلى الببتايد النامي growing peptide. (29)

يعتبر مضاد الـ chloramphenicol من المضادات المؤثرة على البناء البروتيني للخلية، حيث يمتد بتأثير فعال على البكتريا إلا أن النتائج أظهرت مقاومة بكتريا الـ *Salmonella enterica serovar Typhi* لمضادي الـ chloramphenicol, ampiclox وبنسبة (50,58)% على التوالي وهذا يفسر نتيجة للاستخدام الواسع والمتكرر لهذه المضادين أدى إلى ظهور حالة المقاومة البكتيرية لهما، إضافة للاستخدام العشوائي وبدون وصفة طبيب (27) أما النقل الأفقي لجينات المقاومة فهو يلعب دورا فعالا في الانتشار السريع لمقاومة البكتريا للمضادات الحيوية. وقد أوعز (24) إلى أن السبب الرئيسي لمقاومة البكتريا هو امتلاكها لعوامل المقاومة كالـ R-plasmid، وإنزيمات مثل انزيم البيتا لاكتاميز β -lactamase كلها عوامل تزيد من مقاومة البكتريا للمضادات الجرثومية التي كانت حساسة لها سابقا (26,25).

إضافة لهذا فقد بين الجدول (4) أيضا حساسية هذه البكتريا العالية لمضادي الـ Cefotaxime, ciprofloxacin وبنسبة (100)% لكليهما حيث يعتبر مضاد الـ cefotaxim من مضادات الجيل الثالث للسيفالوسبورينات والتي تمتاز بفعاليتها العالية أما مضاد الـ ciprofloxacin فهو من المضادات الواسعة الطيف في تأثيرها على المسببات المرضية البكتيرية وقد بينت دراسة (27) أن مقاومة البكتريا للمضادات الحيوية ciprofloxacin, chloramphenicol كانت (20, 79.6)% على التوالي أما (21) فقد أشارت دراسته إلى نسبة مقاومة الـ *salmonella typhi* للمضادات كانت chloramphenicol (26.6%), ampicillin (72.5%), ciprofloxacin (69%), cotrimazol (56.6%), Amoxicillin (82.9%)

أن المقاومة البكتيرية تجاه المضادات الحيوية تتولد بواسطة اليات مختلفة منها إنتاج إنزيمات معينة تعمل على شل فاعلية المضاد، وتغيير نفاذية أغشية الخلايا البكتيرية لمنع دخول المضاد وزيادة المادة الأساس التي يستهدفها المضاد (28).

مما تقدم يظهر وجود نسب مقاومة مختلفة للبكتريا المعزولة اتجاه المضادات المستخدمة في الدراسة والذي يفسر بسبب الاستعمال العشوائي للمضادات مما أعطى المجال لظهور المقاومة والتي أخذت الانتقال من بكتريا إلى أخرى عن طريق العديد من طرق المقاومة، لذا فإن ارتفاع نسبة البكتريا المقاومة للمضادات الحيوية يؤكد الحاجة إلى ضرورة إجراء فحص الحساسية قبل استخدام المضاد.

ومن ذلك يمكن ان نستنتج :

1. أن الفئة العمرية الثانية (35-25 سنة) كانت الأكثر إصابة بحمى التايفوئيد حيث بلغت نسبتها 49% وتليها الفئة العمرية الثالثة والأولى وبنسبة (33.3, 17.7)% على التوالي وقد فاقت نسبة الإصابة في الذكور 66.5% عما هو في الإناث 33.5% أي نسبة الذكور إلى الإناث كانت 2:1
2. أن نسبة حاملي المرض بالخروج إلى الأدرار كانت 3.5:1 أي أن عصيات التايفوئيد في الزرع الإيجابي للخروج كانت بنسبة (29.1%) مقارنة عما كانت في الزرع الإيجابي للأدرار (8.3%).
3. المصابين بحمى التايفوئيد بالنسبة لزراعي الخروج والبول الإيجابي كان أغلبهم يستخدمون الماء الذي يسحب عن طريق مضخة الماء الكهربائية وبنسبة (43, 50)% على التوالي في حين المستخدمين لماء البئر وماء الحنفية كان كلاهما (28.7)% بالنسبة لزراعي الخروج الإيجابي أما للزرع الإيجابي للبول فقد كان (30, 20)% على التوالي.

4. كان معظم المصابين بالحمى وكللا الزرعين الخروج والبول الايجابي يتناولون وجباتهم خارج المنزل (من المطاعم والباعة المتجولين) بنسبة (60,57) % على التوالي مقارنة بأولئك الذين يتناولون وجباتهم من داخل المنزل وبنسبة (40,43) % على التوالي لزرعي الخروج والإدرار الايجابي.
5. ان 11.4 % من مرضى حمى التايفوئيد من الزرع الايجابي للخروج لديهم تاريخ عائلي بالاصابة مقارنة بـ 88.5 % ليس لديهم تاريخ عائلي في حين الزرع الايجابي للإدرار كان 10 % لديهم تاريخ عائلي مقارنة بـ 90 % ليس لديهم تاريخ عائلي للاصابة بحمى التايفوئيد.
6. تظهر مقاومة البكتريا لمضاد الـ tetracycline بنسبة (98%) في حين كانت العزلات البكتيرية حساسة تجاه الـ ciprofloxacin, cefotaxime وبنسبة (100) %.

التوصيات

1. عدم تناول الوجبات الغذائية من الباعة المتجولين مع الامتناع عن تناول الاطعمة المعاد تجميدها لاسيما في مناطق ذات الانقطاع المستمر للتيار الكهربائي
3. تفادي التلوث الخطير نتيجة استخدام المضخة لسحب الماء مما يؤدي الى تلوثه بمياه المجاري الاسنة خاصة في المناطق التي تعاني من قدم وتشقق انابيب المجاري .
4. عدم تناول المضادات الحيوية دون استشارة طبيب.
5. فحص المخالطين وكل المتقدمين للعمل كعامل في اطعمته والتأكد من خلوصهم من هذا المرض .
6. العناية بمياه الشرب وذلك بإضافة الكلورين لها وحمايتها من التلوث بمياه الصرف الصحي .
7. بسترة أو غلي اللبن أو منتجاته، غلي المحار قبل استعماله
8. التطعيم ضد حمى التايفوئيد لمخالطي المرضى أو حاملي الميكروب أو من يودون السفر إلى مناطق ذات استيطان عالي للمرض.

المصادر

1. Bhan MK, Bahl R, Sazawal S, et al. Association between *Helicobacter pylori* infection and increased risk of typhoid fever. J Infect Dis. 186:1857-1860, (2002).
2. Safdar, Amar ; Harjit Kaur; Linda Elting; Kenneth V.I. Rolston. Antimicrobial Susceptibility of 128 *Salmonella enterica* Seroovar Typhi and Paratyphi A Isolates from Northern India, I.ch.,50:88-91,(2004).
3. Winokur, P. L. ; Vonstein, D. L. ; Hoffman, L. J. Evidence for transfer of CMY-2 AmpC β -lactamase plasmids between *Escherichia coli* and *Salmonella* isolates from food animals and humans. AN. and CH.45: 2716-22, (2001).
4. Vollaard, MD; Albert M.; Soegianto Ali; Henri A. G. H. ;van Asten; Suwandhi Widjaja; Leo G. Visser; Charles Surjadi; Jaap T. van Dissel. Risk Factors for Typhoid and Paratyphoid Fever in Jakarta, In. Af. Journal of Micr. Research, : 033-036,(2004).
5. Lin-Hui Su; Tsu-Lan Wu; Ju-Hsin Chia; Chishih Chu; An-Jing Kuo ; Cheng-Hsun Chiu. Increasing ceftriaxone resistance in *Salmonella* isolates from a university hospital in Taiwan. Journal of Ant..Ch. 55(6):846-852, (2005).

6. Threlfall, E. J. Antimicrobial drug resistance in *Salmonella*: problems and perspectives in food- and water-borne infections. *FEMS Micro.Reviews* 26: 141-8 (2002).
7. Parry, C. M. ; T. T. Hien; G. Dougan; N. J. White;J. J. Farrar. Typhoid fever. *N. Engl. J. Med.* 347:1770-1782 (2002).
8. Na'aya. H. U.; U. E. Eni; C. M. Chama. Typhoid perforation Maiduguri, Nigeria. *Annals of A. M.*, 3, (2): 69 – 72 (2004).
9. Crump JA; Luby SP; Mintz ED. "The global burden of typhoid fever". *Bull World Health Organ.* 82: 346-353 (2004).
- 10.Marzano,-A-V;Mercogliano, -M;Borghi, -A;Facchetti, -M;Caputo,-R.Cutaneous infection caused by *Salmonella typhi*, J-Eur-Acad-Dermatol-Venereol. 17(5): 575-7 (2003).
11. Al-Quarawi SN, el Bushra HE, Fontaine RE, Bubshait SA, el Tantawy NA. Typhoid fever from water desalinized using reverse osmosis. *Epidemiol Infect*: 114(1):41, (1995).
- 12.Senthilkumar;Prabakaran.MultidrugResistant*Salmonella typhi* in symptomatic Typhoid Carriers among Food Handlers in Namakkal District, Tamil Nadu;23, 2,: 92-94,(2005).
13. Ram PK; Naheed A; Brooks WA; Hussein MA; Mintz ED; Breiman RF; Luby SP. Risk factors for typhoid fever in a slum in Dhaka, Bangladesh. *Epidemiol Infect.*:1-8,(2006).
- 14.National Committee for Clinical Laboratory Standards. Performance Standards for Antimicrobial Disk Susceptibility Tests-Seventh Edition: Approved Standard M2-A7. NCCLS, Villanova, PA, USA, (2000).
- 15.Widal, F. Serodiagnostic de la fièvre typhoid. *Semaine Med.* 16:259,(1896).
16. Sunmi Yoo; Hyunjoo Pai;Jeong-hum Byeon; Youn Ho Kang;Shukho Kim; Bok Kwon Lee. Epidemiology of *Salmonella enterica* Serotype Typhi Infections in Korea for Recent 9 Years: Trends of Antimicrobial Resistance. *J Korean Med Sci*; 19: 15-20, ISSN :1011-8934, (2004).
17. Ackers, M. L.; N. D. Puhr; R. V. Tauxe;E. D. Mintz. Laboratory-based surveillance of *Salmonella* serotype Typhi infections in the United States: antimicrobial resistance on the rise. *JAMA.* 283:2668-2673, (2000).

18. Camilo A; Albert MJ; Bhan KM. Background document: the diagnosis, treatment and prevention of typhoid fever. Geneva, World Health Organization, (2003).
19. Marta-Louise Ackers; MD, MPH; Nancy D. Puh; Robert V. Tauxe; Eric D. Mintz .Laboratory-Based Surveillance of Salmonella Serotype Typhi Infections in the United States. JAMA ;283:2668-2673,(2000).
20. Bitar F; Tarpley Y. Intestinal perforation in typhoid fever: historical and state of the art. Rev Infect Dis; 7:257-271.1, (1985).
21. Kubota; T. J. Barrett; M. L. Ackers; P. S. Brachman; E. D. Mint. Analysis of Salmonella enterica Serotype Typhi Pulsed-Field Gel Electrophoresis Patterns Associated with International Travel. Journal of Clinical Microbiology. 43, 3, :1205-1209, (2005).
22. Fouady, A.S; Girgis, S.P.; Gregory; J.M. Omar Wasfy. "Population-Based Surveillance of Typhoid Fever in Egypt", Am. J. Trop. Med. Hyg. 74(1):114-119 (2004).
23. Najah M. AbdelRaheem; Gihan Y. Yousef; Hatem M. Shalaby; Mohammed Eltorky Ahmed AbdelAzziz. Typhoid carries among children in sohag. Public health department,. Sohag University. Pediatric On call [serial online]: http://www.pediatriconcall.com/fordocor/Medical_original_articles/typhoid.asp. (2007).
24. Winokur PL; Canton R; Casellas JM; Legakis N. Variations in the prevalence of strains expressing an extended spectrum β -lactamase Phenotype and characterization of isolates from Europe, the Americas and the Western Pacific region. Clin. Infect. Dis. 32(Suppl. S) :94-10.(2001).
25. Johnson DM; Bieddenbach DJ; Jones RN; Potency .Antimicrobial spectrum update for piperacillin/tazobactam emphasis on its activity against resistant organism populations and generally untested species causing community acquired respiratory tract infections. Diag. Microbial. Infect. Dis. 43:49-60, (2002).
26. Jones RN. Resistance patterns among nosocomial pathogens: Trends over the past few years. Chest 119(suppl. 2):397S-404S, (2001).
27. Doughari, J. H. Retrospective study on the antibiotic resistant pattern of Salmonella typhi from some clinical samples. African Journal of Microbiology Research, 2:033-036,(2007).
28. Jawetz E., Melnick, J.L. Adelberg, E.A, A large Medical Book of Medical Microbiology, 21st ed. Appelton and large, California, (1998).

دراسة القابلية التطهيرية والمضادة للتطهير للمستخلص الفلافوني المنقى جزئياً لنبات الميرمية *Salvia officinalis* باستخدام نظام بكتيري

علي حافظ عباس و عصام فاضل علوان

جامعة بغداد - كلية العلوم - وحدة البحوث البايولوجية للمناطق الحارة

جامعة بغداد - معهد الهندسة الوراثية والتقنية الأحيائية للدراسات العليا

ABSTRACT

This study was carried out in order to determine the toxic and mutagenic and antimutagenic effects for sage (*Salvia officinalis*) against the mutagenic effect of methotrexate (MTX) and The ultraviolet rays. The effect was studied in a bacterial system (G-system). This system consisted of three isolates G₃ *Bacillus* spp., G₁₂ *Arthrobacter* spp. and G₂₇ *Brevibacterium* spp. The study depended on recording survival index as an indicator and induction of streptomycin and rifampicin resistance as a chromosomal marker. Flavonic Extract was prepared from dry sage leaves, Gradual concentrations of plant flavonic extract was used to chose the suitable concentration.

The interactions included three types of treatments (per - MTX, with- MTX and post - MTX) as a chemical mutagen and (per - UV, with- UV and post - UV) as a physical mutagen in order to determine the mechanisms of this plant extract in preventing or reducing the genotoxic effect of MTX and UV.

الخلاصة

أجريت هذه الدراسة للكشف عن التأثيرات السمية والتطهيرية والمضادة للتطهير للمستخلص الفلافوني لنبات الميرمية *Salvia officinalis* إذ كان التركيز الأمثل للمستخلص الفلافوني هو 150 مايكروغرام / مليلتر، ومقارنة فعاليته تجاه العقار Methotrexate (MTX) باعتباره مطفر كيميائي، والأشعة فوق البنفسجية (UV) باعتبارها مطفر فيزيائي وباستخدام نظام الاختبار خارج الجسم الحي (in vitro) بشكل إنفرادي لكل منهما بمعاملات متداخلة للمستخلص مع MTX و UV قبل ومع وبعد المعاملة بالمطفر باستعمال (G-system) بالأعتماد على معامل البقاء Survival fraction (S_x) لدراسة التأثيرات وحث الطفرات المقاومة للمضاد الحيوي الستربتومايسين والريفاميسين كواسمات وراثية Genetic markers.

أظهرت نتائج تأثير التداخل بين التركيز الأمثل للمستخلص والمطفر على معامل البقاء (S_x) ارتفاع قيم معامل بقاء عزلات النظام لتصل إلى قيم مقارنة للطبيعية مقارنة بالسيطرة الموجبة (MTX أو UV فقط)، وكما أظهرت نتائج التداخل بين التركيز الأمثل للمستخلص والمعاملة بالمطفر في حث طفرات المقاومة للمضادين الستربتومايسين والريفاميسين أن MTX لم يكن له أي تأثير في حث الطفرات المقاومة للمضادين الحيويين للمعاملات قبل ومع وبعد المعاملة بالمطفر MTX وللعزلات الثلاث وبذلك عمل المستخلص الفلافوني على إخماد أو تصليح الطفرات ووفر حماية 100% للخلايا البكتيرية.

في حين أظهرت نتائج تأثير التداخل بين التركيز الأمثل للمستخلص والمعاملة بالأشعة فوق البنفسجية بعدم ظهور أي تأثير في حث طفرات المقاومة لمضاد الريفاميسين للمعاملات كافة ولعزلات النظام الثلاثة وكذلك الحال لمضاد الستربتومايسين للمعاملات مع وبعد التعرض للأشعة فوق البنفسجية وللعزلات الثلاثة، في حين ظهرت طفرات مقاومة لمضاد الستربتومايسين عند المعاملة قبل التعرض للأشعة فوق البنفسجية، وبذلك عملت المعاملتان مع وبعد التعرض للأشعة فوق البنفسجية على إخماد أو تصليح الطفرات ووفرت حماية 100% للخلايا البكتيرية في حين كانت نسبة تصليح الطفرات والحماية من التعرض للأشعة للمعاملة قبل التعرض للأشعة فوق البنفسجية تتراوح بين (93.6% - 98.3%)، يمكن الاستنتاج من ذلك أن المستخلص الفلافوني المنقى جزئياً لنبات الميرمية ذي كفاءة عالية تكاد تصل إلى 100% في حماية خلايا النظام المستخدم من التأثيرات السامة للعقار MTX والتعرض للأشعة فوق البنفسجية.

المقدمة

نبات الميرمية من النباتات واسعة الانتشار في مختلف بلدان العالم وفي العراق (المحافظات الشمالية)، والبلدان المجاورة للعراق وكان أول من استخدمه هم الرومان القدماء وأطلق عليه الإغريق إسم (1) Elifages جاءت تسمية الميرمية من اللفظة اللاتينية Salvare التي تعني to save أي الحفاظ على الحياة والتي تشير إلى الخصائص الطبية لهذا النبات (2).

تعد *Salvia officinalis* من أهم أنواع الميرمية من حيث إحتوائها على معظم وأكثر المركبات الفعالة المتواجدة في باقي الأنواع الأخرى ، وتختلف مكونات نبات الميرمية وفقاً للجزء النباتي المستخدم (كالجذور أو الأجزاء الهوائية كالأوراق و الأزهار) ، فأوراق الميرمية غنية بالفلافونيدات Flavonoides إذ تصل نسبتها (1-3%) (3) .

كما تحتوي أوراق الميرمية على مركبات أخرى كالتربينات الثلاثية Triterpenes (بصورة رئيسة Ursolic acid) إذ تصل نسبته إلى 5% ، وتحتوي أيضاً على التربينات الثنائية Diterpenes ، وتحتوي أوراق الميرمية أيضاً على بعض المركبات الفينولية مثل Rosmarinic acid (4) . كما يعد نبات الميرمية من النباتات الغنية بالزيوت الطيارة (Essential oil) تصل نسبتها (1 - 2.5 %) ويمكن الحصول على (8 - 25) مليلتر من الزيوت الطيارة لكل كيلوغرام من أوراق الميرمية (4,5) .

استعملت الميرمية في حفظ الأغذية لما لها من قابلية مضادة للجراثيم و في علاج بعض الأمراض كضعف الذاكرة ، علاج حالات الصرع ، وإرتخاء الأعصاب في حالات التشنجات بإعتبار أن الميرمية تحتوي على مواد مهدئة للأعصاب ، ومعالجة الهذيان المصاحب لإرتفاع درجة حرارة الجسم و معالجة إضطرابات الحبل الشوكي (5,6) ، كما تعد مستخلصات الميرمية كمادة مقلصة للأوعية الدموية فتمنع بذلك حصول النزف المستمر (6,7) .

تستخدم مستخلصات الميرمية في علاج حالات عدم إنتظام الحيض وتقليل تدفق الحليب من الغدد اللبنية في الثدي عند فترة الفطام فضلاً عن إستخدامها في علاج عسر الحيض (6,8) ، كما تستخدم مستخلصات الميرمية كمادة مضادة للتطهير والسرطانات (5,9) .

لنبات الميرمية و مستخلصاتها دور فاعل في القضاء على الكثير من مسببات الإلتهابات البكتيرية أو الفطرية أو الفيروسية إذ أن لها تأثير قاتل ضد بعض أنواع البكتيريا الموجبة و السالبة لصبغة غرام ، في حين أن لها دوراً مثبطاً لنمو باقي الأنواع (10) .

تعد أنظمة الأحياء المجهرية من أكثر الأنظمة انتشاراً في تحديد قابلية المواد على إحداث الطفرات أو قابليتها على منع حدوثها وتشمل هذه الأنظمة البكتيريا والفطريات والخمائر. صُمم نظاماً بكتيرياً أطلق عليه G - System يتضمن ثلاث عزلات بكتيرية تتصف بحساسيتها العالية للمضادين الحيويين الستربتومايسين والريفامبسين (11,12) ، جدول (1) ، واستعمل هذا النظام في الكشف عن قابلية المواد على التطهير وذلك بأستعمال مواد مطفرة قياسية مثل المطفر Nitrosoguanidine (NTG) ، Hydroxylamine (HA) و Acridine Orange (AO) ، 5-Bromouracil (5-BU) وشُخصت هذه العزلات وهي من الأجناس *Bacillus* spp.(G3) ، *Arthrobacter* spp.(G12) و *Brevibacterium* spp.(G27) (11,12) .

جدول 1- صفات عزلات G - System

رقم العزلة	Gram stain	اختبار الحساسية	
		R ₂₀ **	S ₁₀ *
3	-	-	-
12	-	-	-
27	-	-	-

* تركيز الستربتومايسين 10 مايكروغرام/ مليلتر من الوسط الغذائي
** تركيز الريفامبسين 20 مايكروغرام/ مليلتر من الوسط الغذائي
عزلة حساسة.

أختير هذا النظام بالإعتماد على مؤشرات محددة للنظام لعل أهمها صفة المقاومة للمضادات الحيوية الستربتومايسين والريفامبسين بأعتبارها صفات كروموسومية (13) وذلك لثباتية الصفات الكروموسومية مقارنة بالصفات المحمولة على البلازميدات التي يمكن أن تفقد تحت ظروف معينة مثل تعرض الخلايا لعمليات الزرع المتكرر أو تعرض العزلات لبعض المواد الكيفلافونية أو إرتفاع

درجات الحرارة . واختبرت حساسية النماذج الأولية للستربتومايسين والريفامبسين بأستعمال طريقة التدرج في الأطباق (11,12) ووجد أن أنسب التراكيز هي 10 مايكروغرام / مليلتر من الستربتومايسين و 20 مايكروغرام / مليلتر للريفامبسين كما موضح بالجدول (1) .

المواد وطرائق العمل

إستعملت أوراق نبات الميرمية *Salvia officinalis* L. الذي يعود للعائلة الشفوية (Lamiaceae) تم شراؤها من مركز بغداد لطب الأعشاب / وزارة الصحة وتم تصنيفها من قبل المركز نفسه .
خُصر المستخلص الفلافوني لنبات الميرمية على وفق الطريقة المتبعة من قبل (14) بوضع 5 غرامات من الأوراق الجافة في 50 مليلتر من كحول مثيلي بتركيز 80 % لمدة خمس دقائق ، رُشح المستخلص وركّز بأستخدام المبخر الدوار عند درجة حرارة 40 م° ثم تضاف قطرات من حامض الكبريتيك المخفف بعبارية 2N للمزيج على حمام مائي لمدة نصف ساعة ، يستخلص المزيج بالكلوروفورم للحصول على مستخلص يحوي على الفلافونات بنقاوة جزئية وتعاد هذه الخطوة ثلاث مرات بأستخدام قمع فصل ، تؤخذ طبقة الكلوروفورم السفلية بعد الفصل وتبخر الى حد الجفاف للحصول على راسب جاف وتتم إذابتها بأستخدام 50 مليلتر من الماء المقطر ويُعَمَّم المستخلص بأستخدام وحدات ترشيح مفرغة 0.22 Millipore Filter مايكرومتر ويُحفظ في الثلاجة داخل قناني معتمة معقمة مسبقاً (15).

تم الكشف عن وجود الفلافونات في المستخلص بأستخدام كشف الفلافونات العام (16) ، والتشخيص بأستخدام كروموتوغرافيا الطبقة الرقيقة Thin Layer Chromatography (2) ، والتشخيص بأستخدام جهاز كروموتوغرافيا السائل عالي الكفاءة High -Performance Liquid Chromatography (17) ، والتشخيص الطيفي للفلافونات بأستخدام الأشعة فوق البنفسجية Ultraviolet Spectroscopy (2) .

تم الحصول على عزلات G – System من معهد الهندسة الوراثية / جامعة بغداد ، وعومل 5 مليلتر من عالق الخلايا بتركيز مختلفة من المستخلص الفلافوني المنقى جزئياً أولاً لمدة 15 دقيقة ، ثم دُرس تأثير التداخل ما بين التركيز الأمثل للمستخلص و التركيز الأمثل للمطفر الكيميائي Methotrexate (50 مايكروغرام / مليلتر) والمورد من شركة Hixal (Germany) حسب دراسة سابقة (18) بمعاملة عالق الخلايا بالتركيز الأمثل للمستخلص الفلافوني المنقى جزئياً في دارئ الفوسفات (pH 5.5) (11,12,15) لمدة 15 دقيقة ومن ثم المعاملة بالتركيز الأمثل من MTX لمدة 15 دقيقة (قبل المعاملة بالمطفر) ، ومعاملة 5 مليلتر من عالق الخلايا بالتركيز الأمثل للمطفر والمستخلص سوية لمدة 15 دقيقة (مع المعاملة بالمطفر) ، ومعاملة 5 مليلتر من عالق الخلايا بالتركيز الأمثل لمطفر MTX لمدة 15 دقيقة ومن ثم معاملتها بالتركيز الأمثل للمستخلص لمدة 15 دقيقة (بعد المعاملة بالمطفر) ، ودُرس تأثير التداخل ما بين التركيز الأمثل للمستخلص والتطهير بأستخدام الأشعة فوق البنفسجية (19,15) بمعاملة عالق الخلايا بالتركيز الأمثل للمستخلص النباتي في دارئ الفوسفات (pH 5.5) (11,12,15) لمدة 15 دقيقة ومن ثم المعاملة بالأشعة لمدة 15 دقيقة ، ومعاملة 5 مليلتر من عالق الخلايا بالأشعة لمدة 15 دقيقة ومن ثم معاملتها بالتركيز الأمثل للمستخلص الفلافوني المنقى جزئياً لمدة 15 دقيقة .
القوانين و الحسابات (20) .

1. تحديد الجزء الحي المتبقي (Survival frection (S_x)

$$S_x = N_s / N_0$$

(X : تركيز المطفر ، N_s : عدد الخلايا المتبقية بعد المعاملة مباشرة ، N_0 : عدد الخلايا في نموذج السيطرة السالبة)

2. تحديد تردد الطفرات (Mutant frequency (M_x)

$$M_x = N_{mx} / N_0$$

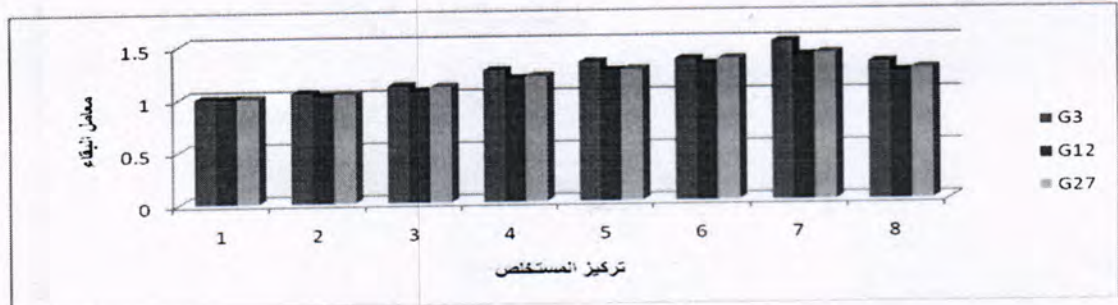
(N_{mx} : عدد الطفرات المستحثة عند التركيز x)

تم تحليل النتائج إحصائياً بإجراء ANOVA Test بتوظيف البرنامج الإحصائي الجاهز SPSS V.11.5 .

النتائج والمناقشة

استعمل المستخلص الفلافوني المنقى جزئياً لنبات الميرمية في دراسة التأثير التطهيري والمضاد للتطهير للمستخلص الفلافوني لنبات الميرمية بعد إجراء الكشوفات الخاصة على الفلافونات . ويوضح الشكل (1) تأثير المستخلص الفلافوني المنقى جزئياً لنبات الميرمية في الجزء المتبقي من الخلايا (S_x) بعد المعاملة بتركيز مختلفة من المستخلص النباتي الفلافوني ويلاحظ من الشكل أن أقل تأثير للمستخلص كان عند التركيز 10 مايكروغرام / مليلتر إذ بلغت قيم معامل البقاء (1.05 ، 1.02 ، 1.04) للعزلات G_3 و G_{12} و G_{27} على التوالي ، وكان أعلى تأثير ملحوظ عند التركيز 150 مايكروغرام / مليلتر إذ بلغت قيم معامل البقاء (1.39 ، 1.37 ، 1.5) للعزلات G_3 و G_{12} و G_{27} على التوالي ، في حين حصل انخفاض لقيمة هذا العامل عند التركيز العالي 200 مايكروغرام / مليلتر ليصل إلى (1.3 ، 1.21 ، 1.24) للعزلات G_3 و G_{12} و G_{27} على التوالي ، ولم تظهر أي طفرة مقاومة للمضادين الستربتومايسين والريفامبسين مما يدل على أن المستخلص الفلافوني للميرمية مادة غير مطفرة .

أثبتت نتائج التحليل الإحصائي لتأثير تراكيز مختلفة من المستخلص على قيم معامل بقاء العزلات وجود هذا التأثير حيث ظهر وجود فرق معنوي (إنخفاض) ($p \leq 0.05$) في قيم معامل بقاء السيطرة السالبة مقارنة مع قيم بقاء المعاملة بالتراكيز (200,150,100,75) مايكروغرام / مليلتر ، بينما ظهر فرق معنوي (ارتفاع) ($p \leq 0.05$) في قيم معامل بقاء المعاملة بالتركيز 150 مايكروغرام / مليلتر مقارنة مع قيم معامل بقاء باقي المعاملات عدا المعاملة بالتركيز 100 مايكروغرام / مليلتر ، في حين لوحظ فرق معنوي (إنخفاض) ($p \leq 0.05$) في قيم معامل البقاء للمعاملة بالتركيز 200 مايكروغرام / مليلتر مقارنة مع قيم معامل بقاء المعاملة بالتركيزين 100 و 150 مايكروغرام / مليلتر .

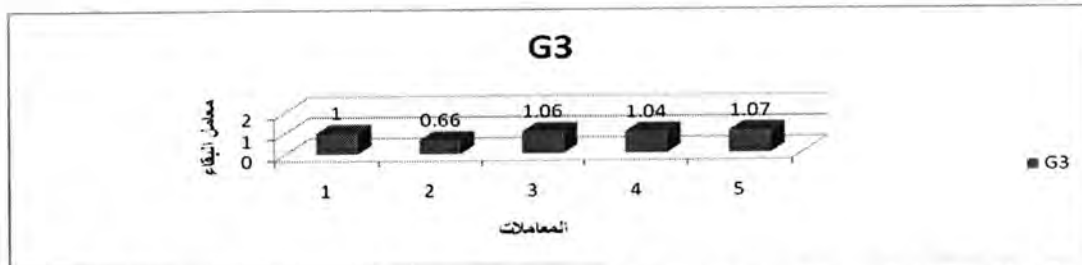


شكل 1- تأثير تراكيز مختلفة من المستخلص الفلافوني لأوراق نبات الميرمية في معامل البقاء لعزلات النظام (1: السيطرة السالبة ، 2: تركيز 10 ، 3: 25 ، 4: 50 ، 5: 75 ، 6: 100 ، 7: 150 ، 8: 200).

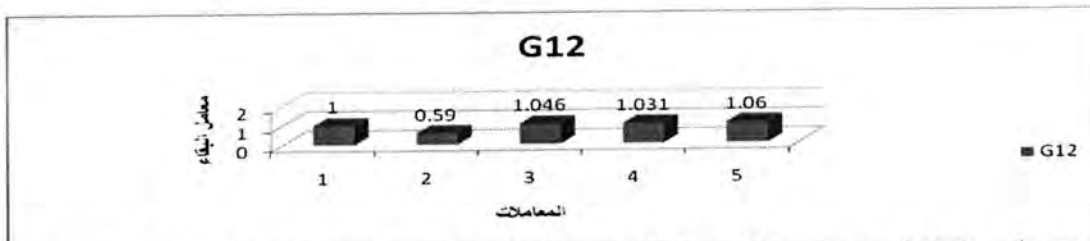
وتوضح الأشكال (2,3,4) تأثير التداخل بين المستخلص الفلافوني المنقى جزئياً لنبات الميرمية والتركيز الأمثل للمطفر MTX في الجزء المتبقي من الخلايا (S_x) . ويلاحظ من الشكل أن المستخلص الفلافوني قد رفع من قيم معامل البقاء لتصل قيمته إلى قيمة مقاربة للسيطرة السالبة ولجميع العزلات البكتيرية المكونة للنظام . إذ بلغت قيم معامل البقاء للمعاملة قبل المعاملة بالمطفر (1.05 ، 1.06 ، 1.046) للعزلات G_3 و G_{12} و G_{27} على التوالي ، بينما بلغت قيم معامل البقاء للمعاملة مع المطفر (1.03 ، 1.031 ، 1.04) للعزلات G_3 و G_{12} و G_{27} على التوالي ، في حين كانت قيم معامل البقاء للمعاملة بعد المعاملة بالمطفر (1.07 ، 1.06 ، 1.055) للعزلات G_3 و G_{12} و G_{27} على التوالي .

وأظهرت نتائج التحليل الإحصائي لتأثير التداخل بين المستخلص الفلافوني و المطفر Methotrexate في قيم معامل بقاء العزلات G_3 ، G_{12} ، G_{27} وجود فرقاً معنوياً (إنخفاضاً) ($p \leq 0.05$) في قيم معامل بقاء السيطرة الموجبة (المعاملة بالمطفر فقط) مقارنة مع قيم بقاء باقي المعاملات عند المعاملة بالمستخلص الفلافوني قبل ومع وبعد المعاملة بالمطفر ، حيث يلاحظ أن المستخلص الفلافوني قد رفع

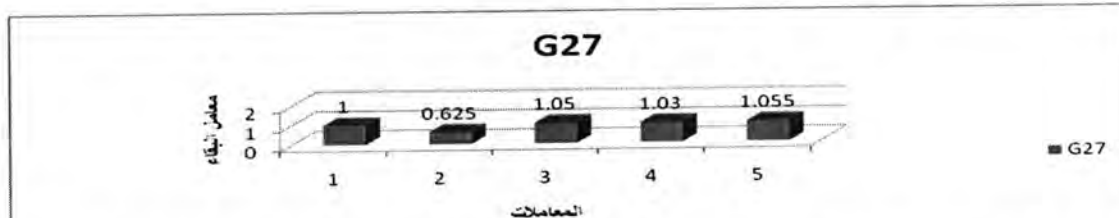
من قيمة معامل البقاء لتصل قيمته إلى قيمة مقارنة للحالة الطبيعية ولجميع العزلات البكتيرية المكونة للنظام ، وبذلك أظهر المستخلص الفلافوني كفاءة عالية في وقاية الخلايا البكتيرية من التأثيرات السمية للمطفر .



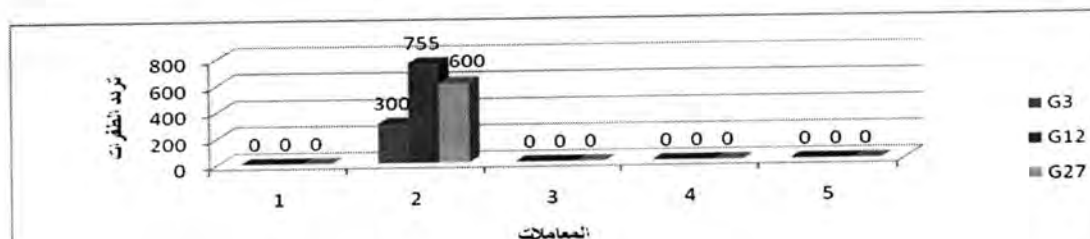
شكل-2: تأثير التداخل بين المستخلص الفلافوني والمطفر Methotrexate على معامل البقاء للعزلة G3 (1: السيطرة السالبة مستخلص فقط ، 2: السيطرة الموجبة MTX فقط، 3: فلافوني قبل المعاملة بالمطفر ، 4: فلافوني مع المعاملة ، 5: فلافوني بعد المعاملة)



شكل-3: تأثير التداخل بين المستخلص الفلافوني والمطفر Methotrexate على معامل البقاء للعزلة G12 (1: السيطرة السالبة مستخلص فقط ، 2: السيطرة الموجبة MTX فقط، 3: فلافوني قبل المعاملة بالمطفر ، 4: فلافوني مع المعاملة ، 5: فلافوني بعد المعاملة)



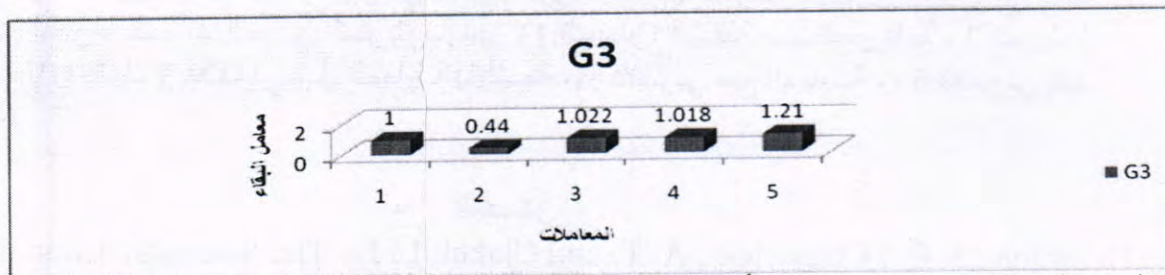
شكل-4: تأثير التداخل بين المستخلص الفلافوني والمطفر Methotrexate على معامل البقاء للعزلة G27 (1: السيطرة السالبة مستخلص فقط ، 2: السيطرة الموجبة MTX فقط، 3: فلافوني قبل المعاملة بالمطفر ، 4: فلافوني مع المعاملة ، 5: فلافوني بعد المعاملة) يوضح الشكل (5) أن المطفر لم يكن له أي تأثير في حث الطفرات المقاومة للمضاد الحيوي الستربتومايسين والريفامبسين للمعاملات قبل ومع وبعد المعاملة بالمطفر MTX والعزلات الثلاث وبذلك عمل المستخلص الفلافوني المنقى جزئياً على إخماد أو تصليح الطفرات ووفر حماية 100% للخلايا البكتيرية .



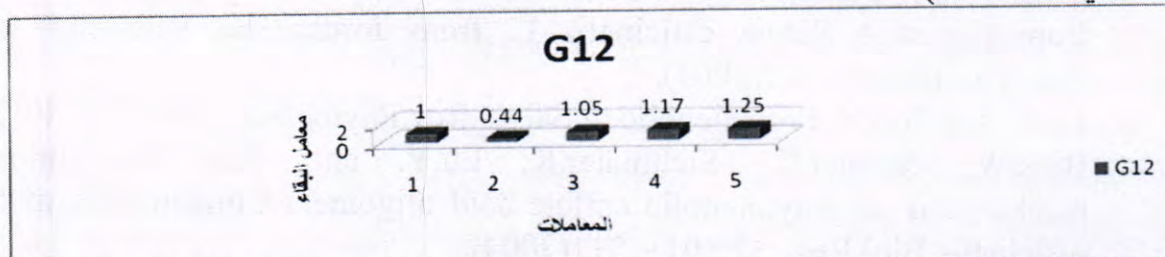
شكل-5: التداخل بين المستخلص والمطفر MTX في حث الطفرات للعزلة G3 ، G12 ، G27 (1: السيطرة السالبة مستخلص فقط ، 2: السيطرة الموجبة MTX فقط، 3: فلافوني قبل المعاملة بالمطفر ، 4: فلافوني مع المعاملة ، 5: فلافوني بعد المعاملة)

وتوضح الأشكال (6،7،8) تأثير التداخل بين المستخلص الفلافوني المنقى جزئياً لنبات الميرمية والتطهير بالأشعة فوق البنفسجية في الجزء المتبقي من الخلايا (S_x) بمعاملة الخلايا بالمستخلص ومن ثم بالأشعة (قبل المعاملة بالمطفر) ، ومعاملة عالق الخلايا بالأشعة والمستخلص سوية (مع المعاملة بالمطفر) ، ومعاملة الخلايا بالأشعة ومن ثم بالمستخلص (بعد المعاملة بالمطفر) ، ويلاحظ أن المستخلص الفلافوني قد رفع قيمة معامل البقاء لتصل قيمته إلى قيمة مقاربة للحالة الطبيعية ولجميع العزلات البكتيرية المكونة للنظام . إذ بلغت قيم معامل البقاء قبل تعريض العزلات للأشعة فوق البنفسجية (1.014, 1.05, 1.022) للعزلات G_3 ، G_{12} ، G_{27} على التوالي ، بينما بلغت قيم معامل البقاء للمعاملة مع التعرض للأشعة (1.15, 1.17, 1.018) للعزلات G_3 ، G_{12} ، G_{27} على التوالي ، في حين كانت قيم معامل البقاء للمعاملة بعد التعرض للأشعة فوق البنفسجية (1.19, 1.25, 1.21) للعزلات G_3 ، G_{12} ، G_{27} على التوالي ، وبذلك أظهر المستخلص الفلافوني كفاءة عالية في وقاية الخلايا البكتيرية من تأثيرات الأشعة فوق البنفسجية.

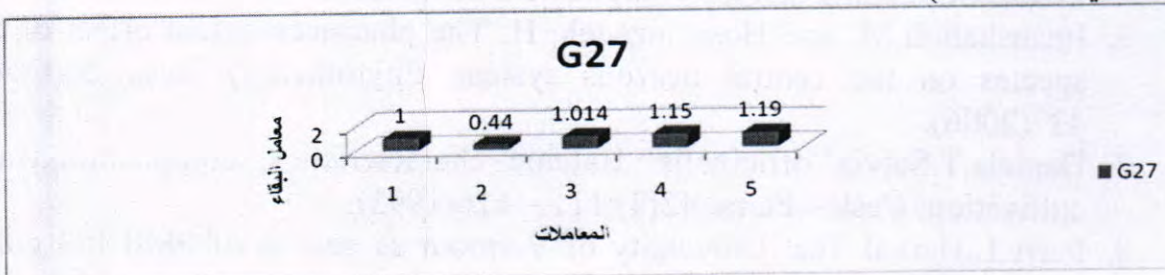
وأظهرت نتائج التحليل الإحصائي لتأثير التداخل بين المستخلص الفلافوني والتعرض للأشعة فوق البنفسجية في قيم معامل البقاء وجود فرق معنوي (إنخفاض) ($p \leq 0.05$) في قيم معامل بقاء السيطرة الموجبة للعزلة G_3 و G_{12} و G_{27} مقارنة مع قيم معامل بقاء باقي المعاملات ، و فرق معنوي (ارتفاع) ($p \leq 0.05$) في قيم كل من المعاملة بالمستخلص مع و بعد التعرض للأشعة فوق البنفسجية مقارنة مع قيم معامل بقاء السيطرة السالبة ، و فرق معنوي (إنخفاض) في معامل بقاء العزلات قبل المعاملة بالأشعة مقارنة بالمعاملة مع وبعد المعاملة بالأشعة لعزلات النظام.



شكل-6: التداخل بين المستخلص والأشعة فوق البنفسجية للعزلة G_3 (1: السيطرة السالبة مستخلص فقط ، 2: السيطرة الموجبة MTX فقط ، 3: فلافوني قبل المعاملة بالمطفر ، 4: فلافوني مع المعاملة ، 5: فلافوني بعد المعاملة) .

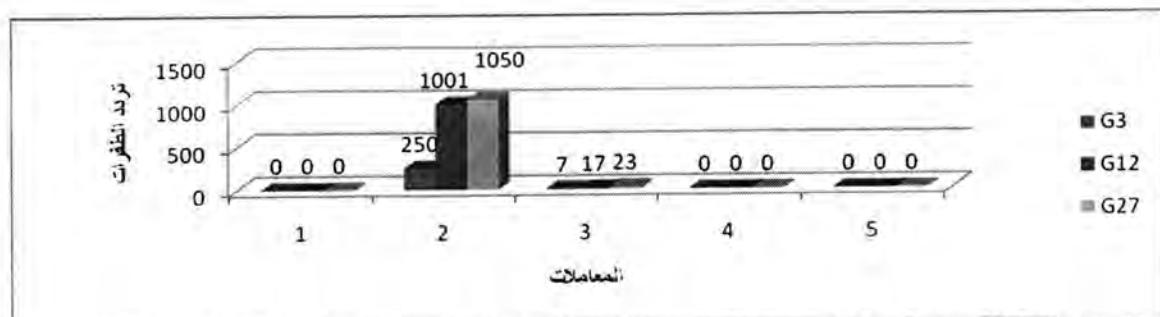


شكل-7: التداخل بين المستخلص والأشعة فوق البنفسجية للعزلة G_3 (1: السيطرة السالبة مستخلص فقط ، 2: السيطرة الموجبة MTX فقط ، 3: فلافوني قبل المعاملة بالمطفر ، 4: فلافوني مع المعاملة ، 5: فلافوني بعد المعاملة) .



شكل-8: التداخل بين المستخلص والأشعة فوق البنفسجية لل عزلة G3 (1: السيطرة السالبة مستخلص فقط ، 2: السيطرة الموجبة MTX فقط، 3: فلافوني قبل المعاملة بالمطفر ، 4: فلافوني مع المعاملة ، 5 : فلافوني بعد المعاملة) .

يوضح الشكل (9) أن المعاملة بالأشعة فوق البنفسجية لم يكن لها أي تأثير في حث طفرات المقاومة لمضاد الريفاميسين لكل المعاملات والستربتومايسين للمعاملات مع و بعد التعرض للأشعة فوق البنفسجية ولل عزلات الثلاثة في حين ظهرت طفرات مقاومة لمضاد الستربتومايسين عند المعاملة قبل التعرض للأشعة فوق البنفسجية ، إذ ظهرت (7 ، 17 ، 23) طفرة للعزلات G_{27} ، G_{12} ، G_3 على التوالي ، وبذلك عملت المعاملتان مع و بعد التعرض للأشعة فوق البنفسجية على إخماد أو تصليح الطفرات ووفرت حماية 100 % للخلايا البكتيرية في حين كانت نسبة تصليح الطفرات والحماية من التعرض للأشعة للمعاملة قبل التعرض للأشعة فوق البنفسجية تتراوح من 93.6 - 98.3 % .



شكل-9: التداخل بين المستخلص والتعرض للأشعة فوق البنفسجية لل عزلة G3, G12, G27 في حث الطفرات المقاومة للمضاد الحيوي الستربتومايسين (1: السيطرة السالبة مستخلص فقط ، 2: السيطرة الموجبة UV فقط، 3: فلافوني قبل المعاملة بالأشعة ، 4: فلافوني مع المعاملة ، 5: فلافوني بعد المعاملة) .

المصادر

1. Simon , J. E. ; Chadwick , A. T. and Clakel, L. E . The Scientific Literatue On Selected Herbs , and Aromatic and Medical Plants of The Temperate Zone. Archon Books, :770(1984) .
2. Dordevic, S.; Cakic, M. and Amr, S. The extraction of apigenin and Luteolin from the sage *Salvia officinalis* L. from Jordan. The Scientific Journal FACTA, 1(5):87 – 93(2001).
3. Lu, Y. and Foo, Y. Polyphenolic of *Salvia*. Rev. Phytochem., 59:117– 140(2002).
4. Bors, W.; Michel, C.; Stettmaier, K; Lu, Y. and Foo, L. Y. Antioxidant mechanisms of polyphenolic caffeic acid oligomers Constituents of *Salvia officinalis*. Biol. Res., 37:301 – 311(2004).
5. Velickovic, A.; Birtic, M. S.; Velickovic, D.; Illic, S. and Mitic, N. The possibilities of the application of some species of sage (*Salvia* L.) as auxiliaries in the treatment of some diseases. J. Ser. Chem. Soc., 68(6):435 – 445(2003).
6. Imanshahidi, M. and Hosseinzadeh, H. The pharmacological effect of *Salvia* species on the central nervous system. Phytotherapy Res., 20(6):427 – 437(2006).
7. Daniela, T. *Salvia officinalis* . Botanic characteristics, composition, use and cultivation. Cesk – Farm, 42(3):111 – 116(1993).
8. Perry, L. Herbal Tea . University of Vermont as part as of PSS1.123 courses , Canada.: 542 – 546(1997).

9. Arima,H.;Ashida,H. and Donno, Gen-ichi Rutin – Enhanced Antibacterial activities of Flavonoides against *Bacillus cereus* and *Salmonella enteritidis*. *Biosci. Biotechnol.Biochem.*,66 (5):1009 – 1014(2002).
10. Willershausen,B.;Cruber,I.and Hamm,G.The influence of herbal ingredients on the plaque index and bleeding tendency of the gingival.*J.Clin. Dent.*,2:75–78 (1991).
11. العزاوي ، غيث لطفي الكشف عن المطفرات في الاغذية والبيئة بأستعمال نظام بكتيري . تقرير دبلوم عالي ، معهد الهندسة الوراثية والتقنيات الاحيائية ، جامعة بغداد(2004) .
12. العزاوي ، غيث لطفي؛ الخفاجي ، زهرة محمود ؛ المشهداني ، ورقاء يحيى والحسن ، أثير احمد مجيد، تطوير نظام بكتيري لتحديد الطفرات في البيئة والاغذية . اولاً : التطهير بالمطفر القياسي Nitrosoguanidine ، مجلة أم سلمة للعلوم . المجلد 2 (3):362-355(2005) .
13. Coleman,D.C.;Pomeray,H.;Estridge,J.K.;Keane,C.T.Cafferky,M.T.;Hone,R. and Foster,T.J Susceptibility to antimicrobial agent and analysis of plasmid in gentamicin and methicillin resistant *Staphylococcus aureus* from Dublin hospitals.*J.Med. Microbio.*, 20: 157-167.(1985).
14. Harbone,J.B.Phytochemical Methods, A Guide to Modern Techniques Of Plant Analysis . 2nd Ed. Chapman and Hall , London(1984).
15. الزبيدي، علي حافظ عباس، دراسة القابلية التطهيرية للمستخلصات المائية والكحولية لنبات الميرمية *Salvia officinalis* بأستعمال نظام بكتيري ، رسالة ماجستير ، معهد الهندسة الوراثية والتقنية الاحيائية ، جامعة بغداد(2007) .
16. Jaffer,H.J.;Mahmod,M.J.;Jawad,A.M.;Naji,A.and AL-Naib, A. Phytochemical and Biological Screening Of Some Iraqi Plants *Fitoterapia Lix* 299 (1983).
17. Redaelli, C. ;Formentini, L. and Santaniello , E. Reversed - Phase high – Preformance liquid chromatography analysisof Apigenin and it's glycosides in flower of *Matricaria chamomilla* and chamomile extract. *Plant. Med.* 42:288 – 292(1981).
18. الشمري ، علي عبيس عبد زنيد. استخلاص وتنقية مركب الكتان من بذور الكتان *Linum usitatissimum* ودراسة قابليته المضادة للتطهير على أنظمة مختلفة ، رسالة ماجستير ، معهد الهندسة الوراثية والتقنية الاحيائية ، جامعة بغداد (2004).
19. Al-Bakri , G. H. ;Umran , M. A. Mutagenesis of a novel Halotolerant bacteria (*Micrococcus* spp.) using Ultraviolet light and N – Methyl – N – Nitro – N – Nitroso Guanidine. *Iraqi Journal of Microbiology*, 6(2):55 – 64(1994)..
20. Eckardt, F. and Haynes , R. H. Quantitation Measures of Induced Mutagenesis.In "Short-Term Tests For Chemical Carcinogens" Eds. Stich, H.F. and San, R.H.C. Springer - verlag: NewYork,Berlin(1981).